

Université Claude - Bernard Lyon 1

Mémoire présenté en vue de l'obtention du
Diplôme d'Habilitation à Diriger des Recherches

Spécialité Sciences de la Terre et de L'Univers

CONTINENTAL AND MARINE ENVIRONMENTAL CHANGES IN EUROPE INDUCED BY GLOBAL CLIMATE VARIABILITY AND REGIONAL PALEOGEOGRAPHY CHANGES

by

Dr. Speranta - Maria POPESCU

UMR 5125 du CNRS

Paléoenvironnements et PaléoBioSphère

Université Claude Bernard Lyon 1

Advisory board

Pr. Jordi AGUSTI, Tarragona University, Tarragona, Spain

Pr. Philip GIBBARD, Cambridge University, Cambridge, Cambridge, UK

Pr. Martin J. HEAD, Brock University, St. Catharines, Canada

Pr. Laurent JOLIVET, Paris 6 University, Paris, France

Pr. Christophe LECUYER, Lyon 1 University, France

Pr. Frederique THEVENARD, Lyon 1 University, France

1st December 2008

SUMMARY

Foreword	
Curriculum Vitae	1
Publication List	9
CHAPTER 1	17
<hr/>	
RESPONSE OF EUROPEAN VEGETATION TO THE GLOBAL CLIMATE CHANGES DURING THE NEOGENE	
1.1. Global climate changes: forcing factors and mechanisms	17
1.2. Miocene global climate changes and European vegetation	21
1.2.1. Global climate variability during the Miocene	21
1.2.2. Vegetation changes in Europe during the Miocene	22
1.3. Pliocene global climate changes and European vegetation	27
1.3.1. Global climate variability during the Pliocene	27
1.3.2. Vegetation changes in Europe during the Early Pliocene	29
1.3.3. Vegetation changes in Europe during the Mid – Late Pliocene and Pleistocene	
PUBLICATIONS	39
CHAPTER 2	155
<hr/>	
PALEO GEOGRAPHY AND MARINE PALEOENVIRONMENTS CHANGES IN EUROPE DURING THE NEOGENE	
2.1. Living dinoflagellates and theirs cysts	155
2.2. Cyst morphology and environmental stress	157
2.3. European paleogeography changes during the Miocene - Pliocene	161
2.3.1. The Pannonian basin paleogeography during the Late Miocene - Early Pliocene	162
2.3.2. Messinian salinity Crisis: connections between Mediterranean and Paratethys seas	168
PUBLICATIONS	173
CHAPTER 3	409
<hr/>	
LATE PLEISTOCENE – HOLOCENE MARINE AND CONTINENTAL ENVIRONMENTS RECONSTRUCTION	
3.1. Mediterranean – Marmara – Black seas connections	409
3.2. Aral Sea – environments during the last 2000 years	431
PUBLICATIONS	433
CONCLUSION	519
<hr/>	
ANNEXES	523
REFERENCES	585

INTRODUCTION

My PhD and post-doctorate researches have focused on paleoclimatic, paleogeographical and paleoenvironmental reconstruction of the Mediterranean Basin and its adjacent seas (i.e. the residual former Paratethys) since 11 Ma, (Figure). During this time-interval the Mediterranean marine and continental environments were affected by significant paleogeographic changes, forced by global climate and sea-level variability, plate tectonics and regional uplift of Alps *s.l.* and Carpathians. Two main important events characterize this period: the isolation and evolution of Paratethys and the almost complete desiccation of the Mediterranean Sea, an event known as the Messinian Salinity Crisis. I selected this region because it is very rich in long and continuous sediment archives, which document: (1) climate evolution of the Northern Hemisphere during the Late Cenozoic with respect to vegetation changes, and (2) progressive evolution of initially marine environments towards brackish and freshwater ones. The brackish to fresh environments had a profound effect on the marine organisms (especially dinoflagellates) that responded to the stress by developing a large variety of cyst morphologies, often described as new genera and/or species.



Methods. The comparative analysis of pollen grains and dinoflagellate cysts from the same samples is rarely performed for such a long time-interval because it needs a deep knowledge in taxonomy and ecology of the both complementary proxies. I reached this parallel expertise, having the benefit of training in (1) botanical identification of pollen grains from the tropical to boreal zones and their ecological significance by Dr. J.-P. Suc, (2) taxonomy and ecology of dinoflagellate cysts by Pr. M. J. Head. To achieve an understanding of the primary factor inducing morphological variations of dinoflagellate cysts, I developed a biological approach (culturing and growing of present-day living dinoflagellates and inducing stress on microcultures experimentations) under supervision of Pr. J. Lewis (Westminster University, London, UK) and Drs. D. Anderson and D. Kulis (WHOI, USA) during my postdoc appointments. The simultaneous work on living and fossil (using biometry and associated statistical analyses) dinoflagellate cysts has allowed me to initiate the

development of a transfer function, widely valid and able for the modelling of the physical parameters of sea-surface waters (salinity, temperature, nutrient contents). Such analyses were performed at high- to very high-chronological resolution, as resulting from the following approach: (1) independently established age-model, based on classical biostratigraphy or radiocarbon ages (for recent sediments), completed by magnetostratigraphy for deposits prior to Mid-Quaternary; (2) comprehensive counting of pollen grains (150 per sample, *Pinus* or any overabundant taxon excepted) and dinoflagellate cysts (200-300 per sample); (3) interpreting the resulting data with respect to ecological requirements. High- to very high-resolution analyses provides results directly comparable with classical oxygen isotope curves. These signals can therefore also be tuned to the frequency of eccentricity, obliquity and precession cycles. Although palynological proxies can be considered as standard, my integrated approach hoists them at the level of the most competitive methods. Another aspect consists in its present-day background, based on many surface samples from the Mediterranean, Marmara and Black seas, taken during several cruises and sampling parties at IFREMER-Brest and WHOI. To develop parallel analyses of pollen grains and dinoflagellate cysts offers additional considerable interests, such as (1) continuous records of climatic changes and sea-level variations independently from sediment types, and (2) quantifications (using transfer functions) of climate for both continental and marine (to brackish) realms as well as of physical oceanic parameters (SST, SSS, nutrient content etc.).

Results and research in progress

Using pollen grains analysis, I developed investigations on **vegetation dynamics and paleoclimate reconstructions** for the whole Mediterranean region and Western Europe extended to the **Late Cenozoic (Jiménez-Moreno *et al.*, 2007; Fauquette *et al.*, 2006)**. Thanks to the high-chronologic resolution:

- a. I established the response of regional vegetation to eccentricity forcing in SW Romania (Dacic Basin) and Black Sea (DSDP Site380) whatever the sediment types (**Popescu, 2001, 2006; Popescu *et al.*, 2006a**);
- b. I was the first to demonstrate the precession forcing on regional vegetation (**Popescu *et al.*, 2006b**) through the Lupoia pollen record (SW Romania);
- c. in the frame of two PhD theses that I co-supervise, pollen grain and dinoflagellate cyst records from DSDP Site 380 (7 - 4 Ma) were completed from 4 Ma to Present in order to evidence the impact of glacial-interglacial cycles over the regional vegetation and to reconstruct the climate variability for the last 7 Ma;
- d. I was the first to demonstrate the solar cycles forcing (Hale and Gleissberg cycles) on the regional vegetation (through the "Thermophilous trees / *Artemisia*" ratio) since the Last Glacial Maximum were evidenced in cored sediments from the Black and Marmara seas (unpublished data), that is a unique outcome.

Using the biometric approach on the dinoflagellate cysts in association with statistical analyses, I demonstrated that fluctuations in salinity are partially responsible for modifying size, shape and ornamentation of the cysts, providing **the first reliable paleoecological and paleobiogeographic reconstructions of the brackish Paratethyan basins (Popescu *et al.*, palynology , in press)**.

Simultaneously, I performed experimental cultures on a living-dinoflagellate species (*Scrippsiella trifida*): suggested relationships between cyst morphological variations

and stress under controlled salinity are confirmed by the preliminary results, while reproduction rate seems also modified (unpublished data).

The multi-proxy (palynology, sedimentology and geochemistry) study on the Aral Sea, done by the first PhD student that I co-supervised, allowed not only the reconstruction of the regional paleoclimate and paleoenvironments, but also permitted to understand the atmosphere dynamics of the last 2 ka over the high latitudes (**Sorrel *et al.*, 2006, 2007**).

Hence, my palynological and biological expertise offers an exclusive tool for establishing a continuous high resolution chronology, paleoclimatic, paleobiogeographic and paleoenvironmental reconstructions. This is particularly important for the basins impacted by important environmental changes, such as the Mediterranean and Black seas, the sediments of the latter being precisely dated for the first time by this approach.

I do not want to close this Introduction Section without addressing my largest acknowledgements to those who supported my researches and expressed their interest in my project, providing personal grants and/or financial assistance for achieving my researches, and especially the PhD and master – graduation students that I appreciated so much to co-supervise.

Curriculum Vitae

Surname: POPESCU SUC

Name: Speranta-Maria

Date of Birth: April, 18th, 1966

Place of Birth: Plostina (Romania)

Marital status: Married, one daughter

Nationality: FRENCH and ROMANIAN

Current Address:

385 Route du Mas Rillier,
69140 Rillieux la Pape, France
Phone: +33 (0)4 72 44 85 86
+33 (0)6 82 14 35 26

E-mail:

Speranta.Popescu@univ-lyon1.fr

Languages: ROMANIAN and FRENCH (*reading, writing, speaking - excellent*)
ENGLISH (*reading, speaking, writing - good*)
RUSSIAN (*reading, writing, speaking - moderately well*)

EDUCATION:

1998 - 2001: DOCTORATE in Earth Sciences with the Highest Distinction at University Lyon 1, supervised by Drs. J.-P. Suc and P. Bernier, **granted by the French Government.** Defence: **December, 17, 2001, with Highest Distinction.**

Title of the PhD: *Vegetation, climate and cyclostratigraphy in Central Paratethys during the Late Miocene and Early Pliocene according to Palynology*

Examiner board:

Christophe LECUYER, Pr., University Lyon 1 (France), President
Henry HOOGHIEMSTRA, Pr., University of Amsterdam (Netherlands), Referee
Silvia IACCARINO, Pr., University of Parma (Italy), Referee
Georges CLAUZON, Lecturer, University Aix-Marseille 1
Georges BARALE, Pr., University Lyon 1
Paul BERNIER, Lecturer, University Lyon 1, Supervisor

1984 - 1989: Engineer in Geology and Geophysics (University of Bucharest, Romania), with the Highest Distinction

Master Project: *Petrography and mineralogy of Paleozoic metamorphic formations and magmas from the Cerna area (Tulcea Department) in order to establish indicators for geological prospection.*

WORK AND ACADEMIC EXPERIENCE

October 2007 to March, 2008 (6 months)

POSTDOCTORAL STAY at Senckenberg Forschungsinstitut und Naturmuseum, Frankfurt am Main, Germany (Pr. V. Mosbrugger). Salary: Senckenberg Forschungsinstitut und Naturmuseum Frankfurt (Germany).

Project: Major climatic events related to vegetation changes (impact on biodiversity) and microfauna evolution (dinoflagellate cyst, foraminifers and calcareous nannoplankton).

January to June, 2007 (6 months)

POSTDOCTORAL STAY at Lyon 1 University, UMR 5125 CNRS (Dr. J.-P. Suc), Lyon France Salary: ANR EGEO Project, (Pr. L. Jolivet, University Paris 6)

Project: Mediterranean - Paratethys exchanges during the Late Cenozoic, using palynological proxies (dinocysts, pollen, and palynofacies).

April to July, 2006 (4 months)

POSTDOCTORAL STAY at Lyon 1 University, UMR 5125 CNRS (Dr. J.-P. Suc), Lyon France, granted by TOTAL OIL COMPANY (M. Bez).

Project: Climate changes during the last 200 ka in the Intertropical Africa: factors controlling the sedimentation of the deep sea fan of the Congo River.

October, 2005 to March, 2006 (6 months)

POSTDOCTORAL STAY at Woods Hole Oceanographic Institution, Department Geology and Geophysics (Dr. L. Giosan) and Biological Department (Dr. D. Anderson), Woods Hole, USA, FULBRIGHT Grant.

Project: Late Cenozoic environmental changes in the Black Sea and Marmara Sea realm according to Palynology.

January to August, 2004 (8 months)

POSTDOCTORAL STAY at Cambridge University, Department of Geography (Dr. M.J. Head), Cambridge (UK), and University of Lyon (UMR5125), (Dr. J.-P. Suc) European Grant within the frame of the Programme ASSEMBLAGE.

Project: Late Miocene to Present dinoflagellate cysts: morphology and taxonomy, comparison with reference Atlantic and Mediterranean Cenozoic assemblages.

November, 2002 to January 2004

Technical Assistant in Palynology, University Lyon 1, France

Research on palynology: identification and counting of pollen grains and dinoflagellate cysts from core's samples, sediments provided by Blason 1 and Blason 2 cruises in the Black Sea). Technical preparation of sediments for palynological analyses

June 2002 (1 month)

POSTDOCTORAL STAY at Westminster University, School of Biosciences (Pr. J. Lewis), London (UK), **granted** by the **European Science Foundation** (EEDEN Programme).

Project: Neogene environmental changes in the Paratethys realm according to morphological changes in dinocysts.

March, 2002 (1 month)

POSTDOCTORAL STAY at **University Lyon 1**, UMR 5125 CNRS, (Dr. J.-P. Suc) **granted** by **CNRS** Programme "Environnements, Vie et Sociétés" (French Institute of Biodiversity).

Working on Pollen database

September, 1998 to December, 2001 granted by the French Government during 3 years for PhD Thesis at University Lyon 1, UMR5125, CNRS, under the supervision of Drs. J.-P. Suc and P. Bernier

Subject: Vegetation, climate and cyclostratigraphy in Central Paratethys during the Late Miocene and Early Pliocene according to Palynology

July, 1989 to September, 1998 - Engineer in the Romanian Coal Company

I acted as manager of a team of about 40 workers, organizing their time schedule of work. In parallel, I continuously calculated stock of coal and, as a consequence, I was narrowly associated to the mining planning.

OTHER AWARDS

November 2002: Short-listed for the Junior Research Fellowship in Science at the St. Catherine College, Cambridge University, UK. **Title of the project: Late Cenozoic environmental changes in the Paratethys realm according to dinocysts**

October, 2007: Short-listed (ranked at the second place) for the position "**Research Associate on pelagic organisms with focus on marine Dinophyceaea**" at the German Center of Marine Biodiversity Research, Senckenberg Forschungsinstitut und Naturmuseum, Frankfurt am Main, Germany.

TECHNICAL AND SCIENTIFIC COMPETENCES

I have a strong experience as manager of drillings and corings on land, get when I was Chief Engineer Geologist in the National Lignite Company of Romania. I was also in charge of core description, sampling and storage.

Then, as Scientist, I have a strong experience in studying marine cored sections, for example from DSDP. I am also used to decide coring setting (INTAS Project on the Caspian Sea), to calculate sampling step of marine cores for reaching the best time-resolution (Marion Dufresne Calypso cores from the Black Sea, cores from the Gulf of Guinea) and to perform it after the detailed sedimentological description.

1. CORE MATERIAL

I have a strong experience as manager of drillings and corings on land, get when I was Chief Engineer Geologist in the National Lignite Company of Romania. I was also in charge of core description, sampling and storage.

Then, as Scientist, I have a strong experience in studying marine cored sections, for example from DSDP. I am also used to decide coring setting (INTAS Project on the Caspian Sea), to calculate sampling step of marine cores for reaching the best time-resolution (Marion Dufresne Calypso cores from the Black Sea, cores from the Gulf of Guinea) and to perform it after the detailed sedimentological description.

2. PALYNOLOGY (MIOCENE – PRESENT)

FOSSIL ASSEMBLAGES

➤ **Pollen Analysis:**

- Taxonomy and paleovegetation reconstruction with respect to present-day ecology (temperature and rainfall conditions).
- Plant diversity by respect to global climate changes, climate forcing on the vegetation dynamics and distribution of relict vegetation areas
- Astronomical and solar forcing of vegetation changes;
- Reconstruction of paleotemperature and paleorainfall using transfer functions based on pollen data (in collaboration)
- Paleoaltitudes reconstruction with respect to the present-day altitudinal organization of vegetation and paleoclimatic parameters (in collaboration)

➤ **Dinoflagellate cyst Analysis:** Taxonomy, paleoecology (with respect to the present day ecological requirements, relationships between theca (motile stage = dinoflagellate) and cysts (encysted stage = dinocyst). I use the morphological - biometrical approach and statistical analyses for establishing the impact of global climate and regional environmental changes (sea-surface temperature = SST, sea-surface salinity = SSS, nutrient contents) on the dinoflagellate cyst morphology.

- Marine, brackish and freshwater paleoenvironment reconstructions
- Research of connections between basins characterized by various paleoenvironmental conditions. Marine sea-surface parameters (sea-surface temperature, sea-surface salinity, upwellings, etc.).

PRESENT-DAY ASSEMBLAGES

➤ **Pollen Analysis**

- Taxonomy, Transport and Sedimentation of pollen grains in marine basins
- Impact of present day global climate warming on plant diversity and distribution of relict areas;

➤ **Living Dinoflagellate Analyses (BIOLOGICAL APPROACH):**

- Relationships between the motile stage (biology) and encysted stage (micropaleontology) of living dinoflagellates, using experimental microcultures
- Induced environmental stress (temperature, salinity, nutrient contents) on the experimental microcultures for analysing the rate of reproduction and

morphological variability of the cysts. This approach allows establishing valid relationships between the cyst morphology and ocean physical parameters (SST, SSS and nutrient variability), that can be used for reconstruction of past climate and environment changes.

- Taxonomy and taphonomy of dinoflagellate cysts.

3. PALEOCLIMATE (MIOCENE - PRESENT)

➤ **Paleoclimate reconstruction:**

- Identification of: (1) major climatic cycles forced by eccentricity, obliquity and precession); (2) short climatic cycles induced by solar activity (Schwabe cycles: 11 yrs, Gleissberg cycles: 88 yrs, Suess cycles: 210 yrs, Hallstattzeit cycles: 2300 yrs) and the climate and sea-level changes (Bond cycles: 900 yrs, Heinrich Events and Dansgaard-Oeschger cycles).
- Quantification of climate (temperature and rainfall) and ocean sea-surface parameters (SST, SSS and nutrient variability) (in collaboration)

➤ **Reconstruction of ocean – atmosphere dynamics using the pollen signal (atmosphere signal) coupled with dinoflagellate cysts signal (ocean signal).**

4. PALEOCEANOGRAPHY – PALEOGEOGRAPHY

- **Vegetation changes induced by global climate changes, regional sea-level variability and regional tectonics.**
- **Evolution of sedimentary basins:** causes and consequences of rapid or progressive transition from marine to brackish/freshwater conditions.

RESEARCH PROGRAMMES TO WHICH I CONTRIBUTED

International Programmes

- 2004-2009: UNESCO-IUGS IGCP 521 project “Black Sea-Mediterranean Corridor during the last 30 ka: Sea-level change and human adaptation”.** Programme leader: V. Yanko-Hombach (Avalon Institute for Applied Science, Canada)
- 2006-2009: NATO- INTAS “The Holocene records of Caspian sea-level change in the offshore Kura Delta, Azerbaijan”.** Programme leader: S. Kroonenberg (Delft University, The Netherlands)
- 2000-2005: EEDEN “Environments and Ecosystem Dynamics of the Eurasian Neogene”** (European Science Foundation Program). Programme leader: J.E. Meulenkamp (Utrecht University, The Netherlands)
- 2003-2006: ASSEMBLAGE “ASSEssMent of the BLAck Sea sedimentary system since the last Glacial Extreme” 5th EC Framework Programme (EVK3-2001-00142).** Programme leader: G. Lericolais (IFREMER, Plouzané, France)

French Programmes

2006-2009: ANR “Rheology and deformation of Aegean lithosphere (EGEO)”. Programme leader: L. Jolivet (University Paris 6)

2004-2007: ECLIPSE II (CNRS) “Spatial-temporal detailed evaluation about the impact of the Messinian Salinity Crisis and its control factors”. Project leaders: J. Deverchère (Brest University, France) and C. Gorini (Lille University, France).

2001-2003: ECLIPSE I (CNRS): “Messinian Salinity Crisis: modality, regional and global consequences, quantifications” Project leaders: J.-P. Suc (Lyon-1 University, France) and J.M. Rouchy (Natural History Museum, Paris, France).

2001-2002: BIODIVERSITY (IFB) “Biodiversity evolution of Mediterranean vegetation since 6 millions years “. Project leaders: S. Fauquette and J.-P. Suc (University Lyon 1, France)

France - China Programme: (Programmes de Recherches Avancés - PRA)

2001-2002: Project (PRA T00-04): “Present-day relictual *Cathaya* forest in southern China. The Mediterranean Pliocene: significant guide to reconstruct its history. Project leaders: J.-P. Suc (University Lyon 1, France) and Z. Zheng (Zhongshan University, Guangzhou, China)

WORKSHOP ORGANISATION

May, 5th – 6th, 2008, Lyon France: Special Session of the Geological Society of France, granted by TOTAL OIL COMPANY, CEA, UCBL, PEPS, CEREGE, GEOSCIENCES AZUR. *“Mio-Pliocene geodynamics and paleogeography of the Mediterranean region: eustasy vs. tectonics”*.

February, 29th – March, 1st, 2008, Bucharest (Romania): French - Romanian Workshop granted by the French Embassy in Romania, TOTAL Oil Company, PEPS, GeoEcoMar Bucarest. *“What happened in southern Romania and Black Sea when the Mediterranean Sea desiccated 5.6 Myrs ago”*

July, 25th – 26th, 2004, Corte (France): International Workshop of the Project ECLIPSE on the Messinian Salinity Crisis, granted by Eclipse 1 French Project and the University of Corte (France). *“The Messinian Salinity Crisis re-visited”*

April, 14th – 20th, 2004, Lyon (France): International Workshop and training session on dinoflagellate cysts, granted by the European Science Foundation (EEDEN Programme) *“Dinocysts: promising markers of Mediterranean - Paratethys relationships”*

November, 16th – 18th, 2000, Lyon (France) International Workshop of the EEDEN Programme (ESF), granted by the *European Scientific Foundation*. “Environments and Ecosystem Dynamics of the Eurasian Neogene: State of the Art”

TEACHING AND TRAINING FOR STUDENTS

2006: Central Michigan University, Department of Geology, Mt. Pleasant, MI 48859 – 3 hours teaching for undergraduate students, I was invited by M. Sirbescu (Assistant Professor)

2007: University Lyon 1, Lyon, France – 3 hours teaching for Master Students, I was invited by Dr. S. Legendre (Director of Research at CNRS)

I co-supervised the following research stages and PhD Theses for undergraduated and graduated students, respectively:

STAGES FOR UNDERGRADUATED STUDENTS:

G. JOUANNIC *Galeacysta etrusca: marker of Mediterranean-Paratethys relationships before and after the Messinian Salinity Crisis: spatial and temporal distribution within Paratethys and Mediterranean Sea (2006 - 2007)*

F. DALESME: *Impact of environmental changes in morphology for brackish dinoflagellate markers: Galeacysta etrusca (2006 - 2007)*

RESEARCH STAGES (MASTER DEGREE)

S. BOROI *Palynological study of Pliocene deposits from Oltenia (Romania). Co-supervised with. N. Ticleanu (Bucharest University, Romania). 2001/2002.*

S. BOROI *Floristic diversity from Late Miocene to Early Pliocene pollen assemblages from DSDP Site 380 A, Leg 42 (Black Sea). Co-supervised with. N. Ticleanu*

F. DALESME *Lingulodinium machaerophorum – impact of environmental stress on the cyst morphology. Co-supervised with G. Escarguel (University Lyon 1, France)*

PhD THESES:

P. SORREL: *The Aral Sea: a paleoclimate archive, 2006. University of Potsdam (Germany). Co-supervised with. R Oberhänsli and H. Oberhänsli (Potsdam University), and. J.-P. Suc (University Lyon 1)*

S. BOROI: *Vegetation changes vs. climate: pollen record of recent glacial-interglacial cycles (0-500,000 yrs) from the Black Sea sediments. Co-supervised with Dr. J.-P. Suc (University Lyon 1).*

- D. BILTEKIN** *Plant diversity and refuges, vegetation and climate changes since 20 Ma in the Anatolian and North-Aegean regions according to pollen records. Co-supervised with J.-P. Suc (University Lyon 1) and N. Çagatay (Istanbul Technical University, Turkey).*
- O. BAZELY** *Black Sea Palaeoclimate and Tephrochronology. Supervisors: Pr. P. Gibbard (Cambridge University, UK) and Pr. D. Pyle (Oxford University, UK). I supervise the palynological work (pollen grains and dinoflagellate cysts) on the Black Sea core.*
- M. DALIBARD:** *Tropical climatology of the Central Africa and Tropical Atlantic during the Last Climatic Cycle. Co-supervised with J.-P. Suc and B. Pittet (University Lyon 1).*

PEER-REVIEWED JOURNAL ARTICLES AND BOOK CHAPTERS

23. Bache, F., **Popescu, S.-M.**, Gorini, C., Suc, J.-P., Clauzon, G., Lofi, J., Olivet, J.-L., Rubino, J.-L., Melinte-Dobrinescu, M.-C., Londeix, L., Armijo, R., Meyer, B., Jouannic, G. *Process of the reflooding of the Mediterranean basin after the Messinian salinity Crisis. Basin Research, in progress*
22. Melinte-Dobrinescu M.-C., Suc, J.-P., Clauzon, G., **Popescu, S.-M.**, Armijo, R., Meyer, B., Biltekin, D., Çağatay N., Uçarkus, G., Jouannic, G., Fauquette, S., Çakir, Z. The Messinian Salinity Crisis in the Dardanelles region: chronostratigraphic constraints. *Palaeogeography, Palaeoclimatology, Palaeoecology, submitted*
21. Mertens, K.N., Ribeiro, S., Bouimetarhan, I., Caner, H., Combourieu-Nebut, N., dale, B., de Vernal, A., Ellegaard, M., Filipova, M., Godhe, A., Groenveld, J., Grøsfjeld, K., Holzwarth, U., Kottoff, U., Leroy, S.A.G., Londeix, L., Marret, F., Matsuoka, K., Mudie, P., Nausts, L., Pena-Manjarrez, J., Persson, A., **Popescu, S.-M.**, Pospelova, V., Sangiorgi, F., Van der Meer, M., Vink, A., Zonneveld, K., Vercauteren, D., Vlassenbroeck, J., Louwye, S. *Lingulodinium machaerophorum* process length in surface sediments. *Marine Micropaleontology, accepted*
20. **Popescu, S.-M.**, Melinte, M.-C., Suc J.-P., Clauzon, G., Quillévéré, F., Süto-Szentai, M. Marine re-flooding of the Mediterranean after the Messinian Salinity Crisis predates the Zanclean GSSP. Reply to the “Comment on ‘Earliest Zanclean age for the Colombacci and uppermost Di Tetto formations of the “latest Messinian” northern Apennines: New palaeoenvironmental data from the Maccarone section (Marche Province, Italy)’ by Popescu et al. (2007) *Geobios* 40 (359-373)” authored by Roveri et al. *Geobios*, 41 (4), **in press**.
19. **Popescu, S.-M.**, Dalesme, F., Joannic, G., Escarguel, G., Head, M.J., Melinte-Dobrinescu, M.C., Süto-Szentai, M., Bakrac, K., Clauzon, G., Suc, J.-P. *Galeacysta etrusca* complex, dinoflagellate cyst marker of Paratethyan influxes into the Mediterranean Sea before and after the peak of the Messinian Salinity Crisis. *Palynology, in press*.
18. Clauzon, G., Suc, J.-P., **Popescu, S.-M.**, Melinte Dobrinescu, M.C., Quillévéré, F., Warny, S., Fauquette, S., Armijo, R., Meyer, J.L., Rubino, J.L., Lericolais, G., Gillet, H., Çağatay, N., Uçarkus, G., Escarguel, G., Jouannic, G., Dalesme, F. Chronology of the Messinian events and paleogeography of Mediterranean region s.l. CIESM, 2008. The Messinian salinity Crisis from mega-deposits to microbiology- A consensus report. N°33 in CIESM Monographs (F. Briand, Ed.), 168 pages, Monaco.
17. Ford, M., Williams, E.A., Malartre, F., **Popescu, S.-M.** Stratigraphic architecture, sedimentology and structure of the Vouraikos Gilbert-type delta, Gulf of Corinth, Greece. In Nichols, G.J., Williams, E.A., Paola, C. (eds.) "Sedimentary Processes, Environments and Basins". *International Association of Sedimentologists Series*, 38 (2007), 49–90.
16. Jimenez-Moreno, G., **Popescu, S.-M.**, Ivanov, D., Suc, J.-P. Neogene flora, vegetation and climate dynamics in Central Eastern Europe according to pollen records. In Williams, M., Haywood, A., Gregory, J. (eds.), “Deep time perspectives on climate change. Marrying the signal from computer models and

- biological proxies". The *Micropalaeontological Society Special Publication, Geological Society of London*, (2007) 393-406, doi: 10.1144/TMS2.19.
15. **Popescu, S.-M.**, Melinte, M.-C. Suc, J.-P., Clauzon, G., Quillevéré, F., Sütö-Szentai, M. Earliest Zanclean age for the Colombacci and uppermost Di Tetto formations of the "latest Messinian" northern Apennines: New palaeoenvironmental data from the Maccarone section (Marche Province, Italy). *Geobios*, 40 (2007), 359–373.
 14. Sorrel, P., **Popescu, S.-M.**, Klotz, S., Suc, J.-P., Oberhänsli, H. Climate variability in the Aral Sea Basin (Central Asia) during the late Holocene based on vegetation changes. *Quaternary Research*, 67, 357–370.
 13. Lericolais, G., Popescu, I., Guichard, F., **Popescu, S.-M.** A Black Sea lowstand at 8500 yr B.P. indicated by a relict coastal dune system at a depth of 90 m below sea level. In Harff, J., Hay, W.W., Tetzlaff, D.M. (eds.), "Coastline Changes: Interrelation of Climate and Geological Processes". *GSA Special Paper*, 426 (2007), 171–189.
 12. Lericolais, G., Popescu, I., Guichard, F., **Popescu, S.-M.**, Manolakakis, L. Water-level fluctuations in the Black Sea since the Last Glacial Maximum. In Yanko-Hombach, V., Gilbert, A.S., Panin N., Dolukhanov, P.M. (eds.), "The Black Sea Flood Question: Changes in Coastline, Climate, and Human Settlement". Springer, Berlin, 2007, 437–452.
 11. Sorrel, P., **Popescu, S.-M.**, Head, M.J., Suc, J.-P., Klotz, S., Oberhänsli, H. Hydrographic development of the Aral Sea during the past 1900 years: results based on a dinoflagellate cyst quantitative analysis. *Palaeogeography, Palaeoclimatology, Palaeoecology*, 234 (2006), 304–327.
 10. **Popescu, S.-M.** Late Miocene and early Pliocene environments in the southwestern Black Sea region from high-resolution palynology of DSDP site 380A (Leg 42B). *Palaeogeography, Palaeoclimatology, Palaeoecology*, 238 (2006), 64–77.
 9. **Popescu, S.-M.**, Krijgsman, W., Suc, J.-P., Clauzon, G., Mărunțeanu, M., Nica, T. Pollen record and integrated high-resolution chronology of the early Pliocene Dacic basin (southwestern Romania). *Palaeogeography, Palaeoclimatology, Palaeoecology*, 238 (2006), 78–90.
 8. **Popescu, S.-M.**, Suc, J.-P., Loutre, M.-F. Early Pliocene vegetation changes forced by eccentricity-precession. Example from Southwestern Romania. *Palaeogeography, Palaeoclimatology, Palaeoecology*, 238 (2006), 340–348.
 7. Fauquette, S., Suc, J.-P., Bertini, A., **Popescu, S.-M.**, Warny, S., Bachiri Taoufiq, N., Perez Villa, M.-J., Chikhi, H., Feddi, N., Subally, D., Clauzon, G., Ferrier, J. How much did climate force the Messinian salinity crisis? Quantified climatic conditions from pollen records in the Mediterranean region. *Palaeogeography, Palaeoclimatology, Palaeoecology*, 238 (2006), 281–301.
 6. Suc, J.-P., **Popescu, S.-M.** Pollen records and climatic cycles in the North Mediterranean region since 2.7 Ma. In M. J. Head, P. L. Gibbard (eds.), "Early-Middle Pleistocene Transitions: The Land-Ocean Evidence". *Special Publication of the Geological Society of London*, 247 (2005), 147–157.
 5. Clauzon, G., Suc, J.-P., **Popescu, S.-M.**, Mărunțeanu, M., Rubino, J.-L., Marinescu, F., Melinte, C.M. Influence of Mediterranean sea-level changes on the Dacic Basin (Eastern Paratethys) during the late Neogene: the

- Mediterranean Lago Mare facies deciphered. *Basin Research*, 17, 3 (2005), 437–562.
4. Lericolais, G., Popescu, I., Panin, N., Guichard, F., **Popescu, S.-M.**, Manolakakis, L. Evidence from recent oceanographic surveys of a last rapid sea level rise of the Black sea. In "Human record of recent geological evolution in the Mediterranean basin-historical and archeological evidence" CIESM Workshop Monograph, 24 (2004), 109–117.
 3. Suc, J.-P., Fauquette S., **Popescu S.-M.**, 2004. L'herbier: un outil indispensable à la recherche palynologique. In R. Pierrel, J.-P. Reduron (eds.), "Les herbiers: un outil d'avenir. Actes du colloque de Lyon 20-22 novembre 2002". AFCEV, Villers lès Nancy, p. 67-87.
 2. **Popescu, S.-M.** Repetitive changes in Early Pliocene vegetation revealed by high-resolution pollen analysis: revised cyclostratigraphy of southwestern Romania. *Review of Palaeobotany and Palynology*, 120 (2001), 181–202.
 1. Roiron, P., Ferrer, J., Linan, E., Rubio, C., Diez, J.-B., **Popescu, S.-M.**, Suc, J.-P. Les flores du bassin lacustre de Rubeilos de Mora. Nouvelles données sur les conditions climatiques au Miocène inférieur dans la région de Teruel (Espagne). *Comptes Rendus de l'Académie des Sciences de Paris, Sciences de la terre et des planètes*, 329 (1999), 897–904.

CONGRESS AND WORKSHOP PAPERS AND ABSTRACTS

- 2008** Clauzon, G., Suc, J.-P., **Popescu, S.-M.**, Melinte-Dobrinescu, M.C., Quillévére, F., Warny, S.A., Fauquette, S., Armijo, R., Meyer, B., Rubino, J.-L., Lericolais, G., Gillet, H., Çağatay, M.N., Uçarkus, G., Escarguel, G., Jouannic, G., Dalesme, F. Chronology of the Messinian events and paleogeography of the Mediterranean region s.l. CIESM Workshop Monographs, 33, 31–37.
- 2008** **Popescu, S.-M.**, Bazeley, O., Boroi, S., Sorrel, P., Dalesme, F., Jouannic, G., Head, M.J., Lericolais, G., Çağatay, N.M., Suc, J.-P. *Mediterranean – Marmara - Black Seas connections during the last 20 ka: palaeoenvironmental reconstruction in the context of global climate change and regional tectonic setting*. 33 IGC, Oslo (Norvège), Symp. HPQ-02.
- Suc, J.-P., Clauzon, G., Bache, F., Cornée, J.-J., Deverchère, J., El Euch-El Koundy, N., Ferry, S., Gillet, H., Gorini, C., Lericolais, G., Lofi, J., Melinte-Dobrinescu, M.C., **Popescu, S.-M.**, Rubino, J.-L., Sage, F. *The latest Miocene – earliest Pliocene Mediterranean mega-cycle in sea-level*. 33 IGC, Oslo (Norvège), Symp. HPS-12.
- Armijo, R., Meyer, B., Suc, J.-P., Clauzon, G., Melinte-Dobrinescu, M.-C., Popescu, S.-M., Uçarkus, G., Çakir, Z., Jouannic, G. The propagation of the North Anatolian fault in the Dardanelles region and the Messinian Salinity Crisis: A new challenge. Special Session of French Geological Society, May 5-6, Lyon, France, 11.
- Clauzon, G., Suc, J.-P., Armijo, R., Meyer, B., Melinte-Dobrinescu, M.-C., Lericolais, G., Gillet, H., **Popescu, S.-M.**, Çağatay, N., Jouannic, G., Uçarkus, G., Çakir, Z., Quillévére, F. Canyons messiniens, Gilbert deltas zancléens et paleogeography de la Mer de Marmara. Special Session of French Geological Society, May 5-6, Lyon, France, 27–28.

Popescu, S.-M., Suc, J.-P., Clauzon, G., Melinte-Dobrinescu, M.-C., Escarguel, G., Quillévère, F., Dalesme, F., Jouannic, G., Head, M., Sütö-Szentai, M., Bakrac, K., Mertes, K., Vercauteren, D. Une nouvelle idée des échanges Paratéthys-Méditerranée et des événements Lago mare à travers le Complexe *Galeacysta etrusca*. Special Session of French Geological Society, May 5-6, Lyon, France, 58–60.

Popescu, S.-M., Jimenez-Moreno, G., Bazeley, O., Boroi, S., Sorrel, P., Dalesme, F., Jouannic, G., Head, M.J., Klotz, S., Giosan, L., Lericolais, G., Çağatay, N., Suc, J.-P. *Mediterranean – Marmara - Black Seas connections during the last 20 k.a.: palaeoenvironmental reconstruction in the context of global climate change and regional tectonic setting*. Turkish Geological Congress, Ankara, Turkey.

Biltekin, D., **Popescu, S.-M.**, Boroi, S., Suc, J.-P. *High-resolution climate and vegetation record in the Anatolian region according to pollen analyses from late Miocene to Late Pleistocene: evidence from DSDP Site 380*. Turkish Geological Congress, Ankara, Turkey.

Armijo, R., Meyer, B., Suc, J.-P., Clauzon, G., Melinte-Dobrinescu, M.C., **Popescu, S.-M.**, Uçarkus, G., Çakir, Z., M. Çağatay, M.N., 2008. *The propagation of the North Anatolian Fault in the Dardanelles Region and the Messinian Salinity Crisis: A new challenge*. Turkish Geological Congress, Ankara, Turkey.

Clauzon, G., Suc, J.-P., Armijo, R., Meyer, B., Melinte-Dobrinescu, M.C., Lericolais, G., Gillet, H., Çağatay, M.N., **Popescu, S.-M.**, Jouannic, G., Uçarkus, G., Çakir, Z., Quillévère, F. *Impact of the Messinian Salinity Crisis in the Marmara Sea region. Did a connection exist between the Aegean and Black seas at that time?* Turkish Geological Congress, Ankara, Turkey.

Popescu, S.-M., Suc, J.-P., Clauzon, G., Melinte-Dobrinescu, M.C., Escarguel, G., Quillévère, F., Sîrbescu, M.-L.C., Dalesme, F., Jouannic, G., Head, M., Sütö-Szentai, M., Bakrac, K., Mertes, K., Vercauteren, D. *Mediterranean - Paratethys connections before and after Messinian Salinity Crisis*. Workshop “What happened in southern Romania and Black Sea when the Mediterranean Sea desiccated 5.6 million years ago”, Bucharest, Romania, 25–28.

Clauzon, G., **Popescu, S.-M.**, Suc, J.-P. *Le Rhin et le Danube : témoins onshore majeurs de la Crise de Salinité Messinienne. Conséquences sur la véritable extension du périmètre affecté par la crise*. Workshop on “What happened in southern Romania and Black Sea when the Mediterranean Sea desiccated 5.6 million years ago”, Bucharest, Romania, 6–9.

Escarguel, G., **Popescu, S.-M.**, Dalesme, F., Jouannic, G., Head, M., Melinte-Dobrinescu, M.C., Sütö-Szentai, M., Bakrac, K., Clauzon, G., Suc, J.-P., Mertes, K., Vercauteren, D. *Galeacysta etrusca complex, dinoflagellate cyst marker of Paratethyan influxes into Mediterranean Sea, before and after the peak of the Messinian Salinity Crisis*. Workshop, “What happened in southern Romania and Black Sea when the Mediterranean Sea desiccated 5.6 million years ago”, Bucharest, Romania, 11

Melinte-Dobrinescu, M.C., Suc, J.-P., Clauzon, G., **Popescu, S.-M.**, Çağatay, N. *Nannofossil records and the impact of the Messinian Salinity Crisis in the North-western Aegean region (NW Turkey)*. Workshop “What happened in

- southern Romania and Black Sea when the Mediterranean Sea desiccated 5.6 million years ago”, Bucharest, Romani, 18–19.
- Suc, J.-P., Clauzon, G., **Popescu, S.-M.**, Melinte-Dobrinescu, M.C., Quillévéré, F., Warny, S.A., Fauquette, S., Rubino, J.-L. *Causes and process of the Messinian Salinity Crisis*. Workshop “What happened in southern Romania and Black Sea when the Mediterranean Sea desiccated 5.6 million years ago”, Bucharest, Romania, 33–35.
- 2007** Suc, J.-P., **Popescu, S.-M.** *Transformations dans la végétation du Pliocène au Quaternaire aux latitudes moyennes de l’hémisphère Nord*. Colloque International Q5, Paris, France.
- Boroi, S., **Popescu, S.-M.**, Jiménez-Moreno, G., Klotz, S., Suc, J.-P. *Végétation et climat d’après les enregistrements polliniques en mer Noire et en mer de Marmara*. Colloque International Q5, Paris, France.
- Popescu, S.-M.**, Klotz, S., Head, M.J. 2005. *Relative sea-level and climate fluctuations in the Marmara and Black Seas during the last 18 kyrs*. Workshop ASSEMBLAGE, Hamburg, Germany.
- Boroi, S., **Popescu, S.-M.**, Jimenez-Moreno, G., Klotz, S., Suc, J.-P. *Vegetation and climate reconstruction in the area of Black and Marmara seas according to pollen records*. Workshop ASSEMBLAGE, Hamburg, Germany.
- Sorrel, P., **Popescu, S.-M.**, Suc, J.-P., Oberhänsli, H. *Paleoclimatic changes in the Aral Sea during the past 1900 years – The vegetation pattern and the moisture conditions*. EGU, Vienna, Austria.
- Suc, J.-P., Clauzon, G., **Popescu, S.-M.** *Late Miocene - Early Pliocene Mediterranean - Paratethys relationships: The Mediterranean Lago Mare deciphered*. 12th R.C.M.N.S. Congress, Vienna, Austria.
- Suc, J.-P., Jiménez-Moreno, G., **Popescu, S.-M.**, Fauquette, S., Klotz, S. *Neogene climate evolution in Europe and peri-Mediterranean regions according to pollen data*. 12th R.C.M.N.S. Congress, Vienna, Austria.
- 2004** **Popescu, S.-M.**, Boroi, S., Head, M., Caner, H., Lericolais, G., Çağatay, N., Algan O. *A new chronology to Mediterranean - Black sea connections during the last 14 ka BP*. EGU - EGS, Nice, France.
- Suc, J.-P., Fauquette, S., **Popescu, S.-M.** L’herbier: un outil indispensable à la recherche palynologique. In Pierrel, R., Reduron, J.-P. (eds.), “Les herbiers: un outil d’avenir. Actes du colloque de Lyon 20-22 novembre 2002”. Edit. Association française pour la Conservation des Espèces Végétales, Nancy, 67–87.
- Popescu, S.-M.**, 2004. *Miocene-Quaternary dinoflagellates cyst, morphological variability linked to environmental changes*. Workshop EEDEN, Lyon, France.
- Clauzon, G., Suc, J.-P., Orzag-Sperber, F., **Popescu, S.-M.** *The Messinian-Zanclean cycle in the Northern Aegean Sea*. 4th Congress “Environment and Identity in the Mediterranean “The Messinian Salinity Crisis re-visited, Corte, France, 27.
- Fauquette, S., Suc, J.-P., Bertini, A., **Popescu, S.-M.**, Warny, S., Bachiri Taoufiq, N., Perez Villa, M.-J., Ferrier, J., Chikhi, H., Subally, D., Feddi, N., Clauzon G. *How much did climate force the Messinian salinity crisis? Quantified climatic conditions from pollen records in the Mediterranean region*.

4th Congress “Environment and Identity in the Mediterranean “The Messinian Salinity Crisis re-visited, Corte, France, 36.

Ferrandini, J., Ferrandini, M., Suc, J.-P., Rouchy, J.-M., Saint Martin, S., **Popescu, S.-M.**, Thimon, I., Jehasse, O. *Late Miocene and early Pliocene deposits of the Aleria area: Livret-guide d'excursion*, 4th Congress “Environment and Identity in the Mediterranean “The Messinian Salinity Crisis re-visited, Corte, France.

Popescu, S.-M. *The dinocysts new markers of Mediterranean - Paratethys connections before and after the Messinian salinity crisis*. 4th Congress “Environment and Identity in the Mediterranean “The Messinian Salinity Crisis re-visited, Corte, France, 72.

Boroi, S., **Popescu, S.-M.**, Suc, J.-P. *Late Glacial - Holocene vegetation in the Black sea region*. 32 International Geological Congress, 44 - G19.02, Florence, Italy, 93.

Popescu, S.-M. *Sea-level changes in the Black Sea region since 14 ka*. 32 International Geological Congress, 72 - T32.03, Florence, Italy, 108.

Clauzon, G., Suc, J.-P., **Popescu, S.-M.** *Late Messinian-Early Zanclean Mediterranean s.l. deposits as a response to outstanding sea-level changes*. 32nd International Geological Congress, 111 - G21.11, Florence, Italy, 131.

Lericolais, G., Popescu, I., Panin, N., Guichard, F. **Popescu, S.-M.** *Was the Last rapid change in the Black Sea linked to a catastrophic event 7500 years ago?* 32nd International Geological Congress, Florence, Italy, 257- G03.03, 208.

Popescu, S.-M. *Vegetation, climate and cyclostratigraphy in Central Paratethys during Late Miocene - Early Pliocene*. 32nd International Geological Congress, 322- T26.01, Florence, Italy.

Sorrel, P., **Popescu, S.-M.**, Head, M.J. *Hydrographic development of the Aral Sea during the past 1,500 yrs-preliminary results based on dinoflagellate cysts*. 32nd International Geological Congress, BW 07, Florence, Italy.

Popescu, S.-M., Boroi, S. *The response of the vegetation in the Black Sea area, during the last 18 ka*. Workshop ASSEMBLAGE, Varna, Bulgaria

Popescu, S.-M., Backrac, K., Süto-Szentai, M., Sorrel, P., Head, M., Galovic, I., 2004. *An overview of the Mediterranean Lago Mare dinoflagellata cysts, their understanding in terms of relationships with the Eastern Paratethys*. Workshop EEDEN/NECLIME, Iraklion, Greece.

Fauquette, S., Suc, J.-P., Bertini, A., **Popescu, S.-M.**, Warny, S., Bachiri Taoufiq, N., Perez Villa, M.-J., Clauzon, G., Ferrier, J., Chikhi, H., Subally, D., Feddi, N. *How much did climate force the Messinian salinity crisis? Quantified climatic conditions from pollen records in the Mediterranean region*. Workshop EEDEN/NECLIME, Iraklion, Greece.

Popescu, S.-M., Suc, J.-P., Jiménez-Moreno, G., Zheng, Z., Favre, E., Boroi, S., Sorrel, P., Deng, Y. *The Late Cenozoic distribution of Cathaya in Europe, North Africa and Middle East*. Guangzhou, China.

2003 Popescu, S.-M. *Holocene Black Sea environments according to palynology*. Geological Society of America Meeting, Seattle, USA.

Popescu, S.-M., Süto-Szentai, M. *The dinocysts, new proxy to understand the environmental changes*. Workshop EEDEN, Stara Lesna, Slovaquia, 69.

- Lericolais, G., Popescu, I., Panin, N., Guichard, F., **Popescu, S.-M.**, Manolakakis, L. *Could the last rapid sea level rise of the Black Sea evidence by oceanographic surveys have been interpreted by Mankind?*. CIESM Workshop, 22-25 October 2003, Fira, Santorini, Greece, 44–53.
- Rubio, C., Roiron, P., Ferrer, J., Díez, J.B., **Popescu S.**, Suc, J.-P. *Paleobotanical and paleoecological data from Lower–Middle Miocene (Burdigalian) basin of Rubielos de Mora*, European Palaeontological Association-Workshop “Exceptional Preservation”, Teruel, Spain, p. 87.
- 2002 Popescu, S.-M.**, Suc, J.-P., Loutre, M.-F. *Lower Pliocene fast and repetitive vegetation changes in southwestern Romania as response to Milankovitch cycles*. 27th General Assembly of the European Geophysical Society, Symposium “Variability at Milankovitch scales”, Nice, France, 326.
- Popescu, S.-M.** *Influence des cycles astronomiques sur la végétation du bassin Dacique au Pliocène inférieur d’après la palynologie*. 3rd French Congress on Stratigraphy, Lyon, France, 186.
- Popescu, S.-M.**, Renaud, S. *Réponse des dinoflagellés au stress provoqué par la confrontation eaux douces locales- eaux salées méditerranéennes inondant la Mer Noire (7150 ans BP)*. 3rd French Congress on Stratigraphy, Lyon, France, 188.
- Suc, J.-P., Fauquette, S., Méon, H., **Popescu, S.-M.** *L’herbier: un outil indispensable à la recherche palynologique*. Colloque “Les herbiers: un outil d’avenir”, Association française pour la conservation des espèces végétales et Société Botanique de France, Lyon, France.
- 2001 Suc, J.-P., Popescu, S.-M.**, Fauquette, S., Bertini, A. *Pliocene vegetation - climate characteristics and evolution in Europe and the Mediterranean region according to pollen data*. I Jornadas Internacionales del Plioceno, Malaga, Spain, 26.
- Popescu, S.-M.** *Messinian and Zanclean vegetation and climate in the Black Sea area compared to the Mediterranean region. Relationships with global climatic evolution and astronomic cyclicities*. Workshop EEDEN/ NECLIME, Praha, Czech Republic, 17–18.
- Popescu, S.-M.** *Messinian and Zanclean pollen records are now available from two areas in Eastern Europe: Dacic basin in south-western Romania and south-western Black Sea*. Workshop EEDEN, Sabadell, Spain, 57.
- 1999 Popescu, S.-M.** *High-resolution pollen record of dacian lignite-clay alternations (mid-lower Zanclean) from the Lupoia quarry (SW Romania): response to precession and cyclostratigraphic calibration*. 11th R.C.M.N.S. Congress, Fes, Morocco, 12.
- Popescu, S.-M.** *Re-interpretation of the Central Paratethys Bosphorian – Dacian - Romanian stages in terms of global climatostratigraphy: relationships with the reference Mediterranean sections*. 11th R.C.M.N.S. Congress, Fes, Morocco, 12.
- Popescu, S.-M.** *Astronomical forcing (eccentricity, precession) of Lower Pliocene vegetation and climate changes in the Central Paratethys: pollen record from the Lupoia section (Dacic Basin)*. Workshop EEDEN, Lyon, France, 52.

Popescu, S.-M., 2000 *Palynologie des sédiments messiniens du Site 380 A du Leg 42B (Mer Noire)*. Journées GFEN-APF “L'événement Messinien : approches paléobiologiques et paléoécologiques”, Rennes, France, 21.

Suc, J.-P., Bertini, A., Clauzon, G., Londeix, L., **Popescu, S.-M.** *Une nouvelle idée du “Lago Mare” à partir de l'approche palynologique*. Journées GFEN-APF “L'événement Messinien: approches paléobiologiques et paléoécologiques”, Rennes, France, 26.

1999 Popescu, S.-M., Fauquette, S. *Lower Pliocene pollen record and climate in the Dacic basin and comparison with the Western Mediterranean data*. Workshop: Neogene Climate Evolution in Eurasia (NECLIME), Tübingen, Germany.

INVITED LECTURES AND SEMINARS

2006 Popescu, S.-M. *Vegetation, Climate and Sea-Level changes in the Mediterranean, Marmara and Black seas since the LGM*. Seminar invited by J. McManus, Department G&G, WHOI, USA, January.

Popescu, S.-M. The Mediterranean – Black Sea connections since the last 20 ka BP., Conference invited by M. Sîrbescu, Central Michigan University, USA., March.

2005 Popescu, S.-M. “*Le Déluge biblique ?*”– *L'invasion des eaux marines méditerranéennes en mer Noire il y a 7, 16 ka BP.*, Seminar invited by M. Kageyama, LSCE Paris, March.

2004 Popescu, S.-M. *Dinocysts: new markers of Mediterranean-Paratethys connections before and after the Messinian Salinity Crisis*. Lecture invited by N. Krstić, Serbian Academy of Science, Belgrad (Serbia), August.

Popescu, S.-M. Variations morphologiques des dinoflagellés, réponse au stress environnemental, Seminar invited by B. David, Dijon University, France, May.

Popescu, S.-M. *Les dinokystes, marqueurs des moments de connexion entre bassins à salinité différente. Leur réponse morphologique au stress environnemental (application à la problématique du déluge)*. Lecture invited by S. Sen, MNHN Paris, France, April.

Popescu, S.-M. *Les dinokystes, marqueurs des moments de connexion entre bassins à salinité différente. Leur réponse morphologique au stress environnemental (application à la problématique du déluge)*. Seminar invited by J. Guiot, CEREGE, France, April.

2003 Popescu, S.-M. What news in the dinoflagellate realm? Conference invited by par J.E. Meulenkamp, EEDEN, Steering Committee Meeting, Bratislava, Slovakia, September.

2001 Popescu, S.-M. *Vegetation, Climate and Cyclostratigraphy in Central Paratethys during Late Miocene and Early Pliocene according to Palynology*. Conference invited by Dr. J. Powel at Joint Meeting of AASP-TMS-NAMS, University College, London, UK.

Popescu, S.-M. Lower Pliocene fast and repetitive vegetation changes in Southwestern Romania as a response to monsoon influence? Asian Monsoons Meeting, Paris-Orsay, France, Presentation invited by F. Bassinot.

RESPONSE OF EUROPEAN VEGETATION TO THE GLOBAL CLIMATIC CHANGES DURING THE NEOGENE

1.1. GLOBAL CLIMATE CHANGES: FORCING FACTORS AND MECHANISMS

The climatic system plays an important role on the distribution of heat energy received from the Sun on the Earth surface and reflects a complex and dynamical interaction between the atmosphere, ocean and land masses in response to insolation. The heating amount and its distribution on the Earth's surface are not constant parameters; their variability is induced by (1) magnetic activity of the Sun, (2) position of the Earth within the solar system, (3) geographic distribution of land masses and (4) ocean- atmosphere dynamics. Any variation of the Sun - Earth system may ultimately cause climatic changes. To understand the present - day climate variability and to predict, using models, the future climatic changes we need to identify the impact of forcing (external and internal) factors and to understand the driving mechanisms.

Among the **external forcing factors** responsible for the global climatic changes, the most important ones are related to the variability of solar irradiance and orbitally modulated insolation.

Relationships between the climatic changes and total solar irradiance were hypothesized in the eighteenth century by William Herschel, who observed a link between sunspots and British grain prices (Foukal *et al.*, 2006). The first convincing evidence was provided later by Willson *et al.*, (1981): their data demonstrate a clear relation between the Total Solar Irradiance (TSI) and dark sunspot formation. Observations show during the last centuries that solar activity varies with a 11-yr periodicity of sunspots (Schwabe cycle), a 22-yr oscillation in solar magnetic polarity (Hale cycle) and an about 88-yr period for a sequence of low sunspot numbers (Gleissberg cycle). Foukal (1994, 1998), then Solansky and Flige (2000) revealed that the ratio between dark sunspot numbers and faculae brightening repartition on the solar disk could be considered as a reliable proxy to calculate the past solar irradiance. In this context, Lean and Foukal, (1988) reconstructed TSI up to 1874. On the total TSI, variability of the Ultraviolet Wavelengths (UV) is significant because they have a prevalent role in atmospheric photochemistry and heating (DeLand *et al.*, 2004), affecting the stratospheric ozone (van Geel *et al.*, 1999) and modulating galactic cosmic ray (Kirkby, 2007). Marsh and Svensmark (2000, 2003) have proposed a correlation between the Galactic Cosmic Ray (GCR) and total amount of low clouds for explaining relationships between climate and solar activity. Directly based on satellite measurements, the increased GCR flux indicated by these authors appear to be associated with increased low cloud cover that, as we know, exerts a strong radiative cooling effect on the Earth. Similar results were obtained by Kristjánsson *et al.* (2002), Sloan and Wolfendale (2008). In addition to the direct measurement of various proxies of solar activity, indirect indicators as cosmogenic radioisotopes (^{10}Be , and ^{14}C) are used to reconstruct solar variation of the past (Beer *et al.*, 1988, 1990; Steig *et al.*, 1996; Bond *et al.*, 2001; Muscler *et al.*, 2004; Braun *et al.*, 2005; Clemens *et al.*, 2005; Vonmoos *et al.*, 2006; Horiuchi *et al.*, 2007). The both isotopes are produced in the upper atmosphere under the influence of cosmic rays of both solar and galactic origin, their fluctuation being caused by changes in solar wind. ^{14}C enters the global carbon

cycle via CO₂ and ¹⁰Be precipitate with aerosols and is washed out by precipitations. Fluctuation of ¹⁰Be in Greenland ice cores was interpreted as a proxy for the precipitation fluctuation and secondarily for solar activity forcing (Mc Hargue and Damon, 1991; Yiou *et al.*, 1997). Finkel and Nishiizumi (1997) have displayed radioisotope records from the GISP 2 core for the time interval between 8 - 5 ka BP, and Bard *et al.* (1997), comparing records of ¹⁴C and ¹⁰Be, concluded that variability of these radioisotopes is explained by solar modulation. Van Geel *et al.* (1999) compared the ¹⁰Be record of Finkel and Nishiizumi (1997) with the $\delta^{18}\text{O}$ (Grootes *et al.*, 1993; Dansgaard *et al.*, 1993) from GISP2 and GRIP ice cores and with ice rafting events provided by Bond and Loti (1995): they concluded that the episodes of reduced solar activity are characterized by increase in cosmic rays (as indicated by high ¹⁰Be values) which coincide with cold phases of Dansgaard-Oeschger events as shown by $\delta^{18}\text{O}$ records. More, recent ¹⁰Be records from the ice sections cored on the two poles (Steig *et al.*, 1996; Muscler *et al.*, 2004; Vonmoos *et al.*, 2006; Horiuchi *et al.*, 2007) show oscillations corresponding to solar cycles of 11-yrs, 22-yrs, 88-yrs and 210-yrs (Suess - de Vries cycles). The second radioisotope ¹⁴C was measured on dendrochronologically dated tree rings (Stuiver 1961, 1965; Baxter and Farmer, 1973) that constitutes the base for the ¹⁴C calibration curve (Stuiver *et al.*, 1993) and reflects the past fluctuations of the atmospheric ¹⁴C. The high production of ¹⁴C could be induced by (1) a lower solar activity that led a cooler climate and higher ¹⁴C, or (2) cooling climate driven by other factors inducing changes in the global carbon cycle and causing increased atmospheric ¹⁴C. Radiocarbon and stable carbon isotope analyses performed on the dendrochronologically dated tree rings (Baxter and Farmer, 1973; Raspopov *et al.*, 2004; Rigozo *et al.*, 2007, 2008; Miyahara *et al.*, 2007, 2008) indicate fluctuations with a periodicity of 11-yrs; 22 yrs, 88 yrs and 200 yrs. This demonstrated that solar activity continuously influences climate. Variations obtained by instrumental measurements on the last centuries may hence be applied to older periods. The impact of solar forcing coupled with general atmospheric circulation on the global climate changes is obvious when regarding the data-sets of the global/regional temperatures (Reid, 1987; Karl and Riebsame, 1984; Newell *et al.*, 1989; Hu *et al.*, 2003; Kofler *et al.*, 2005; Jiang *et al.*, 2005) and hydrodynamic variability, as expressed by (1) North Atlantic Oscillations (NAO) – Northern Hemisphere temperature variability (Kelly, 1977; Gimeno *et al.*, 20003; Geogieva *et al.*, 2007, Mann, 2007), (2) El Niño et Southern Oscillation (ENSO), (Farrar, 2000; Dean and Kemp, 2004; Mann, 2007), (3) monsoon variability (Agnihorti *et al.*, 2002; Fleitmann *et al.*, 2003; Wang *et al.*, 2005; Ji *et al.*, 2006; Liew *et al.*, 2006, Bhattacharyya and Narasimha 2007; Claud *et al.*, 2008): (4) US precipitations (Currie and O'Brien, 1988; Karl and Riebsame, 1984); (5) North China precipitations (Hameed *et al.*, 1983); (6) drought frequency (Mitchel *et al.*, 1979; Yu & Ito, 1999). A simplified mechanism explains the solar forcing on the global climate as related to (1) the solar magnetic activity and variability of TSI directly measured or calculated using radioisotopes (¹⁰Be and ¹⁴C); (2) the distribution of TSI on the Earth surface conditioned in the one hand by the atmospheric variability due to changes into the ozone layer, aerosols, dust veil and clouds and on the second hand by the land masses and ocean-atmosphere dynamics that causes a feedback mechanism on the climatic system. The existence of feedback mechanisms is better illustrated at a long time-scale, by variation of ice sheet (Ruddiman, 2003, 2006a, 2006b) during the glacial – interglacial cycles, related to a very weak annual mean change of insolation (Beer *et al.*, 2006). For example a global cooling leads to growing ice sheet that increase albedo and thus the cooling.

The second external factor which forces the global climate is the *orbitally modulated insolation*. The amount of solar radiation arriving at the top of the atmosphere depends on the energy emitted by the Sun and distance and orientation of the Earth with respect to the Sun. It is demonstrated that the Earth orbit is not only controlled by the gravitational force of the Sun but also influenced by the gravitational force of other planets, responsible of disturbing effects on energy received by the Earth. These disturbing effects depend on the relative position of the Sun, Earth and other planets. Detailed calculation performed by Milankovich (1930) and more recently by Berger (1978) and Lascar *et al.* (2004) reveals that gravitational forces of the planets influence three different orbital parameters of the Earth with different periodicities. They are eccentricity that shows a double periodicity at 100 kyrs and 400 kyrs, the obliquity characterized by a 40 kyr cycle and precession which fluctuate with a 20 kyr periodicity. There are also shorter periodicities (11 kyrs and 5 kyrs) identified within the intertropical band (Berger *et al.*, 2006a, 2006b). The first relationship *between orbit and climate* was provided by Milankovich (1941) who stated that retreats of the northern ice sheet are driven by peaks in northern hemisphere summer insolation resulting in the Late Pliocene-Pleistocene glacial - interglacial cycles. On the Milankovich pioneering model, changes of the solar radiation induce lagged ice-volume responses at the precession and obliquity periods respectively. This first forcing/response model was only partially taken on account later, as by Hays *et al.* (1976), who correlated variation of the last 500 kyr marine δO^{18} values from Southern Hemisphere, with precession, obliquity and eccentricity cycles, concluding that the climatic system responds linearly to the first two parameters and nonlinearly to eccentricity. The critical mechanism of this model (CLIMAP) is the control of ice ablation by insolation during successive warm summers. Later, Imbrie *et al.* (1992, 1993) re-evaluated the climatic changes within the framework of the three orbital signals and added a new element, the greenhouse gases (including CO_2 and CH_4) forcing, providing a new model of orbit-scale climate changes (SPECMAP). This new forcing/response model suggests that the responses initiated on northward by the summer insolation forcing propagated to the Southern Hemisphere via deep-waters, inducing an intermediate response of the climate-system linked to changes in concentration of greenhouse gases (carbon dioxide and methane) which forced later the north ice sheet via CO_2 changes or others feedbacks (Imbrie *et al.*, 1992, 1993). Geochemical data obtained from the Vostok long ice-cores (Petit *et al.*, 1999; EPICA Community Members, 2004) and the establishment of two independent gas-time scales (Bender, 2002; Ruddiman and Raymo, 2003) emphasizes the convergence of different gas signals and δO^{18} at the period of precession and obliquity. According to Ruddiman (2003, 2006a, 2006b) summer insolation forcing on obliquity and precession cycles controls the Northern Hemisphere ice volume with a lag of 6500 and 4500 years, respectively. At the obliquity cycle, ice volume variations induce changes on the Sea-Surface Temperature (SST), dust fluxes and North Atlantic Deep Water flow (NADW), and some of these responses control the atmospheric CO_2 signal, that provides a positive feedback responsible for the amplification of ice-volume changes. At the precession cycle, variability of ice-volume controls the North Atlantic SST. July insolation also forces both north-tropical monsoon and CH_4 changes without any lag and Southern Hemisphere sea ice, SST and CO_2 with a lag of up to 1 kyr. Both CH_4 and CO_2 variability increase directly insolation forcing of ice volume (Ruddiman, 2003).

Among the **internal forcing factors**, the most significant are the *plate tectonics* (at very long time scale) and *igneous activity*.

At global scale, plate tectonics modifies the size, location and altitudinal profile of land masses. These modifications perturb the ocean - atmosphere dynamics causing regional to global climatic disturbances. During the Cenozoic, the most important geotectonic events which are suspected to have altered the global climate are: (1) the acceleration of uplift of the Tibetan Plateau during the Late Miocene (Dettman *et al.*, 2001; Zhisheng *et al.*, 2001; Liu and Yin, 2002; Molnar, 2005; Harris, 2006), that perturbed the atmospheric dynamics, especially causing a strengthening of the Indian monsoon (Harrison *et al.*, 1992, 1993; Molnar *et al.*, 1992); (2) the opening of the Drake Passage (at about 40 Ma) resulting in the onset of the Circumpolar Southern Ocean Circulation; (3) the closure of the Panama Strait (Keigwin, 1982; Haug and Tiedemann, 1998; Haug *et al.*, 2001; Lear *et al.*, 2003; Gussone *et al.*, 2004; Bartoli *et al.*, 2005; Jain and Collins, 2007); and (3) the acceleration of the Red Sea rifting (Ghebream, 1998; Redfield *et al.*, 2003).

The second internal factor which influences global or regional climate is the igneous activity. Basaltic extrusion of long duration (Deccan Plateau at the K/T transition, North Atlantic volcanism at about 55 Ma, Columbia River volcanism at about 16 Ma) and briefer eruptions of single volcanoes influence the global climate in varying degrees. Injection of large volumes of water and carbon dioxide into the atmosphere is responsible for the absorption of heat radiation (infrared) emitted by the Earth and results climate warming (Caldeira and Rampino, 1990). In addition, the water generally condenses out off the atmosphere in rainfall form in a few hours to a few days, and the carbon dioxide quickly dissolves in the oceans or is absorbed by plants. Isolated volcanic eruptions inject within atmosphere large quantities of dust particles, volcanic gases and water vapour which affect the radiative balance (Church *et al.*, 2005). Injection of volcanic dust causes temporary coolings (Robok and Liu, 1994; Robok, 2000), the intensity and duration of such cooling may be related to the amount of dust and size of dust-particles. Dominance of the larger-size particles within the volcanic dust affects the climate at local scale for a short time because these particles land in a few minutes close to the volcanoes. On the contrary, if the volcanic dust is made of thin-size particles, they float around during several hours or days and cause darkness and cooling below the ash cloud. The ejected volcanic gases are mostly composed of sulphur compounds as sulphur dioxide and sulphuric acid aerosols (Rampino and Self, 1984) which easily rise up to the stratosphere, increasing the Earth albedo, reducing the total amount of solar energy and being able to create a significant cooling of the Earth surface after a major eruption. Such an event happened after the 1991 Pinatubo eruption (Minnis *et al.*, 1993; Hansen *et al.*, 1997; Saunders, 1999; Soden *et al.*, 2002; Yang and Schlesinger, 2002; Gleckler *et al.*, 2006), the consequences of which should have been according to models a maximum cooling of about 0.5°C after eruption and 3-4°C if aerosols persisted (Hansen *et al.*, 1997). Similar decreases in temperature between 0.2° and 0.5°C with a duration of one to five years after eruption have been calculated after the Tambora (1815), Krakatau (1883), Santa Maria (1902), Katmai (1912) and Quizapu (1932) eruptions (Self *et al.*, 1981, Oppenheimer, 2003; Church *et al.*, 2005, Gleckler *et al.*, 2006). The Toba eruption, dated at about 73.5 ka BP, was one of the most important volcanic events during the Quaternary. This eruption has been correlated with the Oxygen Isotope Stratigraphy (Ninkovich *et al.*, 1978), from which it has been argued that outburst of such large amounts of ash led to an increase in atmospheric turbidity resulting in a global cooling of about 3-5°C several years. This may have initiated rapid ice grow and related global sea-level fall possibly at the origin of Marine Isotope Stage 5 to 4 (Rampino and Self, 1992).

1.2. MIOCENE GLOBAL CLIMATE AND EUROPEAN VEGETATION

During the Miocene the European vegetation was changed significantly as the regional climate evolved from almost tropical conditions especially developed during the Langhian to subtropical ones which prevailed during the Lower Pliocene. Two main factors are responsible for floristic hecatomb during the Miocene which continued during the Pliocene: (1) the global climate variability leading to its deterioration and (2) upheavals in the European paleogeography.

1.2.1. Global climate variability during the Miocene.

The beginning of the Neogene (Fig. 1) coincides with a transient cooler climate event as response to the intermittent expansion on the East Antarctica Ice Sheet (EAIS), event known as the Mi-1 event (Miller *et al.*, 1987; 1991; Wright *et al.*, 1992; Pagani *et al.*, 1999). This event (as the other Mi-events identified during the Miocene) is characterized by an anomalous positive oxygen isotope excursion (Miller *et al.*, 1987; Wright and Miller, 1993, Zachos *et al.*, 2001) coupled with a deep sea cooling (bottom water temperature was generally between 1 and 2°C, Peakar and DeConto, 2006) and increase of radiative forcing documented by the raise of $p\text{CO}_2$ (Pearson and Palmer, 2000) that momentarily interrupted the long global warming trend (Zachos *et al.*, 2001) initiated at the Eocene/Oligocene transition (Flowers, 1999). Excepted these cooler events (Mi-1 to Mi-3) related to the punctuated expansion of East Antarctic Ice Sheet, the climate was warmer than today during the Lower Miocene (global temperature 3 - 4°C higher) and atmospheric CO_2 concentration was twice as high as today (Naish *et al.*, 2001). Probably, the major agent that helped to maintain relatively warmer conditions during the Early Miocene is the thermohaline circulation which permitted development of equatorial heat transport (Woodruff and Savin, 1989, Wright *et al.*, 1992; Flower and Kenneneth, 1994). The maximum of temperature was reached during the Upper Burdigalian - Lower Langhian (17-15 Ma), episode known as *Miocene Climate Optimum* (MCO). Following this warm episode, an important cooling event, called the *Monterey cooling event* dated at about 14 Ma ago, marked an important step in the transformation of the "greenhouse world" into an "icehouse context". The *Monterey cooling event* coincides with a major ice sheet expansion in Antarctica (Shackleton and Kennett, 1975; Kennett and Barker, 1990; Flower and Kennett, 1993, 1994, 1995; Miller *et al.*, 1991; Zachos *et al.*, 2001, Naish *et al.*, 2001; Bart, 2003; Chow and Bart, 2003; Shevenell *et al.*, 2004; Holbourn *et al.*, 2005). Its processes and causes are still debated. Tectonically driven circulation changes (Kennett, 1975; Hsü and Bernoulli, 1978; Steininger *et al.*, 1985; Woodruff and Savin, 1991, Flower and Kenneneth, 1994) and variations of the atmospheric CO_2 level (Pagani *et al.*, 1999; Raymo and Ruddiman, 1992; Vincent and Berger, 1985) have been suggested as key-mechanisms. These Mid-Miocene global climatic changes (cooling phases corresponding to the Mi 4 to Mi6 events alternated with warmer periods) strongly influenced marine and terrestrial conditions. The most know effects of these climate changes are the increased meridional surface temperature gradient between climatic zones, leading to accentuated aridification in mid-latitude continental regions of Australia, Africa and North and South America that enhanced development of grasslands and stimulated evolution of grazing mammals. An opposite of this cooling trend occurred during the early part of the Late Miocene when low to mid latitude surface water of world oceans warmed up and global climate revitalized. This new reversal of the global climate variability is related to have

been induced by two events: (1) the closure of the Indonesian Seaway (between 8 and 5.2 Ma) and the creation of the early warm pool over the West Pacific that may have a role on the climate modulation (Srinivasan and Sinha 1998; Hall, 2002; Kuhnt *et al.*, 2004; Li *et al.*, 2006) and (2) the onset of a final major episode of Himalayan - Tibetan uplift (Tapponier *et al.*, 2001). The tectonic-induced changes in physiography transformed oceanography and climate to near the modern patterns characterized by strong trade winds and intense Equatorial counter-currents (Kennett *et al.*, 1985). Orbitally-tuned paleoclimate proxies indicate that prior to the Miocene Climate Optimum, climate variability responded to eccentricity (400 and 100 kyrs) and precession (20 kyrs) forcing, the *Monterey Cooling event* (15 -14 Ma) was modulated by obliquity (40 kyrs) and during the time-interval 14 – 6 Ma the forcing factor was eccentricity with a distinct 100 kyr rhythm in climate and circulation patterns.

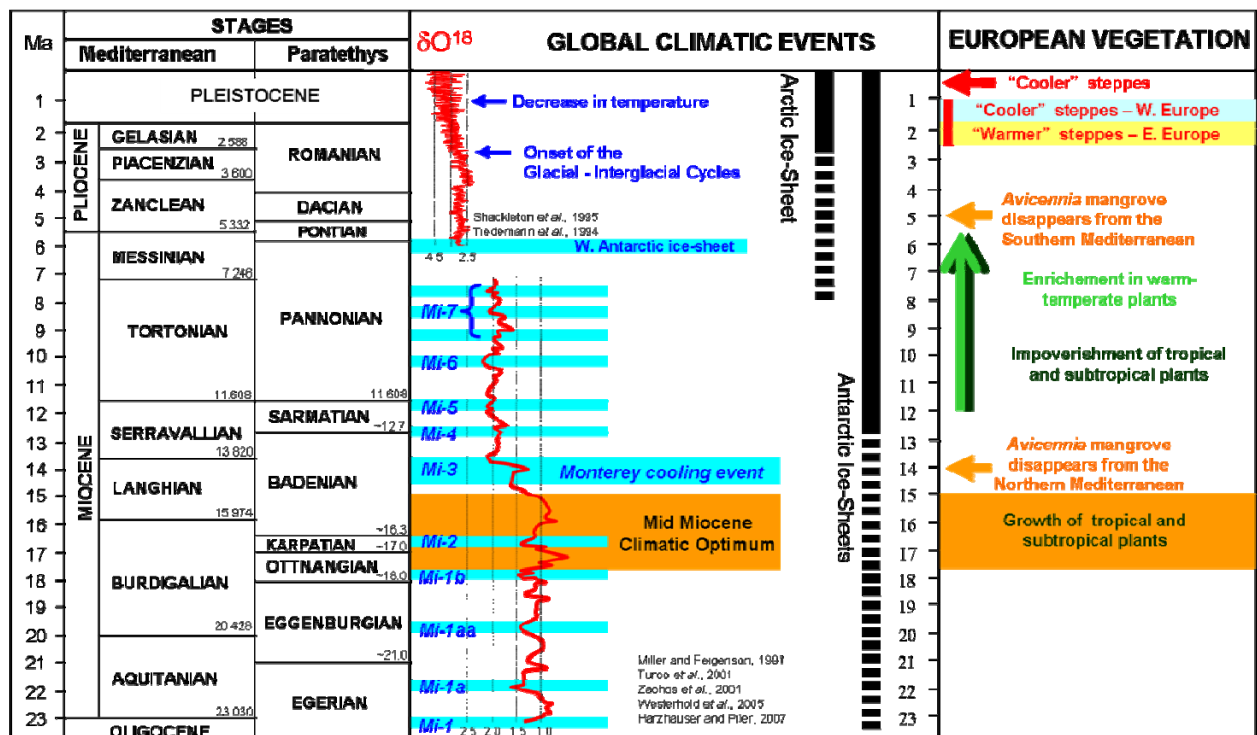


Fig. 1. Neogene global climate events and European vegetation changes

1.2.2. Vegetation changes in Europe during the Miocene

European flora, during the Miocene (Fig. 2) suffered a progressive impoverishment with assemblages rich in tropical elements successively eliminated for the benefit of subtropical and warm-temperate elements which prevailed at the Late Miocene.

During the Early Miocene, southern Europe flora was dominated by tropical and subtropical taxa revealed while subtropical and warm-temperate elements prevailed in the northern Europe according to plant macroremains (Pantic, 1956; Stevanovic and Pantic, 1954; Milovanovic and Mihajlovic, 1984 Fernández Marrón and Alvarez Ramis, 1988; Sanz de Siria Catalán, 1993; Barrón and Sansisteban, 1999; **Roiron *et al.*, 1999¹**; **Rubio *et al.*, 2003**) and pollen records (Bessedik, 1985; **Roiron *et al.*, 1999**; Ivanov *et al.*, 2002; 2007, Jiménez-Moreno *et al.*, 2007a; 2007b ; **2007c**).

¹ The references in bold characters relate to my publications

My preliminary results (**Roiron et al., 1999**) on the Rubielos de Mora Basin (NE Spain) pointed out that the local vegetation was mostly composed by subtropical (*Distylium*, *Engelhardia*, *Platycarya*, Sapotaceae, *Symplocos* Taxodiaceae) and warm-temperate taxa (*Acer*, *Carya*, *Cephalanthus*, *Nyssa* cf. *aquatica* *Populus*, *Quercus*, *Salix*, *Ulmus*, *Zelkova*) accompanied in relative few amounts by high and mid altitude trees (*Abies* and *Cathaya*) and some taxa as *Ceratonia*, *Olea*, *Phillyrea*, *Microtropis fallax*, *Artemisia* indicating that a dry season existed at that time. This study was later enlarged by Jiménez-Moreno (2005) during his PhD thesis on the material from a cored borehole. Local forest vegetation rich in mega- and mesothermic elements was identified in a regional open and xeric context, with also some organization in altitudinal belts (Jiménez-Moreno, 2005, 2007a, 2007b and **2007c**). Pollen flora from this core is constituted of: (1) Megathermic (tropical) elements: Acanthaceae, *Alchornea*, *Amanoa*, *Arecaceae*, *Avicennia*, *Canthium* type, *Bombax*, *Buxus bahamensis* type, *Caesalpiniaceae*, *Mappianthus*, *Meliaceae*, *Passifloraceae*, *Rutaceae*, *Simarubaceae*, *Theaceae*, etc.; (2) Mega-mesothermic (subtropical) elements: *Accacia*, *Araliaceae*, *Celastraceae*, *Chloranthaceae*, *Corylopsis*, *Croton*, *Cyrillaceae–Clethraceae*, *Disanthus*, *Distylium*, *Engelhardia*, *Euphorbiaceae*, *Exbucklandia*, *Fothergilla*, *Hippocastanaceae*, *Menispermaceae*, *Microtropis fallax*, *Mussaenda*, *Nyssa*, *Parthenocissus*, *Platycarya*, *Rhodoleia*, *Rhoiptelea*, *Ricinus*, *Rubiaceae*, *Sapotaceae*, *Symplocos*, *Symplocos paniculata* type, *Taxodium* type, *Taxodiaceae*, etc.; (3) *Cathaya*, a mid-altitude conifer living today in Southern China; (4) Mesothermic (warm-temperate) elements: *Acer*, *Alnus*, *Betula*, *Buxus sempervirens*, *Caprifoliaceae*, *Carpinus*, *Carpinus orientalis*, *Carya*, *Celtis*, *Castanea–Castanopsis* type, *Eucommia*, *Fagus*, *Fraxinus*, *Hamamelidaceae*, *Hamamelis*, *Hedera*, *Ilex*, *Juglans*, *Liquidambar*, *Lonicera*, *Myrica*, *Oleaceae*, *Ostrya*, *Fabaceae–Papilionioideae*, *Parrotia* cf. *persica*, *Platanus*, *Populus Pterocarya*, *Quercus* deciduous type, *Rhamnaceae*, *Rhus*, *Salix*, *Sequoia* type, *Ulmus*, *Zelkova*, *Viburnum*, *Vitis*, etc.; (5) *Pinus* and *Pinaceae*; (6) Mediterranean xerophytes: *Olea*, *Quercus ilex-coccifera* type, *Phillyrea*, etc.; (7) Herbs and shrubs: *Alisma*, *Apiaceae*, *Amaranthaceae–Chenopodiaceae*, *Asteraceae Asteroideae*, *Asteraceae Cichorioideae*, *Brassicaceae*, *Campanulaceae*, *Caryophyllaceae*, *Cistaceae*, *Convolvulaceae*, *Ericaceae*, *Ephedra*, *Geranium*, *Lamiaceae*, *Liliaceae*, *Linum*, *Mercurialis*, *Nitraria*, *Nymphaeaceae*, *Parietaria*, *Poaceae*, *Plantago*, *Potamogeton*, *Polygonaceae*, *Plumbaginaceae*, *Ranunculaceae*, *Resedaceae*, *Rosaceae*, *Rumex*, *Tamarix*, *Thalictrum*, *Tricolporopollenites sibiricum*, *Typha*, *Urticaceae*, etc.

Different paleoclimatic transfer functions (Mosbrugger and Utescher, 1997; Mosbrugger, 1999, Fauquette et al., 1998a) were applied to plant macroremains (Utescher, et al., 2000; Roth-Nebelsik et al., 2004; Mosbrugger et al., 2005) and to pollen records (Ivanov et al., 2002; Jiménez-Moreno et al., 2007b) in order to reconstruct the climate parameters as the mean annual temperature (MAT), mean temperature of the warmest months (MTW), mean temperature of the coldest month (MTC) and mean annual precipitations (MAP). According to pollen record, Jimenez-Moreno et al., (2007) proposed for NE Spain values of MAT between 18°C and 20°C, MTW between 24°C and 27°C, MTC between 9 and 6 °C, and MAP between 900 and 1700mm. According to climate reconstruction using plant macroremains from the Lower Miocene German flora, Roth-Nebelsick et al., (2004) and Utescher, et al., (2000) propose that MAT ranges between 14.1°C (15. 5°C) and 20.8°C (21°C), MTW between 25.7°C and 28.1°C, MTC between 4.7 and 13.3 °C, and MAP between 897-1281 mm. Minor differences between these estimated values for climatic parameters should be related to plant diversity differences.

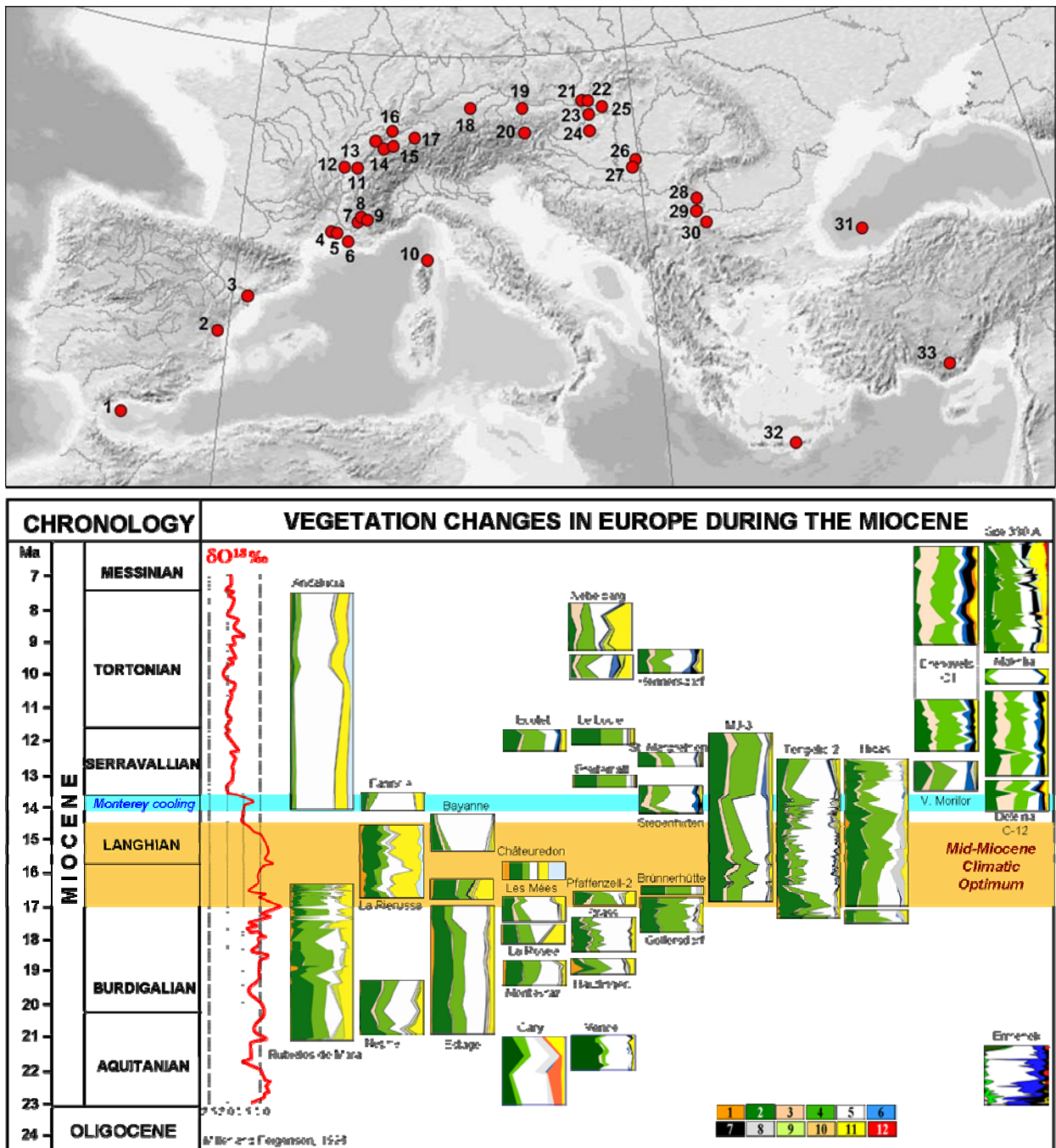


Fig. 2. A. Geographic position of presented sections: 1 Andalusia; 2 Rubielos de Mora; 3 La Rierussa; 4, Estagel; 5 Bayanne; 6, Cary; 7, Les Mées; 8, la Rosée; 9, Châteuredon ; 10, Farinole ; 11, La Nàphe ; 12, Ecotet ; 13, Le Locle ; 14, Montevraz ; 15, Häutlingen; 16, Nebelberg; 17, Breitenmatt; 18, Pfafenzil-II; 19, Strass; 20, Brüner-Hütte; 21, Göllersdorf; 22, Sieberhinten; 23, Hennesdorf; 24, St. Margareten; 25, Moravski Jan -3; 26, Tengelic 2; 27, Hidas-53; 28, Valea Morilor; 29, Drenovets C1; 30, Delenia; 31, Site 380A; 32, Makrilia; 33 Ermenek. (Jimenez- Moreno, 2005; **Jiménez-Moreno, et al., 2007c**); **B. European vegetation changes during the Miocene:** 1, megathermic elements; 2, mega-mesothermic elements, 3 *Cathaya*; 4, mesothermic elements ; 5, *Pinus* and poorly preserved Pinaceae, 6, meso-microthermic (mid-altitude) trees; 7, microthermic (high-altitude) trees; ; 8, non significant pollen grains (undetermined ones, poorly preserved pollen grains, some cosmopolitan or widely distributed elements; 9, Cupressaceae; 10, Mediterranean xerophytes; 11, herbs; 12, steppe elements.

The Middle Miocene vegetation in Europe is well-documented by numerous widely distributed pollen localities (Fig. 2) representative both of climatic changes and of latitudinal-longitudinal organization of vegetation. Plant macroremains mainly concern

central-eastern Europe. Vegetation dynamic and climate evolution is particularly illustrated by some long pollen sequences, such as Tengelic 2 and Hidas in Hungary (Jiménez-Moreno *et al.*, 2005) and La Rierussa in northeastern Spain (Bessedik, 1985; Jiménez-Moreno, 2005).

The Miocene Climatic Optimum is characterized by the highest diversity especially for tropical and subtropical plants supported by their greatest relative frequency in pollen records of Tengelic 2; La Rierussa and Châteaudon sections (Fig.2). The high diversity tropical and subtropical taxa represented by : Euphorbiaceae, Rubiaceae, *Alchornea*, Melastomataceae, *Acacia*, *Sindora*, Rutaceae, *Buxus bahamensis* type, Acanthaceae, Theaceae, etc. Taxodiaceae, *Symplocos*, Arecaceae, *Distylium*, *Platycarya*, *Engelhardia*, Menispermaceae, *Microtropis fallax*, etc. was founded at Tengelic 2 section. At la La Rierussa section, the same tropical elements plus *Avicennia*, *Croton*, *Mappianthus*, Passifloraceae, *Bombax*, *Grewia-Corchorus*, Mimosaceae, Meliaceae, etc., the same subtropical elements plus *Leea*, *Rhoiptelea*, etc. were founded. These two localities have recorded the two thermic maxima of the Miocene Climatic Optimum.

On contrary, the Monterey cooling is directly poorly documented. It has been recorded at Tengelic 2 in continuity to the thermic maximum, being marked by the disappearance of all the tropical elements and the strong decrease of the subtropical ones, respectively replaced by the warm-temperate elements and *Cathaya*. In southern France, few localities show the disappearance of the tropical elements and the coeval increase of the subtropical ones. The following successive minor climatic fluctuations which occurred during Serravallian and Tortonian have been very discontinuously identified (see Nebelberg and Hennersdorf on Fig. 3) in Western-Central Europe, insufficiently detailed in the long records from Eastern Europe (Devronets C1, Makrilia, Deleina: see Fig. 3; Ivanov, 1995; **Jimenez-Moreno *et al.*, 2007c**) because of the lack of effort in identification of thermophilous taxa. Paleoclimatic transfer functions were applied to these pollen records, allowing to estimate at 2-4°C the mean annual temperature drop of the Monterey cooling (Jiménez-Moreno *et al.*, 2005) while the thermic latitudinal gradient was calculated around 0.48°C/° in latitude for the same parameter during the Miocene Climatic Optimum and increased at about 0.6°C/° in latitude at the Late Miocene (Fauquette *et al.*, 2007). The latitudinal gradient in xericity did not change significantly during the same time-interval (Fauquette *et al.*, 2007). Paleotemperature quantifications performed on Bulgarian pollen data do not document a so large drop in temperature for the Monterey cooling but continuously document climatic changes of the Late Miocene (Ivanov *et al.*, 2002). Paleovegetation maps have been elaborated with difficulty when representing only a forest cover (Kovar-Eder *et al.*, 2006), more illustrative when based on contrasting pollen records (Favre, 2007). Such paleovegetation maps may be compared with the first paleovegetation reconstructions proposed by models (François *et al.*, 2006; Favre *et al.*, 2007).

Vegetation of the Messinian Stage (Fig. 3) is well-known thanks to numerous pollen records mostly concentrated in southern Europe (Vai and Ricci Luchi, 1977; Suc, 1989; Bertini *et al.*, 1998; Suc and Bessais, 1990; Bertini, 1992; Chikhi, 1992; Suc *et al.*, 1995a, 1995b; Bachiri-Taoufiq, 2000; **Popescu, 2001**; Warny *et al.*, 2003; **Popescu, 2006**).

Unfortunately, it is incomplete because of the lack of sediments during the peak of the Messinian Salinity Crisis when the Mediterranean and Black seas almost desiccated. The Messinian Antarctic glacials are also difficult to recognize because of the scarcity of pollen grains within the Mediterranean marginal evaporites which deposited at that time.

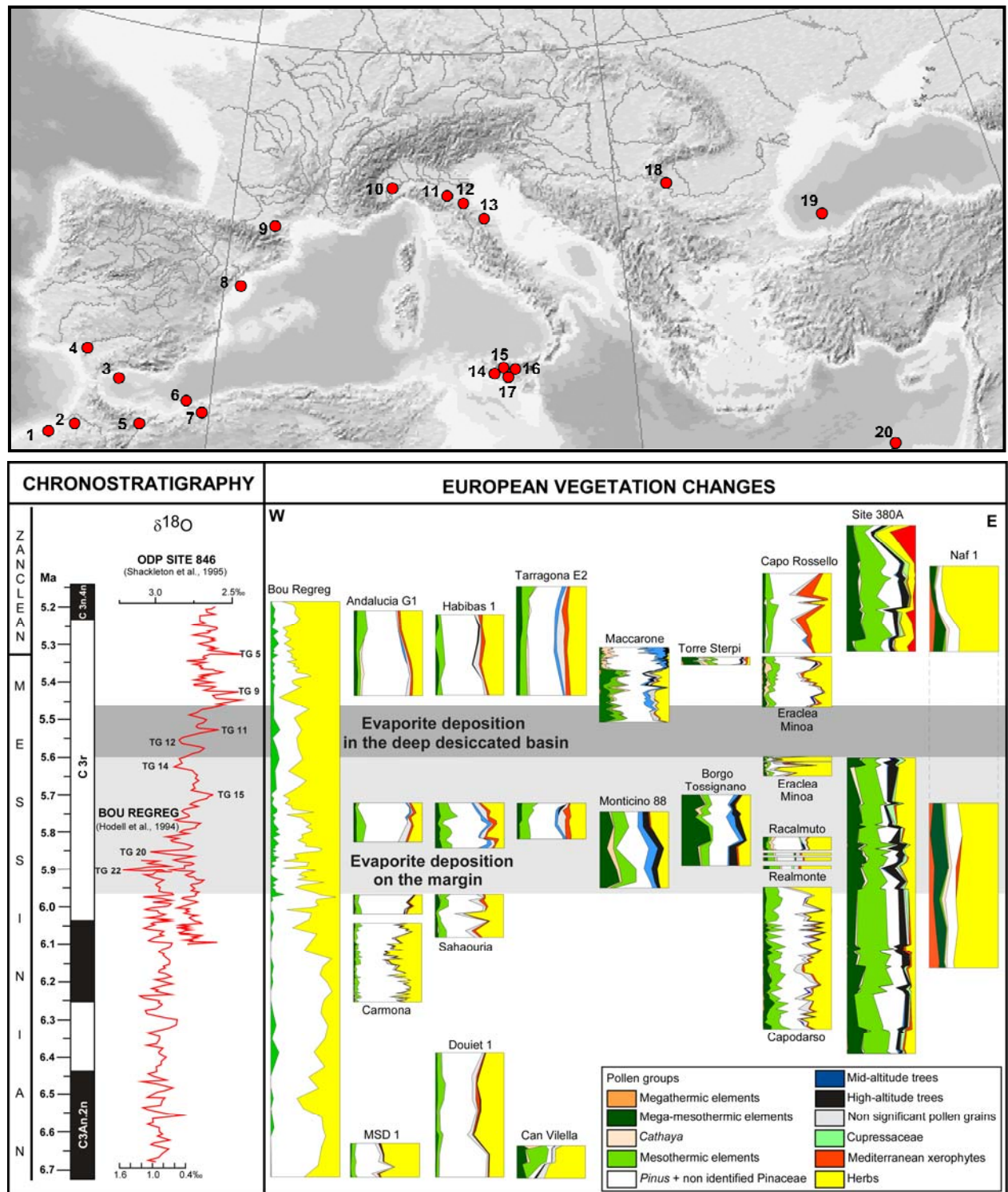


Fig. 3. A. Geographic position of presented sections: 1 Bou Regreg; 2 MSD1; 3 Andalucia G1; 4, Carmona; 5 Douiet 1; 6, Habibas 1; 7, Sahaouria; 8, Tarragona E2; 9, Can Vilella : 10, Torre Sterpi ; 11, Borgo Tossignano ; 12, Monticino ; 13, Macarone ; 14, Eraclea Minoa ; 15, Racalmuto; 16, Capodarso; 17, Realmonte/Capo Rosello; 18, Hinova; 19, Site 380A; 20 Naf1. (Popescu, 2001, 2006; Fauquette et al., 2006); **B. European vegetation changes during the Miocene:** 1, megathermic elements; 2, mege-mesothermic elements, 3 *Cathaya*; 4, mesothermic elements ; 5, *Pinus* and poorly preserved Pinaceae, 6, meso-microthermic (mid-altitude) trees; 7, microthermic (high-altitude) trees; ; 8, non significant pollen grains (undetermined ones, poorly preserved pollen grains, some cosmopolitan or widely distributed elements); 9, Cupressaceae; 10, Mediterranean xerophytes; 11, herbs; 12, steppe elements.

As main results, ones must notice persistence of some tropical elements (*Avicennia*, *Alchornea*, etc.) at the Mediterranean latitude before the peak of the Messinian Salinity Crisis, then the migration to the North of subdesertic herbs and shrubs (*Lygeum*, *Calligonum*, *Ziziphus*, etc.) during the almost complete desiccation phase when they became unable to survive so hard conditions (Fauquette *et al.*, 2006). Anyway, the North-South gradient in temperature and xericity was very pronounced during the Late Miocene, if we do not consider the outstanding epiphenomenon of the Messinian Salinity Crisis. Open vegetation growing under warm and dry conditions developed in south-western Europe and north Africa, whatever the longitude while forests flourished northward under warm and humid conditions (Fig. 4), (Fauquette *et al.*, 2006; Jiménez-Moreno, 2007c). Paleoclimatic reconstruction for the late Miocene (Fauquette *et al.*, 2006) indicate globally warm climate with the MAT between 15- 24°C, with a strong seasonality correlate with high precipitation values (1100 - 1550 mm) for the northern Europe and respectively low seasonality and low precipitation values (320- 680 mm) for the south-western Europe and North Africa. The similar values of MAT and Map were obtained by Kovar - Eder *et al.*, (2006), using plant macroremains data.

1. 3. PLIOCENE GLOBAL CLIMATE AND EUROPEAN VEGETATION

1.3.1. Global climate variability during the Pliocene

The global climate, during the Pliocene (5.332 – 1.808 Ma) was impacted by a major change, related to the onset of the Northern Hemisphere Glaciation at 2.588 Ma. This climate event significantly modified the marine and continental ecosystems.

The Early Pliocene (5.332 - 3.6 Ma) corresponds to a global warm climate both documented by marine (Crowley, 1991; Kenneth and Hodell, 1993; Billups *et al.*, 1998a; 1998b; Ballantyne *et al.*, 2003) and terrestrial records (mammals: Montuire *et al.*, 2006; Fortelius *et al.*, 2006; macroremains: Roiron, 1992 ; Martinetto, 1994; Kovar - Eder *et al.*, 2006; and pollen: Zagwijn, 1960; Suc, 1980 ; Cravatte et Suc, 1981 ; Suc et Cravatte 1982 ; Suc, 1984; Hooghiemstra, 1989 ; Diniz, 1984 ; Clet - Pellerin, 1985; Bessais et Cravatte, 1988; Hooghiemstra et Ran, 1994; Bertini, 1994 ; Suc et Bessais, 1990 ; Combourieu-Nebout, 1990; **Popescu, 2001; 2006 ; Popescu *et al.*, 2006a; 2006b**). Reconstruction of climatic parameters, based on different proxies, indicate at European mid-latitudes a mean annual temperature higher of about 1-5°C than today and mean annual precipitations higher of about 400 -1000 mm (Fauquette *et al.*, 1998, 2006; Montuire *et al.*, 2006; Fortelius *et al.*, 2006; Uhl *et al.*, 2007). This global warm situation was interrupted between 4.7 - 4.5 Ma by a cooling event related to small fluctuations of the Antarctic ice-sheet. This event was identified in the European vegetation and corresponds to the Brunssumian B (Zagwin, 1960) or PIb (Suc, 1984) climatic phases.

The climate remained warm during the Middle Pliocene (3.6 - 2.588 Ma), in spite of several drops in temperature, with a thermic maximum at about 3Ma. Microfaunal records indicate warm surface waters, with SST of about 8°C and 2-3°C higher than today in the North and South Atlantic, respectively (Dowsett and Poore, 1991; Dowsett *et al.*, 1992; 1996; 2005; Cronin *et al.*, 1991; 1993). Data from intertropical Pacific indicate a reduction of the East-West SST gradient suggesting a permanent El Niño phenomenon during the Early-Middle Pliocene (Ravelo *et al.*, 2004; Wara *et al.*, 2005). Mechanism considered explaining this warm climate during Early-Middle Pliocene is still debated. Model simulation (Haywood and Valdes, 2004; Haywood *et al.*, 2007; Chandler

et al., 2008) propose a global temperature warming of 3°C during the Middle Pliocene. These authors propose that the warm climate could be explained by reduced terrestrial ice-sheets in the polar zones (-50% in Greenland, -33% in Antarctica) and sea-ice cover, that caused a strong ice-albedo feedback. Haug (2001) related the warm climate to changes in thermohaline circulation caused by the closure of the Panama seaway (at about 3 Ma ago), while some other authors (Ravelo *et al.*, 2004; Wara *et al.*, 2005; Fedorov *et al.*, 2006) suggested that the permanent El Niño could have contributed to the Pliocene warmth in eliminating stratus clouds, subsequently reducing albedo and increasing atmospheric water vapour. Other hypotheses refer to the strengthening of atmospheric greenhouse and associated feedbacks (Hansen *et al.*, 1984; Soden and Held, 2006, Fedorov *et al.*, 2006) that could have maintained both low- and high-latitude warmth, with a reduced East-West equatorial SST gradient.

The beginning of the Northern Hemisphere Glaciations (NHG) at 2.588 Ma resulted in a global cooling, used to mark the boundary between Middle (Piacenzian) and Late (Gelasian) Pliocene. Several hypotheses were proposed to explain this crucial change of the global climate (Raymo, 1994; Rea *et al.*, 1998; Maslin *et al.*, 1998; Philander and Fedorov, 2003; Ravelo *et al.* 2004a, 2006; Bartoli *et al.*, 2005; Barreiro *et al.*, 2005; Fedorov *et al.*, 2006). An hypothesis refers to the closure of the Panama seaway (Crowley, 1996; Haug and Tiedemann, 1998; Haug, 2001, Bartoli, 2005) that resulted in (1) the gradual restriction of sea-surface water exchanges and high surface salinity contrast between the Atlantic and Pacific oceans (Keigwin, 1982; Haug and Tiedemann, 1998), (2) the intensification of the Gulf Stream, and increasing moisture over the North Atlantic region. According to Driscoll and Haug (1998), the load in humidity of the westerly winds provoked the increase of Eurasian precipitations (rain and snow) and maybe more freshwater input into the Arctic Ocean via Siberian rivers. The lower salinity of the Arctic Ocean facilitated the building of sea-ice than reflected sunlight and heat back to space, induced cooling effect at high latitudes, and finally might lead the onset of NHG (Lunt *et al.*, 2008a, 2008b). Another hypothesis has been suggested by Cane and Molnar (2001) and relates to the impact of closure of the Indonesian seaway (13 – 2.5 Ma) on the global climate. According to these authors, the movement of an island within the Indonesian seaway may have forced the tropical climate reorganization that would may caused the high-latitude cooling and beginning of the NHG. A third hypothesis suggests that the Cenozoic uplift of the Rocky Mountains and Himalaya influenced the atmospheric circulation, in causing larger Rossby wave amplitude and jet-stream deflection able to bring cooler air masses and increased moisture and snowfall over the incipient Greenland ice sheet (Ruddiman and Kutzbach, 1989). Finally, the fourth hypothesis states that a decreased radiative forcing associated with lowered concentration of atmospheric CO₂ led to a cooler melt-season temperature and reduced ablation, causing an annual accumulation of enough snow to grow the ice sheet (Raymo *et al.*, 1996; Kürschner *et al.*, 1996). Each of these hypotheses was tested by Lunt *et al.*, (2008a, 2008b), suggesting that the most probable mechanism at the origin of the NHG should be related to the decrease in atmospheric CO₂, that might have been forced by orbital parameter variability coupled with all the mechanisms previously described.

Anyway, the beginning of the NHG caused important changes in the Late Pliocene (2.558 – 1.8 Ma) climate system, modifying the ocean and atmosphere circulation, in relation with the fluctuation of the Northern Hemisphere ice sheet during glacial-interglacial transition (Raymo *et al.*, 1989; Crowley and North, 1991; Zachos *et al.*, 2001).

In the tropical and subtropical regions, the Late Pliocene climate caused (1) periodically cooler and drier conditions in Africa (Leroy and Dupont, 1994; De Menocal, 1995, 1999; 2004), (2) increase in East-Asian monsoon activity (Clemens *et al.*, 1991; 1996; An *et al.*, 2001; Tian *et al.*, 2006), and (3) acceleration of erosion rate in Himalaya (Huntington *et al.*, 2006).

Looking to the Mediterranean region, xerophytic taxa (*Olea*, *Pistacia*, *Ceratonia*, *Phillyrea*, *Nerium*, *Rhus cotinus*, *Rhamnus*, *Ligustrum*, evergreen *Quercus*, *Cistus*, *Phlomis fruticosa*, Resedaceae, Myrtaceae, etc.) were continuously recorded (sometimes in large quantity) in pollen localities from southern Europe since the beginning of the Miocene, mostly in eastern Spain and southeastern France (Bessedik, 1985; Zheng, 1986; Jiménez-Moreno, 2005). As they are regularly accompanied by subdesertic elements (such as *Prosopis*, *Alchornea*, *Ziziphus*, *Nitraria*, *Lygeum*, *Calligonum*, *Neurada*, Agavaceae, etc.) in a regional landscape largely dominated by herbs, they have been interpreted as inhabiting dry lands in a relatively xeric climatic context characterized by a long drought along the year and low seasonal contrast in temperature within the tropical-subtropical thermic range (Suc, 1989; Pons *et al.*, 1995; Suc *et al.*, 1999). In the Northwestern Mediterranean region, the progressive decline of subtropical plants (Taxodiaceae, *Engelhardia*, Arecaceae, *Distylium*, etc.) occurred during the Early Pliocene and was counterbalanced by the strengthening of xerophytes which benefited from the abandoned areas (Suc *et al.*, 1995). This phenomenon culminated at the Zanclean-Piacenzian passage and is a consequence of the global cooling at 3.6 Ma. It was interpreted as resulting from the onset of the thermic seasonality in the Northwestern Mediterranean region (cool winters, warm summers) which superimposed the pre-existing seasonality in dryness, that resulted in the conjunction of the dry season with the warm season, i.e. in the setting of the Mediterranean climatic rhythm which was experienced in this area up to the earliest glacial at 2.588 Ma (Suc, 1984). Return to such a seasonality was expected at each glacial-interglacial and interglacial-glacial transition according to the model proposed by Combourieu-Nebout (1993), developed from that of Van der Hammen *et al.* (1971). In fact, it was poorly-expressed as shown by the low-amplitude fluctuations of the representatives of the mediterranean ecosystem in the Plio-Pleistocene Crotona series (southern Italy) (Combourieu-Nebout *et al.*, 2000; Klotz *et al.*, 2006; Joannin *et al.*, 2007), being one of the “seven ambiguities in the Mediterranean paleoenvironmental narrative” emphasized by Tzedakis (2007) for the entire Pleistocene. Only the Early Pleistocene pollen record from Camerota (southern Italy) displays the expected development of mediterranean xerophytes and a reliable succession within this ecosystem at a glacial-interglacial transition (Brénac, 1984; **Suc and Popescu, 2005**).

1.3.2. Vegetation changes in Europe during the Early Pliocene

During the Pliocene, Global climate and regional geographic changes particularly influenced the European vegetation. Many studies on macroremains (Roiron, 1992; Martinetto, 1994) and pollen records from the Mediterranean region (Suc, 1980; Cravatte *et al.*, 1981; Suc *et al.*, 1982; Bessais *et al.*, 1988; Zheng *et al.*, 1986; Bertini, 1994; Suc *et al.*, 1990; Combourieu-Nebout, 1990) already documented these changes. Mediterranean long pollen records (Garraf 1 and Autan1: Suc, 1984 Tarragone E2: Bessais and Cravatte, 1988; Stirone: Bertini, 1994; Crotona: Combourieu-Nebout: 1990) have been climatostratigraphically correlated with (1) other European long pollen records (The Netherlands: Zagwijn, 1960; Germany: Menke, 1975; Portugal: Diniz, 1984; Poland: Winter, unpublished; France, Clet- Pellerin,

1985) or Central - America ones (Hooghiemstra, 1989 ; Hooghiemstra and Ran, 1994) and (2) with the global reference oxygen isotopic curve (Combourieu-Nebout and Vergnaud Grazzini, 1991 ; Shackleton *et al.*, 1995 ; Tiedemann *et al.*, 1994). These correlations contributed to demonstrate the impact of global climate changes on the vegetation dynamics.

An important part of my research concentrated (1) on the Early Pliocene of the Dacic Basin (southwestern Romania), a “paleolake” of the residual Paratethys (Fig. 5), offering thick sediments exposed in lignite quarries (Hinova, Valea Visenilor, Husnicioara and Lupoia), and (2) on the Late Miocene - Early Pliocene core drilled on the Black Sea (Site 380A, Leg 42), that was previously studied at low resolution by Traverse (1978). The scientific targets of my work were: (1) to clarify the relationships between East European vegetation changes and global climate; (2) to establish if the cyclic climate variation forced by astronomical factors during the Early Pliocene (Hilgen, 1991) has been intense enough to have caused important changes in the vegetation; (3) to establish the timescale of tropical and subtropical taxa extinction in the studied region which is today a refuge area of several thermophilous plants.

Pollen analysis of the Lupoia section (**Popescu, 2001**) indicates two kinds of cyclic evolution (Fig. 4). The first type of alternations emphasizes warming phases (expansion of low altitude thermophilous forests) in contrast to cooling phases (descent of altitudinal forests). The second type of alternations evokes modern vegetation in Florida and Mississippi Delta where coexist swamps inhabited by trees (*Taxodium distichum*) and marshes occupied by floating herbs (Cyperaceae mostly) including some shrubs (Cyrillaceae, Clethraceae).

Balance of their respective surface (changing along the time) is under control of the fact that marshes require more water than swamps. Based on the previously established chronology according to mammals combined with paleomagnetism, pollen record has been accurately calibrated with respect to eccentricity and precession curves. These correlations suggest that the first type of vegetation variability (thermophilous vs. altitude trees) was induced by eccentricity forcing, with both 100 and 400 kyrs periodicities (**Popescu *et al.*, 2006a, 2006b**). The second types of alternations showed a period of about 20 kyrs and were thus forced by precession. The precession control probably caused variations in humidity in Southeastern Europe directly relating to increasing of East African monsoon influence (**Popescu *et al.*, 2006a, 2006b**). Principal component analysis and spectral analysis have been used, and combined to the ecological significance of taxa according to their modern representatives, a classical approach in palynology resulting in taxa groupings.

Opposition between thermophilous and altitudinal trees is a continuous phenomenon in pollen diagrams from the Dacic Basin. Everywhere, such alternations appear independent from lithology that discard the possible influence of pollen transport. Increases in thermophilous trees correspond to warming up phases and eccentricity minima, increases in altitudinal trees correspond to cooling phases and eccentricity maxima. Relationships have been established with the global reference oxygen isotope curve that confers wide climatostratigraphic significance to the Dacic Basin pollen records and facilitates a high-resolution chronology (Fig. 5). Major climatic phases have been identified and numbered (1 to 23: even numbers = cooling phases; odd numbers = warming up phases) (**Popescu *et al.*, 2006a, 2006b**).

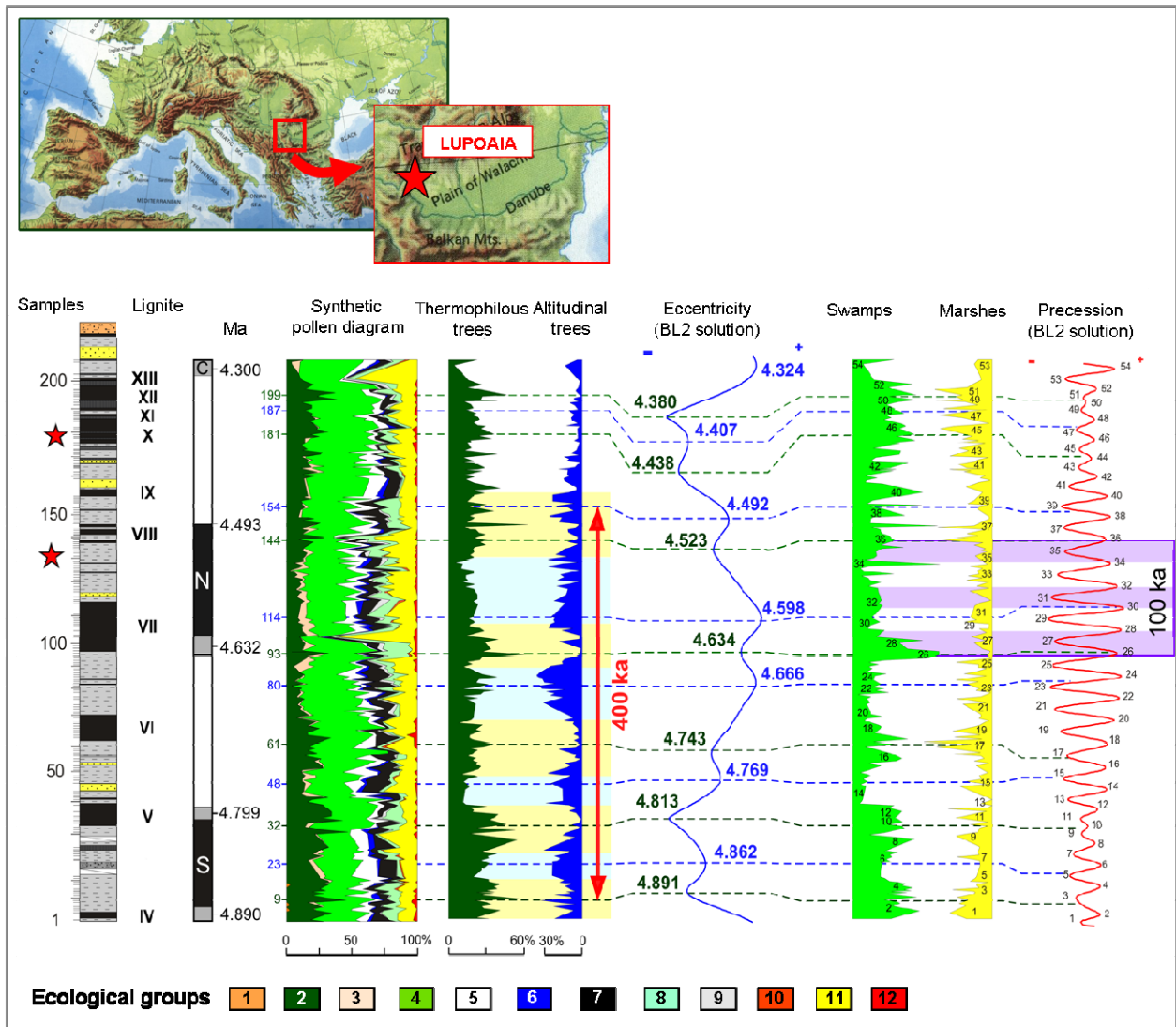


Fig. 4. Lupoia section: vegetation response to orbital forcing (Popescu, 2001; Popescu et al., 2006a, 2006b). Ecological groups represented on the synthetic pollen diagram: 1, megathermic elements (*Euphorbiaceae*, *Amanoa*, *Meliaceae*, *Entada* type, *Pachysandra* type, *Sapindaceae*, *Loranthaceae*); 2, mega-mesothermic elements (*Engelhardia*, *Distylium*, *Parrotiopsis jacquemontiana*, *Microtropis fallax*, *Leea*, *Cyrillaceae-Clethraceae*, *Myrica*, *Taxodium* type, *Cephalanthus*, *Nyssa*); 3, *Cathaya*; 4, mesothermic elements (deciduous *Quercus*, *Carya*, *Pterocarya*, *Parrotia persica*, *Carpinus*, *Ulmus*, *Zelkova*, *Alnus*, *Tilia*, *Vitis*, *Hedera*, etc.); 5, *Pinus*; 6, mid-altitude trees (*Tsuga* and *Cedrus*); 7, high-altitude trees (*Abies* and *Picea*); 8, *Cupressaceae*; 9, taxa without signification; ; 10, mediterranean xerophytes (*Olea*, *Phillyrea*, *Ligustrum*, *Pistacia*, etc.); 11, herbs (*Amaranthaceae-Chenopodiaceae*, *Brassicaceae*, *Polygonaceae*, *Cyperaceae* etc.); 12, steppe elements (*Artemisia*, *Ephedra*).

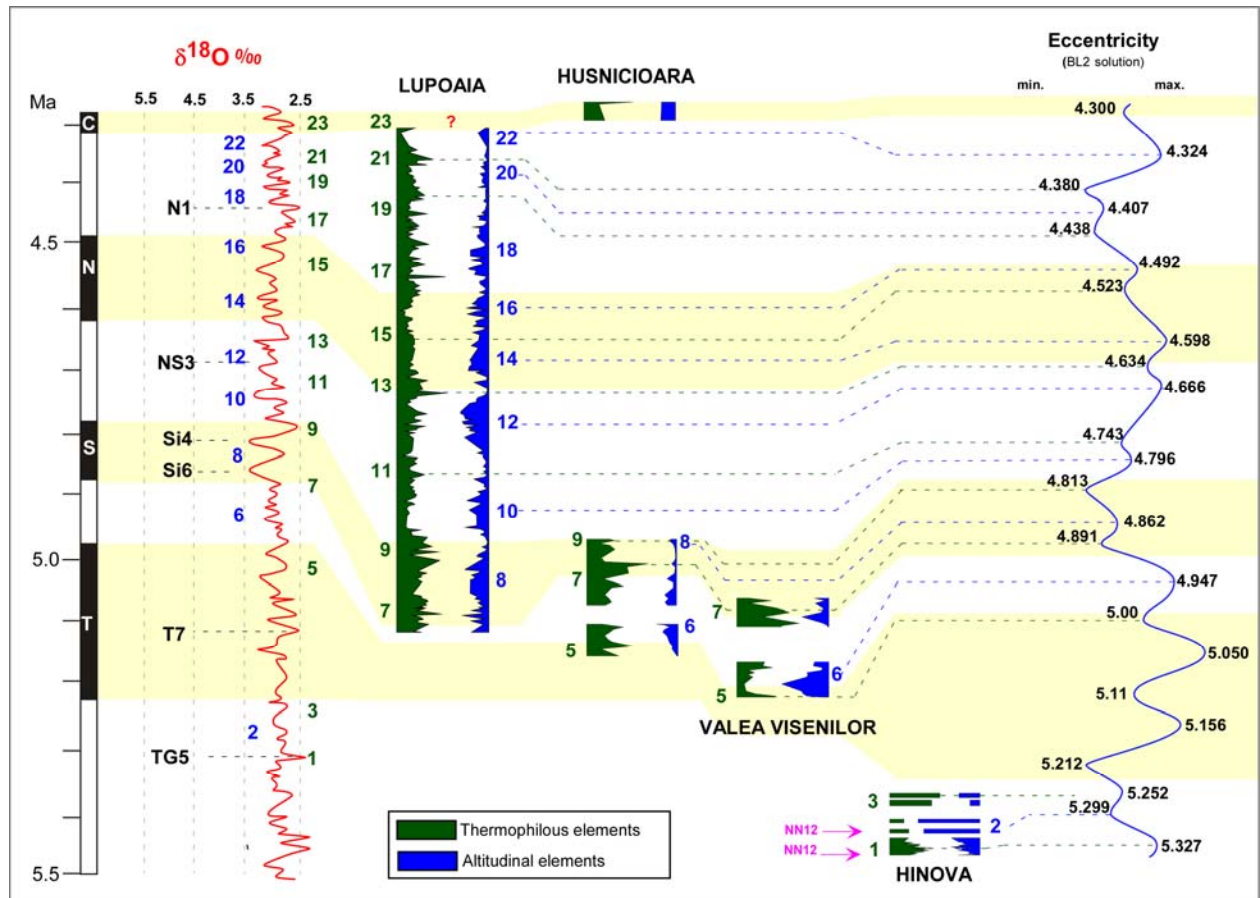


Fig. 5. Climatic relationships and high-resolution chronostratigraphy in the Dacic Basin (Popescu et al., 2006 b).

Similar investigations have been done on the DSDP Site 380A (Leg 42B) located in the Euxinic Basin (i.e. the Black Sea). Its pollen flora (Popescu, 2006) is mainly dominated by Taxodiaceae, deciduous *Quercus*, Cupressaceae, *Cathaya*, *Zelkova*, *Ulmus*, *Alnus*, *Juglans* cf. *cathayensis*, *Abies*, *Pinus*, Poaceae, Asteraceae, Cyperaceae, etc. Development of *Artemisia* and Amaranthaceae-Chenopodiaceae is important above 950 m depth. Some tropical (megathermic) elements are still present in the area, such as *Avicennia* (Verbenaceae), *Amanoa* (Euphorbiaceae), *Fothergilla* and *Exbucklandia* (Hamamelidaceae), Sapindaceae, Acanthaceae. They disappeared at 14 Ma (Serravallian) from the Northwestern Mediterranean region (Suc, 1986, 1996), at 5.6 Ma (Messinian) from the Southern Mediterranean region (Suc and Bessais, 1990; Bachiri Taoufiq et al., 2000).

The Early Pliocene pollen assemblages have been accurately correlated with the major global climatic phases (Suc and Zagwijn, 1983). Such high-resolution pollen records well-correlated with the reference $\delta^{18}\text{O}$ curves, eccentricity and precession curves allow, for the first time, to obtain high-resolution correlations at the European size (Fig. 6).

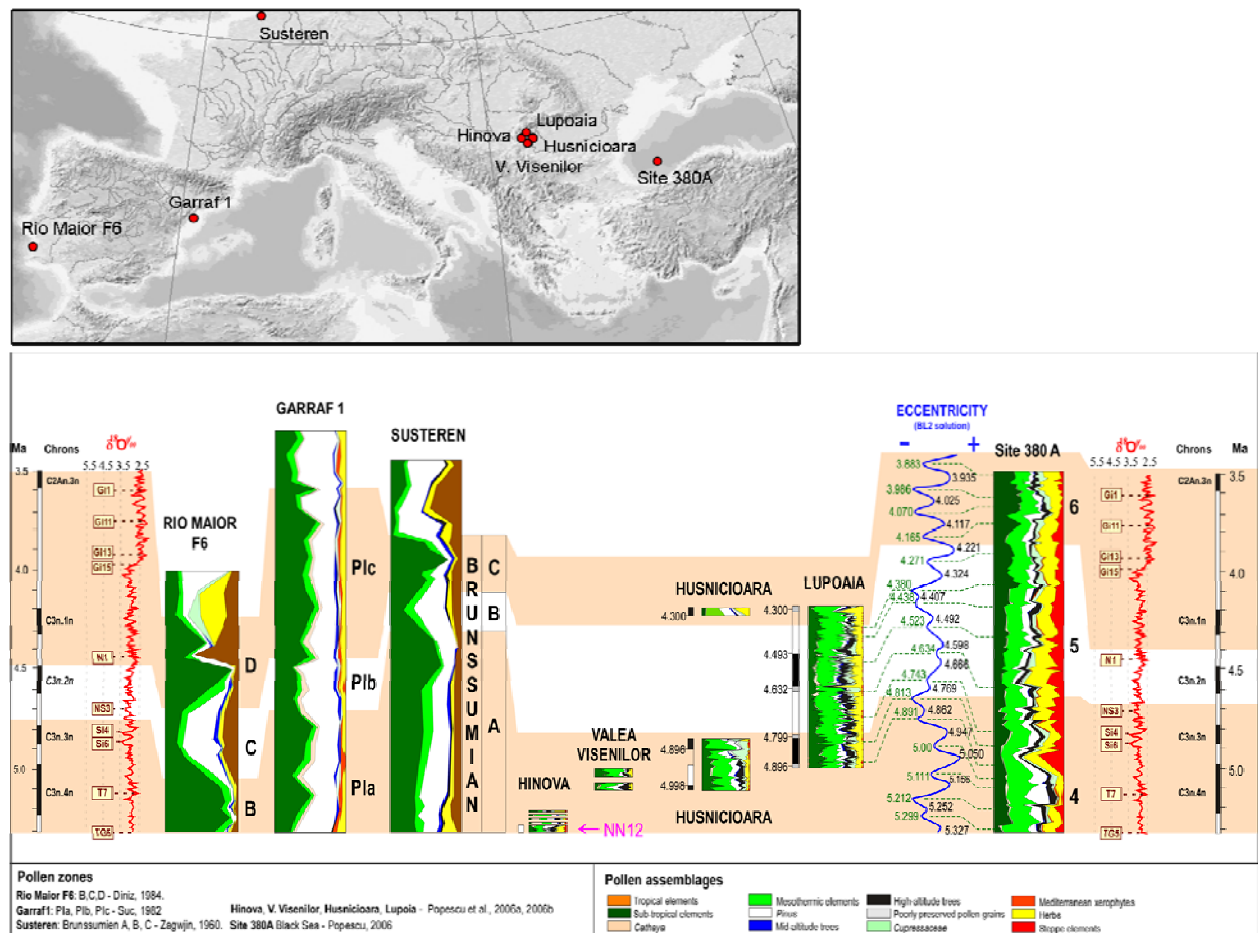


Fig. 6. Early Pliocene European climatostratigraphic relationships (in orange, warm phases; in white, cooler phases)

In addition, pollen floras from the European Early Pliocene allow a refined geographic specification of the different kinds of reconstructed vegetation (Fig. 7). The Northern Mediterranean area is characterized by dominance of arboreal pollen, suggesting a dense forest cover, on contrary to the Southern Mediterranean where herbs were prevalent, signifying a widespread development of open vegetation. Such a contrast in landscape between the North and the South of the Mediterranean is to be related to the latitudinal gradient in humidity. In the North Mediterranean area, the vegetation organization was also closely linked to the relief.

Coastal plains were inhabited by Taxodiaceae swamps (*Glyptostrobus*, *Taxodium*) replaced in some places by marshes (herbs and shrubs). With respect to the geographic position, several plant ecosystems can be distinguished: (1) "salt marshes" along the Atlantic coastline (zone A) as documented at Rio Maior (Diniz, 1984), La Londe (Clet-Pellerin, 1985) and in Northwestern Europe at Susteren (Zagwijn, 1960) and Olenworth (Menke, 1975); (2) marshes mostly made of Cyperaceae evidenced on the Mediterranean coastline at Garraf 1 (Suc and Cravatte, 1982), Stirone (Bertini, 1994) and Maccarone (Bertini, 1992), and within the Dacic Basin at Lupoia (Popescu, 2001, Popescu et al., 2006a; 2006b), Ticleni (Drivaliari et al., 1999) and the Euxinian Basin as shown at Site 380 (Popescu, 2006). Such juxtaposed assemblages resemble the modern vegetation of the Mississippi Delta and Florida (Munaut, 1976). Peculiar vegetation assemblages characterize the Mediterranean coastal plains. In the southeastern Mediterranean region (Zone B: Southwestern Europe, Tunisia, Sicily,

Crete, Egypt and Israel), the open vegetation was composed by herbs (Asteraceae, Poaceae, *Convolvulus*, *Geranium*, etc.) including subdesertic elements such as *Nitraria*, *Neurada*, *Calligonum* and *Lygeum*. Mediterranean xerophytes are only numerically represented in the area of Tarragona and Sicily, their assemblage resemble the modern thermo-mediterranean formation composed mainly by *Olea*, *Pistacia*, *Ceratonia*, *Ziziphus*, etc. (Suc *et al.*, 1995a, 1995b). Close to the mountains (Zone C) vegetation is organized according to an altitudinal gradient. The low altitude vegetation was composed by Taxodiaceae (*Sequoia* humidity) as observed at Saint-Martin du Var (Zheng et Cravatte, 1986, Zheng, 1990) while *Cathaya* and *Cedrus* dominated the mid-altitude belt. *Abies* and *Picea* developed in higher altitude.

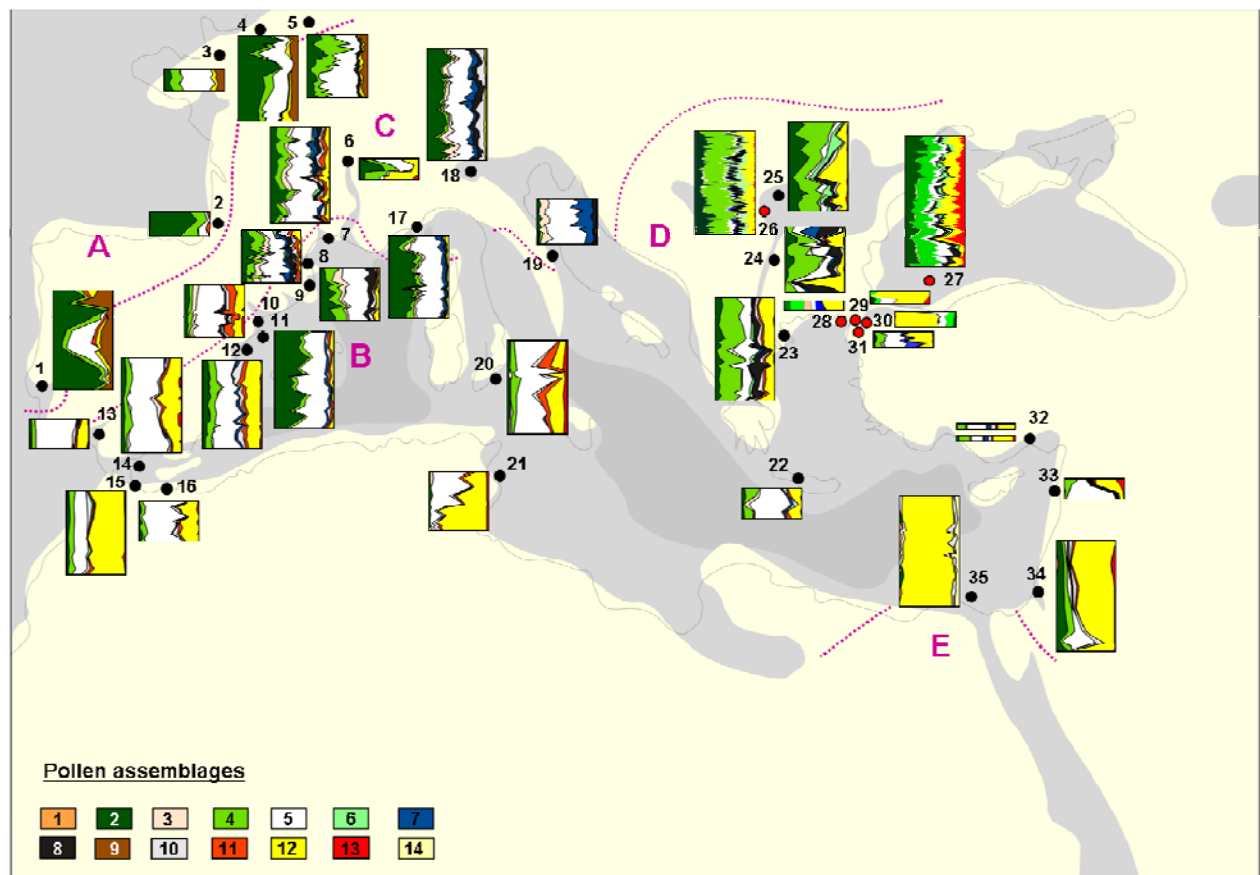


Fig. 7. Lower Pliocene pollen records: 1, Rio-Maior F1 (Diniz, 1984); 2, Arjuzanx (Suc *et al.*, 1986); 3, La Londe (Clet-Pellerin, 1983); 4, Susteren 752.72 (Zagwijn, 1960), 5, Oldensworth (Menke, 1975); 6, Beaune (Méon *et al.*, 1990); 7, Pierrefeu 1 (Suc, 1989); 8, Cap d'Agde 1 (Suc, 1989); 9, Canet 1 (Cravatte *et al.*, 1984); 10, Papiol (Suc and Cravatte, 1982); 11, Garraf 1 (Suc and Cravatte, 1982); 12, Tarragona E1 (Bessais and Cravatte, 1988); 13, Carmona (Suc *et al.*, 1999); 14, Andalucia G1 (Suc *et al.*, 1999); 15, Nador 1 (Suc *et al.*, 1999); 16, Habibas 1 (Suc, 1989); 17, Saint-Martin du Var (Zheng et Cravatte, 1986); 18, Stirone (Bertini, 1994); 19, Maccarone (Bertini, 1994); 20, Capo Rossello (Suc et Bessais, 1990); 21, Oued et Tellil (Suc *et al.*, 1995a); 22, Aghios Vlassios (Drivaliari, 1993); 23, Nestos 2 (Drivaliari, 1993); 24, Ravno Pole S1 (Drivaliari, 1993); 25, Ticleni (Drivaliari *et al.*, 1999); 26, Lupoia (Popescu, 2001); 27, DSDP Site 380A (Popescu, 2006); 28, Enez; 29, Behramli; 30, Eceabat; 31, Intepe (Blitekin, unpublished); 32, 33, Lataquie (Suc, unpublished); 34, Gan Yavne 5 (Drivaliari, 1993); 35, Naf 2 (Drivaliari, 1993). **Pollen assemblages:** 1, tropical evergreen elements; 2, subtropical elements; 3, *Cathaya*; 4, warm-temperate elements; 5, *Pinus* and Pinaceae poorly preserved pollen grains; 6, Cyperaceae; 7, mid-altitude conifers; 8, high-altitude conifers; 9, Ericaceae; 10, paleo-ecologically non significant elements; 11, mediterranean xerophytes; 12, herbs; 13, steppe elements; 14, subdesertic elements.

The Eastern Europe vegetation (zone D) was characterized by coexistent warm-temperate forests (composed by deciduous *Quercus*, *Carya*, *Pterocarya*, *Liquidambar*, *Parrotia persica*, *Carpinus*, *Ulmus*, *Zelkova*, *Celtis*, *Ostrya*, *Platanus*, Juglans, *Juglans* cf. *cathayensis*, *Nyssa*, *Sciadopitys*, *Buxus sempervirens* type, *Acer*, *Tilia*, *Fagus*, *Alnus*, *Salix*, *Populus*, Ericaceae, *Vitis*, *Hedera*, *Lonicera*, *Fraxinus*, *Ligustrum*, *Sambucus*, *Viburnum*, *Rhus*, *Ilex*, *Tamarix*, *Betula*) and open ecosystems (represented by Cyperaceae, Poaceae, Asteraceae, *Plantago*, Brassicaceae, Apiaceae, *Polygonum*, *Rumex*, Amaranthaceae-Chenopodiaceae, Caryophyllaceae, *Linum*, *Erodium*, *Convolvulus*, *Mercurialis*, *Euphorbia*, *Scabiosa*, *Knautia*, Malvaceae, Borraginaceae, *Helianthemum*, *Asphodelus*, Liliaceae, Cannabaceae, Fabaceae, Plumbaginaceae, *Butomus*, *Potamogeton*, Restionaceae, *Myriophyllum*, *Typha*, *Sparganium*, *Thalictrum*, *Nuphar*, *Nymphaea*, Oenotheraceae, *Trapa* and *Utricularia*). Some megathermic elements (Amanoa, Mimosaceae including *Entada* and *Pachysandra* types, Meliaceae, Sapindaceae, Loranthaceae, Arecaceae, Sapotaceae, Tiliaceae) and mega-mesothermic elements (mainly Taxodiaceae, *Engelhardia*, *Cephalanthus*, *Distylium*, *Parrotiopsis jacquemontiana*, *Microtropis fallax*, Cyrillaceae- Clethraceae, *Leea*, *Myrica*, *Nyssa sinensis*, *Parthenocissus henryana*, *Ilex floribunda* type, Anacardiaceae, Araliaceae, *Magnolia*) were persisting (Popescu, 2001; 2006; Popescu et al., 2006a, 2006b). Mediterranean xerophytes were identified in few amounts in the Dacic and Euxinian basins, showing a slight increase according to the latitudinal gradient. Site 380A provides relatively high percentages of *Artemisia* growing in Anatolia, which increased again during the cooler periods. Anatolia probably represents the origin of the repeated steppe expansions which occurred in Europe at each glacial phase. Finally, the Nile region (zone E) documents the presence of savannah (composed mainly by Poaceae and Cyperaceae) including some subdesertic taxa. Nile riparian forests preserved several tropical-subtropical elements (Suc et al.

1.3.3. Vegetation changes in Europe during the Middle- Late Pliocene

On the basis of the climatostratigraphic relationships already established for the Early Pliocene at the European size (Fig. 6), developed in identifying long-distance parallel trends in the evolution of each regional vegetation, it is possible to reproduce the method for the Mid-Pliocene as new pollen records are now available (Wolka Ligezawska in Poland: Winter, unpublished; DSDP Site 380 from the southwestern Black Sea: Popescu et al., in progress) (Fig. 8).

The change in vegetation recorded at the earliest Mid-Pliocene in the five pollen localities is intense and fast, generally characterized by the strong decrease in thermophilous trees counterbalanced by strengthening of herbs (including a few steppe elements) in the Mediterranean region *s.l.* (Garraf 1, Site 380), development of Ericaceae (moors) with herbs on the oceanic side (Susteren, Rio Maior where Cupressaceae also become more important), expansion of cool-temperate (meso-microtherm) trees such as *Betula*, *Fagus* and *Tsuga* northward (Poland). Then, secondary fluctuations are recorded in agreement with the definition of the Reuverian period by Zagwijn (1960): a first complete cyclic succession where coolings prevailed (Reuverian a), a second complete cyclic succession where warmings dominated (Reuverian b), at last a short cooling which marked the transition with the earliest glacial and the onset of Northern Hemisphere glacial-interglacial cycles (Reuverian c) at 2.588 Ma. The forest component of the vegetation recovered a few thermophilous trees at each warming.

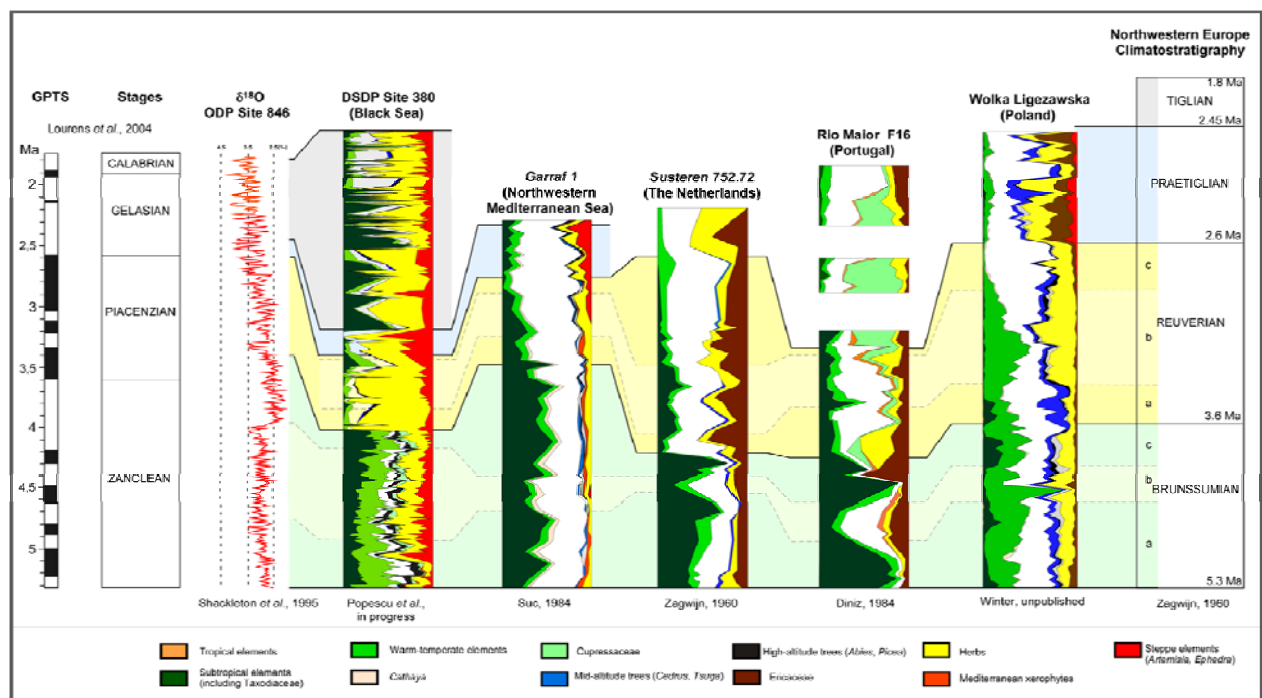


Fig. 8. Pliocene European climatostratigraphic relationships

These relationships show that the climatic subdivision proposed by Zagwijn (1960) already correlated to the Northwestern Mediterranean (Suc and Zagwijn, 1983) have a wide significance. However, southward the latitude of Barcelona, the pollen signal does not show any significant information in terms of vegetation changes and, as a consequence, of climate changes, as herbs monotonously predominated. Some minor changes may have occurred in the South Mediterranean latitudes but they have probably been obscured because of the inability to overall identify herbaceous pollen grains at a finer systematic level than the family.

The time-interval 3.4-2.588 Ma is still too much poorly-documented and needs more attention as it represents the key-moment of the progressive transition from the “greenhouse” climatic context to the “icehouse” one (see also simulations done by Li *et al.*, 1998). Finally, this is also a crucial time-window because it includes the warmth centered at around 3.1 Ma which is generally pointed out as the best past analogue of the present-day warming up (Dowsett and Poore, 1991; Dowsett *et al.*, 1992; Cronin and Dowsett, 1993; Robinson *et al.*, 2008). During this time-interval, contrast in vegetation between North and South European regions exaggerated while the thermic latitudinal gradient increased up to approximately the present-day value ($0.6^{\circ}\text{C}/^{\circ}$ in latitude) (Fauquette *et al.*, 2007).

The Late Pliocene was built up as a chronostratigraphic entity because the global climate evolution is characterized by the appearance of glacial-interglacial cycles at 2.558 Ma, and more precisely by the appearance of glacials in the Northern Hemisphere. The discovery of glacial events in the Northern Hemisphere is due to pollen researches in The Netherlands (Zagwijn, 1960), then correlated with the Mediterranean realm (Suc and Zagwijn, 1983). In the North as well as in the South of Europe, the earliest glacial event has been defined by Suc and Zagwijn (1983) as the first time when pollen diagram is largely dominated by an assemblage of open

vegetation which looks like that of the Last Glacial (tundra-like assemblage in the North with abundant Poaceae, Cyperaceae and Ericaceae; *Artemisia* steppe like assemblage in the South with *Ephedra*) (Fig. 8). This evidence was later validated in the global ocean using oxygen isotope, first by isolated and incomplete data (Shackleton and Opdyke, 1977; Blanc *et al.*, 1983), then by several long and continuously high-resolution records (see among others: Ruddiman *et al.*, 1986; Raymo *et al.*, 1989; Tiedemann *et al.*, 1994; Shackleton *et al.*, 1995) progressively more and more precisely correlated to astronomical parameters.

Today, the palynological definition of the earliest glacial in the Northern Hemisphere must be moderated because (1) highly prevalent open vegetation was documented in the pollen records (but with very low percentage in *Artemisia*) in the Southern Mediterranean since at least the Late Miocene (Suc *et al.*, 1995a, b; Fauquette *et al.*, 2006), (2) relatively large amount of *Artemisia* pollen (significative of *Artemisia* steppe in Anatolia) were found in the Early Pliocene at Site 380 (Popescu, 2006) that I considered in this paper as the putative origin of the *Artemisia* steppe which invaded South Europe during glacials (see Suc and Zagwijn, 1983). Accordingly, the palynological definition of the earliest glacial should be readjusted in adding the notion of “very low representation of the thermophilous (i.e. subtropical and war-temperate) arboreal elements” as it is shown in Figure 8, taking into account the general large over-representation of this vegetation component (see Favre *et al.*, 2008).

The early Northern Hemisphere climatic (i.e. glacial-interglacial) cycles have been referred to obliquity cycles (Ruddiman *et al.*, 1986) while (1) their report by $\delta^{18}\text{O}$ and pollen records was robustly correlated by Combourieu-Nebout and Vergnaud Grazzini (1991), and (2) their status as actual glacial-interglacial cycles according to vegetation dynamics was established by Combourieu-Nebout (1993).

Such 41 kyrs cyclicities are obvious when considering pollen diagrams with a high-chronological resolution such as Site 380 presented in Figure 8 (Popescu *et al.*, in progress). The complete review of Late Pliocene pollen sites was done for Southern Europe in the paper **Suc and Popescu (2005)** which proposes accurate relationships with the reference $\delta^{18}\text{O}$ curves and discusses the variability in vegetation responses according to latitude, longitude and altitude.

Les flores du bassin lacustre de Rubielos de Mora. Nouvelles données sur les conditions climatiques au Miocène inférieur dans la région de Teruel (Espagne)

The flora of the Rubielos de Mora lacustrine basin: climatic conditions during the Lower Miocene in the Teruel region (Spain)

Paul Roiron^a, Javier Ferrer^b, Eladio Liñan^b, Cristóbal Rubio^b, José-Bienvenido Diez^c, Speranta Popescu^d, Jean-Pierre Suc^e

^a Upresa 5059, Institut de botanique, 163, rue A.-Broussonet, 34090 Montpellier, France

^b Area de Paleontología, Departamento de Ciencias de la Tierra, Universidad de Zaragoza, 50009 Zaragoza, Espagne

^c Universidade de Evora, Apartado 94, 7001 Evora codex, Portugal

^d UFR des sciences de la Terre, université Lyon-1, 27-43, bd du 11-Novembre-1918, 69622 Villeurbanne cedex, France

^e Centre de paléontologie stratigraphique et paléoécologie (ERS 2042 CNRS), université Lyon-1, 27-43, bd du 11-Novembre-1918, 69622 Villeurbanne cedex, France

(Reçu le 23 août 1999, accepté après révision le 8 novembre 1999)

Abstract — The stratigraphic and floristic studies of two sections in the lacustrine deposits of the Miocene basin of Rubielos de Mora increase our knowledge of palaeoenvironmental and palaeoclimatic conditions and specify the biochronology of these sites. The lowlands are inhabited by a swampy, or lacustrine, vegetation (*Botryococcus*, *Sparganium*, *Potamogeton*, Taxodiaceae, *Myrica*, *Nyssa*...), whereas the uplands are covered by a *Zelkova* mesophilous forest with other temperate elements (*Acer*, *Betula*, *Carya*...). The scarcity of thermophilous taxa in this vegetation indicates that the climatic conditions were not the warmest in the Miocene. The rodents faunas of this basin suggest a Ramblian–basal Aragonian age (Lower Miocene). (© 1999 Académie des sciences / Éditions scientifiques et médicales Elsevier SAS.)

stratigraphy / leaf flora / pollen flora / lacustrine basin / palaeoclimate / biochronology / Lower Miocene–Ramblian / Lower Aragonian / Rubielos de Mora (Teruel, Spain)

Résumé — De nouvelles études stratigraphiques et floristiques des sédiments lacustres du bassin miocène de Rubielos de Mora permettent de caractériser le paléoenvironnement et le paléoclimat et de préciser la biochronologie des sites. Un milieu palustre, riche en plantes aquatiques et en Taxodiacées, occupait les dépressions, tandis que les zones exondées étaient couvertes d'une forêt mésophile dominée par *Zelkova* avec d'autres éléments tempérés (*Acer*, *Betula*, *Carya*...). La faible présence de taxons thermophiles montre que cette végétation ne correspond pas à la phase la plus chaude du Miocène. Les faunes de rongeurs de sites associés indiquent un âge Ramblien–Aragonien basal (Miocène inférieur). (© 1999 Académie des sciences / Éditions scientifiques et médicales Elsevier SAS.)

stratigraphie / feuilles / pollen / bassin lacustre / paléoclimat / biochronologie / Miocène inférieur / Ramblien / Aragonien inférieur / Rubielos de Mora (Teruel, Espagne)

Note présentée par Édouard Boureau.

* Correspondance et tirés à part.
roiron@crit.univ-montp2.fr

Abridged version

The continental Miocene sediments of Rubielos de Mora are known for their rich fauna (rodents and other mammalians, amphibians, crustaceans, insects, arachnida...) and flora (De Bruijn and Moltzer, 1974; Martínez-Delclòs et al., 1991; Montoya et al., 1996).

The in-filling of the 'Cuenca de Rubielos de Mora' is formed by Lower–Middle Miocene deposits. This basin, elongated in the ENE–WSW direction, with an altitude of 950–1 000 m, is limited and crossed by NW–SE and NE–SW normal faults, giving the region a mosaic aspect (Godoy et al., 1986). Therefore, the correlation between the different fossil localities is difficult to achieve and the floristic remains of each of them should be studied separately.

The subject of this paper is the stratigraphic and floristic study of two sites, Barranco de Alto Ballester and Río Estrecho, the latter being totally new (*figure 1*).

Stratigraphy

The Miocene lacustrine basin of Rubielos de Mora is divided into three sedimentary units (A, B, C, *figure 2*), the upper being the most fossiliferous (Anadón et al., 1988). The lower formation (ca. 300 m) consists of sands with ferruginous nodules and breccic levels. The middle formation (ca. 150 m) is composed of limestone layers with clays or marls intercalations and sometimes lignite beds. The upper formation (more than 300 m) consists of marls and lutites, with occasional limestone or sandy intercalations. Some breccia beds can be discerned in the border facies (Godoy et al., 1986). The sections of Río Estrecho and Barranco de Alto Ballester belong to this unit, which contains most of the flora and fauna remains.

These two sites, whose leaf and pollen floras are studied here, are plotted in the synthetic section (*figure 2*), with the faunal localities RM1 and RM2 (De Bruijn and Moltzer, 1974).

Flora and vegetation

More than 600 samples of leaf remains (and sometimes shoots, fruits or seeds) with preserved organic matter were collected in the two sites. There are no notable differences between the flora from the two sites, even if that of Río Estrecho seems to be less rich (*table 1*).

The identified taxa show a varied macroflora with subtropical (Taxodiaceae, *Comptonia*, *Lomatites*, *Myrica*, *Daphnogene*...) and temperate (*Pinus*, *Alnus*, *Betula*, *Carya*, *Ulmus*, *Zelkova*, *Populus*, *Acer*...) elements. There are also Monocotyledon leaves and one or more aquatic species, characterized by fine tangled filaments (*Potamogeton*?). The marsh (Taxodiaceae, *Myrica*) or riparian (*Alnus*, *Populus*) species should live in or near the lacustrine basin, while the others elements should belong to a deciduous forest on exonded soils and slopes.

The two pollen spectra contain 43 taxa (*table 2*). The swamp (Taxodiaceae, *Myrica*, *Nyssa*, *Cephalanthus*, *Populus*, *Salix*) and aquatic (*Potamogeton*, *Sparganium*, *Botryococcus*) elements are frequent. Other subtropical (Taxodiaceae, *Distylium*, *Engelhardia*, *Platycarya*, Sapotaceae, *Symplocos*) and temperate (*Pinus*, *Acer*, *Carya*, *Nyssa* cf. *aquatica*, *Ulmus*, *Zelkova*, *Quercus*, etc.) taxa are identified.

The pollen and leaf floras are very similar and show the local environment of the sedimentary basin. Few altitudinal (*Abies*, *Cathaya*, *Pinus p. p.*) and xerophytic elements (*Ceratonia*, *Olea*, *Phillyrea*, *Microtropis fallax*, *Artemisia*) are also present in the pollen flora.

Palaeoenvironment and palaeoclimate

The Miocene rodent faunas of the Calatayud–Teruel basin gives evidence of a succession of dry and humid periods during the Ramblian–Aragonian stage, in relation with temperature variations (Daams and Van der Meulen, 1984). In the Rubielos de Mora basin, the fauna of both RM1 and RM2 (*figure 1*) indicate a humid forest environment. Frogs and other batracians remains, as well as rodents of moist biotopes, attest the presence of swamps or lacustrine zones. Nevertheless some open zones should be occupied by Gliridae (De Bruijn and Moltzer, 1974).

The Oligocene flora of Cervera (Bataller and Depape, 1950; Depape and Brice, 1965; Sanz de Siria, 1992) and of Sarreal (Fernández-Marrón, 1973), as well as the Burdigalian floras of the Balearic islands (Arènes and Depape, 1956) and of Martorell (Sanz de Siria, 1981) are still rich in thermophilous taxa (Palmae, Lauraceae, Proteaceae...), indicating warm tropical conditions. In the Lower–Middle Miocene, these megatherm taxa nearly disappear in the Rubielos de Mora basin, which has an altitude close to mountains over 1 300 m high. However, the arboreal Mediterranean xerophytic taxa did not appear as in the Lower Pliocene flora of the area surrounding Barcelona (Almera, 1907; Sanz de Siria, 1983).

The flora of Rubielos characterizes a mesophilous forest vegetation growing under warm to warm-temperate and humid climatic conditions. This is not in contradiction with the dry-season tropical climate of the littoral plains of the northwestern Mediterranean region during the Burdigalian–Langhian (Bessedik, 1985). The mountaneous area of Rubielos de Mora should have been characterized by the existence of greater precipitation and cloudiness than the lowlands.

The pollen flora of Rubielos is close to the Upper Burdigalian floras of Thézan-lès-Béziers and Lospignan II in Languedoc (Bessedik, 1984, 1985). During the Aquitanian and the Burdigalian, the megathermic elements are only weakly represented in the microfloras of the northwestern Mediterranean region, and they become very abundant during the Langhian (Sapotaceae, tropical *Buxus*, Tiliaceae...). The flora of Rubielos takes place in the temperate phase, which characterized the greater part of the Burdigalian of the northwestern Mediterranean region before the Langhian thermic maximum (Bessedik, 1985).

A detailed stratigraphic study of the whole basin is in progress and the comparison of the macroflora with the pollen diagram of the section of Río Estrecho should allow

us to observe the evolution of the vegetation during the course of time.

1. Introduction

Le bassin tertiaire de Rubielos de Mora est bien connu des géologues et des paléontologues, en particulier pour sa richesse en micro- et macromammifères, mais aussi pour sa faune d'Amphibiens, de Crustacés, d'Insectes, d'Arachnides et pour sa flore (De Bruijn et Moltzer, 1974 ; Martínez-Delclòs et al., 1991 ; Montoya et al., 1996).

Le remplissage de la « Cuenca de Rubielos de Mora » est constitué par des dépôts du Miocène inférieur-moyen. Cette cuvette allongée, de direction ENE–WSW, d'altitude moyenne comprise entre 950 et 1 000 m, est limitée et traversée par des failles normales regroupées selon des systèmes de direction NW–SE et NE–SW, qui confèrent à la région un aspect caractéristique de mosaïque de blocs (Godoy et al., 1986). Aussi, les différents gisements apparaissent-ils dispersés et sans continuité verticale, ce qui rend difficile leur corrélation et nécessite des études séparées de chacun des affleurements. Les faunes de mammifères ont permis d'attribuer aux argiles lacustres fossilifères un âge Ramblien–Aragonien inférieur (corrélé au Burdigalien marin : 18 Ma environ).

Une première collection, riche d'environ 300 spécimens récoltés il y a plusieurs années par l'un d'entre nous (J. Ferrer), conservée au laboratoire de paléobotanique de l'université de Saragosse, a été répertoriée et étudiée.

Nous avons d'autre part réalisé de nouveaux échantillonnages de mai 1997 à mai 1999 (récolte d'environ 300 spécimens supplémentaires) dans la coupe de Barranco de Alto Ballester et dans le nouveau site de Río Estrecho (figure 1).

Deux échantillons de sédiment prélevés dans les niveaux à feuilles de Barranco de Alto Ballester et Río Estrecho se sont révélés très riches en pollen. Les résultats palynologiques permettent de comparer les deux approches floristiques.

2. Stratigraphie

Le bassin lacustre miocène de Rubielos de Mora se divise principalement en trois unités sédimentaires (A, B et C), l'unité supérieure (C) étant la plus fossilifère (Anadón et al., 1988) (figure 2). Ces unités sont formées par divers faciès (dépôts fluviaux ou deltaïques, brèches, marnes lacustres). La puissance de ces unités varie, selon que l'on se situe dans la partie orientale (faciès de bordure) ou occidentale (faciès centraux) du bassin.

L'unité inférieure A (environ 300 m) est formée par des sables jaunes, généralement massifs, avec des nodules ferrugineux et des niveaux bréchiques. Dans la zone la plus orientale du bassin, les sables sont plus argileux et de couleur brun-rouge.

L'unité intermédiaire B (environ 150 m) est constituée surtout par des calcaires en strates de faible puissance, par des intercalations d'argiles et de marnes grises, et occasionnellement par des lignites.

L'unité supérieure C (plus de 300 m) est formée principalement par des lutites et des marnes, avec des intercalations sporadiques de calcaires et de sables ou de brèches dans le faciès de bordure (Godoy et al., 1986). C'est dans cette unité que se sont fossilisés des restes de plantes (Hernández-Sampelayo et Cincunegui, 1926 ; Fernández-Marrón et Álvarez-Ramis, 1988 ; Álvarez-Ramis et Fernández-Marrón, 1994 ; Barrón 1997), d'arthropodes (Martínez-Delclòs et al., 1991 ; Peñalver, 1998), de mollusques et de vertébrés amphibiens (Sanchiz, 1977), mammifères (De Bruijn et Moltzer, 1974 ; López Martínez, 1977 ; Montoya et al., 1996) ainsi que des dents de poissons, observées récemment par certains d'entre nous. Les affleurements de Río Estrecho et Barranco de Alto Ballester font partie de cette unité supérieure (figure 2).

La position relative des sites de Río Estrecho et Barranco de Alto Ballester, dont la flore est étudiée dans ce travail, a été indiquée sur la coupe synthétique de la

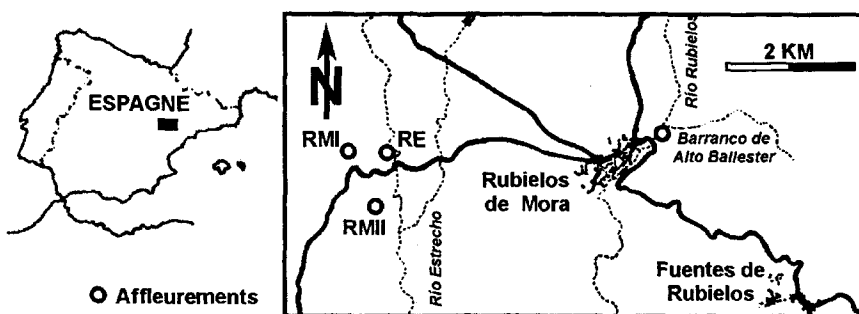


Figure 1. Carte de situation des affleurements de Rubielos de Mora. RE : Río Estrecho ; RMI : Rubielos de Mora I ; RMII : Rubielos de Mora II, Barranco de Alto Ballester.

Location map of the sections of Rubielos de Mora.

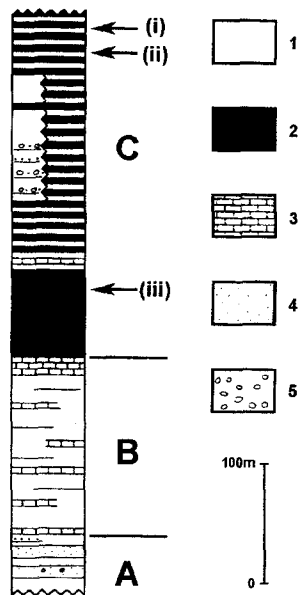


Figure 2. Colonne stratigraphique générale du bassin miocène de Rubielos de Mora, avec la position approximative des gisements (d'après Anadón et al., 1988, modifié). A : unité inférieure ; B : unité intermédiaire ; C : unité supérieure. 1 : lutites massives ; 2 : lutites laminées ; 3 : calcaires ; 4 : sables ; 5 : conglomérat. i) Rubielos de Mora II ; ii) Rubielos de Mora I et Río Estrecho ; iii) Barranco de Alto Ballester.

Schematic stratigraphy of the Miocene basin from Rubielos de Mora with approximate location of the sampling outcrops (after Anadón et al., 1988, amended). A: lower unit; B: middle unit; C: upper unit. 1: thick lutites; 2: laminate lutites; 3: limestone; 4: sands, 5: conglomerates.

figure 2, de même que les gisements à faune appelés traditionnellement RM1 et RM2 (De Bruijn et Moltzer, 1974).

3. Âge

Les faunes de Rubielos de Mora récoltées dans les différents gisements ont été étudiées par divers auteurs qui les ont utilisées comme localités de référence biochronologique (Crusafont-Pairó et al., 1966 ; De Bruijn et Moltzer, 1974 ; Daams, 1976 ; López Martínez, 1977, 1989).

La faune récoltée dans la même unité stratigraphique que la flore de Río Estrecho (RM1) est essentiellement composée d'ossements de grands mammifères et d'oiseaux (Crusafont-Pairó et al., 1966). La présence de restes de Lagomorphes permettrait de corréler cette faune à la zone MN3, correspondant au Ramblen (López Martínez, 1989).

La composition et le degré d'évolution de la faune de rongeurs de Rubielos de Mora 2 (RM2), située stratigraphiquement au-dessus de la localité RM1 (De Bruijn et Moltzer, 1974), la placeraient plutôt dans la zone MN4, à la base de l'Aragonien (Álvarez-Sierra, 1987, López Martínez, 1989).

La présence de dents de *Neocometes* à Rubielos de Mora (RM2), ainsi que dans des sites karstiques du Roussillon (Sud de la France) attribués à la zone MN3, remet en cause l'utilisation de ce genre comme marqueur de la zone MN4 (Aguilar et al., 1997). Ces différents éléments faunistiques semblent concorder pour corréler les niveaux à flore de Río Estrecho avec la zone MN3. L'âge le plus récent de ce dépôt ne pourrait alors excéder la limite MN3/MN4 (Ramblen supérieur-Aragonien inférieur).

4. Flore et végétation

Ce travail fait suite aux études préliminaires de la flore fossile du bassin de Rubielos de Mora. Les premiers travaux concernant la comparaison entre les macrorestes et les pollens avaient montré la présence de Taxodiaceae, Pinaceae, Myricaceae, ainsi que de quelques genres de ligneux caducifoliés, comme *Betula*, *Zelkova*, *Populus*, *Salix*, *Carya*, *Acer...* (Fernández-Marrón et Álvarez-Ramis, 1988 ; Álvarez-Ramis et Fernández-Marrón, 1994).

D'autres sites de ce même bassin (Barranco Casas, Aguarroya, Alto de la Venta, Río Rubielos et Porpol) ont été échantillonnés et ont fait l'objet d'une étude préliminaire des flores foliaire et pollinique (Barrón, 1997). Parmi les pollens, dont les comptages ne sont pas indiqués, les genres *Pinus*, *Carya* et *Ulmus-Zelkova* seraient les plus fréquents. Outre la végétation marécageuse ou lacustre (*Potamogeton*, Sparganiaceae-Typhaceae, *Myrica*) et la forêt caducifoliée avoisinante (Juglandaceae, Ulmaceae, Aceraceae), les autres taxons traduiraient une végétation subtropicale à tempérée-chaude, adaptée à une période sèche (Ephedraceae, Ericaceae, Rosaceae, Buxaceae, Poaceae).

4.1. La flore foliaire

Les nombreux échantillons que nous avons récoltés ont été fossilisés dans un sédiment généralement argileux et laminé. La plupart des spécimens sont sous forme de compressions (avec matière organique), mais l'état de conservation n'est pas toujours excellent. Certains ont été vernis et photographiés ou dessinés avec un stéréomicroscope.

Les spécimens les mieux conservés ont été décrits, puis identifiés, par comparaison avec les feuilles d'autres taxons néogènes et actuels. Il n'y a pas de différence fondamentale entre les flores des deux sites, même si celle de Río Estrecho paraît moins riche pour l'instant (tableau 1).

Les taxons identifiés témoignent d'une macroflore diversifiée qui contient à la fois des éléments subtropicaux (Taxodiaceae, *Comptonia*, *Lomatites*, *Myrica*, *Daphnogene...*) et des éléments tempérés (*Pinus*, *Alnus*, *Betula*, *Carya*, *Ulmus*, *Zelkova*, *Populus*, *Acer...*). On peut noter aussi la présence de feuilles de Monocotylédones (Poa-

Tableau I. Macroflore de Barranco de Alto Ballester et Río Estrecho.

Macroflora of Barranco de Alto Ballester and Río Estrecho.

Taxons	Barranco de Alto Ballester	Río Estrecho
<i>Glyptostrobus europaeus</i>	*	*
<i>Sequoia langsdorfii</i>	*	
<i>Taxodium dubium</i>	*	
<i>Thuja</i> sp.	*	*
<i>Calocedrus</i> aff. <i>decurrens</i>	*	*
<i>Pinus</i> sp.	*	*
cf. <i>Daphnogene</i>	*	
<i>Ulmus</i> cf. <i>campestris</i>	*	
<i>Zelkova zelkovifolia</i>	*	*
<i>Comptonia oeningensis</i>	*	
<i>Myrica lignitum</i>	*	*
<i>Betula insignis</i>	*	
<i>Alnus julianaeformis</i>	*	
<i>Carya minor</i>	*	*
<i>Sorbus</i> cf. <i>aucuparia</i>	*	
<i>Populus</i> cf. <i>tremula</i>	*	*
<i>Lomatites aquensis</i>	*	
cf. <i>Quercus rhenana</i>	*	
<i>Acer</i> sp. aff. <i>A. heldreichii</i>	*	*
<i>Acer tricuspidatum</i>	*	*
Apiaceae		*
cf. <i>Potamogeton</i>	*	*
Graminae ou Cyperaceae	*	*

ceae ou Cyperaceae) et d'une ou plusieurs espèces aquatiques, sous la forme de fins filaments enchevêtrés (*Potamogeton* ?).

4.2. La flore pollinique

La flore pollinique obtenue sur deux échantillons compte 43 taxons (tableau II), les concentrations sont élevées (8 175 grains de pollen par gramme pour l'échantillon RE et 44 662 grains de pollen par gramme pour l'échantillon de Barranco de Alto Ballester). Les éléments palustres (*Taxodiaceae*, *Myrica*, *Nyssa*, *Cephalanthus*, *Populus*, *Salix*) et aquatiques (*Potamogeton*, *Sparganium*, colonies algaires de *Botryococcus*) sont fréquents. Une forêt caducifoliée devait occuper les terrains moins humides, elle devait être riche en Juglandaceae (*Carya*, *Engelhardia* et *Platycarya*) et Ulmaceae (*Ulmus* et *Zelkova*). Les taxons subtropicaux (*Taxodiaceae*, *Distylium*, *Engelhardia*, *Platycarya*, *Sapotaceae*, *Symplocos*) et tempérés (*Pinus*, *Acer*, *Carya*, *Nyssa* cf. *aquatica*, *Ulmus*, *Zelkova*, *Quercus*, etc.) prédominent. La flore pollinique et la macroflore foliaire sont très similaires et traduisent l'environnement assez immédiat du milieu de sédimentation. La flore pollinique livre, en outre, quelques éléments d'altitude (*Abies*, *Cathaya*, *Pi-*

nus p. p.) et des taxons affectionnant une saison sèche (*Ceratonia*, *Olea*, *Phillyrea*, *Microtropis fallax*, *Artemisia*).

5. Paléoenvironnement et paléoclimatologie

L'utilisation de l'écologie des espèces actuelles analogues pour l'interprétation des flores et des faunes fossiles, permet d'obtenir des informations sur les divers milieux dans lesquels vivaient ces plantes et ces animaux. Par ailleurs, la présence, plus ou moins importante, de groupements végétaux thermophiles, mésophiles ou orophiles, de même que celle de rongeurs de climat chaud, tempéré ou frais dans les sites de Rubielos de Mora, donne une idée du climat qui régnait sur la région au moment du dépôt. Des précisions chronologiques peuvent être apportées par la composition ou le degré d'évolution des faunes de rongeurs et par la comparaison avec les courbes des variations de températures et d'humidité du Miocène inférieur et moyen dans le bassin de Calatayud-Teruel (Daams et van der Meulen, 1984 ; Daams et al., 1988 ; Van der Meulen et Daams, 1992 ; Calvo et al., 1993 ; Krijgsman et al., 1994 ; Daams et al., 1999).

5.1. Les faunes

Une étude portant sur de nombreuses faunes de rongeurs miocènes du bassin de Calatayud-Teruel (Daams et Van der Meulen, 1984) a permis de mettre en évidence une succession de périodes sèches et humides au cours du Ramblien et de l'Aragonien, en relation avec une courbe des variations de températures. Dans le bassin de Rubielos, plusieurs gisements à grands mammifères et à rongeurs ont été étudiés (Crusafont-Pairó et al., 1966 ; De Bruijn et Moltzer, 1974 ; López Martínez, 1977 ; Montoya et al., 1996). Bien que non stratigraphiquement corrélables, car situés de part et d'autre d'une faille, les sites RM1 et RM2 (figure 1) contiennent des faunes pratiquement semblables du point de vue paléoclimatologique. Le site de RM2, situé stratigraphiquement au moins 40 m au-dessus de RM1, a livré une faune de rongeurs caractérisant un milieu forestier humide. De nombreux restes de batraciens et de rongeurs de lieux humides confirment la présence de biotopes marécageux et lacustres avec, cependant, des zones plus ouvertes, occupées par les Gliridés (De Bruijn et Moltzer, 1974).

5.2. Les flores

Les flores oligocènes de Cervera (Bataller et Depape, 1950 ; Depape et Brice, 1965 ; Sanz de Siria, 1992) et de Sarreal (Fernández-Marrón, 1973), ainsi que les flores burdigaliennes des îles Baléares (Arènes et Depape, 1956) et de Martorell (Sanz de Siria, 1981), sont encore riches en espèces thermophiles (Palmae, Lauraceae, Pro-

Tableau II. Microflore de Barranco de Alto Ballester et Río Estrecho.

Microflora of Barranco de Alto Ballester and Río Estrecho.

	Barranco de Alto Ballester		Río Estrecho	
	Nombre	%	Nombre	%
<i>Abies</i>			1	0,21
Cupressaceae	2	0,6	4	0,86
<i>Cathaya</i>	3	0,91		
<i>Pinus</i> type <i>diplostellé</i>	50	15,24	139	29,89
<i>Pinus</i> type <i>haploxylon</i>			1	0,21
Taxodiaceae type 1	149	45,42	128	27,52
Taxodiaceae type 2 (grosses verrues) (<i>Cryptomeria</i> ?)	24	7,31	6	1,29
<i>Acer</i>			5	1,07
<i>Ilex</i>	2	0,6		
Araliaceae (non <i>Hedera</i>)			2	0,43
Arecaceae			1	0,21
<i>Ceratonia</i>	1	0,3		
<i>Sambucus</i>	1	0,3		
<i>Microtropis fallax</i>	1	0,3		
Caesalpiniaceae ?			1	0,21
<i>Distylium</i>			2	0,43
Ericaceae			1	0,21
Euphorbiaceae type <i>Ricinus</i>	1	0,3	1	0,21
type <i>Castanea-Castanopsis</i>	1	0,3		
<i>Quercus</i> décidus	5	1,52	6	1,29
<i>Carya</i>	4	1,21	22	4,73
<i>Engelhardia</i>	5	1,52	15	3,22
<i>Platycarya</i>	3	0,91	11	2,36
<i>Myrica</i>	4	1,21	6	1,29
<i>Nyssa</i> cf. <i>aquatica</i>	9	2,74	4	0,86
<i>Nyssa</i> cf. <i>sinensis</i>	1	0,3		
<i>Olea</i>	9	2,74	10	2,15
<i>Phillyrea</i>			1	0,21
Cephalanthus (<i>Rubiaceae</i>)			3	0,64
<i>Populus</i>	1	0,3	4	0,86
<i>Salix</i>	1	0,3	1	0,21
Sapotaceae	1	0,3	2	0,43
<i>Symplocos</i>			4	0,86
<i>Ulmus</i>	5	1,52	15	3,22
<i>Zelkova</i>	3	0,91	20	4,3
Apiaceae	1	0,3		
<i>Artemisia</i>	1	0,3		
<i>Centaurea</i>			1	0,21
Poaceae	5	1,52	10	2,15
<i>Potamogeton</i>	1	0,3	4	0,86
Rosaceae	1	0,3		
<i>Sparganium</i>			2	0,43
Grains indéterminés	6	1,82	5	1,07
Grains indéterminables	27	8,23	27	5,8
Nombre total de grains de pollen	328		465	
Spores monolètes	1	0,29		
Spores trilètes	3	0,87	3	0,63
Autres spores de Ptéridophytes	10	2,9	8	1,68
Spores de Bryophytes	2	0,58		
Nombre total de grains de pollen et de spores	344		476	
Colonies de <i>Botryococcus</i>	13		87	

teaceae...) et traduisent un climat tropical à subtropical. Au Miocène inférieur-moyen, ces taxons mégathermes ont pratiquement disparu du bassin de Rubielos de Mora qui, contrairement aux sites précédents, se trouve dans une région montagneuse, entouré par des sommets dépassant 1 300 m.

On ne voit pas pour autant apparaître dans la macroflore de Rubielos des espèces typiquement méditerranéennes, comme dans la flore du Pliocène inférieur des environs de Barcelone (Almera, 1907 ; Sanz de Siria, 1983). Cette flore ne devait donc pas vivre sous un climat sec. Elle caractérise une végétation forestière méso-

phile, se développant sous un climat chaud à tempéré-chaud et humide. Les espèces palustres (Taxodiaceae, *Myrica*) ou de ripisylve (*Alnus*, *Populus*) devaient vivre aux abords du bassin lacustre, tandis que les autres formaient une forêt caducifoliée ou mixte sur les sols exondés et sur les versants. Les espèces les plus xériques devaient se trouver dans des zones plus ouvertes et bien exposées. On peut noter, cependant, l'absence de la chênaie caducifoliée, comme dans la flore miocène de Buñol, qui ne contient pas non plus de *Zelkova* (Álvarez Ramis et Doubinger, 1981).

Si l'on se réfère aux travaux palynologiques de Bessedik (1984 et 1985) en Languedoc et Provence, il est évident que la flore pollinique obtenue à Rubielos de Mora se rapproche de celles de Thézan-lès-Béziers et de Lespignan II, qui datent du Burdigalien supérieur, à la différence près des conditions édaphiques. Ces microflores, comme celles de l'Aquitainien et du début du Burdigalien, comptent en petit nombre seulement les éléments tropicaux qui seront très abondants au Langhien (Sapotaceae, *Buxus* tropicaux, Tiliaceae, etc.) (Bessedik, 1985 ; Bessedik et Cabrera, 1985). Ces éléments méga-thermes étaient toutefois un peu plus fréquents au début de l'Aquitainien dans des conditions sèches (Bessedik, 1984, 1985). Sur la base de cette comparaison avec les flores polliniques, il est difficile de situer la flore de Rubielos de Mora dans une phase à tendance sèche, d'autant plus que le contexte local traduit des conditions très humides. Cela n'est pas en contradiction avec l'affir-

mation d'un climat tropical à saison sèche marquée au Burdigalien-Langhien (Bessedik, 1985). La région montagneuse de Rubielos devait être mieux arrosée que les basses plaines littorales, avec une nébulosité atmosphérique plus importante. En revanche, il est possible d'affirmer que ce site se place dans la phase tempérée qui caractérisait l'essentiel du Burdigalien nord-ouest méditerranéen avant le maximum thermique du Miocène qui se situe au Langhien (Bessedik, 1985).

6. Conclusion

Les données floristiques concernant le Miocène inférieur en Espagne sont rares. L'étude des restes végétaux de l'unité supérieure du bassin de Rubielos de Mora vient combler en partie cette lacune. Elle met en évidence une végétation palustre ou de ripisylve, ainsi qu'une forêt mésophile traduisant un climat chaud à tempéré chaud et humide. Ces résultats s'accordent avec ceux des faunes. Une étude stratigraphique détaillée de l'ensemble du bassin est en cours. Les difficultés proviennent des différences de sédimentation entre la partie centrale et les zones de bordure, ainsi que des nombreuses failles qui compartimentent ce bassin. La réalisation d'une étude pollinique de l'ensemble de la coupe de Rio Estrecho et la comparaison avec la macroflore devraient permettre d'observer les variations de la végétation au cours du temps.

Remerciements. Les auteurs remercient particulièrement E. Badal, L. Fabre et J.-F. Terral pour leur aide sur le terrain, ainsi que J.-P. Aguilar pour de fructueuses discussions sur les faunes de rongeurs. Ils remercient également la Fundación Conjunto Paleontológico de Teruel pour le financement partiel de ce travail.

7. Références

- Aguilar J.-P., Escarguel G. et Michaux J. 1997. Biochronologie du Miocène inférieur et moyen du Sud de la France à partir des faunes karstiques. Le problème du genre *Neocometes*, in : *Actes du Congrès Biochrom'97*, Mém. Trav. EPHE, Inst. Montpellier, 21, 575-579
- Almera D.J. 1907. Descripción de los terrenos pliocenicos de la cuenca del Bajo Llobregat y llano de Barcelona. III. Flora pliocenica de los alrededores de Barcelona, Mapa geol. prov. Barcelona, 355 p., pl. 19-24
- Álvarez-Ramis C. et Doubinger J. 1981. Sur la paléobotanique du gisement miocène de Buñol (Valencia, Espagne), *Bol. R. Soc. Española Hist. nat. (Geol.)*, 79, 173-179
- Álvarez-Ramis, C. et Fernández-Marrón T. 1994. Conexiones establecidas entre los palinomorfos y los macrorestos vegetales del Mioceno medio de Rubielos de Mora (Teruel), in : *VIII Simposio de Palinología (APLE)*, Irene La-Serna edit., Tenerife, 323-331
- Álvarez Sierra M.A. 1987. Estudio sistemático y bioestratigráfico de los Eomyidae (Rodentia) del Oligoceno superior y Mioceno inferior español, *Scripta Geol.*, Leiden, 86, 1-207
- Anadón P., Cabrera, L. et Julià R. 1988. Anoxic-oxic cyclical lacustrine sedimentation in the Miocene Rubielos de Mora Basin, Spain, in : Fleet A.J., Kelts K. et Talbot M.R. (éds), *Lacustrine Petroleum Source Rocks*, Geological Society London, Special Publication, 40, 353-367
- Arènes J. et Depape G. 1956. La flore burdigalienne des îles Baléares (Majorque), *Rev. gén. Bot.*, Paris, 63, 1-43
- Barrón E. 1997. Estudio paleobotánico de la cuenca miocena inferior de Rubielos de Mora (Teruel, España), in : *Congr. Soc. Paleontología de España*, 149-151
- Bataller J.R. et Depape G. 1950. Flore oligocène de Cervera (Catalogne), *Anales Escuela Peritos Agric. Especialidades Agropecuarias y Servicios Técnicos de Agricultura*, Barcelona, 9, 5-60
- Bessedik M. 1984. The Early Aquitanian and Upper Langhian-Lower Serravallian environments in the Northwestern Mediterranean region, *Paléobiologie continentale*, Montpellier, 14 (2), 153-179
- Bessedik M. 1985. Reconstitution des environnements miocènes des régions nord-ouest méditerranéennes à partir de la palynologie, *Thèse*, Université Montpellier-2, 162 p.
- Bessedik M. et Cabrera L. 1985. Le couple récif-mangrove à Sant-Pau-d'Ordal (Vallès-Penedès, Espagne), témoin du maximum transgressif en Méditerranée nord-occidentale (Burdigalien supérieur-Langhien inférieur), *Newsletters Stratigraphy*, 14 (1), 20-35
- Calvo J.-P., Daams R., Morales J., López-Martínez N., Agustí J., Anadón P., Armenteros I., Cabrera L., Civis J., Corrochano A., Díaz-Molina M., Elizaga E., Hoyos M., Martín-Suarez E., Martínez J., Moissenet E., Muñoz A., Pérez-García A., Pérez-González A., Portero J.M., Robles F., Santisteban C., Torres T., Van der Meulen A.J., Vera J.A. et Mein P. 1993. Up-to-date Spanish continental Neogene

synthesis and paleoclimatic interpretation, *Rev. Soc. Geol. España*, 6 (3-4), 29-40

Crusafont-Pairó M., Gautier F. et Ginsburg L. 1966. Mise en évidence du Vindobonien inférieur continental dans l'Est de la province de Teruel (Espagne), *C. R. somm. Séanc. Soc. géol. France*, fasc. 1, 30-32

Daams R. 1976. Miocene Rodents (Mammalia) from Cetina de Aragón (prov. Zaragoza) and Buñol (prov. Valencia), Spain, *Koninkl. Neder. Akad. Wetensch.*, B 79 (3), 153-182

Daams R. et Van der Meulen A.J. 1984. Paleoenvironmental and paleoclimatic interpretation of micromammal faunal successions in the Upper Oligocene and Miocene of North Central Spain, *Paléobiologie continentale*, Montpellier, 14 (2), 241-257

Daams R., Freudenthal M. et Van der Meulen A.J. 1988. Ecostratigraphy of micromammal faunas from the Neogene of Spain, *Scripta Geol.*, Leiden, Spec. Issue 1, 287-302

Daams R., Van der Meulen A.J., Alvarez Sierra M.A., Peláez-Campomanes P. et Krijgsman W. 1999. Aragonian stratigraphy reconsidered, and a re-evaluation of the Middle Miocene mammal biochronology in Europe, *Earth Planet. Sci. Lett.*, 165, 287-294

De Bruijn H. et Moltzer J.G. 1974. The rodents from Rubielos de Mora: the first evidence of the existence of different biotopes in the Early Miocene of eastern Spain, *Proceedings Koninklijke Nederlandse Akademie Van Wetenschappen*, B, 77, 129-145

Depape G. et Brice D. 1965. La flore oligocène de Cervera (Catalogne). Données complémentaires, *Ann. Soc. Géol. Nord*, 85, 111-117

Fernández-Marrón T. 1973. Nuevas aportaciones a la sistemática y paleoecología de la flora oligocénica de Sarreal (Tarragona), *Estudios Geológicos*, Madrid, 29, 157-169

Fernández-Marrón T. et Álvarez-Ramis C. 1988. Note préliminaire sur l'étude paléobotanique du gisement de Rubielos de Mora (Teruel, Espagne), *Résumé Séminaire de Paléobotanique*, Lille, OFP Informations n° 9, 14

Godoy A., Anadón P., Olivé A., Aguilar M.J., Leal M.C., García J.C., Martín J.M., Meléndez X. et Alvaro M. 1986. Mora de Rubielos, *Memoria del mapa geológico 1/50.000*, Hoja 591, Inst. Geol. Miner. Esp., 1-52

Hernández-Sampelayo P. et Cincúnegui M. 1926. Cuenca de esquistos bituminosos de Ribesalbes (Castellón), *Bol. Inst. Geol. Min. España*, série 3, 6, 3-86

Krijgsman W., Langereis C.G., Daams R. et Van der Meulen A.J. 1994. Magnetostratigraphic dating of the Middle Miocene climate change in the continental deposits of the Aragonian type area in the Calatayud-Teruel basin (Central Spain), *Earth Planet. Sci. Lett.*, 128, 513-526

López-Martínez N. 1977. Revisión sistemática y bioestratigráfica de los Lagomorpha (Mammalia) del Terciario y Cuaternario de España, *Tesis Doctoral*, Univ. Complutense Madrid, 469 p.

López-Martínez N. 1989. Revisión sistemática y bioestratigráfica de los Lagomorpha (Mammalia) del Terciario y Cuaternario de España, *Memorias del Museo Paleontológico de la Universidad de Zaragoza*, 3, 342 p.

Martinez-Delclòs X., Peñalver E. et Belinchón M. 1991. Primeras aportaciones al estudio de los insectos del Mioceno de Rubielos de Mora, Teruel (España), *Revista Española de Paleontología*, n° Extraordinario, 125-137

Montoya P., Peñalver E., Ruiz-Sanchez F.J., Santisteban C. de, Alcalá L., Belinchón M. et Lacomba J.I. 1996. Los yacimientos paleontológicos de la cuenca terciaria continental de Rubielos de Mora (Aragón), *Revista Española de Paleontología*, n° Extraordinario, 215-224

Peñalver E., 1998. Estudio tafonómico y paleoecológico de los insectos del Mioceno de Rubielos de Mora (Teruel), Instituto de Estudios Turolenses, Excma, Diputación Provincial de Teruel, 179 p.

Sanchíz F.B. 1977. Catálogo de los anfibios fósiles de España, *Acta Geológica Hispánica*, 12, 103-107

Sanz de Siria A. 1981. La flora burdigaliense de los alrededores de Martorell (Barcelona), *Paleontologia i Evolució*, Sabadell, 16, 3-13

Sanz de Siria A. 1983. Aportación al conocimiento de la flora pliocénica de los alrededores de Papiol (Barcelona), *Paleontologia i Evolució*, Sabadell, 18, 151-160

Sanz de Siria A. 1992. Estudio de la macroflora oligocena de las cercanías de Cervera (Colección Martí Madern del Museo de geología de Barcelona), *Treb. Mus. Geol. Barcelona*, 2, 269-379

Van der Meulen A.J. et Daams R. 1992. Evolution of Early-Middle Miocene rodent faunas in relation to long-term palaeoenvironmental changes, *Palaeogeogr. Palaeoclim. Palaeoecol.*, 93, 227-253

Neogene flora, vegetation and climate dynamics in southeastern Europe and the northeastern Mediterranean

G. JIMENEZ-MORENO^{1,2,3}, S.-M. POPESCU¹, D. IVANOV⁴ & J.-P. SUC¹

¹*Laboratoire PaléoEnvironnement et PaléobioSphère (UMR CNRS 5125), Université Claude Bernard - Lyon 1, 27-43 boulevard du 11 Novembre, 69622 Villeurbanne, France (e-mail: gonzaloz@ugr.es; popescu@univ-lyon1.fr; jean-pierre.suc@univ-lyon1.fr)*

²*Departamento de Estratigrafía y Paleontología, Universidad de Granada, Avda. Fuente Nueva S/N 18002, Granada, Spain*

³*Center for Environmental Sciences & Education, Box 5694, Northern Arizona University, Flagstaff, AZ 86011USA. (present address) (e-mail: Gonzalo.Jimenez-Moreno@NAU.EDU)*

⁴*Institute of Botany, Bulgarian Academy of Sciences, Acad. G. Bonchev Str., 23, 1113 Sofia, Bulgaria (e-mail: dimiter@bio.bas.bg)*

Abstract: Pollen analysis of Miocene and Pliocene sediments from southeastern Europe and the northeastern Mediterranean is represented in pollen synthetic diagrams based on ecological criteria in order to clearly visualize changes in the composition and structure of the vegetation through time. New pollen data, together with abundant existing palynological information from this area, show a progressive reduction in plant diversity caused by a decrease in the most thermophilous and high-water requirement plants and, on the contrary, an increase in warm-temperate (mesothermic) and seasonal-adapted taxa during the Middle–Late Miocene and Pliocene. At the same time, an increase in high-elevation trees and herbs has been recorded, with a strong augmentation in *Artemisia*, first in the eastern Mediterranean and later on in the western Mediterranean area. This has been interpreted as a response of the vegetation to global and regional processes, including climate cooling related to the development of the East Antarctic Ice Sheet (EAIS), uplift of regional mountains during Alpine orogenesis and progressive movement of Eurasia towards northern latitudes as a result of the northwards collision of Africa.

Pollen analyses dealing with Miocene–Pliocene sediments from the Paratethys are rare. Studies have focused on the Miocene and Pliocene palynology of the Central Paratethys (Petrescu *et al.* 1989a, b; Planderová 1990; Nagy 1991, 1992, 1999; Petrescu & Malan 1992) and Turkey (Benda 1971; Benda *et al.* 1975; Akgün & Akyol 1999), but the lack of any quantitative information render these analyses limited. However, palynological data, with reliable botanical identification, are available for the Miocene (Ivanov 1995; Ivanov & Koleva-Rekalova 1999; Palamarev & Ivanov 2001; Ivanov *et al.* 2002; Jiménez-Moreno *et al.* 2005) and the Pliocene (Drivaliari 1993; Drivaliari *et al.* 1999; Popescu 2001, 2002, 2006; Popescu *et al.* 2006a, b) of the same region. In these studies, pollen was not used for biostratigraphy but for climatic information, as independent biostratigraphic dating was available (see below). Pollen counts and a statistical treatment of the data were made to obtain reliable information about floral diversity, organization of the vegetation and to better visualize vegetation and climate change.

The geographical position of the studied area, between Africa and Eurasia and between a Mediterranean and temperate climate, makes this region of great interest for palaeobotanic studies. Today, the southeastern part of the area is mainly occupied by steppe vegetation rich in *Artemisia* (i.e. the central Anatolian steppes), that is the main refuge area of thermophilous plants (mostly along the Turkish coastlines: Zohary 1973; Quézel & Médail 2003). Alpine tectonics were active during the Neogene, producing uplift of the Carpathians, Dinarides, Balkan, Rhodope and Taurides mountains. Then, important palaeogeographical changes occurred (see below; Rögl 1998; Meulenkamp & Sissingh 2003; Popov *et al.* 2004) that may have contributed to the pattern of vegetation distribution seen today.

In this paper, we present a synthesis of palynological data, interpreted vegetation and climate dynamics based on Miocene and Pliocene deposits from Eastern Europe. New sections of Middle and Late Miocene age from this area have been analysed, adding new information to the already

published data. Changes in vegetation have been observed from the Langhian to the early Pliocene (16.3–3 Ma). These are mainly related to global climatic changes, in temperature and precipitation, that are linked to atmospheric and palaeogeographic changes that were of significant importance during the Neogene.

Regional setting

The studied area comprises Neogene basins formed within the Central–Eastern Paratethys Sea. They were generated during the Neogene, like the rest of the basins belonging to the Paratethys, as a product of the collision of the African plate and Eurasia. These basins are delimited by the Carpathians, Balkan, Dinarides and Taurides, occupying parts of Hungary, Romania, Bulgaria, Serbia,

Greece and Turkey (Fig. 1; Kojumdjieva & Popov 1989; Rögl 1998; Meulenkamp & Sissingh 2003; Goncharova *et al.* 2004; Ilyina *et al.* 2004; Paramonova *et al.* 2004; Khondkarian *et al.* 2004a, b). During the Neogene, the Paratethys displayed a long-term trend of decreasing marine influence and a correlative reduction in size with regard to the marine depositional domains. Marine deposition lasted throughout the Early and Middle Miocene up to approximately 12 Ma, when uplift caused the sea to retreat from the Pannonian basin complex where a brackish lake formed instead (Rögl 1998). However, during the Early and Middle Miocene, connection between the Mediterranean Sea and the Paratethys existed that allowed for a free marine faunal exchange (Harzhauser *et al.* 2003). The first impairment of marine connections is evident in the Late Badenian (Early Serravallian)



Fig. 1. Geographic map of the studied area and location of the sites. 1 Nireas-1; 2 Valea Morilor; 3 Ruzhintsi; 4 Catakbagyaka; 5 Hinova; Husnicioara and Valea Visenilor; 6 Lupoiaia; 7 Ticleni-1; 8 Ravno Pole and Lozenec; 9 Sandanski; 10 Lion of Amphipoli; 11 Nestos-2; 12 Site 380 A; 13 Aghios Vlassios; 14 Avadan; 15 Lataquie; 16 Drenovets C-1; 17 Deleina C-12; 18 Makrilia; 19 Tengelic-2.

when dysaerobic bottom conditions and a stratified water column characterized the Paratethyan realm (Kovac *et al.* 2004). With the onset of the Sarmatian, marine connection to the Mediterranean almost completely ceased, and was reflected by the development of a highly endemic molluscan fauna (Harzhauser & Piller 2004). Finally, at the Sarmatian/Pannonian boundary (Serravallian/Tortonian boundary), the Central Paratethys became entirely restricted and the brackish Lake Pannon was established. Sporadic brief connections occurred during the Late Miocene and Pliocene between the Eastern Paratethys (Dacic and Euxinian basins) and the Mediterranean Sea as documented by nannoplankton influxes (MăruŃeanu & Papaianopol 1998; Semenenko & Olejnik 1995). One of these short connections also concerned the southeastern Pannonian Basin during the so-called Portaferrian regional Stage (Pontian). Some of these connections occurred just before and just after the Messinian salinity crisis (Clauzon *et al.* 2005; Snel *et al.* 2006), resulting in the same responses (i.e. an intense erosion, then the construction of Gilbert-type fan deltas) to the Messinian desiccation and Zanclean flooding as in the Mediterranean Basin itself (Clauzon *et al.* 2005). However, during the late Neogene, most of the Paratethyan basins were disconnected and evolved as isolated lakes, some of them being temporarily connected with the Mediterranean Sea (MăruŃeanu & Papaianopol 1995).

The independent evolution of the different sub-domains of the Paratethys led to the construction of several regional stratigraphies, constituted by stages based on diverse groups of organisms, mainly bivalves and ostracods, and benthic and planktonic foraminifera etc. (Marinescu 1978; Papaianopol & Motas 1978; Papaianopol & Marinescu 1995; Rögl 1998; Fig. 2). Reliable correlations are established between the Eastern Paratethys regional stratigraphy and the Mediterranean standard stratigraphy using nannoplankton (Papaianopol & MăruŃeanu 1993; MăruŃeanu & Papaianopol 1995, 1998; Drivaliari *et al.* 1999; Clauzon *et al.* 2005; Snel *et al.* 2006).

Chronological background

A total of 19 sections and a total of 680 samples have been studied for pollen. Of those 19 sections, 12 (or a part) belong to the Miocene and 14 (or a part) to the Pliocene (Fig. 2). As far as possible, an independent age control has been obtained; it is indicated in Table 1 with the authors of the pollen analyses. The timescale of Gradstein *et al.* (2004) has been used.

Methods

Identification was performed comparing the Neogene pollen grains with those of the living relative plants

using databanks of modern pollen grains and modern and past pollen grain photographs. Based on the results of the pollen spectra, standard synthetic diagrams (Suc 1984) with *Pinus* and Pinaceae have been constructed. In these pollen diagrams, taxa have been arranged into 12 different groups based on ecological criteria in order to obtain some visualization of the vegetation (see below) and more easily compare with reference oxygen isotopic curves. This method has been proven to be a very efficient tool for high-resolution climatic studies characterizing warm–cold alternations related to Milankovitch cycles for both the Miocene (Jiménez-Moreno *et al.* 2005) and the Pliocene (Popescu 2001, 2006; Popescu *et al.* 2006a, b).

Pollen data will be available, after publication, on the web from the ‘Cenozoic pollen and climatic values’ database (CPC) (<http://medias.obs-mip.fr/cpc>).

Results

Plant diversity and vegetation

Even if some parts of the studied region are characterized today by a very diverse flora and are main refuge areas of thermophilous plants (i.e. the Ponto-Euxinian area) (Quézel & Médail 2003), a richer and more diverse flora has been identified for the Mio-Pliocene that consisted of elements found presently in different geographic areas:

- (1) Tropical and subtropical Africa, America and Asia (*Avicennia*, *Bombax*, Caesalpinaceae, *Engelhardia*, *Platycarya*, Taxodiaceae, Hamamelidaceae, *Myrica*, Sapotaceae, etc.).
- (2) Warm-temperate latitudes of the Northern Hemisphere (*Acer*, *Alnus*, *Betula*, Cupressaceae, *Fagus*, *Populus*, deciduous *Quercus*, *Salix*, etc.).
- (3) Mediterranean region (*Olea*, *Phillyrea*, *Ceratonia*, evergreen *Quercus*, etc.).

All of these taxa grew in the Eastern European area during the Miocene.

We use the Chinese flora as a present-day comparison for the southeastern Europe and Middle East flora during the Neogene as it is the closest living example of this floral inventory (Suc 1984). Flora of the broad-leaved evergreen forest was represented by 45 typical tropical and subtropical taxa (i.e. megathermic and mega-mesothermic elements, respectively) in the studied region during the middle Miocene’s warmest phase; only 21 of them persisted until the early Pliocene and have presently disappeared from the area. Flora of the evergreen and deciduous mixed forest was represented by 21 subtropical and warm-temperate taxa (i.e. mega-mesothermic and mesothermic

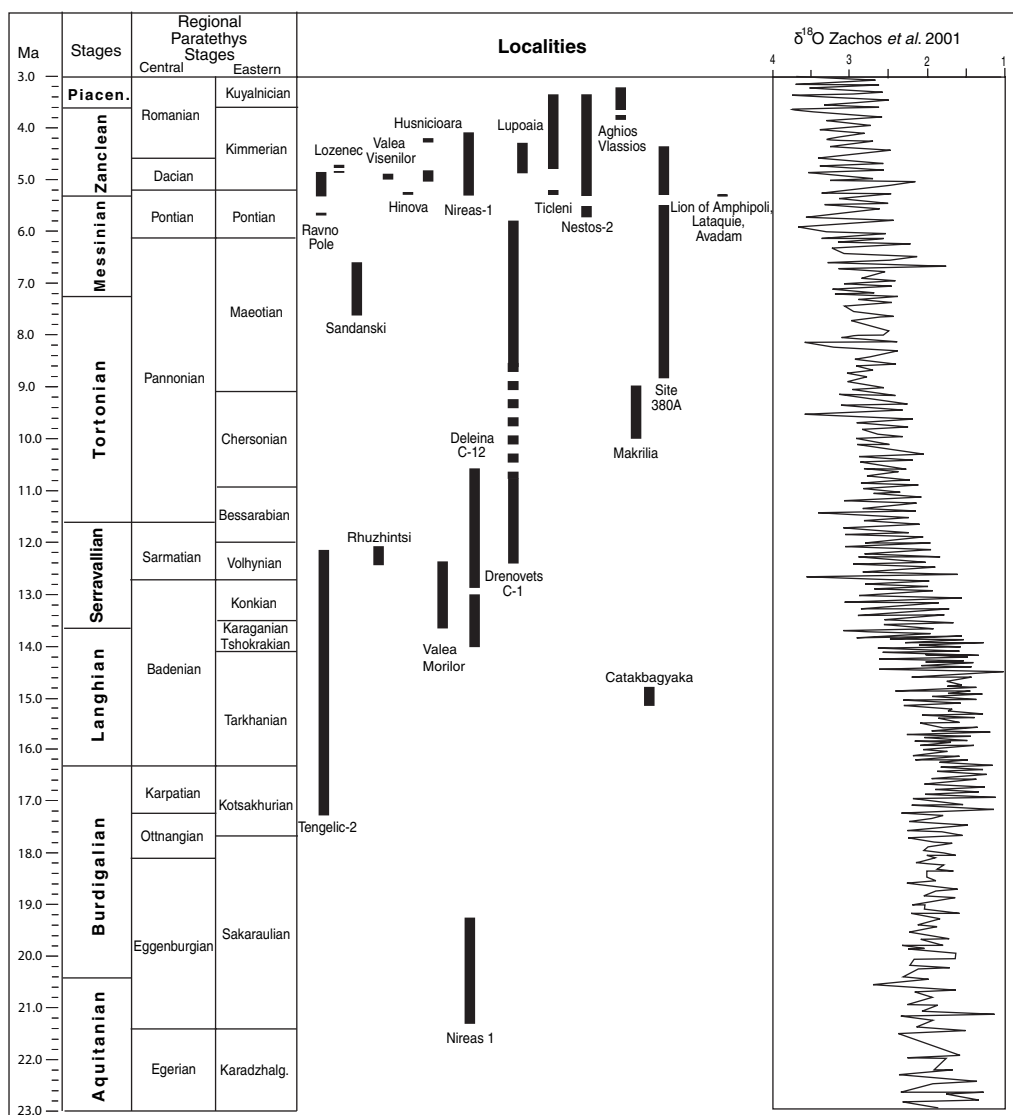


Fig. 2. Miocene and Pliocene chronostratigraphy and temporal situation of the studied sites. Correlations between standard stages and Paratethys stages by Harzhauser & Piller (in press) after data of Steininger (1999), Sprovieri (1992), Sprovieri *et al.* (2002), Fornaciari & Rio (1996) and Fornaciari *et al.* (1996). Oxygen isotope curve after Zachos *et al.* (2001); all stages recalibrated according to Gradstein & Ogg (2004), Gradstein *et al.* (2004) and Lourens *et al.* (2004).

elements, respectively) in the studied region during the Middle Miocene's warmest phase; they persisted here during the Early Pliocene and 17 among them are still living in the area.

The vegetation was characterized by a complex mosaic due to its dependency on several factors (water availability, characteristics of the soils, orientation of relief slopes, etc.) which superimposed its latitudinal–altitudinal organization. The most important factor, similar to

present day, would be altitude, controlling both temperature and precipitation. Therefore, the vegetation would be organized in altitude belts, which have been compared with those found today in subtropical to temperate southeastern China, the most reliable model. The following have been distinguished:

(1) a coastal marine environment characterized by the presence of an impoverished mangrove composed of *Avicennia* which is mainly

Table 1. Age control of the 19 considered pollen localities indicating the authors of the pollen analyses

#	Section	Location	Datation	Age	Pollen analysis by
1	Nireas 1	Greece	* Drivaliari 1993	Aquitanian-Burdigalian	Drivaliari, A.
2	Valea Morilor	Romania	*) Papatanopol <i>et al.</i> 1995	Badenian-Sarmatian	Jiménez-Moreno, G.
3	Ruzhinski	Bulgaria) Kojumdjieva 1976; Palmarev & Ivanov 2001	Sarmatian	Jiménez-Moreno, G.
4	Catakbagyaka	Turkey	i Sickenberg <i>et al.</i> 1975; Heissig 1976	Langhian	Jiménez-Moreno, G.
5	Hinova	Romania) Marinescu 1978	Early Zanclean	Popescu, S.-M.
			* Clauzon <i>et al.</i> 2005	Bosphoritan	
5	Husnicioara	Romania	* § ♣ Popescu <i>et al.</i> 2006a	Early Zanclean Dacian	Popescu, S.-M.
			¶ Ticleanu & Diaconita 1997		
5	Valea Visenilor	Romania	§ ♣ Popescu <i>et al.</i> 2006b	Early Zanclean Dacian	Popescu, S.-M.
			¶ Ticleanu & Diaconita 1997		
6	Lupoaia	Romania	♣ Popescu <i>et al.</i> 2006b	Zanclean Dacian-Romanian	Popescu, S.-M.
			i Radulescu <i>et al.</i> 1997; Apostol & Enache 1979		
			§ Radan & Radan 1998; Van Vugt 2001		
			¶ Ticleanu & Diaconita 1997		
7	Ticleni 1	Romania	♣ Popescu S.-M. 2002; Popescu <i>et al.</i> 2006b	Zanclean Dacian-Romanian	Drivaliari, A. 1993
8	Ravno Pole	Bulgaria	*) Drivaliari <i>et al.</i> 1999	Pontian-Dacian	Drivaliari, A.
8	Lozenc	Bulgaria) Drivaliari 1993	Dacian	Drivaliari, A.
9	Sandanski	Bulgaria	i Gromolard & Guerin 1980; Thomas <i>et al.</i> 1986	Maecotian	Ivanov, D.
10	Lion of Amphipoli	Bulgaria	i Kojumdjieva <i>et al.</i> 1982; Spassov N. (personal information)	Early Zanclean	Suc, J.-P.
11	Nestos 2	Greece	* Melinte, M.C. (personal information)	Messinian-Zanclean	Drivaliari, A.
12	Site 380 A	Black Sea	* + Drivaliari 1993	Late Miocene-Early Pliocene	Popescu, S.-M.
			¶ Hsü 1978; Hsü & Giovanoli 1979; Letouzey <i>et al.</i> 1978		
			♣ Popescu 2006		
13	Aghios Vlassios	Greece	+ Spaak 1983; Drivaliari 1993	Early Pliocene	Drivaliari, A. 1993
14	Avadam	Turkey	¶ Robertson A.H.F. (personal information)	Early Zanclean	Suc, J.-P.
15	Latakie	Syria	¶ Rubino J.-L. (personal information)	Early Zanclean	Suc J.-P.
16	Drenovets C-1	Bulgaria	+) ^ Kojumdjieva <i>et al.</i> 1989	Sarmatian to Pontian	Ivanov, D.
17	Deleina C-12	Bulgaria	+) ^ Kojumdjieva & Popov 1989	Badenian to Pannonian	Ivanov, D.
18	Makrilia	Greece	* Sachse <i>et al.</i> 1999	Tortonian	Sachse, M.
19	Tengelic-2	Hungary	* +) Nagymarosi 1982; Bohn-Havas 1982; Korecz-Laky 1982	Burdigalian Ottnangian to Sarmatian	Jiménez-Moreno, G.

+ Foraminifera ^ Ostracods i Mammals ♣ Climatostratigraphy * Nanoplankton) Bivalves § Palaeomagnetism ¶ Lithostratigraphy

accompanied by halophytes (Amaranthaceae–Chenopodiaceae, *Armeria*, etc.);

(2) a broad-leaved evergreen forest, from sea level to around 700 m altitude characterized by *Taxodium* or *Glyptostrobus*, *Myrica*, *Rhus*, Theaceae, Cyrillaceae–Clethraceae, *Bombax*, Euphorbiaceae, *Distylium*, *Castanopsis*, Sapotaceae, Rutaceae, *Mussaenda*, *Ilex*, *Hedera*, *Ligustrum*, *Jasminum*, Hamamelidaceae, *Engelhardia*, *Rhoiptelea*, etc.;

(3) an evergreen and deciduous mixed forest, above 700 m altitude; characterized by deciduous *Quercus*, *Engelhardia*, *Platycarya*, *Carya*, *Pterocarya*, *Fagus*, *Liquidambar*, *Parrotia*, *Carpinus*, *Celtis*, *Acer*, etc. Within this vegetation belt, riparian vegetation has been identified, composed of *Salix*, *Alnus*, *Carya*, *Carpinus*, *Zelkova*, *Ulmus*, *Liquidambar*, etc. The shrub level was dominated by Ericaceae, *Ilex*, Caprifoliaceae, etc.;

(4) above 1000 m, a mid-altitude deciduous and coniferous mixed forest with *Betula*, *Fagus*, *Cathaya*, *Cedrus*, *Tsuga*.

(5) above 1800 m altitude, a coniferous forest with *Abies* and *Picea*.

Vegetation dynamics

The following description of the Miocene and Pliocene vegetation dynamics in the southern Forecarpathian Basin and Greece–Turkey is a brief summary of the pollen analysis of Drivaliari (1993), Ivanov (1995), Drivaliari *et al.* (1999), Popescu (2001, 2006), Popescu *et al.* (2006a, b), Jiménez-Moreno *et al.* (2005) and Jiménez-Moreno (2005).

Burdigalian–Langhian (20.4–13.6 Ma). The regular occurrence and abundance of thermophilous species typical of the lowest altitudinal belts described above and the relative scarcity of altitudinal elements (Fig. 3) are characteristic for vegetation of this time. The coastal marine environment was then occupied by an impoverished *Avicennia* mangrove and several halophytes (Nagy & Kóky 1991; Nagy 1999; Plaziat *et al.* 2001; Jiménez-Moreno 2005). In the hinterland, lowlands were populated by a broad-leaved evergreen forest, characterized by *Alchornea*, Passifloraceae, *Pandanus*, *Rhus*, Theaceae, Cyrillaceae–Clethraceae, *Bombax*, Rubiaceae, Chloranthaceae, *Reevesia*, Euphorbiaceae, *Distylium*, *Castanopsis*, Sapotaceae, Rutaceae, *Mussaenda*, *Ilex*, *Hedera*, *Itea*, *Alangium*, cf. Mastixiaceae, *Ligustrum*, *Jasminum*, Hamamelidaceae, *Engelhardia*, *Rhoiptelea*, Schizaeaceae, Gleicheniaceae, etc. Within this vegetation belt, swamp forests were also well developed during this time period. Its components, such as *Taxodium* or *Glyptostrobus*, *Nyssa*, *Myrica*, *Planera*, show

comparatively high values in the pollen spectra. Probably the low elevation palaeogeography and very humid conditions at that time in the studied area favoured the wide distribution of swamp forests and of ecologically related riparian forests with *Platanus*, *Liquidambar*, *Zelkova*, *Carya*, *Pterocarya* and *Salix*.

An evergreen and deciduous mixed forest mainly composed of mesothermic elements such as *Quercus*, *Carya*, *Pterocarya*, *Fagus*, Ericaceae, *Ilex*, Caprifoliaceae, *Liquidambar*, *Parrotia*, *Carpinus*, *Celtis*, *Acer*, but also *Engelhardia*, *Platycarya*, etc., characterized areas of higher altitude. Within this vegetation belt, riparian vegetation has been identified, composed of *Salix*, *Alnus*, *Carya*, *Carpinus*, *Zelkova*, *Ulmus*, etc.

It should also be mentioned that conifer pollen, mainly *Pinus* and indeterminate Pinaceae, can be particularly abundant, presumably because of the capacity of saccate pollen for long-distance transport (Heusser 1988; Suc & Drivaliari 1991; Cambon *et al.* 1997; Beaudouin 2003): during the Badenian, the basin developed its largest extension so that the studied sections had the maximum distance from the coastline (Fig. 3). Mid- and high-altitude elements (*Tsuga*, *Cedrus*, *Abies* and *Picea*) and *Cathaya* seem not to vary significantly in sections of this age (Fig. 3).

Serravallian–Tortonian–Messinian (13.6–5.3 Ma). During this time-interval, important changes in the vegetation are observed: *Avicennia*, which populated the coastal areas in previous times, is not found commonly and several megathermic elements (*Buxus bahamensis* group, *Alchornea*, *Bombax*, Iacacinaceae, *Croton*, Melastomataceae, etc.), typical from the broad-leaved evergreen forest, became rare and most of them disappeared (Fig. 3). The evergreen–deciduous mixed forest suffered a great transformation due to the loss and decrease in the abundance of several megathermic evergreen plants. This kind of vegetation was progressively enriched by deciduous mesothermic plants, such as deciduous *Quercus*, and *Fagus*, *Alnus*, *Acer*, *Eucommia*, *Betula*, *Alnus*, *Carpinus*, *Ulmus*, *Zelkova*, *Tilia*, etc. Thus, the vegetation shows a tendency towards increasing proportions of mesothermic deciduous elements coming from higher altitudes.

Even if the thermophilous elements decreased during this period, the swamp forest continued to be well developed. At the same time, the vegetation from mid- (*Cathaya*, *Tsuga* and *Cedrus*) and high-altitude (*Picea* and *Abies*) belts clearly strengthened. For instance, *Tsuga* (mid-altitude indicator) is absent in the Badenian (Langhian and Early Serravallian) or very rare, it is still rare at the base of the Volhynian (approx. 12.7 Ma), but reaches

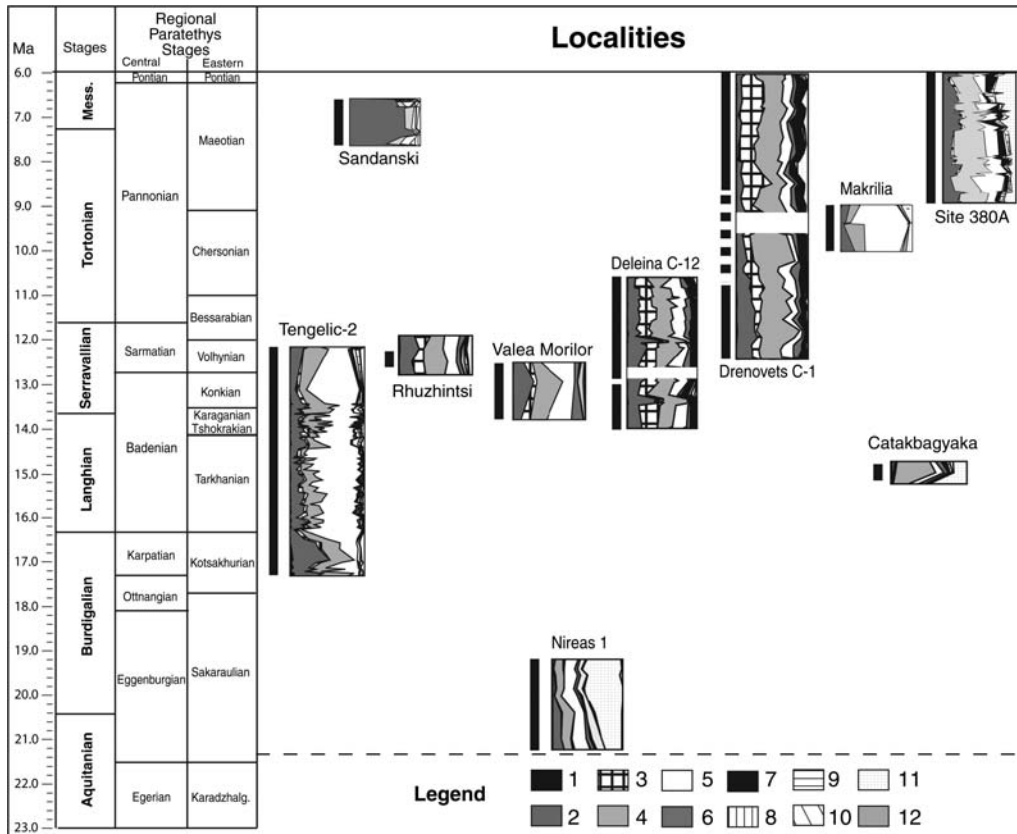


Fig. 3. Synthetic pollen diagrams of the sections spanning the Miocene until 6 Ma. Taxa have been grouped according to their ecological significance as follows: 1 Megathermic (= tropical) elements (*Avicennia*, *Amanoa*, *Alchornea*, *Fothergilla*, *Exbucklandia*, Euphorbiaceae, Sapindaceae, Loranthaceae, Arecaceae, Acanthaceae, *Canthium* type, Passifloraceae, etc.). 2 Mega-mesothermic (= subtropical) elements (Taxodiaceae, *Engelhardia*, *Platycarya*, *Myrica*, Sapotaceae, *Microtropis fallax*, *Symplocos*, *Rhoiptelea*, *Distylium* cf. *sinensis*, *Embolanthera*, *Hamamelis*, Cyrillaceae–Clethraceae, Araliaceae, *Nyssa*, *Liriodendron*, etc.). 3 *Cathaya*, an altitudinal conifer living today in Southern China. 4 Mesothermic (= warm-temperate) elements (deciduous *Quercus*, *Carya*, *Pterocarya*, *Carpinus*, *Juglans*, *Celtis*, *Zekkova*, *Ulmus*, *Tilia*, *Acer*, *Parrotia* cf. *persica*, *Liquidambar*, *Alnus*, *Salix*, *Populus*, *Fraxinus*, *Buxus sempervirens* type, *Betula*, *Fagus*, *Ostrya*, *Parthenocissus* cf. *henryana*, *Hedera*, *Lonicera*, *Elaeagnus*, *Ilex*, *Tilia*, etc.). 5 *Pinus* and poorly preserved Pinaceae pollen grains. 6 Meso-microthermic (= mid-altitude) trees (*Tsuga*, *Cedrus*). 7 Microthermic (= high-altitude) trees (*Abies*, *Picea*). 8 Non-significant pollen grains (undetermined ones, poorly preserved pollen grains, some cosmopolitan or widely distributed elements such as Rosaceae and Ranunculaceae). 9 Cupressaceae. 10 Mediterranean xerophytes (*Quercus ilex* type, *Carpinus* cf. *orientalis*, *Olea*, *Phillyrea*, *Ligustrum*, *Pistacia*, *Ziziphus*, *Cistus*, etc.). 11 Herbs (Poaceae, *Erodium*, *Geranium*, *Convolvulus*, Asteraceae Asteroideae, Asteraceae Cichorioideae, Lamiaceae, *Plantago*, *Euphorbia*, Brassicaceae, Apiaceae, *Knautia*, *Helianthemum*, *Rumex*, *Polygonum*, *Asphodelus*, Campanulaceae, Ericaceae, Amaranthaceae–Chenopodiaceae, Caryophyllaceae, Plumbaginaceae, Cyperaceae, *Potamogeton*, *Sparganium*, *Typha*, Nymphaeaceae, etc.) including some subdesertic elements (*Lyeum*, *Neurada*, *Nitraria*, *Calligonum*). 12 Steppe elements (*Artemisia*, *Ephedra*).

up to 10% in the middle and upper part of the Volhynian (Fig. 3). This palaeofloristic change occurs slowly and gradually without major fluctuations. A similar vegetation change is observed during the same time-interval in other areas of Europe (e.g. Spain, southern France, Switzerland and Austria: Bessedik 1985; Jiménez-Moreno 2005).

The herbs (mainly Poaceae, Amaranthaceae–Chenopodiaceae, *Artemisia*, Caryophyllaceae, Polygalaceae, Lamiaceae, Asteraceae Asteroideae and Asteraceae Cichorioideae) also became more abundant (Fig. 3). This may be due to a somewhat drier climate during that time as is also indicated by macrofloras of the same area (Palamarev 1991; Palamarev &

Ivanov 2004) and confirmed by sedimentological data (Koleva-Rekalova 1994; Ivanov & Koleva-Rekalova 1999): in Bessarabian to Chersonian sediments (12–9.1 Ma) of northeast Bulgaria, aragonite sediments occur which are assumed to have been formed under a seasonally dry climate. This trend continued during the Late Miocene. Presumably, open landscapes covered by more xerophytic herbaceous communities existed during that time.

Pliocene (5.3–c. 3.2 Ma). The vegetation was then characterized by a mosaic of different plant associations inherited from the Miocene. The same vegetation dynamics marked by disappearance of thermophilous plants and increase in mesothermic and micro-mesothermic plants continued. Some of the coastal areas of this region were still inhabited by *Avicennia* mangrove (*Avicennia* pollen at Site 380A at 781.63 m) and several megathermic elements typical from the broad-leaved evergreen forest occupying the lowlands, such as *Amanoa*, *Pachysandra*, *Entada*, Meliaceae, Mimosaceae, Sapindaceae, Tiliaceae, Euphorbiaceae, Acanthaceae and *Fothergilla*, are sporadically present. They disappeared during the early Pliocene (between 4–3.5 Ma) (Popescu 2001). The mega-mesothermic plants, belonging to these plant associations, such as *Engelhardia*, *Microtropis*, *Distylium*, *Parthenocissus*, Sapotaceae, Arecaceae, etc., are still abundant and persisted through the Pliocene (Fig. 4). Swampy (mainly *Taxodium* or *Glyptostrobus*, *Nyssa*, *Myrica*) and marshy (Cyperaceae, Poaceae, Cyrtaceae–Clethraceae, *Myrica*) elements, populating deltaic areas, were very abundant. Trees from the family Taxodiaceae did not disappear from this area until the middle Pleistocene (Mamatsashvili 1975).

The mixed deciduous forest (mainly made up of conifers like *Pinus*, and several deciduous trees such as *Quercus*, *Acer*, *Carpinus*, *Parrotia*, *Carya*, *Pterocarya*, *Liquidambar*, *Platanus*, *Tilia*, *Ulmus*, *Zelkova*, etc.), situated at higher altitude, as well as the trees belonging to the highest altitudinal belts, become more abundant during this period (*Cathaya*, *Cedrus*, *Tsuga*, *Picea* and *Abies*) (increasing percentages of these elements are compared on Fig 3 and 4).

Another important fact that makes a difference between the Pliocene and the Miocene is the strong development of the steppe with *Artemisia* in the Ponto-Euxinian region since the early Pliocene (Site 380A, Fig. 4).

Climatic evolution: regional vs. global climatic change

The high presence of mega- and mega-mesothermic elements during the Early and early Mid-Miocene suggests the existence of a warm, subtropical

climate and a tendency towards slightly cooler conditions in the late Mid-Miocene. Climate was also quite humid, to support the development of such a large association of thermic elements (of present-day 'Asiatic' affiliation and climate) which require very humid conditions all year (Wang 1961). The major change is the impoverishment in plant diversity produced by the disappearance of the most thermophilous plants and the consequent enrichment in mesothermic plants (mainly deciduous *Quercus*, *Alnus*, etc.) and high-elevation conifers, from the Serravallian to the Pliocene.

The floral assemblages during the Early and early Mid-Miocene clearly reflect the Miocene Climatic Optimum (MCO: Zachos *et al.* 2001; Shevenell *et al.* 2004) well-recorded at Tengelic-2 (Jiménez-Moreno *et al.* 2005). The major change registered in plant diversity is related to a gradual decrease in temperature and precipitation after the MCO (Ivanov *et al.* 2002; Jiménez-Moreno *et al.* 2005). This fact is well documented on a worldwide scale and has been correlated with the general decrease in temperature observed by several authors as a gradual increase in the isotopic $\delta^{18}\text{O}$ values of foraminifera from deep-sea sediments (DSDP Sites 608: Miller *et al.* (1991) and 588: Zachos *et al.* (2001)) during this timespan and related to an increase in the size of the EAIS (East Antarctic Ice Sheet) (Zachos *et al.* 2001) (Fig. 2). The isotopic values also indicate that this cooling continued during the Late Miocene and Pliocene (Zachos *et al.* 2001) (Fig. 2).

High-elevation conifers seem not to vary along the sections of early and early Mid-Miocene; however, these elements are abundant in the samples and indicate that the surrounding mountains were already significantly uplifted. Mid- (including *Cathaya*) and high-elevation conifers clearly increase during the late Mid-Miocene and Late Miocene. This can be observed in the boreholes Deleina C-12 and Drenovets C-1 (Fig. 3).

In addition, an augmentation in herbs, mainly *Artemisia*, Amaranthaceae–Chenopodiaceae, Poaceae, Asteraceae, etc., during the Late Miocene and Pliocene, indicates more open vegetation, and drier conditions. Supporting this interpretation is the substitution of thermophilous elements with high humidity requirements all year (Asiatic-like vegetation) by mesothermic (mainly deciduous) elements which can survive under seasonal climate with respect to the precipitation (Popescu 2001; Ivanov *et al.* 2002; Jiménez-Moreno *et al.* 2005).

The noticeable increase in mesothermic plants and high-elevation conifers can be interpreted as a result of climate cooling, or by uplift of surrounding mountains (Kuhlemann & Kempf 2002). In both situations, altitudinal elements would increase.

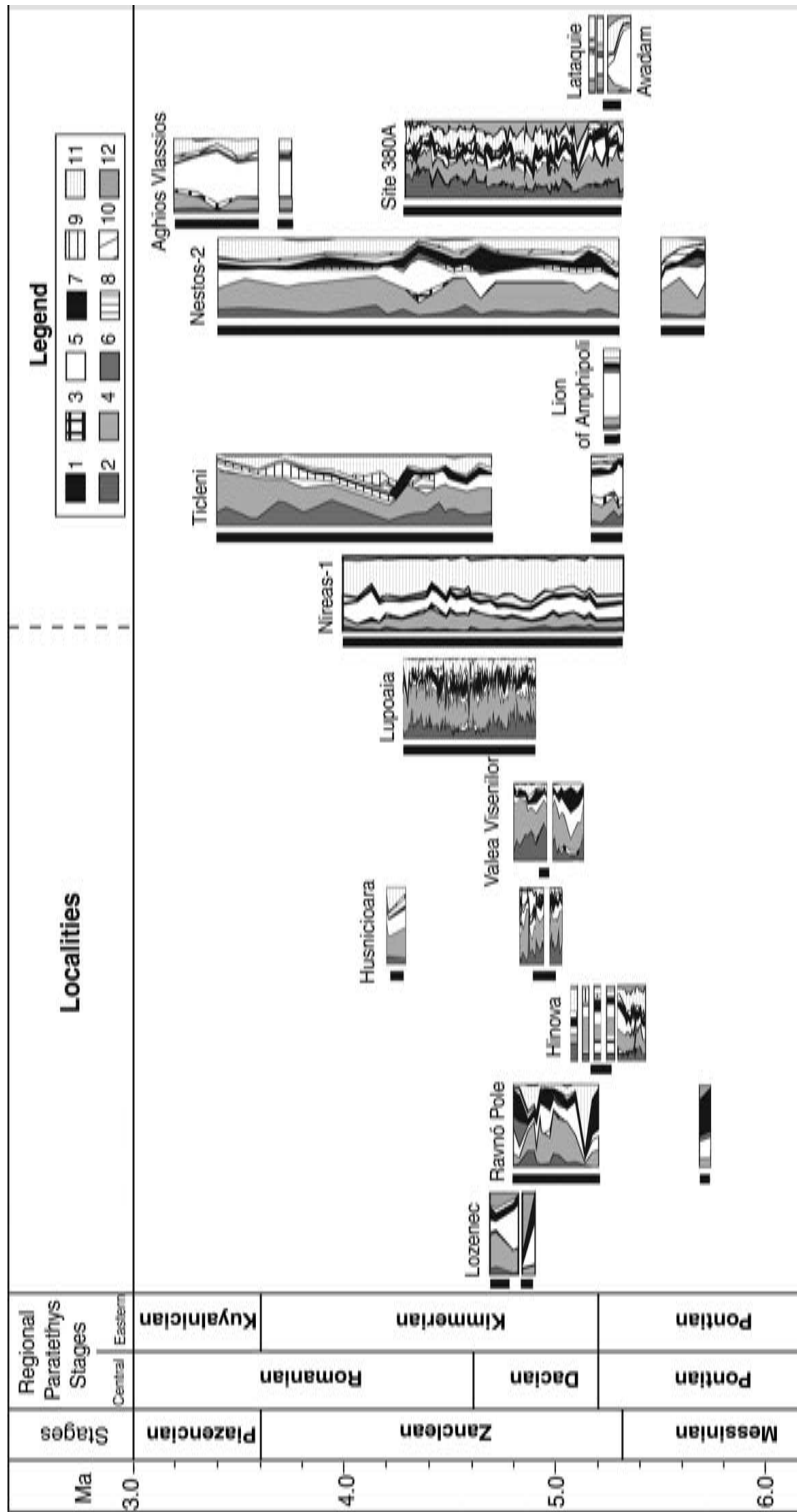


Fig. 4. Synthetic pollen diagrams of the studied sections spanning the Late Miocene (from 6 Ma) and Pliocene. For legend of plant groups, see Figure 3.

It is quite difficult to separate one process from another (global climatic forcing vs. the regional one), due to the tectonic situation of the studied area and the fact that they may have interfered. However, the vanishing of several thermophilous plants, which lived at low elevations and thus were not affected by the regional uplift, and the climate reconstructions using mainly taxa growing at low to middle–low altitude confirm a decrease in mean annual temperatures (Ivanov *et al.* 2002; Jiménez-Moreno *et al.* 2005; Mosbrugger *et al.* 2005). Then, it is clear that even if the uplift of the surrounding mountains may have influenced the regional climate, the evolution of the vegetation during both the Miocene and Pliocene was very dependent on the global climatic signal as shown in previous studies (Popescu 2001, 2002; Ivanov *et al.* 2002; Jiménez-Moreno *et al.* 2005). Hence, according also to the rapid nature of the recorded change in vegetation, we consider that global cooling was the most efficient forcing.

The origin of the steppe with *Artemisia*

Open herbaceous formations in the southern Mediterranean area are known since the Burdigalian (Suc *et al.* 1995a, b; Bachiri Taoufiq *et al.* 2001; Jiménez-Moreno 2005; Jiménez-Moreno & Suc in press). They were already well-developed during the Zanclean in other regions of the Mediterranean area (Suc *et al.* 1999) but were relatively poor in *Artemisia*. It is at the end of the Pliocene, as the climate got cooler and glacial–interglacial cycles appeared in the Northern Hemisphere, when the steppes with *Artemisia* became of significant importance (Suc *et al.* 1995b) during the glacial periods (Suc & Cravatte 1982; Combourieu-Nebout & Vergnaud Grazzini 1991; Beaudouin 2003) and even during interglacials (Subally *et al.* 1999) because of the ambivalent significance of *Artemisia* from the temperature viewpoint (cold vs. warm species: Subally & Quézel 2002).

The presence of steppe vegetation with *Artemisia* in the Ponto-Euxinian region (i.e. in Anatolia according to Site 380A pollen record; Popescu 2001, 2006) in the Late Miocene and their significant strengthening in the Early Pliocene is very informative. Their early presence and development in this region, contrary to the extreme scarcity of *Artemisia* in the Moroccan steppes in the Late Miocene and Early to Middle Pliocene (Bachiri Taoufiq 2000; Suc *et al.* 1999), indicates that Anatolia and neighbouring areas could have been the source area of this kind of vegetation for the rest of the Mediterranean region, a style of vegetation that became very abundant during the cold periods of the Quaternary (Popescu 2001; Suc & Popescu

2005). The early settlement and then development of *Artemisia* steppe vegetation in Anatolia may have resulted from migration from the east of this genus as a consequence of uplift of the Tibetan Plateau (where *Artemisia* species are still abundant today) and the succeeding reinforced Asiatic monsoon (Zhisheng *et al.* 2001).

Conclusions

Pollen data show a progressive reduction in the most thermophilous and high-water requirement plants typical of a broad-leaved evergreen forest and, in contrast, an increase in seasonal-adapted plants coming from higher altitude belts, including mesothermic (mainly deciduous) elements, altitudinal trees and herbs, during the Middle–Late Miocene and Pliocene. This has been interpreted as the response of the vegetation to global climate cooling, accentuated by the regional uplift of the surrounding mountains during Alpine tectonics. This process may also have been favoured by progressive movement of Eurasia towards northern latitudes.

The appearance of steppe vegetation with *Artemisia* on the Anatolian Plateau since the Late Miocene and its development in the Early Pliocene, significantly earlier than in the rest of Southern Europe, is informative. This suggests that the Anatolian *Artemisia*-rich steppes could have been the source area of this kind of open vegetal formation for the rest of the Mediterranean area during the Quaternary.

This paper is a contribution to the French Programme 'Environnement, Vie et Sociétés' (Institut Français de la Biodiversité). The authors thank J. Agustí and M. Harzhauser for their helpful reviews, and the EEDEN Programme (ESF) for invitations to participate in international workshops about the subject. Nurdan Yavuz-Isik is thanked for providing the Miocene samples from Turkey.

References

- AKGÜN, F. & AKYOL, E. 1999. Palynostratigraphy of the coal-bearing Neogene deposits graben in Büyük Menderes Western Anatolia. *Géobios*, **32**, 367–383.
- APOSTOL, L. & ENACHE, C. 1979. Etude de l'espèce *Dicerorhinus megarhinus* (de Christol) du bassin carbonifère de Motru. *Travaux du Musée d'Histoire Naturelle "Grigore Antipa"*, Bucarest, **20**, 533–540.
- BACHIRI TAOUFIQ, N. 2000. Les environnements marins et continentaux du corridor rifain au Miocène supérieur d'après la palynologie. PhD thesis, Université Hassan II – Mohammedia, Casablanca (Morocco).
- BACHIRI TAOUFIQ, N., BARHOUN, N., SUC, J.-P., MEON, H., ELAOUAD, Z. & BENBOUZIANE, A.

2001. Environment, végétation et climat du Messinien au Maroc. *Paleontologia i Evolució*, **32–33**, 127–138.
- BEAUDOUIN, C. 2003. Effets du dernier cycle climatique sur la végétation de la basse vallée du Rhône et sur la sédimentation de la plate-forme du golfe du Lion d'après la palynologie. PhD thesis, Université Claude Bernard Lyon-1, France, 403pp.
- BENDA, L. 1971. Grundzüge einer pollenanalytischen Gliederung des türkischen Jungtertiärs. *Beihefte zum Geologischen Jahrbuch*, **113**, 46pp.
- BENDA, L., HEISSIG, K. & STEFFENS, P. 1975. Die Stellung der vertebraten-faunengruppen der Türkei innerhalb der chronostratigraphischen systeme von Tethys und Paratethys. *Geologische Jahrbuch*, **B**, **15**, 109–116.
- BESSEDIK, M. 1985. Reconstitution des environnements Miocènes de régions nord-ouest méditerranéennes à partir de la palynologie. PhD thesis, Université de Montpellier, France, 162pp.
- BOHN-HAVAS, M. 1982. Mollusca fauna of Badenian and Sarmatian stage from the borehole Tengelic 2. In: NAGY, E., BODOR, E., HAGYAMAROSI, A. ET AL. (eds) *Palaeontological examination of the geological log of the borehole Tengelic 2*. Annales Instituti Geologici Publici Hungarici, **65**, 200–203.
- CAMBON, G., SUC, J.-P., ALOISI, J.-C. ET AL. 1997. Modern pollen deposition in the Rhône delta area (lagoonal and marine sediments) France. *Grana*, **36**, 105–113.
- CLAUZON, G., SUC, J.-P., POPESCU, S.-M., MARUNTEANU, M., RUBINO, J.-L., MARINESCU, F. & MELINTE, M. C. 2005. Influence of the Mediterranean sea-level changes over the Dacic Basin (Eastern Paratethys) in the Late Neogene. *Basin Research*, **17**, 437–462.
- COMBOURIEU-NEBOUT, N. & VERGNAUD GRAZZINI, C. 1991. Late Pliocene Northern hemisphere glaciation: the continental and marine responses in Central Mediterranean. *Quaternary Science Reviews*, **10**, 319–334.
- DRIVALIARI, A. 1993. Images polliniques et paléoenvironnement au Néogène supérieur en Méditerranée orientale. Aspects climatiques et paléogéographiques d'un transect latitudinal (de la Roumanie au Delta du Nil). PhD thesis, Université Montpellier-2, France, 333pp.
- DRIVALIARI, A., ȚICLEANU, N., MARINESCU, F., MĂRUNȚEANU, M. & SUC, J.-P. 1999. A Pliocene climatic record at Ticleni (Southwestern Romania). In: WRENN, J. H., SUC, J.-P. & LEROY, S. A. G. (eds) *The Pliocene: Time of Change*. American Association of Stratigraphic Palynologists Foundation, Dallas, 103–108.
- FORNACIARI, E. & RIO, D. 1996. Latest Oligocene to early Middle Miocene quantitative calcareous nannofossil biostratigraphy in the Mediterranean region. *Micropaleontology*, **42**, 1–36.
- FORNACIARI, E., DI STEFANO, A., RIO, D. & NEGRI, A. 1996. Middle Miocene quantitative calcareous nannofossil biostratigraphy in the Mediterranean region. *Micropaleontology*, **42**, 37–63.
- GONCHAROVA, I. A., SHCHERBA, I. G., KHONDKARIAN, S. O. ET AL. 2004. Lithological-Paleogeographic maps of Paratethys. Map 5: Early Middle Miocene. *Courier Forschungsinstitut Senckenberg*, **250**, 19–21.
- GRADSTEIN, F. M. & OGG, J. G. 2004. Geologic time scale 2004 – why, how, and where next! *Lethaia*, **37**, 175–181.
- GRADSTEIN, F. M., OGG, J. G., SMITH, A. G., BLEEKER, W. & LOURENS, L. J. 2004. A new geologic time scale with special reference to Precambrian and Neogene. *Episodes*, **27**, 83–100.
- GROMOLARD, C. & GUERIN, C. 1980. Mise au point sur *Parabos cordieri* (de Crystol), un Bovidé (Mammalia, Artiodactyla) du Pliocène d'Europe Occidentale. *Géobios*, **13**, 741–755.
- HARZHAUSER, M., MANDIC, O. & ZUSCHIN, M. 2003. Changes in Paratethyan marine molluscs at the Early/Middle Miocene transition: diversity, palaeogeography and palaeoclimate. *Acta Geologica Polonica*, **53**, 323–339.
- HARZHAUSER, M. & PILLER, W. E. 2004. The Early Sarmatian – hidden seesaw changes. *Courier Forschungsinstitut Senckenberg*, **246**, 89–112.
- HARZHAUSER, M. & PILLER, W. E. in press. Benchmark data of a changing sea – palaeogeography, palaeobiography and events in the Central Paratethys during the Miocene. *Palaeogeography, Palaeoclimatology, Palaeoecology*
- HEISSIG, K. 1976. Rhinocerotidae (Mammalia) aus der Anchiitherium-Fauna Anatoliens. *Geologisches Jahrbuch Reihe B*, **19**, 121pp.
- HEUSSER, L. 1988. Pollen distribution in marine sediments on the continental margin of Northern California. *Marine Geology*, **80**, 131–147.
- HSÜ, K. J. 1978. Correlation of Black Sea sequences. In: ROSS, D. A., NEPROCHNOV, Y. P. ET AL. (eds) *Initial Reports of the Deep Sea Drilling Project*, US Government Printing Office, **42**, 489–497.
- HSÜ, K. J. & GIOVANOLI, F. 1979. Messinian event in the Black Sea. *Palaeogeography, Palaeoclimatology, Palaeoecology*, **29**, 75–94.
- ILYINA, L. B., SHCHERBA, I. G., KHONDKARIAN, S. O. ET AL. 2004. Lithological-Paleogeographic maps of Paratethys. Map 6: Mid Middle Miocene. *Courier Forschungsinstitut Senckenberg*, **250**, 23–25.
- IVANOV, D. 1995. Palynological investigations of Miocene sediments from North-West Bulgaria (in Bulgarian, English abstract). PhD thesis, Institute of Botany BAS, Sofia, 45pp.
- IVANOV, D. A. & KOLEVA-REKALOVA, E. 1999. Palynological and sedimentological data about Lake Sarmatian palaeoclimatic changes in the Forecarpathian and Euxinian basins (Northern Bulgaria). *Acta Paleobotanica, Supplement*, **2**, 307–313.
- IVANOV, D., ASHRAF, A. R., MOSBRUGGER, V. & PALAMAREV, E. 2002. Palynological evidence for Miocene climate change in the Forecarpathian Basin (Central Paratethys, NW Bulgaria). *Palaeogeography, Palaeoclimatology, Palaeoecology*, **178**, 19–37.
- JIMÉNEZ-MORENO, G. 2005. Utilización del análisis polínico para la reconstrucción de la vegetación, clima y estimación de paleoaltitudes a lo largo de arco alpino europeo durante el Mioceno (21-8 m.a.). PhD thesis, Univ. Granada and Univ. C. Bernard – Lyon 1, 318pp.
- JIMÉNEZ-MORENO, G., RODRÍGUEZ-TOVAR, F. J., PARDO-IGÚZQUIZA, E., FAUQUETTE, S., SUC, J.-P.

- & MÜLLER, P. 2005. High resolution palynological analysis in the late early-middle Miocene core from the Pannonian Basin, Hungary: climatic changes, astronomical forcing and eustatic fluctuations in the Central Paratethys. *Palaeogeography, Palaeoclimatology, Palaeoecology*, **216**, 73–97.
- JIMÉNEZ-MORENO, G. & SUC, J.-P. in press. Middle Miocene Latitudinal Climatic Gradient in Western Europe: Evidence from Pollen Records. *Palaeogeography, Palaeoclimatology, Palaeoecology*.
- KOJUMDIEVA, E. 1976. Paléocologie des communautés des mollusques du Miocène en Bulgarie du Nord-Ouest. III. Communautés des mollusques du Volhynien (Sarmatien inférieur). *Geologica Balcanica*, **6**, 53–63.
- KOJUMDIEVA, E. & POPOV, N. 1989. Paléogéographie et évolution géodynamique de la Bulgarie Septentrionale au Néogène. *Geologica Balcanica*, **19**, 73–92.
- KOJUMDIEVA, E., NIKOLOV, I., NEDJALKOV, P. & BUSEV, A. 1982. Stratigraphy of the Neogene in the Sandanski Graben. *Geologica Balcanica*, **12**, 69–81.
- KOJUMDIEVA, E., POPOV, N., STANCHEVA, M. & DARAKCHIEVA, S. 1989. Correlation of the biostratigraphic subdivision of the Neogene in Bulgaria after molluscs, foraminifers and ostracods. *Geologica Balcanica*, **19**, 9–22.
- KOLEVA-REKALOVA, E. 1994. Sarmatian aragonite sediments in North-eastern Bulgaria – origin and diagenesis. *Geologica Balcanica*, **25**, 47–64.
- KORECZ-LAKY, I. 1982. Miocene foraminifera fauna from the borehole Tengelic 2. In: NAGY, E., BODOR, E., HAGYAMAROSI, A. ET AL. (eds) *Palaeontological examination of the geological log of the borehole Tengelic 2*, Annales Instituti Geologici Publici Hungarici, **65**, 186–187.
- KOVAC, M., BARATH, I., HARZHAUSER, M., HLAVATY, I. & HUDACKOVA, N. 2004. Miocene depositional systems and sequence stratigraphy of the Vienna Basin. *Courier Forschungsinstitut Senckenberg*, **246**, 187–212.
- KUHLEMANN, J. & KEMPF, O. 2002. Post-Eocene evolution of the North Alpine Foreland Basin and its response to Alpine tectonics. *Sedimentary Geology*, **152**, 45–78.
- LETOUZEY, J., GONNARD, R., MONTADERT, L., KRISTCHEV, K. & DORKEL, A. 1978. Black Sea: Geological setting and recent deposits distribution from seismic reflection data. In: ROSS, D. A., NEPROCHNOV, Y. P. ET AL. (eds) *Initial Reports of the Deep Sea Drilling Project*, US Government Printing Office, **42**, 1077–1084.
- LOURENS, L., HILGEN, F., SHACKLETON, N. J., LASKAR, J. & WILSON, D. 2004. The Neogene Period. In: GRADSTEIN, F., OGG, J. & SMITH, A. (eds) *Geologic Time Scale 2004*. Cambridge University Press.
- MAMATSASHVILI, N. S. 1975. The palynological characteristics of the Kolkhida Quaternary continental deposits (The Georgian SSR). *Metsniereba*, Tbilisi, 114pp.
- MARINESCU, F. 1978. Stratigrafia Neogenului superior din sectorul vestic al Bazinului Dacic. Editura Academiei Republicii Socialista România (in Romanian), 155pp.
- MĂRUNȚEANU, M. & PAPAIAPOPOL, I. 1995. L'association de nannoplankton dans les dépôts roumains situés entre les vallées de Cosmina et de Cricovu Dulce (Munténie, bassin dacique, Roumanie). *Romanian Journal of Paleontology*, **76**, 169–170.
- MĂRUNȚEANU, M. & PAPAIAPOPOL, I. 1998. Mediterranean calcareous nannoplankton in the Dacic Basin. *Romanian Journal of Stratigraphy*, **78**, 115–121.
- MEULENKAMP, J. E. & SINGH, W. 2003. Tertiary palaeogeography and tectonostratigraphic evolution of the Northern and Southern Peri-Tethys platforms and the intermediate domains of the African-Eurasian convergent plate boundary zone. *Palaeogeography, Palaeoclimatology, Palaeoecology*, **196**, 209–228.
- MILLER, K. G., FEIGENSON, M., WRIGHT, J. D. & CLEMENT, B. 1991. Miocene isotope reference section, Deep Sea Drilling Project Site 608: an evaluation of isotope and biostratigraphic resolution. *Palaeoceanography*, **6**, 33–52.
- MOSBRUGGER, V., UTESCHER, T. & DILCHER, D. L. 2005. Cenozoic continental climatic evolution of Central Europe. *PNAS*, **102**, 14964–14969.
- NAGY, E. 1991. Climatic changes in the Hungarian Neogene. *Review of Palaeobotany and Palynology*, **65**, 71–74.
- NAGY, E. 1992. Magyarorszag Neogen sporomorphainak ertekelese. *Geologica Hungarica*, **53**, 1–379.
- NAGY, E. 1999. *Palynological correlation of the Neogene of the Central Paratethys*. Geological Institute of Hungary, Budapest, 149pp.
- NAGY, E. & KÓKAY, J. 1991. Middle Miocene mangrove vegetation in Hungary. *Acta geologica Hungarica*, **34**, 45–52.
- NAGYMAROSI, A. 1982. Badenian-Sarmatian nannoflora from the borehole Tengelic 2. In: NAGY, E., BODOR, E., HAGYAMAROSI, A. ET AL. (eds) *Palaeontological examination of the geological log of the borehole Tengelic 2*, Annales Instituti Geologici Publici Hungarici, **65**, 145–149.
- PALAMAREV, E. 1991. Composition, structure and main stages in the evolution of Miocene paleoflora in Bulgaria. Dsc thesis, (in Bulgarian). BAS, Sofia, 60pp.
- PALAMAREV, E. & IVANOV, D. 2001. Charakterzüge der vegetation des Sarmatien (Mittel- bis Obermiozän im südlichen Teil des Dazischen Beckens (Südost Europa)). *Palaeontographica*, **B259**, 209–220.
- PALAMAREV, E. & IVANOV, D. 2004. Badenian vegetation of Bulgaria: biodiversity, palaeoecology and palaeoclimate. *Courier Forschungsinstitut Senckenberg*, **249**, 63–69.
- PAPAIAPOPOL, I. & MĂRUNȚEANU, M. 1993. Biostratigraphy (molluscs and calcareous nannoplankton) of the Sarmatian and Meotian in eastern Muntenia (dacic basin-Rumania). *Zemni plyn a nafta*, **38**, 9–15.
- PAPAIAPOPOL, I. & MARINESCU, F. 1995. Lithostratigraphy and age of Neogene deposits on the Moesian Platform, between Olt and Danube Rivers. *Romanian Journal of Stratigraphy*, **76**, 67–70.
- PAPAIAPOPOL, I. & MOTAS, I. C. 1978. Marqueurs biostratigraphiques pour dépôt post-chersoniens du Bassin Dacique. *Dari de Seama ale Institutului de Geologie si Geofizica*, Stratigrafie, **64**, 283–294.
- PAPAIAPOPOL, I., JIPA, D., MARINESCU, F., ȚICLEANU, N. & MACALET, R. 1995. Upper Neogene from the

- Dacic Basin – Guide to excursion B2 (post-congress) X congress RCMNS, Bucuresti. *Romanian Journal of Stratigraphy*, **76**, 1–43.
- PARAMONOVA, N. P., SHCHERBA, I. G. & KHONDAKARIAN, S. O. 2004. Lithological-Paleogeographic maps of Paratethys. Map 7: Late Middle Miocene (Late Serravallian, Sarmatian s.s., Middle Sarmatian s.l.). *Courier Forschungsinstitut Senckenberg*, **250**, 27–31.
- PETRESCU, I. & MALAN, L. 1992. *Contributions to the knowledge of Upper Neogene microflora East of Turnu-Severin (Summary)*. Univ. Babeş-Bolyai, Cluj-Napoca Gradina Botanica, Contributii Botanice 1991–1992: 135–143.
- PETRESCU, I., CERNITA, P., MEILESCU, C. *ET AL.* 1989a. Preliminary approaches to the palynology of the Lower Pliocene (Dacian) deposits in the Husnicioara area (Mehedinti county, SW Romania). *Studia Universitatis Babeş-Bolyai Geologia-Geografia*, **34**, 67–74.
- PETRESCU, I., NICA, T., FILIPESCU, S. *ET AL.* 1989b. Paleoclimatical significance of the palynological approach to the Pliocene deposits of Lupoiaia (Gorj county). *Studia Universitatis Babeş-Bolyai Geologia-Geografia*, **34**, 75–81.
- PLANDEROVÁ, E. 1990. *Miocene microflora of slovak Central Paratethys and its biostratigraphical significance*. Dionyz Stur Institute of Geology, Bratislava (Slovakia), 143pp.
- PLAZIAT, J.-C., CAVAGNETTO, C., KOENIGUER, J.-C. & BALTZER, F. 2001. History and biogeography of the mangrove ecosystem, based on a critical reassessment of the paleontological record. *Wetlands Ecology and Management*, **9**, 161–179.
- POPESCU, S.-M. 2001. *Végétation, climat et cyclostratigraphie en Paratéthys centrale au Miocène supérieur et au Pliocène inférieur d'après la palynologie*. PhD thesis. Université Claude Bernard Lyon-1, Lyon, France.
- POPESCU, S.-M. 2002. Repetitive changes in Early Pliocene vegetation revealed by high-resolution pollen analysis: revised cyclostratigraphy of southwestern Romania. *Review of Palaeobotany and Palynology*, **120**, 181–202.
- POPESCU, S.-M. 2006. Upper Miocene and Lower Pliocene environments in the southwestern Black Sea region from high-resolution palynology of DSDP site 380A (Leg 42B). *Palaeogeography, Palaeoclimatology, Palaeoecology*, **238**, 64–77.
- POPESCU, S.-M., KRIJGSMAN, W., SUC, J.-P., CLAUZON, G., MARUNTEANU, M. & NICA, T. 2006a. Pollen record and integrated high-resolution chronology of the early-Pliocene Dacic Basin (Southwestern Romania). *Palaeogeography, Palaeoclimatology, Palaeoecology*, **238**, 78–90.
- POPESCU, S.-M., SUC, J.-P. & LOUTRE, M.-F. 2006b. Early Pliocene vegetation changes forced by eccentricity-precession. Example from Southwestern Romania. *Palaeogeography, Palaeoclimatology, Palaeoecology*, **238**, 340–348.
- POPOV, S. V., RÖGL, F., ROZANOV, A. Y., STEININGER, F. F., SHCHERBA, I. G. & KOVAC, M. (eds) 2004. Lithological-Paleogeographic maps of Paratethys. 10 maps Late Eocene to Pliocene. *Courier Forschungsinstitut Senckenberg*, **250**, 1–46.
- QUÉZEL, P. & MÉDAIL, F. 2003. *Ecologie et biogéographie des forêts du bassin méditerranéen*, Elsevier France, 571pp.
- RADAN, S. C. & RADAN, M. 1998. Study of the geomagnetic field structure in the Tertiary in the context of magnetostratigraphic scale elaboration. I – The Pliocene. *An. Inst. Geol. Rom.*, **70**, 215–231.
- RADULESCU, C., SAMSON, P.-M., SEN, S., STIUCA, E. & HOROI, V. 1997. Les micromammifères pliocènes de Deanic (bassin Dacique, Roumanie). In: AGUILAR, J.-P., LEGENDRE, S. & MICHAUX, J. (eds) *Biochrom'97*, Mémoires Travaux E.P.H.E., Institute Montpellier, **21**, 635–647.
- RÖGL, V. F. 1998. Palaeogeographic considerations for Mediterranean and Paratethys seaways (Oligocene to Miocene), *Annalen des Naturhistorischen Museums in Wien*, **99A**, 279–310.
- SACHSE, M., MOHR, B. & SUC, J.-P. 1999. The Makrilaflora (Crete, Greece) – a contribution to the Neogene history of the climate and vegetation of the Eastern Mediterranean. *Acta palaeobotanica*, **Supplement 2**, 365–372.
- SEMENENKO, V. N. & OLEJNIK, E. S. 1995. Stratigraphic correlation of the Eastern Paratethys Kimmerian and Dacian stages by molluscs, dinocyst and nannoplankton data. *Rom. J. Stratigraphy*, **76**, 113–114.
- SHEVENELL, A. E., KENNETT, J. P. & LEA, D. W. 2004. Middle Miocene southern cooling and Antarctic cryosphere expansion. *Science*, **305**, 1766–1770.
- SICKENBERG, O., BECKER-PLATEN, J. D., BENDA, L. *ET AL.* 1975. Die Gliederung des höheren Jungtertiärs und Altquartärs in der Türkei nach Vertebraten und ihre Bedeutung für die internationale Neogen-Stratigraphie. *Geologisches Jahrbuch Reihe B*, **15**, 167pp.
- SNEL, E., MĂRUNTEANU, M., MACALET, R., MEULENKAMP, J. E. & VAN VUGT, N. 2006. Late Miocene to Early Pliocene chronostratigraphic framework for the Dacic Basin, Romania. *Palaeogeography, Palaeoclimatology, Palaeoecology*, **238**, 107–124.
- SPAACK, P. 1983. Accuracy in correlation and ecological aspects of the planktonic foraminiferal zonation of the Mediterranean Pliocene. *Utrecht Micropalaeontological Bulletin*, **28**, 160pp.
- SPROVIERI, R. 1992. Mediterranean Pliocene biochronology: a high resolution record based on quantitative planktonic foraminifera distribution. *Rivista Italiana di Paleontologia e Stratigrafia*, **98**, 61–100.
- SPROVIERI, R., BONOMO, S., CARUSO, A. *ET AL.* 2002. An Integrated calcareous plankton biostratigraphic scheme and biochronology of the Mediterranean Middle Miocene. *Rivista Italiana di Paleontologia e Stratigrafia*, **108**, 337–353.
- STEININGER, F. F. 1999. Chronostratigraphy, Geochronology and Biochronology of the “European Land Mammal Mega-Zones” (ELMMZ) and the Miocene “Mammal-Zones” (MN-Zones). In: RÖSSNER, G. E. & HEISSIG, K. (eds) *The Miocene Land Mammals of Europe*. Dr. Friedrich Pfeil, München, Germany, 9–24.
- SUBALLY, D., BILLODEAU, G., TAMRAT, E., FERRY, S., DEBARD, E. & HILLAIRE-MARCEL, C. 1999. Cyclic climatic records during the Olduvai subchron (uppermost Pliocene) on Zakynthos Island (Ionian Sea). *Geobios*, **32**, 793–803.

- SUBALLY, D. & QUÉZEL, P. 2002. Glacial or interglacial: *Artemisia* a plant indicator with dual responses. *Review of Palaeobotany and Palynology*, **120**, 123–130.
- SUC, J.-P. 1984. Origin and evolution of the Mediterranean vegetation and climate in Europe. *Nature*, **307**, 429–432.
- SUC, J.-P. & CRAVATTE, J. 1982. Etude palynologique du Pliocène de Catalogne (nord-est de l'Espagne). *Paléobiologie Continentale*, **13**, 1–31.
- SUC, J.-P. & DRIVALIARI, A. 1991. Transport of bisaccate coniferous fossil pollen grains to coastal sediments: an example from the earliest Pliocene Orbria (Languedoc, Southern France). *Review of Palaeobotany and Palynology*, **70**, 247–253.
- SUC, J.-P. & POPESCU, S.-M. 2005. Pollen records and climatic cycles in the North Mediterranean region since 2.7 Ma. In: HEAD, M. J. & GIBBARD, P. L. (eds) *Early–Middle Pleistocene Transitions: The Land–Ocean Evidence*. Geological Society of London, Special Publication, **247**, 147–158.
- SUC, J.-P., DINIZ, F., LEROY, S. *ET AL.* 1995a. Zanclean (~ Brunsumian) to early Piacenzian (~ early-middle Reuverian) climate from 4° to 54° north latitude (West Africa, West Europe and West Mediterranean areas). *Mededelingen Rijks Geologische Dienst*, **52**, 43–56.
- SUC, J.-P., BERTINI, A., COMBORIEU-NEBOUT, N. *ET AL.* 1995b. Structure of West Mediterranean vegetation and climate since 5.3 Ma. *Acta zoologica Cracoviense*, **38**, 3–16.
- SUC, J.-P., FAUQUETTE, S., BESSEDIK, M. *ET AL.* 1999. Neogene vegetation changes in West European and West circum-Mediterranean areas. In: AGUSTÍ, J., ROOK, L. & ANDREWS, P. (eds) *The Evolution of Neogene Terrestrial Ecosystems in Europe*. Cambridge University Press, Cambridge, 378–388.
- THOMAS, H., SPASSOV, N., KODJUMJIEVA, E. *ET AL.* 1986. Résultats préliminaires de la première mission paléontologique franco-bulgare à Dorkovo (arrondissement de Pazardjik, Bulgarie). *Comptes Rendus de l'Académie des Sciences, Paris*, **302**, 1037–1042.
- TICLEANU, N. & DIACONITA, D. 1997. The main coal facies and lithotypes of the Pliocene coal basin, Oltenia, Romania. In: GAYER, R. & PESEK, J. (eds) *European Coal Geology and Technology*, Geological Society, London, Special Publication, **125**, 131–139.
- VAN VUGT, N., LANGEREIS, C. G. & HILGEN, F. J. 2001. Orbital forcing in Pliocene-Pleistocene Mediterranean lacustrine deposits: dominant expression of eccentricity versus precession. *Palaeogeography, Palaeoclimatology, Palaeoecology*, **172**, 193–205.
- WANG, C. W. 1961. The forests of China with a survey of grassland and desert vegetation. Maria Moors Cabot Foundation, **5**, Harvard University Cambridge, Massachusetts, 313pp.
- ZACHOS, J., PAGANI, M., SLOAN, L. & BILLUPS, K., 2001. Trends, rhythms, and aberrations in global climate 65 Ma to present. *Science*, **292**, 686–693.
- ZHISHENG, A., KUTZBACH, J., PRELL, W. L. & PORTER, S. C. 2001. Evolution of Asian monsoons and phased uplift of the Himalaya-Tibetan plateau since Late Miocene times. *Nature*, **411**, 62–66.
- ZOHARY, M. 1973. Geobotanical foundations of the Middle East. Fischer ed., Stuttgart, **2 vol.**, 739pp.



ELSEVIER

Review of Palaeobotany and Palynology 120 (2001) 181–202

**Review of
Palaeobotany
& Palynology**

www.elsevier.com/locate/revpalbo

Repetitive changes in Early Pliocene vegetation revealed by high-resolution pollen analysis: revised cyclostratigraphy of southwestern Romania

Speranta-Maria Popescu *

Laboratoire 'PaléoEnvironnements et PaléobioSphère', Université Claude Bernard - Lyon 1, 27-43 boulevard du 11 Novembre, 69622 Villeurbanne Cedex, France

Received 16 February 2001; received in revised form 11 October 2001; accepted 29 October 2001

Abstract

A high-resolution pollen analysis has been carried out on the Lupoia section (SW Romania) in order to check whether the repetitive clay–lignite alternations correspond to cyclic changes in climate. Increases in altitudinal tree pollen content appear to have been caused by drops in temperature, while developments of thermophilous elements correspond to rises in temperature, still under humid conditions. Such repeated changes in vegetation, on the whole consistent with the clay–lignite alternations, have been forced by cycles in eccentricity. On the basis of a comparison between the Lupoia pollen record and (1) European climatostratigraphy (based on reference pollen diagrams documenting global changes), and (2) global climatic curves (eccentricity, $\delta^{18}\text{O}$), the age of the section has been reconsidered. The Lupoia section (i.e. from lignite IV to lignite XIII) starts just before the C3n.3n Chron and probably ends just before the C3n.1n Chron. The section represents a time span of about 600 kyr, i.e. from about 4.90 Ma to about 4.30 Ma. © 2001 Elsevier Science B.V. All rights reserved.

Keywords: pollen analysis; vegetation; cyclostratigraphy; Pliocene; Romania

1. Introduction

During the last decades, palynological efforts have been made to obtain a good knowledge of the European and Mediterranean Pliocene vegetation and climate (Zagwijn, 1960; Menke, 1975; Diniz, 1984; Suc, 1984a; Zheng and Cravatte, 1986; Drivaliari, 1993; Bertini, 1994). Today, reconstructions of vegetation and climate are coherent for North-European to Mediterranean lati-

tudes during the whole Pliocene, more especially the Early Pliocene (i.e. the Zanclean stage from 5.32 to 3.6 Ma) (Suc and Zagwijn, 1983; Suc et al., 1995). In addition, a climate transfer function, based on pollen records, has been introduced, which underlines subtropical temperatures in southwestern Europe during the Early Pliocene (for example, 16.5°C as mean annual temperature in the Nice area) (Fauquette et al., 1999a).

Early Pliocene pollen data show consistent vegetation changes in Europe from north (Zagwijn, 1960; Menke, 1975) to south (Suc, 1984a; Bertini, 1994; Zheng and Cravatte, 1986), as well as from west (Diniz, 1984) to east (Drivaliari et al., 1999),

* Fax: +33-4-72448382.

E-mail address: popescu@univ-lyon1.fr (S.-M. Popescu).

that allow the subdivision of the period into three main climatic phases. Two main warm phases (Brunssumian A and C of Zagwijn (1960), pollen zones P Ia and P Ic of Suc (1984a)) encompass the first relative cooling episode (Brunssumian B of Zagwijn (1960), pollen zone P Ib of Suc (1984a)). This subdivision is in accordance with the large variations observed in the $\delta^{18}\text{O}$ curve from the ocean record (Tiedemann et al., 1994; Shackleton et al., 1995). Most of the European reference pollen diagrams include secondary fluctuations within the above mentioned climatic phases of the Early Pliocene (Susteren in The Netherlands: Zagwijn, 1960; Oldenswort 9 in Germany: Menke, 1975; Garraf 1 in the north-western Mediterranean shelf off-shore Spain: Suc and Cravatte, 1982; Rio Maior F 14 in Portugal: Diniz, 1984). Unfortunately, these pollen records have been established on a somewhat low number of samples, that do not allow accurate correlation with the continuous $\delta^{18}\text{O}$ record, and therefore with the astronomic parameters.

Van der Zwaan and Gudjonsson (1986) have established the first $\delta^{18}\text{O}$ record at a relative high-resolution for the Pliocene of Sicily which

shows many fluctuations. More recently, Tiedemann et al. (1994) and Shackleton et al. (1995) have demonstrated that such $\delta^{18}\text{O}$ fluctuations are astronomically forced by precession (ca. 20-kyr cycles). In addition, Hilgen (1990, 1991a,b) has established a very accurate time scale for the Mediterranean Lower Pliocene based both on magnetostratigraphy and sedimentological cyclostratigraphy. It was demonstrated that rapid changes in sedimentation were simultaneously forced by precession and eccentricity (100- and 400-kyr cycles).

Certain long, continuous and very propitious land sections can provide high-resolution pollen records that may reveal whether the changes in vegetation are induced by astronomic cycles. The pollen records from Stirone and Monticino (Lower Zanclean of the Po Valley) suggest, despite a low sampling resolution, cyclic variations in the vegetation that are forced by eccentricity (Bertini, 1994). The Lupoia section (southwestern Romania; Fig. 1) offers a long Early Pliocene sedimentary record, characterised by almost regular clay–lignite alternations which have been linked to eccentricity forcing (Van Vugt et al.,

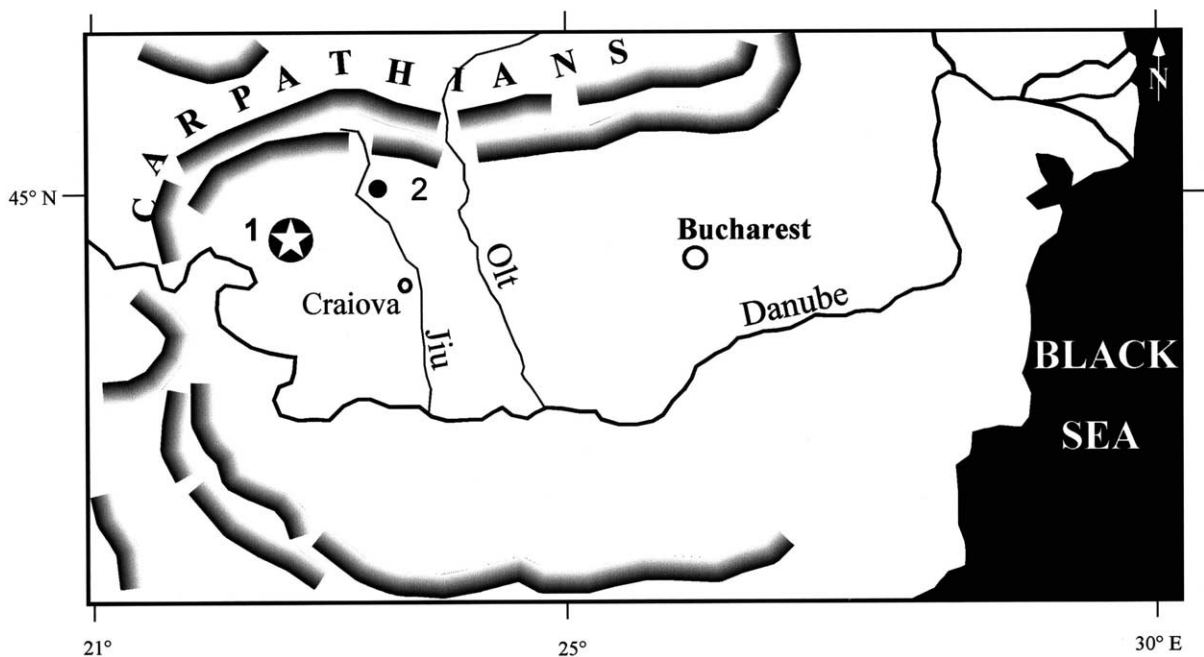


Fig. 1. Location of the Lupoia section in the Dacic Basin. (1) Lupoia, (2) Ticleni borehole.

2001). However, Van Vugt et al. (1998) have demonstrated that the lignite–clay alternations of the Early Pliocene Ptolemais lacustrine basin (north-western Greece) were forced by precession: these lignites would correspond to drier phases and clays to moister phases (Kloosterboer-van Hoeve, 2000).

Accordingly, a high-resolution pollen investigation was carried out on the Lupoia long section in order (1) to know whether Early Pliocene vegetation changes are related to astronomical cycles, and (2) to contribute to the clarification of the climatic significance of lignites located in the eastern Mediterranean region.

2. The Lupoia section

2.1. General characters

The Lupoia quarry is located near the city of Motru (district of Gorj, Romania) close to the Carpathians in Oltenia, some 30 km north of the Danube river (Fig. 1). The quarry is especially characterised by clay–lignite alternations, and includes several sand layers of various thickness. The sedimentary record toward the base of the series has been recovered by cored boreholes.

The Lupoia quarry is 121.50 m high and shows nine major lignite beds corresponding to lignite V to lignite XIII in the regional nomenclature. Some of them have been subdivided into two or three secondary layers as lignites VIII and X (Fig. 2). The underlying sediments cored in boreholes F6 (thickness: 21.20 m) and F11 include the lower layer of lignite V and lignite IV. The present palynological study begins below lignite IV and finishes above lignite XIII (Fig. 2), corresponding to a thickness of 133.70 m. Some other thin lignite or lignitic clay layers have been recorded. Blue-grey clays are abundant in the section and rich in leaf prints (Ticleanu and Buliga, 1992; Ticleanu and Diaconita, 1997). Fluvial sands are mainly concentrated in the mid and the upper part of the section (Fig. 2). The thickness of the different layers varies within the Motru Basin; for example, sands are thicker in the south and the lignite beds contain more subdivisions towards the

south-east. According to Ticleanu and Diaconita (1997), the Motru lignites belong to a deltaic system which, according to Clauzon and Suc (personal information), flowed into the Dacic Sea close to the Zanclean Danube delta, in the area of Dobreta Turnu Severin.

2.2. Chronology

Radan and Radan (1998) have performed palaeomagnetic measurements of samples from both the Lupoia quarry (more than 1000 samples) and two cored boreholes F6 and F11 (about 380 samples). Two normal palaeomagnetic events were identified in the lowermost part (from clays overlying lignite IV to the upper lignite V) and in the mid-part of the section (from about lignite VII to lignite VIII; Fig. 2), respectively. The lower normal episode is preceded by a relatively prolonged undetermined polarity zone, while another one has been identified above lignite XIII (Fig. 2). Some other thin undetermined polarity zones occur along the section but they mostly correspond to lignites which do not constitute a very good lithology for palaeomagnetic measurements. Radan and Radan (1998) have considered these normal episodes to represent the C3n.2n Chron (i.e. the Nunivak Chron) and the C3n.1n Chron (i.e. the Cochiti Chron), respectively. To identify the two normal episodes, the authors used as biostratigraphic argument the presence within lignite VIII (Fig. 2) of a primitive *Mimomys* (*Mimomys rhabonensis*) considered to be representative of the lowermost mammal zone MN 15 (Radulescu et al., 1997). However, it is assumed that the primitive *Mimomys* have appeared in Romania at the same time as in the northwestern Mediterranean region, i.e. after the C3n.1n Chron (locality of Mas Soulet, Nîmes area) (Aguilar and Michaux, 1984; Aguilar et al., 1999). In other words, it is considered that the ‘boundary’ between mammal zones MN 14 and MN 15 is coeval in eastern Europe and western Europe, a concept that is currently topic of strong international discussion (ad hoc Working Group of the Regional Committee on the Mediterranean Neogene Stratigraphy). In northern Greece, the first *Mimomys* (*Mimomys davakosi*) is recorded in the Ptolemais 3 locality

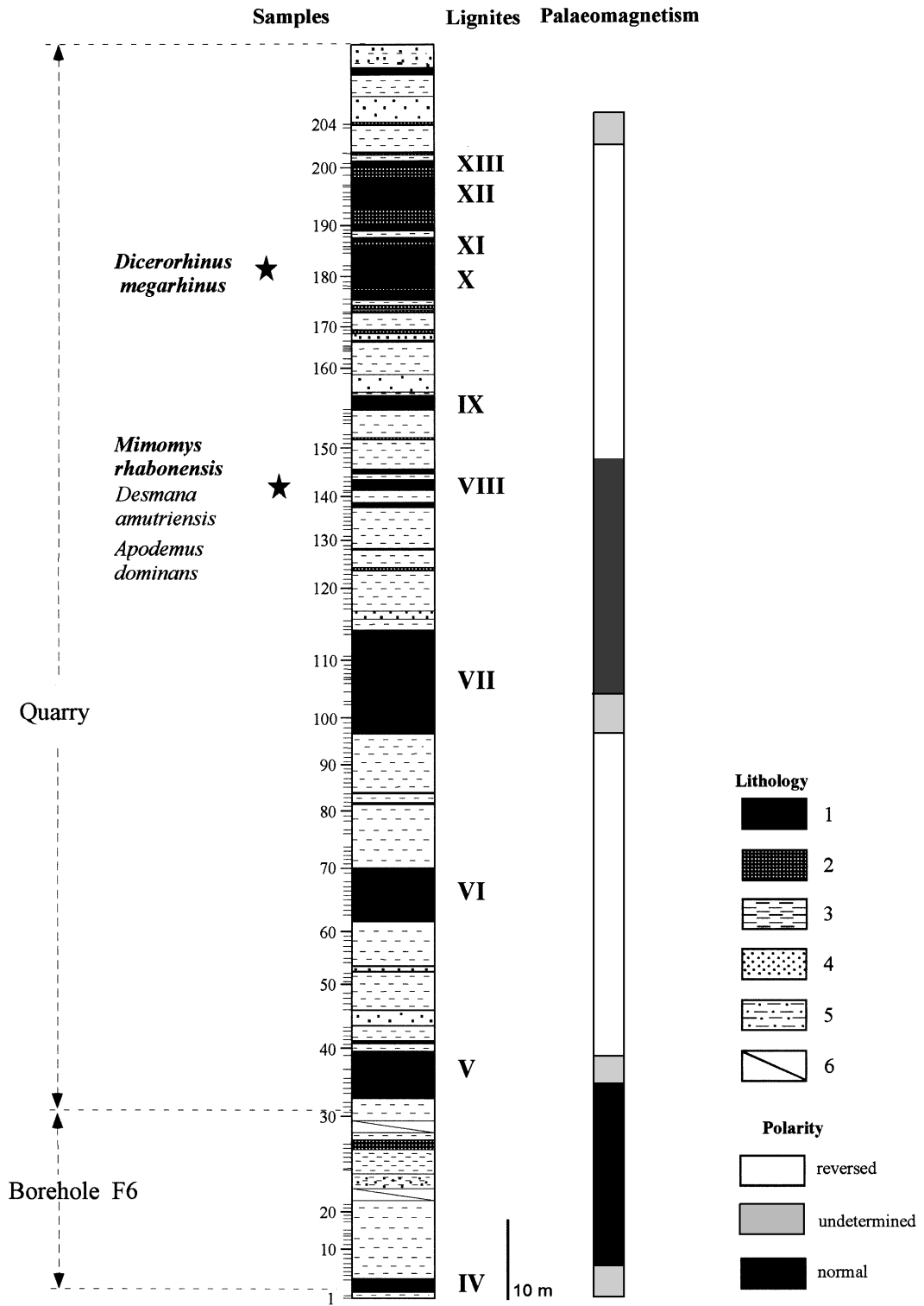


Fig. 2.

(Van de Weerd, 1978) that would belong to the C3n.3n Chron (Van Vugt et al., 1998) according to the stratigraphic information provided by Van de Weerd (1978), Koufos and Pavlides (1988) and Van Vugt et al. (1998). Magnetostratigraphy of the Ptolemais section suggests that *Mimomys* appeared earlier in eastern Europe than in western Europe. This view is also supported by the first appearance of the ancestor of *Mimomys*, *Promimomys insuliferus*, which, in the Ptolemais section (Kardia locality; Van de Weerd, 1978) would occur in a time span including the C3n.4n Chron (Van Vugt et al., 1998) according to the local stratigraphic information (Van de Weerd, 1978; Koufos and Pavlides, 1988; Van Vugt et al., 1998). As a consequence, there is no reliable argument provided by micromammals to support the chronological assignment of the Lupoia section to the successive chrons C3n.2n and C3n.1n. Using a cryogenic magnetometer, Van Vugt et al. (2001) have confirmed the polarity reversals of the Lupoia quarry (78 samples going from lignite V to lignite IX), including two relatively prolonged undetermined polarity zones (within and above lignite V, within lignite VII) (Fig. 2). The authors followed the same chronological interpretation; in their opinion, the reversed episode recorded in the upper part of the section could be assigned, considering its relatively important duration, to the long reversal C2Ar. Such an interpretation does not take into account possible changes in sedimentation rate in the uppermost part of the section, which is richer in lignite and sand beds.

Among the other micromammal remains found in the lignite bed VIII of the quarry, there is *Apodemus dominans*, which is a common species in the European Pliocene, and also found in the three mammal localities of Ptolemais (Van de Weerd, 1978).

Further information is provided by the discovery of *Dicerorhinus megarhinus* remains in the

Horăști mine (Motru Basin) lignite X (Apostol and Enache, 1979). According to Guérin (1980), this species corresponds to the Lower Pliocene (Mammal Zones 14 and 15). The size of the Horăști mine specimen (Apostol and Enache, 1979) is almost similar to that from the specimen of Montpellier (De Serres, 1819). In western Europe, the range of the species should be comprised between about 5 and 4 Ma.

Therefore, mammal fauna does not provide an unquestionable chronological support to the proposed magnetostratigraphic assignment (Radan and Radan, 1998; Van Vugt et al., 2001); on the contrary, the data suggest an age older than that proposed for the Lupoia section.

3. Materials and methods

Numerous samples (231) of clays and lignites have been analysed from the Lupoia section. Most of them (204) have provided a rich pollen flora. Samples 1–31 come from the cored borehole F6, samples 32–204 come from the quarry (Fig. 2).

Clay samples have been prepared following the classic method (successive actions by HCl, HF, etc.; concentration of palynomorphs using ZnCl₂ at density=2, then filtering at 10 μm). Another technical approach has been used for the lignites, starting with a KOH action which replaces the acids. Samples are mounted in glycerine to allow complete observation of palynomorphs, necessary for their proper botanical identification. More than 150 pollen grains (*Pinus*, a generally over-represented element in the pollen flora, excluded) have been counted per sample. Results are given in a simplified detailed pollen diagram where pollen percentages are calculated relative to the total pollen sum (Fig. 3). Spores (pteridophytes, bryophytes, fungi), algae and dinoflagellate cysts have been scored separately. Dry samples have been

Fig. 2. Lithological succession of the Lupoia section (quarry and cored borehole F6) and its magnetostratigraphic subdivision (Radan and Radan, 1998; Van Vugt et al., 2001); stratigraphic locations of mammal remains are indicated. Lithology: (1) lignite; (2) lignitic clay; (3) clay; (4) sand; (5) sandy clay; (6) not recovered interval within borehole F6.

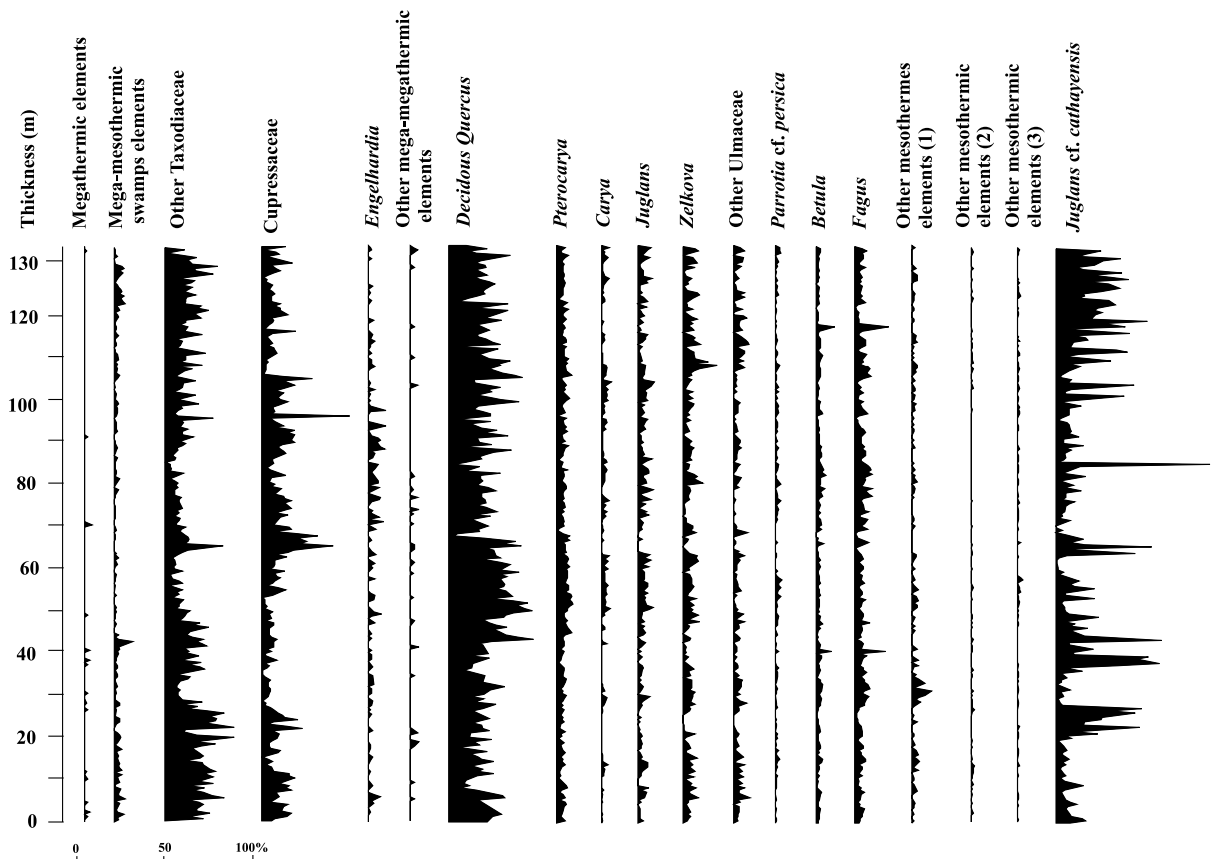


Fig. 3.

weighted, and volumes of residues after treatment were measured in order to calculate pollen concentrations using the method described by [Cour \(1974\)](#). A synthetic pollen diagram has been constructed according to the ecological requirements of taxa ([Fig. 4](#)). Such standard synthetic pollen diagrams ([Suc, 1984a](#)) clearly document temporal changes in pollen content, and aid in comparisons between pollen records throughout Europe and the Mediterranean region; they are generally used for detecting long-distance climatostratigraphic relationships ([Suc et al., 1995](#)).

Interpretations of the pollen records are also supported by statistical analyses (principle component analysis, spectral analysis).

Pollen and spore counts from the Lupoia section are archived at the Laboratory 'PaléoEnvironnements et PaléobioSphère' (University Claude Bernard - Lyon 1) and will be available

from the 'Cenozoic Pollen and Climatic values' database (CPC)¹.

4. Pollen flora and vegetation

The pollen flora is very rich (137 taxa; [Fig. 3](#)), and dominated by trees. These results considerably increase the known floristic palaeodiversity of the area (the delta environment to the altitudinal belts of the Carpathians), when compared to the preliminary palynological study of [Petrescu et al. \(1989\)](#), and the analyses of palaeobotanical macrofossils ([Ticleanu, 1992](#); [Ticleanu and Dia-](#)

¹ For further information, contact Dr. Séverine Fauquette (same address as the author), curator of the CPC database (severine.fauquette@univ-lyon1.fr).

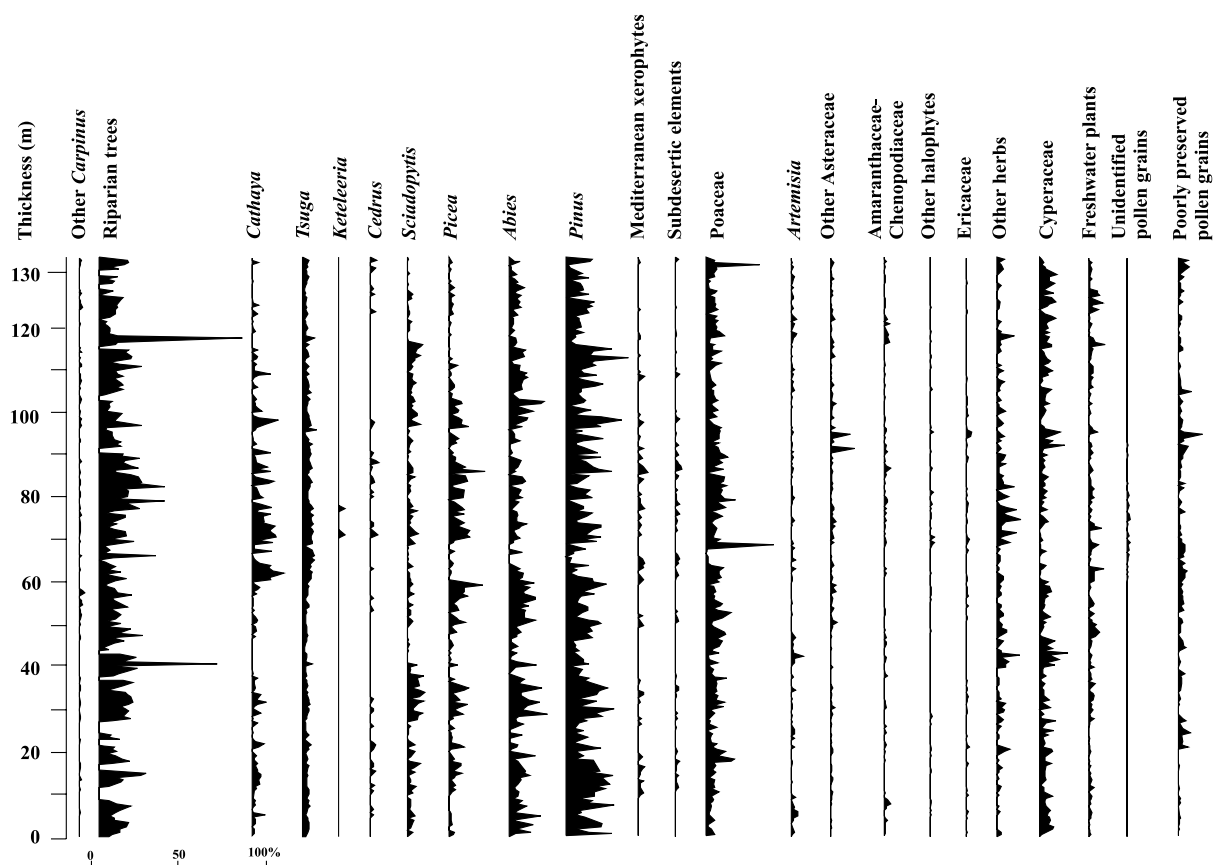
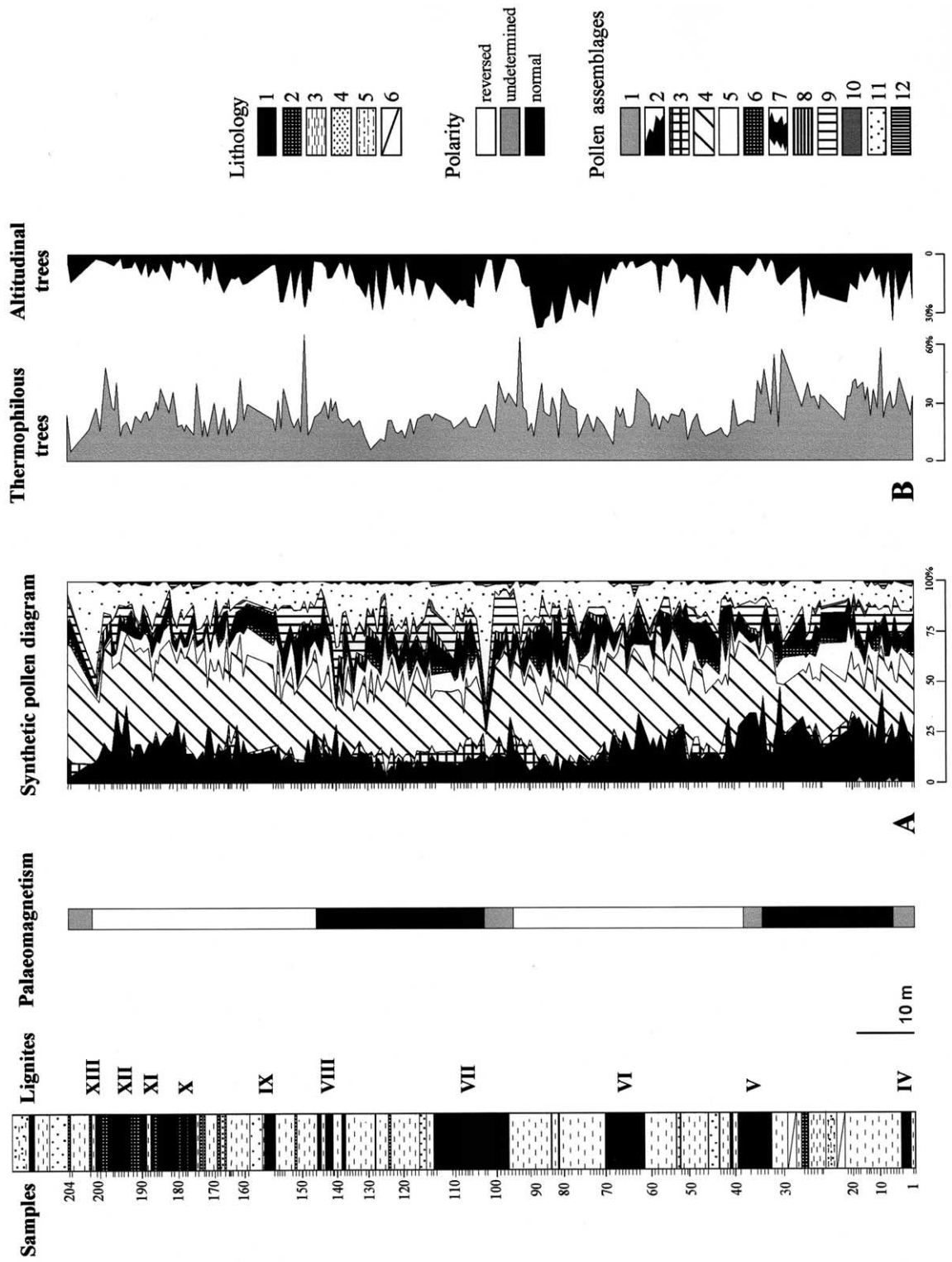


Fig. 3. Simplified detailed pollen diagram of the Lupoia section. Some scarcely represented taxa are grouped into the following sections: (1) megathermic elements: Euphorbiaceae *p.p.*, *Amanoa*, Meliaceae, *Entada* type, other Mimosoideae, *Pachysandra* type, Sapindaceae, Loranthaceae, Tiliaceae *p.p.*; (2) mega-mesothermic swamp elements: Cyrillaceae–Clethraceae, *Myrica*, *Taxodium* type, *Cephalanthus*, *Nyssa* (*Nyssa* cf. *sinensis* and *Nyssa* cf. *aquatica*); (3) other Taxodiaceae: *Sequoia* type, non-identified Taxodiaceae; (4) other mega-mesothermic elements: Arecaceae, Sapotaceae, Anacardiaceae, Araliaceae, *Microtropis fallax*, *Distylium* cf. *sinensis*, *Parrotiopsis* cf. *jacquemontiana*, *Leea*, *Magnolia*; (5) other Ulmaceae: *Celtis*, *Ulmus*, *Ulmus*–*Zelkova* type; (6) other mesothermic elements (1): *Carpinus* cf. *orientalis*, *Platanus*, *Ostrya*, *Liquidambar* (including *Liquidambar* cf. *orinetalis*); (7) other mesothermic elements (2): *Vitis*, *Hedera* (including *Hedera* cf. *helix*), *Lonicera*, *Buxus sempervirens* type, *Ligustrum*; (8) other mesothermic elements (3): *Sambucus*, *Viburnum*, *Rhus*, *Tilia*, *Ilex*, *Acer*, *Tamarix*; (9) other *Carpinus*: *Carpinus* cf. *betulus*, non-identified *Carpinus*; (10) riparian trees: *Alnus*, *Salix*, *Populus*, *Fraxinus*; (11) Mediterranean xerophytes: *Olea*, *Phillyrea*, *Pistacia*, *Quercus ilex* type, *Cistus*, *Periploca*, *Phlomis* cf. *fruticosa*; (12) subdesertic elements: *Nolina*, *Prosopis*; (13) other Asteraceae: Asteroideae, Cichorioideae, *Centaurea*; (14) other halophytes: *Ephedra*, Caryophyllaceae, Plumbaginaceae; (15) other herbs: *Erodium*, *Convolvulus*, *Linum*, *Mercurialis*, *Euphorbia*, Brassicaceae, Apiaceae, *Scabiosa*, *Knautia*, Malvaceae, Boraginaceae, *Helianthemum*, *Plantago*, *Rumex*, *Polygonum* (including *Polygonum* cf. *aviculare* and *Polygonum* cf. *lapatifolium*), Rosaceae, *Asphodelus*, other Liliaceae, *Cannabis*, other Cannabaceae, Papilionoideae; (16) freshwater plants: *Thalictrum*, other Ranunculaceae, *Butomus*, *Restio*, other Restionaceae, *Myriophyllum*, *Potamogeton*, *Sparganium*, *Typha*, *Nuphar*, *Nymphaea*, Oenotheraceae, *Trapa*, *Utricularia*, other Monocotyledones; (17) non-identified pollen grains include *Gymnocardioidites subrotunda* and *Tricolporopollenites sibiricum*. Percentages are calculated relative to the total pollen sum.

conita, 1997). In general, pollen concentration is relatively high (more than 1000 pollen grains/g of sediment), but shows important variations (from 50 up to 83 000 pollen grains/g of sediment).

The dominant taxa have been used to describe and interpret the detailed pollen diagrams in terms of the following vegetational units:

(1) Subtropical swamp forests with the Taxo-



diaceae as main component, in which regular occurrences of *Taxodium* pollen-type are found, including *Taxodium* and *Glyptostrobus*. Today, *Taxodium distichum* is found in the coastal swamps of Northeastern America (Florida and Mississippi delta; George, 1972; Roberts, 1986), and *Glyptostrobus* grows in swampy lowlands within the evergreen broad-leaved forest in China (Wang, 1961). According to macrofossil evidence, the Taxodiaceae living in the Lupoia Pliocene swamps belong to *Glyptostrobus* (*Glyptostrobus europaeus*; Ticleanu, 1992). Cupressaceae pollen grains are also abundant but cannot be identified more accurately. As their frequency trends resemble those of the Taxodiaceae, it is assumed that most Cupressaceae were represented by taxa requiring warm and humid conditions, such as those living today in subtropical Asia (*Chamaecyparis*). This is also supported by the position of Cupressaceae on the second axis of the principle component analysis (Fig. 5). Some other elements formed part of these associations, including *Cephalanthus*, *Myrica* or *Nyssa* cf. *sinensis*. In addition, these assemblages probably contained some subtropical to warm-temperate elements; *Salix p.p.*, *Alnus p.p.*, *Populus p.p.* and a *Juglans* species which is morphologically similar to *Ju-*

glans cathayensis, were found among the plant macrofossils (Ticleanu, personal information). These elements may be the first indicators of the forthcoming warm-temperate swamps of the Middle-Late Pliocene (Drivaliari et al., 1999). Several pteridophytes including *Osmunda* were found in the swamp assemblages.

(2) The abundance of Cyperaceae pollen suggests the presence of herbaceous marshes (see the result of the principle component analysis; Fig. 5). Water plants were also present in such an environment (Restionaceae, *Myriophyllum*, *Potamogeton*, *Trapa*, *Typha*, *Sparganium*, *Nuphar*, Oenotheraceae). These two pollen assemblages have a strong resemblance to the modern vegetation of South Florida (George, 1972) and the Mississippi delta (Roberts, 1986), where swamp forests (with *Taxodium distichum*) and herbaceous marshes (with Cyperaceae mainly) coexist. Their respective floristic composition can also be seen in the modern surface pollen spectra (Rich, 1985; Suc, personal information). Their constitution is in agreement with macroflora (Ticleanu, 1992; Ticleanu and Diaconita, 1997).

(3) Behind such a coastal vegetation, and up to mid-altitude, a mixed subtropical to warm-temperate forest existed with mega-mesothermic and

Fig. 4. (A) Synthetic pollen diagram of the Lupoia section. Pollen grains have been grouped according to ecological significance of the concerned plants. Lithology: see Fig. 2. Pollen assemblages: (1) megathermic elements (unidentified Euphorbiaceae, *Amanoa*, Mimosaceae including *Entada* and *Pachysandra* types, Meliaceae, Sapindaceae, Loranthaceae, Arecaceae, Sapotaceae, Tiliaceae); (2) mega-mesothermic elements (mainly Taxodiaceae, *Engelhardia*, *Cephalanthus*, *Distylium*, *Parrotiopsis jacquemontiana*, *Microtropis fallax*, Cyrillaceae–Clethraceae, *Leea*, *Myrica*, *Nyssa sinensis*, *Parthenocissus henryana*, *Ilex floribunda* type, Anacardiaceae, Araliaceae, *Magnolia*); (3) lower–mid-altitude coniferous elements, *Cathaya*; (4) mesothermic elements (deciduous *Quercus* chiefly, *Carya*, *Pterocarya*, *Liquidambar*, *Parrotia persica*, *Carpinus*, *Ulmus*, *Zelkova*, *Celtis*, *Ostrya*, *Platanus*, *Juglans*, *Juglans* cf. *cathayensis*, *Nyssa*, *Sciadopitys*, *Buxus sempervirens* type, *Acer*, *Tilia*, *Fagus*, *Alnus*, *Salix*, *Populus*, Ericaceae, *Vitis*, *Hedera*, *Lonicera*, *Fraxinus*, *Ligustrum*, *Sambucus*, *Viburnum*, *Rhus*, *Ilex*, *Tamarix*, *Betula*); (5) *Pinus*. Meso-microthermic trees: (6) mid-altitude trees, *Cedrus*, *Keteleeria* and *Tsuga*; (7) montane trees, *Abies* and *Picea*; (8) elements without significance (Rosaceae, Ranunculaceae, unidentified pollen grains, poorly preserved pollen grains); (9) Cupressaceae; (10) ‘Mediterranean’ xerophytes such as *Olea*, *Phillyrea*, *Quercus ilex* type, *Pistacia*, *Cistus*, *Phlomis* cf. *fruticosa*, *Periploca*. Herbs: (11) Cyperaceae, Poaceae, Asteraceae, *Plantago*, Brassicaceae, Apiaceae, *Polygonum*, *Rumex*, Amaranthaceae–Chenopodiaceae, Caryophyllaceae, *Linum*, *Erodium*, *Convolvulus*, *Mercurialis*, *Euphorbia*, *Scabiosa*, *Knautia*, Malvaceae, Boraginaceae, *Helianthemum*, *Asphodelus*, Liliaceae, Cannabaceae, Fabaceae, Plumbaginaceae, *Butomus*, water plants such as *Potamogeton*, Restionaceae, *Myriophyllum*, *Typha*, *Sparganium*, *Thalictrum*, *Nuphar*, *Nymphaea*, Oenotheraceae, *Trapa*, *Utricularia*; (12) steppe elements (*Artemisia*, *Ephedra*). (B) Record of thermophilous trees (i.e. the megathermic elements (such as Mimosaceae including *Propolis* and *Entada* type, *Pachysandra* type, Meliaceae, Euphorbiaceae including *Amanoa*, Sapindaceae, Loranthaceae, Tiliaceae, Arecaceae, Sapotaceae) and the mega-mesothermic elements such as Taxodiaceae (*Sciadopitys* excluded), *Juglans* cf. *cathayensis*, *Engelhardia*, *Myrica*, *Nyssa* cf. *sinensis*, *Distylium*, *Parthenocissus* cf. *henryana*, *Parrotiopsis* cf. *jacquemontiana*, *Microtropis fallax*, *Ilex floribunda* type, Cyrillaceae–Clethraceae, *Leea*, *Magnolia*, *Nolina*, plus Cupressaceae] in contrast to altitudinal trees (*Tsuga*, *Cedrus*, *Cathaya*, *Abies* and *Picea*) along the Lupoia section.

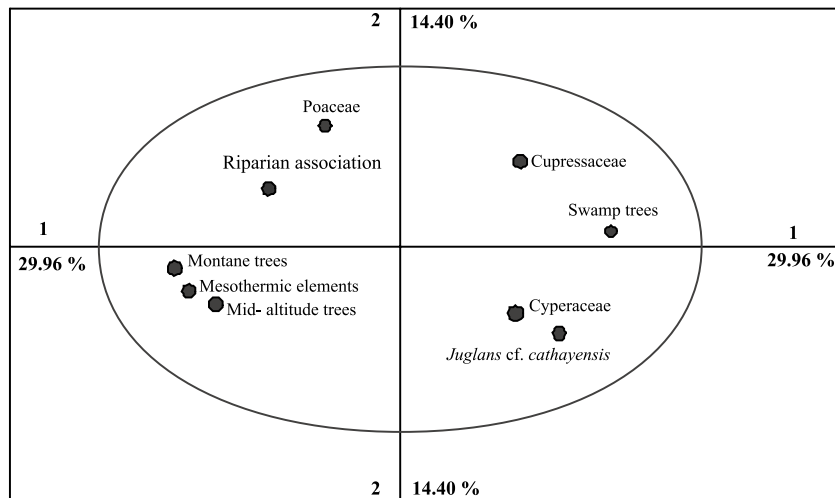


Fig. 5. Principle component analysis applied to some key taxa and some ecological groups recorded in the Lupoia pollen analysis. Axis 1 does not show any clear information. Axis 2 shows two groups which can be interpreted as a selection of the swamp-marsh elements with regard to the other groups. Taxa and groups which have been used in the calculations are those representative of humid (climatic or edaphic) conditions. Pollen groups are those used in the synthetic pollen diagram (Fig. 4), despite the following exceptions in order to test the relative contribution of some elements: (1) swamp trees include Taxodiaceae (*Sciadopitys* excluded) and *Nyssa*; (2) the mesothermic elements have been subdivided into two groups according to their local humidity requirements (this includes a riparian association containing *Alnus*, *Salix*, *Populus*, *Liquidambar* and *Parrotia*). Within the herbs, the two most abundant elements, Poaceae and Cyperaceae, have been tested separately. Megathermic and the other mega-mesothermic elements have not been considered because of their low frequencies.

mesothermic elements such as *Engelhardia*, *Carya*, *Pterocarya*, deciduous *Quercus*, *Fagus*, some Cupressaceae, *Juglans*, *Zelkova*, *Carpinus*, *Acer*, etc. Here, the riparian associations were richer in *Alnus p.p.*, *Salix p.p.*, *Liquidambar*, *Parrotia* and *Populus p.p.* Some other Taxodiaceae, such as *Sciadopitys* and those corresponding to the *Sequoia* pollen type, are represented by a small quantity of pollen grains. As considered by Ticleanu and Diaconita (1997), these elements are included in this vegetation group, taking into account their modern habitat which is often altitudinal and in a lower latitudinal range than in Europe, and because they occur relatively frequently in the Lupoia macroflora (Ticleanu and Diaconita, 1997). Many herbs and shrubs may have been present in such environments, e.g. Asteraceae *p.p.*, Brassicaceae, Polygonaceae, Poaceae *p.p.*, *Buxus*, etc. This vegetation may also have included some Mediterranean elements (*Quercus ilex* type, *Phillyrea*, *Periploca*, *Pistacia*, *Olea*, etc.), as observed in the present-day Colchid vegetation (southern edge of the Caucasus) (Denk

et al., 2002). Finally, the vegetation group contained a variety of megathermic elements at non-significant percentages (Euphorbiaceae including *Amanoa*, Mimosaceae including *Entada*, Meliaceae, Sapindaceae, Loranthaceae, Arecaceae, Sapotaceae, Tiliaceae).

(4) At higher altitudes, the composition of the mixed forest would progressively change, with an increasing presence of gymnosperms. First *Cathaya* and *Sciadopitys* would have been present, replaced subsequently by *Cedrus* and *Tsuga*, and finally by *Abies* and *Picea*. Traditionally, North-European palaeobotanists consider that these trees inhabited lowlands (in association with thermophilous elements) during the Early Pliocene, as documented by cones and seeds in the Lower Rhine fluvial plain (Mai, 1995). Today, *Abies* and *Picea* (still living in northern Europe) would be present above 500 m altitude in this area, according to the latitudinal–altitudinal gradient controlling the modern distribution of trees in Europe (Ozenda, 1975, 1989). Therefore, during the Early Pliocene, these conifers may have been repre-

sented by somewhat ‘thermophilous’ species. However, the presence of *Abies* and *Picea* might indicate cooler conditions in the Middle Pliocene (late Reuverian), when the increase in pollen percentages of these two taxa occurs together with a strong decrease in thermophilous elements (Zagwijn, 1960). At low European latitudes, Early Pliocene floristic conditions were rather different from northern Europe (Zagwijn and Suc, 1984). Indeed, no cones or seeds of *Abies* and *Picea* have been found in lowland or coastal lignites (Rio Maior in Portugal: Diniz, 1984; Arjuzanx in southwestern France: Huard, 1966; Cessenon in southeastern France: Roiron, 1992), and this also applies to the Romanian lignites (Husnicioara, Lupoiaia, etc.: Ticleanu and Diaconita, 1997). In southern Europe, only Zanclean pollen diagrams from areas located at the foot of high massifs (Pyrenees, French Massif Central, Alps, Apennines) show high percentages of *Cathaya*, *Cedrus*, *Tsuga*, *Abies* and *Picea* (Suc et al., 1999). Similar records characterise southwestern Romania (Drivaliari et al., 1999; Popescu, present work and unpublished data). In addition, significant increases in *Abies* and *Picea* represent the earliest Northern Hemisphere glacials in pollen diagrams from the Apennines (Bertini and Roiron, 1997; Pontini and Bertini, 2000); this is also supported by the *Picea* macrofossils found in the lignite quarry of Santa Barbara (Bertini and Roiron, 1997). For these reasons, *Abies* and *Picea* are considered to constitute a South-European montane forest belt, even though its temperature range was somewhat higher than its modern analogue in the European massifs. *Cedrus* is considered as growing in an intermediate altitudinal belt. As previously discussed by Suc (1981), at Cessenon (foot of the south French Massif Central) a lignite has been found which is rich (20–40%) in *Cedrus* pollen, but lacks any macrofossils belonging to this genus. Similarly, *Cathaya*, *Keteleeria* and *Tsuga* can be regarded as mid-altitude conifers.

5. Repetitive vegetation changes

The synthetic pollen diagram suggests repetitive changes (Fig. 4A) between (1) a group consisting

of the thermophilous taxa (i.e. megathermic elements (such as Mimosaceae, Meliaceae, *Amanoa*, Sapindaceae, Loranthaceae, etc.) and mega-mesothermic elements such as Taxodiaceae (*Sciadopitys* excluded), *Juglans* cf. *cathayensis*, *Engelhardia*, *Myrica*, *Nyssa* cf. *sinensis*, *Distylium*, *Parthenocissus* cf. *henryana*, *Parrotiopsis* cf. *jacquemontiana*, *Microtropis fallax*, Cyrillaceae–Clethraceae, *Leea*, etc. plus Cupressaceae), and (2) a group containing the altitudinal trees (*Tsuga*, *Cedrus*, *Cathaya*, *Abies* and *Picea*). Relative frequencies of these groups are shown in Fig. 4B for comparison with changes in lithology.

On the whole, maxima of thermophilous trees correspond to lignite layers, whereas peaks in altitudinal trees occur within clays. A straightforward explanation of the cause of these alternations might be based on differences in pollen transport. Local vegetation may be well-represented in lignite layers, whereas distant vegetation would be better represented in clay layers as a result of long-distance transport of terrigenous material, including pollen, from altitudinal vegetation belts. In this scenario, lignite deposition would have been unpredictable, caused by changes in the alluvial plain morphology resulting from shifts in the course of the river channel. There are, however, several arguments that contradict such an interpretation:

(1) The continuous lignite layers across the entire basin suggest that there were no local effects of changes in the river channel (Ticleanu and Andreescu, 1988).

(2) Some thermophilous tree maxima occur within clay layers (below lignite VI, below lignite VII, below lignite VIII and above lignite IX); some altitudinal tree maxima occur within lignite layers (base of lignite VI, upper lignite VII, lignite IX).

(3) Today, the pollen frequency of montane trees (*Abies* and *Picea*) is not high in prodeltaic clayey areas, as seen in the northwestern Mediterranean region (Fauquette et al., 1999b).

(4) Mesophilous elements (deciduous *Quercus*, *Carya*, *Pterocarya*, *Liquidambar*, *Carpinus*, *Parrotia*, etc.), which inhabited areas relatively distant from the swamps, show, on the whole, a constant abundance (ranging from 20 to 40% of the pollen

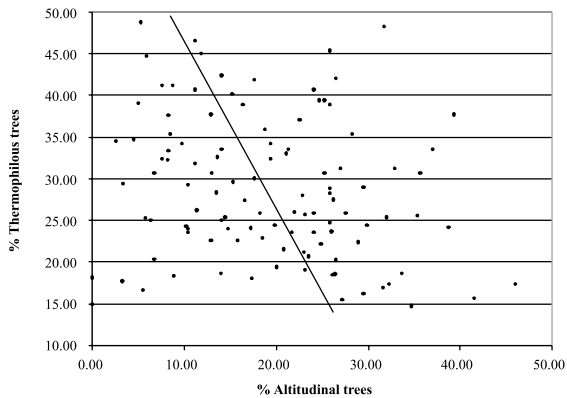


Fig. 6. Linear regression between percentages of thermophilous trees and altitude trees using the reduced major axis method. Regression line is: % thermophilous trees = $(-2.228 \times \text{altitude trees}) + 71.476$ (slope: -2.228 ± 0.522 ; intercept: 71.476 ± 145.8). Unbiased correlation coefficients are: Pearson's $r = -0.199$ ($*P = 0.0375$); Spearman's $r = -0.204$ ($*P = 0.033$).

sum) independent of the clay–lignite alternations.

(5) Similar variations in pollen spectra between thermophilous elements and altitudinal trees have been recorded in homogenous clay from Early Pliocene sections in the Po Valley (Bertini, 1994).

(6) Close to Lupoia, the Hinova section (lowest Pliocene according to nannoplankton evidence; Marunteanu, personal information), entirely constituted by clays, shows very low percentages of altitudinal trees (Popescu, unpublished).

(7) Pollen records between lignites IV and V and above lignite VIII are characterised by relatively low frequencies of altitudinal trees, irrespective of lithology (lignites or clays); on the contrary, frequencies of thermophilous trees are higher in the same intervals. In addition, pollen records between lignites IV and V include some megathermic elements. This suggests that the three main climatic phases of the Early Pliocene could be represented in the Lupoia section (Brunssumian A or phase P Ia in the Lupoia borehole F6 up to lignite V; Brunssumian B or phase P Ib between lignites V and VIII in the Lupoia quarry; Brunssumian C or phase P Ic above lignite VIII in the Lupoia quarry; [Suc and Zagwijn, 1983](#)). The two warm Zanclean

phases (P Ia and P Ic) would be characterised by a larger development of swamps in the Dacic Basin while the Zanclean cooling phase (P Ib) would be characterised by reduced swamps and a moderate lowering of altitudinal vegetation belts in the area. This is consistent with the larger extension in space and in thickness of lignites V and VIII (Jipa, personal information).

On the basis of these arguments, a second and more probable interpretation can be made of the long-term thermophilous–altitudinal tree alternations recorded at Lupoia. These could well indicate successive warm–cool fluctuations corresponding to (1) the development of swamp environments (warmer phases), (2) the descent to lower altitudes of the coniferous forests, with a corresponding increase in their pollen representation in the delta sediments (cooler phases). A correlation analysis has been performed on percentages of thermophilous trees versus those of altitudinal trees for samples 1–110, i.e. in the part of the Lupoia section where clay–lignite alternations are very contrasted; the linear regression is negative (Fig. 6), and supports this interpretation.

Such regular repetitions need to be juxtaposed with fluctuations in eccentricity in order to test the hypothesis of [Van Vugt et al. \(2001\)](#) who suggested a periodicity of 100 kyr for the lignite layers. Fig. 7 focusses on the period considered by [Van Vugt et al. \(2001\)](#) to correspond to the Lupoia section deposition. This period is characterised by great contrasts between eccentricity maxima and minima. The global polarity time scale has been chronologically calibrated on the basis of the eccentricity process. In turn, this time scale has been used to establish a chronology for the $\delta^{18}\text{O}$ curve, taken from a section in which magnetic reversals have been distinctly identified ([Shackleton et al., 1995](#)). The pollen curves may therefore be related to the calibrated time scale using the palaeomagnetic reversals of the Lupoia section. This gives two independent lines of evidence to allow testing of the hypothesis of eccentricity forcing of lignite formation.

In general, the $\delta^{18}\text{O}$ curve indicates a relative cooling phase corresponding to the C3n.2n Chron. However, the pollen record indicates a

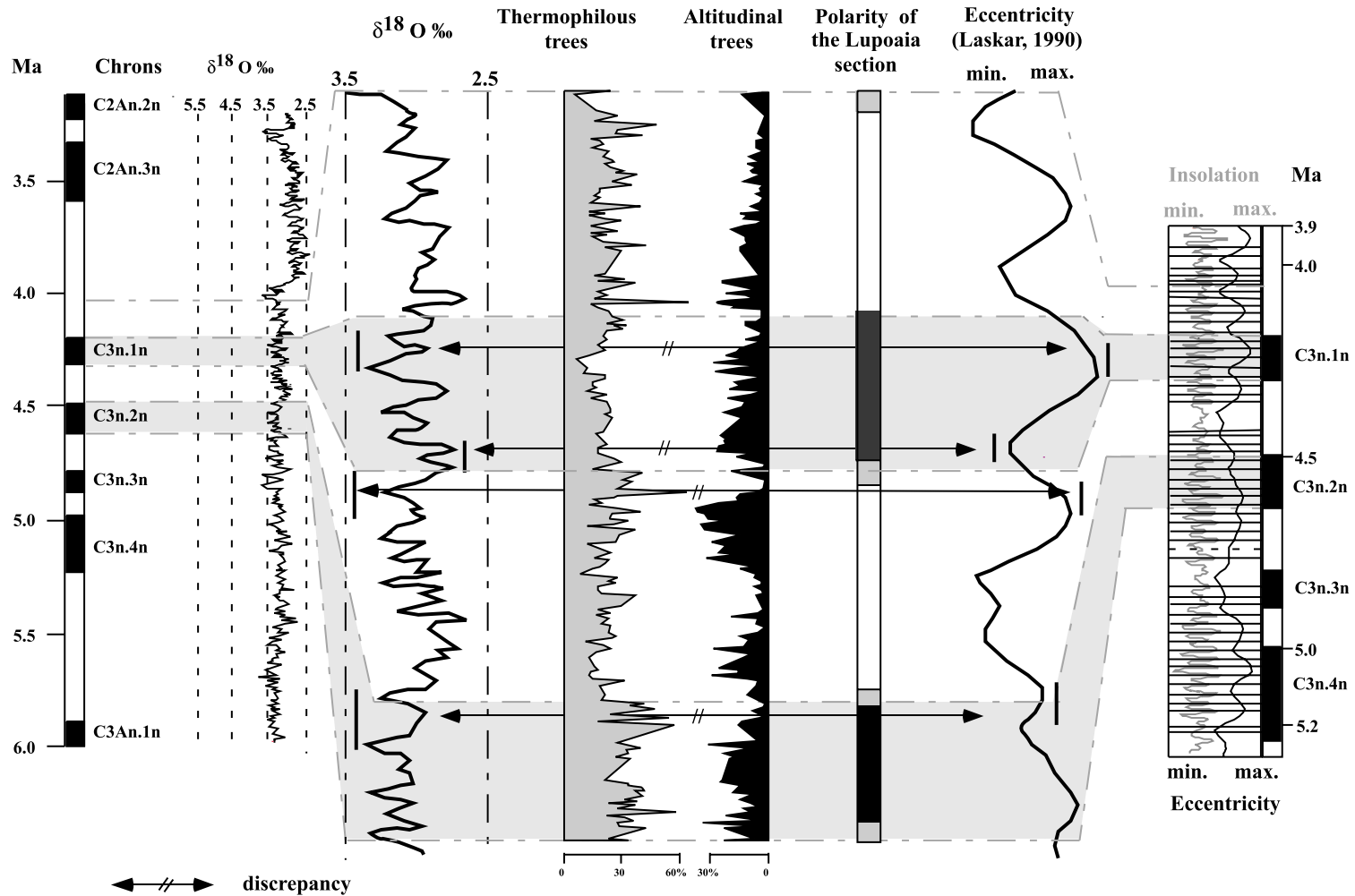


Fig. 7. Curves of thermophilous elements versus altitudinal trees (see Fig. 4B) are compared to eccentricity curve (Laskar, 1990) and to a reference $\delta^{18}\text{O}$ curve (Shackleton et al., 1995) within the chronological frame proposed by Radan and Radan (1998) and Van Vugt et al. (2001). Some discrepancies between pollen curves and $\delta^{18}\text{O}$ and/or eccentricity curves are indicated close to magnetic reversals for comparisons within similar accurate chronological intervals.

warm climate (high percentages of thermophilous trees) during this normal polarity event. The interval between Chrons C3n.2n and C3n.1n corresponds to a warmer period according to the $\delta^{18}\text{O}$ record; this is also supported by changes in eccentricity. However, this is in harmony with pollen data from the reverse interval in the lower part of the Lupoia section, which are indicative of cooler conditions (decrease in thermophilous elements). The same line of reasoning cannot be applied to the upper Lupoia section, since the differences between the pollen record and $\delta^{18}\text{O}$ curve are not so well marked for the time interval between the early C3n.1n Chron and the early C2An.3n Chron. A more detailed examination of the magnetic reversals shows some major discrepancies (points 1, 3, 4 below) between the pollen record and eccentricity and/or $\delta^{18}\text{O}$ curves, and one (point 2) of minor importance:

(1) The reversal at the end of the C3n.2n Chron occurs just before the end of a prolonged maximum in eccentricity and should therefore correspond to a general cooling period (see also the $\delta^{18}\text{O}$ reference curve). This is in contradiction to the high abundance of thermophilous trees in the Lupoia pollen record, which exists for some time prior to this period.

(2) The reversal at the onset of the C3n.1n Chron corresponds to a transition from a maximum eccentricity to a moderate minimum eccentricity, i.e. from a cooler to a warmer period. This is clearly seen in the $\delta^{18}\text{O}$ reference curve, but appears to be in contradiction with high thermophilous tree percentages in the Lupoia pollen record. However, the imprecise definition of the position of this magnetic reversal reduces the strength of this argument.

(3) Following this event, there is a reduction in eccentricity and the $\delta^{18}\text{O}$ curve indicates a warmer climate, in contradiction with the relatively large percentages of altitudinal trees in the Lupoia pollen record.

(4) The upper reversal of C3n.1n Chron corresponds to the transition from a maximum eccentricity to a relative minimum eccentricity, i.e. from cooler to relatively warmer climatic conditions (see also the $\delta^{18}\text{O}$ reference curve). During the same period, however, the Lupoia pollen records

shows an evolution from warmer (high percentages in thermophilous trees) to cooler (increase in altitudinal trees) conditions.

Due to these incompatibilities, an attempt has been made to correlate the Lupoia section with a somewhat earlier period than proposed by Van Vugt et al. (2001). In this concept, tested using a similar comparative approach, the two normal polarity episodes have been assigned to C3n.3n and C3n.2n Chrons, respectively, as indicated on Fig. 8. The period is dominated by a long maximum in eccentricity, interrupted by some brief relative minima. This chronology gives an almost complete correspondence between the Lupoia pollen curves and the global climatic reference curves (eccentricity and $\delta^{18}\text{O}$). This is particularly obvious at the magnetic reversals:

(1) The reversal at the end of the C3n.3n Chron corresponds to a minimum eccentricity, indicating a warm period that is supported by both $\delta^{18}\text{O}$ values and by large percentages of thermophilous trees in the Lupoia pollen record.

(2) The reversal at the onset of the C3n.2n Chron corresponds to a short minimum eccentricity within a long maximum phase, i.e. to warmer conditions within a long cooling period. This is in good agreement with the $\delta^{18}\text{O}$ curve and the maximum of thermophilous trees between two maxima of altitudinal trees in the Lupoia pollen record.

(3) The reversal at the end of the C3n.2n Chron matches the transition from minimum to maximum eccentricity at the end of the long period of maximum eccentricity. This is consistent with the warmer phase expressed both by the $\delta^{18}\text{O}$ reference curve and thermophilous trees in the Lupoia pollen record.

Similar inferences may be made for all the major and minor concordances shown in Fig. 8.

It is therefore proposed that the previously estimated correlation of the Lupoia section (Radan and Radan, 1998; Van Vugt et al., 2001) has to be changed to correspond with the normal Chrons C3n.3n and C3n.2n. In this case, the evolution of the regional climate as reflected by the pollen record is fully consistent with global climatic evolution (insolation and $\delta^{18}\text{O}$ record). Such a chronological assignment is supported by

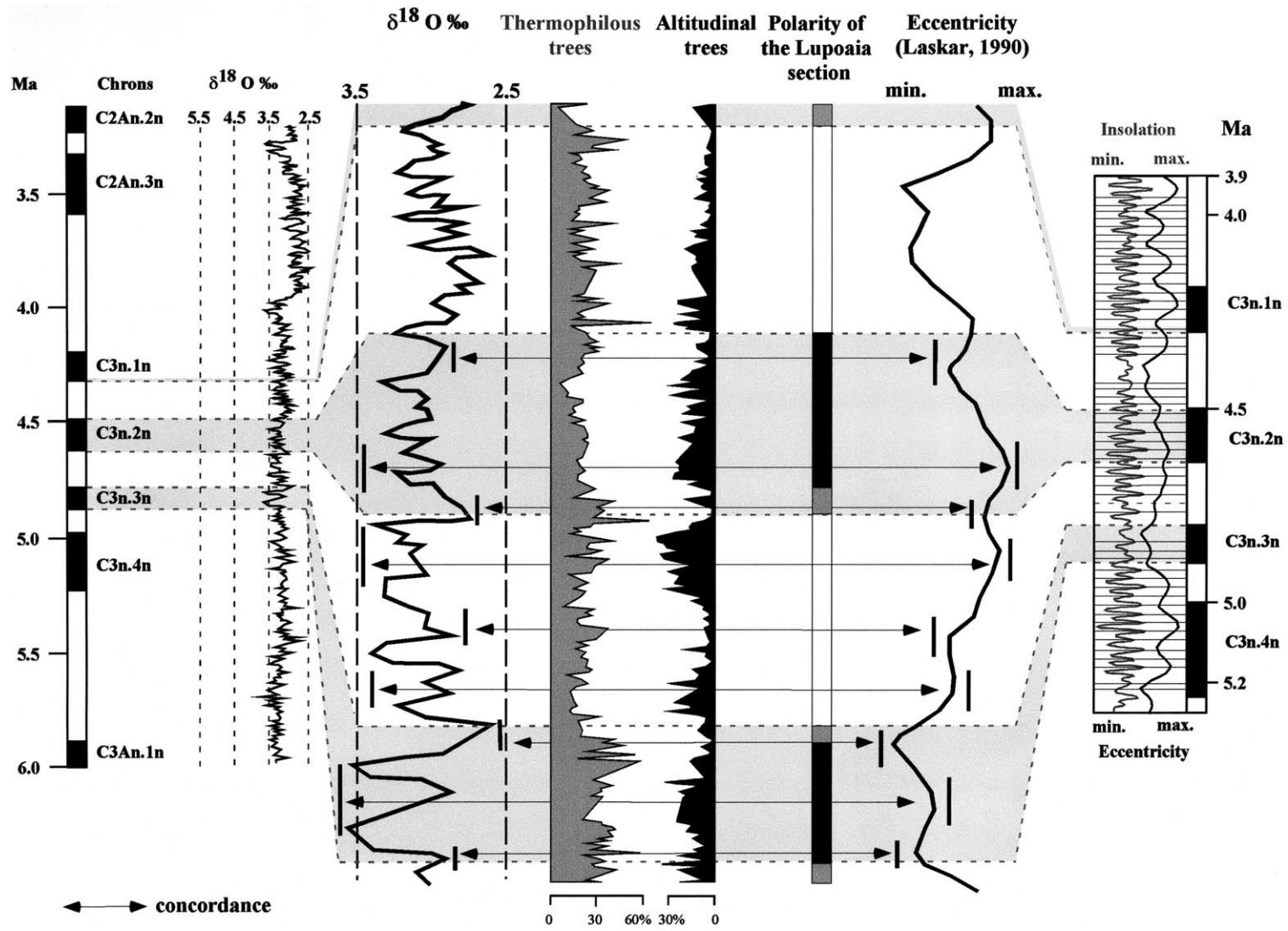


Fig. 8. Curves of thermophilous elements versus altitudinal trees (see Fig. 4B) are compared with the eccentricity curve (Laskar, 1990) and a reference $\delta^{18}\text{O}$ curve (Shackleton et al., 1995) using a chronological frame, which is one chron older than that proposed by Radan and Radan (1998) and Van Vugt et al. (2001). Some concordances between pollen curves and $\delta^{18}\text{O}$ and eccentricity curves are indicated close to magnetic reversals for comparisons within similar accurate chronological intervals.

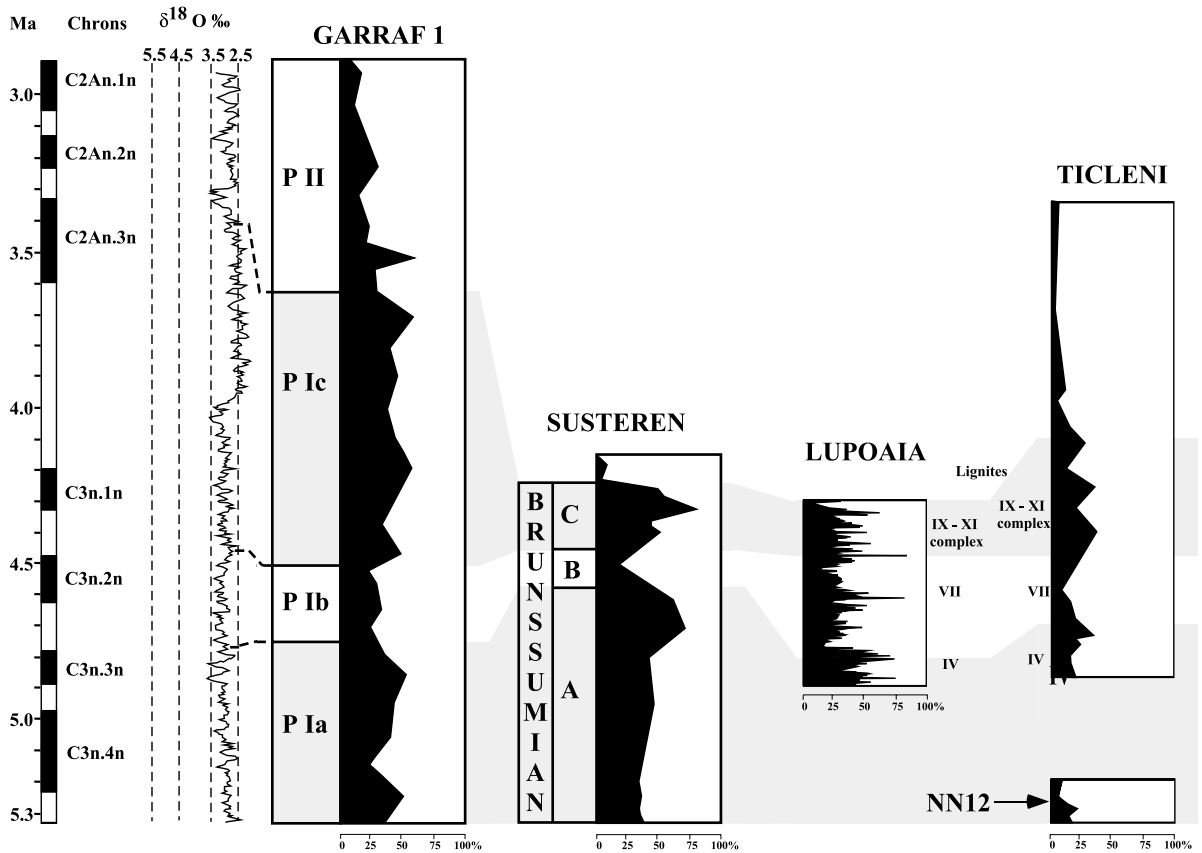


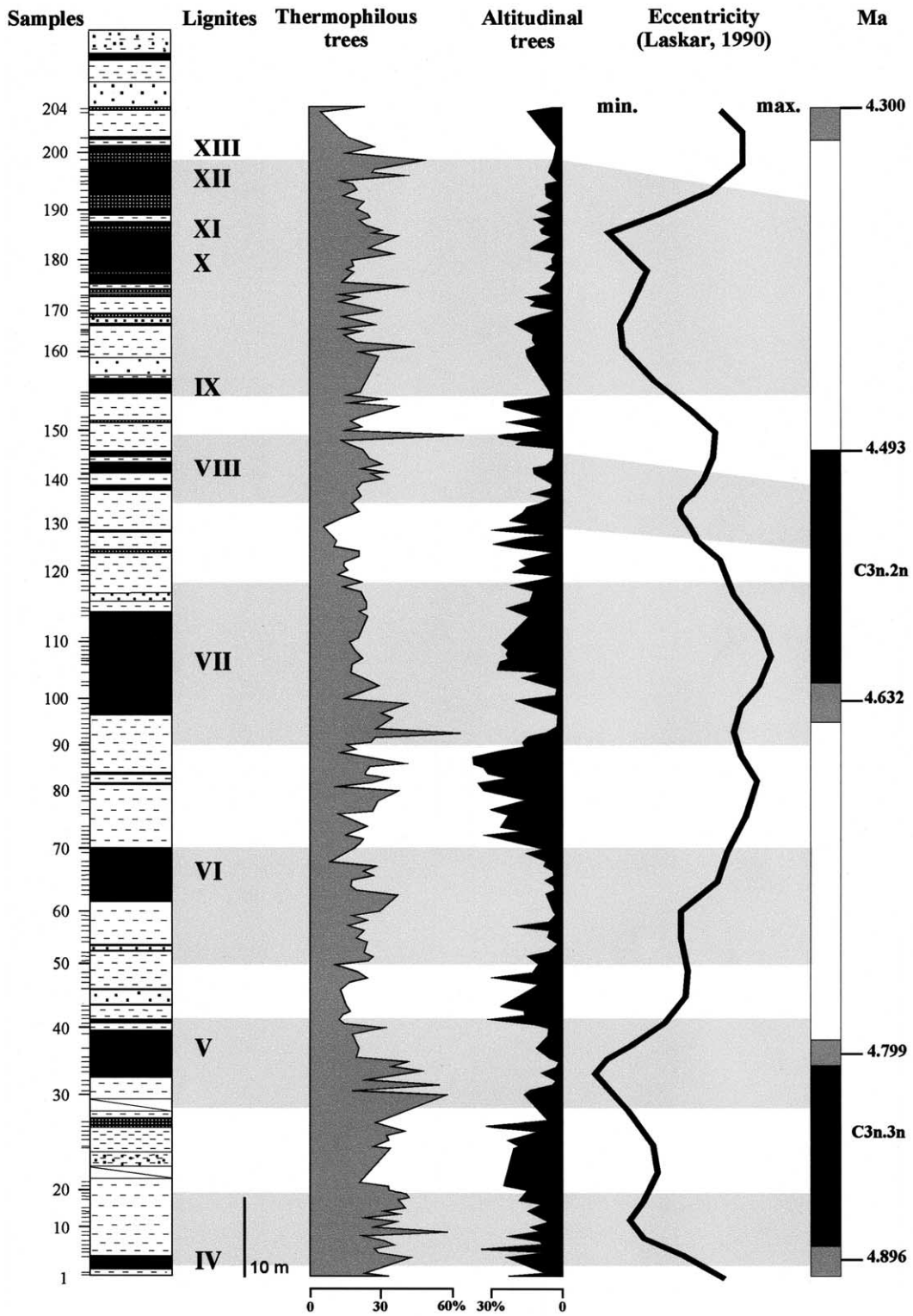
Fig. 9. Place of the Lupoia pollen diagram in the frame of the regional (Ticleni: Drivaliari et al., 1999) and European climatostratigraphies (Susteren in The Netherlands: Zagwijn, 1960; Garraf 1 in the northwestern Mediterranean region: Suc and Cravatte, 1982) and the reference global $\delta^{18}\text{O}$ curve (Shackleton et al., 1995). Climatostratigraphic relationships are based on the respective curves of thermophilous trees focussing on the warm Early Pliocene phase (Brunssumian in The Netherlands, pollen phase P I in the Mediterranean). The Lupoia pollen diagram covers the upper Brunssumian A (pollen zone P Ia in the Mediterranean) to the lower Brunssumian C (pollen zone P Ic in the Mediterranean). Position of lignites IV, VII and IX–XI complex is indicated in support of climatostratigraphic relationships between the Ticleni and the Lupoia sections.

the mammal fauna, especially by the presence of a primitive *Miomys* in lignite VIII. In addition, the proposed age of the Lupoia section would be fully consistent with the climatic subdivision of the Early Pliocene in Europe (Zagwijn, 1960; Suc, 1982; Suc and Zagwijn, 1983), in which a cooling period (Brunssumian B = phase P Ib) is observed between two warm periods (Fig. 9).

The Lupoia section belongs almost completely to this cooling period, which has also been observed in the Ticleni borehole. This is further supported by the regional lignite stratigraphy, cooling being centred around lignite VII (Drivaliari et al., 1999) (Fig. 9).

The Van Vugt et al. (2001) hypothesis is confirmed: lignite layers seem to occur every 100 kyr.

Fig. 10. Cyclic responses in the Lupoia pollen record of thermophilous and altitudinal trees to eccentricity. Chronology of palaeomagnetic reversals after Lourens et al. (1996). Shaded areas represent warm parts of the climatic cycles inferred from comparison of thermophilous tree maxima with eccentricity minima. Lithology: see Fig. 2.



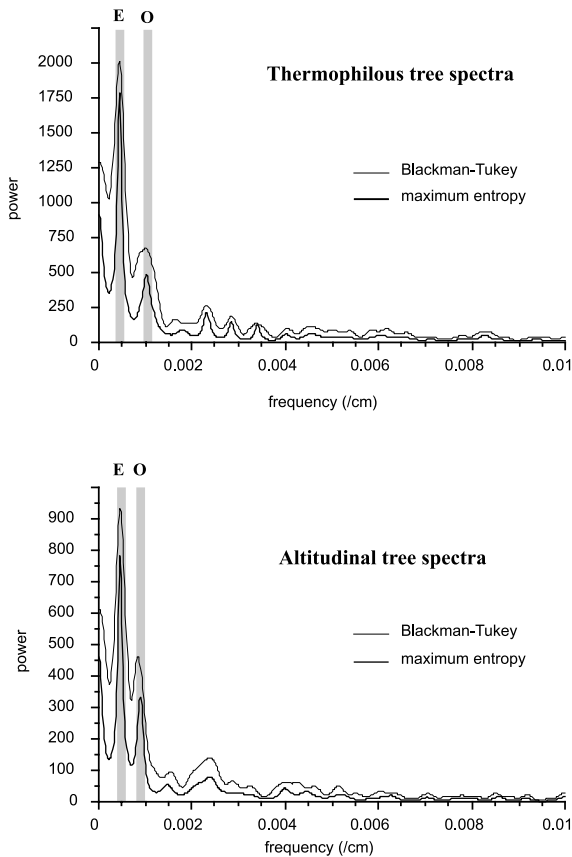


Fig. 11. Spectral analysis of thermophilous elements and altitude trees. E, peak considered as representative of eccentricity period; O, peak considered as representative of obliquity period. The most significant peak E corresponds to 0.0005 as frequency. The correlative period is inverse to frequency (expressed in cm), i.e. 2000 cm.

They are linked to minimum eccentricity. A simple estimate, based on the time separating the two most distant magnetic reversals obviously recorded in the Lupoia section (4.799 (end of C3n.3n Chron)–4.493 Ma (end of C3n.2n Chron) according to Lourens et al., 1996), indicates a period of 306 kyr. This period includes three maxima of altitudinal trees and three relative maxima of eccentricity (100-kyr period) (Fig. 10). A spectral analysis of thermophilous elements and altitudinal trees has been performed with respect to thickness of the section (Analyseries Program: Paillard et al., 1996). Both groups show a strong spectral peak which has been calculated as located at a thickness of 20 m (Fig. 11). This corresponds

to a time period of approximately 87 kyr, and can be considered consistent with the period of eccentricity, when the changes in sedimentation rate that probably differentiated lignites from clays are taken into account.

Pollen concentration can provide information on preservation and/or changes in sedimentation rate (Suc, 1984b); low values may be associated with higher sedimentation rate (pollen grains diluted within a lot of terrigenous particles), and high values with a low sedimentation rate. Fig. 12 shows variations in pollen concentration along the Lupoia section. The highest values (> 10 000 pollen grains/g of sediment) mostly correspond to lignite layers, with the exception of some samples from borehole F6. Examination of the respective thickness of clays and lignites within each eccentricity cycle (sands are excluded because they probably represent a short time-interval), shows that lignites represent less than half a cycle, where one cycle equals the clay layer and the overlying lignite (Fig. 10): lignite V = 25% of the cycle; lignite VI = 40% of the cycle; lignite VII = 25% of the cycle; lignite VIII = 35% of the cycle. For three of these lignites (V, VI, VII), the related minimum eccentricity is considerably shorter in time than the maximum part of the eccentricity curve corresponding to the underlying clays. However, lignite VIII seems thinner as may be expected on the basis of the eccentricity curve, which shows a minimum of longer duration. In contrast, the thickness of lignites IX plus X–XIII (> 60% of the cycle) seems to be in agreement with the relatively long duration of the corresponding minimum in the eccentricity curve. The pollen concentration appears to vary independently of the variation in thickness within the cycles (high pollen concentration for lignites VI, VII and X–XIII; low pollen concentration for lignites V and VIII). As a consequence, pollen concentration seems to be more linked to preservation and possibly to xylite abundance in some lignites. This may explain the scarcity, and occasional absence of pollen grains in some samples.

The eccentricity-forced pollen cycles (thermophilous plants versus altitudinal trees) and lithology cycles (clay–lignite alternations) suggest that the inferred ages throughout the studied section

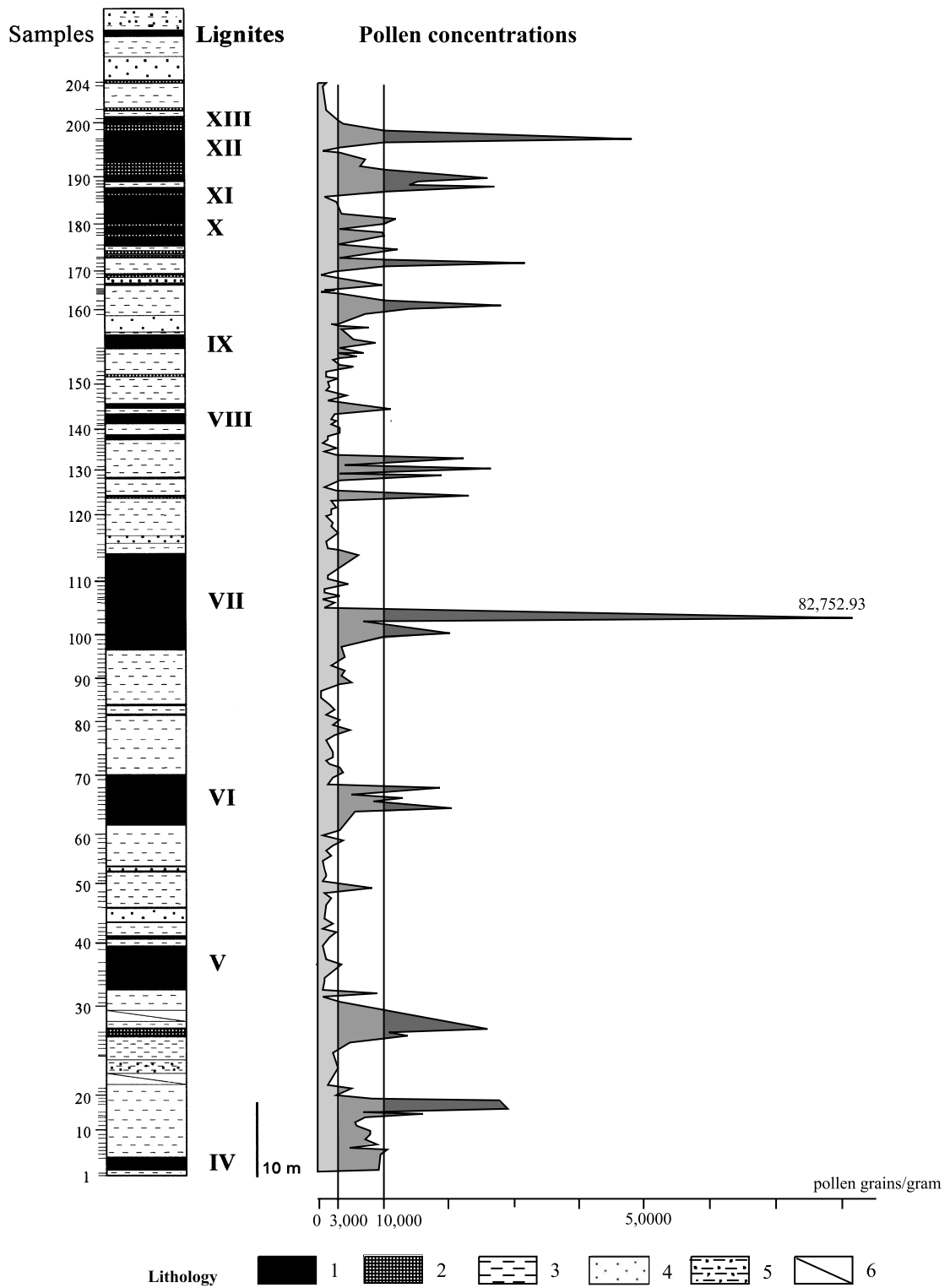


Fig. 12. Pollen concentration along the Lupoia section. Lithology: see Fig. 2.

correspond well with respect to the eccentricity chronology. As a consequence, it is proposed that (1) the undetermined polarity zone in the basal part of the section should belong to the reversed polarity interval prior to C3n.3n Chron (the reversal should occur within the clays located above lignite IV), (2) the reversal at the end of Chron C3n.3n should occur within the undetermined polarity zone, more precisely at the top of lignite V, and (3) the undetermined polarity zone located at the top of the Lupoia section should immediately precede the following normal interval, i.e. the C3n.1n Chron (Fig. 10). The latter inference is based on both the eccentricity chronology and the close relationships between the $\delta^{18}\text{O}$ reference curve and the thermophilous tree curve in the Lupoia pollen record (Fig. 9). Taking this information into account, the studied Lupoia section would represent a time span of about 600 kyr, i.e. from about 4.90 to about 4.30 Ma. The three climatic phases of the Early Pliocene in the Lupoia pollen record (see above: warm phase ending with lignite V, cooler phase between lignites V and VIII, warmer phase starting with lignite VIII; Fig. 10) may be the expression of the 400-kyr cycles of eccentricity overprinting the 100-kyr cycles (see Figs. 8 and 10).

6. Conclusions

High-resolution pollen analyses of the Lupoia section (borehole F6 and quarry) have (1) allowed the reconstruction of the Early Pliocene vegetation of southwestern Romania, and (2) provided evidence of repetitive changes in vegetation. The results show two opposed vegetation belts: thermophilous trees, which were located in low altitudes of the Dacic Basin, and altitudinal trees which probably grew in the Carpathians. During cooling periods, this second group migrated to lower altitudes, and their pollen grains partly masked the local production in the alluvial plain. In this region, lignite deposition corresponds to warm phases under continuously humid conditions.

These vegetation changes and the clay–lignite alternations are forced by eccentricity. A detailed

comparison between pollen data and global climatic fluctuations (provided by eccentricity and $\delta^{18}\text{O}$ curves) has led to a change in the chronological assignment of the section, previously based on a preliminary interpretation of palaeomagnetic measurements (Radan and Radan, 1998; Van Vugt et al., 2001). The revised chronological assignment is in accordance with the mammal fauna, whereas the regional climatic fluctuations are consistent with the global climatic evolution. The Lupoia section covers a period between approximately 4.90 and 4.30 Ma and represents a time span of about 600 kyr. The section completely includes the C3n.3n and C3n.2n Chrons. In addition, it is proposed that the section ends at the onset of the C3n.1n Chron.

Climatically, the Lupoia section covers:

(1) The end of the Early Pliocene warm phase (Brunsumian A in northern Europe and P Ia phase in the northwestern Mediterranean region; Suc and Zagwijn, 1983).

(2) The entire Early Pliocene cooling (Brunsumian B in Northern Europe and P Ib phase in the Northwestern Mediterranean region; Suc and Zagwijn, 1983).

(3) The beginning of the late Early Pliocene warm phase (Brunsumian C in Northern Europe and P Ic phase in the Northwestern Mediterranean region; Suc and Zagwijn, 1983).

The main Early Pliocene climatic subdivisions are now documented for the east of Europe but appear more complex. Other areas (for example at the base of mountains) may provide similarly detailed records when studied with high-resolution pollen investigation.

Acknowledgements

This Ph.D. work was granted by the French Government through its Embassy at Bucharest. This study was supported by the Programme 'Environnement, Vie et Sociétés'. J.-P. Suc and P. Bernier have supervised this work. The manuscript has been improved thanks to the comments of the two referees, Dr. S. Bottema and Dr. V. Mosbrugger. My friends, the Lupoia quarry engineers, provided facilities for sampling. S.C. Ra-

dan gave samples from borehole F6. G. Clauzon, D. Jipa and M. Marunteanu supplied information on palaeogeography and stratigraphy in the Turnu Severin area. I received help from M. Gonzales for performing samples, from G. Escarguel and F. Giraud for statistic treatments. I got a lot of information from P. Mein, C. Guérin, J. Agustí, A.J. Van der Meulen, M. Fortelius and M. Erbajeva on the mammal fauna. P. Bernier, S. Legendre and J.-P. Suc discussed the manuscript, the English edition of which has been made by Dr. Simon Brewer.

References

- Aguilar, J.-P., Legendre, S., Michaux, J., Montuire, S., 1999. Pliocene mammals and climatic reconstruction in the Western Mediterranean area. In: Wrenn, J., Suc, J.-P., Leroy, S.A.G. (Eds.), *The Pliocene: Time of Change*. Am. Assoc. Stratigr. Palynol. Found., pp. 109–120.
- Aguilar, J.-P., Michaux, J., 1984. Le gisement à micromammifères du Mont-Hélène (Pyrénées-Orientales): apports à la connaissance de l'histoire des faunes et des environnements continentaux. Implications stratigraphiques pour le Pliocène du sud de la France. *Paléobiol. Cont.* 14, 19–31.
- Apostol, L., Enache, C., 1979. Etude de l'espèce *Dicerorhinus megarhinus* (de Christol) du bassin carbonifère de Motru. *Trav. Mus. Hist. Nat. Grigore Antipa* 20, 533–540.
- Bertini, A., 1994. Messinian-Zanclean vegetation and climate in North-Central Italy. *Hist. Biol.* 9, 3–10.
- Bertini, A., Roiron, P., 1997. Evolution de la végétation et du climat pendant le Pliocène moyen, en Italie centrale: apport de la palynologie et de la macroflore à l'étude du bassin du Valdarno supérieur (coupe de Santa Barbara). *C. R. Acad. Sci. Paris* 324, 763–771.
- Cour, P., 1974. Nouvelles techniques de détection des flux et des retombées polliniques: étude de la sédimentation des pollens et des spores à la surface du sol. *Pollen Spores* 16, 103–141.
- Denk, T., Frotzler, N., Davitashvili, N., 2002. Vegetational patterns and distribution of relict taxa in humid temperate forests and wetlands of Georgia (Transcaucasia). *Biol. J. Linnean Soc.*, in press.
- Diniz, F., 1984. Apports de la palynologie à la connaissance du Pliocène portugais. Rio Maior: un bassin de référence pour l'histoire de la flore, de la végétation et du climat de la façade atlantique de l'Europe méridionale. Thesis, Université Montpellier 2, p. 230.
- Drivaliari, A., 1993. Images polliniques et paléoenvironnement au Néogène supérieur en Méditerranée orientale. Aspects climatiques et paléogéographiques d'un transect latitudinal (de la Roumanie au delta du Nil). Thesis, Université Montpellier 2, p. 332.
- Drivaliari, A., Ticleanu, N., Marinescu, F., Marunteanu, M., Suc, J.-P., 1999. A Pliocene climatic record at Ticleni (Southwestern Romania). In: Wrenn, J.H., Suc, J.-P., Leroy, S.A.G. (Eds.), *The Pliocene: Time of Change*. Am. Assoc. Stratigr. Palynol. Found., pp. 103–108.
- Fauquette, S., Clauzon, G., Suc, J.-P., Zheng, Z., 1999b. A new approach for paleoaltitude estimates based on pollen records: example of the Mercantour Massif (southeastern France) at the earliest Pliocene. *Earth Planet. Sci. Lett.* 170, 35–47.
- Fauquette, S., Guiot, J., Suc, J.-P., 1999a. A method for climatic reconstruction of the Mediterranean Pliocene using pollen data. *Palaeogeogr. Palaeoclimatol. Palaeoecol.* 144, 183–201.
- George, J.C., 1972. Everglades Wildguide. Natural History Series, Nat. Park Service, US Department of the Interior.
- Guérin, C., 1980. Les Rhinoceros (Mammalia, Perissodactyla) du Miocène terminal au Pléistocène supérieur en Europe occidentale. Comparaison avec les espèces actuelles. *Doc. Sci. Terre Université*, 79, Claude-Bernard Lyon 1, pp. 1–784.
- Hilgen, F.J., 1990. Sedimentary cycles and an astronomically controlled, oscillatory system of climatic changes during the Late Cenozoic in the Mediterranean. *Paléobiol. Cont.* 17, 25–33.
- Hilgen, F.J., 1991a. Astronomical calibration of Gauss to Matuyama sapropels in the Mediterranean and implication for the Geomagnetic Polarity Time Scale. *Earth Planet. Sci. Lett.* 104, 226–244.
- Hilgen, F.J., 1991b. Extension of the astronomically calibrated (polarity) time scale to the Miocene/Pliocene boundary. *Earth Planet. Sci. Lett.* 107, 349–368.
- Huard, J., 1966. Etude anatomique des bois de conifères des couches à lignite néogènes des Landes. *Mém. Soc. Géol. Fr.* 105, 7–85.
- Kloosterboer-van Hoeve, M., 2000. Cyclic changes in the late Neogene vegetation of northern Greece. *LPP Contr. Ser.* 12, 1–131.
- Koufos, G.D., Pavlides, S.B., 1988. Correlation between the continental deposits of the lower Axios valley and Ptolemais basin. *Bull. Geol. Soc. Greece* 20, 9–19.
- Laskar, J., 1990. The chaotic motion of the solar system: a numerical estimate of the size of the chaotic zones. *Ikarus* 88, 266–291.
- Lourens, L.J., Antonarakou, A., Hilgen, F.J., van Hoof, A.A.M., Vergnaud Grazzini, C., Zachariasse, W.J., 1996. Evaluation of the Plio-Pleistocene astronomical time scale. *Paleoceanography* 11, 391–413.
- Mai, D.H., 1995. In: Fischer, G. (Ed.), *Tertiäre Vegetationsgeschichte Europas. Methoden und Ergebnisse*. Jean, Stuttgart, New York, p. 691.
- Menke, B., 1975. Vegetationsgeschichte und Florenstratigraphie Nordwest-Deutschlands im Pliozän und Frühquartär. Mit einem Beitrag zur Biostratigraphie des Weichselfrühglazials. *Geol. Jb. A* 26, 3–151.
- Ozenda, P., 1975. Sur les étages de végétation dans les montagnes du bassin méditerranéen. *Doc. Cart. Ecol.* 16, 1–32.
- Ozenda, P., 1989. Le déplacement vertical des étages de végé-

- tation en fonction de la latitude: un modèle simple et ses limites. *Bull. Soc. Géol. France* 5, 535–540.
- Paillard, D., Labeyrie, L., Yiou, P., 1996. Macintosh Program performs time-series analysis. *Eos Trans. AGU*, 379.
- Petrescu, I., Nica, T., Filipescu, S., Barbu, O., Chira, C., Avram, R., Valaczkai, T., 1989. Paleoclimatical significance of the palynological approach to the Pliocene deposits of Lupoaia (Gorj county). *Stud. Univ. Babeu-Bolyai Geol.-Geogr.* 34, 75–81.
- Pontini, M.R., Bertini, A., 2000. Late Pliocene vegetation and climate in Central Italy: high-resolution pollen analyses from the Fosso Bianco succession (Tiberino Basin). *Geobios* 33, 519–526.
- Radan, S.C., Radan, M., 1998. Study of the geomagnetic field structure in the Tertiary in the context of magnetostratigraphic scale elaboration. I: The Pliocene. *An. Inst. Geol. Rom.* 70, 215–231.
- Radulescu, C., Samson, P.-M., Sen, S., Stiuca, E., Horoi, V., 1997. Les micrommifères pliocènes de Dranic (bassin Dacique, Roumanie). In: Aguilar, J.-P., Michaux, J., Legendre, S. (Eds.), *Actes du Congrès Biochrom'97. Mém. Trav. E.P.H.E., Inst. Montpellier*, 21, pp. 635–647.
- Rich, F.J., 1985. Palynology and Paleoecology of a Lignitic Peat from Trail Ridge, Florida. *Information Circular 100. Florida Geol. Survey*, pp. 1–15.
- Roberts, H.H., 1986. Selected depositional environments of the Mississippi River deltaic plain. *Geol. Soc. of America Centennial Field Guide, Southeastern Sect.*, pp. 435–440.
- Roiron, P., 1992. Flores, végétations et climats du Néogène méditerranéen: apports de macroflores du sud de la France et du nord-est de l'Espagne. Thesis, Université Montpellier 2.
- De Serres, M., 1819. Observations sur divers fossiles de quadrupèdes vivipares nouvellement découverts dans le sol des environs de Montpellier. *J. Phys.* 88, 382, 394, 405, 417.
- Shackleton, N.J., Hall, M.A., Pate, D., 1995. Pliocene stable isotope stratigraphy of Site 846. *Proc. Ocean Drill. Progr.* 138, 337–355.
- Suc, J.-P., 1981. La végétation et le climat du Languedoc (sud de la France) au Pliocène moyen d'après la Palynologie. *Paléobiol. Cont.* 12, 7–26.
- Suc, J.-P., 1982. Palynostratigraphie et paléoclimatologie du Pliocène et du Pléistocène inférieur en Méditerranée nord-occidentale. *C. R. Acad. Sci. Paris* 294, 1003–1008.
- Suc, J.-P., 1984a. Origin and evolution of the Mediterranean vegetation and climate in Europe. *Nature* 307, 429–432.
- Suc, J.-P., 1984b. La signification paléocécologique des restes végétaux. *Bull. Centres rech. Explor.-Prod. Elf-Aquitaine* 8, 97–104.
- Suc, J.-P., Cravatte, J., 1982. Etude palynologique du Pliocène de Catalogne (nord-est de l'Espagne). *Paléobiol. Cont.* 13, 1–31.
- Suc, J.-P., Diniz, F., Leroy, S., Poumot, C., Bertini, A., Dupont, L., Clet, M., Bessais, E., Zheng, Z., Fauquette, S., Ferrier, J., 1995. Zanclean (~ Brunsumian) to early Piacenzian (~ early-middle Reuverian) climate from 4° to 54° north latitude (West Africa, West Europe and West Mediterranean areas). *Meded. Rijks Geol. Dienst.* 52, 43–56.
- Suc, J.-P., Fauquette, S., Bessedik, M., Bertini, A., Zheng, Z., Clauzon, G., Suballyova, D., Diniz, F., Quézel, P., Feddi, N., Clet, M., Bessais, E., Bachiri Taoufiq, N., Méon, H., Combourieu-Nebout, N., 1999. Neogene vegetation changes in West European and West circum-Mediterranean areas. In: Agusti, J., Rook, L., Andrews, P. (Eds.), *Hominoid Evolution and Climatic Change in Europe, vol. 1: The Evolution of Neogene Terrestrial Ecosystems in Europe*. Cambridge University Press, Cambridge, pp. 378–388.
- Suc, J.-P., Zagwijn, W.H., 1983. Plio-Pleistocene correlations between the northwestern Mediterranean region and northwestern Europe according to recent biostratigraphic and paleoclimatic data. *Boreas* 12, 153–166.
- Ticleanu, N., 1992. Main coal-generating paleophytocoenoses in the Pliocene of Oltenia. *Rom. J. Paleontol.* 75, 75–80.
- Ticleanu, N., Andreescu, I., 1988. Considerations on the development of Pliocene coaly complexes in the Jiu-Motru sector (Oltenia). *D. S. Inst. Geol. Geofiz.* 72–73 (2), 227–244.
- Ticleanu, N., Buliga, S., 1992. Paleophytocoenotic researches in Pliocene deposits from the Plostina zone (Gorj district). *Rom. J. Paleontol.* 75, 81–85.
- Ticleanu, N., Diaconita, D., 1997. The main coal facies and lithotypes of the Pliocene coal basin, Oltenia, Romania. In: Gayer, R., Pesek, J. (Eds.), *European Coal Geology and Technology. Geol. Soc. Spec. Publ.* 125, pp. 131–139.
- Tiedemann, R., Sarnthein, M., Shackleton, N.J., 1994. Astronomical timescale for the Pliocene Atlantic $\delta^{18}\text{O}$ and dust flux records of ODP Site 659. *Paleoceanography* 9, 619–638.
- Van der Zwaan, G.J., Gudjonsson, L., 1986. Middle Miocene-Pliocene stable isotope stratigraphy and paleoceanography of the Mediterranean. *Mar. Micropaleontol.* 10, 71–90.
- Van Vugt, N., Langereis, C.G., Hilgen, F.J., 2001. Orbital forcing in Pliocene-Pleistocene Mediterranean lacustrine deposits: Dominant expression of eccentricity versus precession. *Palaeogeogr. Palaeoclimatol. Palaeoecol.* 172, 193–205.
- Van Vugt, N., Steenbrink, J., Langereis, C.G., Hilgen, F.J., Meulenkaamp, J.E., 1998. Magnetostratigraphy-based astronomical tuning of the early Pliocene lacustrine sediments of Ptolemais (NW Greece) and bed-to-bed correlation with the marine record. *Earth Planet. Sci. Lett.* 164, 535–551.
- Wang, C.W., 1961. The Forests of China with a Survey of Grassland and Desert Vegetation, vol. 5. M. Moors Cabot Foundation, p. 313.
- Van de Weerd, A., 1978. Early Ruscinian rodents and lagomorphs (Mammalia) from the lignites near Ptolemais (Macedonia, Greece). *Proc. K. Ned. Akad. Wet.* B82, 127–170.
- Zagwijn, W.H., 1960. Aspects of the Pliocene and early Pleistocene vegetation in The Netherlands. *Meded. Geol. Sticht.* C 3, 1–78.
- Zagwijn, W.H., Suc, J.-P., 1984. Palynostratigraphie du Plio-Pléistocène d'Europe et de Méditerranée nord-occidentales: corrélations chronostratigraphiques, histoire de la végétation et du climat. *Paléobiol. Cont.* 14, 475–483.
- Zheng, Z., Cravatte, J., 1986. Etude palynologique du Pliocène de la Côte d'Azur (France) et du littoral ligure (Italie). *Geobios* 19, 815–823.

Pollen record and integrated high-resolution chronology of the early Pliocene Dacic Basin (southwestern Romania)

Speranta-Maria Popescu^{a,*}, Wout Krijgsman^b, Jean-Pierre Suc^a, Georges Clauzon^c,
Mariana Mărunțeanu^d, Toma Nica^e

^a *Laboratoire PaléoEnvironnements et PaléobioSphère (UMR 5125 CNRS), Université Claude Bernard – Lyon 1, 27-43 boulevard du 11 Novembre, 69622 Villeurbanne Cedex, France*

^b *Paleomagnetic Laboratory “Fort Hoofdijk”, Utrecht University, Budapestlaan 17, 3584 CD Utrecht, The Netherlands*

^c *Centre Européen de Recherche et d'Enseignement sur la Géologie et l'Environnement (UMR 6635 CNRS), Europôle de l'Arbois, BP 80, 13545 Aix-en-Provence Cedex 04, France*

^d *Geological Institute of Romania, str. Caramsebes 1, 79678 Bucharest 32, Romania*

^e *Exploatarea Resurselor Minerale Oltenia, Aleea Muncii 1, Bl.H1, Sc.7, Ap.2, Motru (Gorj), Romania*

Received 2 May 2003; accepted 7 March 2006

Abstract

An integrated stratigraphic study has been performed on four early Pliocene sections in the western Dacic Basin, including the long reference section of Lupoia. Based on the integration of Mediterranean nannoplankton assemblages, the regional lignite stratigraphy, records of large and small mammals, large climatic fluctuations according to pollen grains, and climatostratigraphic relationships at the European scale, it has been possible to establish a magnetostratigraphic correlation of the different sections to the Geomagnetic Polarity Time Scale (GPTS). This correlation suggests that all normal episodes of the early Pliocene (from Thvera to Cochiti chrons) are recorded. Hence, the complete pollen record covers an almost continuous time span from about 5.33 to 4.30 Ma. In addition, the regional Dacian/Romanian stage boundary in the Dacic Basin is located in the Nunivak (C3n.3n) episode with an age of 4.55 ± 0.05 Ma. Our chronologic calibration, combined with high-resolution pollen data, results in a detailed record of paleoclimate in which the ~ 100 kyrs and ~ 400 kyrs eccentricity cycles are clearly identified.

© 2006 Elsevier B.V. All rights reserved.

Keywords: Pliocene; Lignite; Pollen; Magnetostratigraphy; Cyclostratigraphy; Romania

1. Introduction

The western part of the Dacic Basin contains one of the most important stratigraphic successions of Pliocene lignites in Southern Europe. Nevertheless, an accurate and reliable chronology for these deposits – with respect to the global standard timescale – is still lacking. Intense mining exploitation and drilling exploration have led to a complete inventory and mapping of the productive

* Corresponding author.

E-mail addresses: popescu@univ-lyon1.fr (S.-M. Popescu), krijgsma@geo.uu.nl (W. Krijgsman), jean-pierre.suc@univ-lyon1.fr (J.-P. Suc), georges.clauzon@wanadoo.fr (G. Clauzon), marunteanu@igr.ro (M. Mărunțeanu), nica-toma@yahoo.ro (T. Nica).

lignite layers. There are twenty-two main lignite beds (called A to D and I to XVIII), but their thicknesses vary according to geographic location. The lower part of these lignite beds (A to VII) corresponds to the regional Dacian stage, the upper layers (VIII to XVIII) belong to the regional Romanian stage (Marinescu and Papaianopol, 1995; Țicleanu and Diaconița, 1997). The lignite succession is best expressed and most regular in the depocenter of the basin, i.e. in the area delimited by the Carpathians, the Danube and the Olt Rivers (Fig. 1).

In the last decade, several efforts have been made to precise the chronological framework of the Dacic Basin, including fossil mammal studies (Rădulescu et al., 1993), palaeomagnetic measurements (Rădan et al., 1996) and the first systematic pollen analysis (Drivaliari et al., 1999). High-resolution magnetostratigraphic studies on the Lupoiaia reference section have been successively performed by Rădan and Rădan (1998) and Van Vugt et al. (2001). They both recorded two normal and two reversed intervals, and correlated the normal intervals to the Nunivak (C3n.2n) and Cochiti (C3n.1n) episodes of the GPTS. Recently, however, this correlation has been questioned by Popescu (2001), who proposed an alternative correlation of the same normal intervals of Lupoiaia to the Sidufjall (C3n.3n) and Nunivak (C3n.2n) episodes. This latter correlation is supported by a better and more complete use of mammal records and large-scale climatic relationships (Popescu, 2001).

The present paper aims to extend palaeomagnetic measurements to some other reference sections of the

Dacic Basin (Hinova, Husnicioara, Valea Vișenilor; Fig. 1) in order to provide a more accurate chronology for the entire early Pliocene in the area. In addition, high-resolution pollen records have been established for the same sections. Three aspects will be successively displayed and discussed: (1) regional lignite stratigraphy, (2) magnetostratigraphy, (3) climato- and cyclostratigraphy according to pollen records.

2. Regional lignite stratigraphy

The Pliocene of the Dacic Basin, i.e. Dacian–Romanian in regional stage names, consists of a more than 200 m thick succession of almost regular alternations of clays and lignites. It overlies the clayey bottomset beds and the sandy foreset beds of an outstanding Gilbert delta type system, which is perfectly exposed downstream from the Iron Gates of the Danube River near Turmu Severin (Clauzon et al., 2005). The horizontal topset beds of this Gilbert delta system characterize the continental accretion. The silty bottomset beds outcrop downstream near Hinova, where a thin layer supplies a mollusc assemblage of Bosphorian age (late Pontian) and nannoflora characteristic of the earliest Pliocene (zone NN12) (Clauzon et al., 2005). The Pliocene lignite–clay alternations of the west Dacic Basin, may also include some fluvial sands which can be relatively thick such as at Husnicioara. The condition of deposition of these lignites has long been a topic of discussion, but the recent discovery of the Gilbert delta of Turmu Severin on the western border of the Dacic

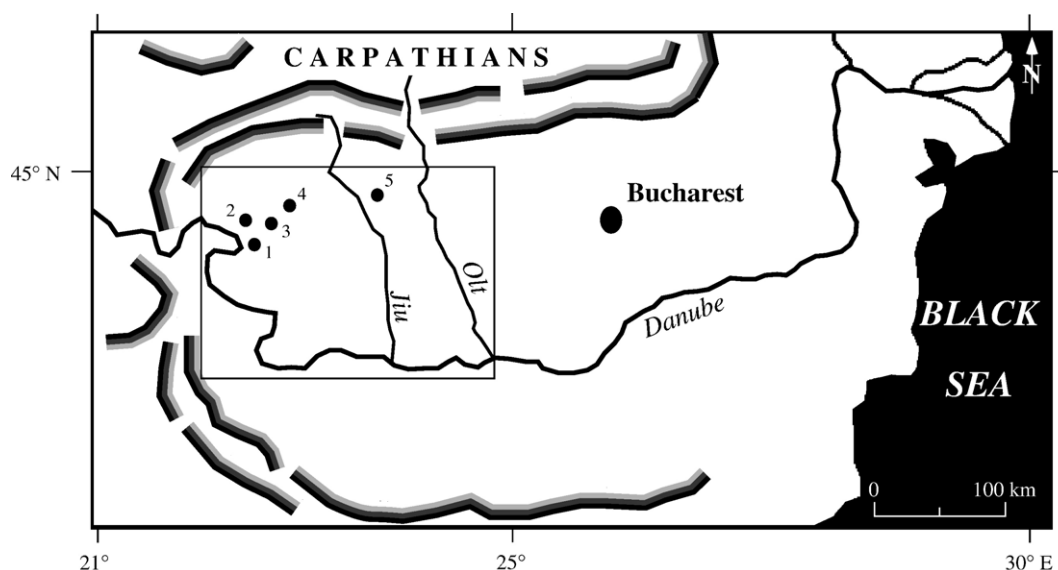


Fig. 1. Location map of the studied localities in southwestern Romania. 1, Hinova; 2, Husnicioara; 3, Valea Vișenilor; 4, Lupoiaia; 5, Țicleni. Rectangle refers to Fig. 2.

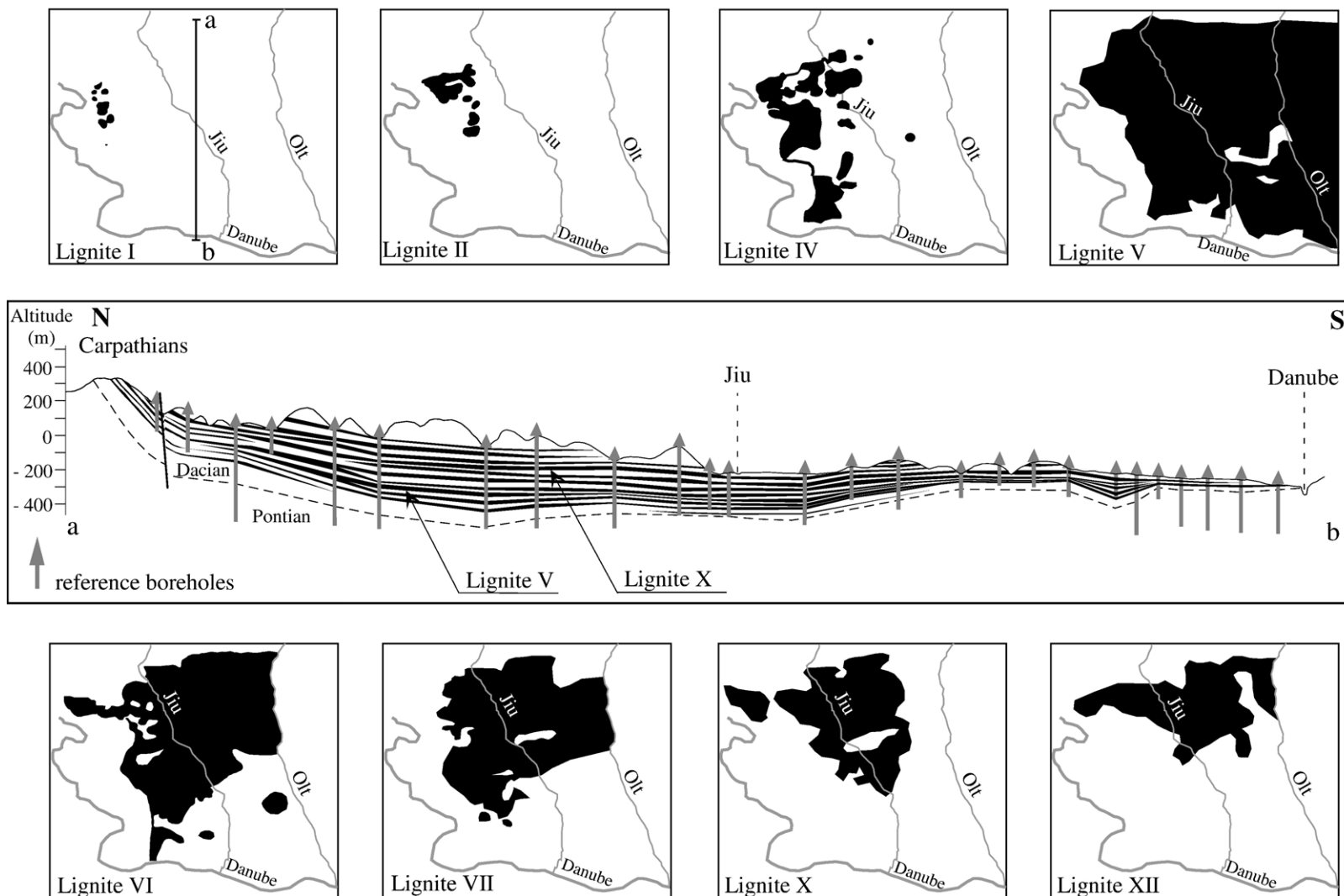


Fig. 2. Stratigraphic and geographic distribution of the most important lignites (in black) in the western Dacic Basin (document from the Romanian Lignite Company). (a–b) North–South profile with reference boreholes.

Basin (momentarily connected to the Mediterranean Sea) now confirms its fluvial origin (Clauzon et al., 2005) as previously suggested by Țicleanu (1995). Țicleanu (1995) has distinguished several types of lignites, based on both their mineral and floristic composition. He considers that the coastal vegetation was very complex and that various modes of lignite formation were controlled by the nature of plants (trees, herbs, and water plants) and by their distribution with respect to the aquatic areas (Țicleanu and Diaconița, 1997). This has been supported by pollen analysis, which evidenced a continuous competition between swamps (made of trees growing over few centimetres of water) and marshes (made of herbs growing over some 50–150 cm of water) (Popescu et al., 2006-this volume). According to Țicleanu (1995), the geographic extension of the lignites was forced by local physiography, water depth, hydrological regime, and possibly also by tectonics. In contrast, however, it has been shown by

Popescu (2001) and Popescu et al. (2006-this volume) that also climate played an important part in lignite deposition and, probably, in space distribution as well.

Despite the ongoing debates on the origin and age of lignite formation, a regional nomenclature of the lignite succession has been established for the mining exploitation, based on the detailed sequences exposed in several quarries and through a dense network of boreholes (every 200 m). This is summarized in Fig. 2, which displays the distribution of the most significant lignite beds in the western part of the Dacic Basin. This regional lignite stratigraphy has consequently been applied to our studied sections (Fig. 3) which start at lignite A (Hinova) and end at lignite XV (Husnicioara). The three uppermost lignite layers (XVI–XVII) are only developed in the central area of the basin (Țicleanu and Diaconița, 1997). This means that an almost complete vertical succession of the early Pliocene has been recovered in the western Dacic Basin, on which

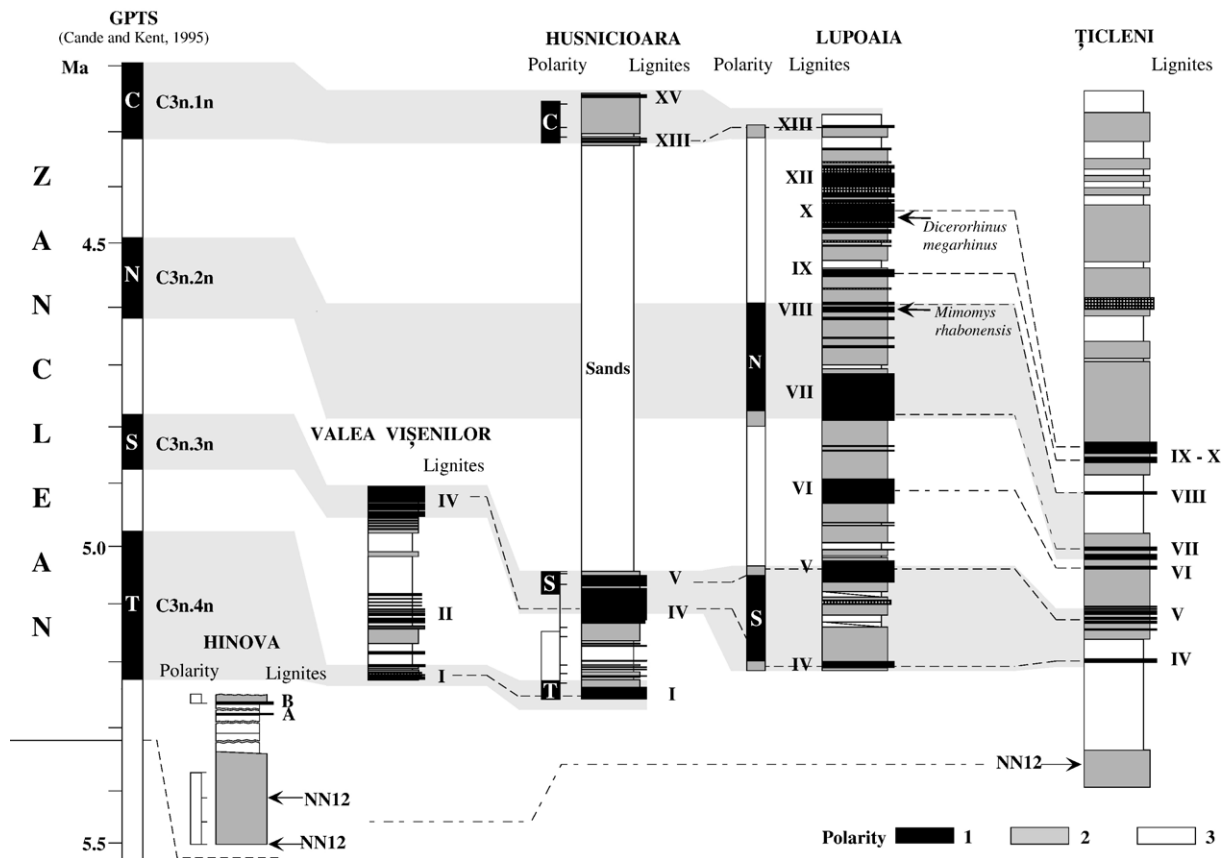


Fig. 3. Stratigraphic succession of lignites (A, B, I to XVIII) from the sections of Hinova, Valea Vișenilor, Husnicioara, Lupoiaia and Țicleni according to the regional nomenclature and chronologic assignment of the studied sections based on regional lignite stratigraphy and palaeomagnetic investigations, with additional biostratigraphic information. For Lupoiaia section, the magnetic polarity column is after Rădan and Rădan (1998) and Van Vugt et al. (2001). 1, lignite; 2, lignite–clay; 3, clay; 4, sand; 5, non-recovered interval; 6, interrupted outline. T, Thvera; S, Sidjufal; N, Nunivak; C, Cochiti (Cande and Kent, 1995).

palaeomagnetic measurements and pollen analysis have been systematically processed (Fig. 3).

3. Magnetostratigraphy

To establish a magnetostratigraphic framework for the early Pliocene of the Dacic Basin, oriented handsamples have been taken from the Hinova (6 levels), Valea Vişenilor (8 levels) and Husnicioara (10 levels) sections. Previous data by Rădan and Rădan (1998) and Van Vugt et al. (2001) from the Lupoia section are also taken into account for a general synthesis. Cores were drilled from the handsamples with compressed air at the palaeomagnetic laboratory Fort Hoofddijk. Unfortunately, the lithology of the Valea Vişenilor section appeared to be unsuitable for drilling, because of the sandy character of the samples. Hence, no palaeomagnetic results have been obtained for this section. Thermal demagnetisation was applied on the samples from Hinova and the lower part of Husnicioara

with small temperature increments of 30–50 °C up to a maximum temperature of 360 °C, in a magnetically shielded furnace. Alternating field demagnetisation was applied on the samples from the upper part of Husnicioara up to a maximum field of 1 T. At least one specimen per sampling level was demagnetised. The natural remanent magnetisation was measured on a 2G Enterprises DC SQUID cryogenic magnetometer.

The samples of the Hinova section have mainly been taken from the clays of the bottom set beds of the Gilbert delta. They have relatively high NRM-intensities, ranging between 1 and 7.5 mA/m, and the NRM is generally composed of two components. First, a small viscous present-day field component is totally removed at a temperature of 150 °C. The second component has a reversed polarity, decays linearly towards to origin, and is largely removed at 360 °C (Fig. 4a,b). Similar thermal demagnetisation behaviour is observed in the samples of the Lupoia section (Van Vugt et al., 2001). There, additional rock magnetic investigations suggested that

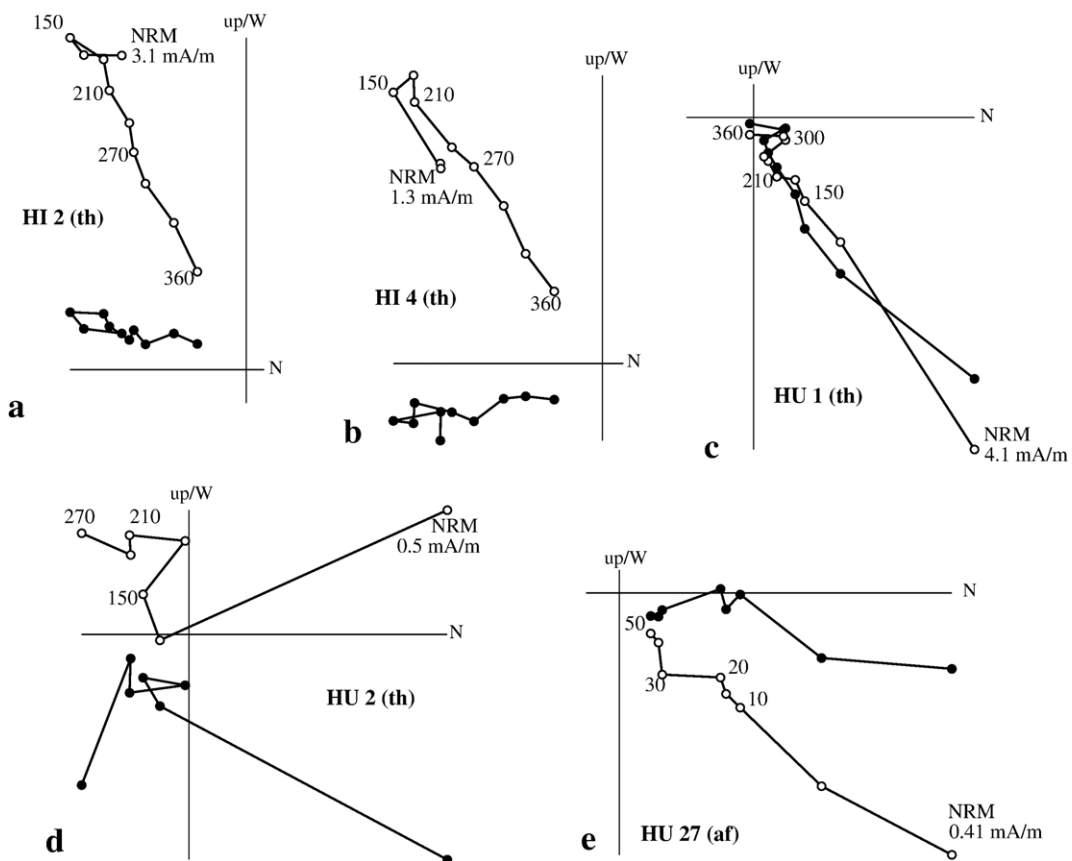


Fig. 4. Zijderveld diagrams for selected samples of the Hinova (HI) and Husnicioara (HU) sections of the west Dacic Basin. Thermal demagnetisation diagrams are indicated with (th), alternating field demagnetisation with (af). Filled symbols denote the projection of the vector end-point on the horizontal plane; open symbols denote projections on the vertical plane; values represent temperatures in °C or in mT.

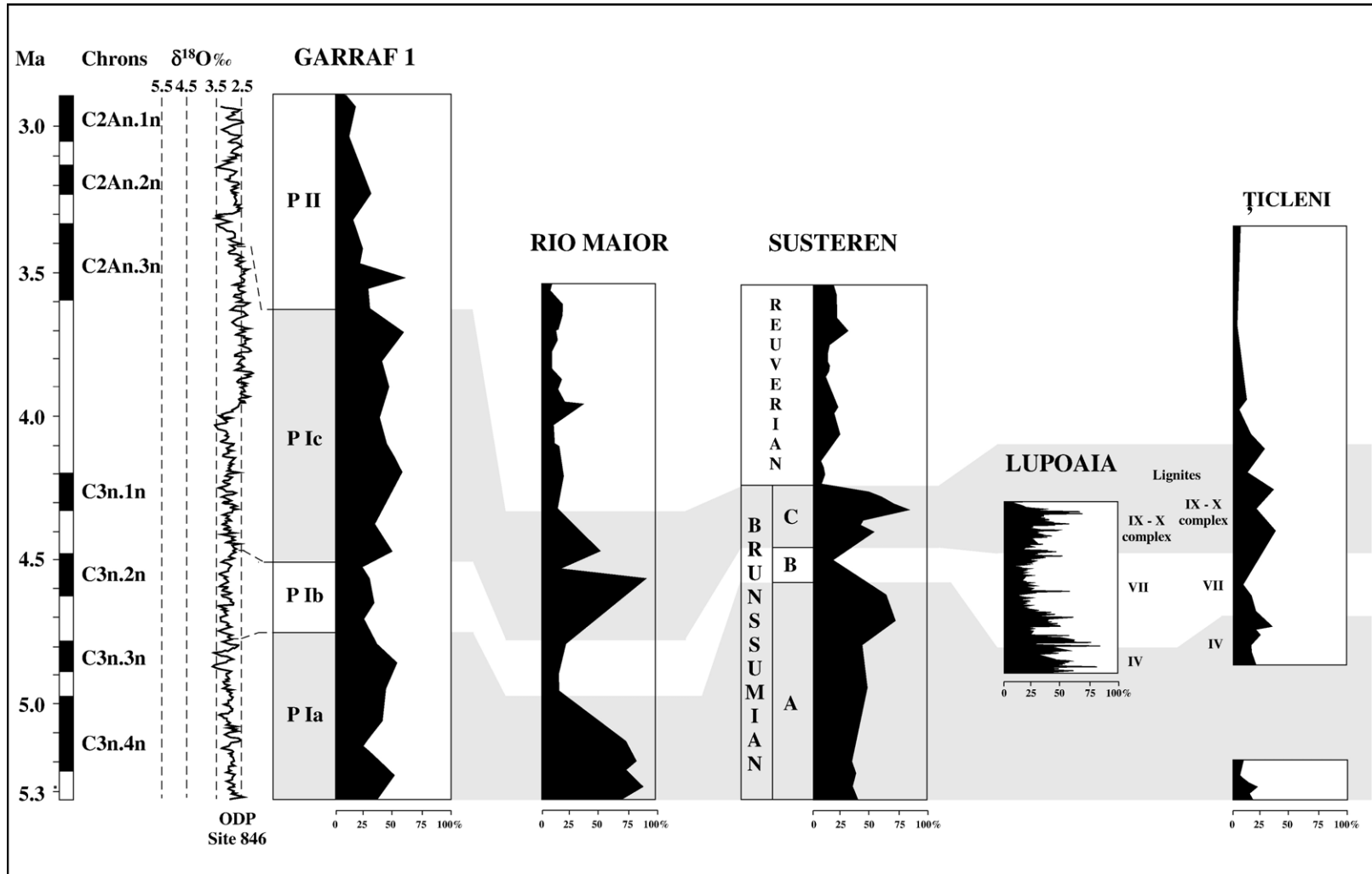


Fig. 5. Early Pliocene climatostratigraphy in Europe according to reference pollen diagrams: Garraf 1 in the Northwestern Mediterranean region (Suc and Cravatte, 1982), Rio Maior F16 in Portugal (Diniz, 1984), Susteren in The Netherlands (Zagwijn, 1960), Lupoia (Popescu, 2001) and Țicleni (Drivalieri et al., 1999) in Romania. Climatostratigraphic relationships are based on the respective curves of subtropical trees compared to the reference oxygen isotope curve from ODP Site 846 (Shackleton et al., 1995).

the magnetic signal was carried by a ferrimagnetic iron sulphide, probably greigite, which is very common in freshwater sediments. Following Van Vugt et al. (2001), we have also interpreted this reversed 150–360 °C component in the Hinova section as a primary component of the NRM, implying that the entire Hinova section was deposited during a period of reversed polarity (Fig. 3).

The samples from the Husnicioara section have been taken at a very propitious moment when the mining excavation reached lignite I. Generally, these samples have a much lower NRM-intensity, and are commonly below 1 mA/m. Consequently, thermal and alternating field demagnetisation show less straightforward diagrams. After removing a viscous component at temperatures of 150 °C (or fields of 150 mT), most samples reveal a second component, which is removed at temperatures up to 360 °C (or fields up to 500 mT). The samples which are taken directly at the top of lignites I and V show a normal polarity component (Fig. 4c). The samples between lignites I and IV reveal demagnetisation diagrams which pass by the origin and gradually merge into the reversed quadrant of the Zijderveld diagrams, suggesting the presence of a reversed component (Fig. 4d). Alternating field demagnetisation diagrams of the samples from the upper part of the section, between lignites XIII and XV are clearly of normal polarity again (Fig. 4e). Consequently, we have interpreted the interval between lignites I and IV of being of reversed polarity, the other intervals of normal polarity (Fig. 3).

High-resolution magnetostratigraphic studies have earlier been performed on the Lupoia section, and the reader is referred to Rădan and Rădan (1998) and Van Vugt et al. (2001) for more detailed information. The main result of these studies was that the lowermost part of the section (lignite V at that time) and the interval from lignite VII up to VIII have a normal polarity (Fig.

4). The middle and uppermost parts are reversed, with the uppermost reversed interval continuing at least up until lignite XV according to Rădan and Rădan (1998).

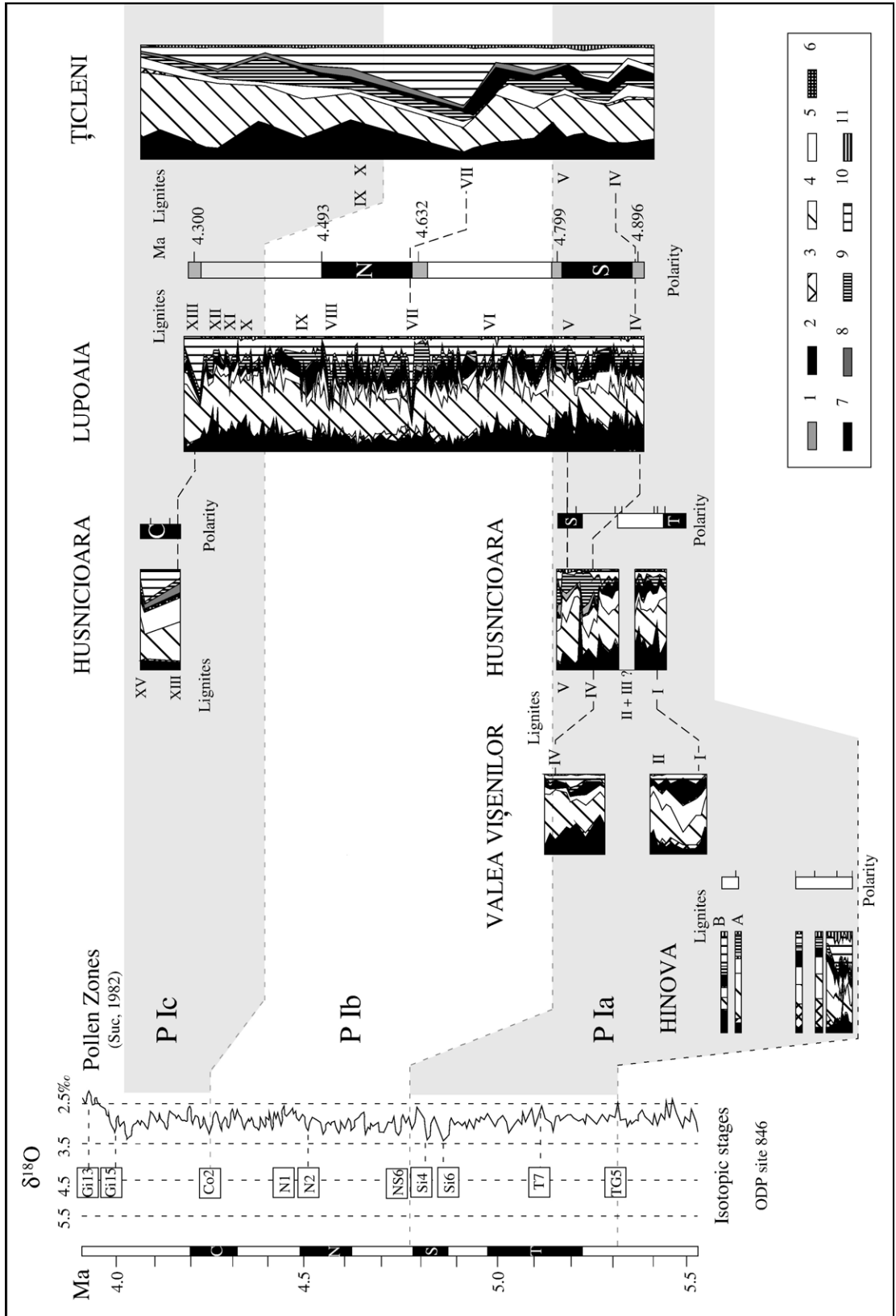
4. Correlation to the GPTS

The magnetic polarity patterns of the studied sections is generally too short to make a straightforward correlation to the GPTS. Nevertheless, there exist many additional stratigraphic constraints to achieve a best-fit correlation. This includes the detailed regional lignite stratigraphy, which allows a correlation between different sections and boreholes, and biostratigraphic constraints from nannoflora and fossil mammals.

In the Hinova section, for instance, the presence of Mediterranean nannoplankton from zone NN12 suggests an earliest Zanclean age. Moreover, the Gilbert type delta that developed along the Danube River was suggested to be related to the Pliocene flooding of the Mediterranean and Eastern Paratethys areas, directly following the Messinian salinity crisis (Clauzon et al., 2005). The observed reversed polarities are in good agreement with this scenario and therefore most likely correlate to the upper part of chron C3r. This implies that the Hinova section has been deposited in the interval between the Pliocene flooding at 5.33 Ma and the base of the Thvera at 5.23 Ma.

The correlation of the Lupoia section to the GPTS has already been the subject of considerable debate. The original magnetostratigraphic correlation by Rădan and Rădan (1998) and Van Vugt et al. (2001) was that the two normal intervals correlate to the Nunivak (C3n.2n) and Cochiti (C3n.1n) episodes. The main argument for this correlation was the presence of a long interval of reversed polarities at the upper part of the Lupoia section, from lignite bed VIII until XV. Later, however, Popescu (2001) proposed an alternative correlation of the two normal intervals to the Sidufjall (C3n.3n) and

Fig. 6. Synthetic pollen diagrams of the early Pliocene sections in the Dacic Basin and their chronological location with respect to the global polarity time-scale and the global climatic evolution. Pollen groups: 1, megathermic (i.e. tropical) elements (unidentified Euphorbiaceae, *Amanoa*, Mimosaceae including *Entada* and *Pachysandra* types, Meliaceae, Sapindaceae, Loranthaceae, Arecaceae, Sapotaceae, Tiliaceae, etc.); 2, megamesothermic (i.e. subtropical) elements (mainly Taxodiaceae, *Engelhardia*, *Cephalanthus*, *Distylium*, *Parrotiopsis jacquemontiana*, *Microtropis fallax*, Cyrillaceae–Clethraceae, *Leea*, *Myrica*, *Nyssa sinensis*, *Parthenocissus henryana*, *Ilex floribunda* type, Anacardiaceae, Araliaceae, *Magnolia*, etc.); 3, a lower-mid-altitude coniferous elements, *Cathaya*; 4, mesothermic (i.e. warm–temperate) elements (deciduous *Quercus* chiefly, *Carya*, *Pterocarya*, *Liquidambar*, *Parrotia persica*, *Carpinus*, *Ulmus*, *Zelkova*, *Celtis*, *Ostrya*, *Platanus*, *Juglans*, *J. cf. cathayensis*, *Nyssa*, *Sciadopitys*, *Buxus sempervirens* type, *Acer*, *Tilia*, *Fagus*, *Alnus*, *Salix*, *Populus*, Ericaceae, *Vitis*, *Hedera*, *Lonicera*, *Fraxinus*, *Ligustrum*, *Sambucus*, *Viburnum*, *Rhus*, *Ilex*, *Tamarix*, *Betula*, etc.); 5, *Pinus*; 6, meso-microthermic (i.e. cool–temperate) trees: *Cedrus*, *Keteleeria* and *Tsuga* growing in mid-altitude; 7, microthermic (i.e. boreal) trees living in high altitude, *Abies* and *Picea*; 8, elements without significance (Rosaceae, Ranunculaceae, unidentified pollen grains, poorly preserved pollen grains); 9, Cupressaceae; 10, herbs: Cyperaceae, Poaceae, Asteraceae, *Plantago*, Brassicaceae, Apiaceae, *Polygonum*, *Rumex*, Amaranthaceae–Chenopodiaceae, Caryophyllaceae, *Linum*, *Erodium*, *Convolvulus*, *Mercurialis*, *Euphorbia*, *Scabiosa*, *Knautia*, Malvaceae, Boraginaceae, *Helianthemum*, *Asphodelus*, Liliaceae, Cannabaceae, Fabaceae, Plumbaginaceae, *Butomus*, water-plants such as *Potamogeton*, Restionaceae, *Myriophyllum*, *Typha*, *Sparganium*, *Thalictrum*, *Nuphar*, *Nymphaea*, Oenotheraceae, *Trapa*, *Utricularia*, etc.; 11, steppe elements (*Artemisia*, *Ephedra*) (Suc, 1984).



Nunivak (C3n.2n). This latter correlation was based on a better fit between the pollen data of Lupoia with global climatic fluctuations provided by the oxygen isotope curves. The only problem with this revised correlation is the apparent absence of the Cochiti (C3n.1n) episode in the upward extension of the Lupoia record. Additional biostratigraphic data at Lupoia comes from fossil mammals, which indicate the presence of a primitive *Miomys* (*Miomys rhabonensis*) and *Apodemus dominans* within lignite VIII (Rădulescu et al., 1993), while *Dicerorhinus megarhinus* is observed within lignite X (Apostol and Enache, 1979). In northern Greece, the first *Miomys* (*Miomys davakosi*) is recorded in the Ptolemais 3 locality (van der Weerd, 1978), which correlates to the Sidufjall (C3n.3n) episode (Van Vugt et al., 1998). Unfortunately, no reliable age constraints (apart from being early Pliocene in age) can be given to the other species. Therefore, this mammal fauna of Lupoia does not provide unambiguous chronological support to distinguish between the two different correlations.

The Husnicioara section is largely overlapping in time with the Lupoia section, although the main part of this section consists of unconsolidated sands, which appeared to be unsuitable for a paleomagnetic study. The upper part of the Husnicioara section, however, consists of a more clay-rich interval and corresponds to the lignites XIII and XV, according to the regional lignite stratigraphy. The demagnetisation results from this interval suggest that lignites XIII–XV were deposited during an interval of normal polarity. Obviously, this is in disagreement again with the reported reversed polarities of the same interval in Lupoia (Rădan and Rădan, 1998). So far, no unambiguous solution is found for this discrepancy, but overprinting of the magnetic signal (either normal or reversed) or errors in the lignite nomenclature (either in Husnicioara or Lupoia) cannot be completely excluded. Nevertheless, the normal polarities of the upper part of Husnicioara are in clear support of the revised correlation of Popescu (2001) and hence they should correspond to the Cochiti (C3n.1n) episode (Fig. 3).

The lower part of the Husnicioara section reveals normal polarities in the lignite–clay interval just below the sands. According to the regional lignite stratigraphy, this interval corresponds to lignites IV and V (Fig. 3). Moreover, these normal polarities are in good agreement with the normal polarities observed in Lupoia between lignites IV and V (Rădan and Rădan, 1998; Van Vugt et al., 2001). Consequently, they correspond to the Sidufjall (C3n.3n) according to the correlation of Popescu (2001). The downward extension of mainly

reversed polarities is in good agreement with this correlation and the normal polarity at the base of the section thus suggests that lignite I was deposited during the uppermost part of the Thvera (C3n.4n) episode.

Summarizing, it can be concluded that the studied Pliocene series of the Dacic Basin covers at least a time span from the earliest Zanclean (about 5.33 Ma) up to the Cochiti normal episode (about 4.2 Ma), including all the normal events of the concerned period (Fig. 3). The onset of lignite deposition in the Dacic Basin is dated at approximately 5.25 Ma, i.e. slightly below the base of the Thvera. This seems to be perfectly synchronous with the marked transition from the carbonates of the “Lower Formation” to the lignite-bearing sediments in the Ptolemais basin in northern Greece, which occurred one precession cycle below the Thvera, suggesting a large-scale regional control on lignite formation. Moreover, the Dacian/Romanian boundary is located between lignites VII and VIII of the Lupoia section (Andreescu, 1981; Alexeeva et al., 1983) and thus correlates to the Nunivak (C3n.3n) episode (Fig. 3). Consequently, the age of the Dacian–Romanian boundary arrives at approximately 4.55 ± 0.05 Ma in the Dacic Basin.

5. Climato- and cyclostratigraphy

The reliability of long-distance relationships based on climatic significance of pollen diagrams has been confirmed by Suc and Zagwijn (1983) and amplified by Suc et al. (1995). At the European mid-latitudes, the early Pliocene is characterized by two warm phases [noted Brunssumian A and C by Zagwijn (1960) and P Ia and P Ic by Suc (1984)] surrounding a moderate cooling phase [Brunssumian B of Zagwijn (1960) = P Ib of Suc (1984)]. Such a subdivision is only slightly expressed in the records of the Southern Mediterranean region where aridity is intense and dominant (Suc et al., 1995). However, it is well pronounced in the records of Portugal in Southwestern Europe (Diniz, 1984) and of the Eastern Paratethys in Southeastern Europe (Drivaliari et al., 1999). The floristic composition of the numerous investigated European regions is rather different, but fluctuations within pollen diagrams are parallel and are distinctly illustrated by the curve of subtropical trees (see the listing below) (Fig. 5). In addition, this pollen curve may be compared with the oxygen isotope reference curve of the open ocean (Shackleton et al., 1995) (Fig. 5). Taking into account the relative weakness of subtropical trees and the relative importance of altitudinal trees in the middle part of the Lupoia pollen diagram (Fig. 6), this section

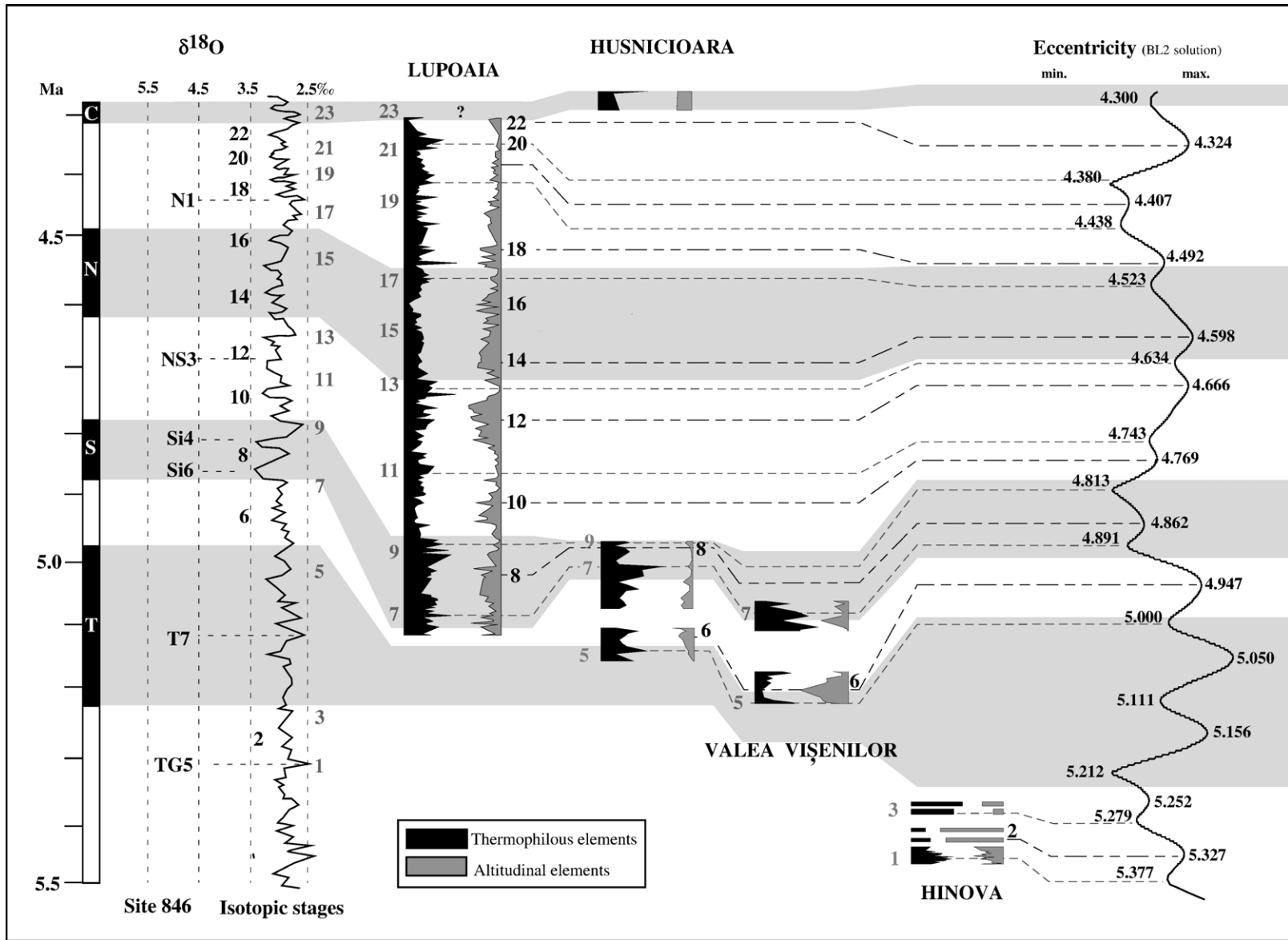


Fig. 7. High-resolution cyclostratigraphy of the early Pliocene sections in the Dacic Basin according to comparison between thermophilous vs. altitudinal element curves and the eccentricity curve (BL2 solution: Loutre and Berger, 1993).

obviously refers to the three Zanclean climatic phases: the upper part of P Ia, the entire P Ib, the lowermost part of P Ic (Figs. 5 and 6). These climatostratigraphic relationships support the magnetostratigraphic assignments discussed above and are wholly consistent with the regional lignite stratigraphy (see relationships between Lupoiaia and Țicleni: Fig. 5). Consequently, it is proposed to correlate the pollen diagrams of the southwestern Romanian sections to obtain climatostratigraphic relationships, thereby including the magnetostratigraphic age constraints and taking into account the regional lignite stratigraphy (Fig. 6).

Detailed pollen counts are deposited at the Laboratory “PaléoEnvironnements et PaléobioSphère” (University Claude Bernard – Lyon 1) and will be shortly on the “Cenozoic Pollen and Climatic values” database (C.P.C.) on the Medias-France website (<http://cpc.mediasfrance.org>). Synthetic pollen diagrams have been used in which taxa are grouped with respect to their climatic and ecological significance (Suc, 1984; Suc et al., 1995). The eleven taxa groupings are given in Fig. 6.

The complete Hinova and Valea Vișenilor sections, the lower part of Husnicioara and the lowermost part of Lupoiaia, belong to the P Ia warm phase (Fig. 6). The warmest period is recorded at Valea Vișenilor, Husnicioara and mostly at Lupoiaia in correspondence with lignite V which, in addition, shows the largest geographic extension; Fig. 2). The middle part of Lupoiaia belongs to the P Ib cooling phase. The coolest period is recorded at Lupoiaia around lignite bed VII, although here it is not so clearly reflected in its geographical extension. The uppermost parts of Lupoiaia and Husnicioara belong to the beginning of the P Ic warm phase (Fig. 6). The Țicleni borehole contains the three climatic phases, which are depicted at a considerably lower resolution but evidently show the “cooler” interval straddling lignite VII (Fig. 6).

Synthetic pollen diagrams can be summarized into two opposite curves, the thermophilous elements (i.e. the megathermic elements plus the mega-mesothermic elements plus the Cupressaceae) on the one hand, the altitudinal elements [*Cathaya* plus meso-microthermic elements (*Tsuga* and *Cedrus*) plus microthermic elements (*Abies* and *Picea*)] on the other hand. Such curves provide very good possibilities of comparison with the oxygen isotopic reference curve, maxima of thermophilous elements (warming events) corresponding to $\delta^{18}\text{O}$ minima and maxima of altitudinal elements (cooling events) corresponding to $\delta^{18}\text{O}$ maxima (Popescu, 2001; Popescu et al., 2006-this volume). In total, 23 major climatic points have been

identified both on the oxygen isotope reference curve and on the pollen records, which have been correlated within the magnetostratigraphic frame during the early Pliocene time window corresponding to the studied sections (Fig. 7). Even numbers indicate cooler events, odd numbers indicate warmer events. The continuous opposition between the two pollen groups evidenced at Lupoiaia (Popescu, 2001) is recurring within the entire basin, whatever the lithology that discards a possible influence of pollen transport. It has been demonstrated by Popescu (2001) and Popescu et al. (2006-this volume) that alternations between these pollen groups were forced by 100 kyr cycles of eccentricity: maxima of thermophilous elements related to minima of eccentricity, maxima of altitudinal elements related to maxima of eccentricity. As a consequence, relationships between pollen curves and the eccentricity curve provide a high-resolution chronology to the Early Zanclean sediments of the Dacic Basin between 5.33 and 4.30 Ma. All the eccentricity cycles have been correlated with pollen records, except those comprised between 5.230 and 5.00 Ma which correspond to sands separating lignites B and I (Țicleanu and Diaconița, 1997) (Fig. 7); i.e. the lowermost top set beds of the Turnu Severin Gilbert delta (Clauzon et al., 2005). In addition, 400 kyr cycles are also obvious: phases of increasing thermophilous elements are exaggerated during the lowest eccentricity minima (climatic events 3, 7 and 9, 19 and 21; Fig. 7), while the altitudinal elements are enriched during the highest eccentricity maxima (climatic events 10, 12, 14 and 16; Fig. 7). This suggests that the large-scale climatic subdivisions proposed by Zagwijn (1960), Suc (1984) and Diniz (1984) and which allow long distance climatostratigraphic relationships (Suc and Zagwijn, 1983; Suc et al., 1995), are dominantly forced by the ~400 kyr eccentricity cycles.

6. Conclusions

Several ways for dating the early Zanclean sediments of the Dacic Basin have been successively used. Mediterranean nannoplankton of zone NN12 immediately overlies a strong erosional surface, which was suggested to have a relation with the Messinian salinity crisis in the Mediterranean (Clauzon et al., 2005), and thus correlates to the earliest Zanclean. The normal polarities of the lignite I and of the lignite XIII–XV interval at Husnicioara seem to confirm the chronological re-calibration of the Lupoiaia reference section to the Sidufjall and Nunivak episodes (Popescu, 2001). This correlation is very consistent with the pollen

records and the resulting climatostratigraphy. In addition, palaeomagnetic measurements have been understood within the frame of the regional lignite stratigraphy and show the presence of the four successive normal events of the Gilbert Chron (Thvera to Cochiti). Consequently, an almost continuous pollen record of the western Dacic Basin is provided for the early Pliocene interval between about 5.33 and 4.30 Ma. Two very significant and still opposite pollen curves (thermophilous elements vs. altitudinal elements) allow a direct comparison with the reference oxygen isotopic curve and with the 100 kyr and 400 kyr eccentricity cycles in the astronomical curve. Recognition of 400 kyr cycles offers large climatostratigraphic subdivisions as previously proposed by Zagwijn (1960), Suc (1984) and Diniz (1984). Recognition of 100 kyr cycles only depends on time resolution of pollen analyses. This emphasizes once again the importance of very high-resolution pollen sampling.

Acknowledgements

This study was supported by the Programme “Environnement, Vie et Sociétés”. WK acknowledges financial support from the Dutch research centre for Integrated Solid Earth Sciences (ISES). The Romanian Lignite Company and D. Jipa are acknowledged for providing underground information. Dr. O. Oms is greatly acknowledged for his review of the paper.

References

- Alexeeva, L.I., Andreescu, I., Brandabur, T., Cepalaga, A., Ghenea, C., Mihaila, N., Trubihin, V., 1983. Correlation of the Pliocene and Lower Pleistocene deposits in the Dacic and Euxinic Basins. *Anu. Inst. Geol. Geofiz., Stratigr. Paleontol.* 59, 143–151.
- Andreescu, I., 1981. Middle–Upper Neogene and Early Quaternary chronostratigraphy from the Dacic Basin and correlation with neighbouring areas. *Ann. Géol. Pays Hellén., h.s.* 4, 129–138.
- Apostol, L., Enache, C., 1979. Etude de l'espèce *Dicerorhinus megarhinus* (de Christol) du bassin carbonifère de Motru. *Trav. Mus. Natl. Hist. Nat. “Grigore Antipa”* 20, 533–540.
- Cande, S.C., Kent, D.V., 1995. Revised calibration of the Geomagnetic Polarity Time Scale for the Late Cretaceous and Cenozoic. *J. Geophys. Res.* 100, 6093–6095.
- Clauzon, G., Suc, J.-P., Popescu, S.-M., Mărunțeanu, M., Rubino, J.-L., Marinescu, F., Melinte, M.C., 2005. Influence of the Mediterranean sea-level changes over the Dacic Basin (Eastern Paratethys) in the Late Neogene. The Mediterranean Lago Mare facies deciphered. *Basin Res.* 17, 437–562.
- Diniz, F., 1984. Etude palynologique du bassin pliocène de Rio Maior. *Paléobiol. Cont.* 14, 259–267.
- Drivaliari, A., Țicleanu, N., Marinescu, F., Mărunțeanu, M., Suc, J.-P., 1999. A Pliocene record at Țicleni (Southwestern Romania). In: Wrenn, J.H., Suc, J.-P., Leroy, S.A.G. (Eds.), *The Pliocene: Time of Change*. Amer. Ass. Stratigr. Palynologist Foundation, pp. 103–108.
- Loutre M.-F., Berger A., 1993. Sensibilité des paramètres astro-climatiques au cours des 8 derniers millions d'années: Scientific Report 93/4, Institut d'Astronomie et de Géophysique G. Lemaître, Université catholique de Louvain, Louvain-la-Neuve: 1–9.
- Marinescu, F., Papaianopol, I., 1995. Chronostratigraphie und Neostatotypen. *Dacien. Edit. Academiei Romane, Bucarest.* 530 pp.
- Popescu, S.-M., 2001. Repetitive changes in early Pliocene vegetation revealed by high-resolution pollen analysis: revised cyclostratigraphy of southwestern Romania. *Rev. Palaeobot. Palynol.* 120, 181–202.
- Popescu, S.-M., Suc, J.-P., Loutre, M.-F., 2006-this volume. Early Pliocene vegetation changes forced by eccentricity–precession. Example from Southwestern Romania. In: Agustí, J., Oms, O., Meulenkamp, J.E. (Eds.), *Late Miocene to early Pliocene environment and climate change in the Mediterranean area*. Palaeogeography, Palaeoclimatology, Palaeoecology, vol. 238, pp. 340–348.
- Rădan, S.C., Rădan, M., 1998. Study of the geomagnetic field structure in the Tertiary in the context of magnetostratigraphic scale elaboration: I. The Pliocene. *An. Inst. Geol. Rom.* 70, 215–231.
- Rădan, S.C., Rădan, M., Rădan, S., Andreescu, I., Vanghelie, I., 1996. Magnetostratigraphic and mineralogical study of Dacian – Romanian formations from Mehedinti area: towards the synonymous nomination of lignite beds related to the Motru zone. *An. Inst. Geol. Rom.* 69 (1), 324–331.
- Rădulescu, S., Samson, P.-M., Stiuică, E., Enciu, P., Popescu, A., 1993. Sur la découverte de nouvelles associations de micromammifères dans le Pliocène d'Olténie. Implications paléobiogéographiques. *An. Univ. Bucur., Geol.* 42, 69–78.
- Shackleton, N.J., Hall, M.A., Pate, D., 1995. Pliocene stable isotope stratigraphy of Site 846. *Proc. Ocean Drill Program, Sci. Res., vol. 138*. U.S. Gov. Print. Off., pp. 337–355.
- Suc, J.-P., 1982. Palynostratigraphie et paléoclimatologie du Pliocène et du Pléistocène inférieur en Méditerranée nord-occidentale. *C. R. Acad. Sci., Paris, Ser. 2* 294, 1003–1008.
- Suc, J.-P., 1984. Origin and evolution of the Mediterranean vegetation and climate in Europe. *Nature* 307, 429–432.
- Suc, J.-P., Cravatte, J., 1982. Etude palynologique du Pliocène de Catalogne (nord-est de l'Espagne). *Paléobiol. Cont.* 13 (1), 1–31.
- Suc, J.-P., Zagwijn, W.H., 1983. Plio-Pleistocene correlations between the northwestern Mediterranean region and northwestern Europe according to recent biostratigraphic and paleoclimatic data. *Boreas* 12, 153–166.
- Suc, J.-P., Diniz, F., Leroy, S., Poumot, C., Bertini, A., Dupont, L., Clet, M., Bessais, E., Zheng, Z., Fauquette, S., Ferrier, J., 1995. Zanclean (~Brunsumian) to early Piacenzian (~early–middle Reuverian) climate from 4° to 54° north latitude (West Africa, West Europe and West Mediterranean areas). *Meded.-Rijks Geol. Dienst* 52, 43–56.
- Țicleanu, N., 1995. Modèle génétique conceptuel des accumulations de charbon du Bassin Dacique. In: Marinescu, F., Papaianopol, I. (Eds.), *Chronostratigraphie und Neostatotypen. Dacien. Edit. Academiei Romane, Bucarest.* pp. 46–54.

- Țicleanu, N., Diaconița, D., 1997. The main coal facies and lithotypes of the Pliocene coal basin, Oltenia, Romania. In: Gayer, R., Pesek, J. (Eds.), *European Coal Geology and Technology*. Geol. Soc. Spec. Publ., vol. 125, pp. 131–139.
- van der Weerd, A., 1978. Early Ruscinian rodents and lagomorphs (Mammalia) from the lignites near Ptolemais (Macedonia, Greece). *Proc. K. Ned. Akad. Wet.* B82, 127–170.
- Van Vugt, N., Steenbrink, J., Langereis, C.G., Hilgen, F.J., Meulenkamp, J.E., 1998. Magnetostratigraphy-based astronomical tuning of the early Pliocene lacustrine sediments of Ptolemais (NW Greece and bed-to-bed correlation with the marine record. *Earth Planet. Sci. Lett.* 164, 535–551.
- Van Vugt, N., Langereis, C.G., Hilgen, F.J., 2001. Orbital forcing in Pliocene–Pleistocene Mediterranean lacustrine deposits: dominant expression of eccentricity versus precession. *Palaeogeogr. Palaeoclimatol. Palaeoecol.* 172, 193–205.
- Zagwijn, W.H., 1960. Aspects of the Pliocene and early Pleistocene vegetation in The Netherlands. *Meded. Geol. Sticht., C 3 (5)*, 1–78.

Early Pliocene vegetation changes forced by eccentricity-precession. Example from Southwestern Romania

Speranta-Maria Popescu^{a,*}, Jean-Pierre Suc^a, Marie-France Loutre^b

^a *Laboratoire PaléoEnvironnements et Paléobiosphère (UMR 5125 CNRS), Université Claude Bernard, Lyon 1, 27-43 boulevard du 11 Novembre, 69622 Villeurbanne Cedex, France*

^b *Institut d'Astronomie et de Géophysique G. Lemaître, Chemin du Cyclotron 2, Université Catholique de Louvain, 1348 Louvain la Neuve, Belgium*

Received 11 June 2003; accepted 7 March 2006

Abstract

Repetitive changes in Early Pliocene marine and continental sediments were forced by astronomical cycles (eccentricity, precession) and related to low amplitude climatic fluctuations as demonstrated at Capo Rossello and Monte San Nicola (Sicily). This work aims to establish if such climatic fluctuations have also controlled changes in the vegetation during the warm Early Pliocene. High-resolution pollen analysis of the Lupoia section (SW Romania) provides evidence of a clear response owing to its location within a delta system which constitutes a reliable area for pollen deposition near the Carpathians (i.e. capable of registering all the vegetation ecosystems from edaphic coastal associations up to the highest altitudinal belts), and owing to its Southeastern European longitude probably where warm–humid air masses arrived regularly, making the region a highly favourable refuge for thermophilous plants. Eccentricity appears to have controlled fluctuations in temperature (development of thermophilous elements during eccentricity minima, and descent of altitudinal trees during eccentricity maxima) while precession appears to have forced changes in humidity (expansion of cypress swamps related to precession maxima, and spread of herbaceous marshes requiring more humidity related to precession minima) with respect to increased precipitation and run-off.

© 2006 Elsevier B.V. All rights reserved.

Keywords: Pollen; Vegetation; Orbital cycles; Pliocene; Romania

1. Introduction

Some Pliocene key sections such as Rossello and Monte San Nicola (Sicily) have had their sedimentation forced by orbital parameters (Hilgen, 1991). The Rossello composite section has become a global reference section for the Early and Middle Pliocene

because of its very detailed sedimentary record (Hilgen, 1987; Hilgen and Langereis, 1989) coupled to a high-resolution palaeomagnetic investigation (Langereis and Hilgen, 1991). The section is mostly a rhythmic succession of grey marls–white marls (or carbonates)–beige marls–white marls (or carbonates) (Hilgen, 1987). Such quadruplets result from intense variations in CaCO₃ content which (1) have been correlated with the precession and eccentricity (both 100 and 400 ka periods) curves and (2) explained by fluctuations in precipitation and consequently in run-off (Hilgen, 1991). Maxima in carbonates have been related to

* Corresponding author.

E-mail addresses: popescu@univ-lyon1.fr (S.-M. Popescu), jean-pierre.suc@univ-lyon1.fr (J.-P. Suc), loutre@astr.ucl.ac.be (M.-F. Loutre).

eccentricity minima, and grey marls (the so-called sapropels) to precession minima (increasing precipitation and run-off) (Hilgen, 1991). Quantified marine organisms (foraminifers, calcareous nannofossils) from the Rossello composite section also show direct relationships with lithological changes, i.e. with precession and eccentricity for the Early–Middle Pliocene (Sprovieri, 1993; Di Stefano et al., 1996). Indeed, stable isotope curves have established that Early–Middle Pliocene astronomical cycles have resulted in variations in temperature (Tiedemann et al., 1994; Shackleton et al., 1995). Rainfall also fluctuated as evidenced by dust flux in Africa (Tiedemann et al., 1994; DeMenocal, 1995).

Similar alternations in lithology, forced both by precession and eccentricity, characterize also the Middle–Late Pliocene passage (at about 2.6 Ma) in Sicily (Rossello composite section, Monte San Nicola; Hilgen, 1991). In contrast, abundance variations of the warm-water planktonic foraminifer *Globigerinoides ruber* recorded for the same time-window at Rossello (Sprovieri, 1993) and Monte San Nicola (Rio et al., 1994) in Sicily and at Singa in Calabria (Lourens et al., 1992), emphasize the progressive dominance of obliquity over the other astronomic parameters, as also supported by oxygen isotope records (Tiedemann et al., 1994; Shackleton et al., 1995). These studies have led to a very accurate chronological calibration of the Pliocene and Early Pleistocene with respect to astronomical parameters (Lourens et al., 1996).

The aim of this paper is to determine whether climatic variations have been intense enough during the Early Pliocene to have induced noticeable changes in vegetation. Pollen analysis has documented Early

Pliocene vegetation changes for the whole of Europe (Zagwijn, 1960; Suc, 1984; Diniz, 1984; Suc et al., 1995). Unfortunately, the low sampling resolution of key sections (Susteren in The Netherlands, Garraf 1 in the Northwestern Mediterranean, Rio Maior F16 in Portugal) does not allow for the assessment of any direct relationship between vegetation changes and orbital cycles (Suc et al., 1995), except with some periods of high-amplitude variations of obliquity (Lourens and Hilgen, 1997). A favourable area for such high-resolution pollen analyses is SW Romania because (1) it is located near the Carpathians where repeated variations in temperature might have caused movements of vegetation belts, and (2) it is part of Southeastern Europe where thermophilous plants requiring some humidity persisted for longer than in the other European and peri-Mediterranean regions (Suc et al., 2004), probably because some warm, humid air masses regularly reached the area. Indeed, up today, coastal Anatolian forests have acted as refuge biotopes for thermophilous plants (Zohary, 1973; Quézel and Médail, 2003).

2. The Lupoaia section

A long well-dated section has been analysed at Motru (44°48' N, 22°58' E) (Fig. 1). The Lupoaia section (133.70 m thick) is mostly made of lignite–clay alternations and corresponds to a delta environment (palaeoaltitude: few meters above lake-level) where various kinds of lignites were generated (Țicleanu and Diaconița, 1997). With respect to the regional lignite stratigraphy which includes 22 coal beds, lignites IV to XIII have been identified in the section (Fig. 2). Two

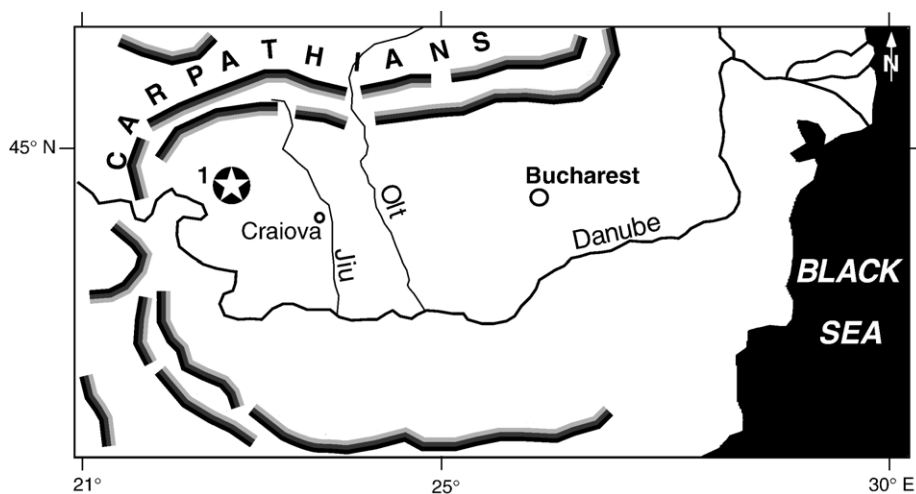


Fig. 1. Location map of the Lupoaia section in Southwestern Romania.

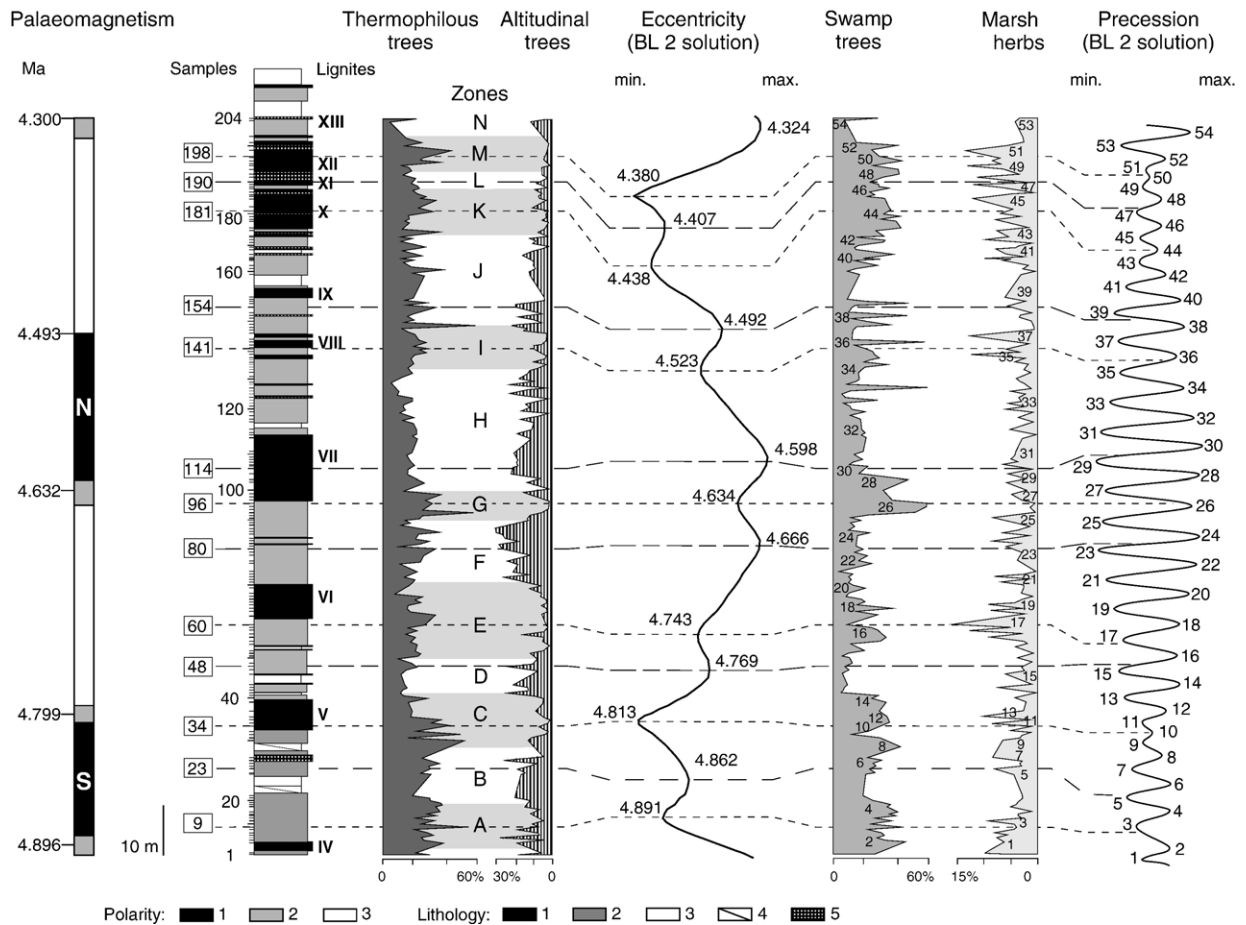


Fig. 2. Response of the pollen record (thermophilous trees vs. altitudinal trees, swamp trees vs. marsh herbs) and lithology (lignite–clay alternations) to orbital forcings (eccentricity and precession) at Lupoia. From left to right: • Lithological succession of the Lupoia section and its magnetostratigraphic control. • Cyclic response of thermophilous elements vs. altitudinal trees with respect to eccentricity (BL2 solution; [Loutre and Berger, 1993](#)) resulting in zones A to N. To the left are outlined samples selected as representative of eccentricity minima and maxima in relation to their inferred astronomical age. • Cyclic response of swamp trees vs. marsh herbs with respect to precession (BL2 solution; [Loutre and Berger, 1993](#)) within the chronological framework related both to magnetostratigraphic control of the Lupoia section and to inferred astronomical ages from thermophilous tree/altitudinal tree curves vs. eccentricity. Respective precession minima and maxima are numbered and correlated to pollen curves. Polarity: 1, normal; 2, undetermined; 3, reverse; S, Sidufjal; N, Nunivak. Lithology: 1, lignite; 2, clays; 3, sand; 4, uncovered zone; 5, lignitic clay.

normal palaeomagnetic events have been documented within the section ([Rădan and Rădan, 1998](#); [Van Vugt et al., 2001](#)) which, according both to local mammal faunas and to climatostratigraphic relationships between the reference European pollen diagrams ([Suc, 1984](#); [Suc et al., 1995](#)) and the Lupoia section, respectively belong to Sidufjal (C3n.3n) and Nunivak (C3n.2n) subchrons ([Popescu, 2001](#); [Popescu et al., 2006-this volume](#)). The section extends from about 4.9 to 4.3 Ma ([Fig. 2](#)).

2.1. Vegetation changes and temperature fluctuations

The Lupoia pollen record shows a continuous competition between plants requiring warm climatic

conditions (mainly subtropical elements: *Taxodiaceae*, *Engelhardia*, *Nyssa*, *Distylium*, *Microtropis fallax*, *Cyrillaceae*–*Clethraceae*, *Leea*, *Magnolia*, etc.; some tropical elements: *Mimosaceae*, *Meliaceae*, *Amanoa*, *Sapindaceae*, *Loranthaceae*, *Arecaceae*, *Sapotaceae*, etc.) and plants living under cool–temperate to cold climatic conditions (*Tsuga*, *Cedrus*, *Cathaya*, *Abies* and *Picea*) ([Fig. 2](#)). The first group of plants probably grew at low altitude (0–500? m), whereas the second group probably inhabited higher elevations (up to 2000–2300 m for *Abies* and *Picea*) ([Fauquette et al., 1999](#)). Such alternations in pollen spectra, more or less consistent with lignite–clay alternations, express changes in temperature respectively characterized in the area by altitudinal shifts of vegetation belts. These

shifts represent the ascending expansion of thermophilous forest towards mid-altitudes when temperature increased, and the descent of altitudinal coniferous forest during cooling phases (Popescu, 2001). Such repetitive fluctuations have also been documented at a lesser chronologic resolution in an Italian Early Pliocene pollen record near the Apennines (Bertini, 1994). The precise chronological framework of the Lupoia section, based on calibrated magnetostratigraphy according to mammals and consistent with the European climatostratigraphy (Popescu, 2001), has allowed us to propose relationships between the climatic evolution as indicated by the pollen record and 100 ka variations in the Earth's orbital eccentricity (Popescu, 2001). Seven alternating well-marked maximum zones of thermophilous trees (shaded areas) or altitudinal trees (white areas) have been regularly recorded along the entire section: they are defined from A to N (Fig. 2). Between the beginning of the Sidufjal Subchron (i.e. the base of the section) and

the end of the Nunivak Subchron, a well-defined time-span of 400 ka includes four clusters of two successive opposed maximum zones, suggesting a time-control of 100 ka (eccentricity cycles) (Popescu, 2001; Popescu et al., 2006-this volume) (Fig. 2).

A spectral analysis has been respectively performed on pollen grains of thermophilous trees and altitudinal trees using the Analyseries Program (Paillard et al., 1996) and already published by Popescu (2001): both groups show a prominent spectral peak located at a thickness of 20 m corresponding to a time period of 87 ka (Fig. 3), that supports the idea of a significant influence of eccentricity in temperature variations. Some effect of obliquity cannot be neglected because of the presence of a moderate peak at a thickness of about 10 m corresponding to a time period of about 43 ka (Fig. 3). Looking to the thermophilous vs. altitudinal tree alternations on Fig. 2, some secondary alternations corresponding to such a period can be

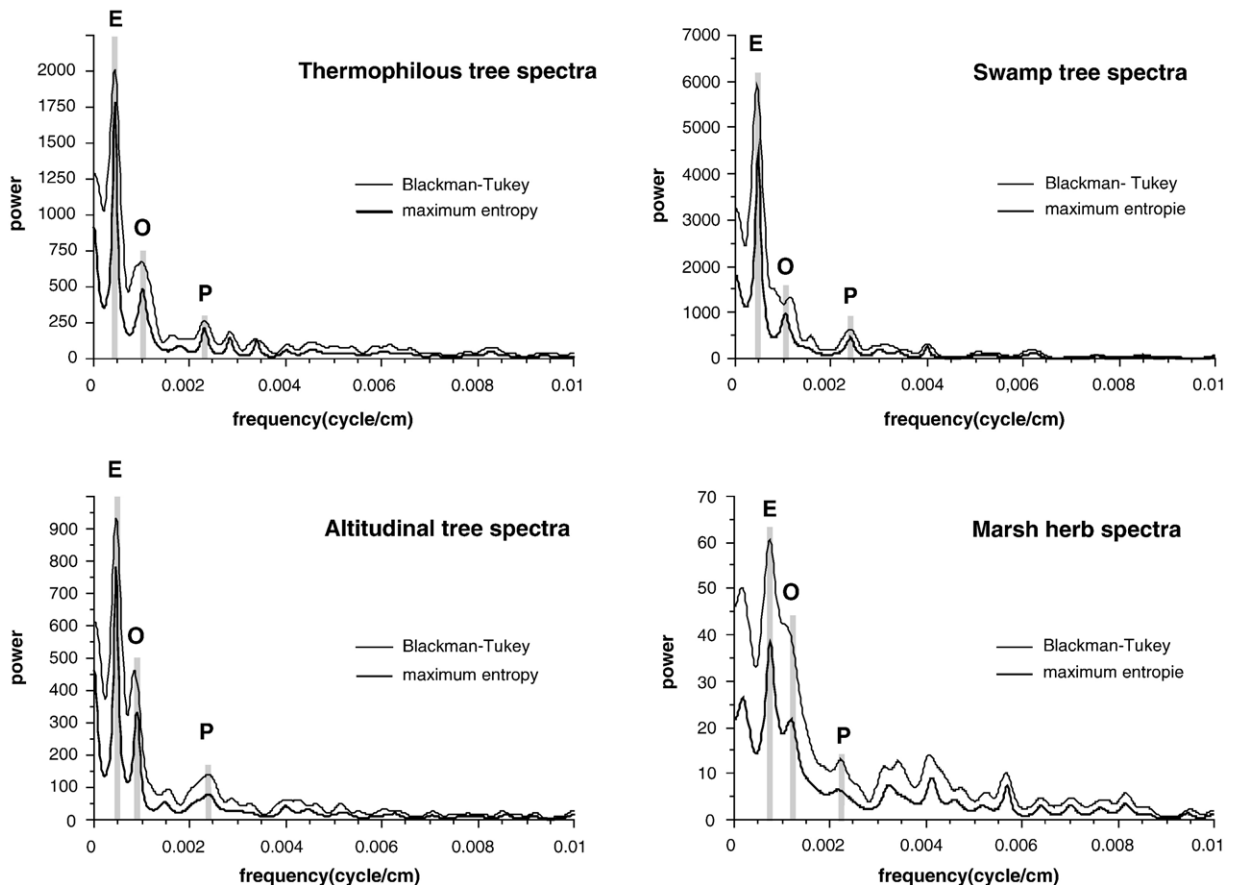


Fig. 3. Spectral analysis of thermophilous elements, altitudinal trees, swamp trees and marsh herbs. The shaded areas indicate the eccentricity (*E*), obliquity (*O*), and precession (*P*) frequencies. Eccentricity peak (*E*) is the most likely expressed for all the pollen groups: it is in phase for thermophilous trees and altitudinal trees with a frequency of 0.0005 cycle/ corresponding on average to 20 m in sediment thickness. Precession peak (*P*) is in phase for swamp trees and marsh herbs with a frequency of 0.00225 cycle/cm, corresponding on average to 4.50 m in sediment thickness.

identified in some of the previously defined zones, for example:

- the moderate maximum in altitudinal trees within the warm zone A,
- a limited maximum in thermophilous trees within the cooler zones F–H–J, where two successive peaks of altitudinal trees are also recorded.

However, our time subdivision of the section will refer in priority to eccentricity cycles because of (1) their continuous almost regular record along the section, (2) the supremacy already established of this orbital parameter in marine Mediterranean coeval sections (Hilgen, 1991).

As explained by Popescu (2001), maxima in thermophilous trees have been related to minima in eccentricity, maxima in altitudinal trees to maxima in eccentricity, respectively, with respect to a reference marine oxygen isotope curve. In addition, we have determined which peak in thermophilous elements represents an eccentricity (relative or absolute) minimum, and reciprocally for altitudinal tree peaks and eccentricity (relative or absolute) maxima. Generally, these peaks are located in the middle part of the concerned shaded or white zone, except for zones H and J where peaks of altitudinal trees are shifted in the lower part of the zone in order to be in agreement with age constrained by palaeomagnetic reversals of the Nunivak Subchron (Fig. 2). The corresponding samples are outlined on Fig. 2 and related to their proposed astronomical age.

2.2. Vegetation changes and humidity fluctuations

The SW Romanian Early Pliocene delta plain was inhabited by trees [Taxodiaceae *p.p.* (the so-called *Taxodium* pollen type which should correspond to *Glyptostrobus* genus according to plant macrofossils; Țicleanu and Diaconița, 1997), Cupressaceae, *Juglans* cf. *cathayensis*, Cyrillaceae–Clethraceae, *Myrica*, *Nyssa*, etc.] and herbs (mostly Cyperaceae and some Poaceae). The modern vegetation analogues providing such a pollen flora are in Florida (Loveless, 1959) and in the Mississippi Delta (Roberts, 1986) where two main kinds of ecosystems are clearly identified: swamps constituted by *Taxodium distichum* forest (including also *Nyssa aquatica*) and marshes mostly inhabited by herbs (such as Cyperaceae) including some shrubs or small trees (such as Cyrillaceae and *Myrica*). Their relative spatial distribution is controlled by water depth and annual hydrological rhythm: sawgrass marshes

require higher water table than forest swamps (Duever et al., 1984; Kushlan, 1990).

In the Lupoia pollen diagram, rapid fluctuations match the swamp tree group (constituting *Taxodium* type, Cupressaceae, *Juglans* cf. *cathayensis*) and the Cyperaceae (considered as representative of the marshy herbaceous association) (Fig. 2). Such groupings are justified by the behaviour of the concerned taxa along the pollen record, as also supported by a principal component analysis which gathers these taxa with respect to axis 2 while separating *Taxodium* type — Cupressaceae from Cyperaceae with respect to axis 1 (Popescu, 2001). The pollen of *T. distichum* predominates in modern swamp sediments whereas the pollen of Cyperaceae predominates in modern marsh sediments (Florida: Willard et al., 2001; Mississippi delta: Chmura et al., 1999). The relative importance of swamp trees vs. Cyperaceae in the pollen record can be considered as representative of surface areas respectively occupied by swamps and marshes.

These alternations have been specified successively within each zone (i.e. time-span) that we have constrained according to the proposed relationships between thermophilous tree vs. altitudinal tree curves and eccentricity minima–maxima, respectively (Fig. 2). Hence, twenty-seven alternations have been numbered on Fig. 2 along the whole Lupoia section.

Spectral analysis was performed on such pollen groups (swamp trees and marsh herbs) independent of any time-constraint and displays three common harmonic peaks which could represent eccentricity, obliquity, and precession cycles, respectively (Fig. 3):

- the peak related to eccentricity does not appear in phase for the two proxies and is more expressed for swamp trees than for marsh herbs; this can be explained by the significant contribution of the former to the thermophilous tree group (see the previous section);
- the peak referred to obliquity is not considerably marked for marsh herbs; the peak referred to precession (about 4.50 m in sediment thickness) is not powerful for the two considered proxies.

In addition, several other peaks of almost equal intensity are recorded for marsh herbs (suggesting cycles of 13.57, 10.61, 7.16 ka, respectively). Such repeated responses may emphasize the excessive sensitivity of herbs to local environmental changes. The response of these plants may also be exaggerated in pollen records because of (1) the extreme coastal location of these herbaceous ecosystems (referring to their present-day

distribution in Florida and within the Mississippi Delta; Duever et al., 1984; Roberts, 1986; Kushlan, 1990), (2) the central situation of the Lupoia section within the basin (see Popescu et al., 2006-this volume): as a result, the serrated variations of herb pollen grains may have been amplified and probably reflect variations in run-off and, as a consequence, lake-level changes (Țicleanu and Diaconița, 1997). For these reasons, we mainly followed as a guideline the prominent variations of swamp tree pollen grains (showing a more coherent relationship with precession: Fig. 3) for identifying alternations “swamp trees vs. marsh herbs” in Fig. 2.

3. Discussion

We have progressively refined the dating of the Lupoia section, starting from a magnetostratigraphic age established both on the basis of mammal remains and on general European climatostratigraphic relationships (Popescu, 2001). A continuous, high-resolution pollen record constrained by this first chronologic framework allows us to propose for the entire Lupoia section (133.70 m thick) a high-resolution chronology tuned first to orbital eccentricity (ca. 7 cycles), and then to precession (ca. 27 cycles) (Fig. 2). We have given priority to the influence of eccentricity over that of obliquity for forcing changes in temperature because:

- (1) long periods (100 ka) in opposition between thermophilous and altitudinal trees have a better expression in pollen curves (as supported by the spectral analysis), in spite of some secondary and discontinuous fluctuations (see above for zones A–F–H–J);
- (2) a prevalent influence of the 100 ka eccentricity cycles has been demonstrated in sedimentary and palaeobiological records for some time interval (see Introduction).

Taking into account the above-mentioned possible secondary responses of vegetation to obliquity (zones A–F–H–J), a direct comparison has been done between eccentricity and obliquity curves (Fig. 4). The position of the related secondary vegetation changes within zones A–F–H–J (indicated by grey areas on Fig. 4) suggests some influence of lowering amplitude phases of obliquity during 400 ka eccentricity cycle maximum.

Another scenario has been proposed for the Early Pliocene lignite deposition at Ptolemais (Northern Greece) where lignite–marl alternations are apparently forced by precession: marls would correspond to

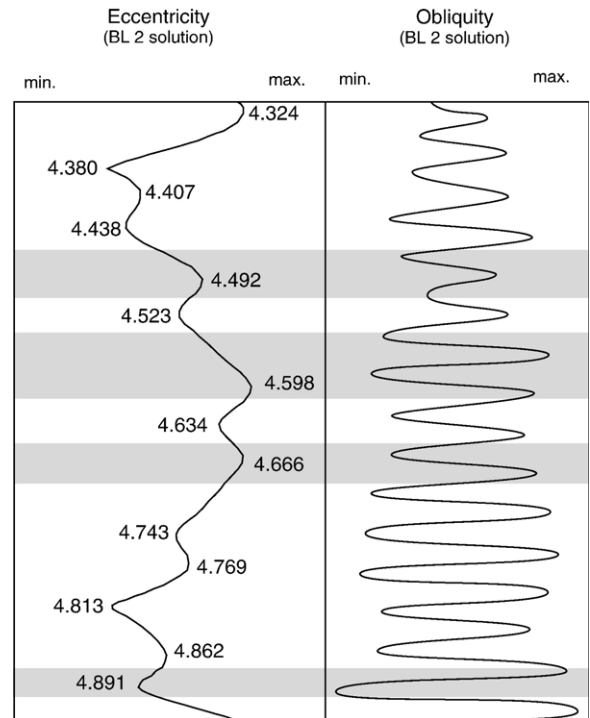


Fig. 4. Compared eccentricity and obliquity curves for the time-window 4.9–4.3 Ma corresponding to the Lupoia section. Grey areas spotlight places where secondary changes in vegetation were recorded within zones A–F–H–J of Fig. 2.

precession minima (wetter phases) and lignites to precession maxima (drier phases) (Van Vugt et al., 2001). As also noted by van Vugt et al. (2001), such a direct scenario appears improbable in Romania where the Early Pliocene lignite deposition was claimed to be linked to minima in eccentricity (i.e. to warmer phases), an assumption moderated by Popescu (2001) and Popescu et al. (2006-this volume). Pollen analysis has been performed on a small part of the Ptolemais section (Kloosterboer-van Hoeve et al., 2005), covering one precession cycle only, where fluctuations of some plant groups suggest to the authors relationships with millennial-scale cycles forced by the North Atlantic Oscillation (with periodicities of 10, 2.5 and 1.5 ka) and to long-period variations in solar activity. As demonstrated above, such cycles do not appear clearly in the Lupoia pollen record, suggesting to us that a different process operated. After a very detailed sedimentological and palaeomagnetic study in the eastern Dacic Basin, Vasiliev et al. (2004) concluded that precession controlled cyclic deposition of sediments expressing changes in water-level.

Nevertheless, some aspects concerning these orbital parameters invite discussion. The study interval (ca. 4.9–

Table 1

Age and numbering of the precession minima and maxima for the time interval 4.914–4.346 Ma

Precession ages (BL2 solution)			
Number	Age	Number	Age
53	4.357	54	4.346
51	4.376	52	4.367
49	4.389	50	4.381
47	4.409	48	4.399
45	4.429	46	4.419
43	4.447	44	4.438
41	4.466	42	4.457
39	4.487	40	4.477
37	4.508-09	38	4.498
35	4.533	36	4.521
33	4.556	34	4.545
31	4.579	32	4.568
29	4.602	30	4.590
27	4.624	28	4.613
25	4.649	26	4.636
23	4.671	24	4.660
21	4.694	22	4.682
19	4.717	20	4.705
17	4.741	18	4.728
15	4.764	16	4.753
13	4.786	14	4.775
11	4.805	12	4.796
9	4.821	10	4.813
7	4.841	8	4.830
5	4.863	6	4.852
3	4.886	4	4.874
1	4.914	2	4.903

4.3 Ma) is characterized by well-marked amplitude of the 400 ka eccentricity cycle. The 100 ka cycle is clearly reduced. As a consequence, some maxima in eccentricity (at 4.769 Ma for example) are lower than some minima (at 4.634 Ma for example) (Fig. 2). Unexpectedly, this did not much restrict the amplitude of response in vegetation groups probably because there existed very contrasting environments (delta plain and high reliefs) over short distances (less than 60 km). Response to the 400 ka cycle is somewhat more pronounced (higher percentages of thermophilous trees during the time intervals 4.90–4.80 and 4.44–4.37 Ma corresponding to small eccentricity maxima; and higher percentages of altitudinal trees during the time interval 4.80–4.44 Ma corresponding to large eccentricity minima) (Popescu, 2001). Our study emphasizes the occurrences of Early Pliocene global warmings during minima in eccentricity. This is different from the situation in the last million years where glacials occurred when eccentricity was minimal. This opposition is consistent with the hypothesis of Li et al. (1998) who proposed that coolings prior to 2.7 Ma corresponded to maxima in eccentricity, and

that coolings later than 2.7 Ma corresponded to minima in eccentricity.

Deposition of anoxic organic-rich sediments in the Central-Eastern Mediterranean, the so-called sapropels, is related to repeated increases in run-off during precession minima and resulting in marine water stratification (Hilgen, 1990, 1991). Repeated increases in Cyperaceae are understood as having resulted from regular increased precipitation and run-off in the Dacic Basin related to precession minima which advantaged herbaceous marshes and caused their enlargement within the southwestern Romanian Early Pliocene delta plain. Accordingly, maxima of Cyperaceae are related to precession minima (Fig. 2). Conversely, maxima of swamp trees belong to phases of decreased moisture and are related to precession maxima.

Precession minima and maxima have been numbered from 1 to 54 for the studied period (odd numbers for precession minima, even numbers for precession maxima) (Fig. 2). Corresponding numbers are also indicated on the respective pollen curves (odd numbers for marsh herb maxima, related to precession minima; even numbers for swamp tree maxima, related to precession maxima); their astronomical age is also given in Table 1. Thirteen chronological marks have been placed in front of the Lupoia samples that we respectively refer to eccentricity minima and maxima (Fig. 2). They constitute a rigid framework for the most detailed relationships based on precession variations (Fig. 2).

Phases of increased precipitation and run-off in the Dacic Basin are supported by the persistence at about 4.6 Ma in southwestern Romania of several tropical elements (*Amanoa*, *Meliaceae*, *Entada*, *Pachysandra*, *Sapindaceae*, *Loranthaceae*, some *Tiliaceae*) which disappeared earlier from the Northwestern Mediterranean region (at about 14 Ma) and from the Central Mediterranean (at about 5.3 Ma) (Suc et al., 2004).

In the Lupoia pollen record, the lowest percentages of marsh herbs (even at their relative maxima) occurred during eccentricity maxima, at around 4.764 (peak 15), 4.694 to 4.557 (peaks 21–33), 4.487 (peak 39), and 4.357 Ma (peak 53) (Fig. 2). At these times, precession minima seem to have induced less humidity in southwestern Romania than during the previous and following phases with eccentricity minima, at around 4.891 (peaks 1, 3), 4.813 (peaks 11, 13), 4.743 (peak 17), 4.523 (peaks 35, 37), and 4.438 to 4.380 Ma (peaks 45–51) (Fig. 2). In contrast, Central Mediterranean Early Pliocene sapropels are better expressed in

correspondence with the eccentricity maxima (Hilgen, 1991). This suggests that, during the eccentricity maxima, run-off might have increased over the Central Mediterranean Basin in contrast to Southeastern Europe. Such an impact could have been more limited to Southeastern Europe during the eccentricity minima. An example of similar differences between Central and Eastern Mediterranean is the recent “cold” sapropel S6 which was deposited at about 170 ka (Kallel et al., 2000) during a relative minimum in eccentricity (Hilgen, 1990; Loutre and Berger, 1993). At this time, surface water salinity appears to have been lower in the Levantine Basin than in the Tyrrhenian Sea. Among the hypotheses to explain this differential are: (1) a greater increase of precipitation in the Eastern Mediterranean than in the Central Mediterranean region and (2) an increase of the Nile River discharge (Kallel et al., 2000; Masson et al., 2000).

Changes in vegetation depend not only on the global climate (temperature, precipitation) but also on space arrangement of plants (regional altitudinal belts and local environments). As a consequence, the choice of any individual peak to be related precisely to an orbital parameter maximum or minimum may be discussed. Anyway, this study has evidenced clear zones (related to eccentricity) and peaks (related to precession minima and maxima) which provide a high-resolution chronologic frame for the Lupoia section.

4. Conclusion

High-resolution pollen analysis of the Lupoia section reveals that significant vegetation changes during the Early Pliocene were controlled by astronomical parameters, these being primarily eccentricity and secondarily precession. Obliquity does not seem to have been a substantial and continuously repeated influence. Eccentricity controlled fluctuations in temperature, while precession forced slight movements in lake-level that were caused by oscillations in precipitation and run-off. The Dacic Basin, and particularly the Lupoia section, are favourably located because they represent coastal environments close to high relief in the Southeastern Europe, and so are able to demonstrate that the Early Pliocene vegetation responded significantly to eccentricity and precession forcing, while sediments and marine organisms were simultaneously affected in the Mediterranean Sea. The present study (see also Popescu et al., *this volume*) has resulted in a very detailed chronology of Late Neogene deposits in the Dacic Basin.

Acknowledgements

This work was funded by the French Government through its Embassy at Bucharest, and was supported by the Programme “Environnement, Vie et Sociétés”. We thank F. Giraud for assistance with statistics, J.E. Meulenkamp for discussion of the results, and P. Bernier and J. Reumer for comments on the manuscript. Anonymous referees are gratefully acknowledged for improvements to the manuscript. Dr. Martin J. Head (Brock University) has improved the English and clarity of the text.

References

- Bertini, A., 1994. Messinian–Zanclean vegetation and climate in North-Central Italy. *Hist. Biol.* 9, 3–10.
- Chmura, G.L., Smirnov, A., Campbell, I.D., 1999. Pollen transport through distributaries and depositional patterns in coastal waters. *Palaeogeogr. Palaeoclimatol. Palaeoecol.* 149, 257–270.
- DeMenocal, P.B., 1995. Plio-Pleistocene African Climate. *Science* 270, 53–59.
- Diniz, F., 1984. Etude palynologique du bassin pliocène de Rio Maior. *Paléobiol. Cont.* 14 (2), 259–267.
- Di Stefano, E., Sprovieri, R., Scarantino, S., 1996. Chronology of biostratigraphic events at the base of the Pliocene. *Palaeopelagos* 6, 401–414.
- Duever, M.J., Meeder, J.F., Duever, L.C., 1984. Ecosystems of the big cypress swamp. In: Ewel, K.C., Odum, H.J. (Eds.), *Cypress Swamps*. University of Florida, Gainesville, USA, pp. 294–303.
- Fauquette, S., Clauzon, G., Suc, J.-P., Zheng, Z., 1999. A new approach for paleoaltitude estimates based on pollen records: example of the Mercantour Massif (southeastern France) at the earliest Pliocene. *Earth Planet. Sci. Lett.* 170, 35–47.
- Hilgen, F.J., 1987. Sedimentary rhythms and high-resolution chronostratigraphic correlations in the Mediterranean Pliocene. *Newsl. Stratigr.* 17 (2), 109–127.
- Hilgen, F.J., 1990. Sedimentary cycles and astronomically controlled oscillatory system of climatic change during the Late Cenozoic in the Mediterranean. *Paléobiol. Cont.* 17, 25–33.
- Hilgen, F.J., 1991. Extension of the astronomically calibrated (polarity) time scale to the Miocene/Pliocene boundary. *Earth Planet. Sci. Lett.* 107, 349–368.
- Hilgen, F.J., Langereis, C.G., 1989. Periodicities of CaCO₃ cycles in the Mediterranean Pliocene: discrepancies with the quasi-periods of the Earth’s orbital cycles? *Terra Nova* 1, 409–415.
- Kallel, N., Duplessy, J.-C., Labeyrie, L., Fontugne, M., Paterne, M., Montacer, M., 2000. Mediterranean pluvial periods and sapropel formation over the last 200 000 years. *Palaeogeogr. Palaeoclimatol. Palaeoecol.* 157, 45–58.
- Kloosterboer-van Hove, M., Steenbrink, J., Visscher, H., Brinkhuis, H., 2005. Millennial-scale climatic cycles in the Early Pliocene pollen record of Ptolemais, northern Greece. *Palaeogeogr. Palaeoclimatol. Palaeoecol.* 229, 321–334.
- Kushlan, J.A., 1990. Freshwater marshes. In: Myers, R.L., Ewel, J.J. (Eds.), *Ecosystems of Florida*. University of Central Florida Press, Orlando, USA, pp. 324–363.
- Langereis, C.G., Hilgen, F.J., 1991. The Rossello composite: a Mediterranean and global reference section for the Early to early Late Pliocene. *Earth Planet. Sci. Lett.* 104, 211–225.

- Li, X.S., Berger, A., Loutre, M.-F., Maslin, M.A., Haug, G.H., Tiedemann, R., 1998. Simulating late Pliocene Northern Hemisphere climate with the LLN-2D model. *Geophys. Res. Lett.* 25, 915–918.
- Lourens, L.J., Hilgen, F.J., 1997. Long-periodic variations in the earth's obliquity and their relation to third-order eustatic cycles and Late Neogene glaciations. *Quat. Int.* 40, 43–52.
- Lourens, L.J., Hilgen, F.J., Gudjonsson, L., Zachariasse, W.J., 1992. Late Pliocene to early Pleistocene astronomically forced sea surface productivity and temperature variations in the Mediterranean. *Mar. Micropaleontol.* 19, 49–78.
- Lourens, L.J., Antonarakou, A., Hilgen, F.J., Van Hoof, A.A.M., Vergnaud Grazzini, C., Zachariasse, W.J., 1996. Evaluation of the Plio-Pleistocene astronomical timescale. *Paleoceanography* 11 (4), 391–413.
- Loutre, M.-F., Berger, A., 1993. Sensibilité des Paramètres Astro-Climatiques au cours des 8 derniers millions d'années: Scientific Report 93/4. Institut d'Astronomie et de Géophysique G. Lemaître, Université catholique de Louvain, Louvain-la-Neuve, pp. 1–9.
- Loveless, C.M., 1959. A study of the vegetation in the Florida Everglades. *Ecology* 40, 1–10.
- Masson, V., Braconnot, P., Jouzel, J., de Noblet, N., Cheddadi, R., Marchal, O., 2000. Simulation of intense monsoons under glacial conditions. *Geophys. Res. Lett.* 27 (12), 1747–1750.
- Paillard, D., Labeyrie, L., Yiou, P., 1996. Macintosh program performs time-series analysis. *Eos, Trans. AGU* 379.
- Popescu, S.-M., 2001. Repetitive changes in Early Pliocene vegetation revealed by high-resolution pollen analysis: revised cyclostratigraphy of southwestern Romania. *Rev. Palaeobot. Palynol.* 120, 181–202.
- Popescu, S.-M., Krijgsman, W., Suc, J.-P., Clauzon, G., Marunþeau, M., Nica, T., 2006. Pollen record and integrated high-resolution chronology of the Early Pliocene Dacic Basin (Southwestern Romania). In: Agustí, J., Oms, O., Meulenkamp, J.E. (Eds.), Late Miocene to Early Pliocene environment and climate change in the Mediterranean area. *Palaeogeogr. Palaeoclimatol. Palaeoecol.* 238, pp. 78–90 (this volume). doi:10.1016/j.palaeo.2006.03.019.
- Quézel, P., Médail, F., 2003. *Ecologie et Biogéographie des Forêts du Bassin Méditerranéen*. Elsevier, France. 571 pp.
- Rădan, S.C., Rădan, M., 1998. Study of the geomagnetic field structure in the Tertiary in the context of magnetostratigraphic scale elaboration. I—The Pliocene. *An. Inst. Geol., Roman* 70, 215–231.
- Rio, D., Sprovieri, R., Di Stefano, E., 1994. The Gelasian Stage: a new chronostratigraphic unit of the Pliocene Series. *Riv. Ital. Paleontol.* 100, 103–124.
- Roberts, H.H., 1986. Selected depositional environments of the Mississippi River deltaic plain. *Geological Society of America Centennial Field Guide—Southeastern Section*, vol. 98, pp. 435–440.
- Shackleton, N.J., Hall, M.A., Pate, D., 1995. Pliocene stable isotope stratigraphy of Site 846. *Proc. Ocean Drill. Prog., Sci. Results*, vol. 138. U.S. Govt. Print. Off., pp. 337–355.
- Sprovieri, R., 1993. Pliocene–Early Pleistocene astronomically forced planktonic foraminifera abundance fluctuations and chronology of Mediterranean calcareous plankton bio-events. *Riv. Ital. Paleontol. Stratigr.* 99, 371–414.
- Suc, J.-P., 1984. Origin and evolution of the Mediterranean vegetation and climate in Europe. *Nature* 307, 429–432.
- Suc, J.-P., Diniz, F., Leroy, S., Poumot, C., Bertini, A., Dupont, L., Clet, M., Bessais, E., Zheng, Z., Fauquette, S., Ferrier, J., 1995. Zanclean (~Brunsumian) to early Piacenzian (~early–middle Reuverian) climate from 4° to 54° north latitude (West Africa, West Europe and West Mediterranean areas). *Meded. Rijks Geol. Dienst* 52, 43–56.
- Suc, J.-P., Fauquette, S., Popescu, S.-M., 2004. L'investigation palynologique du Cénozoïque passe par les herbiers. In: Association française pour la Conservation des espèces végétales, Nancy (Ed.), Actes du Colloque “Les herbiers: un outil d'avenir. Tradition et modernité”, Villeurbanne, pp. 67–87.
- Țicleanu, N., Diaconița, D., 1997. The main coal facies and lithotypes of the Pliocene coal basin, Oltenia, Romania. In: Gayer, R., Pesek, J. (Eds.), *European Coal Geology and Technology*. Geol. Soc. Spec. Publ., vol. 125, pp. 131–139.
- Tiedemann, R., Sarthein, M., Shackleton, N.J., 1994. Astronomical timescale for the Pliocene Atlantic $\delta^{18}\text{O}$ and dust flux records of ODP Site 659. *Paleoceanography* 9 (4), 619–638.
- Van Vugt, N., Langereis, C.G., Hilgen, F.J., 2001. Orbital forcing in Pliocene–Pleistocene Mediterranean lacustrine deposits: dominant expression of eccentricity versus precession. *Palaeogeogr. Palaeoclimatol. Palaeoecol.* 172, 193–205.
- Vasiliev, I., Krijgsman, W., Langereis, C.G., Panaiotu, C.E., Mațenco, L., Bertotti, G., 2004. Towards an astrochronological framework for the eastern Paratethys Mio-Pliocene sedimentary sequences of the Focșani basin (Romania). *Earth Planet. Sci. Lett.* 227, 231–247.
- Willard, D.A., Weimer, L.M., Riegel, W.L., 2001. Pollen assemblages as paleoenvironmental proxies in the Florida Everglades. *Rev. Palaeobot. Palynol.* 113, 213–235.
- Zagwijn, W.H., 1960. Aspects of the Pliocene and early Pleistocene vegetation in The Netherlands. *Meded. Geol. Sticht., ser. C3* 5, 1–78.
- Zohary, M., 1973. *Geobotanical Foundations of the Middle East*, vol. 2. Fischer, G., Stuttgart, pp. 341–739.

Late Miocene and early Pliocene environments in the southwestern Black Sea region from high-resolution palynology of DSDP Site 380A (Leg 42B)

Speranta-Maria Popescu

Laboratoire PaléoEnvironnements et PaléobioSphère, Université Claude Bernard – Lyon 1, 27-43 boulevard du 11 Novembre, 69622 Villeurbanne Cedex, France

Received 9 March 2003; accepted 7 March 2006

Abstract

A high-resolution palynological study has been performed on late Miocene (Messinian) and early Pliocene (Zanclean) sediments cored at DSDP Site 380A (Leg 42B). A late Miocene coastal vegetation has been identified in association with a delta environment. The Pliocene is characterised by competition between the two most important vegetation components, namely humid thermophilous forests and dry steppes, with changes driven by large amplitude climatic variations. These variations are linked to other European reference pollen records and to the global temperature evolution for the early Pliocene, and result in climatostratigraphic relationships at large geographic scale. An orbital tuning is proposed with respect to new data clarifying time control on the section. The Black Sea appears to have dried up in response to the Messinian salinity crisis in the Mediterranean with which it might have been connected during periods of high sea level.

© 2006 Elsevier B.V. All rights reserved.

Keywords: Messinian; Zanclean; Black Sea; Palynology; Climate; Environments

1. Introduction

DSDP Leg 42B has already provided much information on the hydrographic evolution of the Black Sea, especially regarding its interactions with the Mediterranean realm and responses to climatic forcing (Ross et al., 1978a). Among the most important results are (1) the potential reaction of the Black Sea to the Messinian salinity crisis in the Mediterranean (Hsü and Giovanoli, 1979), and (2) the general climatic evolution of the region offered by pollen analysis (Traverse, 1978) (Fig. 1). Unfortunately, these data cannot be undoubtedly used because of the lack of a continuous and reliable

chronostratigraphic framework in the area. Indeed, Hsü and Giovanoli (1979) have suggested that the “Pebbly Breccia” recorded within Site 380A was to be related to the Messinian salinity crisis in the Mediterranean, without any conclusive chronological argument. Recently, new biostratigraphic and magnetostratigraphic data have been provided from the Dacic and the Euxinic Basins (Mărușbeanu and Papaianopol, 1995, 1998; Semenenko and Olejnik, 1995; Clauzon et al., 2005; Snel et al., 2006-*this volume*) that, in association to new field observations in the Dacic Basin (Clauzon et al., 2005), strongly support the idea that the Eastern Paratethys and the Mediterranean Sea were connected (at high sea level) just before and just after the Messinian salinity crisis (Clauzon et al., 2005), i.e. that the Messinian sea-level drop in the Mediterranean

E-mail address: popescu@univ-lyon1.fr.

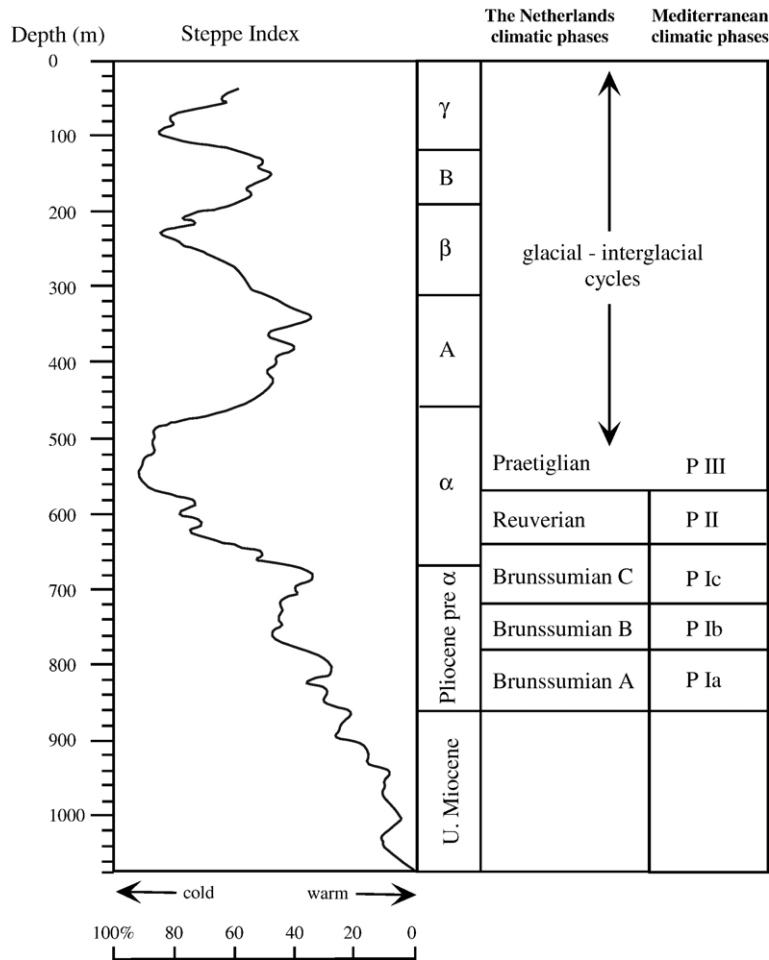


Fig. 1. “Steppe Index” (i.e. *Artemisia* percentages/total thermophilous tree percentages) curve constructed by [Traverse \(1978\)](#) for the entire Site 380A section, and the climatic relationships that I propose with climatostratigraphies developed in The Netherlands ([Zagwijn, 1960](#)) and in the northwestern Mediterranean region ([Suc, 1984](#)).

concerned also the Eastern Paratethys which was led to a temporary desiccation ([Clauzon et al., 2005](#)). A new seismic profile crossing DSDP Sites 381 and 380 corroborated that the Black Sea desiccated, the Messinian erosional surface being evidenced and correlating with the coarse and dolomitic deposits previously considered as belonging to the Messinian salinity crisis within the cores ([Gillet, 2004](#)).

For what concerns the direct dating of the 380A section, some authors felt that the climatostratigraphic approach was the best solution for establishing relationships between the Black Sea records and global change ([Hsü, 1978](#)), but at that time very few stable isotope records (moreover at low resolution) ([Shackleton and Opdyke, 1977](#)) and pollen records (the global value of which was unknown) ([Zagwijn, 1960](#)) were available.

We now have at our disposal combined high-resolution reference isotopic curves ([Tiedemann et al., 1994](#); [Shackleton et al., 1995](#)) and European and Mediterranean pollen records covering the whole Pliocene ([Suc, 1984](#); [Bertoldi et al., 1989](#); [Suc et al., 1995a,b](#)) and, for some of them, the Messinian Stage ([Suc and Bessais, 1990](#); [Bertini, 1994](#); [Suc et al., 1995c](#); [Bertini et al., 1998](#)).

I have therefore performed a high-resolution palynological study of the late Miocene and early Pliocene of DSDP Site 380A (42°05.94'N, 29°36.82'E) in order to establish a precise regional climatic subdivision, to search for long distance climatostratigraphic relationships in the Pliocene, and, as a consequence, to confirm if the Black Sea responded to the Messinian salinity crisis in the Mediterranean.

Site 380A is critical because of (1) its anticipated record covering both latest Miocene and earliest

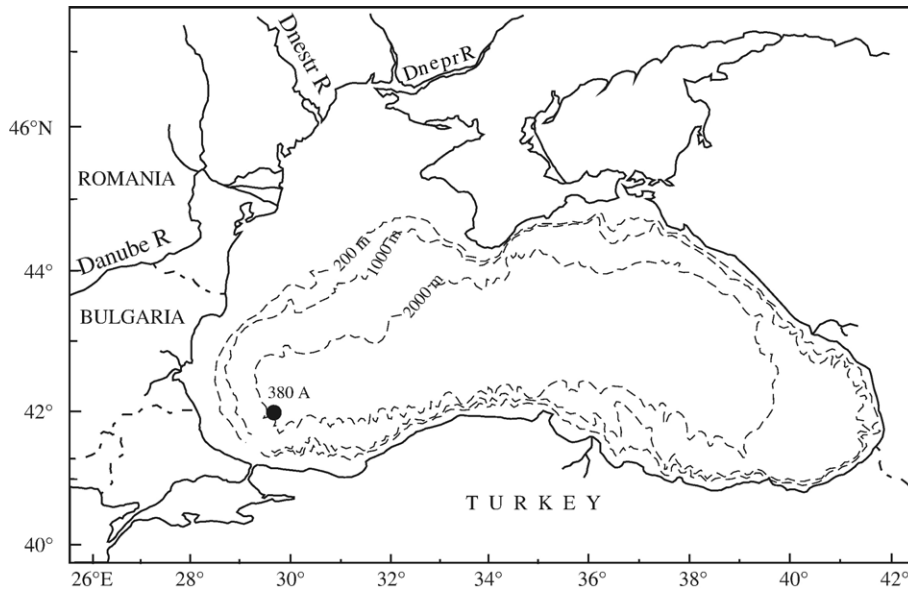


Fig. 2. Geographical location of DSDP Site 380A in the Black Sea.

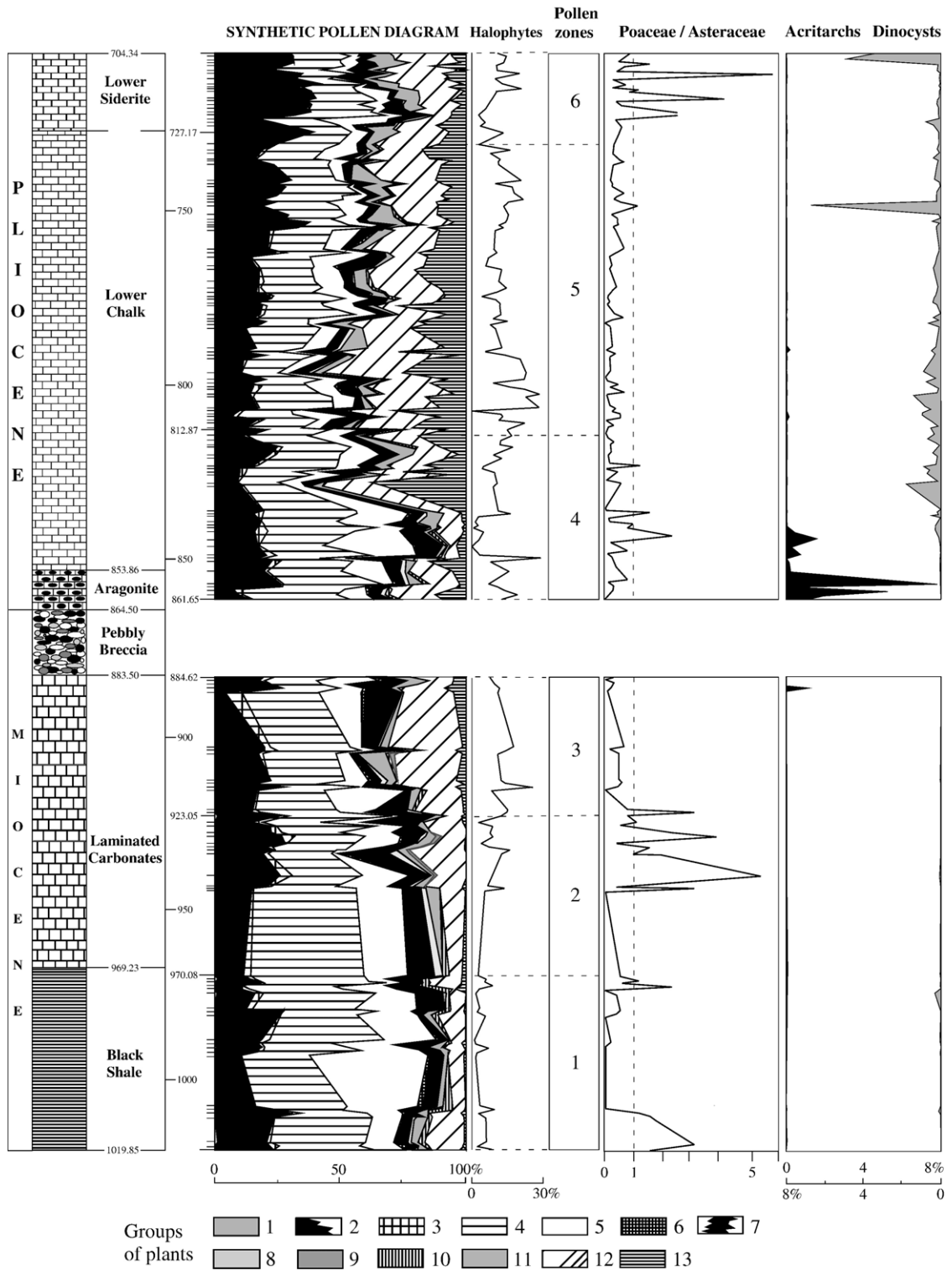
Pliocene (it is the only cored borehole in the Black Sea probably able to provide data on a time window that includes the Messinian salinity crisis), and (2) its geographic location in the southwestern part of the Black Sea (Fig. 2). Indeed, its relatively close proximity to the Bosphorus Strait is crucial for two reasons. First, the question is still open as to which way marine Mediterranean waters entered the Dacic Basin (i.e. the present-day southern Romania), and perhaps occasionally also into the northern Black Sea (Semenenko and Liulieva, 1978), during brief influxes (Mărunțeanu and Papaianopol, 1998). Did direct connections exist in the late Miocene – early Pliocene through a proto-Bosphorus strait (Hsü, 1978; Muratov et al., 1978; Marinescu, 1992)? Were other ways possible such as

southward from the Dacic Basin to the Aegean Sea (Hsü, 1978; Marinescu, 1992)? The study of dinocysts at Site 380A should help in solving this question. Second, the Bosphorus area today is near the junction of two opposed vegetation realms (Zohary, 1973; Noirfalise et al., 1987; Quézel and Médail, 2003): the eastern European and Euxyno-Hyrcanian mesophilous forests (western and southern coasts of the Black Sea) which can extend in some places to the subalpine belt, and the Central Anatolian steppes linked to xeric (dry) climatic conditions. It may be assumed that a more or less similar feature characterised Miocene and Pliocene vegetation in the area (Traverse, 1978): to the north, forest environments rich in Taxodiaceae as evidenced in Bulgaria and southwestern Romania (Drivaliari, 1993;

Fig. 3. Lithology and new synthetic pollen diagram for the lower part of Site 380A (with indication of depth expressed in metres) compared to the halophyte curve (percentages are calculated on the total amount of pollen grains), the corresponding subdivisions in six pollen zones, the ratio Poaceae/Asteraceae pollen grains, and acritarchs (in black) and dinocysts (in grey) (their frequency, sometimes considerable, has been calculated in relation to the total number of pollen grains). Ecological groups of plants: 1, megathermic (=tropical) elements (*Avicennia*, *Amanoa*, *Fothergilla*, *Exbucklandia*, Euphorbiaceae, Sapindaceae, Loranthaceae, Arecaceae, Acanthaceae); 2, mega-mesothermic (=subtropical) elements (Taxodiaceae, *Engelhardia*, *Myrica*, Sapotaceae, *Castanea*–*Castanopsis* type, *Microtropis fallax*, *Distylium* cf. *sinensis*, Araliaceae, *Nyssa*, *Liriodendron*, etc.); 3, *Cathaya*; 4, mesothermic (=warm–temperate) elements (deciduous *Quercus*, *Carya*, *Pterocarya*, *Carpinus*, *Juglans*, *Juglans* cf. *cathayensis*, *Celtis*, *Zekkova*, *Ulmus*, *Tilia*, *Acer*, *Parrotia* cf. *persica*, *Liquidambar* cf. *orientalis*, *Alnus*, *Salix*, *Populus*, *Fraxinus*, *Buxus sempervirens* type, *Betula*, *Fagus*, *Ostrya*, *Parthenocissus* cf. *henryana*, *Hedera*, *Lonicera*, *Elaeagnus*, *Ilex*, *Tilia*, etc.); 5, *Pinus* and poorly preserved Pinaceae pollen grains; 6, mid-altitude trees (*Tsuga*, *Cedrus*); 7, high-altitude trees (*Abies*, *Picea*); 8, non-significant pollen grains (undetermined ones, poorly preserved pollen grains, some cosmopolitan or widely distributed elements such as Rosaceae and Ranunculaceae); 9, Cupressaceae; 10, Mediterranean xerophytes (*Quercus ilex* type, *Olea*, *Phillyrea*, *Ligustrum*, *Pistacia*, *Ziziphus*); 11, a subdesertic element, *Lygeum*; 12, herbs (Poaceae, *Erodium*, *Geranium*, *Convolvulus*, Asteraceae Asteroideae, Asteraceae Cichorioideae, Lamiaceae, *Plantago*, *Euphorbia*, Brassicaceae, Apiaceae, *Knautia*, *Helianthemum*, *Rumex*, *Polygonum*, *Asphodelus*, Campanulaceae, Ericaceae, Amaranthaceae–Chenopodiaceae, Caryophyllaceae, Plumbaginaceae, Cyperaceae, *Potamogeton*, *Sparganium*, *Typha*, Nymphaeaceae); 13, steppe elements (*Artemisia* and *Ephedra*).

Drivaliari et al., 1999; Popescu, 2001); and to the south, steppe environments rich in *Artemisia* as identified in southeastern Anatolia (Suc, personal communication).

A detailed pollen study in such an area must therefore be considered promising for the reconstruction of vegetation change and climate evolution.



2. Previous results from Site 380A, Leg 42B

Fourteen major sedimentary units have been described from this site (Ross, 1978). Those concerning the late Miocene and the early Pliocene are indicated in Fig. 3. Among them, there is a coarse deposit, the so-called “Pebbly Breccia”, which is presented herein. Some micropaleontological analyses have been carried out on this core: from the late Miocene to Present, the most promising methods have appeared to be the pollen analysis (Traverse, 1978) and the diatom analysis (Schrader, 1978).

2.1. The stromatolitic dolomite within the “Pebbly Breccia”

A coarse clastic “Pebbly Breccia” (19 m thick), the genesis of which is uncertain (Ross et al., 1978b), was recovered between 864.5 and 883.5 m depth. It includes blocks of a stromatolitic dolomite (Ross et al., 1978a) which was considered as having formed in an intertidal to supratidal environment (Stoffers and Müller, 1978). This suggests that the Black Sea level was very shallow at that time, in agreement with data from diatoms (less than 50 m water depth) (Schrader, 1978). Hsü and Giovanoli (1979) have interpreted these data as evidence of a drop in the level of the Black Sea to 1600 m below global sea level as a response to the Messinian salinity crisis in the Mediterranean. Such an interpretation was also supported by the record of a seismic reflector (reflector “S”) showing that the “Pebbly Breccia” is related to deltaic deposition and to possible Messinian erosional surface in the Black Sea (Letouzey et al., 1978), the latter being recently confirmed by Gillet (2004).

2.2. The pollen record and its climatic significance

Traverse (1978) established an index, based on the *Artemisia* abundance (i.e. *Artemisia* percentages/total thermophilous tree percentages, for a climatic subdivision of the cores (Fig. 1). Although a relatively small number of samples was studied, the general trends shown by this index revealed consistent subdivisions of the section which appear in good agreement with the large climatic subdivisions in Europe and the Mediterranean region based on pollen analysis (Suc and Zagwijn, 1983). The Mediterranean pollen zones of Suc (1984) can therefore be used to subdivide the Pliocene of Site 380A, as follows: P Ia pollen zone (Brunssumian A) from ca. 860 m to ca. 780 m depth (low amounts of *Artemisia*), P Ib pollen

zone (Brunssumian B) related to the interval ca. 780 – ca. 720 m depth (increase in *Artemisia*), P Ic pollen zone (Brunssumian C) between ca. 720 m and ca. 640 m depth (decrease in *Artemisia*), P II pollen zone (Reuverian) between ca. 640 m and ca. 570 m depth (increase and larger variations in *Artemisia* frequency), and P III pollen zone (Praetiglian) starting at about 570 m depth (predominant *Artemisia*) and followed by glacial–interglacial cycles.

3. New palynological records

One hundred and fifty samples have been analysed from 1019.85 m depth to 704.34 m depth (i.e. from late Miocene to early Pliocene), excluding the interval 883.5–864.5 m (“Pebbly Breccia”, unpropitious to pollen preservation). Sampling density varies according to availability of material, the highest density being in Pliocene sediments (about a sample per metre). Samples (20 g each in general) have been processed according to standard methods (Cour, 1974): acid digestion, concentration using ZnCl₂ and sieving (5 µm), and mounting in glycerine in order to allow rotation of pollen grains for improved examination.

3.1. Pollen flora

The pollen flora contains 119 taxa, that noticeably increases the flora diversity as documented by Traverse (1978). Predominant among the trees are Taxodiaceae (including *Taxodium* type), deciduous *Quercus*, Cupressaceae, *Abies* and *Pinus*; and among the herbs are Poaceae, *Artemisia* and Amaranthaceae–Chenopodiaceae. *Carya*, *Juglans*, *Juglans cf. cathayensis* (a swamp tree), *Alnus*, *Zelkova*, *Ulmus* are also abundant within the arboreal pollen flora; and Asteraceae Cichorioideae, Ericaceae, Cyperaceae are frequent within the non arboreal pollen flora. Detailed pollen counts are deposited at the Laboratory “PaléoEnvironnements et PaléobioSphère” (University Claude Bernard – Lyon 1) and will be shortly on the “Cenozoic Pollen and Climatic values” database (C.P.C.) on the Medias–France website (<http://cpc.mediasfrance.org>). Here (Fig. 3), pollen records are presented in a synthetic pollen diagram, a technical presentation which promotes long distance comparisons of vegetation response to global climatic changes (Suc, 1984; Suc et al., 1995a,b). In such a synthetic pollen diagram (Fig. 3), taxa are grouped according to the ecological significance of their living representatives and to their general behaviour in the Mediterranean Pliocene pollen diagrams (Suc, 1986, 1989), from left to right:

- megathermic (=tropical) elements (*Avicennia*, a mangrove tree; *Amanoa*, *Fothergilla*, *Exbucklandia*, Euphorbiaceae, Sapindaceae, Loranthaceae, Arecaceae, Acanthaceae) are few but mostly recorded in the Miocene sediments, and also in one of the warmest phases of the Pliocene;
- mega-mesothermic (=subtropical) elements [mainly Taxodiaceae (including *Taxodium* type, *Sequoia* type and *Sciadopitys*), *Engelhardia*, *Myrica*, and many other elements as Sapotaceae, *Castanea*–*Castanopsis* type, *Microtropis fallax*, *Distylium* cf. *sinensis*, Araliaceae, *Nyssa*, *Liriodendron*, etc.] are abundant along the entire studied section;
- *Cathaya*, a conifer living today at mid-altitude in tropical China;
- mesothermic (=warm–temperate) elements (deciduous *Quercus*, *Carya*, *Pterocarya*, *Carpinus*, *Juglans* and *Juglans* cf. *cathayensis*, *Celtis*, *Zelkova*, *Ulmus*, *Tilia*, *Acer*, *Parrotia* cf. *persica*, *Liquidambar* cf. *orientalis*, *Alnus*, *Salix*, *Populus*, *Fraxinus*, *Buxus sempervirens* type, *Betula*, *Fagus*, and, with a lower frequency, *Ostrya*, *Parthenocissus* cf. *henryana*, *Hedera*, *Lonicera*, *Elaeagnus*, *Ilex*, *Tilia*, etc.) are abundant along the entire studied interval;
- *Pinus* and poorly preserved Pinaceae pollen grains, representative of various environments (from low to high altitude, for example);
- mid-altitude trees (*Tsuga*, *Cedrus*¹);
- high-altitude trees (*Abies*, *Picea*¹);
- non-significant pollen grains (undetermined ones, poorly preserved pollen grains, some cosmopolitan or widely distributed elements such as Rosaceae and Ranunculaceae);
- Cupressaceae which may include some elements living in warm and humid climatic condition and some others living in dry and warm to cold climatic conditions, impossible to distinguish according to pollen morphology; when Cupressaceae curve is almost parallel to that of Taxodiaceae (as it is here), they can be considered as chiefly represented by subtropical elements as *Chamaecyparis* (Popescu, 2001);
- Mediterranean xerophytes (*Quercus ilex* type mostly, *Olea*, *Phillyrea*, *Ligustrum*, *Pistacia*, *Ziziphus*) are scarce;
- a subdesertic element, *Lygeum* only, is very rare;

- herbs represented by numerous taxa and very abundant pollen grains [Poaceae, *Erodium*, *Geranium*, *Convolvulus*, Asteraceae Asteroideae, Asteraceae Cichorioideae, Lamiaceae, *Plantago*, *Euphorbia*, Brassicaceae, Apiaceae, *Knautia*, *Helianthemum*, *Rumex*, *Polygonum*, *Asphodelus*, Campanulaceae, Ericaceae, etc.; halophytes (Amaranthaceae–Chenopodiaceae, Caryophyllaceae, Plumbaginaceae) are included within the herbs; many of them represent water plants (Cyperaceae p.p., *Potamogeton*, *Sparganium*, *Typha*, Nymphaeaceae)];
- steppe elements (*Artemisia* and *Ephedra*) are separately grouped within the herbaceous pollen grains.

The fossil species *Tricolporopollenites sibiricum* Lubomirova 1972 (also described as *Tricolporopollenites wackersdorfensis* Thiele-Pfeiffer 1980 and *Fupinopollenites wackersdorfensis* (Thiele-Pfeiffer) Liu 1985, the botanical affinity of which is still unknown (Wang and Harley, 2004), has been recorded with near regularity especially within the late Miocene sediments.

Pollen concentration is relatively high for a distal deposit: generally greater than 3000 pollen grains/g of dry sediment, often above 10,000 pollen grains/g, sometimes more than 20,000 pollen grains/g and up to 65,000 pollen grains/g.

Regarding biodiversity, it is worth to emphasize the persistence of some megathermic elements such as *Avicennia* (Verbenaceae), *Amanoa* (Euphorbiaceae), *Fothergilla* and *Exbucklandia* (Hamamelidaceae), Sapindaceae, and Acanthaceae at relatively high latitude. They had disappeared from the northwestern Mediterranean region at 14 Ma (Serravallian) (Suc, 1986; Suc, 1996) whereas they persisted up to about 5.6 Ma (late Messinian) in Sicily (Suc and Bessais, 1990) and North Africa (Chikhi, 1992; Bachiri Taoufiq et al., 2000). Pollen grains of *Avicennia*, a mangrove element, have been very scarcely recorded at Site 380A (at 1018.85 and 781.63 m depth): the presence of this mangrove element which withstands relatively low salinities is in agreement with water salinity deduced from diatom flora and with a suggested water temperature of about 20 °C (Schrader, 1978). This supports the idea that thermophilous plants persisted longer in the southeastern Europe area than elsewhere in the Mediterranean region (Suc, 1996). Indeed, a few relict megathermic elements have also been recorded in the Dacic Basin in the early Pliocene (Popescu, 2001).

Six successive pollen zones have been identified, with special attention to the above-mentioned ecological pollen groups and to halophytes (Fig. 3):

¹ A special attention has been paid to bisaccate pollen grains for a routine and continuous identification in order to refine pollen contents with respect to Traverse's (1978) analyses.

- pollen zone 1, from 1019.85 to 970.08 m depth: characterised by some occurrences of megathermic elements, large amounts of thermophilous trees (mega-mesothermic and mesothermic ones), low percentages of halophytes, and very low percentages of steppe elements; this zone is relatively rich in water plants and Ericaceae;
- pollen zone 2, from 970.08 to 923.05 m depth: same characteristics as pollen zone 1, but scarcity of megathermic elements, clear increase in halophytes, slight increase in steppe elements, *Cathaya* is more common; same representation of water plants and Ericaceae as previously;
- pollen zone 3, from 923.05 to 884.62 m depth: this zone shows a slight decrease in mega-mesothermic and mesothermic elements, megathermic elements are absent; frequency of halophytes significantly increases, and to a lesser extent that of steppe elements; water plants and Ericaceae decrease;
- pollen zone 4, from 861.65 to 819.94 m depth: mega-mesothermic and mesothermic elements increase again in contrast with herbs and especially steppe elements except for their brief maximum in the upper part of the zone; halophytes show moderate frequencies;
- pollen zone 5, from 819.94 to 730.45 m depth: marked by a modest but obvious decrease in mega-mesothermic and mesothermic plants in correspondence with increases in herbs, steppe elements and halophytes;
- pollen zone 6, from 730.45 to 704.34 m depth: new increase in mega-mesothermic and mesothermic trees counterbalanced by decreasing herbs, steppe elements and halophytes. Its base almost corresponds with that of the “Lower Siderite” which has been considered as corresponding to a warm phase within the Pliocene (Traverse, 1978).

3.2. Other palynological constituents

Two kinds of unicellular organisms have been recorded: dinocysts and acritarchs (Fig. 3). They are mostly absent in the late Miocene whereas they are abundant in the Pliocene. Dinocysts (often poorly preserved) include, among others, several types of *Pyxidinospis psilata* (abundant), *Spiniferites*, *Operculodinium*, and scarce specimens of *Lingulodinium machaerophorum*: some of these dinocysts belong to the Mediterranean Sea flora. The following Paratethian endemic species (the most abundant and still well preserved cysts) have been found: *Spiniferites cruciformis* (relatively rare), *Galeacysta etrusca* (very regularly). Acritarchs (light, spherical, echinulate cysts) predomi-

nate in the lowermost Pliocene layers, then they are replaced by dinocysts. On the whole, the frequency of these acritarchs appears positively correlated to halophyte expansion, except in the late Miocene deposits.

4. Discussion

Evolution of the Pliocene vegetation on the whole appears to be characterised by competition between humid and warm forest biotopes and dry (possibly cooler) open vegetation, as experienced in the North-western Mediterranean region (Suc, 1984). This is documented by the contrast between pollen zones 4–6 on the one hand and 5 on the second hand. Along the studied section, mid- and high-altitudinal trees exhibit only moderate variations, probably because the source of their pollen grains is somewhat distant. In more detail, climatic variations appear more complicated, especially when mega-mesothermic elements (mainly Taxodiaceae) are better developed: Poaceae and Asteraceae alternately dominate. Cour and Duzer (1978) have observed along a modern pollen transect from Northern Europe to Central Africa that Poaceae dominate in the more humid latitudes whereas Asteraceae are prevalent in the dry areas. As a consequence, the Poaceae/total Asteraceae ratio in a pollen diagram can be used as a climate index. At Site 380A, strong and repetitive variations of this ratio characterise several parts of the studied section and can be understood as substantial variations in moisture during the warmest phases (Fig. 3). In addition, these variations are consistent with the subdivision in pollen zones (Fig. 3).

Other factors appear to have controlled some changes which are recorded in pollen zones 1–3. Indeed, abundant freshwater plant and Ericaceae pollen grains characterise pollen zones 1 and 2, in association with halophyte pollen grains. This evokes modern edaphic environments in delta systems where freshwater and brackish lagoons coexist. Some representatives of the Taxodiaceae (related to the *Taxodium* type) thrive in such mosaic coastal environments. Pollen analysis of present-day and recent sediments from the Rhône delta documents the coexistence of both kinds of environments and their respective distribution (Cambon et al., 1997; Arnaud-Fassetta et al., 2000). Pollen zone 3 is marked by the reduction of water plants and a significant increase in halophytes which could express a change in the pollen transport from a relatively distant delta source to a nearby brackish lagoon. Such an evolution in coastal environments is consistent with the diatom record from Site 380A: “predominance of benthic species indicates a shallow (less than 50 m water

depth) and polyhaline (salinity: 30 to 40‰) environment” (Schrader, 1978, p. 856). On the whole, curves of steppe elements and halophytes are almost consistent, but some shifts are perceptible. The curve of steppe elements is considered in the Mediterranean region as representative of climatic changes (Suc, 1984) whereas the halophyte curve can be regarded as an index of proximity of shoreline, i.e. as more illustrative of sea-level variations (Poumot and Suc, 1994; Suc et al., 1995c). Nevertheless, much *Artemisia* might participate in coastal associations and much *Amaranthaceae*–*Chenopodiaceae* might belong to steppe associations.

Comparison between *Pinus* and poorly preserved Pinaceae (bisaccate) pollen grains on the one hand, and halophytes on the other, provides information as to whether the sedimentary environment was distal or coastal (Poumot and Suc, 1994; Suc et al., 1995c). These curves are in opposition (Fig. 3): large amounts of *Pinus* and poorly preserved Pinaceae pollen grains indicate a more distal position (pollen zones 1 and 2, middle part of pollen zone 4, and mid to upper part of pollen zone 5), as documented also by the low frequency of halophytes. In contrast, more coastal conditions are indicated by increasing halophytes and low frequency of *Pinus* and poorly preserved Pinaceae pollen grains (pollen zone 3, lower and upper parts of pollen zone 4, lower part of pollen zone 5, and pollen zone 6).

The precise significance of the dinocysts and acritarchs is very difficult to elucidate because many of these organisms are endemic to Paratethian brackish-to-freshwater environments, and their ecological requirements are poorly known. It is best therefore to follow information provided by diatoms as a guide (Schrader, 1978). From 1020 m to about 880 m depth, diatoms indicate a shallow environment (paucity of marine–planktonic species) which can explain the quasi-absence of dinocysts and acritarchs. From about 860 to about 790 m depth, planktonic marine diatoms prevail (*Actinocyclus ehrenbergii* mainly) and the inferred marine conditions (mixoeuryhaline waters: 30–40‰ salinity) can explain the relative abundance of acritarchs and dinocysts. Higher in the core, marine conditions progressively evolved to increasingly lacustrine ones that would correspond to a loss of dinocysts, except for some limited peaks (Fig. 3). An outstanding event occurred at 840–850 m depth and corresponds to an influx of *Synedra indica*, a delicate (coastal) marine diatom (present-day salinity tolerance: 30–40‰), which has been interpreted by Schrader (1978) as a sudden transition from shallow marine to deep marine conditions (entrance of Mediterranean marine waters). The interval 854–860 m depth is characterised by an acme of

acritarchs (continued up to 841 m depth at a lesser intensity) (Fig. 3): this may be understood as the inception of marine conditions in a relatively coastal environment (importance of halophytes). This illuminates initial observations made by Traverse (1978), and supports the idea of a brackish marine environment deduced from aragonite precipitation (Ross et al., 1978b). Today, similar acritarchs are often abundant in the brackish lagoons of the Rhône delta (Suc, personal communication). This was followed by a major influx of Mediterranean dinocysts that, having entered the Black Sea, persisted and became progressively adapted to brackish and maybe nearly(?) freshwater conditions.

It has been proposed to place the base of the Pliocene at Site 380A at the top of the “Pebble Breccia” (864.50 m depth) which might indicate “a shoaling of the sea level with a corresponding subaerial exposure and erosion at Site 381” (Stoffers et al., 1978, p. 387). Hsü and Giovanoli (1979) reinforced this assumption by considering the 883.50–864.50 m depth interval as being equivalent to the Messinian salinity crisis in the Mediterranean Sea, that was recently confirmed by Gillet (2004). This interpretation is supported by the pollen diagram of the overlying interval (pollen zone 4) documenting a climatic phase which appears warmer and moister than the previous pollen zone 3. Climatic differences between pollen zones 3 and 4 are in the same kind of range than those existing between late Messinian (Upper Evaporites) and early Zanclean (Trubi) in Sicily (Fauquette et al., 2006-this volume). Pollen zone 4 is, as a consequence, referred to the early Zanclean). Indeed, pollen diagram appears fully consistent with the early Pliocene reference pollen diagrams in Europe (Susteren, in The Netherlands: Zagwijn, 1960; Garraf 1, offshore Barcelona: Suc and Cravatte, 1982; Rio Maior F16, Portugal: Diniz, 1984), that is in agreement (in finer details of course) with the first climatostratigraphic subdivision that I deduced from the Traverse’s (1978) study (see above and Fig. 1). The arboreal flora is almost the same in these pollen diagrams although the herbaceous vegetation differs according to the area (Suc et al., 1995a). The Zanclean is subdivided into three climatic periods: warm (Brunssumian A=pollen zone P Ia, from 5.33 to ca. 4.75 Ma), cooler (Brunssumian B=pollen zone P Ib, from ca. 4.75 to ca. 4.00 Ma), and the warmest phase (Brunssumian C=pollen zone P Ic, from ca. 4.00 to ca. 3.60 Ma) (Suc and Zagwijn, 1983; Suc et al., 1995a). It is here proposed that Site 380A pollen zones 4, 5 and 6 are respectively correlated to these climatic periods (Fig. 3).

Secondary fluctuations at Site 380A show very precise similarities with various proxies recorded

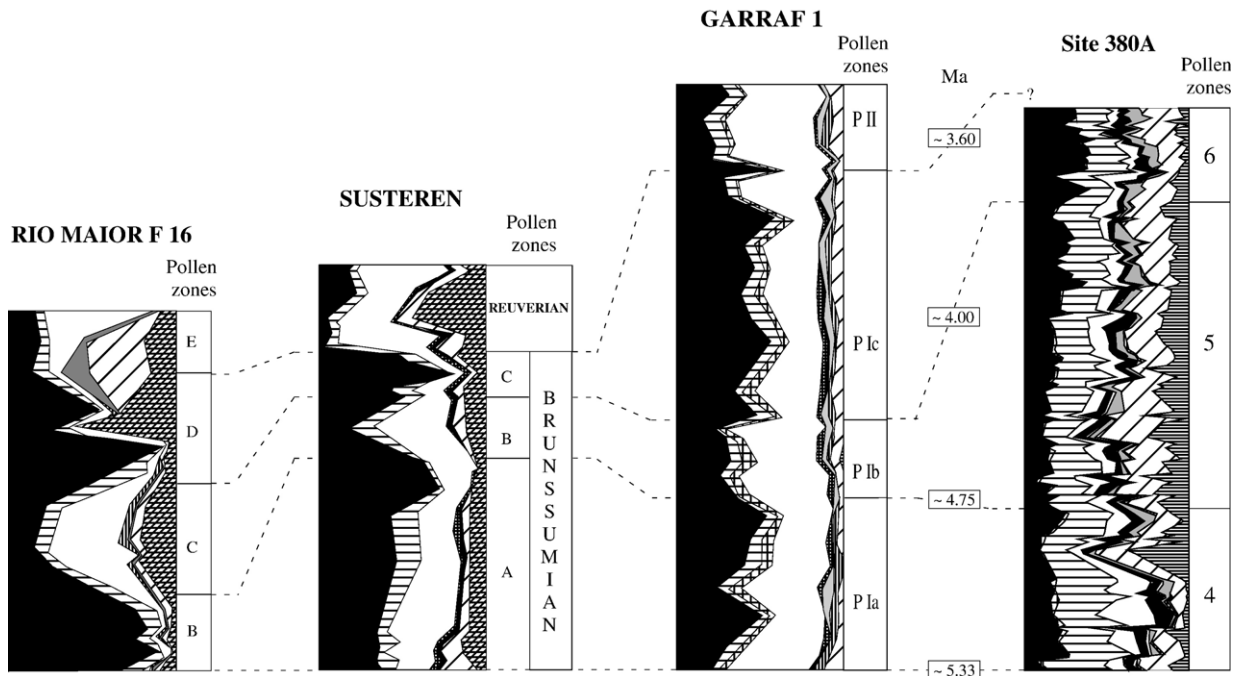


Fig. 4. Climatostratigraphic relationships between the early Pliocene reference pollen diagrams from Western Europe (Rio Maior F16, Portugal: Diniz, 1984; Susteren, The Netherlands: Zagwijn, 1960) and the Northwestern Mediterranean region (Garraf 1, offshore Barcelona: Suc and Cravatte, 1982) and the Site 380A pollen diagram. Respective pollen assemblages and/or climatic phases are indicated to the right of pollen diagrams. Ages in Ma are given for the Garraf 1 borehole with respect to planktonic foraminifer bio- and chronostratigraphy (Cita et al., 1999) and by comparison with the reference isotopic curve (Shackleton et al., 1995) (see Fig. 5). Ecological groups: the same as in Fig. 3, Ericaceae excepted (abundant in the Atlantic side localities, Rio Maior F16 and Susteren) which are illustrated to the right of herbs (in crossed hatching).

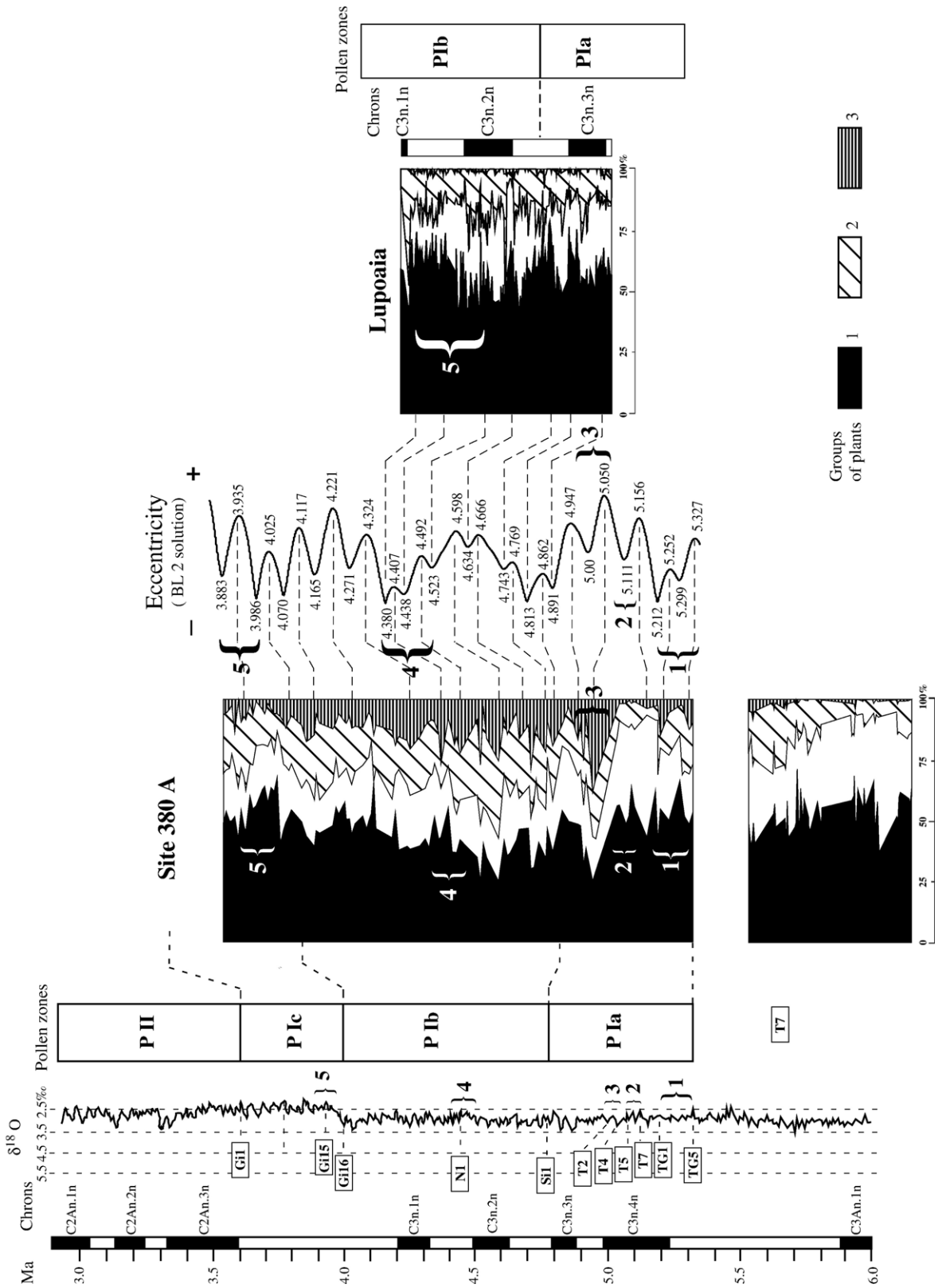
elsewhere. For example, the Brunssumian A starts with a less warm period and a similar warming up occurs in its middle part. The same evolution characterises the Mediterranean pollen zone P Ia and the isotopic curve (Fig. 5), and can be easily recognized at Site 380A (Fig. 4). The Reuverian (=P II pollen zone), a period of moderate cooling, has not been reached in the studied section at Site 380A (Fig. 4). One must emphasize that the late Pliocene Northwestern Mediterranean steppes (rich in *Artemisia*) probably originated from those of the Middle East during the early Pliocene (as recorded in this study), even if the vegetation structure type already existed in the Southwestern Mediterranean region (Suc et al., 1999).

During the early Pliocene, Site 380A seems to have been not too far from the shoreline, and to have been constantly influenced by sea level changes judging from the relative importance of halophytes and their antithetic variations with bisaccate pollen grains (as *Pinus* and

other Pinaceae) (see above and Fig. 3). Following the relatively high Black Sea level of the earliest Pliocene (860–840 m depth interval according to diatoms; Schrader, 1978), variations in distance from the coastline (i.e. changes in sea level) seem to be in agreement with climate evolution: increases in halophytes (and decreases in bisaccate pollen grains) are almost coherent with increases in steppe elements (cooling phases), and presumably correspond to repeated reductions in distance to the coastline (sea level drops). This interpretation is supported by the consistent increases in dinocysts (mostly constituting endemic species) (Fig. 4).

On the whole, such a climatic subdivision is also in agreement with the reference $\delta^{18}\text{O}$ curve (Shackleton et al., 1995), to which large climatostratigraphic subdivisions may be related as shown on Fig. 5: P Ia running between isotopic stages TG5 and Si1, P Ib between isotopic stages Si1 and Gi16, P Ic between isotopic stages Gi16 and Gi1. Indeed, the Site 380A pollen record

Fig. 5. High-resolution proposed relationships between the reference $\delta^{18}\text{O}$ curve with location of several important isotopic stages (Shackleton et al., 1995), Site 380A and the Lupoia section with respect to eccentricity curve (BL2 solution: Loutre and Berger, 1993). The five large-scale climatic phases considered as highly significant are indicated in front of braces. The corresponding Mediterranean reference pollen zones are pointed. Ecological groups of plants: 1, Thermophilous elements (=mega- plus mega-meso- plus mesotherm plants); 2, Herbs; 3, Steppe elements.



displays a significantly higher resolution than the other European and Mediterranean reference pollen diagrams, and offers extensive possibilities to integrate with the $\delta^{18}\text{O}$ record. To check this parallelism, five noteworthy climatic phases have been selected on the $\delta^{18}\text{O}$ curve: 1, warm period from isotopic stages TG5 to TG1; 2, including three short warm phases corresponding to isotopic stages T7 to T5; 3, i.e. two successive cooling phases (isotopic stages T4 and T2); 4, warming in the mid P Ib pollen zone centred around isotopic stage N1; and 5, the warmest phase in the early Pliocene centred around isotopic stage Gi15. These phases are clearly identified in the pollen diagram when reduced to thermophilous elements (mega- plus mega-meso- plus mesotherm plants) in opposition to herbs and steppe elements (Fig. 5). In addition, more precise relationships are achievable with the Lupoia pollen record (southwestern Romania) which is calibrated at high-resolution using magnetostratigraphy and eccentricity (Popescu, 2001). In the Lupoia record, each maximum of thermophilous elements (same presentation as for Site 380A) belongs to a relative or absolute minimum in eccentricity as forced by the palaeomagnetic age control (Fig. 5) (Popescu, 2001). This is consistent with the results of Li et al. (1998) who, after modelling climate evolution, proposed that warmings prior to 2.7 Ma corresponded to minima in eccentricity (and coolings to maxima in eccentricity), and that warmings later than 2.7 Ma corresponded to maxima in eccentricity (and coolings to minima in eccentricity). So, it appears possible to correlate the steppe element maxima of Site 380A (understood as expressive of coolings) with eccentricity maxima (Fig. 5). It can be opposed that not all the steppe maxima have been used: the non-selection of few of them was not arbitrary. I only considered the steppe peaks which clearly alternate with well-identified peaks in thermophilous elements. It results in a tuned chronology to eccentricity which is to be considered as an attempt only because of the lack of an unquestionable age model for Site 380A. Some variability in the sedimentation rate seems to characterise the studied section; nevertheless, the highest values appear to be located in correspondence with cooler phases (5.156–5.050 Ma; 4.769–4.492 Ma; 4.324–4.117 Ma) maybe because of an increased river transport of terrigenous material (Fig. 5).

A similar astronomical tuning of climatic relationships for the late Miocene of Site 380A does not appear attainable because increases in herbs (here mostly halophytes) are coeval with increases in thermophilous elements (see the base of pollen zone 1, the top of pollen zone 2, and the entire pollen zone 3) and not in opposition as would be expected for climatic changes. A lack of samples in some intervals of the Miocene section

in Site 380A also hinder attempts to tune this part of the record (Fig. 3). So the climatic signal in pollen zones 1 to 3 can be effectively reduced to the difference between the edaphic signal in relation with proximity of shoreline.

It is difficult to judge definitively the impact of the Mediterranean Messinian salinity crisis on the Black Sea. Based on diatom and dinocyst–acritarch records augmented by variations in halophyte frequency, it is obvious that a severe sea-level drop and sea-level rise occurred just before the Aragonite layer. This confirms the early observations of DSDP Leg 42B (Ross et al., 1978a). Schrader (1978) proposed that such an event was forced by tectonics, and also considers that “in the case of a totally dried out deep Mediterranean Basin and a depth pattern similar to that of today, it would have been impossible for marine waters and floras to enter the Black Sea from the Mediterranean Sea” (Schrader, 1978, p. 856). A tectonic yo-yo in such a short time interval seems improbable, but water exchanges between the Mediterranean and the Black Sea are also unrealistic, as Schrader (1978) points out. However, new ideas are emerging about exchanges at high sea level between the Mediterranean and the Eastern Paratethys (Dacic Basin, Southwestern Romania) just before and just after desiccation of the deep Mediterranean Basin (Clauzon et al., 2005). These exchanges would have existed in the two directions and are documented both by Mediterranean nannoplankton influxes into the Central Paratethys and by Paratethian dinocyst influxes into the Mediterranean. In this way, the record at Site 380A of marine diatoms and acritarchs within the interval 860–840 m depth would correspond to the second Mediterranean influx (earliest Zanclean in age). Perhaps the first Mediterranean influx, located at 5.6 Ma (i.e. at the TG 15 isotopic stage; Shackleton et al., 1995) in the chronology of the Messinian salinity crisis adopted by Clauzon et al. (1996), corresponds to the initial arrival of acritarchs recorded at 886.10 m depth at Site 380A just below the “Pebbly Breccia” which would mark the Messinian salinity crisis as suggested by Hsü and Giovanoli (1979) and the desiccation of the Black Sea in the same time as the desiccation of the deep Mediterranean Basin. An alternate scenario could be proposed if considering the Krijgsman et al. (1999) age model for the Messinian salinity crisis. This scenario differs from that of Clauzon et al. (1996) in locating the Sicilian Upper Evaporites (latest Messinian) after [and not before as postulated by Clauzon et al. (1996)] the Mediterranean Sea desiccation (i.e. the erosional phase). In this way, the Aragonite layer of Site 380A would belong to the latest Messinian

and not to the earliest Zanclean as proposed above. This hypothesis could be supported by the abundance of acritarchs similar to those generally found in the Caltanissetta Basin (Sicily) within clays interbedded with the Messinian Upper Evaporites. However, such an interpretation is seriously contradicted by the climatostratigraphic relationships on large geographic scale that are established on a clearly identified warm and humid phase at the beginning of the Pliocene (Fig. 4). So, it is preferred to consider that Zanclean started at the Aragonite layer as established by Gillet (2004) and that the Mediterranean marine dinocysts entered the Black Sea in large quantities later (about 170 kyrs) than the first Zanclean marine influxes (Fig. 5).

The location of the passage used by the Mediterranean waters for these influxes remains an unsolved question. Acritarchs entered the Black Sea before the clearly identified Mediterranean dinocysts: this opens the intriguing possibility that the connection between the Mediterranean and Black Seas took place far from the Bosphorus area, probably through the Dacic Basin and Bulgaria (Clauzon et al., 2005).

5. Conclusions

High-resolution palynological study of late Miocene and early Pliocene sediments from Site 380A provides important new information about regional environments and their response to global climate change and desiccation of the Mediterranean Sea. The following results are highlighted:

- (1) the presence of delta environments in the area during the late Miocene where freshwater and brackish lagoons coexisted before saline habitats prevailed in the latest Miocene;
- (2) these edaphic changes aside, vegetation breaks as documented by pollen records chiefly reflect competition between humid thermophilous forests and dry steppes, evoking the present-day antagonisms in regional landscapes;
- (3) pollen analysis of sediments overlying the “Pebby Breccia” shows serious agreements with the standard early Pliocene European pollen diagrams and $\delta^{18}\text{O}$ record, which results in a detailed climatostratigraphy for Site 380A that allows a first attempt of tuning based on a proposed relationship with orbital eccentricity;
- (4) climatic results and the inferred climatostratigraphy of Site 380A support the scenario proposed by Clauzon et al. (1996) for the Messinian salinity crisis;
- (5) so, it is suggested that the Black Sea dried up at 5.6 Ma and that the regional erosion stopped at 5.33 Ma, exactly as the Mediterranean Sea; this constitutes new arguments supporting the actual response of the Black Sea to the Messinian salinity crisis (Gillet, 2004);
- (6) high sea level brief connections between the Mediterranean and the Black Seas were restored after 5.15 Ma only.

Acknowledgements

This study is based on a PhD financed by the French Government through its Embassy at Bucharest, and supported by the French Programmes “Environnement, Vie et Sociétés” and “Eclipse”. J.-P. Suc and P. Bernier kindly supervised this work. I am grateful to G. Clauzon who provided information on his research in the Dacic Basin, and A. Berger and M.-F. Loutre for supplying data on the BL2 solution. I am highly indebted to the referees of this paper (F. J. Hilgen, F. F. Steininger and R. Bertoldi), whom the comments improved significantly the manuscript. M. J. Head is greatly acknowledged for improving some dinocyst identifications, discussing the paper and correcting the English, L. Londeix for discussions about ecological significance of dinocysts and acritarchs. I am grateful to the ODP curatorial staff for provision of samples. M. Gonzales processed the samples.

References

- Arnaud-Fassetta, G., Beaulieu, J.-L., Suc, J.-P., Provansal, M., Williamson, D., Leveau, P., Landuré, C., Gadel, F., Aloisi, J.-C., Giresse, P., Oberlin, C., Duzer, D., 2000. Evidence for an early land use in the Rhône delta (Mediterranean France) as recorded by late Holocene fluvial paleoenvironments (1640–100 B.C.). *Geodyn. Acta* 13, 377–389.
- Bachiri Taoufiq, N., Barhoun, N., Suc, J.-P., Méon, H., Elaouad, Z., Benbouziane, A., 2000. Environnement, végétation et climat du Messinien au Maroc. *Paleontol. Evol.* 32–33, 127–145.
- Bertini, A., 1994. Palynological investigations on Upper Neogene and Lower Pleistocene sections in Central and Northern Italy. *Mem. Soc. Geol. Ital.* 48, 341–443.
- Bertini, A., Londeix, L., Maniscalco, R., Di Stefano, A., Suc, J.-P., Clauzon, G., Gautier, F., Grasso, M., 1998. Paleobiological evidence of depositional conditions in the Salt Member, Gessoso-Solfifera Formation (Messinian upper Miocene) of Sicily. *Micropaleontology* 44 (4), 413–433.
- Bertoldi, R., Rio, D., Thunell, R., 1989. Pliocene–Pleistocene vegetational and climatic evolution of the South-Central Mediterranean. *Palaeogeogr. Palaeoclimatol. Palaeoecol.* 72 (3–4), 263–275.
- Cambon, G., Suc, J.-P., Aloisi, J.-C., Giresse, P., Monaco, A., Touzani, A., Duzer, D., Ferrier, J., 1997. Modern pollen deposition in the Rhône delta area (lagoonal and marine sediments) France. *Grana* 36, 105–113.

- Chikhi, H., 1992. Une palynoflore Méditerranéenne à subtropicale au Messinien pré-évaporitique en Algérie. *Géol. Méditerran.* 19 (1), 19–30.
- Cita, M.B., Rio, D., Sprovieri, R., 1999. The Pliocene series: chronology of the type Mediterranean record and standard chronostratigraphy. In: Wrenn, J.H., Suc, J.-P., Leroy, S.A.G. (Eds.), *The Pliocene: Time of Change*. Amer. Ass. Stratigraphic Palynologists, pp. 49–63.
- Clauzon, G., Suc, J.-P., Gautier, F., Berger, A., Loutre, M.-F., 1996. Alternate interpretation of the Messinian salinity crisis: controversy resolved? *Geology* 24 (4), 363–366.
- Clauzon, G., Suc, J.P., Popescu, S.-M., Mărunțeanu, M., Rubino, J.-L., Marinescu, F., Melinte, M.C., 2005. Influence of the Mediterranean sea-level changes over the Dacic Basin (Eastern Paratethys) in the Late Neogene. *The Mediterranean Lago Mare facies deciphered*. *Basin Res.* 17, 437–562.
- Cour, P., 1974. Nouvelles techniques de détection des flux et de retombées polliniques: étude de la sédimentation des pollens et des spores à la surface du sol. *Pollen Spores* 16 (1), 103–141.
- Cour, P., Duzer, D., 1978. La signification climatique, édaphique et sédimentologique des rapports entre taxons en analyse pollinique. *Ann. Mines Belg.* 7–8, 155–164.
- Diniz, F., 1984. Etude palynologique du bassin Pliocène de Rio Maior. *Paléobiol. Cont.* 14 (2), 259–267.
- Drivaliari, A., 1993. Images polliniques et paléoenvironnements au Néogène supérieur en Méditerranée orientale. Aspects climatiques et paléogéographiques d'un transect latitudinal (de la Roumanie au delta du Nil). Thesis, Univ. Montpellier 2. 333 pp.
- Drivaliari, A., Țicleanu, N., Marinescu, F., Mărunțeanu, M., Suc, J.-P., 1999. A Pliocene climatic record at Ticleni (Southwestern Romania). In: Wrenn, J.H., Suc, J.-P., Leroy, S.A.G. (Eds.), *The Pliocene: Time of Change*. Amer. Ass. Stratigraphic Palynologists Foundation, pp. 103–108.
- Fauquette, S., Suc, J.-P., Bertini, A., Popescu, S.-M., Wany, S., Bachiri Taoufiq, N., Perez Villa, M.-J., Chikhi, H., Subally, D., Feddi, N., Clauzon, G., Ferrier, J., 2006. How much the climate forced the Messinian salinity crisis? Quantified climatic conditions from pollen records in the Mediterranean region. In: Agustí, J., Oms, O., Meulenkamp, J.E. (Eds.), *Late Miocene to Early Pliocene Environment and Climate Change in the Mediterranean Area*. *Palaeogeography, Palaeoclimatology, Palaeoecology*, vol. 238, pp. 281–301. [this volume]. doi:10.1016/j.palaeo.2006.03.029.
- Gillet, H., 2004. La stratigraphie tertiaire et la surface d'érosion messinienne sur les marges occidentales de la mer Noire: stratigraphie sismique haute resolution. Thesis, Univ. Bretagne occidentale. 259 pp.
- Hsü, K.J., 1978. Correlation of Black Sea sequences. In: Ross, D.A., Neprochnov, Y.P., et al. (Eds.), *Initial Report of the Deep Sea Drilling Project*, vol. 42, 2. U.S. Gov. Print. Off., pp. 489–497.
- Hsü, K.J., Giovanoli, F., 1979. Messinian event in the Black Sea. *Palaeogeogr. Palaeoclimatol. Palaeoecol.* 29 (1–2), 75–94.
- Krijgsman, W., Hilgen, F.J., Raffi, I., Sierro, F.J., Wilson, D.S., 1999. Chronology, causes and progression of the Messinian salinity crisis. *Nature* 400, 652–655.
- Letouzey, J., Gonnard, R., Montadert, L., Kristchev, K., Dorkel, A., 1978. Black Sea: geological setting and recent deposits distribution from seismic reflection data. In: Ross, D.A., Neprochnov, Y.P., et al. (Eds.), *Initial Report of the Deep Sea Drilling Project*, vol. 42, 2. U.S. Gov. Print. Off., pp. 1077–1084.
- Li, X.S., Berger, A., Loutre, M.F., Maslin, M.A., Haug, G.H., Tiedemann, R., 1998. Simulating late Pliocene Northern Hemisphere climate with the LLN-2D model. *Geophys. Res. Lett.* 25, 915–918.
- Loutre, M.-F., Berger, A., 1993. Sensibilité des paramètres astro-climatiques au cours des 8 derniers millions d'années. Scientific Report 93/4, Institut d'Astronomie et de Géophysique G. Lemaître, Université catholique de Louvain, Louvain-la-Neuve: 1–9.
- Marinescu, F., 1992. Les bioprovinces de la Paratéthys et leurs relations. *Paleontol. Evol.* 24–25, 445–453.
- Mărunțeanu, M., Papaianopol, I., 1995. The connection between the Dacic and Mediterranean Basins based on calcareous nannoplankton assemblages. *Rom. J. Stratigr.* 76 (7), 169–170.
- Mărunțeanu, M., Papaianopol, I., 1998. Mediterranean calcareous nannoplankton in the Dacic Basin. *Rom. J. Stratigr.* 78, 115–121.
- Muratov, M.V., Neprochnov, Y.P., Ross, D.A., Trimonis, E.S., 1978. Basic features of the Black Sea on the results of Deep-Sea Drilling, Leg 42B. In: Ross, D.A., Neprochnov, Y.P., et al. (Eds.), *Initial Report of the Deep Sea Drilling Project*, vol. 42, 2. U.S. Gov. Print. Off., pp. 1141–1148.
- Noirfalise, A., Dahl, E., Ozenda, P., Quézel, P., 1987. Carte de la végétation naturelle des Etats membres des Communautés européennes et du Conseil de l'Europe. Publ. Communautés Eur., EUR 10970 (78 pp.).
- Popescu, S.-M., 2001. Repetitive changes in lower Pliocene vegetation revealed by high-resolution pollen analysis: revised cyclostratigraphy of southwestern Romania. *Rev. Palaeobot. Palynol.* 120, 181–202.
- Poumot, C., Suc, J.-P., 1994. Palynofaciès et dépôts séquentiels dans des sédiments marins du Néogène. *Bull. Cent. Rech. Explor. Prod. Elf-Aquitaine* 18, 107–119 (spec. publ.).
- Quézel, P., Médail, F., 2003. *Ecologie et biogéographie des forêts du bassin Méditerranéen*. Elsevier, France. 571 pp.
- Ross, D.A., 1978. Black Sea stratigraphy. *Initial Report of the Deep Sea Drilling Project*, vol. 42, 2. U.S. Gov. Print. Off., pp. 17–26.
- Ross, D.A., Neprochnov, Y.P., et al. (Eds.), 1978a. *Initial Report of the Deep Sea Drilling Project*, vol. 42, 2. U.S. Gov. Print. Off. 1244 pp.
- Ross, D.A., et al., 1978b. Site 380. In: Ross, D.A., Neprochnov, Y.P., et al. (Eds.), *Initial Report of the Deep Sea Drilling Project*, vol. 42, 2. U.S. Gov. Print. Off., pp. 119–291.
- Schrader, H.-J., 1978. Quaternary through Neogene history of the Black Sea, deduced from the paleoecology of diatoms, silicoflagellates, ebridians, and chrysomonads. In: Ross, D.A., Neprochnov, Y.P., et al. (Eds.), *Initial Report of the Deep Sea Drilling Project*, vol. 42, 2. U.S. Gov. Print. Off., pp. 789–901.
- Semenenko, V.N., Liulieva, S.A., 1978. Opit priamoi korrelatii Mio-Pliotena Vostocinogo Paratetisa i Tetisa. *Stratigrafia Kainozoiia Severnogo Pricernomia i Krimea. Nauk. Trud.* 2, 95–105.
- Semenenko, V.N., Olejnik, E.S., 1995. Stratigraphic correlation of the Eastern Paratethys Kimmerian and Dacian stages by molluscs, dinocyst and nannoplankton data. *Rom. J. Stratigr.* 76 (7), 113–114.
- Shackleton, N.J., Opdyke, N.D., 1977. Oxygen isotope and paleomagnetic evidence for early Northern Hemisphere glaciation. *Nature* 270, 216–219.
- Shackleton, N.J., Hall, M.A., Pate, D., 1995. Pliocene stable isotope stratigraphy of Site 846. *Proc. Ocean Drill. Prog., Sci. Results*, vol. 138. U.S. Gov. Print. Off., pp. 337–355.
- Snel, E., Mărunțeanu, M., Macaș, R., Meulenkamp, J.E., Van Vugt, N., 2006. Late Miocene to early Pliocene chronostratigraphic framework for the Dacic Basin, Romania. In: Agustí, J., Oms, O., Meulenkamp, J.E. (Eds.), *Late Miocene to Early Pliocene Environment and Climate Change in the Mediterranean Area*.

- Palaeogeogr. Palaeoclimatol. Palaeoecol., vol. 238, pp. 107–124. [this volume]. doi:10.1016/j.palaeo.2006.03.021.
- Stoffers, P., Müller, G., 1978. Mineralogy and lithofacies of Black Sea sediments, Leg 42B Deep Sea Drilling Project. In: Ross, D.A., Neprochnov, Y.P. (Eds.), Initial Report of the Deep Sea Drilling Project, vol. 42, 2. U.S. Gov. Print. Off., pp. 373–390.
- Stoffers, P., Degens, E.T., Trimonis, E.S., 1978. Stratigraphy and suggested ages of Black Sea sediments cored during Leg 42B. In: Ross, D.A., Neprochnov, Y.P., et al. (Eds.), Initial Report of the Deep Sea Drilling Project, vol. 42, 2. U.S. Gov. Print. Off., pp. 483–487.
- Suc, J.-P., 1984. Origin and evolution of the Mediterranean vegetation and climate in Europe. *Nature* 307, 429–432.
- Suc, J.-P., 1986. Flores néogènes de Méditerranée occidentale. Climat et paléogéographie. *Bull. Cent. Rech. Explor. Prod. Elf-Aquitaine* 10 (2), 477–488.
- Suc, J.-P., 1989. Distribution latitudinale et étagement des associations végétales au Cénozoïque supérieur dans l'aire ouest-Méditerranéenne. *Bull. Soc. Géol. Fr., Ser. 8, 5 (3)*, 541–550.
- Suc, J.-P., 1996. Late Neogene vegetation changes in Europe and North Africa. *Eur. Newsl.* 10, 27–28.
- Suc, J.-P., Bessais, E., 1990. Pérennité d'un climat thermo-xérique en Sicile avant, pendant, après la crise de salinité Messinienne. *C. R. Acad. Sci. Paris, Ser. 2 (310)*, 1701–1707.
- Suc, J.-P., Cravatte, J., 1982. Etude palynologique du Pliocène de Catalogne (nord-est de l'Espagne). *Paléobiol. Cont.* 13 (1), 1–31.
- Suc, J.-P., Zagwijn, W.H., 1983. Plio-Pleistocene correlations between the northwestern Mediterranean region and northwestern Europe according to recent biostratigraphic and palaeoclimatic data. *Boreas* 12, 153–166.
- Suc, J.-P., Diniz, J.-P., Leroy, F., Poumot, S., Bertini, C., Dupont, A., Clet, L., Bessais, M., Zheng, E., Fauquette, Z., Ferrier, S., 1995a. Zanclean (~Brunssumian) to early Piacenzian (~ early-middle Reuverian) climate from 4° to 54° north latitude (West Africa, West Europe and West Mediterranean areas). *Meded.-Rijks Geol. Dienst* 52, 43–56.
- Suc, J.-P., Bertini, A., Combourieu-Nebout, N., Diniz, F., Leroy, S., Russo-Ermolli, E., Zheng, Z., Bessais, E., Ferrier, J., 1995b. Structure of West Mediterranean vegetation and climate since 5.3 Ma. *Acta Zool. Cracov.* 38 (1), 3–16.
- Suc, J.-P., Violanti, D., Londeix, L., Poumot, C., Robert, C., Clauzon, G., Gautier, F., Turon, J.-L., Ferrier, J., Chikhi, H., Cambon, G., 1995c. Evolution of the Messinian Mediterranean environments: the Tripoli Formation at Capodarso (Sicily Italy). *Rev. Palaeobot. Palynol.* 87, 51–79.
- Suc, J.-P., Fauquette, J.-P., Bessedik, S., Bertini, M., Zheng, A., Clauzon, Z., Suballyova, G., Diniz, D., Quézel, F., Feddi, P., Clet, N., Bessais, M., Bachiri Taoufiq, E., Méon, N., Combourieu-Nebout, H., 1999. Neogene vegetation changes in West European and West circum-Mediterranean areas. In: Agusti, J., Rook, L., Andrews, P. (Eds.), *Hominid Evolution and Climate in Europe: 1. Climatic and Environmental Change in the Neogene of Europe*. Cambridge University Press, pp. 370–385.
- Tiedemann, R., Sarthein, M., Shackleton, N.J., 1994. Astronomic timescale for the Pliocene Atlantic $\delta^{18}\text{O}$ and dust flux records of Ocean Drilling Program Site 659. *Paleoceanography* 9 (4), 619–638.
- Traverse, A., 1978. Palynological analysis of DSDP Leg 42B (1975) cores from the Black Sea. In: Ross, D.A., Neprochnov, Y.P., et al. (Eds.), Initial Report of the Deep Sea Drilling Project, vol. 42, 2. U. S. Gov. Print. Off., pp. 993–1015.
- Wang, W.M., Harley, M.M., 2004. The Miocene genus *Fupingopollenites*: comparisons with ultrastructure and pseudocolpi in modern pollen. *Rev. Palaeobot. Palynol.* 131, 117–145.
- Zagwijn, W.H., 1960. Aspects of the Pliocene and early Pleistocene vegetation in The Netherlands. *Meded.-Geol. Sticht., Ser. C 3 (5)*, 1–78.
- Zohary, M., 1973. *Geobotanical Foundations of the Middle East*, vol. 2. Fischer, G., Stuttgart, pp. 337–355.

How much did climate force the Messinian salinity crisis? Quantified climatic conditions from pollen records in the Mediterranean region

Séverine Fauquette^{a,b,*}, Jean-Pierre Suc^b, Adele Bertini^c, Speranta-Maria Popescu^b,
Sophie Warny^d, Naïma Bachiri Taoufiq^e, Maria-Jesus Perez Villa^f, Hafida Chikhi^g,
Najat Feddi^h, Danica Suballyⁱ, Georges Clauzon^j, Jacqueline Ferrier^a

^a *Institut des Sciences de l'Evolution (UMR CNRS 5554), Equipe Paléoenvironnements, case courrier 061, Université Montpellier II, Place Eugène Bataillon, 34095 Montpellier cedex 5, France*

^b *Institut Paléoenvironnements et Paléobiosphère (UMR 5125 CNRS), Université Claude Bernard-Lyon 1, Boulevard du 11 Novembre, 69622 Villeurbanne Cedex, France*

^c *Università degli Studi di Firenze, Dipartimento di Scienze della Terra, Via G. La Pira 4, 50121 Firenze, Italy*

^d *Museum of Natural Science and Department of Geology and Geophysics, Louisiana State University, 109 Howe-Russell Building, Baton Rouge, LA 70803, USA*

^e *Département de Géologie, Faculté des Sciences de Ben M'Sik, Université Hassan II — Mohammedia, BP 7955 Sidi Othmane, Casablanca, Morocco*

^f *Institut Paleontologic M. Crusafont, c. Escola Industrial 23, 08201 Sabadell, Spain*

^g *44 bis, rue des Papillons 41000 Blois, France*

^h *Département des Sciences de la Terre, Faculté des Sciences, Université Caddi Ayyad, Avenue Prince Moulay Abdallah, BP S15, Marrakech, Morocco*

ⁱ *Albert-Ludwigs-Universität Freiburg, Botanischer Garten, Schänzlestrasse 1, 79104 Freiburg, Germany*

^j *CEREGE (UMR 6635 CNRS), Université d'Aix-Marseille III, Pôle d'activité commerciale de l'Arbois, BP 80, 13545 Aix-En-Provence Cedex 4, France*

Received 2 April 2003; accepted 7 March 2006

Abstract

The latest Miocene (5.96 to 5.33 Ma) is characterised by an outstanding event: the desiccation of the Mediterranean Sea (Messinian salinity crisis). It has been suggested that this was caused by a tectonic event, with no climatic change playing a role in desiccation. Quantifying the climate of the region during this period will help support or refute this hypothesis. An effective method for reconstructing the climate from Neogene pollen data is the “Climatic Amplitude Method” based on the modern climatic requirements of plants to interpret fossil data. It has been conceived especially for periods devoid of modern vegetation analogue.

Twenty Messinian to Lower Zanclean pollen sequences are now available in the peri-Mediterranean region. Most of them do not cover the whole Messinian interval, particularly those along the Mediterranean shorelines where sedimentation was interrupted during the sea's desiccation. In contrast, sedimentation was almost continuous in such areas as the Atlantic side of Morocco, along the Adriatic coast (including the Po Valley), and to a lesser extent the Black Sea. The Mediterranean sites nonetheless provide a reliable if not a discontinuous record of vegetation variability in time and space.

A first examination of the pollen diagrams reveals a high regional variability controlled by local conditions, and throughout the interval a southward increase in herb pollen frequency in contrast to the tree pollen frequency. This indicates that open and

* Corresponding author. Institut des Sciences de l'Evolution (UMR CNRS 5554), Equipe Paléoenvironnements, case courrier 061, Université Montpellier II, Place Eugène Bataillon, 34095 Montpellier cedex 5, France.

E-mail address: fauquet@isem.univ-montp2.fr (S. Fauquette).

probably dry environments existed in the southern Mediterranean region prior to, during and after the salinity crisis. Trees developed in areas close to mountains such as in the Po Valley, in Cerdanya and in the Black Sea region. Most variations observed in the pollen diagrams are constrained by fluctuations of *Pinus* pollen amounts, indicating eustatic variations. Climatic quantification from pollen data does not show obvious climatic changes due to the desiccation of the Mediterranean Sea, especially in the dry and warm southwestern Mediterranean area (Sicily, southern Spain and North Africa). At Maccarone, along the Adriatic Sea, a decrease in temperatures of the coldest month and, less importantly, a decrease in mean annual temperatures, corresponding to a drastic vegetation change, are reconstructed. These temperature variations are assumed to be controlled by regional environmental changes (massive arrival of waters in this basin) rather than to reflect cooling, because some authors link the second phase of evaporite deposition to a period of global warming. Some migrations of plants probably occurred as a response to Mediterranean desiccation. But the climatic contrast which has probably existed at that time between the central Mediterranean and the peripheral areas might be amplified.

Climatic reconstruction from pollen data in the western Mediterranean area shows that climate is not the direct cause of the Mediterranean desiccation, as the Mediterranean region had experienced continuously high evaporation long before the crisis. Therefore the main factor leading to this event seems to be the successive closures of the Betic and Rifian corridors, isolating the Mediterranean Sea from the Atlantic Ocean.

© 2006 Elsevier B.V. All rights reserved.

Keywords: Messinian; Climate quantification; Pollen; Mediterranean; Black Sea

1. Introduction

The second half of the Messinian stage (5.96 to 5.33 Ma) is characterised in the Mediterranean Basin by a dramatic event: the desiccation of the Mediterranean Sea, i.e. the so-called Messinian salinity crisis. As it is generally accepted, the event corresponds to the interruption of relationships between the Atlantic Ocean and the Mediterranean Sea, causing the desiccation of the Mediterranean and, as a consequence, a thick accumulation of evaporites within the abyssal parts of the basin and the cutting of deep subaerial canyons by rivers.

Since the discovery of the event (Hsü et al., 1973), several scenarios have been debated with most discrepancies concerning chronology and causes of the successive phases of the salinity crisis. Today, after concerted effort on (1) magnetostratigraphy of key-sections [Morocco: Hodell et al. (1994), Cunningham et al. (1997); Southeastern Spain and Sicily: Gautier et al. (1994), Krijgsman et al. (1999b); Po Valley and Adriatic realm: Krijgsman et al. (1999a), G. Napoleone (personal communication)] and (2) radiometric dating [Morocco: Cunningham et al. (1997), Roger et al. (2000), Cornée et al. (2002); Adriatic realm: Odin et al. (1997), H. Maluski (personal communication)], there is general agreement on the age of the onset of the salinity crisis (5.96 Ma) and its termination at 5.33 Ma (Lourens et al., 1996).

The ongoing debate about the Messinian salinity crisis concerns its nature, a two-step event is envisioned by Clauzon et al. (1996) but a synchronous event is

envisioned by Krijgsman et al. (1999b) (Fig. 1). According to Clauzon et al. (1996), marginal evaporites and deep basin evaporites are chronologically disconnected, being separated by 260 kyr. A transgressive event occurred between evaporitic phases which corresponds to the Sicilian Upper Evaporites. In addition, this scenario takes into consideration a regional diversity with appropriate responses to the salinity crisis (perched basins, margins, deep basin) (Clauzon et al., 1996; Clauzon, 1997, 1999) (Fig. 1). The so-called «Lago Mare event» appears as two invasions of the Mediterranean Sea by eastern Paratethyan surface waters during high sea-level phases (Clauzon et al., 2005). This scenario has recently received strong support from oceanographic studies in the southern hemisphere (Vidal et al., 2002; Warny et al., 2003). In contrast, Krijgsman et al. (1999b, 2001) use an astrochronological approach to argue uniformity for the whole Mediterranean, in which marginal basins are isolated between 5.6 and 5.5 Ma by isostatic uplift during the desiccation phase of the Mediterranean (Fig. 1). Their paper concerns only the chronological location of the Sicilian Upper Evaporites, as illustrated by the Eraclea Minoa section. According to Clauzon et al. (1996, 2005), the Sicilian Upper Evaporites represent a transgressive episode at the end of the marginal evaporitic phase, and they precede the desiccation of the Mediterranean Sea (i.e. the deposition of evaporites in the desiccated abyssal plains and the cutting of canyons). According to Krijgsman et al. (1999b), they correspond to the termination of the salinity crisis, i.e. to the transgressive interval which immediately preceded

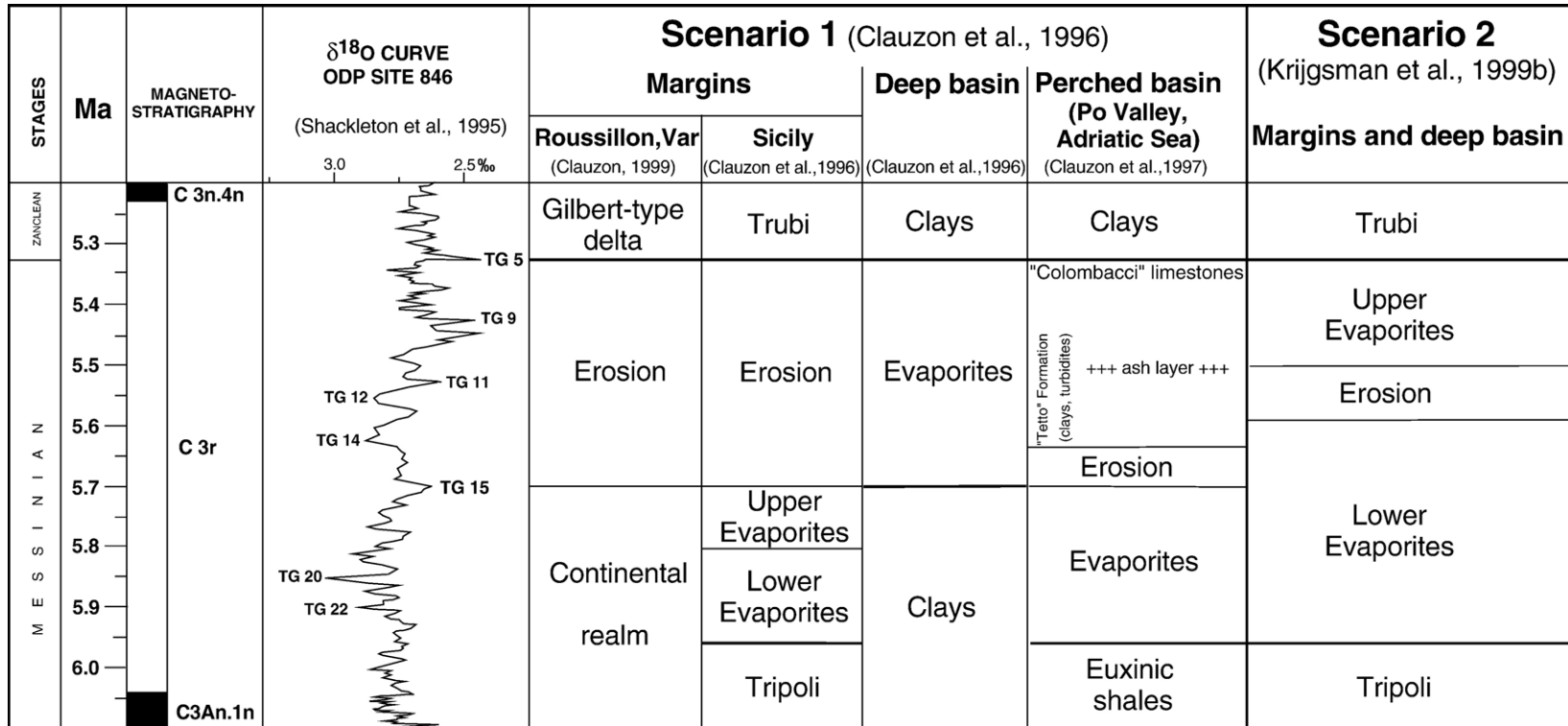


Fig. 1. Comparison of the two principal hypotheses of the Messinian salinity crisis (scenario 1 by Clauzon et al., 1996; scenario 2 by Krijgsman et al., 1999a,b). The thick horizontal lines respectively indicate (1) the onset of the salinity crisis (diachronous in the first scenario according to the basin status, isochronous in the second scenario), (2) the beginning of the Pliocene. The curve from Shackleton et al. (1995) has been chronologically re-calibrated to take into account the new date for the end of C3An.1n Chron established by Krijgsman et al. (1999a,b) at 6.04 Ma.

the flooding of the Mediterranean Basin by the Zanclean sea. This discrepancy has no bearing on climate, and so we choose to follow the scenario of Clauzon et al. (1996, 2005):

- 5.96–ca. 5.8 Ma, moderate global sea-level drop (less than 100 m), a period including two glacial Antarctic isotopic stages TG22 and TG20 (Shackleton et al., 1995; Vidal et al., 2002), causing deposition of Mediterranean marginal evaporites such as those of Sicily, Sorbas, Po Valley, Tyrrhenian realm;
- ca. 5.8–5.7 Ma, sea-level rise, a period including isotopic stage TG15 (Shackleton et al., 1995; Vidal et al., 2002) and corresponding to the Upper Evaporites of Sicily (at the top of which are located the Lago Mare and the Arenazzolo facies);
- 5.7–5.33 Ma, tectonic isolation of the Mediterranean realm, fast desiccation of the Mediterranean Sea, deposition of evaporites in the desiccated abyssal plains, cutting of subaerial canyons;
- 5.33 Ma, instantaneous flooding of the Mediterranean Basin by Atlantic waters (Blanc, 2002).

The question of a climatic cause (increasing dryness) for the desiccation of the Mediterranean Sea, even if not always clearly expressed, is more or less implied for scenarios favouring a deep-water model for basin evaporite deposition (Busson, 1979, 1990; Krijgsman et al., 1999b). Suc and Bessais (1990), Bertini (1994a,b) and Bertini et al. (1998), using pollen analyses, have suggested discarding increasing dryness as an explanation for the salinity crisis. Another climatic change (increasing precipitation) has been considered to explain Lago Mare facies in the Eastern Mediterranean (Orszag-Sperber et al., 2000; Rouchy et al., 2001).

For more than 20 years we have pursued high-quality pollen research on the Messinian deposits around the Mediterranean realm, and results have emerged that contrast with previous and current studies (Trevisan, 1967; Benda, 1971; Bertolani Marchetti and Cita, 1975; Heimann et al., 1975; Traverse, 1978; Bertolani Marchetti, 1984; Ioakim and Solounias, 1985; Mariotti Lippi, 1989; Ediger et al., 1996; Ioakim et al., 1997; etc.). Differences lie in the reliability of botanical pollen identification, in quantity of pollen counted and in density of samples.

The aim of our study is to address some crucial questions concerning the Messinian salinity crisis and the prevailing climate: 1) did climate play a role in triggering the desiccation of the Mediterranean Sea? 2) did climate change in the Mediterranean region during

the salinity crisis and, if so, was it related to the desiccation of the Mediterranean? To help answer these questions, (1) we present a synthesis of Messinian to Early Zanclean pollen records in the Mediterranean realm, and (2) we provide the reconstructed climate of the western Mediterranean area before, during, and after the Messinian salinity crisis, using pollen data from several selected localities in the western Mediterranean region.

2. Pollen data and vegetation reconstruction

Twenty Messinian to Zanclean pollen sequences, all based on high-quality pollen analyses (following the criteria established above), are now available for the peri-Mediterranean region (Fig. 2). Bou Regreg (Atlantic seaboard of Morocco) excepted, none of these sequences covers the entire period 6.7–5.2 Ma (Fig. 3). They provide a reliable but discontinuous record of vegetation variability in time and space. The period of evaporite deposition within deep parts of the desiccated basin (5.7–5.33 Ma) is poorly documented in the Mediterranean region: only the Maccarone section and, in part, the Torre Sterpi section, in the Adriatic Sea–Po Valley area, belong to this interval (Fig. 3). Within this perched basin, sedimentation was continuous because of a positive water balance (Clauzon et al., 1997, 2005) (Fig. 1). The evaporitic phase on the Mediterranean margins is better documented, especially in the Po Valley and in Sicily (Fig. 3). Several pollen diagrams have been generated from offshore boreholes (Andalucia G1, Habibas 1, Tarragona E2, Naf 1) that have been drilled in relatively shallow waters (less than 300 m). For each of these pollen records, the earliest Pliocene is well identified using planktonic foraminifers (*Sphaeroidinellopsis* acme-zone, followed by first appearance of *Globorotalia margaritae*). A gap probably separates the earliest Zanclean sediments from the underlying Messinian ones, corresponding to erosion of the margin during evaporite deposition in deep parts of the desiccated basin. Nevertheless, this gap might be longer than expressed on Fig. 3 owing to possible erosion of the uppermost Messinian deposits before desiccation of the basin.

Deep Sea Drilling Project (DSDP) Site 380A in the Black Sea (Popescu, this volume) has been included in this study as it enlarges our considered area and may help to understand evolution of the Mediterranean climate within a more global framework. Its inclusion is also very useful for validating results based on climate and vegetation modelling (Fluteau et al., 2003; François et al., 2006-this volume). The Black Sea is considered

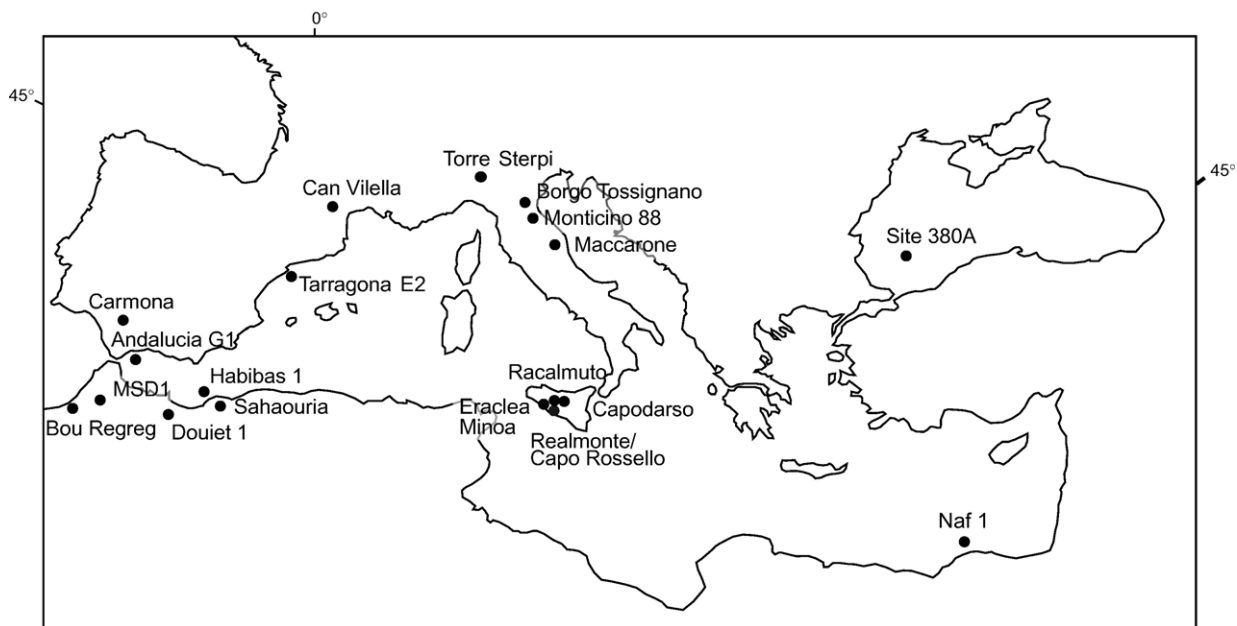


Fig. 2. Location map of the pollen localities considered in this paper.

also to have been involved with the Messinian salinity crisis (Hsü and Giovanoli, 1979), based on erosion observed along seismic lines (Letouzey et al., 1978) and on the presence of a coarse breccia (including blocks of a stromatolitic dolomite) at the same level at DSDP Site 380A (Ross et al., 1978). This borehole was drilled in 2107 m water depth, indicating that it represents abyssal plain upon which the deep desiccated basin evaporites were deposited. This evaporitic phase has probably produced a shorter break in the pollen record (corresponding to the breccia) than on the shelf because it corresponds to an area of sedimentation rather than erosion (Fig. 3). For the same reasons, we have used a section located in southern Spain (at Carmona), on the Atlantic seaboard for comparative purposes and to assess the influence of the Atlantic Ocean on southern Spain's environments and climate before the salinity crisis (Fig. 3).

Some additional information on areas containing our climatically quantified sites is given below before we describe their pollen contents, but more details may be obtained from the literature as most of data have been published.

2.1. Atlantic realm at southern Mediterranean latitude

Two pollen records document this area: Carmona in the Guadalquivir Basin (southern Spain) and Bou Regreg (Salé section, northwestern Morocco) (Fig. 2).

Pollen diagrams from Carmona come from two sections. The lower section is located immediately southward of the city along the road to El Arahal. It belongs to the Andalusian Clays underlying the famous «Calizza Tosca» calcarenite (Perconig, 1974). *G. margaritae* occurs continuously and the deposits are normally magnetised, allowing assignment to Chron C3An.1n (F.J. Sierro and W. Krijgsman, personal communications). This section predates the Messinian salinity crisis (Sierro et al., 1996) (Fig. 3). The upper section has been cored within the Green Clays overlying the «Calizza Tosca» calcarenite; it is reversely magnetised (W. Krijgsman, personal communication) and belongs to Chron C3r but more precise assignment is not possible. This section can therefore be considered as floating between the late Messinian and earliest Pliocene, but its shallow-water status (perhaps in relation with the «Calizza Tosca» regressive conditions) suggests association with the global sea-level fall at 5.9–5.85 Ma (isotopic stages TG22 and TG20) (Fig. 3). Pollen flora of the two sections (analyses by J.-P. Suc, N. Feddi and J. Ferrier, unpublished) is dominated by herbs (alternating Poaceae and Asteraceae mainly) including rare subdesertic elements such as *Lygeum* and *Neurada*. *Pinus* is abundant and shows several fluctuations. Tree frequencies are low and are mostly constituted by deciduous *Quercus*.

The Bou Regreg pollen diagram comes from exposed and cored sections at the Salé Briqueterie (close to

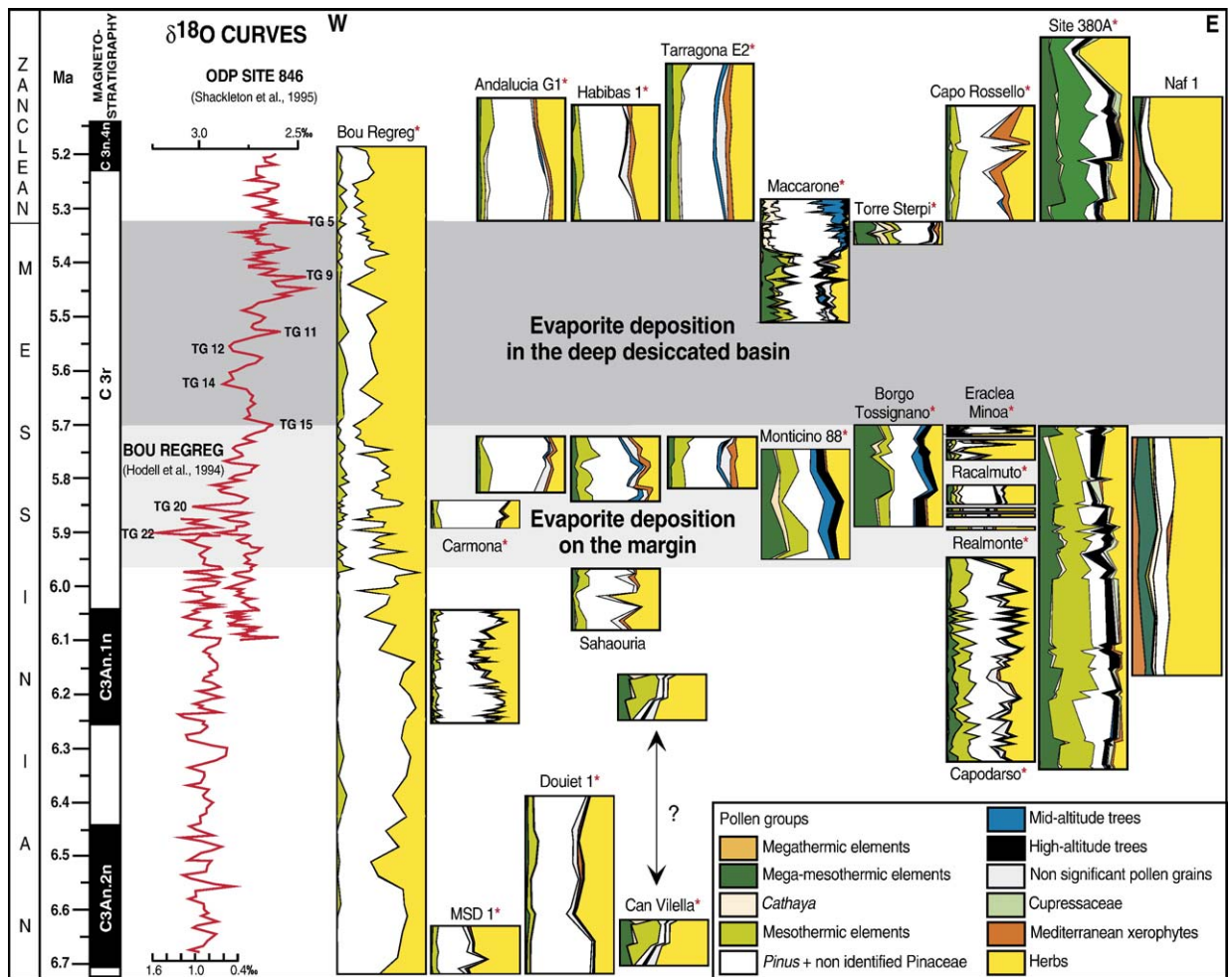


Fig. 3. Synthetic pollen diagrams analyzed in the Mediterranean region between ca. 6.7 and ca. 5.0 Ma according to their chronological location with respect to interrelated $\delta^{18}\text{O}$ curves (Hodell et al., 1994; Shackleton et al., 1995) within the frame of the scenario of the salinity crisis of Clauzon et al. (1996). The two light grey and dark grey strips respectively highlight the two successive evaporitic phases evidenced by Clauzon et al. (1996). Pollen flora on which climate has been quantified is indicated by a red star. Taxa have been grouped according to their ecological significance as follows: 1. megathermic (= tropical) elements (*Avicennia*, *Amanoa*, *Alchornea*, *Fothergilla*, *Exbucklandia*, *Euphorbiaceae*, *Sapindaceae*, *Loranthaceae*, *Areaceae*, *Acanthaceae*, *Canthium* type, *Passifloraceae*, etc.); 2. mega-mesothermic (= subtropical) elements (*Taxodiaceae*, *Engelhardia*, *Platycarya*, *Myrica*, *Sapotaceae*, *Microtropis fallax*, *Symplocos*, *Rhoiptelea*, *Distylium* cf. *sinensis*, *Embolanthera*, *Hamamelis*, *Cyrtillaceae*–*Clethraceae*, *Araliaceae*, *Nyssa*, *Liriodendron*, etc.); 3. *Cathaya*, an altitudinal conifer living today in southern China; 4. mesothermic (= warm-temperate) elements (deciduous *Quercus*, *Carya*, *Pterocarya*, *Carpinus*, *Juglans*, *Celtis*, *Zelkova*, *Ulmus*, *Tilia*, *Acer*, *Parrotia* cf. *persica*, *Liquidambar*, *Alnus*, *Salix*, *Populus*, *Fraxinus*, *Buxus sempervirens* type, *Betula*, *Fagus*, *Ostrya*, *Parthenocissus* cf. *henryana*, *Hedera*, *Lonicera*, *Elaeagnus*, *Ilex*, *Tilia*, etc.); 5. *Pinus* and poorly preserved *Pinaceae* pollen grains; 6. mid-altitude trees (*Tsuga*, *Cedrus*); 7. high-altitude trees (*Abies*, *Picea*); 8. non-significant pollen grains (undetermined ones, poorly preserved pollen grains, some cosmopolitan or widely distributed elements such as *Rosaceae* and *Ranunculaceae*); 9. *Cupressaceae*; 10. Mediterranean xerophytes (*Quercus ilex* type, *Carpinus* cf. *orientalis*, *Olea*, *Phillyrea*, *Pistacia*, *Ziziphus*, *Cistus*, etc.); 11. herbs (*Poaceae*, *Erodium*, *Geranium*, *Convolvulus*, *Asteraceae* *Asteroidae*, *Asteraceae* *Cichorioideae*, *Lamiaceae*, *Plantago*, *Euphorbia*, *Brassicaceae*, *Apiaceae*, *Knautia*, *Helianthemum*, *Rumex*, *Polygonum*, *Asphodelus*, *Campanulaceae*, *Ericaceae*, *Amaranthaceae*–*Chenopodiaceae*, *Caryophyllaceae*, *Plumbaginaceae*, *Cyperaceae*, *Potamogeton*, *Sparganium*, *Typha*, *Nymphaeaceae*, etc.) including some subdesertic elements (*Lygeum*, *Neurada*, *Nitraria*, *Calligonum*) and steppe elements (*Artemisia*, *Ephedra*). (For interpretation of the references to colour in this figure legend, the reader is referred to the web version of this article.)

Rabat) (Warny, 1999). It benefits from a very detailed time control including biostratigraphy, magnetostratigraphy, stable isotope stratigraphy and astrochronological tuning (Hodell et al., 1994, 2001; Warny and

Wrenn, 2002). It covers the uppermost Tortonian, the entire Messinian and reaches the earliest Pliocene (Fig. 3). This section is particularly poor in pollen grains and does not show great taxonomic diversity. *Pinus* is

abundant at the base but strongly decreases from the mid-section up to the top. Pollen analysis evidences an open environment dominated by herbs, especially subdesertic herbs. Arboreal taxa are less well represented than in the other North African sites.

2.2. Alboran Sea area and Rifian Corridor

Five sections document the vegetation in the Rifian Corridor and Alboran Sea regions: MSD1 and Douiet 1 boreholes respectively on the west and east sides of the Rifian Corridor, Andalucia G1 and Habibas 1 boreholes respectively on the north and south shorelines of the Alboran Sea; and Sahaouria in the Chelif Basin (Algeria) (Fig. 2).

The chronostratigraphic position of these sections is well known (Fig. 3). According to planktonic foraminifers (Barhoun, 2000), the MSD1 and Douiet 1 sections refer to the early Messinian, i.e. long before the salinity crisis. Borehole Andalucia G1, where planktonic foraminifers have been studied (Elf-Aquitaine, unpublished data), covers the early Messinian before the desiccation phase and part of the Pliocene, until around 2.4 Ma. Planktonic foraminifers from borehole Habibas 1 have been studied by J. Cravatte (personal communication): the section covers the pre-evaporitic Messinian and the early Pliocene up to around 3.2 Ma. The Sahaouria section is well dated by planktonic foraminifers and immediately predates the Chelif Basin marginal evaporites (Rouchy, 1981).

The pollen content of these sections has been studied as follows: MSD1 and Douiet 1 (Bachiri Taoufiq, 2000), Andalucia G1 (Bessais, unpublished; only Pliocene pollen data have been published: Suc et al., 1995b), Habibas 1 (Suc, 1989), Sahaouria (Chikhi, 1992). Climatic quantification has already been undertaken on the Pliocene parts of the Andalucia G1 and Habibas 1 pollen records (Fauquette et al., 1999).

All these sections show, whatever their age before or after the Messinian salinity crisis, open environments (Fig. 3), rich in herbs, mainly Asteraceae, Poaceae, *Nitraria*, *Neurada* and *Calligonum*, indicating very dry and warm conditions, as these taxa are found today in North Africa under hyper-arid conditions (Saharan elements, with *Neurada* and *Calligonum* indicating dunes). Within the Poaceae, *Lygeum* is also present. This taxon, characteristic of south-Mediterranean steppes, is found today in southern Spain, southern Italy, Sicily, Crete and in North Africa but not in the Sahara (Fauquette et al., 1998a,b). Mediterranean xerophytes are present. Arboreal taxa are frequent, dominated by deciduous *Quercus*, Taxodiaceae, *Myrica*, *Alnus*, indi-

cating the existence of more humid places in the hinterland or moister conditions at higher altitudes. *Pinus* continues to show important percentages.

At MSD 1, Douiet 1, and Sahaouria, megathermic elements (*Canthium* type, Sapotaceae, *Alchornea*, etc.) are regularly represented. More particularly, *Avicennia*, the only mangrove element able to grow out of the tropical zone, has been found within the Messinian sediments of MSD 1, Douiet 1, Habibas 1 and Sahaouria. However, it has never been recorded in northern Africa within the earliest Pliocene sediments (Habibas 1: Suc, 1989; Nador 1: N. Feddi, personal communication).

2.3. Cerdanya

The section of Can Vilella is situated in Cerdanya and comprises lacustrine to palustrine sediments. Paleomagnetism indicates that the section straddles the passage from a reverse event to a normal one (Agusti et al., this volume). The mammal fauna allows us to place the section either at the base of Chron C3An.2n or C3An.1n, i.e. a long time before the salinity crisis (Agusti and Roca, 1987; Agusti et al., 2006-this volume) (Fig. 3).

The pollen flora has been studied by Perez Villa (Agusti et al., 2006-this volume). It reveals a riparian forest environment (Taxodiaceae, *Alnus*, *Myrica*, Cyrtolaceae–Clethraceae, *Engelhardia*, *Cephalanthus*, *Pterocarya*, *Populus*, *Nyssa*, *Salix*, etc.) with many associated herbs (Cyperaceae, Poaceae, *Typha*, etc.) (Fig. 3). *Pinus* has a very low frequency.

2.4. Southern Catalonia

According to planktonic foraminifers, borehole Tarragona E2 covers the late Messinian, just before the desiccation phase of the deep basin, and also most of the Pliocene, up to around 2.4 Ma (Bessais and Cravatte, 1988) (Fig. 3).

Pollen data from borehole Tarragona E2 have been published in Bessais and Cravatte (1988). Climatic quantification has already been undertaken on the Pliocene part of this section (Fauquette et al., 1999).

The pollen flora of the locality (Fig. 3) is characterised by the predominance of herbs (mainly Asteraceae and Poaceae, *Lygeum*, *Nitraria* and *Calligonum*), indicating dry to very dry environments. Mediterranean xerophytes are very frequent, making pollen assemblages very close to the modern thermomediterranean association (Bessais and Cravatte, 1988). The presence of pollen grains of arboreal taxa (mainly deciduous *Quercus*, Taxodiaceae, *Alnus*, *Carya*) indicates

more humid places in the hinterland and along the rivers. *Pinus* is moderately abundant. As for Andalusia G1, pollen data do not show any distinct variation in the vegetation between the Messinian and Pliocene parts of the section.

2.5. The Adriatic Sea–Po Valley area

The Borgo Tossignano and Monticino 88 (also named Cava Li Monti) sections have been sampled in the Vena del Gesso Basin, in eastern Italy (Fig. 2), and correspond to the Gessoso-Solfifera Formation (Vai and Ricci Lucchi, 1977). The age of the sections is well constrained by paleomagnetic and cyclostratigraphic studies (Krijgsman et al., 1999a) (Fig. 3). The pollen data have been established by Bertini (1992, 1994a,b) and illustrate the vegetation during the evaporitic phase. Because of the barren nature of the gypsum beds, only the euxinic shales of the Gessoso-Solfifera Formation were analysed.

The Maccarone section is located southward, in the Marchean outer basin of east-central Italy (Fig. 2). Messinian clays and marls [lower post-evaporitic sequence «p-ev1» of Roveri et al. (2001), also named «di tetto» Formation], which are interbedded at the top of the formation with evaporitic limestones [upper post-evaporitic sequence «p-ev2» of Roveri et al. (2001), also named Colombacci Formation which includes the Lago Mare facies], are overlain by the Argille Azzurre Formation. A volcanic ash layer in the lower part of the section has provided two $^{40}\text{Ar}/^{39}\text{Ar}$ plateau ages of 5.51 and 5.44 ± 0.04 Ma (Odin et al., 1997), a similar age being obtained by H. Maluski (personal communication). Based on this absolute age and biostratigraphy (Carloni et al., 1974), and to its continuously reversed paleomagnetic signal (G. Napoleone, personal communication), the Maccarone section covers the time interval from the end of the Messinian (from ~ 5.6 Ma) to the Early Pliocene. The palynology of the Maccarone section has been published by Bertini (1994a,b, 2002).

The Torre Sterpi section is located in the Po Valley, near Tortone and corresponds to the Lago Mare Formation (Corselli and Grecchi, 1984). The Adriatic–Po region is considered to have evolved as a perched basin in the latest Messinian, i.e. independently from the Central Mediterranean Basin (Corselli and Grecchi, 1984; Clauzon et al., 1997) (Fig. 1). The pollen data have been established by Suc (unpublished) and recently completed by Sachse (2001).

The pollen flora is very diverse (Fig. 3). Tropical elements (i.e. the megathermic elements) living under warm and moist or dry conditions are present in low

quantities in the lower part of Maccarone section (Bertini, 1994a,b), especially those (*Agave*, *Cordyline*, *Nolina*, *Bombax*, *Canthium* type, etc.) that disappeared from the northwestern Mediterranean region in the earliest Serravallian (Bessedik et al., 1984), and from the southwestern Mediterranean region in the latest Messinian [Sicily: Suc and Bessais (1990); North Africa: Chikhi (1992), Bachiri Taoufiq (unpublished)]. Subtropical elements (i.e. the mega-mesothermic elements) and warm-temperate elements (i.e. the mesothermic elements) living under a year-long humid and warm climate (*Engelhardia*, *Taxodium*, *Myrica*, *Nyssa*, etc.) are common and uniformly represented at Borgo Tossignano, Monticino 88, Maccarone and at Torre Sterpi. Deciduous forest elements indicative of warm-temperate and temperate climates (*Quercus*, *Carya*, *Ulmus–Zelkova*, etc.) record a gradual decrease from the Messinian to the Zanclean. The Mediterranean evergreen elements (*Quercus ilex* type, *Olea*, *Phillyrea*, etc.) are sporadic. In the upper part of the Maccarone pollen diagram, *Cathaya*, *Cedrus* and *Tsuga* (the mid-altitude trees), are overall fairly abundant. Mountain elements such as *Picea* and *Abies* are always present but in low quantities. Herbaceous pollen grains (Asteraceae, Poaceae including *Lygeum*, Amaranthaceae–Chenopodiaceae etc.) are numerous in the basal part of the Maccarone succession. *Pinus* is not very abundant, except in the upper part of the Maccarone pollen diagram.

The coastal vegetation was characterised by widespread lagoonal zones, where *Taxodium* thrived alongside *Myrica*, *Nyssa* and others. The size of the basin probably reduced somewhat during the two steps of the salinity crisis, providing a continuous and important record of coastal environments in the distal pollen localities. A break occurred at about 5.4 Ma in the Maccarone section which probably became more distant from the shoreline as it corresponds to an increasing frequency of disaccate pollen grains (*Pinus* and the high altitude elements *Tsuga*, *Cedrus*, *Abies* and *Picea*) which are favoured by transport, compared to non-disaccate pollen grains, and consequently are relatively more abundant offshore (Bertini, 1994a). This pollen flora characterise marine sediments of the early Zanclean high-sea level (Bertini, 1994a).

The pollen flora of the lower half of the Maccarone section shows similarities with the Sicilian herbaceous vegetation (about 5° farther south in latitude), with abundant Poaceae including *Lygeum* and the presence of some megathermic elements (although less important than in Sicily). But abundance of Taxodiaceae and of mid- to high-altitude elements, and scarcity of herbaceous

plants at Torre Sterpi and in the second half of the Maccarone section, make the pollen flora very close to those of Zanclean sections from Liguria and French Southern Alps (Zheng and Cravatte, 1986) but strikingly different from those found for the same time interval at Capo Rossello in Sicily (Suc and Bessais, 1990), as detailed immediately below. This northward migration of thermophilous taxa (some of them being adapted to dryness) will be discussed later.

2.6. The Central Mediterranean margins: example of Sicily

The Capodarso section, situated in the Caltanissetta basin, consists of 170 m of claystones overlain by the Tripoli Formation and the Calcare di Base. This section is overlain by the Lower Sicilian Evaporites. Many samples from the Tripoli Formation were analysed for foraminifers, dinocysts, palynofacies, CaCO₃, pollen grains and clay minerals (Suc et al., 1995c). These data together showed that the general evolution of the basin was from normal marine conditions to confinement and that the sedimentation of the Caltanissetta basin up to the beginning of the Messinian salinity crisis was controlled by global sea level.

The micropaleontology of clayey layers within halite and kainite bodies in the Salt Member of the Lower Evaporitic Complex in the Messinian Gessoso-Solfifera Formation, has been studied in samples taken from the Racalmuto and Realmonte salt mines, also located in the Caltanissetta basin (Bertini et al., 1998). The Upper Evaporites, represented in the reference-section of Eraclea Minoa in the Caltanissetta basin, are composed of six major gypsum–clay alternations (Decima and Wezel, 1973; Mascle and Heimann, 1976), the last one corresponding to clays of the Lago Mare facies and silts of the Arenazzolo Formation. Following the scenario of Clauzon and Suc for the Messinian salinity crisis (see above), a hiatus 370 kyr long exists between the Arenazzolo Formation and the lowermost Zanclean Trubi Formation (Clauzon et al., 1996). A palynological study has been undertaken on 32 samples from clays interbedded with the gypsum, in the clays of the Lago Mare facies, and in the silts of the Arenazzolo Formation.

The early Zanclean in the Caltanissetta basin is represented by the Capo Rossello section, corresponding to the Trubi formation. The pollen data have been collected by Suc and Bessais (Suc and Bessais, 1990; Suc et al., 1995a), and the corresponding climatic reconstruction has already been published (Fauquette et al., 1999).

Hence, so far as the five sections of the Caltanissetta basin are representative of the Messinian succession and the Early Pliocene, with the pre-evaporitic Messinian clays and diatomites (the Tripoli Formation) at Capodarso, the Lower Evaporites at Racalmuto and Realmonte mines, the Upper Evaporites at Eraclea Minoa and finally the Lower Pliocene at Capo Rossello, it is possible to describe the vegetation evolution from the Lower Messinian to the Early Pliocene, keeping in mind that some deficiencies in the pollen record exist (lack of pollen grains within evaporites, hiatus in sedimentation at the top of the Arenazzolo Formation).

The more important variations observed in the pollen diagrams (Fig. 3) are due to relevant variations in *Pinus* pollen percentages. *Pinus* excepted, the pollen spectra are dominated by herbs showing an open and xeric environment, at least on the littoral: arboreal taxa were certainly growing in the hinterland. Megathermic elements are regularly recorded, especially at Capodarso, but they progressively decrease from the Lower Messinian to the Zanclean (Suc and Bessais, 1990). Within these tropical elements is the mangrove taxon *Avicennia*. The last appearance of *Avicennia* is found at Eraclea Minoa, at 3.48 m. No pollen grains of this taxon have been found at Capo Rossello during the Early Pliocene.

2.7. The Eastern Paratethys region

A palynological study has been performed on Upper Miocene to Lower Pliocene sediments cored at DSDP Site 380A, in the southwestern Black Sea (Fig. 2) (Popescu, 2001, 2006-this volume). The borehole at site 380A penetrates a 19 m thick «Pebbly Breccia» including blocks of stromatolitic dolomite (Ross et al., 1978) which is considered to have formed in an intertidal to supratidal environment (Stoffers and Müller, 1978). This suggests, together with diatom data, that the Black Sea was very shallow at that time (Schrader, 1978). This sea-level drop of the Black Sea has been interpreted by Hsü and Giovanoli (1979) as the consequence in the Black Sea of the Messinian salinity crisis.

Pollen data show, through the whole section, a forested environment, dominated by subtropical taxa such as *Engelhardia*, *Myrica*, *Distylium* cf. *sinensis*, Taxodiaceae, Sapotaceae, etc. Mesothermic elements are also abundant. However, the herbaceous elements, and in particular steppe elements (mainly *Artemisia*), are better represented during the Pliocene than during the Late Miocene. Anyway, in this area, steppe elements begin to develop just before the hiatus («Pebbly

breccia») that putatively corresponds to the Messinian salinity crisis. Consequently conditions seem to become drier from the end of the Messinian and during the Pliocene, even if it was initiated before the crisis.

3. Climate quantification

In the present study, climatic reconstructions have been made on the pollen data using the «Climatic Amplitude Method». This method was developed by Fauquette et al. (1998a,b) specifically to quantify the climate of periods for which there are, currently, no modern analogue of the pollen spectra. The basis of this method consists of transposing the climatic requirements of the maximum number of modern taxa to the fossil data.

This method relies on the relationship between the relative pollen abundance of each individual taxon and the climate. The most probable climate for a set of taxa corresponds to the climatic interval suitable for the maximum number of taxa. The climatic estimate is obtained as a climatic interval and a «most likely value», which corresponds to a weighted mean.

Five climatic parameters have been estimated in this study from the pollen data: the mean annual temperature (T_A), the mean annual precipitation (P_A),

the temperature of the coldest and warmest months (T_C and T_W) and the available moisture (i.e. the ratio actual evapotranspiration on potential evapotranspiration, E/PE).

Plants were separated into three groups, looking at their modern distributions, as described in Fauquette et al. (1998a): ubiquitous plants, plants growing under warm conditions (low latitude/altitude taxa) and plants growing under cold conditions (high latitude/altitude taxa). As we want to estimate the climatic parameters for lower altitudes, the two first groups of plants only are used in the reconstruction process.

As in Fauquette et al. (1998a, 1999), the pollen of *Pinus* and non-identified Pinaceae (due to poor preservation) have been excluded from the pollen sum of the fossil spectra because they are over-represented in the marine, and even coastal, deposits due to their prolific production and overabundance from air and water transport (Heusser, 1988; Suc and Drivaliari, 1991; Cambon et al., 1997).

For most of the pollen sequences, climatic estimates have been calculated on the sum of the spectra and are reported on maps (Figs. 4, 7 and 9). For three of the sequences, long «key-sections» (i.e. Maccarone, Bou Regreg and Site 380A in the Black Sea), climatic estimates have been calculated for each pollen spectrum (or for the sum of 3–4 levels at the bottom of Bou

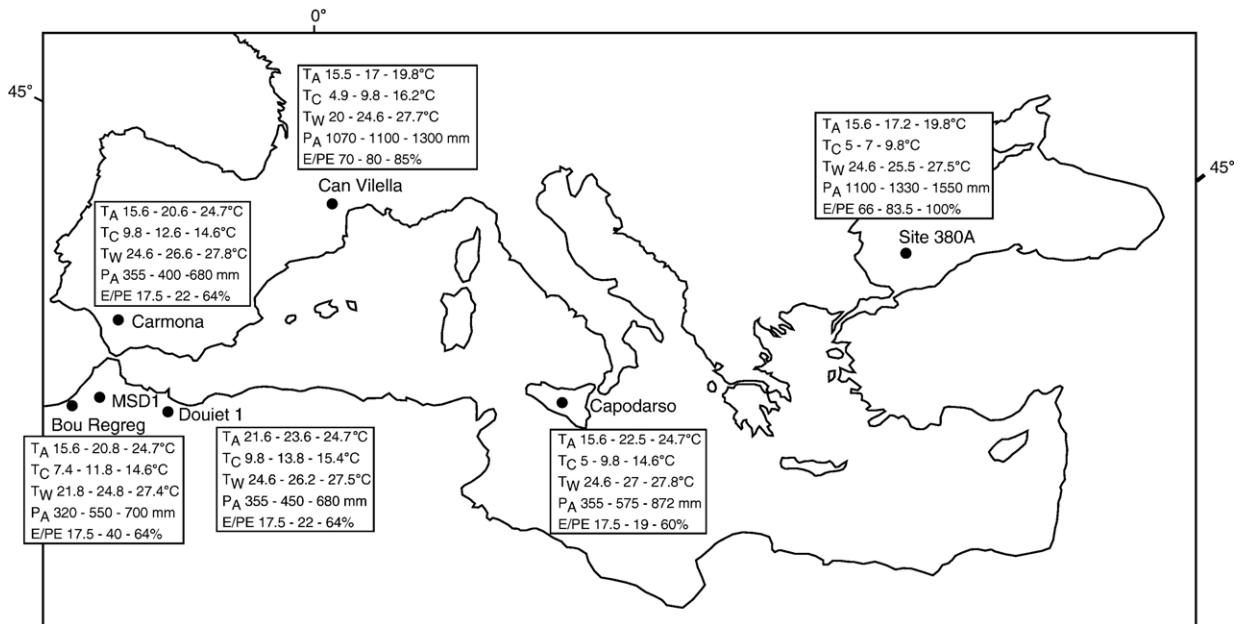


Fig. 4. Climatic quantification results based on pollen data from the period preceding the Messinian salinity crisis (early Messinian). T_A : mean annual temperature, T_C : mean temperature of the coldest month, T_W : mean temperature of the warmest month, P_A : mean annual precipitation, E/PE : ratio

Regreg sequence where pollen spectra are particularly poor) and are given on graphs (Figs. 5, 6 and 8).

3.1. The climate before the Messinian salinity crisis (Figs. 4–6)

In the western Mediterranean region, the climate before the crisis is documented in North Africa (at Douiet 1, MSD 1 sites), Sicily (at Capodarso), Spain (at Can Vilella), along the Atlantic coast (at Carmona and Bou Regreg) and in the Black Sea area.

The climatic reconstruction for this period shows a warm and dry climate in southwestern Spain, North Africa and Sicily. Mean annual temperatures (T_A) were between 15.0–15.5 and 24.7 °C with a most likely value (MLV) ranging between 20.5 and 22.5 °C. Only the Douiet 1 and MSD 1 sites show higher values (21.6 to 24.7 °C with a MLV around 23.7 °C). Temperatures of the coldest (T_C) and warmest (T_W) months are similar

for all the sites (T_C between ~8 and 14.6–15.4 °C with most likely values around 11–14 °C, and T_W between 22 and 27.8 °C with most likely values around 25–26.5 °C). Mean annual precipitation is very low everywhere, even at Carmona along the Atlantic coast (between ~350 and 700 mm with most likely values around 400–500 mm). The lower part of Bou Regreg sequence displays important variations in the most likely value (Fig. 5) due to the presence or absence of such taxa as *Quercus* deciduous type, and *Carya*. However, estimated intervals do not show variations. The ratio E/PE (corresponding to the available moisture) shows low values, comprising between 17.5% and 60–64%, with a MLV around 20%.

At Can Vilella, in Cerdanya, the climate was warm and humid. T_A was around 15 to 19.8 °C with a MLV of 17 °C, T_C between 5 and 12.5 °C with MLV of 9 °C, and T_W between 23.5 and 27.7 °C with a MLV of 25.5 °C. Mean annual precipitation was high, ranging between

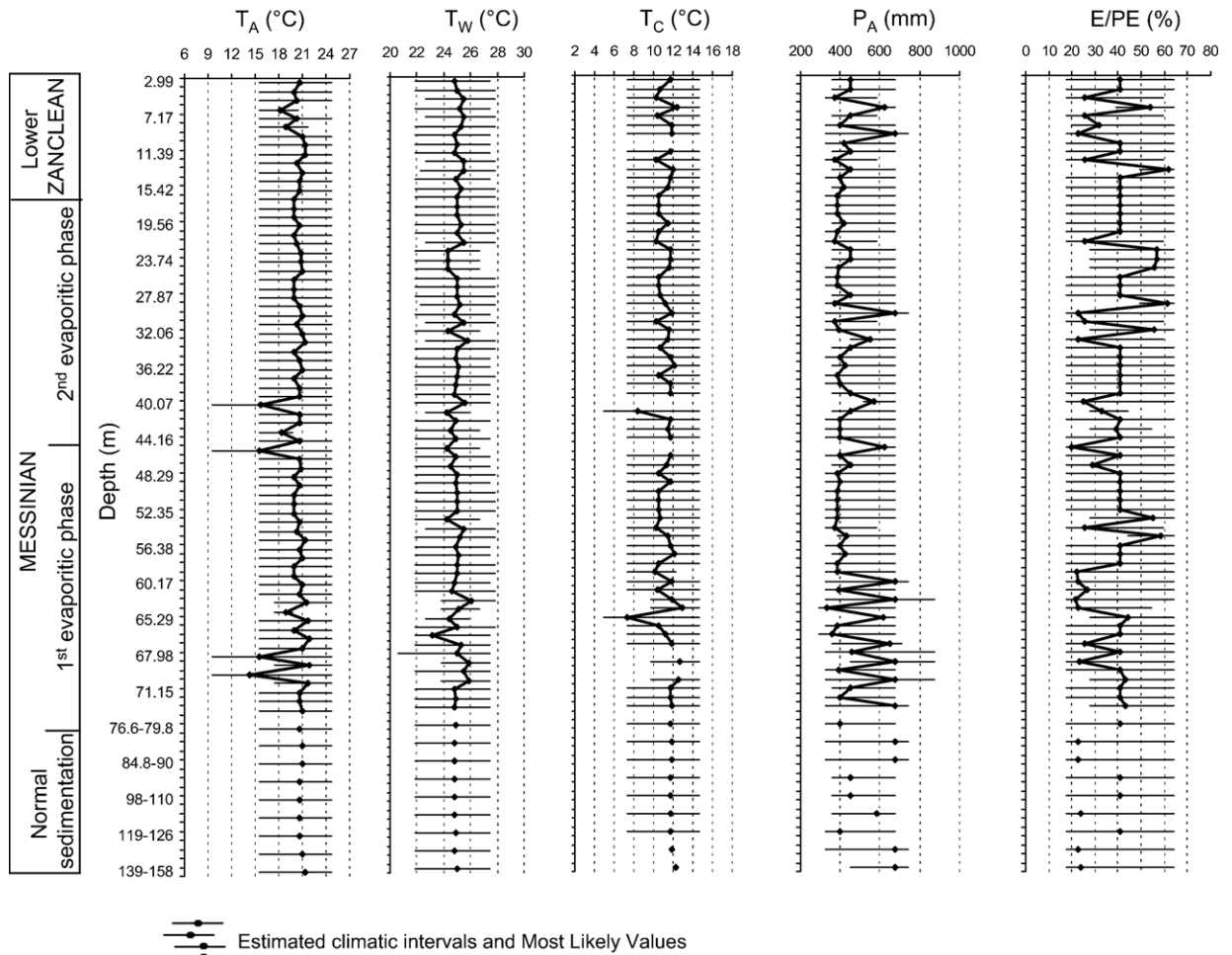


Fig. 5. Climatic quantification results based on pollen data from Bou Regreg for the entire Messinian.

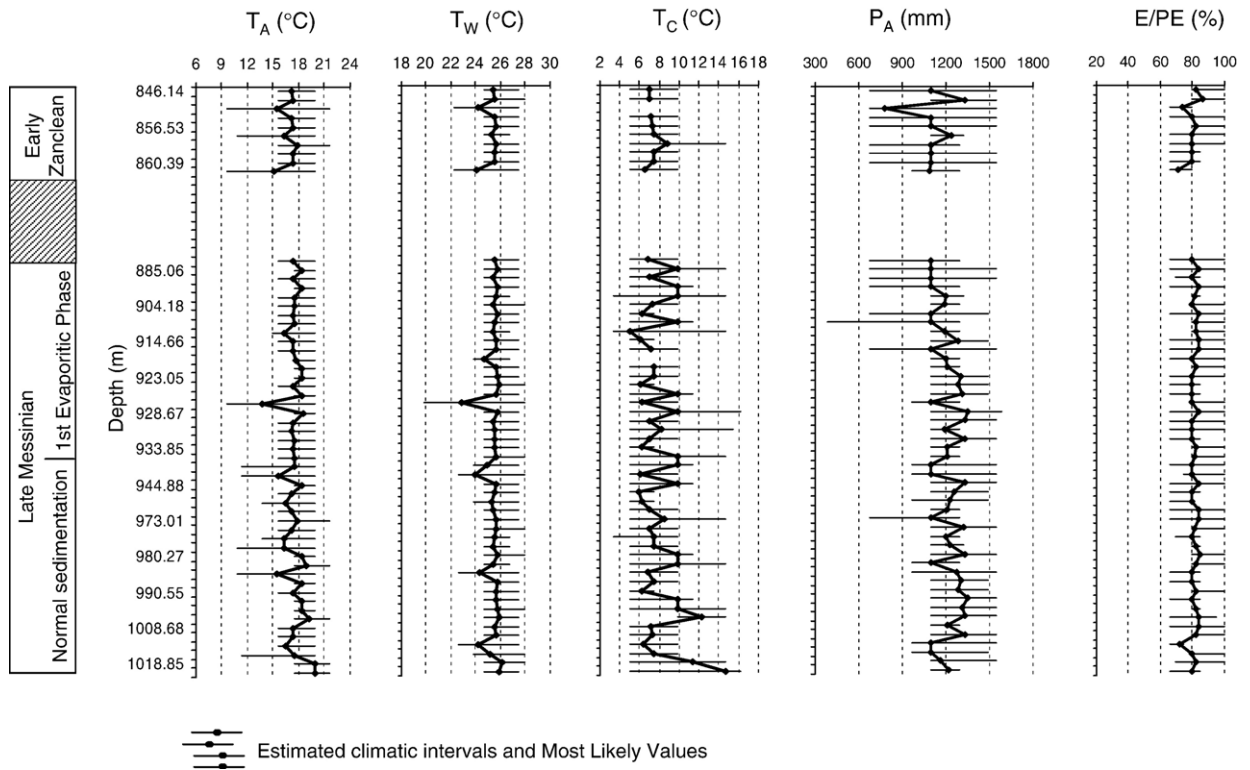


Fig. 6. Climatic quantification results based on pollen data from Site 380A covering the periods just before the Messinian salinity crisis, during the first evaporitic phase and the early Pliocene.

1000 and 1350 mm with a most likely value of 1150 mm. The ratio E/PE was between 66% and 84% with a MLV of 72.5%.

The climate before the Messinian salinity crisis is also documented in the Black Sea area (DSDP Site 380A) (Figs. 4 and 6). There the climate was warm and humid at the beginning of the Messinian. On Fig. 4 are reported values corresponding to a mean climate for this period. Mean annual temperatures were between 15.6 and 19.8 °C with MLV around 17.3 °C (sometimes higher at the beginning of the sequence), temperatures of the coldest month ranged between 5 and 9.8 °C, with a most likely value around 7 °C, temperatures of the warmest month ranged between 24.6 and 27.5 °C with a MLV around 25.5 °C. Mean annual precipitation was between ~1100 and 1550 mm with a MLV around 1200–1300 mm. The available moisture was important, between 66% and 100% with a most likely value of 83.5%. Looking in more detail at Fig. 6, annual precipitation, mean annual temperatures and temperatures of the coldest month show oscillations around the mean values, depending on the presence or absence of megathermic elements in the spectra.

3.2. The climate during the Messinian salinity crisis (Figs. 7 and 8)

The climate during the first desiccation phase of the Messinian salinity crisis in the Mediterranean region is documented for Sicily (Racalmuto and Realmonte mines, Eraclea Minoa), at Carmona, Tarragona, Andalusia, Habibas, Bou Regreg, in the Po Valley, at Borgo Tossignano, Monticino 88 and in the Black Sea area. The end of the Messinian salinity crisis is documented at Torre Sterpi, in the Po Valley and Maccarone, and along the Adriatic coast (Figs. 3 and 7).

At Racalmuto, Realmonte, Eraclea Minoa, Carmona, Andalusia, Tarragona, Habibas and Bou Regreg, the climate during the first desiccation phase was warm and dry, with the same climatic amplitudes as before the crisis. The site of Tarragona, located more to the north, shows slightly higher values of mean annual precipitation (between ~700 and 900 mm with a MLV around 800 mm) and of E/PE with values between 17.5% and 99% (most likely values of 58%).

In the Po Valley, the climate during both first and second evaporitic phases was warm and humid with mean annual temperatures between 15.5 and 19.8 °C

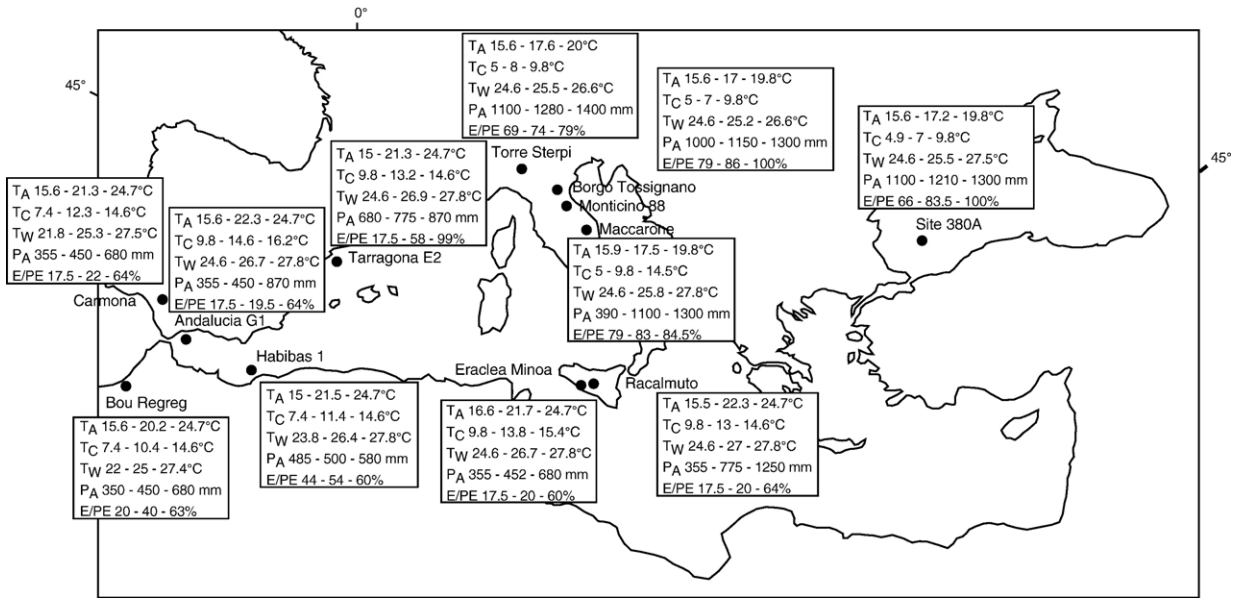


Fig. 7. Climatic quantification results based on pollen data corresponding to the Messinian salinity crisis (1st evaporitic phase: Andaluca, Habibas 1, Tarragona E2, Carmona, Monticino 88, Borgo Tossignano, Eraclea Minoa, Racalmuto, Realmonte mines, Site 380A; 2nd evaporitic phase: Maccarone, Torre Sterpi).

(MLV around 17 °C), mean temperatures of the coldest month between 5.0 and 9.8 °C (MLV around 6.5–7.5 °C), and mean temperatures of the warmest month between 24.6 and 27–28 °C (MLV around 25 °C). Mean annual precipitation was around 1000 and 1300 mm (MLV around 1100–1200 mm), and the available moisture was between 80% and 100% (MLV around 86%).

At Maccarone, one of the «key-site», we present the climatic evolution along the sequence which covers the period from around 5.5 to the Early Pliocene (Fig. 8). Mean annual temperatures were between about 16 and 20 °C for most spectra but up to 23–24.5 °C for some, with most likely values oscillating between 17 and 20 °C (only 1 spectrum shows a lower MLV around 15 °C). Estimated temperatures of the coldest month show significant changes during the first part of the sequence. These temperatures are between 5 and 15 °C or 5 and 10 °C or also 10 and 15 °C. Most likely values are mostly between 7 and 12 °C but up to 15 °C for two samples. On the other hand, during the second part of the sequence, temperatures of the coldest month are more stable, between 5 and 10 °C for most of the spectra, with a MLV of around 7 to 10 °C. Temperatures of the warmest month are relatively stable along the first part of the sequence, between 24.5 and 28 °C with a most likely value oscillating between 25 and 27 °C. Mean annual precipitation is less stable along the

sequence. The first part of the sequence is characterised by both large intervals from around 400 to 1300 mm and a MLV of 1100 mm and smaller intervals from 1100 to 1300 mm whereas the second part of the Messinian stage is characterised by more precise ranges from 700 to 1300 mm with a most likely value around 800 to 1200 mm.

In the Black Sea region, the estimated climate is the same as during the previous period, warm and humid, but with lower values of mean annual precipitation (650 to 1300 mm with MLV ~ 1100 mm) at the very end of the Messinian part of the sequence (Fig. 6).

3.3. The climate after the Messinian salinity crisis, at 5.33 Ma (Figs. 8 and 9)

For some sites (Tarragona, Andaluca, Habibas, Capo Rossello), the climate has already been reconstructed (Fauquette et al., 1999). Values are given again in Fig. 9.

As for the previous interval, the climate was warm and dry in the southwestern Mediterranean region but warm and humid at Maccarone and in the Black Sea region. At Maccarone, along the Adriatic Sea, the climate was exactly as at Stirone in the western part of the Po Valley (Fauquette and Bertini, 2003). However, looking at the detailed climatic reconstruction at Maccarone (Fig. 8), mean annual temperatures and in particular mean temperature of the coldest month show

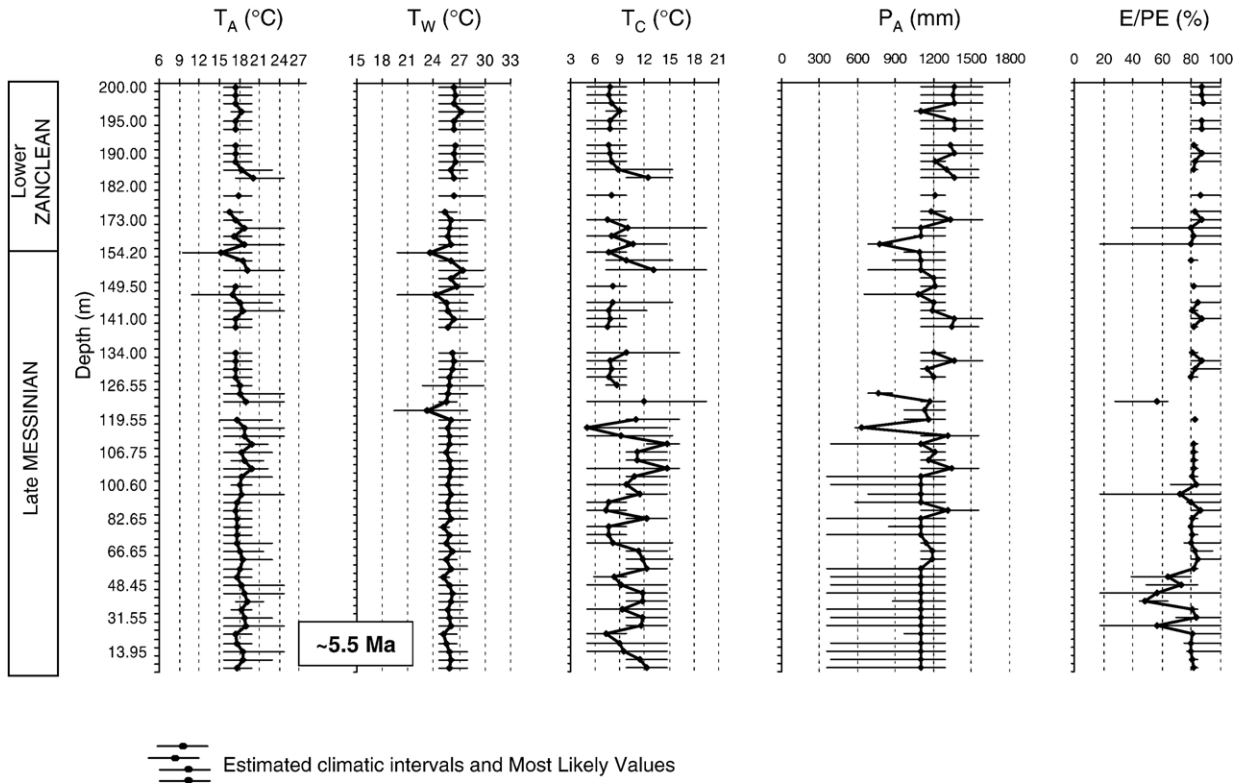


Fig. 8. Climatic quantification results based on pollen data from Maccarone covering the end of the Messinian salinity crisis (from around 5.5 Ma) and the lower Zanclean.

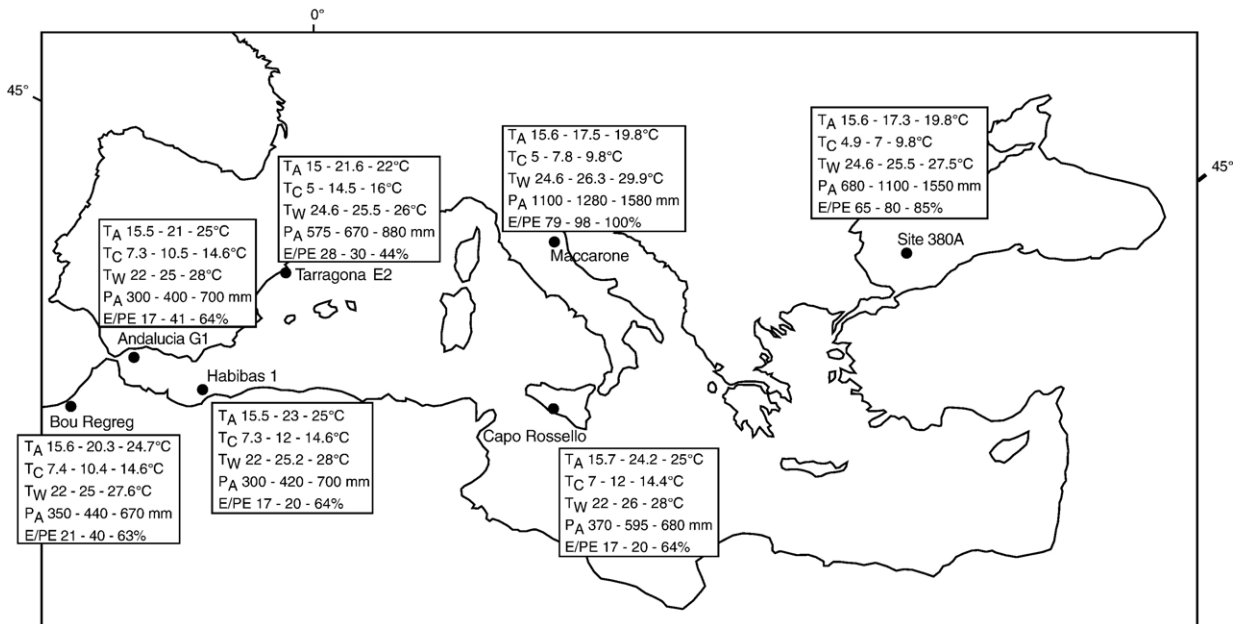


Fig. 9. Climatic quantification results based on pollen data corresponding to the period after the Messinian salinity crisis, i.e. the Early Pliocene.

lower values (except for 2 spectra) which never again exceed 20 and 10 °C respectively. During this period mean annual precipitation shows higher values than during the previous part of the sequence, ranging between 1100 and 1600 mm. Similarly, Fig. 6 shows for the Black Sea region larger ranges of mean annual precipitation than during the previous period, from around 680 to 1550 mm, due to larger amounts of herbs in the spectra. Temperatures of the coldest month never again exceed 10 °C (except for one spectrum), in contrast to the Messinian part.

4. Discussion

A first examination of the synthetic pollen diagrams in Fig. 3 reveals a high regional variability according to geographic location and conditions (latitude, longitude, proximity of highlands, oceanic influence, etc.). Whatever the period, herb frequency increases southward in contrast to tree frequency. This indicates that open and probably dry environments existed in the southern Mediterranean region prior to, during and after the salinity crisis. Trees (including high altitude elements) developed in areas close to mountains such as in the Po Valley (Alps and Apennines), in Cerdanya (Pyrenees) and in Black Sea (Plateau of Anatolia). Nevertheless, the influence of relief appears insufficient to explain high values of thermophilous trees in lands surrounding the Black Sea. The location of this region in southeastern Europe, where the Asian monsoon extended some control, needs also to be considered (Popescu et al., 2006-this volume). Indeed, strengthening of the Asian monsoon over the Eastern Mediterranean region during the late Miocene–earliest Pliocene has been discussed by Griffin (2002).

To the south, herb assemblages are dominated by Poaceae, Asteraceae, *Plantago*, *Erodium* and some very characteristic plants such as *Lygeum*, *Nitraria*, *Calligonum* and *Neurada*. *Lygeum* today characterises the southern Mediterranean region under a thermo-mediterranean climate (from semi-arid to arid conditions, with mean annual precipitation from around 500 to 100 mm, and under high annual temperatures from around 16 to 26°C; Fauquette et al., 1998b). *Nitraria*, *Calligonum* and *Neurada* are found today only in North Africa, in the Sahara, under hyper-arid conditions, with mean annual precipitation under 150 mm. Mediterranean xerophytes are frequent in a latitudinal strip extending from Tarragona to Sicily. In the Nile delta area, the abundance of herbs has a different significance because assemblages are dominated by Cyperaceae and Poaceae which evoke a savannah landscape in the northeastern

Africa realm. The development at so high a latitude of such a vegetation, which requires relatively humid and warm conditions, is also supported by the abundance of megathermic (i.e. tropical elements in the Naf 1 pollen diagram; Poumot and Suc, 1984) taxa. Such a vegetational structure in the southeastern Mediterranean region is in agreement with the hypothesis of Griffin (2002) who proposes an increase of moisture over this area during the salinity crisis but appears to contradict the modelling of climate and vegetation (Fluteau et al., 2003; François et al., 2006-this volume). Perhaps the climatic contrast between central and southeastern Mediterranean regions has many subtle touches, the latter region being less altered by an increase in dryness than the former.

Obviously, most of the variations observed in the pollen diagrams are constrained by fluctuations in the quantity of *Pinus* (Fig. 3). In fact, *Pinus* pollen grains are very effectively transported by air and water, so that variations in percentages indicate variations in the position of the coastline (i.e. eustatic variations). When the littoral zone is far from the sedimentation point, *Pinus* is largely over-represented and inversely, when the littoral zone is close to the site of deposition, *Pinus* is less important compared with the other taxa. Pollen diagrams for Bou Regreg, Carmona, Monticino 88, Maccarone, Capodarso, and Eraclea Minoa demonstrate this effect well. In any case, excluding *Pinus* from the pollen sum results in pollen sequences of almost homogeneous composition, supporting the idea that no relevant climatic change occurred in the Mediterranean region between 6.7 and 5.0 Ma, i.e. just before, during and just after the salinity crisis. This is in good agreement with Münch et al. (2003) who see no climatic variations between 6.9 and 6.0 Ma from the study of coral reefs. Interpreting such pollen diagrams initially in terms of coastline variations (i.e. eustasy fluctuations) is in good agreement with variability in the amounts of halophytes (plants living in saline environments along the shoreline). Pollen of these plants generally increase as *Pinus* percentages decrease (at Capodarso, Eraclea Minoa, in the Messinian part of Site 380A, for example). Interpretation of the pollen diagram of DSDP Site 380A is more complicated because a climatic signal overprints the «eustatic» one. This has been clearly evidenced by Popescu (2006-this volume) for the early Pliocene part of the section where the expected earliest Zanclean age of sediments overlying the breccia has been confirmed using European climatostratigraphic relationships. Just below the breccia, desiccation of the Black Sea is supported by large amounts of halophytes between 935 and 900 m depth interpreted as a moderate lowering of

sea level, probably related to the first step of the salinity crisis (Fig. 3). This is in agreement with the reverse curve of *Pinus*, the greater percentages of which reveal more distal conditions (i.e. probably a higher sea-level). The increase in *Pinus* above 900 m depth could be related to the sea-level rise that corresponds to the Sicilian Upper Evaporites (isotopic stage TG 15) (for more details, see Popescu, this volume).

It is well established that the inverse relationship between *Pinus* and halophytes reflects the distance of the pollen locality to the paleo-coastline (Suc et al., 1995c). But there is some uncertainty about whether to interpret some herbs as halophytes. For example, *Artemisia* may have an edaphic (halophytic) or a climatic significance. This question affects Site 380A. For the Pliocene, large amounts of, and variations in *Artemisia* are clearly linked to climate evolution (Popescu, 2006-this volume). The development of *Artemisia* at the end of the Miocene might have double significance: proximity of the shoreline because of the Messinian sea-level drop and/or increasing dryness in the regional climate (Fluteau et al., 2003; François et al., 2006-this volume). So, the decreasing mean annual precipitation observed on Fig. 6 at the end of the Messinian may be an artefact, or not.

Climatic quantification from pollen data does not show obvious climatic change due to the desiccation of the Mediterranean Sea, especially in the dry southwestern Mediterranean area. Sicily, southern Spain and also North Africa, where the vegetation was subdesertic, are certainly not the best regions to detect climatic variation, especially if small in amplitude. Indeed, a slight change in temperature is certainly not sufficient to modify this type of open vegetation. On the contrary, a small increase in precipitation is sufficient to modify the vegetation in these regions. But there are no real changes in the vegetation composition, or associated changes in precipitation, observed at time of the Messinian salinity crisis (many herbaceous plants and subdesertic plants have been recorded continuously).

We have emphasised the presence in some pollen spectra (Sicily: Capodarso and Eraclea Minoa; North Africa: Douiet 1 and MSD1; Black Sea: Site 380A) of *Avicennia*, a mangrove taxon. Even at very low quantities, the occurrence of *Avicennia* pollen grains indicates the presence of mangrove close to the sampled site, as the taxon is under-represented in the modern pollen floras (Blasco and Caratini, 1973; Lézine, 1996). But it seems that in Sicily and North Africa during the Messinian, the mangrove communities were impoverished compared with modern tropical mangroves. Such impoverished mangroves are found today in the

northern part of the Red Sea area, extending as far as 30°N, i.e. considerably beyond the tropical zone where fully developed mangroves are growing. In fact during Messinian time, the North African, Sicilian and northern Turkish mangroves were certainly highly discontinuous, at their northern limit of distribution, and thus decidedly fragile.

In these regions, *Avicennia* ceases to be recorded in the Lower Zanclean, except in the Black Sea which represents its last appearance in the Mediterranean region (at about 4.7 Ma) owing to the suitable wet and warm climatic conditions in the area (Popescu, 2006-this volume). In fact, the flooding of the Mediterranean makes the sampled sites more distal so that *Avicennia*, whose pollen grains are weakly transported, is less likely to be recorded. In spite of this bias, some Zanclean *Avicennia* pollen have been recorded at Site 380A when the Black Sea was full and the site far from the coastline. It should be mentioned that no pollen of *Avicennia* has been found in the earliest Zanclean coastal localities studied from the southern Mediterranean region (Spain, Morocco, Algeria, Tunisia, Egypt, Israel, Turkey, Syria: Suc et al., 1995b, 1999; Drivaliari, 1993; M. Abdelmalek, pers. com.; Suc, unpublished data; Feddi, unpublished data). Accordingly, we feel that the disappearance of *Avicennia* took place before the earliest Zanclean. The disappearance of *Avicennia* was probably due to severe ecological stress, such as the expansion of hypersaline waters during the desiccation of the Mediterranean, rather than to a climatic deterioration. In Sicily, the disappearance of this taxon occurs between the uppermost Messinian at Eraclea Minoa and the lowermost Zanclean at Capo Rossello. If no gap in sedimentation exists between these two deposits (following Krijgsman's scenario; Fig. 1), there is no climatic deterioration to explain such a crucial disappearance. In contrast, the extinction of *Avicennia* along the southern Mediterranean shorelines could be easily explained by the desiccation, the Caltanissetta basin and other deeper areas becoming very dry and salty. These areas would then have been inhospitable to mangrove which had not survived in refugia within the Mediterranean realm and could not have returned. This argument is used to support the scenario of Clauzon et al. (1996).

Because the causes of this taxon's disappearance are still under discussion, it has not been taken into account in the climate estimates, although it is a good ecological and climatic marker. However, the climate reconstructed without *Avicennia* is consistent with modern climatic conditions prevailing in the northern part of the Red Sea (high temperatures and very low precipitation). And, as

today in the northern part of the Red Sea (Kassas, 1957), the southern Mediterranean vegetation, prior to the complete desiccation of the sea, was composed of an impoverished mangrove zone, an open subdesertic vegetation zone, and a less open vegetation zone of mainly evergreen and mixed mesophilous taxa at higher elevations.

The lower half of the Maccarone section is characterised by the presence, among a large representation of herbaceous plants, of pollen grains of *Lygeum* (up to 7.6%), a Poaceae found today in North Africa, southern Italy, Sicily, southern Spain and Crete, under a thermo-mediterranean semi-arid to arid climate. Thus, this plant indicates very dry conditions in contradiction with the abundance of subtropical plants requiring humidity. This seems to indicate more humid conditions at the foothill and on the slopes of the uplifting Apennines and drier conditions in littoral areas. This hypothesis is reinforced by *Lygeum*'s unique morphology (a relatively big and heavy pollen grain) and, consequently, its weak affinity for transport, so that its presence in the sediments indicates that the plant was living in littoral areas.

Such a composite pollen spectra with plants coming from two different vegetation types lead to very broad climatic estimates, particularly with respect to mean annual precipitation.

It is pertinent to ask whether *Lygeum* was already present at Maccarone before the Messinian salinity crisis. In other words, is the presence of *Lygeum* at so high a latitude (at about 4–5° more than its modern habitat) directly related to the crisis or not? The first possibility is that *Lygeum* was present at Maccarone before the crisis and that a geographic and climatic threshold already existed between Monticino/Borgo Tossignano and Maccarone. The second possibility is that *Lygeum* was not present at Maccarone before the crisis because the harsh ecological conditions imposed by the crisis (expanding saline environments) led to the migration of *Lygeum* with other herbaceous companions from south (Sicily, Calabria) to north, where ecological conditions were more suitable. The apparent absence of *Lygeum* in the pollen record of Moscosi, a thin deposit underlying the Maccarone section, constitutes an argument in favour of the migration to the North of *Lygeum* during the salinity crisis. In any case, the possible migration of subdesertic herbs to the north is considered by Clauzon et al. (2005) as a reliable argument (in addition to the radiometric age of the Maccarone ash) for proposing that the Adriatic–Po realm became a perched basin still supplied by freshwater runoff from

the surrounding mountains when the Mediterranean Sea was desiccated.

Approximately 120 m above the base of the Maccarone section, the strong and sudden decrease in tropical, subtropical, and warm-temperate elements and herbaceous plants, including *Lygeum* (correlated to a decrease in temperatures of the coldest month and, less importantly, to a decrease in mean annual temperatures), viewed against the increase in Pinaceae may be interpreted as a significant paleoenvironmental change. Such a break represents a suddenly increasing distance of the site from the coastline, and has been related to a eustatic/tectonic event by Bertini (1994a, 2002) and Roveri et al. (2001), but to the massive marine transgression in the area by Clauzon et al. (2005). Our understanding of the Maccarone pollen flora may be supported by the data of Vidal et al. (2002) who indicate that the second phase of evaporite deposition should occur during a period of global warming. So, the drastic vegetational changes recorded at Maccarone after 5.5 Ma may not be due to a cooling but rather to regional environmental changes. In fact Maccarone is certainly not a «key-site» for understanding the climate during the Messinian salinity crisis. The pressure of environmental change is so severe that it is difficult to distinguish the relative effects of the climate and/or of the supposed flooding.

The Messinian salinity crisis is a phenomenon in the Mediterranean region, and its influence certainly extends beyond the Mediterranean region, but it is difficult to extricate all the mechanisms involved. Generally, the Messinian salinity crisis is thought to be linked to a eustatic control (Kastens, 1992; Zhang and Scott, 1996), but the timing of the isotope events compared with the chronology of the crisis suggests that global sea-level variations are not alone responsible for the beginning or the end of the crisis (Hodell et al., 2001; Vidal et al., 2002). In the same way, the climatic evolution in the western Mediterranean area shows that the climate is not the direct cause of the Mediterranean desiccation, as the Mediterranean region was subjected long before the crisis to continuously high evaporation (this study; Suc and Bessais, 1990; Bertini, 1994a,b; Bertini et al., 1998; Warny and Wrenn, 2002; Warny et al., 2003). It, therefore, now seems clear that the main factor leading to this event is the closure of the Rifian corridor after that of the Betic corridor, isolating the Mediterranean Sea from the Atlantic Ocean (Clauzon et al., 1996; Krijgsman et al., 1999a,b).

Of course, other mechanisms, all more or less interdependent, are also involved in this event, such as global climate evolution, global eustasy, sea temperatures,

ocean circulation, and ice volume variation (Antarctic and Arctic). Knowing that the Mediterranean Sea is supplied mainly by Atlantic waters, closure of the passage from the Atlantic to the Mediterranean, associated with a known global sea-level drop (Vidal et al., 2002), led to evaporation being more important than filling and, as a consequence, to the desiccation of the basin. On the other hand, it has been proposed that the abrupt regional sea-level rise that reflooded the Mediterranean Sea may have been related to accelerated ice volume reduction caused by a thinning of the Antarctic ice sheet (Warny et al., 2003), and that this facilitated erosion within the Gibraltar Strait and thus its opening (Blanc, 2002).

5. Conclusions

An intensive pollen review allows us to present this first regional synthesis for the period including the Messinian salinity crisis. Two main contrasting areas are evident with respect to the vegetation cover: a southern Mediterranean area characterised by dominant open vegetation growing under dry and warm conditions, and a northern Mediterranean area inhabited by forest assemblages (humid and warm conditions) especially close to upland areas. Few changes are recorded in the pollen diagrams, these being mostly linked to variability in *Pinus* percentages controlled by variations in distance of site from the shoreline, i.e. to eustatic variations. This suggests that no significant climatic change occurred during the studied period, an inference confirmed by climate quantification. Some megathermic elements disappear from the Mediterranean realm at the Messinian–Zanclean transition: the most impressive concerns the mangrove element *Avicennia*. Our observations suggest that its regional extinction was caused by its inability to survive in increasingly saline coastal environments as the Mediterranean Sea was desiccating. A noticeable expansion of herbs (including subdesertic elements such as *Lygeum*) to the north occurred between 5.5 and about 5.4 Ma, i.e. when the Mediterranean Sea had become desiccated. This migration might be related to increasingly harsh conditions in the desiccated areas without the need to invoke a climatic change towards drier conditions some 4–5° northward in latitude. It is probable that migration of plants was induced by a striking increase in dryness over the central Mediterranean. For example, subdesertic herbs could have moved to the north and tropical–subtropical elements to the southeast without climatic conditions in these areas changing significantly as a response to the desiccation of the Mediterranean. So, the proposed increase in

moisture in the southeastern Mediterranean might have been lower than that deduced from the regional geomorphological response to the salinity crisis.

From this study we are able to answer the two questions asked in the introduction: (1) has the climate played a role in triggering the Messinian salinity crisis? and (2) has the Messinian salinity crisis changed the climate in the Mediterranean region?

Regarding the first question, climate was not the direct cause of the Messinian salinity crisis. This is also evident from the $\delta^{18}\text{O}$ records. Indeed, the Mediterranean region was submitted to continuously high evaporation long before the crisis, especially in the south. Given that the Mediterranean Sea is supplied mainly by Atlantic waters, a closure of the passage from the Atlantic to the Mediterranean led to evaporation unrestored by entry of oceanic waters, i.e. to a negative regional hydrological budget.

Regarding the second question, the Messinian salinity crisis seems not to have changed the climate in the Mediterranean region, in particular in the southwestern area, where the climate was very dry and warm before, during and after the event. Some other climatic variations (weak decrease in precipitation at the beginning of the crisis in the Black Sea region, increasing precipitation and decreasing temperatures at the end of the Messinian at Maccarone) may be related to artefacts. Indeed, some vegetation changes are more due to environmental variations (sea-level change) than to climatic changes. This result seems to be confirmed by model simulations (Fluteau et al., 2003) that show no or little changes in the Mediterranean region and in the Rifian area (Atlantic side). On the other hand, these authors show that the Messinian salinity crisis seems to influence deeply the summer monsoon in Asia (shift to the West, temperature decrease over India) and Africa (weakening of precipitation). But the lack of data avoids to validate these results.

Acknowledgements

The climatic quantifications were performed in part at the University of Tübingen (Institute und Museum für Geologie und Paläontologie) during post-doctoral research undertaken by S. Fauquette and funded by the Alexander von Humboldt foundation. Financial support was also provided by the French Programme «Environnement, Vie et Sociétés» and ECLIPSE. Dr. Martin J. Head (University of Cambridge) is thanked for help with the linguistic editing of this paper. Thank you to the two referees, Profs. P. Quézel and J. Agustí, for their helpful comments. The complete pollen counts as

well as results of the climatic quantification have been placed on the Medias-France website in the «Cenozoic Pollen and Climatic values database» (C.P.C., for further information contact S. Fauquette, curator of the database) which is being developed within the framework of the EEDEN Programme. E. Bessais (deceased) generated some of the pollen spectra in the Andalucia G1 and Tarragona E2 sections.

This is ISEM contribution no. 2005-101.

References

- Agusti, J., Roca, E., 1987. Sintesis biostratigrafica de la fosa de la Cerdanya (Pirineos Orientales). *Estud. geol.* 43, 521–529.
- Agusti, J., Oms, O., Furió, M., Pérez-Vila, M.-J., Roca, E., 2006. The Messinian terrestrial record in the Pyrenees: The case of Can Vilella (Cerdanya Basin). *Palaeogeogr. Palaeoclimatol. Palaeoecol.* 238, 179–189. doi:10.1016/j.palaeo.2006.03.024.
- Bachiri Taoufiq, N., 2000. Les environnements marins et continentaux du corridor rifain au Miocène supérieur d'après la palynologie. Thesis, Univ. Casablanca. 206 pp.
- Barhoun, N., 2000. Biostratigraphie et paléoenvironnement du Miocène supérieur et du Pliocène inférieur du Maroc septentrional: Apport des foraminifères planctoniques. Thesis, Univ. Casablanca. 273 pp.
- Benda, L., 1971. Grundzüge einer pollenanalytischen Gliederung des Türkischen Jungtertiärs. *Beih. geol. Jahrb.* 113, 1–45.
- Bertini, A., 1992. Palinologia ed aspetti ambientali del versante adriatico dell'Appennino centro-settentrionale durante il Messiniano e lo Zancleano. PhD Thesis, Firenze University, Italy. 88 p.
- Bertini, A., 1994a. Palynological investigations on Upper Neogene and Lower Pleistocene sections in Central and Northern Italy. *Mem. Soc. Geol. Ital.* 48, 431–443.
- Bertini, A., 1994b. Messinian–Zanclean vegetation and climate in North-Central Italy. *Hist. Biol.* 9, 3–10.
- Bertini, A., 2002. Palynological evidence of upper Neogene environments in Italy. *Acta Univ. Carol., Geol.* 46, 15–25.
- Bertini, A., Londeix, L., Maniscalco, R., Di Stefano, A., Suc, J.-P., Clauzon, G., Gautier, F., Grasso, M., 1998. Paleobiological evidence of depositional conditions in the Salt Member, Gessoso-Solfifera Formation (Messinian, Upper Miocene) of Sicily. *Micropaleontology* 44 (4), 413–433.
- Bertolani Marchetti, D., 1984. Analyse pollinique des intercalations marneuses du Messinien de la «Formazione Gessoso-Solfifera» (Bologne — Italie du Nord). *Paléobiol. Cont.* 14 (2), 143–151.
- Bertolani Marchetti, D., Cita, M.B., 1975. VII) Palynological investigations on Late Messinian sediments recorded at DSDP Site 132 (Tyrrhenian Basin) and their bearing on the deep basin desiccation model. *Riv. Ital. Paleontol.* 81, 281–308.
- Bessais, E., Cravatte, J., 1988. Les écosystèmes végétaux pliocènes de Catalogne méridionale. Variations latitudinales dans le domaine nord-ouest méditerranéen. *Geobios* 21, 49–63.
- Bessedik, M., Guinet, P., Suc, J.-P., 1984. Données paléofloristiques en Méditerranée nord-occidentale depuis l'Aquitainien. *Rev. Paléobiol., Vol. Spec.* 25–31.
- Blanc, P.-L., 2002. The opening of the Plio–Quaternary Gibraltar Strait: assessing the size of a Cataclysm. *Geodin. Acta* 15, 303–317.
- Blasco, F., Caratini, C., 1973. Mangrove de Pichavaram (Tamil Nadu, Inde du Sud). *Phytogéographie et palynologie*. In: Boyé, M., Chamard, P., Fritsch, P., Morin, S., Seurin, M., Blasco, F., Caratini, C. (Eds.), *Cinq études de géomorphologie et palynologie. Travaux et documents de géographie tropicale*, vol. 8, pp. 163–185.
- Busson, G., 1979. Le «géant salifère» messinien du domaine méditerranéen: interprétation génétique et implications paléogéographiques. *Ann. Géol. Pays Hell. Apart Ser. 1*, 227–238.
- Busson, G., 1990. Le Messinien de la Méditerranée... vingt après. *Géol. Fr.* 3–4, 3–58.
- Cambon, G., Suc, J.-P., Aloisi, J.-C., Giresse, P., Monaco, A., Touzani, A., Duzer, D., Ferrier, J., 1997. Modern pollen deposition in the Rhône delta area (lagoonal and marine sediments), France. *Grana* 36, 105–113.
- Carlioni, G.C., Francavilla, F., Borsetti, A.M., Cati, F., D'Onofrio, S., Mezzetti, R., Savelli, C., 1974. Ricerche stratigrafiche sul limite Miocene–Pliocene nelle Marche centro-meridionali. *Giorn. Geol. ser. 2a* 39 (2) 363–392.
- Chikhi, H., 1992. Une palynoflore méditerranéenne à subtropicale au Messinien pré-évaporitique en Algérie. *Géol. Méditerr.* 19 (1), 19–30.
- Clauzon, G., 1997. Detailed morpho-sedimentary recording of the Messinian events in the Betic basin in the light of the two phase model of the salinity crisis. In: Dilibento, E., Di Stefano, A., Maniscalco, R. (Eds.), *Neogene basins of the Mediterranean Region: Controls and Correlation in Space and Time*. R.C.M.N.S. Interim Colloquium, Catania, Abstracts, pp. 40–42.
- Clauzon, G., 1999. L'impact des variations eustatiques du bassin de Méditerranée occidentale sur l'orogène alpin depuis 20 Ma. *Etudes de Géographie Physique* 28, 1–8.
- Clauzon, G., Suc, J.-P., Gautier, F., Berger, A., Loutre, M.-F., 1996. Alternate interpretation of the Messinian Salinity Crisis: controversy resolved? *Geology* 24 (4), 363–366.
- Clauzon, G., Suc, J.-P., Popescu, S.-M., Marunteanu, M., Rubino, J.-L., Marinescu, F., Jipa, D., 2005. Influence of the Mediterranean sea-level changes on the Dacic Basin (Eastern Paratethys) during the late Neogene: the Mediterranean Lago Mare facies deciphered. *Basin Res.* 17, 437–462.
- Cornée, J.-J., Roger, S., Münch, P., Saint-Martin, J.-P., Féraud, G., Conesa, G., Pestrea, S., 2002. Messinian events: new constraints from sedimentological investigations and new ⁴⁰Ar/³⁹Ar ages in the Melilla–Nador basin (Morocco). *Sediment. Geol.* 151, 127–147.
- Corselli, C., Grecchi, G., 1984. The passage from hypersaline to hyposaline conditions in the Mediterranean Messinian: discussion of the possible mechanisms triggering the «lago-mare» facies. *Paléobiol. Cont.* 14 (2), 225–239.
- Cunningham, K.J., Benson, R.H., Rakic-El Bied, K., McKenna, L.W., 1997. Eustatic implications of late Miocene depositional sequences in the Melilla Basin, northeastern Morocco. *Sediment. Geol.* 107, 147–165.
- Decima, A., Wezel, F.C., 1973. Late Miocene evaporites of the central Sicilian basin, Italy. *Initial Rep. Deep Sea Drill. Proj.* 13, 1234–1241.
- Drivaliari, A., 1993. Images polliniques et paléoenvironnements au Néogène supérieur en Méditerranée orientale. Aspects climatiques et paléogéographiques d'un transect latitudinal (de la Roumanie au delta du Nil). PhD Thesis, Univ. Montpellier 2. 333 pp.
- Ediger, V.S., Bati, Z., Kozlu, H., 1996. Tortonian–Messinian palynomorphs from the easternmost Mediterranean region around Iskenderun, Turkey. *Micropaleontology* 42 (2), 189–205.
- Fauquette, S., Bertini, A., 2003. Quantification of the Northern Italy Pliocene climate from pollen data — evidence for a very peculiar climate pattern. *Boreas* 32, 361–369.

- Fauquette, S., Guiot, J., Suc, J.-P., 1998a. A method for climatic reconstruction of the Mediterranean Pliocene using pollen data. *Palaeogeogr. Palaeoclimatol. Palaeoecol.* 144, 183–201.
- Fauquette, S., Quézel, P., Guiot, J., Suc, J.-P., 1998b. Signification bioclimatique de taxons-guides du Pliocène Méditerranéen. *Geobios* 31, 151–169.
- Fauquette, S., Suc, J.-P., Guiot, J., Diniz, F., Feddi, N., Zheng, Z., Bessais, E., Drivaliari, A., 1999. Climate and biomes in the West Mediterranean area during the Pliocene. *Palaeogeogr. Palaeoclimatol. Palaeoecol.* 152, 15–36.
- Fluteau, F., Suc, J.-P., Fauquette, S., 2003. Modelling the climatic consequences of the Messinian Salinity Crisis. *Geophys. Res. Abstr.* 5, 11387.
- François, L., Ghislain, M., Otto, D., Micheels, A., 2006. Late Miocene vegetation reconstruction with the CARAIB model. *Palaeogeogr. Palaeoclimatol. Palaeoecol.* 238, 302–320. doi:10.1016/j.palaeo.2006.03.034.
- Gautier, F., Clauzon, G., Suc, J.-P., Cravatte, J., Violanti, D., 1994. Age et durée de la crise de salinité messinienne. *C. R. Acad. Sci. Paris Ser. 2* (318), 1103–1109.
- Griffin, D.L., 2002. Aridity and humidity: two aspects of the late Miocene climate of North Africa and the Mediterranean. *Palaeogeogr. Palaeoclimatol. Palaeoecol.* 182, 65–91.
- Heimann, K.O., Jung, W., Braune, K., 1975. Schichtenfolge und Flora des Messiniens von Nord-Korfu (Griechenland). *Mitt. Bayer. Staatssamml. Palaeontol. Hist. Geol.* 15, 169–177.
- Heusser, L., 1988. Pollen distribution in marine sediments on the continental margin of Northern California. *Mar. Geol.* 80, 131–147.
- Hodell, D.A., Benson, R.H., Kent, D.V., Boersma, A., Rakic-El Bied, K., 1994. Magnetostratigraphic, biostratigraphic, and stable isotope stratigraphy of an Upper Miocene drill core from the Salé Briqueterie (northwest Morocco): a high-resolution chronology for the Messinian stage. *Paleoceanography* 9, 835–855.
- Hodell, D.A., Curtis, J.H., Sierro, F.J., Raymo, M.E., 2001. Correlation to the Late Miocene to the Early Pliocene sequences between the Mediterranean and North Atlantic. *Paleoceanography* 16 (2), 164–178.
- Hsü, K.J., Giovanoli, F., 1979. Messinian event in the Black Sea. *Palaeogeogr. Palaeoclimatol. Palaeoecol.* 29, 75–94.
- Hsü, K.J., Cita, M.B., Ryan, W.B.F., 1973. The origin of the Mediterranean evaporites. *Initial Reports of the Deep Sea Drilling Project* 13, 1203–1231.
- Ioakim, C., Koutsouveli, A., Tsaila-Monopolis, S., Theodossiou, I., 1997. Palaeoenvironmental and palaeoclimatic conditions during the upper Miocene–lower Pliocene in the Sitia region (Eastern Crete, Greece). *Rev. Paléobiol.* 16 (1), 187–195.
- Ioakim, C., Solounias, N., 1985. A radiometrically dated pollen flora from the Upper Miocene of Samos island, Greece. *Rev. Micropaleontol.* 28 (3), 197–204.
- Kassas, M., 1957. On the ecology of the Red Sea coastal land. *J. Ecol.* 45 (1), 187–203.
- Kastens, K.A., 1992. Did glacio-eustatic sea level drop trigger the Messinian salinity crisis? New evidence from Ocean Drilling Program Site 654 in the Tyrrhenian Sea. *Paleoceanography* 7, 333–356.
- Krijgsman, W., Hilgen, F.J., Marabini, S., Vai, G.B., 1999a. New paleomagnetic and cyclostratigraphic age constraints on the Messinian of the Northern Apennines (Vena del Gesso Basin, Italy). *Mem. Soc. Geol. Ital.* 54, 25–33.
- Krijgsman, W., Hilgen, F.J., Raffi, I., Sierro, F.J., Wilson, D.S., 1999b. Chronology, causes and progression of the Messinian salinity crisis. *Nature* 400, 652–655.
- Krijgsman, W., Fortuin, A.R., Hilgen, F.J., Sierro, F.J., 2001. Astrochronology for the Messinian Sorbas basin (SE Spain) and orbital (precessional) forcing for evaporite cyclicity. *Sediment. Geol.* 140, 43–60.
- Letouzey, J., Gonnard, R., Montadert, L., Kristchev, K., Dorkel, A., 1978. Black Sea: geological setting and recent deposits distribution from seismic reflection data. In: Ross, D.A., Neprochnov, Y.P., et al. (Eds.), *Initial Report of the Deep Sea Drilling Project*, vol. 42, 2. U.S. Gov. Print. Off, pp. 1077–1084.
- Lézine, A.M., 1996. La mangrove ouest africaine, signal des variations du niveau marin et des conditions régionales du climat au cours de la dernière déglaciation. *Bull. Soc. Géol. Fr.* 167 (6), 743–752.
- Lourens, L.J., Antonarakou, A., Hilgen, F.J., Van Hoof, A.A.M., Vergnaud Grazzini, C., Zachariasse, W.J., 1996. Evaluation of the Pliocene to early Pleistocene astronomical time scale. *Paleoceanography* 11, 391–413.
- Mariotti Lippi, M., 1989. Ricerche palinologiche sul Messiniano di Eraclea Minoa (Ag) nel quadro paleofloristico e paleovegetazionale del tardo Miocene italiano. *Webbia* 43 (1), 169–199.
- Masce, G., Heimann, K.O., 1976. Geological observations from Messinian and Lower Pliocene outcrops in Sicily. *Mem. Soc. Geol. Ital.* 16, 127–140.
- Münch, Ph., Saint Martin, J.P., Cornée, J.J., Féraud, G., Pestrea, S., Roger, S., Conesa, G., 2003. Control on facies and sequence stratigraphy of an upper Miocene carbonate ramp and platform, Melilla basin, NE Morocco: comment. *Sediment. Geol.* 3153, 1–4.
- Odin, G.S., Ricci Lucchi, F., Tateo, F., Cosca, M., Hunziker, J.C., 1997. Integrated stratigraphy of the Maccarone section, Late Messinian (Marche region, Italy). In: Montanari, A., Odin, G.S., Coccioni, R. (Eds.), *Miocene Stratigraphy — an Integrated Approach*. Elsevier, Amsterdam, pp. 529–544.
- Orszag-Sperber, F., Rouchy, J.-M., Blanc-Valleron, M.-M., 2000. La transition Messinien–Pliocène en Méditerranée orientale (Chypre): la période du Lago-Mare et sa signification. *C. R. Acad. Sci. Paris, Sci. Terre Planètes* 331, 483–490.
- Perconig, E., 1974. Mise au point du stratotype de l'Andalousien. *Mém. Bur. Rech. Géol. Min.* 78 (2), 659–662.
- Popescu, S.-M., 2001. Végétation, climat et cyclostratigraphie en Paratéthis centrale au Miocène supérieur et au Pliocène inférieur d'après la palynologie. PhD Thesis, Université Claude Bernard — Lyon 1, France. 223 pp.
- Popescu, S.-M., 2006. Late Miocene and early Pliocene environments in the southwestern Black Sea region from high-resolution palynology of DSDP Site 380A (Leg 42B). *Palaeogeogr. Palaeoclimatol. Palaeoecol.* 238, 64–77. doi:10.1016/j.palaeo.2006.03.018.
- Popescu, S.-M., Suc, J.-P., Loutre, M.-F., 2006. Early Pliocene vegetation changes forced by eccentricity-precession. Example from Southwestern Romania. *Palaeogeogr. Palaeoclimatol. Palaeoecol.* 238, 340–348 (this volume). doi:10.1016/j.palaeo.2006.03.032.
- Poumot, C., Suc, J.-P., 1984. Flore pollinique de la fin du Néogène en Méditerranée sud-orientale. *Paléobiol. Cont.* 14 (2), 397–401.
- Roger, S., Münch, P., Cornée, J.-J., Saint-Martin, J.-P., Féraud, G., Pestrea, S., Conesa, G., Ben Moussa, A., 2000. ⁴⁰Ar/³⁹Ar dating of the pre-evaporitic Messinian marine sequences of the Melilla basin (Morocco): a proposal for some biosedimentary events as isochrons around the Alboran Sea. *Earth Planet. Sci. Lett.* 179, 101–113.
- Ross, D.A., Neprochnov, Y.P., Degens, E.T., Erickson, A.J., Hsü, K., Hunt, J.M., Manheim, F., Percival, S., Senalp, M., Stoffers, P., Supko, P., Traverse, A., Trimonis, E.A., 1978. Site 380. In: Ross, D.A., Neprochnov, Y.P., et al. (Eds.), *Initial Report of the Deep Sea Drilling Project*, vol. 42, 2. U.S. Gov. Print. Off, pp. 119–291.

- Rouchy, J.-M., 1981. La genèse des évaporites messiniennes de Méditerranée: un bilan. *Bull. Cent. Rech. Explor. Prod. Elf-Aquitaine* 4, 511–545.
- Rouchy, J.-M., Orszag-Sperber, F., Blanc-Valleron, M.-M., Pierre, C., Rivière, M., Combourieu-Nebout, N., Panayides, I., 2001. Paleoenvironmental changes at the Messinian–Pliocene boundary in the eastern Mediterranean (southern Cyprus basins): significance of the Messinian Lago-Mare. *Sediment. Geol.* 145, 93–117.
- Roveri, M., Bassetti, M.A., Ricci Lucchi, F., 2001. The Mediterranean Messinian salinity crisis: an Apennine foredeep perspective. *Sediment. Geol.* 140, 201–214.
- Sachse, M., 2001. Oleaceous laurophyllous leaf fossils and pollen from the European Tertiary. *Rev. Palaeobot. Palynol.* 115, 213–234.
- Schrader, H.-J., 1978. Quaternary through Neogene history of the Black Sea, deduced from the paleoecology of diatoms, silicoflagellates, ebridians and chrysomonads. In: Ross, D.A., Neprochnov, Y.P., et al. (Eds.), *Initial Report of the Deep Sea Drilling Project*, vol. 42, 2. U.S. Gov. Print. Off., pp. 789–901.
- Shackleton, N.J., Hall, M.A., Pate, D., 1995. Pliocene stable isotope stratigraphy of Site 846. *Proc. Ocean Drill. Program Sci. Results* 138, 337–355.
- Sierro, F.J., Gonzalez Delgado, J.A., Dabrio, C.J., Flores, J.A., Civis, J., 1996. Late Neogene depositional sequences in the foreland basin of Guadalquivir (SW Spain). In: Friend, F., Dabrio, C.J. (Eds.), *Tertiary Basins of Spain*. Cambridge Univ. Press, pp. 329–334.
- Stoffers, P., Müller, G., 1978. Mineralogy and lithofacies of Black Sea sediments, Leg 42B Deep Sea Drilling project. In: Ross, D.A., Neprochnov, Y.P., et al. (Eds.), *Initial Report of the Deep Sea Drilling Project*, vol. 42, 2. U.S. Gov. Print. Off., pp. 373–390.
- Suc, J.-P., 1989. Distribution latitudinale et étagement des associations végétales au Cénozoïque supérieur dans l'aire ouest-méditerranéenne. *Bull. Soc. Géol. Fr. Ser. 8 5 (3)*, 541–550.
- Suc, J.-P., Bessais, E., 1990. Pérennité d'un climat thermoxérique en Sicile, avant, pendant et après la crise de salinité messinienne. *C. R. Acad. Sci. Paris t.310 (II)*, 1701–1707.
- Suc, J.-P., Drivaliari, A., 1991. Transport of bisaccate coniferous fossil pollen grains to coastal sediments: an example from the earliest Pliocene Orb Ría (Languedoc, Southern France). *Rev. Palaeobot. Palynol.* 70, 247–253.
- Suc, J.-P., Bertini, A., Combourieu-Nebout, N., Diniz, F., Leroy, S., Russo-Ermolli, E., Zheng, Z., Bessais, E., Ferrier, J., 1995a. Structure of West Mediterranean and climate since 5,3 Ma. *Acta zool. Cracov.* 38 (1), 3–16.
- Suc, J.-P., Diniz, F., Leroy, S., Poumot, C., Bertini, A., Dupont, L., Clet, M., Bessais, E., Zheng, Z., Fauquette, S., Ferrier, J., 1995b. Zanclean (~Brunsumian) to early Piacenzian (~early-middle Reuverian) climate from 4° to 54° north latitude (West Africa, West Europe and West Mediterranean areas). *Meded. Rijks Geol. Dienst* 52, 43–56.
- Suc, J.-P., Violanti, D., Londeix, L., Poumot, C., Robert, C., Clauzon, G., Gautier, F., Turon, J.-L., Ferrier, J., Chikkhi, H., Cambon, G., 1995c. Evolution of the Messinian Mediterranean environments: the Tripoli Formation at Capodarso (Sicily, Italy). *Rev. Palaeobot. Palynol.* 87, 51–79.
- Suc, J.-P., Fauquette, S., Bessedik, M., Bertini, A., Zheng, Z., Clauzon, G., Suballyova, D., Diniz, F., Quézel, P., Feddi, N., Clet, M., Bessais, E., Bachiri Taoufiq, N., Méon, H., Combourieu-Nebout, N., 1999. Neogene vegetation changes in West European and West circum-Mediterranean areas. In: Agusti, J., Rook, L., Andrews, P. (Eds.), *Hominid Evolution and Climatic Change in Europe*, Vol. 1: *Climatic and Environmental Change in the Neogene of Europe*. Cambridge University Press, pp. 378–388.
- Traverse, A., 1978. Palynological analysis of DSDP Leg 42B (1975) cores from the Black Sea. In: Ross, D.A., Neprochnov, Y.P., et al. (Eds.), *Initial Report of the Deep Sea Drilling Project*, vol. 42, 2. U.S. Gov. Print. Off., pp. 993–1015.
- Trevisan, L., 1967. Pollini fossili del Miocene sup. nei Tripoli del Gabbro (Toscana). *Paleontol. Ital.* 42, 1–78.
- Vai, G.B., Ricci Lucchi, F., 1977. Algal crusts, autochthonous and clastic gypsum in a cannibalistic evaporite basin: a case history from the Messinian of Northern Apennines. *Sedimentology* 24, 211–244.
- Vidal, L., Bickert, T., Wefer, G., Röhl, U., 2002. Late Miocene stable isotope stratigraphy of SE Atlantic ODP Site 1085: relation to Messinian events. *Mar. Geol.* 180, 71–85.
- Warny, S., 1999. Marine and continental environmental changes in the Gibraltar arc area during the late Neogene (8–2.7 Ma) linked to the evolution of global climate and to Atlantic Ocean–Mediterranean Sea relationships. A palynological contribution to the Mediterranean Salinity Crisis through dinoflagellate cysts and pollen analysis. PhD Thesis, Université Catholique de Louvain, Belgium. 295 pp.
- Warny, S., Wrenn, J.H., 2002. Upper Neogene dinoflagellate cyst ecostratigraphy of the Atlantic coast of Morocco. *Micropaleontology* 48, 257–272.
- Warny, S., Bart, P.J., Suc, J.-P., 2003. Timing and progression of climatic, tectonic and glacioeustatic influences on the Messinian Salinity Crisis. *Palaeogeogr. Palaeoclimatol. Palaeoecol.* 202, 59–66.
- Zhang, J., Scott, D.B., 1996. Messinian deep-water turbidites and glacio-eustatic sea-level changes in the North Atlantic: linkage to the Mediterranean Salinity Crisis. *Paleoceanography* 11, 277–297.
- Zheng, Z., Cravatte, J., 1986. Etude palynologique du Pliocène de la Côte d'Azur (France) et du littoral ligure (Italie). *Geobios* 19 (6), 815–823.

Pollen records and climatic cycles in the North Mediterranean region since 2.7 Ma

JEAN-PIERRE SUC & SPERANTA-MARIA POPESCU

Laboratoire PaléoEnvironnements et PaléobioSphère (UMR 5125 CNRS), Université Claude Bernard – Lyon 1, 27–43 boulevard du 11 Novembre, 69622 Villeurbanne Cedex France.

(e-mail: jean-pierre.suc@univ-lyon1.fr; popescu@univ-lyon1.fr)

Abstract: This synthesis incorporates the 16 most important pollen records available across the North Mediterranean region *sensu lato* for the last 2.7 Ma. Their location is discussed with respect to the present-day bioclimatic Mediterranean realm. A special effort has been made to redraw, where necessary, the pollen records in terms of modern cyclostratigraphy. The complexity of the evolution of the Mediterranean flora and vegetation as forced by the climatic cycles is evident. The influence of the latitudinal thermic (and xeric) gradient is confirmed, and the superimposition of a longitudinal gradient, forced by the Asian monsoon, is considered. The Mediterranean flora and vegetation were not altered by any important event during the Early–Middle Pleistocene transition between 1.2 and 0.7 Ma.

This paper presents a synthesis of the vegetational and climatic evolution within the bioclimatically defined Mediterranean realm for the crucial time-window of 1.2–0.7 Ma. During this interval, 40 ka obliquity-forced climatic cycles were progressively replaced by *c.* 100 ka glacial–interglacial oscillations paced by multiples of 20 ka precession cycles (Ruddiman 2003; Maslin & Ridgwell 2005). The aim is to document changes that occurred, or did not occur, in this region in response to this global upheaval in climate pattern, known as the mid-Pleistocene revolution. In order to gain a broad insight based on pollen records, it is necessary to widen the spotlight beyond 1.2–0.7 Ma and include pollen data from 2.7 Ma to the present day. This record starts at the beginning of pronounced climatic cycles in the northern hemisphere, and provides a long chronological record from the Praetiglian Stage to the Holocene (Zagwijn 1975) during which time the effects of successive types of climatic cycle have been experienced.

The bioclimatic Mediterranean realm is today defined using the seasonal distribution of temperature and precipitation, summer (the warmest season) being dry (Quézel & Médail 2003). This realm is clearly delimited (Fig. 1), and is subdivided into several belts according to temperature namely the thermo-Mediterranean ($m > 3^{\circ}\text{C}$), meso-Mediterranean ($0^{\circ}\text{C} < m < 3^{\circ}\text{C}$), supra-Mediterranean ($-3^{\circ}\text{C} < m < 0^{\circ}\text{C}$), mountain-Mediterranean ($-7^{\circ}\text{C} < m < 3^{\circ}\text{C}$) and oro-Mediterranean ($m < -7^{\circ}\text{C}$) belts, where 'm' is the mean of the minima of the coldest month (Quézel & Médail 2003). The thermo-Mediterranean belt is characterized by a plant association rich in *Olea europaea*, *Ceratonia siliqua*, *Chamaerops humilis*, *Pinus halepensis*, *P. brutia*, *Juniperus phoenicea*, *Myrtus communis*, *Pistacia lentiscus*, *P. terebinthus*

and *Lygeum spartium*, while the meso-Mediterranean belt also includes *Olea europaea*, several evergreen species of *Quercus* (e.g. *Q. ilex*, *Q. coccifera*, *Q. suber*), *Pinus halepensis*, *P. brutia*, *Phillyrea* and *Pistacia*. The supra-Mediterranean belt is rich in deciduous *Quercus* with *Ostrya* and *Carpinus orientalis*; the mountain-Mediterranean belt comprises *Pinus nigra*, *Cedrus*, *Abies*, *Fagus* and *Juniperus*; and the oro-Mediterranean belt consists mainly of *Juniperus* and prickly xerophytes (Quézel & Médail 2003). In addition, types of vegetation depend on the superimposition of the amount of rainfall: desert (perarid bioclimate: mean annual precipitation (MAP) < 100 mm); steppe rich in *Artemisia* and other herbs (arid bioclimate: $100 < \text{MAP} < 250$ mm); forest-steppe with *Artemisia*, *Pinus halepensis*, *Juniperus* and scarce evergreen *Quercus* (semiarid bioclimate: $250 < \text{MAP} < 600$ mm); evergreen forest with sclerophilous oaks, *Pinus pinaster* and *P. pinea* (subhumid bioclimate: $600 < \text{MAP} < 800$ mm); and mixed forest with deciduous oaks, *Fagus* and conifers such as *Cedrus* and *Abies* (humid bioclimate: $\text{MAP} > 800$ mm) (MAP values: if $m = 0^{\circ}\text{C}$; Quézel & Médail 2003). However, *Artemisia* steppes are significant in several contexts: they generally correspond to dry environments (steppes with xeric forcing), but others can develop at high Mediterranean altitude under elevated precipitations (steppes with thermal forcing; Quézel & Barbero 1982).

The modern bioclimatic Mediterranean realm is known to have existed since 3.6 Ma (Suc 1984), i.e. the mid-Pliocene, at a time when the Alpine massifs, such as in the French Southern Alps, Calabria, Peloponnesus and South Anatolia, were less elevated than today. For example, a reconstruction based on pollen data and geomorphology indicates that the

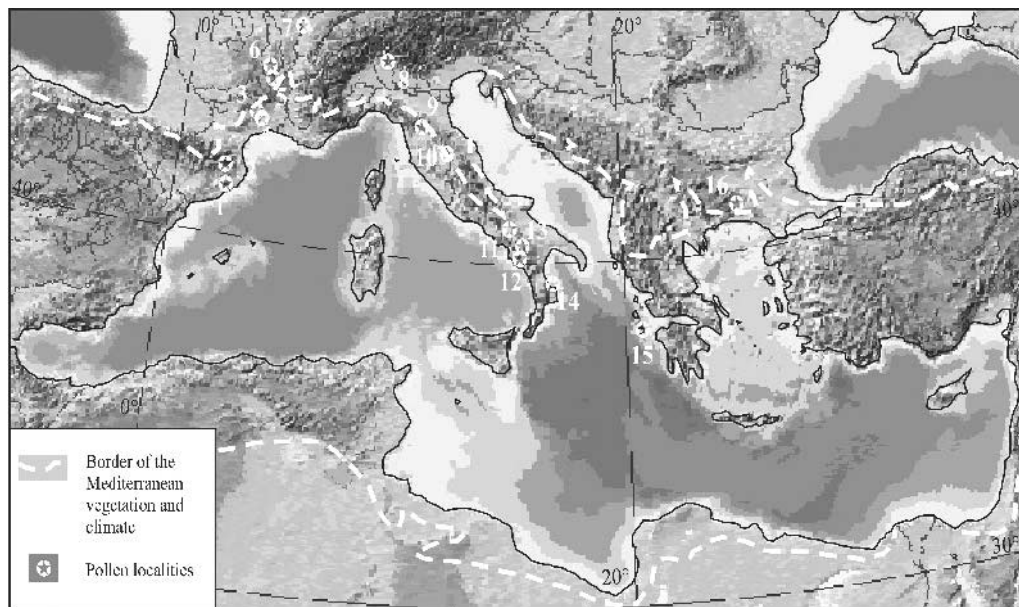


Fig. 1. Map of the Mediterranean region including the pollen localities discussed and the border of the Mediterranean-type vegetation and climate (Quézel & Médail 2003). Localities: 1, Garraf 1; 2, Banyoles; 3, Bernasso; 4, Saint-Macaire; 5, Ceyszac; 6, Senèze; 7, Bresse; 8, Piànico-Sèllere; 9, Upper Valdarno; 10, Colle Curti and Cesi; 11, Acerno; 12, Camerota; 13, Vallo di Diano; 14, Crotone; 15, Zakynthos; 16, Tenaghi Philippon.

Mercantour Massif (French Southern Alps) was 30% less elevated in the Early Pliocene than today (Fauquette *et al.* 1999). Similarly, the Silla Massif (Calabria) is estimated to have been 20% lower during the Early Pleistocene than today (Ciaranfi *et al.* 1983). Nevertheless, despite significant subsequent mountain uplift, the modern bioclimatic subdivision of the Mediterranean realm was already in place at that time (Suc *et al.* 1995*b*) and was merely amplified during the Late Pliocene and Early Pleistocene (Suc *et al.* 1995*a*). Therefore, comparisons will be made in this paper between pollen sites located within the bioclimatic Mediterranean realm and those beyond it (Fig. 1; Quézel & Médail 2003), in order to appreciate fine differences in vegetation irrespective of whether the localities belong to the earliest or most recent glacials and interglacials. In addition, the aforementioned ambivalent significance of modern *Artemisia* steppes was recently emphasized for the Late Pliocene and Early Pleistocene of the north-central Mediterranean region (Subally & Quézel 2002). This also requires comparison between pollen localities of the Mediterranean realm and those beyond.

This synthesis will be used to reinterpret the considered localities in terms of cyclostratigraphy, and to propose a more accurate chronological assignment than was available for most of them when they were published (the exceptions being Senèze,

Crotone, Vallo di Diano, Zakynthos and Tenaghi Philippon). The flora, vegetation and climate will be discussed according to the location of the pollen records. Finally, some relevant discrepancies noted between the northwestern and northeastern Mediterranean climatic patterns will be discussed.

Floral and vegetational changes, and climatic cycles in the North Mediterranean realm

The pollen localities at Garraf 1, Zakynthos and Croton are marine, the last of these being just 30 km from present-day elevations of 1700 m. However, most sites are lacustrine, and some are today located at altitudes below 200 m, i.e. Saint-Macaire, Banyoles, Bresse and Tenaghi Philippon, of which the last three are just 30 km from present high relief of 1000–1500 m. Other localities are now at low altitudes of 200–300 m, i.e. Upper Valdarno, Camerota, and Piànico-Sèllere, but are immediately surrounded by high relief of 1200–2500 m. Some localities are at mid-altitudes of around 500 m, i.e. Bernasso and Senèze, and surrounded by old plateaus of only 700 m, whereas Vallo di Diano is surrounded by still uplifting high massifs of 1000 to 1600 m. Other localities are at rather high altitudes of 700–850 m, i.e. Ceyszac, Cesi, Colle Curti and

Acerno, and are surrounded by high massifs of 1000 to 1600 m; an exception is Ceyszac which belongs to the old French Massif Central, and the present altitude of the surroundings is now probably higher than during the mid-Pleistocene.

Synthetic pollen diagrams have been constructed according to Suc (1984): plants are grouped according to the ecological significance of their modern representative, and/or to their behaviour within the pollen diagrams, e.g. *Cathaya* and the Cupressaceae. The pollen diagrams generally show regular alternations between thermophilous trees and herbs corresponding to successive climatic cycles. These cycles are supported in some cases by oxygen isotope curves obtained from the same sampling, notably at Crotone (Combourieu-Nebout & Vergnaud Grazzini 1991), Vallo di Diano (Russo Ermolli 1994) and Zakynthos (Subally *et al.* 1999) (Figs 2 & 3).

First, the accurate age of each locality will be presented and/or discussed in terms of cyclostratigraphy with respect to the reference oxygen isotope curves of Tiedemann *et al.* (1994) for Ocean Drilling Program (ODP) Site 659 (Central Eastern Atlantic Ocean) and Shackleton *et al.* (1995) for ODP Site 846 (Central Eastern Pacific Ocean) (Figs 2 & 3). Special attention will then be paid to the significance of vegetational changes as documented by pollen data, before examining whether or not the 1.2–0.7 Ma transition from Early to Middle Pleistocene is characterized by change.

Pollen diagrams and cyclostratigraphy since 2.6 Ma (Figs 2 & 3)

The Garraf 1 pollen diagram records the earliest glacial–interglacial cycles as constrained by its reliable biostratigraphy (Suc & Cravatte 1982). The illustrated part of the section shows successive peaks of steppe plants that probably correspond to even numbers of Marine Isotope Stages (MIS) from 108 to 98.

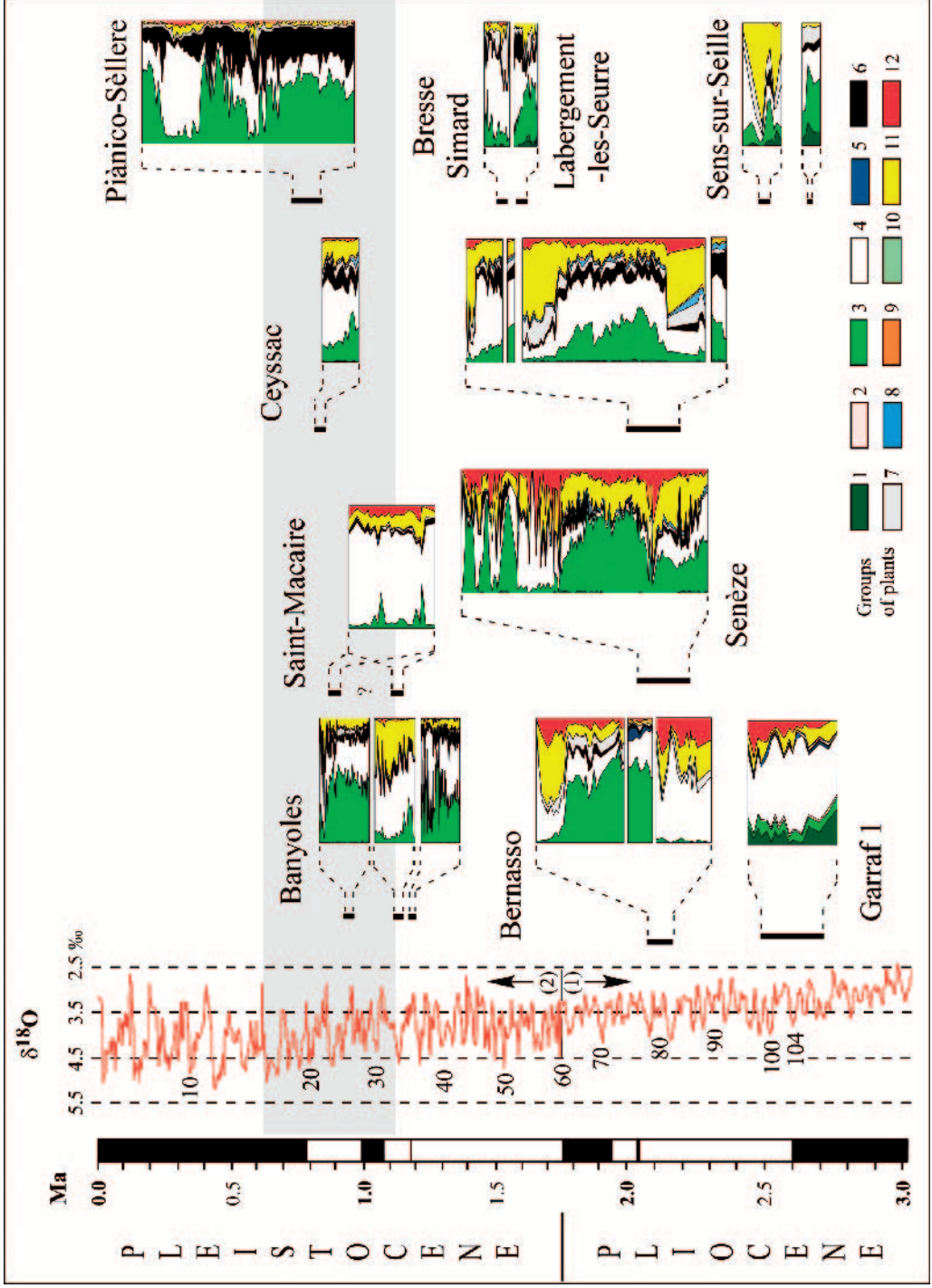
The Bernasso record (Suc 1978) is earlier than the Olduvai Subchron according to radiometric and magnetostratigraphic dating (Ambert *et al.* 1990). It can be considered as extending from MIS 82 to 78 according to the aspect of the pollen record (two strong glacials separated by an interglacial, itself interrupted by a moderate brief cooling). The Senèze record (Elhai 1969) has recently been more accurately constrained by radiometric ages and palaeomagnetism: it belongs to the interval corresponding to MIS 85 to 76 (Roger *et al.* 2000). The Ceyszac composite section is dated at its top by radiometric ages of several volcanic outflows (Ablin 1991). A re-reading of its pollen record suggests that the lower part of the section, which has been correlated with

the Senèze pollen diagram (Ablin 1991), covers a more or less continuous time-span from MIS 83 to 74; its upper part would belong to MIS 21.

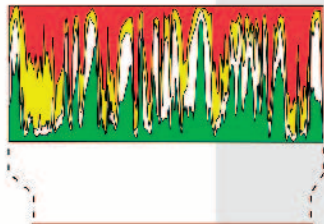
The Bresse succession comprises several localities (including Sens-sur-Seille, Labergement-les-Seurre, and Simard) and exhibits a very discontinuous pollen record dated by rodent biostratigraphy (Chaline & Farjanel 1990); it can be considered as representing MIS 107 or 105 and 100 to 98 for Sens-sur-Seille, extending from MIS 55 to 53 for Labergement-les-Seurre, and representing MIS 50 and 49 for Simard. The Banyoles composite section corresponds to three successive nested palaeolakes dated by mammal remains and palaeomagnetism (Julià Bruguès & Suc 1980; Leroy 1990; Løvlie & Leroy 1995). The discontinuous pollen record could cover MIS 35 to 34 and 25 to 24. Sediments of the Saint-Macaire maar are reverse-magnetized and have an age of between 1.4 and 0.7 Ma (i.e. between two well-dated volcanic outflows; Leroy *et al.* 1994); they correspond to a strong glacial which could belong to MIS 34 or 22.

The Piànico–Sèllere section (Moscariello *et al.* 2000) includes the Matuyama–Brunhes reversal (Pinti *et al.* 2001) and consequently should cover MIS 21 to 17. The composite Crotone series (Semaforo and Vrica sections) benefits from a detailed chronology that is based mainly on biostratigraphy and magnetostratigraphy (Spaak 1983; Pasini & Colalongo 1997; Rio *et al.* 1997) and

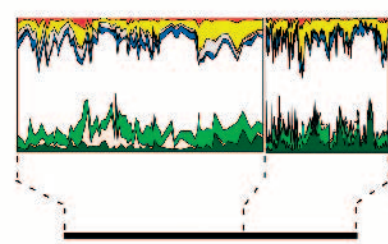
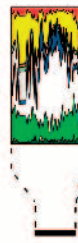
Fig. 2. (overleaf) Synthetic pollen diagrams of selected Late Pliocene to Middle Pleistocene localities from the northwestern Mediterranean region *sensu lato* (localities 1 to 8 in Fig. 1) with respect to their time control: Garraf 1 (Suc & Cravatte 1982), Bernasso (Suc 1978; Leroy & Roiron 1996), Senèze (Elhai 1969), Ceyszac (Ablin 1991), Bresse (Chaline & Farjanel 1990), Banyoles (Julià Bruguès & Suc 1980; Leroy 1990; Løvlie & Leroy 1995), Saint-Macaire (Leroy *et al.* 1994), Piànico–Sèllere (Moscariello *et al.* 2000; Pinti *et al.* 2001). The grey area represents the time window 1.2–0.7 Ma. Two successive reference oxygen isotope curves have been plotted: (1) ODP Site 846 from Shackleton *et al.* (1995); (2) ODP Site 659 from Tiedemann *et al.* (1994). Grouping of plants follows Suc (1984): 1, Mega-mesothermic (e.g. subtropical) elements (e.g. Taxodiaceae, *Engelhardia*, *Myrica*, *Microtropis fallax*, *Distylium*); 2, *Cathaya*; 3, mesothermic (i.e. warm-temperate) elements (e.g. *Quercus*, *Carya*, *Pterocarya*, *Liquidambar*, *Carpinus*, *Ulmus*, *Zelkova*, *Tilia*); 4, poorly preserved pollen grains of *Pinus* and Pinaceae; 5, meso-microthermic (i.e. temperate) elements (*Cedrus*, *Tsuga*); 6, microthermic (i.e. cold-temperate) elements (*Abies*, *Picea*); 7, palaeoecologically insignificant elements; 8, aquatic plants (e.g. *Typha*, *Potamogeton*); 9, Mediterranean xerophytes (e.g. *Olea*, *Phillyrea*, *Pistacia*, *Ceratonia*, *Cistus*, *Quercus ilex* type); 10, Cupressaceae; 11, herbs (e.g. Asteraceae, Poaceae including *Lygeum*, Amaranthaceae–Chenopodiaceae, Brassicaceae, Apiaceae); 12, steppe elements (*Artemisia*, *Ephedra*).



Tenaghi Philippon

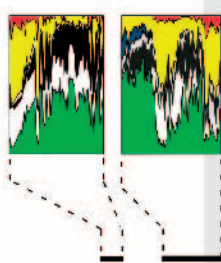


Zakynthos

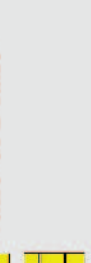


Crotone

Acerno

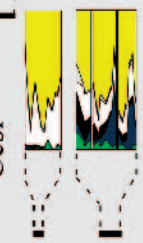


Vallo di Diano



Camerota

Cesi

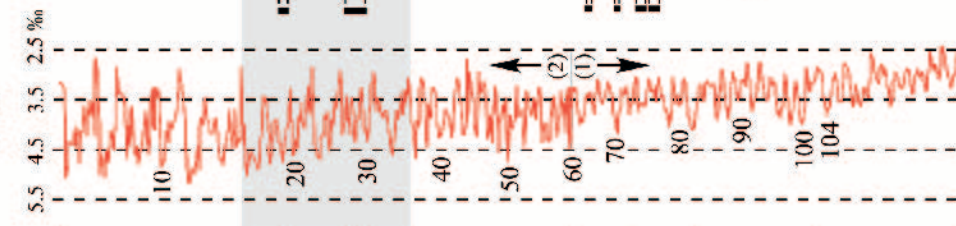


Colle Curti

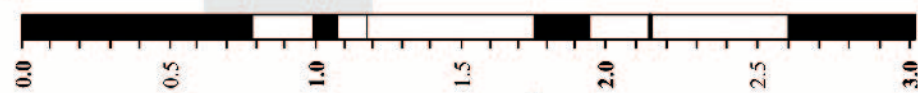


Upper Valdarno

$\delta^{18}O$



Ma



PLEISTOCENE | PLIOCENE



Groups of plants

refined by an oxygen isotope stratigraphy allowing direct correlation to the marine isotope record (Combourieu-Nebout & Vergnaud Grazzini 1991). The series represents a continuous pollen record which runs from MIS 97 to 46 (Combourieu-Nebout & Vergnaud Grazzini 1991; Combourieu-Nebout 1993).

The lower part of the Citadel section on Zakynthos Island has been studied from biostratigraphic, magnetostratigraphic and oxygen isotope perspectives: it represents a time-span from MIS 70 to 63 (Subally *et al.* 1999). The chronological placement of the Upper Valdarno composite section is given by mammal evidence combined with palaeomagnetism (Albianelli *et al.* 1995). Short, discontinuous pollen records (Albianelli *et al.* 1995) might successively belong to MIS 74, 76, 70 and 65 based on their glacial or interglacial status and vegetational dynamics. The Camerota section has no precise time control and its age is still debated (Russo Ermolli 1999). A composite pollen diagram is available which includes the section of Brenac (1984) probably overlain by borehole S1 of Russo Ermolli (1999). The presence, in very low quantities, of Taxodiaceae, *Engelhardia* and Sapotaceae pollen grains, and the absence of *Cathaya*, supports a younger age for the palaeolake of Camerota than for the Crotona series (located in the same area at low altitude). The importance of mesophilous elements seems in agreement with 'warmer' glacial–interglacial cycles and fits well with MIS 43 to 39.

The mid-altitude Colle Curti and Cesi sections contain mammal faunas and are calibrated by palaeomagnetic reversals (Jaramillo–Matuyama and Matuyama–Brunhes; Coltorti *et al.* 1998). The pollen record indicates successive glacial–interglacial cycles (Bertini 2000) that may respectively correlate with MIS 30 to 26 (Colle Curti) and 18 (Cesi). The Vallo di Diano borehole benefits from good age control (radiometric ages and oxygen isotope record): it extends from MIS 16 to 13 (Russo Ermolli

1994). The Acerno section, which includes a trachytic tuff dated at 297 ka, shows a complete climatic cycle (Munno *et al.* 2001) probably running from MIS 10 to 8. The reference Tenaghi Philippon long pollen record (Wijmstra & Groenhart 1983) represents a time interval that is reliably correlated with marine isotope stratigraphy, i.e. from MIS 25 to 1 (Mommersteeg *et al.* 1995).

Changes in the North Mediterranean vegetation and flora between 2.6 Ma and today (Figs 2 & 3)

The actual relevance of the Mediterranean steppe vegetation (herb-dominant pollen assemblages rich in *Artemisia*) to glacial phases has been established according to three distinct approaches:

- its record at Tenaghi Philippon immediately preceding the development of Holocene forest (Van der Hammen *et al.* 1971; Wijmstra & Groenhart 1983);
- its record in the Autan 1 and Garraf 1 boreholes as the first steppe development of the Late Pliocene (Cravatte & Suc 1981; Suc & Cravatte 1982);
- its correspondence with the oxygen isotope record from the Crotona series (Combourieu-Nebout & Vergnaud Grazzini 1991).

A transect of pollen records from northwestern Europe to the Mediterranean allowed Suc & Zagwijn (1983) to reconstruct the vegetation of the Last Glacial: in addition to the continuous prevalence of herbs, this transect shows a southward increase in *Artemisia* with a significant threshold when entering the Mediterranean bioclimatic realm. Such a trend is found again here when comparing the Bresse and Piànico–Sèllere glacial pollen floras (located distinctly outside of the Mediterranean bioclimatic realm with respect to latitude; Fig. 1) with others presented on Figure 2, whatever their age (earliest or most recent climatic cycles). Similar latitudinal and mostly palaeoaltitudinal features discriminate the Colle Curti and Cesi pollen diagrams (North Apennines) from others in southern Italy (Camerota and Vallo di Diano) shown on Figure 3. Hence, the development of *Artemisia* steppe, when represented by widespread herbs, depends not only on the latitude but also the altitude and probably the location of the area with respect to the circulation of air masses. The present-day *Artemisia* steppes are linked to arid and subarid bioclimates (Quézel & Médail 2003). For example, *Artemisia* steppe never expanded significantly at the expense of conifer forest in the Po Valley during glacials. This is explained by the high moisture present in the area

Fig. 3. (*previous page*) Synthetic pollen diagrams of selected Late Pliocene to Middle Pleistocene localities from the central and eastern South Mediterranean region (localities 9 to 16 in Fig. 1) with respect to their time control: Upper Valdarno (Albianelli *et al.* 1995), Colle Curti (Bertini 2000), Cesi (Bertini 2000), Camerota (Brenac 1984; Russo Ermolli 1999), Crotona (Combourieu-Nebout & Vergnaud Grazzini 1991; Combourieu-Nebout 1993), Zakynthos (Subally *et al.* 1999), Vallo di Diano (Russo Ermolli 1994), Acerno (Munno *et al.* 2001), Tenaghi Philippon (Wijmstra & Groenhart 1983). The grey area represents the time window 1.2–0.7 Ma. Two successive reference oxygen isotope curves are plotted: (1) ODP Site 846 from Shackleton *et al.* (1995); (2) ODP Site 659 from Tiedemann *et al.* (1994). Plant groups are as listed in Figure 2 caption.

since the earliest climatic cycles (Fauquette & Bertini 2003; Ravazzi 2003). To the south of the Po Valley (Upper Valdarno, Colle Curti and Cesi), the absence or sparseness of *Artemisia* steppe is probably due to the humidity even during glacials (and still persisting) at mid-altitude localities surrounded by relatively high massifs.

In the Mediterranean realm, glacials are generally characterized by an outstanding increase in herbs, especially *Artemisia*. Nevertheless, the percentage of *Artemisia* varies not only with the geographical features of the pollen site (latitude, palaeoaltitude, palaeoaltitude of the surrounding massifs, etc.) but also with the related time interval. For example, most of the earliest glacials show elevated percentages of *Artemisia* (Garraf 1, Bernasso, Senèze and Ceysac in Fig. 2; Crotona in Fig. 3) that denote drier conditions corresponding to cooler phases as documented by the oxygen isotope record (MIS 100 and 98, 96, 82 and 78 representing higher values of $\delta^{18}\text{O}$). (It should be noted that the high percentages of *Pinus* pollen, which is greatly concentrated by transport to marine sedimentary basins, considerably reduces the percentages of other taxa, including *Artemisia*). The same phenomenon is observed within younger glacials (Saint-Macaire in Fig. 2; Crotona and Camerota in Fig. 3), consecutively relating to MIS 62, 58, 50 and 40, and then 34 or 22.

In contrast, the earliest interglacials are less heterogenous. They generally show a well-developed forest (see Bernasso, Senèze and Ceysac; Fig. 2), characterized by an enrichment southwards in megamesothermic trees such as the Taxodiaceae (Crotona in Fig. 3). The vegetation during younger interglacials was more homogenous (Banyoles and Pianico-Sèllere in Fig. 2) because of the disappearance of mega-mesothermic elements in southern Europe (Camerota, Vallo di Diano, Acerno and Tenaghi Philippon, Fig. 3). Nevertheless, the north-south thermal gradient was not alone in controlling the extinction of thermophilous elements, which may have persisted longer in some protected areas such as the Bresse.

When looking at the long pollen sequences of Crotona and Tenaghi Philippon, which together cover almost all the considered time-span, it is clear that various types of interglacial forests succeeded one another: mixed forests characterized by large amounts of Taxodiaceae (*Sequoia*-type pollen grains), mixed forests where *Cathaya* (an altitudinal conifer living today in subtropical China) prevailed, mixed forests more equitably dominated by Taxodiaceae and deciduous trees, and forests exclusively composed of deciduous trees (Fig. 3). This record respectively concerns: (1) MIS 97 to 75, then (2) 73 to 51, then (3) 49 to 35, and finally (4) 31 to 1. It denotes four long climatic intervals as established by Zagwijn (1975), successively consisting of: (1)

long warm interglacials with cool-temperate glacials (Tiglian A–B); (2) temperate long (Tiglian C) and shorter (Eburonian) interglacials with cooler glacials; (3) warm-temperate long interglacials (Waalian) with cool-temperate glacials; and (4) warm-temperate brief interglacials with longer and colder glacials (Menapian to present). This analysis, obvious in the northern Mediterranean region when considering the amount of subtropical and then warm-temperate trees remaining during glacials, supports the validity of Zagwijn's (1975) subdivisions. These so-called megacycles have recently been relaunched on the basis of oxygen isotope records by Kukla & Cilek (1996).

In addition, it has been demonstrated by Combourieu-Nebout (1993) for the Crotona succession that vegetation dynamics during interglacial-glacial transitions 2.4 Ma ago were almost the same as for the recent climatic cycles, based on the reconstruction of Van der Hammen *et al.* (1971): temperature increased prior to precipitation which continued to increase even when temperature started to decrease. Such vegetational dynamics are obvious not only at Crotona (Fig. 3) but also at Senèze, Ceysac, Vallo di Diano and Camerota, and to a lesser degree at Bernasso (Figs 2 & 3).

However, such a synthetic framework is complicated in the Mediterranean region by the effects of latitudinal (and altitudinal) and longitudinal gradients.

Effects of latitudinal and longitudinal gradients on past Mediterranean vegetation and flora

The influence of a north-south gradient is reflected mainly in the thermophilous trees. Coeval pollen records show an increased quantity of thermophilous elements to the south, a trend that becomes evident when comparing the Senèze (Fig. 2) and Crotona (Fig. 3) pollen records, especially for the Taxodiaceae. Furthermore, the progressive disappearance of these thermophilous elements, which are today absent from the Mediterranean realm, occurred predominantly from north to south (Suc 1996; Popescu 2001; Suc *et al.* 2004) where they persisted until about 1 Ma ago (data from Caltagirone in Sicily: study in progress), i.e. when more severe climatic conditions began in the area.

In parallel, an important influence is also exerted by the Asiatic monsoon which generates a longitudinal gradient that results in the preservation of thermophilous elements in the area, some of these persevering into recent times or even the present day: for example, the Taxodiaceae were still living on the island of Rhodes 500 ka ago (Tsampika section, study in progress), and *Pterocarya*,

Liquidambar, *Zelkova* and *Parrotia* are still extant in this region.

A problem was raised in the work of Subally *et al.* (1999) for the Citadel section of Zakynthos Island, which suggested that glacials are marked by the development of mid- to high-altitude trees (*Cedrus*, *Tsuga*, *Abies* and *Picea*), whereas interglacials are indicated by herbs (including *Artemisia*). This interpretation will be discussed in detail later.

What happened to the Mediterranean flora and vegetation during 1.2–0.7 Ma?

The cooling at 0.9 Ma has been considered severe (Ruddiman *et al.* 1989). It probably corresponds to MIS 22 which reflects strongly increased $\delta^{18}\text{O}$ values. In terms of pollen percentages, and consequently of vegetation changes, this event is not strikingly expressed. For example, in Catalonia and the Po Valley, there is no evidence within the pollen records for a greater expansion of open vegetation during glacials and a reduction of forests during interglacials. It seems that only the composition of the plant ecosystems changed significantly. Because of the low number of pollen data across this interval, only a few regions document what happened at this climatic break: Catalonia, Languedoc and the Po Valley in the northwestern Mediterranean region, and southern Italy.

Suc (1986) has discussed this scenario for the northwestern Mediterranean province. One major step occurred beforehand, at 3.6 Ma, with the establishment of a Mediterranean-like climate (i.e. double seasonality). It caused a severe impoverishment of thermophilous elements requiring humidity all year long (e.g. *Engelhardia*, *Platycarya*, *Rhoiptelea*, *Sapotaceae*, *Menispermaceae*, *Taxodiaceae*, *Symplocos*, *Microtropis fallax*, *Distylium*, *Hamamelis*). However, some elements persisted, such as *Liquidambar*, *Carya*, *Pterocarya*, *Zelkova*, *Parrotia persica*, *Eucommia*, *Cedrus*, *Cathaya* and *Tsuga*. Their disappearance from this area seems to have occurred during the early Middle Pleistocene. Meanwhile, the composition of the *Artemisia* steppes changed considerably: from 2.6 to c. 1 Ma, they included some thermophilous herbs and shrubs, such as *Phlomis fruticosa* and *Cistaceae*. The younger steppes lost these elements but contained more *Cupressaceae* and, especially, *Hippophae rhamnoides*. This probably corresponds to a lowering in temperature.

In southern Italy, a similar scenario characterized the extinction of thermophilous plants, but here it occurred later. *Engelhardia*, *Sapotaceae*, and *Distylium* were still present at Camerota (Brenac 1984; Russo Ermolli 1999) and in a slightly younger Sicilian section (Caltagirone: study in progress)

during the Early Pleistocene. Their extinction probably occurred at about 1 Ma because they are absent from the Vallo di Diano pollen record (Russo Ermolli 1994). *Taxodiaceae*, *Liquidambar*, *Carya*, *Pterocarya*, *Zelkova*, *Eucommia*, *Cedrus*, *Cathaya* and *Tsuga* were still present at Vallo di Diano (Russo Ermolli 1994). Some thermophilous plants (*Zelkova*, *Pterocarya*) were to disappear from the Rome region during the last interglacial (Follieri 1979; Follieri *et al.* 1986). *Zelkova* is still living (in very harsh conditions) in Sicily (Di Pasquale *et al.* 1992). In contrast to the northwestern Mediterranean region, herbs and shrubs associated with the *Artemisia* steppes do not show any change at about 1 Ma. They continued to include many Mediterranean thermophilous xerophytes such as *Lygeum* and *Neurada*.

This overview shows just how important latitude is for understanding vegetational and floral changes in southern Europe during the Early–Middle Pleistocene transition.

Possible discrepancy between the northwestern and northeastern Mediterranean regions

Repeated advances of Mediterranean *Artemisia* steppes have been understood as corresponding to glacials, based on the Last Glacial and earliest glacial records (Suc & Zagwijn 1983). For the earliest glacials, this hypothesis was supported by pollen and oxygen isotope analyses on the same samples from the Crotona series (Combourieu-Nebout & Vergnaud Grazzini 1991). However, this reassuring scenario was contradicted by the results of Subally *et al.* (1999) for Zakynthos Island. Here, oxygen isotope and CaCO_3 measurements were performed on the same samples as those used for pollen analysis. The curves show, for the Olduvai time interval, close similarity to the reference global oxygen isotope curve (Site ODP 846: Shackleton *et al.* 1995) and the oxygen isotope curve recorded by Combourieu-Nebout & Vergnaud Grazzini (1991) for Crotona. Pollen analyses on Zakynthos Island sediments were performed using the same method as for Crotona, and the sediments corresponded to a similar marine environment (rather deep but relatively coastal terrigenous clays). Pollen grains were transported from nearby lands that included elevated relief (the Silla Massif for the Crotona series, the Peloponnesus Massif for Zakynthos). This means that these pollen results can be directly compared, the reliability of pollen data from marine coastal deposits for vegetational reconstruction being long established (Suc *et al.* 1999). For Zakynthos, Subally *et al.* (1999) concluded that *Artemisia* steppe developed during interglacials and *Cedrus* forest during glacials, indicating that glacials were

dry to the west and humid to the east, interglacials humid to the west and dry to the east. The ambiguity in the pollen signal could come from the wide ecological range of the genus *Artemisia sensu lato* which shows the full climatic distribution from perarid and very warm conditions to humid and very cold ones (Subally & Quézel 2002). An intensive investigation is presently underway on the modern pollen of *Artemisia* as well as on fossil specimens from the Late Cenozoic of the Mediterranean area as a means to distinguish 'cool' and 'cold' *Artemisia* species from 'warm' ones using pollen morphology (Suc *et al.* 2004).

Horowitz (1989) suggested that such opposition between eastern and western Mediterranean regions has existed since the earliest climatic cycles, i.e. since 2.6 Ma. His hypothesis was based on the present-day strong climatic difference between the southeastern and the northwestern Mediterranean regions (which may increase further in the context of ongoing global warming: IPCC 2001). He considered that this phenomenon results from variations in the influence of the Asian monsoon that already existed during the Early Pliocene (Zhisheng *et al.* 2001). Bar-Matthews *et al.* (1997) have contested this hypothesis by proposing that the eastern Mediterranean region was characterized by an increase in precipitation during interglacials and a reduction during glacials on the basis of the last deglaciation and Holocene. But this idea was recently moderated somewhat, with maximum rainfall and low temperature being able to be coeval, and likewise a decrease in rainfall and increase in temperature (Bar-Matthews *et al.* 2003). This means that the matter is not completely resolved because some time lags have been evidenced for the Middle Pleistocene: (1) between *Artemisia* maxima and maxima of other herbs for the Middle Pleistocene in the Peloponnese (Okuda *et al.* 2002); and (2) between *Artemisia* maxima and the oxygen isotope curve (Capraro *et al.* 2005).

In addition, an example of the early existence (in the Early Pliocene) of some climatic opposition between southeastern and southwestern Europe is provided by pollen records from SW Romania compared to sapropel deposition in the Central Mediterranean Basin with respect to astronomical cycles (Popescu *et al.* in press). In the latter, sapropels (related to precession minima) are better expressed during eccentricity maxima (Hilgen 1991). In contrast, increasing moisture in SW Romania, characterized by expansion of marshes (also in correspondence with precession minima), is better expressed during minima of eccentricity (Popescu *et al.* in press). Accordingly, the intensity of maxima in humidity (occurring during minima of precession) alternated between the western and eastern Mediterranean regions according to fluctuations in eccentricity.

Conclusions

Sixteen pollen localities have been used for this synthesis which provides a good opportunity to recalibrate selected records in terms of modern cyclostratigraphy.

This overview emphasizes the complexity of changes in flora and vegetation related to climatic cycles in the Mediterranean realm between 2.7 Ma and today. Undoubtedly, the latitudinal thermal (and xeric) gradient (and its altitudinal equivalent) controlled most of this evolution. The timing of disappearances of thermophilous plants in a north-south orientation is a clear consequence of this forcing, as well as the persistence of 'warm' steppes to the south after 1 Ma. In addition, a longitudinal Mediterranean gradient is superimposed on the previous one, reflecting the influence of the Asian monsoon. The question of the existence of some (discontinuous?) discrepancy between northeastern and northwestern Mediterranean regions during glacials and interglacials is not completely resolved and requires further research. No important event characterized the 1.2–0.7 Ma Early–Middle Pleistocene transition in the Mediterranean flora and vegetation.

This paper is a contribution to the French Programme 'Environnement, Vie et Sociétés' (Institut Français de la Biodiversité). It has also been supported by the Italian–French Programme 'Galileo'. M.J. Head is acknowledged for improving the English, and the two reviewers, A. Horowitz and P.C. Tzedakis, are thanked for their constructive comments.

References

- ABLIN, D. 1991. Analyse pollinique des dépôts lacustres de Ceyssac, Plio-Pléistocène du Velay (Massif Central, France). *Cahiers de Micropaléontologie*, **6**(1), 21–38.
- ALBIANELLI, A., BERTINI, A., MAGI, M., NAPOLEONE, G. & SAGRI, M. 1995. Il bacino plio-pleistocenico del Valdarno superiore: eventi deposizionali, paleomagnetici e paleoclimatici. *Il Quaternario*, **8**(1), 11–18.
- AMBERT, P., BOVEN, A., LEROY, S., LØVLIE, R. & SERET, G. 1990. Révision chronostratigraphique de la séquence paléobotanique de Bernasso (Escandorgue, Midi de la France). *Comptes Rendus de l'Académie des Sciences de Paris, ser. 2*, **311**, 413–419.
- BAR-MATTHEWS, M., AYALON, A. & KAUFMAN, A. 1997. Late Quaternary paleoclimate in the eastern Mediterranean region from stable isotope analysis of speleothems at Soreq Cave, Israel. *Quaternary Research*, **47**, 155–168.
- BAR-MATTHEWS, M., AYALON, A., GILMOUR, M., MATTHEWS, A. & HAWKESWORTH, C.J. 2003. Sea-land oxygen isotopic relationships from planktonic foraminifera and speleothems in the Eastern Mediterranean region and their implication for paleorainfall during interglacial intervals. *Geochimica et Cosmochimica Acta*, **67**(17), 3181–3199.

- BERTINI, A. 2000. Pollen record from Colle Curti and Cesi: Early and Middle Pleistocene mammal sites in the Umbro-Marchean Apennine Mountains (central Italy). *Journal of Quaternary Science*, **15**(8), 825–840.
- BRENAC, P. 1984. Végétation et climat de la Campanie du Sud (Italie) au Pliocène final d'après l'analyse pollinique des dépôts de Camerota. *Ecologia Mediterranea*, **10**(3–4), 207–216.
- CAPRARO, L., ASIOLI, A., BACKMAN, J., BERTOLDI, R., CHANNELL, J.E.T., MASSARI, F. & RIO, D. 2005. Climatic patterns revealed by pollen and oxygen isotope records across the Matuyama–Brunhes Boundary in the central Mediterranean (southern Italy). In: HEAD, M.J. & GIBBARD, P.L. (eds) *Early–Middle Pleistocene Transition: The Land–Ocean Evidence*. Geological Society, London, Special Publications, 159–182.
- CHALINE, J. & FARJANEL, G. 1990. Plio–Pleistocene rodent biostratigraphy and palynology of the Bresse Basin, France and correlations within western Europe. *Boreas*, **19**, 69–80.
- CIARANFI, N., GUIDA, M. ET AL. 1983. Elementi sismotettonici dell'Apennino meridionale. *Bollettino della Società geologica Italiana*, **102**, 201–222.
- COLTORTI, M., ALBIANELLI, A., BERTINI, A., FICCARELLI, G., LAURENZI, M.A., NAPOLEONE, G. & TORRE, D. 1998. The Colle Curti Mammal site in the Colfiorito areas (Umbria–Marchean Apennine, Italy): geomorphology, stratigraphy, paleomagnetism and palynology. *Quaternary International*, **47–48**, 107–116.
- COMBOURIEU-NEBOUT, N. 1993. Vegetation response to Upper Pliocene glacial/interglacial cyclicity in the Central Mediterranean. *Quaternary Research*, **40**, 228–236.
- COMBOURIEU-NEBOUT, N. & VERGNAUD GRAZZINI, C. 1991. Late Pliocene Northern Hemisphere glaciations: the continental and marine responses in the Central Mediterranean. *Quaternary Science Reviews*, **10**, 319–334.
- CRAVATTE, J. & SUC, J.-P. 1981. Climatic evolution of North-Western Mediterranean area during Pliocene and Early Pleistocene by pollen-analysis and forams of drill Autan 1. Chronostratigraphic correlations. *Pollen et Spores*, **23**(2), 247–258.
- DI PASQUALE, G., GARFI, G. & QUÉZEL, P. 1992. Sur la présence d'un *Zelkova* nouveau en Sicile sud-orientale (Ulmaceae). *Biocosme mésogéen*, **8–9**, 401–409.
- ELHAL, J. 1969. La Flore sporo-pollinique du gisement villafranchien de Senèze (Massif Central-France). *Pollen et Spores*, **11**, 127–139.
- FAUQUETTE, S. & BERTINI, A. 2003. Quantification of the northern Italy Pliocene climate from pollen data: evidence for a very peculiar climate pattern. *Boreas*, **32**, 361–369.
- FAUQUETTE, S., CLAUZON, G., SUC, J.-P. & ZHENG, Z. 1999. A new approach for palaeoaltitude estimates based on pollen records: example of the Mercantour Massif (southeastern France) at the earliest Pliocene. *Earth Planetary and Science Letters*, **170**, 35–47.
- FOLLIERI, M. 1979. Late Pleistocene floristic evolution near Rome. *Pollen et Spores*, **21**(1–2), 135–148.
- FOLLIERI, M., MAGRI, D. & SADORI, L. 1986. Late Pleistocene *Zelkova* extinction in central Italy. *New Phytologist*, **103**, 269–273.
- HILGEN, F.J. 1991. Extension of the astronomically calibrated (polarity) time scale to the Miocene/Pliocene boundary. *Earth and Planetary Science Letters*, **107**, 349–368.
- HOROWITZ, A. 1989. Continuous pollen diagrams for the last 3.5 MY from Israel: vegetation, climate and correlation with the oxygen isotope record. *Palaeogeography, Palaeoclimatology, Palaeoecology*, **72**, 63–78.
- IPCC 2001. Intergovernmental Panel on Climate Change. World wide web Address: http://ipcc-ddc.cru.uea.ac.uk/cru_data/datadownload/download_index.html.
- JULIÀ BRUGUÈS, R. & SUC, J.-P. 1980. Analyse pollinique des dépôts lacustres du Pléistocène inférieur de Banyoles (Bañolas, site de la Bòbila Ordis – Espagne): un élément nouveau dans la reconstitution de l'histoire paléoclimatique des régions méditerranéennes d'Europe occidentale. *Geobios*, **3**(1), 5–19.
- KUKLA, G. & CILEK, V. 1996. Plio–Pleistocene megacycles: record of climate and tectonics. *Palaeogeography, Palaeoclimatology, Palaeoecology*, **120**, 171–194.
- LEROY, S. 1990. *Paléoclimats plio-pléistocènes en Catalogne et Languedoc d'après la palynologie de formations lacustres*. PhD thesis, Université Catholique de Louvain.
- LEROY, S. & ROIRON, P. 1996. Latest Pliocene pollen and leaf floras from Bernasso palaeolake (Escandorgue Massif, Hérault, France). *Review of Palaeobotany and Palynology*, **94**, 295–328.
- LEROY, S., AMBERT, P. & SUC, J.-P. 1994. Pollen record of the Saint-Macaire maar (Hérault, southern France): a Lower Pleistocene glacial phase in the Languedoc coastal plain. *Review of Palaeobotany and Palynology*, **80**, 149–157.
- LØVLIE, R. & LEROY, S. 1995. Magnetostratigraphy of the Lower Pleistocene Banyoles palaeolake carbonate sediments from Catalonia, NE Spain: evidence for relocation of the Cobb Mountain Sub-Chron. *Quaternary Science Reviews*, **14**, 473–485.
- MASLIN, M.A. & RIDGWELL, A.J. 2005. Mid-Pleistocene revolution and the 'eccentricity myth'. In: HEAD, M.J. & GIBBARD, P.L. (eds) *Early–Middle Pleistocene Transition: The Land–Ocean Evidence*. Geological Society, London, Special Publications, 19–34.
- MOMMERSTEEG, H.J.P.M., LOUTRE, M.-F., YOUNG, R., WIJMSTRA, T.A. & HOOGHIEPSTRA, H. 1995. Orbital forced frequencies in the 975 000 year pollen record from Tenaghi Philippon (Greece). *Climate Dynamics*, **11**, 4–24.
- MOSCARIELLO, A., RAVAZZI, C. ET AL. 2000. A long lacustrine record from the Piànico–Sèllere Basin (Middle–Late Pleistocene, Northern Italy). *Quaternary International*, **73–74**, 47–68.
- MUNNO, R., PETROSINO, P., ROMANO, P., RUSSO ERMOLLI, E. & JUVIGNÉ, E. 2001. A Late Middle Pleistocene climatic cycle in Southern Italy inferred from pollen analysis and tephrostratigraphy of the Acerno lacustrine succession. *Géographie physique et Quaternaire*, **55**(1), 87–99.
- OKUDA, M., VAN VUGT, N., NAKAGAWA, T., IKEYA, M., HAYASHIDA, A., YASUDA, Y. & SETOGUCHI, T. 2002. Palynological evidence for the astronomical origin of lignite-detritus sequence in the Middle Pleistocene Marathousa Member, Megalopolis, SW Greece. *Earth and Planetary Science Letters*, **201**, 143–157.

- PASINI, G. & COLALONGO, M.L. 1997. The Pliocene–Pleistocene boundary-stratotype at Vrica, Italy. In: VAN COUVERING, J. (ed.) *The Pleistocene Boundary and the Beginning of the Quaternary*. Cambridge University Press, Cambridge, 15–45.
- PINTI, D.L., QUIDELLEUR, X., CHIESA, S., RAVAZZI, C. & GILLOT, P.-Y. 2001. K-Ar dating of an early Middle Pleistocene distal tephra in the interglacial varved succession of Piànico–Sèllere (Southern Alps, Italy). *Earth and Planetary Science Letters*, **188**, 1–7.
- POPESCU, S.-M. 2001. *Végétation, climat et cyclostratigraphie en Paratéthys centrale au Miocène supérieur et au Pliocène inférieur d'après la palynologie*. PhD thesis, Université Claude Bernard, Lyon 1.
- POPESCU, S.-M., SUC, J.-P. & LOUTRE, M.-F. Early Pliocene vegetation changes forced by eccentricity–precession in Southwestern Romania. In: AGUSTI, J., OMS, O. & MEULENKAMP, J.E. (eds) *Late Miocene to Early Pliocene environment and climate-change in the Mediterranean area*. *Palaeogeography, Palaeoclimatology, Palaeoecology* (in press).
- QUÉZEL, P. & BARBERO, M. 1982. Definition and characterization of mediterranean-type ecosystems. *Ecologia Mediterranea*, **8**, 15–29.
- QUÉZEL, P. & MÉDAIL, F. 2003. *Ecologie et biogéographie des forêts du bassin méditerranéen*. Elsevier, Paris.
- RAVAZZI, C. 2003. Gli antichi baccini lacustri e i fossili di Leffe, Ranica e Piànico–Sèllere (Prealpi Lombarde). *Quaderni di Geodinamica Alpina e Quaternaria e Quaderni delle Comunità Montana Valle Seriana*, 9–176.
- RIO, D., RAFFI, I. & BACKMAN, J. 1997. Calcareous nannofossil biochronology and the Pliocene–Pleistocene boundary. In: VAN COUVERING, J. (ed.) *The Pleistocene Boundary and the Beginning of the Quaternary*. Cambridge University Press, Cambridge, 63–78.
- ROGER, S., COULON, C. ET AL. 2000. $^{40}\text{Ar}/^{39}\text{Ar}$ dating of a tephra layer in the Pliocene Senèze maar lacustrine sequence (French Massif Central): constraint on the age of the Réunion–Matuyama transition and implications on paleoenvironmental archives. *Earth and Planetary Science Letters*, **183**, 431–440.
- RUDDIMAN, W.F. 2003. Orbital insolation, ice volume, and greenhouse gases. *Quaternary Science Reviews*, **22**, 15–17, 1597–1629.
- RUDDIMAN, W.F., RAYMO, M.E., MARTINSON, D.J., CLEMENT, B.M. & BACKMAN, J. 1989. Pleistocene evolution: Northern Hemisphere ice sheets and North Atlantic Ocean. *Paleoceanography*, **2**(4), 353–412.
- RUSSO ERMOLLI, E. 1994. Analyse pollinique de la succession lacustre pléistocène du Vallo di Diano (Campanie, Italie). *Annales de la Société géologique de Belgique*, **117**(2), 333–354.
- RUSSO ERMOLLI, E. 1999. Vegetation dynamics and climate changes at Camerota (Campania, Italy) at the Pliocene–Pleistocene boundary. *Il Quaternario*, **12**(2), 207–214.
- SHACKLETON, N.J., HALL, M.A. & PATE, D. 1995. Pliocene stable isotope stratigraphy of ODP Site 846. In: PISIAS, G., MAYER, L.A. ET AL. (eds) *Proceedings of the Ocean Drilling Program, Scientific Results*, **138**, 337–355.
- SPAACK, P. 1983. Accuracy in correlation and ecological aspects of the planktonic foraminiferal zonation of the Mediterranean Pliocene. *Utrecht Micropaleontological Bulletin*, **28**, 1–159.
- SUBALLY, D. & QUÉZEL, P. 2002. Glacial or interglacial: *Artemisia* a plant indicator with dual responses. *Review of Palaeobotany and Palynology*, **120**, 123–130.
- SUBALLY, D., BILODEAU, G., TAMRAT, E., FERRY, S., DEBARD, E. & HILLAIRE-MARCEL, C. 1999. Cyclic climatic records during the Olduvai Subchron (Uppermost Pliocene) on Zakyntos Island (Ionian Sea). *Geobios*, **32**(6), 793–803.
- SUC, J.-P. 1978. Analyse pollinique de dépôts plio–pléistocènes du sud du Massif basaltique de l'Escandorgue (série de Bernasso – Lunas, Hérault – France). *Pollen et Spores*, **20**(4), 497–512.
- SUC, J.-P. 1984. Origin and evolution of the Mediterranean vegetation and climate in Europe. *Nature*, **307**, 429–432.
- SUC, J.-P. 1986. Flores néogènes de Méditerranée occidentale. Climat et paléogéographie. *Bulletin des Centres de Recherche et d'Exploration-Production d'Elf-Aquitaine*, **10**(2), 477–488.
- SUC, J.-P. 1996. Late Neogene vegetation changes in Europe and North Africa. *Europal Newsletter*, **10**, 2–28.
- SUC, J.-P. & CRAVATTE, J. 1982. Etude palynologique du Pliocène de Catalogne (nord-est de l'Espagne). *Paléobiologie continentale*, **13**(1), 1–31.
- SUC, J.-P. & ZAGWIJN, W.H. 1983. Plio–Pleistocene correlations between the northwestern Mediterranean region and northwestern Europe according to recent biostratigraphic and paleoclimatic data. *Boreas*, **12**, 153–166.
- SUC, J.-P., BERTINI, A. ET AL. 1995a. Structure of West Mediterranean vegetation and climate since 5.3 Ma. *Acta Zoologica Cracoviense*, **38**(1), 3–16.
- SUC, J.-P., DINIZ, F. ET AL. 1995b. Zanclean (~Brunsumian) to early Piacenzian (~early–middle Reuverian) climate from 4° to 54° north latitude (West Africa, West Europe and West Mediterranean areas). *Mededelingen Rijks Geologische Dienst*, **52**, 43–56.
- SUC, J.-P., FAUQUETTE, S. ET AL. 1999. Neogene vegetation changes in West European and West circum-Mediterranean areas. In: AGUSTI, J., ROOK, L. & ANDREWS, P. (eds) *Hominid Evolution and Climate in Europe, 1. Climatic and Environmental Change in the Neogene of Europe*. Cambridge University Press, Cambridge, 370–385.
- SUC, J.-P., FAUQUETTE, S. & POPESCU, S.-M. 2004. L'investigation palynologique du Cénozoïque passe par les herbiers. *Actes du Colloque "Les herbiers: un outil d'avenir. Tradition et modernité"*, Villeurbanne. Edit. Association française pour la Conservation des Espèces Végétales, Nancy, 67–87.
- TIEDEMANN, R., SARTHEIN, M. & SHACKLETON, N.J. 1994. Astronomic timescale for the Pliocene Atlantic $\delta^{18}\text{O}$ and dust flux records of Ocean Drilling Program Site 659. *Paleoceanography*, **9**(4), 619–638.
- VAN DER HAMMEN, T. WIMSTRA, T.A. & ZAGWIJN, W.H. 1971. The floral record of the Late Cenozoic of Europe. In: TUREKIAN, K. (ed) *The Late Cenozoic Glacial Ages*. Yale University Press, Cambridge, 391–424.

Influence of Mediterranean sea-level changes on the Dacic Basin (Eastern Paratethys) during the late Neogene: the Mediterranean Lago Mare facies deciphered

Georges Clauzon*, Jean-Pierre Suc†, Speranta-Maria Popescu†, Mariana Marunteanu‡, Jean-Loup Rubino¶, Florian Marinescu‡ and Mihaela Carmen Melinte§

*C.E.R.E.G.E. (UMR 6635 CNRS), Université Paul Cézanne, Europôle de l'Arbois, Aix-en-Provence, France

†Laboratoire PaléoEnvironnements et PaléobioSphère (UMR 5125 CNRS), Université Claude Bernard-Lyon 1, Villeurbanne, France

‡Geological Institute of Romania, Bucharest, Romania

¶TOTAL, TG/ISS, CSTTF, Pau, France

§National Institute of Marine Geology and Geoecology, Bucharest, Romania

ABSTRACT

A recently published scenario viewing the Messinian salinity crisis as two evaporitic steps rather than one has led to a search for new indices of the crisis in the Eastern Paratethys. Fluvial processes characterized the southwestern Dacic Basin (Southern Romania, i.e. the Carpathian foredeep) whereas brackish sediments were continuously deposited in its northern part. This is consistent with previously evidenced responses of the Black Sea to the Messinian salinity crisis. High sea-level exchanges between the Mediterranean Sea and Eastern Paratethys are considered to have occurred just before and just after desiccation of the Mediterranean. This accounts for two successive Mediterranean nannoplankton-dinocyst influxes into the Eastern Paratethys that, respectively, belong to zones NN 11 and NN 12. Meanwhile, two separate events that gave rise to Lago Mare facies (with Paratethyan *Congeria*, ostracods and/or dinoflagellate cysts) arose in the Mediterranean Basin in response to these high sea-level exchanges and located 5.52 and 5.33 Ma (isotopic stages TG 11 and TG 5, respectively), i.e. just before and just after the almost complete desiccation of the Mediterranean). These Lago Mare facies formed independently of lakes with ostracods of the *Cyprideis* group that developed in the central basins during the final stages of desiccation. The gateway facilitating these water exchanges is not completely identified. A proto-Bosphorus strait seems unlikely. A plausible alternative route extends from the northern part of the Thessaloniki region up to the Dacic Basin and through Macedonia and the Sofia Basin. The expression 'Lago Mare' is chronostratigraphically ambiguous and should be discontinued for this purpose, although it might remain useful as a palaeoenvironmental term.

INTRODUCTION

The relationships between the Mediterranean Sea and the Paratethys realm have been debated for a long time (Seneš, 1973). Before 16 Ma, connections were unobstructed and faunal exchanges (planktonic and benthic foraminifers, molluscs, dinocysts, etc.) are almost continuously well documented (Rögl & Steininger, 1983). From 12 Ma, Paratethyan conditions evolved into restricted marine environments (Sacchi *et al.*, 1997), and the complete isolation of the Pannonian Basin (Western Paratethys) is generally considered to have occurred in the early Tortonian (Magyar *et al.*, 1999). Then, Paratethys became a succession of more

or less separated brackish to freshwater basins (Stevanović *et al.*, 1990).

Normal connections between the Mediterranean Sea and Paratethys are therefore commonly considered to have ended in the Late Miocene. Nevertheless, Paratethys seems to have had a strong influence on the Mediterranean region during the Messinian salinity crisis, i.e. during the so-called Lago Mare event (Cita *et al.*, 1978a). In many Mediterranean localities, the Lago Mare facies is characterized by the presence of brackish shallow water fauna (molluscs: *Congeria*, *Dreissena*, *Melanopsis*, etc.; ostracods: *Cyprideis pannonica* gr., *Loxoconcha*, *Tyrrhenocythere*, etc.) of Paratethyan origin (Ruggieri, 1967; Cita & Colombo, 1979). More recently, latest Miocene endemic Paratethyan dinocysts including *Galeacysta etrusca* (Müller *et al.*, 1999) have been frequently found in the Mediterranean (Corradini & Biffi, 1988) and added to the Lago Mare biofacies

Correspondence: J.-P. Suc, Laboratoire PaléoEnvironnements et PaléobioSphère (UMR 5125 CNRS), Université Claude Bernard-Lyon 1, 27-43 boulevard du 11 Novembre, 69622 Villeurbanne Cedex, France. E-mail: jean-pierre.suc@univ-lyon1.fr

(Bertini *et al.*, 1995; Bertini, 2002). It has been proposed that the Lago Mare event was caused by the 'capture' of Paratethyan waters by an almost desiccated Mediterranean Basin (Hsü *et al.*, 1973, 1977), the specific process of which is poorly documented (Cita, 1991). Another interpretation is proposed by Orszag-Sperber *et al.* (2000) who consider the Lago Mare event as the development of lakes within depressions caused by strong erosion in the desiccated Mediterranean without any direct linkage with Paratethys. This resulted in a broad confusion between the marginal and deep basin Lago Mare facies that is striking on Fig. 8 of Iaccarino & Bossio (1999, p. 538) who postulate two successive Lago Mare events in the late Messinian.

To explain both the Lago Mare facies in the Mediterranean realm and some Middle Tortonian (Maetotian) Mediterranean brackish mollusks and ostracods in the Eastern Paratethys (Rögl, 1996, 1998), Sprovieri *et al.* (2003) have envisaged a seaway between the Mediterranean Sea and Paratethys in the area of the present Black Sea, and repeated exchanges forced by climate fluctuations since the Tortonian.

An important part of the Eastern Paratethys consists of the Dacic Basin (Fig. 1a, b). It corresponds to the Southern Romania and is delimited to the north and west by the Carpathians, to the south by the Balkan Chain (i.e. the Moesian Platform) and to the east by the Black Sea. This area comprises the foredeep of the Carpathians and it accumulated a very thick succession of terrigenous Neogene sediments (Marinescu *et al.*, 1998). From the Early to Late Miocene (i.e. from about 25 to 10 Ma), the Dacic Basin existed as a transitional basin between the Pannonian Basin (Western Paratethys) and the Euxinian Basin (i.e. the western part of the Eastern Paratethys which extended from the present-day Black Sea across to the Aral Sea) (Rögl & Steininger, 1983; Marinescu, 1992). At about 10 Ma, it became the western appendage of the Euxinian Basin, the connection between the two basins being moderately restricted because of the presence of the Dobrogea horst (Rögl & Steininger, 1983).

The discovery of some late Neogene calcareous nannofossil floras both in Southern Romania (Mărunțeanu, 1992) and the Crimea (Semenenko & Lyuljeva, 1978; Semenenko & Olejnik, 1995) has presented a new means to understand Late Neogene relationships between the Mediterranean Sea and Eastern Paratethys, and has stimulated an intensive and very fruitful research of nannofossils in the Dacic Basin. Hence, almost seventeen recurrent discoveries of Mediterranean nannofossil occurrences have been recorded within the Dacic Basin from about 13.5 Ma up to about 3.5 Ma (Papaianopol & Mărunțeanu, 1993; Mărunțeanu & Papaianopol, 1995, 1998; Drivaliari *et al.*, 1999; Snel *et al.*, in press). This suggests that transient relationships occurred repeatedly between the Mediterranean Sea and the Dacic Basin during the late Neogene.

Accordingly, we can consider the possible influence of Mediterranean sea-level changes over the Eastern Paratethys: some Mediterranean sea-level drops might have caused the fluvial drainage of Paratethyan waters into the

Mediterranean Basin; whereas some Mediterranean sea-level rises might have caused the influx of marine surface water in the Eastern Paratethys (Sprovieri *et al.*, 2003). Such a process would explain the repeated nannofossil records in the Dacic Basin. In particular, two successive Mediterranean nannoplankton influxes have been recorded in Bosphorian sediments of the northern Dacic Basin (Mărunțeanu & Papaianopol, 1998; Snel *et al.*, in press). These sediments belong to the earliest Chron C3r (Snel *et al.*, in press). The first influx correlates to Zone NN11 zone, and the second to Zone NN12 (see Fig. 2 for the chronological assignment of the NN11–NN12 boundary, characterized by the disappearance of *Discoaster quiqueramus* and *Triquetrorhabdulus rugosus* and/or the appearance of *Ceratolithus acutus*: Berggren *et al.*, 1995a, b). These data imply two brief successive connections at high-sea level between the Mediterranean Sea and the Dacic Basin.

In the Black Sea, seismic profiles (Letouzey *et al.*, 1978; Gillet *et al.*, 2003; Gillet, 2004) and the results from three coreholes (Sites 379, 380, 381; Fig. 1a) drilled on DSDP Leg 42B (Ross *et al.*, 1978) suggest that the two main signatures of the Messinian salinity crisis in the Mediterranean exist in this basin: evaporite deposition in the abyssal plain, and an erosional surface on the margin (Hsü & Giovanoli, 1979; Gillet, 2004). Such a similar and coeval response of the Black Sea to the Messinian salinity crisis in the Mediterranean implies that the basins (including the Dacic appendage) were connected at high-sea level just before the crisis.

Several field investigations within the Dacic Basin starting in 1998 (Clauzon & Suc, 1998) were organized to test the hypothesis of Hsü & Giovanoli (1979). The Dacic Basin was chosen because of its dense record of Late Neogene Mediterranean nannofossils that should document the most elevated Mediterranean sea levels in the area. Moreover, the lack of latest Miocene sediments in the Țicleni borehole may be due to an erosional phase consistent with the Messinian salinity crisis (Drivaliari *et al.*, 1999). We focus on the time interval 6–5 Ma, i.e. the period including two major successive global low sea levels (isotopic stages TG 22 and TG 20 of Shackleton *et al.*, 1995) and three main high sea levels (isotopic stages TG 11, TG 9 and TG 5 of Shackleton *et al.*, 1995). Precise ages have been allocated to these isotopic stages by Vidal *et al.* (2002): TG 22 (5.81 Ma), TG 20 (5.76 Ma), TG 11 (5.52 Ma), TG 9 (5.43 Ma) and TG 5 (5.33 Ma). It has been established that the Messinian salinity crisis belongs to the C3r reverse chron (Gautier *et al.*, 1994; Clauzon *et al.*, 1996), its age (5.96–5.33 Ma) being specified by Krijgsman *et al.* (1999a). These successive eustatic events are manifested in the Mediterranean Basin by strong signatures (Clauzon *et al.*, 1996), respectively:

- the deposition of the marginal evaporites caused by a moderate sea-level fall,
- the final phase of carbonate platform deposition on the margins dated at about 5.60 Ma (Cornée *et al.*, 2004) and corresponding to a moderate sea-level rise,

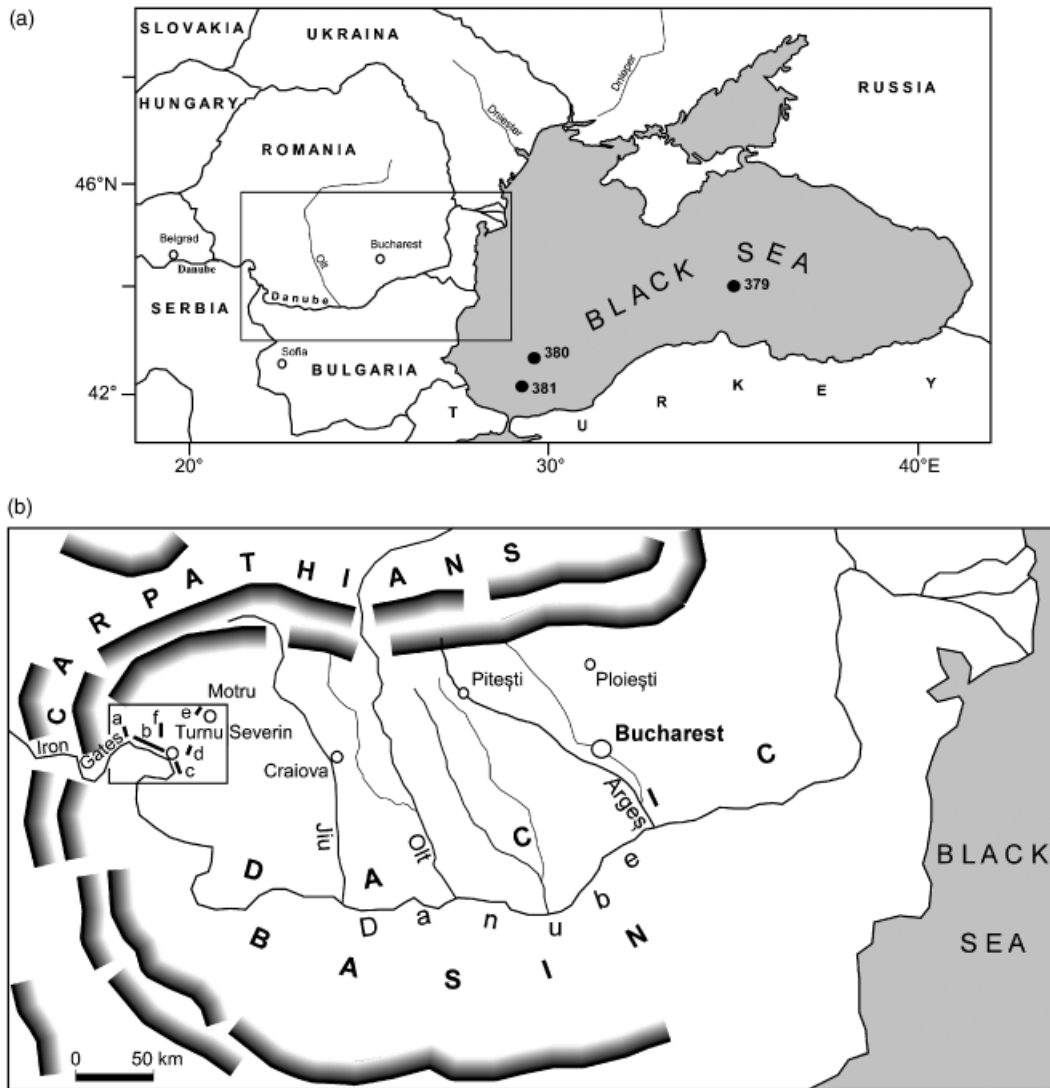


Fig. 1. Map of the Black Sea and its Western edge. (a) Location map of the Dacic Basin (box) with respect to the Black Sea and Sites 379, 380, and 381 of DSDP Leg 42B. (b) Detailed map of the Dacic Basin with the studied sections: a, Gura Vâii; b, Turnu Severin; c, Hinova; d, Husnicioara; e, Motru (Lupoiaia section); f, Vărănic.

- the Messinian erosional surface cutting, depending on the place, carbonate platform and marginal evaporites (Clauzon, 1997), marginal evaporites (Delrieu *et al.*, 1993; Fortuin *et al.*, 1995) or other older deposits (Clauzon, 1999), and corresponding to the deep desiccated basin evaporites (strong sea-level drop),
- the earliest Zanclean high-stand characterized in many places by Gilbert-type fan delta constructions (Clauzon, 1990, 1999).

In the Northwestern Mediterranean region, the two last signatures are obvious at the base of elevations, especially at the outlet of deep transverse valleys (Clauzon, 1999). For this reason, we have developed our field investigations mainly in the area of Turnu Severin where the Danube River achieves its crossing of the Carpathians (Iron Gates) (Fig. 1b). If the Black Sea and Dacic Basin have been affected by the Messinian salinity crisis, similar impacts

must also exist in the Turnu Severin area and on the Northwestern Mediterranean region.

SIGNATURES OF THE MESSINIAN SALINITY CRISIS

The Messinian salinity crisis induced two kinds of results: immediate events as deposition of (marginal and deep basin) evaporites, and erosion of the shelf and downcutting of deep subaerial canyons, and distant effects ranging from the Gilbert-type fan delta mode of sedimentary filling of the Zanclean rias, to the complete rebuilding of the shelf (Lofi *et al.*, 2003). First, we will recount the main immediate and delayed signatures of the Messinian salinity crisis within the Mediterranean Basin and the resulting scenario (Clauzon *et al.*, 1996). We will then describe our field observations in the Dacic Basin and discuss if similar or distinct

signatures might have existed in the Eastern Paratethys and whether characterize the Messinian salinity crisis in this area.

In the Mediterranean Basin

Evaporites deposited in the Mediterranean abyssal plains (reported only by seismic records) are the first consequence of the desiccation of the Mediterranean Sea (Hsü *et al.*, 1973, 1977, 1978b; Ryan *et al.*, 1973). The idea of an almost complete desiccation of the Mediterranean Sea has been supported by the dismantling of the Messinian margins under a generalized erosional surface (Ryan & Cita, 1978; Gorini *et al.*, 1993) and deep subaerial canyons along the course of rivers (Chumakov, 1973; Clauzon, 1973, 1978, 1979, 1982, 1990) because of the strong drop in sea level. The product of this erosion mostly accumulated in detritic cones at the bottom of canyons (Rizzini *et al.*, 1978; Barber, 1981; Savoye & Piper, 1991; Lofi, 2002). The erosion of the margins and their hinterland, especially by rivers, during the Messinian salinity crisis created large voids that were later occupied by Zanclean waters (the so-called Pliocene rias: Denizot, 1952; Clauzon, 1990) and infilled by Zanclean sediments. Such depositional areas possess two peculiarities from a sedimentary viewpoint: (1) they may exceed 1000 m in thickness (Nile and Rhône rias) that is unusual in a margin and (2) in space, interfluves partitioned the deposition realm so that no lateral export of material could occur from one ria to the next. As a consequence, the Zanclean rias have served as outstanding sediment traps, depriving the basin of terrigenous material (Hsü *et al.*, 1973; Cita *et al.*, 1978a, 1999). The flooding of

the Mediterranean Basin by Zanclean marine waters during the global high sea level of cycle TB3.4 (Haq *et al.*, 1987) was sudden as evidenced by the general development of downlap sedimentary constructions, i.e. the absence of any transgressive interval, as observed both within the rias (Clauzon *et al.*, 1995) and in the deep basin (Lofi *et al.*, 2003). Accordingly, the high sea-level prisms are prograding Gilbert-type fan delta constructions (Clauzon, 1990, 1999; Clauzon *et al.*, 1995).

The time interval of the Messinian salinity crisis is now well defined: it started just after the beginning of the Gilbert magnetochron (Chron C3r) (Gautier *et al.*, 1994) and more precisely at 5.96 Ma (Krijgsman *et al.*, 1999a) and ended at 5.33 Ma. (Lourens *et al.*, 1996) in correspondence with isotope stage TG 5 (Shackleton *et al.*, 1995).

A scenario was proposed by Clauzon *et al.* (1996) that reconciles discrepancies between previous models (deep basin–shallow water: Hsü *et al.*, 1973; shallow basin–shallow water: Nesteroff, 1973; deep basin–deep water: Busson, 1990). The so-called ‘two-step’ model has a new chronology constrained by the oxygen isotope curve of Vidal *et al.* (2002) and tuned to the astronomical time-scale. It is also compatible with the cyclostratigraphy proposed by Krijgsman *et al.* (1999b) for the Italian evaporites (Fig. 2). This scenario includes two evaporitic episodes forced by two sea-level drops separated by a brief sea-level rise corresponding to the Upper Evaporites of Sicily (topped by the Lago Mare Formation which is rich in Paratethyan elements Congeria, ostracods, and dinocysts and the Arenazzolo Formation), and culminating in the nearest isotopic low-¹⁸O isotope stage (isotope stage TG 11: Shackleton *et al.*, 1995) (Fig. 2):

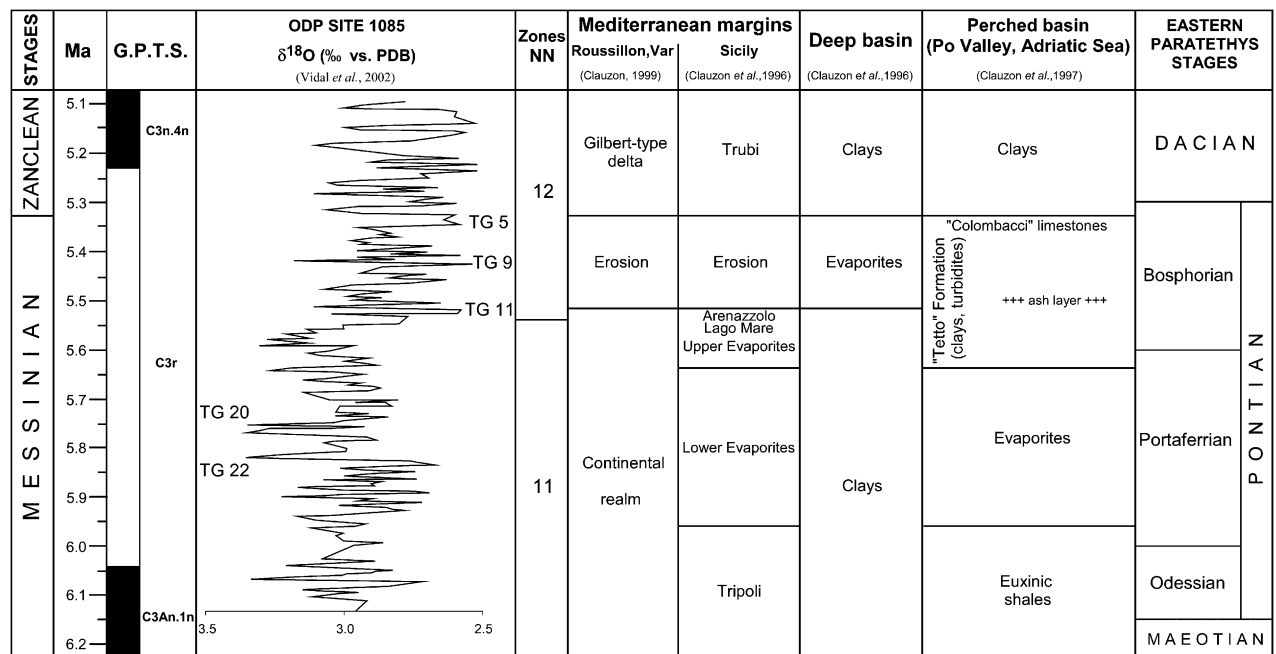


Fig. 2. The two-step scenario for the Messinian salinity crisis (Clauzon *et al.*, 1996) and its various expressions on the margins and in the deep basin. Chronology is based on Vidal *et al.* (2002). Late Miocene–Early Pliocene chronostratigraphic relationships between the Mediterranean Sea and the Dacic Basin revised by Snel *et al.* (in press) are followed in the present work. Age of boundary between nannofossil Zones NN11 and NN12 is from Backman & Raffi (1997).

- the first episode (5.96–5.64 Ma) was a global sea-level drop of moderate amplitude (less than 100 m), including glacial Antarctic isotope stages TG 22 and TG 20 (Shackleton *et al.*, 1995), that precipitated marginal evaporites (Sicily, Sorbas, Po Valley, Tyrrhenian realm) in some more or less isolated basins;
- the second episode (5.52–5.33 Ma) was sea-level drop of very large amplitude (1500–2000 m) that dried up most of the abyssal plains of the Mediterranean Sea, resulting in the deposition of abyssal evaporites and cutting of deep subaerial canyons. Some areas, such as the Po Valley and Adriatic Sea, were not affected by the second sea-level drop, and received persistent and continuous brackish to freshwater sedimentation (Corselli & Grecchi, 1984; Clauzon *et al.*, 1997) (Fig. 2).

This scenario has some basic discrepancies with the models of Rouchy & Saint-Martin (1992), Butler *et al.* (1995), Riding *et al.* (1998) and Krijgsman *et al.* (1999b) that place the Sicilian Upper Evaporites just before the Zanclean flooding. The Sicilian Upper Evaporites (including the Lago Mare and Arenazzolo episodes) are understood by some of these authors as being the transgressive interval before Zanclean flooding (Brolsma, 1976; Butler *et al.*, 1995; Krijgsman *et al.*, 1999b). Such an interpretation is severely contradicted by an absence of any earliest Zanclean transgressive interval within the sedimentary filling of Zanclean rias (Clauzon *et al.*, 1995). New offshore data reinforce the absence of any transgressive interval in the basin during the earliest Pliocene (Lofi *et al.*, 2003). Accordingly, the Sicilian Upper Evaporites (including the Lago Mare and Arenazzolo formations) cannot be considered to onlap the margin at the Messinian/Zanclean transition as considered by Krijgsman *et al.* (1999b). This supports our positioning of the Sicilian Lago Mare at the end of the sea-level rise which tops the first evaporitic phase (Clauzon *et al.*, 1996), i.e. in correspondence with the isotope stage TG 11 according to the adopted chronology (Fig. 2). In some places such as the Rhône Valley, the Barcelona area and the Corsica, a Lago Mare facies undoubtedly belongs to the Zanclean deposits (Rhône Valley: Denizot, 1952; Ballezio, 1972; Barcelona area: Gillet, 1965; Almera, 1894; Corsica: Pilot *et al.*, 1975; Magné *et al.*, 1977), i.e. to isotope stage TG 5 or later.

In the Eastern Paratethys: Dacic and Euxinian Basins

Seismic profiles (Letouzey *et al.*, 1978) and results from three cored boreholes (Sites 379, 380, 381; Fig. 1a) during DSDP Leg 42B (Ross *et al.*, 1978) suggested that the two main signatures of the Messinian salinity crisis in the Mediterranean exist also in the Black Sea: namely, evaporite deposition in the abyssal plain and an erosional surface on the margin (Hsü & Giovanoli, 1979). At Site 380A (cored in the deep basin), a coarse clastic pebbly breccia (19-m thick) was recovered between 864.5- and 883.5-m depth.

It includes blocks of a stromatolitic dolomite considered to have formed in an intertidal to supratidal environment (Stoffers & Müller, 1978). This suggests that the level of the Black Sea was very shallow at that time, in agreement with data from diatoms (less than 50-m water depth) (Schrader, 1978). According to Schrader (1978: p. 856), the comparable horizon at the nearby Site 381, which was cored in a more marginal position 'contains only a few scattered freshwater assemblages, and lies approximately 900 m above the one at Site 380A. Hsü & Giovanoli (1979) have interpreted these data as evidence of the drop in level of the Black Sea to 1600 m below global sea level in association with the Messinian salinity crisis in the Mediterranean. Such an interpretation was also supported by the record of a seismic reflector (reflector 'S') showing that the pebbly breccia is related to a deltaic system, speculatively a Messinian erosional surface in the Black Sea (Letouzey *et al.*, 1978). Such an interpretation is supported by a recent high-resolution pollen study at Site 380A where the lowermost Zanclean age of the aragonite overlying the pebbly breccia is demonstrated according to a global climatostratigraphic approach (Popescu, in press). All the major and secondary climatic variations of the early Zanclean have been recorded at Site 380 and exhibit the same range in intensity as in other European regions regardless of latitude or longitude. In addition, this study confirms the coastal status of the uppermost laminated carbonates underlying the pebbly breccia. Gillet (2004) has evidenced a clear erosional surface below Pliocene and Pleistocene deposits in several seismic profiles of the western Black Sea, especially from Site 380 up to Site 381. This strikingly confirms the previous assumptions of Letouzey *et al.* (1978).

NEW DATA FROM THE WESTERN DACIC BASIN

In order to validate these offshore data on land, the erosional signature of the Messinian salinity crisis was searched in the Dacic Basin along the Danube River that is expected to have offered the same response as the other large rivers (Rhône, Nile). Accordingly, we developed our investigation at the outlet of the Iron Gates (Figs 1 and 3) in the Turnu Severin area. Here, the Danube River has cut a gorge through the Carpathians (Figs 3b and c), the context of which is physiographically similar to Zanclean Gilbert-type fan delta constructions evidenced in the northwestern Mediterranean region, and demonstrates the Messinian age to the underlying erosional surface (Clauzon, 1999).

Evidence of a prominent Danube erosional surface at the outlet of the Iron Gates

At Gura Văii (Figs 1b and 3), a strong erosional surface that we refer to the Messinian salinity crisis cuts Jurassic

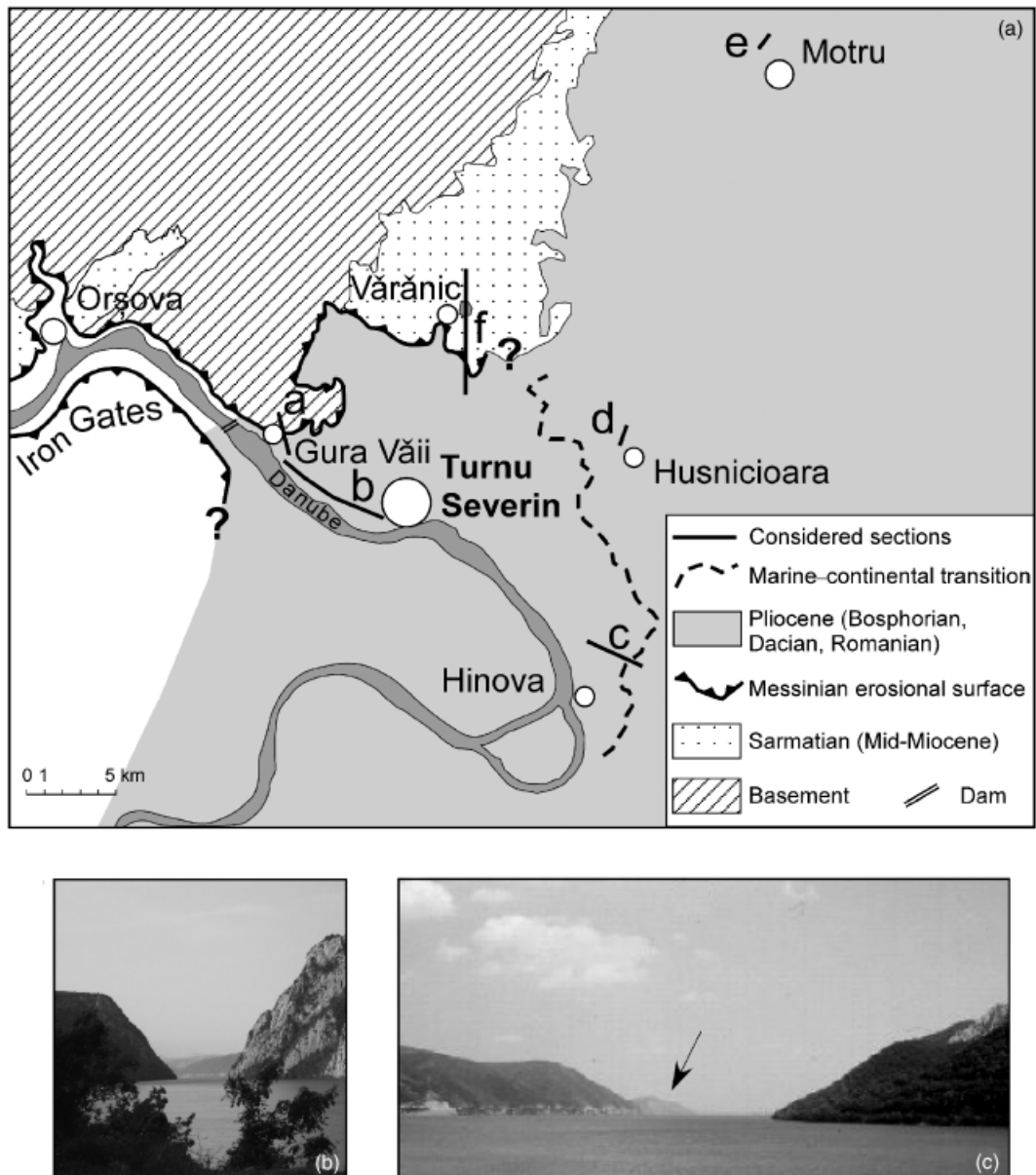


Fig. 3. The Zanclean Gilbert-type fan delta of Turnu Severin. (a) Simplified geological map of the Romanian part of the Iron Gates area. Considered sections: a, Gura Văii; b, Turnu Severin; c, Hinova; d, Husnicioara; e, Motru (Lupoia section); f, Vărănic. Basement comprises Jurassic limestones and metamorphic rocks. (b) The Iron Gates 15-km upstream from Orșova. (c) Outlet of the Iron Gates 5-km downstream from Orșova, with the residual Zanclean deposits (indicated by the arrow).

limestones and is overlain by lateral Zanclean foreset beds (Fig. 4). This erosional surface belongs to a past tributary of the Danube River on its left side. The axial erosional surface cannot be observed but is almost parallel to the Danube's modern thalweg according to geological information given in the Exhibition Hall of the Iron Gates 1 Dam. The dam was built on the Carpathian basement which reached 35 m in altitude. Wells have penetrated conglomerates just in front of the foreset beds. It is deduced that the present-day thalweg, which is less steep than the former one, intersects the erosional surface downstream from the dam. The erosional surface was mapped in this area but is not exposed downstream (Fig. 3a).

The units of the Pliocene Gilbert-type fan delta of Turnu Severin

At the outlet of the Iron Gates (Figs 1b and 3), the Danube River cuts thick conglomerates, dipping 20° eastward on average, that have been erroneously considered as Middle-Late Miocene in age ('Tortonian-Sarmatian': Savu & Ghenea, 1967; Nastaseanu & Bercia, 1968) because of their likeness to a detrital tilted formation overlying Badenian clays 25 km northward (Marinescu, 1978). The Turnu Severin clastic exposure begins close the village of Gura Văii, immediately downstream from the Iron Gates 1 Dam, and is only exposed along the left side of the Danube Valley and valleys of its northern tributaries (Fig. 3).

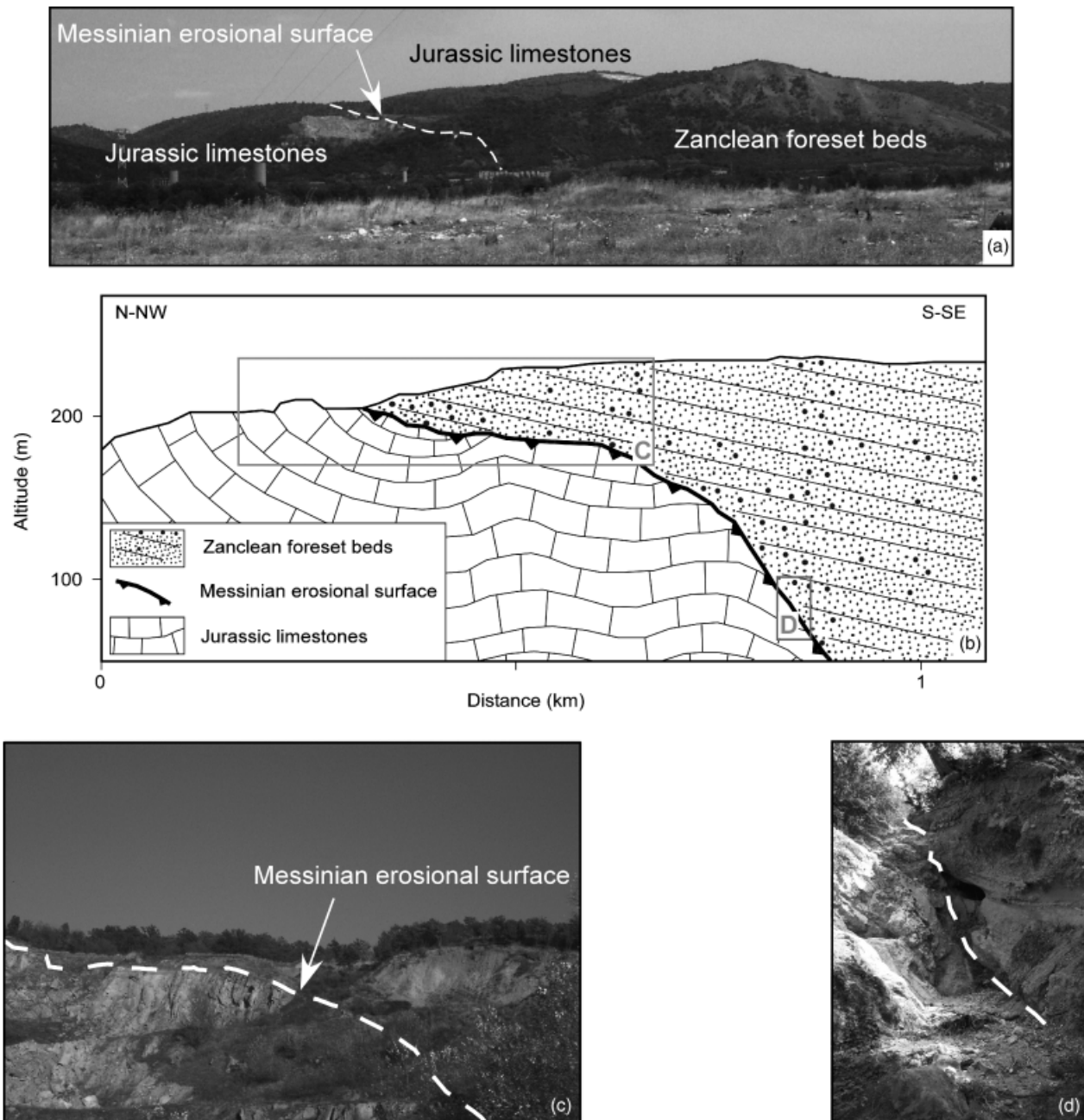


Fig. 4. The Messinian erosional surface and the foreset beds of the Zanclean Gilbert-type fan delta of Turnu Severin at Gura Văii. (a) General view of the area. (b) Cross section at Gura Văii (section 'a' on Figs 1b and 3a). (c) Detail of box C from Fig. 4b (dotted white line: the Messinian erosional surface). (d). Detail of box D from Fig. 4b (dotted white line: the Messinian erosional surface).

These thick conglomerates constitute the foreset beds of a very large Gilbert-type fan delta, and are exposed for more than 20 km. Extending from Gura Văii to the western suburbs of Turnu Severin, they comprise pebbles within a sandy, unevenly cemented matrix (Figs 5a–c, e); and further along the section they become more or less indurated white sands including some conglomeratic channels (Figs 5d and f). They contain rare molluscs.

The silty bottomset beds outcrop upstream from Hino-va where they are overlain by sandy foreset beds (Figs 6a–c) containing a thin layer from which several molluscs have allowed assignment to the Bosphorion regional substage

(Marinescu, 1978) (Table 1). This same layer, and two layers that overlie it have provided us with assemblages of nannofossils and dinocysts (Table 1). In the absence of *Discoaster quinqueramus*, nannofossils are considered as belonging to Zone NN12 which spans the Miocene/Pliocene boundary (Fig. 2; Berggren *et al.*, 1995a, b; Backman & Raffi, 1997). Nevertheless, they reveal an intense Mediterranean sea-level rise and crossing off the sill separating the Mediterranean from the Eastern Paratethys, and illustrate the Zanclean deluge into this Mediterranean appendage. In the Mediterranean, two remarkable successive changes in sea-level occurred within this brief time-window: the

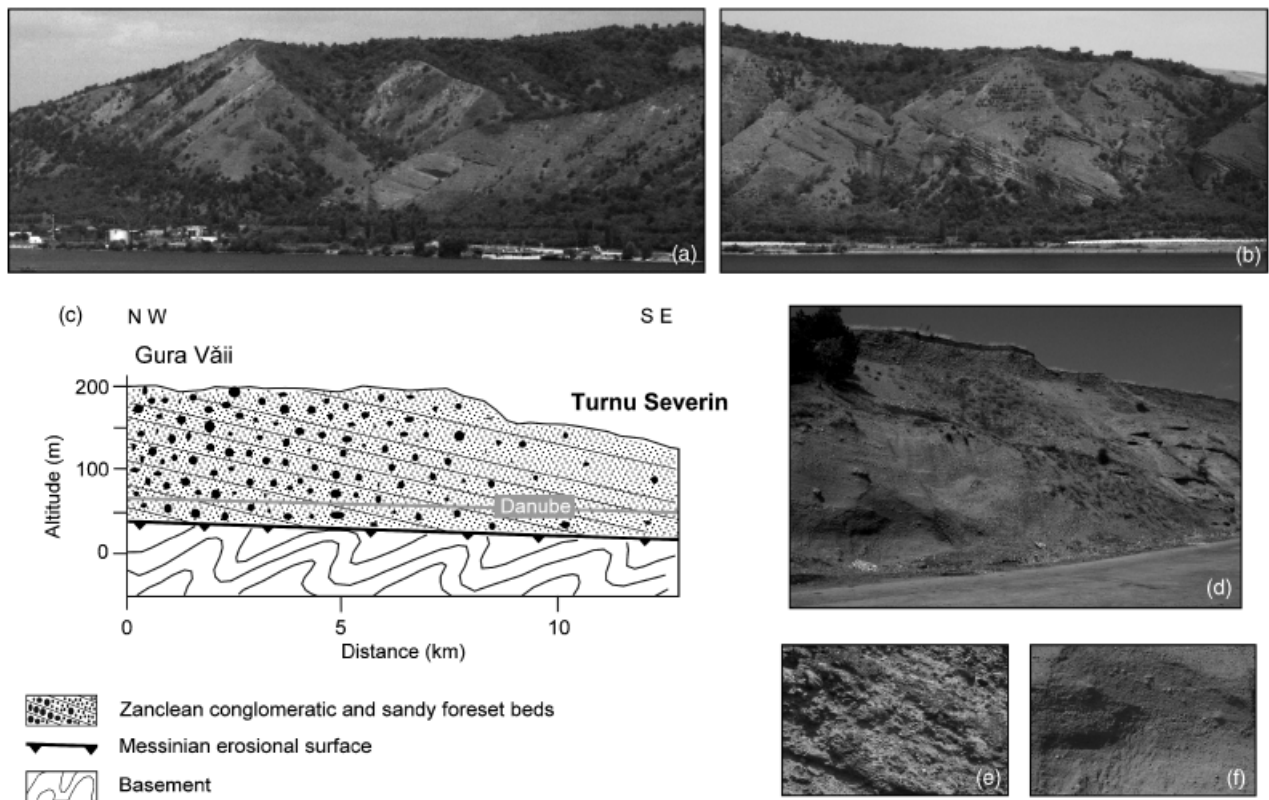


Fig. 5. Foreset beds of the Zanclean Gilbert-type fan delta between Gura Văii and Turnu Severin. (a) Conglomeratic foreset beds at Gura Văii. (b) Conglomeratic foreset beds between Gura Văii and Turnu Severin. (c) Cross section between Gura Văii and Turnu Severin (section 'b' on Figs 1b and 3a). (d) Sandy foreset beds at Turnu Severin (back the swimming pool). (e) Detail of the conglomeratic foreset beds. (f) Detail of the sandy foreset beds.

Messinian draw down and the Zanclean deluge. As a consequence, bottomset beds of the Turnu Severin Gilbert-type fan delta inevitably date the underlying erosional surface of the Messinian salinity crisis. We found at Hinova the same dinocysts as those we found at Cernat Valley in the area of Ploiesti where NN12 nannofossils occur (Snel *et al.*, in press). These floras are characterized by endemic Paratethyan species (Sütőné Szentai, 1989), but also include many typical Mediterranean elements (Table 1).

The top of the overlying sandy foreset beds is marked by (1) an angular discordance ($15\text{--}20^\circ$) at the base of subhorizontal topset beds and (2) a thin lignite layer (Fig. 6d) which probably corresponds to lignite A of Țicleanu & Diaconița (1997). This marks the marine/continental transition that takes place at a present altitude of 220 m. Another lignite (lignite B of Țicleanu & Diaconița (1997) is exposed just above (Fig. 6e). Both clays of the bottomset beds and those clays overlying lignite B are reversely magnetized and belong to Chron C3r (Popescu *et al.*, in press) (Fig. 6c).

Above this submarine deltaic wedge, the topset beds have a total thickness of about 200 m, and comprise alternating sands (with conglomeratic channels) and lignites (20 layers of unequal thickness, including lignites A and B), some of which are intensively worked particularly in the Husnicioara and Motru areas (Țicleanu & Diaconița,

1997; Fig. 3a). At Husnicioara (Fig. 7), lignites I, IV and V of the regional nomenclature are overlain by thick (42 m) fluvial sands indicating the strong, continuous influence of the Danube River. The section shows lignites XIII to XV at its top. Palaeomagnetic measurements have been done (Fig. 7a), and the oldest normal event is related to Chron C3n.4n (Popescu *et al.*, in press), with the others to be interpreted later. In the Motru area, the Lupoia quarry shows a continuous, 137-m thick, succession of lignites, extending from lignite V to lignite XIII (Fig. 8), alternating with clays and some fluvial sands. This section, which represents the almost complete continental accretion in the Carpathian foreland, is Zanclean in age based on the remains of small and large mammals (Fig. 8). Therefore, palaeomagnetic reversals complemented by pollen records (reliably correlated to climatic cycles forced by eccentricity) indicate that the section starts at Chron C3n.3n and includes Chron C3n.2n (Popescu, 2001; Popescu *et al.*, in press). As a consequence, the normal episode recorded at Husnicioara between lignites XIV and XV is Chron C3n.1n (Popescu *et al.*, in press). The high-resolution pollen records evidence the forcing of eccentricity (100-kyr cycles) for the lignite-clay alternations (Popescu, 2001; Popescu *et al.*, in press). According to plant remains (leaves, fruits, pollen grains), the vegetation of the area resembled the modern vegetation of Florida and the Mississippi Delta (Țicleanu & Diaconița, 1997; Popescu, 2001).

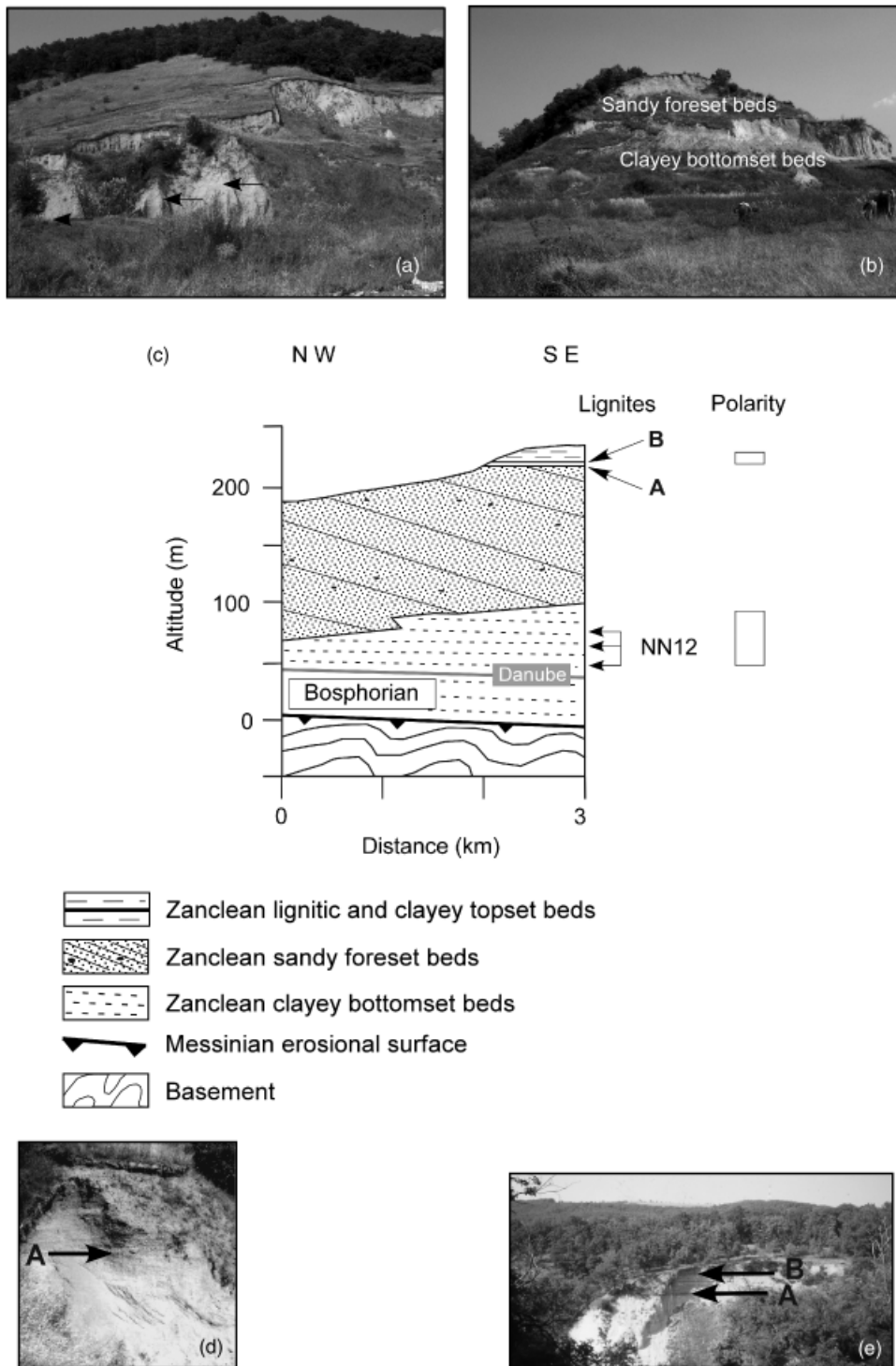


Fig. 6. Distal part of the Zanclean Gilbert-type fan delta of Turnu Severin in the area of Hinova. (a) Clayey bottomset beds (the arrows indicate the levels with Mediterranean nannofossils assigned to Zone NN12). (b) Clayey bottomset beds overlain by sandy foreset beds. (c) Cross section at Hinova (section 'c' on Figs 1b and 3a). (d) Detail of the marine–continental transition (the arrow indicates lignite A). (e) Overlying deposits with the marine–continental transition (i.e. the topset beds overlying the foreset beds; the arrows indicate lignite A corresponding to this transition, and lignite B).

Upstream and to the west of Turnu Severin, material becomes coarser and the continental prism is less than 100-m thick because of Late Pliocene and Pleistocene erosion.

The prism is topped with a conglomeratic abandonment surface marked by some residual siliceous pebbles (Fig. 9a), as can be observed on a topographic bench at

433-m altitude at Vărănic (Fig. 9d) developed on a lapiaz morphology (Fig. 9b). Karstic Jurassic and/or Sarmatian limestones have probably been overlain by the final continental deposits of the Gilbert-type fan delta construction (Fig. 9c). These deposits aggradated up to the beginning of the Plio–Pleistocene cutting which was probably forced

Table 1. Fossil content of the bottomset beds of the Turnu Severin Gilbert-type fan delta at Hinova

Paratethyan molluscs	Mediterranean nannofossils	Paratethyan dinocysts
<i>Limnocardium emarginatum</i>	<i>Reticulofenestra minuta</i>	<i>Galeacysta etrusca</i>
<i>L. petersi</i>	<i>R. pseudoubilicis</i>	<i>Spiniferites cruciformis</i>
<i>Plagiodacna auingeri</i>	<i>R. minutula</i>	<i>Tectatodinium psilatium</i>
<i>Dreissena rostriformis</i> group	<i>R. doronicoides</i>	Mediterranean dinocysts
<i>Dreissenomya aperta</i>	<i>Sphenolithus abies</i>	<i>Achomosphaera andalousiensis</i>
<i>Phyllocardium planum planum</i>	<i>Calcidiscus leptoporus</i>	<i>Operculodinium centrocarpum</i>
	<i>Amaurolithus primus</i>	<i>Impagidinium patulum(?)</i>
	<i>A. amplificus</i>	<i>Spiniferites bentori</i>
	<i>Coccolithus pelagicus</i>	<i>S. elongatus</i>
	<i>Helicosphaera kamptneri</i>	<i>S. hyperacanthus</i>
		<i>S. ramosus</i>
		<i>Nematosphaeropsis labyrinthus</i>
		<i>Tectatodinium pellitum</i>

mostly by the earliest Northern Hemisphere glaciations starting at 2.6 Ma. Indeed, the surface is dated at about 2.2 Ma according to the Slatina mammal faunas which are augmented by magnetostratigraphy (Rădulescu *et al.*, 1997). Such erosion explains the karstic evolution and preservation of siliceous remnants only (Fig. 9a).

The Turnu Severin Zanclean Gilbert-type fan delta compared with the Mediterranean Pliocene Gilbert-type fan deltas

It should be recalled that the only relatively brief and intense drop – rise succession in sea level of profound importance during the Late Miocene–earliest Pliocene interval corresponds to the Messinian salinity crisis followed by the Zanclean deluge (Fig. 2). This assumption is additionally supported strongly by all the chronological data obtained from the topset beds of the Gilbert-type fan delta; namely mammals, magnetostratigraphy and climate fluctuations via pollen records.

The evolution of this Gilbert-type fan delta extending over more than 3 Myrs (from 5.33 to *ca.* 2.10 Ma) is summarized in Fig. 10. This construction, exceeding 400 m in thickness, is strikingly similar to the Western Mediterranean deltas that characterized the Pliocene reflooding after the Messinian desiccation. For example, they are nested within all the earlier Miocene deposits, they rest on an erosional surface (the pronounced fluvial Messinian canyons related to the desiccation phase), and they have clayey bottomset beds of earliest Zanclean age (Zone NN12, Zone MP11) (Clauzon, 1996). They unanimously show three characteristic well-expressed surfaces: the Messinian erosional surface (at 5.33 Ma), the diachronous marine–non-marine transition (because of its prograding genesis) very often expressed by a lignite, and the isochronous abandonment surface expressed everywhere a little earlier than 2 Ma (probably caused by the earliest glacials in the Northern Hemisphere). Such similarities have never been reported outside of the Mediterranean context except in the Dacic Basin. The Dacic Basin Gilbert-type fan delta differs from the Mediterranean Gilbert-type fan deltas in its

number of lignite layers probably owing to the generally humid feature of the region.

It is demonstrated that the Danube River existed a long time before the Pleistocene. Indeed, such an impressive Gilbert-type fan delta system could not be built without the presence of a powerful river. The first appearance of the modern hydrographic network in southern Romania has generally been placed within the Late Pliocene–Early Pleistocene (Jipa, 1997). Our results lower this event to Late Miocene.

Regional extension of the Messinian erosional surface in the Dacic Basin

Exposed sections, such as Valea Văcii and Călugăreni (Ploiești area; Fig. 11), and Badislava (Râmnicu Vâlcea area; Fig. 11), exhibit continuous sedimentation during the Late Miocene and Early Pliocene (Marinescu *et al.*, 1981), as inferred from nannofossil analyses (Mărunțeanu & Papaianopol, 1998) and palaeomagnetic measurements (Snell *et al.*, in press). Subsurface data are consistent with these field observations, with many wells revealing a complete Late Miocene sedimentation (C. Dinu, personal information; Fig. 11). In contrast, some other wells, mostly from the western and southern Carpathian foredeep, are characterized by a hiatus below the Pontian (generally thin) and the Dacian (often easily recognizable because of the presence of lignites). These deposits directly overlie Sarmatian (with the entire Maeotian missing) or older layers such as Oligocene or Cretaceous (Fig. 11). This break in sedimentary record might illustrate an erosional gap because of the ‘proto-Danube’ and its tributaries. Fig. 11 provides an overview of the two palaeogeographically contrasted areas in the Carpathian foreland during the Messinian salinity crisis: (1) an erosional zone resulting from the palaeo-fluvial network and (2) a continuous sedimentary zone within a perched ‘palaeo-lake’. Clarifying the exact expanse of these areas eastward and southward requires examination of additional boreholes.

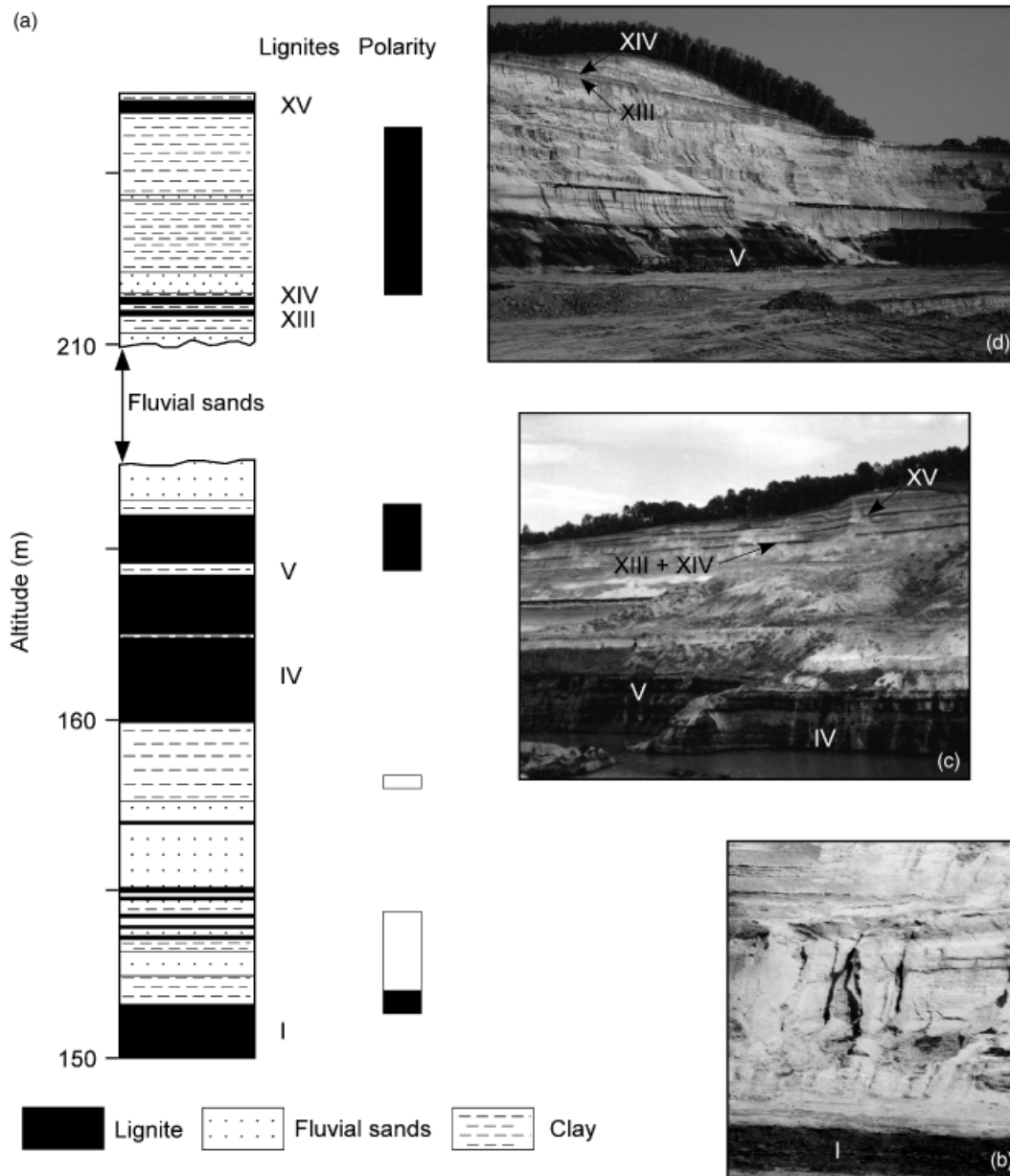


Fig. 7. Vertical section of the Husnicioara quarry (section 'd' on Figs 1b and 3a). (a) Lithological succession and palaeomagnetic polarity. Forty-four metres of fluvial sands represent the time-interval between lignites V and XIII (i.e. about 500 kyr from *ca.* 4.800 to *ca.* 4.300 Ma) during which the Danube flood plain aggradated in the area. (b) Lignite I and of overlying clays. (c) From lignite IV to lignite XV. (d) From lignite V to lignite XIV.

A NEW IDEA ON MEDITERRANEAN – PARATETHYS LATE NEOGENE RELATIONSHIPS

Discoveries of repeated Mediterranean nannoplankton influxes into Paratethys have considerably changed the concept of Mediterranean–Paratethys isolation since the Sarmatian. These influxes occurred (1) from earliest Sarmatian up to Romanian (Dacic Basin: MăruŃeanu, 1992; Papaianopol & MăruŃeanu, 1993; MăruŃeanu & Papaianopol, 1995; MăruŃeanu & Papaianopol, 1998; Drivaliari *et al.*, 1999; Snel *et al.*, in press) and (2) from Maeotian to Kimmerian (regional stage following Pontian) in the Ponto-Caspian Basin (Semenenko & Lyuljeva, 1978;

Semenenko *et al.*, 1995; Semenenko & Olejnik, 1995) (where Mediterranean dinocysts were also found: Semenenko & Olejnik, 1995). It has been proposed that there were many brief incursions of Mediterranean waters into the brackish-freshwaters of the Paratethys, and that 'many species (nannoplankton) died immediately, marking exactly the moment of the connections' (MăruŃeanu & Papaianopol, 1998, p. 121). Such influxes were necessarily forced by high sea levels in the Mediterranean Sea because coccolithophores and many dinoflagellates live within the photic zone of surface waters (Sarjeant, 1974; Winter *et al.*, 1994).

As a consequence, based on two successive records of Mediterranean nannofossils (and dinocysts) in the Eastern Paratethys, we consider the possibility that an inflow of

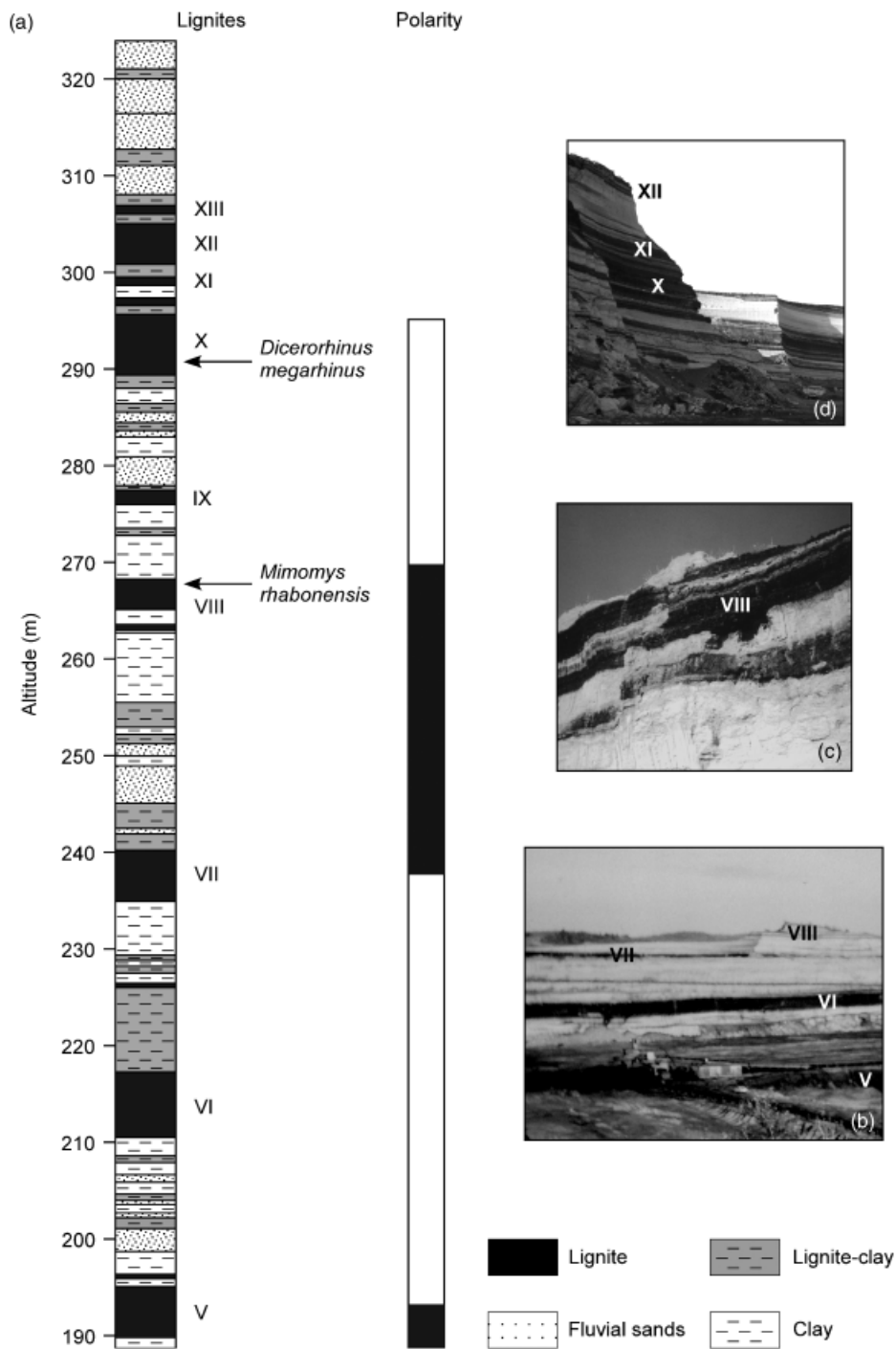


Fig. 8. Vertical section of the Lupoaia quarry (section 'e' on Figs 1b and 3a). (a) Lithological succession and palaeomagnetic polarity from lignite V to lignite XIII and the overlying clays and sands, with indication of the mammal remains. (b) Southern part of the quarry where sediments run from lignite V to lignite VIII. (c) The three layers of lignite VIII. (d) Northern part of the quarry where worked lignites X to XII are located.

Paratethyan waters reached the Mediterranean realm not just once (Hsü *et al.*, 1973) but that two influxes may have occurred via surface currents. The first influx, corresponding to Zone NN11, occurs before a strong erosional surface in the Eastern Paratethys, and just before the deep basin evaporite deposition in the Mediterranean (isotope stage TG 11). The second influx, corresponding to Zone NN12, occurs just above this erosional surface in the Eastern Paratethys (see also Semenenko, 1995; Gillet *et al.*,

2003) and corresponds to the earliest Zanclean in the Mediterranean (starting at isotope stage TG 5) (Fig. 12).

Mediterranean water influxes into Paratethys during the Late Miocene – Early Pliocene

Two influxes of Mediterranean nannoplankton and dinocysts occurred (Mărunțeanu & Papaianopol, 1998; Snel *et al.*, in press). The Late Portaferrian–Borphorian influx

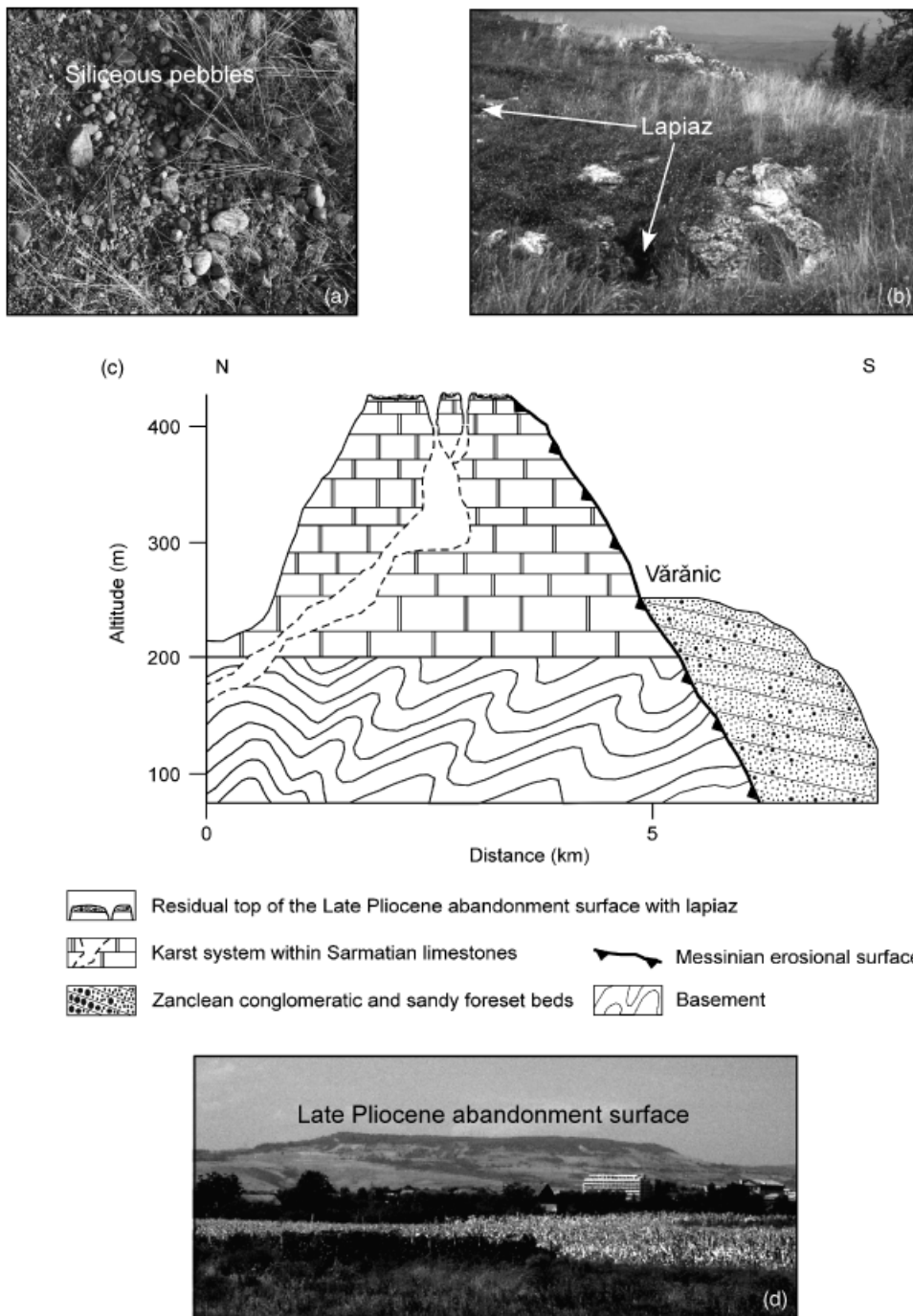


Fig. 9. Residual Late Pliocene abandonment surface near Vărănic. (a) Residual siliceous pebbles at altitude 424m. (b) Lapiaz at altitude 424m. (c) Cross section near Vărănic (section 'f' on Figs 1b and 3a) showing the residual top of the Late Pliocene abandonment surface characterized by remnant siliceous pebbles and lapiaz, the karst system through the Sarmatian limestones and the basement. The conglomeratic and sandy foreset beds of the Turnu Severin Gilbert-type fan delta are separated from the Sarmatian limestones and basement by the Messinian erosional surface. (d) W–E oriented view of the flat morphology of the Late Pliocene residual abandonment surface.

has been recorded at Valea Vacii, Călugăreni and Badislava (Fig. 11), and belongs to Zone NN11. The Bosphorian influx has been recorded at Valea Vacii, Călugăreni, Doicești, Hinova (Fig. 11) and Argova Valley (SE Bucharest, well 68913/67), and belongs to Zone NN12. In contrast to other localities, the nannoplankton (NN12) and dinocyst influx at Hinova overlies an important erosional surface considered to belong to the Messinian salinity crisis. The nanno-

plankton (NN12) influx recorded at Țicleni overlies a gap within Late Pontian deposits (Drivaliari *et al.*, 1999). We therefore conclude that these two successive influxes correspond to two successive high Mediterranean sea levels occurring immediately before and after the Messinian salinity crisis, i.e. to isotope stages TG 11 and TG 5 (Fig. 12) which are referred to high global sea levels (Vidal *et al.*, 2002; Warny *et al.*, 2003).

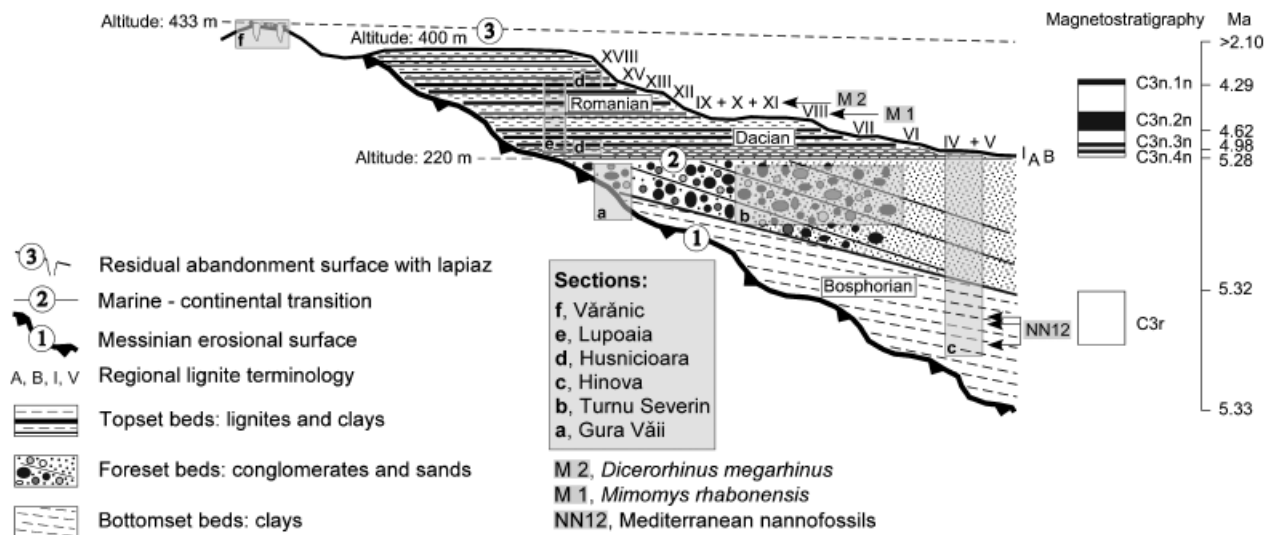


Fig. 10. Location of studied sections 'a'-'f' of the Zanclean Gilbert-type fan delta of Turnu Severin with respect to the structure of a Gilbert-type fan delta as found in the Mediterranean (Clauzon, 1990, 1999; Clauzon *et al.*, 1995) and to the chronology of this exceptionally exposed sedimentary body based on bio- and magnetostratigraphy. Complete details on bio- and chronostratigraphic assignments are given by Popescu (2001) and Popescu *et al.* (in press).

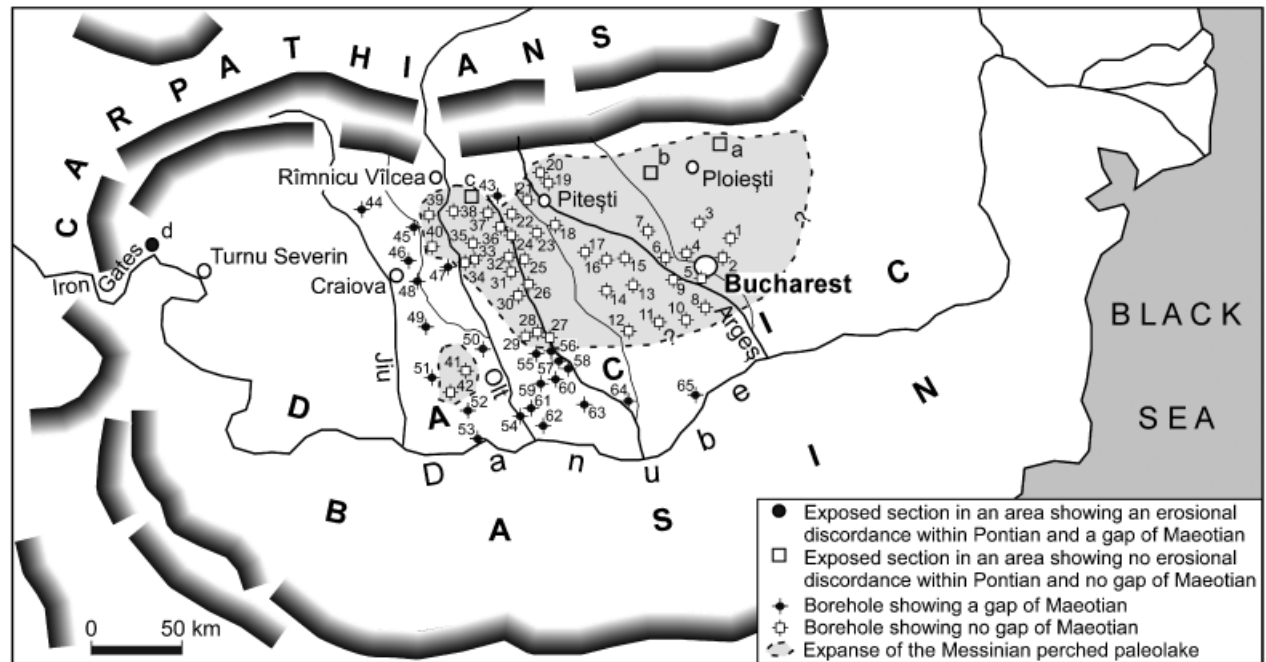


Fig. 11. Considered localities in the Dacic Basin. Exposed sections: a, Valea Vacii; b, Călugăreni; c, Badislava; d, Gura Văii. Boreholes: 1, Moara Vlăsiei; 2, Afumați; 3, Periș 909; 4, Flămanzeni 185; 5, Dumitrana 1483; 6, Potlogi 146; 7, Titu 1690; 8, Singureni 315; 9, Bălaria 590; 10, Ghimpați 2; 11, Videle 96; 12, Orbeasca 255; 13, Ciuperneci 400; 14, Ciolanesti 155; 15, Petrești 1600; 16, Visina 165; 17, Dumbrăveni 166; 18, Humele Buzoesti 2046; 19, Cosești 3275; 20, Mălureni 3300; 21, Giești-Pădureți 75; 22, Spineri 4 and 5030; 23, Gociești 41; 24, Tatulești 5036; 25, Corbu 3; 26, Birla 70; 27, Văleni 7; 28, Boianu 48; 29, Boianu 45; 30, Ciurești 67; 31, Priseaca 3026; 32, Mogoșești 921; 33, Priseaca 2222; 34, Brebeni 28; 35, Optași-Măgura 2; 36, Oprelu 3303; 37, Negreni 3014; 38, Priseaca 3025; 39, Doba 26; 40, Izvoru 39; 41, Caracal 2; 42, Dobrotești 10; 43, Cotmeana 3205; 44, Țicleni; 45, Monrunqlav; 46, GerceȚști 116; 47, Piatra Olt 101; 48, Malu; 49, Leu 105; 50, Caracal 490; 51, Mirșani 31; 52, Caracal 499; 53, Caracal 433; 54, Giuvărăști 16; 55, Stoicănești 43; 56, Stoicănești 44; 57, Bocălești 104; 58, Cărligăți 2; 59, Plăviceni 8; 60, Plăviceni 44; 61, Lita; 62, Turnu Mărgurele; 63, Puțineiu 3; 64, Alexandria; 65, Giurgiu.

Mediterranean nannoplankton influxes into the Central Paratethys are not restricted events because they are also recorded in the Azov Sea region, close to Kerc. Here, they correspond to an interval restricted to Zones NN11 and

NN12 and are located in deposits of latest Pontian – earliest Kimmerian age (i.e. almost reaching the earliest Pliocene) (Semenenko & Lyuljeva, 1978; Semenenko & Pevzner, 1979; Semenenko & Olejnik, 1995). The influxes are sep-

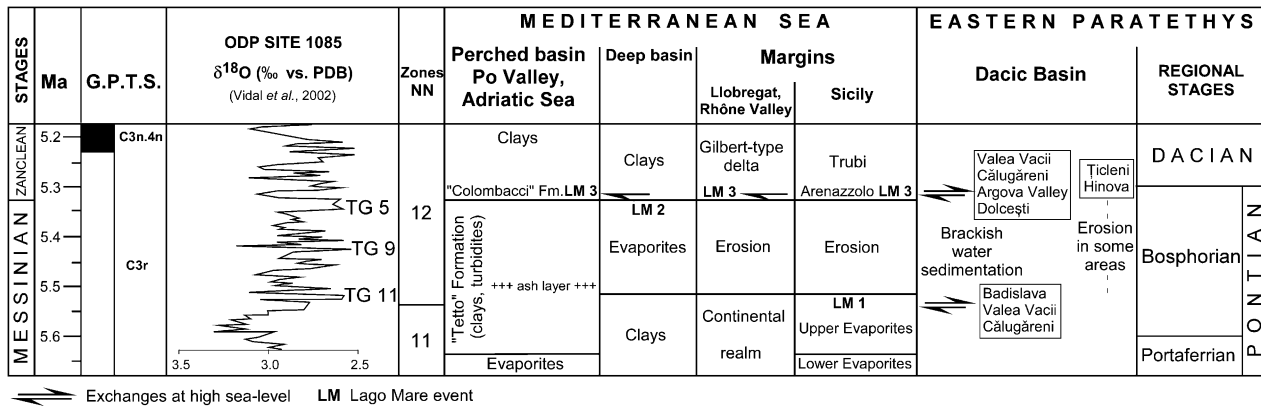


Fig. 12. Proposed evolution of selected basins in the Mediterranean Sea and the Eastern Paratethys during the late Messinian–early Zanclean. Chronological location of the three proposed Lago Mare events. Age of boundary between nanofossil Zones NN11 and NN12 is from Backman & Raffi (1997).

rated by a gap in the deposits that Semenenko (1995) considered as being because of widespread erosion in the northwestern Black Sea, recently confirmed by Gillet *et al.* (2003).

Paratethyan water influxes into the Mediterranean (latest Messinian–earliest Zanclean)

Two Lago Mare events can be distinguished in the Mediterranean realm, the first event occurs at the top of the Sicilian Upper Evaporites (i.e. at the end of the evaporitic phase on the Mediterranean margins; Clauzon *et al.*, 1996), and the second occurs at the beginning of the Zanclean flooding. We relate them to the two successive high Mediterranean sea levels (TG 11 and TG 5) which allowed exchanges of surface waters between the Mediterranean Sea and Paratethys, as supported by the presence of Paratethyan dinocysts (*Galeacysta etrusca* for example) in the two successive Lago Mare events (Fig. 12).

We present a review of many selected Lago Mare Formation localities in the Mediterranean (Fig. 13), taking mainly into account Paratethyan mollusc, ostracod and dinocyst occurrences (Table 2). In this review, deep basal localities (containing only ostracods) are distinguished from marginal ones, which are in turn subdivided into two categories according to the chronological assignment that we propose (late Messinian or earliest Zanclean).

The Messinian localities generally overlie marginal evaporites (*sensu* Clauzon *et al.*, 1996) and/or are overlain by the Messinian erosional surface; in some places, a nanofossil age (NN11) is known (Pasquasia: Cita *et al.*, 1973; Corfou: Vismara Schilling *et al.*, 1976). The calcareous nanofossil assemblages suggest an NN11 age for the Lago Mare Formation and an NN12 age for the Arenazzolo Formation, based on to the disappearance of *Discoaster quinqueramus* between them at Capo Rossello (Cita & Gartner, 1973) and Eraclea Minoa (Bizon *et al.*, 1978; A. Di Stefano, personal information) (Fig. 13). These two formations are separated by the Messinian erosional surface, most conspicuously expressed westward where the uppermost 5 m of the Lago

Mare Formation are missing at the Eraclea Minoa reference section. Such data lead us to reject the classical stratigraphical position of the Arenazzolo Formation (Fig. 2) and to shift it into the earliest Zanclean (Fig. 12), a view previously implied by some authors (Brolsma, 1976; Butler *et al.*, 1995). In this section, cysts of *Galeacysta etrusca* have been recorded only during relative high sea levels (i.e. within the turbiditic layer preceding the last gypsum and within the Arenazzolo Formation) according both to the abundance of *Pinus* vs. halophyte pollen grains (Fauquette *et al.*, in press) and to a sequence stratigraphic analysis (Homewood *et al.*, 1992). It is clear that, at Eraclea Minoa, two successive influxes of Paratethyan elements are recorded in relation to relative high sea levels, respectively: (1) before the almost complete desiccation of the Mediterranean (marked by dinoflagellate cysts including *Galeacysta etrusca* and, at a relative lower sea level, by *Congerina* and ostracods) and (2) after the almost complete desiccation of the Mediterranean (marked by dinoflagellate cysts including *Galeacysta etrusca*). These influxes are separated by the Messinian erosional surface which corresponds to the deep desiccated basin evaporites (Clauzon *et al.*, 1996). Accordingly, these influxes can be respectively related to isotopic stages TG 11 (last occurrence of *Discoaster quinqueramus*, corresponding to the Lago Mare Formation in Sicily) and TG 5 (earliest Zanclean corresponding to the Arenazzolo Formation in Sicily), a gap in sedimentation of 190 kyr separating these two layers (Fig. 12). At Cava Serredi (Livorno, Italy), the uppermost 20 m of the Lago Mare facies are missing from the present-day quarry face at about 400-m north of the section described by Bossio *et al.* (1981). This suggests the presence of the Messinian erosional surface between Messinian and Zanclean deposits, and disputes the continuous deposition claimed by Bossio *et al.* (1981) and Corradini & Biffi (1988).

We distinguished some other earliest Zanclean localities because we observed them above the Messinian erosional surface, as suspected by some previous authors. These localities include Papiol (Almera, 1894; Gillet, 1965), localities from the Rhône Valley (Fontannes, 1883; Denizot, 1952; Ballezio, 1972) and Aleria in Corsica (Magné

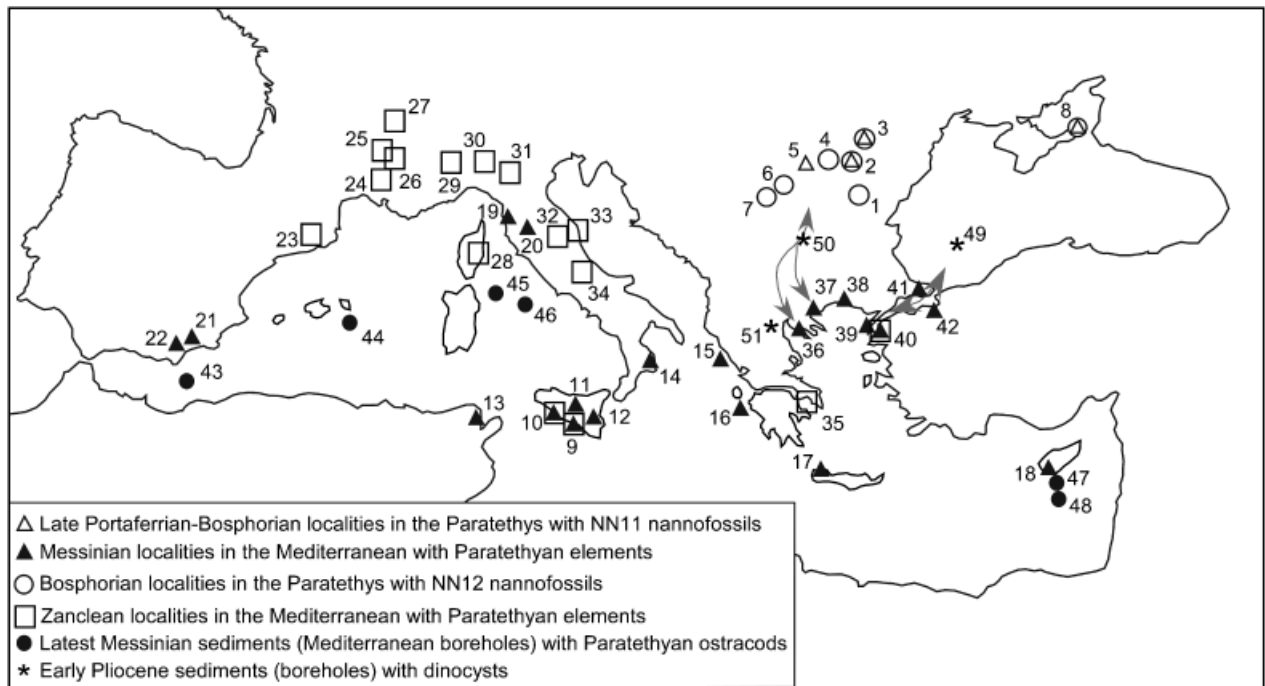


Fig. 13. Selected localities in the Mediterranean and Dacic basins used to propose three Lago Mare events from the late Messinian to earliest Zanclean. The discussed possible gateways between the Aegean Sea and the Eastern Paratethys are indicated by grey double arrows. Localities (some including several sections; references are given in Table 2) are as follows: 1, Argova Valley; 2, Călugăreni; 3, Valea Vacii; 4, Doicești; 5, Badislava; 6, Ticleni; 7, Hinova; 8, Kerc (Azov Sea); 9, Capo Rossello; 10, Eraclea Minoa; 11, Pasquasia; 12, Vizzini; 13, Djebel Kechabta; 14, Zinga; 15, Corfou; 16, Zakynthos; 17, Khairitiana (Crete); 18, Pissouri and Polemi (Cyprus); 19, Cava Serredi; 20, Pomarance; 21, Vera; 22, Sorbas; 23, Papiol; 24, Théziers; 25, Saint-Marcel d'Ardeche; 26, Saint-Restitut; 27, Allex; 28, Aleria; 29, Alba; 30, Torre Sterpi; 31, Monteglino; 32, Maccarone; 33, Ancone; 34, Le Vicenne; 35, Souvala (Aegina); 36, Axios-Thermaikos Basin; 37, Strymon Basin; 38, Xanthi-Kometini Basin; 39, Gelibolu; 40, Intepe; 41, Ambarliköy; 42, Yalakdere; 43, Site 978A; 44, Site 975B; 45, Site 654; 46, Site 974B; 47, Site 968A; 48, Site 967A; 49, Site 380A; 50, Ravno Polé; 51, Ptolemais.

et al., 1977) (Fig. 13). In the Tyrrhenian Sea, the Messinian erosional surface can be followed offshore from Aleria to the basin where it cuts the Messinian evaporites (Aleria, 1980), that are demonstrated as being the marginal ones (Clauzon et al., 1996).

We regard the Colombacci Formation of the Po Valley and the Adriatic realm, classically accepted as latest Messinian in age (Fig. 2), as earliest Zanclean for the following reasons. At Maccarone, this Formation with Paratethyan ostracods and dinoflagellate cysts (including *Galeacysta etrusca*: Bertini, 1992; Popescu, in progress; Table 2) represents a marine environment with planktonic and benthic foraminifers (Carloni et al., 1974) and oceanic dinoflagellate cysts such as *Impagidinium aculeatum* (Bertini, 1992; Popescu, in progress) which began 44 m below the Colombacci Formation. It inevitably belongs to a relative high sea level. The occurrence of *in situ* foraminifers (Carloni et al., 1974) points to a Zanclean age for the Colombacci Formation. This conclusion was previously reached in a confidential study for the TOTAL Company on the Montagna dei Fiori section (near Ascoli, Marche, Italy), an area where the Colombacci Formation is very thick (Selli, 1973; Bassetti et al., 1994).

The age has been unclear for some localities from the Aegean Sea, with assignment to the Messinian (Rögl et al.,

1991; Syrides, 2000) or Zanclean (Karistineos & Georgiades-Dikeoulia, 1985–1986), such as in the Axios-Thermaikos Basin (Fig. 13). The significance of the incursion of Paratethyan waters is also discussed (Syrides, 2000), and the problem is perpetuated because most of the localities have no age control other than molluscan evidence. The matter is nonetheless crucial because these faunas are located in a possible gateway area between the Paratethys and the Mediterranean (Stankovic, 1960; Hsü et al., 1977, 1978a; Kojumdgieva, 1987; Marinescu, 1992). Therefore, after several field investigations in the northern Aegean Sea, we established that localities of the Strymon, Xanthi-Kometini and Gelibolu basins that have Paratethyan elements (Fig. 13) were cut by the Messinian erosional surface (cutting in some places the marginal evaporites, a feature clearly seen also on seismic profiles of the Prinos Basin: Proedrou, 1979; Proedrou & Sidiropoulos, 1993), and overlain by Gilbert-type fan delta deposits showing bottomset beds belonging to nannofossil Zone NN12. A similar situation is suspected for the Ambarliköy area (Fig. 13) based on seismic investigations in the Black Sea (Gillet, 2004). We have recorded Mediterranean calcareous nannofossils continuously along the Intepe section at the western opening of the Dardanelles Strait (Fig. 13). This section belongs to the Messinian Alçitepe Formation

Table 2. Mediterranean Lago Mare localities and their fossil content

Localities	Congeria	Ostracods	Dinocysts
Alboran Sea:			
Vera (Cita <i>et al.</i> , 1980)		+	
Sorbas (Civis <i>et al.</i> , 1979; Ott d'Estevou & Montenat, 1990)	+	+	
Site 978A (Iaccarino & Bossio, 1999)		+	
Northwestern Mediterranean:			
<i>Papiol</i> (Gillet, 1960, 1965; Almera, 1894)	+	+	
<i>Théziers, Saint-Marcel d'Ardèche, Saint-Restitut, Allex (Rhône Valley)</i> (Fontannes, 1883; Ballezio, 1972; Archambault-Guezou, 1976; Carbonnel, 1978)	+	+	
Cava Serredi (Bossio <i>et al.</i> , 1981; Corradini & Biffi, 1988)	+	+	+
Pomarance (Bossio <i>et al.</i> , 1978)	+	+	
<i>Aleria (Corsica)</i> (Pilot <i>et al.</i> , 1975; Magné <i>et al.</i> , 1977)	+	+	+*
Site 975B (Iaccarino & Bossio, 1999)		+	
Site 654 (Cita <i>et al.</i> , 1990)		+	
Site 974B (Iaccarino & Bossio, 1999)		+	
Po Valley and Adriatic Sea:			
<i>Alba</i> (Cavallo & Repetto, 1988)	+		+*
<i>Torre Sterpi</i> (Corselli & Grecchi, 1984)	+	+	+*
<i>Monteglino</i> (Iaccarino & Papani, 1979)	+	+	
<i>Monticino 1987</i> (Marabini & Vai, 1988; Bertini, 1992)	+		+
<i>Ancone</i> (Gillet, 1968)	+	+	
<i>Maccarone</i> (Carloni <i>et al.</i> , 1974; Bertini, 1992)		+	+*
<i>Le Vicenne</i> (Cipollari <i>et al.</i> , 1999; Gliozzi, 1999; Bertini, in progress)	+	+	+
Central Mediterranean:			
Vizzini (Di Geronimo <i>et al.</i> , 1989)	+		
Capo Rossello (Cita & Colombo, 1979; Bonaduce & Sgarrella, 1999)	+	+	+*
Eraclea Minoa (Decima & Sprovieri, 1973; Bonaduce & Sgarrella, 1999)	+	+	+*
Pasquasia (Colalongo, 1968; Cita <i>et al.</i> , 1973)		+	
Zinga (Selli, 1973; Martina <i>et al.</i> , 1979)		+	
Djebel Kechabta (Burolet, 1952; Benson, 1976)		+	
Ionian Sea:			
Corfou (Vismara Schilling <i>et al.</i> , 1976)		+	
Zakynthos (Kontopoulos <i>et al.</i> , 1997)			+
Aegean and Marmara seas:			
Khairitiana (Crete) (Sissingh, 1972)		+	
<i>Souvala</i> (Aegina) (Rögl <i>et al.</i> , 1991)	+	+	
Axios-Thermaikos Basin (Gillet, 1937; Gillet & Geissert, 1971; Syrides, 1998)	+		
Strymon Basin (Syrides, 1995, 1998)	+		
Xanthi-Komotini Basin (Syrides, 1998)	+		
Gelibolu (Gillet <i>et al.</i> , 1978; Görür <i>et al.</i> , 1997)		+	
Intepe (Gillet <i>et al.</i> , 1978; Görür <i>et al.</i> , 1997)		+	
Ambarliköy (Gillet <i>et al.</i> , 1978; Görür <i>et al.</i> , 1997)		+	
Yalacdere (Gillet <i>et al.</i> , 1978; Görür <i>et al.</i> , 1997)		+	
Eastern Levantine Basin:			
Pissouri and Polemi (Cyprus) (Orszag-Sperber <i>et al.</i> , 1980; Di Stefano <i>et al.</i> , 1999; Rouchy <i>et al.</i> , 2001)	+	+	
Site 967 (Spezzaferri <i>et al.</i> , 1998)		+	
Site 968 (Blanc-Valleron <i>et al.</i> , 1998)		+	

A distinction is drawn between the deep basin localities and the marginal ones, and among the latter, between those referred to the late Messinian and those referred to the earliest Zanclean.

Normal characters: deep basin localities **Bold characters**: localities referred to Late Messinian *Italic characters*: localities referred to Early Zanclean.

*Our study.

(Görür *et al.*, 1997), and has two apparently conformable assemblages: the lower part of the succession is assignable to Zone NN11 (co-occurrence of *Triquetrorhabdulus rugosus*, *Reticulofenestra rotaria*, *Amaurolithus primus* and *A. delicatus*),

and the the upper part is assignable to Zone NN12 (indicated by the appearance of *Ceratolithus armatus/C. acutus*, and the disappearance of *Triquetrorhabdulus rugosus*). Moreover, as in other Mediterranean and Atlantic regions

(Backman & Raffi, 1997; Castradori, 1998), the two above-mentioned nannofossil events are not coincident: the extinction of *T. rugosus* is younger than the appearance of *C. armatus/C. acutus*. The two assemblages are separated by a lignite (5-cm thick), a sand (2-cm thick) and a shelly limestone (17-cm thick), which may express the discontinuity observed to the north at Yaylaköy (Gulf of Saros) where clayey bottomset beds belonging to Zone NN12 are nested within the Alçitepe Formation owing to the Messinian erosional surface. Presently, only two localities are of uncertain age: Trilophos (locality 36 on Fig. 13) is assigned to the late Messinian (Gillet & Geissert, 1971; Syrides, 1998) pending nanoplankton data (Fig. 13; Table 2); and Souvala, a locality of the Aegina Island (35 on Fig. 13), is ascribed to the earliest Zanclean (Fig. 13; Table 2) because nannoostracods of Zone NN12 overlie beds containing Congeria, although there is no information on whether an erosional surface is present (Rögl *et al.*, 1991). Hence, despite some missing information on the latter locality, we believe that the two high sea-level exchanges between the Mediterranean Sea and the Paratethys, occurring just before and just after the Mediterranean Sea desiccation, have been recorded in this area.

Re-examination of the Lago Mare localities suggests that two successive influxes of Paratethyan organisms entered the Mediterranean Sea, firstly in the late Messinian and again in the earliest Zanclean. Such influxes were made of surface waters, these being able to transport Congeria and ostracod larvae and where dinoflagellates live in the photic zone. They necessarily correspond to the two opposite influxes of Mediterranean surface waters occurring at high sea level, transporting the calcareous nanoplankton characterizing Zones NN11 and NN12 (Fig. 12). Accordingly, these results suggest the existence of two relatively brief episodes of two-way exchange at high sea level between the Paratethys and the Mediterranean, the brackish to fresh Paratethyan waters exported at the surface, and the Mediterranean saline waters imported below surface (Fig. 12).

DISCUSSION

Two brief influxes of Mediterranean waters (with calcareous nanoplankton and dinoflagellates) have clearly occurred in the late Messinian–earliest Zanclean of the Eastern Paratethys (Dacic and Euxinian basins). They, respectively, belong to the calcareous nannofossil Zones NN11 and NN12. According to palaeomagnetic data in the northern Dacic Basin (Snel *et al.*, in press), they immediately preceded and followed the Messinian salinity crisis. This timing is also attested by the presence of the Messinian erosional surface below the bottomset beds (assigned to Zone NN12) of the Gilbert-type fan delta of Turnu Severin. Because nanoplankton and dinoflagellates are mostly distributed in surface waters (the upper photic zone, i.e. the uppermost 90 m), it is realistic to correlate these influxes with the two successive high global sea levels

illustrated by the isotope stages TG 11 and TG 5 of Shackleton *et al.* (1995) which respectively immediately predate (5.52 Ma) and postdate (5.33 Ma) the Messinian salinity crisis (Vidal *et al.*, 2002; Warny *et al.*, 2003) (Fig. 12). At the same time, brief reverse flows of Paratethyan waters will have entered the Mediterranean, explaining the arrival of Paratethyan elements (Congeria, ostracods and dinoflagellates) and causing the development of two successive Lago Mare facies in the Mediterranean. This scenario resolves the apparently discrepant chronology of this facies that is represented by localities underlying the Messinian erosional surface, but also localities overlying the same surface (Fig. 12). The present-day water exchanges between the Marmara and Black seas through the Bosphorus Strait occurs because brackish waters exit the Black Sea as a surface current that flows over a deeper reverse current of saline Mediterranean waters entering the Black Sea (Fortey, 2000). This presents a realistic analogue for the suggested water exchanges between the Mediterranean Sea and Eastern Paratethys during the Late Neogene. In some areas protected from erosion, the two successive exchanges at high sea level have been recorded within the same vertical section: in the Eastern Paratethys (northern Dacic Basin) and in the Mediterranean (Eraclea Minoa classical section, Intepe) (Fig. 13). In the Mediterranean (except the Po Valley and the Adriatic realm), fluvial erosion during the Mediterranean desiccation resulted in a nesting of Zanclean deposits within Miocene deposits that are generally considerably eroded. Therefore, only one of the two Lago Mare facies caused by high sea-level exchanges can be exposed in each locality, except near Eraclea Minoa and at Cava Serredi (Livorno) where relatively weak erosion occurred. The late Messinian Lago Mare sediments have been protected from erosion in some Mediterranean localities (Fig. 13), whereas the earliest Zanclean Lago Mare deposits are often poorly documented because of the difficulty in observing the oldest Zanclean sediments within the Messinian canyons. In the Po Valley and Adriatic realm, only the second influx (earliest Zanclean) seems documented, considering that, at Maccarone, it significantly postdates an ash bed dated at 5.51 ± 0.04 Ma ($^{40}\text{Ar}/^{39}\text{Ar}$: Odin *et al.*, 1997; H. Maluski, personal information). Such an assumption can be extrapolated across the whole region considering that, for example, at Monticino, the second Lago Mare deposits unconformably overlie the marginal evaporites (Marabini & Vai, 1988); and at Torre Sterpi and Sioneri (near Alba), they overlie the reworked marginal evaporites. These data may support some uplift of the Otrante Sill during the episode that includes the first high sea-level exchange between the Eastern Paratethys and the Mediterranean (5.90–5.40 Ma) (Fig. 14). The connection of the Mediterranean Sea with the Eastern Paratethys at high sea level just before the salinity crisis provides a better explanation for the sea-level drop of the latter than by its drainage into the dried-up Mediterranean as proposed by Hsü *et al.* (1978a). Similar relationships at high sea level occurred repeatedly between the two realms before and after the time-window including

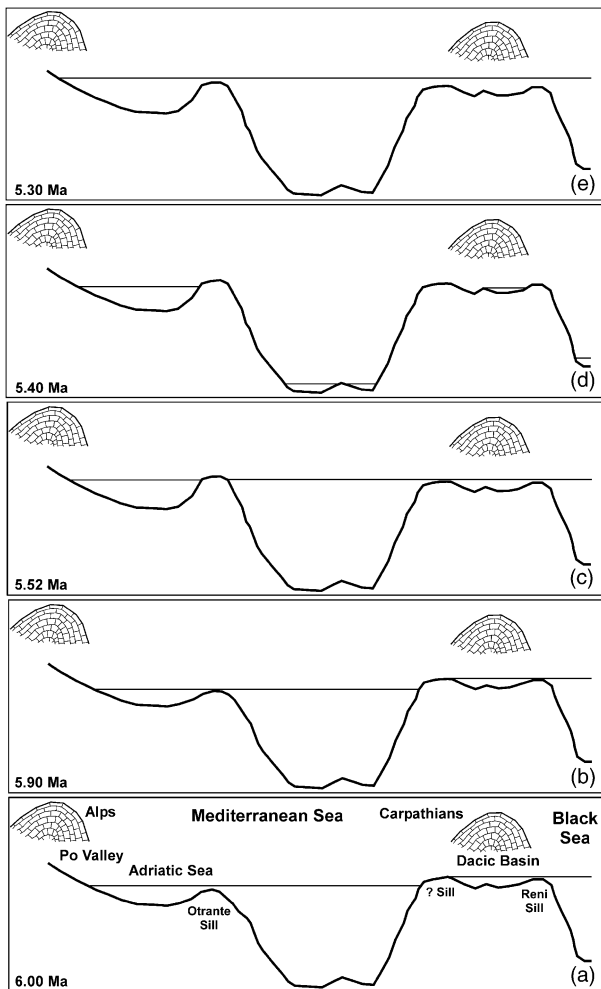


Fig. 14. Proposed sea-level changes in the Mediterranean Sea and the Eastern Paratethys between 6.00 and 5.30 Ma, and their brief connections during episodes of high sea level.

the Messinian salinity crisis as attested by Mediterranean nannofossil records in the Dacic Basin (Mărunțeanu & Păpaianopol, 1998) and by the unusual presence of Paratethyan fauna in the Mediterranean, such as below the Crevillente 6 mammal level (Archambault-Guezou *et al.*, 1979) dated at about 6.1 Ma (Garcés *et al.*, 1998).

The significance of Paratethyan dinocyst influxes into the Mediterranean Basin is different from that of *Congeria* influxes, because they are not recorded simultaneously at some non-coastal localities, such as Eraclea Minoa for instance. At Eraclea Minoa, Paratethyan dinocysts are recorded in the following relatively high sea-level deposits: (1) a turbiditic layer underlying the last gypsum that represents a relative drop in sea level (Homewood *et al.*, 1992) and (2) the Arenazzolo Formation. These two relatively high sea-level deposits are separated by the Lago Mare Formation, which includes *Congeria* only. We believe that dinocyst and *Congeria* migrations have occurred at the same time (as recorded simultaneously in several coastal localities, Torre Sterpi for example). But in some distal localities, such as Eraclea Minoa, dinocysts owing to their greater abundance appear more reliable for identi-

fying the exact influx level. Indeed, *Congeria* beds are a better signature for characterizing more coastal conditions and brackish-water lagoons along the shoreline.

Such exchanges at high sea-level between the Eastern Paratethys and the Mediterranean would correspond to episodic connections not only forced by rises in sea level but also controlled by palaeogeographic features such as very narrow and winding sills and marine currents. Where were such connections located? (Fig. 13). A proto-Dardanelles–Bosphorus gateway was considered by Archambault-Guezou (1976), Kojumdjieva (1987) and Marinescu (1992). The absence of Mediterranean nannofossils from the earliest Pliocene at Site 380A (Percival, 1978), relatively close to the present-day Bosphorus Strait, allows us to discard this hypothesis. An approximately 200-kyr delay in the arrival of Mediterranean diatoms and dinocysts at this site supports our decision (Schrader, 1978; Popescu, in press). According to Carbonnel (1980), a passage in the Black Sea area is untenable because no comparable ostracod faunas are known from wells of DSDP Leg 42B (Benson, 1978; Olteanu, 1978) (Fig. 1a). The morphology of Dacic Basin coccoliths supports a direct connection between the Dacic Basin and the Mediterranean, on the basis of difference in Crimean coccoliths that show some adaptation to Black Sea euxinic conditions because they probably reached this area later. The possibility of a passage through the Serres Basin into Bulgaria, already considered by Kojumdjieva (1987), is discarded according to recent results published by Zagorchev (2002). Nevertheless, a gateway through northern Greece, Macedonia and Bulgaria seems possible (Stankovic, 1960; Hsü *et al.*, 1977, 1978a) because the area was under prevalent extension at that time (Dabovski *et al.*, 2002). Such a possibility, already suggested by Marinescu (1992), should be explored. Assuming such a scenario, the Dacic Basin could have been directly connected to the Mediterranean Sea, being itself episodically connected to the Black Sea north of the Dobrogea horst through the Reni Strait (Semenenko, 1995) (Fig. 14). Such a gateway is supported by morphological adaptations of the dinocysts to the low salinity of the Dacic Basin, which seems to be less important at Hinova than at Cernat or at Site 380A, i.e. at an increased distance away from the connection. A passage through the Sofia Basin is supported by evidence of Mediterranean dinocysts in the Zanclean lacustrine facies from Ravno Polé borehole near Sofia (Drivaliari, 1993). In addition, the canyon of Mezdra to the north of Sofia is a reliable candidate for providing the outlet towards the Danube Plain. We suggest that the most reliable outlet of this gateway in the Aegean Sea is the area of Thessaloniki (i.e. the Axios-Thermaikos Basin) where Syrides (1998) found Paratethyan *Congeria* together with typical Mediterranean organisms (*Mactra*, *Abra*, *Parvivenus widalmi*). This prospective gateway is also supported by the presence in the Zanclean lacustrine layers of Ptolemais, a nearby basin, of *Spiniferites cruciformis*, a typical dinocyst from the Paratethys (Kloosterboer-van Hoeve *et al.*, 2001) at a time when Mediterranean nannofossils of Zone NN13 also penetrated the Dacic Basin (Mărunțeanu &

Papaianopol, 1998). Hence, a passage through the region of Thessaloniki, Macedonia and the Basin of Sofia must be preferred (Fig. 13) and needs to be tested by future investigations.

The evolution of the Mediterranean region (including the Po Valley) and Eastern Paratethys during the interval 6.00–5.30 Ma, as forced by changes in Mediterranean sea level and relationships with the Atlantic Ocean, is summarized in Fig. 14. Some attention is given to the function of sills within the Mediterranean–Eastern Paratethys realm, which controlled exchanges between the basins or caused their isolation. Fig. 14b corresponds to the marginal evaporitic phase, and Fig. 14d to the deep basin desiccation. High sea levels in Fig. 14c (i.e. isotope stage TG 11) and 14 (i.e. isotope stage TG 5) would have produced exchanges between the Mediterranean Sea and Eastern Paratethys, i.e. the Lago Mare events in the Mediterranean realm and simultaneous nannoplankton–dinocyst influxes in the Dacic and Euxinian basins.

The northern part of the Dacic Basin has evolved as a perched basin disconnected both from the Black and Mediterranean seas (Figs 11 and 14), with residual brackish to fresh waters probably caused by the highly positive water budget of the area forced by climatic conditions and proximity of high reliefs. A similar evolution was envisioned for the Po Valley–Adriatic Basin which probably existed during the desiccation of the Mediterranean Sea as a perched freshwater basin (Fig. 14), continuously fed by waters from the Alpine and rising Apennine mountain ranges: during the salinity crisis, the area was characterized by almost continuous sedimentation (Corselli & Grecchi, 1984; Cita & Corselli, 1990; Clauzon *et al.*, 1997; Figs 2 and 12). This hypothesis is supported in the lower part of the Maccarone section by high percentages of certain subdesertic plants (such as *Lygeum*; Bertini, 1994, 2002) that are generally abundant in Sicily before and after the salinity crisis (Suc & Bessaïs, 1990; Bertini *et al.*, 1998). Subdesertic plants probably migrated northwards during the desiccation of the Mediterranean Sea because they could not persist within the evaporitic basin where such dry conditions prevailed (Fauquette *et al.*, in press). The upper part of the section (including the Colombacci Formation) deposited prior to the Zanclean clays has yielded planktonic foraminifers and ostracods that are considered not to be reworked (Carloni *et al.*, 1974), and oceanic dinocysts such as *Impagidinium aculeatum* (Bertini, 1992). We suggest these data indicate that the basin once again received marine waters from the Mediterranean before the officially defined beginning of the Pliocene. Simultaneously, a strong increase in bisaccate pollen grains occurs parallel to a manifold decrease in coastal plants (halophytes), which expresses the sudden establishment of offshore conditions (Bertini, 1994, 2002). This break is so abrupt that it cannot be explained by a tectonic event. We consider that water of the Po Valley–Adriatic lake was at the same level as the Mediterranean Sea, which was now able to overtop the uplifted Otrante Sill (Fig. 14) and introduce surface marine waters during Zanclean flooding, i.e. isotope stage TG 5.

The interpretation of ostracod layers is not easy in terms of invasion of the Mediterranean Basin by Paratethyan waters. There is no ambiguity for the more or less marginal localities where ostracods are generally associated with the other Paratethyan immigrants (Congeria, dinocysts): they really result from brackish water inflows (Fig. 13: localities 9–22 and 36–42 for the first influx, localities 9–10, 23–35 and 40 for the second influx) from the Eastern Paratethys (Table 2). More debatable is the interpretation of ostracod layers found, without any other marker of Paratethyan origin, at the top of the Messinian series in the deep Mediterranean Basin boreholes (Fig. 13: localities 43–48) (Table 2). These ostracods, accepted as being *in situ* because of their fragile carapaces, are thought to represent brackish- or freshwater lakes developed on the deep sea floor just after the desiccation of the Mediterranean Sea (Iaccarino & Bossio, 1999). Such deep deposits are considered to have occurred later than the marginal Lago Mare sediments (Iaccarino & Bossio, 1999, p. 538, Fig. 8). Nevertheless we believe that they result from different events as already suggested by Carbonnel (1980) who put forward the following arguments: the ostracod faunas revealed by deep sea boreholes are less diverse than the marginal ones, and some differences in carapace morphology exist. For us, the presence of lakes on the deep sea floor is incompatible with Mediterranean–Eastern Paratethys exchanges at high sea level. Hence, we consider that such lakes in the deep, almost desiccated Mediterranean Basin had developed immediately at the end of the desiccation or existed during longer periods in some intermediate basins (see ODP Site 652 in the Tyrrhenian Basin; Cita *et al.*, 1990). We suggest that local ecological conditions caused the appearance of *Cyprideis* group ostracods in these deep Mediterranean lakes, as suggested by Rouchy *et al.* (2001) for the southern Cyprus basins. In contrast, the marginal Lago Mare facies seem to have been caused by real influxes of Eastern Paratethys waters during cross exchanges at high sea level between the Mediterranean Sea and the Eastern Paratethys.

Finally, three Lago Mare events occurred in the Mediterranean Sea between 5.96 and 5.30 Ma: they are distinct not only chronologically but also in view of their origin. They have been labelled LM 1, LM 2, and LM 3 on Fig. 12:

- LM 1 occurred at 5.52 Ma and corresponds to isotope stage TG 11; LM 2 occurred at the end of the desiccation, i.e. just before 5.33; and LM 3 occurred at 5.33 Ma and corresponds to isotope stage TG 5;
- LM 1 and LM 3 result from exchanges at high sea level between the Mediterranean Sea and Eastern Paratethys and are characterized by *Congeria*, ostracods and dinocysts; LM 2 reflects ecological changes in the deep Mediterranean lagoons at the end of desiccation, and is marked only by the presence of ostracods.

As a consequence, we recommend restricting the term Lago Mare to a palaeoecological context, and discontinuing its use in chronostratigraphic applications.

Our results resolve the widespread confusion surrounding the old Lago Mare concept (Hsü *et al.*, 1973, 1977; Cita *et al.*, 1978b), which was implied by Fortuin *et al.* (1995, p. 198) in terms of stratigraphic relationships with the Messinian erosional surface, and by Iaccarino & Bossio (1999, p. 538, Fig. 8) as diachronism that we explain by differences between the Mediterranean margins and central basins.

Referring to the map on Fig. 13, LM 1 has a widespread geographic distribution across the Mediterranean margins. In contrast, LM 2 is restricted to the central Mediterranean basins. Lastly, LM 3 appears less widely distributed than LM 1, a feature that could be explained by the insufficient strength of the Paratethyan surface current to oppose the pressure of inflowing Atlantic water.

CONCLUSION

Some classical signatures of the Messinian salinity crisis in the Mediterranean Basin have been found in the Dacic Basin (Eastern Paratethys) in the area of Turnu Severin, close to the course of the modern Danube, namely:

- an erosional surface overlain by clay deposits belonging to calcareous nannofossil Zone NN12,
- an impressive Gilbert-type fan delta.

In addition to evaporite deposition and the presence of an erosional surface in the Black Sea, these new elements located at the outlet of the Iron Gates assert that the Eastern Paratethys was also severely affected by the Messinian salinity crisis.

Influxes of Mediterranean nannofloras and dinocysts penetrated the Dacic Basin and northwestern part of the Euxinian Basin during events corresponding to Zones NN11 and NN12, i.e., just before and just after the desiccation of the Mediterranean. Hence, new data on Mediterranean influxes into the Eastern Paratethys, and new field evidences from the Dacic Basin, suggest that the Mediterranean Sea and the Eastern Paratethys were connected at high sea level just before and just after the crisis, providing another explanation for Black Sea desiccation other than its drainage into the desiccated Mediterranean Basin. Our data suggest that high sea-level cross exchanges existed between the Mediterranean Sea and the Eastern Paratethys.

The Danube River appeared as an immediate consequence of the salinity crisis, and rapidly reached a course similar to its modern one over the Romanian Plain. The Messinian erosional surface developed along the Danube course and along its main tributaries whereas the northern part of the Dacic Basin remained as a perched lake, fed by Carpathian rivers owing to a regional positive hydrologic budget. This area endured continuous sedimentation, as was proposed for the Po Valley and the Adriatic realm.

Henceforth, the Lago Mare must be considered a triple event. Two events, LM 1 and LM 3, affected only the Med-

iterranean margins: one Paratethyan water incursion occurred just before the Mediterranean became desiccated, the other marking the Zanclean reflooding of the Mediterranean; they respectively correspond to isotope stages TG 11 (5.52 Ma) and TG 5 (5.33 Ma). They are only recorded in the marginal and perched satellite basins. They did not affect the deep Mediterranean Basin lakes (containing ostracods of the *Cyprideis* group) which we believe to have developed (LM 2 event) when the Mediterranean was desiccated, just before the Zanclean infilling.

The gateways followed by these water exchanges are more clearly defined. A proto-Bosphorus Strait seems to be unnecessary, but a gateway through Macedonia and Bulgaria seems possible and is being explored.

ACKNOWLEDGMENTS

The following colleagues are acknowledged for discussions and for providing information: M.-P. Aubry, A. Di Stefano, C. Dinu, J.-L. Guendon, D. Jipa, L. Londeix, T. Nica, N. Panin, S.C. Rădan, M. Rădan, N. Țicleanu, M.N. Çağatay and the late I. Papaianopol, C. Rădulescu and P.-M. Samson. W. Krijgsman has performed palaeomagnetic measurements at Hinova and Husnicioara and made some comments on the manuscript. TOTAL provided financial support for the field trip in 1998. PETROM has granted access to some subsurface data. Dr G. Udubaşa, Director of the Romanian Institute of Geology, has provided facilities and R. Maftai some assistance. I. Magyar has offered a fruitful critical review of the manuscript. We greatly appreciate the comments of the two referees, S. Iaccarino and R. Flecker whose suggestions resulted in a significantly improved manuscript. The final English version was edited by Dr Martin J. Head (University of Cambridge).

This work is a contribution to the CNRS ECLIPSE Project on The Messinian Salinity Crisis and to the EEDEN Programme of the European Science Foundation.

REFERENCES

- ALERIA (1980) Le canal de Corse et les bassins nord-tyrrhéniens au Miocène supérieur et terminal (Messinien); leur évolution plio-quadernaire. *Géol. Médit.*, 7(1), 5–12.
- ALMERA, J. (1894) *Descripción de los terrenos pliocénicos de la cuenca del Bajo Llobregat y Llano de Barcelona*. Mapa Geol. Prov, Barcelona.
- ARCHAMBAULT-GUEZOU, J. (1976) Présence de Dreissenidae euxiniques dans les dépôts à Congéries de la vallée du Rhône et sur le pourtour du bassin méditerranéen. Implications biogéographiques. *Bull. Soc. Géol. France*, 18(5, Ser. 7), 1267–1276.
- ARCHAMBAULT-GUEZOU, J., ILINA, L.B., KELLER, J.-P. & MONTENAT, C. (1979) Affinités euxiniques des mollusques messiniens d'Elche (Alicante, Espagne) et implications paléogéographiques. *Ann. Géol. Pays Hellén*, 1(spec. issue), 27–37.
- BACKMAN, J. & RAFFI, I. (1997) Calibration of Miocene nannofossil events to orbitally tuned cyclostratigraphies from Ceara rise. In: *Leg 154* (Ed. by N.J. Shackleton & W.B. Curry, *et al.*) *Proc. Ocean Drill. Progr. Sci. Result*, 154, 83–89.
- BALLESIO, R. (1972) Etude stratigraphique du Pliocène rhodanien. *Doc. Lab. Géol. Fac. Sci. Lyon*, 53, 1–333.

- BARBER, P.M. (1981) Messinian subaerial erosion of the proto-Nile delta. *Mar. Geol.*, **44**(3–4), 253–272.
- BASSETTI, M.A., RICCI LUCCHI, F. & ROVERI, M. (1994) Physical stratigraphy of the Messinian post-evaporitic deposit in Central-Southern Marche area (Appennines, Central Italy). *Mem. Soc. Geol. It.*, **48**, 275–288.
- BENSON, R.H. (1976) Changes in the ostracodes of the Mediterranean with the Messinian salinity crisis. *Palaeogeogr. Palaeoclimatol. Palaeoecol.*, **20**, 147–170.
- BENSON, R.H. (1978) Preliminary examination of the ostracodes of DSDP Leg 42B. In: *Leg 42B* (Ed. by D.A. Ross & Y.P. Neprochnov, et al.) *Init. Rep. Deep Sea Drill. Proj.* **42**(2), 1039–1040.
- BERGGREN, W.A., HILGEN, F.J., LANGEREIS, C.G., KENT, D.V., OBRADOVICH, J.D., RAFFI, I., RAYMO, M.E. & SHACKLETON, N.J. (1995a) Late Neogene chronology: new perspectives in high-resolution stratigraphy. *Geol. Soc. Am. Bull.*, **107**(11), 1272–1287.
- BERGGREN, W.A., KENT, D.V., SWISHER, C.C. & AUBRY, M.-P. (1995b) A revised Cenozoic geochronology and chronostratigraphy. In: *Geochronology Time Scales and Global Stratigraphic Correlation SEPM Spec. Publ.*, **54**, 141–212.
- BERTINI, A. (1992) *Palinologia ed aspetti ambientali del versante Adriatico dell'Appennino centro-settentrionale durante il Messiniano e lo Zancleano*. PhD Thesis, University of Florence.
- BERTINI, A. (1994) Palynological investigations on Upper Neogene and Lower Pleistocene sections in Central and Northern Italy. *Mem. Soc. Geol. It.*, **48**, 431–443.
- BERTINI, A. (2002) Palynological evidence of Upper Neogene environments in Italy. *Acta Univ. Carolinae, Geol.*, **46**(4), 15–25.
- BERTINI, A., CORRADINI, D. & SUC, J.-P. (1995) On *Galeacysta etrusca* and the connections between the Mediterranean and the Paratethys. *Rom. J. Stratigr.*, **76**(Suppl. 7), 141–142.
- BERTINI, A., LONDEIX, L., MANISCALCO, R., DI STEFANO, A., SUC, J.-P., CLAUZON, G., GAUTIER, F. & GRASSO, M. (1998) Paleobiological evidence of depositional conditions in the Salt Member, Gessoso-Solfifera Formation (Messinian, Upper Miocene) of Sicily. *Micropaleontology*, **44**(4), 413–433.
- BIZON, J.-J., BIZON, G. & MÜLLER, C. (1978) Données tirées de l'étude des foraminifères et des nannofossiles du Messinien en affleurement et dans le domaine marin. *Bull. Mus. Nat. Hist. Nat., Paris*, **518**(70, ser. 3), 123–135.
- BLANC-VALLERON, M.-M., ROUCHY, J.-M., PIERRE, C., BADAUT-TRAUTH, D. & SCHULER, M. (1998) Evidence of Messinian nonmarine deposition at Site 968 (Cyprus lower slope). In: *Leg 160* (Ed. by A.H.F. Robertson & K.-C. Emeis, et al.) *Proc. Ocean Drill. Progr. Sci. Results*, **160**, 437–445.
- BONADUCE, G. & SGARRELLA, F. (1999) Paleocological interpretation of the latest Messinian sediments from southern Sicily (Italy). *Mem. Soc. Geol. It.*, **54**, 83–91.
- BOSSIO, A., ESTEBAN, M., GIANNELLI, L., LONGINELLI, A., MAZZANTI, R., MAZZEI, R., RICCI LUCCHI, F. & SALVATORINI, G. (1978) Some aspects of the Upper Miocene in Tuscany. In: *Messinian Seminar 4, Rome* (Ed. by Pacini), p. 88. IGCP Project 96 & CNR.
- BOSSIO, A., GIANNELLI, L., MAZZANTI, R., MAZZEI, R. & SALVATORINI, G. (1981) Gli strati alti del Messiniano, il passaggio Miocene-Pliocene e la sezione plio-pleistocenica di Nugola nelle colline a NE del Monti Livornesi. In: *9th Congress of Society of Paleontology, Italy* (Ed. by Pacini), p. 199. Società Paleontologica Italiana.
- BROLSMA, M.J. (1976) Discussion of the arguments concerning the palaeoenvironmental interpretation of the Arenazzolo in Capo Rossello and Eraclea Minoa (S. Sicily, Italy). *Mem. Soc. Geol. It.*, **16**, 153–157.
- BUROLLET, P.F. (1952) *Porto Farina*. Carte géologique de la Tunisie au 1/50.000ème, 7.
- BUSSON, G. (1990) Le Messinien de la Méditerranée vingt après. *Géol. France*, **3–4**, 3–58.
- BUTLER, R.W.H., LICKORISH, W.H., GRASSO, M., PEDLEY, H.M. & RAMBERTI, L. (1995) Tectonics and sequence stratigraphy in Messinian basins, Sicily: Constraints on the initiation and termination of the Mediterranean salinity crisis. *Geol. Soc. Am. Bull.*, **107**(4), 425–439.
- CARBONNEL, P. (1978) La zone à *Loxococoncha djaffarovi* SCHNEIDER (Ostracoda, Miocène supérieur) ou le Messinien de la vallée du Rhône. *Rev. Micropaléontol.*, **21**(3), 106–118.
- CARBONNEL, P. (1980) L'ostracofaune du Messinien: une preuve de la vidange de la Paratéthys. *Géol. Médit.*, **7**(1), 19–24.
- CARLONI, G., FRANCAVILLA, F., BORSETTI, A.M., CATI, F., D'ONOFRIO, S., MEZZETTI, R. & SAVELLI, C. (1974) Ricerche stratigrafiche sul limite Miocene-Pliocene nelle Marche centro-meridionali. *Giorn. Geol.*, **39**(2, Ser. 2), 363–392.
- CASTRADORI, D. (1998) Calcareous nannofossils in the basal Zanclean of the Eastern Mediterranean Sea: remarks on paleoceanography and sapropel formation. In: *Leg 180* (Ed. by A.H.F. Robertson, K.-C. Emeis, C. Richter & A. Camerlenghi), *Proc. Ocean Drill. Progr., Sci. Res.*, **180**, 113–123.
- CAVALLO, O. & REPETTO, G. (1988) Un nuovo giacimento della facies a Congerie nell'Albese. *Riv. Piemont. Stor. Nat.*, **9**, 43–62.
- CHUMAKOV, I. (1973) Geological history of the Mediterranean at the end of the Miocene—the beginning of the Pliocene according to new data. In: *Leg 13* (Ed. by W.B.F. Ryan & K.J. Hsü, et al.) *Init. Rep. Deep Sea Drill. Proj.*, **13**(2), 1241–1242.
- CIPOLLARI, P., COSENTINO, D., ESU, D., GIROTTI, O., GLIOZZI, E. & PRATURLON, A. (1999) Thrust-top lacustrine-lagoonal basin development in accretionary wedges: late Messinian (Lago-Mare) episode in the central Apennines (Italy). *Palaeogeogr. Palaeoclimatol. Palaeoecol.*, **151**, 149–166.
- CITA, M.B. (1991) Development of a scientific controversy. In: *Controversies in Modern Geology* (Ed. by DW. Muller, J.A. McKenzie & H. Weissert), pp. 13–23. Academic Press. Limited, London.
- CITA, M.B. & COLOMBO, L. (1979) Sedimentation in the latest Messinian at Capo Rossello (Sicily). *Sedimentology*, **26**, 497–522.
- CITA, M.B. & CORSELLI, C. (1990) Messinian paleogeography and erosional surfaces in Italy: an overview. *Palaeogeogr. Palaeoclimatol. Palaeoecol.*, **77**, 67–82.
- CITA, M.B. & GARTNER, S. (1973) Studi sul Pliocene e sugli strati di passaggio dal Miocene al Pliocene. IV. The stratotype Zanclean foraminiferal and nannofossil biostratigraphy. *Riv. Ital. Paleont.*, **79**(4), 503–558.
- CITA, M.B., RACCHETTI, S., BRAMBILLA, R., NEGRI, M., COLOMBAROLI, D., MORELLI, L., RITTER, M., ROVIRA, E., SALA, P., BERTARINI, L. & SANVITO, S. (1999) Changes in sedimentation rates in all Mediterranean drillsites document basin evolution and support starved basin conditions after early Zanclean flood. *Mem. Soc. Geol. It.*, **54**, 145–159.
- CITA, M.B., RYAN, W.B.F. & KIDD, R.B. (1978a) Sedimentation rates in Neogene deep sea sediments from the Mediterranean and geodynamic implications of their changes. In: *Leg 42A* (Ed. by K.J. Hsü & L. Montadert, et al.) *Init. Rep. Deep Sea Drill. Proj.*, **42**(1), 991–1002.
- CITA, M.B., SANTAMBROGIO, S., MELILLO, B. & ROGATE, F. (1990) Messinian paleoenvironments: new evidence from the

- Tyrrhenian Sea (ODP Leg 107). In: *Leg 107* (Ed. by K.A. Kastens & J. Mascle, et al.) *Init. Rep. Deep Sea Drill. Proj., Sci. Res.*, **107**, 211–227.
- CITA, M.B., STRADNER, H. & CIARANFI, N. (1973) Studi sul Pliocene e sugli strati di passaggio dal Miocene al Pliocene. III. Biostratigraphical investigations on the Messinian stratotype and on the overlying “Trubi” Formation. *Riv. Ital. Paleont.*, **79**(3), 393–446.
- CITA, M.B., VISMARA SCHILLING, A. & BOSSIO, A. (1980) Studi sul Pliocene e sugli strati di passaggio dal Miocene al Pliocene. XII. Stratigraphy and paleoenvironment of the Cuevas del Almanzora section (Vera basin). A re-interpretation. *Riv. Ital. Paleont.*, **86**(1), 215–240.
- CITA, M.B., WRIGHT, R.C., RYAN, W.B.F. & LONGINELLI, A. (1978b) Messinian paleoenvironments. In: *Leg 42A* (Ed. by K. Hsü & L. Montadert, et al.) *Init. Rep. Deep Sea Drill. Proj., Sci. Res.*, **42**(1), 1003–1025.
- CIVIS, J., MARTINELLI, J. & DE PORTA, J. (1979) Presencia de *Cyprideis pannonica pseudoagrigentina* DECIMA en el Miembro Zorreras (Sorbas, Almería). *Studia Geol.*, **15**, 57–62.
- CLAUZON, G. (1973) The eustatic hypothesis and the pre-cutting of the Rhone Valley. In: *Leg 13* (Ed. by W.B.F. Ryan & K.J. Hsü, et al.) *Init. Rep. Deep Sea Drill. Proj.*, **13**(2), 1251–1256.
- CLAUZON, G. (1978) The Messinian Var canyon (Provence, Southern France). Paleogeographic implications. *Mar. Geol.*, **27**(3–4), 231–246.
- CLAUZON, G. (1979) Le canyon messinien de la Durance (Provence, France): une preuve paléogéographique du bassin profond de dessiccation. *Palaeogeogr. Palaeoclimatol. Palaeoecol.*, **29**(1–2), 15–40.
- CLAUZON, G. (1982) Le canyon messinien du Rhône: une preuve décisive du “desiccated deep-basin model” (Hsü, Cita et Ryan, 1973). *Bull. Soc. Géol. France*, **24**(3, Ser. 7), 597–610.
- CLAUZON, G. (1990) Restitution de l'évolution géodynamique néogène du bassin du Roussillon et de l'unité adjacente des Corbières d'après les données écostratigraphiques et paléogéographiques. *Paléobiol. Cont.*, **17**, 125–155.
- CLAUZON, G. (1996) Limites de séquence et évolution géodynamique. *Géomorphologie*, **1**, 3–22.
- CLAUZON, G. (1997) Detailed morpho-sedimentary recording of the Messinian events in the betic basin in the light of the two phase model of the Salinity Crisis. In: *Neogene Basins of the Mediterranean Region: Controls and Correlation in Space and Time* (Ed. by E. Diliberto, A. Di Stefano & R. Maniscalco). R.C.M.N.S. Inter.-Coll., Catania, *Program Abstracts*, 40–42.
- CLAUZON, G. (1999) L'impact des variations eustatiques du bassin de Méditerranée occidentale sur l'orogène alpin depuis 20 Ma. *Et. Géogr. Phys.*, **28**, 1–8.
- CLAUZON, G., RUBINO, J.-L. & CASERO, P. (1997) Regional modalities of the Messinian Salinity Crisis in the framework of a two phases model. In: *Neogene Basins of the Mediterranean Region: Controls and Correlation in Space and Time* (Ed. by E. Diliberto, A. Di Stefano & R. Maniscalco). R.C.M.N.S. Inter.-Coll., Catania, *Program Abstracts*, 44–46.
- CLAUZON, G., RUBINO, J.-L. & SAVOYE, B. (1995) Marine Pliocene Gilbert-type fan deltas along the French Mediterranean coast. Field Trip Guide Book, 16th IAS regional meeting of Sedimentology. *Publ. Ass. Séd. Fr.*, **23**, 143–222.
- CLAUZON, G. & SUC, J.-P. (1998) Peut-on appliquer au couple Mer Noire – Danube le modèle de dévolution du bassin de Méditerranée occidentale – Rhône lors de la crise de salinité messinienne? Rapport TOTAL – Conventions TEP/DEG-1546-1551, 62pp.
- CLAUZON, G., SUC, J.-P., GAUTIER, F., BERGER, A. & LOUTRE, M.-F. (1996) Alternate interpretation of the Messinian salinity crisis: controversy resolved? *Geology*, **24**(4), 363–366.
- COLALONGO, M.L. (1968) Ostracodi del neostratotipo del Messiniano. *Giorn. Geol.*, **35**(2, Ser. 2), 67–72.
- CORNÉE, J.-J., SAINT-MARTIN, J.-P., CONESA, G., MUNCH, P., ANDRE, J.-P., SAINT-MARTIN, S. & ROGER, S. (2004) Correlations and sequence stratigraphic model for Messinian carbonate platforms of the western and central Mediterranean. *Int. J. Earth Sci.*, **93**, 621–633.
- CORRADINI, D. & BIFFI, U. (1988) Etude des dinokystes à la limite Messinien–Pliocène dans la coupe Cava Serredi, Toscane, Italie. *Bull. Centres Rech. Explor.-Prod. Elf-Aquitaine*, **12**(1), 221–236.
- CORSELLI, C. & GRECCHI, G. (1984) The passage from hypersaline to hyposaline conditions in the Mediterranean Messinian: discussion of the possible mechanisms triggering the “lago-mare” facies. *Paléobiol. Cont.*, **14**(2), 225–239.
- DABOVSKI, C., BOYANOV, I., KHRISCHEV, K., NIKOLOV, T., SAPOUNOV, I., YANEV, Y. & ZAGORCHEV, I. (2002) Structure and Alpine evolution of Bulgaria. *Geol. Balcanica*, **32**(2–4), 9–15.
- DECIMA, A. & SPROVIERI, R. (1973) Comments on late Messinian microfaunas in several sections from Sicily. In: *Messinian Events in the Mediterranean* (Ed. by C.W. Drooger), *Kon. Ned. Akad. Wetenschappen, Geodynam. Sci. Rep.* **7**, 229–234.
- DELRIEU, B., ROUCHY, J.-M. & FOUCAULT, A. (1993) La surface d'érosion fini-messinienne en Crète centrale (Grèce) et sur le pourtour méditerranéen: rapports avec la crise de salinité méditerranéenne. *C. R. Acad. Sci. Paris*, **316**(ser. 2), 527–533.
- DENIZOT, G. (1952) Le Pliocène dans la vallée du Rhône. *Rev. Géogr. Lyon*, **27**(4), 327–357.
- DI GERONIMO, I., ESU, D. & GRASSO, M. (1989) Gli strati a “Congerie” del Messiniano superiore del margine nord-occidentale Ibleo. Caratteristiche faunistiche e possibili implicazioni paleogeografiche e paleoclimatiche. *Atti Acad. Peloritana dei Pericolanti*, **67**(Suppl. 1), 129–150.
- DRIVALIARI, A. (1993) Images polliniques et paléoenvironnements au Néogène supérieur en Méditerranée orientale. Aspects climatiques et paléogéographiques d'un transect latitudinal (de la Roumanie au delta du Nil). PhD Thesis, University of Montpellier 2.
- DRIVALIARI, A., ȚICLEANU, N., MARINESCU, F., MARUŢEANU, M. & SUC, J.-P. (1999) A Pliocene climatic record at Țicleni (Southwestern Romania). In: *The Pliocene: Time of Change* (Ed. by J.H. Wrenn, J.-P. Suc & S.A.G. Leroy), pp. 103–108. Amer. Ass. Stratigr. Palynologists Foundation.
- FAUQUETTE, S., SUC, J.-P., BERTINI, A., POPESCU, S.-M., WARNY, S., BACHIRI TAOUFIQ, N., PEREZ VILLA, M.-J., CHIKHI, H., SUBALLY, D., FEDDI, N., CLAUZON, G. & FERRIER, J. (in press) How much did the climate force the Messinian salinity crisis? Quantified climatic conditions from pollen records in the Mediterranean region. *Palaeogeogr. Palaeoclimatol. Palaeoecol.*
- FONTANNES, F. (1883) Note sur l'Extension et la Faune de la mer pliocène dans le sud-est de la France. *Bull. Soc. Géol. France*, **11**(Ser. 3), 103–142.
- FORTEY, R. (2000) La mer Noire, fille du Déluge? *La Recherche*, **327**, 54–57.
- FORTUIN, A.R., KELLING, J.M.D. & ROEP, TH.B. (1995) The enigmatic Messinian–Pliocene section of Cuevas del Almanzora (Vera Basin, SE Spain) revisited – erosional features and strontium isotope ages. *Sedim. Geol.*, **97**, 177–201.

- GARCÉS, M., KRIJGSMAN, W. & AGUSTI, J. (1998) Chronology of the late Turolian deposits of the Fortuna basin (SE Spain): implications for the Messinian evolution of the eastern Betics. *Earth Planet. Sci. Lett.*, **163**, 69–81.
- GAUTIER, F., CLAUZON, G., SUC, J.-P., CRAVATTE, J. & VIOLANTI, D. (1994) Age et durée de la crise de salinité messinienne. *C. R. Acad. Sci. Paris*, **318**(ser. 2), 1103–1109.
- GILLET, H. (2004) La stratigraphie tertiaire et la surface d'érosion messinienne sur les marges occidentales de la Mer Noire: Stratigraphie sismique haute résolution. PhD Thesis, University of Bretagne Occidentale (Brest).
- GILLET, H., LERICOLAIS, G., REHAULT, J.-P. & DINU, C. (2003) La stratigraphie oligo-miocène et la surface d'érosion messinienne en mer Noire, stratigraphie sismique haute résolution. *C. R. Geosciences*, **335**, 907–916.
- GILLET, S. (1937) Sur la présence du Pontien s. str. Dans la région de Salonique. *C. R. Acad. Sci. Paris*, **205**, 1243–1245.
- GILLET, S. (1960) Observations sur de jeunes coquilles de Mollusques du Pliocène saumâtre du Llobregat (Barcelone). *Bull. Soc. Géol. France*, **1**(Ser. 7), 731–733.
- GILLET, S. (1965) Los Limnocardidos del Plioceno de Papiol (Barcelona). *Mem. y Commun.*, **1**(Ser. 2), 3–81.
- GILLET, S. (1968) La faune messinienne des environs d'Ancona. *Giorn. Geol.*, **36**(Ser. 2), 69–100.
- GILLET, S. & GEISSERT, F. (1971) La faune de mollusques du Pontien de Trilophos (SW de Thessaloniki). *Ann. Géol. Pays Hellén.*, **23**(Ser. 1), 123–164.
- GILLET, S., GRAMANN, F. & STEFFENS, P. (1978) Neue biostratigraphische Ergebnisse aus dem brackischen Neogen an Dardanellen und Marmara-Meer (Türkei). *Newslett. Stratigr.*, **7**(1), 53–64.
- GLIOZZI, E. (1999) A late Messinian brackish water ostracod fauna of Paratethyan aspect from Le Vicenne Basin (Abruzzi, central Apennines, Italy). *Palaeogeogr. Palaeoclimatol. Palaeoecol.*, **151**, 191–208.
- GORINI, C., LE MARREC, A. & MAUFFRET, A. (1993) Contribution to the structural and sedimentary history of the Gulf of Lions (western Mediterranean), from the ECORS profiles, industrial seismic profiles and well data. *Bull. Soc. Géol. France*, **164**(3), 353–363.
- GÖRÜR, N., CAGATAY, N., SAKINC, M., SUMENGEN, M., SENTURK, K., YALTIRAK, C. & TCHAPALYGA, A. (1997) Origin of the Sea of Marmara deduced from Neogene to Quaternary paleogeographic evolution of its frame. *Int. Geol. Rev.*, **39**, 342–352.
- HAQ, B.U., HARDENBOL, J. & VAIL, P.R. (1987) Chronology of fluctuating sea levels since the Triassic. *Science*, **235**, 1156–1167.
- HOMWOOD, P., GUILLOCHEAU, F., ESCHARD, R. & CROSS, T.A. (1992) Corrélations haute résolution et stratigraphie génétique: une démarche intégrée. *Bull. Centres Rech. Explor.-Prod. Elf-Aquitaine*, **16**, 357–381.
- HSÜ, K.J., CITA, M.B. & RYAN, W.B.F. (1973) The origin of the Mediterranean evaporites. In: *Leg 13* (Ed. by W.B.F. Ryan & K.J. Hsü, et al.) *Init. Rep. Deep Sea Drill. Proj.* **13**, 1203–1231.
- HSÜ, K.J. & GIOVANOLI, F. (1979) Messinian event in the Black Sea. *Palaeogeogr. Palaeoclimatol. Palaeoecol.*, **29**(1–2), 75–94.
- HSÜ, K.J., MONTADERT, L., BERNOULLI, D., CITA, M.B., ERICKSON, A., GARRISON, R.E., KIDD, R.B., MELIERES, F., MULLER, C. & WRIGHT, R. (1977) History of the Mediterranean salinity crisis. *Nature*, **267**, 399–403.
- HSÜ, K.J., MONTADERT, L., BERNOULLI, D., CITA, M.B., ERICKSON, A., GARRISON, R.E., KIDD, R.B., MELIERES, F., MULLER, C. & WRIGHT, R. (1978a) History of the Mediterranean salinity crisis. In: *Leg 42A* (Ed. by K.J. Hsü & L. Montadert, et al.) *Init. Rep. Deep Sea Drill. Proj.*, **42**(1), 1053–1078.
- HSÜ, K.J. & MONTADERT, L., et al (eds.) (1978b) *Leg 42A. Init. Rep. Deep Sea Drill. Proj.*, **42**, 1.
- IACCARINO, S. & BOSSIO, A. (1999) Palaeoenvironment of uppermost Messinian sequences in the Western Mediterranean (Sites 974, 975, and 978). In: *Leg 161* (Ed. by R. Zahn, M.C. Comas & A. Klaus), *Proc. Ocean Drill. Progr., Sci. Results*, **161**, 529–541.
- IACCARINO, S. & PAPANI, G. (1979) Il Messiniano dell'Appennino settentrionale dalla Val d'Arda alla Val Secchia: stratigrafia e rapporti con il substrato e il Pliocene. In: *Volume Dedicato a Sergio Vénzo* (Ed. by G. Step), pp. 15–46. University of Parma.
- JIPA, D. (1997) Late Neogene – Quaternary evolution of Dacian Basin (Romania). An analysis of sediment thickness pattern. *Geo-Eco-Marina*, **2**, 127–134.
- KARISTINEOS, N.K. & GEORGIADES-DIKEOULIA, E. (1985–86) The marine transgression in the Serres Basin. *Ann. Géol. Pays Hellén.*, **33**(1), 221–232.
- KLOOSTERBOER-VAN HOEVE, M.L., STEENBRINK, J. & BRINKHUIS, H. (2001) A short-term cooling event, 4.205 million years ago, in the Ptolemais Basin, Northern Greece. *Palaeogeogr. Palaeoclimatol. Palaeoecol.*, **173**, 61–73.
- KOJUMDIEVA, E. (1987) Evolution géodynamique du bassin égéen pendant le Miocène supérieur et ses relations à la Paratéthys Orientale. *Geol. Balcanica*, **17**(1), 3–14.
- KONTOPOULOS, N., ZELILIDIS, A., PIPER, D.J.W. & MUDIE, P.J. (1997) Messinian evaporites in Zakynthos, Greece. *Palaeogeogr. Palaeoclimatol. Palaeoecol.*, **129**, 361–367.
- KRIJGSMAN, W., HILGEN, F.J., RAFFI, I., SIERRA, F.J. & WILSON, D.S. (1999a) Chronology, causes and progression of the Messinian Salinity Crisis. *Nature*, **400**, 652–655.
- KRIJGSMAN, W., HILGEN, F.J., MARABINI, S. & VAI, G.B. (1999b) New paleomagnetic and cyclostratigraphic age constraints on the Messinian of the Northern Apennines (Vena del Gesso Basin, Italy). *Mem. Soc. Geol. It.*, **54**, 25–33.
- LETOUZEY, J., GONNARD, R., MONTADERT, L., KRISTCHEV, K. & DORKEL, A. (1978) Black Sea: geological setting and recent deposits distribution from seismic reflection data. In: *Leg 42B* (Ed. by D.A. Ross & Y.P. Neprochnov, et al.) *Init. Rep. Deep Sea Drill. Proj.*, **42**(2), 1077–1084.
- LOFI, J. (2002) La Crise de Salinité Messinienne: Conséquences directes et différées sur l'évolution sédimentaire de la marge du Golfe du Lion. PhD Thesis, University of Sciences et Techniques. Lille.
- LOFI, J., RABINEAU, M., GORINI, C., BERNE, S., CLAUZON, G., DE CLARENS, P., DOS REIS, T., MOUNTAIN, G.S., RYAN, W.B.F., STECKLER, M. & FOUCHET, C. (2003) Plio-Quaternary prograding clinoform wedges of the Western Gulf of Lions continental margin (NW Mediterranean) after the Messinian Salinity Crisis. *Mar. Geol.*, **198**, 289–317.
- LOURENS, L.J., ANTONARAKOU, A., HILGEN, F.J., VAN HOOF, A.A.M., VERGNAUD GRAZZINI, C. & ZACHARIASSE, W.J. (1996) Evaluation of the Pliocene to early Pleistocene astronomical time scale. *Paleoceanography*, **11**, 391–413.
- MAGNÉ, J., ORSZAG-SPERBER, F. & PILOT, M.-D. (1977) Nouvelles données sur le Pliocène de Corse: le problème de la limite Miocène-Pliocène. *Bull. Bur. Rech. Géol. Min.*, **3**(Ser. 2, sect. 1), 209–218.
- MAGYAR, I., GEARY, D.H. & MÜLLER, P. (1999) Paleogeographic evolution of the Late Miocene Lake Pannon in Central Europe. *Palaeogeogr. Palaeoclimatol. Palaeoecol.*, **147**, 151–167.

- MARABINI, S. & VAL, G.B. (1988) Geology of the Monticino Quarry, Brisighella, Italy. Stratigraphic implications of its late Messinian mammal fauna. In: *Fossil Vertebrates in the Lamone Valley, Romagna Apennines – Field Trip Guidebook* (Ed. by C. De Giuli & G.B. Vai), pp. 39–57. Faenza.
- MARINESCU, F. (1978) *Stratigrafia Neogenului Superior Din Sectorul Vestic Al Bazinului Dacic*. Edit. Acad. R.S.R., Bucharest.
- MARINESCU, F. (1992) Les bioprovinces de la Paratéthys et leurs relations. *Paleontologia i Evolució*, 24–25, 445–453.
- MARINESCU, F., GHENEA, C. & PAPAIAPOPOL, I. (1981) Stratigraphy of the Neogene and the Pleistocene Boundary. Guide Excursion A6, Guidebook ser. 20, 12th Congr. Carpatho-Balkan, Inst. Geol. Geophys. Bucharest, p. 111.
- MARINESCU, F., MARUŢEANU, M., PAPAIAPOPOL, I. & POPESCU, G. (1998) Tables with the correlations of the Neogene deposits in Romania. *Rom. J. Stratigr.*, 78, 181–186.
- MARTINA, E., CASATI, P., CITA, M.B., GERSONDE, R., D'ONOFRIO, S. & BOSSIO, A. (1979) Notes on the Messinian stratigraphy of the Crotona basin, Calabria (Italy). *Ann. Géol. Pays Hellén.*, 2(spec. issue), 755–765.
- MĂRUNŢEANU, M. (1992) Distribution of the Miocene calcareous nannofossils in the Intra- and Extra-Carpathian areas of Romania. *Knivovnicka ZPN*, 14b(2), 247–261.
- MĂRUNŢEANU, M. & PAPAIAPOPOL, I. (1995) The connection between the Dacic and Mediterranean Basins based on calcareous nannoplankton assemblages. *Rom. J. Stratigr.*, 76(7), 169–170.
- MĂRUNŢEANU, M. & PAPAIAPOPOL, I. (1998) Mediterranean calcareous nannoplankton in the Dacic Basin. *Rom. J. Stratigr.*, 78, 115–121.
- MÜLLER, P., GEARY, D.H. & MAGYAR, I. (1999) The endemic molluscs of the Late Miocene Lake Pannon: their origin, evolution, and family-level taxonomy. *Lethaia*, 32, 47–60.
- NASTASEANU, S. & BERCIA, I. (1968) *Baia de Arama. Carte géologique de Roumanie au 1/200.000*, Vol. 32. Institut géologique, Bucharest.
- NESTEROFF, W.D. (1973) Un modèle pour les évaporites messiniennes en Méditerranée, des bassins peu profonds avec des dépôts d'évaporites lagunaires. In: *Messinian events in the Mediterranean* (Ed. by C.W. Drooger), *Kon. Ned. Akad. Wetensch., Geodynam. Sci. Rep.*, 7, 68–81.
- ODIN, G.S., RICCI LUCCHI, F., TATEO, F., COSCA, M. & HUNZIKER, J.C. (1997) Integrated stratigraphy of the Maccarone section, Late Messinian (Marche region, Italy). In: *Miocene Stratigraphy – An Integrated Approach* (Ed. by A. Montanari, G.S. Odin & R. Coccioni), pp. 529–544. Elsevier, Amsterdam.
- OLTEANU, R. (1978) Ostracoda from DSDP Leg 42B. In: *Leg 42B* (Ed. by D.A. Ross & Y.P. Neprochnov, et al.) *Init. Rep. Deep Sea Drill. Proj.*, 42(2), 1017–1038.
- ORSZAG-SPERBER, F., ROUCHY, J.-M., BIZON, G., BIZON, J.-J., CRAVATTE, J. & MULLER, C. (1980) La sédimentation messinienne dans le bassin de Polemi (Chypre). *Géol. Médit.*, 7(1), 91–102.
- ORSZAG-SPERBER, F., ROUCHY, J.-M. & BLANC-VALLERON, M.-M. (2000) La transition Messinien-Pliocène en Méditerranée orientale (Chypre): la période du Lago-Mare et sa signification. *C. R. Acad. Sci. Paris., Earth Planet. Sci.*, 331, 483–490.
- OTT D'ESTEVOU, P. & MONTENAT, C. (1990) Le bassin de Sorbas – Tabernas. *Doc. et Trav. IGAL*, 12–13, 101–128.
- PAPAIAPOPOL, I. & MĂRUNŢEANU, M. (1993) Biostratigraphy (molluscs and calcareous nannoplankton) of the Sarmatian and Meotian in Eastern Muntenia (Dacic basin – Romania). *Zemni plyn a nafta*, 38(1), 9–15.
- PERCIVAL JR, S.F. (1978) Indigenous and reworked coccoliths from the Black Sea. In: *Leg 42B* (Ed. by D.A. Ross & Y.P. Neprochnov, et al.) *Init. Rep. Deep Sea Drill. Proj.*, 42(2), 773–781.
- PILOT, M.-D., BREBION, P. & LAURIAT-RAGE, A. (1975) Les gisements fossilifères du Néogène récent et du Quaternaire de la région d'Aléria-Vadina. *Bull. Soc. Sc. Hist. Nat. Corse*, 61–77.
- POPESCU, S.-M. (2001) Repetitive changes in Early Pliocene vegetation revealed by high-resolution pollen analysis: revised cyclostratigraphy of southwestern Romania. *Rev. Palaeobot. Palynol.*, 120, 181–202.
- POPESCU, S.-M. (in press) Upper Miocene and Lower Pliocene environments in the southwestern Black Sea region from high-resolution palynology of DSDP site 380A (Leg 42B). *Palaeogeogr. Palaeoclimatol. Palaeoecol.*
- POPESCU, S.-M., KRIJGSMAN, W., SUC, J.-P., CLAUZON, G. & MĂRUNŢEANU, M. (in press) Early Pliocene integrated stratigraphy and high-resolution chronology of the Dacic Basin (Southwestern Romania). *Palaeogeogr. Palaeoclimatol. Palaeoecol.*
- PROEDROU, P. (1979) The evaporites formation in the Nestos-Prinos graben in the Northern Aegean Sea. *Ann. Géol. Pays Hellén.*, 2(spec. issue), 1013–1020.
- PROEDROU, P. & SIDIROPOULOS, T. (1993) Prinos Field – Greece, Aegean Basin. In: *Treatise of Petroleum Geology, Atlas of Oil and Gas Fields* (Ed. by N.H. Foster & E.A. Beaumont), pp. 275–291. American Association of Petroleum Geologists, Tulsa.
- RĂDULESCU, C., SAMSON, P.-M., SEN, S., STIUCA, E. & HOROI, V. (1997) Les micromammifères pliocènes de Drănic (Bassin Dacique, Roumanie). In *BiochroM'97* (Ed. by J.-P. Aguilar, S. Legendre & J. Michaux), *Mém. Trav. E.P.H.E., Inst. Montpellier*, 21, 635–647.
- RIDING, R., BRAGA, J.C., MARTIN, J.M. & SANCHEZ-ALMAZO, I.M. (1998) Mediterranean Messinian Salinity Crisis: constraints from a coeval marginal basin. Sorbas, SE Spain. *Mar. Geol.*, 146, 1–20.
- RIZZINI, A., VEZZANI, F., COCOCETTA, V. & MILAD, G. (1978) Stratigraphy and sedimentation of a Neogene-Quaternary section in the Nile delta area (A.R.E.). *Mar. Geol.*, 27, 327–348.
- RÖGL, F., BERNOR, R.L., DERTMIZAKIS, M.D., MULLER, C. & STANCHEVA, M. (1991) On the Pontian correlation in the Aegean (Aegina Island). *Nemslitt. Stratigr.*, 24(3), 137–158.
- RÖGL, F. (1996) Stratigraphic correlation of the Paratethys Oligocene and Miocene. *Mitt. Ges. Geol. Bergbaustud. Österr.*, 41, 65–73.
- RÖGL, F. (1998) Palaeogeographic considerations for Mediterranean and Paratethys seaways (Oligocene to Miocene). *Ann. Naturhist. Mus. Wien*, 99(A), 279–310.
- RÖGL, F. & STEININGER, F.F. (1983) Vom Zerfall der Tethys zu Mediterran und Paratethys. Die neogene Paläogeographie und Palinspastik des zirkul-mediterranen Raumes. *Ann. Naturhist. Mus. Wien*, 85(A), 135–163.
- ROSS, D.A. & Neprochnov, Y.P., et al. (eds) (1978) *Leg 42B. Init. Rep. Deep Sea Drill. Proj.*, 42, 2.
- ROUCHY, J.-M., ORSZAG-SPERBER, F., BLANC-VALLERON, M.-M., PIERRE, C., RIVIERE, M., COMBOURIEU-NEBOUT, N. & PANAYIDES, I. (2001) Palaeoenvironmental changes at the Messinian-Pliocene boundary in the Eastern Mediterranean (southern Cyprus basins): significance of the Messinian Lago-Mare. *Sedim. Geol.*, 145, 93–117.

- ROUGHY, J.-M. & SAINT-MARTIN, J.-P. (1992) Late Miocene events in the Mediterranean as recorded by carbonate-evaporite relations. *Geology*, **20**, 629–632.
- RUGGERI, G. (1967) The Miocene and later evolution of the Mediterranean Sea. In: *Aspects of Tethyan Biogeography* (Ed. by C.G. Adams & D.V. Ager), *Syst. Assoc. Publ.*, **7**, 283–290.
- RYAN, W.B.F. & CITA, M.B. (1978) Messinian erosional surfaces in the Mediterranean. *Mar. Geol.*, **27**(3–4), 193–230.
- RYAN, W.B.F. & HSÜ, K.J., *et al* (eds) (1973) *Leg 13. Init. Rep. Deep Sea Drill. Proj.*, **13**.
- SACCHI, M., HORVATH, F., MAGYAR, I. & MÜLLER, P. (1997) Problems and progress in establishing a Late Neogene chronostratigraphy for the Central Paratethys. *Neogene Newsletter*, **4**, 37–46.
- SARJEANT, W.A.S. (1974) *Fossil and Living Dinoflagellates*. Academic Press, London.
- SAVOYE, B. & PIPER, D.J.W. (1991) The Messinian event on the margin of the Mediterranean Sea in the Nice area, southern France. *Mar. Geol.*, **97**, 279–304.
- SAVU, H. & GHENEA, C. (1967) Turnu Severin. Carte géologique de Roumanie au 1/200.000, 40, Institut géologique, Bucharest.
- SCHRADER, H.-J. (1978) Quaternary through Neogene history of the Black Sea, deduced from the paleoecology of Diatoms, Silicoflagellates, Ebridians, and Chrysomonads. In: *Leg 42B* (Ed. by D.A. Ross & Y.P. Neprochnov, *et al*) *Init. Rep. Deep Sea Drill. Proj.*, **42**(2), 789–901.
- SELLI, R. (1973) An outline of the Italian Messinian. In: *Messinian Events in the Mediterranean* (Ed. by C.W. Drooger), *Kon. Ned. Akad. Wetensch., Geodynam. Sci. Rep.*, **7**, 150–171.
- SEMENENKO, V.N. (1995) Geological events at the Miocene/Pliocene boundary in the Eastern Paratethys. *Geol. Soc. Greece*, **4**(Spec Publ), 264–268.
- SEMENENKO, V.N., ILJINA, L.B. & LYULJEVA, S.A. (1995) About zonal correlation of the Meotian stage of the Eastern Paratethys. *Rom. J. Stratigr.*, **76**(7), 115–116.
- SEMENENKO, V.N. & LYULJEVA, S.A. (1978) Opit priamoj korelacji moi-pliotena Vostocinogo Paratetisa i Tetisa. *Stratigrafia Kainozoa Severnogo Pricernomoria i Krima. Nauk. Trud.*, **2**, 95–105.
- SEMENENKO, V.N. & OLEJNIK, E.S. (1995) Stratigraphic correlation of the Eastern Paratethys Kimmerian and Dacian stages by molluscs, dinocyst and nannoplankton data. *Rom. J. Stratigr.*, **76**(7), 113–114.
- SEMENENKO, V.N. & PEVZNER, M.A. (1979) Correlation of Miocene and Pliocene of the Ponto-Caspian on the biostratigraphic and paleomagnetic data. *Proc. USSR Acad. Sci., Geol. Ser.*, **1**, 5–15.
- SENEŠ, J. (1973) Correlation hypotheses of the Neogene Tethys and Paratethys. *Giorn. Geol.*, **39**(2), 271–286.
- SHACKLETON, N.J., HALL, M.A. & PATE, D. (1995) Pliocene stable isotope stratigraphy of Site 846. In: *Leg 138* (Ed. by K. Sonder), *Proc. Ocean Drill. Progr., Sci. Results*, **138**, 337–355.
- SISSINGH, W. (1972) Late Cenozoic ostracoda of the South Aegean island arc. *Utrecht Micropaleontol. Bull.*, **6**, 1–187.
- SNEL, E., MARUNȚEANU, M., MACALET, R., MEULENKAMP, J.E. & VAN VUGT, N. (in press) Late Miocene to Early Pliocene chronostratigraphic framework for the Dacic Basin, Romania. *Palaeogeogr. Palaeoclimatol. Palaeoecol.*
- SPEZZAFERRI, S., CITA, M.B. & MCKENZIE, J. (1998) The Miocene/Pliocene boundary in the Eastern Mediterranean: results from Sites 967 and 969. In: *Leg 160* (Ed. by A.H.F. Robertson & K.-C. Emeis, *et al*) *Proc. Ocean Drill. Progr., Sci. Results*, **160**, 9–28.
- SPROVIERI, M., SACCHI, M. & ROHLING, E.J. (2003) Climatically influenced interactions between the Mediterranean and the Paratethys during the Tortonian. *Paleoceanography*, **18**(2), 1–10.
- STANKOVIC, S. (1960) *The Balkan Lake Ohrid and its Living World. Monographiae Biologiae, Vol. 9*. Uitgeverij Dr W. Junk, The Hague, p. 357.
- STEVANOVIĆ, P.M., NEVESSKAYA, L.A., MARINESCU, F., SOKAC, A. & JAMBOR, A (eds) (1990) *Chronostratigraphie und Neostratotypen, Neogen der Westlichen ("Zentrale") Paratethys, Vol. 8* (pp. 1–952. Jazu and Sanu, Zagreb–Belgrad, Pontien.
- STOFFERS, P. & MÜLLER, G. (1978) Mineralogy and lithofacies of Black Sea sediments, Leg 42B Deep Sea Drilling Project. In: *Leg 42B* (Ed. by D.A. Ross & Y.P. Neprochnov, *et al*) *Init. Rep. Deep Sea Drill. Proj.* **42**(2), 373–390.
- SUC, J.-P. & BESSAIS, E. (1990) Pérennité d'un climat thermique en Sicile, avant, pendant, après la crise de salinité messinienne. *C. R. Acad. Sci. Paris*, **310**(ser. 2), 1701–1707.
- SÜTÖNÉ SZENTAI, M. (1989) Microplankton flora of the Pannonian sequence of the Szentlorinc-XII structure exploratory well. *Földtani Közlemény*, **119**, 31–43.
- SYRIDES, G.E. (1995) Neogene mollusk faunas from Strymon basin, Macedonia, Greece. First results for biochronology and palaeoenvironment. *Geobios*, **18**(sp. issue), 381–388.
- SYRIDES, G.E. (1998) Paratethyan mollusc faunas from the Neogene of Macedonia and Thrace, Northern Greece. *Rom. J. Stratigr.*, **78**, 171–180.
- SYRIDES, G.E. (2000) Neogene marine cycles in Strymon basin, Macedonia, Greece. *Geol. Soc. Greece*, **9**(sp. publ), 217–225.
- ȚICLEANU, N. & DIACONIȚA, D. (1997) The main coal facies and lithotypes of the Pliocene coal Basin, Oltenia, Romania. In: *European Coal Geology and Technology* (Ed. by R. Gayer & J. Pesek), *Geol. Soc. Sp. Publ.*, **125**, 131–139.
- VIDAL, L., BICKERT, T., WEFER, G. & ROHL, U. (2002) Late Miocene stable isotope stratigraphy of SE Atlantic ODP Site 1085: Relation to Messinian events. *Mar. Geol.*, **180**, 71–85.
- VISMARA SCHILLING, A., STARDNER, H., CITA, M.B. & GAETANI, M. (1976) Stratigraphic investigations on the late Neogene of Corfou (Greece) with special reference to the Miocene/Pliocene boundary and to its geodynamic significance. *Mem. Soc. Geol. Iter.*, **16**, 279–317.
- WARNY, S., BART, P.J. & SUC, J.-P. (2003) Timing and progression of climatic, tectonic and glacioeustatic influences on the Messinian Salinity Crisis. *Palaeogeogr. Palaeoclimatol. Palaeoecol.*, **202**, 59–66.
- WINTER, A., JORDAN, R.W. & ROTH, P.H. (1994) Biogeography of living coccolithophores in ocean waters. In: *Coccolithophores* (Ed. by A. Winter & W.G. Siesser), pp. 161–177. Cambridge University Press, Cambridge.
- ZAGORCHEV, I. (2002) Neogene fluviolacustrine systems in the Northern Peri-Aegean region. *Geol. Balcanica*, **32**(2–4), 139–144.

Manuscript received 8 May 2002; Manuscript accepted 10 May 2005.

Original article

Earliest Zanclean age for the Colombacci and uppermost Di Tetto formations of the “latest Messinian” northern Apennines: New palaeoenvironmental data from the Maccarone section (Marche Province, Italy)

La Formation de Colombacci et le sommet de la Formation Di Tetto (« Messinien terminal » des Apennins septentrionaux) sont d’âge zancéen : Nouvelles données paléoenvironnementales sur la coupe de Maccarone (Marche, Italie)

Speranta-Maria Popescu^{a,*}, Mihaela-Carmen Melinte^b, Jean-Pierre Suc^a, Georges Clauzon^c, Frédéric Quillévéré^a, Maria Sütö-Szentai^d

^a UMR 5125 PEPS CNRS, université Lyon 1, campus de la Doua, bâtiment Géode, 69622 Villeurbanne cedex, France

^b National Institute of Marine Geology and Geo-ecology (GEOECOMAR), 23–25, Dimitrie-Onciul Street, 024053 Bucharest, Romania

^c CEREGE (UMR 6635 CNRS), université Paul-Cézanne, europôle de l’Arbois, BP 80, 13545 Aix-en-Provence cedex 04, France

^d Natural History Collection of Komlo, Városház tér 1, 7300 Komlo, Hungary

Received 5 September 2006; accepted 15 November 2006

Available online 30 April 2007

Abstract

The occurrence of planktonic foraminifers in the latest Messinian deposits (uppermost Di Tetto Formation and Colombacci Formation) of the Marche Province (Apennine foredeep, Italy) has stimulated a debate since the 1970s. An earlier palynological study of the entire Maccarone section revealed a pronounced, and a sudden increasing frequency of saccate pollen grains which indicates more distal conditions, and thus a transgression. At first attributed to tectonic activity, this transgression is now interpreted as representing the Zanclean marine transgression after the discovery of *Ceratolithus acutus*, the calcareous nannofossil marker of the earliest Zanclean in the Mediterranean Sea. Evidence from marine dinoflagellate cysts and planktonic foraminifers supports this result. The Colombacci Formation and uppermost part of the Di Tetto Formation (i.e. the entire p–ev2 stratigraphic unit) belong to the earliest Zanclean. The so-called Lago Mare no longer has a regional chronostratigraphic sense, and should be understood as the invasion of Paratethyan organisms via surface waters owing to a connection at high sea-level between the Aegean Sea and the Eastern Paratethys (Dacic Basin). A new robust environmental reconstruction of the northern Apennine foredeep is proposed, which respectively considers the effects of tectonics and Mediterranean eustasy.

© 2007 Elsevier Masson SAS. All rights reserved.

Résumé

La présence de foraminifères planctoniques dans les dépôts du Messinien terminal (sommet de la Formation Di Tetto et Formation à Colombacci) de l’avant-fosse apenninique (Italie, région adriatique) est sujette à discussion depuis les années 1970. L’étude palynologique de la coupe de Maccarone avait révélé une soudaine et forte augmentation des pollens à ballonnets traduisant un milieu plus distal dans sa moitié supérieure. Cette transgression, qui a d’abord été attribuée à l’activité tectonique, est ici établie comme étant la transgression marine du Zancéen après la découverte de *Ceratolithus acutus*, le marqueur chez les nannofossiles du Zancéen basal en Méditerranée. La présence conjointe de kystes de dinoflagellés marins et de foraminifères planctoniques appuie ce résultat. En conséquence, la Formation à Colombacci et la partie sommitale de la Formation Di Tetto, c’est-à-dire l’intégralité de l’unité stratigraphique p–ev2, relèvent du Zancéen basal. Les dépôts qui étaient attribués au

* Corresponding author.

E-mail address: popescu@univ-lyon1.fr (S.-M. Popescu).

Lago Mare n'ont plus de sens chronostratigraphique mais reflètent l'invasion d'organismes paratéthysiens à la suite d'échanges d'eaux de surface lors de connexions à haut niveau marin entre la mer Egée et le bassin Dacique (Paratéthys orientale). Une nouvelle reconstitution environnementale de l'avant-fosse apenninique septentrionale est proposée, qui prend solidement en compte les effets conjugués de l'activité tectonique et des variations du niveau marin méditerranéen.

© 2007 Elsevier Masson SAS. All rights reserved.

Keywords: Zanclean transgression; Calcareous nannofossils; Marine dinoflagellate cysts; Lago Mare

Mots clés : Transgression zancléenne ; Nannofossiles calcaires ; Kystes de dinoflagellés marins ; Lago Mare

1. Introduction

In the northern Apennines, the Messinian-Zanclean sedimentary succession overlying the evaporitic Gessoso-Solfifera Formation has been described as comprising of three clastic formations (Roveri et al., 1998), from the base to top:

- the Di Tetto Fm. consisting of clays and turbidites, including a volcanic ash dated at about 5.50 Ma (Odin et al., 1997); this formation is the lower unit of the post-evaporitic depositional sequence (Bassetti, 2000; Roveri et al., 2001); it has been assigned to the latest Messinian with respect to $^{39}\text{Ar}/^{40}\text{Ar}$ dating of the volcanic ash, and is constrained by the astronomical age of the Miocene-Pliocene boundary at 5.33 Ma (Lourens et al., 1996, 2004);
- the Colombacci Fm. consists of alternating thin limestones and clays, containing remains from the Paratethys (ostracods: mostly of *Cyprideis*; molluscs), and assimilated into the so-called Lago Mare (Cita and Colombo, 1979; Orszag-Sperber, 2006); this is the upper unit of the post-evaporitic depositional sequence (Roveri et al., 2001), which is assigned to the latest Messinian in agreement with the classical understanding of the Lago Mare facies, and because of the Zanclean fossil content of the overlying clays; a geometrical unconformity separates this formation from the underlying one (Bassetti, 2000);
- the Argille Azzurre Fm. which constitutes the widespread early Zanclean facies, including the relevant planktonic foraminifers (Selli, 1973).

Recently, another subdivision was proposed on the basis of detailed sedimentological investigations (Roveri et al., 2001; Manzi et al., 2005; Roveri and Manzi, 2006):

- a post-evaporitic unit 1 (p-ev₁) that overlies the Gessoso-Solfifera Fm., and comprises the ash layer and some turbidites; it has an estimated time-span of 5.60 to 5.40 Ma;
- a post-evaporitic unit 2 (p-ev₂) i.e. separated from the underlying unit by a minor discontinuity; rich in turbiditic layers, it includes in its upper part the Colombacci limestones; it has an estimated time-span of 5.40 to 5.33 Ma, terminating where the Argille Azzurre conformably overlies the Colombacci Fm.

One of the reference localities for this succession is the Maccarone section (close to Apiro: 43°24'20" N, 0°39'00" E, top of the section 430 m asl; Fig. 1), where the ash bed was

dated (Odin et al., 1997). At Moscosi, the Messinian gypsum underlying the Maccarone section is resedimented (Bassetti et al., 1994; Roveri et al., 1998, 2001; Bassetti, 2000; Manzi et al., 2005). The well-exposed section here (Fig. 2) has been the subject of several investigations, including those on foraminifers (Carloni et al., 1974a), and palynology (Bertini, 1992, 1994, 2002, 2006).

Results from these studies raised several inconsistencies:

- Relatively diverse if not abundant planktonic (and some benthic) foraminifers found discontinuously at about 60 m (and more continuously at about 20 m) below the Zanclean clays (Fig. 2; Carloni et al., 1974a). Moreover, a marine microfauna was found in several sections (sometimes associated with coccoliths) but systematically interpreted as reworked because of incompatibilities with the ostracod *Cyprideis* (Casati et al., 1976; Bassetti et al., 2003). Colalongo et al. (1976) admittedly expressed a more moderate viewpoint, and Carloni et al. (1974a) accepted the co-existence of this fauna with *Cyprideis*;
- Dinoflagellate cysts (including marine species such as *Impagidinium aculeatum*, *Lingulodinium machaerophorum*, *Spiniferites ramosus*) show a sudden improvement preservation, and increase in diversity 60 m below the Zanclean clays (Fig. 2; Bertini, 1992, 2006);

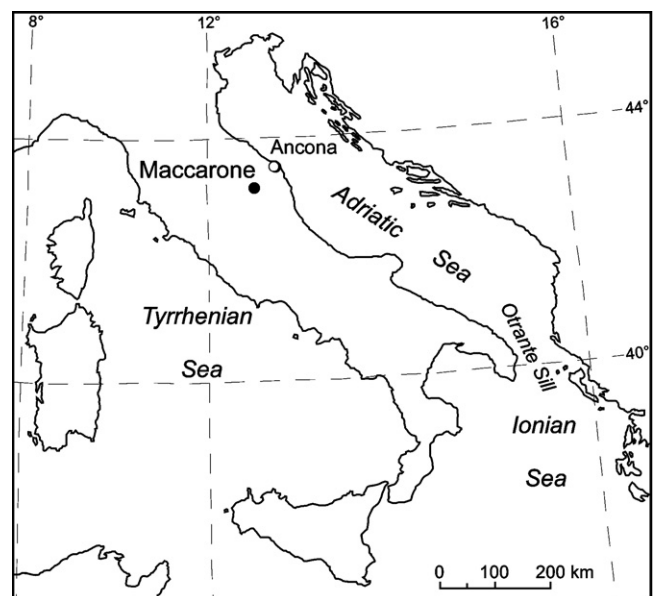


Fig. 1. Location map of the Maccarone section.

Fig. 1. Localisation géographique de la coupe de Maccarone.

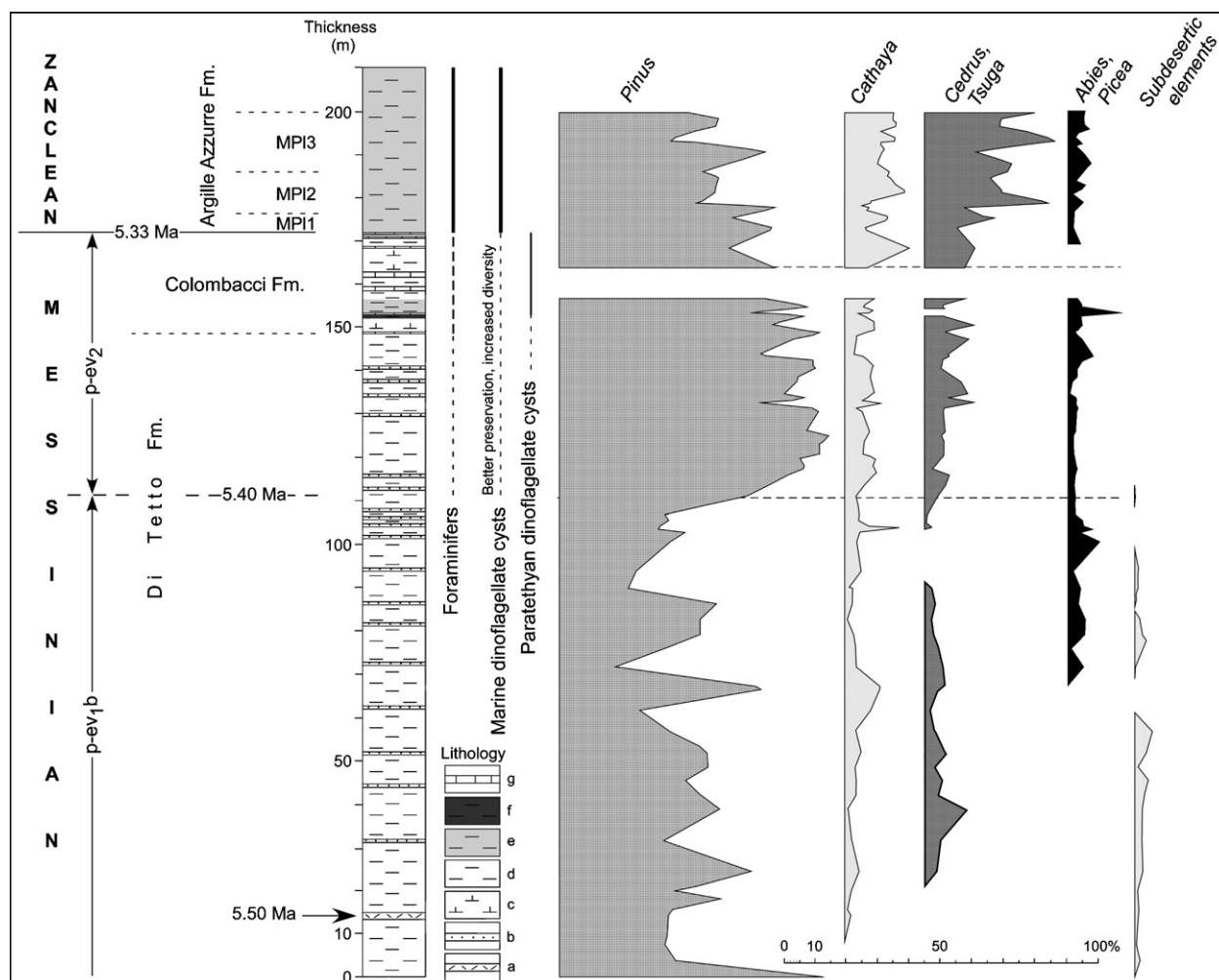


Fig. 2. Lithology and traditional bio-chronostratigraphy of the Maccarone section with some micropaleontological data and pollen marker taxa. The updated chronostratigraphy proposed in the present work is shown in Fig. 3. Lithology after Bertini (2006), modified according to our observations: a, Volcanic ash; b, Turbiditic layer; c, Calcareous clay; d, Light clay; e, Grey clay; f, Black clay; g, Limestone. Bio- and chronostratigraphy is from Carloni et al. (1974a, 1974b), Bassetti et al. (1994), Odin et al. (1997), Roveri et al. (1998), Manzi et al. (2005), Bertini (2006), Roveri and Manzi (2006). Foraminiferal records are from Carloni et al. (1974a) with a discontinuous record of rare specimens from their sample 22A (i.e. at about the pev_1b – pev_2 formation boundary), and continuous record of frequent specimens from their sample 42 (i.e. at the Di Tetto-Colombacci formation boundary), and continuous record of abundant specimens from their sample 49 (i.e. at the base of the Argille Azzurre Fm.). Dinoflagellate cysts are from Bertini (1992, 2006) who indicated a better preservation, and a slightly higher diversity in marine dinoflagellate cysts 40 m below the Colombacci Fm., and fully marine conditions (with the abrupt appearance of *Impagidinium patulum*) at the base of the Argille Azzurre Fm. Bertini (1992, 2006) also pointed out the early presence of Paratethyan dinoflagellate cysts (the so-called *Impagidinium* sp. 1) with respect to the Colombacci Fm. (somewhat 10 m below the first carbonate layer) in which they are frequent. Pollen records are from Bertini (1992): *Pinus*, *Cathaya*, *Cedrus*, *Tsuga*, *Abies*, and *Picea* have an amplified signal owing to their buoyancy (facilitated by the presence of bladders) during aquatic transport; subdesertic elements: *Ziziphus*, *Croton*, *Agavaceae*, *Agave*, *Cordyline*, *Nolina*, *Prosopis*, *Lygeum*, *Calligonum*.

Fig. 2. Lithologie et bio-chronostratigraphie classique de la coupe de Maccarone complétée de quelques données micropaléontologiques et des taxons marqueurs dans la flore pollinique. La nouvelle chronostratigraphie déduite de ce travail est donnée dans la Fig. 3. Lithologie d'après Bertini (2006), modifiée selon nos observations : a, Cinérite ; b, Niveaux turbiditiques ; c, Argile calcaire ; d, Argile claire ; e, Argile grise ; f, Argile noire ; g, Calcaire. Bio- chronostratigraphie d'après Carloni et al. (1974a, 1974b), Bassetti et al. (1994), Odin et al. (1997), Roveri et al. (1998), Manzi et al. (2005), Bertini (2006), Roveri et Manzi (2006). Données sur les foraminifères d'après Carloni et al. (1974a), avec un enregistrement discontinu de rares spécimens à partir de leur échantillon 22A (à peu près la limite entre les formations pev_1b – pev_2), un enregistrement davantage continu de spécimens fréquents à partir de leur échantillon 42 (limite entre les formations Di Tetto et Colombacci), et un enregistrement continu de spécimens abondants à partir de leur échantillon 49 (base de la Formation des Argille Azzurre). Kystes de dinoflagellés d'après Bertini (1992, 2006), montrant une meilleure préservation et une diversité légèrement plus élevée des éléments marins 40 m sous la Formation à Colombacci, et des conditions franchement marines (avec l'apparition soudaine d'*Impagidinium patulum*) à la base de la Formation des Argille Azzurre. De plus, Bertini (1992, 2006) souligne la présence de kystes de dinoflagellés paratéthysiens (sous l'appellation *Impagidinium* sp. 1) antérieurement à la Formation à Colombacci (10 m environ sous le premier lit carbonaté) dans laquelle ils sont fréquents. Données polliniques d'après Bertini (1992) : *Pinus*, *Cathaya*, *Cedrus*, *Tsuga*, *Abies* et *Picea* ont un signal amplifié dû à leur flottabilité facilitée par leur(s) ballonnet(s) remplis d'air ; éléments subdésertiques : *Ziziphus*, *Croton*, *Agavaceae*, *Agave*, *Cordyline*, *Nolina*, *Prosopis*, *Lygeum*, *Calligonum*.

- A rapid increase in abundance of *Pinus* pollen (from 30 to 75% on average) occurs also at about 60 m below the Zanclean clays, and 37 m below the first Colombacci limestone (Bertini, 1992, 1994, 2002, 2006), and the consequence of a tectonic event (Bertini, 2002, 2006) is discarded (Clauzon et al., 2005);
- Pollen of *Lygeum spartum*, a typical subdesertic plant (Brullo et al., 2002), was almost continuously recorded in association with other subdesertic elements (Agavaceae including *Agave*, *Nolina*, and *Cordyline* as well as *Croton*, *Prosopis*, and *Calligonum*) at such a high latitude along the lowermost 110 m of the section (sometimes up to 5%: Fig. 2; Bertini, 1992, 2006) in an humid palaeoclimatic context (Fauquette et al., 2006).

These discrepancies have prompted the present study. High-resolution sampling was performed on the lowermost Argille Azzurre, Colombacci, and uppermost Di Tetto formations at almost regular intervals (0.80–1 m) following deep excavations (45 samples versus 20 in the same interval by Bertini, 1992, 2002, 2006), and stopped when solifluction disturbed observation in the middle part of the Di Tetto Formation (Fig. 3).

Our investigations concern the nanoplankton (not previously documented in the section), dinoflagellate cysts, and planktonic foraminifers, focussing on an interval about 40 m thick including the uppermost part of the Di Tetto Fm., the entire Colombacci Fm. (i.e. the major part of the p-ev₂ unit), and the beginning of the Argille Azzurre Fm. (Fig. 3). Two modest geometrical unconformities have been reported,

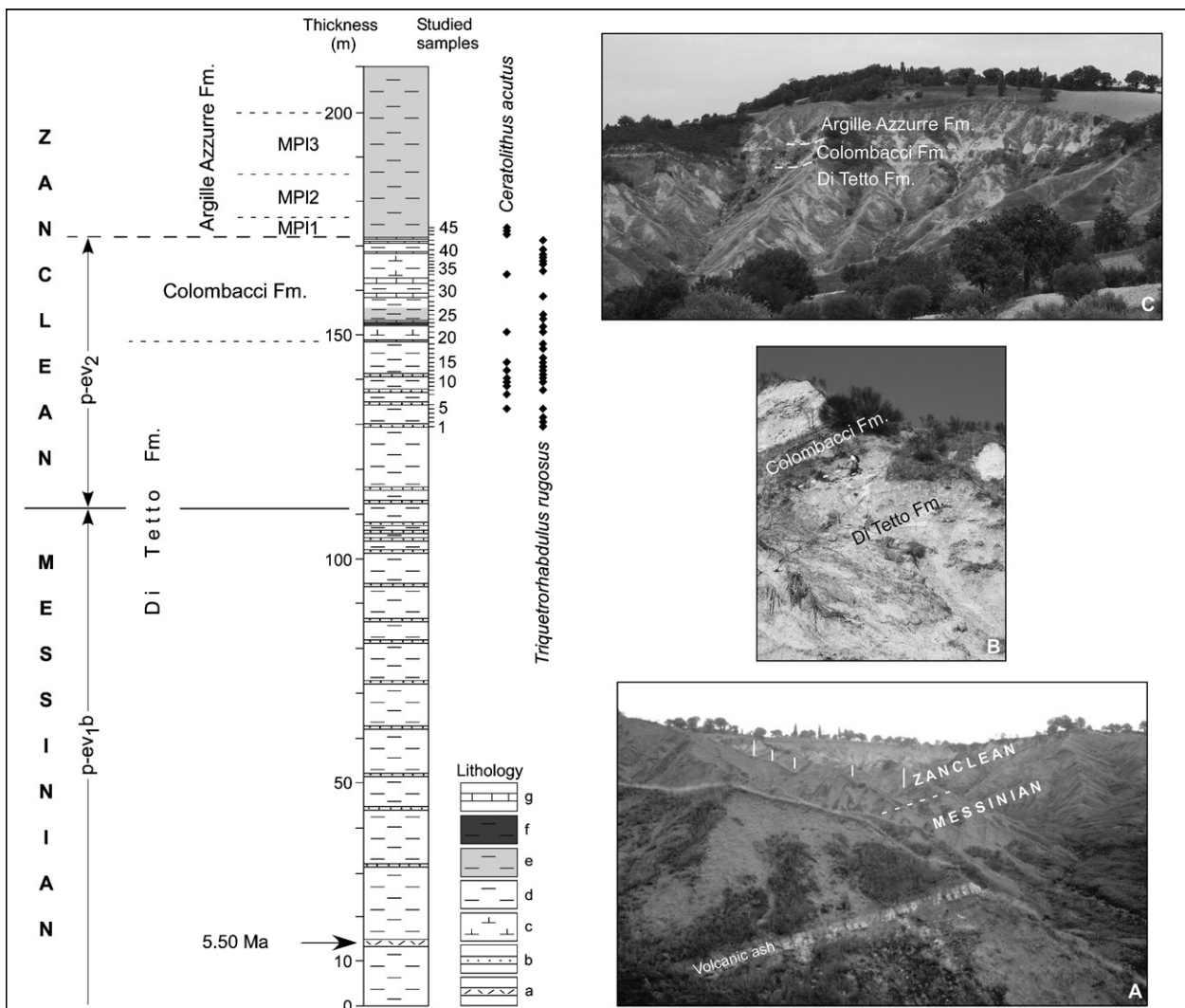


Fig. 3. Revisited chronostratigraphy of the Maccarone section with the location of the studied samples and the recorded occurrences of the calcareous nanofossil stratigraphic markers *Ceratolithus acutus* and *Triquetrorhabdulus rugosus*. Lithology after Bertini (2006), and modified from our observations: a, Volcanic ash; b, Turbiditic layer; c, Calcareous clay; d, Light clay; e, Grey clay; f, Black clay; g, Limestone. Photographs: A, The entire Maccarone section (the vertical lines indicate sampled segments); B, The boundary between the Di Tetto and Colombacci formations; C, Upper part of the Maccarone section.

Fig. 3. Chronostratigraphie révisée de la coupe de Maccarone avec l'emplacement des échantillons étudiés et les enregistrements des nanofossiles calcaires marqueurs stratigraphiques *Ceratolithus acutus* et *Triquetrorhabdulus rugosus*. Lithologie d'après Bertini (2006), modifiée selon nos observations : a, Cinérite ; b, Niveaux turbiditiques ; c, Argile calcaire ; d, Argile claire ; e, Argile grise ; f, Argile noire ; g, Calcaire. Photographies : A, Ensemble de la coupe de Maccarone (les lignes verticales indiquent les segments échantillonnés) ; B, Limite entre les formations Di Tetto et Colombacci ; C, Partie supérieure de la coupe de Maccarone.

respectively in the upper part of the Di Tetto Fm. (i.e. at the boundary between the p-ev₁ and p-ev₂ units (Roveri and Manzi, 2006), and at the boundary between the Di Tetto and Colombacci formations (Bassetti, 2000) (i.e. within the p-ev₂ unit). They are related to the regional tectonic activity, that is well-recognized in marginal areas (Roveri et al., 1998, 2001) but not directly expressed in the Maccarone section itself.

2. Calcareous nannofossils

Calcareous nannofossils are generally abundant, except in the Colombacci Fm. (samples 20–35). Preservation is on the whole moderate, except in the Colombacci Fm., and the four lowermost samples of the studied section where it is poor, and

in some samples where it is relatively good (Fig. 4). The assemblages are dominated by *Coccolithus pelagicus*, *Reticulofenestra pseudoumbilicus*, *Sphenolithus abies*, *S. moriformis*, *Triquetrorhabdulus rugosus*, and the small reticulofenestrids (Fig. 4). Of particular biostratigraphic significance are (1) *Triquetrorhabdulus rugosus* (nearly continuous occurrence from sample 1 to 25 and 34 to 42, and an isolated occurrence in sample 29), and (2) *Ceratolithus acutus* (nearly continuous occurrence from sample 5 to 15, isolated occurrences in samples 21 and 33, and a continuous record at the top of the section from sample 43) (Fig. 4).

The top of the calcareous nannofossil Zone NN11 is defined by the disappearance of *Discoaster quinquerramus* (Berggren et al., 1995a), the age of which was estimated at about 5.537 Ma

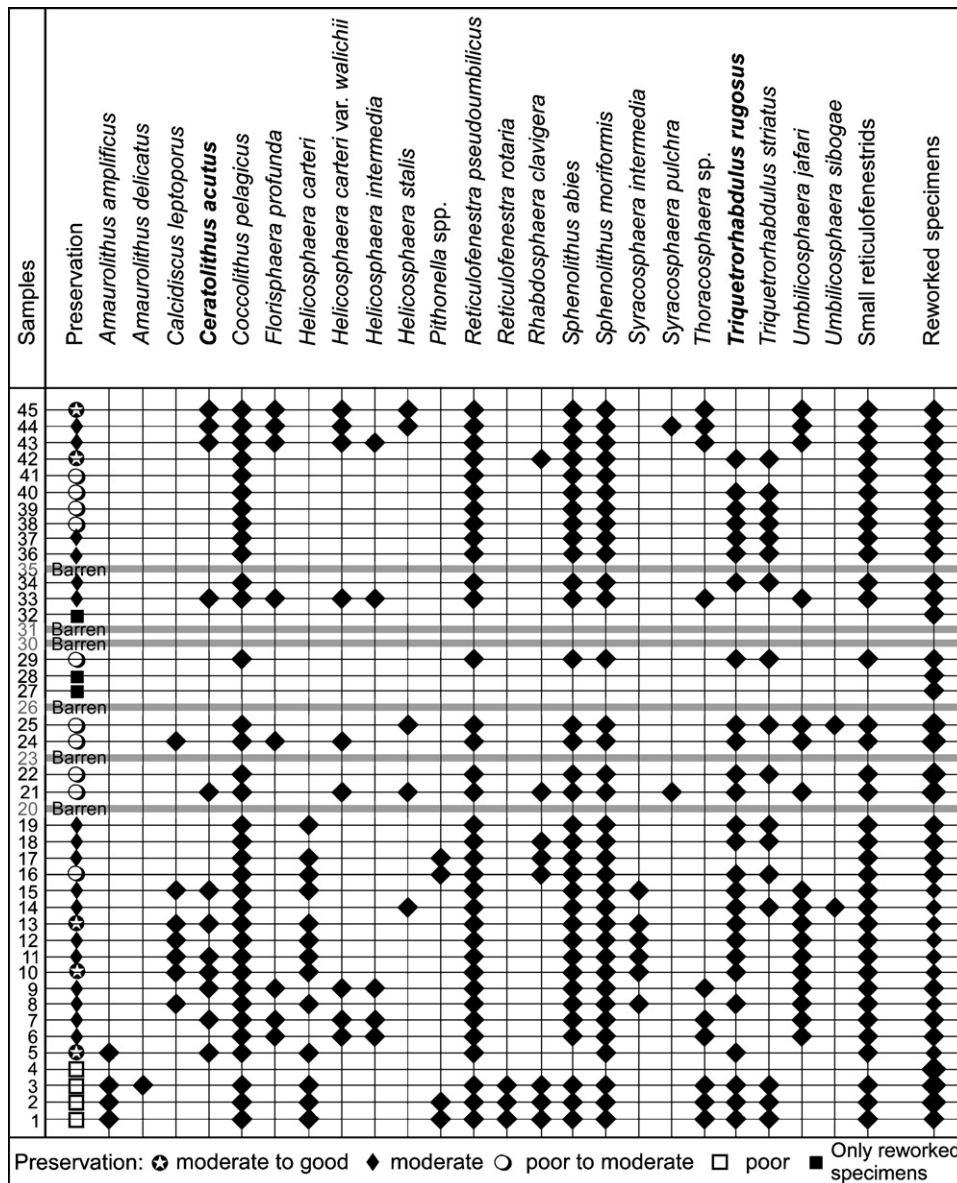


Fig. 4. Recorded occurrences of calcareous nannofossils in the present study. Key taxa are in bold face. For the reworked specimens, the size of the black rhombs relates to the amount of reworking.

Fig. 4. Distribution des nannofossiles calcaires trouvés dans notre étude. Les taxons marqueurs sont en caractères gras. Spécimens remaniés : la taille des symboles est en relation avec l'importance du remaniement.

Ma	Polarity	Epochs	Stages	Planktonic Foraminifer Zones		Calcareous Nannofossil Zones	
				Mediterranean Sea	Global time scale	Mediterranean Sea	Global time scale
3		PLIOCENE	Piacenzian	MPI5	PL4-PL5	MNN16	NN16
	MPI4			PL3			
4			Zanclean	MPI3	PL2	MNN14-15	NN13-15
	MPI2			PL1	MNN12		
5					MPI1		
6		MIOCENE	Messinian	Non Distinctive Zone	Non Distinctive Zone	c	b
	MM13			M13b-14	MNN11		
7			Tortonian	MM12	a	a	
8							

Fig. 5. Comparison of Late Miocene and Early Pliocene bio- and chronostratigraphy in the Mediterranean Sea according to the “EEDEN Integrated Neogene Correlation Table” coordinated by Iaccarino, S. and Steininger, F.F. (unpublished) with the global time scale of Lourens et al. (2004).

Fig. 5. Bio- et chronostratigraphie du Miocène supérieur et du Pliocène inférieur de Méditerranée selon la charte établie par le Programme “EEDEN” coordonnée par Iaccarino et Steininger (inédit) comparée à la charte globale de Lourens et al. (2004).

by Backman and Raffi (1997), and precisely recalculated at 5.58 Ma by Lourens et al. (2004) (Fig. 5), although this species is very rare or even absent in the Mediterranean area (Rio et al., 1984). In the studied samples, only a few broken specimens of *D. quinqueramus* were observed, and are probably reworked. *Ceratolithus acutus* had a proposed range of 5.372–5.046 Ma in the equatorial Atlantic (Backman and Raffi, 1997) which was recalculated 5.35–5.04 Ma by Lourens et al. (2004) (Fig. 5). This datum precedes the disappearance of *Triquetrorhabdulus rugosus* (Berggren et al., 1995a, 1995b) placed at 5.28 Ma by Lourens et al. (2004). In the Mediterranean region, the first appearance of *C. acutus* was delayed until the beginning of the Pliocene (Cita and Gartner, 1973; Castradori, 1998) because of the isolation of the basin during the Messinian salinity crisis, the so-called “Non Distinctive Zone” of Iaccarino and Salvatorini (1982) (Fig. 5). Moreover, as in other Mediterranean and Atlantic sites (Backman and Raffi, 1997; Castradori, 1998), the two above-mentioned nannofossil events are not coincident: the extinction of *T. rugosus* is younger than the appearance of *C. acutus*. As a consequence, the presence of *C. acutus* in any Mediterranean sediment means that this deposit necessarily belongs to the earliest Zanclean (Fig. 5). At first sight, the studied interval from the Maccarone section, which records both *Triquetrorhabdulus rugosus* (samples 1–42), and *Ceratolithus acutus* (samples 5–45), belongs to the MNN12 Calcareous Nannofossil Zone of Rio et al. (1990) who emended the standard zonation of Martini (1971), that is, to the earliest Zanclean (Fig. 5).

Even we assume that highest occurrences of *T. rugosus* might represent reworking, the almost continuous presence of *C. acutus* throughout the investigated succession (except its base and some barren intervals) is referable to MNN12.

Also notable is the increased frequency of *Coccolithus pelagicus* towards the base of the study successions (samples

5–10). Siesser and Kaenel (1999) also reported an increased abundance of *C. pelagicus* (considered to be more related to cool surface waters, during the Pliocene; Bukry, 1981) in the Western Mediterranean area, within the lower part zone NN12. By contrast, the paracme of *Reticulofenestra pseudumbilicus*, a bio-event reported in the lowermost zone MNN12 by such authors as Rio et al. (1990) and Di Stefano (1998) was not encountered in the studied section. This may be due to the reworking, which could have modified the original nannofloral composition. Alternatively, the basal Zanclean *R. pseudumbilicus* paracme may have a limited applicability in the Mediterranean area (Van Couvering et al., 2000).

3. Dinoflagellate cysts

More than 200 dinoflagellate cysts have been counted per sample, yielding a total of 45 taxa. The preservation of specimens is on the whole poor to moderate in the Di Tetto Fm. (samples 1–19) and moderate to good in the Colombacci Fm., and the lower part of the Argille Azzurre Fm. (samples 26–45).

Particular effort have been made to identify the brackish stenohaline Paratethyan species: *Galeacysta etrusca*, *Impagidinium globosum*, *Millioudinium bacculatum*, *Millioudinium baltessii*, *Millioudinium dektense*, *Millioudinium pelagicum*, *Millioudinium punctatum*, *Pontiadinium inequicornutum*, *Pontiadinium obesum*, *Pontiadinium pecsvaradense*, *Pyxidinospis psilata*, *Romanodinium areolatum*, *Spiniferites balcanicus*, *Spiniferites bentorii* subsp. *budajenoensis*, *Spiniferites bentorii* subsp. *coniunctus*, *Spiniferites bentorii* subsp. *oblongus*, *Spiniferites bentorii* subsp. *pannonicus*, *Spiniferites cruciformis*, *Spiniferites galeaformis*, *Spiniferites inaequalis*; *Spiniferites maisensis*, *Spiniferites sagittarius*, *Spiniferites tihanyensis*, *Spiniferites validus*, *Spiniferites virgulaeformis*. This was done by directly comparing the Maccarone specimens with topotypes of Paratethyan taxa as well as their corresponding original iconography and description. The following species are invalid, and a study is in progress with M.J. Head for their emendation: *Impagidinium globosum* Sütö-Szentai, 1985, *Millioudinium baltessii* Sütö-Szentai, 1990, *Millioudinium dektense* Sütö-Szentai, 1990, *Millioudinium pelagicum* Sütö-Szentai, 1990, *Millioudinium punctatum* Baltes, 1971, *Spiniferites balcanicus* Baltes, 1971, *Spiniferites bentorii* subsp. *budajenoensis* Sütö-Szentai, 1986, *Spiniferites bentorii* subsp. *coniunctus* Sütö-Szentai, 1988, *Spiniferites bentorii* subsp. *oblongus* Sütö-Szentai, 1986, *Spiniferites bentorii* subsp. *pannonicus* Sütö-Szentai, 1986, *Spiniferites sagittarius* Sütö-Szentai, 1990, *Spiniferites tihanyensis* Sütö-Szentai, 1988. One result of our taxonomic studies is that the *Impagidinium* sp. 2 of Corradini and Biffi (1988), also illustrated by Bertini (1992: Pl. 3, Fig. 9), is a morphotype of *Spiniferites cruciformis* (Wall et al., 1973): see Marret et al. (2004) and Mudie et al. (2004) for illustrative photographs. Corradini and Biffi (1988) suggested that *Impagidinium* sp. 1 may be equivalent to *Millioudinium (Leptodinium) bacculatum* but did not consult the reference material of Baltes (1971). Our taxonomic investigations now indicate that *Impagidinium* sp. 1, as illustrated also by Bertini (1992: Pl. 3, Fig. 10) from the Maccarone section, is indeed

Millioudodinium bacculatum, and not *Caspidium rugosum* of Marret et al. (2004) (see also Sorrel et al., 2006) as claimed by Bertini (2006). Results are presented in a detailed dinoflagellate cyst occurrence diagram (Fig. 6a,b).

Fig. 7 displays the relative frequency of some marker taxa according to their ecological significance (marine euryhaline and stenohaline species, brackish stenohaline species). The reworked dinoflagellate cysts contain such taxa as *Achomosphaera alcicornu* (Eisenack, 1954), Davey and Williams, 1966, *Homotryblium oceanicum* (Eaton, 1976), Bujak et al., 1980, *Deflandrea* spp., *Spiniferites granulatus* (Davey, 1969b), Lentin and Williams, 1973), *Achomosphaera ramulifera* (Deflandre, 1937), and specimens that show an increased uptake of safranin stain. Their percentage is based on the total number of in situ plus reworked cysts (Fig. 7).

In contrast to Bertini (2006) we consider our quantitative study of dinoflagellate cysts (Fig. 7) to show an important environmental change in surface-water salinity. To characterize these environmental changes, taxa have been grouped according to their ecological significance (Fig. 7): (1) marine stenohaline dinoflagellate cysts indicated in bold characters on Fig. 6a, (2) marine euryhaline dinoflagellate cysts incorporating other marine taxa presented in Fig. 6a, (3) brackish stenohaline Paratethyan dinoflagellate cysts based on independent curves of marker taxa (*Spiniferites cruciformis*, *Galeacysta etrusca*, and *Pyxidiniopsis psilata*), and one curve for the other taxa listed in Fig. 6b, (4) the fresh-water alga *Pediastrum*. Reworked dinoflagellate cysts are also plotted on Fig. 7. A morphological study of *Galeacysta etrusca*, *Spiniferites balcanicus*, and *Romanodinium areolatum*, originating from different well-

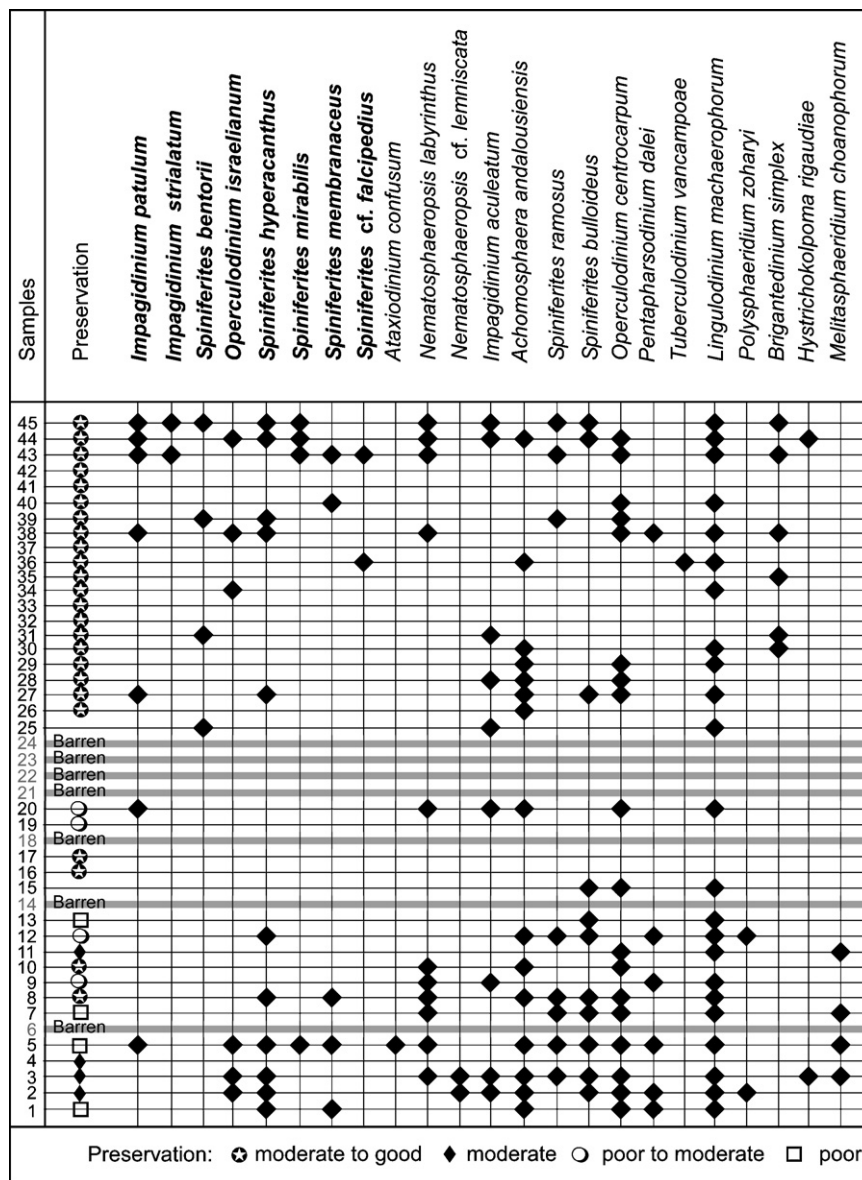


Fig. 6. Recorded occurrences of dinoflagellate cysts in the present study: a, marine species; b, brackish Paratethyan species. Key taxa are in bold characters. Fig. 6. Distribution des kystes de dinoflagellés trouvés dans notre étude : a, espèces marines ; b, espèces saumâtres paratéthysiennes. Les taxons marqueurs sont en caractères gras.

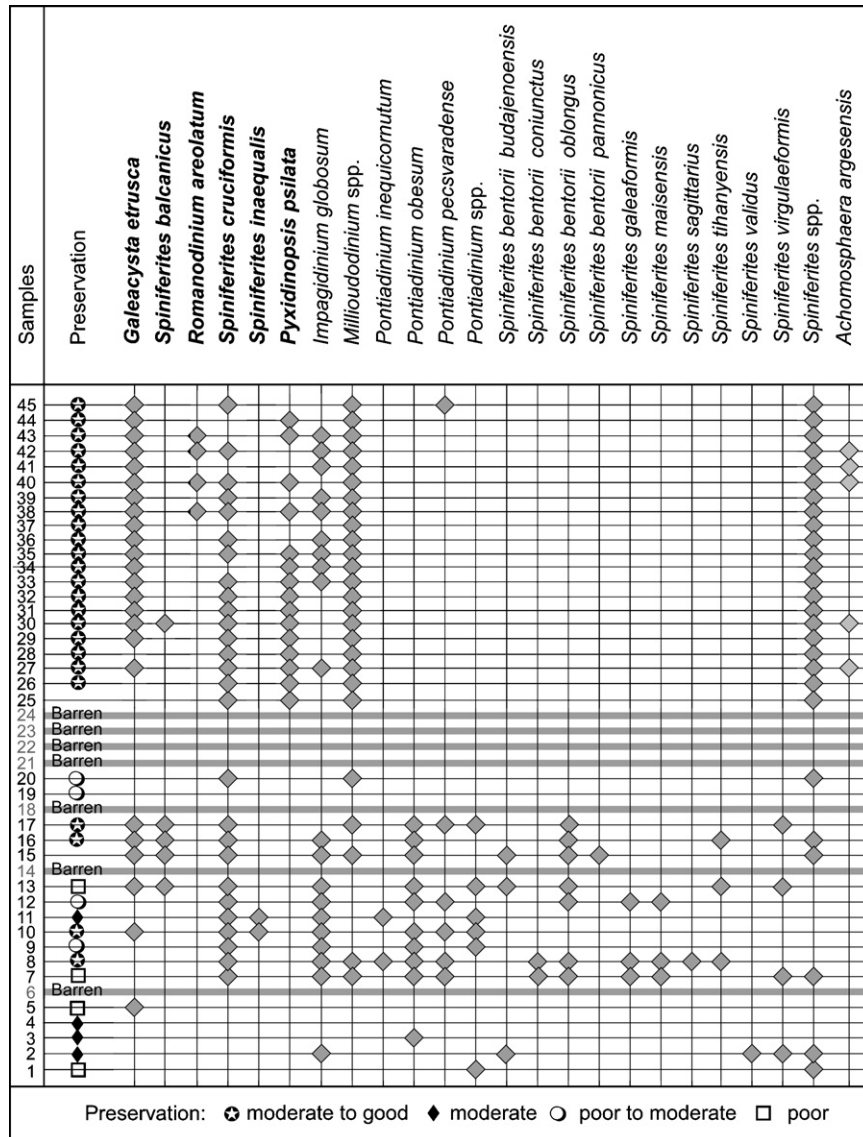


Fig. 6. (Continued).

dated Mediterranean and Paratethyan sections, suggests that these species probably represented different steps in evolution/adaptation to environmental changes (probably in surface-water salinity) of the same species (Popescu, unpublished). As a consequence, these taxa have been grouped within the *Galeacysta etrusca* curve (Fig. 7). It is also notable that the specimens identified in the present study as *Spiniferites cruciformis* and *Pyxidiniopsis psilata* display a range of morphologies just as they do in the Black Sea Holocene sediments (Wall et al., 1973). Our data from the entire Neogene of Paratethys show that the transition from oval to cruciform body, and the well- to poorly-expressed tabulation characterizes reduced surface-water salinity.

The lower and upper parts of the studied section (samples 1–5 and 43–45, respectively) are dominated by the marine euryhaline (80%), and stenohaline (15%) dinoflagellate cysts documenting a typical marine environment (Fig. 7). The middle part of the studied section (samples 7–42) is characterized by

prevalent brackish Paratethyan species, indicating a decrease in surface-water salinity.

The freshwater alga *Pediastrum* is frequent in the lower part of the studied section (samples 1–20) with an acme in samples 7 and 8 (in equal number to the dinoflagellate cysts), exactly where this event was also identified by Bertini (2006). It is noteworthy that the vertical distribution of *Pediastrum* is practically in phase with the greatest amounts of reworked dinoflagellate cysts (Fig. 7), and a palynofacies dominated by coaly microdebris and woody microfragments (samples 1 to 12), documenting an important arrival of freshwater probably because of an intensified river input (Poumot and Suc, 1994).

4. Planktonic foraminifers

This study only relates to the Colombacci Fm. and the lowermost Argille Azzurre Fm. On the whole, preservation is moderate to poor. Planktonic foraminifers are abundant and

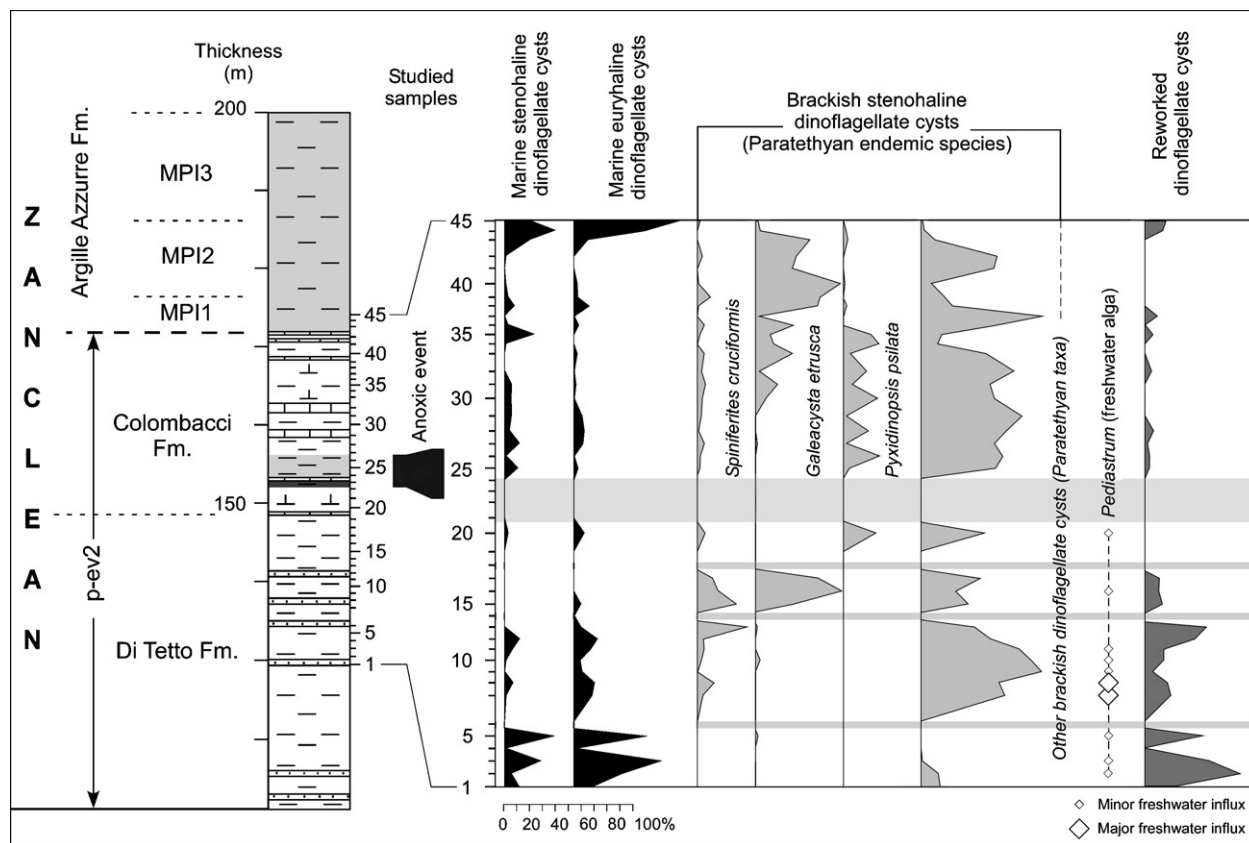


Fig. 7. Distribution and relative frequency of dinoflagellate cyst markers in the present study, with location of the anoxic layer. Barren intervals are indicated by grey bands. Lithology: see Figs. 2 and 3.

Fig. 7. Distribution et fréquence relative des kystes de dinoflagellés marqueurs trouvés dans notre étude, avec l'emplacement du niveau anoxique. Les intervalles dépourvus de kystes de dinoflagellés sont indiqués par des bandes grises. Lithologie : voir Figs. 2 et 3.

diverse only in samples 41 (Colombacci Fm.), and 43–45 (Argille Azzurre Fm.). Reworked specimens are frequent. Results are given on Fig. 8, and are consistent with those published by Carloni et al. (1974a). However, planktonic foraminifers from sample 24 to 40 display a small size (found only within the <250 μm fraction), a peculiarity also noticed by Colalongo et al. (1976) in the Colombacci Fm. of Cella, that indicates unfavourable environmental conditions. Ostracods are abundant in samples 38 to 42, as already pointed out by Carloni et al. (1974a) and Casati et al. (1976).

5. Discussion

Many consistent lines of evidence reveal the evolution of aquatic and continental environmental conditions in the area of Maccarone, which can be extended to the entire Adriatic foredeep, and Po Basin by integrating the available information.

Marine Zanclean Mediterranean waters entered this region before the arrival of the planktonic foraminifers *Sphaeroidinellopsis* and then *Globorotalia margaritae*, the marker species of zones MP11 and 2, respectively, which belong to the early Zanclean (Cita and Gartner, 1973). This is attested by (1) the first appearance of *Ceratolithus acutus*, the nannofossil marker for the base of the Pliocene in the Mediterranean which cannot

be explained by reworking (Fig. 3), (2) the almost regular occurrence of non-reworked planktonic foraminifers (Fig. 8), and (3) marine dinoflagellate cysts (Figs. 6 and 7). The early arrival of Zanclean foraminifers might be detected through the record in the uppermost Di Tetto Fm. of the benthic species *Uvigerina rutila* (Carloni et al., 1974a: sample 22A), which being a marker for the Zanclean (Iaccarino, 1967; Cita and Gartner, 1973), likewise cannot be suspected of reworking. Additional evidence of the normal marine condition of the Colombacci Fm. was recently provided by Carnevale et al. (2006a) who studied otoliths of euryhaline marine fish from the Ca' Ciuccio section close to Montecalvo in Foglia. These authors proposed that the marine refilling of the Mediterranean preceded the Miocene-Pliocene boundary.

The marine incursion operated in two pronounced steps:

- the first one occurred in the upper Di Tetto Fm. (starting before sample 1 and lasting through sample 15) based on (1) the abundance of marine euryhaline dinoflagellate cysts (*Impagidinium aculeatum*, *Nematosphaeropsis labyrinthus*, *N. cf. lemniscata* *Spiniferites ramosus*, *S. bulloideus*, *Lingulodinium machaerophorum*, *Operculodinium centrocarpum*, *Pentapharsodinium dalei*) accompanied by marine stenohaline taxa (*Impagidinium patulum*, *I. striatum*, *Spiniferites bentorii*, *S. mirabilis*, *S. hyperacanthus*,

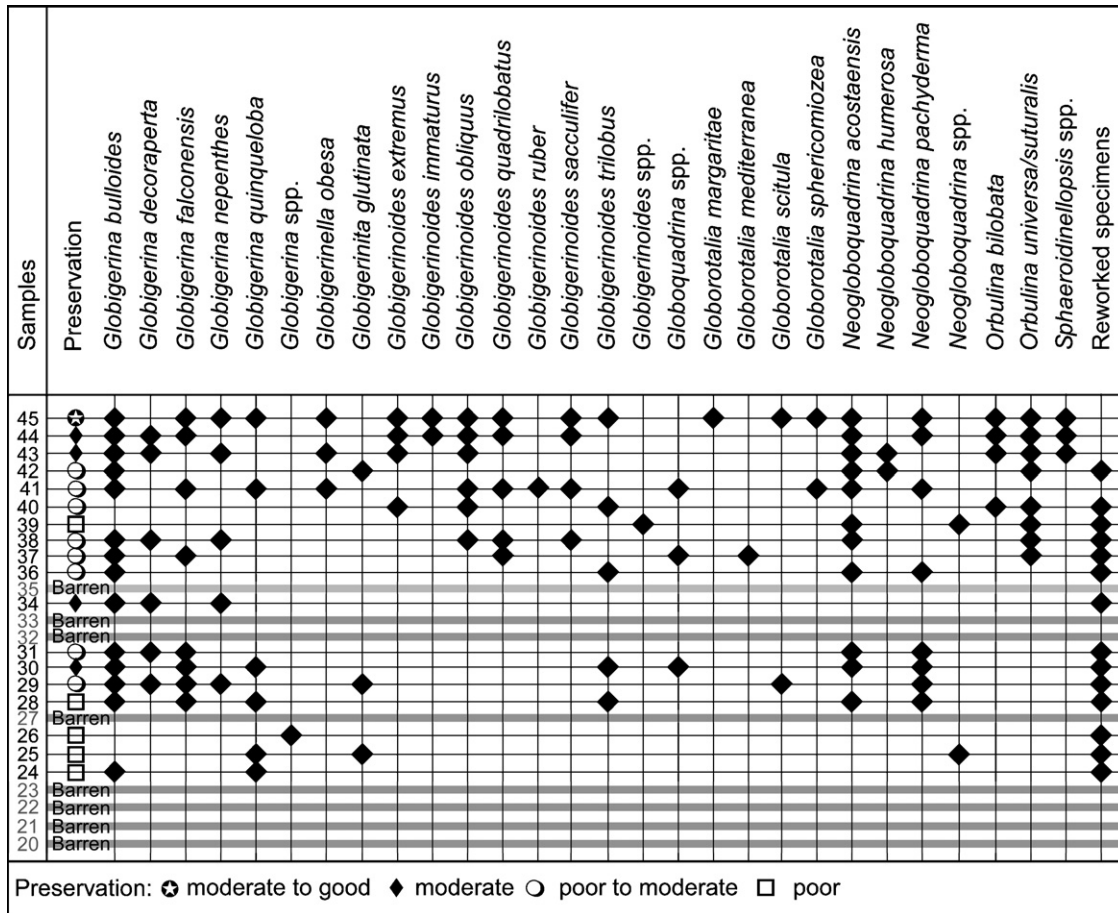


Fig. 8. Recorded occurrences of planktonic foraminifera in the studied samples of the Colombacci and Argille Azzurre fms.

Fig. 8. Distribution des foraminifères planctoniques dans les échantillons étudiés des formations à Colombacci et des Argille Azzurre.

S. membranaceus, *S. cf. falcipediis*, *Achomosphaera andalousiensis*) (Fig. 7), and (2) the coeval diversity in calcareous nannofossils including the appearance of *Ceratolithus acutus* (Figs. 3 and 4);

- the second step occurred in the Colombacci Fm., and intensified in the Argille Azzurre Fm. (samples 23–45); it is marked (1) by strongly anoxic conditions (about 80% of a yellow and fleecy amorphous organic matter in the palynofacies of samples 23–26 corresponding to black and grey clays) probably caused by a contrasted water stratification (Poumot and Suc, 1994) (Fig. 7), (2) marine euryhaline dinoflagellate cysts which increase again in parallel to the marine stenohaline species (Fig. 7), (3) diversity of calcareous nannofossils more manifest from sample 33 (Fig. 4), (4) increasing diversity in planktonic foraminifera, these displaying a normal size from sample 41 (Fig. 8).

Between these two steps, influx of marine water continued as evidenced by dinoflagellate cysts, in sample 20 for example (Fig. 7), and more continuously by calcareous nannofossils (Fig. 4). The process is characteristic of an influx of marine waters overflowing a sill (the Otrante Sill in this case), surface waters entering first the isolated basin with dinoflagellates and coccoliths, followed by deeper waters with more abundant

foraminifera. Among the latter, the planktonic marker species entered the Apennine foredeep when salinity reached a sufficiently elevated level for their persistent presence. At the beginning of the transgression, the euryhaline dinoflagellate cysts are more abundant than the stenohaline ones, as explained by their great capacity to adapt within a large salinity and temperature range (Marret and Zonnerveld, 2003).

The dinoflagellate cyst record shows that the so-called Lago Mare event (corresponding to the Colombacci Fm.: Cita and Colombo, 1979; Bassetti et al., 2003; Orszag-Sperber, 2006) is sandwiched within the marine transgression here referred to the earliest Zanclean (Figs. 3 and 7). Accordingly, the classical interpretation of a Lago Mare event as resulting from the draining of Paratethyan brackish waters into an almost desiccated Mediterranean Basin (Hsü et al., 1973; Cita et al., 1978: Fig. 12, p. 1018) is fully disproved as already demonstrated by Clauzon et al. (2005) on the basis of such evidence as the coeval inflow of Mediterranean marine waters into the Eastern Paratethys. Actually, two Lago Mare events happened in the Mediterranean Sea as a result of cross exchanges with the Eastern Paratethys at high sea-level, the first event just before the Mediterranean desiccation, and the second event caused by the reflooding of the Mediterranean Sea during the earliest Zanclean (Clauzon et al., 2005). The Lago Mare

event recorded at Maccarone is that of the earliest Zanclean. It documents the existence of high sea-level connections with the Eastern Paratethys allowing inflow to the Mediterranean of reduced salinity surface waters originating from the Paratethys, transporting stenohaline dinoflagellates, and larvae of ostracods and molluscs. As also corroborated by fish remains, the Lago Mare events occurred when the Mediterranean Sea was full of water: see Carnevale et al. (2006b) for the first Lago Mare event, and Carnevale et al. (2006a) for the Zanclean one. As a consequence, the systematic dismissal of marine elements as reworked within the Lago Mare events (in accordance with the conventional assumption that it is impossible to record ecologically mixed fossil assemblages), must be abandoned. The records of foraminifers and calcareous nannofossils within the Colombacci deposits, such as at Cella (Colalongo et al., 1976), Gualdo (Casati et al. (1976), and Monticino (Rio and Negri, 1988) regain their full significance. The small size of planktonic foraminifers testify to the unfavourable quality of waters. The significance of the ostracod species in the region has been clarified by Bassetti et al. (2003) who demonstrated their weak relationship with the contemporaneous Paratethyan species. These results pointed out the risk to define the Lago Mare events on the basis of the ostracods only, and reinforced the ecological significance of such events.

In the middle part of the Maccarone section, the relative frequency of *Pinus* pollen rapidly (within just a 5.5 m thick interval) increases from 33 to 78% in parallel with a moderate increase in the other saccate pollen grains (*Cathaya*, *Cedrus*, *Tsuga*, *Abies*, and *Picea*: Fig. 2; Bertini, 2002, 2006). *Pinus* in particular but also other saccate pollen grains are known to be over-represented in distal aquatic sediments because they are more buoyant during water and air transport (Heusser, 1988; Beaudouin et al., 2007). Such a shift has been correctly understood as reflecting a transgressive trend resulting in an increasing distance of the locality from shore (Bertini, 2002). However, this event was attributed to tectonic activity in the northern Apennines (Bertini, 2006), and associated with the regional unconformity separating p-ev2 from p-ev1 units (Bertini, 2002). This break appears too abrupt to be explained by a tectonic event, especially when considering the unlikelihood of a transgressive trend occurring in an area undergoing compression (the Maccarone subaquatic sediments of the Colombacci Fm. have been uplifted to 380 m asl). It is much more plausible to explain a rapid retreat of the shoreline by the sudden marine Zanclean transgression, as documented herein.

The lower part of the studied section (samples 1–17) is characterized both by large numbers of reworked dinoflagellate cysts, a palynofacies rich in coaly microparticles and woody microfragments, and presence of abundance of *Pediastrum*. The intense river input could relate to the tectonic phase to which interstratified marginal deltaic conglomerates belong consistently (Roveri et al., 2001; Manzi et al., 2005). This tectonic phase was still active when the Zanclean marine flooding occurred, as recorded at the base of unit p-ev2. At the end of deposition of the Colombacci Fm., a decrease in tectonic activity might have caused a rise in sea level at the beginning of

the Argille Azzurre deposition, thereby allowing the late arrival of the planktonic foraminifer markers of the early Zanclean.

The two step scenario of the Messinian salinity crisis as conceived by Clauzon et al. (1996) is based on the following basic observations: all around the Mediterranean Basin, the Messinian marginal evaporites are cut by an impressive erosional surface itself overlain by early Zanclean Gilbert-type fan deltas (Clauzon et al., 1996, 2005, in progress). These features prove that two successive drops in sea-level occurred: the first was a minor one that caused the deposition of the marginal evaporites; then, a severe drawdown resulted in the cutting of deep fluvial canyons joining the central basin evaporites in the almost desiccated abyssal plains (Lofi et al., 2005). Signs of these two steps are detected in the Maccarone area: the resedimented evaporites from marginal areas document the first sea-level drop; and the unexpected presence (with significant percentages) of subdesertic plants at such a high latitude during the time-span 5.50–5.40 Ma (Fig. 2) at a time when the scenario of Clauzon et al. (1996, 2005) places the almost complete desiccation of the Mediterranean Sea. Today, *Lygeum spartum* (the most abundant subdesertic element recorded at Maccarone) does exceed a latitude of 40°30' N in the Italian Peninsula (Brullo et al., 2002). Bertini (2006) invokes a drier climatic episode to explain this northward expansion of subdesertic elements, a hypothesis fully contradicted by (1) the regional floral context denoting humid warm-temperate conditions (abundance of Taxodiaceae, *Engelhardia*, *Quercus*, etc.; Bertini, 1992) as also supported by palaeoclimatic quantification (Fauquette et al., 2006), (2) the absence of any drier phase at that time in North Africa where, on the contrary, a wetter episode is documented (Griffin, 2002; Fauquette et al., 2006). It is more plausible to accept that subdesertic plants moved northward because the southern Italian Peninsula had become uninhabitable during the paroxysmic phase of desiccation: indeed, a subdesertic plant, adapted to very xeric conditions, thrives when it receives a large quantity of water but is alone having survived a very dry climate.

Two of the debated scenarios of the Messinian salinity crisis have considered the question of the Adriatic and Po region where shallow-water primary evaporites are still in place on the margin but were resedimented later within the Apennine foredeep which never desiccated (Roveri et al., 1998, 2001; Bassetti, 2000):

- it was proposed by Manzi et al. (2005) and Roveri and Manzi (2006) to enlarge the Adriatic foredeep model to the whole Mediterranean Basin, postulating that “a large part of the evaporites lying on the Mediterranean floor could have a clastic origin” (Manzi et al., 2005: p. 899). This implies that the Mediterranean Sea never dried out, a proposal that fully contradicts the nature, and thickness of the Mediterranean central basins evaporites inferred from seismic profiles (Savoie and Piper, 1991; Gorini et al., 2005; Sage et al., 2005; Bertoni and Cartwright, 2006), and the presence of deep fluvial (i.e. subaerial) canyons separated by a well-expressed erosional surface on the interfluves (Chumakov,

1973; Clauzon, 1973, 1978; Savoye and Piper, 1991; Gorini et al., 2005; Lofi et al., 2005; Bertoni and Cartwright, 2006);

- Clauzon et al. (1997, 2005) suggested that the Adriatic and Po region persisted as a perched lake (because they display a continuous subaquatic sedimentation during the time-interval of the Mediterranean desiccation), isolated from the desiccated Mediterranean Sea as a result of the combined effects of the Otrante Sill, and the positive hydrologic budget of the region surrounded by uplifting massifs. A significant part of the Dacic Basin experienced a similar evolution (Clauzon et al., 2005) when both the Mediterranean Sea and Black Sea simultaneously desiccated (Gillet, 2004). The Marmara Sea probably persisted too as a perched isolated lake based on the palaeogeography published by Çağatay et al. (2006), and our own recent field observations.

Combining the former data from Bertini (1992, 1994, 2002, 2006), especially those concerning the lower part of the Maccarone section, together with our new data focussing on the upper part of the section with a higher sampling resolution (including dinoflagellate cysts, calcareous nannofossils, and planktonic foraminifers) as well as data recently published on the area (micropaleontological and geochemical information by Bassetti et al., 2003, 2004, respectively, and fish records from Carnevale et al., 2006a), it is possible to reconstruct a reliable environmental evolution of the Apennine foredeep in the late Messinian through early Zanclean. This evolution, which is fully consistent with the geodynamic reconstruction depicted by Roveri et al. (1998, 2001), is summarized in Fig. 9, and may be described as follows. Two main geodynamic events significantly influenced the environments during a period of relatively stable warm and wet climate (Fauquette et al., 2006):

- a powerful tectonic activity continuously affected the region during the Mediterranean Sea desiccation at a time when the Adriatic–Po basin was a perched lake surrounded by uplifting landmasses. This is clearly evidenced by geological observations (Roveri et al., 1998, 2001; Bassetti, 2000), and is supported by strong signs of an intense run-off in the palynological residues (abundant reworked palynomorphs, coaly and woody microparticles, presence of *Concentricystes*, abundance of *Pediastrum*). The continuity of this intense tectonic activity during a relatively long interval explains the absence of any unconformity in the foredeep as reported for the Maccarone section. During the earlier part of this phase, subdesertic plants spread northwards. This should be understood as an epiphenomenon caused by the desiccation of the Mediterranean (Fauquette et al., 2006);
- a marine transgression conceals the effects of tectonism within the sedimentary record because of its suddenness and considerable amplitude. This is undoubtedly the Zanclean transgression as revealed by the coccolith marker *Ceratolithus acutus*. In the Maccarone area, the effects of run-off are henceforth less well expressed probably because the deltaic zones and shoreline were pushed back inland. As another consequence of this event, turbiditic layers progressively disappeared from the foredeep. Tectonic activity probably

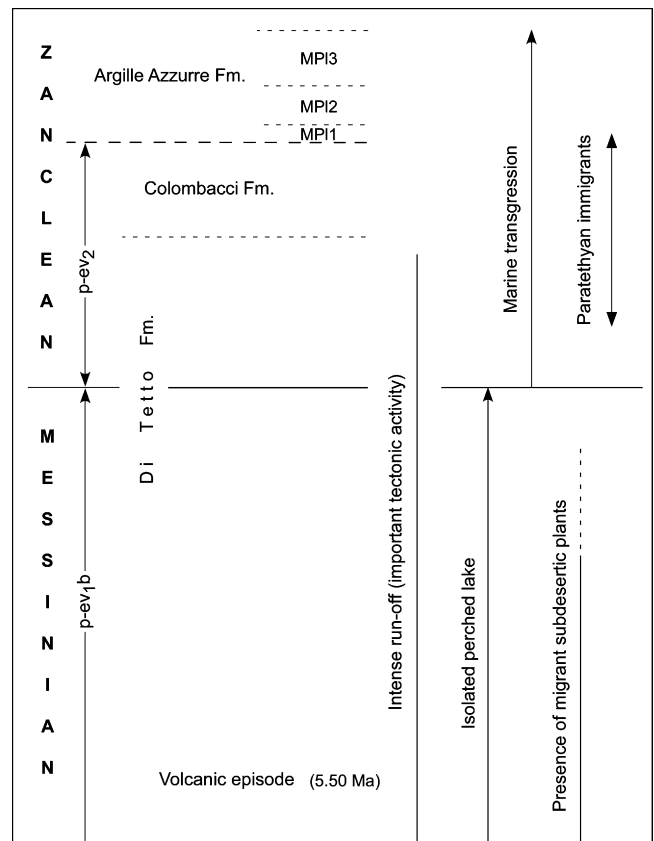


Fig. 9. Proposed environmental evolution of the Apennine foredeep area in the late Messinian and early Zanclean.

Fig. 9. Évolution environnementale de la région de l'avant-fosse des Apennins à la fin du Messinien et au début du Zancéen.

continued but it was less obvious in the sedimentary record. The Zanclean transgression re-established relationships with the Eastern Paratethys through a gateway going from northern Greece up to the Dacic Basin via the Macedonian and Bulgarian basins (Clauzon et al., 2005). This connection allowed brackish surface waters originating from the eastern Paratethys to reach the Adriatic–Po region with their cortege of immigrant living organisms. Evidence for the invasion of Paratethyan dinoflagellates ceases in the second metre of the Argille Azzurre Fm. presumably because of the tectonic closure of the North Aegean–Dacic Basin gateway. In the earliest Zanclean (i.e. the youngest Di Tetto and the entire Colombacci deposits), salinity was probably low in the Apennine foredeep, favouring the immigrant dinoflagellates while creating unfavourable conditions for the already-arrived planktonic foraminifers. The water column rapidly stratified, and led to anoxic deposits (black layers rich in amorphous organic matter: possibly representing sapropels). The alternation between calcareous beds (“colombacci”), and clays might be understood as resulting from variations in salinity as foreseen by Bassetti et al. (2004). The somewhat ambiguous environmental conditions reported for the Colombacci Fm. by geochemists (Casati et al., 1976; Molenaar and De Feyter, 1985; Bassetti et al., 2004) probably originate in the difficulty for waters of various

quality to mix. Such waters would have included locally-sourced former freshwater enriched by a continuous intense run-off, normal marine Mediterranean waters entering the basin, and surface Paratethyan brackish waters.

A final consequence of these results is the necessary revision of the regional stratigraphy, chronostratigraphy, and geological mapping caused by moving the p-ev2 unit into the Zanclean Stage.

6. Conclusion

We emphasize the importance of the Maccarone section, part of which was revisited in our investigations. Our study demonstrates the value of multiple approaches, and exposes the danger of systematically rejecting data simply because it contradicts classical assumptions. Two meaningful advances characterize this work:

- a closing of the debate initiated in Bologna in 1967 at the 4th Congress of the Regional Committee on Mediterranean Neogene Stratigraphy about whether the Colombacci Formation is Messinian or Pliocene in age. It unequivocally belongs to the earliest Pliocene, as does the underlying uppermost part of the Di Tetto Fm. (i.e. the entire p-ev2 stratigraphic unit);
- the lowering in the regional stratigraphy of the Zanclean transgression. This allows, after integrating all available data, a new reconstruction of terrestrial and aquatic environments that is fully compatible with the regional geodynamic picture (Roveri and Manzi, 2006), recent advances in regional palaeoenvironmental studies (Bassetti et al., 2004; Carnevale et al., 2006a), and the Lago Mare scenario formulated by Clauzon et al. (2005). The invasion of Paratethyan species is clearly the consequence of the Zanclean high sea-level that connected the Mediterranean to the Eastern Paratethys.

The failings of the Lago Mare as chronostratigraphic unit are manifest. Within the Apennine foredeep, an area under strong geodynamic control, the respective effects of local tectonics and Mediterranean eustasy have been clarified. Because of the suddenness and amplitude of the Zanclean transgression, it is the Mediterranean eustatic signature that prevails in the sedimentary and palaeobiological records.

Acknowledgements

This work benefited from the support of the French-Italian Galilée cooperative Program. The EEDEN Program of the ESF granted a meeting in Lyon devoted to “Dinoflagellate cysts as promising markers of the Mediterranean-Paratethys relationships” that was attended by several of the authors. This paper is a contribution to the EEDEN Program of the ESF, and the Messinian Project of the C.N.R.S. ECLIPSE Program. We are very grateful to referees, M.J. Head and an anonymous one, who suggested several improvements of the manuscript. In addition, M.J. Head edited the English. Contribution UMR 5125-07.013.

References

- Backman, J., Raffi, I., 1997. Calibration of Miocene nannofossil events to orbitally tuned cyclostratigraphies from Ceara Rise. In: Shackleton, N.J., Curry, W.B. et al. (Eds.), Leg 154. Proceedings of the Ocean Drilling Program, Scientific Results 154, pp. 83–89.
- Baltes, N., 1971. Pliocene Dinoflagellata and Acritarcha in Romania. In: Farinacci, A. (Ed.), Proceedings of the 2nd International Conference on Planktonic Microfossils. Edizioni Tecnoscienza, Rome, pp. 1–16.
- Bassetti, M.A., 2000. Stratigraphy, Sedimentology and paleogeography of Upper Messinian (“post-evaporitic”) deposits in Marche area (Apennines, Central Italy). *Memorie di Scienze Geologiche* 52, 319–349.
- Bassetti, M.A., Manzi, V., Lugli, S., Roveri, M., Longinelli, A., Ricci Lucchi, F., Barbieri, M., 2004. Palaeoenvironmental significance of Messinian post-evaporitic lacustrine carbonates in the northern Apennines, Italy. *Sedimentary Geology* 172, 1–18.
- Bassetti, M.A., Miculan, P., Ricci Lucchi, F., 2003. Ostracod faunas and brackish-water environments of the late Messinian Sapigno section (northern Apennines, Italy). *Palaeogeography, Palaeoclimatology, Palaeoecology* 198, 335–352.
- Bassetti, M.A., Ricci Lucchi, F., Roveri, M., 1994. Physical stratigraphy of the Messinian post-evaporitic deposit in Central-Southern Marche area (Apennines, Central Italy). *Memorie della Società Geologica Italiana* 48, 275–288.
- Beaudouin, C., Suc, J.-P., Escarguel, G., Arnaud, M., Charmasson, S., 2007. The significance of pollen signal in present-day marine terrigenous sediments: The example of the Gulf of Lions (western Mediterranean Sea). *Geobios* 40, 159–172.
- Berggren, W.A., Hilgen, F.J., Langereis, C.G., Kent, D.V., Obradovich, J.D., Raffi, I., Raymo, M.E., Shackleton, N.J., 1995a. Late Neogene chronology: New perspectives in high-resolution stratigraphy. *Geological Society of America Bulletin* 107, 1272–1287.
- Berggren, W.A., Kent, D.V., Swisher, C.C., Aubry, M.-P., 1995b. A revised Cenozoic geochronology and chronostratigraphy. In: Berggren, W.A. (Ed.), *Geochronology Time Scales and Global Stratigraphic Correlation*. SEPM, Society for Sedimentary Geology, Special Publication, Tulsa 54, pp. 141–212.
- Bertini, A., 1992. *Palinologia ed aspetti ambientali del versante adriatico dell’Appennino centro-settentrionale durante il Messiniano e lo Zancleano*. PhD thesis, University of Florence, Florence.
- Bertini, A., 1994. Palynological investigations on Upper Neogene and Lower Pleistocene sections in central and northern Italy. *Memorie della Società Geologica Italiana* 48, 431–443.
- Bertini, A., 2002. Palynological evidence of Upper Neogene environments in Italy. *Acta Universitatis Carolinae. Geologica* 46, 15–25.
- Bertini, A., 2006. The northern Apennines palynological record as a contribute for the reconstruction of the Messinian palaeoenvironments. *Sedimentary Geology* 188/189, 235–258.
- Bertoni, C., Cartwright, J.A., 2006. Controls on the basin wide architecture of late Miocene (Messinian) evaporites on the Levant margin (Eastern Mediterranean). *Sedimentary Geology* 188/189, 93–114.
- Bruno, S., Giusso del Galdo, G., Guarino, R., 2002. Phytosociological notes on the *Lygeum spartum* grasslands from Crete. *Lazaroa* 23, 65–72.
- Bukry, D., 1981. Pacific coast coccolith stratigraphy between Point Conception and Cabo Corrientes. In: Yeats, R.S., Haq, B.U. et al. (Eds.), Leg 63. Initial Reports of the Deep Sea Drilling Project 63, U.S. Government Printing Office, Washington, pp. 445–471.
- Çağatay, M.N., Görür, N., Flecker, R., Sakiç, M., Tünoğlu, C., Ellam, R., Krijgsman, W., Vincent, S., Dikbaş, A., 2006. Paratethyan-Mediterranean connectivity in the Sea of Marmara region (NW Turkey) during the Messinian. *Sedimentary Geology* (188/189), 171–187.
- Carlone, G.C., Francavilla, F., Borsetti, A.M., Cati, F., D’Onofrio, S., Mezzetti, R., Savelli, C., 1974a. Ricerche stratigrafiche sul limite Miocene-Pliocene nelle Marche Centro-meridionali. *Giornale di Geologia* 39 (ser 2), 363–392.
- Carlone, G.C., Cati, F., Borsetti, A.M., Francavilla, F., Mezzetti, R., Savelli, C., 1974b. Il limite Miocene-Pliocene nelle Marche Centro-meridionali. *Bolletino della Società Geologica Italiana* 93, 823–836.

- Carnevale, G., Caputo, D., Landini, W., 2006a. Late Miocene fish otoliths from the Colombacci Formation (Northern Apennines Italy): Implications for the Messinian ‘Lago-mare’ event. *Geological Journal* 41, 1–9.
- Carnevale, G., Landini, W., Sarti, G., 2006b. Mare versus Lago-mare: marine fishes and the Mediterranean environment at the end of the Messinian Salinity Crisis. *Journal of the Geological Society of London* 163, 75–80.
- Casati, P., Bertozzi, P., Cita, M.B., Longinelli, A., Damiani, V., 1976. Stratigraphy and paleoenvironment of the Messinian “Colombacci” Formation in the periadriatic trough. A pilot study. *Memorie della Società Geologica Italiana* 16, 173–195.
- Castradori, D., 1998. Calcareous nannofossils in the basal Zanclean of the Eastern Mediterranean Sea: remarks on paleoceanography and sapropel formation. In: Robertson, A.H.F., Emeis, K.-C., Richter, C., Camerlenghi, A. (Eds.), Leg 180. Proceedings of the Ocean Drilling Program, Scientific Results 180. pp. 113–123.
- Chumakov, I., 1973. Geological history of the Mediterranean at the end of the Miocene-the beginning of the Pliocene according to new data. In: Ryan, W.B.F., Hsü, K.J. et al. (Eds.), Leg 13. Initial Reports of the Deep Sea Drilling Project 13. U.S. Government Printing Office, Washington, pp. 1241–1242.
- Cita, M.B., Colombo, L., 1979. Sedimentation in the latest Messinian at Capo Rossello (Sicily). *Sedimentology* 26, 497–522.
- Cita, M.B., Gartner, S., 1973. Studi sul Pliocene e gli strata di passaggio dal Miocene al Pliocene IV. The stratotype Zanclean foraminiferal and nannofossil biostratigraphy. *Rivista Italiana di Paleontologia e Stratigrafia* 79, 503–558.
- Cita, M.B., Wright, R.C., Ryan, W.B.F., Longinelli, A., 1978. Messinian paleoenvironments. In: Hsü, K.J., Montabert, L. et al. (Eds.), Leg 42. Initial reports of the Deep Sea Drilling Project 42. U.S. Government Printing Office, Washington, pp. 1003–1035.
- Clauzon, G., 1973. The eustatic hypothesis and the pre-cutting of the Rhone Valley. In: Ryan, W.B.F., Hsü, K.J. et al. (Eds.), Leg 13. Initial Reports of the Deep Sea Drilling Project 13, U. S. Government Printing Office, Washington, pp. 1251–1256.
- Clauzon, G., 1978. The Messinian Var canyon (Provence Southern France). Paleogeographic implications. *Marine Geology* 27, 231–246.
- Clauzon, G., Rubino, J.-L., Casero, P., 1997. Regional modalities of the Messinian Salinity Crisis in the framework of two phases model. In: Grasso, M. (Ed.), Neogene basins of the Mediterranean region: controls and correlation in space and time, RCMNS. Interim-Colloquium, Catania, Program and Abstracts. pp. 44–46.
- Clauzon, G., Suc, J.-P., Gautier, F., Berger, A., Loutre, M.-F., 1996. Alternate interpretation of the Messinian salinity crisis: Controversy resolved? *Geology* 24, 363–366.
- Clauzon, G., Suc, J.-P., Popescu, S.-M., Marunteanu, M., Rubino, J.-L., Marinescu, F., Melinte, M.C., 2005. Influence of the Mediterranean sea-level changes over the Dacic Basin (Eastern Paratethys) in the Late Neogene. The Mediterranean Lago Mare facies deciphered. *Basin Research* 17, 437–462.
- Colalongo, M.L., Cremonini, G., Farabegoli, E., Sartori, R., Tampieri, R., Tomadin, L., 1976. Palaeoenvironmental study of the “Colombacci” Formation in Romagna (Italy): the cella section. *Memorie della Società Geologica Italiana* 16, 197–216.
- Corradini, D., Biffi, U., 1988. Étude des dinokystes à la limite Messinien-Pliocène dans la coupe Cava Serredi, Toscane, Italie [Dinocyst study at the Messinian-Pliocene boundary in the Cava Serredi section, Tuscany, Italy]. *Bulletin des Centres de Recherches Exploration-Production Elf-Aquitaine* 12, 221–236.
- Di Stefano, E., 1998. Calcareous Nannofossil Quantitative Biostratigraphy of Holes 969E and 963B (Eastern Mediterranean). In: Robertson, A.H.F., Emeis, K.-C., Richter, C., Camerlenghi, A. (Eds.), Leg 160. Proceedings of the Ocean Drilling Program, Scientific Results 160, pp. 99–112.
- Fauquette, S., Suc, J.-P., Bertini, A., Popescu, S.-M., Warny, S., Bachiri Taoufik, N., Perez Villa, M.-J., Chikhi, H., Feddi, N., Subally, D., Clauzon, G., Ferrier, J., 2006. How much did climate force the Messinian salinity crisis? Quantified climatic conditions from pollen records in the Mediterranean region. *Palaeogeography, Palaeoclimatology, Palaeoecology* 238, 281–301.
- Gillet, H., 2004. La stratigraphie tertiaire et la surface d’érosion messinienne sur les marges occidentales de la mer Noire : stratigraphie sismique haute résolution. Thèse de l’université de Bretagne occidentale, Brest.
- Gorini, C., Lofi, J., Duvail, C., Tadeu Dos Reis, A., Guennoc, P., Lestrat, P., Mauffret, A., 2005. The Late Messinian salinity crisis and Late Miocene tectonism: Interaction and consequences on the physiography and post-rift evolution of the Gulf of Lions margin. *Marine and Petroleum Geology* 22, 695–712.
- Griffin, D.L., 2002. Aridity and humidity: two aspects of the late Miocene climate of North Africa and the Mediterranean. *Palaeogeography, Palaeoclimatology, Palaeoecology* 182, 68–91.
- Heusser, L.E., 1988. Pollen distribution in marine sediments on the continental margin off northern California. *Marine Geology* 80, 131–147.
- Hsü, K.J., Cita, M.B., Ryan, W.B.F., 1973. The origin of the Mediterranean evaporites. In: Initial Reports of the Deep Sea Drilling Project 13, U. S. Government Printing Office, Washington, pp. 1203–1231.
- Iaccarino, S., 1967. Les Foraminifères du stratotype du Tabianien (Pliocène inférieur) de Tabiano Bagni (Parma). *Memorie della Società Italiana di Scienze Naturali* 15, 165–180.
- Iaccarino, S., Salvatorini, G., 1982. A framework of planktonic foraminiferal biostratigraphy for early Miocene to late Pliocene in the Mediterranean area. *Paleontologia Etracografia ed Evoluzione* 2, 115–125.
- Lofi, J., Gorini, C., Berné, S., Clauzon, G., Tadeu Dos Reis, A., Ryan, W.B.F., Steckler, M.S., 2005. Erosional processes and paleoenvironmental changes in the Western Gulf of Lions (SW France) during the Messinian Salinity Crisis. *Marine Geology* 217, 1–30.
- Lourens, L.J., Antonarakou, A., Hilgen, F.J., Van Hoof, A.A.M., Vergnaud Grazzini, C., Zachariasse, W.J., 1996. Evaluation of the Pliocene to early Pleistocene astronomical time scale. *Paleoceanography* 11, 391–413.
- Lourens, L.J., Hilgen, F.J., Laskar, J., Shackleton, N.J., Wilson, D., 2004. The Neogene Period. In: Gradstein, F., Ogg, J., Smith, A. (Eds.), *A Geological Time Scale*. Cambridge University Press, Cambridge. pp. 409–440.
- Manzi, V., Lugli, S., Ricci Lucchi, F., Roveri, M., 2005. Deep-water clastic evaporites deposition in the Messinian Adriatic foredeep (northern Apennines Italy): did the Mediterranean ever dry out? *Sedimentology* 52, 875–902.
- Marret, F., Leroy, S., Chalié, F., Gasse, F., 2004. New organic-walled dinoflagellate cyst from recent sediments of Central Asian seas. *Review of Palaeobotany and Palynology* 129, 1–20.
- Marret, F., Zonnerveld, K.A.F., 2003. Atlas of modern organic-walled dinoflagellate cyst distribution. *Review of Palaeobotany and Palynology* 125, 1–200.
- Martini, E., 1971. Standard Tertiary and Quaternary calcareous nannoplankton zonation. In: Farinacci, A. (Ed.), Proceedings of the 2nd International Conference on Planktonic Microfossils. Edizioni Tecnoscienza, Rome, pp. 739–785.
- Molenaar, N., De Feyter, A.J., 1985. Carbonates associated with alluvial fans: an example from the Messinian Colombacci Formation of the Pietrarubbia Basin, Northern Marche, Italy. *Sedimentary Geology* 42, 1–23.
- Mudie, P.J., Rochon, A., Aksu, A.E., Gillespie, H., 2004. Late glacial Holocene and modern dinoflagellate cyst assemblages in the Aegean-Marmara-Black Sea corridor: statistical analysis and re-interpretation of the early Holocene Noah’s Flood hypothesis. *Review of Palaeobotany and Palynology* 128, 143–167.
- Odin, G.S., Ricci Lucchi, F., Tateo, F., Cosca, M., Hunziker, J.C., 1997. Integrated stratigraphy of the Maccarone section, Late Messinian (Marche region, Italy). In: Montanari, A., Odin, G.S., Coccioni, R. (Eds.), *Miocene Stratigraphy—An Integrated Approach*. Elsevier, Amsterdam, pp. 529–544.
- Orszag-Sperber, F., 2006. Changing perspectives in the concept of “Lago-Mare” in Mediterranean Late Miocene evolution. *Sedimentary Geology* 188/189, 259–277.
- Poumot, C., Suc, J.-P., 1994. Palynofaciès et dépôts séquentiels dans des sédiments marins du Néogène. *Bulletin des Centres de Recherche Exploration-Production Elf-Aquitaine* 18, publication spéciale 107–119.
- Rio, D., Negri, A., 1988. Calcareous nannofossils (Monticino Quarry, Faenza). In: De Giulio, C., Vai, G.B. (Eds.), *Fossil Vertebrates in the Lamone Valley, Romagna Apennines*. Field Trip Guidebook of the International Workshop

- “Continental faunas at the Miocene/Pliocene boundary”, Faenza, pp. 55–57.
- Rio, D., Raffi, I., Villa, G., 1990. Pliocene-Pleistocene calcareous nannofossil distribution patterns in the Western Mediterranean. In: Kastens, K.A., Mascle, J. et al. (Eds.), Leg 107. Proceedings of the Ocean Drilling Program, Scientific Results 107, pp. 513–533.
- Rio, D., Sprovieri, R., Raffi, I., 1984. Calcareous plankton biostratigraphy and biochronology of the Pliocene-lower Pleistocene succession of the Capo Rossello area, Sicily. *Marine Micropaleontology* 9, 135–180.
- Roveri, M., Bassetti, M.A., Ricci Lucchi, F., 2001. The Mediterranean Messinian salinity crisis: an Apennine foredeep perspective. *Sedimentary Geology* 140, 201–214.
- Roveri, M., Manzi, V., 2006. The Messinian salinity crisis: Looking for a new paradigm? *Palaeogeography, Palaeoclimatology, Palaeoecology*.
- Roveri, M., Manzi, V., Bassetti, M.A., Merini, M., Ricci Lucchi, F., 1998. Stratigraphy of the Messinian post-evaporitic stage in eastern Romagna (northern Apennines, Italy). *Giornale di Geologia* 60 (ser 3), 119–142.
- Sage, F., Von Gronefeld, G., Deverchère, J., Gaullier, V., Maillard, A., Gorini, C., 2005. Seismic evidence for Messinian detrital deposits at the western Sardinia margin, northwestern Mediterranean. *Marine and Petroleum Geology* 22, 757–773.
- Savoie, B., Piper, D.J.W., 1991. The Messinian event on the margin of the Mediterranean Sea in the Nice area, southern France. *Marine Geology* 97, 279–304.
- Selli, R., 1973. An outline of the Italian Messinian. In: Drooger, C.W. (Ed.), Messinian events in the Mediterranean. Koninklijke Nederlandse Akademie Van Wetenschappen, Geodynamics Scientific Report, 7. pp. 150–171.
- Siesser, W.G., Kaenel de, E.P., 1999. Neogene Calcareous nannofossil: Western Mediterranean Biostratigraphy and Paleoclimatology. In: Zahn, R., Comas, M.C., Kalus, A. (Eds.), Leg 161. Proceedings of the Ocean Drilling Program, Scientific Results 161, pp. 223–237.
- Sorrel, P., Popescu, S.-M., Head, M.J., Suc, J.-P., Klotz, S., Oberhänsli, H., 2006. Hydrographic development of the Aral Sea during the last 2000 years based on a quantitative analysis of dinoflagellate cysts. *Palaeogeography, Palaeoclimatology, Palaeoecology* 234, 304–327.
- Van Couvering, J.A., Castradori, D., Cita, M.B., Hilgen, F.J., Rio, D., 2000. The base of the Zanclean Stage and of the Pliocene Series. *Episodes* 23, 179–186.
- Wall, D., Dale, B., Harada, K., 1973. Descriptions of new fossil dinoflagellates from the Late Quaternary of the Black Sea. *Micropaleontology* 19, 18–31.

Comment on

Marine reflooding of the Mediterranean after the Messinian Salinity Crisis predates the Zanclean GSSP. Reply to the “Comment on ‘Earliest Zanclean age for the Colombacci and uppermost Di Tetto formations of the “latest Messinian” northern Apennines: New palaeoenvironmental data from the Maccarone section (Marche Province, Italy)’ by Popescu et al. (2007) Geobios 40 (359–373)” authored by Roveri et al.

La réinvasion marine de la Méditerranée après la crise de salinité Messinienne est antérieure au GSSP du Zancéen. Réponse au « commentaire sur ‘La Formation de Colombacci et le sommet de la Formation Di Tetto (« Messinien terminal » des Apennins septentrionaux) sont d’âge zancéen : nouvelles données paléoenvironnementales sur la coupe de Maccarone (Marche, Italie)’ par Popescu et al. (2007) Geobios 40 (359–373) » par Roveri et al.

Speranta-Maria Popescu^{a,*}, Mihaela-Carmen Melinte^b, Jean-Pierre Suc^a,
Georges Clauzon^c, Frédéric Quillévéré^a, Maria Sütő-Szentai^d

^a UMR 5125 CNRS, laboratoire paléoenvironnements et paléobiosphère, université de Lyon et de Lyon-1, 69622 Villeurbanne, France

^b National Institute of Marine Geology and Geoecology (GEOECOMAR), 23–25 Dimitrie Onciul Street, 024053 Bucharest, Romania

^c UMR 6635 CNRS, CEREGE, université Paul-Cézanne, pôle de l’Arbois, BP 80, 13545 Aix-en-Provence cedex 04, France

^d Natural History Collection of Komlo, Városház tér 1, 7300 Komlo, Hungary

Received 16 May 2008; accepted 23 May 2008

Available online 29 August 2008

Abstract

After some deontological considerations, we confirm that evidence of Mediterranean reflooding by Atlantic waters occurs significantly below the formally defined base of the Zanclean Stage at 5.332 Ma, as shown by the lowest occurrence of the calcareous nannofossil *Ceratolithus acutus* (illustrated) in the lower part of the p-ev₂ Formation in the Maccarone section. This species can be detected only after prolonged investigations of the smear slides. Hence, the cyclostratigraphy of the Marche late Messinian requires revision.

© 2008 Elsevier Masson SAS. All rights reserved.

DOIs of original articles: 10.1016/j.geobios.2006.11.005, 10.1016/j.geobios.2008.01.002.

* Corresponding author.

E-mail address: speranta.popescu@univ-lyon1.fr (S.-M. Popescu).

0016-6995/\$ – see front matter © 2008 Elsevier Masson SAS. All rights reserved.

doi:10.1016/j.geobios.2008.05.001

Résumé

Après quelques commentaires d'ordre déontologique, nous confirmons que la réinvasion du bassin méditerranéen par les eaux atlantiques est intervenue bien avant la base « officielle » de l'étage Zancéen placée à 5,332 Ma. Cela est notamment illustré par la présence du nannofossile *Ceratolithus acutus* (photographies à l'appui) dans la partie inférieure de la Formation p-ev₂ à Maccarone. La présence de cette espèce ne peut être établie qu'après une recherche au microscope plus longue que de coutume. La cyclostratigraphie du Messinien supérieur de la Province des Marches doit être révisée en conséquence.

© 2008 Elsevier Masson SAS. All rights reserved.

Keywords: Pre-Zanclean transgression; *Ceratolithus acutus*; Stratigraphy

Mots clés : Transgression anté-zancléenne ; *Ceratolithus acutus* ; Stratigraphie

1. Introduction

Our reply to the comment of Roveri et al. is concise because our data are essentially self-evident. First, we wish to make a deontological observation. Roveri et al. in their Introduction wrote: “Popescu et al. (2007) **derive palaeoenvironmental implications supporting the Messinian salinity crisis scenario proposed by the same Authors** group in previous papers (Clauzon et al., 2005)”. The two-step scenario for the Messinian Salinity Crisis (Clauzon et al., 1996) was proposed after comprehensive field observations in the Sorbas Basin and other Mediterranean peripheral basins where well-dated Messinian marginal evaporites are cut by a huge erosional surface overlain by lower Zanclean deposits (see also Gautier et al., 1994). Such a situation which clearly documents two successive sea-level falls, a moderate one corresponding to the marginal evaporites followed by an outstanding one that caused the central basin evaporites and an intense coeval subaerial erosion (including fluvial canyons) of the margins, is observed all around the Mediterranean and **does not necessitate an adjustment of the data as additional support** as suspected by Roveri et al. This assumption written by Roveri et al. curiously resembles that of Bertini (2006: p. 250, line 11): “It is a fact that such event [i.e. “an additional Lago-Mare event” as indicated five lines above] **is indispensable to validate the two diachronous steps-model** proposed by Clauzon et al. (1996)”. Such assumptions seem to run counter to the deontological approach in science. Our concept of stratigraphy is to consider all the data and not merely select those in agreement with our so-called previously edified scenario. The alternative would allow any new data, even contradictory, to be integrated and serve to validate or modify our interpretation. It happens, however, that our two-step scenario (Clauzon et al., 1996) was fully accepted by a group of specialists of the Messinian Salinity Crisis during the **CIESM Workshop in Almeria (November, 7–10, 2007)**, i.e. before submission of the comment by Roveri et al., an agreement recently published in a CIESM paper, the editing of which was curiously led by M. Roveri himself (**CIESM Workshop Monographs, 2007**; see especially its Fig. 4, p. 17).

2. The post Salinity Crisis reflooding of the Mediterranean and the Zanclean GSSP

Our contradictors are correct to emphasize that the marine records in the Di Tetto and Colombacci formations cannot be

related to the early Zanclean Stage as clearly defined by the Zanclean Global Stratotype Section and Point (GSSP) at Eraclea Minoa (Van Couvering et al., 2000). The Zanclean GSSP is dated at 5.332 Ma in the Sicilian Series and has its echo in the Argille Azzurre overlying the Colombacci Formation in the Marche Series.

But the signs of marine reflooding of the Mediterranean prior to the Zanclean GSSP are not isolated, as they are also suggested in Morocco (Cornée et al., 2006), Calabria (Cavazza and DeCelles, 1998), Sicily (Londeix et al., 2007), Gulf of Lions (Bache, 2008), northeastern Aegean Sea (Clauzon et al., 2008), etc.

Our somewhat provocative title (Popescu et al., 2007) aimed to show again how greatly the Zanclean GSSP (Van Couvering et al., 2000) is compromised, given that it immediately follows a sedimentary hiatus on the Mediterranean margins and is complicated by a marine reflooding that is now known to occur in two steps. Can such a GSSP be appropriate when linked to such an exceptional succession of major events?

3. The Maccarone fossil records

Roveri et al. announce a more complete study of the Maccarone section by their group that is based on a dense sampling. We may expect very promising discussions arising from the paleobiological records and forthcoming geochemical measurements.

It is not necessary to repeat descriptions of the dinoflagellate cyst flora (Bertini, 1992, 2006; Popescu et al., 2007) recalled by Roveri et al. Additional new details on this flora are provided by Popescu et al. (in press). In any case, a complete understanding of ecological variations within Lago Mare facies as reflected in the dinoflagellate cyst record requires a detailed comparison with the type specimens from the Pannonian Basin, these being available only in Komlo and Lyon.

Foraminifers from the Di Tetto and Colombacci formations are considered by Roveri et al. as reworked, and they are rejected only on the weak argument that their presence is in contradiction with the ostracod record which has a freshwater signature. Such contradictory coexisting faunas are not exceptional in coastal environments within the Lago Mare context, as pointed out in Corsica (Casabianda locality) by Saint Martin et al. (2007) for sediments also containing *Ceratolithus acutus*, the marker of the nannofossil subzone NN12b (Popescu et al., 2007).

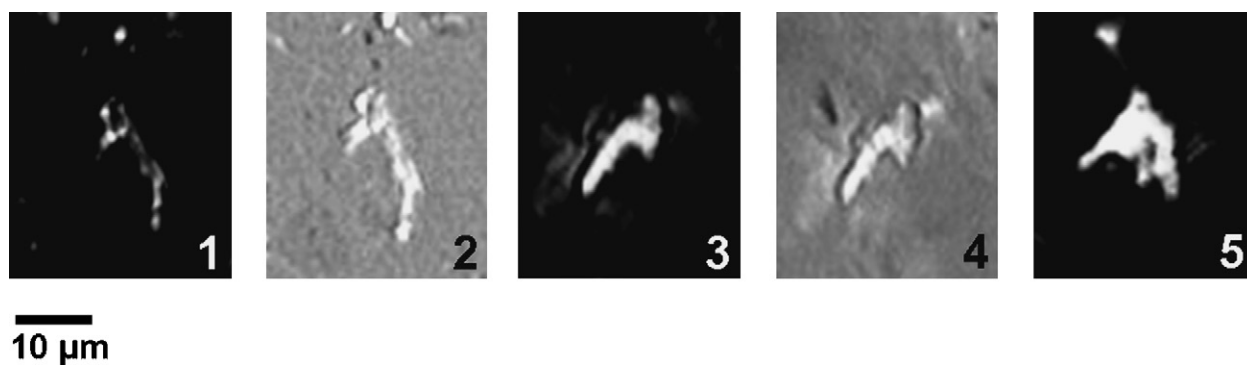


Fig. 1. 1. *Ceratolithus acutus* Gartner and Bukry, sample 5 (Popescu et al., 2007), crossed nicols. 2. *Ceratolithus acutus* Gartner and Bukry, sample 5 (Popescu et al., 2007), parallel light. 3. *Ceratolithus acutus* Gartner and Bukry, sample 13 (Popescu et al., 2007), crossed nicols. 4. *Ceratolithus acutus* Gartner and Bukry, sample 13 (Popescu et al., 2007), parallel light. 5. *Ceratolithus acutus* Gartner and Bukry, sample 21 (Popescu et al., 2007), crossed nicols.

C. acutus is actually present, even if very scarce, in the Colombacci and underlying upper Di Tetto formations with similar morphology to that found in the Argille Azzurre deposits. Sediment caving cannot be invoked as we sampled in late August 2004, at the bottom of deep excavations made a few days earlier by the Roveri group. The presence of *C. acutus* almost continuously in our samples 5–15, and then episodically (samples 21 and 33) and finally continuously from sample 43, is fully consistent with the succession of bioevents recorded in the Maccarone section (Bertini, 1992, 2006; Popescu et al., 2007) as in many other peri-Mediterranean sections (Clauzon et al., 2008):

- at about 110 m from the base of the section, large increases in *Pinus* (indicative of more distal environment) and the coeval presence of foraminifers and marine dinoflagellate cysts;
- record of *Triquetrorhabdulus rugosus* from at least 130 m;
- first record of *C. acutus* at about 135 m;
- full marine conditions at 172 m (Argille Azzurre Fm.).

Roveri et al. argue that *C. acutus* is a very scarce species in the lower Zanclean of the Mediterranean where they mention it has been recorded only by Castradori (1998). This is inaccurate because the species was reported not only in several Mediterranean regions [i.e. at Capo Rossello by Cita and Gartner (1973), in the Aegean region (Acropotamos locality, northern Greece) by Snel et al. (2006b) and regularly by us everywhere in the Mediterranean Basin (Clauzon et al., 2008; Popescu et al., in press), as well as in the Paratethys (Dacic Basin: Mărunţeanu and Papaianopol, 1998; Snel et al., 2006a). In agreement with E. Di Stefano et al. (1996) who declare that “Due to the rare presence of the species [i.e. *C. acutus*], in the Mediterranean sequence this bioevent [i.e. the First Occurrence of *C. acutus*] can be identified only with a longer than routine investigation of the smear slides, but its recognition at the base of the Mediterranean Pliocene sequence is extremely important” (p. 408, lines 18–21), we performed a very careful analysis of each sample from the Maccarone section. Notably, the nannofossil *C. acutus* was recorded with very low frequency throughout the lower part of the studied

section, where it is extremely rare (i.e., one specimen per more than 50 fields of view [FOV]) (Fig. 1(1–5)). Moreover, in the investigated sequence, it was not recorded in all samples. The absence of *C. acutus* in these samples is probably due to non-preservation, as its absence is coincident with those samples that yielded a poor or poor-to-moderately preserved nannofossil assemblages. A higher abundance of *C. acutus* (one specimen per 30–50 FOV) was observed towards the upper part of the section. However, a careful calcareous nannoplankton investigation could not omit specimens of *C. acutus*. On the other hand, the “typical Pliocene species widely documented in Late Miocene (e.g. *Discoaster tamalis*, *Helicosphaera sellii*)”, according to Roveri et al., were not found by us in the Maccarone section.

Roveri et al. question our record of *C. acutus* at Maccarone on the basis of their cyclostratigraphy of the Colombacci Fm. This cyclostratigraphy is calibrated using two ages: that of the base of the Argille Azzurre Formation at 5.33 Ma which is reliable, and that at the boundary between p-ev₁ and p-ev₂ Formations at 5.42 Ma which is only speculative (see also Gennari et al., 2008). We conclude that our oldest specimens of *C. acutus* in the lower p-ev₂ Formation provide at last another reliable age (5.35 Ma; Lourens et al., 2004; 5.345: Raffi et al., 2006) for revising the cyclostratigraphic interpretation of the late Messinian in the Marche Province, taking also into account the radiometric age of the ash layer at 5.50 Ma.

4. Conclusion

Although there are many other aspects to counter assumptions made by Roveri et al., we consider that our detailed arguments are clearly sufficient to objectively establish the presence of early influxes of Mediterranean marine waters into the previously isolated Apennines foredeep. Such influxes occurred significantly before the formally-defined base of the Zanclean Stage, and resulted from what was probably an almost complete reflooding of the Mediterranean Basin significantly before 5.332 Ma. We appreciate the opportunity provided by Roveri et al. to reiterate our conclusions.

References

- Bache, F., 2008. Évolution Oligo-Miocène des marges du micro-océan Liguro-Provençal. PhD thesis, Université de Bretagne occidentale, Brest.
- Bertini, A., 1992. Palinologia ed aspetti ambientali del versante adriatico dell'Appennino centro-settentrionale durante il Messiniano e lo Zancleano. PhD Thesis, University of Florence.
- Bertini, A., 2006. The northern Apennines palynological record as a contribute for the reconstruction of the Messinian palaeoenvironments. *Sedimentary Geology* 188/189, 235–258.
- Castradori, D., 1998. Calcareous nannofossils in the basal Zanclean of the Eastern Mediterranean Sea: remarks on paleoceanography and sapropel formation. In: Robertson, A.H.F., Emeis, K.-C., Richter, C., Camerlenghi, A. (Eds.), Leg 180, Proceedings of the Ocean Drilling Program, Scientific Results 180, 113–123.
- Cavazza, W., DeCelles, P.G., 1998. Upper Messinian siliciclastic rocks in southeastern Calabria (southern Italy): palaeotectonic and eustatic implications for the evolution of the central Mediterranean region. *Tectonophysics* 298, 223–241.
- CIESM Workshop Monographs (Antón, J., Briand, F., Çağatay, M.N., De Lange, G.J., Flecker, R., Gaullier, V., Guiliano, L., Gunde-Cimerman, N., Hübscher, C., Krijgsman, W., Lambregts, P., Lofi, J., Lugli, S., Manzi, V., McGenity, T.J., Roveri, M., Sierro, F.J., Suc, J.-P.), 2007. The Messinian Salinity Crisis from mega-deposits to microbiology – A Consensus Report. CIESM Workshop Monographs 33, 7–28.
- Cita, M.B., Gartner, S., 1973. Studi sul Pliocene e gli strati di passaggio dal Miocene al Pliocene, IV. The stratotype Zanclean foraminiferal and nannofossil biostratigraphy. *Rivista Italiana di Paleontologia e Stratigraphia* 79, 503–558.
- Clauzon, G., Suc, J.-P., Gautier, F., Berger, A., Loutre, M.-F., 1996. Alternate interpretation of the Messinian salinity crisis: Controversy resolved? *Geology* 24, 363–366.
- Clauzon, G., Suc, J.-P., Armijo, R., Meyer, B., Melinte-Dobrinescu, M.C., Lericolais, G., Gillet, H., Çağatay, M.N., Popescu, S.-M., Jouannic, G., Ucarus, G., Çakir, Z., Quillévéré, F., 2008. Impact of the Messinian Salinity Crisis in the region of the Marmara Sea. Did a connection exist between the Aegean and Black seas at that time? 61th Turkish Geological Congress, Ankara, Abstracts book, pp. 136–137.
- Clauzon, G., Suc, J.-P., Popescu, S.-M., Mărunțeanu, M., Rubino, J.-L., Marinescu, F., Melinte, M.C., 2005. Influence of the Mediterranean sea-level changes over the Dacic Basin (Eastern Paratethys) in the Late Neogene. The Mediterranean Lago Mare facies deciphered. *Basin Research* 17, 437–462.
- Cornée, J.-J., Ferrandini, M., Saint Martin, J.-P., Münch, P., Moullade, M., Ribaud-Laurenti, A., Roger, S., Saint Martin, S., Ferrandini, J., 2006. The late Messinian erosional surface and the subsequent reflooding in the Mediterranean: New insights from the Melilla-Nador basin (Morocco). *Palaeogeography, Palaeoclimatology, Palaeoecology* 230, 129–154.
- Di Stefano, E., Sprovieri, R., Scarantino, S., 1996. Chronology of biostratigraphic events at the base of the Pliocene. *Palaeopelagos* 6, 401–414.
- Gennari, R., Iaccarino, S.M., Roveri, M., Manzi, V., Grossi, F., 2008. Integrated biostratigraphic and physical stratigraphic framework: a high definition correlative tool for the Lago Mare deposits. Specialized Session of the French Geological Society on “Mio-Pliocene geodynamics and paleogeography of the Mediterranean region: eustacy–tectonics interference”, Lyon, Abstracts Volume, pp. 39–41.
- Gautier, F., Clauzon, G., Suc, J.-P., Cravatte, J., Violanti, D., 1994. Âge et durée de la crise de salinité messinienne. *Comptes rendus de l'Académie des sciences de Paris* 320 (2), 1103–1109.
- Londeix, L., Benzakour, M., Suc, J.-P., Turon, J.-L., 2007. Messinian paleoenvironments and hydrology in Sicily (Italy): The dinoflagellate cyst record. *Geobios* 40, 233–250.
- Lourens, L.J., Hilgen, F.J., Laskar, J., Shackleton, N.K., Wilson, D., 2004. The Neogene Period. In: Gradstein, F., Ogg, J., Smith, A. (Eds.), *A Geological Time Scale*. Cambridge University Press, Cambridge, pp. 409–440.
- Mărunțeanu, M., Papaianopol, I., 1998. Mediterranean calcareous nannoplankton in the Dacic Basin. *Romanian Journal of Stratigraphy* 78, 115–121.
- Popescu, S.M., Dalesme, F., Jouannic, G., Escarguel, G., Head, M.J., Melinte-Dobrinescu, M.C., Sütő-Szentai, M., Bakrac, K., Clauzon, G., Suc, J.-P., in press. *Galeacysta etrusca* complex, dinoflagellate cyst marker of Paratethyan influxes into the Mediterranean Sea before and after the peak of the Messinian Salinity Crisis. *Palynology*.
- Popescu, S.M., Melinte, M.C., Suc, J.-P., Clauzon, G., Quillévéré, F., Sütő-Szentai, M., 2007. Earliest Zanclean age for the Colombacci and uppermost Di Tetto formations of the “latest Messinian” northern Apennines: New palaeoenvironmental data from the Maccarone section (Marche Province, Italy). *Geobios* 40, 359–373.
- Raffi, I., Backman, J., Fornaciari, E., Pălike, H., Rio, D., Lourens, L., Hilgen, F., 2006. A review of calcareous nannofossil astrobiochronology encompassing the past 25 million years. *Quaternary Science Reviews* 25, 3113–3137.
- Saint Martin, S., Saint Martin, J.-P., Ferrandini, J., Ferrandini, M., 2007. La microflore de diatomées au passage Mio-Pliocène en Corse. *Geobios* 40, 375–390.
- Snel, E., Mărunțeanu, M., Macaleț, R., Meulenkamp, J.E., Van Vugt, N., 2006a. Late Miocene to Early Pliocene chronostratigraphic framework for the Dacic Basin, Romania. *Palaeogeography, Palaeoclimatology, Palaeoecology* 238, 107–124.
- Snel, E., Mărunțeanu, M., Meulenkamp, J.E., 2006b. Calcareous nannofossil biostratigraphy and magnetostratigraphy of the Upper Miocene and Lower Pliocene of the Northern Aegean (Orphanic Gulf-Strimon Basin areas), Greece. *Palaeogeography, Palaeoclimatology, Palaeoecology* 238, 125–130.
- Van Couvering, J.A., Castradori, D., Cita, M.B., Hilgen, F.J., Rio, D., 2000. The base of the Zanclean Stage and of the Pliocene Series. *Episodes* 23, 179–186.

The Messinian Salinity Crisis in the Dardanelles region: Chronostratigraphic constraints

Mihaela Carmen Melinte-Dobrinescu^a, Jean-Pierre Suc^b,
Georges Clauzon^c, Speranța-Maria Popescu^b, Rolando Armijo^e, Bertrand Meyer^f,
Demet Biltekin^d, M. Namık Çağatay^d, Gülsen Ucarkus^d, Gwénaél Jouannic^f,
Séverine Fauquette^g, Ziyadin Çakir^d

- a, National Institute of Marine Geology and Geo-ecology (GEOECOMAR), 23-25 Dimitrie Onciul Street, RO-024053 Bucharest, Romania,
e-mail: melinte@geoecomar.ro
- b, UMR 5125 PEPS, CNRS, France; Université Lyon 1, Campus de La Doua, Bâtiment Géode, 69622 Villeurbanne Cedex, France
e-mail: jean-pierre.suc@univ-lyon1.fr, speranta.popescu@univ-lyon1.fr
- c, C.E.R.E.G.E. (UMR 6635 6635 CNRS), Université Paul Cezanne, 13545 Aix-en-Provence Cedex, France
e-mail: clauzon@cerege.fr
- d, Istanbul Technical University, School of Mines and Eurasia Institute of Earth Sciences, Istanbul, Turkey
e-mail: cagatay@itu.edu.tr, ucarkus1@itu.edu.tr, ziyadin.cakir@itu.edu.tr
- e, Laboratoire de Tectonique, Institut de Physique du Globe de Paris (UMR 7154 CNRS), 75252 Paris Cedex, France
e-mail: armijo@ipgp.jussieu.fr
- f, Laboratoire de Tectonique (UMR 7072 CNRS), Université Paris 6, 75252 Paris Cedex 05, France
e-mail: bmeyer@ccr.jussieu.fr; jouannic.gwenael@neuf.fr
- g, Institut des Sciences de l'Evolution (UM2-CNRS), CC 061, Université Montpellier 2, Place Eugène Bataillon, 34095 Montpellier Cedex 05, France
e-mail: severine.fauquette@univ-montp2.fr

Abstract.

An intense controversy on chronostratigraphy of Late Miocene – Early Pliocene deposits and the Messinian Salinity Crisis in the Dardanelles area led to a systematic investigation of calcareous nannoplankton content of 10 key-sections representative of the most relevant regional Kirazlı and Alçıtepe formations. Our study shows clearly that the Kirazlı Formation deposits predate the Messinian Salinity Crisis while those of the Alçıtepe Formation postdate this outstanding event, which severely impacted the region as widely known around the Mediterranean Basin. Fluvial canyon cutting or gap in sedimentation linked to the peak of the Messinian Salinity Crisis separate the two formations. Detailed palaeoenvironmental investigations allow reconstructing the regional palaeogeography before, during and after the Messinian Salinity Crisis. No passage existed in the area during the Messinian Salinity Crisis between the Mediterranean Sea and Eastern Paratethys.

Key words: Calcareous nannoplankton, Chronostratigraphy, Messinian Salinity Crisis, Palaeogeography, NE Aegean region.

1. Introduction

During the Late Neogene, very significant paleobiogeographical changes have taken place in the Mediterranean region *s.l.*, fundamentally because the connection of the Atlantic Ocean with the Mediterranean Sea and the Paratethys (a residual continental sea which covered large areas of the Central and Eastern Europe) Sea was restricted and sometimes completely interrupted (Seneš, 1973; Rögl and Steininger, 1983; Marinescu, 1992; Rögl, 1998; Popov et al., 2004; Mărunțeanu and Papaianopol, 1995; Sprovieri et al., 2003; Clauzon et al., 2005; Popescu, 2006; Melinte, 2006). The latest Miocene is characterized by an exceptional event, which is the severe sea-level drop of the Mediterranean Sea, leading to the Messinian Salinity Crisis (MSC). This event is characterized throughout the Mediterranean basin by both, deposition of thick evaporites in its deep basins and cutting of huge fluvial canyons across its margins (Hsü et al., 1973; Clauzon, 1973; Cita et al., 1978; Clauzon et al., 1996). Such a prominent geological event produced significant changes in the palaeobiological assemblages, mirrored especially by the marine planktonic organisms (such as planktonic foraminifers, calcareous nannoplankton and dinoflagellates), which are very sensitive to environmental changes.

Consequently, the Messinian Salinity Crisis is now recognized as the most prominent event marking paleobiogeographical change in the Mediterranean. Examples of case studies of spectacular features associated with the MSC are widespread over the entire Mediterranean area (for an overview, see: Agusti et al., 2006; Rouchy et al., 2006; Suc et al., 2007; CIESM, 2008). The present study is devoted to improve our knowledge of the MSC in the Dardanelles region (Fig. 1A), which is crucial for our understanding of the evolution of the linkage between the Aegean Sea and the Black Sea. The existence of a gateway at the time of the MSC is subject of controversy (in support of such a gateway, see: Esu, 2007; Faranda et al., 2007; Gliozzi et al., 2007; Stoica et al., 2007; in opposition of such a gateway, see: Clauzon et al., 2005; Popescu, 2006; Gillet et al., 2007; Popescu et al., 2008). However, most studies of the regional stratigraphy are at odds with the mere existence of a good record of the MSC in the Dardanelles (see, for examples: Görür et al., 1997, 2000; Çağatay et al., 1998, 2006; Türkecan and Yurtsever, 2002; Sakıncı and Yalıtırak, 2005). The consensus among regional stratigraphers is that the rocks outcropping in the Dardanelles are chiefly sediments of Eocene to Middle-Late Miocene age and that the region is basically devoid of marine sediments of Pliocene age (Figs. 1B, 1C). The typical strong marginal signature of the MSC is present all around the Mediterranean (including the Aegean Sea), with an erosional surface and deeply incised fluvial canyons, subsequently covered and filled with marine Pliocene sediments (examples from the Western Mediterranean: Clauzon, 1973, 1978, 1980a, 1980b, 1982, 1990; Gautier et al., 1994; Guennoc et al., 2000; Lofi et al., 2003, 2005; Cornée et al., 2006; Maillard and Mauffret, 2006; Sage et al., 2005 – example from the Central Mediterranean: El Euch – El Koundi et al., accepted – examples from the Eastern Mediterranean: Chumakov, 1973; Delrieu et al., 1993; Poisson et al., 2003). Even if these erosional effects of the MSC were suspected in the Dardanelles region (Çağatay et al., 2006), they were not clearly evidenced until today, mapped and recognized as such by the conventional stratigraphy.

Defying the stratigraphical consensus, the study by Armijo et al. (1999) presented evidence for a widespread erosion surface and a prominent canyon that parallels the present-day Dardanelles Strait. These authors interpreted explicitly these features as possibly resulting from the MSC, given the large uncertainties in the ages of the

formations mapped in the area (Ternek, 1964). Both the erosion surface and the canyon appear carved into the sediments of the Kirazlı Formation and filled by sediments of the Alçıtepe Formation (Armijo et al., 1999). Consequently, Armijo et al. (1999) deduced for these two formations a possible Messinian and an early Pliocene age, respectively (Fig. 2). The study by Armijo et al. (1999) includes a geological map that shows strong folding affecting layers of the Kirazlı Formation, but not those of the overlying Alçıtepe Formation. Therefore, that important unconformity would also correlate roughly with the MSC, providing an invaluable constraint for the age of the propagation of the North Anatolian Fault across the region (Armijo et al., 1999). The work by Armijo et al. (1999) has been strongly criticized (e.g., Yalıtırak et al., 2000 vs. Armijo et al., 2000) and its main stratigraphic inferences dismissed (e.g., Sakıncı and Yalıtırak, 2005; Çağatay et al., 2006).

In order to clarify the significance of the Messinian Salinity Crisis and its geological imprint in the Dardanelles region, we revised the stratigraphy by a systematic sampling of the most critical sedimentary units and by dating them using calcareous nannofossils. We studied ten key-sections (Enez and Yaylaköy in the Gulf of Saros; Burhanlı, Eceabat, Poyraztepe, Kilitbahir, Seddülbahir, Intepe, Yenimahalle and Truva in the Dardanelles Strait) where Late Neogene deposits are well exposed (Figs. 1B, 1C). Our study aims are: (1) dating these sections with respect to global bio- chronostratigraphy using calcareous nannofossils, (2) reconstructing marine and continental palaeoenvironments using nannoplankton, dinoflagellate cysts and pollen grains, and (3) setting up a reliable chronostratigraphic basis for current and future studies of the Messinian Salinity Crisis in the Dardanelles region, as well as for studies using the MSC as a chronometer for deformation associated with the North Anatolian Fault.

The age of the Alçıtepe Formation is the crucial question for the ongoing controversy (Fig. 2). The Alçıtepe Formation is described as being composed of brackish- to fresh-water carbonates, interbedded with marine sandstones and siltstones (Görür et al., 1997; Çağatay et al., 1999) as more or less conformably overlying the Kirazlı Formation (Çağatay et al., 2006). It is overlain by shallow fluvio-marine siliciclastic rocks (Göztepe Fm. in the North Marmara region, Truva Fm. in the South Marmara region: Görür et al., 2000; Çağatay et al., 2006). A brackish Paratethyan fauna (i.e. *Mactra* sp., *Paradacna abichi*, *Dreissena* sp., *Cardium* sp., and *C. edulis*) was reported from the Alçıtepe Formation, suggesting that these deposits belong to the Pontian Paratethyan Stage (Gillet et al., 1978; Taner, 1979; Çağatay et al., 2006) and, as a consequence, to the so-called “late Messinian Lago Mare” (Sakıncı and Yalıtırak, 2005; Çağatay et al., 2006). Some intercalations of layers with Mediterranean marine faunas (*Ostrea*, *Pecten*) were also reported (Sakıncı and Yalıtırak, 2005), that emphasizes the dual, Paratethyan and Mediterranean, influence in the area. To characterize the MSC in the region, we focussed our study on the passage between the Alçıtepe Formation and the underlying Kirazlı Formation.

2. Material and methods

Qualitative nannofloral investigations were performed for the sections Enez, Yaylaköy, Burhanlı, Eceabat, Poyraztepe, Kilitbahir, Seddülbahir, Intepe, Yenimahalle and Truva, while quantitative analyses were undertaken on the Intepe section. In all, 35 samples from >34 m of sediments of the Intepe section were investigated. To retain the original sample composition, smear slides were prepared directly from untreated samples. The

calcareous nannofloral analyses were performed using a light polarizing microscope at x1600 magnification. We estimated the degree of preservation as follows: P = poor, severe dissolution, fragmentation and/or overgrowth; the specific identification is hindered up to 70%; M = moderate, dissolution and/or overgrowth; the specific identification is hindered up to 30%; G = good, little dissolution and/or overgrowth; diagnostic characteristics are preserved, and the specimens could be identified to species level (up to 90%). For the semi-quantitative nannofloral analyses, at least 300 specimens were counted in each sample. Abundances of the taxa encountered were recorded as follows: R, rare, 1 specimen/>20 fields of view; F, few, 1s/11-20 FOV; C, common, 1s/2-10 FOV; A, abundant, >1s/FOV. The nannofloral taxonomic identification follows Perch-Nielsen (1985) and Young (1998).

Palynological samples were analysed from some of these sections: Burhanlı (1 sample), Eceabat (1 sample), Seddülbahir (2 samples), Intepe (9 samples). Each sample (20 g of dry sediment) was processed using standard method (Cour, 1974): acid digestion, concentration using ZnCl₂ (at density 2.0) and sieving at 10 µm. A 50 µl volume of residue was mounted between the coverslip and microscope slide using glycerine in order to allow rotation of palynomorphs for their complete examination resulting in their proper identification. Counting of palynomorphs was performed using a light microscope, their identification was done at x1000 magnification. Pollen grains were identified with a botanical approach. 150 pollen grains except those of *Pinus* were identified and counted per sample. The pollen slides showing very poor concentrations in dinoflagellate cysts, a new sieving at 20 µm was performed on the pollen residue that permitted to concentrate the dinoflagellate cysts and a new slide was obtained using 50 µl from the new residue. Only the nine samples from the Intepe sections were analysed: all the specimens present on a slide were identified and counted. The freshwater algae *Pediastrum* and *Botryococcus* were considered as transported by rivers, and were also counted. Their vertical distribution documents duration and intensity of freshwater inputs.

3. Results

3.1. Bio- and chrono-stratigraphy

The calcareous nannoplankton offers an accurate way of biostratigraphic dating based on successive appearance-disappearance events within the time-window 8-4 Ma, which is of interest to this study. It uses the classical nannoplankton Zonation of Martini (1971), the major events of which are now precisely dated (Backman and Raffi, 1997; Lourens et al., 2004; Raffi et al., 2003; Raffi et al., 2006). They are summarized on Figure 3. Five of the concerned taxa have been recorded in the studied sections: *Amaurolithus primus* (First Appearance Datum, FAD: 7.424 Ma; Last Appearance Datum, LAD: 4.50 Ma), *Reticulofenestra rotaria* (FAD: ca. 7.41 Ma; LAD: imprecise, up to ca. 6 Ma), *Triquetrorhabdulus rugosus* (FAD: 12.671 Ma; LAD: 5.279 Ma), *Ceratolithus acutus* (FAD: 5.345 Ma; LAD: 5.040 Ma), and *Reticulofenestra pseudoumbilicus* (FAD: 8.761 Ma; LAD: 3.839 Ma). It should be noted that, when different ages were proposed by Raffi et al. (2006), we considered those proposed for the Eastern Mediterranean when available. Combining appearance-disappearance datum of these taxa allowed us to easily distinguish nannoplankton Zones 11 to 13 (Fig. 3).

3.1.1. Gulf of Saros

Near Enez, the studied section is located on the eastern shoreline of the Enez lagoon (40°46'24" N latitude, 26°04' E longitude; Fig. 1B), an area described as covered by deltaic deposits of the Meriç River overlying the Kirazlı Formation (Çağatay et al., 1998, 2006) while Sakıncı et al. (1999) indicates some bioclastic carbonate rocks attributed to the Alçitepe Fm., the upper part of which could belong to Zanclean. Here, brownish clays with a thickness of about 8 m have provided a poorly to moderately preserved nannoflora analysed within 7 samples. The joint presence of *Triquetrorhabdulus rugosus* and *Ceratolithus acutus* specifies the beginning of the NN12b nannofossil Subzone (Table 1), representing the extreme end of Messinian (after the MSC) to early Zanclean (Fig. 3).

At Yaylaköy, blue clays are exposed along the beach (40°36'22" N latitude, 26°21'28" longitude E; Fig. 1B) below coquina beds with *Ostrea* and interbedded with *Cardium*-bearing sands of Zanclean age (Çağatay et al., 1998, 2006). This section probably corresponds to the upper third of the Erikli section of Sakıncı et al. (1999) and Sakıncı and Yalıtırak (2005) that the authors refer to the Alçitepe Formation. The studied sample of the blue clays includes *Ceratolithus acutus* and *Triquetrorhabdulus rugosus*. Reworked specimens are rare. This moderately preserved nannoflora also belongs to the beginning of the nannofossil Subzone NN12b (Table 1), i.e. the extreme end of Messinian (after the MSC) to early Zanclean (Fig. 3).

3.1.2. Dardanelles Strait

At Burhanlı (40°18'17" N latitude, 26°33'08" E longitude; Fig. 1C), five samples from the variegated clays of the Kirazlı Formation provided a moderately preserved nannoflora with *Amaurolithus primus*, *Reticulofenestra pseudoumbilicus*, *R. rotaria* and *Triquetrorhabdulus rugosus* (Table 1). Reworkings from Cretaceous, Eocene, Oligocene and Miocene have been observed. Such an assemblage belongs to the lower part of the nannofossil Subzone NN11b (i.e. to the latest Tortonian – early Messinian) (Table 1, Fig. 3).

Northward Eceabat (40°11'30" latitude N, 26°21'18" E longitude; Fig. 1C), four samples have been studied from the whitish clayey base (40 m thick) belonging to the Kirazlı Formation, and one sample from a clayey intercalation within calcareous tabular deposits of the Alçitepe Formation (Sakıncı et al., 1999). All of them display a nannoflora characterized by a poor to moderate preservation and few reworked specimens. It includes *Amaurolithus primus*, *Reticulofenestra pseudoumbilicus*, *R. rotaria*, and *Triquetrorhabdulus rugosus* (Table 1). As for Burhanlı, such an assemblage belongs to the lower part of the nannofossil Subzone NN11b (i.e. to the latest Tortonian – early Messinian) (Table 1, Fig. 3).

In the nearby Poyraztepe hill (40°12'27.6" N latitude, 26°21'59.9" E longitude; Fig. 1B), the upper part of the section belonging to the Alçitepe Formation and with a stratigraphic position higher than the top of the Eceabat section, provided a nannoflora from its uppermost clayey intercalations underlying the topmost limestone. They contain, among an important amount of reworked specimens, *Triquetrorhabdulus rugosus* and *Reticulofenestra pseudoumbilicus*, a nannoflora of the upper NN11b Subzone (Table 1), i.e. the late Messinian (Fig. 3).

Near Kilitbahir, two thin sections were investigated: the one on the seashore (40°10'08.8" E longitude, 26°22'16" N latitude) belongs to the Kirazlı Fm. and that along a path above the castle (40°08'35" E longitude, 26°22'10" N latitude) to the Alçitepe Fm. (Sakıncı et al., 1999; Sakıncı and Yalıtırak, 2005) (Fig. 1C). The coastal

locality is made of 1.50 m of blue clays rich in mollusc shells overlain by about 20 m of sands including, 4 m over their base, a blue clayey bed (1 m thick). Of the four samples collected, the three lowermost samples contain *Triquetrorhabdulus rugosus* and *Reticulofenestra pseudoumbilicus* (Table 1); reworking is important in these samples. The fourth sample (intercalated clays) provided the same calcareous nannofossil assemblage plus *Ceratolithus acutus*, a nannoflora unchanged above the castle (Table 1). The two samples yielding *C. acutus* are characterized by a weak reworking. They belong to Subzone NN12b (Table 1), i.e. the extreme end of Messinian to early Zanclean (Fig. 3). The three coastal samples belong to Subzone NN12a (i.e. to the latest Messinian) (Table 1, Fig. 3). As it has been demonstrated that the Mediterranean reflooding anticipated the base of the Zanclean Stage (Popescu et al., 2007, 2008) as defined by its GSSP (Global Stratotype and Point Section: Van Couvering et al., 2000) and in the absence of any unconformity between samples of Subzones NN12b and NN12a, we consider that all these samples postdate the MSC.

At the beach of Seddülbahir, there are two distinct sections both referring to the Alçıtepe Fm. (Sakinç and Yaltrak, 2005), of which the second section constitutes the reference exposure: (1) to the East (40°02'30" N latitude, 26°11'12.1" E longitude; Fig. 1C), a thin section (5 m thick) mostly made of sands, clays and marls, yielded within five samples an homogenous nannoflora with few reworking, including *Triquetrorhandulus rugosus*, *Reticulofenestra pseudoumbilicus*, *R. rotaria*, referring to lower part of Subzone NN11b (i.e. latest Tortonian to early Messinian in age) (Table 2, Fig. 3); (2) to the West (40°02'38" N latitude, 26°10'55" E longitude; Fig. 1C), the second section, made of thick clays (about 30 m) rich in mollusc shells, provided *Triquetrorhabdulus rugosus* and *Reticulofenestra pseudoumbilicus* in its lowermost 7 metres (samples 1-7; Table 1) plus *Ceratolithus acutus* in the overlying sediments (samples 8-12; Table 1). Reworking is weak. As there is no unconformity within the West Seddülbahir section, nannoflora evidences the continuous passage from Subzone NN12a to NN12b (Table 2), i.e. from the latest Messinian (after the peak of the MSC, as at the Kilitbahir seashore section) to the early Zanclean (Fig. 3). However, the Seddülbahir West section is discordant over the Seddülbahir East one.

The Intepe section (40°1'27" N latitude, 26°20'33" E longitude; Fig. 1C) (Gillet et al., 1978; Sakinç and Yaltrak, 2005) is about 77 m thick, of which we studied the 36 m thick central part (Figs. 4A, 4C). The studied section is made up of sands, clays, calcareous sandstones and thin limestones. It is topped by yellow sands and pebbly sandstones and a thick calcareous flagstone which constitutes a local reference surface. The section is rich in *Maetra* shells and displays also gastropod shells such as *Melanopsis*. In its middle part, the section displays a thin lignite (5 cm thick) (Gillet et al., 1978) overlain by a sand (2 cm thick) and a *Maetra coquina* (17 cm thick). Thirty five samples were studied: all of them provided a relatively well-preserved nannoflora (Fig. 5). From the biostratigraphic point of view, *Reticulofenestra rotaria* was found discontinuously up to sample 18, *Triquetrorhabdulus rugosus* continuously recorded from sample 1 to sample 31, *Ceratolithus acutus* from sample 24 to sample 35 (Table 3; Fig. 4C). Hence, the lower part of the studied section (samples 1-18) belongs to the beginning of the NN11b calcareous nannofossil Subzone according to the joint occurrence of *R. rotaria* and *T. rugosus*, while its upper part (i.e. from sample 24 where *C. acutus* appears) represents a large part of Subzone NN12b including the disappearance level of *T. rugosus* (Table 3; Fig. 4C). As a consequence, the interval between samples 18 and 24 belongs to the

continuing NN11b Subzone and maybe to NN12a Subzone for the uppermost layers just preceding sample 24 (Fig. 3). Distinction between Messinian and Zanclean can be placed around samples 23-24 according to the first appearance level of *Ceratolithus acutus*. If some changes in sea-level have been recorded in the section with respect to an impact of the MSC, they concern the layers immediately underlying the appearance of *C. acutus* (Fig. 4C). Our research focussed on the lignite corresponding to our sample 21 (Figs. 4C, 4D) as a first candidate because of its deposition under few centimetres of water. The lignite has an erosional contact with the overlying fine sand (Fig. 4E). But the expected gap in sedimentation is obvious in a lateral outcrop where the lignite is directly overlain on a long distance by reddish clays indicative of an emersion phase (Fig. 4F), because in present-day lignite quarries, lignites catch fire readily upon exposure, cooking the overlying clays, thus producing ‘porcellanite’ (Fig. 4G). This is the obvious signature of an emersion event that occurred just before the appearance of *C. acutus*. Accordingly, we may consider that (1) the lignite corresponds to the first step of the MSC (5.960-5.760 Ma; Fig. 3) characterized by a weak fall in sea-level (ca. 150 m), (2) the immediately overlying clays correlate with the sea-level rise separating the two steps of the MSC (5.76-5.60 Ma; Fig. 3), (3) the erosion of these clays or their cooking (when being partly preserved during the duration of exposure) signs the huge drop in sea-level (ca. 1,500 m) of the peak of the MSC (5.60-5.46 Ma; Fig. 3) (Clauzon et al., 1996).

About 34 m thick, the Yenimahalle section (39°57’51” N latitude, 26°17’46” E longitude; Fig. 1C), is mostly composed of sands, sandstones and limestones including some clayey intercalations. It was described by Çağatay et al. (2006) who included it into the Alçitepe and Truva formations. Palaeomagnetic measurements performed here by W. Krijgsman (Çağatay et al., 2006) revealed a continuous reverse signal and the section was assigned to Chron C3r, and more precisely to its Messinian part. However, the Yenimahalle section should be relatively younger than the Intepe section because it overlies an obvious morphological surface atop the Intepe section, an assumption also supported by the absence of any calcareous coccolith at Yenimahalle. *Ceratolithus acutus* is recorded without *Triquetrorhabdulus rugosus* in the upper part of the Intepe section (Fig. 4C) which could belong to the upper part of Chron C3r, and possibly Chron C3n.4n (see Fig. 3). As a consequence, the Yenimahalle section should be assigned at least to the next reverse chron, i.e. Chron C3n.3r.

The Truva section (39°57’30” N latitude, 26°14’47” E longitude; Fig. 1C), with a thickness of only 5 m, and composed of limestones and intercalated clays, tops the Truva Fm. No calcareous nannoplankton was found in the two studied samples.

The above results of this nannofossil biostratigraphic study allows us to date in detail several reference sections of the formations in NW Turkey and relate them precisely with respect to the events of the MSC.

3.2. Palaeoenvironmental reconstructions

3.2.1. Marine palaeoenvironments

3.2.1.1. Calcareous nannofossil fluctuations

For the nannofloral semi-quantitative analyses of the Intepe section, seven taxonomic groups were counted, as follows:

(1) The *Discoaster* group, generally inhabits the lower photic zone (Flores et al., 2005), it may occupy the same ecological niche as *Florisphaera profunda* which was found in tropical and subtropical waters in the modern ocean (Okada and McIntyre, 1977) or in Mediterranean sapropels (Negri et al., 1999; Castradori, 1998). The discoasterids are commonly related to the warm surface-waters (Backman and Pestiaux, 1987), although some discoasterids (such as *D. asymmetricus*, *D. tamalis* and *D. variabilis*) seem to be more related to cool waters, while *D. brouweri* is seen as a proxy of warm surface waters (Bukry, 1981; Raffi et al., 1998) during the Neogene. This group indicates oligotrophic conditions in the upper part of the photic zone (Chepstow-Lusty et al., 1989).

(2) The “small sized” reticulofenestrads (with the long axis <3 µm), are assumed to be indicative of hypereutrophic and schizohaline conditions (Wade and Bown, 2006, referring to *Reticulofenestra minuta*) presenting similar trend as the cold-water species *Coccolithus pelagicus* (Kouwenhoven et al., 2006). Negative correlation between the “small sized” and the “large-sized” reticulofenestrads was observed in the late Messinian of the Pissouri Basin (Cyprus).

(3) *Reticulofenestra pseudumbilicus* is a diagenetic resistant and long-ranging Neogene nannofossil. In the Western Mediterranean Late Messinian sequences, high abundance of *R. pseudumbilicus* is coeval with peaks in opal, diatoms and cold-eutrophic foraminifers, indicating generally high productivity and relatively cool conditions (Flores et al., 2005). Blooms of *R. pseudumbilicus* associated with increase in discoasterid relative abundance, identified in Early Miocene, are regarded as indicative of an oligotrophic setting and warm water surface conditions (Melinte, 2005).

(4) *Coccolithus pelagicus* lives today in the cold waters of the North Hemisphere (Ziveri et al., 2004) and is considered as a cold surface-water proxy (Raffi and Rio, 1981) indicating mesotrophic conditions (Flores et al., 2005). It was supposed that *C. pelagicus* changed its trophic preference along time. During the Early Tertiary and Miocene, it was a cosmopolitan coccolith, abundant in warm and cool surface waters (Bukry, 1981). Since the Late Neogene, *C. pelagicus* developed an affinity for cool waters, and could be used as a palaeotemperature proxy (Bukry, 1981; Raffi and Rio, 1981).

(5) *Sphenolithus abies* is more related to mesotrophic conditions and normal marine surface water (Wade and Bown, 2006). The sphenoliths seem to have shallower water preference (Perch-Nielsen, 1985). Some authors (Gibbs et al., 2004; Flores et al., 2005) assumed that the sphenoliths document oligotrophic warm surface waters.

(6) The calcareous dinoflagellate *Thoracosphaera* is a ‘disaster’ taxon which blooms under stressful marine conditions (i.e. just above the K/T boundary: Perch-Nielsen, 1985; Gardin, 2002). Its increased abundance was interpreted to reflect unusual environmental conditions, as high amount of CO₂, salinity decrease and probably pH fluctuation of the surface waters, accompanied by episodes of considerable warming (Hildebrand-Hubel et al., 1999; Lamolda et al., 2005). Because *Thoracosphaera* spp. is usually fragmented, we counted as one specimen either a whole coccosphere, or fragments which represented at least 3/4 of a coccosphere.

(7) *Braarudosphaera bigelowii*, the blooms of which indicate lowering salinity intervals (i.e. just above the Cretaceous/Tertiary boundary event: Lamolda et al., 2005; or in basal Oligocene deposits of the Central Paratethys area: Melinte, 2005). It is also assumed that this taxon prefers marginal seas (Cunha and Shimabukuro, 1997).

The lower 3.8 m of the section (samples 1-7) are characterized by a relative high diversity, the number of the identified taxa belonging from 19 to 25, the maximum of

diversity was observed at the base of this interval (Table 4). The nannofloral assemblages are dominated by *Coccolithus pelagicus* (~30%) accompanied by *Reticulofenestra pseudoumbilicus* and small sized reticulofenestrids, which make together up to 30%, *Discoaster* spp. and *Sphenolithus abies* are common (Fig. 5). Rare reworked Cretaceous and Palaeogene nannofossils are also present. Probably this represents the last Messinian interval where normal marine conditions prevailed in the studied area, most likely accompanied by a mesotrophic setting.

The next 2.50 m (samples 8-13) are characterized by a slow and continuous decline of the diversity, from 17 up to 13 taxa (Table 4). A substantial decrease of the taxa related to open marine conditions, such as the discoasterids and sphenoliths (which make together no more than 1%), was observed. The small sized reticulofenestrids show slow fluctuations (between 11-16%), while *Reticulofenestra pseudoumbilicus* has an ascending trend and reaches at the top of this interval 30%. *Coccolithus pelagicus* continuously decreases from 28% to 14%. Notably, *Braarudosphaera bigelowii* and *Thoracosphaera* have a more consistent frequency as in the older interval, the former up to 7%, and the latter up to 9%, indicating stressfully conditions in relation probably with the drop in salinity (Fig. 5). The reworked Cretaceous-Paleogene-Miocene taxa are common.

The paleoenvironmental deterioration is more pronounced in the next 4.0 m of the Intepe section, running from samples 14 to 21. The diversity decreases drastically (Table 4), from 14 to only 5 taxa at the top of the interval (sample 21). The sphenoliths and the discoasterids are vanished; the abundance of the small sized reticulofenestrids significantly decreases from 15% at the base of this interval below 2% towards the top, like *Coccolithus pelagicus* and *Reticulofenestra pseudoumbilicus*, which shift from 19% to 4% and 30% to 7%, respectively (Fig. 5). Notably, at the beginning of this interval, a significant increase of the calcareous dinoflagellate *Thoracosphaera* (with a peak at 21%) was observed. *Thoracosphaera* decreases at the top of this interval, up to 1%, and its lowermost abundance corresponds to the highest frequency of *Braarudosphaera bigelowii*, representing almost 60% of the total nannoflora. The significant decrease of *Thoracosphaera*, coincident with the *Braarudosphaera bigelowii* bloom, indicates an important decrease in salinity. The collapse of the calcareous nannofossil assemblage and the progressive decrease in salinity probably indicate the transition from less saline (brackish) environment to continental one, marked by a lignite layer (sample 21). Hence, we may assume that a brackish environment prevailed in the studied area just before the beginning of the MSC.

The next 2 m (samples 22-26) are characterized by a revitalization of the marine assemblages. The nannofloral diversity abruptly increases from 5 to 19 taxa at the base of this interval, and afterwards reaches the value of 23 (Table 4). Very few reworked taxa were encountered. *Braarudosphaera bigelowii* represents a minor component of the nannoflora and does not exceed 3% (Fig. 5). *Thoracosphaera*, after a peak at 15%, recorded at the base of this interval, drops to values below 5%. *Coccolithus pelagicus* increases more than twofold (from 5% to 11%), while *Reticulofenestra pseudoumbilicus* has a decreasing trend (from 16% to 10%). Discoasterids recover from 0.5% to 11%, as well as sphenoliths, which have a maximum of abundance (21%) at the top of this interval. Interestingly, the sphenolith maximum is synchronous with the maximum of the small-sized reticulofenestrids, which shift from 2% to 20%. All these data indicate reflooding by marine waters and progressive re-establishment of normal marine

conditions. Additionally, the high sphenolith frequency could be indicative for a mesotrophic setting.

The youngest 11 m (samples 27-35) of the studied succession are characterized by a moderate diversity (18-21 taxa), low fluctuation of *Reticulofenestra pseudoumbilicus* (between 11-15%), and higher fluctuation in abundance of the small-sized reticulofenestrids (from 16% to 24%). As in the subjacent interval, only few reworked nanofossils were observed. In this interval, as in the whole studied section, the small-sized reticulofenestrids could be negatively correlated with *Reticulofenestra pseudoumbilicus*. The single interval where no correlation could be evidenced between these two nanofloral groups is placed in the middle part of the Intepe section (i.e. the 2 m characterized by the calcareous nannoplankton collapse, samples 17-21; Fig. 5). The abundance of *Coccolithus pelagicus* slightly varies (between 11-16%). *Braarudosphaera bigelowii* and *Thoracosphaera* represent minor component of the assemblages. The former is between 0.5% and 5%, and almost vanished towards the topmost interval, while the latter is between 0.9-3%. The discoasterids increased throughout this interval, from 11% at the base up to 17% towards the top. The sphenolith abundance decreases from 24% at the base of this interval up to 16% towards the top. Taking into account the paleoceanographic significance of the discoasterids and sphenoliths (i.e., Castradori, 1998; Flores et al., 2005; Kouwenhoven et al., 2006) we may assume a progressive shift from mesotrophic to oligotrophic conditions towards the top of the Intepe section.

To summarize, three main ecostratigraphic intervals have been identified within the Intepe section (Fig. 5):

- interval 1 (samples 1-13) denoting almost normal marine conditions;
- interval 2 (samples 14-21) illustrative of a sea-level fall associated with a decrease in salinity (probably brackish conditions), and some emersion at its top;
- interval 3 (samples 22-35) indicating a return to almost normal marine conditions in spite of some deterioration in the uppermost layers.

3.2.1.2. Dinoflagellate cysts

The dinoflagellate cyst flora comprises only 13 taxa, to which can be added freshwater algae as *Pediastrum* and *Botryococcus* colonies that are interpreted as markers of freshwater input. Preservation of dinoflagellate cysts is poor to moderate. The dinoflagellate cyst assemblage is constituted by: (1) oceanic species and other neritic species as *Spiniferites mirabilis* and *S. membranaceus*, (2) marine autotrophic cosmopolitan species such as *Lingulodinium machaerophorum*, *Operculodinium centrocarpum* sensu Wall and Dale, *Spiniferites bentorii*, *S. bentorii* subsp. *truncates*, *S. hyperacanthus*, *S. ramosus*, *S. bulloideus*, *Spiniferites* spp., and (3) Paratethyan brackish species as *Galeacysta etrusca* and *Impagidinium globosum*. despite dinoflagellate cyst scarcity in the Intepe section, their assemblage distribution, completed by the relative frequency of freshwater algae documents palaeoenvironmental changes.

During the time-interval corresponding to samples 15-19, the dinoflagellate cyst flora was dominated by marine euryhaline species as *O. centrocarpum*, *L. machaerophorum*, *Spiniferites bulloideus*, *S. ramosus*, *S. bentorii*, *S. bentorii* subsp. *truncates*, *S. hyperacanthus*. The high relative abundance of *Spiniferites* spp. (more than 50 %), characterized by short processes, denotes the deterioration of marine conditions, in relation with a drop in salinity (Kokinos and Anderson, 1995; Hallett, 1999; Ellegaard, 2000; Sorrel et al., 2006; Popescu et al., 2008). We need to mention the presence of *S.*

mirabilis within sample 15 (one specimen), and that presence of the Paratethyan brackish dinoflagellate cysts *Galeacysta etrusca* in sample 17 (one specimen) and *Impagidinium globosum* in samples 17 and 19 (one specimen per sample). Morphology of *G. etrusca* denotes that this specimen belongs to the morphological group “C” (small endocyst / exocyst ratio) of Popescu et al. (2008). Its record in sample 17 (1) indicates that the age of this sediment is significantly older than the MSC and a fortiori than the formal “Lago Mare” event(s) (Clauzon et al., 2005), and (2) supports that no passage between the Aegean Sea and Eastern Paratethys existed through the Bosphorus Strait area before and after the Messinian Salinity Crisis, in agreement with the assumption of Clauzon et al. (2005), Popescu (2006) and Popescu et al. (2008).

Samples 20 to 23 are characterized by the absence of dinoflagellate cysts and a huge increase (acme) of *Pediastrum* that indicates a new change in the local environments marked now by fresh- to brackish-water conditions. Salinity at that time is probably less than 4.6 pps, according to minimum of salinity tolerance of *S. ramosus* (Marret and Zonneveld, 2003), identified as the most tolerant marine eurihaline species within the Intepe assemblage. This interpretation is consistent with the absence of calcareous nannoplankton and deposition of a lignite layer (sample 21) when shallow water and freshwater conditions prevailed. *Pediastrum* was also found in sample 24, with a high relative abundance indicating continuous fresh- to brackish-water conditions, sometimes interrupted by incursions of marine waters. Sample 25 is characterized by increase in diversity of marine dinoflagellate cysts and their relative abundance in opposition to a decrease of *Pediastrum*, that indicates increased salinity. Sample 26 is characterized by the absence of marine dinoflagellate cysts and increase of freshwater algae, that indicates the return of prevalent freshwater input.

According to the dinoflagellate cyst record, we may propose a more detailed evolution of the environmental conditions during the time-interval corresponding to samples 14-26, as summarized:

- from sample 14 to 19 (i.e. interval 2 of nannoflora; Fig. 5) the local environment was characterized by low saline conditions and evolved progressively to brackish ones at the top of the interval; this decrease in salinity of surface-waters caused unfavourable conditions for marine plankton;
- samples 20 to 23 indicate an huge input of freshwater resulting in brackish to freshwater conditions in the local environment, sometimes interrupted by some marine incursion revealed by the calcareous nannoplankton;
- samples 24 and 26 display the progressive increase in salinity in relation with the reflooding by marine waters and some freshwater inputs.

3.2.2. Continental palaeoenvironments

Sixteen samples from the Dardanelles Strait area provided pollen grains in sufficient quantity. They inform on the vegetation of the region just before and after the MSC. Herbs (Asteraceae, Poaceae, Amaranthaceae-Chenopodiaceae, Caryophyllaceae, *Artemisia*, etc.) predominated before the MSC (Burhanlı, Eceabat, Intepe *p.p.*) while trees were mostly composed of warm-temperate elements (*Quercus*, *Carya*, *Zelkova*, etc.) with few subtropical elements (Taxodiaceae, *Engelhardia*) (Fig. 6). After the MSC (Intepe *p.p.*, Seddülbahir), subtropical trees (with *Cathaya*) show larger percentages as *Pinus* and altitudinal trees (*Cedrus*, *Abies*, *Picea*) do (Fig. 6). Increase in disaccate pollen grains (*Pinus*, *Cedrus*, *Abies*, *Picea*) could indicate a more distal location of the upper part of

the Intepe section with respect to the palaeoshoreline, i.e. in relation with marine water invasion after the MSC. However, the larger representation of halophytes (Amaranthaceae-Chenopodiaceae) and freshwater plants (*Sparganium*, Alismataceae, *Potamogeton*) after the MSC points out nearby coastal environments.

As a consequence, we suggest that the increase in conifer pollen grains (*Cedrus* mainly, with *Abies* and *Picea*) could be significative of some relief uplift resulting in a larger representation of altitudinal conifers in coastal pollen records. Southward Intepe, the Kayaci Mount which is made of Eocene-Oligocene volcanic rocks does not bear evidence for uplift during the latest Miocene. *Cedrus* does not like silice-rich soils but prefers limestones, dolomites and flyschs (Quézel, 1998; Quézel and Médail, 2003) and the Kayaci relief, whatever its elevation, is not a likely source of *Cedrus* pollen grains. Armijo et al. (1999) suggested that the Ganos-Gelibolu Mountain, situated to the North of the Dardanelles and mostly constituted by Eocene-Oligocene flysch and volcanics, has been uplifted during the Messinian as a response to the propagation of the North Anatolian Fault (Fig. 1B). This relief appears to be a good candidate for the habitat of *Cedrus* forests as they exist today in southern Turkey (Quézel, 1998; Quézel and Médail, 2003). Uplift occurred during the late Messinian as significant percentages in *Cedrus* plus *Abies* and *Picea* were recorded at Intepe after the MSC (samples 22-26) at the difference of the older deposits (Burhanlı, Eceabat and Intepe samples 15-20) (Fig. 6). Reconstruction of the mean annual temperature by palaeoclimatic transfer function (Fauquette et al., 1998) in the coastal area using a selection of the pollen assemblage (altitudinal trees are not employed for this calculation) offers a possibility to estimate minimum palaeoaltitude of the nearby massif (Fauquette et al., 1999) as altitudinal elevation of conifer belts is narrowly linked to temperature and, as a consequence, to latitude of the massif (Ozenda, 1989). This estimate was done using the pollen record of Intepe after the MSC. The most probable mean annual temperature calculated for the Intepe samples 22-26 is 16.5°C (range: 15-18.5°C). This temperature is recorded today, in Turkey at low altitude, at around 38.5° of North latitude. We applied the method described by Fauquette et al. (1999) where the estimated palaeotemperatures are shifted into present-day latitudes. The obtained latitudes are projected onto the altitudinal elevation gradient of the *Abies-Picea* belt with respect to decreasing latitude (100 m in altitude per degree in latitude; Ozenda, 1989) and provide a range from 1,800 to 2,400 m for the minimum altitude of the Ganos Mountain with a most probable value at 2,000 m.

4. Discussion

The new bio- and ecostratigraphic data provide consistent information on the impact of the MSC in the Dardanelles which must be discussed in terms of palaeogeographic inferences and palaeoenvironments.

4.1. Palaeogeographic inferences

This study allows to date precisely some key-sections defining the regional stratigraphic framework, which was previously established by rather loose correlations of lithological units, using mollusc macrofossils which may have a large range of salinity tolerance and duration (Sakinç et al., 1999).

The most important outcome concerns the Alçitepe Fm. which is younger than the Messinian Salinity Crisis according to its two reference sections:

- at Seddülbahir, the Alçıtepe Fm. deposits (i.e. the Seddülbahir West section) are separated from the Kirazlı Fm. deposits (i.e. the Seddülbahir East section) by an unconformity which hence corresponds to the Messinian Erosional Surface (Figs. 7B, 7C);
- at Intepe, the Alçıtepe Fm. deposits conformably overlie those of the Kirazlı Fm., but we established that they were separated by a lack of sediments resulting from emersion and probably some erosion in relation with the peak of the MSC, this is what we called the Messinian discontinuity (Figs. 4, 7B).

In addition, the Eceabat section plus its uppermost part at Poyraztepe hill, which were conventionally attributed to the Alçıtepe Fm. on the basis of lithological similarities, have a late Messinian age and must belong to the Kirazlı Fm. (Figs. 3, 7B, 7D). Beds of the Eceabat and Poyraztepe sections are horizontal and culminate at altitude 143 m (Fig. 7D). Southward, between Eceabat and Kilitbahir (Fig. 7D), sediments younger than the MSC start from the seashore and relate to the early Zanclean up to the altitude 125 m where calcareous nannoplankton (*Triquetrorhabdulus rugosus* and *Ceratolithus acutus*) was recorded above the Kilitbahir castle (Figs. 3, 7B, 7D, 7G). As they are also almost horizontal and covered by the Alçıtepe calcareous flagstone, they are obviously nested within the Messinian succession of Eceabat-Poyraztepe from which they are separated by the Messinian Erosional Surface (Figs. 7B, 7D). The extremity of the Gelibolu Peninsula obviously corresponds to the sedimentary filling of a fluvial valley incised during the peak of the MSC (Fig. 7A), as suggested by Armijo et al. (1999). Many places in this area, such as at Nuriyamut (Figs. 7A, 7B), show thick early Zanclean sands with gravels with an organization in foreset beds dipping (25-30° at Nuriyamut) in the direction of the axis of the Messinian valley (Fig. 7F). Such a sedimentary organization is typical of a Gilbert-type fan delta which is the widespread feature of sediments within the Messinian canyons after the Mediterranean reflooding (Clauzon, 1990; Clauzon et al., 1990). Clayey deposits at Seddülbahir West and Kilitbahir seashore constitute the bottomset beds of the Dardanelles Gilbert-type fan delta more or less imbricated with coarser foreset beds (Fig. 7B). The calcareous topmost plateau of Alçıtepe constitutes the abandonment surface of the Gilbert-type fan delta.

On the southern coastline of the Dardanelles Strait, the horizontal sediments observed in the Intepe section are suddenly (300 m northward the section) replaced by sands and gravels organized in foreset beds dipping (25°) in direction of the Dardanelles Gilbert-type fan delta (Fig. 7E). The contact is obviously erosional as it has been precisely followed onland back to the Güzelyalı village (Fig. 7A). This Gilbert-type fan delta construction fills a canyon cut by a tributary of the main Dardanelles fluvial drain during the peak of the MSC (Figs. 7A, 7B). Here, the Messinian Erosional Surface incises deposits of the Kirazlı Fm. and laterally evolves into a discontinuity in an interfluvial context (Intepe section) as drawn on Figure 7B.

Accordingly, the impact of the MSC is obvious in the region and must henceforth be considered in the stratigraphic setting and palaeogeographic reconstructions. The gap in sedimentation because of erosion (Dardanelles and tributary Messinian canyons) or non-deposition (Intepe) is chronostratigraphically located in the extremely latest Messinian, i.e. during the peak of the MSC, and not in the Zanclean as repeatedly assumed as by Sakıncı et al. (1999) and Sakıncı and Yaltrak (2005). Nesting of post-MSD deposits within the pre-MSD ones must allow to distinguish the Alçıtepe Fm. from the Kirazlı Fm. without using the often misleading facies characteristics.

In the Gulf of Saros, nesting of the post-MSC sediments within the older ones is not very pronounced, probably because of a relatively weak fluvial activity. The most intense fluvial activity during the MSC located in the Dardanelles Strait area and rapidly diminished when passing to an interfluvial context, as supported by the palaeoenvironmental data.

In spite of its reverse palaeomagnetic signal and the record of Paratethyan organisms, the Yenimahalle section cannot be considered as representative of the MSC in the region. Clearly overlying the topmost flagstone of Intepe, which has a similar significance as the abandonment surface of the Dardanelles Gilbert-type fan delta, the Yenimahalle section has a younger Zanclean age and represents the end of the Pliocene sedimentation in the region (Fig. 7B).

4.2. Palaeoenvironments

The present-day southern shoreline of the Dardanelles Strait is a key-area because of the proximity of distinct environments during the peak of the MSC (a fluvial canyon and an interfluvial domain) and after it (a subaquatic delta system and a coastal domain). Such a coexistence is somewhat normal but the accuracy of its record over a short distance is infrequent. At Intepe, the local environment fluctuated between marine and almost freshwater conditions in relation with moderate to intense fluvial freshwater inputs. Blooms of *Thoracosphaera* are situated at the base and towards the top of the interval characterized by the calcareous nannoplankton collapse (Fig. 5). Such blooms may reflect unstable marine conditions, associated with a high nutrient input and the lack of other marine planktonic competitors. Bloom of *Braarudosphaera bigelowii* at the top of the Messinian layers at Intepe is probably a local event relating to the palaeogeographic context. As they are more sensitive to environmental changes than the nannoplankton, dinoflagellate cysts require that the Intepe locality was very close to the paleoshoreline. A bay head (Fig. 7A) seems to be the probable palaeogeography before and after the MSC while the varying freshwater inputs depended from the nearby river. Such a relatively isolated context was significantly impacted by the successive fluctuations in Mediterranean sea-level and the resulting steps of the MSC (Clauzon et al., 1996). The moderate sea-level fall of the first step of the MSC is marked by the lignite and some development of marsh conditions (5.96-5.76 Ma; Fig. 3). The following sea-level rise is indicated by the overlying clays (5.76-5.60 Ma; Fig. 3), mostly eroded or cooked during the episode of emersion corresponding to the huge sea-level drop of the peak of the MSC during which the nearby fluvial canyon was cut (5.60-5.46 Ma). Climatic conditions are warm and relatively dry out of the riverbanks as supported by the large percentages of herb pollen grains. Some relief uplifted during the MSC, which supports the idea of creation of important relief in the Ganos-Gelibolu Massif.

According to these results, the generally suggested gateway between the Black Sea (i.e. the Eastern Paratethys) and Aegean Sea through the Marmara realm during the MSC (Görür et al., 1997; Çağatay et al., 2006) cannot be perpetuated. Indeed, a connection between these domains is incompatible with a coeval subaerial erosion both on the Black Sea side (Gillet et al., 2007) and the Dardanelles area (this work) during the peak of the MSC. Connection would have been only possible during times of high sea level, i.e. before and after the peak of the MSC (Clauzon et al., 2005) or before its first step. However, the extreme scarcity of Paratethyan dinoflagellate cysts in the Intepe sediments does not support such a connection, as they are representative of surface waters. For the

same reason, a one-way passage resulting in influx of Paratethyan organisms only into the Mediterranean realm (see discussion in: CIESM, 2008) is questionable. The almost continuous presence of the Paratethyan bivalves and ostracods before and after the MSC in the region (Çağatay et al., 2006) needs to be explained. It has been suggested that their arrival was caused by an episode of high sea-level just before the peak of the MSC (Clauzon et al., 2005; Popescu et al., 2008) and that their persistence was favoured in some relatively isolated environments (lagoons, bays) at the frontier between marine, brackish and freshwater conditions (Çağatay et al., 2006). Testing the scarcity or absence of Paratethyan dinoflagellate cysts, which should be the first immigrants, appears to be an appropriate diagnosis.

5. Conclusion

The chronological constraints presented in this work provide a sound background for new prospects on the late Miocene – Pliocene stratigraphy and palaeogeography in the Dardanelles region. Evidence of the strong impact of the MSC in the region, as elsewhere around the Mediterranean, indicates that the Dardanelles Strait was a fluvial collector eroding the older rocks during the peak of the MSC. Systematic use of calcareous nannoplankton results in a clarified regional stratigraphy, unbiased by lithological similarities and where the peak of the MSC may be used as a robust chronological reference. The study in progress aims at reconstructing the Messinian fluvial network in the Marmara region and deciphering the role of the MSC on the North Anatolian Fault propagation across the region. At last, the Dardanelles-Marmara region is to be discarded as a connection between the Eastern Paratethys and Mediterranean Sea during the Messinian Salinity Crisis.

Acknowledgements

This research started within the frame of the CNRS-INSU ECLIPSE II Programme and was mostly developed thanks to the ANR EGEO Project. One of us (D. Biltekin) was granted by the French Embassy in Turkey for her PhD thesis.

This paper is the contribution UMR 5125-08- **, and ISEM contribution n°200*-**.

References

- Agusti, J., Oms, O., Meulenkamp, J.E., 2006. Introduction to the Late Miocene to Early Pliocene environment and climate change in the Mediterranean area. *Palaeogeography, Palaeoclimatology, Palaeoecology*, 238, 1–4.
- Armijo, R., Meyer, B., Hubert, A., Barka, A., 1999. Westward propagation of the North Anatolian fault into the northern Aegean: Timing and kinematics. *Geology*, 27, 267–270.
- Armijo, R., Meyer, B., Hubert, A., Barka, A., 2000. Westward propagation of North Anatolian fault into the northern Aegean: Timing and kinematics: Reply. *Geology*, 28, 188–189.
- Backman, J., Pestiaux, P., 1987. Pliocene Discoaster abundance variations, Deep Sea Drilling Project Site 606: biochronology and paleoenvironmental implications. Initial Reports of the Deep Sea Drilling Project 94, 903–910.
- Backman, J., Raffi, I., 1997. Calibration of Miocene nannofossil events to orbitally tuned cyclostratigraphies from Ceara Rise. *Proceedings of the Ocean Drilling Program. Scientific Results* 154, 83–89.
- Bukry, D., 1981. Pacific coast coccolith stratigraphy between Point Conception and Cabo Corrientes. Initial Reports of the Deep Sea Drilling Project 63, 445–471.
- Çağatay, N.M., Görür, N., Alpar, B., Saatçılar, R., Akkök, R., Sakıncı, M., Yüce, H., Yaltrak, C., Kuşçu, İ., 1998. Geological evolution of the Gulf of Saros, NE Aegean Sea. *Geo Marine Letter* 18, 1–9.
- Çağatay, N.M., Görür, N., Flecker, R., Sakıncı, M., Tünoğlu, C., Ellam, R., Krijgsman, W., Vincent, S., Dikbaş, A., 2006. Paratethyan–Mediterranean connectivity in the Sea of Marmara region (NW Turkey) during the Messinian. *Sedimentary Geology* 188–189, 171–187.
- Castradori, D., 1998. Calcareous nannofossils in the basal Zanclean of the Eastern Mediterranean Sea: remarks on paleoceanography and sapropel formation. *Proceedings of the Ocean Drilling Program, Scientific Results* 160, 113–123.
- Chepstow-Lusty, A., Backman, J., Shackleton, N.J., 1989. Comparison of upper Pliocene Discoaster abundance variations from North Atlantic Sites 552, 607, 658, 659 and 662: further evidence for marine plankton responding to orbital forcing. *Proceedings of the Ocean Drilling Program. Scientific Results* 108, 121–141.
- Chumakov, I.S., 1973. Geological history of the Mediterranean at the end of the Miocene – the beginning of the Pliocene according to new data. Initial Reports of the Deep Sea Drilling Project, 13, 2, 1241–1242.
- CIESM¹, 2008. Executive Summary. In: *The Messinian Salinity Crisis from mega-deposits to microbiology – A consensus report* (Briand, F., ed.), CIESM Workshop Monographs, 33, 7–28.
- Cita, M.B., Gartner, S., 1973. Studi sul Pliocene e sugli strati al passaggio dal Miocene al Pliocene, IV. The stratotype Zanclean foraminiferal and nannofossil biostratigraphy. *Rivista Italiana di Paleontologia e Stratigrafia* 79, 503–558.
- Cita, M.B., Ryan, W.B.F., Kidd, R.B., 1978. Sedimentation rates in Neogene deep sea sediments from the Mediterranean and geodynamic implications of their changes. Initial Reports of the Deep Sea Drilling Project 42A, 991–1002.

¹ Roveri, M., Krijgsman, W., Suc, J.-P., Lugli, S., Lofi, J., Sierro, F.J., Manzi, V., Flecker, R., and others.

- Clauzon, G., 1973. The eustatic hypothesis and the pre-Pliocene cutting of the Rhône Valley. Initial Reports of the Deep Sea Drilling Project 13, 2, 1251–1256.
- Clauzon, G., 1978. The Messinian Var canyon (Provence, Southern France) – Paleogeographic implications. *Marine Geology*, 27, 231–246.
- Clauzon, G., 1980a. Le canyon messinien de la Durance (Provence, France): une preuve paléogéographique du bassin profond de dessiccation. *Palaeogeography, Palaeoclimatology, Palaeoecology*, 29, 15–40.
- Clauzon, G., 1980b. Révision de l'interprétation géodynamique du passage Miocène-Pliocène dans le bassin de Vera (Espagne méridionale): les coupes d'Antas et de Cuevas del Almanzora. *Rivista Italiana di Paleontologia*, 86, 1, 203–214.
- Clauzon, G., 1982. Le canyon messinien du Rhône: une preuve décisive du “desiccated deep-basin model” (Hsü, Cita et Ryan, 1973). *Bulletin de la Société Géologique de France*, ser. 7, 24, 3, 597–610.
- Clauzon, G., 1990. Restitution de l'évolution géodynamique néogène du bassin du Roussillon et de l'unité adjacente des Corbières d'après les données écostratigraphiques et paléogéographiques. *Paléobiologie continentale*, 17, 125–155.
- Clauzon, G., 1999. L'impact des variations eustatiques du bassin de Méditerranée occidentale sur l'orogène alpin depuis 20 Ma. *Etudes de Géographie Physique* 28, 1–8.
- Clauzon, G., Suc, J.-P., Aguilar, J.-P., Ambert, P., Cappetta, H., Cravatte, J., Drivaliari, A., Doménech, R., Dubar, M., Leroy, S., Martinell, J., Michaux, J., Roiron, P., Rubino, J.-L., Savoye, B., Vernet, J.-L., 1990. Pliocene geodynamic and climatic evolutions in the French Mediterranean region. *Paleontologia i Evolucio*, Mém. spéc., 2, 132–186.
- Clauzon, G., Suc, J.-P., Gautier, F., Berger, A., Loutre, M.-F., 1996. Alternate interpretation of the Messinian salinity crisis: controversy resolved? *Geology* 24, 363–366.
- Clauzon, G., Suc, J.-P., Popescu, S.-M., Mărunțeanu, M., Rubino, J.-L., Marinescu, F., Melinte, M.C., 2005. Influence of the Mediterranean sea-level changes over the Dacic Basin (Eastern Paratethys) in the Late Neogene. The Mediterranean Lago Mare facies deciphered. *Basin Research* 17, 437–462.
- Cornée, J.-J., Ferrandini, M., Saint Martin, J.-P., Münch, Ph., Moullade, M., Ribaud-Laurenti, A., Roger, S., Saint Martin, S., Ferrandini, J., 2006. The late Messinian erosional surface and the subsequent reflooding in the Mediterranean: New insights from the Melilla–Nador basin (Morocco). *Palaeogeography, Palaeoclimatology, Palaeoecology*, 230, 1-2, 129–154.
- Cour, P., 1974. Nouvelles techniques de détection des flux et de retombées polliniques: étude de la sédimentation des pollens et des spores à la surface du sol. *Pollen et Spores*, 16, 1, 103–141.
- Cunha, A.S., Shimabukuro, S., 1997. *Braarudosphaera* blooms and anomalous enrichments of *Nannoconus*: evidence from the Turonian south Atlantic, Santos basin, Brazil. *Journal of Nanoplankton Research* 19, 51–55.
- Delrieu, B., Rouchy, J.M., Foucault, A., 1993. La surface d'érosion finimessinienne en Crète centrale (Grèce) et sur le pourtour méditerranéen: Rapport avec la crise de salinité méditerranéenne. *Comptes-Rendus de l'Académie des Sciences de Paris*, ser. 2, 318, 1103–1109.
- Dewey, J.F., Şengör, A.M.C., 1979. Aegean and surrounding regions, complex multiplate and continuum tectonics in a convergent zone. *Bulletin of Geological Society of America* 90, 84–92.

- Di Stefano, E., Sprovieri, R., Scarantino, S., 1996. Chronology of biostratigraphic events at the base of the Pliocene. *Palaeopelagos* 6, 401–414.
- El Euch – El Koundi, N., Ferry, S., Suc, J.-P., Clauzon, G., Melinte-Dobrinescu, M.C., Gorini, C., Safra, A., El Koundi, M., Zargouni, F., accepted. Messinian deposits and erosion in Northern Tunisia: Inferences on Strait of Sicily Turing the Messinian Salinity Crisis. *Terra Nova*.
- Ellegaard, M., 2000. Variations in dinoflagellate cyst morphology under conditions of changing salinity during the last 2000 years in the Limfjord, Denmark. *Review of Palaeobotany and Palynology*, 109, 65–81.
- Esu, D., 2007. Latest Messinian “Lago-Mare” Lymnocardiinae from Italy: Close relations with the Pontian fauna from the Dacic Basin. *Geobios*, 40, 291–302.
- Faranda, C., Gliozzi, E., Ligios, S., 2007. Late Miocene brackish Loxoconchidae (Crustacea, Ostracoda) from Italy. *Geobios*, 40, 303–324.
- Fauquette, S., Guiot, J., Suc, J.-P., 1998. A method for climatic reconstruction of the Mediterranean Pliocene using pollen data. *Palaeogeography, Palaeoclimatology, Palaeoecology*, 144, 183–201.
- Fauquette, S., Clauzon, G., Suc, J.-P., Zheng, Z., 1999. A new approach for paleoaltitude estimates based on pollen records: example of the Mercantour Massif (southeastern France) at the earliest Pliocene. *Earth and Planetary Science Letters*, 170, 35–47.
- Fornaciari, E., Di Stefano, A., Rio, D., and Negri, A., 1996. Middle Miocene quantitative calcareous nanofossil biostratigraphy in the Mediterranean region. *Micropaleontology* 42, 37–63.
- Flores, J.A., Sierro, F.J., Filippelli, G.M., Bárcena, M.A., Pérez-Folgadoa, M., Vázquez, A., Utrilla, R., 2005. Surface water dynamics and phytoplankton communities during deposition of cyclic late Messinian sapropel sequences in the western Mediterranean. *Marine Micropaleontology* 56, 50–79.
- Gardin, S., 2002. Late Maastrichtian to early Danian calcareous nanofossil at Élles (Northwest Tunisia). A tale of one million years across the K-T Boundary. *Palaeogeography, Palaeoclimatology, Palaeoecology* 178, 211–231.
- Gautier, F., Clauzon, G., Suc, J.-P., Cravatte, J., Violanti, D., 1994. Age et durée de la crise de salinité messinienne. *Comptes-Rendus de l’Académie des Sciences de Paris*, ser. 2, 318, 1103–1109.
- Gibbs, S.J., Shackleton, N.J., Young, J.R., 2004. Orbitally-forced climate signals in mid Pliocene nanofossil assemblages. *Marine Micropaleontology* 51, 39–56.
- Gillet, H., Lericolais, G., Réhault, J.-P., 2007. Messinian event in the black sea: Evidence of a Messinian erosional surface. *Marine Geology*, 244, 142–165.
- Gillet, S., Gramann, F., Steffens, P., 1978. Neue biostratigraphische Ergebnisse aus dem brackischen Neogen an Dardanellen und Marmara-Meer (Türkei). *Newsletters of Stratigraphy* 7, 53–64.
- Gliozzi, E., Ceci, M.A., Grossi, F., Ligios, S., 2007. Paratethyan Ostracods immigrants in Italy during the Late Miocene. *Geobios*, 40, 325–337.
- Göktaşan, E., Ergin, M., Özyalvaç, M., Sur, H.I., Tur, H., Görüm, T., Ustraömer, T., Batuk, F.G., Alp, H., Birkan, H., Türker, A., Gezgin, E., Özturan, M., 2008. Factors controlling the morphological evolution of the Çanakkale Strait (Dardanelles, Turkey). *Geo-Marine Letters*, 28, 107–129.
- Görür, L., Çağatay, M.N., Sakıncı, M., Tchapylyga, A., Akkök, R., Natalin, B., 2000. Neogene Paratethyan succession in Turkey and its implications for paleogeographic

- evolution of the Eastern Paratethys. In: Bozkurt, E., Winchester, J.A., Piper, J.A.D. (Eds.), *Tectonics and Magmatism in Turkey and Surrounding Area*. Geological Society of London Special Publication 173, pp. 251–269.
- Görür, L., Çağatay, Sakıncı, M., Sumengen, M., Senturk, K., Yaltırak, C., Tchapylyga, A., 1997. Origin of the Sea of Marmara deduced from Neogene to Quaternary paleogeographic evolution of its frame. *International Geological Review* 39, 342–352.
- Guennoc, P., Gorini, C., Mauffret, A., 2000. Histoire géologique du Golfe du Lion et cartographie du rift oligo-aquitainien et de la surface messinienne. *Géologie de la France*, 3, 67–97.
- Hallett, R.I., 1999. Consequences of environmental change on the growth and morphology of *Lingulodinium polyedrum* (Dinophyceae) in culture. Thesis, Westminster Univ. London, 109 pp.
- Hildebrand-Hubel, T., Williems, H., Versteegh, G.J.M., 1999. Variations in calcareous dinoflagellate associations from the Maastrichtian to Middle Eocene of the western South Atlantic Ocean (São Paulo Plateau, DSDP Leg 39, Site 356). *Review of Palaeobotany and Palynology* 106, 57–87.
- Hsü, K.J., Cita, M.B., Ryan, W.B.F., 1973. The origin of the Mediterranean evaporites. *Initial Reports of the Deep Sea Drilling Project* 42, 1203–1231.
- Kokinos, J.P., Anderson, D.M., 1995. Morphological development of resting cysts in cultures of the marine dinoflagellate *Lingulodinium polyedrum* (= *L. machaerophorum*). *Palynology*, 19, 143–166.
- Kouwenhoven T.J., Morigi C., Negri A., Giunta S., Krijgsman W., Rouchy J.-M., 2006. Paleoenvironmental evolution of the eastern Mediterranean during the Messinian: Constraints from integrated microfossil data of the Pissouri Basin (Cyprus). *Marine Micropaleontology* 60, 17–44.
- Lamolda, M.A., Melinte, M.C., Kaiho, K., 2005. Nannofloral extinction and survivorship across the K/T boundary at Caravaca, southeastern Spain. *Palaeogeography, Palaeoclimatology, Palaeoecology* 224, 27–52.
- Lofi, J., Rabineau, M., Gorini, C., Berné, S., Clauzon, G., De Clarens, P., Dos Reis, T., Mountain, G.S., Ryan, W.B.F., Steckler, M., Fouchet, C., 2003. Plio-Quaternary prograding clinoform wedges of the Western Gulf of Lions continental margin (NW Mediterranean) after the Messinian Salinity Crisis. *Marine Geology*, 198, 289–317.
- Lofi, J., Gorini, C., Berné, S., Clauzon, G., Dos Reis, A.T., Ryan, W.B.F., Steckler, M.S., 2005. Erosional processes and paleo-environmental changes in the western gulf of Lion (SW France) during the Messinian salinity crisis. *Marine Geology*, 217, 1–30.
- Lourens, L.J., Hilgen, F.J., Laskar, J., Shackleton, N.J., Wilson, D., 2004. The Neogene period. In: Gradstein, F.M., Ogg, J.G., Smith, A.G. (Eds.), *A geological Time Scale 2004*. Cambridge University Press, Cambridge, pp. 409–440.
- Maillard, A., Mauffret, A., 2006. Relationship between erosion surfaces and Late Miocene Salinity Crisis deposits in the Valencia Basin (northwestern Mediterranean): evidence for an early sea-level fall. *Terra Nova*, 18, 321–329.
- Marinescu, F., 1992. Les bioprovinces de la Paratéthys et leurs relations. *Paleontologia i Evolució*, 24–25, 445–453.
- Marret, F., Zonneveld, K.A.F., 2003. Atlas of modern organic-walled dinoflagellate cyst distribution. *Review of Palaeobotany and Palynology*, 125, 1–200.

- Martini, E., 1971. Standard Tertiary and Quaternary calcareous nannoplankton zonation, In: Farinacci, A. (Ed.), Proceedings of the 2nd International Conference on Planktonic Microfossils, Roma 1970, 2, editura Tecnoscienza, Rome, pp. 739–785.
- Mărunțeanu, M., Papaianopol, I., 1995. The connection between the Dacic and Mediterranean Basins based on calcareous nannoplankton assemblages. *Romanian Journal of Stratigraphy* 76, 169–170.
- Melinte M.C., 2005. Oligocene palaeoenvironmental changes in the Romanian Carpathians, revealed by calcareous nannofossil fluctuation. In: Tyszka, J., Oliwkiewicz-Miklasinska, M., Gedl, P., and Kaminski, M.A. (Eds.), *Methods and Application in Micropalaeontology*. *Studia Geologica Polonica* 124, 15–27.
- Melinte, M.C., 2006. Cretaceous-Cenozoic paleobiogeography of the southern Romanian Black Sea onshore and offshore areas. *Geo-Eco-Marina* 12, 79–90.
- Negri, A., Giunta, S., Hilgen, F.J., Krijgsman, W., Vai, G.B., 1999. Calcareous nannofossil biostratigraphy of the M. del Casino section (northern Apennines, Italy) and paleoceanographic conditions at times of late Miocene sapropel formation. *Marine Micropaleontology* 36, 13–30.
- Okada, H., McIntyre, A., 1977. Modern coccolithophores of the Pacific and North Atlantic Oceans. *Micropaleontology* 23, 1–55.
- Okada, H., Bukry, D., 1980. Supplementary modification and introduction of code numbers to the low-latitude coccolith biostratigraphic zonation (Bukry, 1973; 1975). *Marine Micropaleontology* 5, 321–325.
- Ozenda, P., 1989. Le déplacement vertical des étages de végétation en fonction de la latitude: un modèle simple et ses limites. *Bulletin de la Société Géologique de France*, ser. 8, 5, 83, 535–540.
- Parke, J.R., Minshull, T.A., Anderson, G., White, R.S., McKenzie, D., Kuşçu, I., Bull, J.M., Görür, N., Şengör, C., 1999. Active faults in the Sea of Marmara, western Turkey, imaged by seismic reflection profiles. *Terra Nova*, 11, 223–227.
- Perch-Nielsen, K., 1985. Cenozoic calcareous nannofossils. In: Bolli, H.M., Saunders, J.B., Perch-Nielsen, K. (Eds.), *Plankton Stratigraphy*, Cambridge University Press, Cambridge, pp. 427–554.
- Poisson, A., Wernli, R., Sağular, E.K., Temiz, H., 2003. New data concerning the age of the Aksu Thrust in the south of the Aksu valley, Isparta Angle (SW Turkey): consequences for the Antalya Basin and the Eastern Mediterranean. *Geological Journal*, 38, 311–327.
- Popescu, S.-M., 2006. Upper Miocene and Lower Pliocene environments in the southwestern Black Sea region from high-resolution palynology of DSDP site 380A (Leg 42B). *Palaeogeography, Palaeoclimatology, Palaeoecology* 238, 64–77.
- Popescu, S.-M., Suc, J.-P., Melinte, M., Clauzon, G., Quillévéré, F., Sütő-Szentai, M., 2007. Earliest Zanclean age for the Colombacci and uppermost Di Tetto formations of the “latest Messinian” northern Apennines: New palaeoenvironmental data from the Maccarone section (Marche Province, Italy). *Geobios*, 40, 3, 359–373.
- Popescu, S.-M., Dalesme, F., Jouannic, G., Escarguel, G., Head, M.J., Melinte-Dobrinescu, M.C., Sütő-Szentai, M., Bakrac, K., Clauzon, G., Suc, J.-P., 2008. *Galeacysta etrusca* complex, dinoflagellate cyst marker of Paratethyan influxes into the Mediterranean Sea before and after the peak of the Messinian Salinity Crisis. *Palynology*.

- Popov, S.V., Neveeskaya, L.A., 2000. Late Miocene brackish water mollusks and the history of the Aegean basin. *Stratigraphy and Geological Correlation* 8 (2), 195–205.
- Quézel, P., 1998. Cèdres et cédraies du pourtour méditerranéen: signification bioclimatique et phytogéographique. *Forêt méditerranéenne* 19 (3), 243–260.
- Quézel, P., Médail, F., 2003. *Ecologie et biogéographie des forêts du bassin méditerranéen*. Elsevier, Paris, 570 pp.
- Raffi, I., Rio, D., 1979. Calcareous nannofossil biostratigraphy of DSDP Site 132, Leg 13 (Tyrrhenian Sea, Western Mediterranean). *Rivista Italiana di Paleontologia e Stratigrafia* 85, 127–172.
- Raffi I., Rio, D., 1981. *Coccolithus pelagicus* (Wallich): a paleotemperature indicator in the late Pliocene Mediterranean deep sea record. In: Wezel F.C. (Ed.), *Sedimentary Basins of Mediterranean Margins*, Pitagora, Bologna, pp. 187–190.
- Raffi, I., Backman, J., Rio, D., 1998. Evolutionary trends of tropical calcareous nannofossils in the Late Neogene. *Marine Micropaleontology* 35, 17–41.
- Raffi, I., Backman, J., Fornaciari, E., Pälike, H., Rio, D., Lourens, L., Hilgen, F., 2006. A review of calcareous nannofossil astrobiochronology encompassing the past 25 million years. *Quaternary Science Review*, 25, 3113–3137.
- Rio, D., Fornaciari, E., Raffi, I., 1990. Late Oligocene through early Pleistocene calcareous nannofossils from western equatorial Indian Ocean. *Proceedings of the Ocean Drilling Programme. Scientific Results*, 115, 175–235.
- Raffi, I., Mozzato, C., Fornaciari, E., Hilgen, F.J., Rio, D., 2003. Late Miocene calcareous nannofossil biostratigraphy and astrobiochronology for the Mediterranean region. *Micropaleontology*, 49, 1, 1–26.
- Rögl, F., 1998. Palaeogeographic considerations for Mediterranean and Paratethys seaways (Oligocene to Miocene). *Annalen des naturhistorischen Museums in Wien* 99(A), 279–310.
- Rouchy, J.-M., Suc, J.-P., Ferrandini, J., Ferrandini, M., 2006. The Messinian Salinity Crisis revisited. *Sedimentary Geology*, 188–189, 1–8.
- Sage, F., Von Gronefeld, G., Déverchère, J., Gaullier, V., Mailalrd, A., Gorini, C., 2005. Seismic evidence for Messinian detrital deposits at the western Sardinia margin, northwestern Mediterranean. *Marine and Petroleum Geology*, 22, 757–773.
- Sakinç, M., Yaltrak, C., Oktay, F.Y., 1999. Palaeogeographical evolution of the Thrace Neogene Basin and the Tethys–Paratethys relations at northwestern Turkey (Thrace). *Palaeogeography, Palaeoclimatology, Palaeoecology*, 153, 17–40.
- Sakinç, M., Yaltrak, C., 2005. Messinian crisis: What happened around the northeastern Aegean? *Marine Geology* 221, 423–436.
- Seneš, J., 1973. Correlation hypotheses of the Neogene Tethys and Paratethys. *Giornale di Geologia* 39, 271–286.
- Snel E., Mărunțeanu M., Meulenkamp J.E., 2006. Calcareous nannofossil biostratigraphy and magnetostratigraphy of the Upper Miocene and Lower Pliocene of the Northern Aegean (Orphanic Gulf-Strimon Basin areas), Greece. *Palaeogeography, Palaeoclimatology, Palaeoecology* 238, 107–124.
- Sorrel, P., Popescu, S.-M., Head, M.J., Suc, J.-P., Klotz, S., Oberhänsli, H., 2006. Hydrographic development of the Aral Sea during the last 2000 years based on a quantitative analysis of dinoflagellate cysts. *Palaeogeography, Palaeoclimatology, Palaeoecology*, 234, 304–327.

- Sprovieri, M., Bellanca, A., Neri, R., Mazzola, S., Bonanno, A., Patti, B., Sorgente, R., 1999. Astronomical calibration of late Miocene stratigraphic events and analysis of precessionally driven paleoceanographic changes in the Mediterranean basin. *Memorie della Società Geologica Italiana* 54, 7–24.
- Sprovieri, M., Sacchi, M., Rohling, E.J., 2003. Climatically influenced interactions between the Mediterranean and the Paratethys during the Tortonian. *Paleoceanography*, 18, 2, 12-1–12-10.
- Stoica, M., Lazaçr, I., Vasiliev, I., Krijgsman, W., 2007. Mollusc assemblages of the Pontian and Dacian deposits from the Topolog-Arges area (southern Carpathian foredeep – Romania). *Geobios*, 40, 391–405.
- Suc, J.-P., Rouchy, J.M., Ferrandini, M., Ferrandini, J., 2007. Editorial. The Messinian Salinity Crisis revisited. *Geobios*, 40, 3, 231–232.
- Taner, G., 1979. Die Molluskenfauna der Neogenen Formationen der Halbinsel – Gelibolu. *Annales Géologiques des Pays Helléniques*, out of series, 3, 1189–1194.
- Ternek, Z., 1964. Geological map of Turkey at 1/500.000: Istanbul. Maden Tetkik ve Arama Enstitüsü Hazırlamış ve Yayınlamıştır, Ankara.
- Türkecan, A., Yurtsever, A., 2002. Geological map of Turkey at 1/500.000: Istanbul. Maden Tetkik ve Arama Genel Müdürlüğü, Ankara.
- Ustaömer, T., Gökaşan, E., Tur, H., Görüm, T., Batuk, F.G., Kalafat, D., Alp, H., Ecevitoglu, B., Birkan, H., 2008. Faulting, mass-wasting and deposition in an active dextral shear zone, the Gulf of Saros and the NE Aegean Sea, NW Turkey. *Geo-Marine Letters*, 28, 171–193.
- Van Couvering, J.A., Castradori, D., Cita, M.B., Hilgen, F.J., Rio, D., 2000. The base of the Zanclean Stage and of the Pliocene Series. *Episodes*, 23, 3, 179–187.
- Wade, B.S., Bown, P.R., 2006. Calcareous nannofossils in extreme environments: The Messinian Salinity Crisis, Polemi Basin, Cyprus. *Palaeogeography, Palaeoclimatology, Palaeoecology* 233, 271–286.
- Yaltırak, C., Sakıncı, M., Oktay, F.Y., 2000. Westward propagation of North Anatolian fault into the northern Aegean: Timing and kinematics: Comment. *Geology*, 28, 187–188.
- Young, J.R., 1998. Chapter 9: Neogene. In: Bown, P.R. (Ed.), *Calcareous Nannofossils Biostratigraphy*. British Micropaleontological Society Publications Series, Kluwer Academic Press, Dordrecht, pp. 225–265.
- Ziveri P., Baumann, K.-H., Böckel, B., Bollmann, J., Young, J.R., 2004. Present day coccolithophore biogeography of the Atlantic Ocean. In: Thierstein H.R., Young J.R., (Eds.), *Coccolithophores-From Molecular Processes to Global Impact*. Springer-Verlag, pp. 529–562.

Figure captions

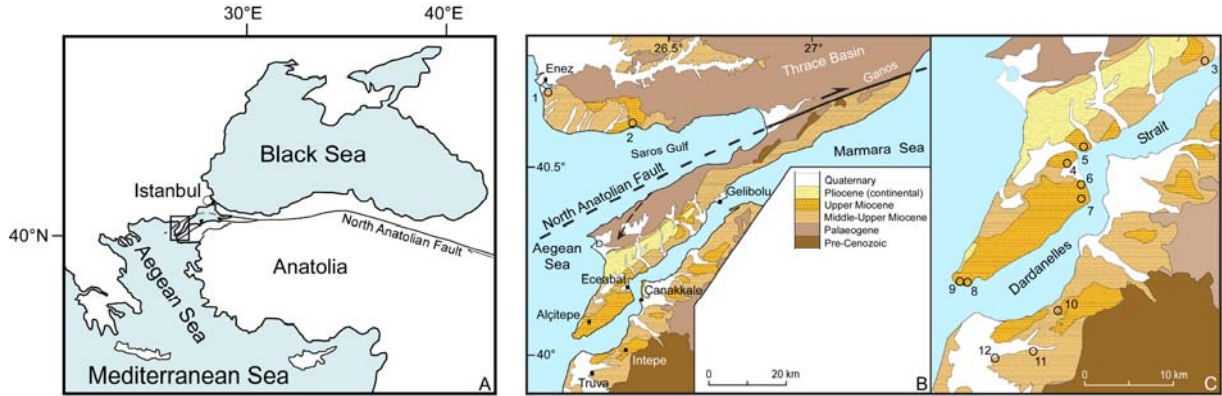


Fig. 1. Location and geological maps.

A, Study area.

B, Geological map of the studied area according to Türkecan and Yurtsever (2002).

Localities: 1, Enez; 2, Yaylaköy.

C, Geological map of the area surrounding the Dardanelles Strait according to Türkecan and Yurtsever (2002).

Localities: 3, Burhanlı; 4, Eceabat; 5, Poyraztepe; 6, Kilitbahir (seashore); 7, Kilitbahir (castle); 8, Seddülbahir East; 9, Seddülbahir West; 10, Intepe; 11, Yenimahalle; 12, Truva.

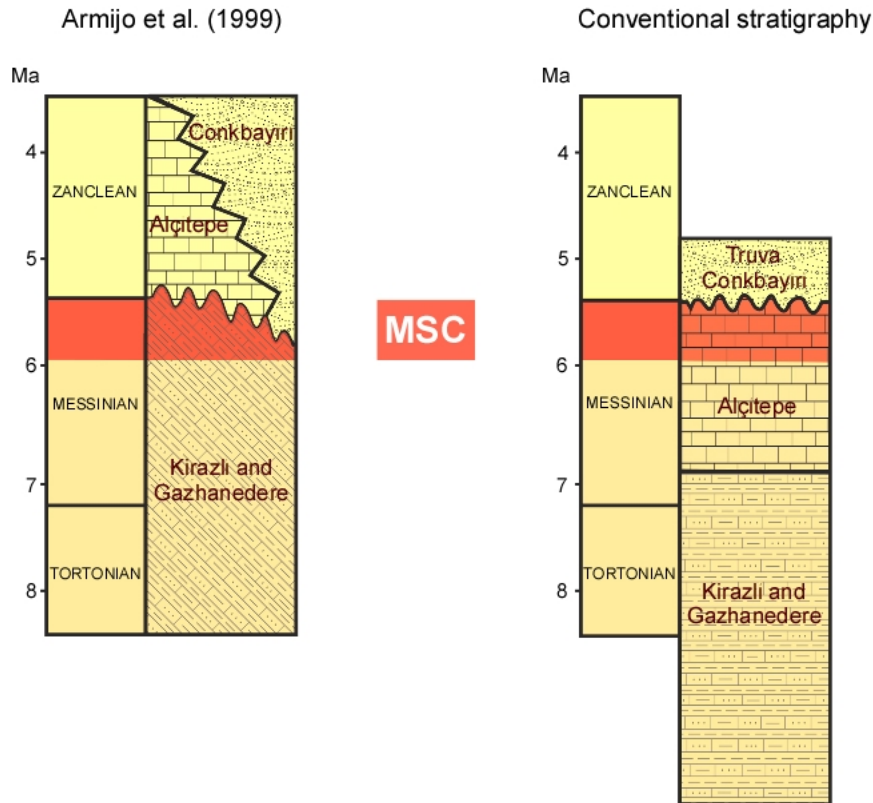


Fig. 2. Controversed age of the Neogene formations in the Dardanelles Strait area. Time-interval corresponding to the Messinian Salinity Crisis (MSC) is indicated by a red band. Defining the stratigraphic position of the Alçitepe Formation with respect to the MSC is critical. The hypothesis represented to the left (Armijo et al., 1999) assigns a Pliocene age (post MSC) to the Alçitepe Formation. The hypothesis that is currently proposed in the conventional stratigraphy (e.g., Görür et al., 1997; Sakiñç et al., 1999; Türkecan and Yurtsever, 2002; Çağatay et al., 2006) assigns a Miocene age (pre MSC and partly coeval with it) to the Alçitepe Formation. The undulating line represents an important erosion and tectonic unconformity in the hypothesis of Armijo et al. (1999), only a slight unconformity in the conventional stratigraphy.

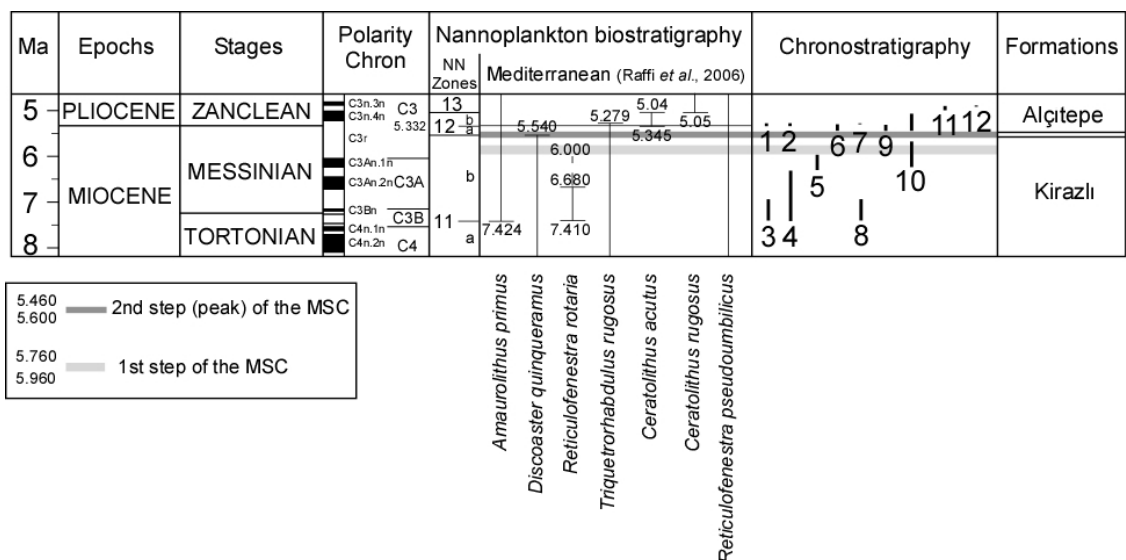


Fig. 3. Chronostratigraphy, calcareous nannoplankton biostratigraphy of the Late Miocene and Early Pliocene and inferred age of the studied sections. Chronology refers to Lourens et al. (2004), calcareous nannoplankton events to Raffi et al. (2006).

The grey strips correspond to two steps of the MSC (Clauzon et al., 1996) accepted by a representative community working on the Messinian Salinity Crisis (CIESM, 2008). Locality numbers, see Figs. 1B, 1C.

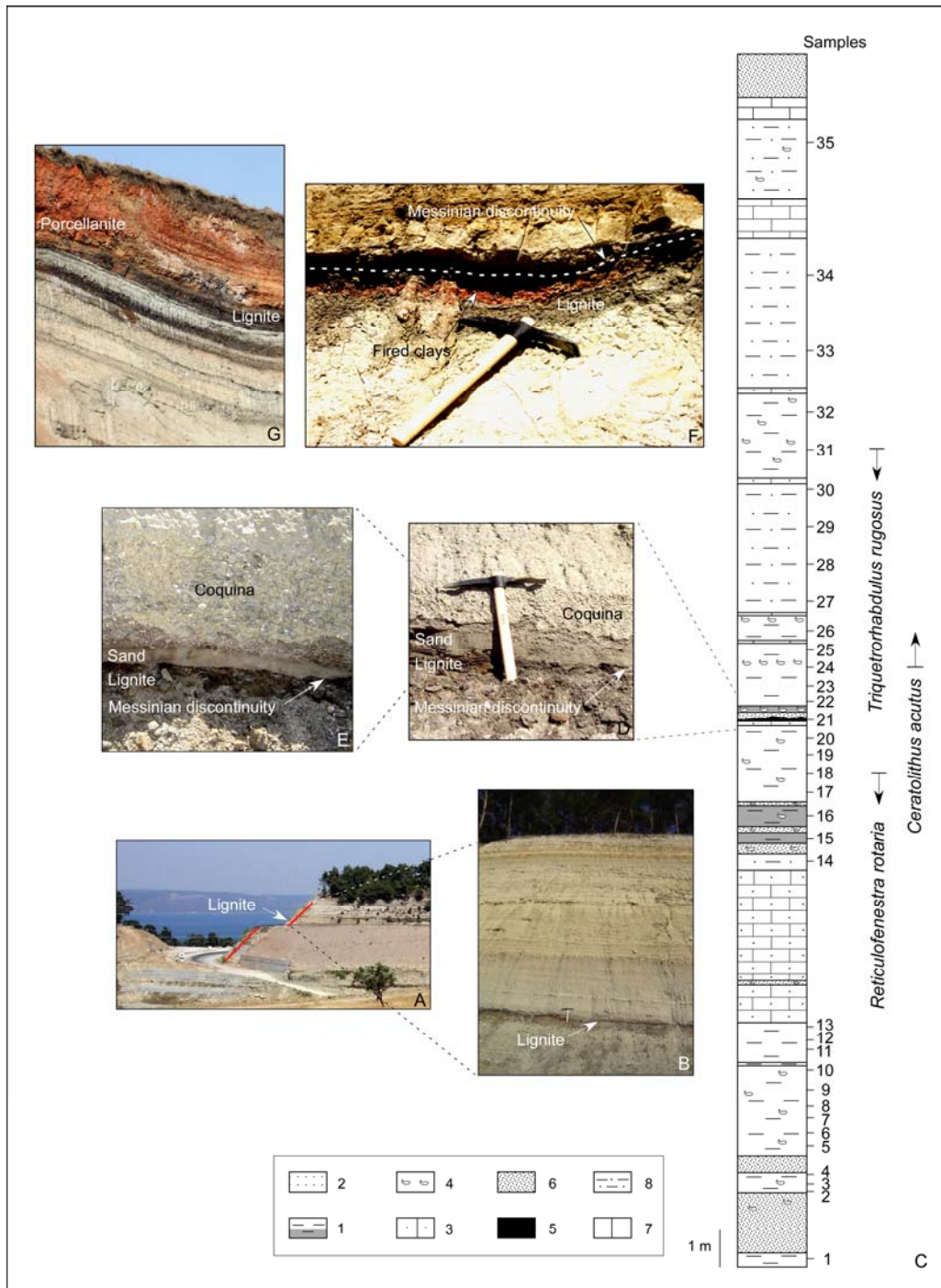


Fig. 4. Lithostratigraphy and calcareous nannoplankton biostratigraphy of the central part of the Intepe section.

A, General view of the Intepe section where red lines indicate the studied part of the section;

B, Upper part of the studied section;

C, Lithological log of the studied section, location of samples, extension of three calcareous nannofossil species providing biostratigraphic information;

1, Dark-light clay; 2, Sand; 3, Calcareous sandstone; 4, Mollusc shells; 5, Lignite; 6, Sandstone; 7, Limestone; 8, Silt.

D, Lignite-coquina interval including the discontinuity caused by the peak of the MSC;

E, Detail of Figure 4D;

F, Fired clays (porcellanite) overlying the lignite and marking the discontinuity caused by the peak of the MSC;

G, Present-day analogue from the S Romania lignite Lupoia quarry showing clays transformed into porcellanite after being naturally fired by the underlying lignite.

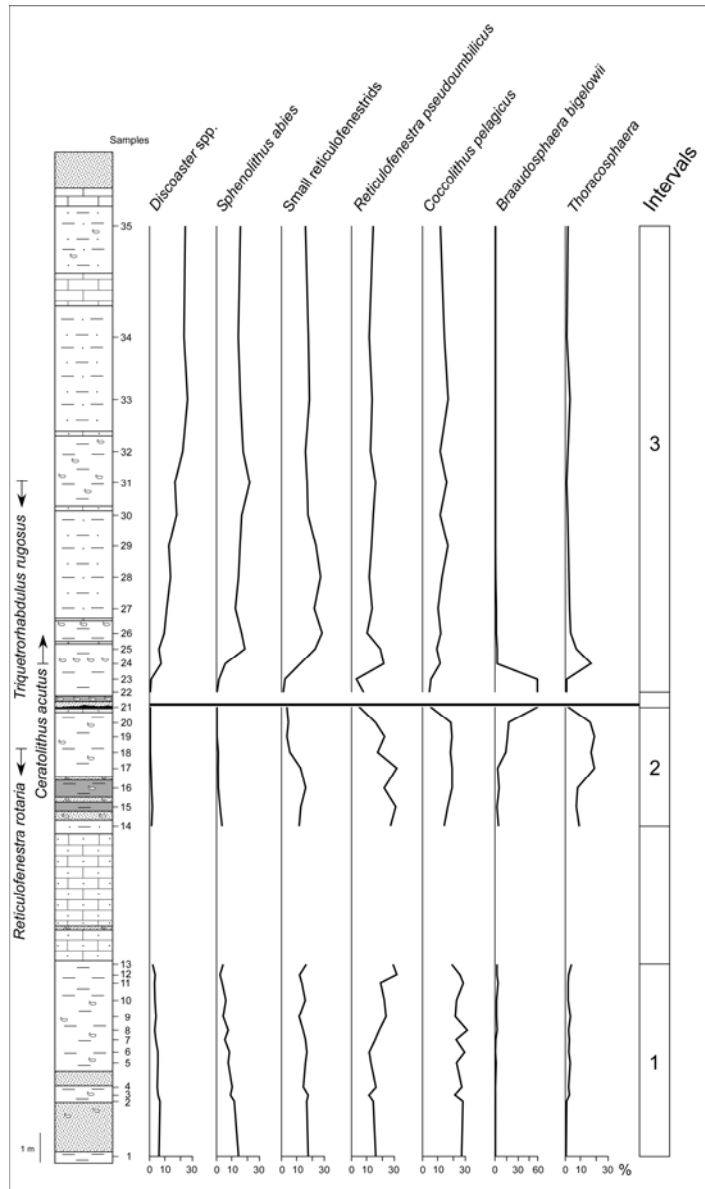


Fig. 5. Fluctuation of the selected calcareous nannofossil groups in the Intepe section (NW Turkey).
Legend, see Figure 4C.

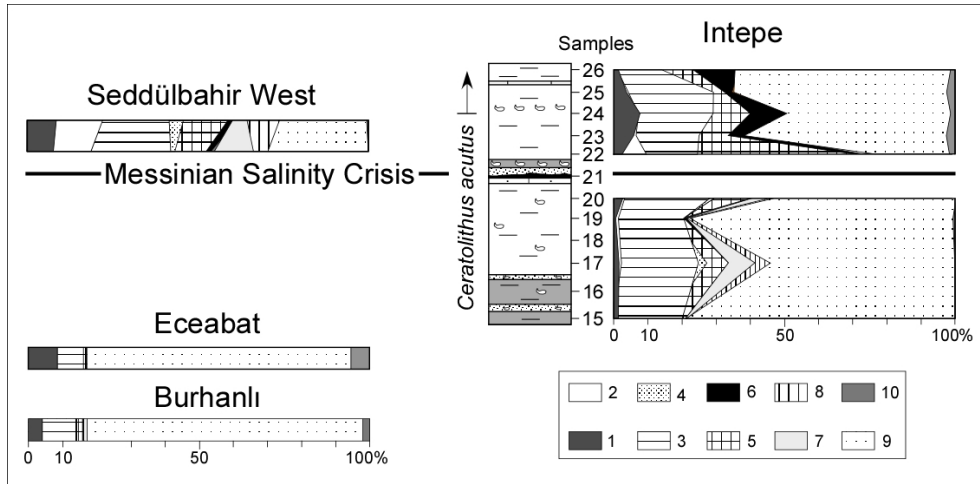


Fig. 6. Synthetic pollen diagram from some localities before and after the peak of the MSC.

- 1, Subtropical trees; 2, *Cathaya*; 3, Warm-temperate trees; 4, Cupressaceae; 5, Cool-temperate trees (*Cedrus* mainly); 6, Boreal trees (*Abies* and *Picea*); 7, Elements without signification; 8, Mediterranean xerophytes; 9, Herbs; 10, Steppe elements (*Artemisia* mainly).

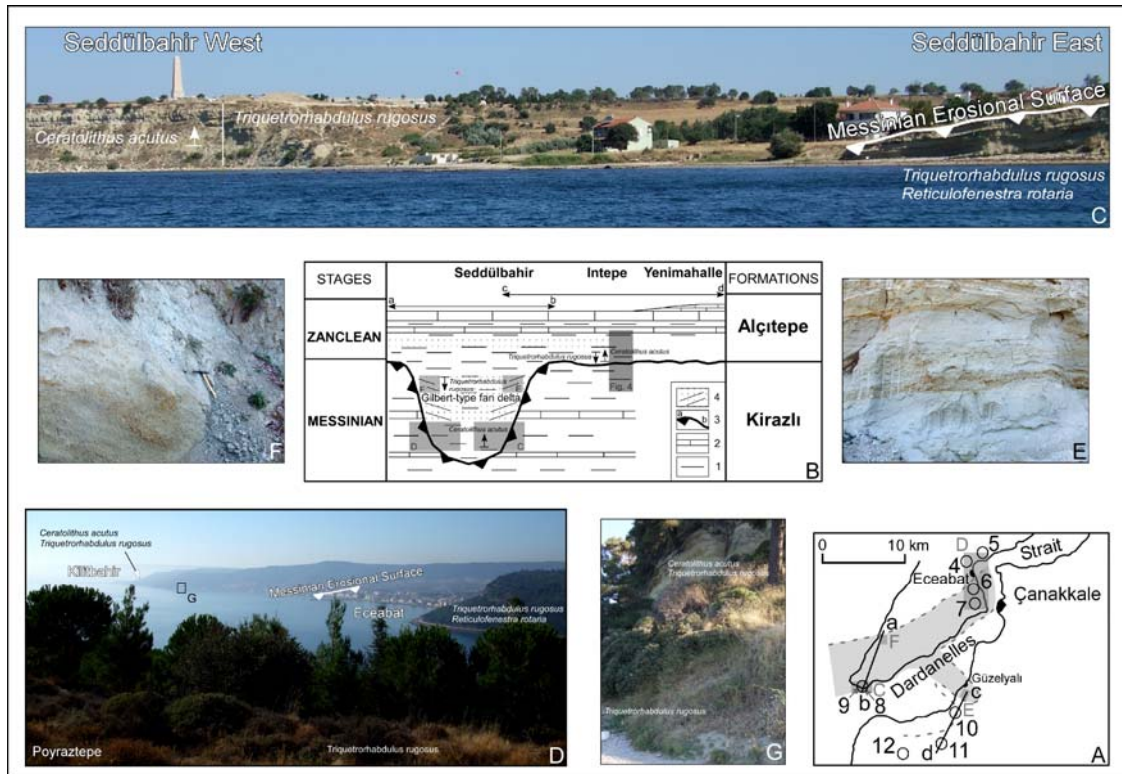


Fig. 7. The Messinian fluvial canyon in the western part of the Dardanelles Strait.

A, Map showing the main Messinian fluvial canyon and a tributary (grey surface), the Early Zanclean coastline (dotted grey line), and location of photographs C-F. Sections: 4, Eceabat; 5, Poyraztepe; 6, Kilitbahir (seashore); 7, Kilitbahir (castle); 8, Seddülbahir East; 9, Seddülbahir West; 10, Intepe; 11, Yenimahalle; 12, Truva.

B, Reconstructed composite cross-section (a-b, c-d) in the Dardanelles Strait and the extremity of the Gelibolu Peninsula through the Zanclean Gilbert-type fan delta with calcareous nannoplankton events and location of photographs C-F and Fig. 4.

1, Clay; 2, Limestone; 3a, Messinian Erosional Surface; 3b, Messinian discontinuity; 4, Sandy and gravelly foreset beds.

C, Photograph of the beach of Seddülbahir showing the Messinian Erosional Surface cutting the clays and sands of the Seddülbahir East section and overlain by the clayey bottomset beds of the Seddülbahir West section. Nannoplankton markers are indicated.

D, View of the surroundings of Eceabat showing the Alçıtepe Formation deposits imbedded within the Eceabat-Poyraztepe sections now reported to the Kirazlı Formation. Nannoplankton markers and the Messinian Erosional Surface are indicated.

E, Sandy and gravelly foreset beds near the Intepe section.

F, Sandy and gravelly foreset beds at Nuriyamut.

G, Kilitbahir (seashore) section with calcareous nannoplankton markers.

1 **GALEACYSTA ETRUSCA COMPLEX, DINOFLAGELLATE CYST MARKER**
2 **OF PARATETHYAN INFLUXES INTO THE MEDITERRANEAN SEA**
3 **BEFORE AND AFTER THE PEAK OF THE MESSINIAN SALINITY CRISIS**
4

5
6 SPERANTA-MARIA POPESCU*
7 UMR 5125 PEPS, CNRS, France ;
8 Université Lyon 1, Campus de La Doua
9 Bâtiment Géode, 69622 Villeurbanne cedex, France
10 popescu@univ-lyon1.fr

11 *and:
12 Senckenberg Forschungsinstitut und Naturmuseum
13 Senckenberganlage 25
14 60325 Frankfurt am Main, Germany
15

16 FLORENT DALESME
17 UFR des Sciences de la Terre
18 Université Lyon 1, Campus de La Doua
19 Bâtiment Géode, 69622 Villeurbanne cedex, France
20 florent.dalesme@wanadoo.fr
21

22 GWÉNAËL JOUANNIC
23 UFR des Sciences de la Terre
24 Université Lyon 1, Campus de La Doua
25 Bâtiment Géode, 69622 Villeurbanne cedex, France
26 gwenaeljouannic@aol.com
27

28 GILLES ESCARGUEL
29 UMR 5125 PEPS, CNRS, France
30 Université Lyon 1, Campus de La Doua
31 Bâtiment Géode, 69622 Villeurbanne cedex, France
32 Gilles.Escarguel@univ-lyon1.fr
33

34 MARTIN J. HEAD
35 Department of Earth Sciences
36 Brock University
37 500 Glenridge Avenue
38 St. Catharines
39 Ontario L2S 3A1, Canada
40 mjhead@brocku.ca
41

42 MIHAELA CARMEN MELINTE-DOBRINESCU
43 National Institute of Marine Geology and Geo-ecology (GEOECOMAR)
44 23-25 Dimitrie Onciul Street
45 024053 Bucharest, Romania
46 melinte@geoecomar.ro
47

48 MARIA SÜTŐ-SZENTAI
49 Natural History Collection of Komlo
50 Városház tér 1, 7300 Komlo, Hungary

51 suto.zoltanne@freemail.hu,

52

53 KORALJKA BAKRAC

54 Croatian Geological Survey

55 HGI-CGS

56 Sachsova 2

57 10000 Zagreb, Croatia

58 Koraljka.Bakrac@hgi-cgs.hr

59

60 GEORGES CLAUZON

61 C.E.R.E.G.E. (UMR 6635 CNRS)

62 Université Paul Cézanne, Europôle de l'Arbois

63 BP 80, 13545 Aix-en-Provence Cedex 04, France

64 clauzon@cerege.fr

65

66 JEAN-PIERRE SUC

67 UMR 5125 PEPS, CNRS, France

68 Université Lyon 1, Campus de La Doua

69 Bâtiment Géode, 69622 Villeurbanne cedex, France

70 jean-pierre.suc@univ-lyon1.fr

71

72

73 **ABSTRACT**

74

75 More than a thousand specimens of *Galeacysta etrusca* complex from eleven Upper Miocene
76 and Lower Pliocene localities of the Paratethyan and Mediterranean realms have been studied
77 using a biometric approach in part relating to the degree of separation between endocyst and
78 ectocyst. Four stable biometric groups have been statistically distinguished, the occurrence or
79 prevalence of which appears closely linked to environmental conditions irrespective of the
80 realm. Group “a” is related to brackish conditions, group “b” to marine conditions, group “c”
81 to freshwater, and group “d” to high nutrient levels. Based on an accurate chronology
82 provided by calcareous nannoplankton bioevents and recognition of the Messinian Erosional
83 Surface, this study reveals:

84 - the high sensitivity of *Galeacysta etrusca* complex for reconstructing paleoenvironments
85 and the connection–isolation phases of basins;

86 - the detailed history of this species which originated in the Pannonian Basin at ca. 8 Ma
87 before invading the Dacic Basin at about 6 Ma, then migrating into the Mediterranean during
88 high sea-level connections (the “Lago Mare” events just before and after the peak of the
89 Messinian Salinity Crisis, i.e. at 5.60 Ma and during the interval 5.48–5.33 Ma, respectively)
90 and, finally, into the Black Sea at 5.13 Ma;

91 - an improved paleogeographic reconstruction for the Mediterranean and Paratethyan realms
92 with focus on the location of corridors and the timing of when they were active.

93 Field observations and dinoflagellate cyst data lead us to consider that the reflooding of the
94 Mediterranean Basin by Atlantic waters occurred at ca. 5.48 Ma, about 150 kyrs before the
95 Zanclean GSSP (5.33 Ma).

96

97

98 **Key words:** *Galeacysta etrusca* complex; Paratethys–Mediterranean; Messinian; Zanclean;
99 “Lago Mare”.

100

INTRODUCTION

101
102 The dinoflagellate cyst *Galeacysta etrusca* Corradini & Biffi 1988 is considered to have
103 migrated from the Paratethys into the Mediterranean Sea during the latest Messinian (Text-
104 Figure 1A). It was first described from the latest Messinian age at Cava Serredi (Livorno
105 Province, Italy; Text-Figure 1B) by Corradini and Biffi (1988). Morphologically close
106 dinoflagellate cysts are known from the Lower Pliocene of southern Romania as
107 *Thalassiphora balcanica* Balteş 1971 and *Romanodinium areolatum* Balteş 1971; these
108 differing from *Galeacysta etrusca* only by a reduced expression of the tabulation. Based on
109 studies of the Pannonian Basin (Central Paratethys), Sütő-Szentai (1988) attempted to transfer
110 *Thalassiphora balcanica* to the genus *Spiniferites*, although the resulting combination was not
111 validly published until later as *Spiniferites balcanicus* (Balteş, 1971) Sütő-Szentai 2000. Sütő-
112 Szoltánné (1994) maintained *Spiniferites balcanicus* and *Galeacysta etrusca* as separate
113 species, but considered *Galeacysta etrusca* as a planktonic (thecate) form. *Nematosphaeropsis*
114 *bicorporis* Sütő-Szentai 1996 is also morphologically close to *Galeacysta etrusca* and was
115 described from the Upper Pannonian (regional Stage) in the Central Paratethys by Sütő-
116 Szentai (1990). The name *Nematosphaeropsis bicorporis* was not validly published by Sütő-
117 Szentai (1990) because the author did not state the location of the holotype. This information
118 was later provided by the same author (under the name Sütőné Szentai, 1996), thereby
119 completing requirements for valid publication.

120 Hence, *Galeacysta etrusca*, *Romanodinium areolatum*, *Spiniferites balcanicus*, and
121 *Nematosphaeropsis bicorporis* are all validly published names relating to morphologically
122 close, if not identical cyst forms. The spatial and temporal distribution of *Galeacysta etrusca*,
123 *Romanodinium areolatum*, *Spiniferites balcanicus*, and *Nematosphaeropsis bicorporis* is
124 associated with major paleogeographic changes that led to fragmentation of the Paratethys
125 Sea (Text-Figure 1A) into separate basins (i.e. Pannonian, Dacic, Euxinian and Caspian) as a
126 result of the Carpathian uplift (Pomérol, 1973; Rögl and Steininger, 1983; Piller et al., 2007).
127 This fragmentation implies important paleoenvironmental changes marked by progressive
128 decrease in salinity from west to east in these basins.

129 It has been demonstrated that dinoflagellates are sensitive to environmental change, and
130 their cyst morphologies may become modified in response to environmental stress. The
131 appearance of cruciform endocysts and variations in septal development (Wall et al., 1973;
132 Wall and Dale, 1974) or reductions in process length (de Vernal et al., 1989; Dale, 1996;
133 Ellegaard, 2000; Lewis et al., 1999; 2003; Head, 2007) have been correlated to reduced
134 salinities of surface waters. Laboratory experiments on living specimens have confirmed the
135 morphological changes observed in the fossil record, and show that certain species vary in
136 process length (Kokinos and Anderson, 1995) and process morphology (Lewis and Hallett,
137 1997) even under stable salinity conditions, indicating that cyst morphological changes are
138 controlled by multiple factors such as salinity, temperature and nutrients.

139 The presence of transitional morphologies between *Galeacysta etrusca*, *Romanodinium*
140 *areolatum*, *Spiniferites balcanicus* and *Nematosphaeropsis bicorporis*, strongly suggests that
141 all these taxa could be considered as morphological variants of the same species. As a
142 working hypothesis in this study, we therefore group them in the *Galeacysta etrusca* complex.
143 Hereafter, we will abbreviate *Galeacysta etrusca* complex to *Galeacysta etrusca*, except when
144 referring to the species described by Corradini and Biffi indicated as *Galeacysta etrusca*
145 Corradini and Biffi 1988. We provisionally use the name *Galeacysta etrusca* Corradini and
Biffi 1998 because the type material is illustrated and described unambiguously, although we
acknowledge that the name *Romanodinium areolatum* Balteş 1971 has priority. The type
materials of these morphotypes are under investigation, and formal synonymies will be
presented in due course.

In the Pannonian Basin, the appearance of *Galeacysta etrusca* Corradini & Biffi 1988, at about 8 Ma (Magyar et al., 1999a), then followed by its high abundance up to ca. 5 Ma, allows this species to be considered as the marker for the uppermost regional biozone of the Upper Miocene (Sütő-Szentai, 1990; Magyar et al., 1999a; Müller et al., 1999; Sacchi and Horváth, 2002; Popov et al., 2006; Piller et al., 2007). In the Mediterranean area, *Galeacysta etrusca* occurred within the late Messinian–early Zanclean interval which includes the Messinian Salinity Crisis that led to the almost complete desiccation of the Mediterranean Sea. The regular occurrence of *Galeacysta etrusca* Corradini & Biffi 1988 in the latest Messinian deposits brought this species to becoming the microplankton reference for the “Lago Mare” biofacies (Bertini et al., 1995).

The present study aims to show that during Messinian and Zanclean times, *Galeacysta etrusca* developed a wide range of morphological variability including (1) the degree of separation between ectocyst and endocyst (the parameter used in this paper) representing the same morphological response to environmental stress as process length of chorate dinoflagellate cysts, (2) the overall size and length/width ratio of endocyst and ectocyst, and (3) shape of endocyst from oval to cruciform (here disregarded). This variability is documented by a biometric and statistic analysis of a data set made of 1144 specimens of *Galeacysta etrusca* from Central-Eastern Paratethys and Mediterranean sections located within the Upper Miocene and Lower Pliocene (Text-Figure 1B). Two complementary aspects are most particularly worked out: (1) the geographic and hydrographic reconstruction of the Paratethys and Mediterranean realm around the Messinian Salinity Crisis, and (2) the morphological and biometric characterization of *Galeacysta etrusca* as a response to environmental (salinity and nutrient) changes. These two research axes lead us to answer two main questions:

- (1) Is it possible to distinguish between the two “Lago Mare” events evidenced by Clauzon et al. (2005) using the morphological and biometric range of *Galeacysta etrusca* complex in the Mediterranean realm?
- (2) Do the interfered *Galeacysta etrusca* migrations give information about the complicated paleogeographical changes within the Mediterranean and Central-Eastern Paratethys during this period?

THE MESSINIAN SALINITY CRISIS AND THE “LAGO MARE” EVENTS

The Mediterranean experienced dramatic changes during the Late Miocene when it became temporarily isolated as a result of tectonic activity (Hsü et al., 1973; Duggen et al., 2003; Jolivet et al., 2006). Isolation led to the Messinian Salinity Crisis, peaking with a severe drop in Mediterranean sea-level which resulted in the deposition of thick evaporites in central basins (Hsü et al., 1973; Rouchy and Caruso, 2006) and intense subaerial erosion of the margins (Clauzon, 1999). During the almost complete desiccation of the Mediterranean Sea, the Paratethys was considered to be a suspended basin full of water (Hsü et al., 1978; Cita et al., 1978). The drainage of Paratethys into Mediterranean Sea was considered as a single isochronous event by Hsü et al. (1973) and is evidenced by the “Lago Mare” biofacies characterized by Paratethyan fossil assemblages. This hypothesis was contradicted by (1) the discovery of latest Messinian and earliest Zanclean Mediterranean marine calcareous nannoplankton in the Eastern Paratethys (Dacic Basin: Mărunțeanu and Papaianopol, 1995; 1998; Drivaliari et al., 1999; Snel et al., 2006; Azov Sea: Semenenko and Olejnik, 1995) within the time-frame encompassing the Messinian Salinity Crisis; and (2) by the clear evidence of two successive falls in sea level (Clauzon et al., 1996). The first was from 5.960 to about 5.760 Ma, when a minor sea-level drop caused the deposition of evaporites in the more-or-less isolated marginal basins (gypsum, halite and potash salts in such areas as Sicily

where they constitute the Lower Evaporites) and some erosion in the most proximal parts of river valleys. The second was from 5.640 to 5.480 Ma when a major sea-level drop resulted in: (1) the almost complete desiccation of the Mediterranean Sea, (2) deposition of the central basin evaporites, and (3) massive subaerial erosion (deep river canyons and intense dismantling of the margins) that strongly cut the marginal evaporites and extended to the base of the central basin evaporites. These two sea-level drops were separated by an intermediate transgressive and cyclic episode corresponding to the Upper Evaporites of Sicily, where, as at Eraclea Minoa, relatively low sea-levels caused the deposition of six gypsum beds.

Similar events (deposition of marginal evaporites followed by huge erosion) also impacted the Eastern Paratethys (Gillet et al., 2003; 2007; Clauzon et al., 2005) which had been connected almost continuously to the Mediterranean Sea during the high sea-level episodes of the Neogene since about 14 Ma (Mărunțeanu and Papaianopol, 1995; 1998). Popescu (2006) used the late arrival of marine dinoflagellate cysts at DSDP Site 380, Leg 42 in the Black Sea to demonstrate that the supposed “proto-Bosphorus” was closed during the Late Neogene, and that the gateway was instead located in the Balkans area (Clauzon et al., 2005). The presence of Paratethyan organisms: (1) molluscs (dreissenids and lymnocyprids), (2) ostracods (*Cyprideis pannonica* group), (3) dinoflagellate cysts (*Galeacysta etrusca*, *Spiniferites cruciformis*, *Pyxidinospis psilata* etc.) in the Mediterranean (Clauzon et al., 2005); simultaneously with the presence of Mediterranean planktonic microorganisms: (1) coccoliths (Mărunțeanu and Papaianopol, 1995, 1998; Semenenko and Olejnik, 1995; Clauzon et al., 2005; Snel et al., 2006), (2) foraminifers, (3) dinoflagellate cysts (Popescu, 2006; Popescu et al., 2006) in the Paratethys implies that these two seas communicated during high sea-levels before and after the Messinian Salinity Crisis. This connection resulted in two “Lago Mare” events, the first indicated at the top of the Messinian marginal evaporites and the second in the lowermost Zanclean (Clauzon et al., 2005). This leads to the new concept of the “Lago Mare” events (Clauzon et al., 2005) depicted in Text-Figure 2. Contrasting the various concepts related to the term Lago Mare, we put it within inverted commas when it concerned the peculiar related Mediterranean biofacies or the event at the origin of the invasion of Paratethyan organisms into the Mediterranean [two high sea-level exchanges, and an intermediate dilution episode; see Clauzon et al., 2005 for more details], and we wrote it without inverted commas when a stratigraphic formation described as such is concerned. These two “Lago Mare” events are in agreement with the two-step scenario of Clauzon et al. (1996; 2005), as summarized above. This scenario contrasts with: (1) Krijgsman et al.’s (1999) scenario which considers the marginal evaporites as coeval with the central basin evaporites without any sea-level fall at the beginning of the crisis (in addition to a discrepancy over the precise location of the erosional surface in Sicily), (2) Rouchy and Caruso’s (2006) scenario that invokes a polyphased erosion even though a single erosion event is marked on the Mediterranean margins (Lofi et al., 2005), and (3) Braga et al.’s (2006) scenario where the marginal pre-evaporitic paleotopography is confused with the Messinian erosional surface which everywhere postdates the marginal evaporites (Clauzon et al., 1996).

STUDIED LOCALITIES AND THEIR CHRONOSTRATIGRAPHIC SETTING

According to Clauzon et al. (2005), within the time-interval 6–5 Ma two phases of water exchanges existed between Mediterranean and Paratethys seas, each high-sea level connections generating a “Lago Mare” event in Mediterranean margins. The first episode preceded the desiccation phase of the Messinian Salinity Crisis and refers to the NN11b calcareous nannoplankton subzone (Text-Figure 2), causing during highest intensity the arrival of *Galeacysta etrusca* Corradini & Biffi 1988 recorded at Cava Serredi, Eraclea Minoa (first influx) and Aghios Sostis. The second episode immediately followed the desiccation

phase of the Messinian Salinity Crisis in the late NN12a and earliest NN12b calcareous nannoplankton zone (Text-Figure 2); the resulting invasion of *Galeacysta etrusca* lasted about 180 kyrs (as calculated at Eraclea Minoa between the above proposed age for the base of Arenazzolo and that of the base of the acme of *Sphaeroidinellopsis*; Lourens et al., 2004) while the two-way water-exchange continued sporadically until ca. 5 Ma as evidenced at DSDP Hole 380A (Popescu, 2006) (Text-Figure 2).

In this paper we studied fourteen localities (Majs 2, Krajačići, Krašić, Cernat, Valea Vacii, Eraclea Minoa, Hinova, Maccarone, San Donato and DSDP Hole 380A, Malunje, Torre Sterpi, Sioneri and Casabianda) distributed on the Central and eastern Paratethys and Mediterranean margins. The last four localities were not retained for final statistical analyses and comparisons because *Galeacysta etrusca* is scarce. The chronostratigraphic positions of studied localities are reported below.

The Central Paratethys (Pannonian Basin)

The earliest appearance of *Galeacysta etrusca* is at 8 Ma in the Pannonian Basin (Central Paratethys), where it persisted for 3 myrs, until 5 Ma. This species has been used as a chronostratigraphic indicator throughout the Pannonian Basin (Magyar et al., 1999a, b; Müller et al., 1999). Because the late Miocene stratigraphy of this basin is still in discussion (Sacchi and Horváth, 2002; Piller et al., 2007), we will follow here the classical assumption which discards the Pontian Stage in the Pannonian Basin (Magyar et al., 1999a; Müller et al., 1999) (Text-Figure 2).

In this basin, four localities were selected in order to observe: (1) the morphology of the “oldest” representatives *Galeacysta etrusca* in typical low salinity condition (Majs 2 section), and (2) the possible morphological modification in relation with a relative increase in salinity, indicated by the presence of marine dinoflagellate cysts (Malunje, Krašić and Krajačići sections) and meaningless coccoliths (Krajačići). The Majs2 samples analyzed in this study have been selected from the oldest beds of the *Galeacysta etrusca* Zone at ca. 8 Ma (Text-Figure 2; Magyar et al., 1999a, b). The low salinity condition at this time is indicated by the presence of typically Paratethyan dinoflagellate cysts assemblages and the absence of marine dinoflagellate cysts. The Malunje, Krašić and Krajačići sections from the Pannonian Basin belong to the Upper Pannonian (Text-Figure 2; Magyar et al., 1999a; Kovačić et al., 2004). The presence of marine microorganisms suggests a connection between the Pannonian Basin and Mediterranean Sea at that time.

The Eastern Paratethys (Dacic and Euxinian Basins)

In the Eastern Paratethys (Dacic and Euxinian Basins), *Galeacysta etrusca* represents a common species recorded in sediments belonging to the regional Pontian Stage (Text-Figure 2). In spite of an intensive effort in magnetostratigraphy under biostratigraphic control by molluscs, the age boundaries of the regional stages in the Dacic Basin are still disputed (Maeotian–Pontian: 6.15–5.75 Ma; Pontian–Dacian: 5.30–4.70 Ma; Vasiliev et al., 2004; Snel et al., 2006; Stoica et al., 2007; see also: Clauzon et al., 2005; Popescu et al., 2006); discrepancies are indicated on Text-Figure 2. Age boundaries of the regional substages have only been proposed by Snel et al. (2006) and are reported for indicative purpose in Text-Figure 2: 6 Ma for the Odessian–Portaferrian and 5.60 Ma for the Portaferrian–Bosphorian. In this study, we chronologically calibrate the sections using the global nannoplankton biostratigraphy and considering their position with respect to the Messinian Erosional Surface identified in both basins. Four localities were analyzed for these two basins, respectively Cernat, Valea Vacii and Hinova in the Dacic basin, and DSDP Hole 380A in the Black sea (Euxinian Basin). The Cernat and Valea Vacii sections (Text-Figure 2) belong to the Portaferrian and Bosphorian substages, respectively. Both sections contain calcareous

nannoplankton of the NN11b subzone (Mărunțeanu and Papaianopol, 1998; Snel et al., 2006) since the basin was at that time connected with the Mediterranean (Clauzon et al., 2005) and are considered corresponding to the Late Messinian. The Hinova section contains a Bosphorinan mollusc fauna and includes calcareous nannoplankton assignable to zone NN12a (Popescu, 2001; Clauzon et al., 2005; Popescu et al., 2006). More precisely, they have an astronomical age from 5.40 to 5.34 Ma according to vegetation cycles identified in the pollen record (Popescu et al., 2006) (Text-Figure 2). This section overlies a massive erosional surface referred to the desiccation phase of the Messinian Salinity Crisis (Clauzon et al., 2005). Sediments from the Black Sea DSDP Hole 380A considered in this study overlie the Messinian Erosional Surface (Gillet et al., 2007) and cover an astronomically dated time-window from 5.11 to 5.00 Ma, as also indicated by the pollen record (Popescu, 2006) (Text-Figure 2).

The Mediterranean realm

In the Mediterranean margins, *Galeacysta etrusca* is recorded at Cava Serredi (Corradini and Biffi, 1988), Maccarone (Bertini, 2006; Popescu et al., 2007) and San Donato (Bassetti, 1997) in Central Italy; Torre Sterpi and Sioneri (Popescu, unpublished) in Northern Italy; at Eraclea Minoa in Sicily (Londeix et al., 2007) and Casabianda in Corsica (Popescu, unpublished) (Text-Figure 1B). According to their biostratigraphic chronology and their position with respect to the Messinian Erosional Surface (Text-Figure 1B), Cava Serredi and Agios Sostis are considered as Messinian localities, corresponding to the first “Lago Mare” event (Clauzon et al., 2005); on contrary, Maccarone, San Donato, Torre Sterpi, Sioneri and Casabianda are post Messinian Salinity Crisis localities and correspond to the second “Lago Mare” event (Clauzon et al., 2005). A special case is Eraclea Minoa section that includes the two “Lago Mare” events. Cava Serredi, Eraclea Minoa, Maccarone and Casabianda sections were restudied in order to better understand their chronostratigraphic position with respect to the Messinian Salinity Crisis. The new obtained bio- and chronostratigraphic data are presented below.

At the **Cava Serredi** quarry, a Lago Mare deposit of about 26 m in thickness was described in the 1980s, sandwiched between the uppermost thick gypsum bed and the Zanclean clays (Bossio et al., 1981). It was clearly subdivided into two parts: the lower part (7.50 m thick), dreissenid-rich, including some highly concentrated beds (coquinas), is considered to indicate brackish conditions; whereas the upper part (about 18 m thick) was rich in *Melanopsis* and *Theodoxus* shells and corresponds to a more freshwater environment (Text-Figure 3A, B; Bossio et al., 1981). Today, the working face of the quarry has moved about 2 km northward, and only 6.60 m of Lago Mare separates the highest gypsum bed from the lowermost Zanclean clays that are well-characterized by our lowest record of *Ceratolithus acutus* 3 m above their base, which precedes that of *Sphaeroidinellopsis* evidenced by Bossio et al. (1981) (Text-Figure 3B, C). The Lago Mare is composed only of dreissenid-rich sediments (including coquinas). The *Melanopsis* layer is absent. We conclude that the missing ca. 19 m of Lago Mare (i.e. the entire *Melanopsis* layer plus ca. 1 m of dreissenid-rich sediment) were eroded during the desiccation phase of the Messinian Salinity Crisis and that, accordingly, the Messinian Erosional Surface corresponds here to moderate erosion and must be placed at the top of the Lago Mare (Text-Figure 3). This section was presented as showing a continuous passage from the Messinian to Zanclean by Bossio et al. (1981), Corradini and Biffi (1988) and Carnevale et al. (2006). In fact, the *Galeacysta etrusca* Corradini & Biffi 1988 layer of Cava Serredi documents what we consider as an episode of high sea-level and intensive exchange between the Mediterranean and Eastern Paratethys just preceding the Mediterranean desiccation phase (Text-Figure 2) (Clauzon et al., 2005). The marine

conditions of the Cava Serredi dreissenid beds have recently been supported by the presence of marine fish remains (Carnevale et al., 2006).

Eraclea Minoa is the only Mediterranean section where *Galeacysta etrusca* has been recorded before and after the Messinian desiccation phase (Clauzon et al., 2005; Londeix et al., 2007). Here, the desiccation is not expressed by well-marked erosion, probably because the locality occupied an interfluvial position in a semi-arid area (Suc and Bessais, 1990; Fauquette et al., 2006). However, a discontinuity has been reported as shown in Text-Figure 4. Two sections have been examined near the global stratotype section and point (GSSP) of the Zanclean Stage (Van Couvering et al., 2000) (Text-Figure 4A). Section 1 starts with clays and diatomitic turbidite underlying the highest gypsum bed of the Sicilian Upper Evaporites, followed by the clayey Lago Mare Formation (7.80 m thick) including in its upper part three characteristic layers (two dreissenids coquinas, 25 cm and 40 cm thick respectively, bordering a white sand 32 cm thick). This is followed by the silty Arenazzolo Formation (5.60 m thick) comprising 7.5 dark–light cycles, which is itself overlain by the carbonate–marly cyclic Trubi Formation at the base of which the Zanclean GSSP has been placed (Text-Fig. 4C, E). Nannofloral assemblages from the Lago Mare Formation contain, among other taxa, *Amaurolithus amplificus*, *Amaurolithus primus*, *Coccolithus pelagicus*, *Helicosphaera carteri* s.l., *Helicosphaera intermedia*, *Pontosphaera multipora*, small-sized reticulofenestrads, *Reticulofenestra pseudoumbilicus*, *Sphenolithus* group *abies/moriformis*, *Triquetrorhabdulus striatus* and *Triquetrorhabdulus rugosus*, and may be related to the subzone NN11b. *Galeacysta etrusca* has been reported only in the diatomitic turbidite underlying the highest gypsum and within the Arenazzolo Formation (Londeix et al., 2007). We studied specimens from four samples, one from the diatomitic turbidite and three from the Arenazzolo Formation (Text-Figure 4C). At section 2, major differences have been observed with respect to section 1: (1) the Lago Mare Formation is significantly reduced (1.50 m thick only) and does not show the three aforementioned reference layers in its upper part (Text-Figure 4D, E), and (2) the Arenazzolo deposits clearly onlap the Lago Mare clays (Text-Figure 4E). We suggest that the upper part of the Lago Mare of section 1 has been eroded in section 2. As a consequence, we place the Messinian Erosional Surface at the top of the Lago Mare Formation, an assumption also supported by the onlapping nature of the Arenazzolo silts. This proposal is fully consistent with new offshore data from the Strait of Sicily which sharply contradict the proposed Messinian erosion in Sicily as sandwiched between the Lower and Upper Evaporites (Butler et al., 1995; Krijgsman et al., 1999), an interpretation resulting from confusion with the effects of local tectonics (Clauzon et al., 1996). In agreement with Brolsma (1975; 1976), we consider that the Arenazzolo Formation represents the reflooding of the Mediterranean Basin by Atlantic waters, recorded below the base of the Trubi Formation, i.e. earlier than the Zanclean GSSP. The related time-interval should be of about 150 kyrs, taking the 7.5 dark–light cycles of the Arenazzolo Formation as precessional cycles just as those of the immediately overlying Trubi Formation (Hilgen and Langereis, 1993). Hence, the base of the Arenazzolo Formation would date from 5.48 Ma, that should be the age of the Mediterranean reflooding after the Messinian Salinity Crisis (Text-Figure 2), an assumption consistent with the new concept of the “Lago Mare” events as representing repeated exchanges during high sea-level between the Mediterranean and Paratethys (Clauzon et al., 2005). The *Galeacysta etrusca* occurrences at Eraclea Minoa are limited to episodes of rising sea-level represented by the diatomitic turbidite and Arenazzolo Formation (Londeix et al., 2007) that we consider bordering the peak of the Messinian Salinity Crisis.

At **Maccarone** (Adriatic realm), *Galeacysta etrusca* has been recorded within a stratigraphic interval including the uppermost Di Tetto, Colombacci, and lowermost Argille Azzurre formations (Bertini, 2006; Popescu et al., 2007). The studied specimens are from the uppermost Di Tetto (samples 15-18) and Colombacci (samples 30-42) formations (Popescu et

al., 2007; Table 1). The Argille Azzurre Formation characterizes the beginning of the Zanclean in the area (Selli, 1973) but the recent recording of *Ceratolithus acutus* both in the uppermost Di Tetto and entire Colombacci formations significantly lowers the reflooding by marine waters in this stratigraphic succession (Popescu et al., 2007). As a consequence, all the specimens of *Galeacysta etrusca* from the Maccarone section are younger than the Messinian Salinity Crisis (Text-Figure 2). The studied *Galeacysta etrusca* specimens from San Donato belong to the upper Colombacci Formation (Bassetti, 1997) and, accordingly, refer to the same episode (Text-Figure 2). A similar stratigraphic position characterizes the Torre Sterpi locality near Tortona (Corselli and Grecchi, 1984) and the Sioneri locality near Alba (Cavallo and Repetto, 1988).

At **Casabianda**, the Aleria Formation overlies an erosional surface (Saint Martin et al., 2007) that we refer to the Messinian Erosional Surface because of our discovery of *Ceratolithus acutus* (accompanied, inter alia, by *Triquetrorhabdulus rugosus*) within the diatomitic sediments directly overlying those containing dreissenids and *Galeacysta etrusca*. The Casabianda diatomites obviously deposited after the end of the Messinian Salinity Crisis (Text-Figure 2).

METHODS

Within the framework of the previously discussed chronostratigraphy, 47 samples (Table 1) were selected from most of the localities mentioned above (Majs 2, Krajačići, Krašić, Cernat, Valea Vacii, Eraclea Minoa, Hinova, Maccarone, San Donato and DSDP Hole 380A). Malunje, Torre Sterpi, Sioneri and Casabianda were not retained for final statistical analyses and comparisons because *Galeacysta etrusca* is scarce at these localities. We did not examine the *Galeacysta etrusca* specimens from Agios Sostis. We did not recover the *Galeacysta etrusca* Corradini & Biffi 1988 horizon at Cava Serredi at the top of the dreissenids layers in the present-day working face of the quarry, probably eroded during the desiccation phase (Text-Figure 3). Hence, we used for this locality the photographs published by Corradini and Biffi (1988).

Each sample (20 g of dry sediment) was processed using standard methods (Cour, 1974): acid digestion, concentration using $ZnCl_2$ (at density 2.0) and sieving at 10 μm . A 50 μl volume of residue was mounted between the coverslip and microscope slide using glycerine in order to allow rotation of dinoflagellate cysts for their complete examination and homogeneity in measurements. *Galeacysta etrusca* was identified using a light microscope at x600 and x1000 magnifications.

For each specimen we took four measurements at the light microscope (Plate 1): the length and width of the endocyst (L_{EN} and W_{EN} , respectively) and the length and width of the ectocyst (L_{EC} and W_{EC} , respectively). To obtain homogenous measurements, all specimens were rotated into dorso-ventral orientation. Based on these four log-transformed variables, we first performed a one-way Multiple Analysis of Variance between all the studied sections (complete data set: 1,144 individuals), coupled with a Canonical Variate Analysis (a multigroup Discriminant Analysis; Text-Figure 5) (Legendre & Legendre, 1998). Log-transformation was used in order to normalize initially right-skewed distributions and to linearize possible allometric relations within the biometric space. This preliminary analysis returned highly significant results indicating two main sources of biometric variation between samples: the overall dinocyst size on the first canonical variate axis, and the relative size of ectocyst vs. endocyst on the second canonical variate axis.

We thus defined two simple log-transformed synthetic descriptors:

$$X = \log\left(\sqrt[4]{L_{EN} \times W_{EN} \times L_{EC} \times W_{EC}}\right), \text{ and}$$

$$Y = \log(D_{EN/EC}) = \log\left(\frac{L_{EN} \times W_{EN}}{L_{EC} \times W_{EC}}\right) = \log(L_{EN} \times W_{EN}) - \log(L_{EC} \times W_{EC}).$$

X is the log-transformed geometric mean of the four initial variables; it is an estimate of the overall size of the dinoflagellate cyst. Y is the log-transformed ratio (i.e., the Simpson Ratio; see Simpson et al., 1960: 356-358) of the endocyst and ectocyst length and width products (i.e., the $D_{EN/EC}$ ratio, expressed in percentage of ectocyst's length \times width), allowing the comparison of the relative (*not* absolute) dimensions of these two dinocyst structures. Y directly co-varies with the relative distance of ectocyst from endocyst: all size being equal, the greater the separation, i.e. the smaller the endocyst with respect to the ectocyst, the smaller Y and $D_{EN/EC}$. Thus, it is an estimate of one of the main “shape parameters” classically used to describe and discriminate the dinoflagellate cyst taxa considered in this work (see the Introduction section).

We then further analyzed each sampled Y -distribution for multi-normality using mixture analysis (Redner and Walker, 1984; Titterton et al., 1985). In each case, the mixture with the lowest associated Akaike Information Criterion value was selected in order to favour the solution that produces the best fit without overfitting.

Most comparisons were achieved using Student t -tests and one-way analyses of variance (ANOVA), including in both cases a Welch-Satterthwaite correction for unequal variances between samples when necessary (Satterthwaite, 1946; Welch, 1947; Sokal and Rohlf, 1995). All statistical analyses were performed using the PAST software, v. 1.64 (Hammer et al., 2001).

RESULTS

X and Y distributions were first analyzed for the two most intensively sampled early Zanclean sections: Maccarone (13 samples, 698 individuals) and Hinova (16 samples, 247 individuals) (Text-Figure 6). One-way ANOVAs of X and Y indicate a very high inter-level heterogeneity for both descriptors in the Maccarone section (X : $F = 87.9$; $d.f. = 12, 97$; $p = 2 \times 10^{-46}$; Y : $F = 13.9$; $d.f. = 12, 99$; $p = 2 \times 10^{-16}$ [both ANOVAs include a Welch-Satterthwaite correction]). Conversely, no heterogeneity is found in the Hinova section (X : $F = 1.15$; $d.f. = 15, 231$; $p = 0.31$; Y : $F = 1.04$; $d.f. = 15, 231$; $p = 0.41$). After the Messinian Salinity Crisis, no significant changes thus appear at Hinova in the size and shape of *Galeacysta etrusca*, with individuals showing a mean $D_{EN/EC}$ ratio of about 35%. In contrast, a three-step sequence is evidenced at Maccarone. At the beginning of the analyzed series of samples (levels 15 to 18: Popescu et al., 2007), assemblages are made of rather small-sized individuals with a mean $D_{EN/EC}$ ratio of about 34%, identical at the 95% confidence level to that observed at Hinova (Student t -test: $t = 1.87$; $d.f. = 323$; $p = 0.063$). At the end of the sequence (samples 35 to 42: Popescu et al., 2007), assemblages comprise rather large individuals with a mean $D_{EN/EC}$ ratio of about 41%, both X and Y mean values being significantly greater than observed previously (Student t -test on X : $t = 28.6$, $d.f. = 564$, $p = 3 \times 10^{-47}$; Student t -test on Y : $t = 7.14$, $d.f. = 564$, $p = 3 \times 10^{-12}$). Between these two sets of assemblages, intermediate samples illustrate a gradual compositional transition from assemblages dominated by small individuals with a mean $D_{EN/EC}$ ratio close to 34%, to assemblages dominated by large-sized individuals with a mean $D_{EN/EC}$ ratio of about 41%. Hence, the “transition effect” observed between the lower and upper parts of the Maccarone section is not the result of a gradual biometric change of individuals, but is the simple consequence of the gradual changing in relative abundance of smaller-sized and smaller- $D_{EN/EC}$ individuals (characteristic of the lower part of the analyzed time series) and larger-sized and larger- $D_{EN/EC}$ individuals (characteristic of the upper part of

the analyzed section). Thus, these first results clearly indicate that at least two stable, dimensionally homogeneous biometric groups (hereafter named “groups”) with mean D_{ENEC} ratios of about 34% and 41%, respectively, can be statistically distinguished at Maccarone, whereas a single one can be evidenced throughout the Hinova section.

At the level of the complete analyzed data set, mixture analyses of the 39 sampled Y -distributions allowed us to identify four distinct such stable biometric groups (named “a” to “d”; Plate 2) although these partly overlap one another (Table 2; Text-Figure 7). Groups “a”, “b” and “c” are characterized by individuals with a small, intermediate, and large D_{ENEC} ratio, with mean values of ca. 32–36%, 47–53%, and 60%, respectively, inversely related to the relative distance between the endocyst and ectocyst – the greater D_{ENEC} , the smaller distance. These three groups do not differ from one another in their mean size (X) values (see below). In contrast, group “d” is characterized by large individuals with a D_{ENEC} ratio of ca. 39–43%, intermediate between the mean values of groups “a” and “b”. Individuals from the previously described assemblages of the Hinova section and the lower part of the Maccarone section are referred to group “a”, while those of the upper part of the Maccarone section belong to group “d”.

In several localities, only one of the four biometric groups occurs (e.g., Valea Vacii and Hinova for group “a”, Krajačići and Eraclea Minoa for group “b”, Majs 2 for group “c”, and Maccarone samples 35 to 42 (Popescu et al., 2007) for group “d”, allowing us to draw an XY scatter plot for the corresponding individuals (Table 2; Text-Figure 8). A small, but highly significant positive linear relationship between X and Y is observed only for group “a” ($R^2 = 0.081$, $n = 333$, $p_{[H_0: R^2=0]} = 1.3 \times 10^{-7}$), whereas for both groups “b” and “d”, X and Y appear linearly independent (“b”: $R^2 = 1.6 \times 10^{-3}$, $n = 107$, $p = 0.68$; “d”: $R^2 = 2.4 \times 10^{-3}$, $n = 482$, $p = 0.29$). From this point of view, group “d”, which is observed only in the upper part of the Maccarone section (samples 35 to 42: Popescu et al., 2007), can be regarded as a local adaptation directly replacing group “a” (samples 15 to 18: Popescu et al., 2007). Actually, group “d” is characterized by X -values noticeably (ca. 30%) greater than the three other groups, indicating larger individuals, and Y -values slightly larger than for group “a”. Conversely, groups “a” and “b” (and also “c”) cannot be distinguished based on X -values, but can be statistically identified based on Y . A one-way ANOVA of Y between groups “a”, “b” and “d” (group “c” is not considered due to its scarcity in the data set) indicates a highly significant global heterogeneity between the three groups: $F = 102.5$, $d.f. = 2, 284$; $p = 3 \times 10^{-34}$ (including a Welch-Satterthwaite correction). A post-hoc contrast analysis, using Tukey’s HSD test, returns highly significant p -values for all three couples of groups ([a-b], [a-d] and [b-d]: $p = 2.2 \times 10^{-5}$ in all three cases), indicating significant pairwise differences between the three groups.

In some samples, two biometric groups occur together (e.g., Krašić and DSDP Hole 380A for groups “a” and “b”, Cernat for groups “a” and “c”). The way groups “a” and “b” are identified in such mixed samples is exemplified in Text-Figure 9. These two examples illustrate the fact that when these two groups are found simultaneously, their Y distribution partially overlaps. This first indicates that the rather large amount of superposition of groups “a” and “b” in Text-Figure 9 is partially, but very likely not completely, “real”. It could actually be, at least partially, an artificial consequence of failure of the mixture analysis to detect the joint occurrence of these two groups, leading to a false identification of individuals from group “b” as belonging to group “a” (or vice versa) when one of them markedly dominates the sample assemblage. Second, both Text-Figures 8 and 9 thus illustrate the fact that these biometric groups can only be identified and distinguished by statistical means, and by no means correspond to discrete morphotypes referable to distinct dinoflagellate cyst species. Statistically different stable biometric variants of *Galeacysta etrusca* do exist, but these variants describe a morphological continuum with no clear limits between them.

In summary, the following observations can thus be made (Table 2; Text-Figure 7).

Prior to the Messinian Salinity Crisis, group “b” is recorded alone at Krajačići (Plate 2, fig. 1), and group “c” at Majs 2 (Plate 2, figs. 8–9). At Krašić (Plate 2, fig. 5), group “a” is prevalent but group “b” is significantly represented. Groups “a” and “c” are unequally represented at Cernat and group “a” alone has been recorded at Valea Vacii. The *Galeacysta etrusca* specimens which are represented in the Mediterranean Basin as recorded at Cava Serredi and Eraclea Minoa belong to group “b”.

After the Messinian Salinity Crisis, the *Galeacysta etrusca* assemblage from Hinova (Plate 2, figs. 2–3) comprises only specimens of group “a”, but that from DSDP Hole 380A is represented by groups “a” (dominant) and “b”. Specimens recorded at Eraclea Minoa belong entirely to group “b” (Plate 2, fig. 4). Assemblages from Maccarone are more diverse and have changed along the interval during which *Galeacysta etrusca* is recorded: at the beginning of invasion, only group “a” (Plate 2, fig. 6) is present; then, three groups are recorded at the same levels (mostly group “d”, with “a” and “c” as subordinate groups); and finally only group “d” remains (Plate 2, figs. 7, 10–12). At San Donato, the *Galeacysta etrusca* specimens measured within the interval preceding its disappearance belong exclusively to group “b”.

DISCUSSION

Paratethyan and Mediterranean *Galeacysta etrusca* history around the Messinian/Zanclean boundary

In this study, the oldest *Galeacysta etrusca* specimens originate from the late Pannonian age (Majs 2 section in the Pannonian Basin) and belong to the biometric group “c”, i.e., specimens with rather high $D_{EN/EC}$ ratio values corresponding to dinocysts with a relatively small distance between the endocyst and ectocyst (Plate 2, figs. 8–9). Within this basin, we then distinguish groups “a” and “b” in the latest Pannonian Krašić section (Plate 2, fig. 1) and group “b” in the Krajačići section (Plate 2, fig. 5). Differences between these assemblages cannot be explained by time alone but, more probably, by an already existing paleoenvironmental diversification within the Pannonian Basin. The exclusive occurrence of group “c” at Majs 2, although based only on five specimens (Table 2), suggests that *Galeacysta etrusca* was living in fresh to brackish conditions just before the marine connection between the Pannonian Basin and the Mediterranean Sea (see above). This assumption is in agreement with the absence of any other marine organisms (including other dinoflagellate cyst species) and is consistent with the high $D_{EN/EC}$ ratio of *Galeacysta etrusca*. Groups “a” and “b”, identified at the Krajačići and Krašić sections (Plate 2, figs. 1, 5) show decreases in their $D_{EN/EC}$ ratio, probably in response to increased salinity as a result of the connection at high-sea level between the Pannonian Basin and Mediterranean Sea. This connection is supported by the presence in the Pannonian sections of Mediterranean calcareous nannoplankton and marine dinoflagellate cysts (*Achomosphaera andalousiensis*, *Nematosphaeropsis labyrinthus*) as at Krajačići.

In the Dacic Basin, at Cernat, *Galeacysta etrusca* shows two morphological groups: (1) group “c”, characterized by a high $D_{EN/EC}$ ratio, is represented in low percentages (11%) and corresponds to the “old” Pannonian stock, and (2) group “a”, which is dominant (89%) and could be related to more saline conditions than that associated to group “c”, induced by the connection between the Dacic Basin and Mediterranean Sea during the Portaferrian–Bosphorlian, as indicated by the presence of NN11b calcareous nannoplankton subzone in the same samples. The persistence only of group “a” in the early Bosphorlian Valea Vacii section suggests that environmental conditions in the Dacic Basin were stable and more saline in the early Bosphorlian than in the Portaferrian.

Before the Messinian Salinity Crisis, the southwestern Euxinian Basin was characterized by freshwater conditions according to Schrader's (1978) diatom record at DSDP Hole 380A (Text-Figure 1). Indeed, we found no marine or brackish dinoflagellate cyst, including *Galeacysta etrusca*, in the same intervals of DSDP Hole 380A (Popescu, 2006). However, the presence in the Crimea of calcareous nannoplankton of subzone NN11b (Semenenko and Olejnik, 1995) indicates that the Euxinian and Dacic basins were probably connected in the early Bosphorion; the gateway was located at the Reni Strait according to Semenenko and Olejnik (1995).

In the Mediterranean Basin, only *Galeacysta etrusca* group "b" was recorded at Cava Serredi and Eraclea Minoa, in sediments dating from the latest Messinian. At Cava Serredi, *Galeacysta etrusca* Corradini & Biffi 1988 is accompanied by *Impagidinium* sp. 1 and 2 of Corradini and Biffi (1988), which may be referable to *Millioudodinium bacculatum* and *Spiniferites cruciformis*, respectively (Popescu et al., 2007), two species with Paratethyan affinities. Group "b" recorded in the Mediterranean Basin probably represents an adaptation of *Galeacysta etrusca* to a new environment after its arrival from the Paratethys during the high sea-level just preceding the peak of the Messinian Salinity Crisis (i.e. the desiccation phase delimited on Text-Figure 7). Group "a" has lower $D_{EN/EC}$ ratio than group "b", but as shown above, these groups can occur simultaneously and do not correspond to clearly discrete morphotypes. The presence of *Galeacysta etrusca* in the Mediterranean Basin before the Messinian Salinity Crisis peak documents the connection between the Mediterranean and Paratethys in the late Messinian corresponding to the first "Lago Mare" event (Clauzon et al., 2005).

Connections between the remnant Paratethys and the Mediterranean between 8 and 5 Ma are debated intensely, as are the connections between the Paratethyan basins themselves (Stevanović, 1974; Archambault-Guézou, 1976; Rögl and Steininger, 1983; Kojumdgieva, 1987; Marinescu, 1992; Magyar et al., 1999b; Müller et al., 1999; Meulenkamp and Sissingh, 2003; Popov et al., 2006; and Piller et al., 2007). Based on the evidence of similar fossils (mainly *Congeria rhomboidea*) in the Pannonian and Dacic basins, Stevanović (1951) proposed the opening of a gateway between these basins in the area of the Iron Gates and created the Portaferrian Regional substage (from the French *Portes de Fer* for Iron Gates). In fact, the Portaferrian Stage *sensu* Stevanović (1951) corresponds partly to the upper part of the Pannonian Stage in the Lake Pannon (Magyar et al., 1999a; Müller et al., 1999; Piller et al., 2007), the waters of which momentarily entered the Dacic Basin.

The presence of Mediterranean calcareous nannoplankton in the Maeotian of the Dacic Basin (Mărunțeanu and Papaionopol, 1998; Snel et al., 2006) but also the Pannonian Basin at Krajačići, simultaneously with the presence of Mediterranean marine dinoflagellate cysts, suggests that these Paratethyan basins were connected to the Mediterranean Sea at high sea-level at around 7 Ma. It has been demonstrated that the Iron Gates passage through the Carpathians, constantly refuted by Marinescu (1992), was in fact made by fluvial downcutting during the peak of the Messinian Salinity Crisis (Clauzon et al., 2005; Leever, 2007). In addition, it has been established by Clauzon et al. (2005) that the connection between the Dacic Basin and the Mediterranean Sea, passing by Thessaloniki, Skopje, Niš and the modern Timok Valley (Text-Figure 10A, B), was probably active from 13.5 Ma until about 4 Ma based on the occurrence of Mediterranean calcareous nannoplankton in the Dacic Basin (Mărunțeanu and Papaionopol, 1995; 1998). As a consequence, we propose that this corridor extended through a western branch entering the Pannonian Basin in the area of Niš–Belgrade up to 5.60 Ma exclusively (Text-Figure 10A). As the western branch of this corridor was probably already active at about 7 Ma, based on the marine dinoflagellate cysts and coccoliths recorded at Krajačići (Text-Figure 2), one must envisage some delay in the arrival of the sublittoral to lacustrine *Congeria rhomboidea* in the Dacic Basin. Anyway, all the data are in

agreement with the closure of this branch at the beginning of the Bosphorion (Text-Figure 2). A two-way current probably worked in such gateways, as today in the Bosphorus Strait where the marine Mediterranean water inflows through the corridor as bottom water, where it brings marine organisms to the Black Sea, while less saline Black Sea water outflows at the surface and transports brackish organisms into the Mediterranean (Guibout, 1987; Bethoux and Gentili, 1999). Such similar opposed currents may have existed in the past and explain the repeated entries of *Galeacysta etrusca* into the Mediterranean Basin.

During the Messinian Salinity Crisis, important paleogeographic changes impacted Europe: the Mediterranean and the Black Sea (i.e. the Euxinian Basin) almost desiccated; the Dacic Basin, the Adriatic and Po realm persisted as suspended lakes (Clauzon et al., 2005, Popescu et al., 2007) and became brackish to freshwater; and the Pannonian Basin became very reduced as it was also affected by an intensive fluvial erosion (Csato et al., 2007).

Galeacysta etrusca group “a” (Plate 2, figs. 2-3), because it was prevalent in the Dacic Basin before the peak of the Messinian Salinity Crisis, probably survived when this basin partly shrank as a suspended lake during the paroxysm of the crisis (Clauzon et al., 2005) and, as a consequence, was alone in the basin at the earliest Zanclean (Hinova section). As soon as the connection between the Dacic Basin and the Mediterranean Sea was re-established at the end of the Messinian Salinity Crisis, this species re-invaded the Mediterranean realm. At that time, group “b”, which replaces group “a” when salinity increases, is recorded at Eraclea Minoa in fully marine waters accompanied by the other Paratethyan species: *Spiniferites cruciformis*, *Pterocysta cruciformis* and *Seriliodinium explicatum* (Londeix et al., 2007).

Fresh- to brackish-water conditions existed in the Adriatic–Po realm in the latest Messinian as indicated at the Maccarone section (Popescu et al., 2007). But Popescu et al. (2007 text-fig. 7) have shown that two major marine incursions were recorded at Maccarone: (1) below the Colombacci Formation (i.e. the second “Lago Mare” event) as supported by abundant marine dinoflagellate cysts and a high diversity of calcareous nannoplankton including the marker *Ceratolithus acutus* (Text-Figure 2), and (2) above the Colombacci Formation as supported by such marine organisms as dinoflagellate cysts, calcareous nannoplankton and more abundant planktonic foraminifers. The first marine incursion probably modified the previous freshwater conditions into brackish water ones, similar to those of the Dacic Basin, thus permitting the immigrant Paratethyan species to colonize this basin without changing their morphology. Indeed, *Galeacysta etrusca* was first represented by group “a” (Plate 2, fig. 6; Text-Figure 7). Then, continuous freshwater river input and brief minor marine influxes within the Colombacci Formation induced weak fluctuations in salinity and nutrient content that might explain the morphological diversification of *Galeacysta etrusca* into groups “c” and “d” while accompanied by the persisting group “a” (Plate 2, figs. 7, 10–12; Text-Figures 6, 7). Finally, the development of stable environmental conditions produced group “d” in the uppermost Colombacci Formation before its disappearance at the second major marine invasion (Plate 2, figs. 10-12; Text-Figure 7). With respect to the recent chronology established for the Maccarone section (Popescu et al., 2007), this adaptation process lasted only about 50 kyrs, i.e., between the first appearance of *Ceratolithus acutus* (5.35 Ma) and that of the planktonic foraminifer *Sphaeroidinellopsis* (5.30 Ma: Lourens et al., 2004). Northward, at San Donato (Text-Figure 1), *Galeacysta etrusca* arrived later (in the uppermost layer of the Colombacci Formation), without other Paratethyan immigrants, when marine conditions were almost completely established. This explains why group “b” alone is recorded, as at Eraclea Minoa.

Later on (at ca. 5.13 Ma), dinoflagellates of the Dacic Basin entered the Black Sea (Euxinian Basin) when the sea level rose to overflow the Reni Sill, developing predominant cysts of group “a” accompanied by fewer specimens of group “b” (Plate 2, fig. 4).

Environmental, hydrographic and geographic insights from *Galeacysta etrusca*

Based on the above-discussed scenario, it is now possible to answer the questions challenged in the Introduction.

First, it appears unrealistic to distinguish from the available evidences the two “Lago Mare” events in the Mediterranean Basin on the basis of *Galeacysta etrusca* morphology and biometry as we have observed and measured it. Indeed, this study establishes that each invasion of Paratethyan dinoflagellates is represented by *Galeacysta etrusca* individuals exclusively belonging to biometrical group “a” (corresponding to specimens with a relatively large distance between the endocyst and ectocyst), which probably reflects a stable morphology related to more saline conditions, as found in the Paratethyan sections and in the lower part of the studied Maccarone section. When the species faces marine conditions, group “a” is replaced by group “b”, as recorded at Cava Serredi and Eraclea Minoa. Group “d” seems to be linked to increases both in salinity and nutrient content. Finally, group “c” appears to characterize freshwater environments.

Second, the accurate chronologic location of the studied materials and the high environmental sensitivity of *Galeacysta etrusca* undoubtedly refine our knowledge of the Central–Eastern Mediterranean and Paratethys during the time-interval 6–5 Ma as detailed below.

From ca. 8 Ma to 5.60 Ma (Text-Figures 2, 7), the connection of the Pannonian Basin both with the Dacic Basin and the Mediterranean Sea should be envisaged as a Y-shaped corridor with two northern branches diverging northward of Niš (Text-Figure 10A). This reconstruction is consistent with geological maps (Kräutner and Krstić, 2003) and some previous assumptions (see for example: Stanković *in* Hsü et al., 1978, p. 1073, except that we attribute the “Lago Mare” events to exchanges at high sea-level between the Mediterranean and Paratethys; see also: Marinescu *in* Hsü, 1978, p. 517, except that their map was proposed for the Pliocene and shows another passage at the place of the Iron Gates, a possibility quite rightly refuted by Marinescu, 1992). The gateway proposed here not only allowed Pannonian Basin–Mediterranean and Dacic Basin–Mediterranean exchanges but also Pannonian–Dacic basin exchanges. Southward, this corridor passed through Skopje to reach the Aegean Sea at present-day Gulf of Thermaikos (Clauzon et al., 2005). Along this corridor (Text-Figure 10A) we observe several Messinian and Zanclean Mediterranean marine deposits separated by a strong erosional surface. After the Messinian Salinity Crisis, the corridor was re-established without its western branch, probably because of uplift in the southwestern Carpathians. Water-mass exchanges at high sea-level resumed, but were limited to the Mediterranean and the Dacic Basin while the Pannonian Basin was isolated and significantly restricted (Text-Figure 10B). The corridor probably joined the Dacic Basin in the area of the present-day Timok Valley, i.e. at the distal part of the Zanclean Gilbert-type fan delta constructed by the proto-Danube River, which cut the Carpathians during the Messinian desiccation phase at the place of the present-day Iron Gates Gorge (Text-Figure 10B; Clauzon et al., 2005; Leever, 2007). This proto-Danube River probably originated from the western edge of the Carpathians, where some important latest Miocene fluvial erosion has been evidenced (Csato et al., 2007).

The late arrival of Mediterranean dinoflagellate cysts in the southern Black Sea requires explanation. Because the Black Sea desiccated at the same time as the Mediterranean, one must consider: (1) a connection with the Mediterranean Sea prior to the Messinian Salinity Crisis, and (2) the emerging drier climatic regional conditions evidenced by Popescu (2006), which were likely reinforced considerably by the Mediterranean desiccation in progress. It has been demonstrated that no connection was possible through the area of the present-day Bosphorus Strait before or after the crisis (Popescu, 2006), an assumption reinforced by evidence of the Messinian Erosional Surface at DSDP Sites 381 and 380, i.e. extending from

the southwestern Black Sea shelf to the basin (Gillet et al., 2007). Hence, the connection between the Black Sea and the Mediterranean seems to have been through the Dacic Basin and the Reni Strait in the area of the Dobrogea horst, as proposed by Semenenko and Olejnik (1995). No Mediterranean calcareous nannoplankton were recorded at Site 380 before or after the crisis, and no Mediterranean dinoflagellate cysts were found before the crisis although they invaded this basin after a delay of 200 kyrs in the early Zanclean. However, Mediterranean marine calcareous nannoplankton arrived at the Crimea before and after the Messinian Salinity Crisis (subzones NN11b and NN12b, respectively) through the Dacic Basin (Semenenko and Olejnik, 1995). One must thus conceive that: (1) at Site 380, the Messinian beds presumably containing Mediterranean calcareous nannoplankton and dinoflagellate cysts were eroded during the desiccation phase, and (2) the post-desiccation (subzone NN12b) calcareous nannoplankton from the Crimea are coeval with the first marine dinoflagellate cysts and diatoms at Site 380 (i.e. 5.13 Ma, consistent with the temporal range of *Ceratolithus acutus*; Text-Figure 2). The fluvial erosion that dismantled the northern shelf of the Black Sea during the desiccation phase did not impact the Dobrogea horst (Gillet et al., 2003). The supposed obstacle of the Reni Sill (Text-Figure 10A) was crossed again by marine Mediterranean waters at 5.13 Ma, which could explain the delayed arrival of Zanclean marine Mediterranean calcareous nannoplankton, dinoflagellates, and diatoms into the Euxinian Basin (Schrader, 1978; Popescu, 2006).

In the Central Mediterranean, the first invasion by Paratethyan dinoflagellates occurred almost simultaneously as recorded at Eraclea Minoa, Cava Serredi, and Aghios Sostis (Zakynthos Island). This invasion only relates to the Mediterranean Basin itself as no record of this pre-desiccation “Lago Mare” phase has ever been documented in the Adriatic–Po realm. The Paratethyan immigrants did not enter this realm before the Zanclean probably because of important uplift in the area during the first stage of the Messinian Salinity Crisis (Scarselli et al., 2006). During the desiccation phase, the Adriatic–Po realm persisted as a suspended freshwater basin with a continuous clayey to turbiditic sedimentation in the Apennine foredeep (Clauzon et al., 1997, 2005; Scarselli et al., 2006). Simultaneously, Messinian marginal evaporites were reworked in the Apennine foredeep (Manzi et al., 2007). Owing to the well-dated succession of bioevents in the nannoflora (Text-Figure 2), it is possible to refine the paleogeographic reconstruction by the precise timing of the successive arrivals of Paratethyan dinoflagellates into the Mediterranean. The new Paratethyan immigrants arrived at about 5.48 Ma in the Central Mediterranean as indicated by the Eraclea Minoa section, but they reached the Adriatic realm about 50 kyrs later (Text-Figure 7), when the Mediterranean sea-level was high enough to overflow the uplifting Otranto Sill (Text-Figure 10), a barrier created by the offshore extension of the Apulia shelf margin in conjunction with a major NE–SW transcurrent fault system (Clauzon et al., 1997).

To summarize, the role of straits and sills appears essential for deciphering paleogeographic changes in the crucial 8–5 Ma time-interval during which enormous changes in sea-level interplayed with intense tectonic movements. It has been possible to constrain the successive values of the Mediterranean sea-level during this time (Clauzon, 1996; 1999). Estimates are based on: (1) the global sea-level before the onset and after the end of the Messinian Salinity Crisis (i.e., when the Mediterranean was connected to the Atlantic Ocean) as given by Haq et al. (1987), and (2) meticulous field studies allowing the relative effects of sea-level change and regional tectonic movement throughout the Mediterranean (marginal and central basins) to be differentiated, including the interval during which it was isolated. These estimates are (see Text-Figure 2 for the precise chronology; asl–bsl = above–below the present global sea-level) (Clauzon, 1996; 1999; Clauzon et al., 1996):

- 40 m asl at 6 Ma; ca. 110 m bsl between 5.96 and about 5.70 Ma, especially for marginal basins relatively isolated by sills (i.e. the marginal episode of the crisis);

- 40 m asl between about 5.70 and 5.60 Ma, a sea-level rise mostly recorded in marginal basins (corresponding in particular to the Sicilian Upper Evaporites ending with the first “Lago Mare” event at high sea-level; Text-Figure 1);
- about 1500 m bsl between about 5.60 and 5.48 Ma (deep-basin episode of the crisis; see also: Savoye and Piper, 1991; Lofi et al., 2005; Sage et al., 2005);
- 80 m asl at 5.48–5.33 Ma, after the post-Messinian Salinity Crisis reflooding (starting with the second “Lago Mare” event at high sea-level).

Dinoflagellates are here shown to be highly effective organisms for establishing connection and/or isolation phases of the various basins adjacent to the Mediterranean. As the opposing migrations of Paratethyan and Mediterranean dinoflagellates must necessarily occur during phases of high sea-level, they are potentially useful for discriminating between the effects of local tectonic movements and regional sea-level changes. Among the Paratethyan dinoflagellate cysts, *Galeacysta etrusca* appears the most sensitive marker of the “Lago Mare” events because its migration is narrowly linked to high sea-level phases. This is particularly true when comparing the vertical distribution of *Galeacysta etrusca* and dreissenids at Eraclea Minoa: *Galeacysta etrusca* is recorded in the relative high sea-level deposits represented by diatomitic turbidites preceding the last gypsum bed and in the Arenazzolo Formation, while dreissenids occur within the Lago Mare Formation which corresponds to a relative lowering of sea-level (Text-Figure 4). As dreissenids may develop in invading coastal lagoon environments, they are more significant of local brackish conditions (possibly continuing after the invasion event) than *Galeacysta etrusca*, which precisely demarcates the exchange events at high sea-level between basins. *Galeacysta etrusca* appears also more effective in signalling such exchanges than ostracods of the *Cyprideis pannonica* group, which shows a wider distribution in both space and time. These ostracods were used alone to define a dilution phase by river input recorded in the almost desiccated Mediterranean basins and ending the peak of the Messinian Salinity Crisis (McCulloch and De Deckker, 1989; Rouchy et al., 2001). This brief dilution event has been used wrongly to change the significance of the “Lago Mare” events (Orszag-Sperber, 2006); it does not result from an exchange at high sea-level between the Mediterranean and Paratethys but more probably from a colonization of new freshwater habitats.

Galeacysta etrusca was also recorded in Late Pliocene deposits from ODP Site 898 in the Atlantic Ocean westward of the Iberian Peninsula coastline (McCarthy and Mudie, 1996). The authors invoke either a possible reworking or some transport in the Mediterranean overflow water. As the published photograph (McCarthy and Mudie, 1996: pl. 2, fig. 12) is not particularly convincing, we are cautious about this record. However, it might be an extra-Mediterranean signal of a “Lago Mare” event more recent than those discussed in this paper, a prospect not unrealistic if considering the almost continuous record of Mediterranean calcareous nannoplankton in the Dacic Basin up to Late Pliocene zone NN16 (Mărunțeanu and Papaianopol, 1995; 1998; Lourens et al., 2004). Indeed, the “Lago Mare” events resulting from exchanges at high sea-level between the Mediterranean and Paratethys may have occurred at any time during the Late Neogene so long as a gateway was active between these basins. An older example of Mediterranean–Paratethys connection was documented by Archambault-Guézou et al. (1979) according to an euxinic mollusc fauna found just below the Crevillente 6 mammal level in southeastern Spain, i.e. prior to 6.10 Ma (Garcés et al., 1998). This mollusc fauna shows affinities with the Maeotian mollusc fauna from the Eastern Paratethys (Archambault-Guézou et al., 1979).

CONCLUSION

The high specificity of dinoflagellate cysts for reconstructing paleoenvironments is emphasized in this study, which reveals the extreme sensitivity of *Galeacysta etrusca*. Indeed, new biometric analyses and previously documented records of *Galeacysta etrusca* from the Late Neogene of the Paratethys and Mediterranean allow us to reconstruct the history of the species within the framework of paleogeographic changes that occurred from 8 to 5 Ma. The associated chronology of calcareous nannoplankton bioevents, and the stratigraphic location of the studied deposits with respect to the isochronous Messinian Erosional Surface (formed at the peak of the Messinian Salinity Crisis), have together been particularly useful for depicting the chronological framework that underpins this study. This results in a reliable history of this species, especially regarding its significance as an immigrant from the Paratethys into the Mediterranean, its migration during high sea-level episodes (i.e. the “Lago Mare” events), the timing of such episodes, and the locations and courses of the gateways contra Orszag-Sperber, (2006, p. 270).

Galeacysta etrusca originated from the Pannonian Basin in the Late Miocene. It invaded the Dacic Basin during the interval 6–5.60 Ma, from where it migrated into the Mediterranean at least twice (major phases at ca. 5.60 and 5.48–5.33 Ma, i.e. just before and just after the peak of the Messinian Salinity Crisis, respectively) and, later (at ca. 5.13 Ma), towards the Black Sea.

Among the four statistically defined stable biometric groups (Text-Figure 7), group “a” appears to characterise brackish environments, accompanied by group “c” when freshwater input increases, while group “b” immediately replaces group “a” when salinity increases. The large size of individuals in group “d” developed in peculiar nutrient-rich conditions. This diversification into morphological groups developed irrespective of the realm (Paratethyan or Mediterranean) and period, with the possible exception of group “d” which has presently been recorded only from the latest Messinian of the Adriatic.

From a paleogeographic perspective, the Portaferrian connection (6–5.60 Ma) between the Pannonian and Dacic basins is supported by this study, and its location specified: a Y-shaped corridor with two northern branches joining the Pannonian and Dacic basins together, and both to the Aegean Sea (Text-Figure 10A). The status of the Adriatic–Po realm as a suspended and isolated basin during the desiccation phase of the Mediterranean (as was probably the Dacic Basin in part) is supported by our data which document a delayed arrival (50 kyrs) of *Galeacysta etrusca* compared to the Mediterranean Basin. The late arrival of the Mediterranean marine dinoflagellates accompanied by *Galeacysta etrusca* into the Black Sea at ca. 5.13 Ma documents paleogeographic assumptions about its relationship with the nearby Dacic Basin (Text-Figure 10).

Finally, field observations (Text-Figure 4) and dinoflagellate cyst data indicate the reflooding of the Mediterranean Basin by Atlantic waters at 5.48 Ma, i.e. significantly earlier than the GSSP of the Zanclean Stage at 5.33 Ma.

ACKNOWLEDGEMENTS

We are indebted to A. Bossio who provided his old photograph from Cava Serredi; to M.-A. Bassetti who provided her palynological residues from San Donato; to the late F. Marinescu and I. Papaianopol who guided J.-P.S and G.C. in 1998 at Cernat and Valea Vacii; and to the directors of the Cava Serredi Factory and Casabianda Prison who authorized several visits to the exposed deposits. The Ocean Drilling Program provided the samples from Hole 380A. The manuscript has been significantly improved by the comments done by the reviewers, L. Edwards and W. Piller, and the Editor of the issue, F. McCarthy. This paper is a

publication of the French Programs ECLIPSE II CNRS and ANR EGEO. Contribution UMR 5125-08.007.

References cited

ARCHAMBAULT-GUÉZOU, J.

1976 Présence de Dreissenidae euxiniques dans les dépôts à Congéries de la vallée du Rhône et sur le pourtour méditerranéen. Implications biogéographiques. *Bulletin de la Société Géologique de France*, ser. 7, 18(5): 1267–1276.

ARCHAMBAULT-GUÉZOU, J., ILINA, L.B., KELLER, J.-P., and MONTENAT, C.

1979 Affinités euxiniques des mollusques messiniens d'Elche (Alicante, Espagne) et implications paléogéographiques. *Annales Géologiques des Pays Helléniques*, hors série, 1: 27–37.

BALTEŞ, N.

1971 Pliocene Dinoflagellata and Acritarcha in Romania. In Farinacci, A. (ed.). *Proceedings of the Second Planktonic Conference*, Rome 1970, p. 1–16.

BASSETTI, M.A.

1997 *Il Messiniano clastico post-evaporitico nelle Marche (Bacino Interno)*. Unpublished Ph.D. thesis, University of Bologna, Bologna, Italy, 163 p.

BERTINI, A.

2006 The northern Apennines palynological record as a contribute for the reconstruction of the Messinian palaeoenvironments. *Sedimentary Geology*, 188/189: 235–258.

BERTINI, A., CORRADINI, D., and SUC, J.-P.

1995 On *Galeacysta etrusca* and the connections between the Mediterranean and the Paratethys. *Romanian Journal of Stratigraphy*, 76(7): 141–142.

BETHOUX, J.P., and GENTILI, B.

1999 Functioning of the Mediterranean Sea: past and present changes related to freshwater input and climate changes. *Journal of Marine Systems*, 20: 33–47.

BOSSIO, A., GIANNELLI, L., MAZZANTI, R., MAZZEI, R., and SALVATORINI, G.

1981 Gli strati alti del Messiniano, il passaggio Miocene–Pliocene e la sezione plio-pleistocenica di Nugola nelle colline a NE dei Monti Livornesi. *Abstracts from the 9th Congress of the Società Paleontologica Italiana*, Pacini, Pisa, 1981: 55–90 [excursion guide-book].

BRAGA, J.C., MARTÍN, J.M., RIDING, R., AGUIRRE, J., SÁNCHEZ-ALMAZO, I.M., and DINARÈS-TURELL, J.

2006 Testing models for the Messinian salinity crisis: The Messinian record in Almería, SE Spain. *Sedimentary Geology*, 188/189: 131–154.

BROLSMA, M.J.

1975 Lithostratigraphy and foraminiferal assemblages of the Miocene–Pliocene transitional strata of Capo Rossello and Eraclea Minoa (Sicily, Italy). *Proceedings of the Koninklijke Nederlandse Akademie Van Wetenschappen*, Series B, 78(5): 341–380.

BROLSMA, M.J.

1976 Discussion of the arguments concerning the palaeoenvironmental interpretation of the Arenazzolo in Capo Rossello and Eraclea Minoa (S. Sicily, Italy). *Memorie della Società Geologica Italiana*, 16: 153–157.

BUTLER, R.W.H., LICKORISH, W.H., GRASSO, M., PEDLEY, H.M. and RAMBERTI, L.

- 1995 Tectonics and sequence stratigraphy in Messinian basins, Sicily: Constraints on the initiation and termination of the Mediterranean salinity crisis. *Geological Society of America Bulletin*, 107: 425–439.
- CARNEVALE, G., LANDINI, W., and SARTI, G.
2006 Mare versus Lago-Mare: marine fishes and the Mediterranean environment at the end of the Messinian Salinity Crisis. *Journal of the Geological Society of London*, 163: 75–80.
- CAVALLO, O., and REPETTO, G.
1998 Un nuovo giacimento della facies a Congerie nell'Albese. *Rivista Piemontese di Storia Naturale*, 9: 43–62.
- CITA, M.B., WRIGHT, R.C., RYAN, W.B.F., and LONGINELLI, A.
1978 Messinian paleoenvironments. *Initial Reports of the Deep Sea Drilling Project*, 42(1): 1003–1035.
- CLAUZON, G.
1996 Limites de séquences et évolution géodynamique. *Géomorphologie*, 1: 3–22.
- CLAUZON, G.
1999 L'impact des variations eustatiques du bassin de Méditerranée occidentale sur l'orogène alpin depuis 20 Ma. *Etudes de géographie physique*, 28: 1–8.
- CLAUZON, G., RUBINO, J.-L., and CASERO, P.
1997 Regional modalities of the Messinian Salinity Crisis in the framework of two phases model. *Abstracts from the R.C.M.N.S. Interim-Colloquium on Neogene basins of the Mediterranean region: controls and correlation in space and time, Catania, November 1997*: 44–46 (abstract).
- CLAUZON, G., SUC, J.-P., GAUTIER, F., BERGER, A., and LOUTRE, M.-F.
1996 Alternate interpretation of the Messinian salinity crisis: Controversy resolved? *Geology*, 24(4): 363–366.
- CLAUZON, G., SUC, J.-P., POPESCU, S.-M., MĂRUNȚEANU, M., RUBINO, J.-L., MARINESCU, F., and MELINTE, M.C.
2005 Influence of the Mediterranean sea-level changes over the Dacic Basin (Eastern Paratethys) in the Late Neogene. The Mediterranean Lago Mare facies deciphered. *Basin Research*, 17: 437–462.
- CORRADINI, D., and BIFFI, U.
1988 Etude des dinokystes à la limite Messinien-Pliocène dans la coupe Cava Serredi, Toscane, Italie. *Bulletin des Centres de Recherche Exploration-Production Elf-Aquitaine*, 12 (1): 221–236.
- CORSELLI, C., and GRECCHI, G.
1984 The passage from hypersaline to hyposaline conditions in the Mediterranean Messinian: Discussion of the possible mechanisms triggering the “Lago Mare” facies. *Paléobiologie continentale*, 14 (2): 225–239.
- COUR, P.
1974 Nouvelles techniques de détection des flux et de retombées polliniques: étude de la sédimentation des pollens et des spores à la surface du sol. *Pollen et Spores*, 16(1): 103–141.
- CSATO, I., KENDALL, C.G.St C., and MOORE, P.D.
2007 The Messinian problem in the Pannonian Basin, Eastern Hungary – Insights from stratigraphic simulations. *Sedimentary Geology*, 201: 111–140.
- DALE, B.,
1996 Dinoflagellate cyst ecology: modeling and geological applications. In: Jansonius, J., McGregor, D.C. (Eds.), *Palynology: Principles and Applications*. American Association of Stratigraphic Palynologists Foundation, Dallas, pp. 1249–1276.

- DE VERNAL, A., GOYETTE, C., RODRIGUES, C.G.
 1989 Contribution palynostratigraphique (dinokystes, pollen et spores) à la connaissance de la mer de Champlain: coupe de Saint Cezaire, Québec. *Canadian Journal of Earth Sciences* 26, 2450–2464.
- DRIVALIARI, A., ȚICLEANU, N., MARINESCU, F., MARUNȚEANU, M., and SUC, J.-P.
 1999 A Pliocene climatic record at Țicleni (Southwestern Romania). In: Wrenn, J.H., Suc, J.-P. and Leroy, S.A.G (eds.). *The Pliocene: Time of Change*, American Association of Stratigraphic Palynologists Foundation, Dallas, Texas, U.S.A., p.103–108.
- DUGGEN, S., HOERNLE, K., VAN DEN BOGAARD, P., RÜPKE, L., and MORGAN, J.P.
 2003 Deep roots of the Messinian salinity crisis. *Nature*, 422: 602–604.
- ELLEGAARD, M.
 2000 Variations in dinoflagellate cyst morphology under conditions of changing salinity during the last 2000 years. *Review of Palaeobotany and Palynology* 109: 65– 81.
- FAUQUETTE, S., SUC, J.-P., BERTINI, A., POPESCU, S.-M., WARNY, S., BACHIRI TAOUFIQ, N., PEREZ VILLA, M.-J., CHIKHI, H., FEDDI, N., SUBALLY, D., CLAUZON, G., and FERRIER, J.
 2006 How much did climate force the Messinian salinity crisis? Quantified climatic conditions from pollen records in the Mediterranean region. *Palaeogeography, Palaeoclimatology, Palaeoecology*, 238(1–4): 281–301.
- GARCÉS, M., KRIJGSMAN, W., and AGUSTÍ, J.
 1998 Chronology of the late Turolian deposits of the Fortuna basin (SE Spain): implications for the Messinian evolution of the eastern Betics. *Earth and Planetary Science Letters*, 163: 69–81.
- GILLET, H., LERICOLAIS, G., RÉHAULT, J.-P., and DINU, C.
 2003 La stratigraphie oligo–miocène et la surface d'érosion messinienne en mer Noire, stratigraphie sismique haute résolution. *Comptes Rendus Geosciences*, 335: 907–916.
- GILLET, H., LERICOLAIS, G., and RÉHAULT, J.-P.
 2007 Messinian events in the Black Sea: Evidence of a Messinian erosional surface. *Marine Geology*, 244: 142–165.
- GUIBOUT, P.
 1987 *Atlas hydrologique de la Méditerranée*. SDP IFREMER, Brest, 150 p.
- HAMMER, Ø., HARPER, D.A.T., and RYAN, P.D.
 2001 PAST: Paleontological Statistics Software Package for Education and Data Analysis. *Palaeontologia Electronica*, 4: 9 p.
- HAQ, B.U., HARDENBOL, J., and VAIL, P.R.
 1987 Chronology of fluctuating sea levels since the Triassic (250 million years ago to present). *Science*, 235: 1156–1167.
- HEAD, M.J.
 2007 Last Interglacial (Eemian) hydrographic conditions in the southwestern Baltic Sea based on dinoflagellate cysts from Ristinge Klint, Denmark. *Geological Magazine*, 44:
- HILGEN, F.J., and LANGEREIS, C.G.
 1993 A critical re-evaluation of the Miocene/Pliocene boundary as defined in the Mediterranean. *Earth and Planetary Science Letters*, 118: 167–179.
- HSÜ, K.J., CITA, M.B., and RYAN, W.B.F.
 1973 The origin of the Mediterranean evaporites. *Initial Reports of the Deep Sea Drilling Project*, 13: 1203–1231.
- HSÜ, K.J.

- 1978 Stratigraphy of the lacustrine sedimentation in the Black Sea. *Initial Reports of the Deep Sea Drilling Project*, 42(2): 509–524.
- HSÜ, K.J., MONTADERT, L., BERNOULLI, D., CITA, M.B., ERICKSON, A., GARRISON, R.E., KIDD, R.B., MELIÈRES, F., MÜLLER, C., and WRIGHT, R.
- 1978 History of the Mediterranean salinity crisis. *Initial Reports of the Deep Sea Drilling Project*, 42(1): 1053–1078.
- JOLIVET, L., AUGIER, R., ROBIN, C., SUC, J.-P., and ROUCHY, J.M.
- 2006 Lithospheric-scale geodynamic context of the Messinian salinity crisis. *Sedimentary Geology*, 188–189, 9–33.
- KOJUMDGIEVA, E.
- 1987 Evolution géodynamique du bassin Egéen pendant le Miocène Supérieur et ses relations à la Paratéthys Orientale. *Geologica Balcanica*, 17(1): 3–14.
- KONTOPOULOS, N., ZELILIDIS, A., PIPER, D.J.W., and MUDIE, P.J.
- 1997 Messinian evaporites in Zakynthos, Greece. *Palaeogeography, Palaeoclimatology, Palaeoecology*, 129: 361–367.
- KOVÁČIC, M., ZUPANIČ, J., BABIĆ, L.J., VRDALJKO, D., MIKNIĆ, M., BAKRAČ, K., HEĆIMOVIĆ, I., AVANIĆ, R., and BRKIĆ, M.
- 2004 Lacustrine basin to delta evolution in the Zagorje Basin, a Pannonian sub-basin (Late Miocene: Pontian, NW Croatia). *Facies*, 50: 19–33.
- KRÄUTNER, H.G., and KRSTIĆ, B.
- 2003 *Geological map of the Carpatho–Balkanides between Mehadia, Oravița, Niš and Sofia*. Geoinstitut, Belgrade, map at scale 1/300,000.
- KRIJGSMAN, W., HILGEN, F.J., RAFFI, I., SIERRO, F.J. and WILSON, D.S.
- 1999 Chronology, causes and progression of the Messinian salinity crisis. *Nature*, 400: 652–655.
- LEEVEER, K.
- 2007 Foreland of the Romanian Carpathians. Controls on late orogenic sedimentary basin evolution and Paratethys paleogeography. Published Ph.D. thesis, NSG publication n° 20071204, Vrije University of Amsterdam, 182 p.
- LEGENDRE, P., and LEGENDRE, L.
- 1998 *Numerical ecology*. Elsevier, Amsterdam, 853 p.
- LEWIS, J., and HALLETT, R.
- 1997 *Lingulodinium polyedrum (Gonyaulax polyedra)*, a blooming dinoflagellate. *Oceanography and Marine Biology Annual Review*, 35: 97–161.
- LEWIS, J., ROCHON, A., and HARDING, I.
- 1999 Preliminary observations of cyst-theca relationships in *Spiniferites ramosus* and *Spiniferites membranaceus* (Dinophyceae). *Grana*, 38: 113–124.
- LEWIS, J., ELLEGAARD, M., HALLETT, R., HARDING, I., ROCHON, A.
- 2003 Environmental control of cyst morphology in gonyaulacoid dinoflagellates. In: Matsuoka, K., Yoshida, M., and Iwataki, M. (eds.). *Dino7*, Seventh International Conference on Modern and Fossil Dinoflagellates, Nagasaki, Japan, September 21–25; Program, Abstracts & Participants Volume, Additional Abstract.
- LOFI, J., GORINI, C., BERNÉ, S., CLAUZON, G., TADEU DOS REIS, A., RYAN, W.B.F., and STECKLER, M.S.
- 2005 Erosional processes and paleo-environmental changes in the Western Gulf of Lions (SW France) during the Messinian Salinity Crisis. *Marine Geology*, 217: 1–30.
- LONDEIX, L., BENZAKOUR, M., SUC, J.-P., and TURON, J.-L.
- 2007 Messinian paleoenvironments and hydrology in Sicily (Italy): The dinoflagellate cyst record. *Geobios*, 40(3): 233–250.

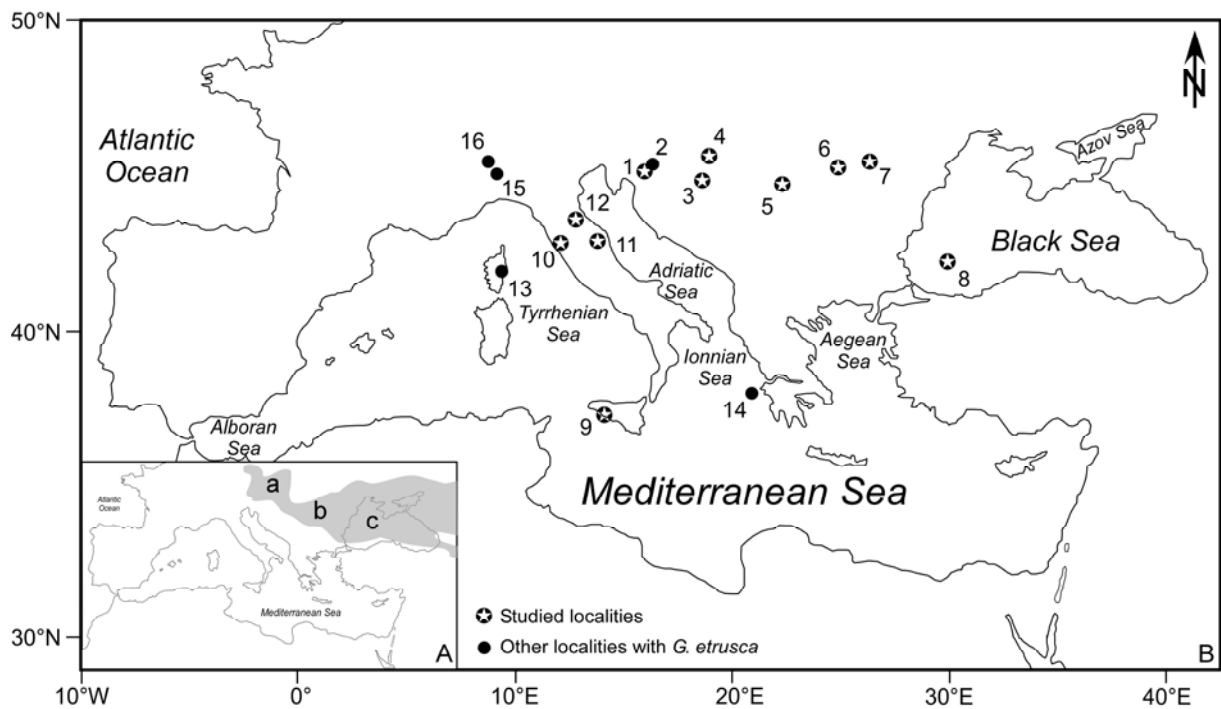
- LOURENS, L.J., HILGEN, F.J., LASKAR, J., SHACKLETON, N.J., and WILSON, D.
2004 The Neogene Period. *In*: Gradstein, F., Ogg, J., and Smith, A. (eds.). *A Geological Time Scale*, Cambridge University Press, p. 409–440.
- MAGYAR, I., GEARY, D.H., SÜTŐ-SZENTAI, M., LANTOS, M., and MÜLLER, P.
1999a Integrated bio-, magneto- and chronostratigraphic correlations of the Late Miocene Lake Pannon deposits. *Acta Geologica Hungarica*, 42: 5–31.
- MAGYAR, I., GEARY, D.H., and MÜLLER, P.
1999b Paleogeographic evolution of the Late Miocene lake Pannon in Central Europe. *Palaeogeography, Palaeoclimatology, Palaeoecology*, 147: 151–167.
- MANZI, V., ROVERI, M., GENNARI, R., BERTINI, A., BIFFI, U., GIUNTA, S., IACCARINO, S.M., LANCI, L., LUGLI, S., NEGRI, A., RIVA, A., ROSSI, M.E., and TAVIANI, M.
2007 The deep-water counterpart of the Messinian Lower Evaporites in the Apennine foredeep: the Fananello section (Northern Apennines, Italy). *Palaeogeography, Palaeoclimatology, Palaeoecology*, 251(3-4): 470–499.
- MARINESCU, F.
1992 Les bioprovinces de la Paratéthys et leurs relations. *Paleontologia i Evolució*, 24-25: 445–453.
- MĂRUNȚEANU, M., and PAPAIANOPOL, I.
1995 The connection between the Dacic and Mediterranean Basins based on calcareous nannoplankton assemblages. *Romanian Journal of Stratigraphy*, 76(7): 169–170.
- MĂRUNȚEANU, M., and PAPAIANOPOL, I.
1998 Mediterranean calcareous nannoplankton in the Dacic Basin. *Romanian Journal of Stratigraphy*, 78: 115–121.
- MCCARTHY, F.M.G., and MUDIE, P.J.
1996 Palynology and dinoflagellate biostratigraphy of Upper Cenozoic sediments from Sites 898 and 900, Iberia abyssal plain. *Proceedings of the Ocean Drilling Program, Scientific Results*, 149: 241–265.
- MCCULLOCH, M.T., and DE DECKKER, P.
1989 Sr isotope constraints on the Mediterranean environment at the end of the Messinian salinity crisis. *Nature*, 342: 62–65.
- MEULENKAMP, J.E., and SISSINGH, W.
2003 Tertiary palaeogeography and tectonostratigraphic evolution of the Northern and Southern Peri-Tethys platforms and the intermediate domains of the African–Eurasian convergent plate boundary zone. *Palaeogeography, Palaeoclimatology, Palaeoecology*, 196: 209–228.
- MÜLLER, P., GEARY, D.H., and MAGYAR, I.
1999 The endemic molluscs of the late Miocene Lake Pannon: their origin, evolution, and family-level taxonomy. *Lethaia*, 32: 47–60.
- ORSZAG-SPERBER, F.
2004 Changing perspectives in the concept of “Lago Mare” in Mediterranean Late Miocene evolution. *Sedimentary Geology*, 188–189: 259–277.
- PILLER, W.E., HARZHAUSER, M., and MANDIC, O.
2007 Miocene Central Paratethys stratigraphy – current status and future directions. *Stratigraphy*, 4 (2–3): 151–168.
- POMEROL, C.
1973 *Stratigraphie et paléogéographie. Ère Cénozoïque*. Doin, Paris: 269 p.
- POPESCU, S.-M.

- 2001 Végétation, climat et cyclostratigraphie en Paratéthys centrale au Miocène supérieur et au Pliocène inférieur d'après la palynologie. Unpublished PhD thesis, University Lyon 1, Villeurbanne, France, 223 p.
- 2006 Late Miocene and early Pliocene environments in the southwestern Black Sea region from high-resolution palynology of DSDP Site 380A (Leg 42B). *Palaeogeography, Palaeoclimatology, Palaeoecology*, 238(1–4): 64–77.
- POPESCU, S.-M., MELINTE, M.-C., SUC, J.-P., CLAUZON, G., QUILLEVERE, F., and SÜTŐ-SZENTAI, M.
- 2007 Earliest Zanclean age for the Colombacci and uppermost Di Tetto formations of the “latest Messinian” northern Apennines: New palaeoenvironmental data from the Maccarone section (Marche Province, Italy). *Geobios*, 40(3): 359–373.
- POPESCU, S.-M., KRIJGSMAN, W., SUC, J.-P., CLAUZON, G., MĂRUNȚEANU, M., and NICA, T.
- 2006 Pollen record and integrated high-resolution chronology of the Early Pliocene Dacic Basin (Southwestern Romania). *Palaeogeography, Palaeoclimatology, Palaeoecology*, 238(1–4): 78–90.
- POPOV, S.V., SHCHERBA, I.G., ILYINA, L.B., NEVESSKAYA, L.A., PARAMONOVA, N.P., KHONDKARIAN, S.O., and MAGYAR, I.
- 2006 Late Miocene to Pliocene palaeogeography of the Paratethys and its relation to the Mediterranean. *Palaeogeography, Palaeoclimatology, Palaeoecology*, 238(1–4): 91–106.
- REDNER, R.A., and WALKER, H.F.
- 1984 Mixture Densities, Maximum Likelihood and the EM Algorithm. *SIAM Review*, 26 (2): 195–239.
- RÖGL, F., and STEININGER, F.F.
1983. Vom Zerfall der Tethys zu Mediterran und paratethys. Die neogene Paläogeographie und Palinspastik des zirkum-mediterranean Raumes. *Annales des Naturhistorischen Museums in Wien*, 85(A): 135–163.
- ROUCHY, J.M., and CARUSO, A.
- 2006 The Messinian salinity crisis in the Mediterranean basin: A reassessment of the data and an integrated scenario. *Sedimentary Geology*, 188–189: 35–67.
- ROUCHY, J.M., ORSZAG-SPERBER, F., BLANC-VALLERON, M.-M., PIERRE, C., RIVIÈRE, M., COMBOURIEU-NEBOUT, N., and PANAYIDES, I.
- 2001 Palaeoenvironmental changes at the Messinian–Pliocene boundary in the eastern Mediterranean: southern Cyprus basins. *Sedimentary Geology*, 145: 93–117.
- SACCHI, M., and HORVÁTH, F.
- 2002 Towards a new time scale for the Upper Miocene continental series of the Pannonian basin (Central Paratethys). *EGU Stephan Mueller Special Publications Series*, 3: 79–94.
- SAGE, F., VON GRONFELD, G., DEVERCHÈRE, J., GAULLIER, V., MAILLARD, A., and GORINI, C.
- 2005 Seismic evidence for Messinian detrital deposits at the western Sardinia margin, northwestern Mediterranean. *Marine and Petroleum Geology*, 22: 757–773.
- SAINT MARTIN, S., SAINT MARTIN, J.-P., FERRANDINI, J., and FERRANDINI, M.
- 2007 La microflore de diatomées au passage Mio–Pliocène en Corse. *Geobios*, 40(3): 375–390.
- SATTERTHWAITE, F.E.
- 1946 An Approximate Distribution of Estimates of Variance Components. *Biometrics Bulletin*, 2: 110–114.
- SAVOYE, B., and PIPER, D.J.W.

- 1991 The Messinian event on the margin of the Mediterranean Sea in the Nice area, southern France. *Marine Geology*, 97: 279–304.
- SCARSELLI, S., SIMPSON, G.D.H., ALLEN, P.A., MINELLI, G., and GAUDENZI, L.
2006 Association between Messinian drainage network formation and major tectonic activity in the Marche Apennines (Italy). *Terra Nova*, 19: 74–81.
- SCHRADER, H.-J.
1978 Quaternary trough Neogene history of the Black Sea, deduced from the paleoecology of diatoms, silicoflagellates, ebridians and chrysomonads. *Initial Reports of the Deep Sea Drilling Project*, 42(2): 789–901.
- SELLI, R.
1973 An outline of the Italian Messinian. In: Drooger, C.W. (ed.), Messinian events in the Mediterranean. *Koninklijke Nederlandse Akademie Van Wetenschappen, Geodynamics Scientific Report 7*: 150–171.
- SEMENENKO, V.N., and OLEJNIK, E.S.
1995 Stratigraphic correlation of the Eastern Paratethys Kimmerian and Dacian stages by molluscs, dinocyst and nannoplankton data. *Romanian Journal of Stratigraphy*, 76(7): 113–114.
- SIMPSON, G.G., ROE, A., and LEWONTIN, R.C.
1960 *Quantitative Zoology*, revised edition. Harcourt, Brace, and World, New York.
- SNEL, E., MARUNȚEANU, M., MACALEȚ, R., MEULENKAMP, J.E., and VAN VUGT, N.
2006 Late Miocene to Early Pliocene chronostratigraphic framework for the Dacic Basin, Romania. *Palaeogeography, Palaeoclimatology, Palaeoecology*, 238(1–4): 107–124.
- STEVANOVIĆ, P.M.
1951 Pontische Stufe im engeren Sinne – Obere Congerienschichten Serbiens und der angrenzenden Gebiete. *Serbische Akademie der Wissenschaften, Sonderausgabe, Mathematisch-Naturwissenschaftliche Klasse*, 2, 187: 1–351.
- STOICA, M., LAZĂR, I., VASILIEV, I., and KRIJGSMAN, W.
2007 Mollusc assemblages of the Pontian and Dacian deposits from the Topolog-Argeș area (southern Carpathian foredeep – Romania). *Geobios*, 40(3): 391–405.
- SOKAL, R.R., and ROHLF, F.J.
1995 *Biometry* (3rd edition). Freeman and Co. Edit., New York, 887 p.
- SUC, J.-P., and BESSAIS, E.
1990 Pérennité d'un climat thermo-xérique en Sicile, avant, pendant, après la crise de salinité messinienne. *Comptes Rendus de l'Académie des Sciences de Paris* (2), 310: 1701–1707.
- SÜTÖNÉ SZENTAI, M.
1996 Micropaleontological type material of Natural Historical Collection at Komló. *Földtani Közlöny*, 126(2–3): 267–278.
- SÜTŐ-SZENTAI, M.
1988 Microplankton zones of organic skeleton in the Pannonian *s.l.* stratum complex and in the upper part of the Sarmatian strata. *Acta Botanica Hungarica*, 34(3–4): 339–356.
1990 Mikroplanktonflora der pontischen (oberpannonischen) Bildungen Ungarns. In: Stevanović, P., Neveškaya, L., Marinescu, F., Sokać, A., and Jámbor, Á. (eds.), *Chronostratigraphie und Neostatotypen, Neogen der Westlichen* (“Zentrale”) *Paratethys*. Band VIII, Pontien. Jazu and Sanu, Zagreb–Belgrade, p. 842–869.

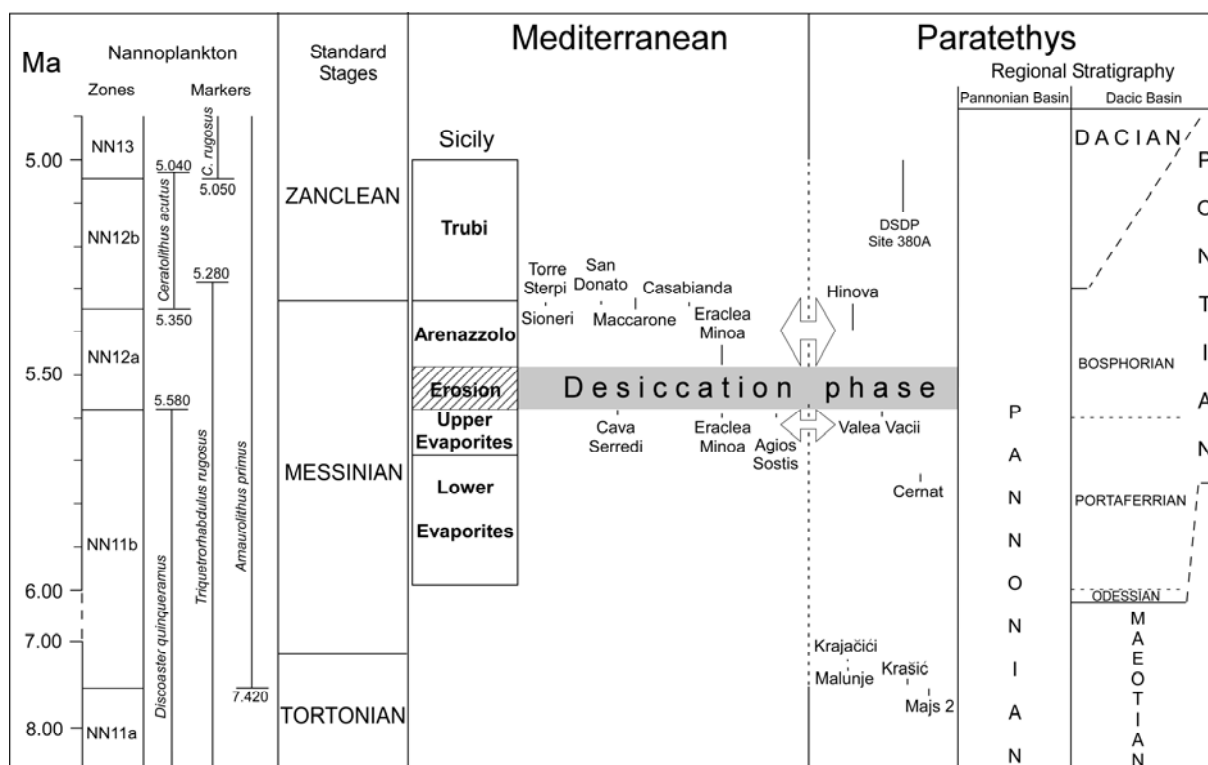
- 2000 Organic walled microplankton zonation of the Pannonian *s.l.* in the surroundings of Kaskantyú, Paks and Tengelic (Hungary). Annual Report of the Geological Institute of Hungary, 1994–1995/II, p. 153–175.
- SÜTŐ ZOLTÁNNÉ, M.
 1994 Microplankton associations of organic skeleton in the surroundings of Villány Mts. Szerves vázú mikroplankton a Villányi-hegség környezetében. *Földtani Közlöny*, 124(4): 451–478.
- TITTERINGTON, D., SMITH, A., and MAKOV, U.
 1985 *Statistical Analysis of Finite Mixture Distributions*. John Wiley & Sons, Chichester, U.K., 254 p.
- VAN COUVERING, J.A., CASTRADORI, D., CITA, M.B., HILGEN, F.J., and RIO, D.
 2000 The base of the Zanclean Stage and of the Pliocene Series. *Episodes*, 23(3): 179–187.
- VASILIEV, I., KRIJGSMAN, W., LANGEREIS, C.G., PANAIOTU, C.E., MAȚENCO, L., and BERTOTTI, G.
 2004 Towards an astrochronological framework for the eastern Paratethys Mio–Pliocene sedimentary sequences of the Focșani basin (Romania). *Earth Planetary and Science Letters*, 227: 231–247.
- WALL, D., DALE, B., and HARADA, K.
 1973 Descriptions of new fossil dinoflagellates from the late Quaternary of the Black Sea. *Micropaleontology*, 19: 18–31.
- WALL, D., and DALE, B.
 1974 Dinoflagellates in late Quaternary deep-water sediments from the Black Sea. In: Degens, E.T., and Ross, D.A. (eds.), *The Black Sea: Its Geology, Chemistry and Biology*. American Association of Petroleum Geologists, Memoir 20, p. 364–380.
- WELCH, B.L.
 1947 The generalization of "student's" problem when several different population variances are involved. *Biometrika*, 34: 28–35.

Figure captions

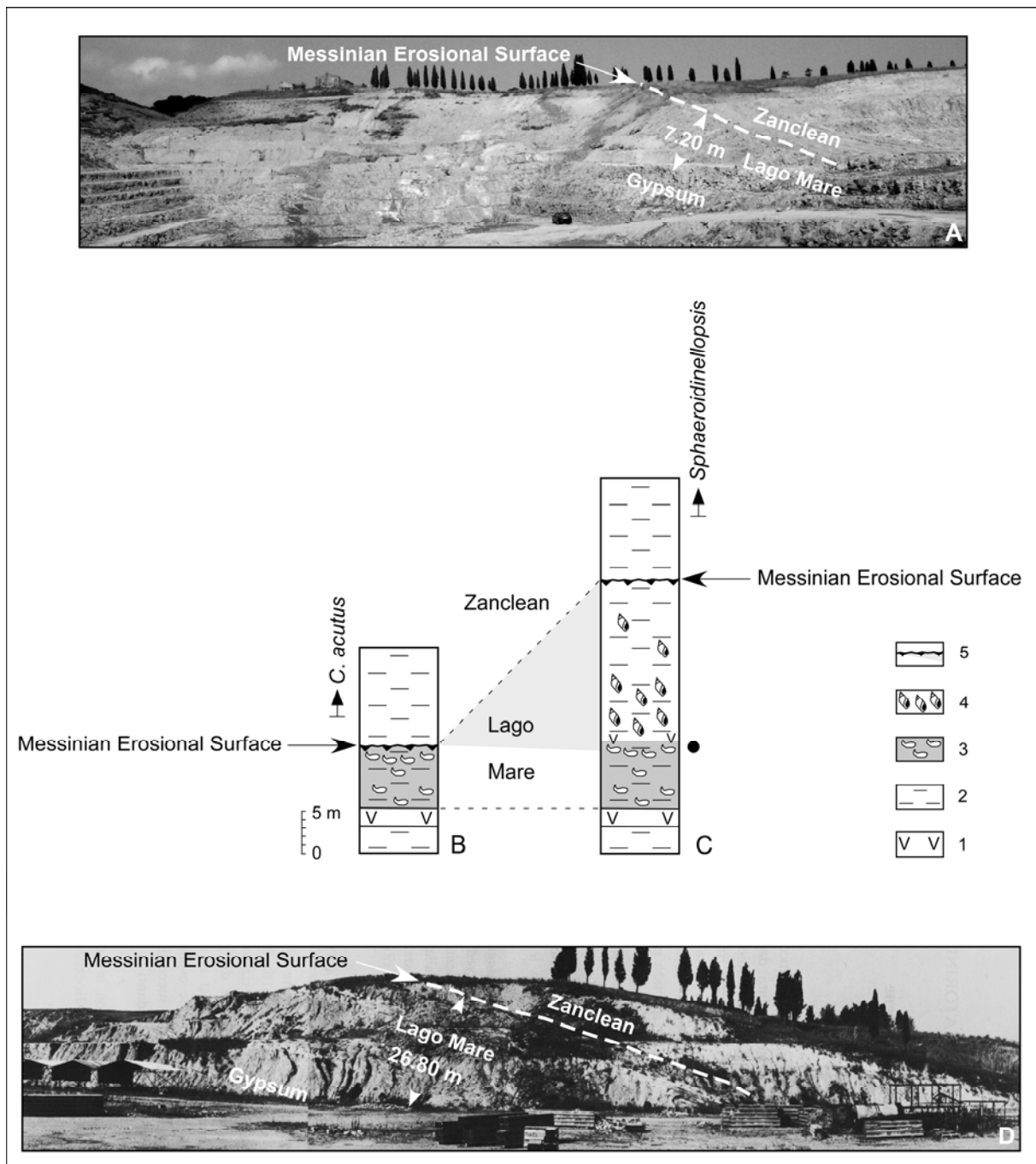


Text-Figure 1. Location maps. A, Paleogeographic location of the Paratethyan basins in gray (a, Pannonian; b, Dacic; and c, Euxinian and Caspian) with respect to the present-day Mediterranean Sea.

B, Localities yielding *Galeacysta etrusca*: 1, Krašić; 2, Malunje; 3, Krajačići; 4, Majs 2; 5, Hinova; 6, Cernat; 7, Valea Vacii; 8, DSDP Site 380; 9, Eraclea Minoa; 10, Cava Serredi; 11, Maccarone; 12, San Donato; 13, Casabianda; 14, Agios Sostis; 15, Torre Sterpi; 16, Sioneri.



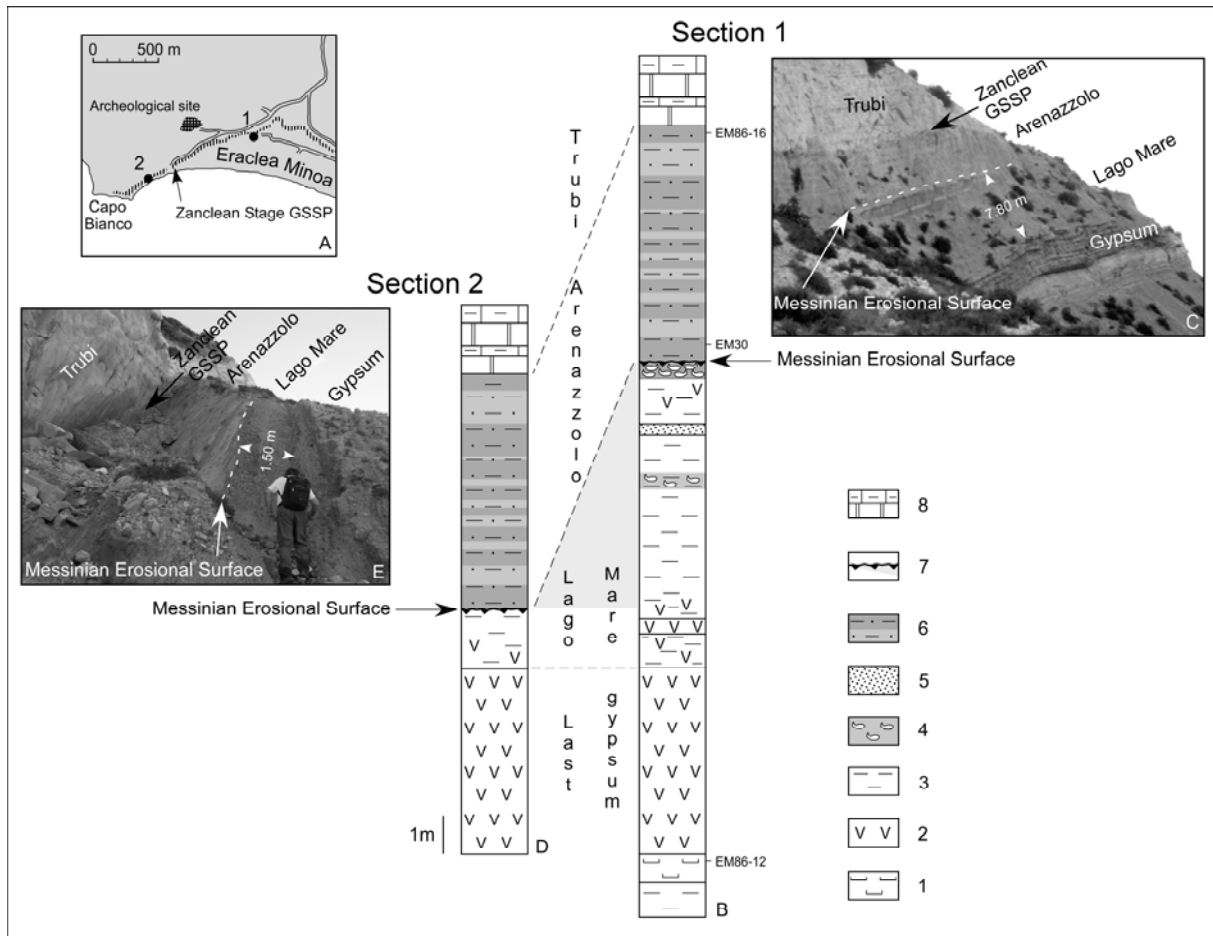
Text-Figure 2. Chronostratigraphic position of the localities yielding any specimen of the *Galeacysta etrusca* based on the two-step scenario of the Messinian Salinity Crisis (Clauzon et al., 1996; 2005). Calcareous nannoplankton biochronology is from Lourens et al. (2004). Age boundaries of regional stages in the Dacic Basin show the discrepancies between the authors (Vasiliev et al., 2004; Clauzon et al., 2005; Popescu et al., 2006; Snel et al., 2006; Stoica et al., 2007). Age boundaries of regional substages in the Dacic Basin are after Snel et al. (2006). Double arrows specify the major interconnection episodes (“Lago Mare” events: Clauzon et al., 2005) between the Mediterranean and Paratethys within a phase of discontinuous water-exchanges as indicated by the dashed line separating the Mediterranean and Paratethys columns.



Text-Figure 3. Stratigraphy of the upper Messinian and lowermost Zanclean deposits at Cava Serredi in the early 1980s compared to today, with the location of the Messinian Erosional Surface.

A, Photograph of the present-day working face of the quarry. B, Present-day section. C, Section published by Bossio et al. (1981) with the black circle indicating the *Galeacysta etrusca* Corradini & Biffi 1988 layer ; D, Photograph (courtesy of A. Bossio) showing the working face of the quarry in the early 1980s.

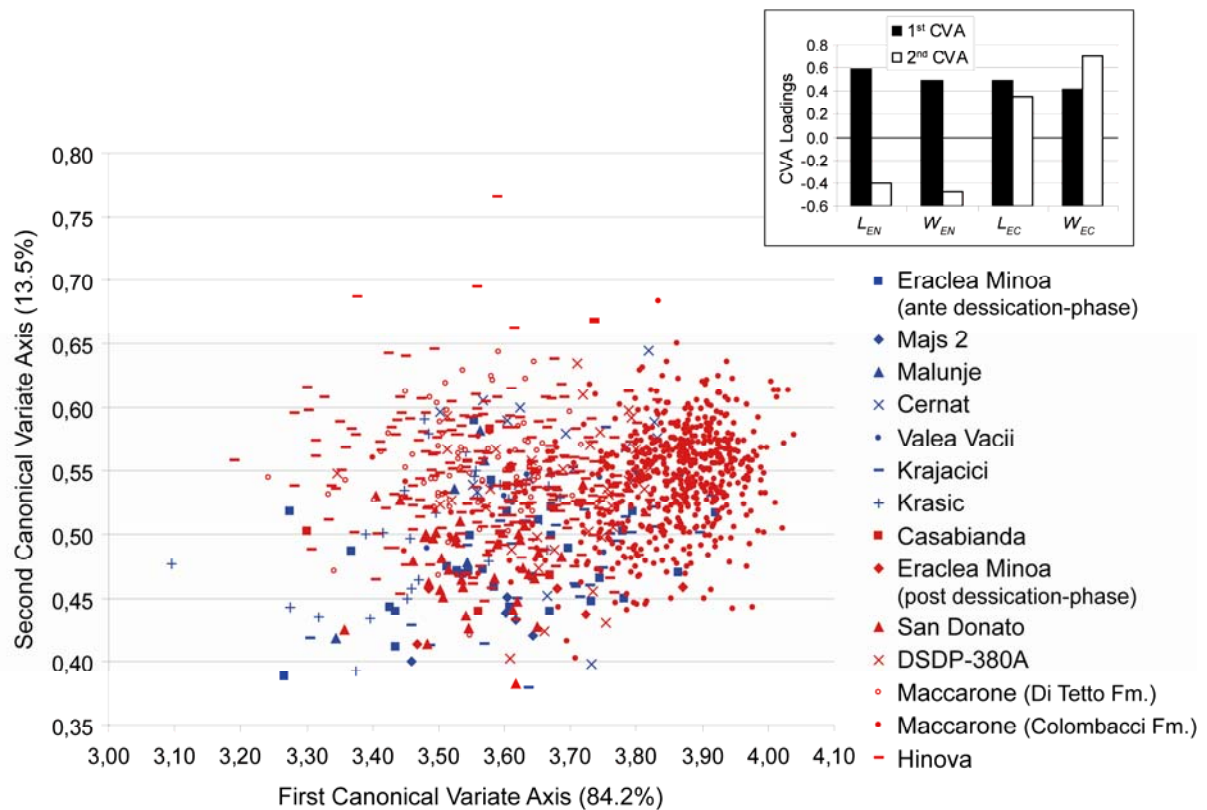
1, Gypsum; 2, Clay; 3, Dreissenid bed; 4, *Melanopsis* bed; 5, Messinian Erosional Surface (in gray, the eroded sediments missing from the present-day working face of the quarry).



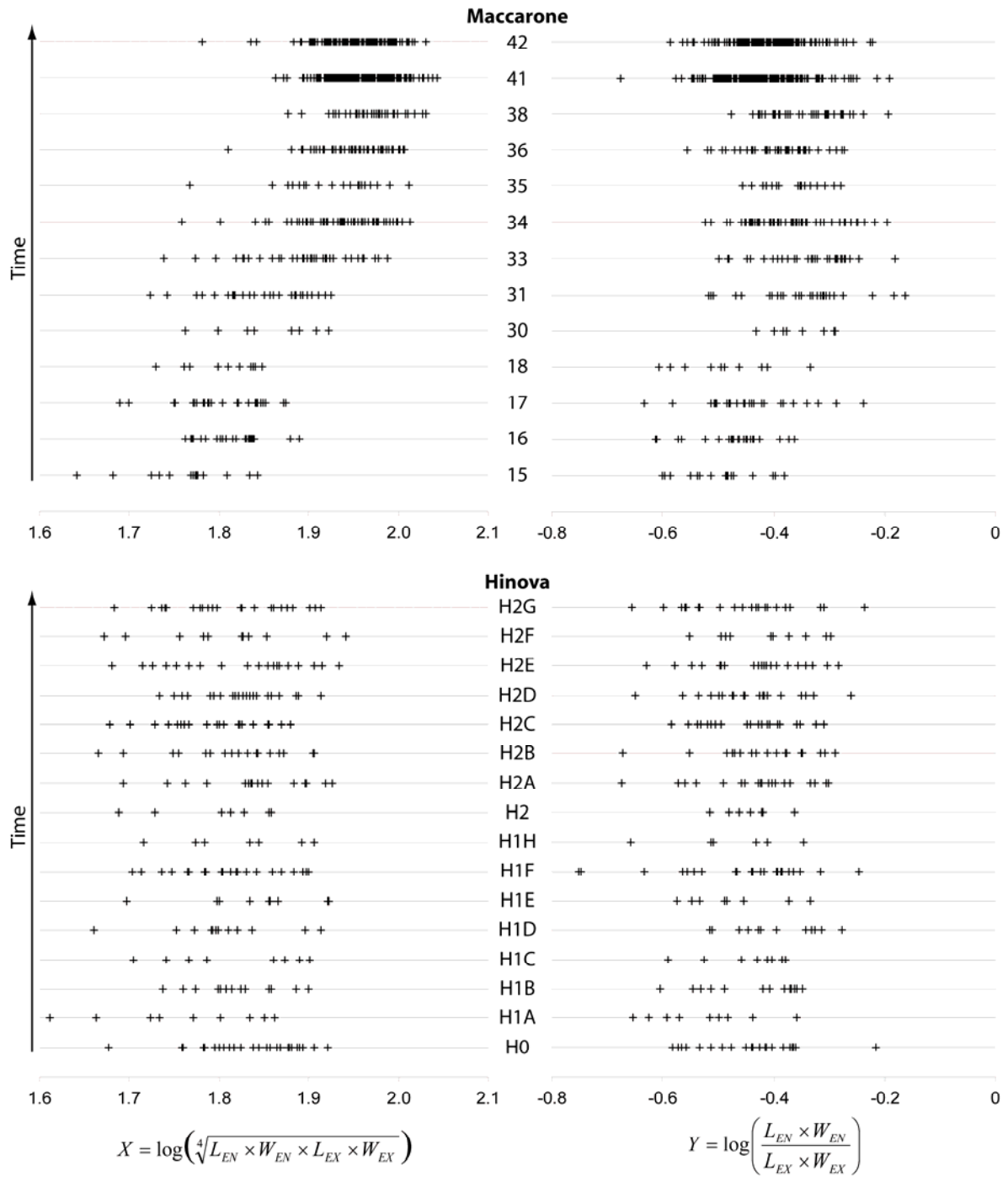
Text-Figure 4. The Eraclea Minoa sections 1 and 2.

A, Location of studied sections and of the Zanclean Stage global stratotype section and point (GSSP) (Van Couvering et al., 2000); B, Stratigraphic succession of section 1 with location of the three samples from which specimens of *Galeacysta etrusca* complex have been studied; C, Photograph of section 1; D, Stratigraphic succession of section 2; E, Photograph of section 2.

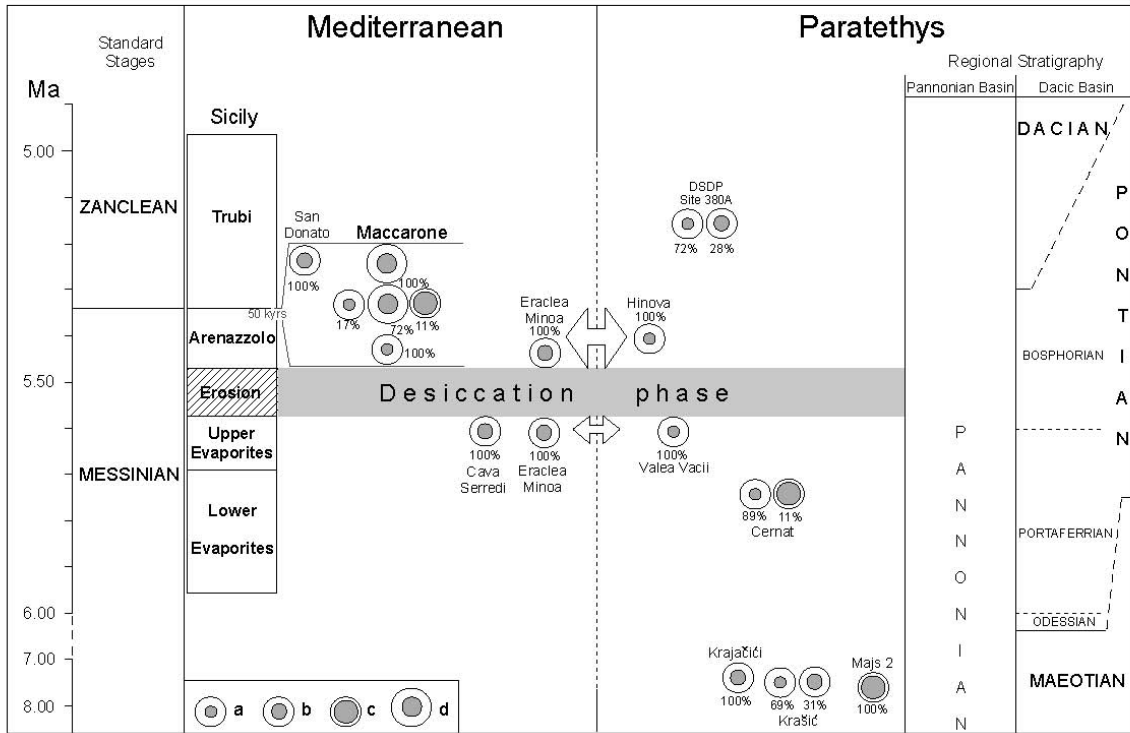
1, Diatomitic turbidite; 2, Gypsum; 3, Clays; 4, Dreissenid coquina; 5, Sand; 6, Light–dark cycles of the silts of the Arenazzolo Formation; 7, Messinian Erosional Surface (in gray, the eroded sediments missing in section 2); 8, carbonate–marly cycles of the Trubi Formation.



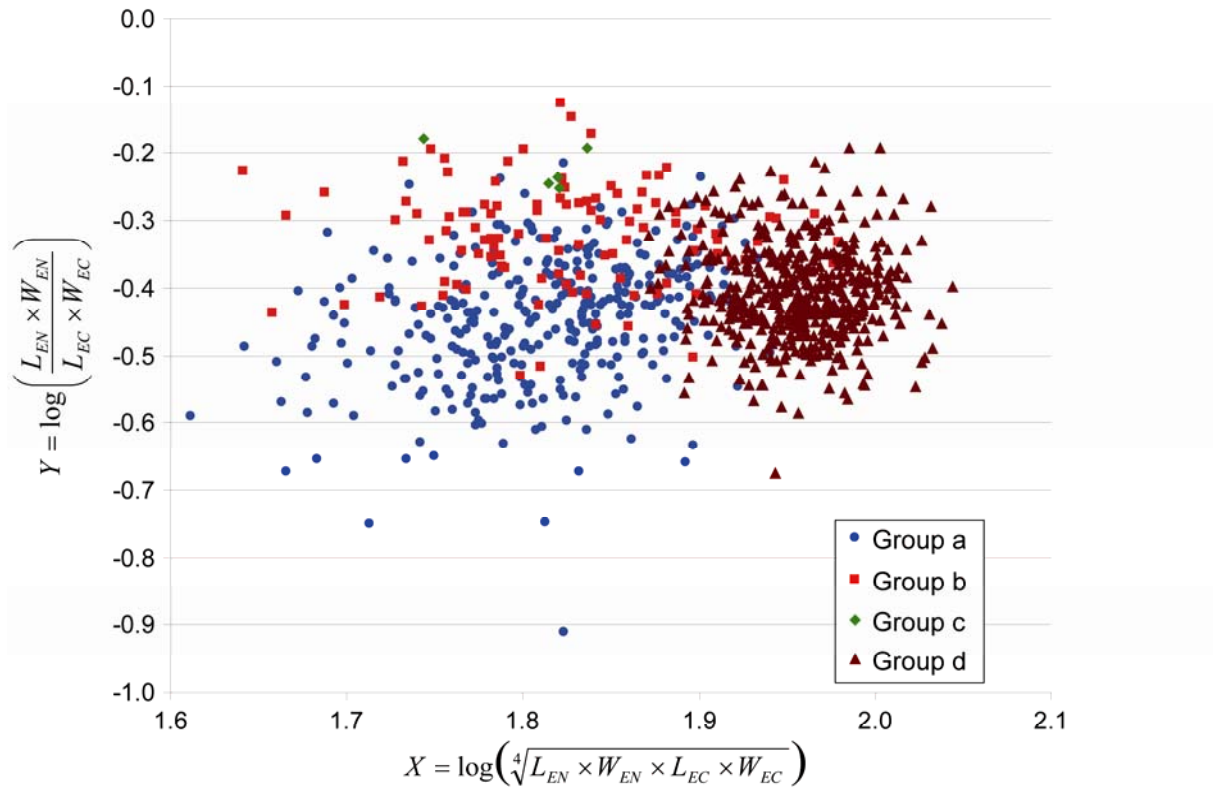
Text-Figure 5. First canonical plane resulting from a one-way Multiple Analysis of Variance based on the four log-transformed initial variables: length and width of the endocyst (noted L_{EN} and W_{EN} , respectively) and length and width of the ectocyst (noted L_{EC} and W_{EC} , respectively). MANOVA's highly significant results (Wilk's $\lambda = 0.455$; $d.f. = 48, 4347$; $F = 20.5$, $p = 5 \times 10^{-156}$) allow the identification of two main sources of biometric variation: overall dinoflagellate cyst size on the first canonical variate axis, and $D_{EN/EC}$ ratio on the second canonical variate axis (inset; see text for details).



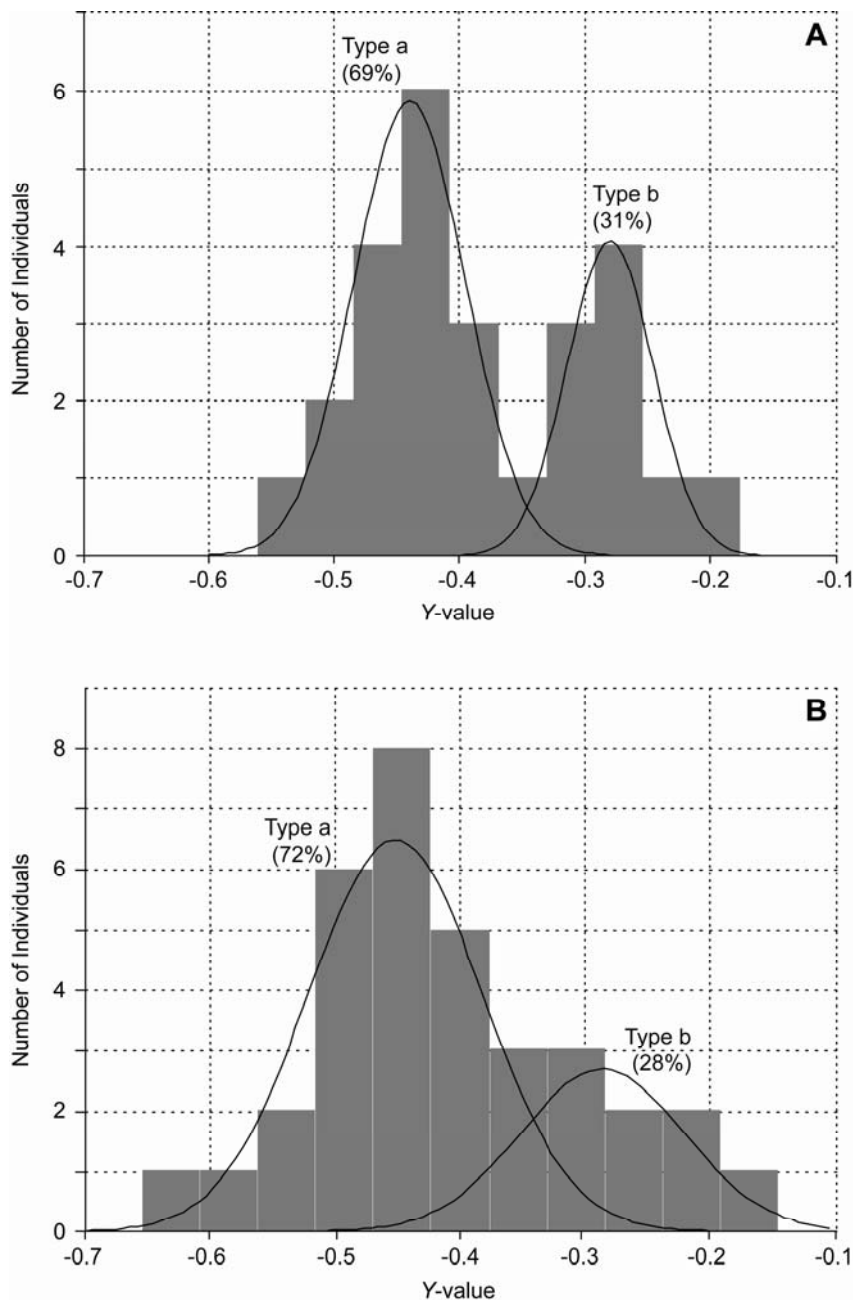
Text-Figure 6. Evolution of X (the dinocyst log-transformed geometric mean size) and Y (the dinocyst log-transformed $D_{EN/EC}$ ratio) distribution through early Zanclean times at Maccarone (up, 694 individuals) and Hinova sections (down, 248 individuals).



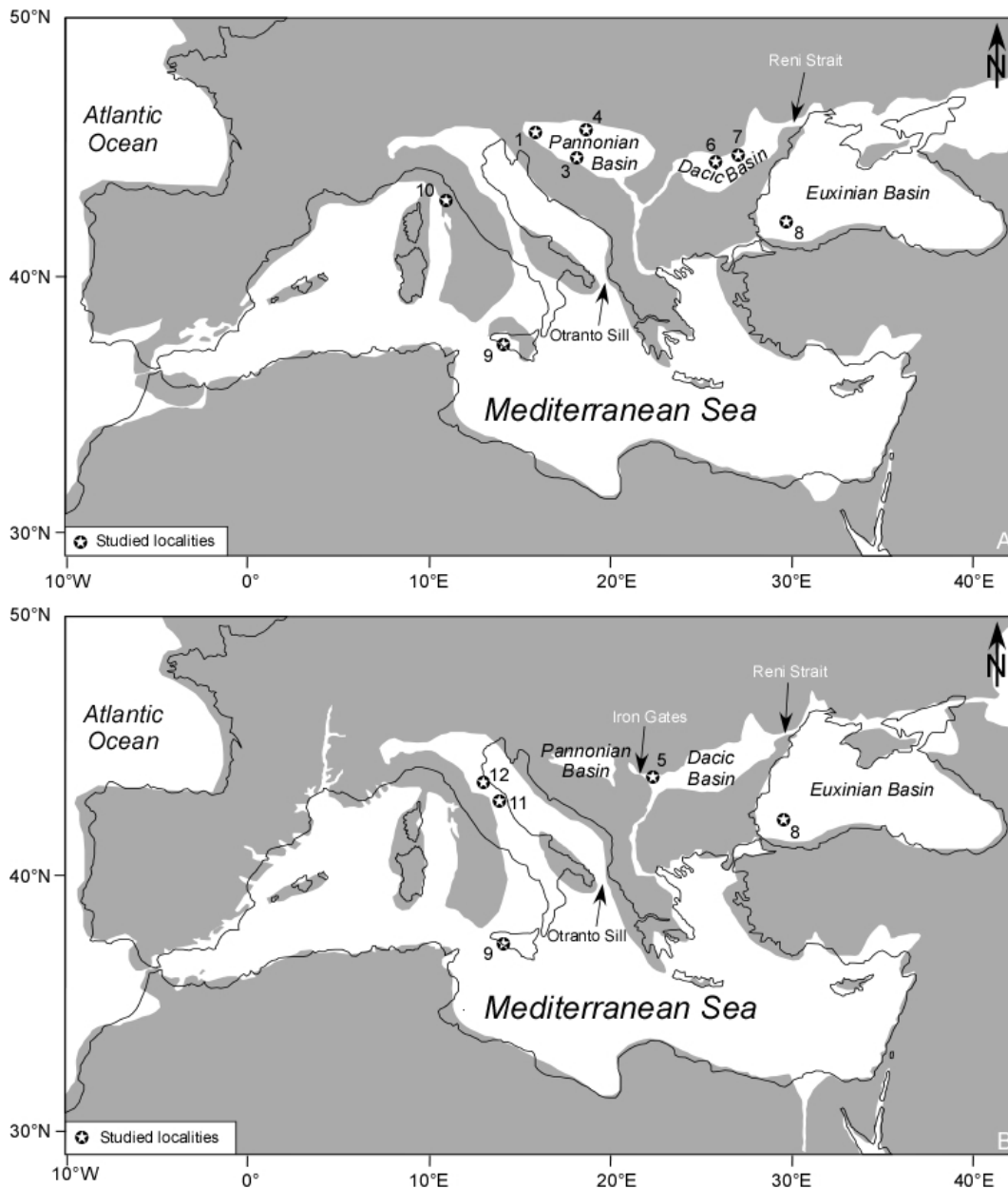
Text-Figure 7. Distribution of the *Galeacysta etrusca* biometric groups recorded in the studied localities with their respective percentages. Same legend as Text-Figure 2. The time-interval corresponding to the Colombacci Formation in the Apennine foredeep (Maccarone and San Donato sections) is enlarged. Groups: “a”, small individuals with small (ca. 32–36%) D_{ENEC} ratio; “b”, small individuals with intermediate (ca. 47–53%) D_{ENEC} ratio; “c”, small individuals with large (ca. 60%) D_{ENEC} ratio; “d”, large individuals with small to intermediate (ca. 39–43%) D_{ENEC} ratio.



Text-Figure 8. XY scatter plot of the single-group samples (see Table 2 and explanations in the text).



Text-Figure 9. *Y*-distribution histograms of *Galeacysta etrusca* assemblages showing Gaussian distributions superimposed for groups “a” and “b” (see Table 2 for the numerical values of estimated distribution parameters). Assemblages from: A, Krašić (Messinian); and B, DSDP Hole 380A (Zanclean).



Text-Figure 10. Paleogeography of the Mediterranean and central–eastern Paratethys (land areas in gray) based on Popov et al. (2006) but revised in accordance with our observations and deductions.

A, Late Messinian, before the peak of the Messinian Salinity Crisis.

B, Latest Messinian – Early Zanclean, after the peak of the Messinian Salinity Crisis.

Corresponding studied localities with specimens of the *Galeacysta etrusca* are shown: 1, Krašić; 3, Krajačići; 4, Majs 2; 5, Hinova; 6, Cernat; 7, Valea Vacii; 8, DSDP Site 380; 9, Eraclea Minoa; 10, Cava Serredi; 11, Maccarone; 12, San Donato.

Region	Locality	Samples	Nannoplankton	References
Eastern Paratethys	Dacic Basin	Hinova	H0, H1a, b, c, d, e H2, H2a, b, c, d, e H2f, g	Subzone NN12a Popescu et al. (2006) Clauzon et al. (2005)
	Euxinian Basin	DSDP Hole 380A (depth in m)	828.02, 829.06, 837.06, 839.08, 840.07, 841.91	No Popescu (2001; 2006)
Mediterranean	Casabianda	CO.08 (Aleria Formation)	Subzone NN12b	Saint Martin et al. (2007)
	San Donato	SD21 (Colombacci Formation)	Not searched	Bassetti (1997)
	Maccarone	38, 41, 42(Colombacci Formation) 34, 35, 36(Colombacci Formation) 30, 31, 33(Colombacci Formation) 15, 16, 17, 18 (Di Tetto Formation)	Subzones NN12a and b	Popescu et al. (2007)
	Eraclia Minoa	EM86-16, EM30 (Arenazzolo Formation) EM86-12 (Diatomitic turbidites underlying the last gypsum)	Subzone NN12a Subzone NN11b	
	Cava Serredi	7.2 of Corradini and Biffi (1988)	Subzone NN11b	Bossio et al. (1981)
Eastern Paratethys	Dacic Basin	Cernat	P1, P4	Subzone NN11b Mărunțeanu and Papaianopol (1998)
		Valea Vacii	3, 4	Subzone NN11b Snel et al. (2006)
Central Paratethys	Pannonian Basin	Krajačići	Krajačići I 1/1, 1/3	Meaningless Kováčic et al. (2004)
		Krašić	Krašić I 1/1	No Kováčic et al. (2004)
		Malunje	MAL I 1/1	No Magyar et al. (1999a)
		Majs 2 (depth in m)	257.3	No Sütő Zoltánné (1994)

Table 1. Studied samples and their respective sections and nannoplankton biostratigraphic assignment.

Sample	N	Group "a"		Group "b"		Group "c"		Group "d"	
		$\mu \pm \sigma$	%	$\mu \pm \sigma$	%	$\mu \pm \sigma$	%	$\mu \pm \sigma$	%
Eraclea Minoa (M)	30	---	---	-0.324±0.069	100	---	---	---	---
Majs 2	5	---	---	---	---	-0.221±0.030	100	---	---
Cernat	18	-0.478±0.062	89	---	---	-0.212±0.042	11	---	---
Valea Vacci	8	-0.396±0.040	100	---	---	---	---	---	---
Krajačići	27	---	---	-0.317±0.073	100	---	---	---	---
Krašić	26	-0.434±0.061	69	-0.277±0.032	31	---	---	---	---
Eraclea Minoa (Z)	7	---	---	-0.275±0.069	100	---	---	---	---
San Donato	37	---	---	-0.308±0.070	100	---	---	---	---
DSDP-380A	33	-0.452±0.069	72	-0.287±0.066	28	---	---	---	---
Hinova – H0	26	-0.444±0.084	100	---	---	---	---	---	---
Hinova – H1A	9	-0.426±0.089	100	---	---	---	---	---	---
Hinova – H1B	13	-0.438±0.083	100	---	---	---	---	---	---
Hinova – H1C	8	-0.447±0.070	100	---	---	---	---	---	---
Hinova – H1D	13	-0.391±0.006	100	---	---	---	---	---	---
Hinova – H1E	9	-0.475±0.074	100	---	---	---	---	---	---
Hinova – H1F	22	-0.463±0.126	100	---	---	---	---	---	---
Hinova – H1H	7	-0.459±0.102	100	---	---	---	---	---	---
Hinova – H2	8	-0.433±0.050	100	---	---	---	---	---	---
Hinova – H2A	19	-0.434±0.096	100	---	---	---	---	---	---
Hinova – H2B	18	-0.428±0.095	100	---	---	---	---	---	---
Hinova – H2C	20	-0.446±0.078	100	---	---	---	---	---	---
Hinova – H2D	21	-0.444±0.085	100	---	---	---	---	---	---
Hinova – H2E	20	-0.433±0.091	100	---	---	---	---	---	---
Hinova – H2F	11	-0.413±0.078	100	---	---	---	---	---	---
Hinova – H2G	23	-0.451±0.099	100	---	---	---	---	---	---
Maccarone – 15	16	-0.496±0.067	100	---	---	---	---	---	---
Maccarone – 16	24	-0.474±0.063	100	---	---	---	---	---	---
Maccarone – 17	29	-0.438±0.082	100	---	---	---	---	---	---
Maccarone – 18	10	-0.488±0.081	100	---	---	---	---	---	---
Maccarone – 30	8	---	---	---	---	---	---	-0.354±0.050	100
Maccarone – 31	27	-0.494±0.025	18	---	---	-0.188±0.024	11	-0.341±0.041	71
Maccarone – 33	36	-0.487±0.008	7	---	---	---	---	-0.334±0.061	93
Maccarone – 34	59	---	---	---	---	-0.253±0.030	18	-0.399±0.055	82
Maccarone – 35	19	---	---	---	---	---	---	-0.368±0.048	100
Maccarone – 36	44	---	---	---	---	---	---	-0.390±0.064	100
Maccarone – 38	35	---	---	---	---	---	---	-0.344±0.064	100
Maccarone – 41	236	---	---	---	---	---	---	-0.421±0.066	100
Maccarone – 42	155	---	---	---	---	---	---	-0.409±0.066	100

Table 2. Mixture analysis results of the 38 sampled distributions of the dinoflagellate cyst shape parameter: $Y = \log\left(\frac{L_{EN} \times W_{EN}}{L_{EC} \times W_{EC}}\right)$. N: sample size; $\mu \pm \sigma$, %: Y mean \pm standard deviation and relative abundance of the identified biometric groups.

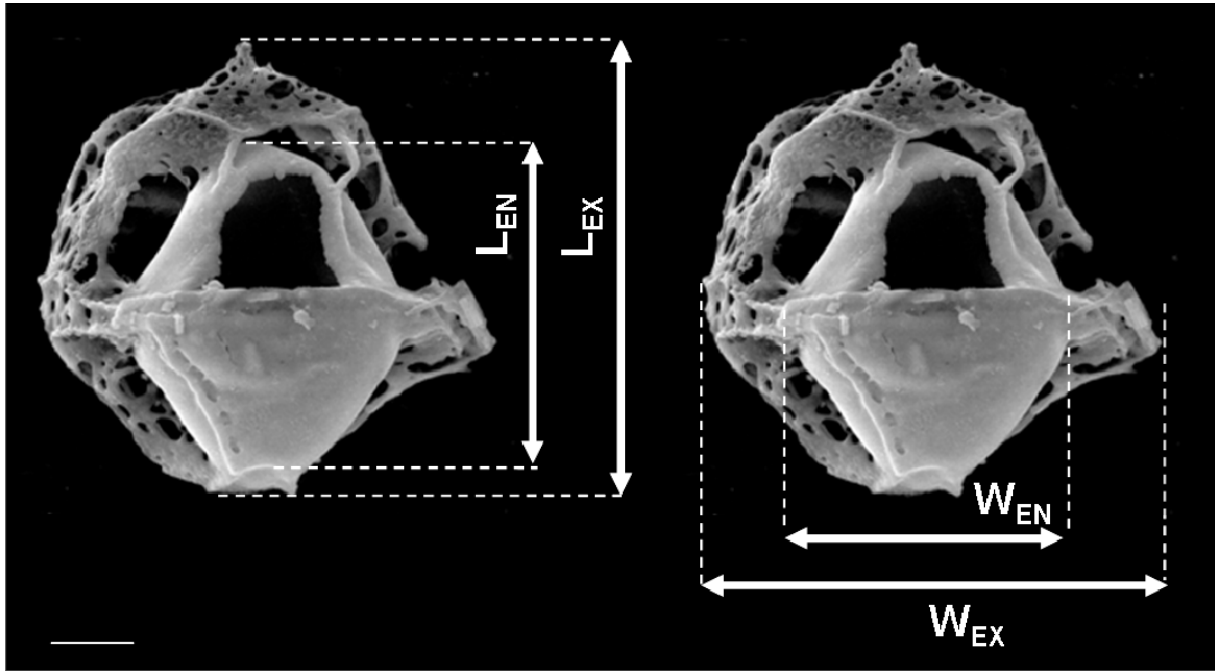


PLATE 1. The four measured parameters shown on a specimen of the *Galeacysta etrusca*.

L_{EN} , Length of the endocyst; W_{EN} , Width of the endocyst; L_{EX} , Length of the ectocyst;
 W_{EX} , Width of the ectocyst.

The scale bar represents 20 μm .

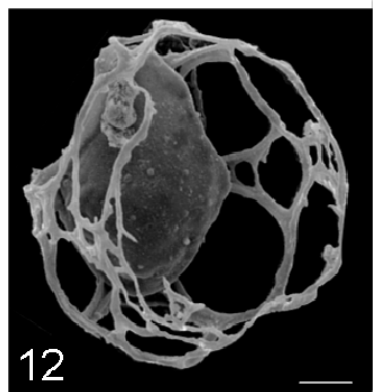
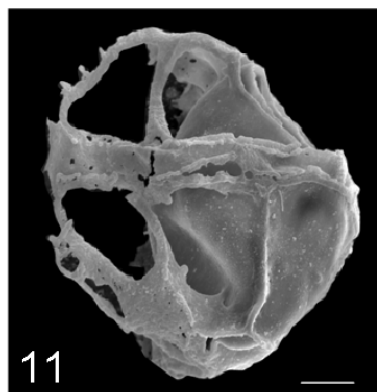
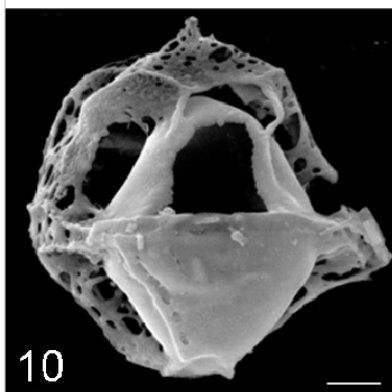
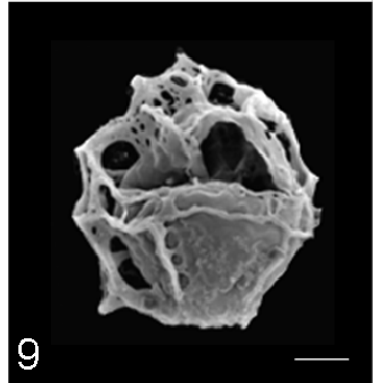
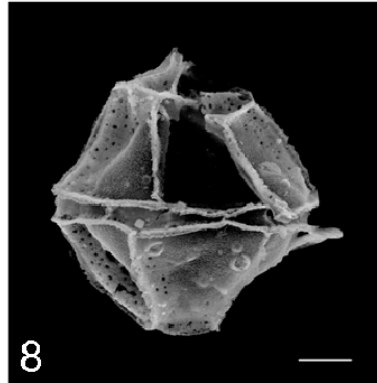
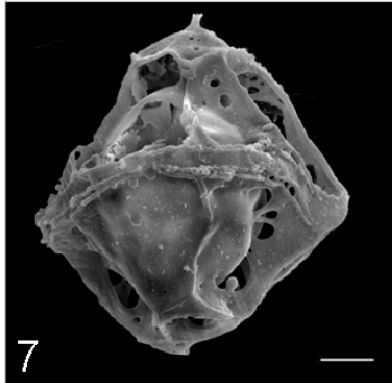
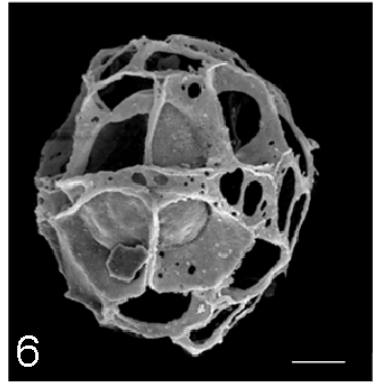
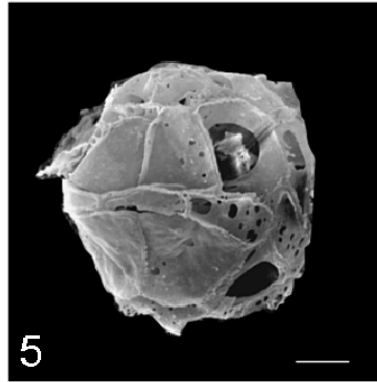
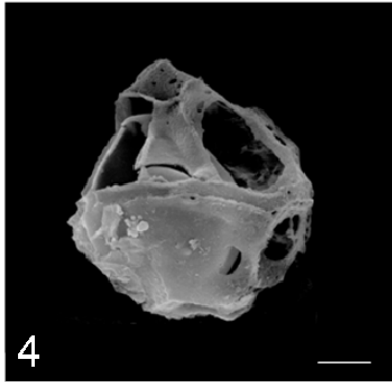
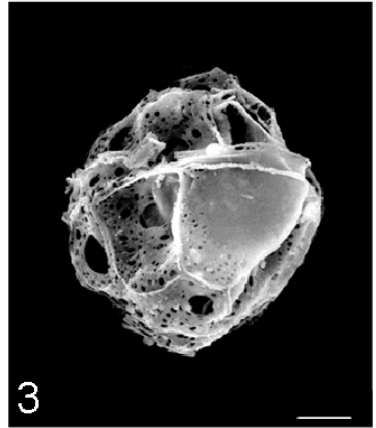
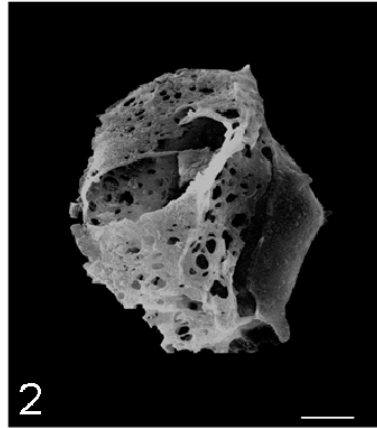
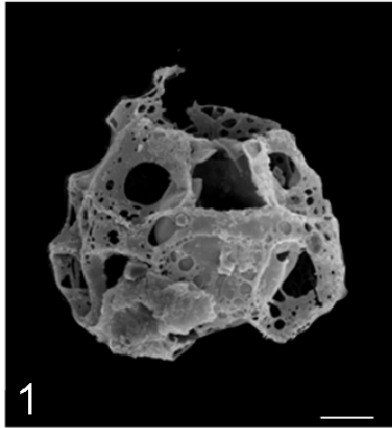


PLATE 2.

Scanning electron microphotograph of specimens of the *Galeacysta etrusca*.

Specimens are assigned to morphological groups as defined in this study by biometric analysis. The scale bar represents 20 μm .

Fig. 1, Specimen of group "b" recorded from Krajačići (Pannonian Basin), sample I 1/1.

Fig. 2, Specimen of group "a" recorded from Hinova (Dacic Basin), sample H2.

Fig. 3, Specimen of group "a" recorded from Hinova (Dacic Basin), sample H2.

Fig. 4, Specimen of group "b" recorded from DSDP Site 380 (Black Sea), sample 828.02 m depth.

Fig. 5, Specimen of group "a" recorded from Krašić (Pannonian Basin), sample I 1/1.

Fig. 6, Specimen of group "a" recorded from Maccarone (central Italy), sample 33.

Fig. 7, Specimen of group "b" recorded from Maccarone (central Italy), sample 33.

Fig. 8, Specimen of group "c" recorded from Majs 2 (Pannonian Basin), sample 257.30 m depth.

Fig. 9, Specimen of group "c" recorded from Majs 2 (Pannonian Basin), sample 257.30 m depth.

Fig. 10, Specimen of group "d" recorded from Maccarone (central Italy), sample 42.

Fig. 11, Specimen of group "d" recorded from Maccarone (central Italy), sample 42.

Fig. 12, Specimen of group "d" recorded from Maccarone (central Italy), sample 42.



Contents lists available at ScienceDirect

Marine Micropaleontology

journal homepage: www.elsevier.com/locate/marmicro

Process length variation in cysts of a dinoflagellate, *Lingulodinium machaerophorum*, in surface sediments: Investigating its potential as salinity proxy

Kenneth N. Mertens^{a,*}, Sofia Ribeiro^{b,bb}, Ilham Bouimetarhan^c, Hulya Caner^d, Nathalie Combourieu Nebout^e, Barrie Dale^f, Anne De Vernal^g, Marianne Ellegaard^b, Mariana Filipova^h, Anna Godhe^{cc}, Evelyne Goubert^j, Kari Grøsfjeld^k, Ulrike Holzwarth^c, Ulrich Kotthoff^l, Suzanne A.G. Leroy^m, Laurent Londeixⁿ, Fabienne Marret^o, Kazumi Matsuoka^p, Peta J. Mudie^q, Lieven Naudts^r, José Luis Peña-Manjarrez^s, Agneta Perssonⁱ, Speranta-Maria Popescu^t, Vera Pospelova^u, Francesca Sangiorgi^v, Marcel T.J. van der Meer^w, Annemiek Vink^x, Karin A.F. Zonneveld^y, Dries Vercauteren^z, Jelle Vlassenbroeck^{aa}, Stephen Louwye^a

^a Research Unit Palaeontology, Ghent University, Krijgslaan 281 s8, 9000 Ghent, Belgium

^b Department of Biology, Aquatic Biology Section, Faculty of Sciences, University of Copenhagen, Øster Farimagsgade 2D DK-1353 Copenhagen K, Denmark

^c Centre for Marine Environmental Sciences (Marum), University of Bremen, P.O. Box 330440, D-28334, Germany

^d Institute of Marine Sciences and Management, Istanbul University, Vefa 34470, Turkey

^e LSCE/IPSU UMR CEA-CNRS-UVSQ, Domaine du CNRS, Avenue de la Terrasse Bat. 12, F-91198 Gif sur Yvette Cedex, France

^f Department of Geosciences, University of Oslo, PB 1047 Blindern, N-0316 Oslo, Norway

^g GEOTOP, Université du Québec à Montréal, P.O. Box 8888, Montréal, Québec, Canada H3C 3P8

^h Museum of Natural History, 41 Maria Louisa Blvd., 9000 Varna, Bulgaria

ⁱ Department of Marine Ecology, Marine Botany, University of Gothenburg, PO Box 461, SE 405 30, Göteborg, Sweden

^j Université Européenne de Bretagne, Université de Bretagne Sud, Lab-STICC, Campus Tohannic, 56 000 Vannes, France

^k Geological Survey of Norway, N-7491 Trondheim, Norway

^l Institute of Geosciences, University of Frankfurt, Altenhöferallee 1, D-60438 Frankfurt/M., Germany

^m Institute for the Environment, Brunel University (West London), Uxbridge UB8 3PH, UK

ⁿ Université Bordeaux 1, UMR 5805 EPOC, avenue de Facultés, 33405 Talence cedex, France

^o Department of Geography, University of Liverpool, Liverpool L69 7ZT, UK

^p Institute for East China Sea Research (ECSER), 1-14, Bunkyo-machi, Nagasaki 852-8521, Japan

^q Geological Survey Canada Atlantic, Dartmouth, Nova Scotia, Canada B2Y 4A2

^r Renard Centre of Marine Geology (RCMG), Ghent University, Krijgslaan 281 s8, B-9000 Ghent, Belgium

^s Centro de Estudios Tecnológicos del Mar No. 11. Km. 6.5 carretera Ensenada-Tijuana, Ensenada, Baja California, México

^t Université Claude Bernard Lyon 1, Laboratoire Paléoenvironnements et Paléobiosphère, UMR 5125 CNRS, 2 Rue Raphaël, Dubois, 69622 Villeurbanne Cedex, France

^u School of Earth and Ocean Sciences, University of Victoria, Petch 168, P.O. Box 3055 STN CSC, Victoria, B.C., Canada V8W 3P6

^v (Institute of Environmental Biology) Laboratory of Palaeobotany and Palynology Utrecht University, Utrecht, The Netherlands

^w Marine Organic Biogeochemistry, NIOZ Royal Netherlands Institute for Sea Research, P.O. Box 59, 1790 AB Den Burg, Texel, The Netherlands

^x Federal Institute for Geosciences and Natural Resources, Alfred-Bentz-Haus, Stilleweg 2, 30 655 Hannover, Germany

^y Fachbereich 5-Geowissenschaften, University of Bremen, P.O. Box 330440, D-28334, Germany

^z Laboratory of General Biochemistry and Physical Pharmacy, Ghent University, Harelbekestraat 72, 9000 Ghent, Belgium

^{aa} UGCT, Ghent University, Proeftuinstraat 86, 9000 Ghent, Belgium

^{bb} Departamento de Geologia Marinha, LNEG, Estrada da Portela, Zambujal 2721-866 Alfragide, Portugal Faculdade de Ciências, Universidade de Lisboa, Instituto de Oceanografia, Campo Grande 1749-016 Lisboa, Portugal

^{cc} Department of Marine Ecology, University of Gothenburg, PO Box 461, SE 405 30, Göteborg, Sweden

* Corresponding author. Tel.: +3292644613; fax: +3292644608.

E-mail address: Kenneth.Mertens@ugent.be (K.N. Mertens).

ARTICLE INFO

Article history:

Received 30 July 2008

Received in revised form 10 October 2008

Accepted 17 October 2008

Available online xxxxx

Keywords:

Lingulodinium machaerophorum

Processes

Lingulodinium polyedrum

Biometry

Palaeosalinity

Dinoflagellate cysts

ABSTRACT

A biometrical analysis of the dinoflagellate cyst *Lingulodinium machaerophorum* [Deflandre, G., Cookson, I.C., 1955. Fossil microplankton from Australia late Mesozoic and Tertiary sediments. Australian journal of Marine and Freshwater Research 6: 242–313.] Wall, 1967 in 144 globally distributed surface sediment samples revealed that the average process length is related to summer salinity and temperature at a water depth of 30 m by the equation (salinity/temperature) = (0.078*average process length+0.534) with $R^2=0.69$. This relationship can be used to reconstruct palaeosalinities, albeit with caution. The particular ecological window can be associated with known distributions of the corresponding motile stage *Lingulodinium polyedrum* (Stein) Dodge, 1989. Confocal laser microscopy showed that the average process length is positively related to the average distance between process bases ($R^2=0.78$), and negatively related to the number of processes ($R^2=0.65$). These results document the existence of two end members in cyst formation: one with many short, densely distributed processes and one with a few, long, widely spaced processes, which can be respectively related to low and high salinity/temperature ratios. Obstruction during formation of the cysts causes anomalous distributions of the processes. From a biological perspective, processes function to facilitate sinking of the cysts through clustering.

© 2008 Elsevier B.V. All rights reserved.

1. Introduction

Salinity contributes significantly to the density of seawater, and is an important parameter for tracking changes in ocean circulation and climate variation. Palaeosalinity reconstructions are of critical importance for better understanding of global climate change, since they can be linked to changes of the thermohaline circulation (Schmidt et al., 2004). Quantitative salinity reconstructions have been proposed on the basis of several approaches that use, for example, foraminiferal oxygen isotopes (e.g. Wang et al., 1995), $\delta^{18}\text{O}_{\text{seawater}}$ based on foraminiferal Mg/Ca ratios and $\delta^{18}\text{O}$ (e.g. Schmidt et al., 2004; Nürnberg and Groeneveld, 2006), alkenones (e.g. Rostek et al., 1993), the modern analogue technique applied to dinoflagellate cyst assemblages (e.g. de Vernal and Hillaire-Marcel, 2000) and δD in alkenones (e.g. Schouten et al., 2006; van der Meer et al.,

2007, 2008). However, none of these approaches is unequivocal (e.g. alkenones; Bendle et al. 2005).

Some planktonic organisms are known to show morphological variability depending on salinity, e.g. variable nodding in the ostracod *Cyprideis torosa*, van Harten (2000) and morphological variation in the coccoliths of *Emiliania huxleyi* (Bollman and Herrle, 2007). A similar dependence has been reported for *Lingulodinium machaerophorum* (Deflandre and Cookson, 1955) Wall, 1967, the cyst of the autotrophic dinoflagellate *Lingulodinium polyedrum* (Stein) Dodge, 1989 which forms extensive harmful algal blooms reported from California (Sweeney, 1975), Scotland (Lewis et al., 1985), British Columbia (Mudie et al., 2002), Morocco (Bennouna et al., 2002), West Iberia (Amorim et al., 2001) and other coastal areas. This species can be considered a model dinoflagellate since it is easily cultured and has been the subject of numerous

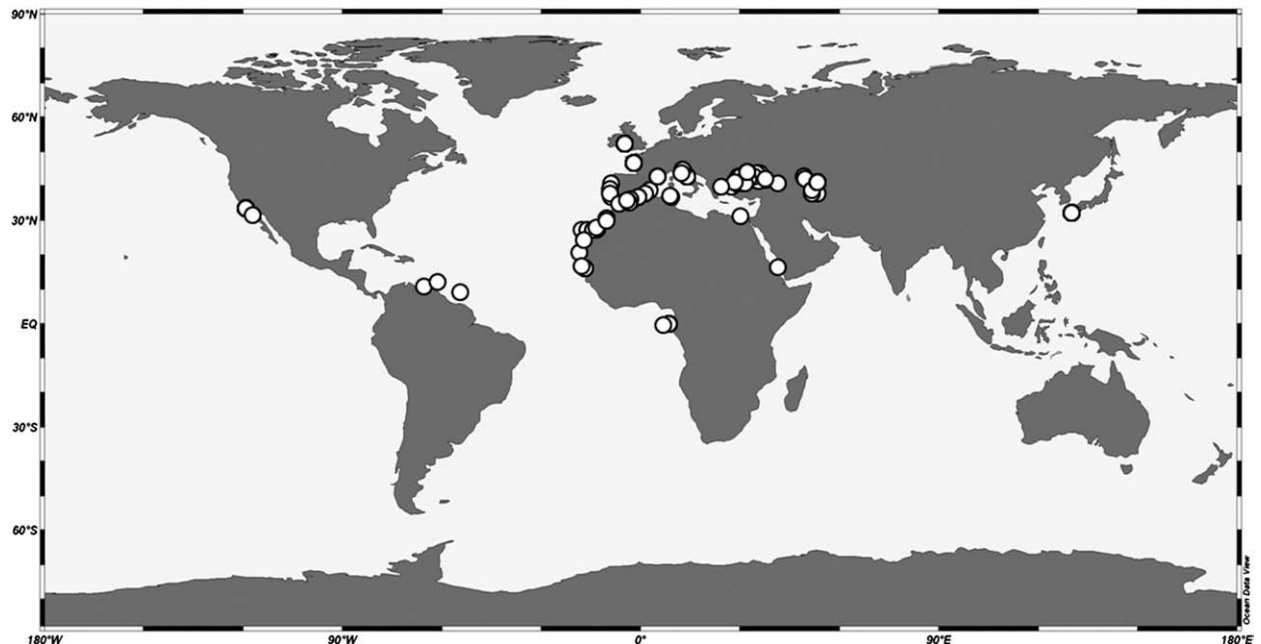


Fig. 1. Distribution of the 144 surface samples where *Lingulodinium machaerophorum* process lengths were studied.

Table 1

Average process length from LM measurements, standard deviation, body diameter and standard deviation, average summer temperature and salinity at 30 m water depth, ratio between both and density calculated from both

Region	# samples	Processes measured	Average process length (µm)	Stdev (µm)	Average body diameter (µm)	Stdev (µm)	Average summer $T_{30\text{ m}}$	Average summer $S_{30\text{ m}}$	$S_{30\text{ m}}/T_{30\text{ m}}$	Density (kg/m ³)	Preservation	Reference
Caspian Sea–Aral Sea	13	1320	5.6	3.4	48.1	6.1	15.72	12.72	0.81	1008.87	Bad to good	Marret et al. (2004), Sorrell et al. (2006), Leroy et al. (2006) and Leroy (unpublished data), Leroy et al. (2007)
Etang de Berre	2	300	7.5	2.5	44.9	4.5	19.91	26.10	1.31	1018.14	Average	Leroy (2001) and Robert et al. (2006)
Japan	5	735	8.0	1.9	45.3	5.7	24.54	33.72	1.37	1022.64	Good	Matsuoka (unpublished data)
Caribbean–West Equatorial Atlantic	6	306	13.0	4.4	44.1	6.4	26.19	36.08	1.38	1023.92	Average	Vink et al. (2000), Mertens et al. (2008) and Vink et al. (2001)
Scandinavian Fjords–Kattegat–Skagerrak	26	2271	13.2	4.2	47.9	6.4	16.55*	24.14*	1.46*	1017.43	Bad to good	Grøsfjeld and Harland (2001), Gundersen (1988), Ellegaard (2000), Christensen et al. (2004) and Persson et al. (2000)
East Equatorial Atlantic–Dakar Coast	7	903	13.2	3.4	46.6	6.2	22.88	35.52	1.55	1024.49	Bad to good	Marret (1994) and Bouimetarhan et al. (unpublished data).
Black Sea and Marmara Sea	35	5196	15.0	4.1	46.3	4.6	12.22	20.08	1.64	1015.14	Good	Verleye et al. (2008), Caner and Algan (2002), Caner (unpublished data), Cagatay et al. (2000), Naudts (unpublished data), Popescu et al. (unpublished), Mudie et al. (2007) and van der Meer et al. (2008)
Portugal–Brittanny	9	1350	16.8	3.6	45.3	5.5	16.53	35.22	2.13	1025.93	Good	Ribeiro et al. (unpublished data), Goubert (unpublished data)
NW Africa	12	1749	18.4	3.8	48.1	6.3	19.47	36.36	1.87	1026.07	Average to good	Holzwarth et al. (unpublished data); Kuhlmann et al. (2004), Richter et al. (2007)
Mediterranean–Red Sea	36	3507	19.6	4.4	45.6	6.1	18.39	37.57	2.04	1027.28	Average to good	Sangiorgi et al. (2005), Londeix (unpublished data), Combourieu-Nebout et al. (1999), Pirlet (unpublished data), Schoel (1974) and Kothoff et al. (2008)
Pacific	9	1224	21.2	4.3	47.7	6.1	14.39	33.45	2.32	1025.04	Good	Pospelova et al. (2008) and Peña-Manjarrez et al. (2005)
Celtic Sea	6	750	21.8	4.1	47.8	5.7	13.50	34.30	2.54	1025.88	Good	Marret and Scource (2002)

Results are sorted by short to long process length.

*For this region data from 0 m water depth is used.

investigations. An extensive review of these studies was given by Lewis and Hallett (1997).

Process length variation of *L. machaerophorum* was initially related to salinity variations in the Black Sea by Wall et al. (1973), and subsequently investigated in other regions (Turon, 1984; Dale, 1996; Matthiessen and Brenner, 1996; Nehring, 1994, 1997;

Ellegaard, 2000; Mudie et al., 2001; Brenner, 2005; Sorrel et al., 2006; Marret et al., 2007). Kokinos and Anderson (1995) were the first to demonstrate the occurrence of different biometrical groups in culture experiments. Later culture experiments (Hallett, 1999) revealed a linear relationship between average process length and salinity, but also temperature.

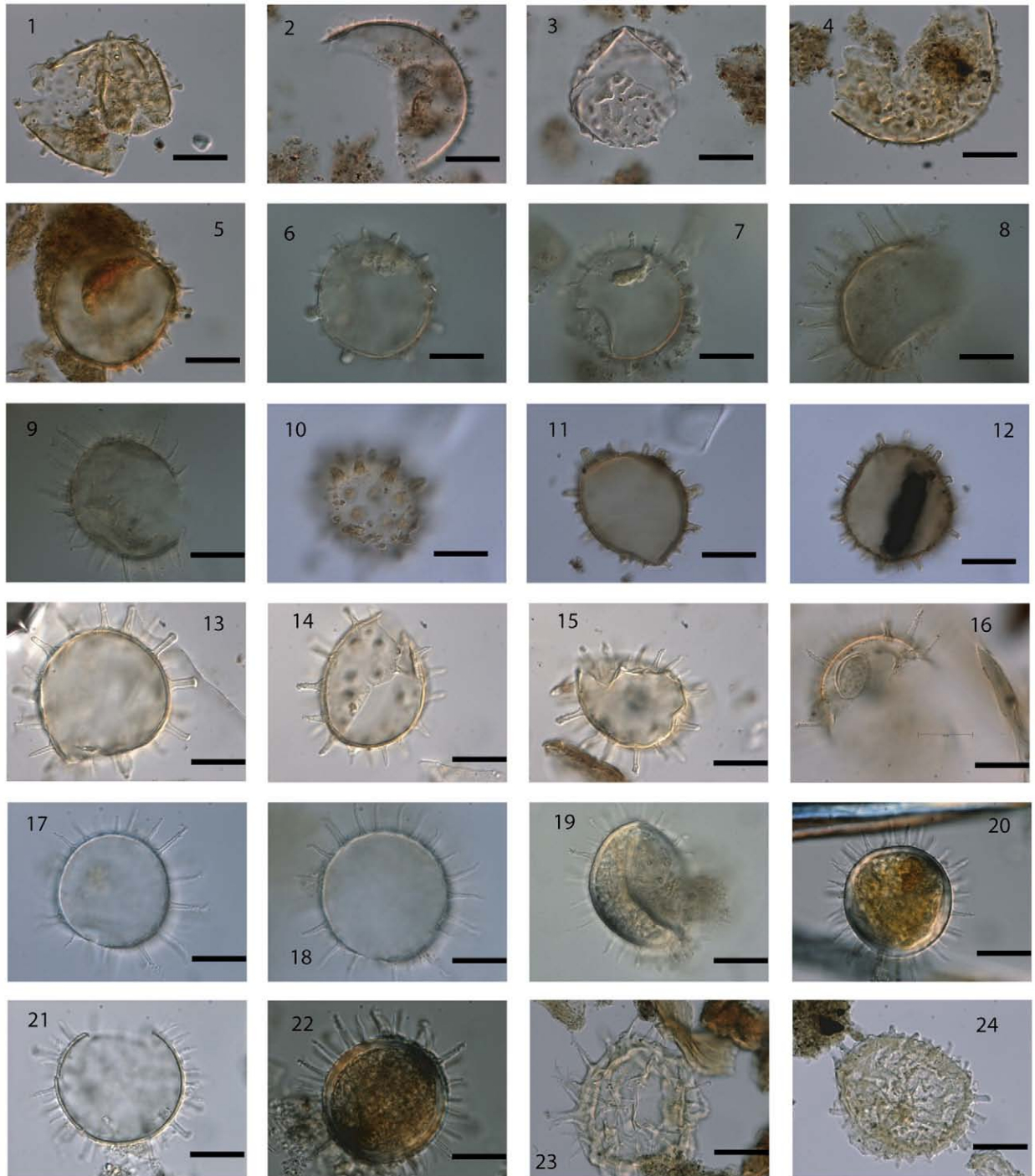


Plate I. *Lingulodinium machaerophorum* cysts from Caspian sea (1–5), Aral Sea (6–9), Etang de Berre (10–12), Baltic Sea (13–15) and Scandinavian Fjords (16–24). Specific sample names are 1–4. CPO4. 5.US02. 6–7. AR23. 8–9.AR17. 10–12. Etang de Berre (19). 13. NG6.14.NG.7.15.NG9.16. Limfjord. Note inclusion of *Nannobarbophora* acritarch. 17. Havstenfjorden 18–19. Guumar Fjord 20–21. G2.22.K2. 23–24. Risor Site. All scale bars are 20 μ m.

The process length of *L. machaerophorum* as a salinity proxy represents a large potential for palaeoenvironmental studies, since this species occurs in a wide range of marine conditions (Marret and Zonneveld, 2003), and can be traced back to the Late Paleocene (Head et al., 1996). The aim of the present study was to evaluate whether the average process length shows a linear relationship to salinity and/or temperature, and to assess its usability for palaeosalinity reconstruction. To achieve this goal, *L. machaerophorum* cysts were studied from surface sediments collected in numerous coastal areas. Confocal laser microscopy was used for the reconstruction of the complete distribution of the processes on the cyst wall, which has important implications for cyst formation.

2. Material and methods

2.1. Sample preparation and light microscopy

A total of 144 surface sediment samples were studied for biometric measurements of *L. machaerophorum* cysts from the Kattegat–Skagerrak, Celtic Sea, Brittany, Portuguese coast, Etang de Berre (France), Mediterranean Sea, Marmara Sea, Black Sea, Caspian and Aral Seas, northwest African coast, Canary Islands, coast of Dakar, Gulf of Guinea, Caribbean Sea, Santa Monica Bay (California), Todos Santos Bay (Mexico) and Isahaya Bay (Japan) (Fig. 1). Most samples were core top samples from areas with relatively high sedimentation rates, and can be considered recent, i.e. representing a few centuries (see Supplementary data). Five samples have a maximum age of a few thousand years, but since process lengths are as long as processes of recent, nearby samples, these were also considered representative. In general, the studied cysts provide us a global view of the biometric variation of cysts formed during the last few centuries by *L. polyedrum*. It is assumed here that the environmental conditions steering the morphological changes within the cysts are similar to recent environmental conditions.

All the cysts were extracted from the sediments according to maceration methods that are described in the literature shown in Table 1. Most methods used standard maceration techniques involving hydrochloric acid and hydrofluoric acid, sieving and/or ultrasonication. Regardless of the method used, the cysts all appeared similar in terms of preservation (Plates I–IV).

All measurements were made using a Zeiss Axioskop 2 and an Olympus BH-2 light microscope, equipped with an AxioCam RC5 digital camera (Axiovision v. 4.6 software) and Color View II (Cell F Software Imaging System) respectively, and 100x oil immersion objectives. All measurements were performed by Kenneth Mertens, except for the samples from Portugal, which were measured by Sofia Ribeiro. Observer bias did not influence the measurements.

For each sample, the length of the three longest visible processes and the largest body diameter were measured of 50 cysts for each sample. Measuring 50 cysts gave reproducible results: in sample GeoB7625-2 from the Black Sea, three process lengths per cyst for 50 cysts were measured, and was then repeated on 50 different cysts, showing no significant differences ($\bar{x} = 13.50 \mu\text{m} \pm 2.99 \mu\text{m}$ and $\bar{x} = 13.21 \mu\text{m} \pm 2.62 \mu\text{m}$, *t*-test: *p* = 0.37). The length of each process was measured from the middle of the process base to the process tip. The absolute error in process measurement was 0.4 μm . Within each cyst, three processes could always be found within the focal plane of the

light microscope, and for this reason this number seemed a reasonable choice. Three reasons can be advanced for choosing the longest processes. Firstly, the longest processes reflect unobstructed growth of the cyst (see below). Secondly, the longest processes allowed to document the largest variation, and this enhanced the accuracy of the proxy. Thirdly, since only a few processes were parallel to the focal plane of the microscope, it was imperative to make a consistent choice. Sometimes fewer than 50 cysts were measured, if more were not available. Fragments representing less than half of a cyst were not measured, nor were cysts with mostly broken processes.

2.2. Salinity and temperature data

The biometric measurements on cysts from the different study areas were compared to both seasonal and annual temperature and salinity at different depths – henceforth noted as $T_{0\text{ m}}$, $T_{10\text{ m}}$, ... and $S_{0\text{ m}}$, $S_{10\text{ m}}$, ..., using the gridded 1/4° World Ocean Atlas 2001 (Stephens et al. 2002; Boyer et al., 2002) and the Ocean Data View software (Schlitzer, R., <http://odv.awi.de>, 2008). For the Scandinavian Fjords, in situ data were available from the Water Quality Association of the Bohus Coast (<http://www.bvuf.com>).

2.3. Confocal laser microscopy

Confocal microscopy was performed using a Nikon C1 confocal microscope with a laser wavelength of 488 nm and laser intensity of 10.3%. No colouring was necessary since the cysts were sufficiently autofluorescent. The Z-stack step size was 0.25 μm with a Pixel dwell time of 10.8 μs . The objective used was a 60 \times /1.40/0.13 Plan-Apochromat lens with oil immersion. After correcting the z-axis for differences in refractive index between the immersion oil and glycerine jelly (here a factor of 78% of correction was used), images were rendered to triangulated surfaces (.stl files) with Volume Graphics VGStudioMax© software. These were imported in Autodesk 3DsMax©, where XYZ coordinates of the base and top of the processes were recorded. From these coordinates Euclidean distances were calculated, enabling the calculation of the process length and the distances between the processes. Distances to the two closest processes of each process were calculated, and by averaging these numbers, the average distance between processes was calculated. A more detailed description of the methodology is given at <http://www.paleo.ugent.be/Confocal.htm>.

3. Results

3.1. Preservation issues

To establish the validity of the measurements, preservation needs to be taken into account. Two types of degradation were considered: mechanical and chemical. Three categories were used to describe the mechanical degradation of the cysts: bad (most cysts were fragmented or torn, and processes were broken), average (about half of the cysts were fragmented or torn, and few processes were broken, and good (few cysts were torn or fragmented, and were often still encysted) (see Table 1).

The differences in mechanical breakdown were, from our experience, largely caused by post-processing treatments such as sonication. Prolonged sonication, however, does not

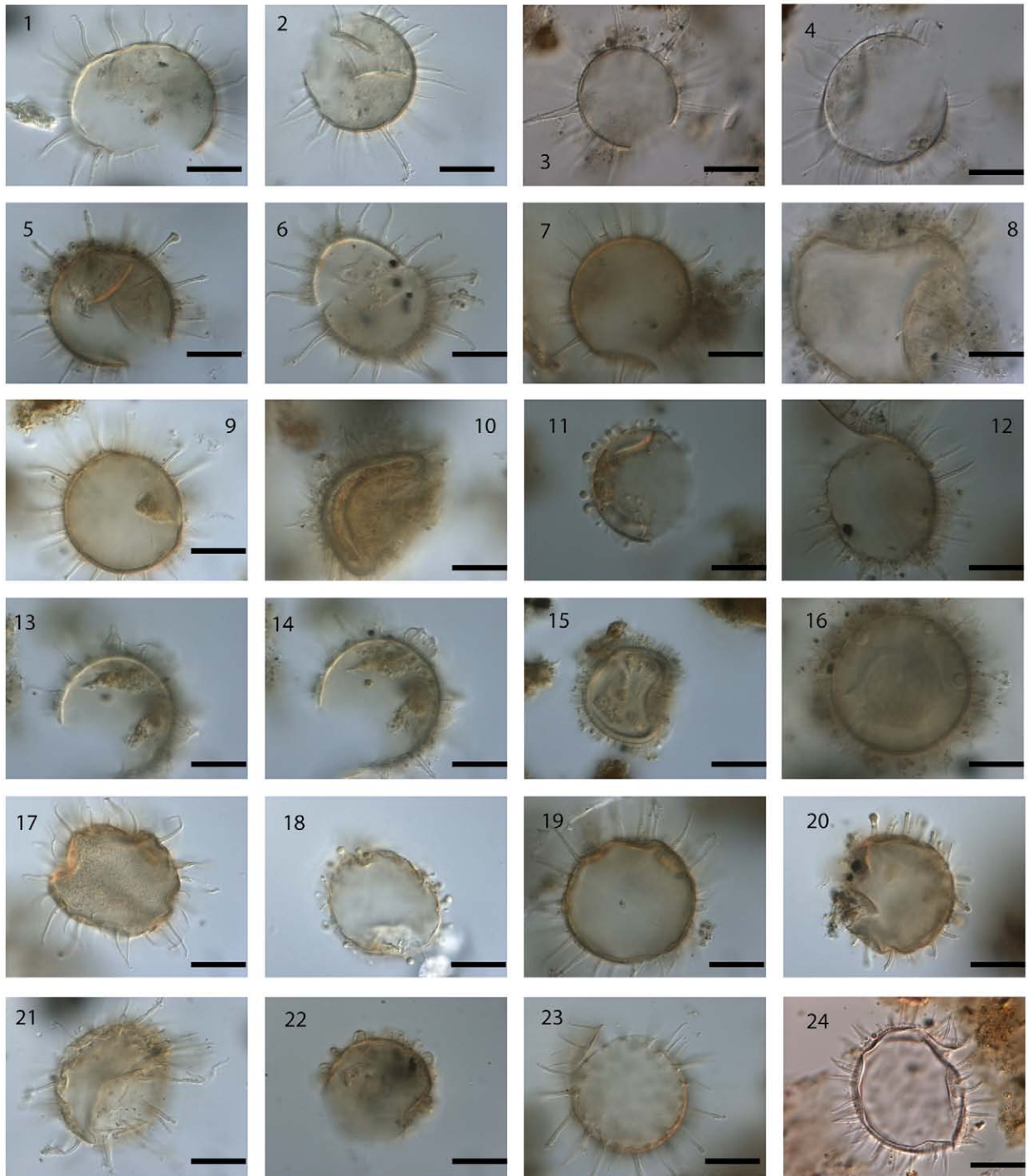


Plate II. *Lingulodinium machaerophorum* cyst from Marmara Sea (1–4) and Black Sea (5–24). Note the wide range of morphotypes occurring in these samples. Specific samples names are: (1–2) Dm 13 (3–4) Dm5 (5–6) Knorr 134.72. (7) Knorr 134.51. (8) GGC18 Swollen cyst due to use of acetolysis. (9–10) Knorr 134.35. (11–12) Knorr 134.2. (13–15) B2KS33 0-1. Note merged process in 13 and 14. (16) B2 KS 01 0-1. Note globules at basis of processes. (17–18) All 1464. (19) All 1443. (20–21) All 1438. (22) All 434. Note merged processes. (23) All145.1. (24) GeoB7625. Coloured with Safranin-O. All scale bars are 20 μ m.

significantly change process length variation. The sample from Gullmar Fjord (average process length of 14.6 μ m, standard deviation SD 4.0) was sonicated in an ultrasonic bath for two

minutes and the results were not significantly different from samples that were not sonicated (average process length of 14.3 μ m, SD 4.1) (t -test: $p=0.38$).

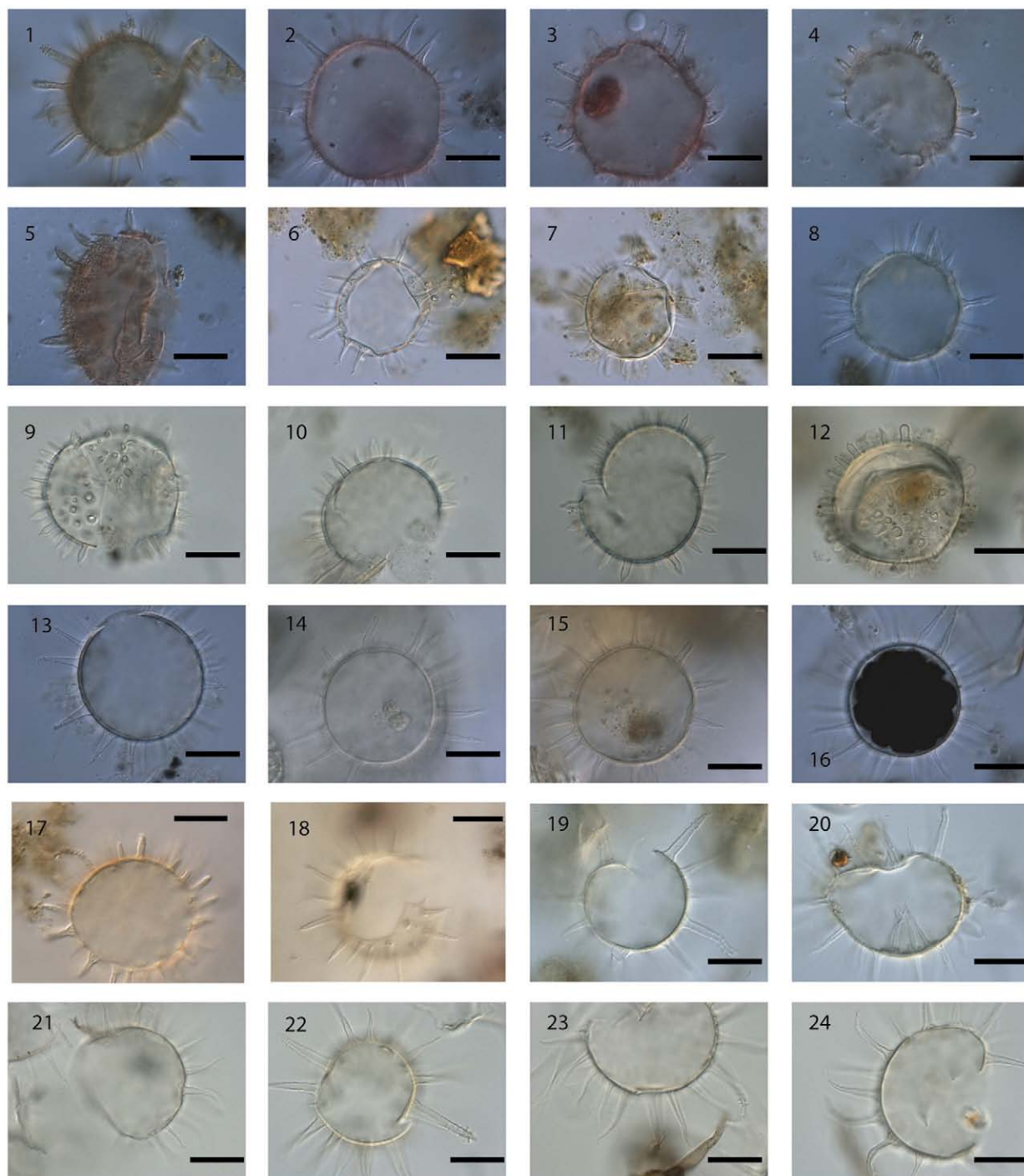


Plate III. *Lingulodinium machaerophorum* cyst from East Equatorial Atlantic (1–7), West Equatorial Atlantic (8), Japan (9–12), Brittany (13–16), Portugal (17–18) and NW Africa (19–24). Specific sample names are: (1) 6437-1, (2–3) 6847-2, (4–5) 6875-1, (6–7) Geob9503 Dakar, (8) M35003-4, (9–10) AB22, (11) AB40, (12) ISA2, (13) BV1, (14–15) BV3, (16) BV5, (17–18) Tejo, (19–20) Geob4024-1 (21) Geob5539-2, (22–24) Geob5548. All scale bars are 20 μ m.

Chemical breakdown, on the other hand, could be caused by oxidation or acid treatment. *L. machaerophorum* is moderately sensitive to changes in oxygen availability (Zonneveld et al., 2001). Cysts from samples treated with acetolysis were clearly swollen (Plate II.8). Most interestingly, both processes and cyst

body swell proportionately. These samples were not used for analysis. Similar results were noted after treatment with KOH. These maceration methods are not suitable for biometric studies. Cysts extracted using warm HF showed traces of degradation (see Plate I.23, I.24), but process length did not change.

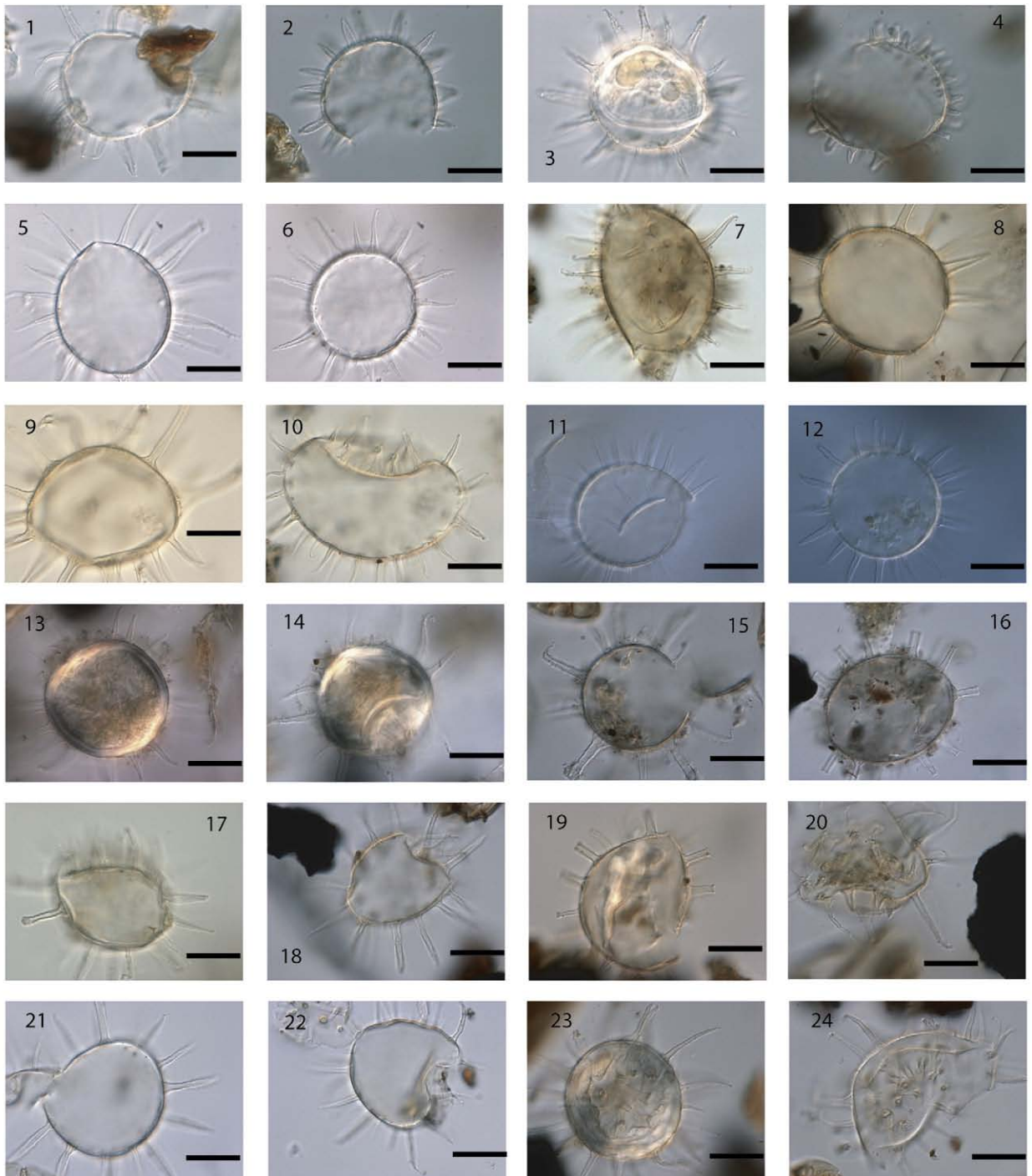


Plate IV. *Lingulodinium machaerophorum* cyst from Mediterranean (1–11), Red Sea (12) Celtic Sea (13–16) and Pacific Ocean (17–24). Note the widely distributed very long processes in Celtic Sea and Pacific Ocean samples. Specific samples are: (1) North Adriatic AN71. (2–4) North Adriatic AN71. (5–6) Nile Delta. (7) 273.4. (8) 5153. (9) 516.6. (10) 521.3. (11–12) Red Sea VA01–200P. (13–14) Station9 6.99. (15) Station 9 5.00 (16) Station 9 2.99 with truncated processes. (17) Todos Santos Bay (Mexico). (18–19) Santa Monica Bay, UVic07-896 18 with truncated processes. (20) UVic07-897. (21–22) UVic07-898.22 with truncated processes. (23–24) UVic07-902. All scale bars are 20 μm .

3.2. Overall cyst biometrics for the multi-regional dataset

The 19,611 process length measurements resulted in a global average of 15.5 μm with a standard deviation of 5.8 μm ,

and a range from 0 to 41 μm (Fig. 2). Most cysts encountered were comparable to the forms described by Kokinos and Anderson (1995), and bald cysts were rare. The range found is clearly broader than the 2 to 21 μm range postulated by Reid

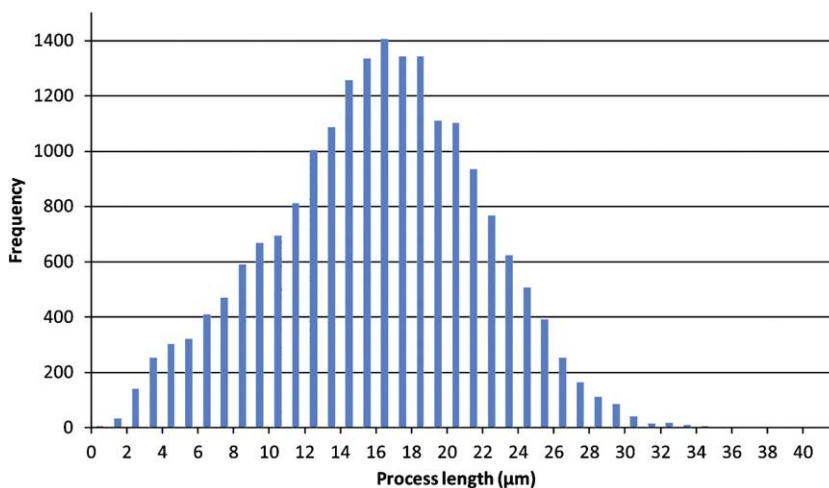


Fig. 2. Size-frequency spectrum of 19,611 process measurements.

(1974). The skewness of the distribution was -0.12 , since there is some tailing at the left side of the size frequency curve (Fig. 2). The asymmetric distribution was due to the fact that standard deviation increased with average process length. This could be explained partly by the methodological approach – errors on the larger measurements were larger, since larger processes were more often curved or tilted – and by the more common occurrence of cysts with relatively shorter processes in samples that mostly contain cysts with longer processes (also evident in regional size-spectra, Fig. 4).

The 6537 body diameter measurements resulted in an average body diameter of $46.6 \mu\text{m}$ with a standard deviation of $5.8 \mu\text{m}$, over a range from 26 to $77 \mu\text{m}$. This was again a broader range than the 31 to $54 \mu\text{m}$ given by Deflandre and Cookson (1955) and Wall and Dale (1968). This discrepancy could be explained partly by cysts sometimes being compressed or torn, yielding an anomalously long body diameter. This mechanical deformation of the cyst explains also a positive skewness of the size-frequency spectrum (Fig. 3).

The averaged data of *L. machaerophorum* cysts in every region is given in Table 1, sorted from low to high average process length. Individual size-frequency spectra are shown in Fig. 4 and the cysts are shown in Plate I–IV. All measurements are available as Supplementary data.

3.3. Comparison of process length with salinity and temperature

Data from the Scandinavian Fjords and the Kattegat-Skagerrak were excluded from all relations since they significantly increased the scatter on all regressions. The reason is given in the Discussion (Section 4.3).

The relation of the average process length of *L. machaerophorum* with only the salinity data, fitted best with the winter $S_{0 \text{ m}}$ ($R^2=0.54$). When compared to temperature data alone, the best relationship was with the winter $T_{50 \text{ m}}$ ($R^2=0.06$). A much stronger relationship could be found with salinity divided by temperature at a water depth of 30 m from July to September (summer). This relationship is expressed as $(S_{30 \text{ m}}/T_{30 \text{ m}}) = (0.078 * \text{average process length} + 0.534)$, and has a $R^2=0.69$ (Fig. 5) and the standard error is $0.31 \text{ psu}/^\circ\text{C}$. Since seawater density is dependent on salinity and temperature, it could be expected that density would have a similar relationship with process length. However, the regression with water density at 30 m water depth shows a stronger relation to process length ($R^2=0.50$) than with salinity alone ($R^2=0.42$ with summer $S_{30 \text{ m}}$), but not better than with $S_{30 \text{ m}}/T_{30 \text{ m}}$.

An overview of the results in the studied areas is given in Table 1. Next to average process length, salinity, temperature and $S_{30 \text{ m}}/T_{30 \text{ m}}$, seawater density data are given, and illustrate that

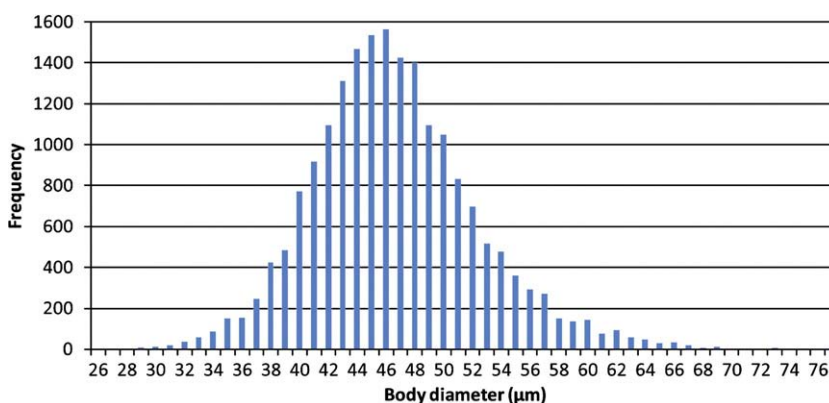


Fig. 3. Size-frequency spectrum of 6211 body diameter measurements.

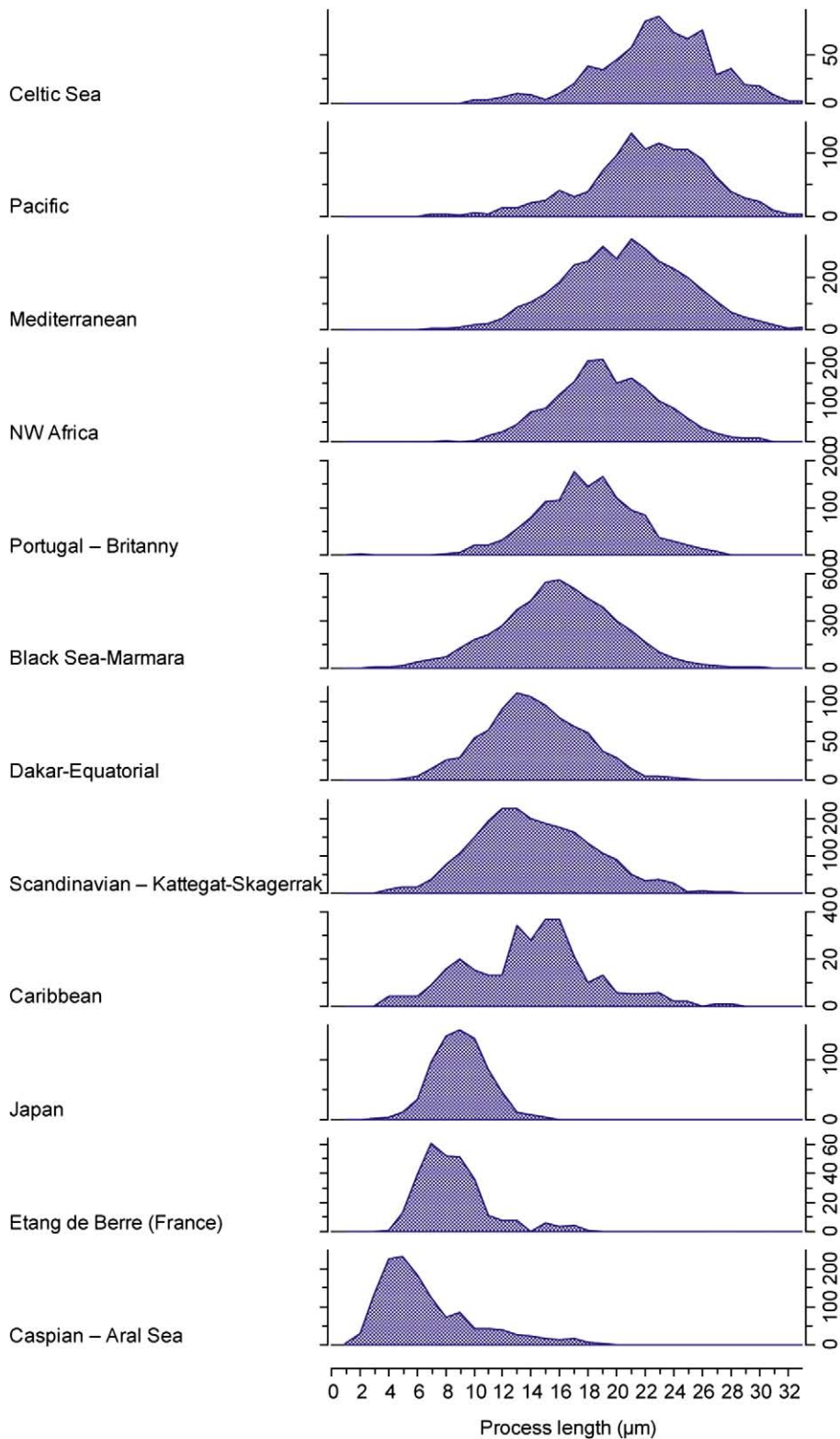


Fig. 4. Size-frequency spectra of regional process measurements, sorted from top (long average processes) to bottom (short average processes).

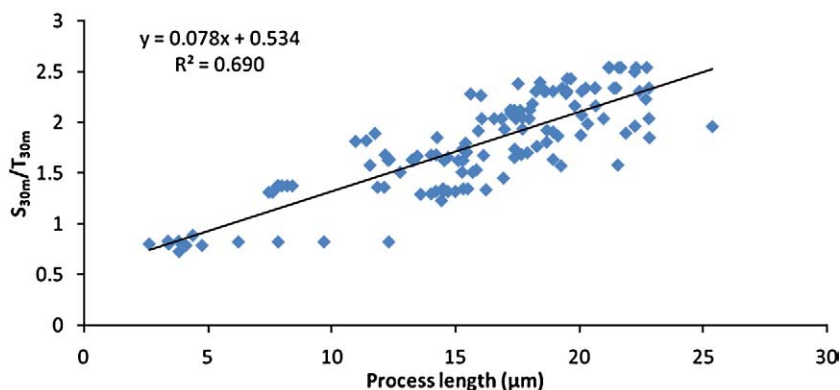


Fig. 5. Regression between average process length and summer $S_{30\text{ m}}/T_{30\text{ m}}$ for the 144 surface samples.

this parameter does not show a better fit than the $S_{30\text{ m}}/T_{30\text{ m}}$ ratio. The regression between this averaged data from each region is $(S_{30\text{ m}}/T_{30\text{ m}}) = (0.085 \cdot \text{average process length} + 0.468)$, $R^2 = 0.89$ (Fig. 6).

3.3.1. Process length in relation to body diameter

No relation between the process length and cyst body diameter was found ($R^2 = 0.002$). This was expected since culture experiments also revealed no relation between the body diameter and the salinity (Hallet, 1999). Furthermore, no significant relation was found between body diameter with the ratio between salinity and temperature at different depths. Variations in cyst body diameter are probably caused mainly by germination of the cyst or compression.

3.3.2. Process length in relation to relative cyst abundance

Mudie et al. (2001) found a correlation of $R^2 = 0.71$ between the relative abundance of *L. machaerophorum* and increasing salinity between 16 and 21.5 psu for Holocene assemblages in Marmara Sea core M9. To check this relationship in our dataset, the relative abundances of *L. machaerophorum* were determined in 92 surface samples. No significant linear relation between relative abundances in the assemblages and either the process length or the body diameter was found. No significant relationship between relative abundance and temperature or salinity data was found. This is not surprising since the relationship between relative abundances and environmental parameters is not linear, but unimodal (Dale,

1996), and several other factors play a role in determining the relative abundances on such a global scale, mostly relative abundances of other species (closed-sum problems).

3.4. Confocal laser microscopy

All processes on 20 cysts from the North Adriatic Sea (samples AN71 and AN6b) and one from the Gulf of Cadiz (sample GeoB9064) were measured, resulting in 1460 process measurements. The average distances between the processes were also calculated. A summary of the results is given in Table 2. Process length ranged from 0 to 31 μm , which differs from the 1983 process lengths from the North Adriatic Sea samples measured with transmitted light microscopy (6 to 34 μm). The shift in the frequency size spectra was obviously due to the fact that only the longest processes were measured (Fig. 7). Most remarkable was the large peak around 3 μm for the confocal measurements. Apparently, a large number of shorter processes were present on most of these cysts.

It is noteworthy that the number of processes was significantly inversely related to the average process length ($R^2 = 0.65$) (Fig. 8) and the average process length was significantly related to the average distance between the processes ($R^2 = 0.78$) (Fig. 9), and that. The lower R^2 can be explained by the incompleteness of the cysts: all cysts were germinated and thus lacking opercular plates, which can number between one and five or more in the case of epicystal archeopyles (Evitt, 1985). This implies that a large number of

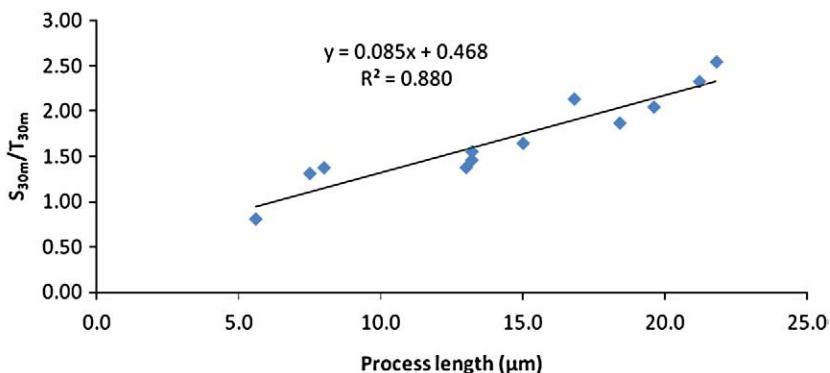


Fig. 6. Regression between average process length and summer $S_{30\text{ m}}/T_{30\text{ m}}$ averaged for every region separately.

Table 2

Average process length, standard deviation, number of processes measured and average distance between process bases from confocal microscopy in full measurements

Cyst number	Sample	Average length (µm)	Stdev length (µm)	# Processes measured	Body diameter (µm)	Average distance (µm)
2	AN71	9.82	5.78	79	44.53	4.35
4	AN71	7.26	5.72	89	39.84	3.76
5	AN71	15.87	5.06	50	56.89	5.79
7	AN71	9.80	6.36	72	45.11	4.68
9	AN71	17.79	6.41	62	43.25	6.78
10	AN71	10.32	6.49	67	39.95	4.55
11	AN71	12.25	1.90	56	43.26	6.21
12	AN71	6.85	4.82	107	39.34	3.98
13	AN71	11.50	7.26	89	43.32	4.76
14	AN71	15.88	7.27	61	51.76	6.90
15	AN71	13.20	6.19	28*	40.54	5.67
16	AN71	15.43	4.19	59	41.93	5.61
17	AN71	12.44	5.43	71	44.69	4.95
2	AN6B	11.79	6.09	71	36.38	4.40
4	AN6B	9.86	5.47	103	45.60	4.88
5	AN6B	9.14	7.13	102	42.87	4.05
6	AN6B	12.17	4.72	76	47.13	4.71
8	AN6B	12.53	4.53	58	57.84	5.66
9	AN6B	13.07	3.50	51	40.77	5.40
10	AN6B	10.30	4.68	76	41.20	4.44
1	GeoB9064	18.16	6.76	33	36.10	6.24
Average		12.16	5.51	69.52	43.92	5.13
Stdev		3.11	1.33	21.06	5.68	0.91

*This number was not used in the regression with process length, since less than half of this cyst was preserved.

processes can be missing, and it would be subjective to attempt a correction for the missing processes. It was not possible to use encysted specimens since the strong autofluorescence of the endospore of these specimens obscured many of the least autofluorescent processes. No significant relation was found between the body diameter and the average process length ($R^2=0.04$), which supports the observation with transmitted light microscopy.

4. Discussion

4.1. Process length correlated to summer $S_{30\text{ m}}/T_{30\text{ m}}$: is it realistic?

The quasi unimodal size frequency spectrum of both process length and cyst body diameter (Figs. 2 and 3), plus the correlation between the average process length and the summer $S_{30\text{ m}}/T_{30\text{ m}}$, strongly confirm that all recorded cysts are ecophenotypes of a single species. It is furthermore not surprising that the most significant relation was found with the summer $S_{30\text{ m}}/T_{30\text{ m}}$ depth. These three extra parameters – seasonality, temperature and depth – are discussed below.

Late summer–early autumn is generally the time of maximum stratification of the surface waters. Reduced salinity would enhance the water column stability with the generation of a pycnocline, and lowered water column turbulence, conditions that favour growth of *L. polyedrum* (Thomas and Gibson, 1990). In most upwelling regions, this would coincide with periods of upwelling relaxation (Blasco, 1977). Late summer–early autumn is the time of the exponential growth phase of *L. polyedrum*, which coincides with peak production of *L. machaerophorum* cysts, at least in Loch Creran, northwest Scotland (Lewis et al., 1985), and in Todos Santos Bay, Mexico (Peña-Manjarrez et al., 2005). Culturing suggests that the cyst production is triggered by nutrient depletion, and influenced by temperature (Lewis and Hallett, 1997).

The relationship found between process length and both temperature and salinity is not surprising since the formation of processes can be considered a biochemical process (Hallett, 1999), dependent on both temperature (negative relation) and salinity (positive relation). The culture experiments by Hallett (1999) confirm a positive relation to salinity and a negative relation to temperature.

Moreover, the cysts are probably formed deeper in the water column, which would explain the fit to a 30 m depth. It is well known that *L. polyedrum* migrates deep in the water column (Lewis and Hallett, 1997). A similar vertically migrating dinoflagellate, *Peridiniella catenata*, also forms cysts deeper in the water column, mostly at 30–40 m depth (Spilling et al.,

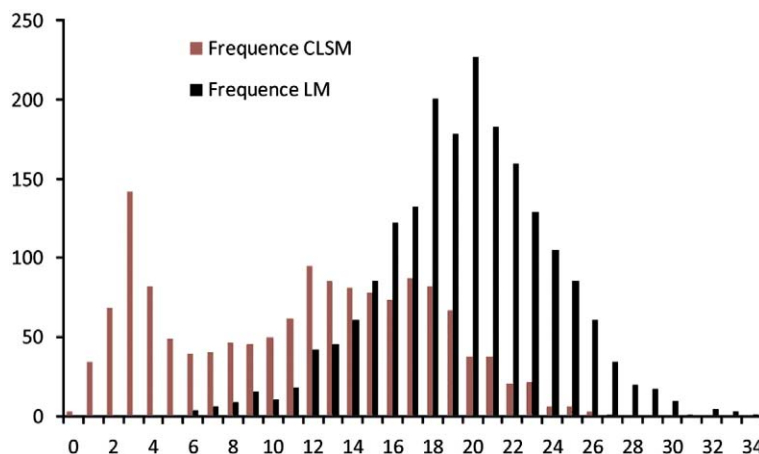


Fig. 7. Comparison between the size-frequency spectra from 1460 confocal measurements (CLSM) from the North Adriatic Sea (samples AN71 and AN6b) and from the Gulf of Cadiz and 1983 light microscope (LM) measurements from the North Adriatic.

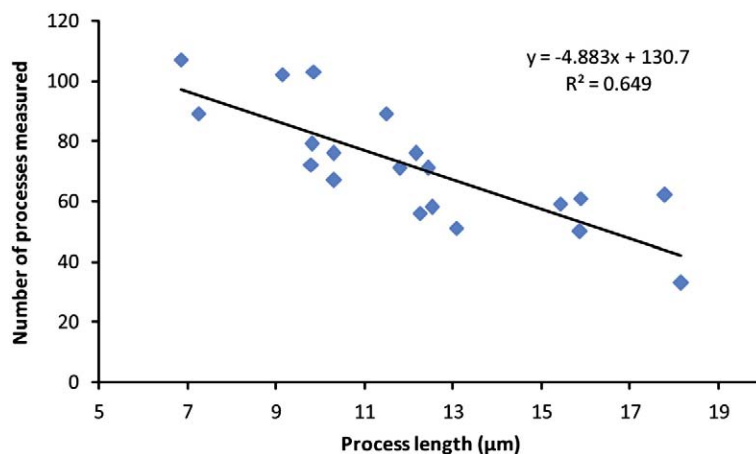


Fig. 8. Regression between average process length and the number of processes for the cysts measured with confocal microscopy.

2006). These cysts are probably formed within a range of water depths, and with 30 m depth reflecting an average depth.

The ranges of temperature (9–31 °C) and salinity (12.4–42.1 psu) at 30 m represent the window in which cyst formation takes place. Cultures show that *L. polyedrum* forms cysts at salinities ranging from 10 to 40 psu (Hallett, 1999), which fits with the results obtained in this study. The relation to deeper salinity and temperature data suggests that cyst formation more often than not takes place deeper in the water column, where salinities may be higher and temperatures lower, which suggests that caution is needed before linking *L. machaerophorum* cyst abundances directly to near surface data. This could explain the occurrence of cysts of *L. polyedrum* in regions with surface salinities as low as 5 psu (e.g. McMinn, 1990, 1991; Dale, 1996; Persson et al., 2000).

No better relation was found with density despite its dependence on salinity and temperature. Apparently, density as calculated from salinity and temperature, and pressure (water depth) by Fofonoff and Millard (1983) is much more determined by salinity, and less by temperature, whereas we assume that measured average process length is influenced by a combination of these parameters.

4.2. Transport issues

L. polyedrum occurs in estuaries, coastal embayments and neritic environments of temperate to subtropical regions (Lewis and Hallett, 1997). However, transport of the cysts into other areas by currents must be considered, and the records of *L. machaerophorum* in oceanic environments have been attributed to reworking or long-distance transport (Wall et al., 1977). A classic example is the upwelling area off northwest Africa where the cyst has been recorded over a much wider area than the thecate stage (Dodge and Harland, 1991). In this study, it was assumed that long-distance transport was not an important factor, since the transported cysts would be transported from areas with minor salinity and temperature differences, which would, according to the equation (see 2.3), be reflected in negligible changes in process length.

4.3. The Problematic Kattegat–Skagerrak and Scandinavian Fjord samples

It is noteworthy that the inclusion of the Kattegat–Skagerrak and Scandinavian samples increased the scatter of the regression

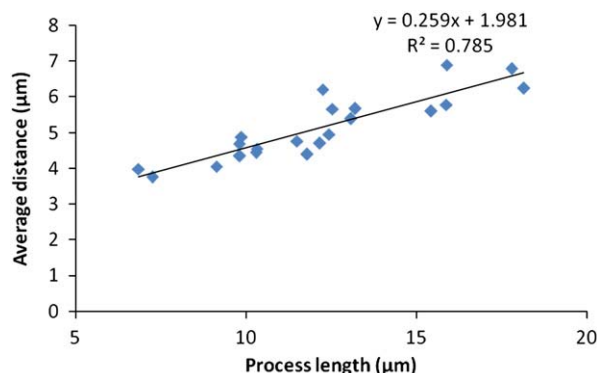


Fig. 9. Regression between average process length and the average distance between process bases for the cysts measured with confocal microscopy.

significantly. Two causes can be suggested. Firstly, since most samples plotted above the regression line, the average process length could be anomalously short. Most probably this is not linked to a preservation issue, since the average preservation was average to good (except for the Risør site), and broken processes were rare. All recovered cysts are from the uppermost section of box cores, and are thus recently formed. One possible explanation is that these specimens are genetically different which could result in slightly different morphologies. However, there is no *a priori* reason why this should be so, and this conflicts with the unimodal size-frequency distribution of process length.

Secondly, the used summer $S_{30\text{ m}}/T_{30\text{ m}}$ data could be incorrect, and this can be attributed to several causes. On one hand, the cyst production could have taken place at different water depths. When surface data ($S_{0\text{ m}}/T_{0\text{ m}}$) for the Kattegat–Skagerrak and Scandinavian samples is included in the global dataset of summer $S_{30\text{ m}}/T_{30\text{ m}}$, the relation between average process length is more significant ($R^2=0.61$). On the other hand, the timing of cyst production might be different. *L. polyedrum* blooms in fjords are probably short-lived, followed by a long resting period (Godhe and McQuoid, 2003). As for the Kattegat–Skagerrak, salinity-driven stratification, with higher salinity bottom waters and low salinity surface waters, could result in a very particular environment. In this way, the cysts are formed probably under specific salinity and temperature conditions, which could explain the increase in scatter.

4.4. Confocal measurements and implications for cyst formation

The results of this study lead to enhanced insight into the process of cyst formation of *L. machaerophorum*. Before discussing the implications of our study in detail we summarise the state of the art knowledge on cyst formation as described by Lewis & Hallett (1997) and Kokinos and Anderson (1995). The studies of these authors indicate that at the start of the cyst formation process, the motile planozygote ceases swimming, ejects its flagella, and the outer membrane swells. Then, the thecal plates of the planozygote dissociate and are pulled away from the cytoplasm by the ballooning of the outer membrane and underneath this, the formation of the cyst wall occurs. A layer of globules (each ~5 μm across) surround the cytoplasm and the spines grow outwards taking the globules with them. These terminal globules collapse to form spine tips and variations in this process confer the variable process morphology observed. Probably, membrane expansion is activated by osmosis (Kokinos, 1994), which causes a pressure gradient. According to Hallett (1999) the outer membrane always reaches full expansion, both for short and long process-bearing individuals. Measurements with confocal laser microscopy clearly show that a positive relation exists between the process length and the distance between processes, and a negative relation between the processes length and the number of processes.

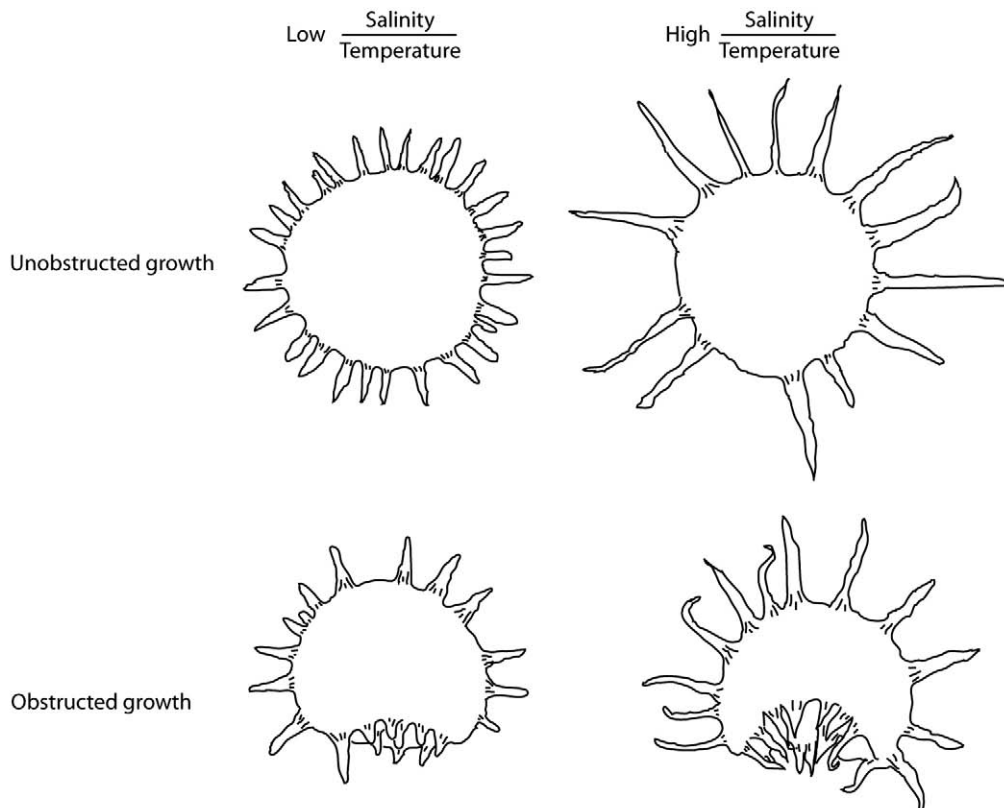


Fig. 10. Conceptual model for process formation.

These findings lead towards three implications. Firstly, the amount of dinosporin necessary for constructing the processes would be constant, at least for the studied cysts from the Mediterranean Sea. However, one needs to assume that the amount of dinosporin is proportionate to the number of processes, multiplied by the average process length. This entails that the amount of dinosporin needed for formation of the periplasm is constant, which is reasonable since the body diameter is independent of process length. Secondly, the good correlation between the average distance and the process length, together with the observation that globules are all forming simultaneously (Hallett, pers. comm.), suggests that the process length is predetermined. Thirdly, these observations suggest the existence of two end members: one with many closely spaced short processes, and one with a few, more widely spaced, long processes (Fig. 10). This gradient in biometrical groups can also be visually observed in transmitted light microscopy (Plate I–IV) and the suggested formation process for the two end members is illustrated in Fig. 11.

In order to reconcile these observations with observations from cultures, the physico-chemical properties of dinosporin have to be considered. According to Kokinos (1994), dinosporin consists of a complex aromatic biopolymer, possibly made of tocopherols. However, upon re-analysis, De Leeuw et al. (2006) showed the tocopherol link to be untrue. It can now be speculated that a certain fixed amount of this precursor monomer (probably a sugar, Versteegh, pers. comm.) for dinosporin is distributed across the sphere, in such a way that a minimum of energy is necessary for this process. This can occur through a process of flocculation (Hemsley et al. (2004)), and is dependent on both temperature and salinity. Fewer but larger colloids of the monomer will be formed when $S_{30\text{ m}}/T_{30\text{ m}}$ is higher and these will coalesce on the cytoplasmic membrane. When many small colloids are formed, it might occur that two or more colloids merge, and form one larger process (Plates II.13, II.15 and II.22). This theory can also explain the rare occurrence of crests on cyst species such as *Operculodinium centrocarpum*, where crests are formed when processes are closely spaced. In the next step, the visco-elastic dinosporin is synthesized on the globules, and stretches out in a radial direction. This stretching is clearly visible in the striations at the base of the processes. Another result of this stretching is the

formation of tiny spinules at the distal tip. These are more apparent on the longer processes, and could be the result of a fractal process: what happens at a larger scale, namely the stretching of the processes, is repeated here at a smaller scale as, stretching of the spinules. However, it is unlikely that the stretching is solely caused by membrane expansion. Hallett (1999) indicated that the outer membrane expansion is independent of the definitive process length. Thus the stretching is most probably caused by the combination of outer membrane expansion and a chemical process, similar to the swelling of cysts caused by acetolysis or KOH (see Section 2.1).

Two types of cysts deserve special attention. Clavate or bulbous process bearing cysts (Plate I.6; Plate II.11, II.20) were frequently encountered in surface sediments from low salinity environments (Black Sea, Caspian Sea, Aral Sea and the Kattegat–Skagerrak). They were frequently encountered in culture by Kokinos and Anderson (1995), but rarely by Hallett (1999). These only seem to differ from normal processes, in that the globules were not able to detach from these processes. This is supported by the fact that the length of normal processes on cysts bearing clavate processes is the same as for clavate processes.

The second type of cysts deserving attention are the bald or spheromorphic cyst. Lewis and Hallett (1997) observed that these cysts are not artefacts of laboratory culturing, since cysts devoid of processes occur in the natural environment of Loch Creran in northwest Scotland. Moreover, Persson (unpubl. experiment, 1996) noted inculturing experiments, that these cysts are viable, and thus cannot be regarded as malformations. Apart from the Aral Sea, very few bald cysts were recorded in surface sediments. It appears that on these cysts, process development did not take place. It can be speculated that this could be caused by a very early rupture of the outer membrane or the inability of the precursor monomer to flocculate at a very reduced $S_{30\text{ m}}/T_{30\text{ m}}$.

4.5. Process distribution

The process distribution on *L. machaerophorum* has been considered intratabular to non-tabular (Wall and Dale, 1968), although some authors noted alignment in the circular area (Evvit and Davidson, 1964, Wall et al., 1973). Marret et al. (2004) showed a remarkable reticulate pattern in the ventral area on

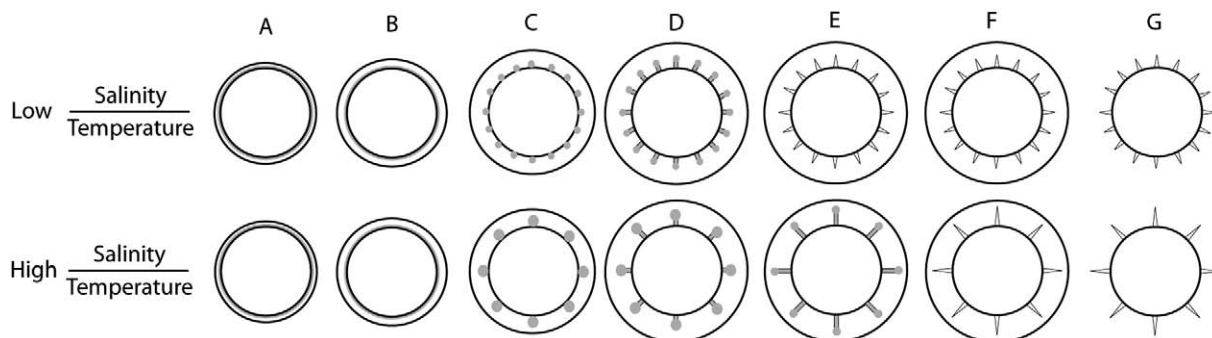


Fig. 11. Suggested formation process for the two end members based on observation and documentation by Kokinos and Anderson (1995) and Hallett (1999), and theoretical consideration by Hemsley et al. (2004). Monomer is shown in grey, membranes and polymerised coat in black. (A–B) The outer membrane starts to expand, a fixed amount of monomer is formed and starts to coalesce on the cytoplasmic membrane. (C) Depending on environmental parameters (salinity and temperature), a lot of small or a few large colloids of the monomer are formed. (D) Visco-elastic dinosporin is synthesized on the globules and stretches in a radial direction. (E) Membrane expansion often comes to a stop before radial stretching ends. (F) Formation of longer process takes longer than shorter process formation. (G) Membrane rupture occurs.

cysts with very short processes from the Caspian Sea, suggestive of a tabular distribution. Our findings indicate a regular and equidistant distribution of the processes, with evidence of a tabulation pattern lacking.

The process length distribution is not uniform. In cultures, cysts are formed at the bottom of the observation chambers, resulting in an asymmetrical distribution of the processes on the cysts, where shorter processes are formed at the obstructed side, and longer processes at the unobstructed side (Kokinis and Anderson, 1995; Hallett, 1999). When assuming that a constant amount of dinosporin is distributed over the cyst body, aberrantly long processes would form at the unobstructed side, and aberrantly short processes at the obstructed side. Our observations confirm this phenomenon: cysts from shallow areas show a similar asymmetry. The frequent occurrence of short processes on cysts from shallow areas in the Mediterranean Sea can be explained in a similar way (Fig. 7). If one measures the longest processes on these cysts, values will be slightly larger than expected from our equation. This obstruction factor needs to be incorporated into our conceptual model (Fig. 10). It is furthermore noticeable that many of the non-shallow cysts show this asymmetry to a certain degree (Plate I–IV), suggesting that this obstruction could be occurring more generally. The frequent occurrence of short processes along the cingulum could also be explained in a similar way, if the cysts were to be formed in a preferred orientation, with the obstructed side along the archeopyle.

4.6. Biological function of morphological changes?

The final consideration deals with the biological function of the processes. Possible functions of spines on resting stages have been proposed by Belmonte et al. (1997), and include flotation, clustering and enhanced sinking, passive defence, sensory activity and/or chemical exchanges and dispersal. Since the link between process length and $S_{30\text{ m}}/T_{30\text{ m}}$ exists and density is also dependent on $S_{30\text{ m}}/T_{30\text{ m}}$, it is obvious that either flotation or clustering and enhanced sinking will be the most important biological function of morphological changes of the processes. Longer processes increase the drag coefficient of the cyst and thus increase floating ability according to Stokes' law, but also increase cluster ability. However, the longest processes occur in high water density (high $S_{30\text{ m}}/T_{30\text{ m}}$) environments, where flotation would be easier, which is counterintuitive. It seems more logical, then, that longer processes are developed to facilitate sinking (through clustering) in environments with high water density.

5. Conclusions

- A total of 19,611 measurements of *L. machaerophorum* from 144 globally distributed surface samples showed a relationship between process length and both summer salinity and temperature at 30 m water depth, as given by the following equation: $(S_{30\text{ m}}/T_{30\text{ m}}) = (0.078 * \text{average process length} + 0.534)$ with $R^2 = 0.69$. For salinity the range covered is at least 12.5 to 42 psu, and for temperature 9 to 31 °C. To establish the accuracy of this salinity proxy, future culture studies will hopefully further constrain this relationship.
- Confocal microscopy shows that distances between processes are strongly related to average process length, and

that the number of processes is inversely related to average process length. This suggests a two end-member model, one with numerous short, closely spaced processes and one with relatively few, widely spaced, long processes.

- Processes of *L. machaerophorum* are hypothesized to biologically function mainly as a clustering device to enhance sinking rates.

Acknowledgements

Warner Brückmann and Silke Schenk (IFM Geomar), Rusty Lotti Bond (Lamont Doherty Earth Observatory), Chad Broyles and Walter Hale (IODP), Jim Broda Braddock Linsley (University at Albany-State), Larry Benson (USGS), Aurélie Chambouvet and Nathalie Simon (Station Biologique, Roscoff) and Liviu Giosan (WHOI), Gilles Lericolais (IFREMER, France), Katrien Heirman and Hans Pirlet (RCMG), Jean-Pierre Arrondeau (IAV) and Rex Harland are kindly acknowledged for providing samples.

Marie-Thérèse Morzadec-Kerfourn is kindly thanked for providing detailed information on sampling locations from Brittany and Philippe Picon (GIPREB) for providing salinity data from Etang de Berre. We are grateful to Zoë Verlaak for helping out with the confocal measurements and Richard Hallett for stimulating discussions on *Lingulodinium machaerophorum* process development.

We express gratitude to Martin Head and one anonymous reviewer for detailed reviews of an earlier version of this manuscript.

Appendix A. Supplementary data

Supplementary data associated with this article can be found, in the online version, at doi:10.1016/j.marmicro.2008.10.004.

References

- Amo rim, A., Palma, A.S., Sampayo, M.A., Moita, M.T., 2001. On a *Lingulodinium polyedrum* bloom in Setúbal bay, Portugal. In: Hallegraeff, G.M., Blackburn, S.I., Bolch, C.J., Lewis, R.J. (Eds.), Harmful Algal Blooms 2000. Intergovernmental Oceanographic Commission of UNESCO, pp. 133–136.
- Bendle, J., Rosell-Mele, A., Ziveri, P., 2005. Variability of unusual distributions of alkenones in the surface waters of the Nordic seas. *Paleoceanography* 20. doi:10.1029/2004PA001025.
- Bennouna, A., Berland, B., El Attar, J., Assobhei, O., 2002. *Lingulodinium polyedrum* (Stein) Dodge red tide in shellfish areas along Doukkala coast (Moroccan Atlantic). *Oceanologica Acta* 25 (3), 159–170.
- Belmonte, G., Miglietta, A., Rubino, F., Boero, F., 1997. Morphological convergence of resting stages of planktonic organisms: a review. *Hydrobiologia* 355, 159–165.
- Blasco, D., 1977. Red tide in the upwelling region of Baja California. *Limnology and Oceanography* 22, 255–263.
- Bollmann, J., Herrie, J.O., 2007. Morphological variation of *Emiliania huxleyi* and sea surface salinity. *Earth and Planetary Science Letters* 255, 273–288.
- Boyer, T.P., Stephens, C., Antonov, J.I., Conkright, M.E., Locarnini, R.A., O'Brien, T.D., Garcia, H.E., 2002. World Ocean Atlas 2001, Volume 2: salinity. In: Levitus, S. (Ed.), NOAA Atlas NESDIS, vol. 50. U.S. Government Printing Office, Wash., D.C. 165 pp., CD-ROMs.
- Brenner, W., 2005. Holocene environmental history of the Gotland Basin (Baltic Sea) – a micropaleontological model. *Palaeogeography, Palaeoclimatology, Palaeoecology* 220, 227–241.
- Cagatay, M.N., Görür, N., Algan, O., Eastoe, C., Tchapalyga, A., Ongan, D., Kuhn, T., Kuscu, I., 2000. Late Glacial–Holocene palaeoceanography of the Sea of Marmara: timing of connections with the Mediterranean and the Black Seas. *Marine Geology* 167, 191–206.
- Caner, H., Algan, O., 2002. Palynology of sapropelic layers from the Marmara Sea. *Marine Geology* 190, 35–46.
- Christensen, J.T., Cedhagen, T., Hylleberg, J., 2004. Late-Holocene salinity changes in Limfjorden, Denmark. *Sarsia* 89, 379–387.

- Combourieu-Nebout, N., Londeix, L., Baudin, F., Turon, J.-L., von Grafenstein, R., Zahn, R., 1999. Quaternary marine and continental paleoenvironments in the western Mediterranean (site 976, Alboran Sea): Palynological evidence. Proceedings of the Ocean Drilling Program. Scientific Results, 161, pp. 457–468.
- Dale, B., 1996. Dinoflagellate cyst ecology: modelling and geological applications. In: Jansonius, J., McGregor, D.C. (Eds.), *Palynology: Principles and Applications*, vol. 3. AASP Foundation, Dallas, TX, pp. 1249–1275.
- Deflandre, G., Cookson, I.C., 1955. Fossil microplankton from Australia late Mesozoic and Tertiary sediments. *Australian Journal of Marine and Freshwater Research* 6, 242–313.
- de Leeuw, J.W., Versteegh, G.J.M., van Bergen, P.F., 2006. Biomacromolecules of algae and plants and their fossil analogues. *Plant Ecology* 182, 209–233.
- de Vernal, A., Hillaire-Marcel, C., 2000. Sea-ice cover, sea-surface salinity and halo/thermocline structure of the northwest North Atlantic: modern versus full glacial conditions. *Quaternary Science Reviews*, 19 (5), 65–85.
- Dodge, J.D., Harland, R., 1991. The distribution of planktonic dinoflagellates and their cysts in the eastern and northeastern Atlantic Ocean. *New Phytologist* 118, 593–603.
- Ellegaard, 2000. Variations in dinoflagellate cyst morphology under conditions of changing salinity during the last 2000 years in the Limfjord, Denmark. *Review of Palaeobotany and Palynology* 109, 65–81.
- Evitt, W.R., Davidson, S.E., 1964. Dinoflagellate cysts and thecae. Stanford University Publications Geological Sciences 10, 1–12.
- Evitt, W.R., 1985. Sporopollenin dinoflagellate cysts. Their morphology and interpretation. Dallas: American Association of Stratigraphic Palynologists Foundation.
- Fofonoff, P., Millard Jr., R.C., 1983. Algorithms for computing of fundamental properties of seawater. *Unesco Technical Papers in Marine Sciences* 44, 1–53.
- Godhe, A., McQuoid, 2003. Influence of benthic and pelagic environmental factors on the distribution of dinoflagellate cysts in surface sediments along the Swedish west coast. *Aquatic Microbial Ecology* 32, 185–201.
- Grøsfjeld, K., Harland, R., 2001. Distribution of modern dinoflagellate cysts from inshore areas along the coast of southern Norway. *Journal of Quaternary Science* 16 (7), 651–659.
- Gundersen, N., 1988. En palynologisk undersøkelse av dinoflagellatcyster langs en synkende salinitetsgradient i recente sedimenter fra Østersjøområdet. Unpublished candidata scientiarum thesis, University of Oslo, 1–96.
- Hallett, R.I. 1999. Consequences of environmental change on the growth and morphology of *Lingulodinium polyedrum* (Dinophyceae) in culture. PhD thesis 1–109. University of Westminster.
- Head, M.J., 1996. Late Cenozoic dinoflagellates from the Royal Society borehole at Ludham, Norfolk, Eastern England. *Journal of Paleontology* 70 (4), 543–570.
- Hemsley, A.R., Lewis, J., Griffiths, P.C., 2004. Soft and sticky development: some underlying reasons for microarchitectural pattern convergence. *Review of Palaeobotany and Palynology* 130, 105–119.
- Kokinos, J.P., 1994. Studies on the cell wall of dinoflagellate resting cysts: morphological development, ultrastructure, and chemical composition. PhD thesis, Massachusetts Institute of Technology/Woods Hole Oceanographic Institution.
- Kokinos, J.P., Anderson, D.M., 1995. Morphological development of resting cysts in cultures of the marine dinoflagellate *Lingulodinium polyedrum* (= *L. machaerophorum*). *Palynology* 19, 143–166.
- Kotthoff, U., Pross, J., Müller, U.C., Peyron, O., Schmiedl, G., Schulz, H., Bordon, A., 2008. Climate dynamics in the borderlands of the Aegean Sea during formation of sapropel S1 deduced from a marine pollen record. *Quaternary Science Reviews* 27, 832–845.
- Kuhlmann, H., Freudenthal, T., Helmke, P., Meggers, H., 2004. Reconstruction of paleoceanography off NW Africa during the last 40,000 years: influence of local and regional factors on sediment accumulation. *Marine Geology* 207 (1–4), 209–224.
- Leroy, S.A.G., Marret, F., Giralt, S., Bulatov, S.A., 2006. Natural and anthropogenic rapid changes in the Kara-Bogaz Gol over the last two centuries reconstructed from palynological analyses and a comparison to instrumental records. *Quaternary International* 150, 52–70.
- Leroy, S.A.G., Marret, F., Gibert, E., Chalié, F., Reyss, J.L., Arpe, K., 2007. River inflow and salinity changes in the Caspian Sea during the last 5500 years. *Quaternary Science Reviews* 26 (25–28), 3359–3383.
- Leroy, V., 2001. Traceurs palynologiques des flux biogéniques et des conditions hydrographiques en milieu marin cotier: exemple de l'étang de Berre. DEA, Ecole doctorale Sciences de l'environnement d'Aix-Marseille, 30 pp.
- Lewis, J., Tett, P., Dodge, J.D., 1985. The cyst-theca cycle of *Gonyaulax polyedra* (*Lingulodinium machaerophorum*) in Creran, a Scottish west coast Sea-Loch. In: Anderson, D.M., White, A.W., Baden, D.G. (Eds.), *Toxic dinoflagellates*. Elsevier Science Publishing, pp. 85–90.
- Lewis, J., Hallett, R., 1997. *Lingulodinium polyedrum* (*Gonyaulax polyedra*) a blooming dinoflagellate. In: Ansell, A.D., Gibson, R.N., Barnes, M. (Eds.), *Oceanography and Marine Biology: An Annual Review*, vol. 35. UCL Press, London, pp. 97–161.
- Marret, F., 1994. Distribution of dinoflagellate cysts in recent marine sediments from the east Equatorial Atlantic (Gulf of Guinea). *Review of Palaeobotany and Palynology* 84, 1–22.
- Marret, F., Scurce, J., 2002. Control of modern dinoflagellate cyst distribution in the Irish and Celtic seas by seasonal stratification dynamics. *Marine Micropaleontology* 47, 101–116.
- Marret, F., Leroy, S.A.G., Chalié, F., Gasse, F., 2004. New organic-walled dinoflagellate cysts from recent sediments of Central Asian seas. *Review of Palaeobotany and Palynology* 129, 1–20.
- Marret, F., Zonneveld, K.A.F., 2003. Atlas of modern organic-walled dinoflagellate cyst distribution. *Review of Palaeobotany and Palynology* 125, 1–200.
- Marret, F., Mudie, P., Aksu, A., Hiscott, R.N., 2007. A Holocene dinocyst record of a two-step transformation of the Neoeuxinian brackish water lake into the Black Sea. *Quaternary International* 193. doi:10.1016/j.quaint.2007.01.010.
- Matthiessen, J., Brenner, W., 1996. Chlorococcalgen und Dinoflagellaten-Zysten in rezenten Sedimenten des Greifswalder Boddens (südliche Ostsee). *Senckenbergiana Maritima* 27 (1/2), 33–48.
- Mertens, K., Lynn, M., Aycard, M., Lin, H.-L., Louwye, S., 2008. Coccolithophores as paleoecological indicators for shift of the ITCZ in the Cariaco Basin during the Late Quaternary. *Journal of Quaternary Science*. doi:10.1002/jqs.1194.
- McMinn, A., 1990. Recent dinoflagellate cyst distribution in eastern Australia. *Review of Palaeobotany and Palynology* 65, 305–310.
- McMinn, A., 1991. Recent dinoflagellate cysts from estuaries on the central coast of New South Wales, Australia. *Micropaleontology* 37, 269–287.
- Mudie, P.J., Aksu, A.E., Yasar, D., 2001. Late Quaternary dinoflagellate cysts from the Black, Marmara and Aegean seas: variations in assemblages, morphology and paleosalinity. *Marine Micropaleontology* 43, 155–178.
- Mudie, P.J., Rochon, A.E., Levac, E., 2002. Palynological records of red tide-producing species in Canada: past trends and implications for the future. *Palaeogeography, Palaeoclimatology, Palaeoecology* 180 (1), 159–186.
- Mudie, P.J., Marret, F., Aksu, A.E., Hiscott, R.N., Gillespie, H., 2007. Palynological evidence for climatic change, anthropogenic activity and outflow of Black Sea water during the Late Pleistocene and Holocene: centennial- to decadal-scale records from the Black and Marmara Seas. *Quaternary International* 167–168, 73–90.
- Nehring, S., 1994. Spatial distribution of dinoflagellate resting cysts in recent sediments of Kiel Bight, Germany (Baltic Sea). *Ophelia* 39 (2), 137–158.
- Nehring, S., 1997. Dinoflagellate resting cysts from recent German coastal sediments. *Botanica Marina* 40, 307–324.
- Nürnberg, D., Groeneveld, J., 2006. Pleistocene variability of the subtropical convergence at East Tasman Plateau: evidence from planktonic foraminiferal Mg/Ca (ODP Site 1172A). *Geochemistry, Geophysics, Geosystems* 7–4, Q04P11. doi:10.1029/2005GC000984.
- Peña-Manjarrez, J.L., Helenes, J., Gaxiola-Castro, G., Orellano-Cepeda, E., 2005. Dinoflagellate cysts and bloom events at Todos Santos Bay, Baja California, México, 1999–2000. *Continental Shelf Research* 25, 1375–1393.
- Persson, A., Godhe, A., Karlson, B., 2000. Dinoflagellate cysts in recent sediments from the West coast of Sweden. *Botanica Marina* 43, 66–79.
- Pospelova, V., de Vernal, A., Pedersen, T.F., 2008. Distribution of dinoflagellate cysts in surface sediments from the northeastern Pacific Ocean (43–25°N) in relation to sea-surface temperature, productivity and coastal upwelling. *Marine Micropaleontology* 68 (1–2), 21–48. doi:10.1016/j.marmicro.2008.01.008.
- Reid, P.C., 1974. Gonyaulacean dinoflagellate cysts from the British Isles. *Nova Hedwigia* 25, 579–637.
- Richter, D., Vink, A., Zonneveld, K.A.F., Kuhlmann, H., Willems, H., 2007. Calcareous dinoflagellate cyst distributions in surface sediments from upwelling areas off NW Africa, and their relationships with environmental parameters of the upper water column. *Marine Micropaleontology* 63, 201–228.
- Robert, C., Degiovanni, C., Jaubert, R., Leroy, V., Reyss, J.L., Saliège, J.F., Thouveny, N., de Vernal, A., 2006. Variability of sedimentation and environment in the Berre coastal lagoon (SE France) since the first millennium: natural and anthropogenic forcings. *Journal of Geochemical Exploration* 88, 440–444.
- Rostek, F., Ruhland, G., Bassinot, F.C., Muller, P.J., Labeyrie, L.D., Lancelot, Y., Bard, E., 1993. Reconstructing sea-surface temperature and salinity using $\delta^{18}\text{O}$ and alkenone records. *Nature* 364, 319–321.
- Sangiorgi, F., Fabbri, D., Comandini, M., Gabbianelli, G., Tagliavini, E., 2005. The distribution of sterols and organic-walled dinoflagellate cysts in surface sediments of the North-western Adriatic Sea (Italy). *Estuarine, Coastal and Shelf Science* 64, 395–406.
- Schmidt, M.W., Spero, H.J., Lea, D.W., 2004. Links between salinity variation in the Caribbean and North Atlantic thermohaline circulation. *Nature* 428, 160–163.

- Schoell, M., 1974. Valdivia VA 01/03, Hydrographie II und III. Bundesanstalt für Bodenforschung, Hannover, Germany.
- Schouten, S., Ossebaar, J., Schreiber, K., Kienhuis, M.V.M., Langer, G., Benthien, A., Bijma, J., 2006. The effect of temperature, salinity and growth rate on the stable hydrogen isotopic composition of long chain alkenones produced by *Emiliania huxleyi* and *Gephyrocapsa oceanica*. *Biogeosciences* 3, 113–119.
- Sorrell, P., Popescu, S.-M., Head, M.J., Suc, J.-P., Klotz, S., Oberhänsli, H., 2006. Hydrographic development of the Aral Sea during the last 2000 years based on a quantitative analysis of dinoflagellate cysts. *Palaeography, Palaeoclimatology, Palaeoecology* 234, 304–327.
- Spilling, K., Kremp, A., Tamelander, T., 2006. Vertical distribution and cyst production of *Peridiniella catenata* (Dinophyceae) during a spring bloom in the Baltic Sea. *Journal of Plankton Research* 28 (7), 659–665.
- Stephens, C., Antonov, J.I., Boyer, T.P., Conkright, M.E., Locarnini, R.A., O'Brien, T.D., Garcia, H.E., 2002. World Ocean Atlas 2001, Volume 1: temperature. In: Levitus, S. (Ed.), NOAA Atlas NESDIS, vol. 49. U.S. Government Printing Office, Wash., D.C. 167 pp., CD-ROMs.
- Sweeney, B.M., 1975. Red tides I have known. In *toxic dinoflagellate blooms*. In: LoCicero, V.R. (Ed.), Massachusetts Science and Technology Foundation, Wakefield, Massachusetts, pp. 225–234.
- Thomas, W.H., Gibson, C.H., 1990. Quantified small-scale turbulence inhibits a red tide dinoflagellate, *Gonyaulax polyedra* Stein. *Deep-Sea Research* 37, 1538–1593.
- Turon, J.-L., 1984. Le palynoplankton dans l'environnement actuel de l'Atlantique nord-oriental. Evolution climatique et hydrologique depuis le dernier maximum glaciaire. Mémoire de l'institut de Géologie du Bassin d'Aquitaine 17, 1–313.
- van der Meer, M.T.J., Sangiorgi, F., Baas, M., Brinkhuis, H., Sinninghe-Damsté, J.S., Schouten, S., 2008. Molecular isotopic and dinoflagellate evidence for Late Holocene freshening of the Black Sea. *Earth and Planetary Science Letters* 267, 426–434.
- Van der Meer, M.T.J., Baas, M., Rijpstra, W.I.C., Marino, G., Rohling, E.J., Sinninghe Damsté, J.S., Schouten, S., 2007. Hydrogen isotopic compositions of long-chain alkenones record freshwater flooding of the Eastern Mediterranean at the onset of sapropel deposition. *Earth and Planetary Science Letters* 262, 594–600.
- van Harten, D., 2000. Variable nodding in *Cyprideis torosa* (Ostracoda, Crustacea): an overview, experimental results and a model from Catastrophe Theory. *Hydrobiologia* 419 (1), 131–139. doi:10.1023/A:1003935419364.
- Verleye, T., Mertens, K.N., Louwye, S., Arz, H.W., 2008. Holocene Salinity changes in the southwestern Black Sea: a reconstruction based on dinoflagellate cysts. *Palynology* 32.
- Vink, A., Rühlemann, C., Zonneveld, K.A.F., Mulitza, S., Hüls, M., Willems, H., 2001. Shifts in the position of the North Equatorial Current and rapid productivity changes in the western Tropical Atlantic during the last glacial. *Paleoceanography* 16 (1), 1–12.
- Vink, A., Zonneveld, K.A.F., Willems, H., 2000. Organic-walled dinoflagellate cysts in western equatorial Atlantic surface sediments: distributions and their relation to environment. *Review of Palaeobotany and Palynology* 112, 247–286.
- Wall, D., Dale, B., 1968. Modern dinoflagellate cysts and the evolution of the Peridinales. *Micropaleontology* 14, 265–304.
- Wall, D., Dale, B., Harada, K., 1973. Description of new fossil dinoflagellates from the Late Quaternary of the Black Sea. *Micropaleontology* 19, 18–31.
- Wall, D., Dale, B., Lohman, G.P., Smith, W.K., 1977. The environmental and climatic distribution of dinoflagellate cysts in modern marine sediments from regions in the North and South Atlantic Ocean and adjacent seas. *Marine Micropaleontology* 2, 121–200.
- Wang, L., Sarntheim, M., Duplessy, J.C., Erlenkeuser, H., Jung, S., Pfaumann, U., 1995. Paleo sea surface salinities in the low-latitude Atlantic: the $\delta^{18}\text{O}$ record of *Globigerinoides ruber* (White). *Paleoceanography* 10, 749–761.
- Zonneveld, K.A.F., Versteegh, G.J.M., de Lange, G.J., 2001. Palaeoproductivity and post-depositional aerobic organic matter decay reflected by dinoflagellate cyst assemblages of the Eastern Mediterranean S1 sapropel. *Marine Geology* 172, 181–195.

LATE PLEISTOCENE – HOLOCENE MARINE AND CONTINENTAL ENVIRONMENTS RECONSTRUCTION

3.1. MEDITERANEAN - BLACK - MARMARA SEA REGION

The Late Glacial and Holocene were times of important changes in the Mediterranean region. Both episodes witnessed significant vegetation dynamics driven by global climate changes, and the transition from Late Glacial to Holocene was characterized by a sea-level rise of more than 100 m. During this time-span, the Marmara and Black seas were affected by an outstanding event related to their successive flooding by the marine Mediterranean waters at 12 ka BP and 8.4 ka BP respectively. They provoked impressive changes on the previous brackish environments, coastal agricultural practices and human diaspora (Ryan and Pittman, 1999). For what concerns the flooding of the Marmara Sea, the most accepted hypothesis relates to a progressive process caused by the global rise in sea-level during the last deglaciation. As for the Black Sea flooding, a intense international debate is opened and concerns: (1) the gateway supposed to have connected the Black and Marmara seas (Bosporus Strait or Sakarya River); (2) the causes of the opening of this gateway; and (3) the character, progressive or catastrophic, of this event. According to ^{14}C ages, some authors assume previous connections between the Black and Marmara seas through the valley of the Sakarya River at 7230 ^{14}C yrs BP (Görür *et al.*, 2001), i.e. significantly before the opening of the Bosporus Strait that would be dated at 5300 ^{14}C yrs BP (Çağatay *et al.*, 2000). The factors which caused the inundation of the Black Sea refer to the collapse of the Bosporus Strait forced by the regional tectonic activity (Gökaşan *et al.*, 1997; Demirbağ *et al.*, 1999) or to the global sea-level rise and the resulting erosion of the strait (Ross and Degens, 1974; Demirbağ *et al.*, 1999). As a consequence, whatever the location of the initial channel, two scenarios have been opposed: (1) the “deep sill model” that assumes the abrupt flooding of the Black Sea (Ryan *et al.*, 1997), and (2) the “shallow sill model” that refers to a more progressive invasion by the Mediterranean marine waters (Aksu *et al.*, 1999).

In the frame of the European Project ASSEMBLAGE (EVK3-CT-2002-00090) axed on the Last Glacial Cycle evolution of the Black Sea Basin, different cores have been studied (Fig. 22), using a full palynological approach (pollen grains, dinoflagellate cysts and palynofacies features) that permits to contribute to answer the previous questions. The pollen analyses provided an accurate idea on the vegetation dynamics which was controlled by global climate changes and hence a reconstruction of variability of the climate parameters such as the mean annual temperature (MAT), mean temperature of the coldest (MTC) and warmest (MTW) months, and mean annual precipitations (MAP) based on a transfer functions applied to pollen records (in collaboration with S. Klotz, Tübingen University, Germany). Pollen analyses and climate reconstruction were achieved for three cores: BLKS 98-10 and B2KS33 from the Black sea and C10 from the Marmara Sea. Several other cores are partially analysed on the moment. The dinoflagellate cyst analysis was used to characterize the flooding and its consequences on the marine realm. Two transfer functions, using the dinoflagellate cysts, are in progress, in order to reconstruct the physical parameters of sea-surface waters as sea-surface salinity (SSS), sea-surface temperature (SST) and nutrient content. The first transfer function takes into account the relative frequency of dinoflagellate cysts in the assemblages and global sea-surface parameter ranges (SST, SSS and nutrient content)

for each species. This method was first developed for the North Atlantic and it is difficult to apply on the environments submitted to important fluctuations of sea-surface parameters, such as the intercontinental seas (Black, Marmara, Caspian and Aral seas). This method was used for quantifying the parameters of marine water input during the short connections. A second transfer function, developed in collaboration with K. Mertens (Gent University, Belgium), aims to reconstruct the SSS and SST using the morphological modification of some selected species (*Lingulodinium machaerophorum* and *Operculodinium centrocarpum*). Preliminary results were obtained on the core BLKS 98-10 (Black sea) by F. Dalesme (my Master 1 student). The palynofacies analyses provide information on the variability of oxic/anoxic conditions in the two basins and on sea-level variation.

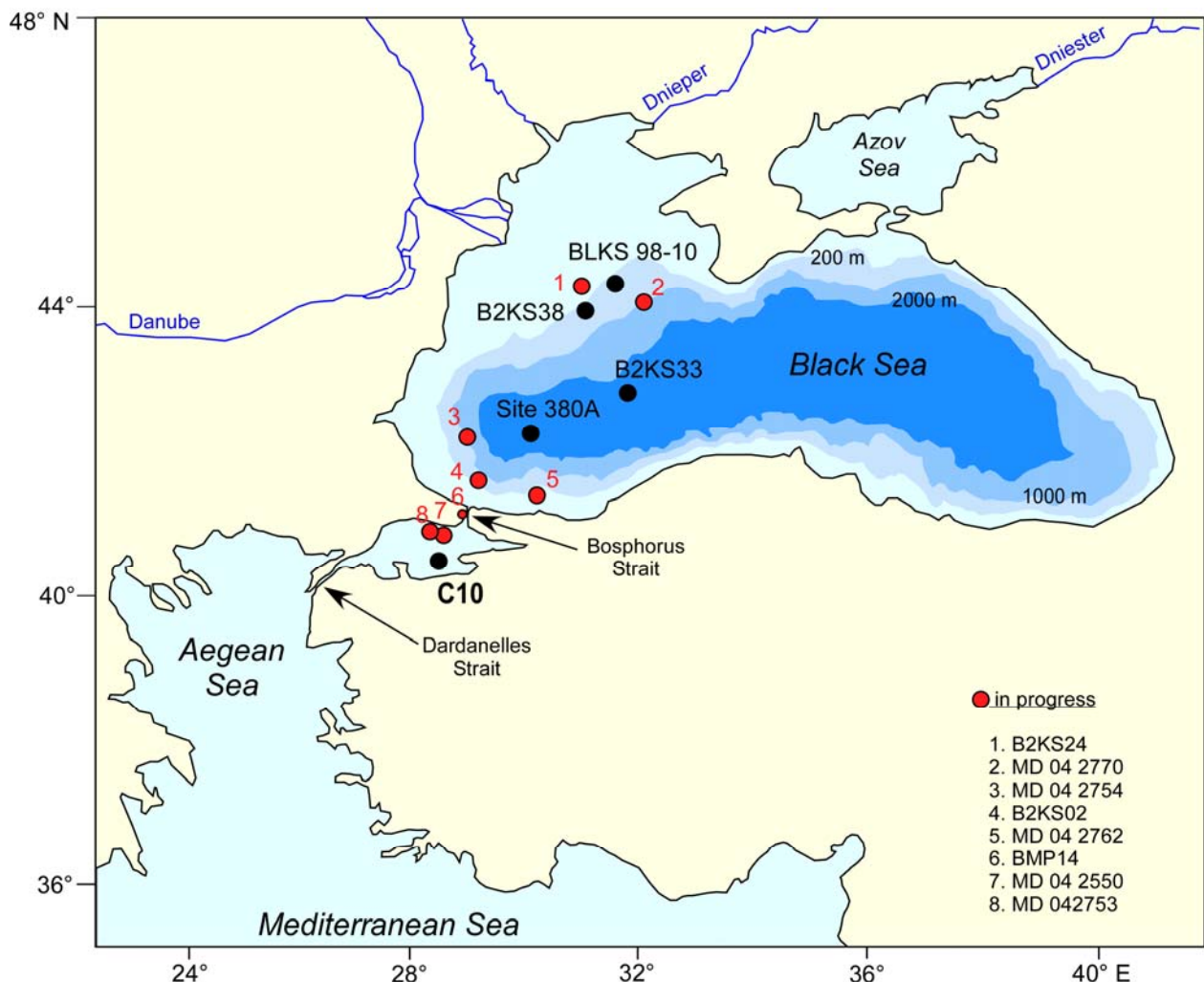


Fig. 22. Geographical position of the studied cores: BLKS and B2KS cores were drilled during BLASON 1 and BLASON 2 French cruises, MD – cores were drilled during the ASSEMBLAGE European Project, C-10 (Marmara Sea) was provided by N. Çagatay (Technical Istanbul University) and BMP 14 core (drilled in the Bosphorus Strait) was provided by O. Algan (Istanbul University).

3.1.1. Global climate changes, impact on the regional vegetation.

The studied region is today at the intersection of four vegetation realms (Fig. 23): (1) at mid-altitude, deciduous temperate forests (with oaks and beeches) develop and are replaced higher in altitude by conifers (mainly pines, firs, junipers and spruces); (2) dry

grasslands characterize the north Black and Marmara sea region; (3) meso-Mediterranean ecosystems with evergreen oaks and shrubs are located around the Marmara Sea; and (4) *Artemisia* steppes inhabit the Anatolian Plateau and South Crimea (Bohn *et al.*, 2004; Zohary, 1973; Quézel and Médail, 2003). Such a vegetation organizing is identified in the region since the Late Miocene (Popescu 2006, Popescu *et al.*, in progress; Biltekin *et al.*, in progress). Its dynamics was forced by astronomical factors, as revealed by the Early Pliocene of Site 380 (Popescu, 2006) or for the last climatic cycles from the Tenaghi Philippon core (Wijmstra and Groenhart, 1983). To understand the taphonomic aspect of pollen grain sedimentation, surface samples from Romania and Black Sea top cores (provided by the ASSEMBLAGE Project, or sampled during my postdoc at WHOI, USA) were collected and partly analysed. The geographic location of the studied cores is shown in Fig. 23. Preliminary results suggest that the pollen content represents the local vegetation as documented by the Romanian samples, the understanding of Black sea-surface samples seems to be more complicated, the signal being probably impacted by the internal circulation of the Black Sea (Rim Current?).

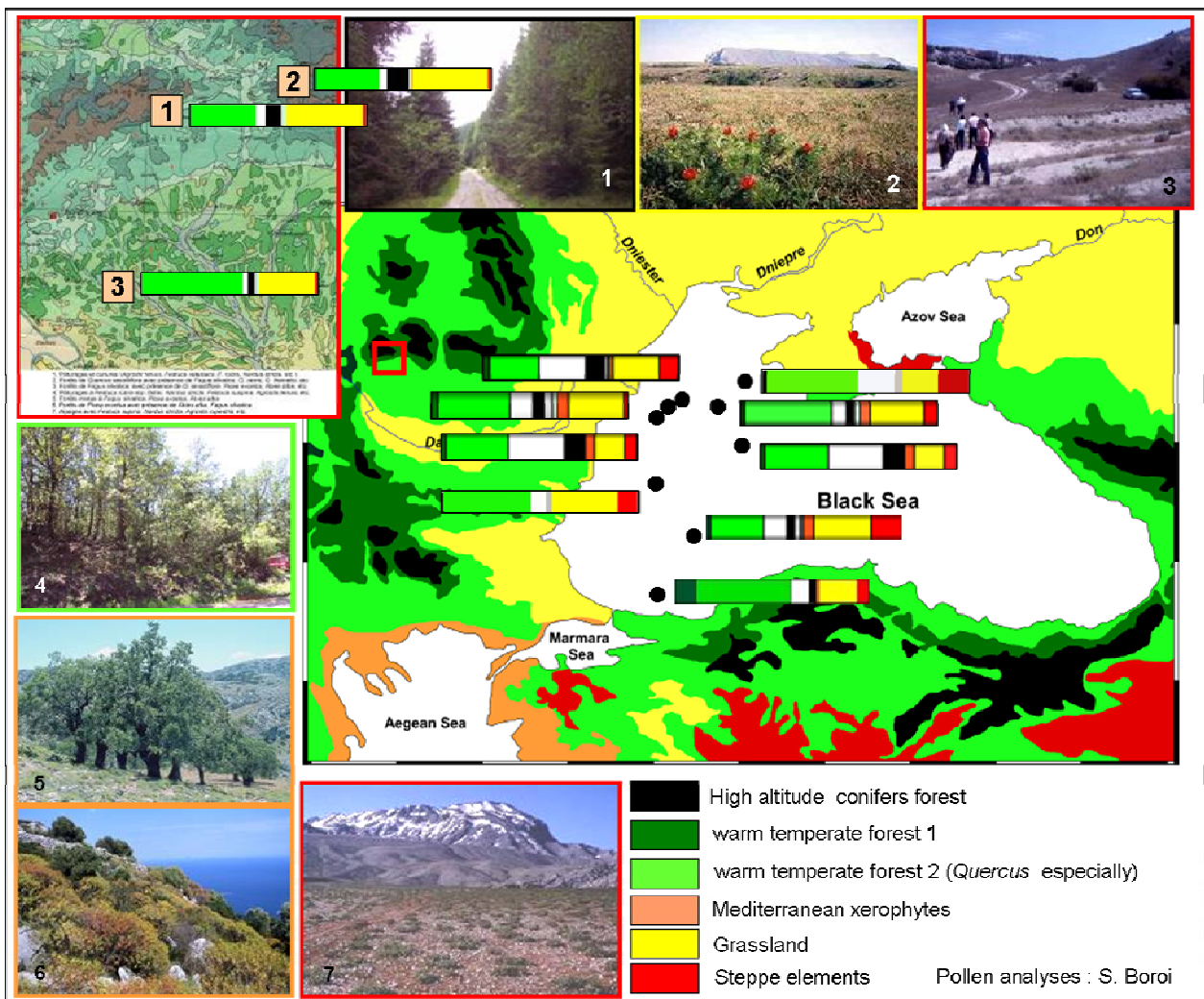


Fig. 23. Present-day simplified vegetation map of the studied region, geographic location of surface-samples and the corresponding pollen spectra. Photographs refer to vegetation types: 1, altitudinal forest (Site 2); 2, Crimea grassland; 3, Crimea steppe; 4, warm temperate deciduous *Quercus* forest (Site 3); 5, 6, meso-Mediterranean vegetation, 7, *Artemisia* steppe of the Anatolian Plateau.

In terms of vegetation dynamics of the studied area, the development of open vegetation marked by high frequency of herbs, including halophytes and steppe elements (*Artemisia*, mainly), is related to cooler and drier climate conditions, while the development of thermophilous elements corresponds to warmer and more humid conditions (Fig. 24). Such an opposition between wet and dry vegetations results in very contrasted pollen diagrams documenting a highly variable vegetation.

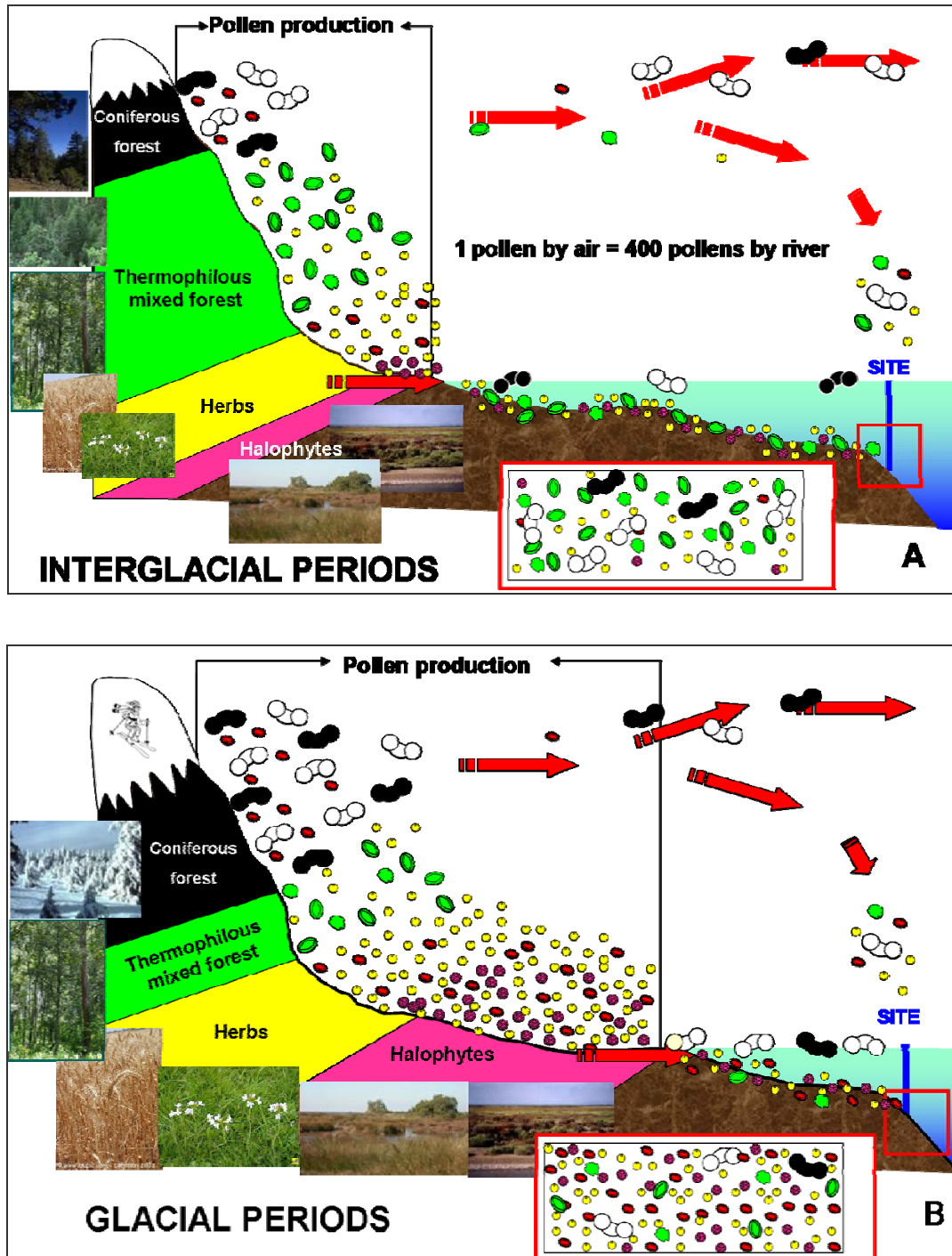


Fig. 24. Vegetation distribution with respect to altitudinal gradient and climate context (A, interglacial period; B, glacial period), pollen transport by air and by river, according to the quantified model from the Rhône Delta, and representative pollen floras (on the slide) of glacial or interglacial phases.

Two indexes, almost similar, are used to represent the vegetation changes with respect to global climate fluctuations: the first one is based on the ratio between total arboreal pollen, including *Pinus*, and steppe elements (somewhat equivalent to the “steppe index” of Traverse, 1973); the second one is based on the ratio between pollen grains of thermophilous elements (*Pinus* and other conifers such as *Picea*, *Abies*, *Cathaya*, are excluded) and those of steppe elements (*Artemisia*, *Ephedra*, etc.). *Pinus* has been excluded because it can only be identified at the genus level using pollen grains, it represents a variety of environments ranging from warm-temperate to cold-temperate conditions and it generally almost disappears within sapropels for still unclear reasons, although probably related to taphonomy. Surface sediment studies (Heusser and Balsam, 1977) and laboratory experiments (Holmes, 1994) suggest that the distribution of pollen grains in the surface sediments is directly dependent on pollen density and morphology (Holmes, 1994). Heusser and Balsam (1977) suggest that small and dense pollen grains generally accumulate with highest percentages (50 to 80%) in proximal areas (e.g. littoral, prodeltaic sediments), while coniferous bissetate less dense pollen grains (e.g. *Pinus*, *Abies*) are more dominant in the distal areas (basin sediments).

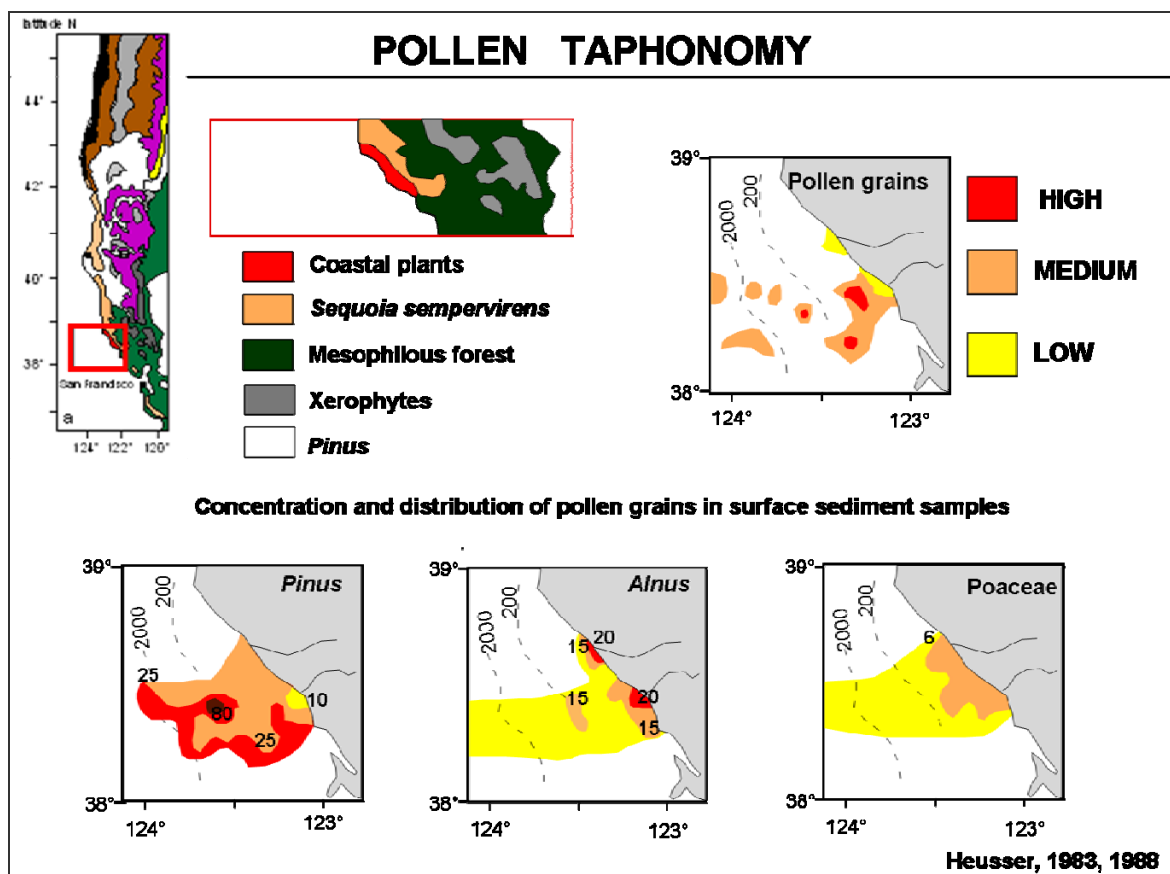


Fig. 25. Pollen taphonomy according to Heusser, 1983, 1988.

According to these studies (Fig. 25), we may use the relationships between the relative abundance of *Pinus* (and on the whole the bissetate pollen grains) and halophytes (i.e. Amaranthaceae-Chenopodiaceae) to indicate sea-level variation. Generally, high percentages of *Pinus* associated to low percentages of halophytes reflect distal conditions and may correlate with high relative sea-level, while a decrease in *Pinus* consistent with an increase in halophytes may correlate with low relative sea-level.

High-resolution pollen records obtained from different Black Sea (BLKS 98-10, B2KS 38) and Marmara Sea cores (C10) (see Fig. 22 for the core location) by myself and/or my PhD students.

BLKS 98-10 (Black sea) core was drilled on the upper continental slope of the western Black Sea (44°04.04'N and 30°50.68'E) at a water depth of 378 m during the BlaSON cruise in 1998. The core is long of 7.55 m and shows a continuous sedimentation according to seismic record. This core benefits from five ^{14}C datings (Major *et al.*, 2002), that permitted to establish a high-chronological resolution. The age model was constructed using the Calib 5 software (Reimer *et al.*, 2004). Pollen records show a high-diversified flora composed of 111 taxa which are presented on a semi-detailed diagram in Figure 24.

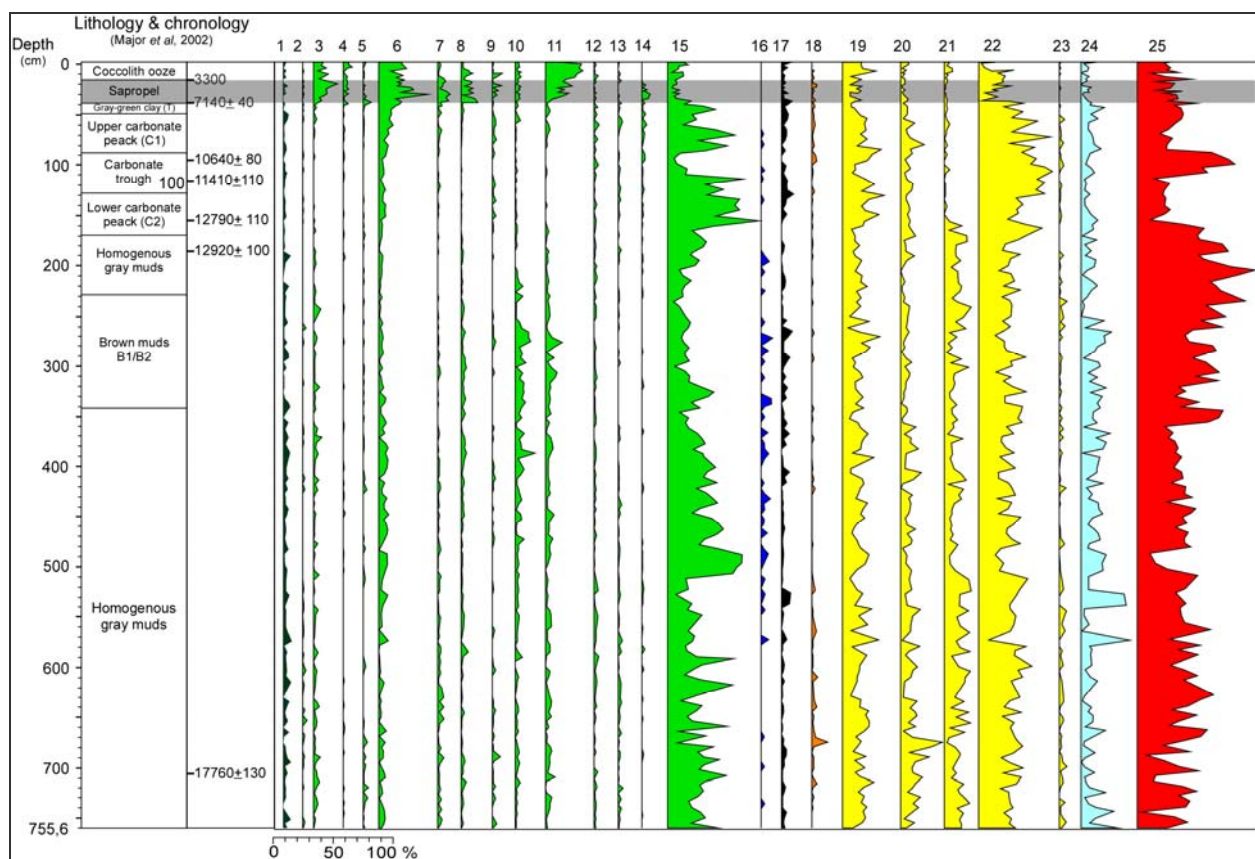


Fig. 24. Semi-detailed pollen diagram, core BLKS 98-10: 1, Taxodiaceae; 2, *Acer*; 3, *Carpinus*; 4, *Fagus*; 5, other mesothermic taxa: *Buxus sempervirens*, Rutaceae, *Platanus*, *Ostrya*, *Liquidambar*, *Liquidambar orientalis*, *Ilex*, *Tilia*, Vitaceae; 6, *Quercus*; 7, Ulmaceae: *Celtis*, *Ulmus*, *Zelkova*; 8, *Corylus*; 9, Juglandaceae: *Carya*, *Juglans*, *Juglans cathayensis*, *Pterocarya*; 10, *Betula*; 11, *Alnus*; 12, *Salix*; 13, *Fraxinus*; 14, *Populus*; 15, *Pinus*; 16, Mid-altitude trees: *Sciadopytis*, *Tsuga*, *Cedrus*; 17, High-altitude trees: *Picea*, *Abies*; 18, Mediterranean xerophytes: Oleaceae, *Olea*, *Quercus ilex* type, Rhamnaceae; 19, Poaceae; 20, Asteraceae; 21, other herbs: Rosaceae, *Sanguisorba*, *Geranium*, *Hypericum*, Papaveraceae, *Papaver*, *Argemone*, *Erodium*, Lamiaceae, Cereals, Primulaceae, *Euphorbia*; Cistaceae; *Echinops*, *Rumex*, Brassicaceae, Apiaceae, Crassulaceae, Boraginaceae, *Borrago*, Polygonaceae, *Polygonum cf. aviculare*, *Polygonum cf. lapatifolium*, *Gallium*, *Asphodellus*, Cannabaceae, Amaryllidaceae, *Helianthemum*, Ericaceae, *Euonymus*, Campanulaceae, Solanaceae, Fabaceae, *Ziziphus*, Liliaceae, *Knautia*, *Tamarix*, Fabaceae Papilionioideae, Urticaceae; 22, Amarantaceae-Chenopodiaceae; 23, other halophytes: Caryophyllaceae, Plumbaginaceae; 24, freshwater plants: *Sparganium*, *Utricularia*, *Typha*, *Potamogeton*, *Myriophyllum*, Ranunculaceae, *Ranunculus*, *Plantago*, Cyperaceae; 25, *Artemisia*.

The taxa identified were grouped according to their ecological requirements and represented in a synthetic pollen diagram (Fig. 25). Development of warm-temperate elements is coeval with increase in temperature and precipitation. According to our age model, these periods were correlated to the global warm climatic phases Bølling-Allerød, Atlantic and Subatlantic, respectively. The cooler climatic phases (i.e. the Last Glacial Maximum, Younger Dryas and Boreal) are characterized by the development of open vegetation (made of herbs and steppe elements) and cooler and drier climate as documented by the climate quantification.

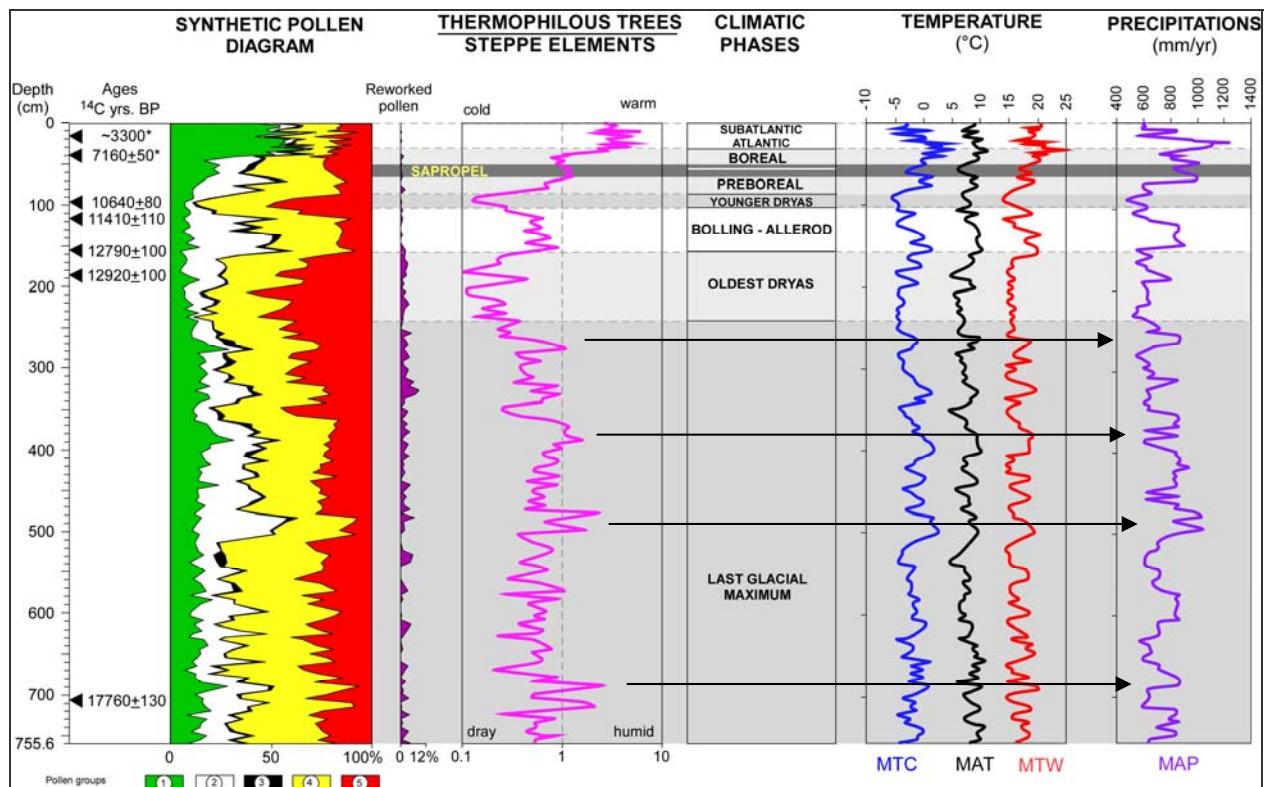


Fig. 25. BLKS 98-10: vegetation and climate reconstruction: 1, subtropical and warm-temperate taxa, 2, *Pinus*, 3, herbs, 4, *Artemisia*; MAT: mean annual temperature; MTC: mean temperature of the coldest month; MTW: mean temperature of the warmest month; MAP: mean annual precipitation.

In the pollen diagram we observe an increase in *Pinus* percentages at about 500 cm depth and during the Bølling- Allerød time-interval. The oldest increase in *Pinus* (500 cm depth) corresponds to the “red layer” deposits in the Black Sea which are correlated with the “chocolate clays” of the Caspian Sea, regarded by some authors as a probable moment of connection between the Black and Caspian seas (Tchepaliga, 1984). Other authors suggest that these deposits are related to the increase of fluvial transport from the eastern part of the Black Sea (Bahr *et al.*, 2004), forced by the melt water pulses. Our data indicate clearly a limited warming and an increase in precipitations. These two conditions probably provoked a little sea-level rise and more distal conditions at the core place, documented by increase in relative abundance of *Pinus*

B2KS 38 (Black Sea) is located at 43°48.424’N, 30°24.111’E (Black Sea) and was drilled at 355 m depth. I choose to analyse the B2KS33 core because it reports a very dilated sediment-interval (9.55 m thick) tanks to its position in the Danube prodelta on the west edge of the Viteaz Canyon (Popescu *et al.*, 2001, 2004), mostly deposited during a low sea-level. An age control has been obtained for the uppermost 250 cm of

CHAPTER 3

Marine and continental East European environmental changes since the Last Glacial

the core, done by radiocarbon datations and previous published ages corresponding to the widespread sapropel layer (Major *et al.*, 2002 and references therein). The very high-resolution pollen record (every 5 cm) indicates a very rich flora composed of 87 taxa, almost equally distributed between trees and herbs with shrubs (Fig. 26). A peculiar feature of the flora is the presence (in few quantities) of thermophilous trees such as *Taxodiaceae*, *Engelhardia*, *Carya*, *Tsuga* and *Cathaya* which are not living today in the region. Pollen record (Fig. 26) shows a clear succession of steppe (in the lower part of the pollen diagram) and forest (in the upper part of the diagram). The turnover is located at the base of the sapropel at 130 cm depth. According to the pollen content, the major part of the core might however have recorded a dilated Younger Dryas preceded by Allerød.

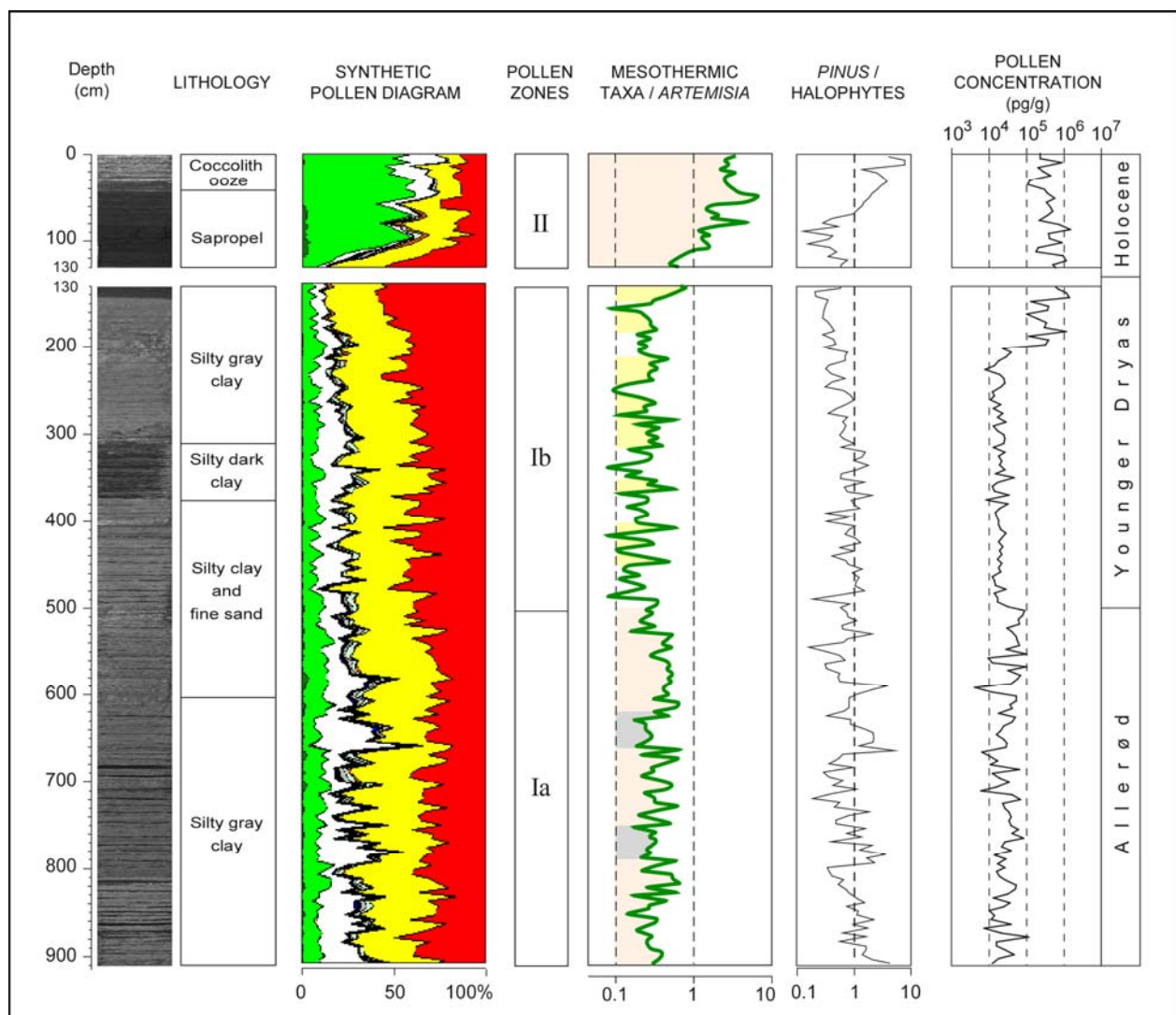


Fig. 26. Pollen record of the core B2KS33 (pollen analyses was done by S. Boroi).

The fine sensibility of the mesothermic taxa vs. *Artemisia* (mt/A) curve at a so high-chronological resolution allows a direct and fruitful comparison with the GRIP oxygen isotope curve (Fig. 27). In the latter, Holocene is easily distinguishable from the Younger Dryas, itself clearly discernible from the Allerød-Bølling and Oldest Dryas. An equivalent shift is obvious on the curve mt/A at the Holocene – Younger Dryas passage (here abrupt because of the gap in sedimentation at 130 cm): the ratio is >1 for the Holocene,

CHAPTER 3

Marine and continental East European environmental changes since the Last Glacial

still <1 for the Younger Dryas. From 500 cm depth to the base of the core, this ratio shows maximum and particularly minimum values higher than during the Younger Dryas. This phase, corresponding to the pollen zone Ia (Fig. 26), belongs to a warmer period than the Younger Dryas and can be related to the Allerød-Bølling. Such a relationship is also supported by the detailed comparison feasible between the mt/A curve and the zoomed GRIP curve for the Younger Dryas interval where groups of the most prominent maxima-minima of similar amplitude may be tentatively correlated (Fig. 27). Below, the mt/A curve shows three relatively warmer intervals only, which can be related to the Allerød equivalent phases (Fig. 26). As a consequence, core B2KS38 would reach only the earliest Allerød period and an age of 13,800 ka (cal. BP) or 11,800 ^{14}C ka BP is supposed for the base of the core.

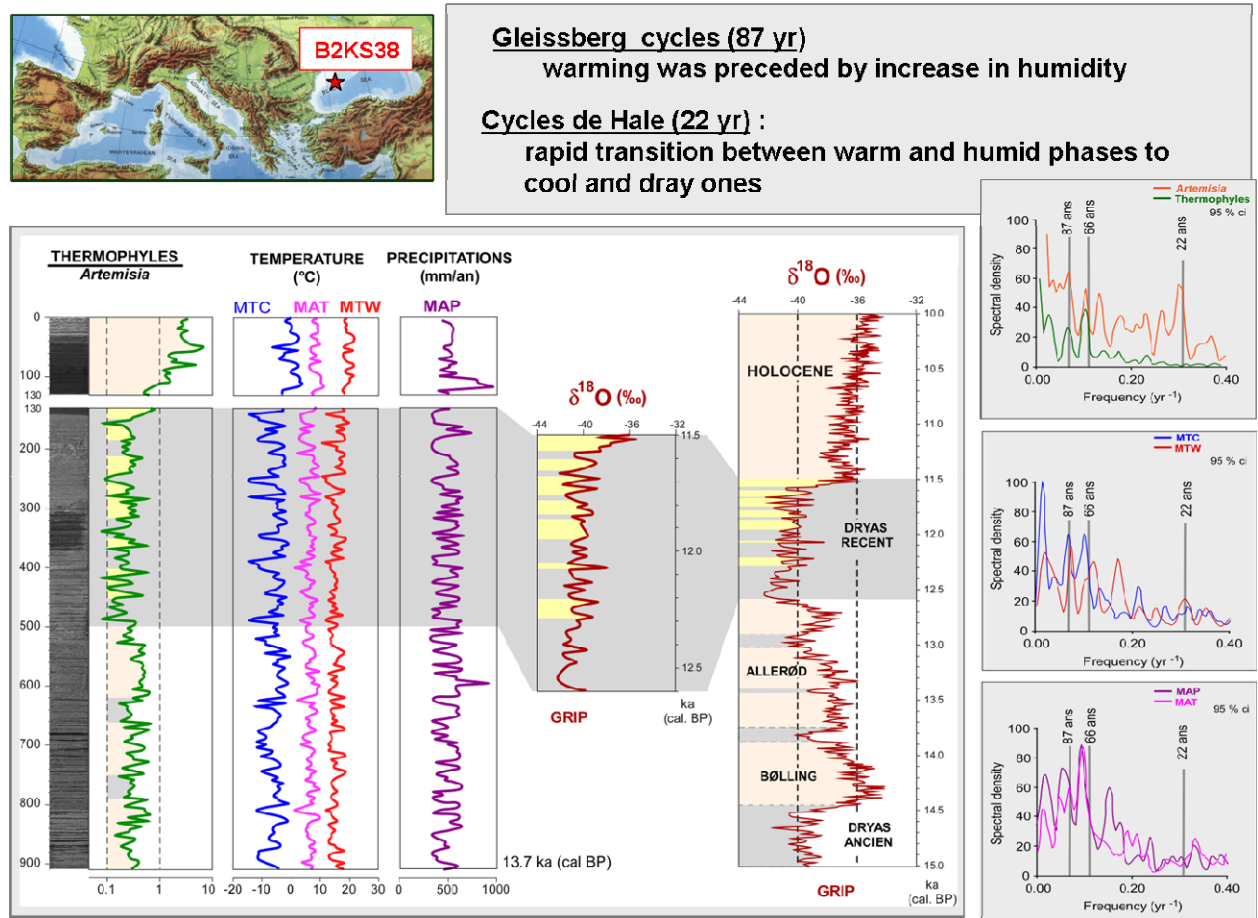


Fig. 27. Correlation between pollen record of the core B2KS38 and the global reference oxygen isotope curve (GRIP), spectral analyses on selected taxa or pollen groups indicate the solar forcing on the vegetation changes.

The climatic interpretation of the fossil pollen floras using the PCS method provides quantitative estimates for several climate parameters (Fig. 27): mean temperature of the coldest month (MTC), mean annual temperature (MAT), mean temperature of the warmest month (MTW), and mean annual precipitation (MAP). On a general trend, from the base until 500 cm in depth, the average MTC is -6°C , MAT is 6.7°C , MTW is 15°C , and MAP is about 620 mm. Interval from 500 cm to 130 cm in depth is characterized by an average MTC of -5.9°C , MAT of 6.4°C , MTW of 15.5°C , and MAP of about 600 mm. In contrast, above 130 cm, the average MTC is 0.3°C , MAT is 8.6°C , MTW is 19.5°C , and MAP is about 655 mm. As a result, the climatic comparison between pollen zones Ia and Ib yields a somewhat lower continentality during pollen zone Ia, evidenced by a

~0.7°C higher MTC and 0.5°C lower MTW, as well as higher minimum MTC (-11.5°C against -14°C) and lower maximum MTC values (18.6°C against 20°C). Despite of these differences, on climatic view pollen zones Ia and Ib are documented to be relatively similar in this Black Sea record. In contrast, considerable higher temperatures but similar precipitation is documented for pollen zone II. The average rise for MTC from pollen zone Ib to pollen zone II is 6.2°C, for MAT is 2.2°C and for MTW is 4°C. Within all periods covered by the record, no significant trends of medium-term climatic changes can be determined. With view on short-term climatic oscillations (less to 200 years), the pollen floras and the climate estimates consistently indicate several strong changes during the high-resolution intervals of pollen zones Ia and Ib. Strongest pronounced by changes in MTC, repeated cyclic climatic patterns become obvious which exemplarily may be seen during the intervals 820.5 cm to 895.5 cm in depth, or from 355.5 cm to 295.5 cm in depth. Correspondingly, such a cycle includes a cool phase which is followed by a longer warm phase until temperatures are again decreasing. In relation to MTC, changes in MAP seem to show a time lag.

The repeated maxima-minima of curve *mt/A* suggest some cyclic variations in climate during a relative short time-slice. Solar cycles of 11, 22, 90 or 200 yrs may have forced changes in temperature. Such an influence is to be tested on the time-interval defined by the three ¹⁴C ages, corresponding to a sediment thickness of 771 cm (from 916 to 145 cm in depth). To determine cyclic climate patterns recorded in the sequence, spectral analyses have been applied on different parameters (Fig. 27). Most notable, it is revealed that the units *Artemisia*, mega-mesothermic elements, specific altitudinal elements, and herbs, significantly responded to the forcing of ~87 yr, ~66 yr, and ~22 yr periodicities. Especially, *Artemisia* shows a strong sensitivity to changes on the ~87 yr and ~22 yr band. A similar, but even more clear pattern is obtained when considering the power spectra of the reconstructed climate parameters, evidencing the effect of the ~87 yr Gleissberg-cycle and the ~22 yr Hale-cycle, and suggesting that the documented ~66 yr cycle may rely on an amplification of the ~22 yr cycle. Since the reconstruction integrates the paleoclimatic signals from the individual taxa, the overall power spectra characteristics are more pronounced.

Using the ratio between *Pinus* and halophytes and the concentration of the pollen grains calculated on the core B2KS38 (Fig. 26), we can inform about sea-level variation. Generally, *Pinus* is more abundant in pollen records distant from the shoreline because its pollen is easily transported on sea surface. On contrary, halophyte pollen grains (Amaranthaceae-Chenopodiaceae, Caryophyllaceae, *Ephedra*, Plumbaginaceae and *Tamarix*) are produced by plants living near the seashore (salted environments). Some *Artemisia* specimens probably inhabited the coastal environments and could have been included within halophytes. But, I preferred in this case study to consider all the pollen grains of *Artemisia* as belonging more to ecosystems inferred to climate than to edaphic (i.e. azonal) ones. This is also supported by the frequent opposition between the Amaranthaceae-Chenopodiaceae and *Artemisia* curves. Abundance of halophyte pollen grains in marine sediments indicates a nearby coastline. In core B2KS38, *Pinus* curve continuously contrasts with that of halophytes, allowing to draw the curve of their ratio to be used as a rough proxy of the shoreline distance and, accordingly, of the sea-level variation (Poumot and Suc, 1994; Suc *et al.*, 1995). In some parts of pollen zones Ia and II, this ratio is significantly superior to 1, that supposes relatively an higher sea level in agreement with the climate of Allerød and Holocene, respectively.

Pollen concentration informs on river transport of terrigenous material. Slightly higher and more or less varying concentration in pollen characterizes the Allerød period (Fig.

26). Such variations appear in agreement with the *Pinus*/halophytes ratio (Fig. 26), i.e. with the sea-level changes. Increased concentrations in pollen grains could express rise in sea-level in relation with melt water pulses (e.g. increased river input forced by warmer conditions). Indeed, the pollen concentration curve is almost consistent with the mesothermic taxa/*Artemisia* curve and reflects changes in temperature (higher pollen concentration during warmer phases) (Fig. 26). Climate quantification points out the winter temperature as the most relevant factor (Fig. 27). Lower and relatively stable values in pollen concentration have been recorded during the Younger Dryas except within its uppermost part (195.5-130 cm in depth) (Fig. 26). As pointed out by the *Pinus*/halophytes curve, this lower sea-level phase may be related to increasing erosion on land providing more terrigenous elements because of colder conditions and more open vegetation. An important break in the pollen concentration occurs at 195.5 cm (more than 10^5 pg/g) (Fig. 26) when sea-level was minimum according to the *Pinus*/halophyte ratio, as was also the temperature according to strengthening of the *Artemisia* steppe (Fig. 26). Such conditions could correspond to a maximum of ice extension and a reduced fluvial transport in terrigenous material.

Core C10 (4 m length) was drilled on the eastern ridge separating the Central and Çınarcık basins of the Marmara Sea ($28^{\circ} 24.000'$ N, $40^{\circ} 45.000'$ E, 364 m water depth) (Fig. 28). Two lithological units constitute the core: the lower part (Unit II: from 400 to 200 cm depth) was deposited under brackish conditions, the upper part (Unit I: from 200 to 0 cm depth) under marine conditions. Unit II is a grey to dark grey mud whereas Unit I is a green mud and includes a dark olive–green sapropel layer (from 200 to 80 cm depth) (Fig. 28). The early Holocene sapropel has a generally accepted age in the Marmara Sea of 10,600 ^{14}C years BP at its base and 6,400 ^{14}C years BP at the top (Mudie *et al.*, 2001, 2002a, 2002b; 2004; Canner and Algan, 2002, Çagatay *et al.*, 2000). Our age model of core C10, based on radiocarbon dating of mollusc shells (Table 1), is consistent with the previous datations of the sapropel (Fig. 28).

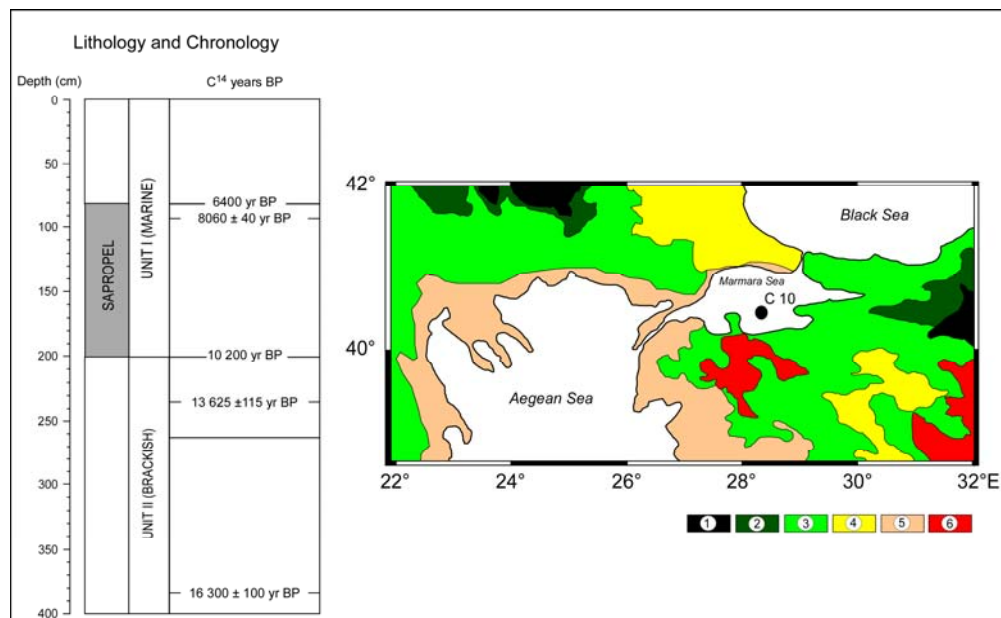


Fig. 28. Simplified vegetation map of the studied region: 1, High-altitude forest, 2, mixed warm-temperate forest; 3, warm-temperate forest; 4, grassland; 5, thermo-Mediterranean vegetation; 6, *Artemisia* steppe; Core C12, geographic location, chronology and lithology

The pollen flora consists of 83 taxa (Figs. 29a and 29b), of which 39 are trees (Fig. 29a) and 45 are herbs and shrubs (Fig. 29b).

CHAPTER 3

Marine and continental East European environmental changes since the Last Glacial

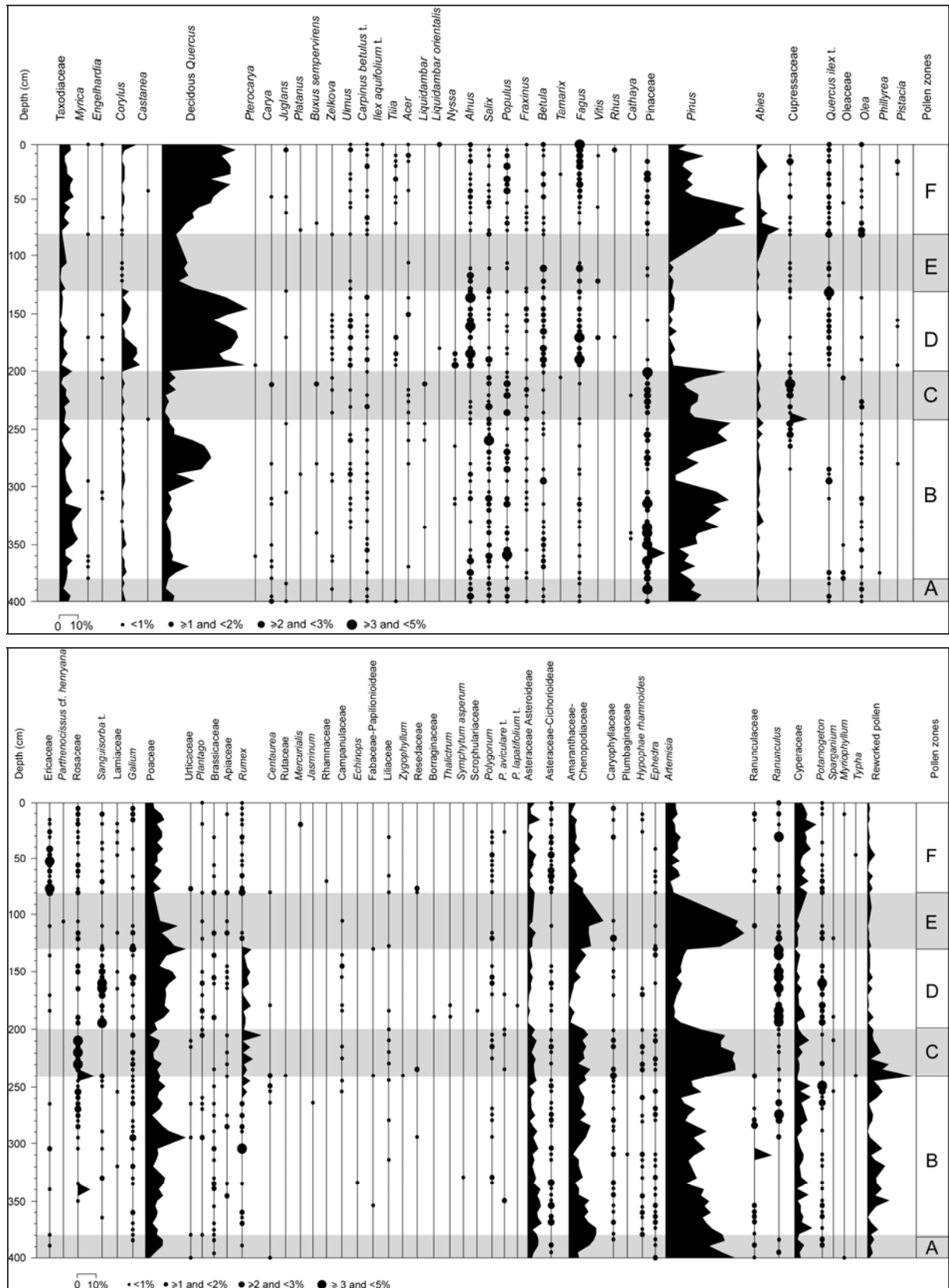


Fig. 29. Detailed pollen diagram of the core C10

Preliminary remarks can be made regarding the presence of warm–temperate to subtropical plants. Some of these are sporadic (*Myrica*, *Engelhardia*, *Pterocarya*, *Carya*,

Liquidambar, *Zelkova*, *Nyssa*, *Cathaya*), whereas others are continuously present with variable contribution (Taxodiaceae) and suggest that the Marmara Sea hinterland was a refuge area for thermophilous plants (Zohary, 1973). Our studies of Black Sea sediments show a continuous record of Taxodiaceae. The presence today of *Pterocarya*, *Liquidambar* and *Zelkova* in southern Turkey and in the southern Caucasus edge (the Colchide region) supports the status of this region as a refuge area. The possibility of reworking for these pollen grains is easily discounted because of their very well-preserved condition and their abundance curves that are consistent with the warmest phases (for example, see Taxodiaceae, *Zelkova* and *Nyssa* on Figure 29). These observations from low duration cores are fully confirmed by the long pollen record from Site 380 which documents a highly reliable story of these “exotic” thermophilous taxa in the region (Popescu *et al.*, in progress; Biltekin *et al.*, in progress). Previous pollen analyses of the study area showed only the presence of *Carya* (Mudie *et al.*, 2002a), the difference in flora diversity being due to a problem of ability in pollen identification. Accordingly, our pollen records constitute a serious advancement in the knowledge and understanding of thermophilous plant extinction in Southeastern Europe along a North–South and West–East gradient, and the Middle East where these plants probably suffered from anthropogenic activities (Suc *et al.*, 2004).

Six pollen zones, A to F, have been established based on pronounced variations in the contribution of selected marker plants in the detailed pollen data (Fig. 29). Zones are described below and the data are further used to calculate climatic values via transfer function (Fig. 30).

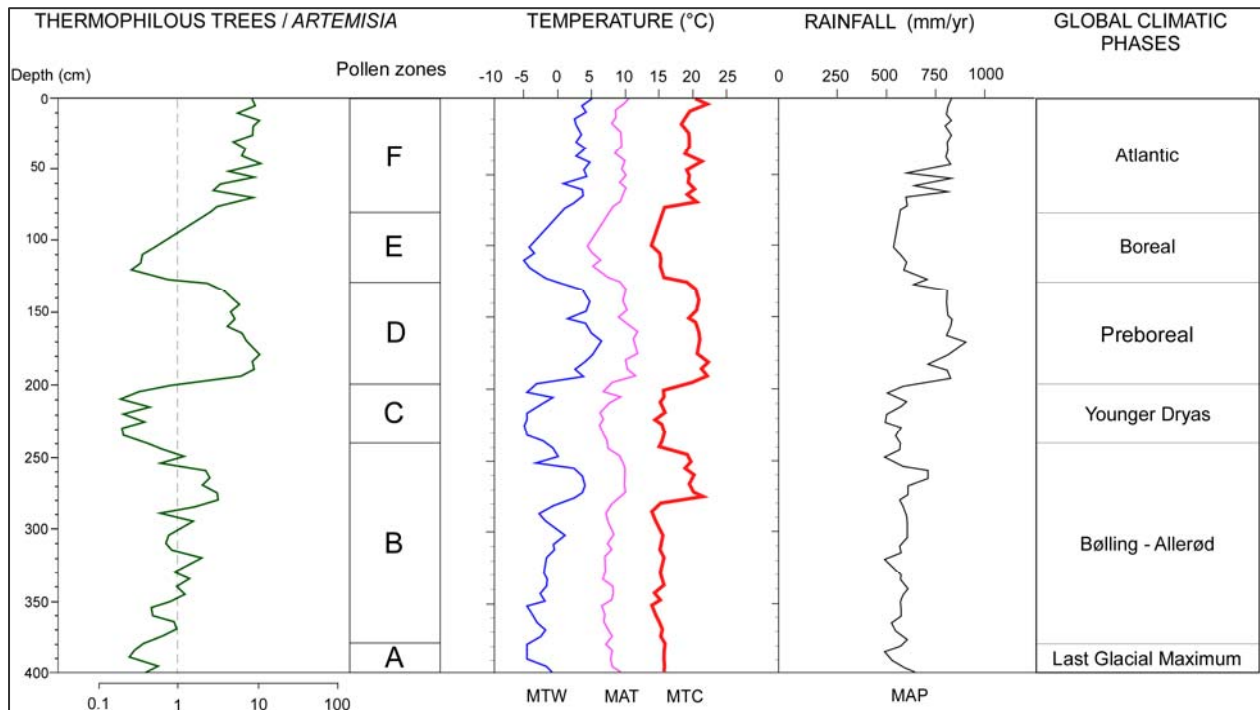


Fig. 30. Thermophilous trees vs. *Artemisia* ratio and paleoclimate quantifications. MTW = mean temperature of the warmest month, MAT = mean annual temperature, MTC = mean temperature of the coldest month, and MAP = mean annual precipitation

A climate index has been established using the ratio of “thermophilous trees / *Artemisia*”, the “thermophilous trees” grouping *Quercus*, *Corylus* and Taxodiaceae (the most abundant taxa).

- Zone A, from 400 to 380 cm, is characterized by large amounts of *Artemisia* pollen and Amaranthaceae-Chenopodiaceae (halophytes) and low percentages of thermophilous trees such as the Taxodiaceae and deciduous *Quercus*. The ^{14}C age at 390 cm ($16,300 \pm 100$ yrs BP) supports the correlation of this zone with the end of the Last Glacial Maximum. Zone A does not show a low mean annual temperature, but it seems to be characterized by high-seasonality (low temperature for the coldest month) and relatively low rainfall.
- Zone B, from 380 to 240 cm, corresponds to an increased frequency of thermophilous trees (Taxodiaceae, deciduous *Quercus*) accompanied by pioneer elements (Cupressaceae), and to a strong decrease in *Artemisia*. More forested conditions and two bounding ^{14}C ages (the younger indicating $13,625 \pm 115$ yrs BP at 247 cm depth) suggest that this zone corresponds to the Bølling–Allerød interval. This phase does not initially differ greatly from the previous one, but represents a warming that is clearly marked by all the parameters, and is accompanied by some increased precipitation.
- Zone C, from 240 to 200 cm, shows a dramatic fall in deciduous *Quercus* precisely balanced by a new expansion of *Artemisia*; such features are characteristic of the Younger Dryas. This episode appears to correspond to an important cooling mostly concentrated on winters and a noticeable decrease in rainfall which began before the decline in temperature.
- Zone D, from 200 to 130 cm, is marked by a rapid and impressive development of deciduous *Quercus* accompanied by *Corylus*, *Alnus*, *Fagus* and to some extent *Ulmus* and counterbalanced by the decline of *Artemisia*, Asteraceae Asteroideae and Amaranthaceae-Chenopodiaceae. Some herbs (*Rumex*) and shrubs (Rosaceae, including *Sanguisorba* type), that were previously frequent, continued to be present. Overall the pollen record of this zone, which corresponds to the Preboreal, reflects a rapid reforestation. Both temperature (summer and winter) and precipitation increased greatly.
- Zone E, from 130 to 80 cm, indicates again a brief opening of forest ecosystems (lowered percentages of deciduous *Quercus* and other thermophilous trees) and strengthening of *Artemisia* steppe accompanied by halophytes (Amaranthaceae-Chenopodiaceae). Increases in open vegetation indicate a cooler and drier climate. The temperature fall is concentrated more on winters, and there is a less intense drop in rainfall than during the Younger Dryas.
- Zone F, from 80 to 0 cm, reflects a progressive expansion of forests (spread of *Abies* followed by that of deciduous *Quercus*) and a reduction of *Artemisia* steppes. This is the Atlantic warm phase, ending with some spreading of *Fagus* and *Abies* (Subboreal phase?). The episode appears to have more elevated temperatures, regardless of season, in spite of some irregularities in rainfall at its beginning. The present-day climatic conditions at Istanbul validate estimated conditions for the core top, except for (1) a slightly higher mean annual temperature ($+2^\circ\text{C}$) and mean temperature of the warmest month ($+2^\circ\text{C}$), and (2) some reduction in rainfall (-200 mm/yr) that may be explained by the present-day warming.

Pinus has not been considered in the above subdivision because its frequency is often biased by taphonomic (Holmes, 1994) aspects that are independent of climate fluctuations. Because of its buoyancy, phases of high abundance are generally related to high relative sea levels: in the middle and upper pollen zone B, uppermost pollen

zone C and lower pollen zone F (Holmes, 1994; Heusser and Balsam, 1977). Conversely, low percentages of *Pinus* may be related to a low relative sea level (Heusser and Balsam, 1977), as for pollen zone B, especially at 290 cm. However, very low frequencies of *Pinus* are often recorded within sapropel (Combourieu-Nebout, 1990; Combourieu-Nebout *et al.*, 1998) but not always (Rossignol-Strick and Paterne, 1999). Such a variability is not yet explained and does not seem to be related to the origin of the sapropel formation (increasing run-off in the Mediterranean Sea, invasion of marine Mediterranean waters into the brackish Marmara Sea).

To conclude, the vegetation from the Marmara – Black sea region responds to the global climate fluctuations. The cooler periods are marked by the developments of open vegetation while the warmer periods correspond to the forest developments. I mentioned the regional aspect of the vegetation marked by the strengthening of the *Artemisia* steppe that existed in this area since the Late Miocene (Popescu, 2006) and probably invaded the Mediterranean coastal environments during the glacials (Suc and Popescu, 2004). A particular aspect is represented by its capacity to act as refuge area for many subtropical - warm temperate trees.

3. 1.2. Flooding of the Marmara Sea: progressive or catastrophic event?

From the hydrologic point of view, the Marmara Sea has an intermediate position between the Aegean Sea (i.e. the Mediterranean Sea) and the Black Sea (Fig. 22), being separated from them by two straits, the Dardanelles (present-day depth of the sill: –75 m) and the Bosphorus (present-day depth of the sill: –35 m), respectively. Today, salinity of the Marmara Sea waters is 21 pps on average, i.e. an intermediate value between that of the Aegean (37–39 pps) and Black seas (15–20 pps) (Mudie *et al.*, 2001; 2002b; 2004). The warm (15–20°C) hypersaline Mediterranean waters plunge into the Marmara Sea after passing the Dardanelles Sill and circulate towards the Black Sea. Cold (5–15°C) and low saline surface waters originating from the Black Sea cross the Marmara Sea and reach for a part the Aegean Basin. Hence the Marmara Sea is a domain of intense water circulation controlled by exchanges with the nearby basins. This results in a stratification of waters with a very obvious halocline at about 10–20 m depth with overlying waters at 22–24 pps, and underlying waters at and 37–39 pps. Fluctuations are observed in relation with seasonality. During the last lowstand, the Marmara and Black seas were isolated and evolved into brackish lakes (Degens and Ross, 1972; Ryan *et al.*, 1997, 2003; Aksu *et al.*, 2002; Görür *et al.*, 2001; Çağatay *et al.*, 2000). Understanding the processes and time schedule of their infilling by marine Mediterranean waters after the Last Glacial Maximum is of major importance for the reconstruction of the recent Black Sea history, a matter of an intense debate (Degens and Ross, 1972; Ryan *et al.*, 1997, 2003; Aksu *et al.*, 2002; Görür *et al.*, 2001) related both to the global sea-level rise Çağatay *et al.*, 2000) and regional tectonics (Yaltırak *et al.*, 2000).

Palynological analyses (dinoflagellate cysts and palynofacies) were performed on C10 core (Marmara Sea) in order (1) to characterize the progressive or rapid process of its flooding, and (2) to reconstruct the impact of these respective events on the marine ecosystems.

In the C10 core, the dinoflagellate cyst flora comprises 32 marine taxa, to which can be added freshwater algae. The relative percentages (calculated from the total dinoflagellate cyst sum) are plotted in a detailed dinoflagellate cyst diagram (Fig. 31).

CHAPTER 3

Marine and continental East European environmental changes since the Last Glacial

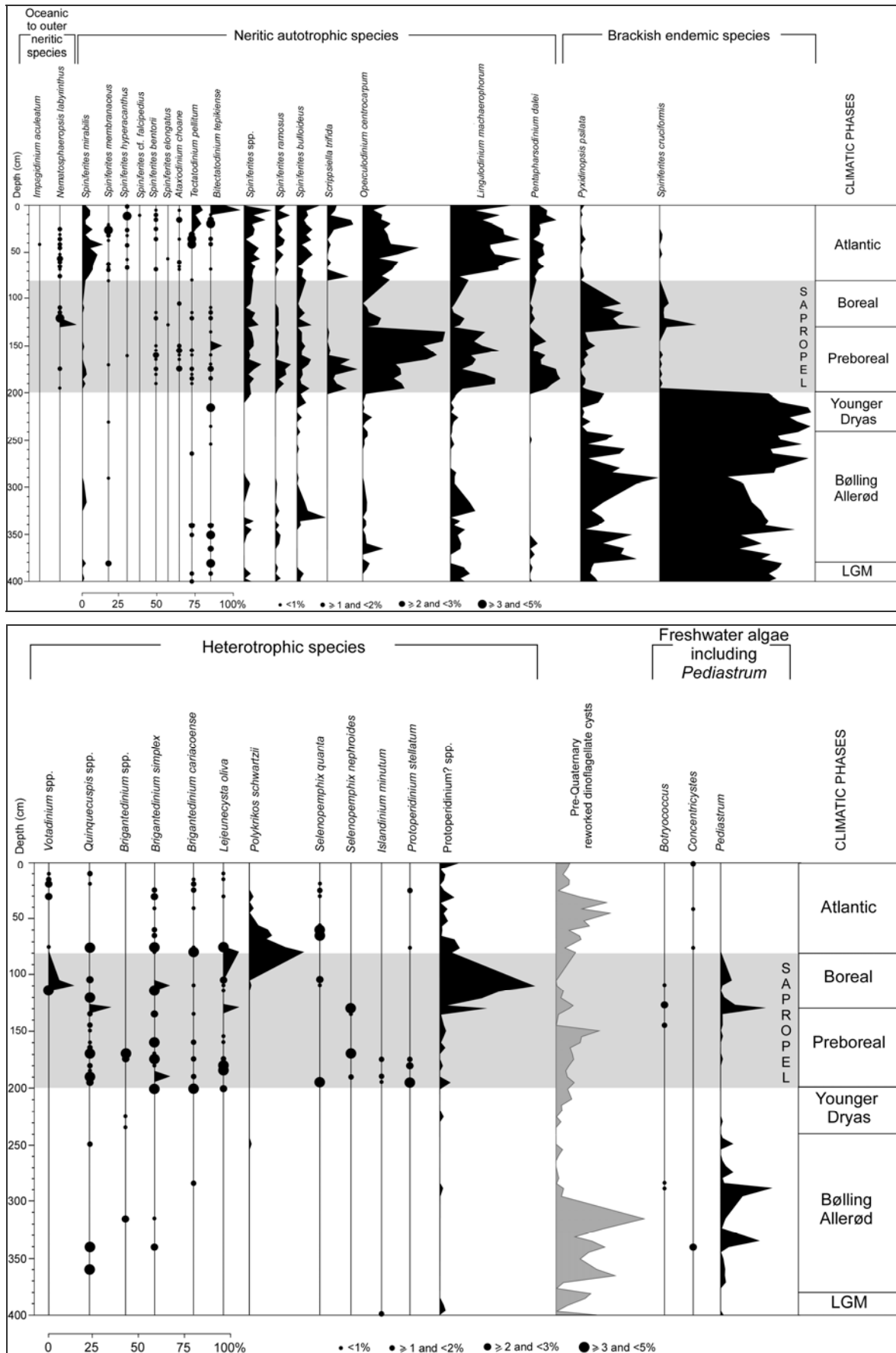


Fig. 31. Detailed dinoflagellate cyst diagram from C10 core (Marmara Sea)

This diagram shows also the relative values of freshwater algae and pre-Quaternary reworked dinoflagellate cysts (calculated from the sum of dinoflagellate cysts plus, respectively, the sum of the freshwater algae or that of the pre-Quaternary reworked dinoflagellate cysts). A strong break separates the diagram into two successive parts.

The lower part of diagram (from 400 to 200 cm) corresponds to the end of the Last Glacial Maximum, Bølling-Allerød and Younger Dryas global climatic phases. These intervals are dominated by the brackish endemic species *Pyxidinoopsis psilata* and *Spiniferites cruciformis* and denote the “low salinity lake” status of the Marmara Sea before 10,600 ¹⁴C years BP (12,000 years cal. BP). The permanent opposition between the two endemic species might be correlated with minor changes in surface waters conditions generated by increases in temperature and by some meltwater pulses decreasing salinity during the Bølling-Allerød climatic phase (Weaver *et al.*, 2003). The increase in *Pyxidinoopsis psilata* is synchronous with that of the freshwater alga *Pediastrum* and may signify a freshening of surface waters especially during the middle of the Bølling-Allerød time. This interval is also marked by the rare presence of oceanic to other neritic species (Marret and Zonneveld, 2003): *Spiniferites mirabilis* (1.04 % at 395 cm; 2.13% at 380 cm; 2.5% at 315 cm and 1% at 295 cm depth), *S. membranaceus* (2.13 % at 380 cm; 0.87% at 290 cm and 0.98% at 230 cm depth), *Tectatodinium pellitum* (1.85 % at 265 cm, 2.22% at 340 cm, 1.54% at 350 cm, 1.02 at 390 cm, 1.08% at 400 cm depth), *Bitectatodinium tepikiense* (5.55% at 210 cm, 0.9% at 235 cm, 1% at 255, 2.23% at 340 cm, 3.07% at 350 cm, 2.13% at 365 cm, 4.25% at 380 cm and 1.42% at 385 cm depth) accompanied by marine autotrophic cosmopolitan species: *Spiniferites ramosus* (between 0.9% and 3.1%), *S. bulloideus* (between 0.8 and 18%), *Operculodinium centrocarpum* sensu Wall and Dale (between 0.9 and 12.76 %) and *Lingulodinium machaerophorum* (0.96–15.90 %) which suggests the earliest connection between the Marmara and Aegean seas. The high percentages of pre-Quaternary reworked dinoflagellate cysts might signify brief marine influxes or freshwater river input (erosion of Neogene sediments).

The upper part of the diagram (from 200 to 0 cm) is characterized by a more diverse, open-marine flora and includes the first appearance of several heterotrophic dinoflagellate species. There is also an important decrease in brackish endemic species. In agreement with ¹⁴C ages and climatostratigraphy based on pollen grains, this part of the diagram corresponds to the Preboreal, Boreal, and Atlantic global climatic phases.

The Preboreal warmer climatic phase is characterized by an increasing diversity in dinoflagellate cysts (28 taxa). The autotrophic cosmopolitan species (Fig. 31) increase in percentage and diversity, some of them making their first appearance (*Spiniferites hyperacanthus*, *S. bentorii*, and *Ataxodinium choane*) in Marmara surface waters. Significantly, the outer neritic species *Nematosphaeropsis labyrinthus* also has its first appearance at the beginning of this interval.

The sudden rise to dominance of the autotrophic cosmopolitan species *Operculodinium centrocarpum*, *Lingulodinium machaerophorum* and *Pentapharsodinium dalei*, shows a first rapid marine Mediterranean influx into the Marmara Sea at that time (10,600 ¹⁴C years BP, i.e. ~12 cal ka BP), and is consistent with increasing diversity in heterotrophic species as well as a rapid increase in percentages of pre-Quaternary reworked dinoflagellate cysts (Fig. 31). The brackish endemic dinoflagellate cysts show an important concomitant decrease in percentages. The salinity must have exceeded ca. 20 psu. judging from the diversity of species present, but the abundance of the

euryhaline species *Operculodinium centrocarpum* and *Lingulodinium machaerophorum* (Head *et al.*, 2005) suggests that open-marine conditions were not yet established. The sharp rise in cysts of the spring–blooming species *Pentapharsodinium dalei* reflects the rise in salinity but may also suggest relatively cool surface waters during spring (Dale, 2001).

During the Boreal cooler climatic phase, the dinoflagellate cyst record shows an increase in endemic brackish species and heterotrophic species, and a decrease in percentages of autotrophic cosmopolitan species and pre-Quaternary reworked elements. The increase in the brackish species *Pyxidinosia psilata* and *Spiniferites cruciformis* reflects a freshening of surface water due to (1) the global freshening of marine waters (Dale, 2001; Thunell and Williams, 1989; Duplessy *et al.*, 1992; Rhamstorf, 1995; Barber *et al.*, 1999; Keigwin and Boyle, 2000) (2) a possible outflow of Black Sea waters (Aksu *et al.*, 1999), or (3) a connection with some coastal lagoons. An increase in cysts of *Polykrikos schwartzii* (heterotrophic species) between 80 and 60 cm might be correlated with the high productivity episode that marks the end of the sapropel (Aksu *et al.*, 1999) in the Marmara Sea.

The highest 80 cm of core C10 corresponds to the final warmer climatic period (Atlantic to Present). The dinoflagellate cyst assemblages show an increase in percentages of autotrophic cosmopolitan species, and the endemic brackish species almost disappear. The abundance of *Lingulodinium machaerophorum*, *Operculodinium centrocarpum* and *Pentapharsodinium dalei* is coeval with increases in pre-Quaternary reworked dinoflagellate cysts, which suggests a second strong invasion of the Marmara Sea by marine Mediterranean waters just after the cooling at 8.2 ka BP, and finally results in establishing the present marine conditions.

Character of lacustrine–marine transition at 10,600 ¹⁴C years BP. Invasion of the Marmara Sea by marine Mediterranean waters at 10,600 ¹⁴C years BP is represented by the beginning of the sapropel layer formation (at 200 cm depth) which illustrates the first major environmental change. Abrupt increase in diversity and relative values of marine dinoflagellate cysts accompanied by a bloom of marine autotrophic species (at 200 cm depth), that replaced the brackish endemic ones (Fig. 31), suggests a fast increase in sea-surface salinity waters. The time-span between the last “brackish” dinoflagellate assemblage (at 205 cm depth) and the first “marine” dinoflagellate assemblage (at 200 cm depth), suggests that the lacustrine–marine transition represents a very short event (114 yrs, obtained by extrapolation between the ¹⁴C ages at the base and upper part of the lacustrine unit in our core). The transition from cooler and dry Younger Dryas to warmer and wet Preboreal climatic phase, with increasing in the summer and winter temperature and rainfall correlates with increase in sea-surface salinity and makes more contrasted the beginning of the sapropel in the Marmara Sea.

Earlier connection between the Mediterranean and Marmara seas (16,300 –10,600 ¹⁴C years BP) is suggested by the presence of neritic dinoflagellate species (*Spiniferites mirabilis*, *S. membranaceus*, *Tectatodinium pellitum*, *Bitectatodinium tepikiense*) during the “brackish lake” period as recorded in the C10 core (Fig. 31). We discount any contamination of the samples because each sample has been cleaned before the chemical process; and no contamination by thermophilous tree pollen that are considerably more frequent in the upper half of the core was found in the lower part of the pollen record. Similarly, no reworking can be invoked because the dinoflagellate cysts are excellently preserved and they do not occur correlated with the colder phases (relative low sea-level) when erosion increased (Fig. 32).

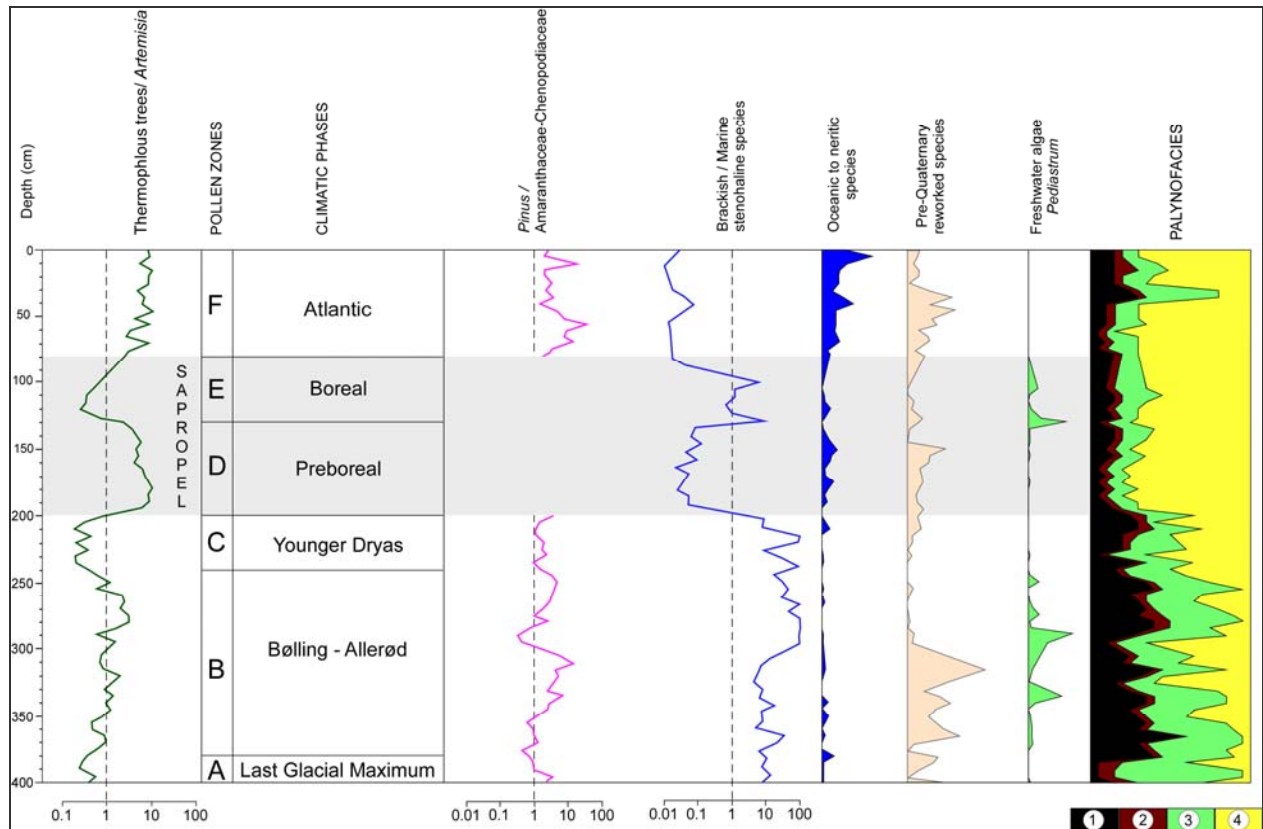


Fig. 32. Grouped dinoflagellate cysts according to salinity and nutrient requirements, and palynofacies synthetic diagram with respect to climatostratigraphy according to pollen data. 1, Black organic matter (BO.M.); 2, Woody organic matter (W.O.M.); 3, Cellular organic matter (C.O.M.); 4, Amorphous organic matter (A.O.M.)

Similar records have been discussed by Mudie *et al.* (2002b, 2004) in their corresponding dinocyst zone D2. Without discarding the possibility of earlier influxes of Mediterranean marine waters into the Marmara Sea, Mudie *et al.* discuss the possibility that the neritic species might have survived in the brackish Marmara Basin during the Last Glacial Maximum as a memory of the last period during which the Marmara was connected to the Aegean Sea, i.e. since the Marine Isotope Stage 5e (Hiscott *et al.*, 2002). Such a long survival seems inconceivable for ecologically sensitive taxa. Culture experiments on different living taxa show that germination is at maximum 75 days (Binder and Anderson, 1987; Kokinos and Anderson, 1995) and the required time to maintain a culture of living species capable to produce the resting cysts is about 2 years (Kokinos and Anderson, 1995). I prefer to consider the possibility of brief influxes of marine waters flooding over the Dardanelles Sill during the relaxation phases of the uplifting area. This hypothesis is consistent with the coeval episodic increases in amorphous organic matter within core C10 suggesting early episodes of anoxia (Fig. 32) and with the high speed of the global sea-level rise just after the Last Glacial Maximum (Chappell and Shackleton, 1986; Waelbroeck *et al.*, 2002; Siddall *et al.*, 2003) combined to continuous uplift of the Dardanelles Sill since 300 ka BP, underlining propitious conditions for such episodic influxes (Yaltirak *et al.*, 2002).

3. 1.3. Flooding of Black Sea: progressive or catastrophic event?

Flooding of the Black Sea by Mediterranean waters is currently shaped by two hypotheses: a slow and progressive invasion¹ resulting from the global post-glacial transgression (Aksu *et al.*, 2002) or a rapid invasion (Ryan *et al.* 1997, 2003) as resulting from the sudden opening of the Bosphorus Strait (Gökasan *et al.*, 1997). This caused an extensive drowning of the surrounding coastal lands of the Black Sea. The proposed catastrophic inundation of the broad shelf surrounding the Black Sea culminating at about 8.4 cal ka BP has been linked to a historical Noah's Flood (Ryan and Pittman, 1999). Evidence for flooding comes principally from features associated with a widespread erosion surface on the shelf that is overlain by marine deposits. Coastal dunes (Lericolais *et al.*, 2004; 2006; 2007) are preserved on this erosion surface at a depth between -80 and -100 m: their preserved morphology sealed by a mud drape can only be explained by an accelerated inundation of the basin at 8.4 kyrs BP (Aksu *et al.*, 1999). Rapid flooding is contingent upon a sudden opening of the Bosphorus Strait, coupled with a relatively low water level for the Black Sea. Most criticisms of rapid flooding have been addressed (Aksu *et al.*, 2002), but the history of Mediterranean inflows that preceded the flood, and the significance of basin-wide sapropel formation that immediately followed it, are less well understood. Previous research has been hindered by reduced fossil diversity that characterizes most Late Quaternary Black Sea sediments, a consequence of the prevailing low-salinity lacustrine conditions during the Neoeuxinian period.

Our dinoflagellate cyst record and palynofacies analyses, coupled with reconstructions of the paleovegetation and paleoclimate parameters, try to explain the causes, the mechanisms and the impact on marine and continental ecosystems of this important event.

The dinoflagellate cysts records on the core BLKS 98-10 are represented by at least 37 species belonging to 18 genera and comprising 66 separate morphotypes. The cysts are subdivided into eight ecological groups, and a ninth represents the predominantly freshwater chlorococcalean genus *Pediastrum* (Fig. 33). The distribution of these groups allows the core to be subdivided into two local assemblage zones D1 and D2 (Fig. 33). Zone D1 (755 cm – 40 cm) spans the base of the core to the base of the sapropel. It represents a low-salinity assemblage characterized by the co-dominance of *Spiniferites cruciformis* and *Pyxidinopsis psilata*, species essentially endemic to the Black Sea at this time. Fluctuations in dominance between these two species may reflect changes in hydrography or in sea-surface temperature. However, the temperature requirements of these two species are not yet known, and the several peaks of *Spiniferites cruciformis* within Zone D1 may reflect a complex interplay of factors including changes in proximity to shore. The *Pediastrum* a freshwater alga is interpreted as indicator of freshwater input, the increase of relative abundance of this alga during the warmer intervals confirmed the increase of freshwater input. The maximum of abundance of *Pediastrum* is remarked during the Bølling warm interval and could be correlated with the meltwater pulse 1A, responsible for a rapid rise (25m) of global sea level of about 20m (Weaver *et al.*, 2003). A reduction in *Pediastrum* during the Younger Dryas signals reduced river input, and agrees with evidence from pollen for a drier climate and a more proximal shoreline during this interval. Occurring in small but increasing numbers upwards through Zone D1 are *Lingulodinium machaerophorum* (with normal and reduced processes) and occasional specimens of *Ataxodinium choanum*, *Operculodinium centrocarpum sensu* Wall and Dale, 1966, *Scrippsiella* cf. *trifida*, *Spiniferites bentorii bentorii*, *S. bentorii truncatum* *S. hyperacanthus*, and *S.*

ramosus. These together give evidence of a minor, and possibly intermittent inflow of Mediterranean waters into the Black Sea during this interval. Salinities of about 7 or less are indicated for this interval based on contemporaneous molluscs from the Black Sea (Wall and Dale, 1974), but the presence of *Lingulodinium machaerophorum* which is found only where surface salinities exceed about 8 (Wall and Dale, 1974) suggests somewhat higher salinities for Zone D1.

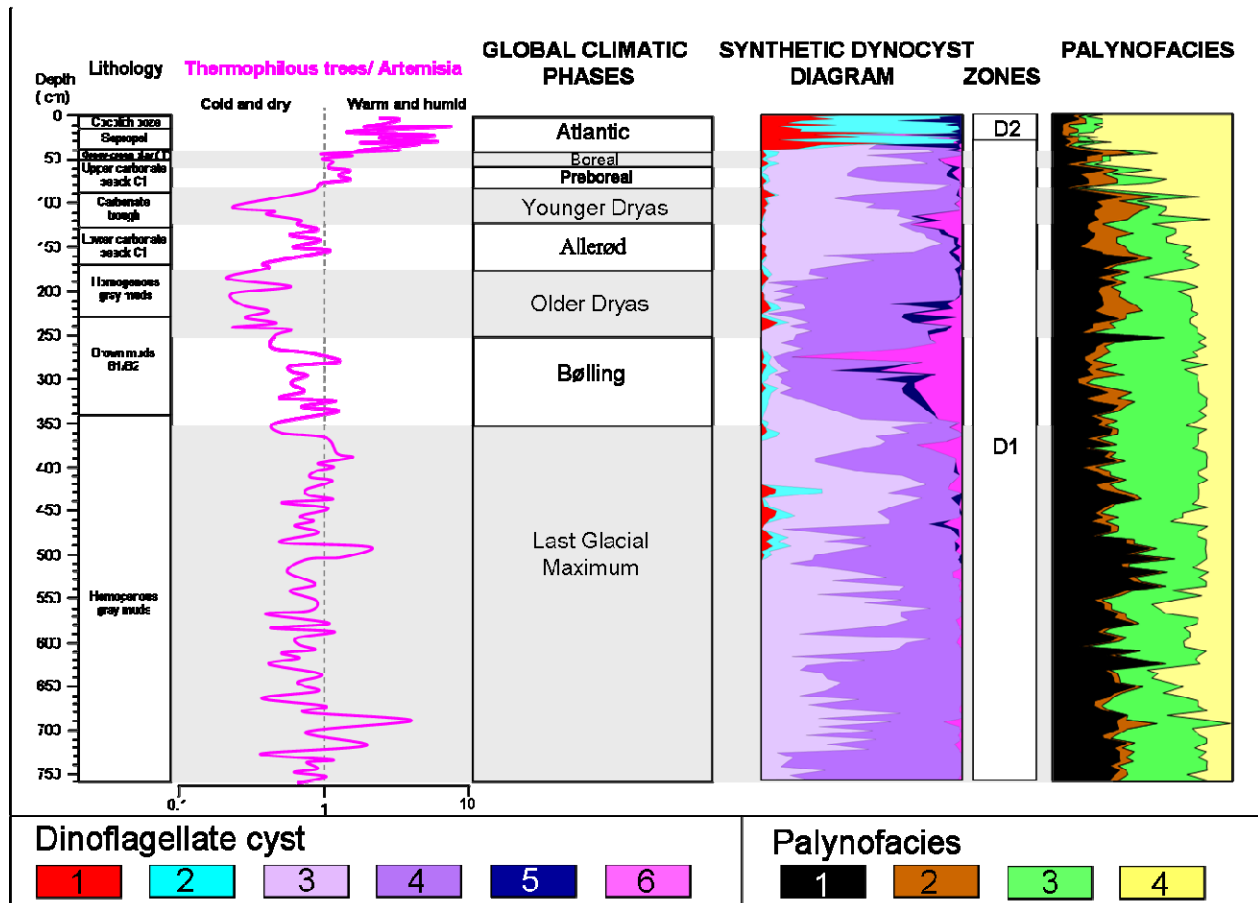


Fig. 33. Climate variability, dinoflagellate ecological groups and *Pediastrum*: 1. Mediterranean species: *Achomosphaera* sp., *A. andalusiensis*, *Ataxodinium choanum*, *Capisocysta lata*, *Capisocysta* cf. *lata*, *Operculodinium centrocarpum* sensu Wall and Dale, 1966, *Spiniferites bentorii bentorii*, *S. bentorii truncata*, *S. mirabilis*, *S. cf. falcipidius*, *S. hyperacanthus*, *Tectatodinium pellitum*, *S. bulloideus*, *S. ramosus*, *Spiniferites* spp., *Pentapharsodinium dalei*; 2. *Lingulodinium machaerophorum*, *Scrippsiella* spp.: mostly cysts of *Scrippsiella* cf. *trifida*; 3. *Spiniferites cruciformis*; 4. *Pyxidionopsis psilata*; 5. Heterotrophic spp.: *Brigantedinium cariacense*, *Brigantedinium* sp., *Colchidinium* sp., *Polykrikos* cf. *schwartzii*, *Protoperidinium compressum*, *Protoperidinium* sp., *Quinquecuspidis* spp., *Stelladinium* sp., *Votadinium* sp., *Xandarodinium xanthum*. 6. freshwater alga *Pediastrum* and **Palynofacies**: COM: cellular organic matter; WOM: woody organic matter; BOM: black organic matter; AOM: amorphous organic matter.

Zone D2 (40–0 cm) occurs from the base of the sapropel to the top of the core. It is marked by an abrupt change in dominance of *Lingulodinium machaerophorum*, *Scrippsiella* spp., and taxa of the Mediterranean species group. Species making their first appearance in this zone are *Achomosphaera andalusiensis*, *Capisocysta* spp.,

Pentapharsodinium dalei, *Tectatodinium pellitum*, and the heterotrophic species *Cochlodinium* sp., *Polykrikos* cf. *schwartzii*, *Protoperidinium compressum*, *Quinquecuspis* spp., *Stelladinium* sp., *Votadinium* sp., and *Xandarodinium xanthum*. *Spiniferites mirabilis* and *S. hyperacanthus* are also characteristic of Zone D2. This zone represents an abrupt shift to significantly more saline surface waters. The immigrant species almost completely replace the endemic Black Sea species *Spiniferites cruciformis* and *Pyxidinoopsis psilata*, which are sparse in the lowest sample and rare or absent thereafter. The increase in Mediterranean species is accompanied by their diversification into many morphotypes. All of the Mediterranean species are euryhaline but some are especially tolerant of reduced salinities (e.g. *Ataxodinium choane*, *Operculodinium centrocarpum* sensu Wall and Dale, 1966, *Spiniferites bentorii*, *S. bulloideus*, *Tectatodinium pellitum*), whereas others (*L. machaerophorum* and heterotrophic species) reflect elevated nutrient levels. Salinities approximating at least present-day values of 18 are indicated for Zone D2.

Four constituents are considered in the palynofacies (Combaz, 1991): cellular organic matter (C.O.M.) mainly made of pollen grains, spores, dinoflagellate cysts, cuticle fragments, etc.; woody organic matter (W.O.M.) showing pieces of wood; black organic matter (B.O.M.) constituted by coaly organic fragments and sometimes pyrite grains; amorphous organic matter (A.O.M.) which results from the disintegration of the organic matter from the living organisms by bacteria under anoxic conditions on the sea floor. A prevalent C.O.M. indicates a relatively short transport of particles from the land, a more important one when W.O.M. is frequent; large quantity of B.O.M. is linked to low sea-level stand and intense fluvial erosion; abundance in yellow and fleecy A.O.M. is generally related to water stratification (Poumot and Suc, 1994). In the Mediterranean sediments, increases in yellow-fleecy A.O.M. generally correspond to sapropel formation, but it has been established that the sapropel formation is the ultimate term of such a sedimentary process and that water marine stratification and anaerobic conditions on the sea floor can be expressed by large amount of yellow-fleecy A.O.M. in the palynofacies without any change in the sediment (Suc *et al.*, 1991). Anoxic conditions have occurred on the NW slope of the Black Sea before (and after) its sedimentary expression as sapropel, during cold and dry climatic phases as well as during warm-temperate and humid ones (e.g. independently from climatic changes). Accordingly, water stratification cannot be related to freshwater fluvial input over the Black Sea brackish waters.

Our data indicate that the flooding of the Black sea was a very rapid event that lasted less than 200 years, according to our high- resolution sampling. New samples, at 50 year resolution are in progress.

To conclude, these high-resolution studies on the Black and Marmara sea cores show that:

1. changes in regional vegetation were forced by global climate changes: the cooler period were characterized by the development of open vegetation, the warm climatic phases were dominated by forests;
2. the Marmara and Black seas evolved in less saline conditions before their respective flooding by Mediterranean waters;
3. early short unidirectional influxes of marine Mediterranean waters were for the first time documented, being probably induced by the regional tectonic activity;

4. flooding of the Marmara and Black seas were very fast events, respectively, provoking “environmental crises” marked by “blooms” of morphologically adapted species.

3.2. THE ARAL SEA: CLIMATE AND PALEOENVIRONMENT RECONSTRUCTIONS FOR THE LAST 2000 YEARS

The reconstruction of marine and continental environments of the Aral Sea region was done by my first PhD student, P. Sorrel, during his thesis. This study integrated a European Program (CLIMAN) under coordination of Dr. H. Oberhänsli (GFZ Potsdam). I co-supervised (with J.-P. Suc, Lyon 1 University) the palynological work (pollen grains and dinoflagellate cysts) on a CH1 core drilled in the Chernyshov Bay (NW part of the modern Large Aral Sea) (Fig. 34). During the last 2000 yrs, the marine and continental environments of this region suffered important changes, related to the impact of global climate and human occupation. High-resolution palynological records (pollen grains and dinoflagellate cysts) permitted to reconstruct environmental changes in the region, and more to identify the most forcing factors responsible for the Aral Sea evolution during the late Holocene.

The pollen record and climatic parameters reconstruction (in collaboration with S. Klotz, Tübingen University, Germany) suggest that cold and arid conditions prevailed in western central Asia during ca. 0-400 AD, 900-1150 AD and 1500 – 1650 AD, as documented by the extension of xeric vegetation dominated by steppe elements. Conversely, warmer and less arid conditions occurred during ca. 400-900 AD and 1150-1450 AD, when steppe vegetation was enriched in plants requiring moister conditions (Sorrel, 2006; **Sorrel et al., 2007**). Changes in precipitation pattern in the Aral Sea region were related to the Eastern Mediterranean cyclonic system, that provoked increasing humidity in the Middle East and Western Central Asia during winters and early springs. Sedimentological and geochemical analyses (Sorrel, 2006) confirm the pollen record and climate parameters reconstruction, suggesting as forcing factor the spatial movements of the Siberian High Pressure system.

The high-resolution dinoflagellate cyst record permitted to evidence the sea-level variation of the Aral Sea during the studied time-period, to propose an evolution of the surface water salinity and to deduce its impact on cyst morphology (i.e. short process of *L. machaerophorum* corresponding to increased salinity, contrarily to observations done in the Black and Marmara seas), and to establish which were the main factors controlling these changes (**Sorrel et al. 2006**). Lake lowstand and polysaline conditions were documented at about 0–400 AD, 725–1260 AD, 1500 AD, 1600 AD, 1800 AD and since the 1960s, whereas oligosaline conditions associated to higher lake levels.

A Black Sea lowstand at 8500 yr B.P. indicated by a relict coastal dune system at a depth of 90 m below sea level

Gilles Lericolais*

Institut français de recherche pour l'exploitation de la mer, Centre de Brest, BP 70, F 29200 Plouzané cedex, France

Irina Popescu

Renard Centre of Marine Geology, University of Ghent, Department of Geology and Soil Science, Krijgslaan 281 S8, B-9000 Gent, Belgium

François Guichard

Laboratoire des Sciences du Climat et de l'Environnement, Centre National de la Recherche Scientifique—Commissariat à l'Énergie Atomique, Avenue de la Terrasse, BP 1, F 91198 Gif-sur-Yvette cedex, France

Speranta Maria Popescu

Université Claude Bernard Lyon 1, 43, boulevard du 11 Novembre 1918, F 69 622 Villeurbanne cedex, France

ABSTRACT

Oceanographic surveys in the Black Sea during 1998, 2002, and 2004 in the framework of a French-Romanian joint project, and recently in the framework of the European project ASSEMBLAGE, complement previous seabed mapping and subsurface sampling studies undertaken in the Black Sea by various international expeditions. Until the Ryan and Pitman flood theory and prior to this project, it was proposed that the Black Sea was predominantly a fresh-water lake interrupted by possible marine invasions coincident with high sea level during the Quaternary.

From the recent surveys carried out on the western part of the Black Sea it is evident that the Black Sea's lake level rose on the shelf to at least the isobath -40 to -30 m as ascertained by the landward limit of extent of the *Dreissena* layer characteristic of brackish to fresh-water conditions. This rise in the lake level could coincide with the answer of the Black Sea catchment's basin to the meltwater drained from the thawing of the ice cap ensuing Melt Water Pulse 1A (Bard et al., 1996). It is possible that at that time the lake level filled by fresh water reached the level of its outlet and spilled into the Mediterranean Sea. Later, in the mid-Holocene at 7.5 k.y. B.P., the onset of salt-water conditions is clearly evident in the Black Sea. From these observations Ryan et al. (1997) came to the conclusion that the Black Sea could have been filled by salt water cascading from the Mediterranean. Even though this hypothesis has been challenged (Aksu et al., 2002b, 1999b), the recent confirmation of the excellent preservation of drowned beaches, sand dunes, and soils during Ifremer (Institut français de recherche pour l'exploitation de la mer) surveys seems to support the Ryan and Pitman hypothesis (Ryan and Pitman, 1999).

*Gilles.Lericolais@ifremer.fr

The multibeam echo-sounding and the seismic reflection profiles acquired on the Romanian margin during our surveys revealed wave-cut terraces at an average water depth of 100 m. More evidence of seawater penetration is marked at the Bosphorus outlet by the presence of recent canyon heads mapped during the last cruise in 2002. The cores recovered on the Romanian continental shelf penetrated an erosion surface, indicating subaerial exposure well below the level of the modern Bosphorus outlet. The ^{14}C ages documented a simultaneous colonization of the terrestrial surface by marine mollusks at 7.1 k.y. B.P. The most recent palynology analysis and studies of the dynocyst population (Popescu, 2004) document a real onset of fresh-water arrival during the Younger Dryas and abrupt replacement of Black Sea dynocyst by Mediterranean population, coincident with the onset of the marine mollusks.

Keywords: rapid transgression, Younger Dryas, seismic stratigraphy, multibeam geomorphology, Bosphorus outlet, Black Sea continental shelf.

INTRODUCTION

In 1997, Ryan et al. published results of a joint Russian-American expedition carried out in 1993 on the continental shelf south of the Kerch Strait and west of the Crimea (Major, 1994; Ryan et al., 1997). They had evidence in support of a catastrophic flood of the Black Sea 7500 yr ago. Their interpretation was deduced from high-resolution seismic reflection profiles, and ^{14}C accelerator mass spectrometry (AMS) dating of faunas sampled from cores targeted on these profiles. This joint Russian-American survey revealed a buried erosional surface of shelly gravel extending across the broad continental margin of the northern Black Sea to beyond the shelf break (Evsylekov and Shimkus, 1995; Major, 1994). The cores recovered evidence of subaerial mud cracks at -99 m, algae remains at -110 m, and the in situ roots of shrubs in desiccated mud at -123 m. Each site lay well below the -70 m level of the Bosphorus bedrock sill (Algan et al., 2001; Gökasan et al., 1997). From these results Ryan et al. (1997) proposed that a drowning event in the Black Sea 7500 yr ago may have been the consequence of Mediterranean water penetration into a lowstand lake. This rapid Black Sea transgression is characterized by the deposition of a uniform marine mud drape on the terrestrial surface equally as thick in depressions as on dune crests with no sign of landward-directed onlap of the sedimentary layers in the drape (Ryan et al., 2003). The ^{14}C ages documented a simultaneous subaqueous colonization of the terrestrial surface by marine mollusks at 7100 yr B.P.¹ This age was assigned to the Holocene flooding event. However, flooding precludes the possibility of outflow to the Sea of Marmara during the prior lowstand lake stage. Recently, Aksu et al. (2002b) presented arguments for persistent Holocene outflow from the Black Sea to the eastern Mediterranean and (2002c) for noncatastrophic variations in Black Sea water level during the last 10,000 yr B.P. This contradicts the flood hypothesis.

In the meantime, international and European projects in the Black Sea facilitated two Ifremer oceanographic surveys onboard

RV *Le Suroît* in 1998 and 2002 and a survey onboard *Le Marion Dufresne* in 2004, completing previous international studies of seabed mapping and of subsurface sampling. The main objectives of these cruises, which were supported by the European ASSEMBLAGE (ASSESSment of the BLACK Sea sedimentary system since the last Glacial Extreme) project, are the assessment of the Black Sea sedimentary system since the Last Glacial Maximum (LGM) and the quantification of the impacts of climate change and the sensitivity of the Black Sea system to external force. These surveys, which were carried out on the northwestern continental shelf of the Black Sea, complement systematic high-resolution seismic prospecting done in the 1990s by the Romanian GeoEcoMar institute (National Institute of Marine Geology and Geo-ecology). The preliminary subsurface analysis of the Romanian continental shelf (Popescu, 2002; Popescu et al., 2004) correlated with the results of these last surveys point out that Black Sea lake levels rose on the shelf to at least the -40 to -30 m isobath as indicated by the landward limit of extent of the brackish fauna encountered in the *Dreissena* layer. Since the Black Sea was an important catchment basin for the meltwater drained from the Fennoscandian ice cap ensuing Melt Water Pulse 1A (MWP 1A) in the Bølling-Allerød period (Bard et al., 1990), it is possible that at that time the water level of the lake filled with melt freshwater, rose to the level of its outlet, and spilled into the Mediterranean. However, the onset of salt-water conditions in the Black Sea during the mid-Holocene (7500 yr B.P.) has been clearly indicated. Although contradictory hypotheses have been discussed (Aksu et al., 1999b, 2002a, 2002b, 2002c), lowstand-incised anastomosed channels mapped on the Romanian shelf and recent discoveries of well-preserved drowned beaches, sand dunes, and soils provide new support for the Ryan and Pitman flood hypothesis.

BACKGROUND

General Setting

The northwestern part of the Black Sea receives water and sediment discharge from the largest European rivers—the Danube, the Dniepr, the Dniestr, and the Southern Bug. 817,000

¹“yr B.P.” means years before present (1950) with neither correction for reservoir age nor calibration to calendar years. In Ryan et al. (1997) and Ryan and Pitman (1999a), ages were expressed in calendar years with 7500 cal yr B.P. equivalent to 7100 yr B.P.

km² of the drainage basin for the Danube alone represents the expanse of these river basins. The shelf is particularly wide in this part of the basin (~140 km with a maximum of 170 km off the mouth of the Dniepr River) and narrows to both the east and west (Fig. 1). The total average sediment discharge from the Danube subsequent to damming is estimated to be around 30–35 million t/yr, out of which only 4–6 million t/yr consists of sandy material (Panin, 1997). During the glacial lowstands and especially at the beginning of interglacials, sediment discharge from these rivers was probably much higher.

The Black Sea is a marginal basin, connected to the external Mediterranean Sea over a sill located in the Bosphorus Strait (with a current 32 m sill depth). It has long been recognized that the Black Sea was isolated from the Marmara Sea and the Mediterranean during glacial intervals when levels of the latter seas

fell below the sill depth of the Bosphorus (Degens and Ross, 1974). It has been postulated that the Black Sea water level oscillated independently of the global eustasy, as the Black Sea was an isolated basin for any water level below the depth of the strait. Consequently, lowstand periods in the Black Sea do not necessarily correspond to lowstands in the world ocean, but are related to regional wet-dry cycles (Major, 2002; Tchepalyga, 1984). The role that the Bosphorus Strait has played in controlling the salinity and stratification of both seas and for the production intervals of anoxia has been widely discussed (Arkhangelskiy and Strakhov, 1938; Lane-Serff et al., 1997; Muramoto et al., 1991; Rohling, 1994; Scholten, 1974). The general view is that during periods of low global sea level, connection between the Black Sea and the ocean was lost. The Black Sea, freshened from river discharge, expanded to become a well-ventilated vast lake and established

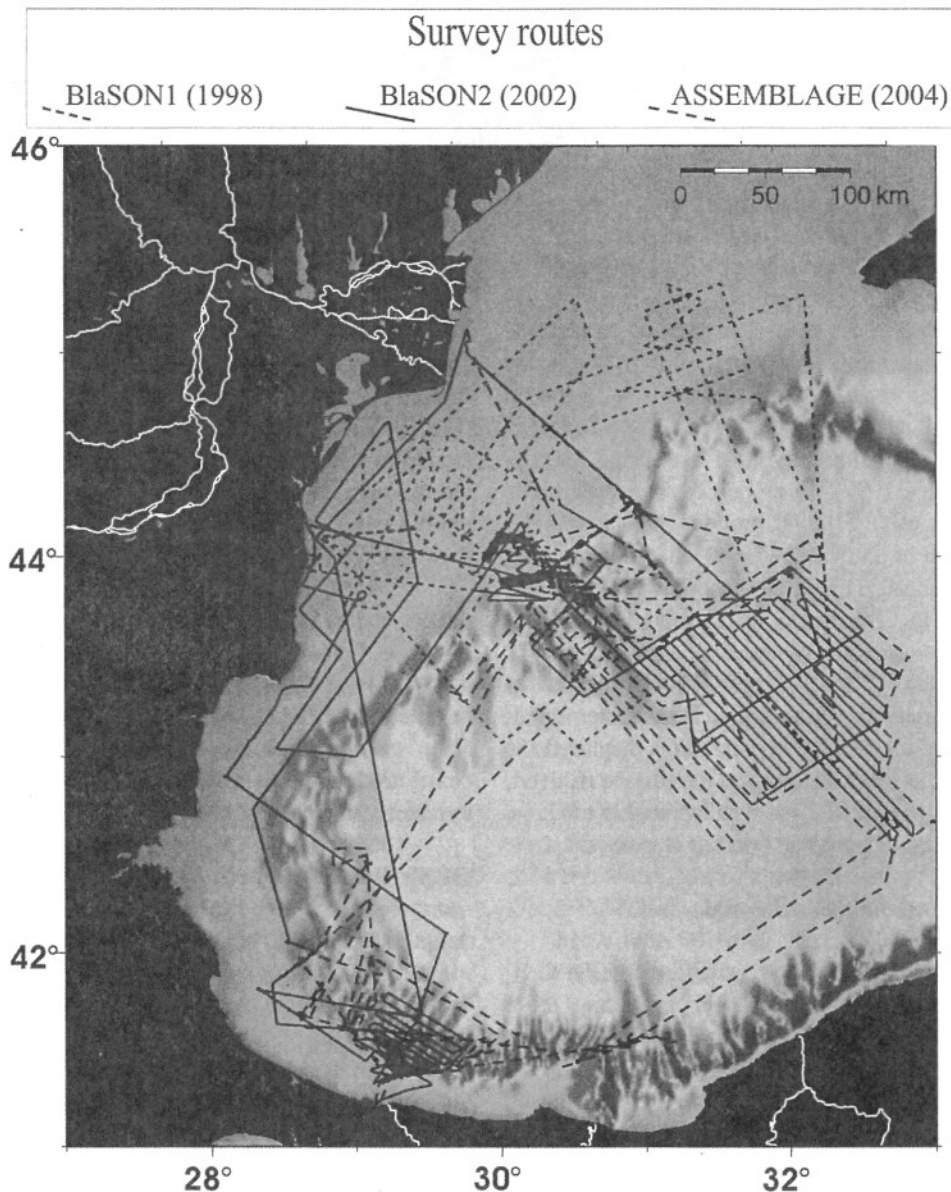


Figure 1. Bathymetry of the semi-enclosed Black Sea basin and Ifremer survey route locations.

a shoreline at the level of its outlet (Hodder, 1990; Tchepalyga, 1984) in order to export excess water to the Mediterranean. Another widely accepted hypothesis regarding the connection of the Black Sea with the external oceans postulates that this inland sea had always maintained a continuous outflow through the Bosphorus and Dardanelles Straits, even during the highly arid glacial intervals (Kvasov and Blazhchishin, 1978; Tchepalyga, 1984). According to this hypothesis, precipitation and river input into the Black Sea exceeded any loss from local evaporation. Indeed, meltwater from former ice caps in Fennoscandia, northern Asia (Grosswald, 1980), and the central Alps transformed the Black Sea into a giant fresh-water lake a number of times in the past (Federov, 1971; Ross et al., 1970), most recently during the Neoeuxinian stage of the Late Pleistocene (Arkhangelskiy and Strakhov, 1938; Federov, 1971; Nevesskaja, 1965; Nevesskaja and Nevesskiy, 1961; Ross et al., 1970).

In 1997, Ryan et al. underlined the occurrence of a widespread unconformity interpreted as an erosional surface subaerially exposed during the last glacial. Using new AMS ^{14}C dates, and abrupt changes in the organic carbon content, water content, and $\delta^{18}\text{O}$ from core material, these authors presented evidence that the Black Sea was a fresh-water lake 7500 yr ago (Ryan et al., 1997). In 2003 Ryan et al. proposed using strontium isotopes to show that the salinization was initiated earlier at 8.4 k.y. B.P. and that the 7.14 k.y. B.P. only reflected a threshold in salinity.

Various aged sapropels sampled from the eastern Mediterranean and the Black Sea are used as arguments against the hypothesis favoring a catastrophic flooding. Sapropel S_1 in the Aegean is generally interpreted to have been deposited between ~8000 and 5500 yr B.P. (Aksu et al., 1999a, 1999b; Fontugne et al., 1994), although deposition may have lasted until 5300 yr B.P. (Rohling and de Rijk, 1999). To support the noncatastrophic flood hypothesis, Aksu et al. (1999a) propose that fresh water from the Black Sea rich in nutrients reduced the surface salinity of the eastern Mediterranean. This phenomenon, which decreases the deep circulation of this sea, favors high surface productivity with restricted circulation, providing good conditions for sapropel formation. However, Rohling (1994) suggests that sapropel formation in the Black Sea started ~550 yr later than in the eastern Mediterranean, when the denser Mediterranean waters displaced the nutrient-rich waters in the Black Sea toward the surface (Calvert, 1990; Calvert and Fontugne, 1987). This lag is probably too large to be accounted for by the catastrophic flooding hypothesis.

Paleorivers on the Romanian Continental Shelf

From previous Romanian surveys carried out by the GeoEcoMar institute, several recent paleoriver channels have been identified that incise the continental shelf down to a 90 m water depth (Popescu et al., 2004) (Fig. 2). These paleochannels are completely filled by sediments and are no longer visible in the bathymetry. These erosive features reach 400–1500 m in width and 20–30 m in depth; they present conventional asymmetry on some cross sections with point-bar- and cut-side- like structures

(Fig. 3). These paleochannels are also sealed by the mud drape described by Major et al. (2002), Popescu et al. (2004), and Ryan et al. (2003), which is parallel to the sea bottom and which corresponds to the marine sedimentation (Lericolais et al., 2003). For Popescu et al. (2004) the stratigraphic position of these incisions lying directly under the discontinuity at the base of the Holocene strongly suggests that they formed during the last lowstand. The cartography of these buried channels shows that they are concentrated around two main directions. This distribution leads to their interpretation as anastomosed fluvial systems corresponding to two distinct drainage systems (Fig. 2). These would correspond to former paleo-Danube River flooding on the shelf to the outer shelf where they apparently split into several arms similar to a fluvial deltaic structure comparable in size to the modern Danube delta and lie close to the Danube Canyon (Popescu et al., 2004), which is also known as the Viteaz Canyon.

Paleocoastline on the Romanian Continental Shelf

Terraces have been recognized on many Black Sea margins, including the narrow Caucasus shelves (Ostrovskiy et al., 1977a; Shimkus et al., 1980) and the Northern Turkish shelf (Algan et al., 2002; Ballard et al., 2000). Among these terraces, shells belonging to past littoral environments were dated between 19–9 k.y. B.P. (Dimitrov, 1982; Ostrovskiy et al., 1977a; Shcherbakov et al., 1978; Tchepalyga, 1984). On the Romanian continental shelf, Popescu et al. (2004) have noticed the absence of incised river channels below 90 m water depth where a wave-cut terrace-like morphology was mapped ~100 km far from the Danube delta (Fig. 2). Wave-cut terraces are erosional surfaces created by erosion from wave action indicating the vicinity of the shoreline. Since rivers do not always generate continuous incised valleys along the entire shelf (Lericolais et al., 2001; Talling, 2000; Wescott, 1993), their absence below the isobath –90 m does not necessarily indicate the location of the paleocoastline. A good indicator of the paleocoastline is the wave-cut terrace wrapping around the head of Viteaz Canyon and present between isobath –98 and isobath –112 m (Popescu et al., 2004). Northward of Viteaz Canyon the terrace deepens again to –97 m while the height increases to 10–15 m and splits into two distinct steps. The last lowstand paleocoastline should thus have been situated between this submerged terrace and the deepest buried fluvial channels (Fig. 2).

OBSERVATIONS

Acquisition and Processing of Data

During the two campaigns on board the RV *Le Suroît*, precise positioning was given by a Differential Global Positioning System (DGPS). In some areas (i.e., dune field mosaics), real-time navigation processing within a few meters' accuracy made it possible to follow parallel track lines spaced 200 m apart at a speed of 4 knots. The vessel was equipped with EM1000 and EM300 swath bathymetry systems, and high-resolution seismic

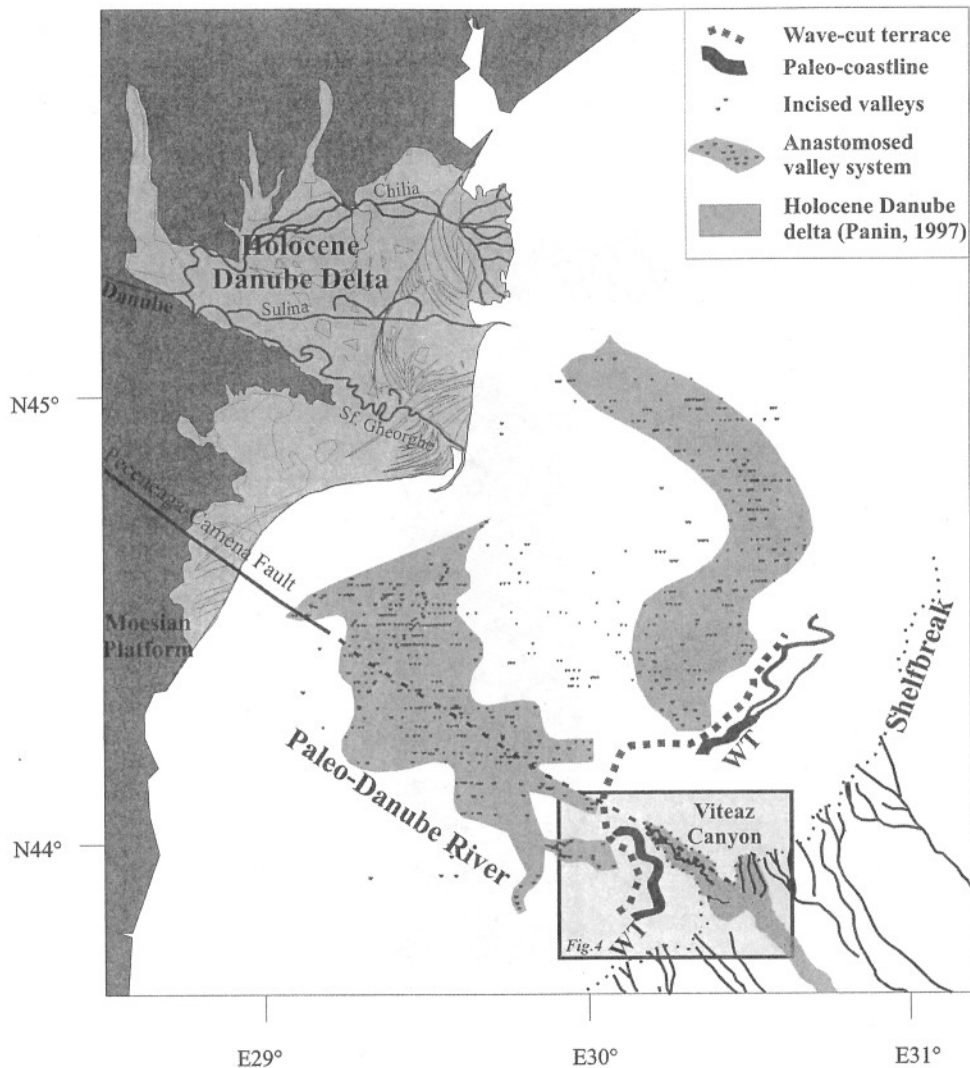


Figure 2. Paleogeographic map of the northwestern Black Sea margin during the last sea-level lowstand. Individual incised paleochannels identified on shallow seismic profiles were shot by the GeoEcoMar institute and interpreted by Popescu et al. (2004). Areas characterized by dense occurrence of buried channels cluster in two main paleo-drainage systems. The presumed position of the Peceneaga-Camena fault is drawn after Winguth et al. (2000) and Dinu et al. (2002, 2005). WT—Location of the submerged wave-cut terrace.

lines were shot simultaneously using a Chirp sonar system. All data acquisition was synchronized and digitally recorded.

The Simrad multibeam echo-sounders provided the mapped bathymetry by processing the returned echo of each sonic transmission through a selection of preformed beams trained across a strip of seafloor effectively four to seven times as wide as the water depth. Each beam gives a depth resolution in the order of 10 cm in a footprint 5 m across and 2 m long along the swath at the selected 4 knots survey speed. An image of backscatter reflectance energy was generated along with the digital elevations. Navigation, bathymetry, and image data were processed and synthesized in order to plot positions automatically, to produce bathymetric maps, and to produce an image mosaic.

The high-resolution seismic reflection source was a Chirp sonar single channel, with a frequency sweeping from 1.8 to 5.3 kHz. The digital data acquisition was done in real time on the Delph PC-based system.

More than 90 cores were recovered during these cruises. They were done using a Kullenberg piston core and in some cases by using a vibrocorer.

Surficial Features

Bathymetry data were provided by multibeam echo-sounder (Fig. 4). In 1998, the Viteaz Canyon (Popescu et al., 2004) and zone A (Fig. 4) were surveyed. On the zone A mosaic, a sea-

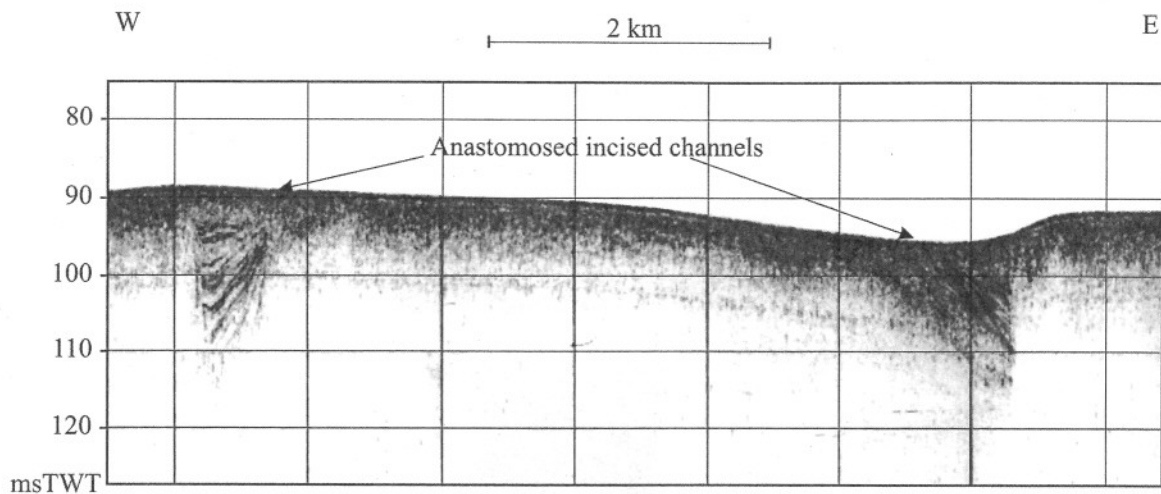


Figure 3. Paleovalleys with small cut side and point bar incised in the brackish layer (from Popescu et al., 2004). msTWT—Two Way Time (ms).

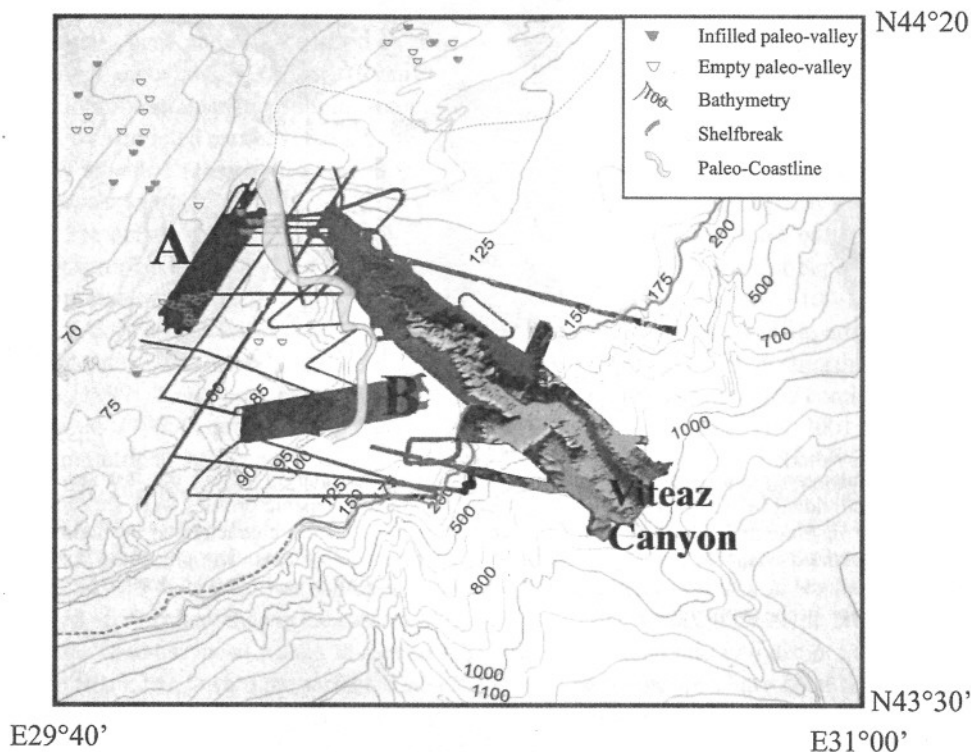


Figure 4. The multibeam bathymetry showing the 1998 (zone A) and 2002 (zone B) mosaic realized around the Viteaz Canyon head.

bed populated by sand ridges and small depressions overlying and sculpted into the eroded remains of a former terrestrial floodplain was revealed. Results were presented by Lericolais et al. (2007). These ridges located at the crest and landward of a shoreface recognized at depths of 85 to 100 m have stronger correspondence to aspect ratios of modern linear beach ridges than to those of underwater sand waves. The depressions among

this first mosaic are similar in size and shape to blowouts formed through wind deflation. The ridges and depressions sit on a surface exposed by a lowstand of the Black Sea's glacial and postglacial lake. Seismic sections present forced regression sequences eroded by a wave-cut terrace at a depth of 100 m. Submergence without destruction and infilling suggests a rapid rise in the lake's surface.

In 2002, zone B (Fig. 5) was recognized. In the northeastern part of this mosaic, linear ridges 4–5 m in relief and with an average spacing of 250 m are prominent. They strike almost uniformly obliquely to a berm-like step along a north-south axis of the mosaic. In addition, depressions with a diameter from 100 to 500 m and a negative relief of 5 to 10 m are present in the southwestern half of the corridor. Parabolic features have been revealed inside these depressions (D on Fig. 5). The wave-cut terrace described as unique on the outer shelf in previous works (Major et al., 2002; Popescu et al., 2004; Ryan et al., 2003) is clearly evident on the presented mosaic. The upper surface of the berm varies around 90 m b.s.l. This is consistent with a major lowstand level situated somewhere around 100 m below the sea surface.

Subsurface Features

The ridges and depressions can be viewed in cross section using high-resolution seismic reflection profiles. The Chirp sonar provides seismic penetration to tens of meters and defines layering to the sub-meter scale. The profiles indicate that the ridges are superimposed on a reverberant “bottomset” constituted of prograding reflectors whose morphology is interpreted as forced reflection system tract (Posamentier et al., 1992) (Fig. 6). These last reflectors deepen seaward and are truncated by an erosional surface described as the wave-cut terrace on the multibeam mosaic. From the seismic profiles, it is clear that the entire area is covered by a drape of less than one meter thick, confirming that the dune system is no longer active. Everywhere

across the mid and outer shelf the ridges, mounds, and depressions are draped by this thin layer of sediment with a remarkably uniform thickness of no more than a meter (Fig. 6).

Seismic profiles across the parabolic features show that these sand bodies developed inside a trough. Their seismic facies is similar to sand dune facies and can be interpreted as barchane sand dunes (Fig. 7).

Sediment Cores

Sediments, obtained by coring, provide evidence in support of the reflection profiles. During the BlaSON (Black Sea Over Neoeuxinian) and ASSEMBLAGE campaigns, an important set of gravity cores has been recovered. Here we present only results obtained on the dune fields bringing important information on the age of the onset of these sand bodies. Sampling into the interior of a ridge on the zone A dune field mosaic done by Lericolais et al. (2006) (Fig. 4) (i.e., core BLKS9837 taken in a water depth of 68 m, core length 190 cm, position N44°00.54'–E29°58.87') recovered dark sand rich in opaque heavy minerals and shell fragments (Fig. 8). Sampled minerals include quartz, garnet, and ilmenite. Shell fragments belong to the fresh-water mussels of the *Dreissena* species. Cores into the bedded sediments, on which the dunes have formed, sampled silty red and brownish clay with thin lenses containing fresh to slightly brackish water mollusks (*Dreissena* and *Monodacna* sp., respectively). These mollusk specimens return AMS radiocarbon dates spanning from 8585 ± 50 yr B.P. to 10,160 ± 90 yr B.P. (without reservoir and dendrochronologic calibration).

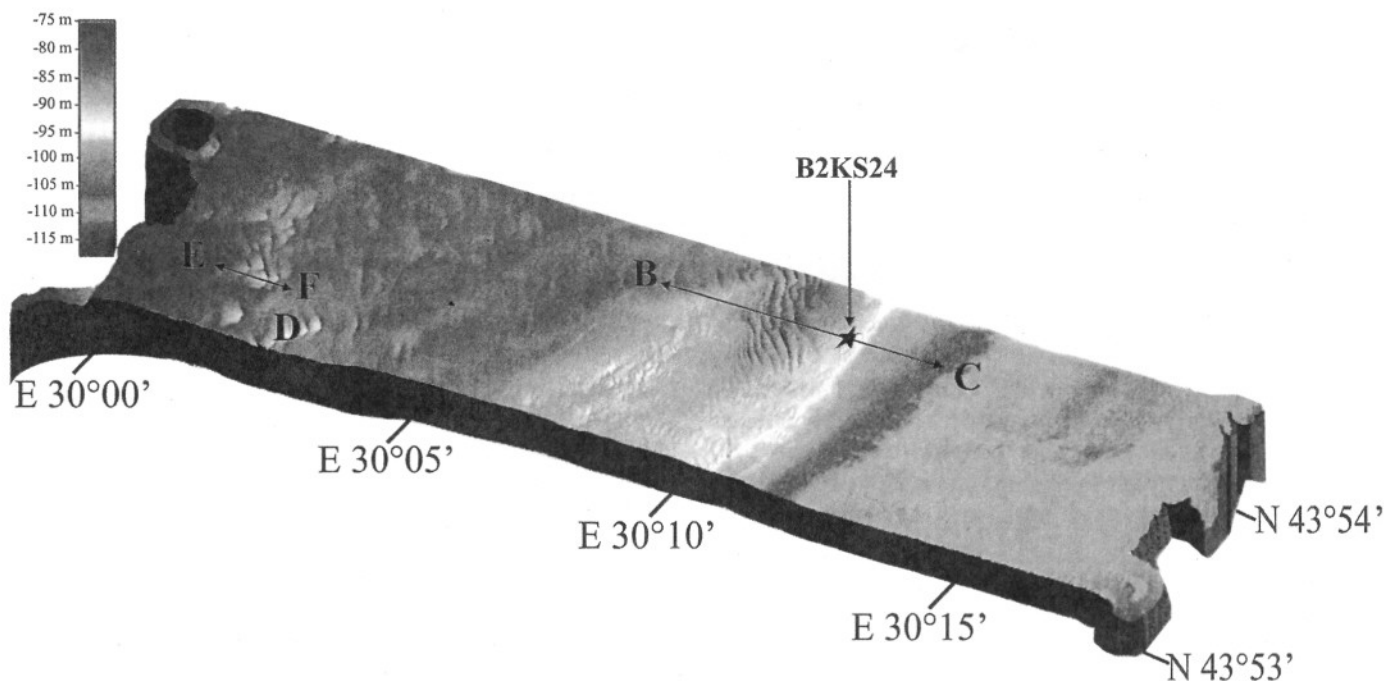


Figure 5. The multibeam bathymetry covering a sand dune field (zone B, Fig. 4). B–C—seismic profile across the sand dunes (Fig. 6); B2KS24—name and location of the core (Fig. 9); D—depression location; E–F—seismic profile across a trough with a parabolic dune (Fig. 7).

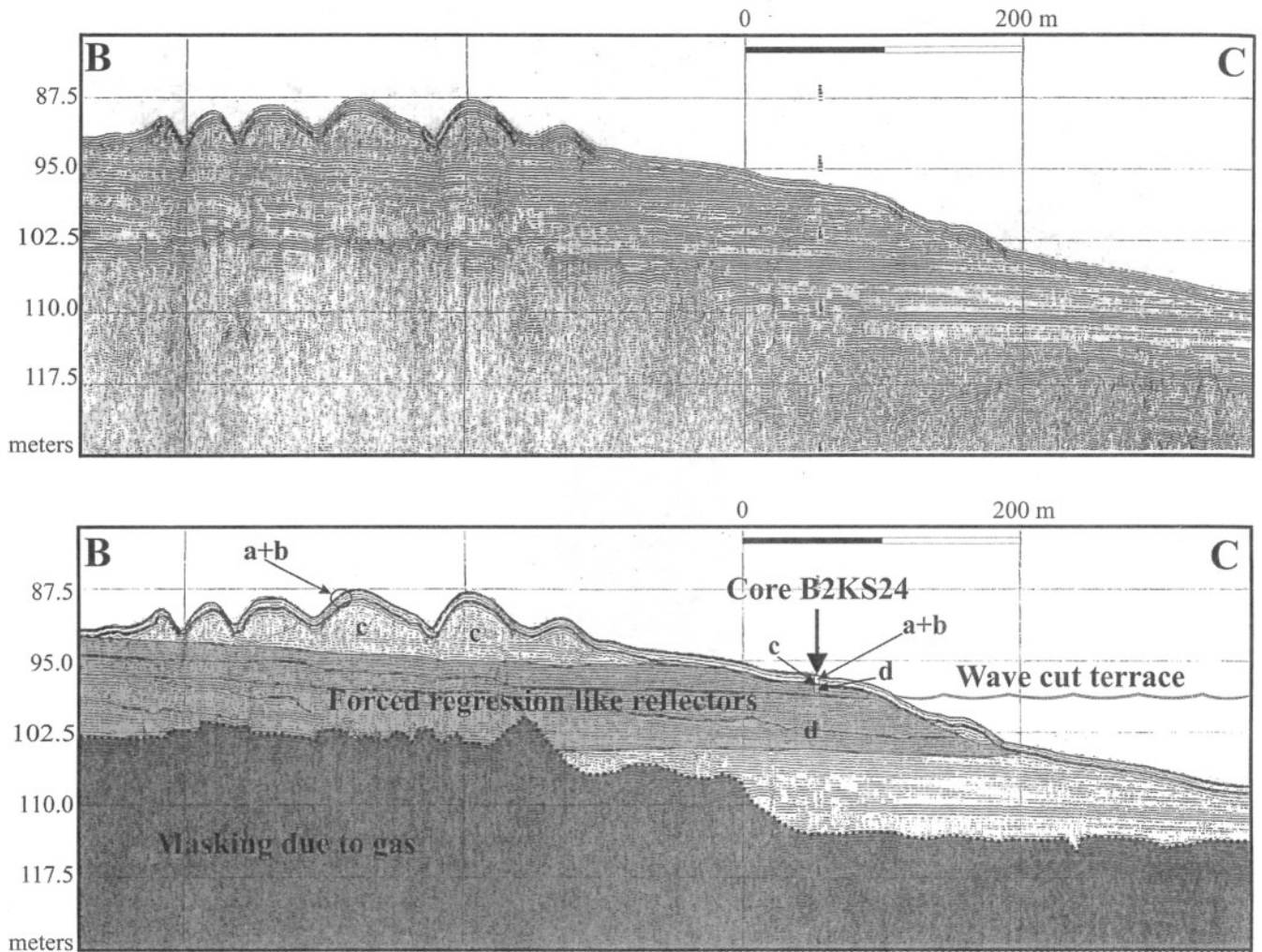


Figure 6. Seismic profile across a sand dune (B–C on Fig. 5). Core B2KS24 is presented in Figure 9; a+b corresponds to the marine layer; c—hash layer with *Dreissena*; and d—limnic sediment layer.

Sampling the top of the wave-cut terrace by piston coring (B2KS24 taken in a water depth of 96 m, core length 401 cm, position N43°53.79'–E30°11.00') provides evidence in support of the reflection profile (Fig. 9). Coring of the bedded sediments underlying the dunes and upon which they formed extracted a complete section similar to the description made by Major et al. (2002) of a core obtained during the first French-Romanian survey in 1998. The sequences can be described as follows: (1) the bottom of the core presents silty laminated clay (unit d) containing fresh to slightly brackish water mollusks (*Dreissena distincta*). These specimens return AMS radiocarbon dates of $11,040 \pm 50$ C¹⁴ B.P. (without reservoir and dendrochronologic calibration). (2) Above, marked by a sharp basal contact is a 15-cm-thick light gray layer rich in *Dreissena* sp. detritus dated between 8760 ± 40 C¹⁴ B.P. and 8620 ± 50 C¹⁴ B.P. (described as the hash layer by Major et al., 2002). Above the layer rich in *Dreissena* sp. detritus is a marine sequence characterized by a mollusk assemblage that is exclu-

sively salt-water species, such as *Mytilus edulis* (also known as *Mytilaster*) and *Cerastoderma edule*. Those last shells sampled near the base of the uppermost drape, which is dated 2820 ± 30 C¹⁴ B.P., date between 6520 ± 40 C¹⁴ B.P. and 5525 ± 35 C¹⁴ B.P. Recent palynological and dinocyst analyses (Popescu, 2004) on samples from within these cores indicate an abrupt fresh-water transition during the Younger Dryas followed by an abrupt replacement of the endemic Black Sea dinocysts by a Mediterranean population at 7150 C¹⁴ B.P.

INTERPRETATION

Interpretation of the Linear Ridges

Are They Sand Waves?

In underwater environments the asymmetrical linear ridges would be classified as sand waves (Allen, 1982) or large dunes (Ashley, 1990). One observes sand waves in many places on

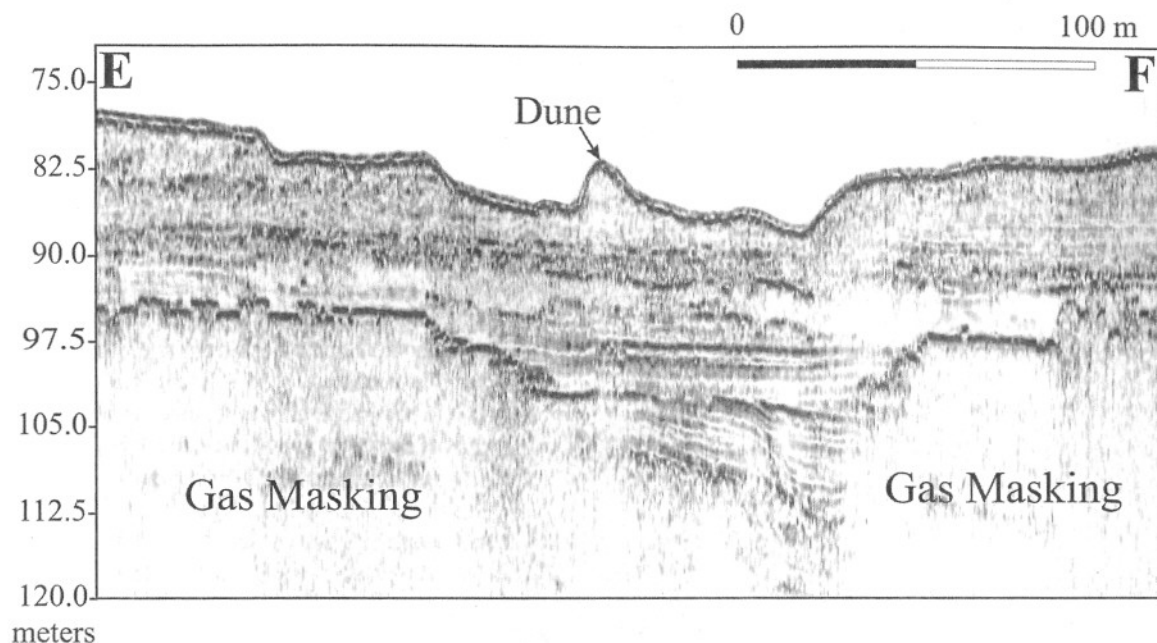


Figure 7. Seismic profile across a barchane dune inside a trough; E–F on Figure 5.

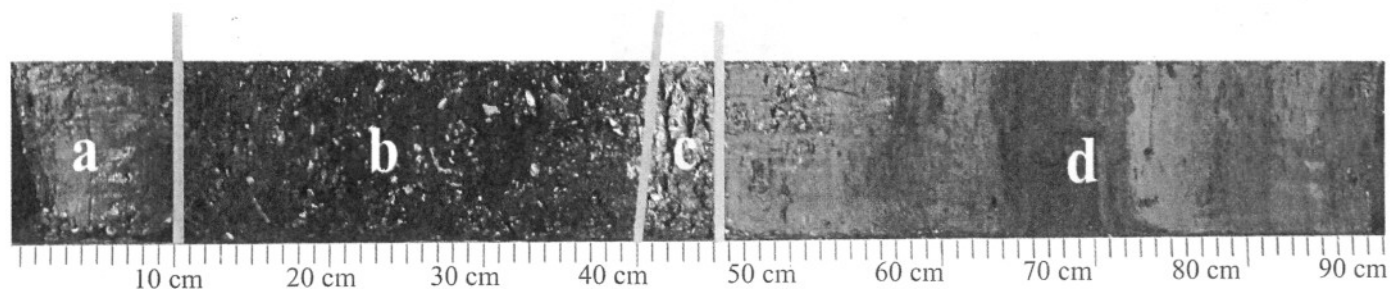


Figure 8. Core BLKS9837 (N 44°0.54'–E 29°58.87') recovered on the dune field at a depth of 68 m (Lericolais et al., 2006): (a) Layer with *Modiulus* dated from 3000 yr B.P. to present; (b) layer with *Mytilus edulis* dates between 6900 and 3000 yr B.P.; (c) layer with *Dreissena*—the youngest is dated 7500 yr B.P.; and (d) limnic sediment layer dated 10,160 yr B.P.

the continental shelf. Examples include the Bay of Fundy (Dalrymple, 1984), the English Channel off the Normandy coast of France (Berné et al., 1988), the North Sea (McCave, 1971), and the East Coast of the United States (Swift and Freeland, 1978). Sand waves are products of sedimentary environments characterized by high-energy bottom currents (Allen, 1982). The strongest currents are generated by the ebb and flood of tides through inlets (Berné et al., 1998; Kenyon and Stride, 1968; McCave, 1971; Terwindt and Brouwer, 1986). Such currents tend to amplify within estuaries (Kostaschuk and Villard, 1996). Sand waves also form in wave-dominated environments (Berné et al., 1988) or by oceanic currents (Flemming, 1988). In seas without significant tide, such as the Mediterranean, sand bodies are generally found as wedges built of shoreface deposits. But dunes are also observed around major delta systems such as the Rhône (Amorosi et al., 1999) and the Nile (Stanley, 1996).

Sand waves in estuary settings have varying asymmetries depending upon whether they are flood or ebb dominated. Their internal inclined beds show reversals in dip direction as flood-dominated sand ridges become ebb-dominated and vice versa. Active sand waves are features of the shallow inner shelf (Swift and Field, 1981) and its coastal bays. Sand waves on the outer shelf in depths of 110 to 140 m on the southern Celtic margin (Berné et al., 1998) are relict bedforms deposited when the sea surface lay more than 100 m below its present level. Sand waves are flow-transverse bedforms whereas linear ridges are flow parallel. The Black Sea's linear ridges are also relict as shown by the drape that covers them.

Are They Longshore Bars?

Longshore bars are described in lake environments, such as Lakes Michigan, Huron, and Erie (Davidson-Arnott et al., 1996). These bars form depths less than 4 m. They are typically 10 km long, 25–50 m wide, and 0.2–0.75 m high (Wattrus and Rausch,

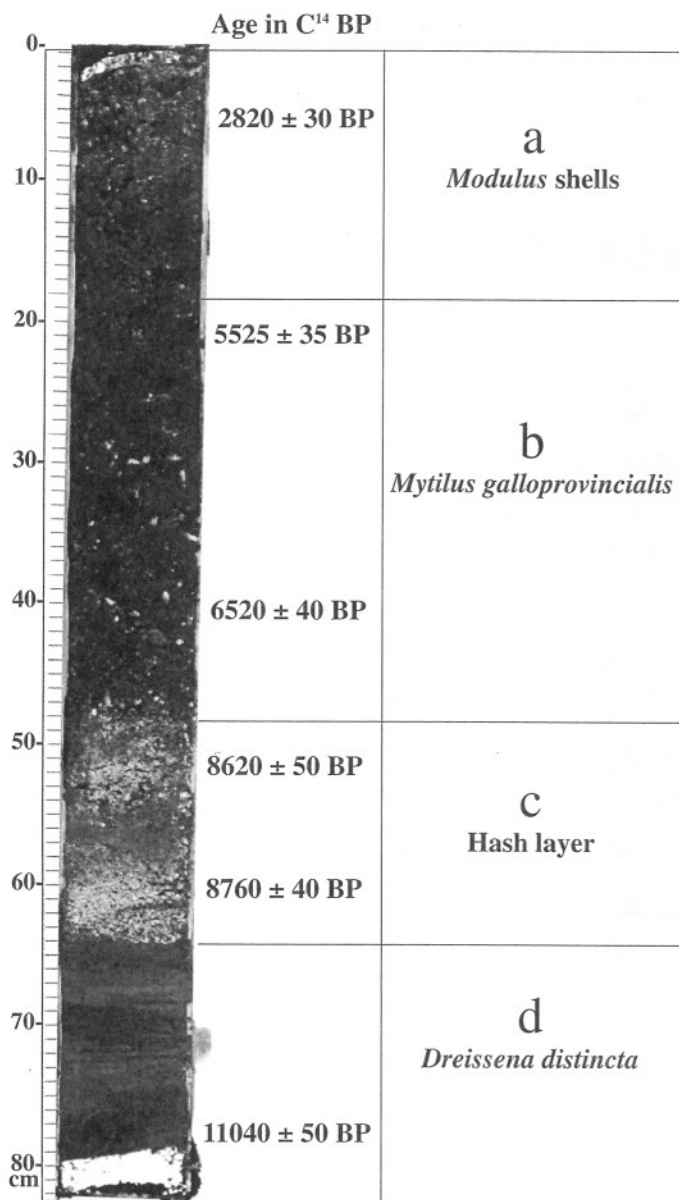


Figure 9. Core B2KS24 (N43°53.79'–E30°11.00') recovered on dune field B (Fig. 4) and on top of the wave-cut terrace (Fig. 6).

2001) and develop as multiple sets of ridges, which are aligned parallel to the shore. The linear ridges surveyed in this study are aligned somewhat obliquely to the regional bathymetric contour and to the paleoshoreline outlined by wave-cut terraces (Figs. 4 and 5). The striking characteristic of shoreface-attached ridges is that they orient at an oblique angle to the shoreline with their seaward tips directed toward the prevailing current (Snedden and Bergman, 1999). If the Black Sea's linear ridges correspond to relict-drowned, shoreface-attached sand ridges, then they should have formed when the Black Sea level lay 5 m above the crests. The level of the Black Sea would have been approximately –60 to –75 m at the time of their formation.

Are They Delta Mouth Bars?

The Black Sea's linear ridges could be interpreted as successive mouth bars of a deltaic body constructed during a lowstand of sea level. Such mouth bars are present today within the Saint George II distributary channel of the Danube delta (Panin, 1997). Wave-dominated deltas present a series of shore-parallel sand ridges forming as mouth bars built up and out to form a new beach. This results from a net supply of bedload material from the river. In any case, the utilization of such ridges as water-level indicators presupposes a recognizable interface between the wave-built foreshore and the overlying aeolian forest within a given ridge (Otvos, 2000). For the Black Sea's ridges to be mouth bars, they had to have been constructed during a regression that brought the shoreline to where they are now found, confirming a lowstand at that position.

Are They Coastal Dunes?

Coastal dunes *sensu lato* result from the accumulation of sand transported along the shore by the combined action of winds and waves (Carter et al., 1990a) in littoral environments (Carter et al., 1990b). Foredunes and parallel dunes, beach ridges and cheniers are long, linear, ridge-forming formations representing the locations of ancient shorelines (Meldahl, 1995). They occur on low-relief coastal plains, standing with several meters of relief above their surroundings. In terrestrial sand seas, aeolian dunes are classified on the basis of shape and the number of facies (McKee, 1979). The abundant dune type is linear, with the long axes oriented parallel to the prevailing or dominant wind and resultant sand drift direction (Wilson, 1972). Linear dunes, accumulating rather than migrating during active phases, tend to develop in wind regimes with a significant degree of directional variability and where sand supply is minimal (Thomas, 1997).

Coastal dune formation is enhanced by the input of littoral sediments during periods of low sea level. Foredune ridges have an aeolian (foredune) cap on the accreted berm that indicates the occurrence of winds sufficiently strong to transport beach sand (Roy et al., 1994). Beach ridges are low-relief, wave-formed berms that rarely rise more than 3 m above mean sea level, but foredune ridges and swale have greater amplitude (3–5 m) and crest elevations of 7–10 m (Thom and Hall, 1991). For the linear ridges on the Black Sea's shelf to be coastal dunes, they had to have been constructed during a regression that exposed the surface upon which they grew, and they had to survive intact any subsequent shoreface erosion as they became submerged.

Interpretation of the Hollows

In subsea environments, small enclosed and unfilled hollows are rare. The exception is for substrate which is easily eroded, where bedforms may climb at a negative angle and cannibalize the substrate. If these bedforms are sinuous or crescentic, they will produce swale by scouring to the lee face of the depression (Berné et al., 1998). Another exception is the small circular pockmark left by venting gas. Bathymetric surveys in other oceans and seas have

not revealed hollows displaying the size and shape interconnectedness as those mapped on the Romanian shelf. However, enclosed depressions like those in the surveyed corridor are characteristic of windy and arid environments (Shaw and Thomas, 1997). The cavities are eroded into the substrate by deflation processes, with the magnitude of the excavation ultimately limited by the groundwater table (Laity, 1994). The depressions at the scale of those mapped on the Romanian shelf are similar to pans. Pan initiation and growth depend on materials susceptible to deflation such as poorly consolidated clay-rich material that curls, flakes, and blows away upon desiccation. Pans in dune settings may occur as a string of depressions aligned along a former river course and its braid plain. Pans often transform into ponds during wet phases, generally from groundwater recharge. Pond and marsh sediments have been reported from between the dunes of sand seas during intervals of substantially increased moisture (Lancaster et al., 1994). Present-day ponds are reported in the desert seas of northwestern China (Wang et al., 2002). In coastal domains, pans correspond to blowouts formed when strong onshore winds erode

gaps in a single foredune or series of beach ridges (Giles et al., 1997). Leakage of sand occurs mainly through erosion of the dune front by storm waves or by landward movement of sand through blowouts or parabolic dune migration (Carter et al., 1990a) or by a combination of these factors.

Subsea or Subaerial Origin?

To evaluate an origin for the Black Sea's linear ridges their dimensions and spacing are compared to subaerial dunes and subsea sand waves. In Figure 10, the height and spacing of the linear ridges on the Romanian and Ukrainian margins fall within and along the trend of the population defined for sedimentary coasts, where combined wind and wave action shape coastal ridges on the barrier surface with dimensions and spacing situated at the border between aeolian and subaqueous features. Various subsea sand ridges on the European Atlantic margin have an average height around 4.7 m (Berné et al., 1998) and are comparable to the 4.25 m calculated from a bibliographic synthesis (Allen, 1982).

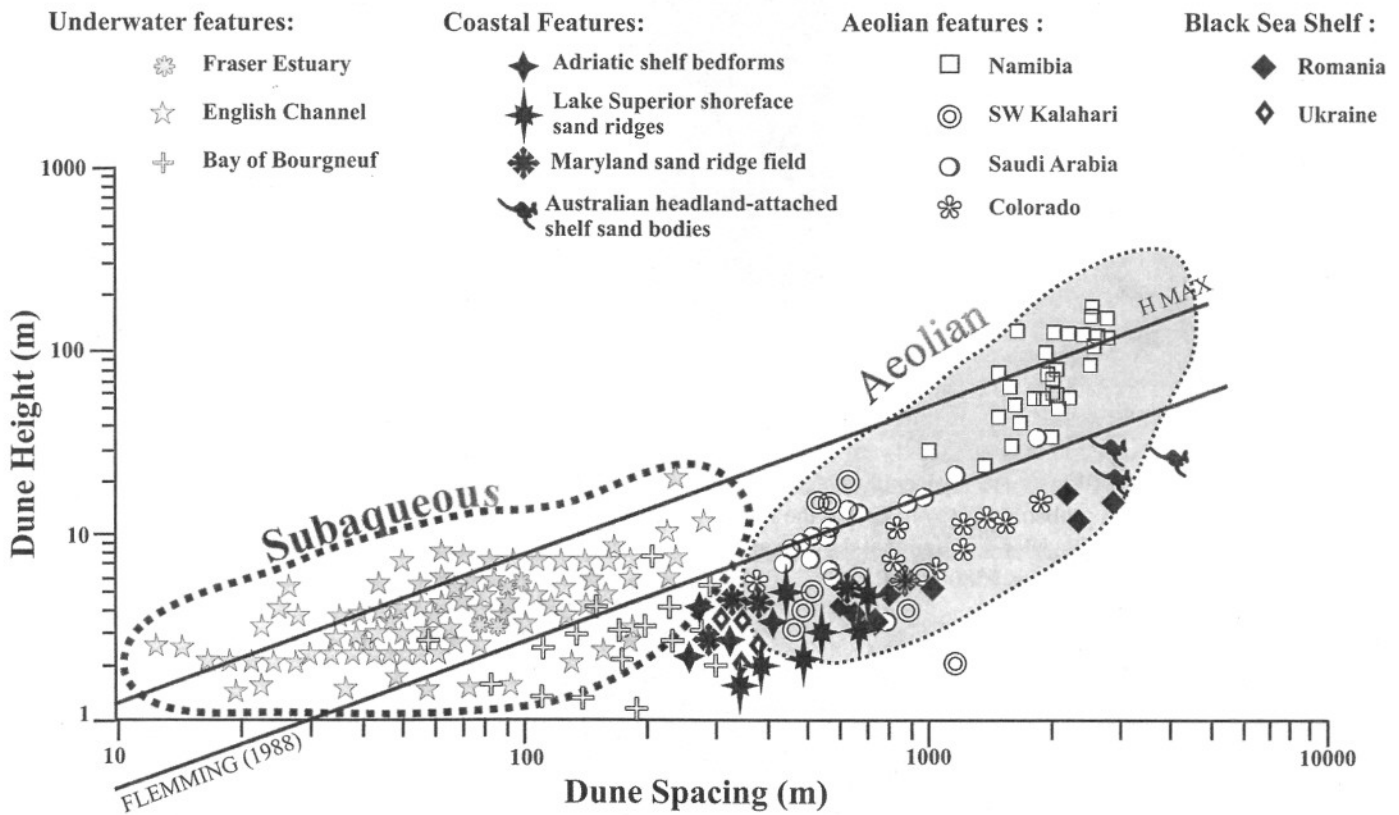


Figure 10. Dune height (m) versus dune spacing (m). Logarithmic diagram of aeolian and subaqueous dunes. The surveyed dunes of the Romanian and Ukrainian shelf are presented among other dunes from both origins (aeolian and subaqueous). The lower and the upper lines have been established by Flemming (1988) for subaqueous dunes; $H = 0.0677 \cdot L^{0.8098}$ and $H_{max} = 0.16 \cdot L^{0.84}$. References used for:

- Underwater features: Kostaschuk and Villard (1996) for Fraser River, Berné et al. (1998) for English Channel, Berné (1991) for Bay of Bourgneuf;
- Coastal features: Correggiari et al. (1996) for Adriatic shelf bedforms, Wattrus and Rausch (2001) for Lake Superior shoreface sand ridges, Swift and Field (1981) for Maryland sand ridge field, and Roy et al. (1994) for Australian headland-attached shelf sand bodies;
- Aeolian features: Lancaster (1998) for Namibian dunes, Thomas (1997) for dunes from the Kalahari desert, Fryberger et al. (1983) for the Saudian sand sea, and Fryberger et al. (1979) for Colorado eolian "sand-sheet" deposit; and
- Black Sea shelf: this paper for the Romanian shelf and Ryan et al. (1997) for the Ukrainian shelf.

The height/spacing ratio of subsea ridges (Berné et al., 1998; Flemming, 1988) is parallel to but offset from the trend of the aeolian features. The height and spacing of the linear ridges on the Romanian and Ukrainian margins are more representative of the coastal population than the subsea one. Similar features to the studied dune formation have been reported at the southern part of Cape Flattery (Australia), where currently active parabolic dunes are transgressing over an older strandplain surface (Pye, 1993). The Romanian-surveyed dune fields are located directly foreshore the wave-cut bluff delineating the paleoshoreline situated at 100 m deep. Waves, wave-dominated currents, and winds are mechanisms for moving and depositing sand on shorefaces and beaches of the open coast. In the case of a rapid sea-level rise, coastal processes only have time to build low, discontinuous foredunes on the barrier surface that provide little impediment to storm washover and wind deflation resulting in the formation of blowouts or pans.

Age of the Ridges and Depressions

A grip on the age of the Black Sea's linear ridges is obtained by analysis of the materials beneath and above them. The uniform drape of the euryhaline mollusk-bearing mud across the erosion surface provides an upper minimum limit, and the brackish mollusks in the shell hash with a marine strontium isotopic signature (Ryan et al., 1997) refine the end of ridge and depression activity at 8.5 k.y. B.P. The materials within the dunes consisting of shell-bearing sand with *Dreissena* fragments give dates of 8.5 k.y. B.P., but dune formation could have commenced earlier because core penetration into the sand was very limited. The prograding reflectors upon which the dunes sit and into which the depressions have eroded as well as how the wave-cut terrace is marked provide a lower limit. The red-brown clay in core BLKS9814 at -55m and lying 1.2 m below the erosion surface contains a lens rich in *Monodacna* dated at 9580 yr B.P. (Ryan et al., 2003). Since the linear ridges in the surveyed corridor lie landward of this core and their substrate may not have been as deeply eroded as that of the outermost shelf, it is probably safe to infer that the ridges have been constructed after this later date and that they migrated over floodplain deposits as young as 9580 yr B.P.

Evidence of Subaerial Exposure

An erosion surface is present everywhere across the Romanian, Ukrainian, and Turkish shelves (Demirbag et al., 1999). The erosion truncates the sediment fill of river channels, some of which display the point-bar bedding geometry of meandering streams (Fig. 3). The sediments corresponding to the eroded substrate are found to possess high bulk density (1.8–2.2 g/cm³) and low water content (<30%), compatible with de-watering in a terrestrial setting (Ryan et al., 1997). Root casts and desiccation cracks have also been observed in soils below the erosion surface (Major, 1994). The strata cut by erosion are stiff clays with occasional silt/sand lenses containing mollusks that have been dated on the Ukrainian

and Bulgarian shelf to glacial periods in the late to middle Pleistocene. The erosion has even cut into Neogene strata (Kuprin et al., 1974; Shcherbakov and Babak, 1979; Shopov et al., 1986).

The dry sediment and desiccation features on the erosion surface are compatible with the superimposed ridges and depressions forming in coastal, river mouth, and shoreface environments.

DISCUSSION

The transition of the Black Sea system from a fresh-water lake to a marine environment was perhaps one of the most dramatic Late Quaternary environmental events in the world. During the Last Glacial Maximum, 21,000 yr ago, the Black Sea was probably a giant fresh-water lake as proposed by Arkhangel'skiy and Strakhov (1938) or at least a brackish enclosed basin; its water level stood more than 120 m below today's level. As early as 2001, analysis of high-resolution seismic reflection profiles, Chirp and side-scan data, together with piston cores from the first BlaSON survey realized on the Danube fan (Popescu et al., 2001), provided new insight into the recent sedimentation processes in the deep northwestern Black Sea. It was determined that the last channel-levee system on the Danube fan developed during the Neoeuxinian lowstand (stage 2) in a semi-fresh-water basin with a water level ~120 m lower than today. Sediments supplied by the Danube were transported to the deep basin through the Viteaz Canyon (Fig. 4). A definite relationship exists between water level and Danube fan sedimentation: When water level is close to the shelf break during lowstands, fluvial sediments are transported to the deep-sea fan, while fan construction is essentially interrupted during water-level highstands (Fig. 11). Functioning of the deep-sea fan is a good indicator of lowstand periods (Popescu et al., 2001; Winguth et al., 2000; Wong et al., 1997).

Since the Black Sea was in close vicinity to the Scandinavian-Russian ice cap, the supply of the melting water from the glaciers into the Black Sea through the major drainage system constituted by the large European rivers (Danube, Dniepr, Dniestr, and Bug) was assimilated into the brownish layers described in cores (Bahr et al., 2005; Major et al., 2002). The water brought to the Black Sea after Melt Water Pulse 1A (MWP 1A) at ~12,500 C¹⁴ B.P. (14,500 yr cal. B.P.) (Bard et al., 1990) was supposed to have a large enough impact that the water level rose to between


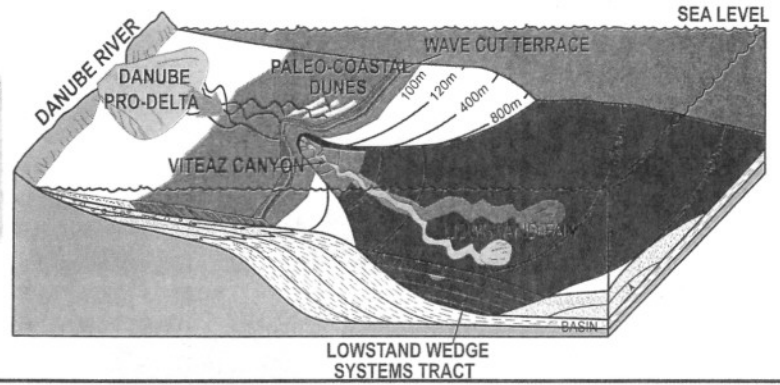
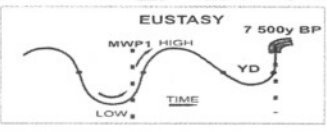
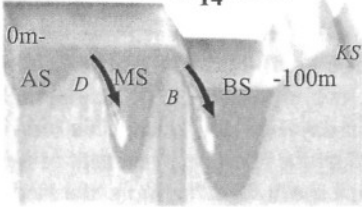
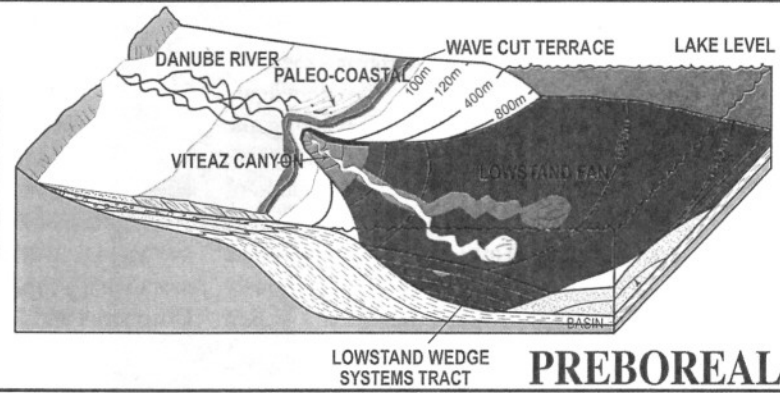
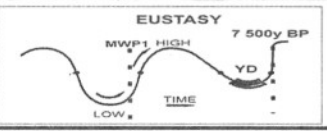
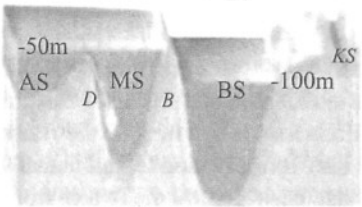


Figure 11. Schematic scenario inspired by Posamentier and Vail (1988) of the water-level fluctuations in the Black Sea since the Last Glacial Maximum deduced from geomorphological results, supported by the Danube deep-sea fan functioning (Popescu et al., 2001), the results from palynology and dinoflagellates (Popescu, 2004), and the paleocoastline position. LGM—Last Glacial Maximum; MWP1—Melt Water Pulse 1; YD—Younger Dryas; AS—Aegean Sea; MS—Marmara Sea; BS—Black Sea; KS—Kerch Strait; D—Dadanelles; B—Bosphorus.

7 500 C₁₄ BP

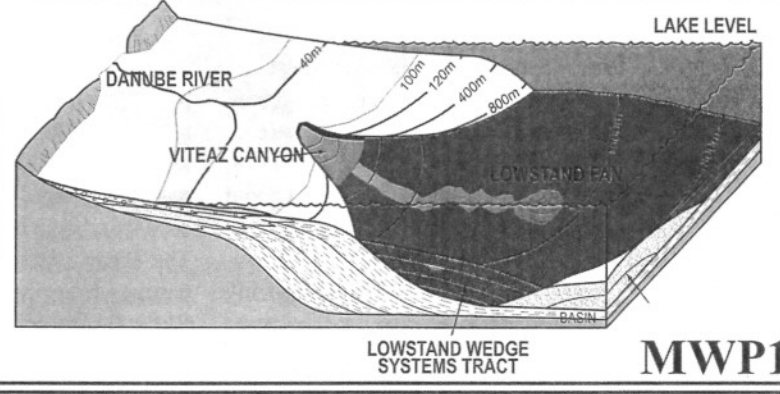
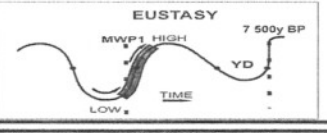
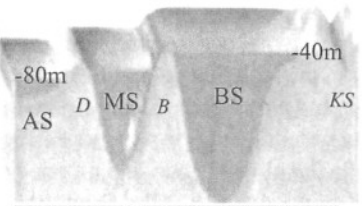


8 600 C₁₄ BP



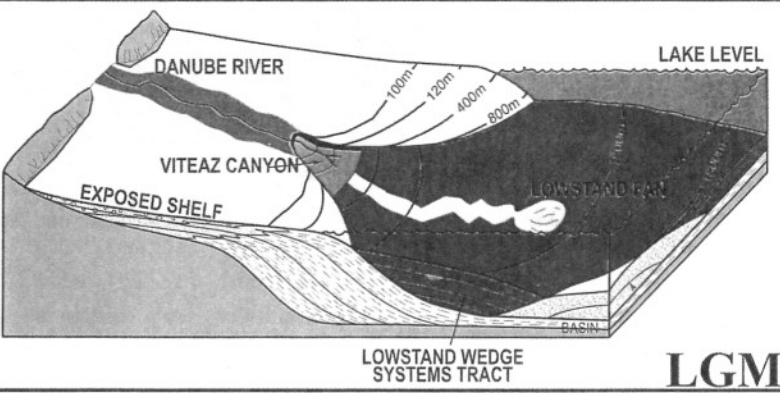
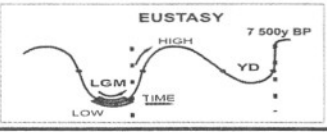
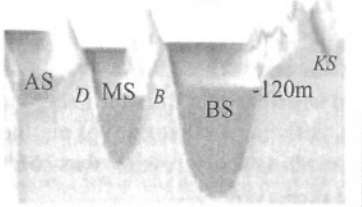
PREBOREAL

12 000 C₁₄ BP



MWP1

18 000 C₁₄ BP



LGM

- 
SUBMARINE FAN FACIES
- 
OLD SUBMARINE FAN
- 
FLUVIAL FACIES
- 
COASTAL SEDIMENTS
- 
OFFSHORE MARINE FACIES

–40 m to –20 m, where the *Dreissena* layers were deposited. The –40 m upper limit is interpreted from our records, which are not exhaustive, and the –20 m limit is provided by Valentina Yanko-Hombach (Yanko, 1990). This last value for the transgression upper limit would have brought the level of the Black Sea even higher to the Bosphorus sill, and possible inflow of marine species like Mediterranean dinoflagellate population can be envisaged (Popescu, 2004). The rise in the Black Sea water level, which stayed between fresh and brackish conditions, stopped the deep-sea fan sedimentation (Fig. 11).

Palynological studies done on BlaSON cores (Popescu, 2004) show that during the Younger Dryas a cool and drier climate prevailed. Northeastern rivers converged to the North Sea and to the Ancylus Lake (Baltic Sea) (Jensen et al., 1999), giving reduced river input to the Black Sea and resulting in a receding shoreline. This is consistent with some evaporative drawdown of the Black Sea and correlates to the evidence of an authigenic aragonite layer present in all the cores studied (Jermannau, 2004). This drawdown is also confirmed by the determination of the forced regression-like reflectors recognized on the dune field mosaics and dated from this period. This lowered sea level in the Black Sea persisted afterward as implied by (1) the continuously dry climatic conditions in the region starting around 13 k.y. B.P. and lasting till 8 k.y. B.P. (large percentages of herbs and steppe elements were described in the cores [Popescu, 2004]), and (2) the dune formation between 9.7 k.y. B.P. and 8.5 k.y. B.P. on the desiccated northwestern Black Sea shelf at –100 m. The Younger Dryas climatic event had lowered the Black Sea water level and the presence of the coastal sand dunes and wave-cut terrace confirmed this lowstand (Fig. 11). Numerous Russian authors (e.g., Ostrovskiy et al., 1977b; Shcherbakov et al., 1978, and 1979; Shimkus et al., 1980) have indicated a sea-level lowstand at about –90 m, based on the location of offshore sand ridges described at the shelf edge south of Crimea. The anastomosed buried fluvial channels described by Popescu et al. (2004), which suddenly disappear below 90 m depth, and a unique wave-cut terrace on the outer shelf, with an upper surface varying between –95 and –100 m, are therefore consistent with a major lowstand level situated somewhere around 100 m deep. Around Viteaz Canyon the paleocoastline was forming a wide gulf in which two rivers were flowing (Fig. 2). Previous studies have proposed a depth of 105 m for this lowstand according to a regional erosional truncation recognized on the southern coast of the Black Sea (Demirbag et al., 1999; Gorur et al., 2001) and also based on evidence from a terrace on the northern shelf edge (Major et al., 2002).

Preservation of these sand dunes and buried small incised valleys can be linked with a rapid transgression during which the ravinement processes related to the water-level rise have no time to sufficiently erode the sea bottom (Benan and Kocurek, 2000; Lericolais et al., 2004). Around 7.5 k.y. B.P., the surface waters of the Black Sea suddenly attained present-day conditions owing to an abrupt flooding of the Black Sea by Mediterranean waters, as shown by dinoflagellate cyst records (Popescu, 2004) and supposed by Ryan et al. (2003, 1997). This can also be related to

the beginning of the sapropel deposit, which was widespread and synchronous across slope and basin floor. Popescu (2004) demonstrated that at 7160 yr B.P. a sudden (<760 yr according to the resolution of their data) inflow of a large volume of marine Mediterranean waters caused an abrupt increase in salinity, which attained the present-day euxinic values. This inflow of marine waters is confirmed by the abrupt replacement of fresh to brackish species by marine species. Furthermore, the model developed by Siddall et al. (2004) shows that ~60,000 m³/s of water must have flowed into the Black Sea basin after the sill broke and it would have taken 33 yr to equalize water levels in the Black Sea and the Sea of Marmara. Such a sudden flood would have preserved lowstand marks on the Black Sea's northwestern shelf.

CONCLUSION

The results presented here confirm that the Holocene climate modifications in the intercontinental setting of Eastern Europe had significant implications for the behavior of the Black Sea water-level fluctuations. Rare preservation of an intact regressional surface, a big drainage basin fed by meltwater from the Fennoscandian ice cap, and the two-way exchange of water through the Bosphorus and Dardanelles Straits are the major consequences resulting from reconnection between the Marmara Sea and the Black Sea. The sand dune fields and associated wave-cut terrace are interpreted as coastal zone relicts that persisted between 9580 and 8585 yr B.P. A wave-cut terrace presently at –100 m and dunes and pans between –80 and –65 m would have lain well below the level of the external ocean (Fairbanks, 1989; Lambeck and Bard, 2000). As the Black Sea moved from an enclosed to a semi-enclosed basin, and as it was the receiving basin of the meltwaters, it is clear that water fluctuation was more directly linked to climate change while the global ocean had a stronger hysteresis. The water issued from the melting of the Fennoscandian ice cap ensuing from the Bølling-Allerød warming was drained to the Black Sea by major European rivers (Dniepr, Dniestr, and Bug) and the Danube drained part of the meltwater from the Alps. The Black Sea, whose brackish water level was under –120 m at that time, rose up to –40 or even –20 m. The onset of the Younger Dryas cool and drier climate favored the regression processed in the Black Sea and the level went down to –100 m as witnessed by the coastal dunes and the anastomosed river system. These conditions prevailed till the water level of the Marmara Sea reached the sill of the Bosphorus, initiating the entrance of marine waters into the Black Sea. The resulting transgression was so rapid that the coastal features were preserved.

A Black Sea lake preserved below global sea level would have needed a Bosphorus barrier shallower than the external ocean. Burial of the dunes and pans by a drape of mud is not sufficient to imply a sudden infilling of the depression once the Bosphorus barrier was breached. But taken with evidence of an abrupt transition from shell hash (the very condensed layer with brackish fauna) to mud, and the impressive preservation of dunes and pans with no preferential infilling of the depression, it seems likely that

the Black Sea experienced a rapid terminal transgression. The Caspian Sea, which seems to have encountered a similar phenomenon, with the exception of the last reconnection, has similar sand dunes as high as 20 m that lie parallel to the seashore and that contain sandy particles and fragments of shells in the coastal regions of Mazandaran and Gilan (Iran). The relict Black Sea dunes are occasionally cut across by wind blows witnessing a lowstand. The Black Sea water-level fluctuations appear to be directly linked to climate variability (Kvasov, 1975; Svitoch et al., 2000). The Black Sea, like other enclosed basins, when not connected to the Mediterranean, reacted by reaching highstand after the melt-water pulses, which were directly connected to the drainage of the Fennoscandian ice cap and lowstand through evaporation in dry periods as was the Younger Dryas in this region (Popescu, 2004). Such behavior is additionally reported for Turkish lakes during the same period, which followed a water-level fluctuation directly linked to climate variability and encountered a drawdown in the Younger Dryas (Fontugne et al., 1999; Kashima, 2003), as did the giant Black Sea lake. In addition, the fresh water provided by the melting of the ice was stopped during the Younger Dryas and the former fresh-water-providing rivers were diverted to the north—the North Sea and the Baltic Sea were free of ice.

ACKNOWLEDGMENTS

Our research was supported by the French ministry of foreign affairs in the context of a bi-lateral collaboration between France and Romania, and was prolonged by a European project of the fifth framework program called ASSEMBLAGE (EVK3-CT-2002-00090). We are grateful to Nicolae Panin, who started and supported the project. We also thank Eliane Le Drezen and Alain Normand for their work in multibeam data processing, Hervé Nouzé and Hervé Gillet for seismic processing, as well as the crew of the vessels *Le Suroît* and *Le Marion Dufresne*. We extend special thanks to Yvon Balut. We also thank William R.F. Ryan and Candace Major for having shared their ideas at the beginning of these oceanic cruises and for their help in the core dating.

REFERENCES CITED

- Aksu, A.E., Abrajano, T., Mudie, P.J., and Yasar, D., 1999a, Organic geochemical and palynological evidence for terrigenous origin of the organic matter in Aegean Sea sapropel S1: *Marine Geology*, v. 153, no. 1–4, p. 303–318, doi: 10.1016/S0025-3227(98)00077-2.
- Aksu, A.E., Hiscott, R.N., and Yasar, D., 1999b, Oscillating Quaternary water levels of the Marmara Sea and vigorous outflow into the Aegean Sea from the Marmara Sea Black Sea drainage corridor: *Marine Geology*, v. 153, no. 1–4, p. 275–302, doi: 10.1016/S0025-3227(98)00078-4.
- Aksu, A.E., Hiscott, R.N., Kaminski, M.A., Mudie, P.J., Gillespie, H., Abrajano, T., and Yasar, D., 2002a, Last glacial-Holocene paleoceanography of the Black Sea and Marmara Sea: Stable isotopic, foraminiferal and coccolith evidence: *Marine Geology*, v. 190, no. 1–2, p. 119–149, doi: 10.1016/S0025-3227(02)00345-6.
- Aksu, A.E., Hiscott, R.N., Mudie, P.J., Rochon, A., Kaminski, M.A., Abrajano, T., and Yasar, D., 2002b, Persistent Holocene outflow from the Black Sea to the eastern Mediterranean contradicts Noah's flood hypothesis: *GSA Today*, v. 12, no. 5, p. 4–10, doi: 10.1130/1052-5173(2002)012<0004:PHOFTB>2.0.CO;2.
- Aksu, A.E., Hiscott, R.N., Yasar, D., Isler, F.I., and Marsh, S., 2002c, Seismic stratigraphy of Late Quaternary deposits from the southwestern Black Sea shelf: Evidence for non-catastrophic variations in sea-level during the last ~10000 yr: *Marine Geology*, v. 190, no. 1–2, p. 61–94, doi: 10.1016/S0025-3227(02)00343-2.
- Algan, O., Çağatay, N., Tchepalyga, A.L., Ongan, D., Eastoe, C., and Gökasan, E., 2001, Stratigraphy of the sediment infill in Bosphorus Strait: Water exchange between the Black and Mediterranean Seas during the last glacial-Holocene: *Geo-Marine Letters*, v. 20, no. 4, p. 209–218, doi: 10.1007/s003670000058.
- Algan, O., Gokasan, E., Gazioglu, C., Yucel, Z.Y., Alpar, B., Guneyso, C., Kirci, E., Demirel, S., Sari, E., and Ongan, D., 2002, A high-resolution seismic study in Sakarya Delta and Submarine Canyon, southern Black Sea shelf: *Continental Shelf Research*, v. 22, no. 10, p. 1511–1527, doi: 10.1016/S0278-4343(02)00012-2.
- Allen, J.R.L., 1982, *Sedimentary Structure: Their Character and Physical Basis*: Amsterdam and New York, Elsevier, 663 p.
- Amorosi, A., Colalongo, M.L., Pasini, G., and Preti, D., 1999, Sedimentary response to Late Quaternary sea-level changes in the Romagna coastal plain (northern Italy): *Sedimentology*, v. 46, no. 1, p. 99–121, doi: 10.1046/j.1365-3091.1999.00205.x.
- Arkhangel'skiy, A.D., and Strakhov, N.M., 1938, Geological structure and history of the evolution of the Black Sea: *Izvestiia Akademii Nauk SSSR. Seriya Khimicheskaya*, v. 10, p. 3–104.
- Ashley, G.M., 1990, Classification of large-scale subaqueous bedforms: A new look at an old problem: *Journal of Sedimentary Petrology*, v. 60, no. 1, p. 160–172.
- Bahr, A., Lamy, F., Arz, H., Kuhlmann, H., and Wefer, G., 2005, Late glacial to Holocene climate and sedimentation history in the NW Black Sea: *Marine Geology*, v. 214, no. 4, p. 309–322, doi: 10.1016/j.margeo.2004.11.013.
- Ballard, R.D., Coleman, D.F., and Rosenberg, G., 2000, Further evidence of abrupt Holocene drowning of the Black Sea shelf: *Marine Geology*, v. 170, no. 3–4, p. 253–261, doi: 10.1016/S0025-3227(00)00108-0.
- Bard, E., Hamelin, B., Fairbanks, R.G., and Zinder, A., 1990, A calibration of the ¹⁴C timescale over the past 30,000 years using mass spectrometric U-Th ages from Barbados corals: *Nature*, v. 345, p. 405–410, doi: 10.1038/345405a0.
- Bard, E., Hamelin, B., Arnold, M., Montaggioni, L., Cabiocch, G., Faure, G., and Rougerie, F., 1996, Deglacial sea-level record from Tahiti corals and the timing of global meltwater discharge: *Nature*, v. 382, no. 6588, p. 241–244, doi: 10.1038/382241a0.
- Benan, C.A.A., and Kocurek, G., 2000, Catastrophic flooding of an aeolian dune field: Jurassic Entrada and Todilto Formations, Ghost Ranch, New Mexico, USA: *Sedimentology*, v. 47, no. 6, p. 1069–1080, doi: 10.1046/j.1365-3091.2000.00341.x.
- Berné, S., 1991, *Architecture et dynamique des dunes tidales: Exemples de la marge atlantique française* [thèse de sciences]: Université de Lille 1, 295 p.
- Berné, S., Auffret, J.-P., and Walker, P., 1988, Internal structure of subtidal sand waves revealed by high-resolution seismic reflection: *Sedimentology*, v. 35, p. 5–20, doi: 10.1111/j.1365-3091.1988.tb00902.x.
- Berné, S., Lericolais, G., Marsset, T., Bourillet, J.-F., and De Batist, M., 1998, Erosional offshore sand ridges and lowstand shorefaces: Examples from tide and wave dominated environments of France: *Journal of Sedimentary Research*, v. 68, no. 4, p. 540–555.
- Calvert, S.E., 1990, Geochemistry and origin of the Holocene sapropel in the Black Sea., in Ittekkot, V., Kempe, S., Michaelis, W., and Spitz, A., eds., *Facets of Modern Biogeochemistry*: Berlin, Federal Republic of Germany, Springer-Verlag, p. 326–352.
- Calvert, S.E., and Fontugne, M.R., 1987, Stable carbon isotopic evidence for the marine origin of the organic matter in the Holocene Black Sea sapropel: *Chemical Geology*, v. 66, no. 3–4, p. 315–322.
- Carter, R.W.G., Hesp, P.A., Nordstrom, K.F., and Psuty, N.P., 1990a, Erosional landforms in coastal dunes, in Nordstrom, K.F., Psuty, N.P., and Carter, R.W.G., eds., *Coastal Dunes: Form and Process*: Chichester, UK, John Wiley & Sons, p. 217–250.
- Carter, R.W.G., Nordstrom, K.F., and Psuty, N.P., 1990b, The study of coastal dunes, in Nordstrom, K.F., Psuty, N.P., and Carter, R.W.G., eds., *Coastal Dunes: Form and Process*: Chichester, UK, John Wiley & Sons, p. 1–14.
- Correggiari, A., Field, M.E., and Trincardi, F., 1996, Late Quaternary transgressive large dunes on the sediment-starved Adriatic shelf, in De Batist, M., and Jacobs, P., eds., *Geology of Siliciclastic Shelf Seas*: Geological Society [London] Special Publication 117, p. 155–169.

- Dalrymple, R.W., 1984, Morphology and internal structure of sand waves in the Bay of Fundy: *Sedimentology*, v. 31, p. 365–382, doi: 10.1111/j.1365-3091.1984.tb00865.x.
- Davidson-Arnott, R.G.D., Law, M.N., and Stone, G.W., 1996, Measurement and prediction of long-term sediment supply to coastal foredunes, in R. W. G. (Bill) Carter memorial edition: *Journal of Coastal Research*, v. 12, no. 3, p. 654–663.
- Degens, E.T., and Ross, D.A., 1974, *The Black Sea—Geology, Chemistry and Biology*: Tulsa, Oklahoma, American Association of Petroleum Geologists, 633 p.
- Demirbag, E., Gökasan, E., Oktay, F.Y., Simsek, M., and Yüce, H., 1999, The last sea level changes in the Black Sea: Evidence from the seismic data: *Marine Geology*, v. 157, no. 3–4, p. 249–265, doi: 10.1016/S0025-3227(98)00158-3.
- Dimitrov, P.S., 1982, Radiocarbon datings of bottom sediments from the Bulgarian Black Sea Shelf: *Bulgarian Academy of Sciences Oceanology*, v. 9, p. 45–53.
- Dinu, C., Wong, H.K., and Tambrea, D., 2002, Stratigraphic and tectonic syntheses of the Romanian Black Sea shelf and correlation with major land structures, in Dinu, C., and Monacu, V., eds., *Geology and Tectonics of the Romanian Black Sea Shelf and Its Hydrocarbon Potential*: Bucharest, Bucharest Geoscience Forum, p. 101–117.
- Dinu, C., Wong, H.K., Tambrea, D., and Matenco, L., 2005, Stratigraphic and structural characteristics of the Romanian Black Sea shelf: *Tectonophysics*, v. 410, no. 1–4, p. 417–435, doi: 10.1016/j.tecto.2005.04.012.
- Evsylekov, Y.D., and Shimkus, K.M., 1995, Geomorphological and neotectonic development of outer part of continental margin to the south of Kerch Strait: *Oceanology (Moscow)*, v. 35, p. 623–628.
- Fairbanks, R.G., 1989, A 17,000-year glacio-eustatic sea level record: Influence of glacial melting rates on the Younger Dryas event and deep-ocean circulation: *Nature*, v. 342, no. 6250, p. 637–642, doi: 10.1038/342637a0.
- Federov, P.V., 1971, Postglacial transgression of the Black Sea: *International Geology Review*, v. 14, no. 2, p. 160–164.
- Flemming, B.W., 1988, Pseudo-tidal sedimentation in a non-tidal shelf environment (Southeast African continental margin), in de Boer, P.L. de., Gelder, A. van, and Nio, S.D., eds., *Tide-Influenced Sedimentary Environments and Facies*: Dordrecht, Netherlands, D. Reidel Publishing Co., p. 167–180.
- Fontugne, M.R., Arnold, M., Labeyrie, L., Paterne, M., Calvert, S.E., and Duplessy, J.-C., 1994, Paleoenvironment, sapropel chronology, and Nile river discharge during the last 20,000 years as indicated by deep-sea sediment records in the eastern Mediterranean: *Radiocarbon*, v. 34, p. 75–88.
- Fontugne, M.R., Kuzucuoglu, C., Karabiyikoglu, M., Hatte, C., and Pastre, J.-F., 1999, From Pleniglacial to Holocene: A ¹⁴C chronostratigraphy of environmental changes in the Konya Plain, Turkey: *Quaternary Science Reviews*, v. 18, no. 4–5, p. 573–591, doi: 10.1016/S0277-3791(98)90098-1.
- Fryberger, S.G., Dean, G., and McKee, E.D., 1979, *Dune Forms and Wind Regime: A Study of Global Sand Seas*: Reston, Virginia, U.S. Geological Survey.
- Fryberger, S.G., Al Sari, A.M., and Clisham, T.J., 1983, Eolian dune, interdune, sand sheet, and siliciclastic sabkha sediments of an offshore prograding sand sea, Dhahran area, Saudi Arabia: *American Association of Petroleum Geologists Bulletin*, v. 67, no. 2, p. 280–312.
- Giles, P.T., McCann, S.B., and Wolfe, S., 1997, Fore-dune development on Iles de la Madeleine (Quebec), Atlantic Canada, in Wolfe, S., ed., *Eolian processes in supply-limited and nondesert environments—Processus éoliens dans les milieux non-désertiques et d'alimentation entravée*: *Canadian Journal of Earth Sciences—Journal Canadien des Sciences de la Terre*, v. 34, no. 11, p. 1467–1476.
- Gökasan, E., Demirbag, E., Oktay, F.Y., Ecevitoglu, B., Simsek, M., and Yüce, H., 1997, On the origin of the Bosphorus: *Marine Geology*, v. 140, no. 1–2, p. 183–199, doi: 10.1016/S0025-3227(97)0022-4.
- Gorur, N., Çagatay, M.N., Emre, O., Alpar, B., Saking, M., Islamoglu, Y., Algan, O., Erkal, T., Kecer, M., Akkok, R., and Karlik, G., 2001, Is the abrupt drowning of the Black Sea shelf at 7150 yr BP a myth?: *Marine Geology*, v. 176, no. 1–4, p. 65–73, doi: 10.1016/S0025-3227(01)00148-7.
- Grosswald, M.G., 1980, Late Weichselian ice sheet of northern Eurasia: *Quaternary Research*, v. 13, no. 1, p. 1–32, doi: 10.1016/0033-5894(80)90080-0.
- Hodder, I., 1990, *The Domestication of Europe: Structure and Contingency in Neolithic Societies (Social Archaeology)*: Oxford, Blackwell Publishers, 331 p.
- Jensen, J.B., Bennike, O., Witkowski, A., Lemke, W., and Kuijpers, A., 1999, Early Holocene history of the southwestern Baltic Sea: The Ancylus Lake stage: *Boreas*, v. 28, no. 4, p. 437–453, doi: 10.1080/030094899421966.
- Jermannaud, P., 2004, *Etude sédimentologique et sismique des dépôts quaternaires de l'éventail profond du Danube [master 2 thesis]*: Université de Bordeaux 1, 50 p.
- Kashima, K., 2003, The quantitative reconstruction of salinity changes using diatom assemblages in inland saline lakes in the central part of Turkey during the Late Quaternary: *Quaternary International*, v. 105, no. 1, p. 13–19, doi: 10.1016/S1040-6182(02)00145-3.
- Kenyon, N.H., and Stride, A.H., 1968, The crest length and sinuosity of some marine sand waves: *Journal of Sedimentary Petrology*, v. 38, p. 255–259.
- Kostaschuk, R.A., and Villard, P., 1996, Flow and sediment transport over large subaqueous dunes: Fraser River, Canada: *Sedimentology*, v. 43, no. 5, p. 849–863, doi: 10.1111/j.1365-3091.1996.tb01506.x.
- Kuprin, P.N., Scherbakov, F.A., and Morgunov, I.I., 1974, Correlation, age, and distribution of the postglacial continental terrace sediments of the Black Sea: *Baltica*, v. 5, p. 241–249.
- Kvasov, D.D., 1975, *Late Quaternary History of Major Lakes and Inland Seas of Eastern Europe*: Leningrad, Nauka Press.
- Kvasov, D.D., and Blazhchishin, A.I., 1978, The key to sources of the Pliocene and Pleistocene glaciation is at the bottom of the Barents Sea: *Nature*, v. 273, no. 5658, p. 138–140, doi: 10.1038/273138a0.
- Laity, J.E., 1994, Landforms of aeolian erosion, in Abrahams, A.D., and Parsons, A.J., eds., *Geomorphology of Desert Environments*: London, Chapman and Hall, p. 506–535.
- Lambeck, K., and Bard, E., 2000, Sea-level change along the French Mediterranean coast for the past 30 000 years: *Earth and Planetary Science Letters*, v. 175, p. 203–222, doi: 10.1016/S0012-821X(99)00289-7.
- Lancaster, N., 1998, Dune morphology, chronology and Quaternary climate change, in Alsharan, A., Glennie, K.W., Wintle, G.L., and Kendall, C.G.S., eds., *Quaternary Deserts and Climate Change*: Rotterdam, Netherlands, Balkema, p. 339–350.
- Lancaster, N., Nickling, W.G., Wyatt, V.E., and McKenna Neuman, C.K., 1994, Sediment flux and airflow on the stoss slope of aeolian dunes: *Eos (Transactions, American Geophysical Union)*, v. 75, no. 44, p. 302.
- Lane-Serff, G.F., Rohling, E.J., Bryden, H.L., and Charnock, H., 1997, Post-glacial connection of the Black Sea to the Mediterranean and its relation to the timing of sapropel formation: *Paleoceanography*, v. 12, no. 2, p. 169–174, doi: 10.1029/96PA03934.
- Lericolais, G., Berné, S., and Feniès, H., 2001, Seaward pinching out and internal stratigraphy of the Gironde incised valley on the shelf (Bay of Biscay): *Marine Geology*, v. 175, no. 1–4, p. 183–197.
- Lericolais, G., Popescu, I., Panin, N., Guichard, F., Popescu, S.M., and Manolakakis, L., 2003, Could the last rapid sea level rise of the Black Sea evidence by oceanographic surveys have been interpreted by mankind?, in *CIESM Workshop Monographs*, vol. 24, 22–25 October, Fira, Santorini, Greece, p. 44–53.
- Lericolais, G., Chivas, A.R., Chiocci, F.L., Uscinowicz, S., Jom, B.J., Lemke, W., and Violante, R.A., 2004, Rapid transgressions into semi-enclosed basins since the Last Glacial Maximum, in 32nd International Geological Correlation Program Florence 2004, Florence, p. Session 249: T05.03—Continental shelves during the last glacial cycle 249–4.
- Lericolais, G., Popescu, I., Guichard, F., Popescu, S.M., and Manolakakis, L., 2007, Water-level fluctuations in the Black Sea since the Last Glacial Maximum, in Yanko-Hombach, V., Gilbert, A.S., Panin, N., and Dolukhanov, P.M., eds., *The Black Sea Flood Question: Changes in Coastline, Climate, and Human Settlement*: New York: Springer-Verlag, p. 437–452.
- Major, C.O., 1994, *Late Quaternary sedimentation in the Kerch area of the Black Sea shelf: Response to sea level fluctuation [B.A. thesis]*: Middletown, Connecticut, Wesleyan University, 116 p.
- Major, C.O., 2002, *Non-eustatic controls on sea-level change in semi-enclosed basin [Ph.D. thesis]*: New York, Columbia University, 223 p.
- Major, C.O., Ryan, W.B.F., Lericolais, G., and Hajdas, I., 2002, Constraints on Black Sea outflow to the Sea of Marmara during the last glacial-interglacial transition: *Marine Geology*, v. 190, no. 1–2, p. 19–34, doi: 10.1016/S0025-3227(02)00340-7.
- McCave, I.N., 1971, Sand waves in the North Sea off the coast of Holland: *Marine Geology*, v. 10, p. 199–225, doi: 10.1016/0025-3227(71)90063-6.
- McKee, E.D., 1979, *Sedimentary structures in dunes: A study of global sand seas*: Reston, Virginia, U.S. Geological Survey.

- Meldahl, K.H., 1995, Pleistocene shoreline ridges from tide-dominated and wave-dominated coasts: Northern Gulf of California and western Baja California, Mexico: *Marine Geology*, v. 123, no. 1–2, p. 61–72, doi: 10.1016/0025-3227(95)80004-U.
- Muramoto, J.A., Honjo, S., Fry, B., Hay, B.J., Howarth, R.W., Cisne, J.L., and Murray, J.W., 1991, Sulfur, iron and organic carbon fluxes in the Black Sea: Sulfur isotopic evidence for origin of sulfur fluxes, *in* Black Sea oceanography: Results from the 1988 Black Sea Expedition: Deep-Sea Research, v. Part A: Oceanographic Research Papers, vol. 38, suppl. 2A, p. 1151–1187.
- Neveeskaja, L.A., 1965, Late Quaternary bivalve mollusks of the Black Sea: Their systematics and ecology: *Akademy Nauk USSR Paleontology Institute Trudi*, v. 105, p. 1–390.
- Neveeskaja, L.A., and Neveeskiy, Y.N., 1961, Relationship between the Karangat and Neoeuxine beds in littoral regions of Black Sea: *Akad. Nauk USSR Doklady*, v. 137, no. 4, p. 934–937.
- Ostrovskiy, A.B., Izmaylov, Y.A., Balabanov, I.P., Skiba, S.I., Skryabina, N.G., Arslanov, S.A., Gey, N.A., and Suprunova, N.I., 1977a, New data on the paleohydrological regime of the Black Sea in the Upper Pleistocene and Holocene, *in* Kaplin, P.A., and Shcherbakov, F.A., eds., *Paleogeography and Deposits of the Pleistocene of the Southern Seas of the USSR*: Moscow, Nauka Press, p. 131–141.
- Ostrovskiy, A.B., Sccheglo, A.P., Arslanov, S.A., and Shchelinskiy, V.Y., 1977b, New data on the stratigraphy and geochronology of Pleistocene marine terraces of the Black Sea coast, Caucasus, and Kerch-Taman region, *in* Kaplin, P.A., and Shcherbakov, F.A., eds., *Paleogeography and Deposits of the Pleistocene of the Southern Seas of the USSR*: Moscow, Nauka Press, p. 61–99.
- Otvos, E.G., 2000, Beach ridges—Definitions and significance: *Geomorphology*, v. 32, p. 83–108, doi: 10.1016/S0169-555X(99)00075-6.
- Panin, N., 1997, On the geomorphologic and geologic evolution of the river Danube: Black Sea interaction zone: *Geo-Eco-Marina*, v. 2, p. 31–40.
- Popescu, I., 2002, Analyse des processus sédimentaires récents dans l'éventail profond du Danube (mer Noire) [Ph.D. thesis]: Brest, Université de Bretagne Occidentale—Université de Bucarest, 282 p.
- Popescu, I., Lericolais, G., Panin, N., Wong, H.K., and Droz, L., 2001, Late Quaternary channel avulsions on the Danube deep-sea fan: *Marine Geology*, v. 179, no. 1–2, p. 25–37, doi: 10.1016/S0025-3227(01)00197-9.
- Popescu, I., Lericolais, G., Panin, N., Normand, A., Dinu, C., and Le Drezen, E., 2004, The Danube Submarine Canyon (Black Sea): Morphology and sedimentary processes: *Marine Geology*, v. 206, no. 1–4, p. 249–265, doi: 10.1016/j.margeo.2004.03.003.
- Popescu, S.M., 2004, Sea-level changes in the Black Sea region since 14 ka BP, *in* 32nd International Geological Correlation Program Florence 2004, Florence, p. Session: T34.02—Sea-level change since the last glacial maximum.
- Posamentier, H.W., and Vail, P.R., 1988, Eustatic controls on clastic deposition II—Sequence and systems tracts models, *in* Wilgus, C.K., Hastings, B.S., Kendall, H.W., Posamentier, H.W., Ross, C.A., and Van Wagoner, J.C., eds., *Sea-level Changes—An Integrated Approach*: Society of Economic Paleontologists and Mineralogists: Tulsa, Oklahoma, Barbara H. Lidz, p. 125–154.
- Posamentier, H.W., Allen, G.P., James, D.P., and Tesson, M., 1992, Forced regressions in a sequence stratigraphic framework: Concepts, examples, and exploration significance: *American Association of Petroleum Geologists Bulletin*, v. 76, no. 11, p. 1687–1709.
- Pye, K., 1993, Late Quaternary development of coastal parabolic megadune complexes in northeastern Australia, *in* Pye, K., and Lancaster, N., eds., *Aeolian Sediments; Modern and Ancient*: Special Publication of the International Association of Sedimentologists: Oxford, Blackwell Scientific Publications, p. 23–44.
- Rohling, E.J., 1994, Review and new aspects concerning the formation of eastern Mediterranean sapropels: *Marine Geology*, v. 122, no. 1–2, p. 1–28, doi: 10.1016/0025-3227(94)90202-X.
- Rohling, E.J., and de Rijk, S., 1999, Holocene Climate Optimum and Last Glacial Maximum in the Mediterranean: The marine oxygen isotope record: *Marine Geology*, v. 153, no. 1–4, p. 57–75, doi: 10.1016/S0025-3227(98)00020-6.
- Ross, D.A., Degens, E.T., and MacIrvine, J., 1970, Black Sea: Recent sedimentary history: *Science*, v. 170, no. 9, p. 163–165.
- Roy, P.S., Cowell, P.J., Ferland, M.A., Thom, B.G., Carter, R.W.G., and Woodroffe, C.D., 1994, Wave-dominated coasts, *in* Carter, R.W.G., and Woodroffe, C.D., eds., *Coastal Evolution: Late Quaternary Shoreline Morphodynamics*: Cambridge, UK, Cambridge University Press, p. 121–186.
- Ryan, W.B.F., and Pitman, W.C., III, 1999, Noah's Flood: The New Scientific Discoveries about the Event That Changed History: New York, Simon and Schuster, 319 p.
- Ryan, W.B.F., Pitman, W.C., III, Major, C.O., Shimkus, K.M., Moskalenko, V., Jones, G.A., Dimitrov, P.S., Gorür, G., Saking, M., and Yüce, H., 1997, An abrupt drowning of the Black Sea shelf: *Marine Geology*, v. 138, no. 1–2, p. 119–126, doi: 10.1016/S0025-3227(97)00007-8.
- Ryan, W.B.F., Major, C.O., Lericolais, G., and Goldstein, S.L., 2003, Catastrophic flooding of the Black Sea: *Annual Review of Earth and Planetary Sciences*, v. 31, no. 1, p. 525–554, doi: 10.1146/annurev.earth.31.100901.141249.
- Scholten, R., 1974, Role of the Bosphorus in Black Sea chemistry and sedimentation, *in* Degens, E.T., and Ross, D.A., eds., *The Black Sea: Geology, Chemistry, and Biology*: Tulsa, Oklahoma, American Association of Petroleum Geologists, p. 115–126.
- Shaw, P.A., and Thomas, D.S.G., 1997, Pans, playas and salt lakes, *in* Thomas, D.S.G., ed., *Arid Zone Geomorphology: Process, Form and Change in Drylands*: New York, John Wiley & Sons, p. 293–317.
- Shcherbakov, F.A., and Babak, Y.V., 1979, Stratigraphic subdivision of the Neoeuxinian deposits in the Black Sea: *Oceanology (Moscow)*, v. 19, no. 3, p. 298–300.
- Shcherbakov, F.A., Kuprin, P.N., Potapova, L.I., Polyakov, A.S., Zabelina, E.K., and Sorokin, V.M., 1978, Sedimentation on the Continental Shelf of the Black Sea: Moscow, Nauka Press, 211 p.
- Shimkus, K.M., Evsyukov, Y.D., and Solovjeva, R.N., 1980, Submarine terraces of the lower shelf zone and their nature, *in* Malovitsky, Y.P., and Shimkus, K.M., eds., *Geological and Geophysical Studies of the Pre-Oceanic Zone*: Moscow, Petr Petrovich Shirshov Institute of Oceanology of the Russian Academy of Sciences, USSR, p. 81–92.
- Shopov, V., Chochov, S., and Georgiev, V., 1986, Lithostratigraphy of Upper Quaternary sediments from the northwestern Black Sea shelf between the parallels of the Cape Emine and Danube River mouth: *Geologica Balcanica*, v. 16, no. 6, p. 99–112.
- Siddall, M., Pratt, L.J., Helfrich, K.R., and Giosan, L., 2004, Testing the physical oceanographic implications of the suggested sudden Black Sea infill 8400 years ago: *Paleoceanography*, v. 19, no. PA1024, p. 1–11, doi: 10.1029/2003PA000903.
- Snedden, J.W., and Bergman, K.M., 1999, Isolated shallow marine sand bodies; deposits for all interpretations, *in* Bergman, K.M., and Snedden, J.W., eds., *Isolated Shallow Marine Sand Bodies; Sequence Stratigraphic Analysis and Sedimentologic Interpretation*: Society for Sedimentary Geology Special Publication 64, p. 1–11.
- Stanley, D.J., 1996, Nile delta: Extreme case of sediment entrapment on a delta plain and consequent coastal land loss: *Marine Geology*, v. 129, no. 3–4, p. 189–195, doi: 10.1016/0025-3227(96)83344-5.
- Svitoch, A.A., Selivanov, A.O., and Yanina, T.A., 2000, Paleohydrology of the Black Sea Pleistocene Basins: *Water Resources*, v. 27, no. 6, p. 594–603, doi: 10.1023/A:1026661801941.
- Swift, D.J.P., and Field, M.E., 1981, Evolution of a classic sand ridge field: Maryland sector, North American inner shelf: *Sedimentology*, v. 28, p. 461–482, doi: 10.1111/j.1365-3091.1981.tb01695.x.
- Swift, D.J.P., and Freeland, G.L., 1978, Current lineations and sand waves on the inner shelf, Middle Atlantic Bight of North America: *Journal of Sedimentary Petrology*, v. 48, no. 4, p. 1257–1266.
- Talling, P.J., 2000, Self-organization of river networks to threshold states: *Water Resources Research*, v. 36, no. 4, p. 1119–1128, doi: 10.1029/1999WR900339.
- Tchepalyga, A.L., 1984, Inland sea basins, *in* Velichko, A.A., Wright, H.E.J., and Barnosky, C.W., eds., *Late Quaternary Environments of the Soviet Union*: Minneapolis, Minnesota, University of Minnesota Press, p. 229–247.
- Terwindt, J.H.J., and Brouwer, M.J.N., 1986, The behaviour of intertidal sand waves during neap-spring tide cycles and the relevance for paleoflow reconstructions: *Sedimentology*, v. 33, p. 1–31, doi: 10.1111/j.1365-3091.1986.tb00742.x.
- Thom, B.G., and Hall, W., 1991, Behaviour of beach profiles during accretion and erosion dominated periods: *Earth Surface Processes and Landforms*, v. 16, no. 2, p. 113–127.
- Thomas, D.S.G., 1997, *Arid Zone Geomorphology: Process, Form and Change in Drylands*: New York, John Wiley & Sons, 732 p.

- Wang, X., Dong, Z., Zhang, J., and Chen, G., 2002, Geomorphology of sand dunes in the Northeast Taklimakan Desert: *Geomorphology*, v. 42, no. 3–4, p. 183–195, doi: 10.1016/S0169-555X(01)00085-X.
- Wattus, N.J., and Rausch, D.E., 2001, A preliminary survey of relict shoreface-attached sand ridges in Western Lake Superior: *Marine Geology*, v. 179, no. 3–4, p. 163–177, doi: 10.1016/S0025-3227(01)00221-3.
- Wescott, W.A., 1993, Geomorphic thresholds and complex response of fluvial systems: Some implications for sequence stratigraphy: *American Association of Petroleum Geologists Bulletin*, v. 77, no. 7, p. 1208–1218.
- Wilson, I.G., 1972, Aeolian bedforms—Their development and origins: *Sedimentology*, v. 19, no. 3–4, p. 173–210, doi: 10.1111/j.1365-3091.1972.tb00020.x.
- Winguth, C., Wong, H.K., Panin, N., Dinu, C., Georgescu, P., Ungureanu, G., Krugliakov, V.V., and Podshuveit, V., 2000, Upper Quaternary water level history and sedimentation in the northwestern Black Sea: *Marine Geology*, v. 167, no. 1–2, p. 127–146, doi: 10.1016/S0025-3227(00)00024-4.
- Wong, H.K., Winguth, C., Panin, N., Dinu, C., Wollschläger, M., Ungureanu, G., and Podshuveit, V., 1997, The Danube and Dniepr fans, morphostructure and evolution: *GeoEcoMarina*, v. 2, p. 77–102.
- Yanko, V., 1990, Stratigraphy and paleogeography of Marine Pleistocene and Holocene deposits of the Southern Seas of the USSR: *Memorie Società Geologica Italiana*, v. 44, p. 167–187.

WATER-LEVEL FLUCTUATIONS IN THE BLACK SEA SINCE THE LAST GLACIAL MAXIMUM

Gilles Lericolais¹, Irina Popescu², François Guichard³, Speranta-Maria Popescu⁴, Laurence Manolakakis⁵

¹ IFREMER (Institut Français de Recherche pour l'Exploitation de la Mer), Centre de Brest, BP 70, F29200 Plouzané cedex, France

² RCMG (Renard Centre of Marine Geology), Department of Geology and Soil Science, University of Ghent, Ghent, Belgium

³ LSCE (Laboratoire des Sciences du Climat et de l'Environnement), CNRS-CEA, Avenue de la Terrasse, BP 1, F 91198, Gif-sur-Yvette cedex, France

⁴ Centre de Paléontologie Stratigraphique et Paléoécologie, Université Claude Bernard – Lyon 1, 43, blvd du 11 Novembre 1918, F69622 Villeurbanne cedex, France

⁵ UMR (Unité Mixte de Recherche) 7041 CNRS, Equipe Protohistoire européenne, 21 Allée de l'Université, F92023 Nanterre cedex, France

Abstract:

Two IFREMER oceanographic surveys carried out in the northwestern Black Sea in 1998 and 2002 complement previous seabed mapping and subsurface sampling by various international expeditions. They show that the lake level rose on the continental shelf to at least the –40 to –30 m isobath based on the landward limit of a *Dreissena* layer representative of very low salinity conditions (< 5‰). The Black Sea then shows clear evidence for an onset of marine conditions at 7150 BP. From these observations, Ryan *et al.* (1997) concluded that the Black Sea could have filled abruptly with saltwater cascading in from the Mediterranean. Despite critical discussions of this interpretation, recent IFREMER discoveries of well preserved drowned beaches, sand dunes, and soils appear to lend support to the flood hypothesis. This new evidence includes (1) multibeam echo-sounding and seismic reflection profiles that reveal wave-cut terraces at about –100 m, (2) Romanian shelf cores that show an erosion surface indicating subaerial exposure well below the sill of the modern Bosphorus, (3) ¹⁴C ages documenting a colonization of the former terrestrial shelf surface by marine molluscs at 7150 BP, (4) evidence of sea water penetration into the Black Sea in the form of recent canyon heads at the Bosphorus outlet, and (5) palynological analysis and

dinocyst studies that pinpoint the arrival of freshwater during the Younger Dryas and, later, the rapid replacement of Black Sea dinocysts by a Mediterranean population.

Keywords : Rapid transgression, Younger Dryas, Seismic stratigraphy, multibeam geomorphology, Bosphorus outlet, Black Sea continental shelf

1. INTRODUCTION

In 1997, Ryan and Pitman (Ryan *et al.* 1997) presented astonishing evidence supporting a catastrophic flooding of the Black Sea basin about 7500 years ago and speculated on the role it may have played in the spread of early farming into Europe and much of Asia. Their book, *Noah's Flood: The New Scientific Discoveries About The Event That Changed History* (Ryan and Pitman 1998), proposed that the Black Sea flood could have cast such a long shadow over succeeding cultures that it inspired the deluge account in the Babylonian Epic of Gilgamesh and, in turn, the story of Noah in the Book of Genesis.

This hypothesis resulted from a joint Russian-American expedition conducted in 1993 on the continental shelf south of the Kerch Strait (Major 1994; Ryan *et al.* 1997). High-resolution seismic reflection profiles, cores precisely targeted on these profiles, and ^{14}C accelerator mass spectrometry (AMS) dating of recovered fauna permitted several conclusions. The survey revealed a buried erosional surface strewn with shell gravel that extended across the broad continental margin of the northern Black Sea and beyond the shelf break (Evsylekov and Shimkus 1995; Major 1994). The cores revealed evidence of subaerial mud cracks at 99 m beneath the sea surface, algal remains at 110 m, and *in situ* roots of shrubs in desiccated mud at ~123 m. Each site lay well below the 70 m depth of the Bosphorus bedrock sill (Alpar 2001; Göktaşan *et al.* 1997).

The combined evidence suggested to the research team that a drowning event in the Pontic basin may have resulted from a marine transgression into a vastly shrunken lake. It appeared that this inundation subsequently deposited a uniform drape of marine mud upon the former terrestrial surface, creating a sapropel layer equally thick in depressions as on crests of dunes, and with no sign of landward-directed onlap of the sedimentary layers in the drape (Ryan *et al.* 2003). The ^{14}C age determinations documented a simultaneous subaqueous colonization of the terrestrial surface by marine molluscs at 7100 BP,¹ and this date was assigned to the flooding event.

The previous shrunken lake stage and subsequent flooding preclude the possibility of outflow to the Sea of Marmara at that time. Recently, however, Aksu *et al.* (2002c) presented arguments for persistent Holocene outflow from the Black Sea to the eastern Mediterranean and for non-catastrophic variations in the level of the Black Sea during the last 10,000 years (Aksu *et al.* 2002a).

These findings are in direct contradiction to the flood hypothesis.

In 1998 and 2002, two Black Sea projects, one European and the other more broadly international, enabled IFREMER to conduct two oceanographic surveys that afforded the opportunity to complete work previously begun on seabed mapping and subsurface sampling. The main objectives of these cruises were to prepare for the European ASSEMBLAGE Project, which would assess Black Sea sedimentation since the Last Glacial Maximum (LGM), quantify the impacts of climate change, and evaluate the sensitivity of the Black Sea system to external forcing. Progress in resolving these major issues can be achieved only through examination of geomorphology and stratigraphy from the shelf to the abyssal deep in the northwestern corner of the Black Sea.

These surveys revealed that lake level in the Pontic basin rose on the shelf to at least the -40 to -30 m isobath, which corresponds to the landward limit of a layer containing the shelly debris of *Dreissena rostriformis distincta*, a mollusc indicative of freshwater conditions. This rise in freshwater suggests that the lake which preceded the formation of the Black Sea served as an important catchment for meltwater draining out of the Fennoscandian ice cap: Melt Water Pulse 1A during the Bölling-Allerød interval (Bard *et al.* 1990). Possibly, the lake level at this time broke over the sill of its outlet and spilled into the Mediterranean through the Marmara Sea, however, the onset of salt water conditions creating the Black Sea during the mid-Holocene (7150 BP) has been clearly demonstrated. Although opposing hypotheses have been proposed (Aksu *et al.* 1999b, 2002a, b, c), recent discoveries of well preserved drowned beaches, sand dunes, and soils provide new evidence supporting the Ryan and Pitman flood hypothesis.

2. GEOLOGICAL BACKGROUND

The Black Sea is a 2.2 km deep basin with a wide continental shelf in its northwestern corner (Figure 1). External connection to the Mediterranean Sea is over a sill within the Bosphorus Strait. The role played by this strait in controlling the salinity and stratification of both seas as well as the production of anoxia in the Black Sea has been often discussed (Arkhangel'sky and Strakhov 1938; Scholten 1974; Muramoto *et al.* 1991; Rohling 1994; Lane-Saunders 1997; Abrajano *et al.* 2002). The general view is that during periods of low global sea level, the connection between the Black Sea and the ocean was severed. The Black Sea then freshened as a result of continued river discharge, expanding into a vast, well ventilated lake with a shoreline established at the level of its outlet (Chepalyga 1984; Hodder 1990), from which excess water was exported to the Mediterranean.

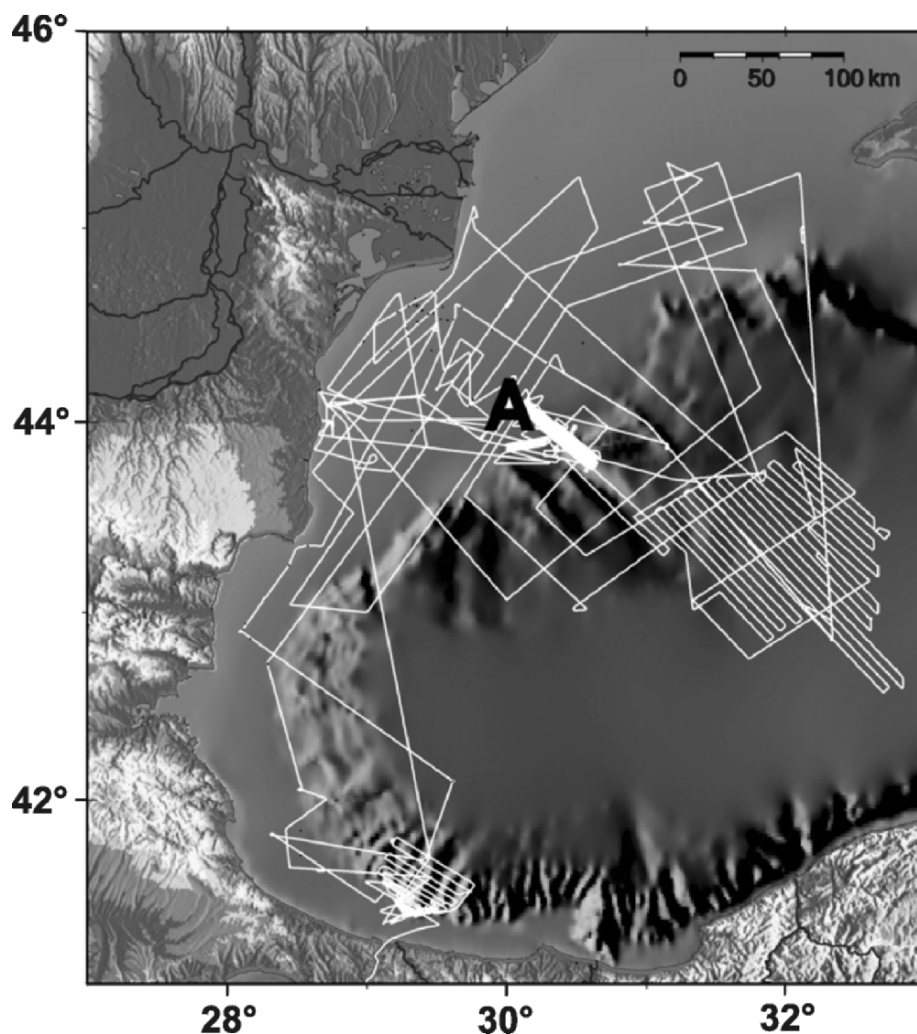


Figure 1. Bathymetry of the semi-enclosed Black Sea basin and IFREMER survey route locations. “A” represents location depicted in Figure 3.

The largest European rivers, the Danube, Dnieper, and Dniester, deliver their water and deposit their sediment loads into the northwestern Black Sea. The Danube drainage basin, 817,000 km² in areal extent, charges the Black Sea at an estimated rate of 6047 m³/s (almost 190 km³/yr), while the river’s sediment discharge at its mouth was about 51.7 million tons per year (t/yr) before the river was dammed in 1970 and 1983 (Bondar 1998). Estimates of total sediment discharge subsequent to damming average less than 30–35 million t/yr, of which only 4–6 million t/yr is sandy material (Panin 1997). During glacial lowstands, and especially at the beginning of interglacials, sediment discharge from these

rivers was probably much higher.

It has long been recognized that the Black Sea became isolated from the Marmara and Mediterranean Seas during glacial intervals when the world ocean level fell below the Bosphorus sill depth (–35 m). It has also been postulated that water level in the Black Sea began to rise in step with that of the Marmara and Mediterranean Seas during times when the level of the world ocean had risen above the Bosphorus sill depth (Degens and Ross 1974). Recent sediment analyses along the margins of the Black Sea suggest, however, that water-level fluctuations in the Pontic basin were somewhat more complex, with high lake levels occurring during the wet intervals of late glacial stages and low lake levels occurring during the drier intervals of early interglacials (Chepalyga 1984).

Another widely accepted hypothesis postulates that the Black Sea had always maintained a continuous outflow through the Bosphorus and Dardanelles Straits, even during highly arid glacial intervals (Chepalyga 1984; Kvasov and Blazhchishin 1978). This perspective essentially assumes that precipitation and river input into the Pontic basin always exceeded loss from local evaporation. Indeed, meltwater from the former ice sheets in Fennoscandia, northern Asia (Grosswald 1980), and the central Alps transformed the Black Sea into a giant freshwater lake a number of times during the past (Federov 1971; Ross *et al.* 1970), most recently during the Late Pleistocene Neoeuxinian stage of the LGM, between 25–18 ky BP (Arkhangel'sky and Strakhov 1938; Nevevskaya and Nevevsky 1961; Nevevskaya 1965; Ross *et al.* 1970; Fedorov 1971).

Ryan *et al.* (1997) published evidence suggesting that the Black Sea became a giant freshwater lake during the LGM. This evidence included new AMS ^{14}C dates, abrupt changes in the organic carbon content, water content, and $\delta^{18}\text{O}$ from core material dated approximately 7150 BP, as well as the occurrence of a widespread unconformity interpreted as an erosional surface subaerially exposed during the last glacial. The distribution of recorded depths for this unconformity implies that the surface of the freshwater lake must have fallen to levels greater than 100 m below its outlet. Ryan *et al.* (1997) inferred from this that, by about 7150 BP, the sill depth of the Bosphorus was breached by the rising world ocean, and a catastrophic flooding of the continental shelf of the Black Sea occurred (Figure 2).

Evidence that does not support the catastrophic flood hypothesis includes variously aged sapropels sampled from the eastern Mediterranean and the Black Sea. Sapropel S1 in the Aegean is generally thought to have been deposited between about 8000 and 5500 BP (Aksu *et al.* 1999a, b; Fontugne *et al.* 1994), although deposition may have lasted until 5300 BP (Rohling and de Rijk 1999). Aksu *et al.* (1999a) suggest that during this time, nutrient-rich freshwater from the Black Sea reduced the surface salinity of the eastern Mediterranean, thereby increasing the stability between the surface and deep waters and decreasing deep circulation. As a result, high surface productivity and restricted

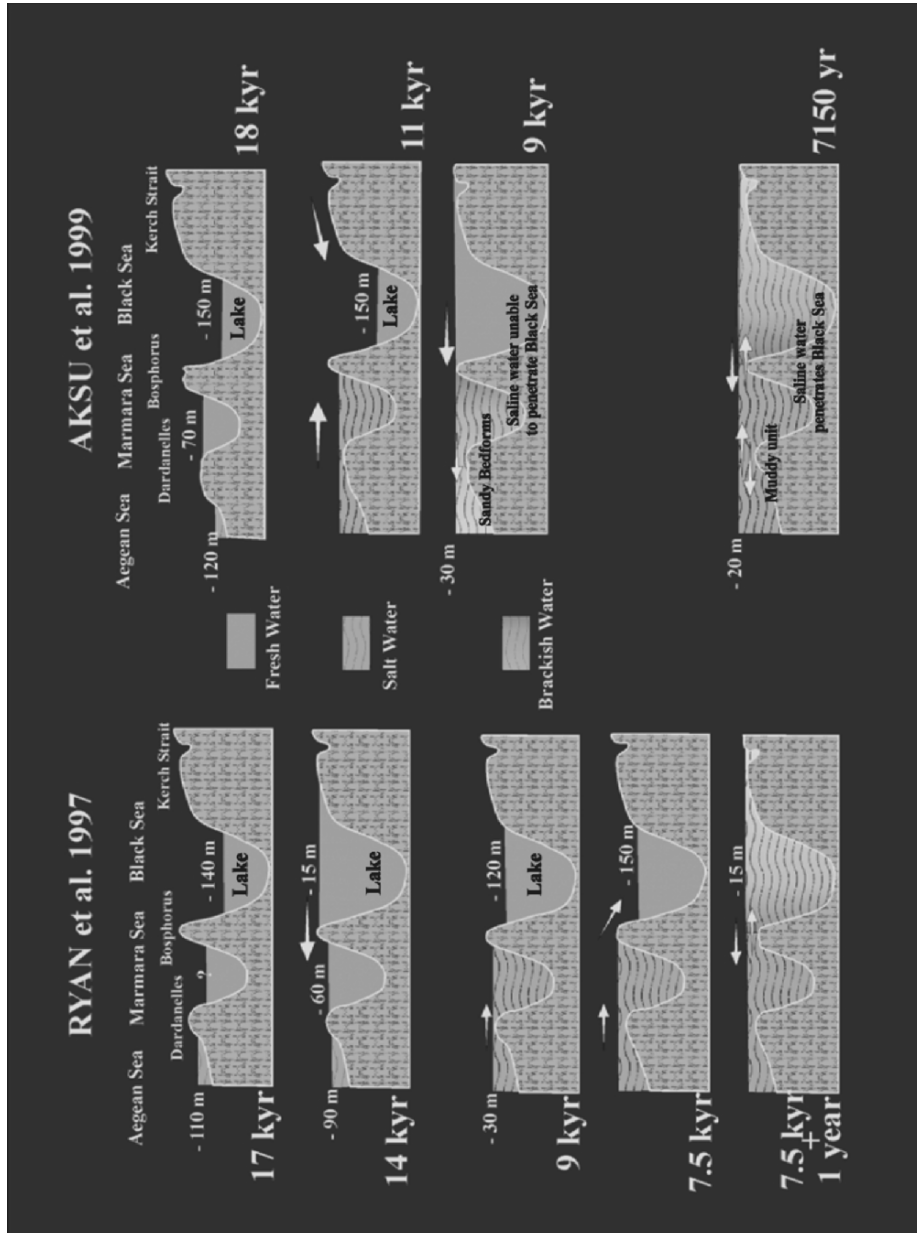


Figure 2. Alternative schemes of reconnection between the Black and Mediterranean Seas.

circulation provided conditions favorable for sapropel formation. Rohling (1994), however, suggests that sapropel formation in the Black Sea started about 550 years later than it did in the eastern Mediterranean, when denser water from the Mediterranean, upon entering the Pontic basin, displaced the nutrient-rich waters in the Black Sea upward toward the surface (Calvert 1990; Calvert and Fontugne 1987). This lag is probably too large to be accounted for by the catastrophic flooding hypothesis.

3. OBSERVATIONS

3.1 Acquisition and Processing of Data

During the two campaigns on board the *R/V Le Suroîta* DGPS system afforded precise positioning. In some areas (for example, the dune field of Figure 3), real-time navigation processing with an accuracy of a few meters made it possible to follow parallel track lines spaced 200 m apart at a speed of 4 knots. The vessel was equipped with a Simrad EM 1000 swath bathymetry system, and very high resolution seismic lines were shot simultaneously using a mud-penetrator and Chirp sonar system. All data acquisition was synchronized and digitally recorded.

An EM 1000 multibeam echo-sounder provided mapped bathymetry by processing the returned echo of each sonic transmission through a selection of 68 pre-formed beams trained across a strip of sea floor effectively four times as wide as the water depth. Each beam gives a depth resolution on the order of 10 centimeters over a five by two meter footprint along the surveyed swath, and all obtained at the survey speed of 4 knots. An image of backscatter reflectance energy was generated along with the digital elevations. Navigation, bathymetry, and image data were processed and synthesized in order to plot positions automatically, and thereby produce bathymetric maps and an image mosaic.

The very high resolution seismic reflection sources were a single channel mud-penetrator with a central frequency around 2500 Hz and an XSTAR Chirp sonar, sweeping between 4 and 16 kHz. The digital data acquisition was done in real time on the Triton-Elics Delph PC-based system.

Coring was achieved using a Kullenberg piston core and, in some cases, a vibrocorer.

3.2 Topography

Bathymetry data provided by the multibeam echo-sounder are illustrated in Figure 4. Prominent in the northern half of the survey area are linear ridges

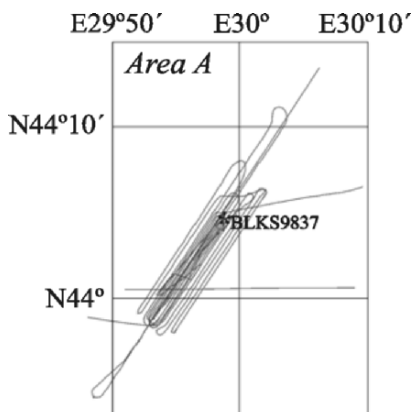


Figure 3. Map showing the location of profiles acquired on the dune field of Area A (indicated on Figure 1).

four to five meters in relief with an average spacing of 750 m. The ridges strike almost uniformly at an azimuth of $75 \pm 10^\circ$, they typically reveal asymmetrical cross-sections with the steeper sides facing to the southeast, and they possess a length to width ratio exceeding four. Numerous depressions 100 to 1800 m in diameter and 3 to 9 m deep also populate

the southern half of the corridor. Depths of individual depressions are greatest at the base of their northeast walls, and they shoal to the southwest. In the center of the surveyed corridor, some depressions align within the troughs between the linear ridges.

3.3 Subsurface Structure

The ridges and depressions can be viewed in cross-section using high resolution seismic reflection profiles. The sub-bottom profiler and Chirp sonar provide seismic penetration to tens of meters and define layering to the sub-meter scale. The profiles indicate that the ridges in the north are asymmetrical, and with one exception, their steeper side faces to the southeast. These ridges are superimposed on a reverberant “bottomset” reflector that is sometimes conformable with subjacent strata, but in many cases truncates them (Figure 5). Although the high ground in the south has a mound-like appearance, seismic surveys show an asymmetrical cross-section with the crest and steeper slope predominantly located on the south side. The interiors of the ridges and mounds contain steeply-dipping “foreset” clinoforms with the same asymmetry and orientation as the cross-section topographic profiles.

The ridges, mounds, and depressions of the mid and outer shelf are everywhere draped by a thin layer of sediment of remarkably uniform thickness, no more than a meter (Figure 5). The linear ridges surveyed in this study are aligned somewhat obliquely to the regional bathymetric contour and to the paleo-shoreline outlined by wave-cut terraces (Figure 6).

3.4 Sediment Cores

Sediments obtained by coring provide ground truth for the reflection profiles. Sampling into the interior of a ridge on the dune field (core BLKS9837

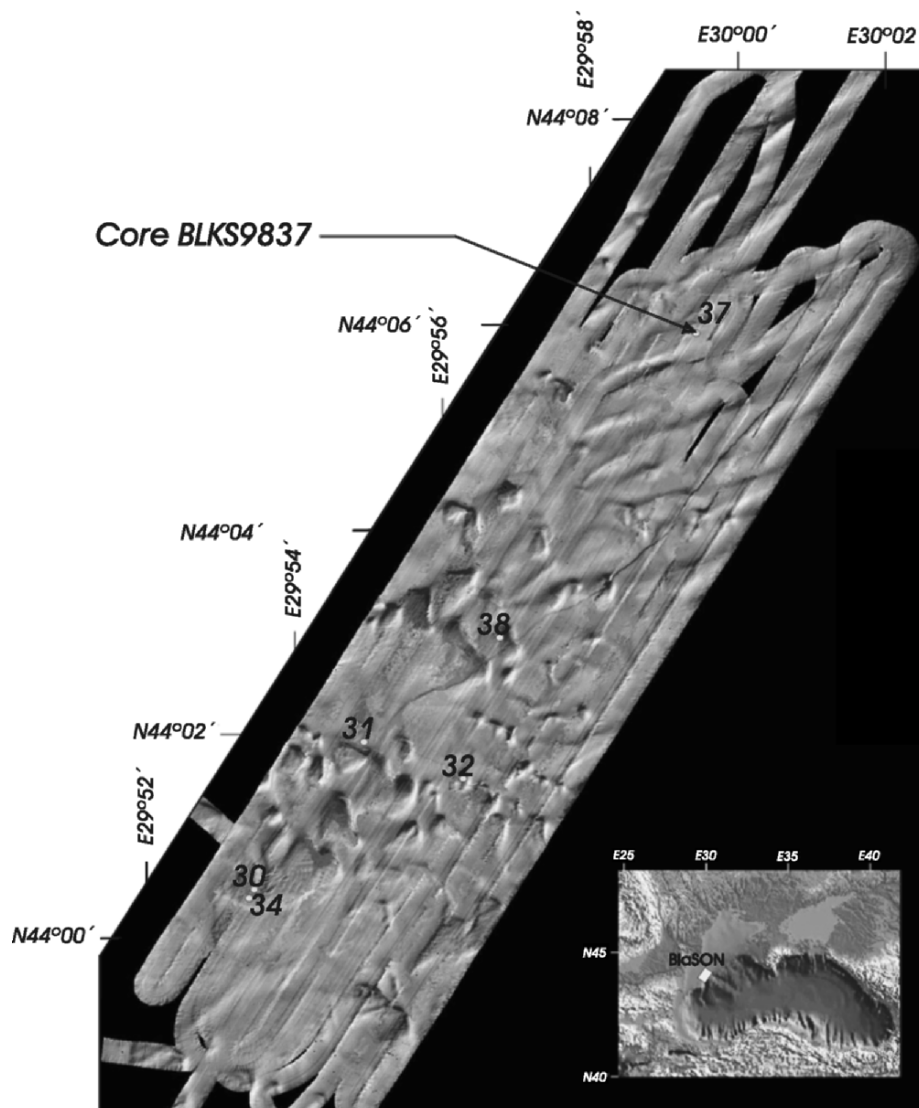


Figure 4. Multibeam bathymetry of the sand dune field and the location of core BLKS9837.

taken in a water depth of 68 m, core length 190 cm, position N44°00.54'-E029°58.87') recovered dark sand rich in opaque heavy minerals and shell fragments (Figure 7). Sampled minerals include quartz, garnet, and ilmenite. Shell fragments belong to freshwater mussels of *Dreissena rostriformis distincta*. Coring of the bedded sediments underlying the dunes and upon which they formed extracted silty red and brownish clay with thin lenses containing fresh to slightly brackish water molluscs (*Dreissena* and *Monodacna* spp., respectively).

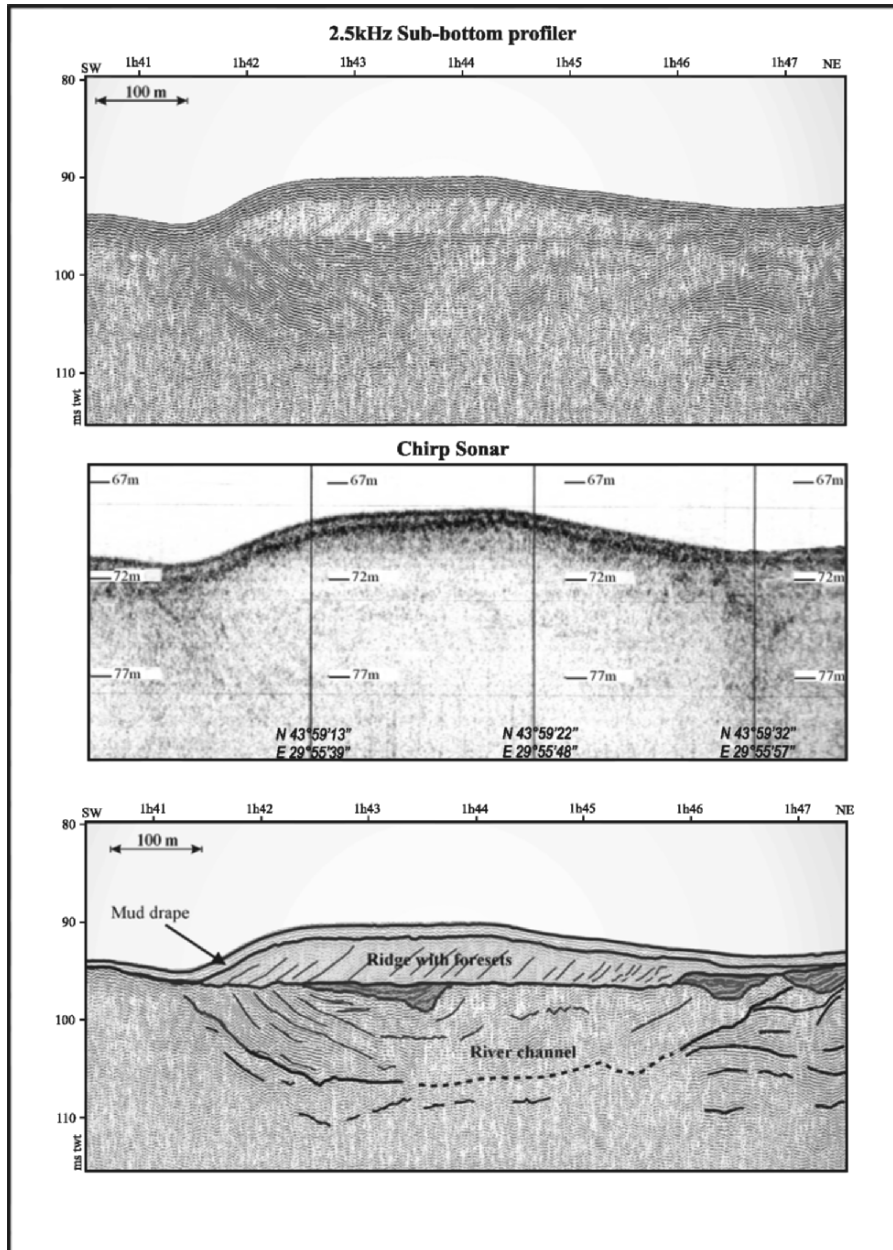


Figure 5. Seismic profiles across a sand dune.

These molluscan specimens return AMS radiocarbon dates spanning the interval 8585 to 10,160±90 BP (without reservoir and dendro-chronologic calibration).

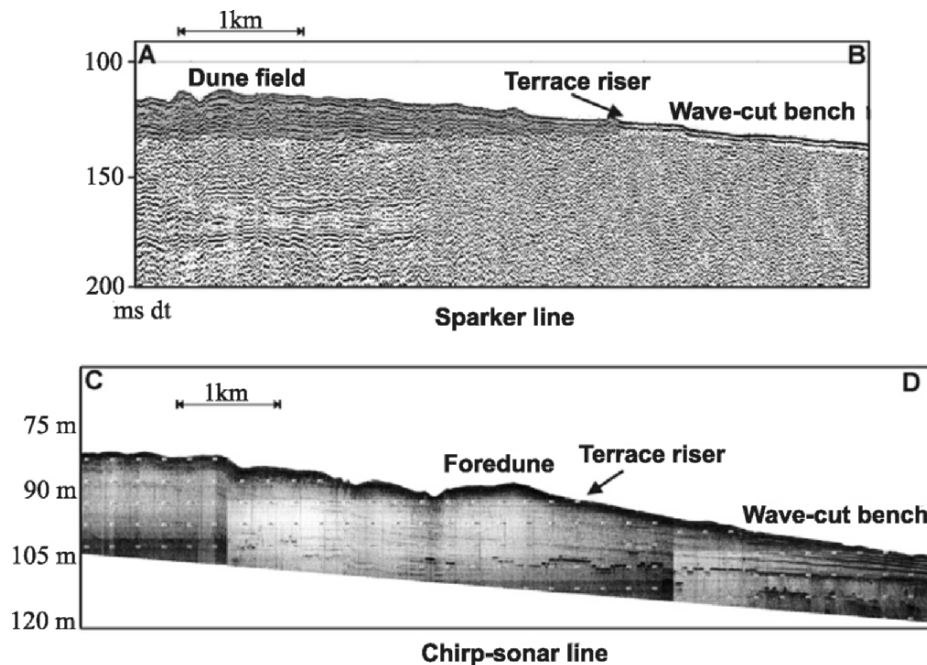


Figure 6. Seismic profiles across the wave-cut terrace.

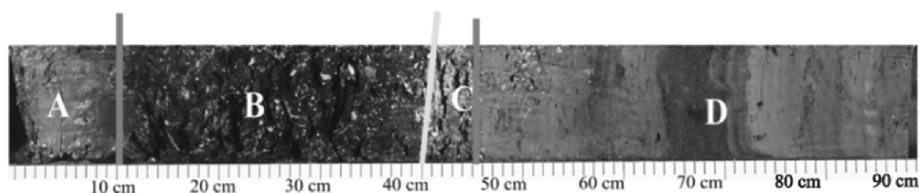


Figure 7. Core BLKS9837 (N44°00.54'-E29°58.87') recovered from dune field; A = layer with Modulus dated from 3000 BP to present; B = layer with *Mytilus edulis* dating between 6900 and 3000 BP; C = layer with *Dreissena* sp., the youngest dating 7150 BP.

Molluscs recovered in the cores from within the uniform surface drape reveal exclusively saltwater species, such as *Mytilus edulis* (also known as *Mytilaster*) and *Cerastoderma edule*. Those sampled near the base of the drape date between 6590 and 7770±80 BP.

Cores that penetrated through the drape reveal a sharp basal contact between the overlying organic mud with its marine molluscs and an underlying sand of variable thickness, rich in *Dreissena* sp. detritus. Recent palynological and dinocyst analyses by Speranta-Maria Popescu (Popescu *et al.* nd) on samples from within these cores indicate an abrupt freshwater transition during the

Younger Dryas followed by an abrupt replacement of the Black Sea dinocysts by a Mediterranean population at 7150 BP.

4. DISCUSSION

The sand dune fields and associated wave-cut terrace are interpreted as coastal zone relics that have persisted since 9680 to 8360 BP. At that time, a wave-cut terrace presently at -100 m with dunes and pans between -80 and -65 m would have lain well below the level of the external ocean (Fairbanks 1989). A lake could have existed below global sea level only if the Bosphorus barrier was higher than the external ocean, thereby preventing outflow. Burial of the dunes and pans by a drape of mud is not sufficient to imply a sudden infilling of the depression once the Bosphorus barrier was breached, but considering the evidence of (1) an abrupt transition from shell hash (a very condensed layer with brackish fauna) to mud, and (2) the impressive preservation of dunes and pans with no preferential infilling of the depression, a rapid terminal transgression of the Black Sea seems a compelling interpretation. The Caspian Sea, which appears to have experienced similar phenomena (with the exception of the last reconnection), reveals in the Iranian coastal regions of Mazandaran and Gilan comparable sand dunes on the terrestrial surface as high as 20 m that lie parallel to the seashore and which contain sandy particles and fragments of shells. The relic Black Sea dunes are occasionally cut across by aeolian deflation, which testifies to a previous lowstand.

Water-level fluctuations in the Black Sea appear to be directly linked to climate variability (Kvasov 1975; Svitoch *et al.* 2000). The Caspian Sea, another enclosed basin, reacted similarly. When not connected to the Mediterranean via the Black Sea, it reached highstands and achieved outflow in cold periods and drew down to lowstands through evaporation in warm periods. When the Mediterranean Sea penetrated the Dardanelles Strait at 12,000 BP, the level of the Marmara was below its outlet (Aksu *et al.* 1999b, 2002b).

Whether catastrophic flooding is hydraulically possible remains open to question. Lane-Serff *et al.* (1997) modeled the events following the connection of the Black Sea to the Mediterranean hydraulically and assumed that the sill cross-section has remained more-or-less unchanged. They showed that significant freshwater outflow from the Black Sea occurred only 500–1000 years after sea level in the Mediterranean reached the Bosphorus sill depth. A two-layer exchange between the two seas was initiated when an upper limit to the water flux was able to pass over the sill. This delay corresponds in order of magnitude to the lag between the onset of sapropel deposition in the Mediterranean and that in the Black Sea. Furthermore, they also demonstrated that it took 2500–3500 years for the bulk of the freshwater in the Black Sea to be replaced by salty

Mediterranean water and for euryhaline-marine conditions to be established. This period corresponds to the time of eastern Mediterranean sapropel deposition.

Debate continues about whether a catastrophic flood in the Black Sea significantly impacted habitation, migration, and cultural practices of European Neolithic populations. The archaeological interpretations presented by Ryan and Pitman (1998) depend upon the principal archaeological assumption that after the onset of agriculture, the ancient Near East suffered a drought that forced the first farmers to find refuge in a more hospitable climate, that of the pre-flood Black Sea coast. Kalish *et al.* (2003) suggest that a more realistic picture of the Neolithic diaspora into Europe consists of various waves, currents, and eddies of people, bringing animals and plants. In some areas, an influx of migrating farmers replaced sparse local foraging populations with Neolithic agricultural communities. Elsewhere, early farming communities appeared as isolated pioneer outposts within a multicultural landscape of foragers and farmers.

5. CONCLUSION

Recent surveys carried out on the northwestern continental shelf of the Black Sea imply that the early Holocene lake level rose on the shelf to at least the -40 to -30 m isobath as evidenced by the landward limit of the *Dreissena* layer, which is characteristic of freshwater conditions. This rise in freshwater level is consistent with interpretations of the Pontic basin as an important catchment for meltwater drained from ice caps during Melt Water Pulse 1. It is possible that the lake, having filled with freshwater at this time, rose to the level of its outlet and spilled into the Mediterranean. However, in the mid-Holocene, at 7150 BP, the onset of salt water conditions is clearly evidenced in the Black Sea. From these observations, Ryan *et al.* (1997) came to the conclusion that the Black Sea could have been filled by saltwater cascading from the Mediterranean.

Despite discussions to the contrary, recent IFREMER seismic surveys indicate the presence of well preserved drowned beaches, sand dunes, and soils supporting the interpretations of Ryan and Pitman that the Black Sea was rapidly filled with marine water from the Mediterranean during the mid-Holocene.

ACKNOWLEDGMENTS

Our research was supported by the French Ministry of Foreign Affairs in the context of a bilateral collaboration between France and Romania, and

continued by a European project of the 5th framework program called ASSEMBLAGE. We thank Nicolae Panin for the important role he played in this collaboration. We also thank William Haxby, Eliane Le Drezen, and Alain Normand for their work in multibeam data processing; Hervé Nouzé and Hervé Gillet for seismic processing; and the crew of the vessel *Le Suroît*. We also thank William B.F. Ryan and Candace Major for having shared their ideas at the beginning of these oceanic cruises and for their help in core dating. Appreciation is expressed to Renée Hetherington for her help in editing.

ENDNOTES

1. The abbreviation BP means radiocarbon years before present (1950) with neither correction for reservoir age nor calibration to calendar years. In Ryan *et al.* (1997) and Ryan and Pitman (1998), ages were expressed in calendar years, with 7500 calBP (= 5550 BC) equivalent to 7100 BP.

REFERENCES

- Abrajano, T., A.E. Aksu, R.N. Hiscott, and P.J. Mudie
 2002 Aspects of carbon isotope biogeochemistry of late Quaternary sediments from the Marmara Sea and Black Sea. *Marine Geology* 190:151–164.
- Aksu, A.E., T. Abrajano, P.J. Mudie, and D. Yaşar
 1999a Organic geochemical and palynological evidence for terrigenous origin of the organic matter in Aegean Sea sapropel S1. *Marine Geology* 153:303–318.
- Aksu, A.E., R.N. Hiscott, and D. Yaşar
 1999b Oscillating Quaternary water levels of the Marmara Sea and vigorous outflow into the Aegean Sea from the Marmara Sea–Black Sea drainage corridor. *Marine Geology* 153: 275–302.
- Aksu, A.E., R.N. Hiscott, D. Yaşar, F.I. İşler, and S. Marsh
 2002a Seismic stratigraphy of Late Quaternary deposits from the southwestern Black Sea shelf: evidence for non-catastrophic variations in sea-level during the last ~10 000 yr. *Marine Geology* 190:61–94.
- Aksu, A.E., R.N. Hiscott, M.A. Kaminski, P.J. Mudie, H. Gillespie, T. Abrajano, and D. Yaşar
 2002b Last glacial-Holocene paleoceanography of the Black Sea and Marmara Sea: stable isotopic, foraminiferal and coccolith evidence. *Marine Geology* 190:119–149.
- Aksu, A.E., R.N. Hiscott, P.J. Mudie, A. Rochon, M.A. Kaminski, T. Abrajano, and D. Yaşar
 2002c Persistent Holocene outflow from the Black Sea to the Eastern Mediterranean contradicts Noah's Flood Hypothesis. *GSA Today* 12(5):4–10.
- Algan O., N. Çağatay, A. Tchepalyga, D. Ongan, C. Eastoe, and E. Gökaşan
 2001 Stratigraphy of the sediment infill in Bosphorus Strait: water exchange between the Black and Mediterranean Seas during the last glacial Holocene. *Geo-Marine Letters* 20(4):209–218.
- Arkhangel'sky, A.D., and N.M. Strakhov
 1938 *Geologicheskoe stroenie i istoriia razvitiia Chernogo moria* [*Geological Structure and History of the Black Sea*]. Izdatel'stvo Akademiia Nauk SSSR, Moscow and Leningrad. (In Russian)

- Bard, E., B. Hamelin, R.G. Fairbanks, and A. Zindler
 1990 Calibration of the ^{14}C timescale over the past 30,000 years using mass spectrometric U–Th ages from Barbados corals. *Nature* 345(6274):405–410.
- Bondar, C.
 1998 Hydromorphological relation characterizing the Danube river mouths and the coastal zone in front of the Danube delta. *Geo-Eco-Marina* 3:99–102.
- Calvert, S.E.
 1990 Geochemistry and origin of the Holocene sapropel in the Black Sea. In *Facets of Modern Biogeochemistry*, V. Ittekkot, S. Kempe, W. Michaelis, and A. Spitzzy, eds, pp. 326–352. Springer-Verlag, Berlin.
- Calvert, S.E. and M.R. Fontugne
 1987 Stable carbon isotopic evidence for the marine origin of the organic matter in the Holocene Black Sea sapropel. *Chemical Geology* 66(3–4):315–322.
- Chepalyga, A.L.
 1984 Inland sea basins. In *Late Quaternary Environments of the Soviet Union*, A.A. Velichko, ed., H.E. Wright, Jr., and C.W. Barnowsky, eds, English edition, pp. 229–247. University of Minnesota Press, Minneapolis.
- Degens, E.T., and D.A. Ross, eds
 1974 *The Black Sea—Geology, Chemistry, and Biology*. Memoir 20, American Association of Petroleum Geologists, Tulsa.
- Evsylekov, Y.D. and K.M. Shimkus
 1995 Geomorphological and neotectonic development of outer part of continental margin to the south of Kerch Strait. *Oceanology* 35:623–628.
- Fairbanks, R.G.
 1989 A 17,000-year glacio-eustatic sea level record: influence of glacial melting rates on the Younger Dryas event and deep-ocean circulation. *Nature* 342(6250):637–642.
- Fedorov, P.V.
 1971 Postglacial transgression of the Black Sea. *International Geology Review* 14(2):160–164.
- Fontugne, M.R. M. Arnold, L. Labeyrie, M. Paterne, S.E. Calvert, and J.-C. Duplessy
 1994 Paleoenvironment, sapropel chronology and Nile river discharge during the last 20,000 years as indicated by deep-sea sediment records in the eastern Mediterranean. In *Late Quaternary Chronology and Paleoclimates of the Eastern Mediterranean*, O. Bar-Yosef and R.S. Kra, eds, pp. 75–88. RADIOCARBON and the American School of Prehistoric Research, Tucson, Arizona, and Cambridge, Massachusetts.
- Gökaşan, E., E. Demirbağ, F.Y. Oktay, B. Ecevitoglu, M. Şimşek, and H. Yüce
 1997 On the origin of the Bosphorus. *Marine Geology* 140:183–199.
- Grosswald, M.G.
 1980 Late Weichselian ice sheet of northern Eurasia. *Quaternary Research* 13(1):1–32.
- Hodder, I.
 1990 *The Domestication of Europe: Structure and Contingency in Neolithic Societies*. Blackwell Publishers, Oxford.
- Kalis, A.J., J. Merkt, and J. Wunderlich
 2003 Environmental changes during the Holocene climatic optimum in central Europe - human impact and natural causes. *Quaternary Science Reviews* 22(1):33–79.
- Kvasov, D.D.
 1975 *Pozdnechetvertichnaia istoriia krupnykh ozer i vnutrennikh morei Vostochnoi Evropy* [*The Late Quaternary History of the Large Lakes and Inland Seas of Eastern Europe*]. Nauka, Moscow.
- Kvasov, D.D. and A.I. Blazhchishin
 1978 The key to sources of the Pliocene and Pleistocene glaciation is at the bottom of the

- Barents Sea. *Nature* 273(5658):138–140.
- Lane-Serff, G.F., E.J. Rohling, H.L. Bryden, and H. Charnock
 1997 Postglacial connection of the Black Sea to the Mediterranean and its relation to the timing of sapropel formation. *Paleoceanography* 12(2):169–174.
- Major, C.O.
 1994 Late Quaternary Sedimentation in the Kerch Area of the Black Sea Shelf: Response to Sea Level Fluctuation. BA Thesis, Wesleyan University, Middletown, Connecticut.
- Muramoto, J.A., S. Honjo, B. Fry, B.J. Hay, R.W. Howarth, and J.L. Cisne
 1991 Sulfur, iron and organic carbon fluxes in the Black Sea—sulfur isotopic evidence for origin of sulfur fluxes. In Black Sea oceanography; results from the 1988 Black Sea Expedition. *Deep-Sea Research Part A. Oceanographic Research Papers* 38(Supplement 2A): S1151–S1187.
- Neveeskaya, L.A.
 1965 *Pozdnechetvertichnye dvustvorchatye molliuski Chernogo Moria, ikh sistematika i ekologiya* [Late Quaternary Bivalve Molluscs of the Black Sea, their Systematics and Ecology]. Trudy Paleontologicheskogo Instituta Akademii Nauk SSSR 105. Nauka, Moscow.
- Neveeskaya, L.A., and Yu.N. Neveesky
 1961 O sootnoshenii karangatskikh i novoevksinskikh sloev v pribrezhnykh raionakh Chernogo moria [Correlation between the Karangatian and Neoeuxinian layers in littoral regions of the Black Sea]. *Doklady Akademii Nauk SSSR* 137(4):934–937.
- Panin, N.
 1997 On the geomorphologic and geologic evolution of the river Danube–Black Sea interaction zone. *Geo-Eco-Marina* 2:31–40.
- Popescu, S.-M., M.J. Head, J.-P. Suc, G. Lericolais, and M.N. Çağatay
 and Rapid flooding of the Black Sea at 7,160 yrs BP after progressive salinity increase since 12,800 yrs BP. Ms. Submitted for publication.
- Rohling, E.J.
 1994 Review and new aspects concerning the formation of eastern Mediterranean sapropels. *Marine Geology* 122:1–28.
- Rohling, E.J., and S. de Rijk
 1999 Holocene Climate Optimum and Last Glacial Maximum in the Mediterranean: the marine oxygen isotope record. *Marine Geology* 153:57–75.
- Ross, D.A., E.T. Degens, and J. MacIlvaine
 1970 Black Sea: recent sedimentary history. *Science* 170(3954):163–165.
- Ryan, W., and W.C. Pitman
 1998 *Noah's Flood: The New Scientific Discoveries About the Event that Changed History*. Simon & Schuster, New York.
- Ryan, W.B.F., W.C. Pitman, III, C.O. Major, K. Shimkus, V. Moskalenko, G.A. Jones, P. Dimitrov, N. Görür, M. Sakinç and H. Yüce
 1997 An abrupt drowning of the Black Sea shelf. *Marine Geology* 138:119–126.
- Ryan, W.B.F., C.O. Major, G. Lericolais, and S.L. Goldstein
 2003 Catastrophic flooding of the Black Sea. *Annual Review of Earth and Planetary Science* 31:525–554.
- Scholten, R.
 1974 Role of the Bosphorus in Black Sea chemistry and sedimentation. In *The Black Sea—Geology, Chemistry, and Biology*, E.T. Degens and D.A. Ross, eds, pp. 115–126. American Association of Petroleum Geologists, Memoir 20, Tulsa, Oklahoma.
- Svitoch, A.A., A.O. Selivanov, and T.A. Yanina
 2000 Paleohydrology of the Black Sea Pleistocene basins. *Water Resources* 27:594–603.

Hydrographic development of the Aral Sea during the last 2000 years based on a quantitative analysis of dinoflagellate cysts

P. Sorrel^{a,b,*}, S.-M. Popescu^b, M.J. Head^{c,1}, J.P. Suc^b, S. Klotz^{b,d}, H. Oberhänsli^a

^a GeoForschungsZentrum, Telegraphenberg, D-14473 Potsdam, Germany

^b Laboratoire PaléoEnvironnements et PaléobioSphère (UMR CNRS 5125), Université Claude Bernard—Lyon 1, 27-43, boulevard du 11 Novembre, 69622 Villeurbanne Cedex, France

^c Department of Geography, University of Cambridge, Downing Place, Cambridge CB2 3EN, UK

^d Institut für Geowissenschaften, Universität Tübingen, Sigwartstrasse 10, 72070 Tübingen, Germany

Received 30 June 2005; received in revised form 4 October 2005; accepted 13 October 2005

Abstract

The Aral Sea Basin is a critical area for studying the influence of climate and anthropogenic impact on the development of hydrographic conditions in an endorheic basin. We present organic-walled dinoflagellate cyst analyses with a sampling resolution of 15 to 20 years from a core retrieved at Chernyshov Bay in the NW Large Aral Sea (Kazakhstan). Cysts are present throughout, but species richness is low (seven taxa). The dominant morphotypes are *Lingulodinium machaerophorum* with varied process length and *Impagidinium caspiense*, a species recently described from the Caspian Sea. Subordinate species are *Caspidium rugosum*, *Romanodinium areolatum*, *Spiniferites cruciformis*, cysts of *Pentapharsodinium dalei*, and round brownish protoperidiniacean cysts. The chlorococcalean algae *Botryococcus* and *Pediastrum* are taken to represent freshwater inflow into the Aral Sea.

The data are used to reconstruct salinity as expressed in lake level changes during the past 2000 years. We quantify and date for the first time prominent salinity variations from the northern part of the Large Aral Sea. During high lake levels, *I. caspiense*, representing brackish conditions with salinities of about 10–15 g kg⁻¹ or less, prevails. Assemblages dominated by *L. machaerophorum* document lake lowstands during approximately 0–425 AD (or 100? BC–425 AD), 920–1230 AD, 1500 AD, 1600–1650 AD, 1800 AD and since the 1960s. Because salinity in the Aral Sea is mostly controlled by meltwater discharges from the Syr Darya and Amu Darya rivers, we interpret changes in salinity levels as a proxy for temperature fluctuations in the Tien Shan Mountains that control snow melt. Significant erosion of marine Palaeogene and Neogene deposits in the hinterland, evidenced between 1230 AD and 1400 AD, is regarded as sheet-wash from shore. This is controlled by the low pressure system that develops over the Eastern Mediterranean and brings moist air to the Middle East and Central Asia during late spring and summer. We propose that the recorded environmental changes are related primarily to climate, but perhaps to a lesser extent by human-controlled irrigation activities. Our results documenting climate change in western Central Asia are fairly consistent with reports elsewhere from Central Asia.

© 2006 Elsevier B.V. All rights reserved.

Keywords: Aral Sea hydrology; Late Holocene; Dinoflagellate cysts; Lake level changes; Glacial meltwater discharge; Mediterranean low-pressure system

* Corresponding author. GeoForschungsZentrum, Telegraphenberg, D-14473 Potsdam, Germany. Tel.: +49 331 288 1347; fax: +49 331 288 1349. E-mail address: psorrel@gfz-potsdam.de (P. Sorrel).

¹ Present address: Department of Earth Sciences, Brock University, 500 Glenridge Avenue, St. Catharines, Ontario, Canada L2S 3A1.

1. Introduction

The Aral Sea is a large saline lake in the Aral–Sarykamish depression in Central Asia and bordered by Kazakhstan and Uzbekistan (Fig. 1). After about

14 ka, when the Aral and Caspian seas became separated from one another (Tchepaliga, 2004), the Aral Sea level developed a strong dependence upon the inflow of its two main tributaries, the Syr Darya and Amu Darya rivers. These rivers originate from the

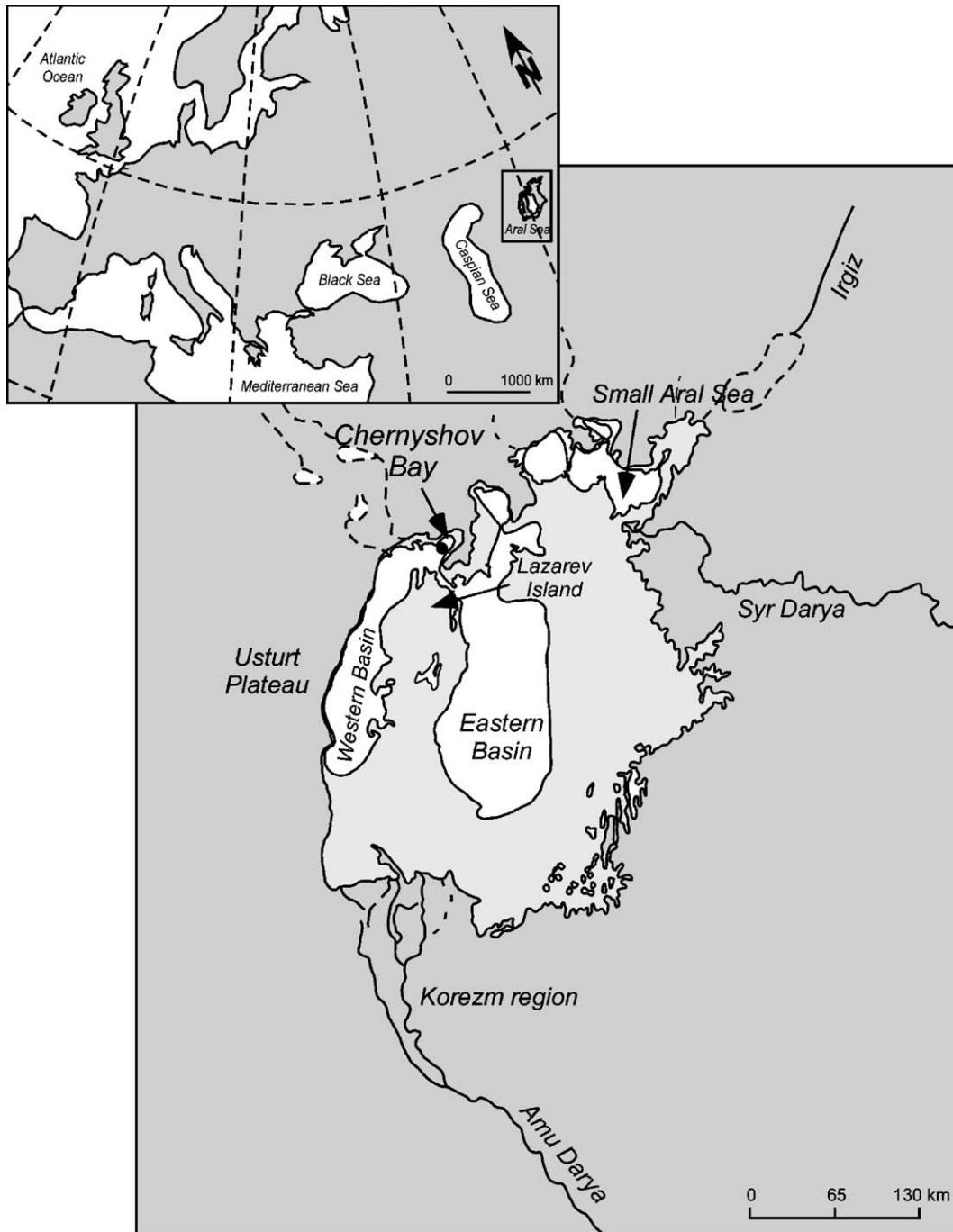


Fig. 1. Location map of the present Aral Sea (in white) and the study area. The light grey shading indicates the sea level from the early 1960s, whereas the dashed lines represent the former courses of episodic local rivers (after Létolle and Mainguet, 1993). The Eastern and Western basins constitute the Large Aral Sea.

highest part of the Pamir and Tien Shan mountains, 1500 km southeast of the Aral Sea. Nowadays, the Aral Sea is an endorheic lake with low freshwater inflow from rivers and low precipitation due to the extremely arid continental climate ($\sim 100 \text{ mm year}^{-1}$ on average; [Létolle and Mainguet, 1993](#)). As a result of extreme insolation-forced heating leading to desert conditions, the mechanical and chemical weathering of sediments is accentuated and erosional processes are enhanced.

During the past 40 years the Aral Sea, which was the fourth largest inland lake in the world, has suffered a dramatic reduction in size due to intensive irrigation activities in the hinterland ([Boomer et al., 2000](#)). As a consequence, its area has diminished more than fourfold, and the volume more than tenfold. The lake level has in fact stabilised during the last 3 to 4 years, as irrigation has decreased ([Zavialov, 2005](#)). Nonetheless, the lake level dropped by 22.5 m from its value in 1965, and the Aral Sea became split into two major water bodies, namely the Large Aral Sea represented by its western and eastern basins which are connected only through a short (3 km) and shallow (8 m) channel ([Nourgaliev, pers. comm. in Zavialov, 2005](#)), and the Small Aral Sea in the North ([Fig. 1](#)). Today, the lake level is at 30.5 m above sea level (a.s.l.) ([Zavialov et al., 2003](#)), whereas it was at 53 m a.s.l. in 1960 ([Létolle and Mainguet, 1993](#)). As a result of the considerable reduction in water volume and the reduced freshwater influx into the Aral Sea, salinity levels have increased more than eightfold. Surface-water salinity rose from 10.4 g kg^{-1} in 1960 to more than 80 g kg^{-1} in 2002–2003 ([Zavialov et al., 2003](#); [Friedrich and Oberhänsli, 2004](#)). The salinification had recently considerable consequences for the flora and fauna ([Mirabdullayev et al., 2004](#)), thus showing that the Aral Sea represents an ecosystem highly sensitive to climate changes and anthropogenic impact.

The palaeoenvironmental development of the Aral Sea has been studied from sediments since the late 1960s. [Maev et al. \(1999\)](#) dated changes in palaeoenvironmental conditions over the past 7000 years from two cores retrieved in the central part of the eastern basin. They reported phases of major regression during approximately 450–550 AD and 1550–1650 AD. This was further confirmed by [Aleshinskaya et al. \(1996\)](#) using palaeontological proxies and by [Boroffka et al. \(2005\)](#) from archaeological and geomorphological observations. [Boroffka et al. \(2005\)](#) also documented a low lake level from 800 AD to 1100 AD. However, interpretation remains ambiguous for the time window 1000–1500 AD. [Aleshinskaya et al. \(1996\)](#) suggested

deep-water conditions between 1100 AD and 1500 AD, whereas historical data point to a severe (or even complete) drying-out of the lake between the 13th and the 16th centuries ([Boroffka et al., 2005](#)).

Regarding environmental changes during the Holocene, the present state of knowledge is fairly good for the region south of the Aral Sea but rather poor for the northern part. During a field campaign in the summer of 2002, sediment cores were retrieved for the first time from the northwest shore of the Large Aral Sea (Chernyshov Bay; [Fig. 1](#)) (www.CLIMAN.gfz-potsdam.de). Using this cored material, we present new palaeontological data covering the past 2000 years with a time resolution of 15 to 20 years. Based on a quantitative analysis of organic-walled dinoflagellate cysts, we provide evidence for large palaeosalinity and lake water level variations.

2. Material and methods

2.1. Sedimentological description

In August 2002, two piston cores (composite cores CH1 and CH2 with respective total lengths of 11.04 m and 6.0 m) taken with a Usinger piston corer (<http://CLIMAN.gfz-potsdam.de>) and six gravity cores were retrieved from Chernyshov Bay ([Fig. 1](#)). These cores were collected 1 km from the shoreline ($45^{\circ}58'528''\text{N}$, $59^{\circ}14'459''\text{E}$) at a water depth of 22 m. Composite Core CH1 consists of sections 21, 22, 23, 27, 28 and 29, whereas composite core CH2 consists of sections 30, 31 and 32. Cores CH1 and CH2 were retrieved from the same coring location at about 1 m apart. In this study, we conducted our analyses on sections 30, 31 and 32 from Core CH2 and on sections 27, 28 and 29 from Core CH1. We then named this composite section CH2/1, whose total length is 10.79 m. The correlation between Cores CH1 and CH2 was performed by matching laminations using photographs, physical properties (bulk sediment density, magnetic susceptibility) and XRF scanning.

Sediments from this site ([Fig. 2A](#)) consist of greenish to greyish silty clays and dark water-saturated organic muds with sporadically intercalated more sandy material. The sediments, which are finely laminated, comprise material of variable origin (terrigenous, biogenic and chemogenic) and size (from clay and fine silt to fine sand with mollusc shell fragments). Chemical precipitates, such as gypsum (G), occur both as dispersed microcrystals in the sediment (G_3 , G_4 ; [Fig. 2B](#)) and as discrete layers (G_1 , G_2). Neither erosive discontinuity, nor features of bottom traction are ob-

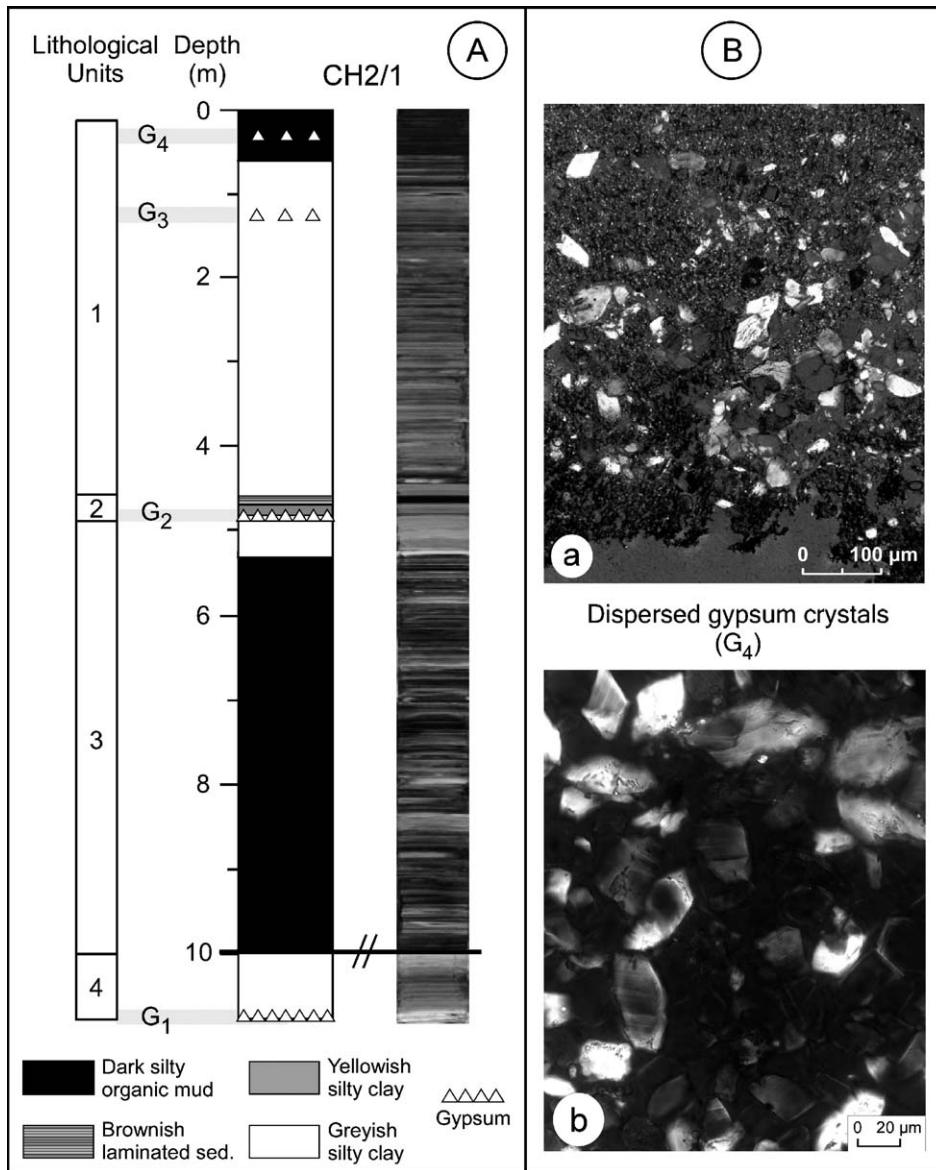


Fig. 2. A: Lithology of section CH2/1 (total depth=10.79 m). Note the break in core between Units 3 and 4 corresponding to a coring gap of unknown extent. B: Microfacies photographs. a: Dispersed gypsum crystals in a fine clayey matrix (G₄ [0.2–0.3 m]); b: Gypsum crystals showing characteristic monoclinic structures and cleavages (G₄ [0.2–0.3 m]).

served in the core. The laminated character of section CH2/1 indicates probable settling of various autochthonous and allochthonous particles from the water column during seasonally varying hydrographic conditions. Four lithological units are recognized. Between 0.0 and 4.5 m (Unit 1), the sediment is mostly silty to sandy clay with rare macrofossil remains although the uppermost part (0.0–0.5 m) consists of a dark, organic, finely laminated mud. Unit 2 is characterized by a horizon of laminated gypsum at its base (G₂: 1-cm thick) overlain by a 13-cm thick interval of yellowish

thinly laminated sediments which in turn are abruptly interrupted by brownish laminated sediments (10.5-cm thick interval). Downcore, between 4.86 and 9.7 m depth (Unit 3), the sediments consist of a dark silty organic mud, often water-saturated and very rich in organic matter including allochthonous aquatic plant remains. The plant remains occur both as a dispersed phase in the matrix and as partly decayed fragments that constitute organic horizons. These sediments, which are characteristic of dysoxic to anoxic bottom-water conditions, are separated from a lower sequence

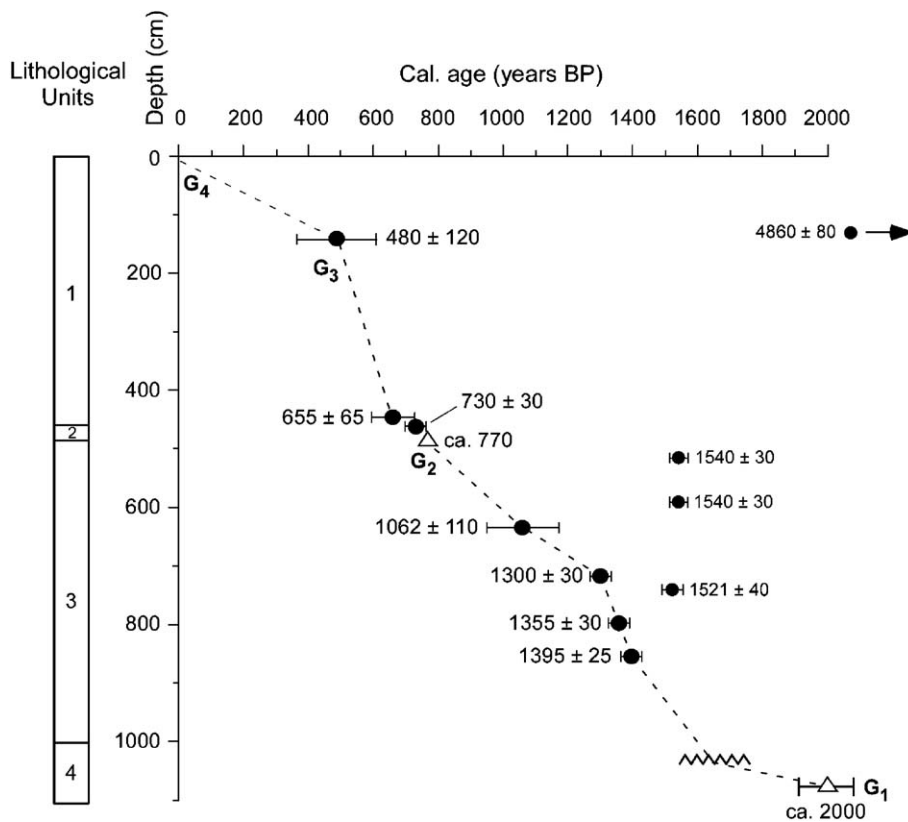


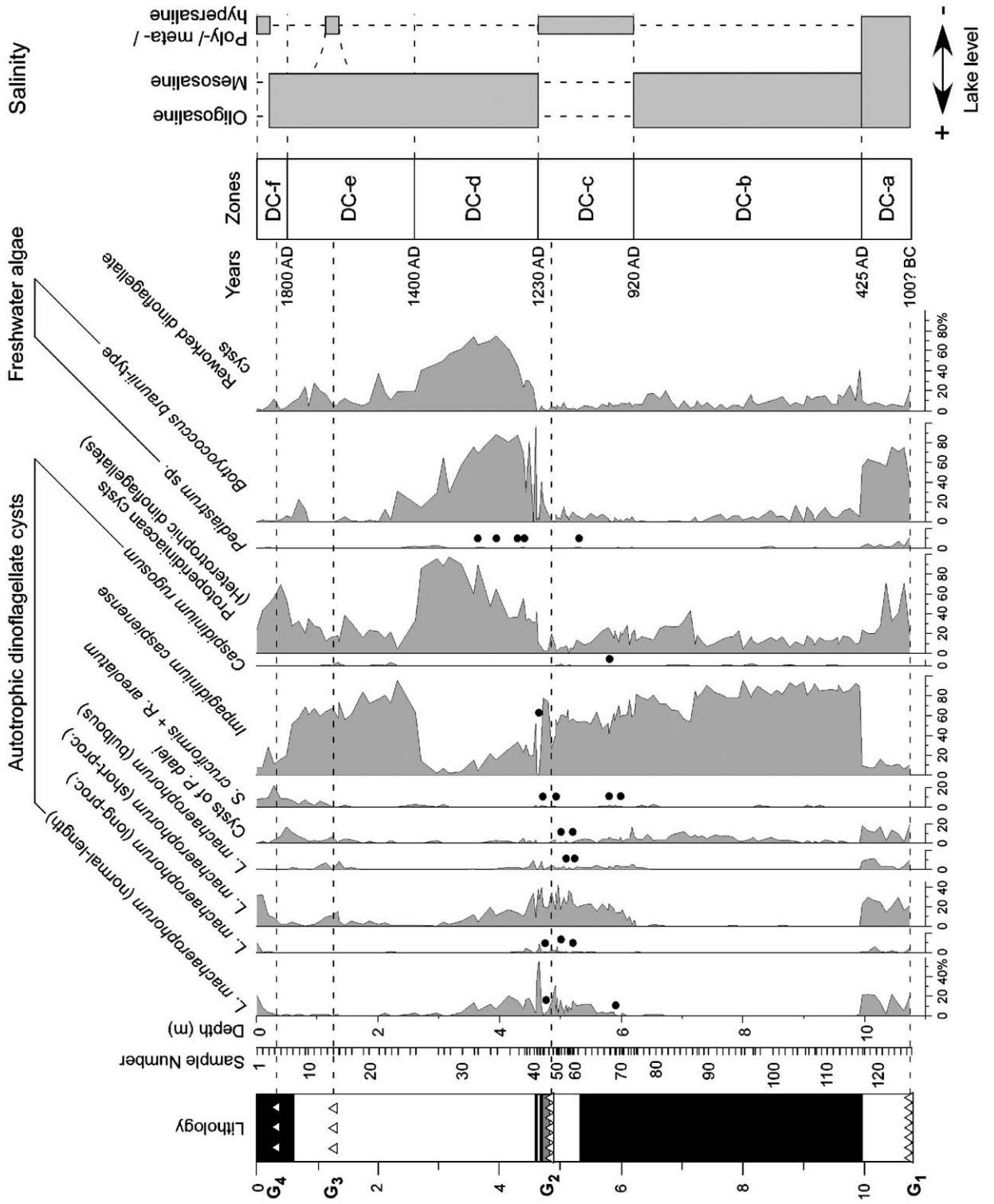
Fig. 3. Age model for section CH2/1 based on AMS ^{14}C dating on the filamentous green alga *Vaucheria* sp.: 480 ± 120 cal. yr BP, 655 ± 65 cal. yr BP (Nourgaliev et al., 2003); 108.6 ± 0.3 pMC (Poz-4753), 1062 ± 110 yr BP (Poz-12279), 1300 ± 30 cal. yr BP (Poz-4762), 1395 ± 25 cal. yr BP (Poz-4760), 1521 ± 40 cal. yr BP (Poz-4764), 1540 ± 30 cal. yr BP (Poz-4756/59), 4860 ± 80 cal. yr BP (Poz-4760), on TOC: 730 ± 30 yr BP (Poz-13511), and on CaCO_3 of mollusc shells: 1355 ± 30 cal. yr BP (Poz-9662). AMS ^{14}C dating was measured in the Poznań Radiocarbon Laboratory (Poland).

(9.97–10.79 m, Unit 4) by a coring gap of unknown extent. Unit 4 consists of thinly laminated grey silty clays that include at the base, laminated gypsum (G_1) interbedded with clayey layers. No turbiditic sediments have been recognized. The hydrochemical conditions at Chernyshov Bay today are very pronounced. A strong pycnocline has developed that maintains and stabilises an underlying body of anoxic deep-water (Friedrich and Oberhänsli, 2004) that in turn influences sedimentation by preventing bioturbation (except in the top-most part of the core [0.0–0.05 m]). Hence, sediments from Chernyshov Bay show well-preserved laminations (Friedrich and Oberhänsli, 2004).

2.2. Age model

In section CH2/1, AMS radiocarbon ages were determined using the filamentous green alga *Vaucheria* sp. and CaCO_3 from mollusc shells which were picked from the sediment sample and carefully washed. Algae were stored in water within a glass vessel. For each sample, AMS ^{14}C dating was performed using between 0.2 and 1.0 mg of pure extracted carbon. Radiocarbon ages were corrected to calibrated (cal) ages using the IntCal04 calibration curve published in Reimer et al. (2004). These determinations resulted in sedimentation rate estimates for

Fig. 4. Relative abundance of dinoflagellate cysts and freshwater algae from the Chernyshov Bay Core CH2/1, ecostratigraphic zonation based on the dinoflagellate cysts, and schematic salinity fluctuations. Each species and morphotype is expressed as a proportion of the total in-situ dinoflagellate cysts. *Pediastrum* sp. and *Botryococcus braunii*-type are expressed as a proportion of the total in-situ dinoflagellate cysts plus freshwater taxa. Reworked dinoflagellate cysts are expressed as a proportion of total in-situ dinoflagellate cysts plus reworked dinoflagellate cysts. Solid dots indicate rare occurrence (0.5% or less). Each sample represents a ~ 10 cm interval of core and is plotted by its mean depth. Oligosaline conditions represent salinities of $0.5\text{--}5$ g kg^{-1} ; mesosaline conditions salinities of $5\text{--}20$ g kg^{-1} and poly- to meta-/hypersaline conditions salinities $>20/30$ g kg^{-1} . See Fig. 2 for explanation of lithology.



the different lithological units. A preliminary age model for section CH2/1 based on AMS radiocarbon dating is proposed in Fig. 3. Reliable dating for the upper 6 m of section CH2/1 was obtained by correlation with the magnetic susceptibility record from parallel cores 7, 8 and 9 retrieved 50 m apart from the studied cores (Nourgaliev et al., 2003). AMS ^{14}C dating on cores 7, 8 and 9 was performed on the green alga *Vaucheria* sp. This correlation gives an age of 480 ± 120 years BP (cal. years) at 1.4 m depth for section CH2/1. In addition, the time interval represented by Unit 2 is temporally constrained between 655 ± 65 years BP (cal. years) at 4.5 m depth and 770 yr BP at 4.86 m for the laminated gypsum, as correlated to a decrease in tree-ring width from the Tien Shan Mountains (see Fig. 11). This time range is further constrained by an age of 730 ± 30 yr BP (cal. years) at 4.65 m. These results imply high sedimentation rates during the deposition of Unit 1 (1.6 cm year^{-1} from 1.36 m to 4.43 m) but conversely very low sedimentation rates for Unit 2 ($\sim 0.3 \text{ cm year}^{-1}$). Supplementary ^{14}C dating performed on *Vaucheria* sp. provides an age of 1062 ± 110 cal. years BP at 6.34 m, 1300 ± 30 cal. years BP at 6.94 m and of 1395 ± 25 cal. years BP at 8.25 m, while ^{14}C dating from mollusc shells indicates an age of 1355 ± 30 years BP at 7.73 m. Relatively high sedimentation rates are implied for Unit 3 ($\sim 1.4 \text{ cm year}^{-1}$ from 5.69 m to 10.36 m). Based on this adjustment, a linear extrapolation along Unit 3 would suggest an average age of ca. 2000 years BP (100? BC to 100 AD) for the base of section CH2/1 (G₄) corresponding to a major lake level drop. This is consistent with others studies (see Aleshinskaya et al., 1996 on radiocarbon-dated cores 15 and 86 from the Large Aral, and Boomer et al., 2000, p. 1269) that report on an important lake regression at 2000 years BP. Accordingly, a sampling interval of 10 cm, which represents a time resolution of 15 to 20 years, was selected. The top of the core (uppermost 40 cm) has been dated as post-1963, as based on a peak in ^{137}Cs at 0.44 m reflecting the climax of the bomb period (ca. 1963–1964 AD) (Heim, 2005) and this is confirmed by a date on *Vaucheria* sp. that reveals an age of 108.6 ± 0.3 pMC at 0.47 m. The dates 4860 ± 80 years BP at 1.30 m, 1540 ± 30 years BP at 5.16 m, 1540 ± 30 years BP at 5.90 m and 1521 ± 40 years BP at 7.40 m, respectively, reflect reworking of older material from shore. This is confirmed by reworked dinoflagellate cysts that are conspicuously abundant at these depths (see Fig. 4). Ages between 1521 and 1540 years BP typically represent sediment ages of a high lake-level stand. Due to a lack of dating of living algae sampled from the near-

shore, no reservoir correction can be applied yet. This is work in progress.

2.3. Sample processing and palynological analysis

For the study of dinoflagellate cysts, 125 sediment samples each consisting of 15 to 25 g dry weight were treated sequentially with cold HCl (35%), cold HF (70%) and cold HCl (35%) after Cour's method (1974). Denser particles were then separated from the organic residue using ZnCl_2 (density=2.0). After additional washing with HCl and water, the samples were sieved at 150 μm to eliminate the coarser particles including macro-organic remains, and then sieved again at 10 μm following brief (about 30 s) sonication. The residue was then stained using safranin-o, homogenized, and mounted onto microscope slides using glycerol. Finally, the coverslips were sealed with LMR histological glue.

Dinoflagellate cysts was identified and enumerated under a light microscope at $\times 1000$ magnification. Between 200 and 400 dinoflagellate cysts were counted for intervals of elevated salinity since specimens are generally abundant in such intervals. In other slides, where dinoflagellate cysts occur very sparsely, a minimum of 100 dinoflagellate cysts per sample were counted. Light photomicrographs (LM) were taken using a Leica DMR microscope fitted with a Leica DC300 digital camera. For scanning electron micrographs, residues were sieved at 20 μm , washed with distilled water and air-dried onto small circular metal blocks for 2 h, mounted onto metal stubs, and sputter-coated with gold.

Calculation of dinoflagellate cyst concentrations per gram of dry sediment was performed according to Cour's method (1974). Dinoflagellate cysts were found in every sample examined and preservation varies from poor (crumpling of cysts) to very good in intervals of elevated salinity. The dinoflagellate cyst record is shown by relative abundances of each taxon in a detailed diagram to emphasize palaeoenvironmental changes in the core (Fig. 4). Also shown are concentrations of in-situ cysts (per gram dry weight) of other palynomorphs and of reworked taxa (Fig. 5). Counts are archived at the Laboratory 'PaléoEnvironnements et PaléobioSphère' (University Claude Bernard—Lyon 1, France). The dinoflagellate cyst zones (DC-a–DC-f; Figs. 4 and 5) have been established using Statistica 6.0 according to a canonical correspondence analysis performed on selected taxa representing variables, in order to determine major ecological trends across section CH2/1. In addition, to examine whether relative abundance could be

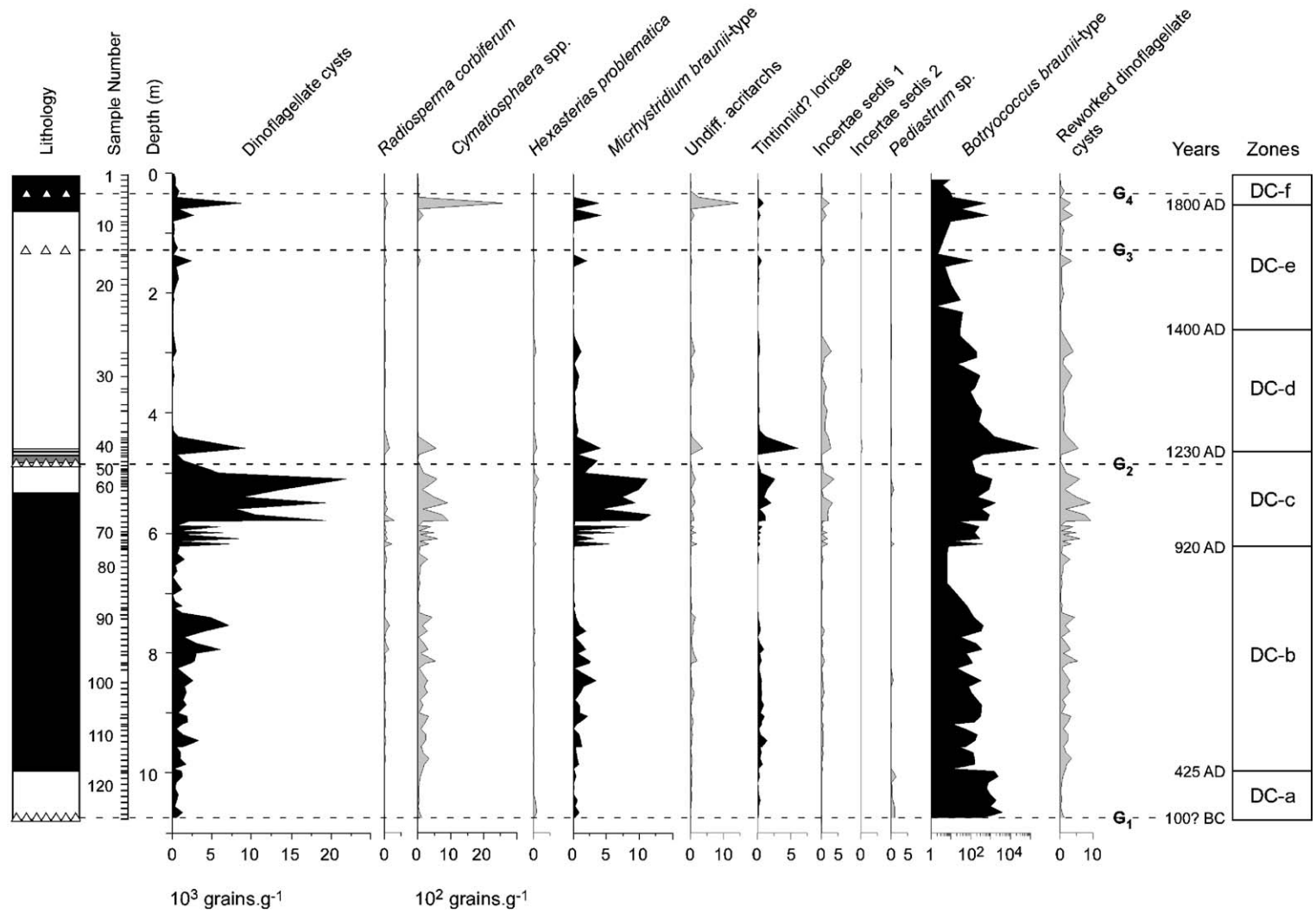


Fig. 5. Concentrations (per gram of dry sediment) of all aquatic palynomorphs counted in section CH2/1. Black-shaded curves: 10^3 grains g^{-1} . Grey-shaded curves: 10^2 grains g^{-1} . Note that concentrations of *Botryococcus braunii*-type are expressed in a logarithmic scale. Each sample represents a ~ 10 cm interval of core and is plotted by its mean depth. The zones refer to the dinoflagellate cyst ecostratigraphy described herein. See Fig. 2 for explanation of lithology.

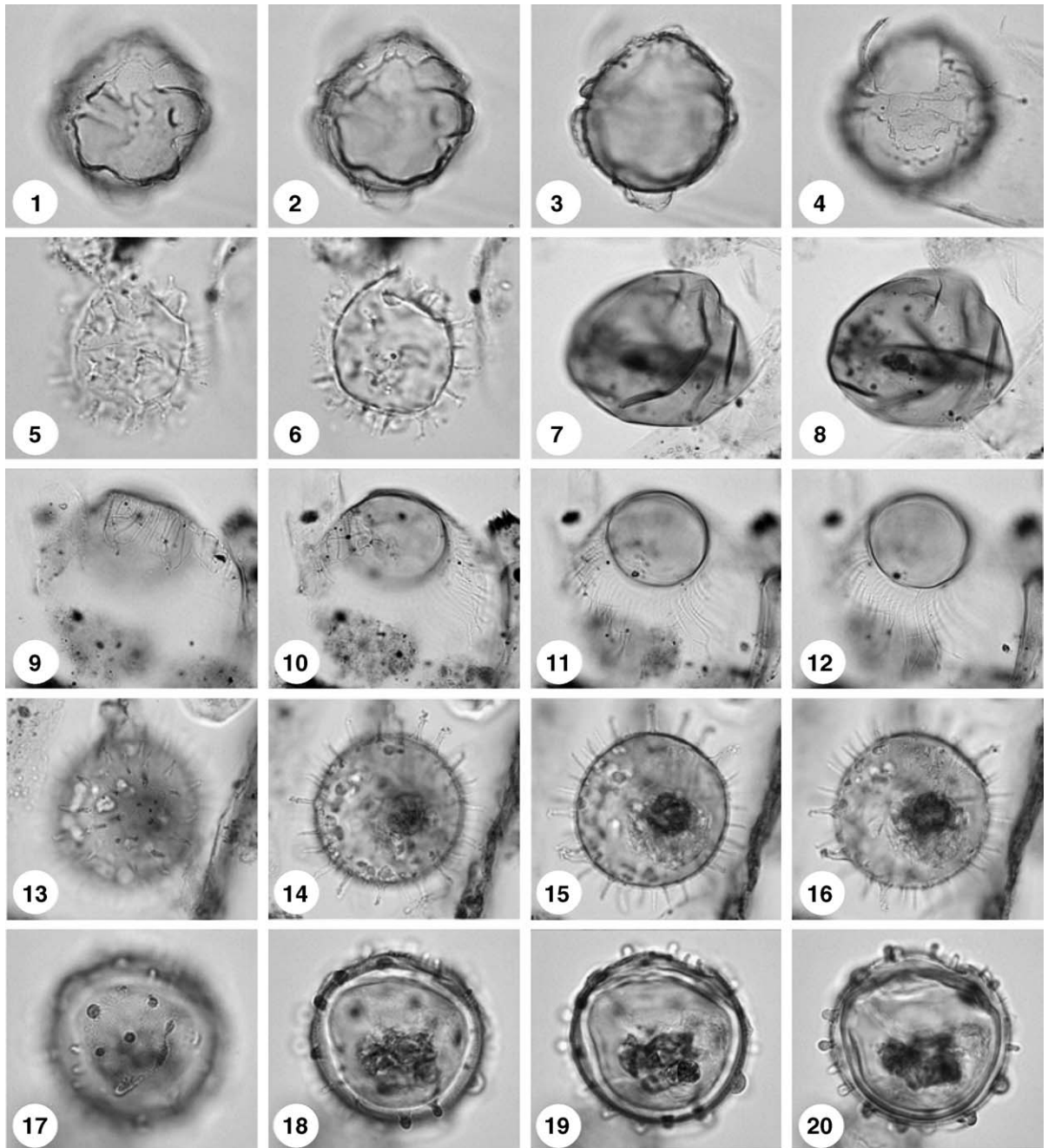


Fig. 6. Dinoflagellate cysts and other aquatic palynomorphs from Chernyshov Bay. Light micrographs in bright-field. An England Finder reference is given after the sample number. (1–4) *Impagidinium caspiense* Marret, 2004. Ventral view of ventral surface (1–2), mid-focus (3), and dorsal surface (4) showing archeopyle; max. dia. 45 μ m; sample 1A (M20/3); depth 537.5–540.5 cm. (5–6) Cyst of *Pentapharsodinium dalei* (Indelicato and Loeblich, 1986), upper and mid foci; central body max. dia. 23 μ m; sample 11A (K20/3); depth 507.5–510.5 cm. (7–8) Protoperidiniacean cyst, upper and low foci; max. dia. 44 μ m; sample 9A (N43/3); depth 537.5–540.5 cm. (9–12) *Radiosperma corbiferum* Meunier, 1910 (=Sternhaarstatoplast of Hensen, 1887), upper (9–10), mid (11) and low (12) foci; central body max. dia. 38 μ m; sample 9A (M10/0); depth 537.5–540.5 cm. (13–20) *Lingulodinium machaerophorum* (Deflandre and Cookson, 1955). (13–16) Specimen with processes of normal length (8–10 μ m); upper (13–14), mid (15) and low (16) foci; central body max. dia. 51 μ m; sample 9A (F35/4); depth 537.5–540.5 cm. (17–20) Specimen with bulbous processes; upper (17–18) and mid (19–20) foci; central body max. dia. 46 μ m; sample 9A (J51/0); depth 537.5–540.5 cm.

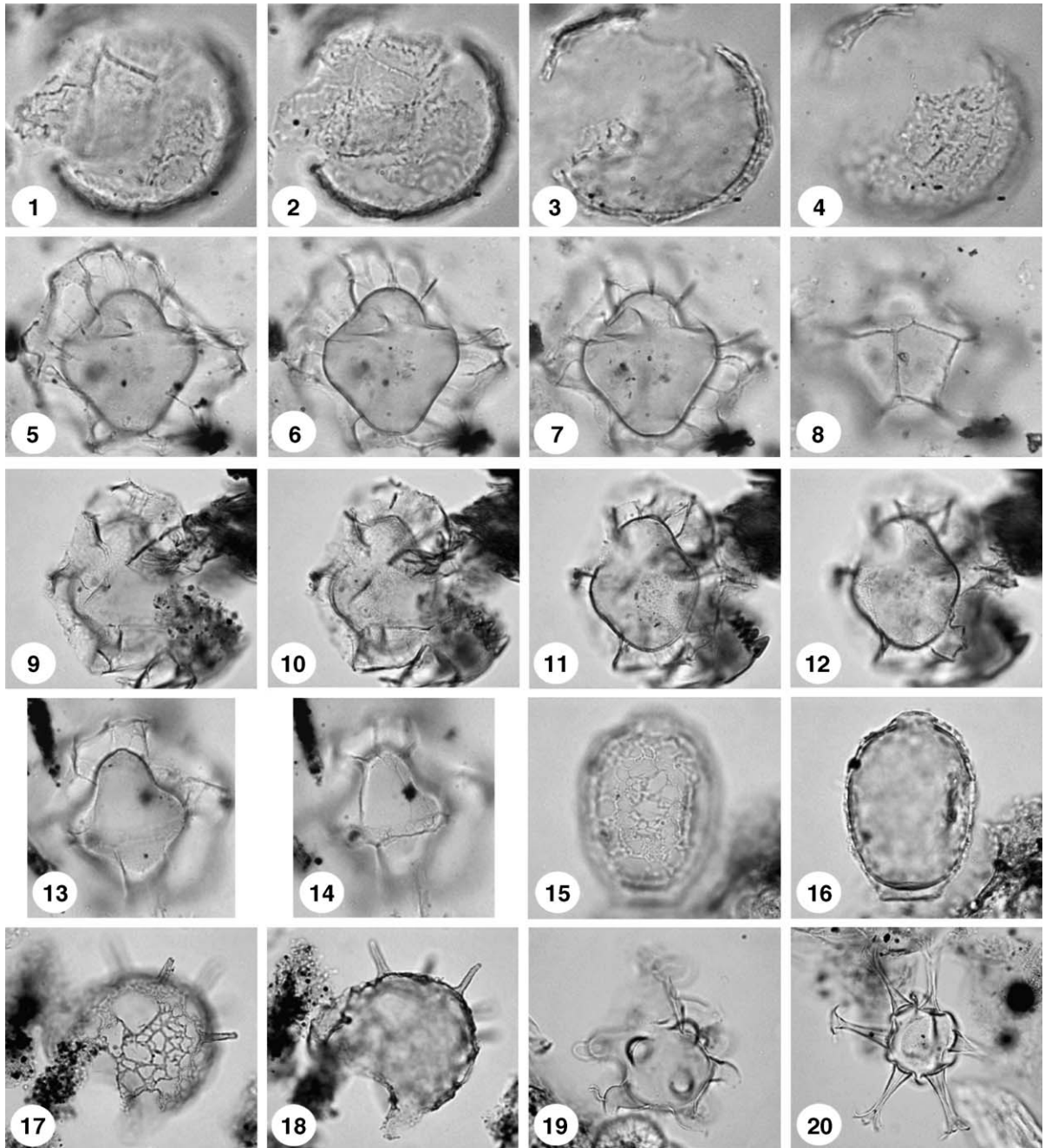


Fig. 7. Dinoflagellate cysts and other aquatic palynomorphs from Chernyshov Bay. Light micrographs in bright-field. An England Finder reference is given after the sample number. (1–4) *Caspidinium rugosum* Marret, 2004. Upper (1–2), mid (3) and low (4) foci; central body max. dia. 52 μ m; sample 32A3; depth 607.5–610 cm. (5–8) *Spiniferites cruciformis* Wall et al., 1973, ventral view showing ventral surface (5), mid focus (6–7) and dorsal surface (8); sample 32A3; central body max. dia. 52 μ m; depth 587.5–590 cm. (9–12) *S. cruciformis* Wall et al., 1973, ventral view showing ventral surface (9–10), mid focus (11) and dorsal surface (12); central body length 51 μ m; sample 9A (J25/0); depth 537.5–540.5 cm. (13–14) *S. cruciformis* Wall et al., 1973, low focus (13) and slightly lower focus of the dorsal surface in ventral view (14) showing archeopyle; central body max. dia. 51 μ m; sample 32A3; depth 547.5–550.5 cm. (15–16) Tintinniid? lorica, upper (15) and mid (16) foci; total length 53 μ m; sample 1A (P27/0); depth 457.5–459.5 cm. (17–18) Incertae sedis 1, upper (17) and mid (18) foci; central body maximum diameter 77 μ m; sample 1A (P27/0); depth 457.5–459.5 cm. (19) Incertae sedis 2, upper focus; total length 62 μ m; sample 9A (M10/0); depth 537.5–540.5 cm. (20) *Hexasterias problematica* Cleve, 1900, mid-focus; central body max. dia. 38 μ m; sample 11A (J31/3); depth 507.5–510.5 cm.

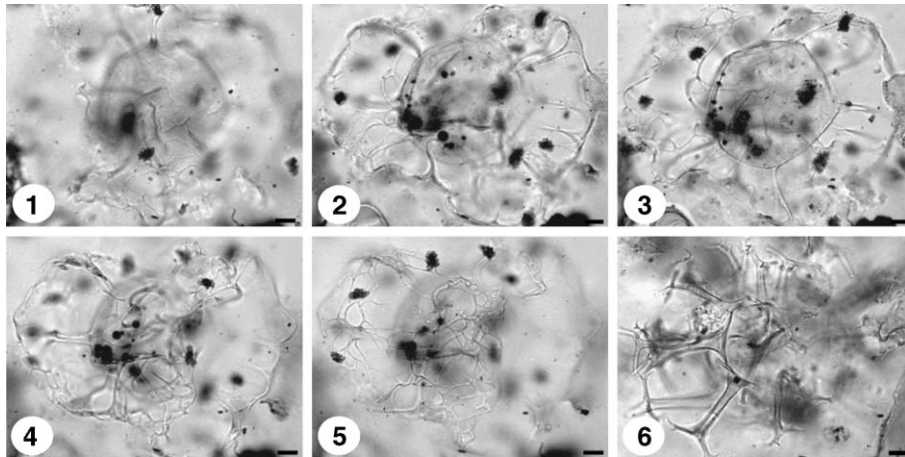


Fig. 8. Dinoflagellate cysts from Chernyshov Bay. Light micrographs in bright-field. (1–5) *Romanodinium areolatum* Baltes, 1971b, upper (1–2), mid (3) and lower (4–5) foci; central body max. dia. 63 μm ; sample 32A3; depth 587.5–590 cm. (6) Reworked specimen of *Spiniferites validus* Sütö-Szentai, 1982 low focus; central body max. dia. 71 μm sample 32A3; depth 607.5–610 cm.

biased by concentration values, a principal component analysis was performed on selected variables using the software “Past”. The results revealed that no relevant link exists between the different variables.

2.4. Ecological groupings of dinoflagellate cysts and other palynomorphs

The in-situ dinoflagellate cyst flora is of low diversity and comprises the following taxa: *Impagidinium caspiense* (Fig. 6.1–6.4), cysts of *Pentapharsodinium dalei* (Fig. 6.5–6.6), protoperidiniacean cysts (Fig. 6.7–6.8), *Lingulodinium machaerophorum* (Figs. 6.13–6.20 and 9), *Caspidinium rugosum* (Figs. 7.1–7.4 and 10.1–10.3), *Spiniferites cruciformis* (Figs. 7.5–7.8 and 10.4–10.7) and morphotypes assigned to *Romanodinium areolatum* (Fig. 8.1–8.5). The species are grouped according to their ecological preferences. Additional aquatic palynomorph taxa recorded are specimens of the chlorophycean (green algal) taxon *Botryococcus braunii*-type (Fig. 10.9) and *Pediastrum* sp.; the prasinophycean (green flagellate) species *Hexasterias* (al. *Polyasterias*) *problematica* (Fig. 7.20) and genus *Cymatiosphaera*; loricae of the ciliate order Tintinniida (Fig. 7.15–7.16); and incertae sedis taxa including *Michrystidium* (a probable algal cyst), Incertae sedis sp. 1 (Fig. 7.17–7.18), Incertae sedis sp. 2 (Fig. 7.19) and *Radiosperma corbiferum* (Figs. 6.9–6.12 and 10.9).

- *L. machaerophorum* (Figs. 6.13–6.20 and 9) is a euryhaline species that can tolerate salinities as low as about 10–15 g kg^{-1} (see Head et al., 2005, pp. 24–25 for review) and as high as about 40 g kg^{-1} based on laboratory culturing studies (Lewis and

Hallett, 1997), or indeed higher than 40 g kg^{-1} and approaching 50 g kg^{-1} as indicated by its distribution in surface sediments of the Persian Gulf (Bradford and Wall, 1984). The motile stage of this species blooms in late summer, and has a tropical to temperate distribution, with a late-summer minimum temperature limit of about 10–12 $^{\circ}\text{C}$ (Dale, 1996; Lewis and Hallett, 1997). Since *L. machaerophorum* develops different morphotypes with respect to changing temperature (–3 to 29 $^{\circ}\text{C}$) and salinity of surface-waters, it is regarded as a reliable indicator of environmental changes in a water body. These morphotypes are characterized by large variations in process length and shape (Fig. 4). Up to 15 different process types have been found for *L. machaerophorum* in previous studies (Wall et al., 1973; Harland, 1977; Kokinos and Anderson, 1995; Lewis and Hallett, 1997; Hallett, 1999). Most of these process types are also found in the late Holocene sediments of Chernyshov Bay. Typical specimens (Figs. 6.13–6.16 and 9.7–9.8) have processes of moderate length (5–15 μm) that taper distally to points, while other specimens may have long processes (15–20 μm ; Fig. 9.1–9.3) again tapering to points and often bearing small spinules at their distal ends. Some specimens with long, curved processes are also seen. Specimens with reduced processes ($\leq 5 \mu\text{m}$; Fig. 9.4–9.6) are found with terminations that are columnar, pointed or bulbous (Figs. 6.17–6.20 and 9.9).

- *P. dalei* (Fig. 6.5–6.6) is a spring-blooming species (Dale, 2001) most common in high northern latitudes (Rochon et al., 1999; de Vernal et al., 2001; Marret and Zonneveld, 2003). It tolerates a wide

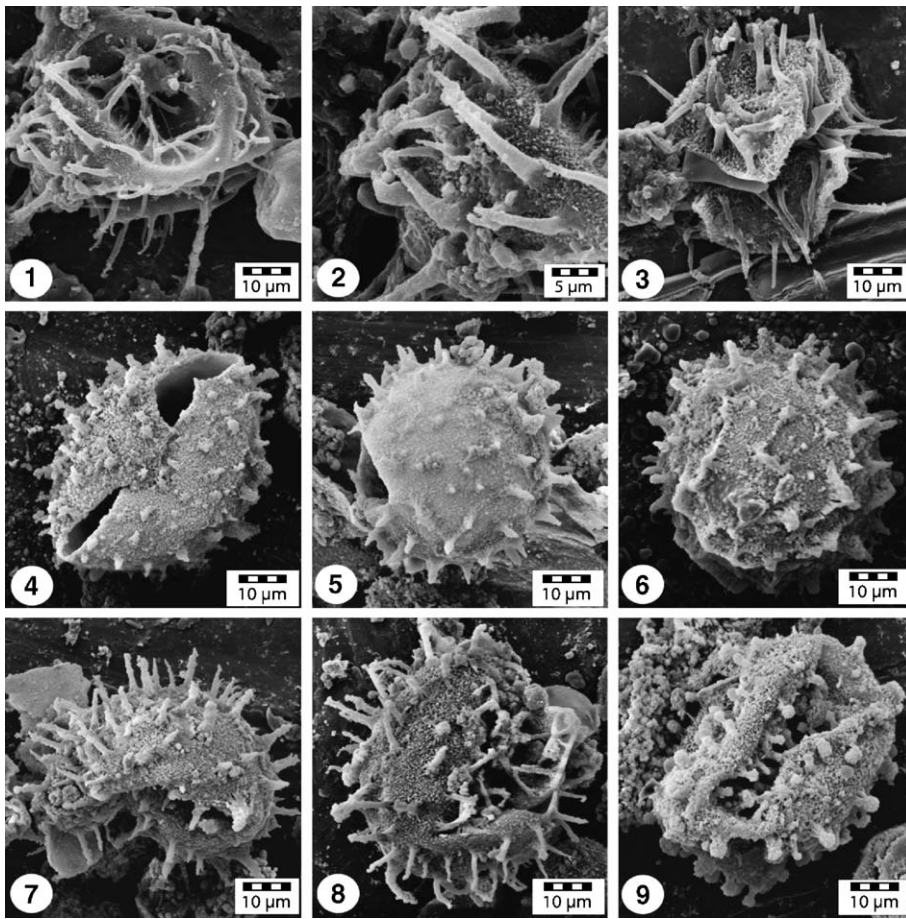


Fig. 9. Morphotypes of *Lingulodinium machaerophorum* from Chernyshov Bay. Scanning electron micrographs. (1–3) *L. machaerophorum* with long processes; sample 11A; depth 507.5–510.5 cm. (4–6) *L. machaerophorum* with reduced processes; sample 11A; depth 507.5–510.5 cm. (7–8) *L. machaerophorum* with processes of normal length; sample 11A; depth 507.5–510.5 cm. (9) *L. machaerophorum* with bulbous processes; sample 11A; depth 507.5–510.5 cm.

range of salinities (21–37 g kg⁻¹) and nutrient concentrations judging from a literature compilation of its cyst distribution (Marret and Zonneveld, 2003), although the small size and inconspicuous morphology of these cysts suggest the possibility of misidentification. Its presence in the Aral Sea core may be related to cool spring surface-waters resulting from cold winters (<0 °C).

- *S. cruciformis* (Figs. 7.5–7.14 and 10.4–10.7) in our section shows similar morphological variability to that described from the Holocene of the Black Sea by Wall et al. (1973) and Wall and Dale (1974), and as that described for modern and sub-modern specimens of the Caspian Sea (morphotypes A, B and C; Marret et al., 2004). *S. cruciformis* was first described from Late Pleistocene to early Holocene (23 to 7 ky BP) sediments from the Black Sea (Wall et al., 1973). The ecological affinities of *S. cruciformis* have already been discussed

in several papers because this species has been found in other Eurasian water bodies, such as the Black, Marmara and Aegean seas (Aksu et al., 1995a,b; Mudie et al., 1998, 2001, 2002; Popescu, 2001), and the Caspian Sea (Marret et al., 2004), but also in Lake Kastoria sediments of Late Glacial and Holocene ages (Kouli et al., 2001). Its occurrence was also reported from Upper Miocene/Lower Pliocene sediments of the Paratethys (Popescu, 2001; Popescu, in press) and Mediterranean realms (Kloosterboer-van Hove et al., 2001). The shape and size of sutural septa, ridges and processes have been all described as extremely variable (Wall et al., 1973; Mudie et al., 2001). Such variations may be linked to fluctuations in salinity (Dale, 1996). In this study, specimens assigned to *S. cruciformis* vary widely in body shape and degree of development of sutural septa and flanges. The size of the central body is rather

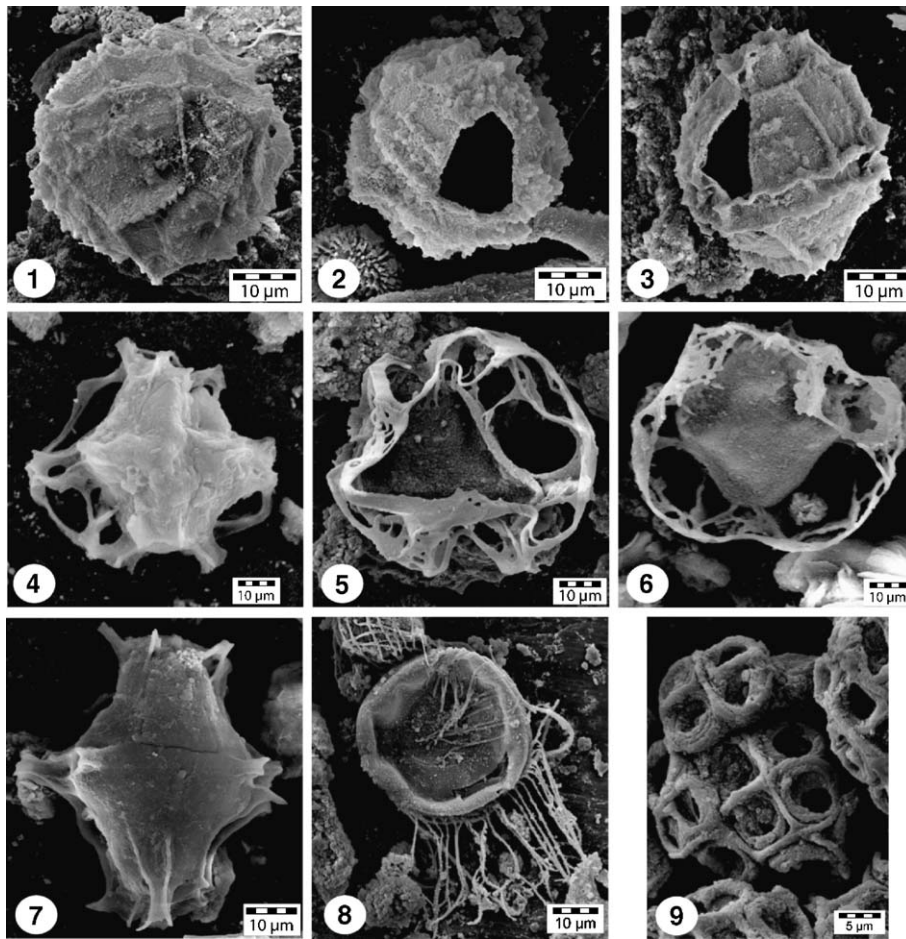


Fig. 10. Dinoflagellate cysts and other aquatic palynomorphs from Chernyshov Bay. Scanning micrographs. (1–3) *Impagidinium caspiense* Marret, 2004. Antapical view (1) and dorsal views showing archeopyle (2–3); sample 11A; depth 507.5–510.5 cm. (4–7) *Spiniferites cruciformis* Wall et al., 1973. (4) Cruciform/ellipsoidal body with a well-developed and perforated flange, ventral view; sample 24B; depth 49–51 cm. (5) Cruciform body with well-developed and perforated flange, ventral view; sample 24B; depth 4951 cm. (6) Cruciform/ellipsoidal body with well-developed and perforated flange, ventral view; sample 24B; depth 49–51 cm. (7) Cruciform body with incipient flange formed by incomplete development of low septa, dorsal view; sample 24B; depth 49–51 cm. (8) *Radiosperma corbiferum* Meunier, 1910 (=Sternhaarstatoplast of Hensen, 1887), dorsal view showing pylome; sample 11A; depth 507.5–510.5 cm. (9) *Botryococcus braunii*-type; sample 11A; depth 507.5–510.5 cm.

similar between specimens (length 40–50 µm; width 30–40 µm). The central body is either cruciform or ellipsoidal to pentagonal in shape. The degree of variation in the development of the flanges/septa consists of: (1) no development (Fig. 10.7), (2) low, fenestrate septa and incipient flange development (Fig. 10.4), or (3) well-developed and perforate–fenestrate flanges and septa (Figs. 7.5–7.14 and 10.5–10.6). However, there is a full range of intermediate variability. Specimens assignable to *R. areolatum* (Baltes, 1971a,b) are presented in Fig. 8.1–8.5. Because of the presence of morphologies intermediate between *S. cruciformis* and *R. areolatum* in our material, we have grouped these two species together in the counts (Fig. 4).

- *I. caspiense* (Figs. 6.1–6.4 and 10.1–10.3) and *C. rugosum* (Fig. 7.1–7.4) have recently been described from surface and subsurface sediments of the Caspian Sea by Marret et al. (2004). These species are apparently endemic to Central Asian Seas. However, since they might respond to different controls, they were plotted separately (Fig. 4). *I. caspiense* is the most abundant species encountered in sediments from section CH2/1, although our detailed understanding of its ecological requirements is poor. It thrives in low salinity waters (Marret et al., 2004).
- Proteroperidiniacean cysts are also frequent (Fig. 6.7–6.8). These are large, smooth, spherical to subspherical pale brownish cysts, often folded, and with a rarely visible archeopyle. They are considered het-

erotrophic, and their presence may be related to elevated nutrient levels from river inflow. Because they typically feed on diatoms and other primary producers, protoperidiniacean cysts, such as those of the genus *Protoperidinium*, are regarded as paleoproductivity indicators (Dale and Gjellsa, 1993; Dale, 1996). Moreover, since they are very sensitive to post-depositional oxygen-related decay, they give crucial information on past variations in bottom water and/or pore water circulation in the sediment (Zonneveld et al., 2001). As we expect anoxic conditions (oxygen-depleted conditions) to have prevailed on the lake bottom during the time window studied (resulting from the highly stratified waters), we can therefore here use protoperidiniacean cysts as a paleoproductivity indicator.

- Freshwater algal taxa are represented by coenobia of the chlorococcalean (green algae) genus *Pediastrum*, and by colonies of the chlorococcalean *B. braunii*-type (Fig. 10.9). *Pediastrum* is a predominantly freshwater genus (Parra Barientos, 1979; Bold and Wynne, 1985), although records from brackish habitats are documented (Brenner, 2001). *Botryococcus* is mostly associated today with freshwater environments, although records from brackish habitats are also known (Batten and Grenfell, 1996). On the grounds of probability (see also Matthiessen et al., 2000), we regard *Pediastrum* and *B. braunii*-type as indicators of freshwater discharge into Chernyshov Bay.

In addition to the groups discussed above, other aquatic taxa occur in low quantities. The distributions of these taxa are listed individually in Fig. 5.

- *Radiosperma corbiferum* (Figs. 6.9–6.12 and 10.8) is a marine to brackish organism previously recorded from the living plankton of the South-Western Baltic Sea (as Sternhaarstatoblast in Hensen, 1887), Baltic Sea proper including the eastern Gulf of Finland where summer surface salinities are below 3 g kg⁻¹ (Leegaard, 1920) and the Barents Sea (Meunier, 1910). It has been reported also from modern sediments of the brackish Baltic Sea where it occurs in nearly all samples from a transect representing low salinity (<6 g kg⁻¹) in the western Gulf of Finland to relatively high salinity (about 25 g kg⁻¹) in the Skagerrak (as Organismtype A in Gundersen, 1988, pl. 4, fig. 4). Highest concentrations were recorded in the central Baltic Sea where summer surface salinities are around 6–7 g kg⁻¹. Elsewhere, *R. corbiferum* has been reported from modern surface sediments of the Laptev Sea (Kunz-Pirrung, 1998,

1999), where this species has highest values north and east of the Lena delta and in front of the Yana river mouth (Kunz-Pirrung, 1999). It is also known from modern sediments of the Kiel Bight, South-Western Baltic Sea (as Sternhaarstatoblast of Hensen, 1887, in Nehring, 1994) and from sediments of Guanabara Bay at Rio de Janeiro, Brazil (Brenner, 2001). In the fossil record, *R. corbiferum* has been reported from Holocene deposits of the central Baltic Sea (Brenner, 2001) and Last Interglacial deposits of the South-Western Baltic Sea (Head et al., 2005). This distinctive but biologically enigmatic organism evidently has a broad salinity tolerance and, although it has been reported mostly from brackish-marine environments, factors additional to salinity may also control its distribution (Brenner, 2001).

- *Hexasterias* (al. *Polyasterias*) *problematica* (Fig. 7.20) has been recorded previously from Baffin Bay fjords where it is one of several species that increase towards the meltwater plumes (Mudie, 1992). It has also been found in modern sediments of the Laptev Sea (Kunz-Pirrung, 1998, 1999) and the plankton of the North Sea region (Cleve, 1900) as well as in the same general area (as “Röhrenstatoblast” in Hensen, 1887). It appears to be a brackish or euryhaline species (Matthiessen et al., 2000).
- The other aquatic groups (Fig. 7.15–7.16 and 7.17–7.18) here identified have either broad or uncertain environmental preferences.

Reworked specimens were found to occur generally within intervals of increased freshwater inflow. One group includes *Charlesdownia coleothrypta*, *Enneadocysta arcuata*, *Deflandrea phosphoritica*, *Phthanoperidinium comatum*, *Dapsilidinium pseudocolligerum*, *Areosphaeridium diktyoplokum*, and *Spiniferites* spp. (Fig. 8.6), and represents Palaeogene reworking. These specimens are often distinguished by an increased absorption of safranin-o stain, which probably reflects the oxidation history of these reworked specimens. A second group of reworked taxa, notably *Spiniferites* cf. *falcipediis*, *S. bentorii* (a single specimen), *S. hyperacanthus*, *S. membranaceus*, *S. ramosus*, *S. bulloideus*, *Spiniferites* sp., *Operculodinium centrocarpum* sensu Wall and Dale, 1966, is characterized by thin-walled cysts generally not affected by the safranin-o stain. Most of these specimens (*Spiniferites* cf. *falcipediis*, *S. bentorii*, *S. hyperacanthus*, *O. centrocarpum* sensu Wall and Dale, 1966) represent a typical Mediterranean assemblage that occurs in peak frequencies when river transport is implicated. We therefore

presume that they have been reworked from upper Neogene or Quaternary deposits, and their presence is probably linked to Plio-Pleistocene connections between the Aral, Caspian, Black and Mediterranean seas.

3. Results

Seven ecostratigraphic zones have been distinguished by statistically assessing major changes in the composition of the dinoflagellate cyst assemblage (Figs. 4 and 5). These ecostratigraphic zones mostly coincide with the lithological units previously defined.

Zone DC-a (10.75–9.97 m) is characterized by the dominance of *L. machaerophorum* as a whole, with maximum total values of 63% at 10.16 cm. Morphotypes bearing short- and normal-length processes are abundant (respectively up to 29% and 21% at 10.06 m) while specimens with long and bulbous processes are present (respectively up to 6% and 8% at 10.16 m). Frequencies of protoperidiniacean cysts fluctuate at relatively high numbers and oscillate between 18% at 9.97 m and 70% at 10.36 m. Note the reciprocating fluctuations in the frequencies of *L. machaerophorum* and protoperidiniacean cysts. Counts of *B. braunii*-type depict a somewhat decreasing trend through this zone, with relative abundances of 75% at 10.66 m to 57% at 9.97 m, as do numbers of *Pediastrum*, decreasing from 10.6% at 10.75 m to 1.7% at 9.97 m. Abundances of *I. caspiense* are relatively low throughout this zone where they average 10%, when frequencies in cysts of *P. dalei* display maximum values of 18% at 10.75 m. Reworked taxa are also present in low abundances, amounting to 20% at 10.75 m. Preservation is good throughout this zone and the dinoflagellate cyst concentration is relatively low (300–1300 specimens g^{-1}). The abrupt shift that characterizes the upper limit of this zone at 9.97 cm is related not to natural causes but to a coring failure.

Zone DC-b (9.97–6.18 m) is dominated by the species *I. caspiense*, which averages 70% to 80% for most of the zone. The previously dominant species *L. machaerophorum* disappears almost totally at the base, but occurs discretely again upwards (10% in total at 6.22 m). Counts of protoperidiniacean cysts are relatively constant throughout this zone (10–20%) but nevertheless exhibit a marked increase around 7.13 m (41%). Freshwater taxa, as well as cysts of *P. dalei*, are present as well, the latter increasing in abundances from the lower part to the top, attaining 15% at 6.18 m. Low abundances of *C. rugosum* (up to 2%) are also

recorded. Dinoflagellate cyst concentrations are medium (500–7250 cysts g^{-1}) and the preservation is poor due to crumpling of cysts.

Zone DC-c (6.18–4.64 m) documents the co-occurrence of two dominant taxa: *L. machaerophorum* and *I. caspiense*. While *I. caspiense* values remain relatively constant throughout this interval (50–60% on average), relative abundances of *L. machaerophorum* depict a progressive increase from 14% at bottom up to 91% at 4.64 m in total (respectively minimal and maximal values of 0–30%, 0–6%, 0–41.5% and 0–8% from morphotypes with normal length, long, short and bulbous processes). Conversely, relative abundances of protoperidiniacean cysts decrease from 27% at 6.09 m to 2% at 4.71 cm (0% at 5.14 m). Also, cysts of *P. dalei* (0–5%) and freshwater taxa (<10% on average but 40% at 4.695 m) occur in low numbers throughout this zone. *S. cruciformis* including *R. areolatum* is mostly found in the lowermost part (between 5.99 and 5.69 m; 1–2%) although they also occur in low frequencies near the top. *C. rugosum* is rare (up to 1.5%). Preservation is very good in this zone; correlatively the dinoflagellate cyst concentration is relatively high (from 800 to ca. 22,000 cysts g^{-1} ; Fig. 5). There is also a noticeable increase in the concentration of *Michrystidium braunii*-type organisms throughout this zone (up to ca. 12,000 specimens g^{-1} at the top). The transition from Zone DC-c to DC-d coincides with the transition from lithological Unit 2 to 3 (Fig. 2).

Zone DC-d (4.64–2.62 m) is characterized by an abrupt increase in the relative abundance of protoperidiniacean cysts, with a maximum of 95.8% at 3.18 m and frequencies fluctuating around 70% between 3.95 m and 2.72 m. Correspondingly, after an abrupt increase in the frequencies of freshwater species (notably *B. braunii*-type) with average values increasing up to 96.5% at 4.59 m, the abundance shows a progressive decreasing trend upwards (18% at 2.62 m). Abundances of reworked dinoflagellate cysts are also high in this zone, increasing to 75% at 3.75 m and at 3.58 m, before progressively decreasing further upwards. Abundances of *L. machaerophorum* show a stepwise decrease from 91% at 4.64 m (ecozonal boundary Zones DC-c/d) to 1% at 2.72 m. Relative abundances of cysts of *P. dalei* remain very low (<5%) in this zone. *S. cruciformis* including *R. areolatum* is found in low abundances (1–3%), mostly between 3.08 and 2.62 m. Also present are reworked specimens of *Spiniferites* species, including *S. ramosus* and *S. bulloideus*, which occur as smooth, thin-walled and delicate specimens. This zone is characterized by very low concentrations of dinoflagellate cysts (30–600 specimens g^{-1}) and poor preservation.

Zone DC-e (2.62–0.5 m) is characterized by the replacement of protoperidiniacean cysts (20% on average but 4% at 2.32 m) by *I. caspiense* that becomes conspicuously dominant, with average values amounting to 60%. Correspondingly, relative abundances of reworked taxa significantly decline (ca. 20% at 2.62 m to 8% at 0.6 m). Frequencies of *L. machaerophorum* are low throughout this zone, although a slight increase is noticeable between 1.36 m and 1.05 m (10–20%). *S. cruciformis* including *R. areolatum* is more scarcely represented in this zone with contributions never exceeding 2% of the dinoflagellate cyst assemblage. Relative abundances of cysts of *P. dalei* are relatively constant (~5%) but conspicuously increase at the top (16% at 0.5 m). Rare cysts of *C. rugosum* are also present (1–3%). Dinoflagellate cyst concentrations are again low (70 to 800 specimens g^{-1}) although the preservation is much better.

Zone DC-f (0.5–0 m) is characterized by the dominance of *L. machaerophorum* morphotypes whose relative abundances abruptly increase from 0.5 m upwards (normal length processes: 20%; long processes: 10%; short processes: 30%; bulbous processes: 1% at the very top). Conversely, relative abundances of *I. caspiense*, protoperidiniacean cysts and morphotypes of *S. cruciformis* noticeably decrease between 0.5 m and the topmost part of this zone, with respective values of 16% at 0.5 m to 8% at 0 m for *I. caspiense*, 68% to 23% for the protoperidiniacean cysts and 21% to 7% for the morphotypes of *S. cruciformis*. Cysts of *P. dalei* progressively disappear with values ranging from 16% at 0.5 m to 0% at the top. Dinoflagellate cyst preservation is very good throughout this zone but the concentration remains relatively low (200–8000 cysts g^{-1}).

4. Discussion

4.1. Palaeoenvironmental reconstruction

For the past 2000 years, two contrasting environmental states can be distinguished, each with distinct extremes. Transiently highly saline (poly- to meta-/hypersaline) conditions are inferred by specific dinoflagellate cyst assemblages characterized by increasing/high abundances of *L. machaerophorum*. Coevally, gypsum starts to precipitate from the water column as soon as the salinity reaches 28 $g\ kg^{-1}$ (Brodskaya, 1952; Bortnik and Chistyayeva, 1990). Since the motile stage of *L. machaerophorum* commonly blooms in late summer, persistently higher abundances of this species may imply sustained levels of enhanced evaporation. Conversely, periods of decreasing salinity (oligo-/meso-

saline conditions: 0.5–25 $g\ kg^{-1}$) are inferred from dinoflagellate cyst assemblages characterized by decreasing frequencies of *L. machaerophorum* (and reduced processes: <5 μm) but increased abundances of other autotrophic (notably *I. caspiense*) and heterotrophic (protoperidiniacean cysts) species. Higher abundances of freshwater algae (*Pediastrum*, *B. braunii*-type) imply river discharge and periods of freshening of the lake. Furthermore, due to its ecological preferences, *P. dalei* may serve as a proxy for cool spring surface-waters following cold winters. The dinoflagellate cyst record can thus be used to infer surface-water variations in salinity, palaeoproductivity and potentially also temperature. Because these changes imply fluctuations in lake water level, coeval changes in sedimentation and environmental processes should have occurred. The palaeoenvironmental changes are discussed here in terms of contrasting environmental states, notably salinity and lake water levels (see Fig. 4).

Today, salt concentrations in the Western Basin have increased to 82 $g\ kg^{-1}$ in surface-waters and 110 $g\ kg^{-1}$ at depth (Friedrich and Oberhänsli, 2004). This is reflected in the topmost sediment of section CH2/1 by an abrupt increase in abundance of the autotrophic species *L. machaerophorum* (especially morphotypes with long, i.e. >15 μm and normal length, i.e. 5–15 μm , processes; Zone DC-f) within a trend strengthened at the very top. Based on this observation and the aforementioned ecological tolerances of the species, we confirm *L. machaerophorum* as a reliable environmental indicator indicating salinity increase in surface-water layers. It must be understood, however, that the motile stage of *L. machaerophorum* blooms mostly in late summer (Lewis and Hallett, 1997) and its cyst record therefore does not necessarily reflect conditions at other times of the year.

4.1.1. Zone DC-a (10.75–9.97 m: 100? BC–425 AD)

This zone is interpreted as representing a period of low lake level due to evaporative drawdown, indicated by high levels of *L. machaerophorum* and deposition of gypsum (G_1). In the Aral Sea, gypsum precipitates out in the water column once salinity attains 28 $g\ kg^{-1}$ (Brodskaya, 1952; Bortnik and Chistyayeva, 1990), which thus suggests that surface water salinity during Zone DC-a was above 28 $g\ kg^{-1}$. This is in agreement with the salinity tolerance of *L. machaerophorum*, a species grown in the laboratory in salinities up to 40 $g\ kg^{-1}$ (Lewis and Hallett, 1997; Hallett, 1999) and whose modern distribution in surface sediments of the Gulf of Persia implies a tolerance to salinities exceeding 40 $g\ kg^{-1}$ and indeed approaching 50 $g\ kg^{-1}$ (Bradford

and Wall, 1984). *L. machaerophorum* blooms in late summer, and high numbers indicate sustained periods of enhanced summer evaporation during Zone DC-a. At the same time, abundant fresh-water algae *B. braunii*-type and *Pediastrum* sp., and nutrient-dependent (protoperidiniacean) cysts, also characterise this zone and indicate freshwater inflow and increased palaeoproductivity. The source of the freshwater inflows remains debatable. These episodic freshwater influxes are possibly linked to phases of stronger discharges of the Syr Darya and Amu Darya rivers in late spring/early summer. They can also originate from local rivers episodically flushing into the bay (Fig. 1), such as the Irgiz River in the north (see Aleshinskaya et al., 1996). The seasonal contrast in sea-surface temperatures, when judging from significant numbers of cysts of the spring-blooming, cool-tolerant species *P. dalei*, was probably higher between 100? BC and 425 AD, with relatively cool spring surface-water temperatures following cold winters.

4.1.2. Zone DC-b (9.97–6.18 m: 425–920 AD)

I. caspiense is a brackish species judging from its modern distribution in the Caspian Sea, although it overlaps ecologically with *L. machaerophorum* in the lower range of the latter species' salinity tolerance (Marret et al., 2004). The dominance of *I. caspiense* in this zone and near absence of *L. machaerophorum* indicates that the surface water salinity was below 15 g kg⁻¹ and probably around 10 g kg⁻¹ (the approximate lower limit for *L. machaerophorum*). The presence of *P. dalei* and protoperidiniacean cysts is not inconsistent with this interpretation, as these species are present in the low-salinity Caspian Sea today (Marret et al., 2004). The reduction in salinity during Zone DC-b implies that the lake level had risen substantially (although we do not know if this was gradual or abrupt because of the coring break). Because of the low topography of the shorelines around the lake, even a slight rise in lake level will have a substantial effect on the position of the shoreline. It will have expanded outwards considerably in all directions, and will have moved substantially away from the coring site. This may explain why Zone DC-b has low representations of *B. braunii*-type and *Pediastrum* sp.—the river discharges supplying these allochthonous palynomorphs being further away.

4.1.3. Zone DC-c (6.18–4.64 m: 920–1230 AD)

A relatively steady increase in *L. machaerophorum* and reciprocal decrease in the brackish species *I. caspiense* together evidences a progressive salinity increase in this zone, with precipitation of gypsum (G₂)

near the top. A pronounced increase in dinoflagellate cyst concentration within this zone probably signifies increased productivity as a response to the rise in salinity. Judging from the presence of gypsum deposits and tolerance of *L. machaerophorum* to high salinities, it would seem that salinities rose above 28 g kg⁻¹. The increasing salinity throughout this zone suggests progressive lowering of the lake level.

4.1.4. Zone DC-d (4.64–2.62 m: 1230–1400 AD)

This zone represents a progressive decline in salinity, as evidenced by a reduction in *L. machaerophorum* to near disappearance at the top of the zone. This was evidently caused by freshwater inflow into the lake, as indicated by abundant *B. braunii*-type. This zone is also characterized by a drastic change in sedimentation from the deposition of laminated sediments to silty clays (Fig. 2) rather poor in palynomorphs (Fig. 5). The coring site was clearly receiving significant river discharges because reworked cysts are also abundant. These reworked cysts attest to active erosion of Neogene and late Quaternary deposits during periods of elevated sheet-wash from shore, and account for the high sediment accumulation rates in this zone (16 mm year⁻¹, see also Nourgaliev et al., 2003). Nutrient input at this time is reflected in the high levels of protoperidiniacean cysts. However, general productivity is likely to have been lower in this zone than Zone DC-c because of the declining salinity. The low values of *I. caspiense* seem to be caused by reciprocally high values of protoperidiniacean cysts. The progressive decline in both *B. braunii*-type and reworked cysts probably relates to the expansion of the lake as it continued to fill, which will have caused rivers supplying freshwater to the lake to recede from the core site. Judging from low numbers of the cool-tolerant species *P. dalei*, spring surface-water temperatures were probably higher between 1230 AD and 1400 AD, implying relatively mild winters.

4.1.5. Zone DC-e (2.62–0.5 m: 1400–1800 AD)

The lower part of this zone represents a continuance of reduced salinities established at the top of Zone DC-d, marked by low levels of *L. machaerophorum* and high levels of *I. caspiense*. Conditions were comparable to those in DC-b, with salinity probably around 10–15 g kg⁻¹ or slightly less. The abrupt decline in protoperidiniacean cysts (causing a reciprocally abrupt increase in *I. caspiense*) might be explained in terms of a gradual lowering of salinity that abruptly exceeded the physiological limit of the protoperidiniaceans. Salinities were evidently increas-

ing through the lower part of Zone DC-e (1500 and 1600–1650 AD), as evidenced by increased values of *L. machaerophorum* and declining values of *I. caspiense*. This seems to have culminated in the gypsum layer G₃ in the middle of the zone. The upper part of Zone DC-e is more difficult to reconstruct but salinities were certainly above 10 g kg⁻¹, judging from the persistence of *L. machaerophorum*, yet remained brackish given the high values of *I. caspiense*.

4.1.6. Zone DC-f (0.5–0 m: 1800–1980 AD)

A return to progressively more saline conditions, as prevails today, is evidenced by an increase in *L. machaerophorum*, reduced levels of *I. caspiense*, and the formation of gypsum (G₄) within this zone. Also cooler spring surface-water temperatures following harsher winter conditions are reflected by higher abundances of cysts of *P. dalei* around 1900 AD.

4.2. Palaeoclimatic changes inferred from dinoflagellate cysts

Numerous previous studies indicate that climates of the Central Asian deserts and semi-deserts have experienced different changes from hyper-arid deserts to more humid semi-arid conditions at various temporal scales during the late Quaternary and Holocene (e.g. Tarasov et al., 1998; Velichko, 1989). During the past few thousand years these changes have resulted in multiple lake level changes (e.g. Létolle and Mainguet, 1993; Boomer et al., 2000; Boroffka et al., 2005). The present-day climate in western Central Asia is mainly controlled by the Westwind Drift carrying moist air to the mountain ranges which condenses as snow in the Pamir and Tien-Shan, the catchment areas of the two tributaries feeding the Aral Sea. Thus the meltwater discharged by Syr Darya and Amu Darya rivers largely controls the hydrological balance in the lake during late spring and early summer. In addition, local precipitation occurs during late winter and early spring when depressions, developing over the Eastern Mediterranean, subsequently move along a northeast trajectory where they may even replenish moisture over the Caspian Sea (Lioubimtseva, 2002). This adds to the water balance in the Aral Sea. Hence the relative abundance of reworked dinoflagellate cysts is expected to increase during periods of elevated sheet-wash from shore caused by enhanced moisture derived from the Mediterranean Sea. A third factor of importance, though difficult to quantify is the seasonally changing evaporation rate probably due to short-term changes in solar insolation. During the past few thousand years these

factors have exerted control on the water balance to varying degrees.

The dinoflagellate cyst record indicates prominent salinity increases during the intervals ca. 0–425 AD (or 100? BC–425 AD), 920–1230 AD, 1500 AD, 1600–1650 AD, 1800 AD and the modern increase (Fig. 11). The lowermost sequence (Zone DC-a, Unit 4), which represents the first few centuries AD, characterizes as a whole elevated salinity levels resulting in gypsum precipitation (G₁) during an important phase of lake level lowering (27–28 m a.s.l.; see Nurtaev, 2004). During this time period, salinity increases mainly occurred at around 0 AD, 100–200 AD and 350–425 AD, probably resulting from considerably lowered meltwater run-off supplied by the rivers due to lowered late spring and summer temperatures in the mountains of the high altitude catchment. This is contemporaneous with glacier expansion during 2100–1700 yr BP in the northern and western Tien Shan (Savoskul and Solomina, 1996) and in the Pamir-Alay mountains (Zech et al., 2000). Coevally, at approximately 2000 years BP, a lake level recession is reported from Lake Van (Turkey) based on detailed palaeoclimatological studies (Landmann et al., 1996; Lemcke and Sturm, 1996) that demonstrate a period of decreasing humidity beginning at about 3500 and culminating at 2000 years BP. Similarly in Syria (Bryson, 1996) and Israel (Schilman et al., 2002), declining rainfall leading to dry events is also reported at around 2000 years BP. The decrease of rainfall is possibly related to a waning of the low-pressure system that developed over the Eastern Mediterranean and/or to a shift of the trajectories bringing moist air from the Eastern Mediterranean to the Middle East and Western Central Asia. In the Aral Sea hinterland, low levels of rainfall are inferred from low abundances of reworked dinocysts hence suggesting reduced on-land sheet-wash too.

The causes driving the progressive increase in salinity at ca. 920–1230 AD (Middle Ages) may be climatically controlled as well. The increase in salinity is accompanied by a progressive and extensive lake-level fall of the Aral Sea, as a pronounced regression was also recorded in Tschebas Bay (Wünnemann et al., submitted for publication), thus reflecting long-term declining discharges from the Syr Darya and the Amu Darya rivers around 1200 AD. These results are fairly consistent with the tree-ring width record of Esper et al. (2002) (Fig. 11) and Mukhamedshin (1977), where several short-lasting events can be correlated with our salinity curve (Fig. 11). These authors report a notable decrease in ring width from 800 AD to 1250 AD, corresponding to a colder phase in the Tien Shan and

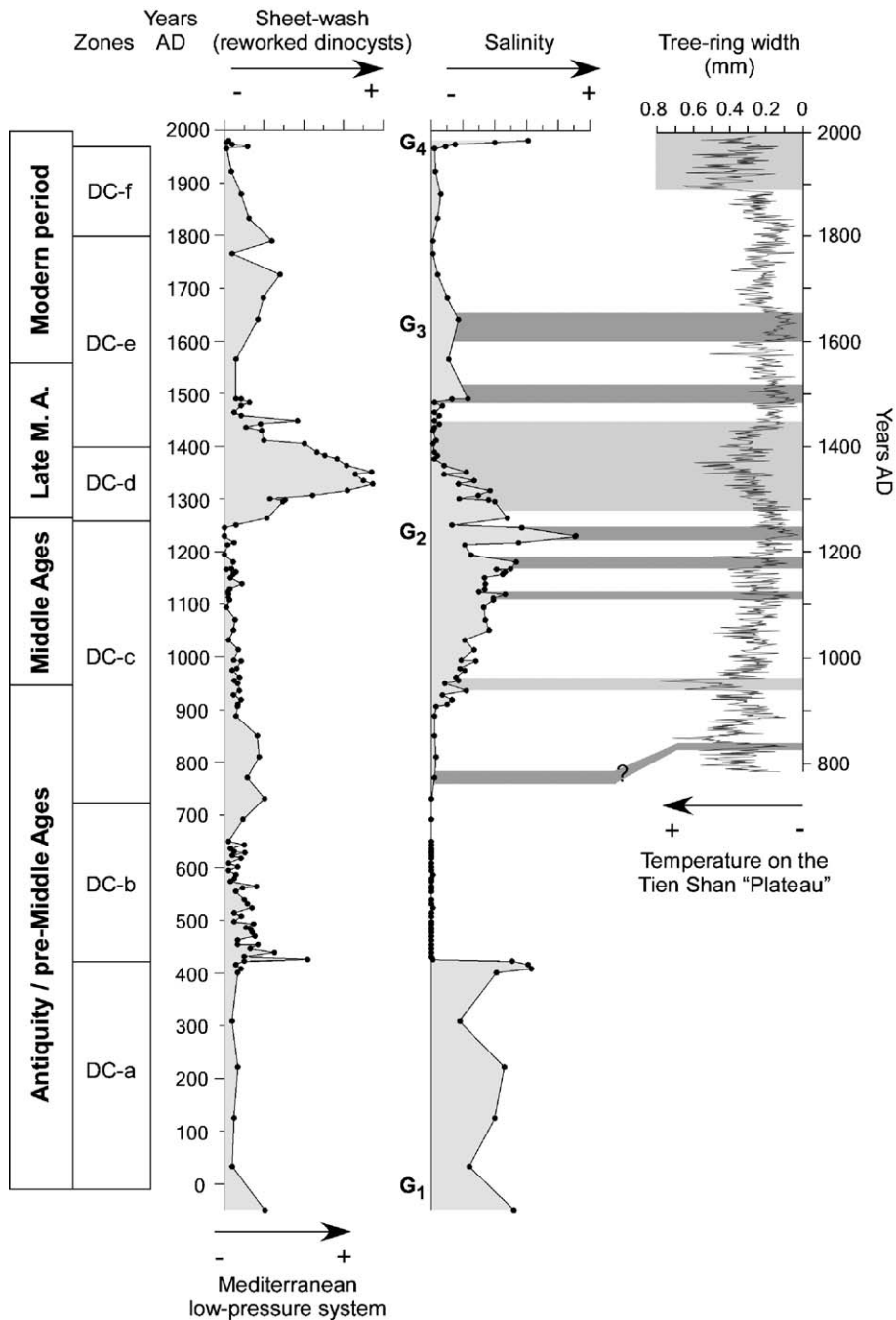


Fig. 11. Correlation of palaeoenvironmental changes during the last 2000 years as inferred from section CH2/1 with the tree-ring width record of Esper et al. (2002). The salinity reconstruction is estimated from the relative abundance of *L. machaerophorum*. Data are plotted according to the age model as detailed in Section 2.2 (Fig. 4). G₁ to G₄ refer to chemical precipitates of gypsum in section CH2/1 (see Section 2.1; Fig. 2).

Pamir-Alay mountains, respectively, with lowered late spring and summer temperatures. This is further supported by preliminary pollen analyses conducted on section CH2/1, which reflects cool and arid conditions in the Aral Sea Basin after 1000 AD. This aridification

of the climate matches relatively well with variations observed in the western Tibetan Plateau by Bao et al. (2003). From air-temperature reconstructions, these authors report warming conditions during the intervals 800–1050 AD and 1250–1400 AD (Medieval Warm/

Wet Period) with a short colder phase during ca. 1050–1250 AD, and especially at around 1200 AD. The salinity increase intervening between 920 AD and 1230 AD in our record is accompanied by very low abundances of reworked dinoflagellate cysts (Fig. 11) suggesting again considerably reduced sheet-wash from the shore and thus lowered moisture derived from the Eastern Mediterranean region during the late winter and early spring seasons. This is well-supported through palaeoenvironmental records from the Eastern Mediterranean Sea (Issar et al., 1990; Schilman et al., 2002) that document colder conditions resulting in a decrease of evaporation and reduced rainfall as inferred from $\delta^{18}\text{O}$ variations of pelagic foraminifera and carbonate cave deposits (Soreq cave, Israel).

A progressive decrease in salinity (oligo-/mesosaline conditions) and a return to higher lake levels characterize the period 1230–1450 AD. Coevally, tree-ring width conspicuously increased, growing at similar rates during ca. 1360–1370 AD to those observed for the last 100 years (Esper et al., 2002). This is further confirmed by Kotlyakov et al. (1991) who reported a warming phase between the 11th and 14th–15th centuries, based on tree-ring data from the Tien Shan. Increased growing rates thus characterize higher temperatures in the mountains that result in elevated meltwater discharges to the Aral Sea in late spring/early summer. Moreover, higher abundances of reworked dinoflagellate cysts of Neogene/late Quaternary ages reflect enhanced regional spring precipitation in Central Asia from 1230–1400 AD. They document the intensified erosion of shore sediments which occurred frequently during extreme sheet-wash events linked to intensified low pressure systems over the Eastern Mediterranean. The latter is confirmed by Schilman et al. (2002) who documented higher rainfall over Israel between 1250 AD and 1500 AD.

Similarly, the two slight increases in salinity as recorded at ca. 1500 AD and 1600–1650 AD from the dinoflagellate cysts are probably climatically driven as well. The interval from 1500 to ca. 1650 AD includes the coldest decades according to the mean annual temperature reconstruction for the Northern Hemisphere (Bradley, 2000). New archaeological findings from the south Aral Sea (Boroffka et al., 2005; Shirinov et al., 2004) indicate that the lake level lowered to as much as 31 m a.s.l. at that time. A similar brief drying event has been reported at about 1650 AD by Boomer et al. (2003) from their studies on ostracods. Besides, these events are well-constrained with other records from Central Asia. Two successive decreases in tree-ring width are reported

from Esper et al. (2002) between 1500 AD and 1600–1650 AD. These events match well with two salinity increases in the Aral Sea (Fig. 11) and reflect reduced meltwater inflow from the catchment area. This also closely matches a cooler phase from the Western Tibetan Plateau at ca. 1500–1550 AD and 1600–1650 AD when glaciers advanced on the southern Tibetan Plateau (Bao et al., 2003). We thus propose that this event widely expressed north of 35°N may correspond to a short-lived Little Ice Age signature in the Aral Sea sediments.

After 1650 AD, salinity slightly fluctuated around lower levels (oligo-/mesosaline conditions) suggesting higher lake levels up to 1900 AD, with nevertheless a short-lasting salinity increase around 1800 AD. This is again consistent with the tree-ring record for this time window (Esper et al., 2002), where climatic conditions appear relatively favourable for growth, except around 1800 AD where a decrease in the tree-ring width can be observed. Precipitation frequency, as inferred from the reworked dinoflagellate cysts, fluctuated slightly during this period, with probably higher rainfall at ca. 1650 and 1700 AD, but declined afterwards. Near to the top of section CH2/1, a strong environmental shift (Zone DC-f; Figs. 4 and 11) documents the onset of the modern lake level regression. Though this disaster is mostly due to the intensification of irrigation in the hinterland since the early 1960s, instrumental data already document a lake whose level was starting to lower in the late 1950s (Krivonogov, pers. comm., 2005).

4.3. Human influence on hydrography

Climate variability is probably the dominant factor controlling the hydrology in western Central Asia and thus the salinity in the Aral Sea, but one might expect human influence (irrigation activities) to also have exerted an important role in this densely settled region along the Silk Route during the past 2000 years. Since Early Antiquity (4th–2nd centuries BC) up to the pre-Islamic Middle Ages (4th–6th centuries AD), water from the Syr Darya and the Amu Darya rivers has been used on a large scale for irrigation, mostly in open canals (see Boroffka et al., 2005, *in press*). According to Létolle and Mainguet (1993), the hydraulic installations on the Amu Darya were completely destroyed after the invasion of Mongol warriors (the Huns Hephtalites) around 380–400 AD. Thus at that time the Aral Sea was reported to be cut-off from its main source of freshwater. Historical reports from Greek sources (Barthold, 1910) further indicate that

the Amu Darya discharged into the Caspian Sea during this period. However, this event may not be at the origin of the lake regression observed at ca. 2000 years BP because a time lag of almost 400 years would be implied. Instead it may have only amplified the retreat of the water body witnessed by an aridification in Central Asia. Similar considerations may be regarded concerning the period 920–1230 AD (Zone DC-c), which records the Middle Ages' regression. Although irrigation gradually declined up to the 13th century AD (Boroffka et al., 2005), historical reports document a total destruction of the hydraulic installations in the Khorezm region after Genghis Khan's invasion documented at 1221 AD (Létolle and Mainquet, 1993). This catastrophic event led again to a severing of the Amu Darya from the Aral Sea, which was reported as discharging into the Caspian Sea at that time. Nonetheless, our dinoflagellate cyst record rather reflects a gradual regressive phase which would not match with a catastrophic event resulting from the destruction of dams in the Amu Darya delta. We thus propose that the progressive lake level lowering inferred for the period 920–1230 AD is again most probably climatically driven, but that human activities might have further strengthened the lake level fall.

5. Conclusions

This is the first ecostratigraphic study using dinoflagellate cysts from the late Quaternary of the Aral Sea and has led to an improved understanding of the mechanisms that control environmental changes in the Aral Sea during the Late Holocene. It has also helped to unravel the influence of climate and anthropogenic activities on the hydrographic development of the Aral Sea during the past 2000 years. The results suggest that the successive lake level fluctuations are indeed climatically triggered, and result from different factors controlling the water balance in Central Asia, notably the Westwind Drift controlling temperatures in the montane regions, and local to regional rainfall sourced by migrating moisture from the Eastern Mediterranean Sea. Other factors may have influenced climate conditions over the Aral Sea Basin, such as variable solar activity, as suggested by Crowley (2000) based on climate-modelled simulations over the Northern Hemisphere. Testing this proposal would require higher-resolution analyses than presently undertaken. However, the degree of lake-level lowering may have been amplified by humans responding to changing environmental conditions. Irrigation systems were probably extended during periods of more arid

conditions. Documentary evidence shows the existence of irrigation activities already during Early Classical Antiquity (before 0 BC) (Boroffka et al., 2005), indicating that lake water levels strongly depended on climate conditions at that time too. As to changes during the early to middle Holocene, ongoing research aims to unravel the respective impacts of climate and tectonics on the hydrology of the Aral Sea ecosystem.

Acknowledgments

The CLIMAN project is funded by the INTAS organization of the European Union (Project No. Aral 00-1030) and the German Science Foundation (DFG Project 436 RUS 111/663-OB 86/4). We are grateful for this support. We wish to thank especially Dr. Francois Demory for excellent support in the field. We acknowledge Dr. Gilles Escarguel, Dr. Jean-Jacques Cornée, Dr. Pierpaolo Zuddas and Samuel Mailhot (University Claude Bernard—Lyon 1) for valuable discussions and insights. The manuscript reviewers are also acknowledged for helping to improve the paper.

References

- Aksu, A.E., Yasar, D., Mudie, P.J., 1995a. Palaeoclimatic and paleoceanographic conditions leading to development of sapropel layer S1 in the Aegean Sea. *Palaeogeography, Palaeoclimatology, Palaeoecology* 116, 71–101.
- Aksu, A.E., Yasar, D., Mudie, P.J., Gillespie, H., 1995b. Late glacial–Holocene paleoclimatic and paleoceanographic evolution of the Aegean Sea: micropaleontological and stable isotope evidence. *Marine Geology* 123, 33–59.
- Aleshinskaya, Z.V., Tarasov, P.E., Harrison, S.P., 1996. Aral Sea, Kazakhstan–Uzbekistan. *Lake Status Records FSU and Mongolia*, p. 108–114.
- Baltes, N., 1971a. Tertiary plant microfossil assemblages from the Pannonian depression (Rumania) and their paleoecology. *Review of Palaeobotany and Palynology* 11, 125–158.
- Baltes, N., 1971b. Pliocene dinoflagellata and acritarcha in Romania. In: Farinacci, A. (Ed.), *Proceedings, Second Planktonic Conference, Rome vol. 1970 (1)*. Edizioni Tecnoscienza, Rome, pp. 1–19.
- Bao, Y., Bräuning, A., Yafeng, S., 2003. Late Holocene temperature fluctuations on the Tibetan Plateau. *Quaternary Science Reviews* 22, 2335–2344.
- Barthold, W., 1910. *Nachrichten über den Aral-See und den unteren Lauf des Amu-darja von den ältesten Zeiten bis zum XVII. Jahrhundert. Quellen und Forschungen zur Erd- und Kulturkunde vol. 2*. Otto Wigand m.b.H., Leipzig.
- Batten, D.J., Grenfell, H.R., 1996. Green and blue-green algae. 7D—*Botryococcus*. In: Jansonius, J., McGregor, D.C. (Eds.), *Palynology: Principles and Applications vol. 1*. American Association of Stratigraphic Palynologists Foundation, Dallas, Texas, pp. 205–214.
- Bold, H.C., Wynne, M.J., 1985. *Introduction to the Algae*, (2nd edition). Prentice-Hall, Englewood Cliffs, NJ. 720 pp.

- Boomer, I., Aladin, N., Plotnikov, I., Whatley, R., 2000. The palaeolimnology of the Aral Sea: a review. *Quaternary Science Reviews* 19, 1259–1278.
- Boomer, I., Home, D.J., Slipper, I., 2003. The use of ostracodes in palaeoenvironmental studies, or What can you do with an ostracod shell? *Palaeontological Society Papers* 9, 153–180.
- Boroffka, N.G.O., Oberhänsli, H., Achatov, G.A., Aladin, N.V., Bapakov, K.M., Erzhanova, A., Hoernig, A., Krivonogov, S.K., Lobas, D.A., Savel'eva, T.V., Wuennemann, B., 2005. Human settlements on the northern shores of lake Aral and water level changes. *Mitigation and Adaptation Strategies for Global Change* 10, 71–85.
- Boroffka, N.G.O., Oberhänsli, H., Sorrel, P., Reinhardt, C., Wünnemann, B., Alimov, K., Baratov, S., Rakhimov, K., Saparov, N., Shirinov, T., Krivonogov, S.K., in press. *Archaeology and climate: Settlement and lake level changes at the Aral Sea*. *Geoarchaeology*.
- Bortnik, V.N., Chistyayeva, S.P. (Eds.), 1990. *Hydrometeorology and hydrochemistry of the USSR seas, The Aral Sea vol. VII*. *Gidrometeoizdat, Leningrad*. 196 pp. (in Russian).
- Bradford, M.R., Wall, D.A., 1984. The distribution of Recent organic-walled dinoflagellate cysts in the Persian Gulf, Gulf of Oman, and northwestern Arabian Sea. *Palaeontographica Abteilung B Paläophytologie* 192, 16–84.
- Bradley, R.S., 2000. 1000 years of climate change. *Science* 288, 1353–1354.
- Brenner, W.W., 2001. Organic-walled microfossils from the central Baltic Sea, indicators of environmental change and base for ecostratigraphic correlation. *Baltica* 14, 40–51.
- Brodskaya, I.G., 1952. *Data and Processes on Sedimentary Deposits of the Aral Sea*. tr. In-Ta Geol. Nauk, AN SSSR vol. 115. 140 pp. (in Russian).
- Bryson, R.A., 1996. Proxy indications of Holocene winter rains in southwest Asia compared with simulated rainfall. In: Dalfes, H.N., Kukla, G., Weiss, H. (Eds.), *Third Millennium BC: Climate Change and Old World Collapse*, NATO ASI Series I vol. 49. Springer Verlag, pp. 465–473.
- Cleve, P.T., 1900. The plankton of the North Sea, the English Channel, and the Skagerrak in 1898. *Kungl. Svenska Vetenskapsakademien Handlingar* 32 (8), 1–53.
- Cour, P., 1974. Nouvelles techniques de détection des flux et de retombées polliniques: étude de la sédimentation des pollens et des spores à la surface du sol. *Pollen et Spores* 23 (2), 247–258.
- Crowley, T.J., 2000. Causes of climate change over the past 1000 years. *Science* 289, 270–277.
- Dale, B., 1996. Dinoflagellate cyst ecology: modelling and geological applications. In: Jansonius, J., McGregor, D.C. (Eds.), *Palynology: Principles and Applications* vol. 3. American Association of Stratigraphic Palynologists Foundation, Dallas TX, pp. 1249–1275.
- Dale, B., 2001. The sedimentary record of dinoflagellate cysts: looking back into the future of phytoplankton blooms. *Scientia Marina* 65 (Suppl. 2), 257–272.
- Dale, B., Gjellsa, A., 1993. Dinoflagellate cysts as paleoproductivity indicators: state of the art, potential, and limits. In: Zahn, R., Pedersen, T.F., Kaminski, M.A., Labeyrie, L. (Eds.), *Carbon Cycling in the Glacial Ocean: Constrains on the Ocean's Role in Global Change: Quantitative Approaches in Paleoceanography*, NATO ASI Series I, Global Environmental Change. Springer, Berlin, pp. 521–537.
- Deflandre, G., Cookson, I.C., 1955. Fossil microplankton from Australian Late Mesozoic and Tertiary sediments. *Australian Journal of Marine and Freshwater Research* 6, 242–313.
- de Vernal, A., Henry, M., Matthiessen, J., Mudie, P.J., Rochon, A., Boessenkool, K.P., Eynaud, F., Grösfeld, K., Guiot, J., Hamel, D., Harland, R., Head, M.J., Kunz-Pirring, M., Levac, E., Loucheur, V., Peyron, O., Pospelova, V., Radi, T., Turon, J.-L., Voronina, E., 2001. Dinoflagellate cyst assemblages as tracers of sea-surface conditions in the northern North Atlantic, Arctic and sub-Arctic seas: the new 'n=677' data base and its application for quantitative palaeoceanographic reconstruction. *Journal of Quaternary Sciences* 16, 681–698.
- Esper, J., Schweingruber, F.H., Winiger, M., 2002. 1300 years of climate history for Western Central Asia inferred from tree-rings. *Holocene* 12, 267–277.
- Friedrich, J., Oberhänsli, H., 2004. Hydrochemical properties of the Aral Sea water in summer 2002. *Journal of Marine Systems* 47, 77–88.
- Gundersen, N., 1988. En palynologisk undersøkelse av dinoflagellatcyster langs en synkende salinitetsgradient i recente sedimenter fra Østersjø-området. *Cand. Scient. Dissertation, Geologisk Institutt, Universitetet i Oslo*.
- Hallett, R.I., 1999. Consequences of environmental change on the growth and morphology of *Lingulodinium polyedrum* (Dinophyceae) in culture. PhD Thesis, University of Westminster, London.
- Harland, R., 1977. Recent and Late Quaternary (Flandrian and Devensian) dinoflagellate cysts from marine continental shelf sediments around the British Isles. *Palaeontographica Abteilung B Paläophytologie* 164, 87–126.
- Head, M.J., Seidenkrantz, M.-S., Janczyk-Kopikowa, Z., Marks, L., Gibbard, P.L., 2005. Last Interglacial (Eemian) hydrographic conditions in the southeastern Baltic Sea, NE Europe, based on dinoflagellate cysts. *Quaternary International* 130, 3–30.
- Heim, C., 2005. Die Geochemische Zusammensetzung der Sedimente im Aralsee und Sedimentationsprozesse während der letzten 100 Jahre. Diploma thesis, Alfred-Wegener-Institut Bremerhaven.
- Hensen, V., 1887. Über die Bestimmung des Planktons oder des im Meere treibenden Materials an Pflanzen und Thieren. *Berichte der Kommission zur wissenschaftlichen Untersuchung der deutschen Meere in Kiel* 5, 107.
- Issar, A.S., Govrin, Y., Geyh, A.M., Wakshal, E., Wolf, M., 1990. Climate changes during the upper Holocene in Israel. *Israel Journal of Earth Sciences* 40, 219–223.
- Kloosterboer-van Hoeve, M.L., Steenbrink, J., Brinkhuis, H., 2001. A short-term cooling event, 4.205 million years ago, in the Ptolemais basin, northern Greece. *Palaeogeography, Palaeoclimatology, Palaeoecology* 173, 61–73.
- Kokinos, J.P., Anderson, D.M., 1995. Morphological development of resting cysts in cultures of the marine dinoflagellate *Lingulodinium polyedrum* (= *L. machaerophorum*). *Palynology* 19, 143–166.
- Kotlyakov, V.M., Serebryanny, R., Solomina, O.N., 1991. Climate change and glacier fluctuation during the last 1000 years in the southern mountains of the USSR. *Mountain Research and Development* 11 (1), 1–12.
- Kouli, K., Brinkhuis, H., Dale, B., 2001. *Spiniferites cruciformis*: a fresh water dinoflagellate cyst? Review of Palaeobotany and Palynology 133, 273–286.
- Kunz-Pirring, M., 1998. Rekonstruktion der Oberflächenwassermassen der östlichen Laptevsee im Holozän anhand von aquatischen Palynomorphen. *Berichte zur Polarforschung* 281, 1–117.
- Kunz-Pirring, M., 1999. Distribution of aquatic palynomorphs in surface sediments from the Laptev Sea, Eastern Arctic Ocean. In: Kassens, H., Bauch, H.A., Dmitrenko, I., et al., (Eds.), *Land-Ocean Systems in the Siberian Arctic: Dynamics and History*. Springer-Verlag, Berlin, pp. 561–575.

- Landmann, G., Reimer, A., Lemcke, G., Kempe, S., 1996. Dating late glacial abrupt climate changes in the 14,570-yr long continuous varve record of Lake Van, Turkey. *Palaeogeography, Palaeoclimatology, Palaeoecology* 122, 107–118.
- Leegaard, C., 1920. Microplankton from the Finnish waters during the month of May 1912. *Acta Societatis Scientiarum Fennicae* 48, 1–44.
- Lemcke, G., Sturm, M., 1996. ^{18}O and trace element measurements as proxy for the reconstruction of climate changes at Lake Van (Turkey). In: Dalfes, H.N., Kukla, G., Weiss, H. (Eds.), *Third Millennium BC; Climate Change and Old World Collapse*, NATO ASI Series I vol. 49. Springer Verlag, pp. 653–678.
- Létoille, R., Mainguet, M., 1993. Aral. Springer Verlag, Paris.
- Lewis, J., Hallett, R., 1997. *Lingulodinium polyedrum* (*Gonyaulax polyedra*) a blooming dinoflagellate. *Oceanography and Marine Biology: An Annual Review* 35, 97–161.
- Lioubimtseva, E., 2002. Arid environments. In: Shahgedanova, M. (Ed.), *Physical Geography of Northern Eurasia*. Oxford University Press, Oxford. 571 pp.
- Maev, E.G., Karpychev, Yu, A., 1999. Radiocarbon dating of bottom sediments in the Aral Sea: age deposits and sea level fluctuations. *Water Resources* 26/2, 187–194.
- Marret, F., Zonneveld, K.A.F., 2003. Atlas of modern organic-walled dinoflagellate cyst distribution. *Review of Palaeobotany and Palynology* 125, 1–200.
- Marret, F., Leroy, S., Chalié, F., Gasse, F., 2004. New organic-walled dinoflagellate cysts from recent sediments of Central Asian seas. *Review of Palaeobotany and Palynology* 129, 1–20.
- Matthiessen, J., Kunz-Pirrung, M., Mudie, P.J., 2000. Freshwater chlorophycean algae in recent marine sediments of the Beaufort, Laptev and Kara Seas (Arctic Ocean) as indicators of river runoff. *International Journal of Earth Sciences* 89, 470–485.
- Meunier, A., 1910. *Microplankton des Mers de Barents et de Kara*. Charles Bulens, Imprimerie Scientifique, Bruxelles.
- Mirabdullayev, I.M., Joldasova, I.M., Mustafaeva, Z.A., Kazakhbaev, S.K., Lyubimova, S.A., Tashmukhamedov, B.A., 2004. Succession of the ecosystems of the Aral Sea during its transition from oligosaline to polyhaline conditions. *Journal of Marine Systems* 47, 101–107.
- Mudie, P.J., 1992. Circum-arctic Quaternary and Neogene marine palynofloras: paleoecology and statistical analysis. In: Head, M.J., Wrenn, J.H. (Eds.), *Neogene and Quaternary Dinoflagellate Cysts and Acritarchs*. American Association of Stratigraphic Palynologists, Foundation, Dallas, TX, pp. 347–390.
- Mudie, P.J., Aksu, A.E., Duman, M., 1998. Late Quaternary dinocysts from the Black, the Marmara and Aegean seas: variations in assemblages, morphology and paleosalinity. In: Smelror, M. (Ed.), *Abstracts from the Sixth International Conference on Modern and Fossil Dinoflagellates* Dino 6, Trondheim, June 1998, Norges teknisk-naturvitenskapelige universitet Vitenskapsmuseet, Rapport botanisk serie vol. 1998-1.
- Mudie, P.J., Aksu, A.E., Yasar, D., 2001. Late Quaternary dinoflagellates cyst distribution. *Review of Palaeobotany and Palynology* 125, 1–200.
- Mudie, P.J., Rochon, A., Aksu, A.E., Gillespie, H., 2002. Dinoflagellate cysts, freshwater algae and fungal spores as salinity indicators in Late Quaternary cores from Marmara and Black seas. *Marine Geology* 190, 203–231.
- Mukhamedshin, K.D., 1977. Tien Shan juniper forests and their economic significance (Archevniki Tian'-Shanya I ikh lesokhoziaistvennoye znachenije). Ilim, Frunze.
- Nehring, S., 1994. Spatial distribution of dinoflagellate resting cysts in recent sediments of Kiel Bight, Germany (Baltic Sea). *Ophelia* 39, 137–158.
- Nourgaliev, D.K., Heller, F., Borisov, A.S., Hajdas, I., Bonani, G., Iassonov, P.G., Oberhänsli, H., 2003. Very high resolution paleosecular variation record for the last 1200 years from the Aral Sea. *Geophysical Research Letters* 30 (17), 4-1–4-4.
- Nurtaev, B., 2004. Aral Sea Basin evolution: geodynamic aspect. In: Nihoul, J.C.J., Zavialov, P.O., Micklin, Ph.P. (Eds.), *Dying and Dead Seas: Climatic Anthropogenic Causes*. Proceedings of the NATO Advanced Research Workshop, Liège, Belgium, 7–10 May, 2003, Nato Science Series: IV. Earth and Environmental Sciences vol. 36. Springer-Verlag, Berlin, pp. 91–97.
- Parra Barientos, O.O., 1979. Revision der Gattung *Pediastrum* Meyen (Chlorophyta). *Bibliotheca Phycologia* 48 (1-186), 1–55.
- Popescu, S.-M., 2001. Végétation, climat et cyclostratigraphie en Paratéthys centrale au Miocène supérieur et au Pliocène inférieur d'après la palynologie. Thèse de doctorat, Université Claude Bernard—Lyon 1.
- Popescu, S.-M., in press. Upper Miocene and Lower Pliocene environments in the southwestern Black Sea region from high-resolution palynology of DSDP site 380A (Leg 42B). *Palaeogeography, Palaeoclimatology, Palaeoecology*.
- Reimer, P.J., Baillie, M.G.L., Bard, E., Bayliss, A., Beck, J.W., Bertrand, C.J.H., Blackwell, P.G., Buck, C.E., Burr, G.S., Cutler, K.B., Damon, P.E., Lawrence Edwards, R., Fairbanks, R.G., Friedrich, M., Guilderson, T.P., Hogg, A.G., Hughen, K.A., Kromer, B., McCormac, G., Manning, S., Bronk Ramsey, C., Reimer, R.W., Remmele, S., Southon, J.R., Stuiver, M., Talamo, S., Taylor, F.W., van der Plicht, J., Weiyhenmeyer, C.E., 2004. IntCal04 terrestrial radiocarbon age calibration, 0–26 cal. yr BP. *Radiocarbon* 46 (3), 1029–1058.
- Rochon, A., de Vernal, A., Turon, J.-L., Matthiessen, J., Head, M.J., 1999. Distribution of Recent Dinoflagellate Cysts in Surface Sediments from the North Atlantic Ocean and Adjacent Seas in Relation to Sea-Surface Parameters. *American Association of Stratigraphic Palynologists, Contributions Series No. 35*, pp. 1–150.
- Savoskul, O.S., Solomina, O.N., 1996. Late Holocene glacier variations in the frontal and inner ranges of the Tien Shan, central Asia. *The Holocene* 6 (1), 25–35.
- Schilman, B., Ayalon, A., Bar-Matthews, M., Kagan, E.J., Almogil-Labin, A., 2002. Sea–land palaeoclimate correlation in the eastern Mediterranean region during the Late Holocene. *Israel Journal of Earth Sciences* 51, 181–190.
- Shirinov, T., Alimov, K., Baratov, S., Rakhimov, K., Saporov, N., Boroffka, N., Vjunnemann, B., Rajnkhardt, Khr., Sorrel, P. and Krivonogov, S., 2004. Polevye raboty po proektu INTAS Aral No. 00-130: “Klimaticheskie izmenenija v epochu golocena i razvitie poselenij cheloveka v bassejne Aral'skogo Morja” “Holocene climatic variability and evolution of human settlement in the Aral Sea basin (CLIMAN)”. *Arkeologicheskie issledovanija v Uzbekistane* 2003 goda, 4, 197–205.
- Tarasov, P.E., Webb III, T., Andreev, A.A., Afanas'eva, N.B., Berezina, N.A., Bezusko, L.G., Blyakharchuk, T.A., Bolikhovskaya, N.S., Cheddadi, R., Chernavskaya, M.M., Chernova, G.M., Dorofeyuk, N.I., Dirksen, V.G., Elina, G.A., Filimonova, L.V., Glebov, F.Z., Guiot, J., Gunova, V.S., Harrison, S.P., Jolly, D., Khomutova, V.I., Kvavadze, E.V., Osipova, I.M., Panova, N.K., Prentice, I.C., Saarse, L., Sevastyanov, D.V., Volkova, V.S., Zernitskaya, V.P., 1998. Present-day and mid-Holocene biomes reconstructed from pollen and plant macrofossil data from the

- former Soviet Union and Mongolia. *Journal of Biogeography* 25, 1029–1053.
- Tchepaliga, A., 2004. Late Glacial great flood in the Black Sea and Caspian Sea. Geological Society of America Annual Meeting, Seattle, 2–5 November 2003, Abstract, session No 189.
- Velichko, A.A., 1989. The relationship of the climatic changes in the high and low latitudes of the Earth during the Late Pleistocene and Holocene. In: Velichko, A.A., et al., (Eds.), *Paleoclimates and Glaciation in the Pleistocene*. Nauka Press, Moscow, pp. 5–19.
- Wall, D., Dale, B., 1966. “Living fossils” in Western Atlantic plankton. *Nature* 211 (5053), 1025–1026.
- Wall, D., Dale, B., 1974. Dinoflagellates in late Quaternary deep-water sediments of the Black Sea. In: Degens, R.T., Ross, D.A. (Eds.), *The Black Sea—Geology, Chemistry and Biology*, Memoir vol. 20. American Association of Petroleum Geologists, pp. 364–380.
- Wall, D., Dale, B., Harada, K., 1973. Description of new fossil dinoflagellates from the Late Quaternary of the Black Sea. *Micropaleontology* 19, 18–31.
- Wünnemann, B., Riedel, F., Keyser, D., Reinhardt, C., Pint, A., Sorrel, P., Oberhänsli, H., submitted for publication. The limnological development of the Aral Sea since the early Middle Ages inferred from sediments and aquatic organism. *Quaternary Research*.
- Zavialov, P.O., 2005. *Physical Oceanography of the Dying Aral Sea*. Springer Verlag, Chichester, UK. 146 pp.
- Zavialov, P.O., Kostianoy, A.G., Emelianov, S.V., Ni, A.A., Ishniyazov, D., Khan, V.M., Kudyshkin, T.V., 2003. Hydrographic survey in the dying Aral Sea. *Geophysical Research Letters* 30 (13), 2.1–2.4.
- Zech, W., Glaser, B., Ni, A., Petrov, M., Lemzin, I., 2000. Soils as indicators of the Pleistocene and Holocene landscape evolution in the Alay Range (Kyrgyzstan). *Quaternary International* 65/66, 161–169.
- Zonneveld, K.A.F., Versteegh, G.J.M., de Lange, G.J., 2001. Palaeo-productivity and post-depositional aerobic matter decay reflected by dinoflagellate cyst assemblages of the Eastern Mediterranean S1 sapropel. *Marine Geology* 172, 181–195.

Corrigendum

Corrigendum to “Hydrographic development of the Aral Sea during the last 2000 years based on a quantitative analysis of dinoflagellate cysts”

P. Sorrel ^{a,b}, S.-M. Popescu ^b, M.J. Head ^{c,*}, J.P. Suc ^b, S. Klotz ^{b,d}, H. Oberhänsli ^a

^a *GeoForschungsZentrum, Telegraphenberg, D-14473 Potsdam, Germany*

^b *Laboratoire PaléoEnvironnements et Paléobiosphère (UMR CNRS) 5125, Université Claude Bernard – Lyon 1, 27–43, boulevard du 11 Novembre, 69622 Villeurbanne Cedex, France*

^c *Department of Earth Sciences, Brock University, 500 Glenridge Avenue, St. Catharines, Ontario, Canada L2S 3A1*

^d *Institut für Geowissenschaften, Universität Tübingen, Sigwartstrasse 10, 72070 Tübingen, Germany*

Accepted 16 May 2006

A recent publication by Sorrel et al. (2006) on the hydrographic development of the Aral Sea during the last 2000 years refers in the Abstract to a “low pressure system that develops over the Eastern Mediterranean and brings moist air to the Middle East and Central Asia during late spring and summer”. In fact, the timing of seasonal rainfall is during late winter and spring, and not late spring and summer as published. This error is not duplicated elsewhere in the publication, but its presence in the Abstract is sufficiently prominent to warrant correction here.

Pollen evidence from the Aral Sea (Sorrel et al., in press) supports arguments that the North Atlantic oscillation, when in negative mode, is a controlling factor for humidity reaching Central Asia (Mann, 2002). Hence, moisture loading can only occur in the eastern Mediterranean during late winter and early spring (Hurrell, 1995; Hurrell and van Loon, 1997; Hurrell et al., 2003). The moist air follows a WSW–WNE trajectory where it subsequently reaches the Middle East (Cullen et al., 2002) and the Aral Sea Basin (Aizen et al., 2001; Lioubimtseva, 2002).

References

- Aizen, E.M., Aizen, V.B., Melack, J.M., Nakamura, T., Ohta, T., 2001. Precipitation and atmospheric circulation patterns at mid-latitudes of Asia. *International Journal of Climatology* 21, 535–556.
- Cullen, H.M., Kaplan, A., Arkin, P.A., de Menocal, P.B., 2002. Impact of the North Atlantic Oscillation on Middle Eastern climate and streamflow. *Climatic Change* 55, 315–338.
- Hurrell, J.W., 1995. Decadal trends in the North Atlantic Oscillation: regional temperatures and precipitation. *Science* 269, 676–679.
- Hurrell, J.W., van Loon, H., 1997. Decadal variations in climate associated with the North Atlantic Oscillation. *Climate Change* 36, 301–326.
- Hurrell, J.W., Kushnir, Y., Ottensen, G., Visbeck, M., 2003. An overview of the North Atlantic Oscillation. In: Hurrell, J.W., Kushnir, Y., Ottensen, G., Visbeck, M. (Eds.), *The North Atlantic Oscillation: Climate Significance and Environmental Impact*. Geophysical Monograph Series, vol. 134, pp. 1–36. Washington DC.
- Lioubimtseva, E., 2002. Arid environments. In: Shahgedanova, M. (Ed.), *Physical Geography of Northern Eurasia*. Oxford University Press, Oxford. 571 pp.
- Mann, M.E., 2002. Large-scale climate variability and connections with the Middle East in the past. *Climatic Change* 55, 287–314.
- Sorrel, P., Popescu, S.-M., Head, M.J., Suc, J.P., Klotz, S., Oberhänsli, H., 2006. Hydrographic development of the Aral Sea during the last 2000 years based on a quantitative analysis of dinoflagellate cysts. *Palaeogeography, Palaeoclimatology, Palaeoecology*.
- Sorrel, P., Popescu, S.-M., Klotz, S., Suc, J.P., Oberhänsli, H., in press. Climate variability in the Aral Sea Basin (Central Asia) during the late Holocene. *Quaternary Research*.

DOI of original article: [10.1016/j.palaeo.2005.10.012](https://doi.org/10.1016/j.palaeo.2005.10.012)

* Corresponding author.

E-mail address: mjhead@brocku.ca (M.J. Head).

Climate variability in the Aral Sea basin (Central Asia) during the late Holocene based on vegetation changes

Philippe Sorrel^{a,*}, Speranta-Maria Popescu^b, Stefan Klotz^{b,c}, Jean-Pierre Suc^b, Hedi Oberhänsli^a

^a *GeoForschungsZentrum Potsdam, Telegraphenberg, D-14473 Potsdam, Germany*

^b *Laboratoire PaléoEnvironnements et PaléobioSphère (UMR 5125 CNRS), Université Claude Bernard-Lyon 1, 27–43 boulevard du 11 Novembre, F-69622 Villeurbanne Cedex, France*

^c *Institut für Geowissenschaften, Universität Tübingen, Sigwartstrasse 10, D-72070 Tübingen, Germany*

Received 21 November 2006

Available online 25 January 2007

Abstract

High-resolution pollen analyses (~50 yr) from sediment cores retrieved at Chernyshov Bay in the NW Large Aral Sea record shifts in vegetational development from subdesertic to steppe vegetation in the Aral Sea basin during the late Holocene. Using pollen data to quantify climatic parameters, we reconstruct and date for the first time significant changes in moisture conditions in Central Asia during the past 2000 yr. Cold and arid conditions prevailed between ca. AD 0 and 400, AD 900 and 1150, and AD 1500 and 1650 with the extension of xeric vegetation dominated by steppe elements. These intervals are characterized by low winter and summer mean temperatures and low mean annual precipitation ($P_{\text{mm}} < 250$ mm/yr). Conversely, the most suitable climate conditions occurred between ca. AD 400 and 900, and AD 1150 and 1450, when steppe vegetation was enriched by plants requiring moister conditions ($P_{\text{mm}} \sim 250$ –500 mm/yr) and some trees developed. Our results are fairly consistent with other late Holocene records from the eastern Mediterranean region and the Middle East, showing that regional rainfall in Central Asia is predominantly controlled by the eastern Mediterranean cyclonic system when the North Atlantic Oscillation (NAO) is in a negative phase. © 2006 University of Washington. All rights reserved.

Keywords: Pollen analysis; Vegetation; Climate; Aral Sea; Late Holocene; Central Asia; Negative NAO

Introduction

Numerous biostratigraphic, geomorphological and archaeological proxy data document that climate of Central Asian deserts and semi-deserts experienced many changes at various time scales through the Pleistocene and Holocene (e.g., Velichko, 1989; Tarasov et al., 1998a; Boomer et al., 2000; Boroffka et al., 2005, 2006). Climatic variations resulted in multiple shifts from hyper-arid to semi-arid deserts and even steppe vegetations with development of shrubs (Kremenetski and Tarasov, 1997; Kremenetski et al., 1997; Tarasov, 1992; Tarasov et al., 1997, 1998a). Whereas environmental and climate changes are well documented in southwestern Siberia

and Kazakhstan during the Pleistocene and early Holocene (Kremenetski and Tarasov, 1997; Kremenetski et al., 1997; Tarasov et al., 1997), however, they are still scarce for the Aral Sea (e.g., Rubanov et al., 1987; Boomer et al., 2000). Using pollen and tree macrofossil records, Tarasov et al. (1998a) reconstructed vegetation biomes at ca. 6000 ¹⁴C yr BP and documented dry conditions similar to present-day ones around the Aral Sea. Distinct vegetation changes occurred in north-eastern Kazakhstan (Kremenetski and Tarasov, 1997). From two peatlands and two lakes sections, they document a milder climate between 6000 and 4500 ¹⁴C yr BP, followed by drier and more continental conditions during 4500–3600 ¹⁴C yr BP, and a “less continental” climate during 3300–2700 ¹⁴C yr BP. Recently, Esper et al. (2002) published a high-resolution climate record from the Karakorum and Tien-Shan Mountains based on tree-ring width, documenting prominent temperature changes for the last 1200 yr. They reported relatively warm conditions during AD 800–1000, AD 1300–

* Corresponding author. Present address: Laboratoire « Morphodynamique continentale et côtière (M2C) » (UMR 6143 CNRS), Université de Caen Basse-Normandie, 24 rue des Tilleuls, F-14000 Caen, France. Fax: +33 231 565 757.

E-mail address: philippe.sorrel@unicaen.fr (P. Sorrel).

1450, and during the past century. In contrast, lowered temperatures were inferred during AD 1000–1200 and during the “Little Ice Age” (AD 1450–1900).

In the Aral Sea area, high-resolution climatic studies have been recently undertaken in the context of the project CLIMAN (Nourgaliev et al., 2003; Sorrel et al., 2006). In this study, we present a new pollen record covering the last 2000 yr with a time resolution of ca. 50 yr. Based on quantitative pollen analyses, we use pollen data to show significant changes in moisture conditions, temperature, and vegetation patterns in the Aral Sea basin. Our objective is to identify climatically induced shifts in the terrestrial vegetation surrounding the lake and to compare them to other records from the Middle East and Central Asia. These data are then critically evaluated in order to initially assess late Holocene climatic changes in Central Asia.

Geological and climatic frame of the Aral Sea basin

The Aral Sea, situated in Central Asia (Fig. 1), represents an ideal sedimentary archive for studying environmental and climate changes in the past. The present-day climate is marked by extreme continental conditions that are mediated by a complex topography around the Aral Sea. The Central Asian arid region (=Aral Sea basin) comprises the Turan Lowland and the Kyzyl Kum, and it is surrounded in the north by the southern margin of the Kazakh Hills (at ca. 48°N), the Middle Asian Mountains on its southern and southeastern edges (Pamir, Tien Shan), and the lower mountains of the Kopet Dagh (2000 m altitude) in the southwest (Fig. 1). In the north, the Turan Lowland descends progressively northward and westward and opens towards the Caspian lowland (Lioubimtseva et al., 2005). In the Aral Sea basin, ecosystems mostly represented by steppes (including shrubs) are the



Figure 1. Location map of the Aral Sea and the study area (modified after Lioubimtseva et al., 2005).

prevailing landscapes. Some isolated trees (e.g., poplar, tamarisk, elm, oak), which are typical for riparian ecosystems, are restricted to the banks of two major Central Asian rivers, the Syr Darya and the Amu Darya. Winters, dominated by the Siberian High Pressure Cell (Zavialov, 2005), are cold. Severe frosts, with mean temperatures of $-26\text{ }^{\circ}\text{C}$ and absolute minimum of $-40\text{ }^{\circ}\text{C}$ are common (Lioubimtseva et al., 2005). In contrast, summers are hot, cloudless and dry. In autumn, a rapid cooling of the land tends to stabilize the atmosphere, protracting the dry season. Therefore, rain is rare in the basin with maximum precipitation in winter and early spring (Lioubimtseva, 2002; Nezhlin et al., 2005), whereas almost no rain occurs between May and October (e.g., Létolle and Mainguet, 1993; Zavialov, 2005). Overall, the characteristic number of rainy days is 30–45 per yr (Bortnik and Chistyayeva, 1990), and precipitation over the Aral Sea tends to increase northwards (Zavialov, 2005).

Materials and methods

Site, sediments and chronology

During a field campaign in the summer 2002, piston cores CH1 (11.04 m) and CH2 (6.0 m) ($45^{\circ}58.528'\text{N}$, $59^{\circ}14.459'\text{E}$; water depth 22 m) were retrieved with a Usinger piston corer (<http://www.uwitec.at>) about one km off the shoreline at Chernyshov Bay (Fig. 1). We investigated the composite

sediment core CH2/1 (Cores CH1 and CH2), whose total length is 10.79 m. The correlation between Cores CH1 and CH2 was performed by matching laminations, using photographs, physical properties and XRF scanning data. Detailed lithological description of section CH2/1 is given in Sorrel et al. (2006). A simplified lithological profile and the age model for section CH2/1 are presented in Figure 2.

In section CH2/1, reliable dating for the upper 5 m was obtained by correlation with the magnetic susceptibility record from parallel cores 7, 8 and 9 retrieved ca. 50 m apart from the studied cores (Nourgaliev et al., 2003). This correlation provides an age of 480 ± 120 cal yr BP at 1.4 m depth and 655 ± 65 cal yr BP at 4.48 m in section CH2/1 (Table 1). For the lower part of section CH2/1 [5.00–10.79 m], AMS radiocarbon ages were determined using the green alga *Vaucheria* sp. and CaCO_3 from mollusc shells, which were successively picked from the washed sediment sample and carefully cleaned from adhering particles. Algae were stored in distilled water within a glass vessel. For each sample, AMS ^{14}C dating was performed using between 0.2 and 1.0 mg of pure extracted carbon. Extrapolation of sedimentation rates below 8.3 m provides an age of ca. 2000 ^{14}C yr BP for the basement of section CH2/1. A sampling interval of 30 to 40 cm was selected, which provides a time resolution of ca. 50 yr. The top of the core (uppermost 40 cm) has been dated as post-AD 1963, as based on a peak in ^{137}Cs at 0.46 m reflecting the bomb period (ca. AD 1963–1964) (Heim,

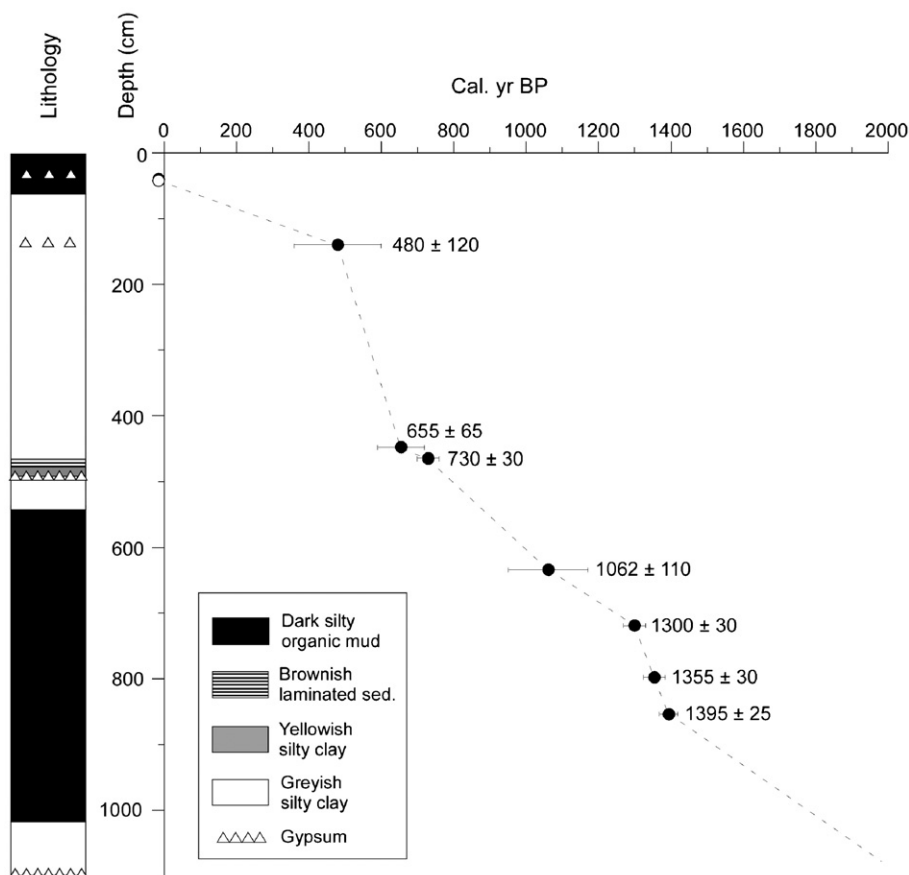


Figure 2. Simplified lithological profile and age model for section CH2/1 based on AMS ^{14}C dating (full dots). Open dot: peak in ^{137}Cs [AD 1963–1964].

Table 1
Radiocarbon dates for section CH2/1. AMS ^{14}C ages were measured at Poznań Radiocarbon Laboratory (Poland)

Sample name	Core depth (m)	Lab. no.	^{14}C yr BP	2 Std. dev. (95% confidence interval)	cal. yr BP	Dated material
Nourgaliev et al. (2003) ¹	1.4	KSU 2	435	120	480	<i>Vaucheria</i> sp.
Nourgaliev et al. (2003) ²	4.48	KSU 3	640	65	655	<i>Vaucheria</i> sp.
Aral 32 134.5–138.5 cm	4.65	Poz-13511	815	30	730	TOC
Aral 27 209–212 cm	6.34	Poz-12279	1160	110	1062	<i>Vaucheria</i> sp.
Aral 27 269–271 cm	6.93	Poz-4762	1395	30	1300	<i>Vaucheria</i> sp.
Aral 28 40–45; 52–54 cm	~7.73	Poz-9662	1480	30	1355	molluscs
Aral 28 112–114 cm	8.28	Poz-4760	1515	25	1395	<i>Vaucheria</i> sp.

Radiocarbon ages were corrected to calibrated (cal) ages using the IntCal04 calibration curve (Reimer et al., 2004).

2005). Our age model is very similar to that established on Core CH1 for the diatom-inferred palaeoconductivity record of Austin et al. (2007). It diverges only on a few points and these discrepancies are mostly due to the fact that: (1) different cores from Chernyshov Bay were investigated, i.e., Core CH1 in Austin et al. (2007) and section CH2/1 in this study; (2) different calibration methods were used, i.e., OxCal v. 3.10 (Bronk Ramsey, 2005) in Austin et al. (2007) whereas the IntCal04 calibration curve (Reimer et al., 2004) has been used here. However, the source of the ^{14}C dating remains the same (project CLIMAN; <http://climan.gfz-potsdam.de/>). For further detail on the chronology of section CH2/1, we refer to Sorrel et al. (2006).

Sample processing

Pollen slide preparation followed the Cour's method (Cour, 1974). 35 sediment samples (15–25 g dry weight) were treated with cold HCl (35%) and cold HF (70%) to remove carbonates and silicates. Denser particles were separated from the organic residue using ZnCl_2 (density=2.0). Residues were filtered through a 150- μm nylon sieve to eliminate the coarser particles including organic macroremains. Palynomorphs were further concentrated using a 10- μm nylon sieve after a brief sonication (about 30 s). The final residue was then homogenized, and mounted onto microscope slides with glycerol. A transmitting light microscope using 400 \times and 1000 \times magnifications was used for pollen identification. Pollen identification was performed using the pollen photograph bank and several atlases of the 'Laboratoire PaléoEnvironnements et PaléobioSphère' (Lyon) as well as its pollen database, "Photopal" (<http://medias.obs-mip.fr/photopal>). Pollen grains are very well preserved in late Holocene sediments from section CH2/1 and abundant in all samples. Pollen concentration was estimated using the Cour's method (Cour, 1974). Concentration in palynomorphs varies from <500 to >45,000 grains/g. Pollen zones were assessed using a canonical correspondence analysis performed on selected taxa representing variables. Pollen enumeration was conducted at the Laboratory 'PaléoEnvironnements et PaléobioSphère', and data are stored in the C.P.C. database (<http://cpc.mediasfrance.org>).

Taxonomy and ecological grouping of pollen grains

Since pollen grains found in modern sediments and transported either by air or by rivers reflect the local to regional

vegetation, we used the botanical determination of pollen grains to reconstruct palaeovegetation in the Aral Sea basin. A minimum of 100 pollen grains, excluding Amaranthaceae–Chenopodiaceae and *Artemisia*, which are usually over-represented in arid environments, and non-determinable (i.e., poorly preserved) pollen grains, were counted in each sample. Generally more than 25 different taxa were found in each sample. 74 taxa have been identified (Table 2), and 17,356 pollen grains were enumerated.

Two different diagrams were developed from these data:

- A detailed pollen diagram (Fig. 3) displays percentages of the most frequent taxa, which were calculated relative to the total pollen sum;
- A standard synthetic diagram (Fig. 4), in which pollen taxa are represented in 10 relevant groups of taxa based on their ecological preferences (Table 2), to visualize changes in the vegetation pattern (composition, structure).

Climate reconstruction

For the quantification of palaeoclimate signals recorded in plant assemblages, the "probability mutual climatic spheres" (PCS) method described in detail by Klotz and Pross (1999) and Klotz et al. (2003, 2004) was favoured over modern analogue methods (e.g., Guiot, 1987, 1990; Prentice et al., 1992, 1996; Peyron et al., 1998; Tarasov et al., 1998a,b; Klotz, 1999). Generally, modern analogue methods (MAM) are based primarily on comparing past pollen spectra with present-day analogues. In this study, the main restriction in applying this technique is the general poorness of the underlying available database of surface pollen spectra from the Aral Sea region (only 91 in Kazakhstan; Tarasov et al., 1998a) that could serve as modern analogues for reliable climate reconstructions. Besides, the usefulness of these methods is restricted when no present-day analogues exist for past pollen floras, as is the case for the association Amaranthaceae–*Artemisia*–*Taxodium* found in this record. In addition, climate reconstructions with modern analogue methods may be significantly influenced by taphonomic effects when applied, for instance, on records from areas such as the Aral Sea basin, which experiences numerous dust storms throughout the year (Seredkina, 1960; Létolle and Mainguet, 1993; Zvialev, 2005). Hence, the use of the PCS method is more suitable than MAM for reconstructing climate changes in this study.

Table 2

List of the taxa identified within section CH2/1

Mega-mesothermic (=subtropical) elements	<i>Pterocarya</i>	<i>Rumex</i>
<i>Engelhardia</i>	<i>Eucommia ulmoides</i>	<i>Polygonum</i>
<i>Myrica</i>		Caryophyllaceae
Taxodiaceae (including <i>Taxodium</i> -type)	Meso-microthermic (=mid-latitude) elements	<i>Phlomis</i>
	<i>Tsuga</i>	Cyperaceae
Other mega-mesothermic elements:	<i>Cathaya</i>	
<i>Nyssa</i>		Other herbs:
<i>Mappianthus</i>	Microthermic (=high-latitude) elements	Asteraceae Cichorioideae type
Euphorbiaceae	<i>Abies</i>	<i>Polygonum</i>
		<i>Gallium</i>
Mesothermic (=warm temperate) elements	<i>Pinus</i>	Cannabaceae
<i>Quercus</i>		Fabaceae
<i>Alnus</i>	Schlerophyllous elements	Plumbaginaceae
<i>Liquidambar</i>	Cupressaceae	<i>Urtica</i>
<i>Juglans</i>	evergreen <i>Quercus</i>	Zygophyllaceae
<i>Ulmus</i>		Brassicaceae
<i>Carpinus</i>	Aquatic plants	<i>Helianthemum</i>
<i>Populus</i>	<i>Sparganium</i> + <i>Typha</i>	Geraniaceae
<i>Betula</i>	<i>Potamogeton</i>	<i>Sambucus</i>
<i>Corylus</i>		Papaveraceae
Other mesothermic elements:	Other aquatic plants:	<i>Plantago</i>
<i>Buxus sempervirens</i> type	<i>Myriophyllum</i>	Apiaceae
<i>Vitis</i>	<i>Aristolochia</i>	Ericaceae
<i>Juglans cf. cathayensis</i>	<i>Alisma</i>	Liliaceae
<i>Zelkova</i>	<i>Nymphaea</i>	<i>Narcissus</i>
<i>Tilia</i>		
<i>Taxus</i>	Non-significant (=cosmopolitan) elements	<i>Calligonum</i>
<i>Salix</i>	Rosaceae	<i>Nitraria</i>
<i>Fagus</i>	Ranunculaceae	<i>Ziziphus spina-christi</i>
<i>Platanus</i>		
<i>Fraxinus</i>	Herbs	Steppe elements
<i>Acer</i>	Amaranthaceae–Chenopodiaceae	<i>Artemisia</i>
<i>Carya</i>	Asteraceae Asteroidae	<i>Ephedra</i>
	Poaceae	

Taxa are grouped according to their ecological requirements. The different groups are plotted in the synthetic pollen diagram.

The PCS method is independent of relative proportions of plants, considering only their presence (at a minimum level of 0.5% abundance). Generally, “mutual climatic range” methods (including the PCS) determine the climatic tolerance of past taxa by means of mutual present-day ranges of the climatic tolerances of the nearest living relatives (NLR) of the taxa represented in the past assemblages. It has been recognized a considerable advantage of this reconstruction method to be independent from the availability of modern analogues and from taphonomic influences (Mosbrugger and Utescher, 1997). Especially, the PCS method calculates probability intervals within the mutual climatic spheres by comparison with the spheres calculated for a multitude of present-day floras. These probability intervals result from the observation that the climatic preferences of the present-day floras are considerably restricted as compared to their potential range.

The quality of PCS has been tested on the basis of a multitude of present-day floras (Klotz et al., 2003, 2004) documenting the large agreement between reconstructed and actual grid climate values, with correlation coefficients and mean average error of 0.95 and 1.1 °C for summer temperatures, 0.95 and 1.7 °C for winter temperatures, 0.95 and 1.1 °C for mean annual

temperature and 0.86 and 100 mm for mean annual precipitation. Therefore, the PCS is considered to represent a very sensitive method for the interpretation of climate variability.

Results

Five ecostratigraphic pollen zones have been distinguished based on major changes in pollen assemblages, labelled as P1 to P5 (Figs. 3 and 4).

Pollen zone P1 (10.75–9.97 m; ca. AD 0–400)

This zone is characterized by a large supremacy of herbs (45–47.6%), mainly represented by Amaranthaceae–Chenopodiaceae (35–40%) and steppe elements (43–47%), with frequencies of *Artemisia* fluctuating between 42.7 and 46.8%. Among other herbaceous plants (Caryophyllaceae, Asteraceae Asteroidae, *Rumex*, Cyperaceae), Poaceae are abundant with values increasing towards the top (2.5–5.8%). Conversely, arboreal taxa are extremely rare (mega-mesothermic elements: <2%, mesothermic elements: <5%), mostly represented by Taxodiaceae (1.2% at 9.97 m), *Betula* (1.2% at 9.97 m) and few *Alnus* (<1%). Pollen grains of *Quercus*, *Carpinus*, *Populus*,

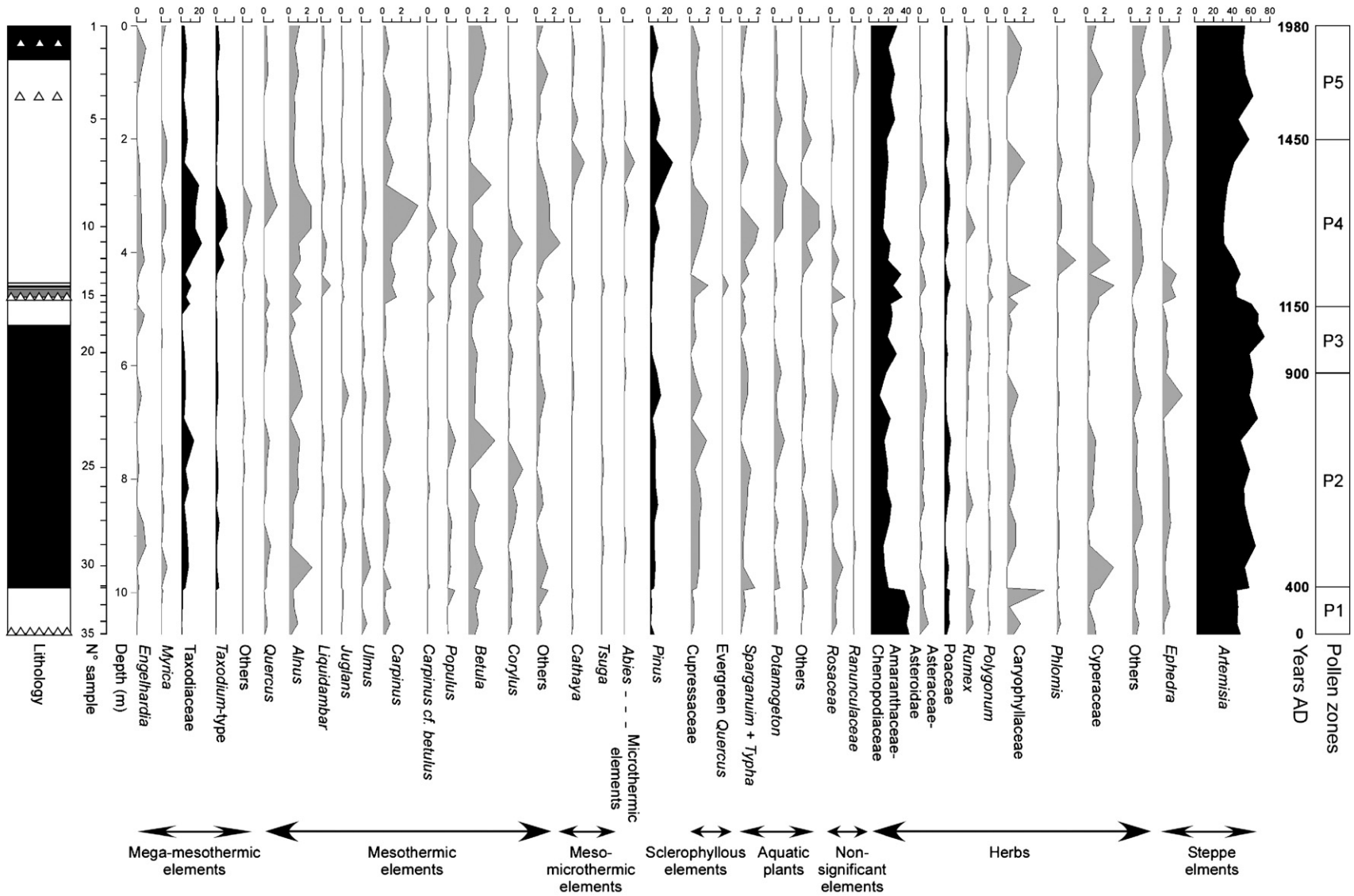


Figure 3. Pollen detailed diagram for section CH2/1. Black-filled lines indicate percentage abundance and gray-filled lines give 10× exaggeration (i.e., per mill abundance). Pollen zones P1 to P5 are based on the present study. For lithology, see Figure 2.

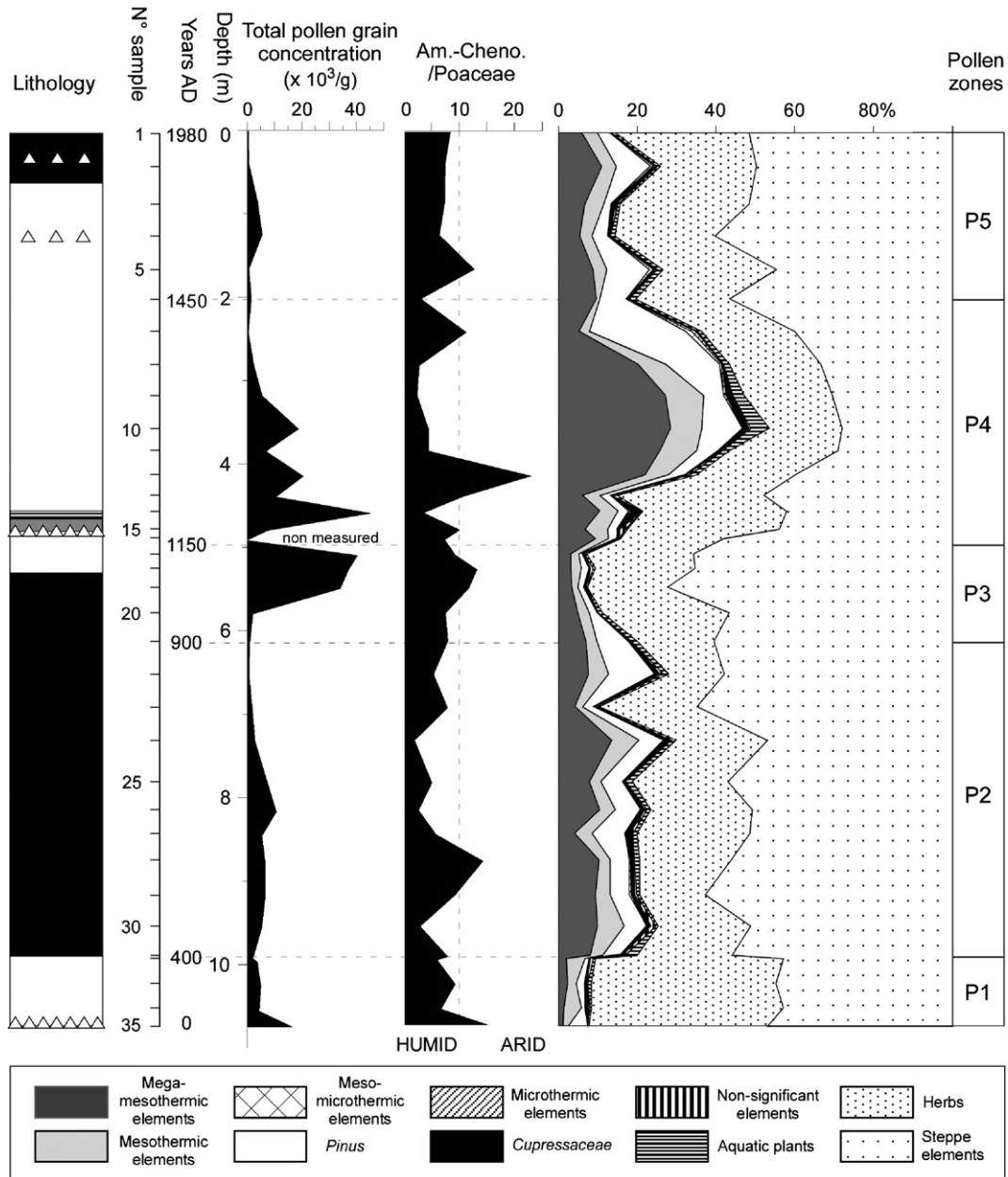


Figure 4. Pollen synthetic diagram for section CH2/1. Grouping was performed with regard to the ecology of the plants (see Table 2). Concentrations (per gram of dry sediment) are relative to the total pollen sum. Each sample represents a 30- to 40-cm interval and is plotted by its mean depth (see text for details). The ratio Amaranthaceae–Chenopodiaceae/Poaceae is regarded as representing a semi-quantitative index of aridity. For lithology, see Figure 2.

Corylus and Cupressaceae are also present at low percentages, with values never exceeding 1%. *Pinus* is found at low abundances (<5%), as are pollen of Rosaceae and aquatic plants (>1%). Total pollen concentration is relatively high in the lowermost part of this zone (16,600 grains/g at 10.75 m) but decrease upwards (<4000 grains/g at 9.97 m) (Fig. 4).

Pollen zone P2 (9.97–6.13 m; ca. AD 400–900)

This zone shows a conspicuous increase in percentages of arboreal taxa characterized by higher abundances of mega-mesothermic (Taxodiaceae: 13.3% at 7.33 m) and mesothermic (6.8% at 7.33 m) elements. Among other warm-temperate trees,

Betula, *Alnus* and *Corylus* are most abundant (Figs. 3 and 4). Frequency of Cupressaceae also slightly increases (1.7% at 7.33 m), while values of *Pinus* become more important (mean: 6.2%; 11.7% at 6.53 m). This zone is also characterized by a drastic decrease in percentages of Amaranthaceae–Chenopodiaceae (9–21%), and numbers of Poaceae also slightly decrease. Relative abundances of *Artemisia* (steppe) remain stable at relative high levels, even showing higher values than in zone P1 (47–65%). Non-significant pollen grains are also present in low values (<1.5%) and abundance of aquatic plants slightly increases (0.6–3%). Total pollen concentration is lower in this zone and fluctuates between 2000 and 10,500 grains/g (Fig. 4).

Pollen zone P3 (6.13–4.92 m; ca. AD 900–1150)

This zone is characterized by a general decrease in mega-mesothermic and mesothermic elements, with respective values of 2.8–9% and 1.5–3.4% (Fig. 4). In particular, abundances of Taxodiaceae (mean: 3.1%) and *Taxodium*-type (0–1.6%) show pronounced lower values compared to the previous zone. Among the mesothermic elements, *Alnus*, *Betula* and to a lesser extent *Quercus* and *Carpinus* are the most represented taxa, with values rarely exceeding 1%. Though frequencies of herbs (Amaranthaceae–Chenopodiaceae, Asteraceae Asteroidae, *Rumex*, *Phlomis*, Cyperaceae) remain stable compared to zone P2 (19.5–32%) with a slight decrease in Poaceae (1.5–3.6%), abundance of steppe elements conspicuously increases through elevated frequency of *Artemisia* (56–72%). Percentages of Cupressaceae, non-significant elements and aquatic plants are again relatively low (<2%), while *Pinus* frequency clearly decreases (mean: 2.7%). Total pollen concentration increases towards the top of this zone, with a maximum value of 40,000 grains/g at 5.1 m (Fig. 4).

Pollen zone P4 (4.92–2.02 m; ca. AD 1150–1450)

Following the increase in steppe elements in zone P3, this zone emphasizes a pronounced increase in percentages of trees and notably of mega-mesothermic elements with a maximum of 28.3% at 3.58 m (Figs. 3 and 4). Noticeably, relative abundances of Taxodiaceae fluctuate between 5% in the lowermost part of the zone (4.8 m) up to 21.7% at 3.85 m, while maximal values of *Taxodium*-type (12.2%) are recorded at 3.58 m. Pollen of *Engelhardia* and *Myrica* is also found but in low numbers (<1%), while rare specimens of *Nyssa* and *Mappianthus* have been recorded as well. Mesothermic elements are common (3.5–9.8%) and mostly represented, among other warm-temperate taxa, by *Carpinus* (3.7% at 3.18 m), *Alnus* (2.35% at 3.58 m), *Quercus* (1.4% at 3.18 m), *Betula* (1.15% at 3.85 m) and *Corylus* (1.5% at 3.85 m). *Populus* ($\leq 1\%$) and higher frequency of *Liquidambar* (<1%) also occur in this zone. *Pinus* becomes more abundant upwards, with a maximum of 24.3% at 2.42 m, while few pollen grains of *Tsuga* and *Abies* also have been found. Though frequency of Poaceae noticeably increases (6.5% at 4.59 m, 6% at 3.18 m; 5.6% at 2.82 m), as do values of Cyperaceae (0.2–2.8%), percentages of *Artemisia* conspicuously drop, with a minimum of 28.3% at 3.58 m and with values fluctuating around 40% throughout the zone. Abundances of Amaranthaceae–Chenopodiaceae are relatively similar as in zones P2 and P3 (14.8–32%). Aquatic plants increase noticeably (4.7% at 3.58 m), as does Cupressaceae (1.9% at 4.59 m). Total pollen concentration decreases in this zone from 45,000 grains/g at 4.59 m to less than 500 at 2.42 m (Fig. 4).

Pollen zone P5 (2.02–0.00 m; ca. AD 1450–1980)

This zone is characterized by the transition to present-day vegetation types, with an abrupt decrease in percentages of mega-mesothermic elements (5.15–10.6%) and to a lesser

extent of warm temperate trees (1–4.8%), correlative with an increase in herbs (23.8–33.6%) and steppe (45% to ca. 52% at the top) frequencies (Figs. 3 and 4). Mega-mesothermic elements are mainly represented by Taxodiaceae (including *Taxodium*-type) that nonetheless never exceed 10%, while other taxa from this group become scarce. Among the mesothermic elements, only abundance of *Betula* regularly exceeds 1%, whereas *Quercus*, *Alnus*, *Liquidambar*, *Populus* and *Corylus* mostly run below 1%. Percentages of Cupressaceae slightly decrease (0.2–1.1%), as does *Pinus* from 10.8% at 1.66 m to 3% at the top. *Tsuga*, *Abies* and non-significant elements still occur, but at very low numbers (<1%). Although Amaranthaceae–Chenopodiaceae yield a pronounced increase in this zone (16.7–27.7%), the frequency of Poaceae decreases (2–5.3%). Total pollen concentration is relatively low in this zone (<500–5550 grains/g) (Fig. 4).

Vegetation patterns derived from the pollen record

Herbs, predominant in all samples (Fig. 4), are characterized by an overwhelming presence of *Artemisia* that accounts for 28–72% of the pollen sum, and pollen of Amaranthaceae–Chenopodiaceae (20–25%). Poaceae (mean: 3.5%) is also common. Studies of pollen composition in aerosols indicate that both *Artemisia* and Amaranthaceae–Chenopodiaceae are high pollen producers (Van Campo et al., 1996; Cour et al., 1999), whereas Poaceae are rare in arid regions (Cour and Duzer, 1978; Van Campo et al., 1996). At present in Central Asia, *Artemisia* and Amaranthaceae–Chenopodiaceae are characteristic elements of steppe, semi-desert and desert environments (Tarasov et al., 1998a,b). Since Amaranthaceae–Chenopodiaceae are commonly present under saline and desert conditions but can be easily replaced, even during periods of minor elevation in precipitation, a slight increase in abundance can be interpreted as an increase in salinity and/or aridification (El Moslimany, 1990).

Pollen data suggest that open vegetation types with typical steppe elements (shrubs, herbs) were always predominant in the Aral Sea basin during the last 2000 yr. This implies that xeric conditions prevailed in the region, interrupted by periods of slightly enhanced moisture as reflected by slightly increased values of Poaceae. Based on the above ecological significance of Amaranthaceae–Chenopodiaceae (indicative of dry conditions) and Poaceae, whose abundance generally increases with rain, we use the ratio Amaranthaceae–Chenopodiaceae/Poaceae as a semi-quantitative index of aridity (Fig. 4). In this diagram, high values of the ratio (>10) are considered indicative of arid conditions that favour semi-desert-steppe vegetation, whereas low values (<10) reflect periods of slightly elevated moisture conditions and the development of few trees in a less arid steppe. This is concurrent with abundance of aquatic plants and Cyperaceae, which reflect some extension in aquatic environment (Fig. 3). Therefore, correspondence between low ratio values, sedimentological data and changes in lake water levels (Sorrel et al., 2006) validate the use of the ratio as a proxy for relative moisture availability in the Aral Sea basin.

Halophytes (Amaranthaceae–Chenopodiaceae, *Ephedra*, partly *Artemisia*) probably contribute to the predominant vegetation along the Aral Sea shoreline. However, the presence of aquatic plants is also common in the pollen flora. In general, frequency of aquatic plants is almost parallel to that of Poaceae (Fig. 3). Increasing frequency of these taxa may be thus representative of some extension of local marshes accompanied by some development of herbs requiring less dry conditions, reflecting a slight increase in humidity.

Trees are a minor component of the pollen flora, averaging 20% on the whole downcore, with a maximum value of 28% in zone P4. Each arboreal group is indicative of specific environmental conditions, permitting us to trace the probable origin of each taxon according to its ecology and present-day distribution. *Pinus* was probably not an eminent component of the regional vegetation; its frequency, even being modest, may be caused by its prolific production and overabundance in air and water transport. Warm-temperate elements (2–10%), also common in the pollen record, comprise some elements today restricted to the Middle East, such as *Liquidambar* and *Pterocarya*. The presence of these mesothermic elements may reflect the past development of some riparian vegetation in the Aral Sea basin. More surprisingly, in a region where such dry climate conditions predominated (judging from the overwhelming dominance of herbs in the pollen record), some mega-mesothermic elements indicative of relatively warmer and wetter environments have been found in every sample analysed. These elements are mostly represented by Taxodiaceae (including the *Taxodium*-type pollen, a swamp element) and to a lesser extent by *Engelhardia* and *Myrica*. Considering the regional, near sub-arid conditions in the basin during the last 2000 yr, the presence of these relictuous elements in the Aral Sea sediments requires comment. Similarly, the presence of *Cathaya* (a past conifer restricted today in a few mid-altitude environments of the southwestern subtropical China) among the mid-altitude elements would be unexpected in such conditions.

Because the Aral Sea is surrounded by older deposits mostly of Paleogene and Neogene age, we might expect increased reworking of older material from shore during periods of sheet wash erosion, as it is the case for dinoflagellate cysts (see Fig. 6). However, from several samples of Miocene marls collected nearby the Chernyshov Bay, no pollen grains of *Taxodium*-type, Taxodiaceae, *Cathaya*, *Engelhardia*, *Myrica* were found. On the contrary, in section CH2/1, most of these pollen grains are found well preserved, rarely broken or damaged, and exhibit all the criteria characteristic of fresh pollens. For further reliability, we carefully examined them under fluorescence light, a method that is currently used by palynologists to distinguish fresh from reworked specimens. Results showed that the pollen grains of *Cathaya*, *Taxodium*-type and other relictuous taxa display whitish to yellow tints that are usually characteristic of non-reworked pollen grains (unpublished data). Similar observations resulted from tests conducted on *Artemisia* and pollen grains of Amaranthaceae–Chenopodiaceae. Hence, the presence of mesothermic and mega-mesothermic relictuous taxa in sediments from Chernyshov

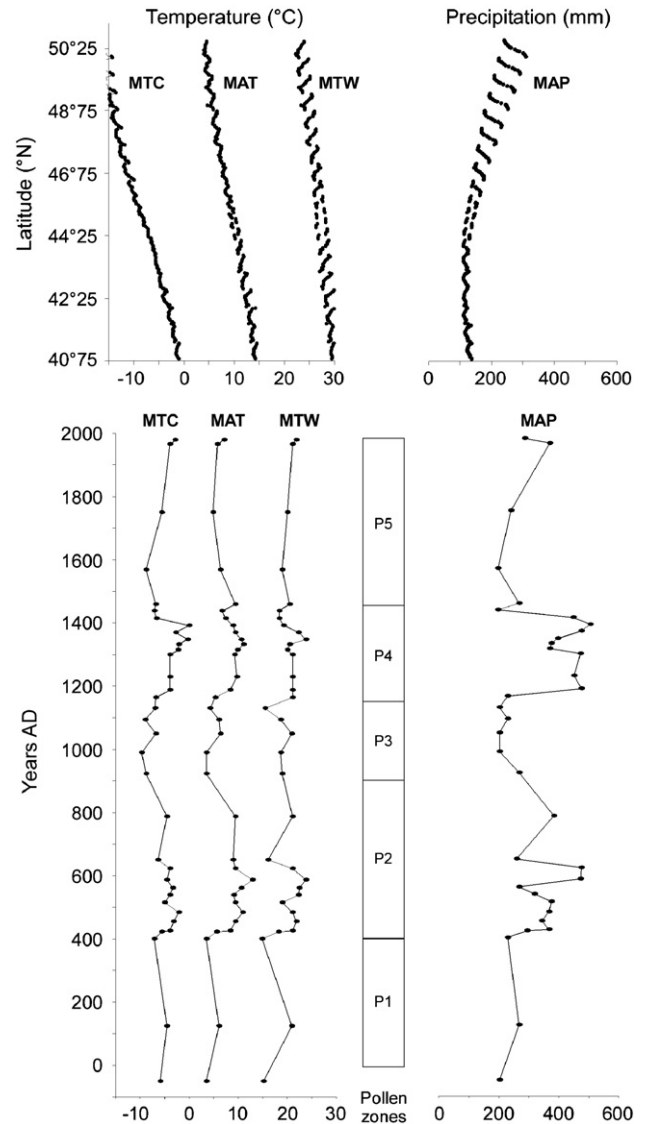


Figure 5. Reconstructed climate parameters: mean annual temperature (MAT in °C), mean temperature of the coldest month (MTC in °C), mean temperature of the warmest month (MTW in °C) and mean annual precipitation (MAP in mm/yr) for section CH2/1 during the last 2000 yr (lower diagram). Taxodiaceae and *Taxodium*-type have not been included for climate quantification (see text for detail). The upper figure represents instrumental data for present-day different temperature parameters, and mean annual precipitation in Central Asia. Data have been plotted along the latitudinal gradient [40°75'–50°25'N] (y). Data were extracted from New et al. (1999).

Bay is probably linked with mid- to long-distance wind transport, respectively.

Climate reconstruction

The composite pollen diagram (Fig. 4) suggests that some limited but significant changes in the vegetation pattern have occurred in the Aral Sea basin over the last 2000 yr. Changes in the pollen flora document switches between sub-desertic conditions (steppe almost completely constituted of *Artemisia*) and less dry environments (steppe enriched in Poaceae) coeval

to the establishment of some riparian trees. Since the expansion of open vegetation and the development of trees are controlled by climate conditions, we used the pollen data to reconstruct climate variability in terms of different temperature parameters and mean annual precipitation during the last 2000 yr (Fig. 5). For the climate reconstruction, all taxa recorded in samples from section CH2/1 have been included with the exception of Taxodiaceae. Indeed, *Taxodium* is naturally found today only in very restricted regions of southeast Asia, making the derived climatic sphere (e.g., coldest and warmest spheres of the species and their relationship) based on its geographical distribution very approximate. This is in contrast to the climate spheres of the other azonal vegetation elements used in the reconstruction whose present-day distributions are well known, and which are therefore of higher resolution.

Because the source of some pollen grains may be distant from the central depression of the basin, this quantitative reconstruction of climatic parameters gives a regional wide-spread picture of the changes in moisture conditions rather than a local signal restricted to the Aral Sea and its nearest adjacent areas. To further constrain our climatic reconstruction, we compared the reconstructed values to modern instrumental data from Central Asia along the latitudinal gradient [40°75′–50°25′N] across the Aral Sea basin (Fig. 5).

Pollen zone P1 (10.75–9.97 m; ca. AD 0–400): basal arid interval

High values of the ratio Amaranthaceae–Chenopodiaceae/Poaceae concurrently with high frequency of steppe element *Artemisia* and Amaranthaceae–Chenopodiaceae indicate that prevailing climate from ca. AD 0 to 400 was colder and more arid than today, with mean annual temperatures of 4–6 °C, temperatures of the coldest month averaging –6 °C and mean annual precipitation never exceeding 300 mm/yr. The general feature of such climatic conditions is supported by sedimentological data and precipitation of gypsum interbedded with fine clays in the lowermost part of this zone. The transition between pollen zones P1 and P2 is probably characterized by a very short coring gap.

Pollen zone P2 (9.97–6.13 m; ca. AD 400–900): increasing humidity

Decreasing xeric conditions are inferred from low values of the ratio Amaranthaceae–Chenopodiaceae/Poaceae (<10) between ca. AD 400 and 900. Coevally, an increase in the abundance of warm-temperate elements and aquatic plants suggests that the climate became moderately moister and potentially warmer. Reconstructed climate conditions indeed document that mean annual precipitation fluctuated between 270 and 475 mm/yr, whereas temperatures of the warmest month averaged 21 °C (coldest month: –5 °C) and mean annual temperatures 9 °C. Increase in moisture conditions are concurrent with the evidence of lake-level rise, inferred from dinoflagellate cyst assemblages (Sorrel et al., 2006), and may have favoured the expansion of some riparian trees.

Pollen zone P3 (6.13–4.92 m; ca. AD 900–1150): strong aridification

This zone documents a return to strong arid conditions, as reflected by the progressive decrease in warm-temperate trees and the expansion of steppe elements *Artemisia* and Amaranthaceae–Chenopodiaceae. This is concurrent with high values of the aridity index (>10) and declined rainfall (200–230 mm/yr). Climate reconstruction document lower temperatures during this interval (coldest month: –7° to –10 °C; warmest month: 15°–21 °C; mean annual temperature: 4°–6 °C). Further evidence for a long-term aridification is provided by a gypsum layer at 4.86 m (Fig. 4).

Pollen zone P4 (4.92–2.02 m; ca. AD 1150–1450): increasing humidity

Increasing moisture conditions are inferred from a drop in the abundance of both steppe herbs and shrubs coincident with higher percentages of Poaceae and trees. Based on the ratio Amaranthaceae–Chenopodiaceae/Poaceae (<10), prevailing climate conditions were noticeably moister than at present. This is concurrent with enhanced precipitation (370–505 mm/yr). Reconstructed temperatures for this interval were higher (mean annual: 7°–11 °C; coldest month: –4 °C). Increasing moisture conditions are consistent with rising lake levels and important freshwater discharges in the Aral Sea, as indicated in the dinoflagellate cyst assemblages (Sorrel et al., 2006). Higher-water availability between ca. AD 1150 and 1450 probably favoured the expansion of trees onshore, with a possible development of a riparian association comprising warm-temperate trees (*Ulmus*, *Alnus*, *Populus*, *Corylus*) and maybe few mega-mesothermic elements (*Taxodium*-type, *Engelhardia*). The last sample records the onset of more arid conditions resulting in lower precipitation rates (<200 mm/yr).

Pollen zone P5 (2.02–0.00 m; ca. AD 1450–1980): brief aridification followed by present-day climate conditions

A third arid interval is recorded during ca. AD 1450–1550, as reflected by increasing abundance of steppe element *Artemisia* and slightly higher values of the ratio Amaranthaceae–Chenopodiaceae/Poaceae. This short phase is characterized by low precipitation rates (200–270 mm/yr) but more contrasting temperatures. Whereas both mean annual values (6°–9 °C) and temperatures for the warmest month (18.9°–20.5 °C) suggest warmer conditions in this interval, mean values for the coldest month decrease from –7 °C around AD 1450 to –9 °C at AD 1550. This interpretation is confirmed by sedimentological data, with precipitation of gypsum crystals in clay sediments around AD 1500. Reconstructed climatic parameters from the pollen content of surface sediments (AD 1550–1980) indicate contrasting precipitation rates (240–370 m/yr) and a slight warming trend (coldest month: –6° to –3 °C; warmest month: 20°–22 °C; mean annual temperature: 7 °C). Observations of present-day landscapes along the northern shore of the Aral Sea corroborate pollen evidence of enhanced aridity and higher

temperatures in recent decades. The reconstructed climate parameters in the uppermost sample (i.e., AD 1980) are in accordance with present-day instrumental data from Central Asia (Fig. 5), where mean annual temperature and precipitation respectively decrease/increase from 14 °C/110 mm at 40°75'N to 4 °C/310 mm at 50°25'N, validating the ranges of values obtained in our climate quantification. However, whether reconstructed temperature for the coldest month (−3 °C) fairly overlaps instrumental values (−1° to −16 °C), the estimated value for the warmest month (22 °C) appears slightly lower than the instrumental ones (22°–30 °C). An explanation for this could be the rapid warming trend observed during the past 20 yr, which is not documented in our pollen record.

Discussion and conclusions

Today, the climate in the deserts of Central Asia is mostly controlled by the shifts of the westerly cyclonic circulation and depends on the position of the Siberian High during winter and spring (Zavialov, 2005). In addition, local precipitation occurs during winter and early spring when depressions, developing over the eastern Mediterranean, subsequently move along a northeast trajectory where they may replenish moisture over the Caspian Sea (Létolle and Mainguet, 1993; Roberts and Wright,

1993; Aizen et al., 2001; Lioubimtseva, 2002). Therefore, we may expect elevated precipitation in Central Asia when moisture-transporting storms are stronger in the eastern Mediterranean region and, if so, we should find similar pattern of humidity between areas influenced by eastward moving storms (Israel, Turkey, Iran) and the Aral Sea basin during the last 2000 yr. Detailed palaeoclimatological studies based on $\delta^{18}\text{O}$ measurements from carbonate deposits of the Soreq Cave (Israel) (Schilman et al., 2002) provide a reliable record for comparison with the pollen-derived climate reconstruction presented here (Fig. 6). We also use the relative abundance of reworked dinoflagellate cysts, which is expected to increase during periods of elevated sheet wash from shore, as a further proxy of the rainfall intensity (Sorrel et al., 2006).

Whereas a cold and arid period (mean annual rainfall <300 mm) has been inferred from the pollen flora during AD 0–400, Schilman et al. (2002) document declining rainfall leading to dry events in Israel around AD 0. A similar phenomenon was reported in Syria, with reduced winter/spring rains (Bryson, 1996). Coevally, a decrease in lake level is reported from Lake Van in Turkey, evidencing a period of decreasing humidity between ca. 1500 BC and AD 0 (Landmann et al., 1996; Lemcke and Sturm, 1996). The decrease of rainfall is possibly related to a change in the mode of the North Atlantic Oscillation

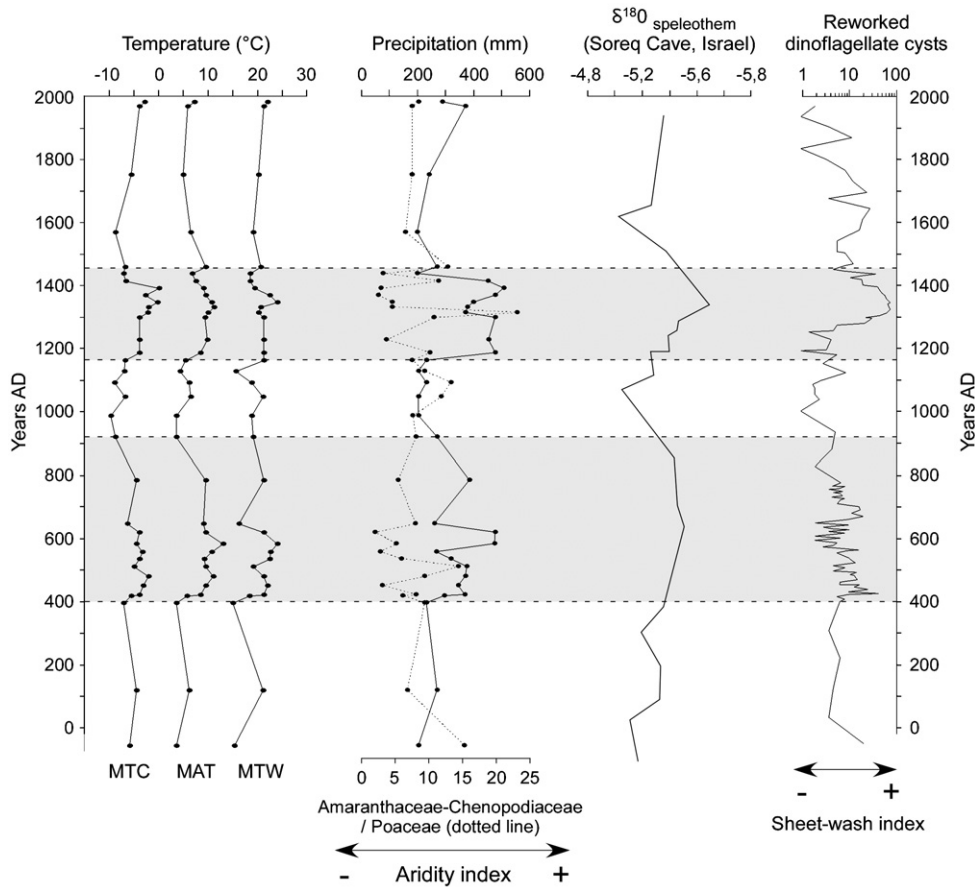


Figure 6. Comparison between reconstructed climate parameters (temperature, precipitation: black full lines) from section CH2/1, the $\delta^{18}\text{O}$ record from carbonate deposits in the Soreq Cave (Israel; Schilman et al., 2002) and the sheet wash index derived from the relative abundance of reworked dinoflagellate cysts at Chernyshov Bay (Sorrel et al., 2006). Grey shadings represent periods of increased temperature and rainfall in the Aral Sea basin when moisture-transporting storms are stronger from the Eastern Mediterranean Sea.

(NAO) that reduced cyclonic activity over the eastern Mediterranean, being high during a negative NAO mode (Hurrell, 1995; Hurrell et al., 2003). This is in accordance with Aizen et al. (2001), who found that the NAO has a statistically significant inverse relationship with moisture availability over mid-latitudes of continental Asia. Based on correlation analyses between atmospheric circulation patterns and regional precipitation, they reported that a negative (positive) difference in sea-level pressure anomalies between the Azores and the Iceland is favourable (unfavourable) for precipitation development over the middle plains of Asia.

Following this aridification, the time interval ca. AD 400–900 is characterized by some warmer and wetter climate conditions in the Aral Sea basin, which favoured the development of some arboreal vegetation in the less dry edaphic areas. This is supported by a conspicuous decrease in the $\delta^{18}\text{O}$ of carbonate deposits from the Soreq Cave (Schilman et al., 2002; Fig. 6), which infers elevated precipitation rates in Israel during AD 400–900 linked to stronger storms over the eastern Mediterranean. Other evidences document a period of maximum precipitation around AD 700, as inferred from land records including tree assemblages (Lipschitz et al., 1981), high-stand levels of the Dead Sea (Frumkin et al., 1991) and carbonate cave deposits in Israel (Bar-Matthews et al., 1998).

The period AD 900–1150 is characterized by a return to colder and more arid conditions in the Aral Sea basin concurrently with declining rainfall (<270 mm/yr) and low mean annual temperatures, suggesting lowered moisture derived from the eastern Mediterranean in winter and early spring during a possible positive phase of the NAO. This is in accordance with other palaeoenvironmental records from the eastern Mediterranean which document colder conditions and reduced precipitation between AD 850 and 1200 (Issar et al., 1991; Schilman et al., 2002).

After AD 1150, elevated moisture conditions during a warmer period are inferred with precipitation rates frequently beyond 400 mm/yr, although the associated change in the vegetation pattern was not registered in the C:N ratio (<10) of organic isotopes from Chernyshov Bay (Austin, unpublished data). It coincides, however, with elevated sheet wash from shore as reflected by higher abundance of reworked dinoflagellate cysts. A similar pattern to increasing humidity is inferred from lowered $\delta^{18}\text{O}$ values in speleothems from the Soreq Cave between AD 1200 and 1500 (Fig. 6), suggesting higher rainfall over the eastern Mediterranean region during the Medieval Warm Period. This event also corresponds to high-stand levels of the Dead Sea (Issar et al., 1991) and the Sea of Galilee (Frumkin et al., 1991).

A brief aridification occurred again during AD 1450–1550. This short-term change towards colder/drier conditions probably coincide with the Little Ice Age, whose signature has been previously recorded in $\delta^{18}\text{O}$ values from the foraminiferan *G. ruber* in the eastern Mediterranean Sea (Schilman et al., 2001) and in carbonate deposits from Israel (Bar-Matthews et al., 1998; Schilman et al., 2002). From AD 1550 onwards, increased temperatures document a progressive warming. For

the last 2000 yr, no human activity exerting control on vegetation change has been detected from the pollen record of Chernyshov Bay.

Despite a time-resolution of ca. 50 yr, the climate reconstruction provides compelling evidence that centennial-scale events are recorded during the last 2000 yr (Fig. 6). In the Aral Sea basin, climate conditions may fluctuate with a periodicity of ~400 yr, with intervals of relatively elevated moisture conditions alternating with more arid phases. Since our data match fairly well with the Soreq cave record from Israel (Schilman et al., 2002), we thus conclude that the precipitation pattern in the Aral Sea basin is directly linked to atmospheric changes in the eastern Mediterranean region, modulating moisture distribution towards the Middle East and Western Central Asia. This link may document a teleconnection to the NAO during negative phases. Modelling of Holocene climatic scenarios would improve our understanding of atmosphere–biosphere interactions in this vast arid region and identify important thresholds between climate changes and landscape responses.

Acknowledgments

The CLIMAN project was funded by INTAS (European Union) (Project No. Aral 00-1030), the German Science Foundation (DFG Project 436 RUS 111/663-OB 86/4) and NATO CLG Ref. 980445. We are grateful for this support. We wish to thank especially Dr. François Demory for excellent support in the field. The authors gratefully acknowledge Dr. Derek B. Booth and two anonymous reviewers for their constructive comments which have helped to improve the manuscript.

References

- Aizen, E.M., Aizen, V.B., Melack, J.M., Nakamura, T., Ohta, T., 2001. Precipitation and atmospheric circulation patterns at mid-latitudes of Asia. *International Journal of Climatology* 21, 535–556.
- Austin, P., Mackay, A., Palagushkina, O., Leng, M., 2007. A high-resolution diatom-inferred palaeoconductivity and sea-level record of the Aral Sea for the last ca. 1600 years. *Quaternary Research*. *Quaternary Research* 67, 383–393.
- Bar-Matthews, M., Ayalon, A., Kaufmann, A., 1998. Middle to late Holocene (6500 years period) palaeoclimate in the eastern Mediterranean region from stable isotopic composition of speleothems from Soreq Cave, Israel. In: Issar, A.S., Brown, N. (Eds.), *Water, Environment and Society in Time of Climate Change*. Kluwer Academic Publishers, pp. 203–214.
- Boomer, I., Aladin, N., Plotnikov, I., Whatley, R., 2000. The palaeolimnology of the Aral Sea: a review. *Quaternary Science Reviews* 19, 1259–1278.
- Boroffka, N.G.O., Oberhänsli, H., Achatov, G.A., Aladin, N.V., Baipakov, K.M., Erzhanova, A., Hoernig, A., Krivonogov, S.K., Lobas, D.A., Savel'eva, T.V., Wuennemann, B., 2005. Human settlements on the northern shores of Lake Aral and water level changes. *Mitigation and Adaptation Strategies for Global Change* 10, 71–85.
- Boroffka, N.G.O., Oberhänsli, H., Sorrel, P., Demory, F., Reinhardt, C., Wuennemann, B., Alimov, K., Baratov, S., Rakhimov, K., Saparov, N., Shirinov, T., Krivonogov, S.K., 2006. Archaeology and climate: Settlement and lake level changes at the Aral Sea. *Geoarchaeology* 21 (7), 721–734.
- Bortnik, V.N., Chistyeva, S.P. (Eds.), 1990. *Hydrometeorology and Hydrochemistry of the USSR Seas. The Aral Sea, vol. VII. Gidrometeoizdat, Leningrad*. 196 pp. (in Russian).

- Bronk Ramsey, C., 2005. OxCal version 3.10.
- Bryson, R.A., 1996. Proxy indications of Holocene winter rains in southwest Asia compared with simulated rainfall. In: Dalfes, H.N., Kukla, G., Weiss, H. (Eds.), *Third Millennium BC; Climate Change and Old World Collapse*. NATO ASI Series I, vol. 49. Springer Verlag, pp. 465–473.
- Cour, P., 1974. Nouvelles techniques de détection des flux et de retombées polliniques: étude de la sédimentation des pollens et des spores à la surface du sol. *Pollen et Spores* 23 (2), 247–258.
- Cour, P., Duzer, D., 1978. La signification climatique, édaphique et sédimentologique des rapports entre taxons en analyse pollinique. *Annales des Mines de Belgique* 7/8, 155–164.
- Cour, P., Zheng, Z., Duzer, D., Calleja, M., Yao, Z., 1999. Vegetational and climatic significance of modern pollen rain in northwestern Tibet. *Review of Palaeobotany and Palynology* 104, 183–204.
- El Moslimany, A.P., 1990. Ecological significance of common non-arboreal pollen: examples from drylands of the Middle East. *Review of Palaeobotany and Palynology* 76 (2–4), 343–350.
- Esper, J., Schweingruber, F.H., Winiger, M., 2002. 1300 years of climate history for Western Central Asia inferred from tree-rings. *Holocene* 12, 267–277.
- Frumkin, A., Magaritz, M., Carmi, I., Zak, I., 1991. The Holocene climatic record of the salt caves of Mount Sedom, Israel. *Holocene* 1, 191–200.
- Guiot, J., 1987. Late Quaternary climatic change in France estimated from multivariate pollen time series. *Quaternary Research* 28, 100–118.
- Guiot, J., 1990. Methodology of the last climatic cycle reconstruction in France from pollen data. *Palaeogeography, Palaeoclimatology, Palaeoecology* 80, 49–69.
- Heim, C., 2005. Die Geochemische Zusammensetzung der Sedimente im Aralsee und Sedimentationsprozesse während der letzten 100 Jahre. Diploma thesis, Alfred-Wegener-Institut Bremerhaven, 89 pp.
- Hurrell, J., 1995. Decadal trends in the North Atlantic Oscillation—Regional temperatures and precipitation. *Science* 269, 676–679.
- Hurrell, J., Kushnir, Y., Ottersen, G., Visbeck, M., 2003. An overview of the North Atlantic Oscillation. In: Hurrell, J., Kushnir, Y., Ottersen, G., Visbeck, M. (Eds.), *The North Atlantic Oscillation: Climatic Significance and Environmental Impact*. AGU, Washington, pp. 1–35.
- Issar, A.S., Govrin, Y., Geyh, A.M., Wakshal, E., Wolf, M., 1991. Climate changes during the Upper Holocene in Israel. *Israelian Journal Earth Sciences* 40, 219–223.
- Klotz, S., 1999. Neue Methoden der Klimarekonstruktion—angewendet auf quartäre Pollensequenzen der französischen Alpen. *Tübinger Mikropaläontologische Mitteilungen* 21, 169 pp.
- Klotz, S., Pross, J., 1999. Pollen-based reconstructions in the European Pleistocene: the modified indicator species approach as a tool for quantitative analysis. *Acta Palaeobotanica, Supplementum* 2, 481–486.
- Klotz, S., Guiot, J., Mosbrugger, V., 2003. Continental European Eemian and early Würmian climate evolution: comparing signals using different quantitative reconstruction approaches based on pollen. *Global and Planetary Change* 36, 277–294.
- Klotz, S., Müller, U., Mosbrugger, V., de Beaulieu, J.L., Reille, M., 2004. Eemian to early Würmian climate dynamics: history and pattern of changes in Central Europe. *Palaeogeography, Palaeoclimatology, Palaeoecology* 211, 107–126.
- Kremenetski, C.-V., Tarasov, P.E., 1997. Postglacial development of Kazakhstan pine forests. *Géographie Physique et Quaternaire* 51 (3), 391–404.
- Kremenetski, C.-V., Tarasov, P.E., Cherkinsky, A.E., 1997. The latest Pleistocene in Southwestern Siberia and Kazakhstan. *Quaternary International* 41/42, 125–134.
- Landmann, G., Reimer, A., Lemcke, G., Kempe, S., 1996. Dating Late Glacial abrupt climate changes in the 14,570-yr long continuous varve record of Lake Van, Turkey. *Palaeogeography, Palaeoclimatology, Palaeoecology* 122, 107–118.
- Lemcke, G., Sturm, M., 1996. ^{18}O and trace element measurements as proxy for the reconstruction of climate changes at Lake Van (Turkey). In: Dalfes, H.N., Kukla, G., Weiss, H. (Eds.), *Third Millennium BC; Climate Change and Old World Collapse*. NATO ASI Series I, vol. 49. Springer Verlag, pp. 653–678.
- Létolle, R., Mainguet, M., 1993. *Aral*. Springer Verlag, Paris, 358 pp.
- Lioubimtseva, E., 2002. Arid environments. In: Shahgedanova, M. (Ed.), *Physical Geography of Northern Eurasia*. Oxford University Press, Oxford, 571 pp.
- Lioubimtseva, E., Cole, R., Adams, J.M., Kapustin, G., 2005. Impacts of climate and land-cover changes in arid lands of Central Asia. *Journal of Arid Environments* 62, 285–308.
- Lipschitz, N., Lev-Yadun, S., Waisel, Y., 1981. Dendroarchaeological investigations in Israel (Asada). *Israel Exploration Journal* 31, 230–234.
- Mosbrugger, V., Utescher, T., 1997. The coexistence approach—A method for quantitative reconstructions of Tertiary terrestrial palaeoclimate data using plant fossils. *Palaeogeography, Palaeoclimatology, Palaeoecology* 134, 61–86.
- New, M., Hulme, M., Jones, P., 1999. Representing twentieth century space-time climate variability. I: development of a 1961–1990 mean monthly terrestrial climatology. *Journal of Climate* 12, 829–856.
- Nezlin, N.P., Kostianoy, A.G., Li, B.-L., 2005. Inter-annual variability and interaction of remote-sensed vegetation index and atmospheric precipitation in the Aral Sea region. *Journal of Arid Environments* 62, 677–700.
- Nourgaliev, D.K., Heller, F., Borisov, A.S., Hajdas, I., Bonani, G., Iassonov, P.G., Oberhänsli, H., 2003. Very high resolution paleosecular variation record for the last 1200 years from the Aral Sea. *Geophysical Research Letters* 30 (17), 4-1–4-4.
- Peyron, O., Guiot, J., Cheddadi, R., Tarasov, P., Reille, M., de Beaulieu, J.L., Bottema, S., Andreu, V., 1998. Climate reconstruction in Europe for 18,000 yr B.P. from pollen data. *Quaternary Research* 49, 183–196.
- Prentice, I.C., Cramer, W., Harrison, S.P., Leemans, R., Monserud, R.A., Solomon, A.M., 1992. A global biome model based on plant physiology and dominance, soil properties and climate. *Journal of Biogeography* 19, 117–134.
- Prentice, I.C., Guiot, J., Huntley, B., Jolly, D., Cheddadi, R., 1996. Reconstructing biomes from palaeoecological data: a general method and its application to European pollen data at 0 and 6 ka. *Climate Dynamics* 12, 185–194.
- Reimer, P.J., Baillie, M.G.L., Bard, E., Bayliss, A., Beck, J.W., Bertrand, C.J.H., Blackwell, P.G., Buck, C.E., Burr, G.S., Cutler, K.B., Damon, P.E., Lawrence Edwards, R., Fairbanks, R.G., Friedrich, M., Guilderson, T.P., Hogg, A.G., Hughen, K.A., Kromer, B., McCormac, G., Manning, S., Bronk Ramsey, C., Reimer, R.W., Remmele, S., Southon, J.R., Stuiver, M., Talamo, S., Taylor, F.W., van der Plicht, J., Weihsenmeyer, C.E., 2004. IntCal04 terrestrial radiocarbon age calibration, 0–26 cal. yr BP. *Radiocarbon* 46 (3), 1029–1058.
- Roberts, N., Wright, H.E., 1993. Vegetational, lake-level, and climatic history of the Near East and Southwest Asia. In: Wright, H.E. (Ed.), *Global Climates since the Last Glacial Maximum*. University of Minnesota Press, pp. 194–220.
- Rubanov, I.V., Ischniyanov, D.P., Baskakova, M.A., 1987. *Geology of the Aral Sea*. Tashkent, 248 pp. (in Russian).
- Schilman, B., Bar-Matthews, M., Almogi-Labin, A., Luz, B., 2001. Global climate instability reflected by Eastern Mediterranean marine records during the Late Holocene. *Palaeogeography, Palaeoclimatology, Palaeoecology* 176, 157–176.
- Schilman, B., Ayaly, A., Bar-Matthews, M., Kagan, E.J., Almogi-Labin, A., 2002. Sea-land palaeoclimate correlation in the Eastern Mediterranean region during the Late Holocene. *Israel Journal of Earth Sciences* 51, 181–190.
- Seredkina, E.A., 1960. Dust storms in Kazakhstan (Pyl'nie buri v Kazakhstane). *Proceedings of KazNIGMI* 15, 54–59 (in Russian).
- Sorrel, P., Popescu, S.-M., Head, M.J., Suc, J.P., Klotz, S., Oberhänsli, H., 2006. Hydrographic development of the Aral Sea during the last 2000 years based on a quantitative analysis of dinoflagellate cysts. *Palaeogeography, Palaeoclimatology, Palaeoecology* 234 (2–4), 304–327.
- Tarasov, P.E., 1992. *Holocene palaeogeography of the steppe zone of Northern and Central Kazakhstan*. Thesis, Moscow University, 213 pp.
- Tarasov, P.E., Jolly, D., Kaplan, J.O., 1997. A continuous Late Glacial and Holocene record of vegetation changes in Kazakhstan. *Palaeogeography, Palaeoclimatology, Palaeoecology* 136, 281–292.
- Tarasov, P.E., Webb III, T., Andreev, A.A., Afanas'eva, N.B., Berezina, N.A., Bezusko, L.G., Blyakharchuk, T.A., Bolikhovskaya, N.S., Cheddadi, R., Chernavskaya, M.M., Chernova, G.M., Dorofeyuk, N.I., Dirksen, V.G.,

- Elina, G.A., Filimonova, L.V., Glebov, F.Z., Guiot, J., Gunova, V.S., Harrison, S.P., Jolly, D., Khomutova, V.I., Kvavadze, E.V., Osipova, I.M., Panova, N.K., Prentice, I.C., Saarse, L., Sevastyanov, D.V., Volkova, V.S., Zernitskaya, V.P., 1998a. Present-day and mid-Holocene biomes reconstructed from pollen and plant macrofossil data from the former Soviet Union and Mongolia. *Journal of Biogeography* 25, 1029–1053.
- Tarasov, P.E., Cheddadi, R., Guiot, J., Bottema, S., Peyron, O., Belmonte, J., Ruiz-Sanchez, V., Saadi, F.A., Brewer, S., 1998b. A method to determine warm and cool steppe biomes from pollen data; application to the Mediterranean and Kazakhstan regions. *Journal of Quaternary Sciences* 13, 335–344.
- Van Campo, E., Cour, P., Sixuan, H., 1996. Holocene environmental changes in Bangong Co Basin (Western Tibet). Part 2: The pollen record. *Palaeogeography, Palaeoclimatology, Palaeoecology* 120, 49–63.
- Velichko, A.A., 1989. The relationship of the climatic changes in the high and low latitudes of the Earth during the Late Pleistocene and Holocene. In: Velichko, A.A., et al. (Ed.), *Paleoclimates and Glaciation in the Pleistocene*. Nauka Press, Moscow, pp. 5–19.
- Zavialov, P.O., 2005. *Physical oceanography of the dying Aral Sea*. Springer Verlag, published in association with Praxis Publishing, Chichester, UK, 146 pp.

CONCLUSION

This manuscript synthesizes my scientific work from my PhD (1998-2001), including my postdoc stages (2002-2008). Being pollen analyst, my postdoc stages aimed in developing my second expertise concerning the organic walled dinoflagellate cysts, which resulted in paleogeographic reconstructions and characterization of the marine paleoenvironmental changes. My researches focussed on the impact of global climate on continental and marine environments in Europe and Mediterranean realms during the Late Cenozoic, as promoted by 23 publications in international journals and more than 50 presentations in international meetings. During the last six years, I was co-supervising 6 PhD students and 4 graduate and undergraduate students' research (see publication listing). My scientific work developed within the frame of several national and international scientific projects (see CV).

Using pollen grains analysis, I reconstructed the vegetation dynamics and paleoclimate evolution in Eastern Europe for the Late Miocene - Early Pliocene times, the extension of which to the entire Late Cenozoic was favoured by several collaborations. Thanks to investigations marked by a high- and very-high chronogological resolution, I identified the impact of astronomical (eccentricity and for the first time, precession forcing) and solar control on the vegetation changes, and the past climate parameters were reconstructed in collaboration.

Using dinoflagellate cyst analysis, my work concentrated on the characterization of important fluctuations of sea-surface parameters (salinity, temperature and nutrient content) in Paratethys (intercontinental endemic sea, almost completely isolated from the Mediterranean since about 11 Ma years, its evolution marking the passage from marine to less saline conditions) and its present-day relict seas (i.e. Black, Caspian and Aral seas). The main target of this work was to characterize the paleoenvironment and paleoclimatic changes. Narrowly linked to sea-surface parameters, dinoflagellates have appeared as very sensitive organisms to environmental changes, and their strategy to adapt to new environmental conditions was written over their cyst morphology. To understand biological aspect of this group of organisms, especially during my two postdoc stages (Westminster University, London and WHOI, USA), I performed cultures of a living-dinoflagellate species, that I continued in Lyon. Preliminary results on *Scrippsiella trifida* (see Chap. 2) clearly point out the impact of salinity on reproduction rate and cyst morphology. Concerning the fossil dinoflagellates (some of them being considered as extinct today), I performed high-resolution exhaustive countings at different time-scales, and for some selected species such as *Galeacysta etrusca* and *Lingulodinium machaerophorum*, I promoted biometrical and statistic analyses that permitted to obtain new and relevant paleoecological, paleobiological and paleogeographic reconstructions.

The multi -proxy approach (palynology, sedimentology and geochemistry) developed on the Aral Sea sediments by my first co-supervised PhD student allowed us not only to reconstruct the regional paleoclimate and paleoenvironments, but also to understand the atmosphere dynamics of the last 2 ka over the high latitudes of the Northern Hemisphere.

As a perspective, I will extend my researches to the intertropical area in order to reconstruct and understand the atmosphere-ocean dynamics and climate impact on the intertropical area and mid-latitudes. Two PhD theses in progress, that I am co-

supervising (M. Dalibard and A. Safra), focus on this topic. The first one concerns the Guinea Gulf (Eastern intertropical Atlantic) and the second (A. Safra) the Mediterranean region (Gulf of Lions and Adriatic Sea). The major goal of these PhD researches is to understand the ocean – atmosphere dynamics during the Last Climatic Cycle through a multi-proxy approach (pollen grains, dinoflagellate cysts and organic geochemistry).

The second direction of my future researches concerns the dinoflagellates, and is related to the development of relationships between living organisms and their cyst in order to provide a reliable transfer function for reconstructing sea-surface parameters able to be applied to any type of basin. As far as this work is supported by the development of microculture experiments on selected species under stress control, I aim to perform an associated biometrical and statistic aspect on both the cysts resulting from cultures and those recorded in past sediments.

ANNEXES

L'investigation palynologique du Cénozoïque passe par les herbiers

Jean-Pierre Suc¹, Séverine Fauquette²
et Speranta-Maria Popescu³

Université Claude Bernard – Lyon 1, Laboratoire PaléoEnvironnements et
PaléobioSphère (UMR 5125 CNRS), 27-43 boulevard du 11 Novembre, F-
69622 Villeurbanne Cedex
(jean-pierre.suc@univ-lyon1.fr; fauquet@isem.univ-montp2.fr; popescu@univ-
lyon1.fr)

RESUME

Les palynologues du Cénozoïque qui se posent la question de l'identification botanique des grains de pollen sont des utilisateurs assidus des herbiers pour l'obtention du matériel comparatif de référence qui sera examiné au microscope photonique et, éventuellement, au microscope électronique à balayage. Il en résulte une maîtrise des caractères morphologiques du pollen permettant une identification indiscutable. Les banques de données relayent à présent les atlas iconographiques. Les résultats scientifiques résultant de ce type d'approche sont sans précédent et concernent aussi bien la diversité floristique, la végétation, le climat que la chronologie à très haute résolution. Ces données ont récemment abouti à des quantifications qui ouvrent sur de nouvelles perspectives.

Introduction.

Depuis 1960, un important changement est intervenu dans la philosophie des Palynologues du Néogène [période comprise entre 23,8 et 1,77 Ma (millions d'années)] : il s'agit de l'extension au Pliocène (de 5,33 à 1,77 Ma) de l'approche palynologique quaternariste qui repose sur trois critères (l'identification botanique des grains de pollen, leur comptage effectif et en nombre significatif dans les résidus de sédiments après traitement, la multiplication des échantillons étudiés sur une coupe verticale) (Zagwijn, 1960). Cette méthode a été ensuite intensifiée par les travaux de A. Pons (1964) puis de J.-P. Suc (1980) et Hooghiemstra (1989). Cela avait pour corollaire l'abandon de tout objectif de datation des terrains à priori par leur contenu pollinique (Suc et Bessedik, 1981). M. Bessedik (1985) a ensuite étendu la méthode au Miocène (de 23,8 à 5,33 Ma) avant que des auteurs essayent de l'appliquer avec succès aux périodes immédiatement antérieures (Eocène et Oligocène : de 54,8 à 23,8 Ma) (Gruas-Cavagnetto, 1987 ; Schuler, 1988). Cette réussite a sonné le glas d'une méthode totalement désuète mais combien tenace, dite « morphographique », dans laquelle les caractères polliniques étaient réduits à leur portion élémentaire et où un binôme « linnéen » artificiel (en dépit de l'indication éventuelle d'affinités botaniques souvent grossières) conférait l'illusion d'une identification spécifique totalement irréaliste (Thomson et Pflug, 1953 ; Krutzsch, 1970, 1971). Cette révolution n'a été possible, chez les Géologues, que grâce à l'utilisation soutenue par certains Palynologues du matériel pollinique comparatif provenant des herbiers.

Dans cet article, nous aborderons à travers quelques exemples les bienfaits de l'identification botanique des grains de pollen du Cénozoïque, puis nous indiquerons quelques exemples de banques de données en Palynologie avant d'évoquer quelques unes des applications spectaculaires des données polliniques du Cénozoïque.

L'IDENTIFICATION BOTANIQUE DES GRAINS DE POLLEN DU CENOZOÏQUE.

Le Palynologue prélève des fleurs dans des parts d'herbier et en extrait le pollen qu'il monte entre lame et lamelle pour observation au microscope photonique. Des collections de référence de pollen des plantes actuelles se sont ainsi développées, les plus importantes se trouvant à Montpellier, Stockholm, Amsterdam. Elles permettent d'une part l'élaboration d'atlas iconographiques (exemples parmi les plus connus : Maley, 1970 ; Richard,

1970 ; Nilsson *et al.*, 1977 ; Bonnefille et Riollet, 1980 ; Thanikaimoni, 1987 ; Reille, 1992, 1995, 1998 ; Tissot *et al.*, 1994 ; Jones *et al.*, 1995 ; Fuhsiong *et al.*, 1997), d'autre part l'examen simultané au microscope à pont de comparaison des grains de pollen du Cénozoïque à ceux des plantes actuelles auxquelles on les rapporte. Dans l'ensemble, on peut identifier au niveau du genre (quelquefois de l'espèce) les grains de pollen des arbres (ou des ligneux plus généralement), au niveau de la famille (occasionnellement du genre, rarement de l'espèce) ceux des herbes. Cette limitation vient appuyer le bien-fondé de la démarche basée sur la nomenclature botanique car toutes les familles actuelles et pratiquement tous les genres actuels existaient peu après le début du Cénozoïque (début de l'Eocène à 54,5 Ma), la période antérieure du Paléogène, le Paléocène (de 65 à 54,5 Ma), soulevant beaucoup de questions du point de vue floristique. Un examen complémentaire peut être réalisé en utilisant le microscope électronique à balayage qui permet surtout la comparaison des éléments très fins de l'ornementation et, en conséquence, la certitude ou non d'une attribution au niveau de l'espèce.

Il est certain que cette démarche ne va pas sans risque car beaucoup d'espèces ont une origine relativement récente et que certaines autres, plus anciennes, ont pu voir leur écologie se modifier au cours du temps (Kvacek, 2003). Il n'en demeure pas moins vrai que certaines espèces ont peu ou pas évolué depuis plusieurs millions d'années et que leurs exigences écologiques sont demeurées les mêmes. C'est le cas, par exemple, d'*Avicennia marina* Vierh. (Verbenaceae) dont le pollen du Miocène moyen (16 Ma) qui lui est rapporté est en tous points semblable au pollen actuel de l'espèce (Bessedik, 1981) (Fig. 1). Cette identification a permis de restituer (1) les écosystèmes littoraux méditerranéens au cours du Néogène, (2) l'histoire de la manrove à *Avicennia* en Méditerranée, notamment sa disparition des littoraux nord-méditerranéens à 14 Ma puis des littoraux sud-méditerranéens (incluant la Sicile) à 5,6 Ma (Bessedik, 1985 ; Suc et Bessais, 1990).

Dans la description détaillée du grain de pollen qu'il fait, le Palynologue considère de nombreux caractères (jusqu'à 200 voire plus) ayant trait aux ouvertures, à la structure, à l'ornementation et à la forme du pollen. Il réalise l'examen par la méthode dite de la « L.O. analyse » (Lumière-Ombre analyse) qui consiste dans la pénétration optique très progressive de la membrane pollinique (l'exine) (Erdtman, 1966). Cet examen complet n'est possible qu'au microscope optique et nécessite une expérience bien acquise. L'examen au microscope électronique à balayage ne peut concerner que quelques caractères de certains des aspects observés (l'ornementation surtout, les ouvertures pour leur forme externe seulement, la forme générale du pollen). Il ne saurait donc être déterminant dans l'identification botanique a priori du pollen mais doit venir en appui de l'observation comparative au microscope photonique lorsque celle-ci est concluante.

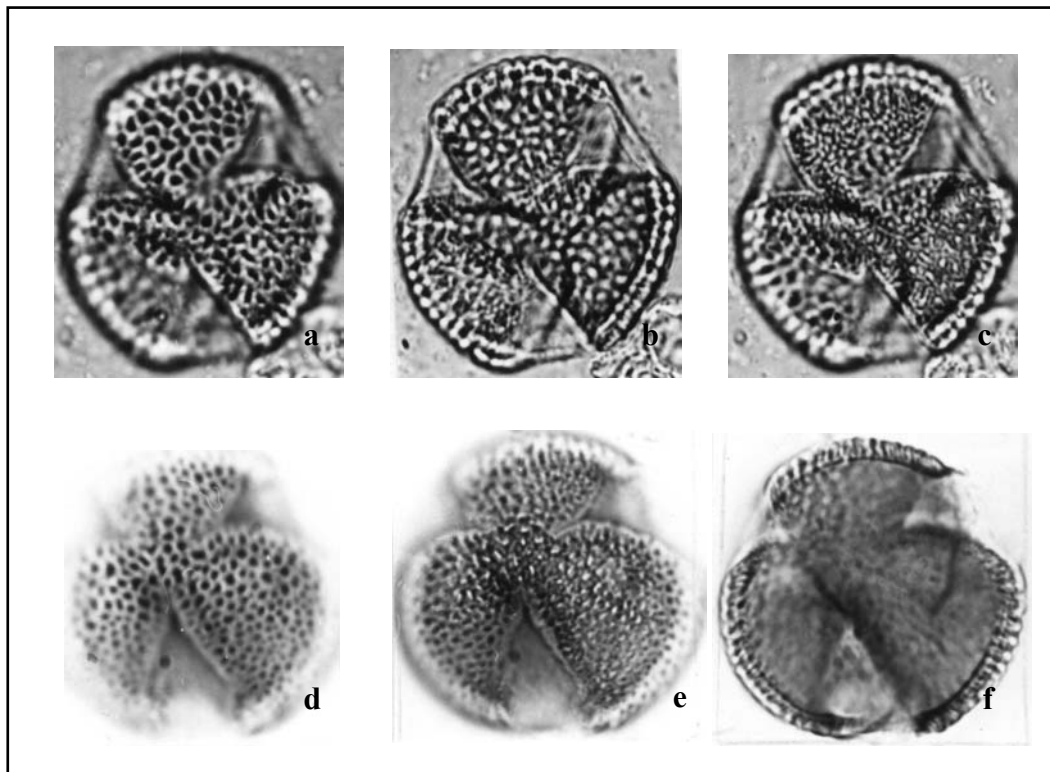


Fig. 1. Pollen actuel d'*Avicennia marina* Vierh. (Verbenaceae) (a à c) comparé au pollen du Langhien méditerranéen (16 Ma) qui lui est attribué (d à f). Les vues ont été prises aux mêmes niveaux optiques (x1000) : a et d, surface de l'ornementation (on remarquera la grande similitude du réseau : murs en blanc, mailles en noir) ; b et e, base des columelles (à noter l'épaisseur croissante des murs du réseau en noir par rapport aux mailles en blanc) ; c et f, coupe optique équatoriale des grains (voir l'analogie des trois sillons et la répartition semblable des columelles).

Le problème majeur réside dans la méconnaissance (ou la négligence) par certains Palynologues de caractères morphologiques qui ont une sens taxonomique essentiel. Cela vient d'une carence dans la formation morphologique de Palynologues qui n'ont pas fréquenté les grandes écoles de morphologie pollinique (G. Erdtman, J. Praglowski et S. Nilsson à Stockholm ; M. Van Campo et P. Guinet à Montpellier ; W. Punt à Utrecht). Un des exemples les plus frappants est la confusion possible entre *Olea* (Oleaceae) et *Microtropis fallax* Pitard (Celastraceae) qui ne subsiste plus aujourd'hui que dans deux stations du Viêt-Nam et qui était très fréquent dans le Néogène d'Europe méridionale et centrale (Lobreau-Callen et Suc, 1972 ; G. Jimenez Moreno, communication personnelle). La forte potentialité de confusion vient de la présence de replis de l'endexine dans l'aperture du pollen tricolporé de *Microtropis fallax* L. (difficiles à voir si l'on ne peut pas faire mouvoir les grains dans un milieu de montage liquide comme le glycérol), caractère qui n'existe

pas dans le pollen tricolpé d'*Olea*. On mesure pleinement combien les reconstitutions environnementales peuvent être faussées par ce genre d'erreur.

L'observation au microscope électronique à balayage peut efficacement appuyer celle faite préalablement au microscope photonique. Un des meilleurs exemples est donné par la distinction entre *Cathaya* et certaines espèces de *Pinus*. Le microscope photonique suffit dans la plupart des cas à identifier le pollen de *Cathaya* sur la structure des alvéoles des ballonnets (un seul niveau d'alvéoles à paroi épaisse et contournée chez *Cathaya*, trois niveaux d'alvéoles à paroi fine et davantage rectiligne chez *Pinus*), la forme du grain (ballonnets emboîtants chez *Cathaya*, non emboîtants chez *Pinus*) et le plancher des ballonnets (à granulations chez *Cathaya*, lisse chez *Pinus*) (Fig. 2). Toutefois, il existe des grains (souvent un peu plus grands) de *Pinus* qui présentent pratiquement la même structure que ceux de *Cathaya* et qui en sont difficilement discernables au microscope photonique (Fig. 3). Leur observation au microscope électronique à balayage permet de lever cette interrogation (les grains de pollen de *Pinus* ont une ornementation verruqueuse assez grossière) (Fig. 3).

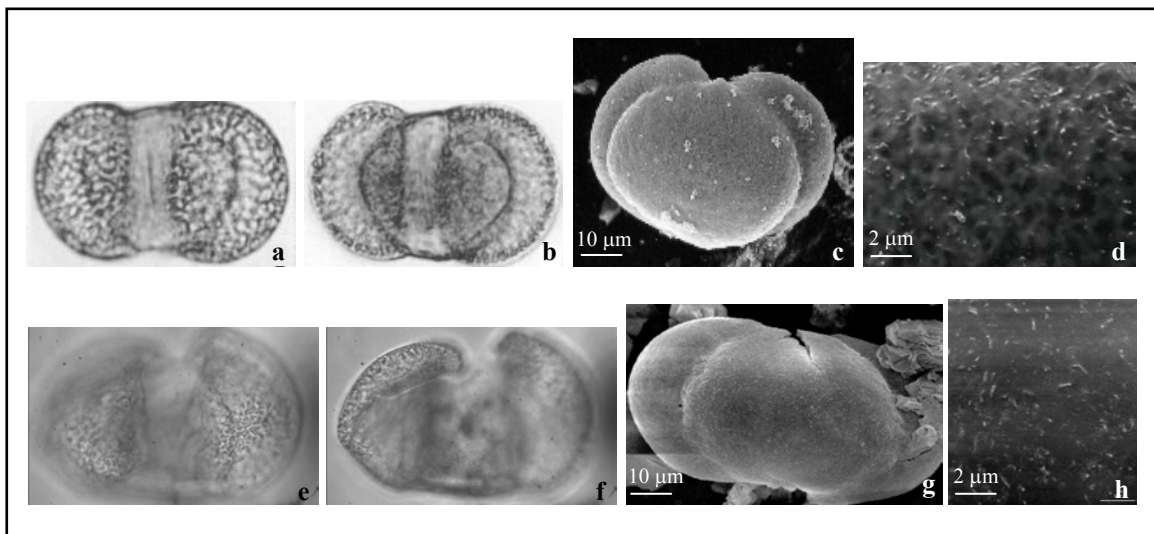


Fig. 2. Pollen actuel de *Cathaya argyrophylla* Chung et Kuang (a à d) comparé au pollen du Zancéen méditerranéen (5 Ma) qui lui est attribué (e à h). Les vues a et b, e et f (microscope photonique) sont au même niveau (vues distales), les vues a, b, c, e, f et g sont au même grossissement (indiqué par une échelle sur les vues c et g) : a et e, structure alvéolaire (alvéoles à paroi épaisse et contournée, granulations du plancher des ballonnets) ; b et f, coupe optique (ballonnets emboîtants) ; c et g, vues proximales au microscope électronique à balayage (ballonnets emboîtants) ; d et h, détails de l'ornementation au microscope électronique à balayage (micro-épines caractéristiques).

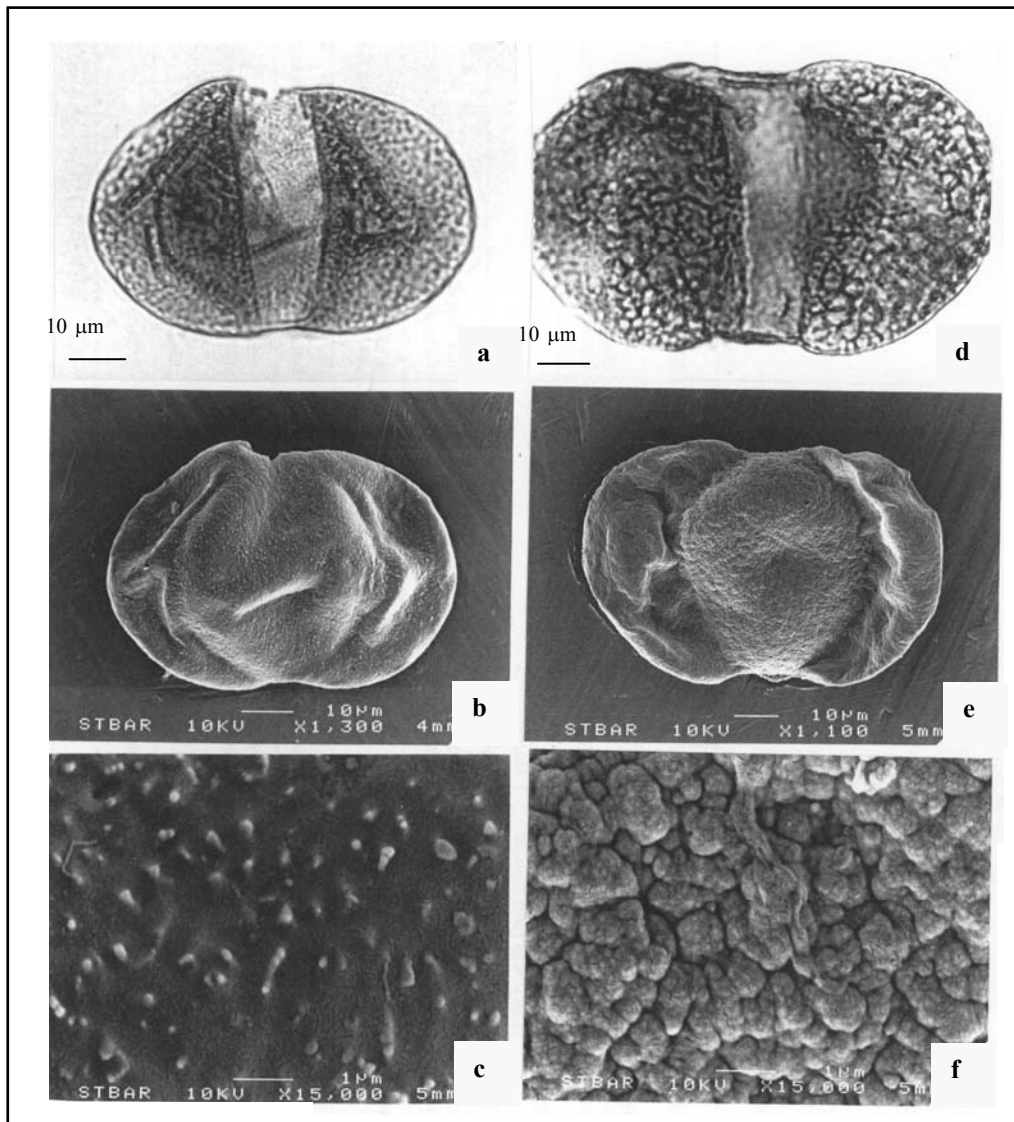


Fig. 3. Grains de pollen du Gélasien méditerranéen (2 Ma) respectivement attribués à *Cathaya* (a à c) et à *Pinus* (d à f). Les photographies au microscope photonique a et d sont au point sur la structure alvéolaire (très similaire) des ballonnets en vue distale ; b et e, vues proximales au microscope électronique à balayage montrant le caractère emboîtant des ballonnets ; c et f, détails de l'ornementation au microscope électronique à balayage (micro-épines caractéristiques chez *Cathaya*, verrues grossières chez *Pinus*).

Le lecteur mesurera combien le Palynologue acquis à cette démarche a besoin d'échantillons d'herbiers bien identifiés. Toute la crédibilité des reconstitutions qu'il déduit de ses flores polliniques en dépend.

LES BANQUES DE PHOTOGRAPHIES DIGITALISEES EN PALYNOLOGIE.

Les banques de photographies digitalisées de grains de pollen sont venues supplanter les atlas iconographiques. Certaines sont déjà disponibles sur *Internet*, comme l'*African Pollen Database* (<http://medias.obs-mip.fr/apd>: auteur, A.-M. Lézine), qui met à disposition des chercheurs un nombre élevé de photographies du pollen actuel d'espèces de diverses familles africaines. Il s'agit d'un outil d'identification rapide constitué d'images sur papier scannées sans commentaire morphologique ni tri de caractères.

La banque d'images digitalisées de pollen PHOTOPAL (auteurs : J.-P. Suc, G. Bucciatti et B. Brémond) a été construite selon une philosophie différente. Elle fonctionne en français et en anglais. Des espèces de toutes familles botaniques, d'origine géographique variée et d'écologie diverse y sont illustrées. Les photographies se présentent sous la forme de fiches (contenant jusqu'à 20 images en noir et blanc sur un demi-écran), chacune de ces images pouvant être observée successivement, à grand format, sur le second demi-écran (Fig. 4).

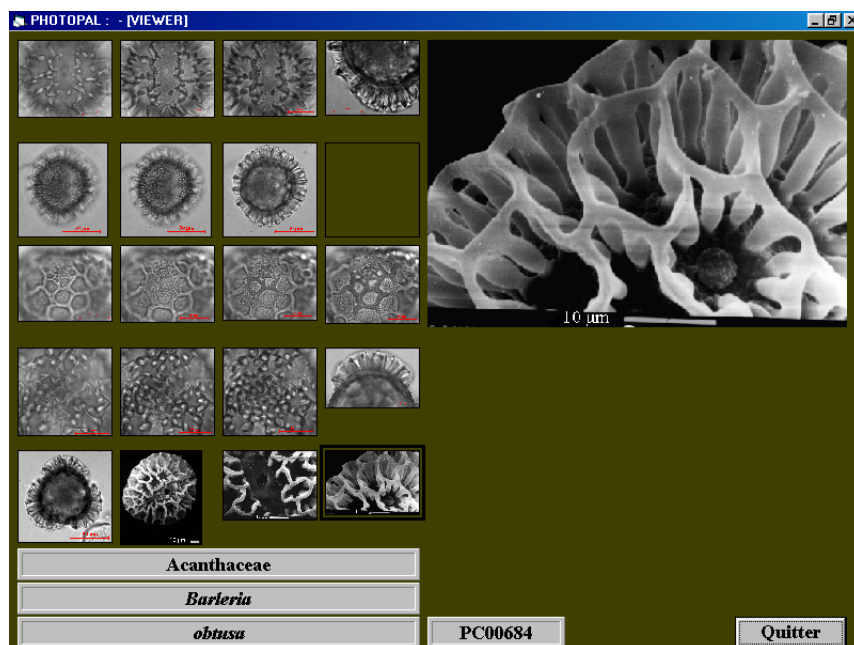


Fig. 4. Banque PHOTOPAL. Exemple de présentation du pollen de *Barleria obtusa* Nees (Acanthaceae) à travers des images en microscopie photonique et électronique à balayage.

Ces images, provenant toutes de prises de vue faites au laboratoire avec une caméra CCD, sont à haute résolution (Super VGA: 756 x 581 pixels - 256 niveaux de gris). Les fiches sont pour l'essentiel constituées de vues en microscopie photonique (grossissement 1000, parfois 400) et incluent aussi des vues en microscopie électronique à balayage (Fig. 4).

Une fiche d'information sur la plante (origine de l'échantillon, distribution géographique, écologie, synonymies, phénologie de l'espèce) et une fiche de description morphologique du pollen sont aussi disponibles pour chaque espèce. L'utilisateur accède aux espèces dont il désire observer les photographies du pollen soit directement par la voie systématique, soit par l'intermédiaire d'un procédé de tri des caractères très performant pour l'identification des pollens trouvés dans les sédiments (Fig. 5). PHOTOPAL, qui est aussi un excellent outil de formation à la morphologie pollinique, s'adresse aux Palynologues (de la recherche fondamentale comme de la recherche appliquée) travaillant sur les sédiments du Cénozoïque ou sur les pollens actuels (Systématique, aéropalynologie, mélioppalynologie). Actuellement disponible sur CDROM et comptant 200 espèces, la banque est progressivement enrichie et sera prochainement installée sur le site de Médias-France.

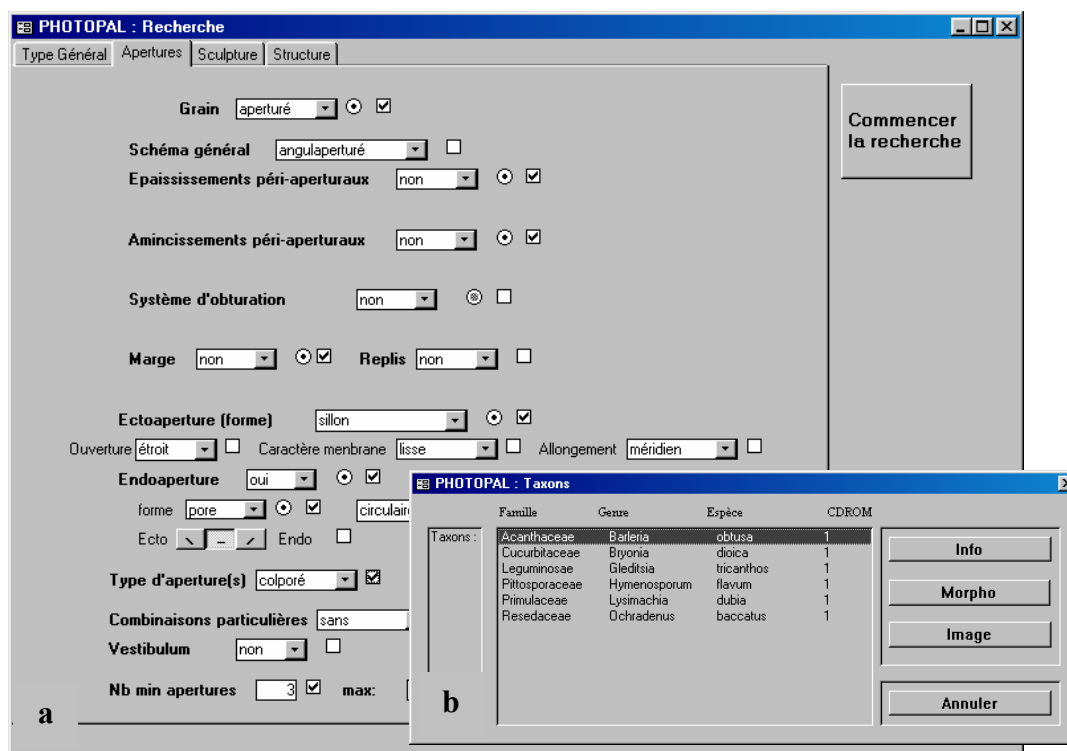


Fig. 5. Identification d'un grain de pollen dans la Banque PHOTOPAL.
a, Tri de ses caractères morphologiques.
b, Résultat de la recherche.

LES APPLICATIONS DES DONNEES POLLINIQUES DU CENOZOÏQUE.

Celles-ci se sont considérablement développées au cours des vingt dernières années et ont dépassé toutes les espérances d'alors.

Du point de vue de la diversité floristique, la flore du Néogène d'Europe et du pourtour méditerranéen est à présent très largement inventoriée et montre de plus en plus d'affinités avec la flore actuelle de Chine tropicale et subtropicale. Près de 200 taxons y ont été identifiés dont plus d'une cinquantaine n'habitent plus aujourd'hui ces régions (*Avicennia*, *Amanoa*, Sapotaceae, Taxodiaceae, *Bombax*, *Sindora*, *Engelhardia*, *Platycarya*, *Rhoiptelea*, plusieurs genres d'Hamamelidaceae, etc.).

Le calendrier et les modalités de leur extinction sont bien connus (Fig. 6): celle-ci s'est opérée du Nord vers le Sud sous l'effet des refroidissements répétés (glaciations arctiques régulières depuis 2,6 Ma) avec des reliquats à l'est et à l'ouest du domaine méditerranéen, vraisemblablement sous l'influence protectrice respective des moussons ouest-africaine et asiatique (Suc, 1996 ; Popescu, 2001a).

La distribution actuelle des plantes reliques sur le pourtour méditerranéen ou à ses abords reflète bien le calendrier des extinctions de la région méditerranéenne des représentants des groupes de végétaux thermophiles (Fig. 6) : les éléments mégathermes (tropicaux) (*Avicennia*, *Bombax*, *Amanoa*, Sapindaceae, *Sindora*, Rubiaceae, etc.) ont disparu les premiers du nord de la Méditerranée (14 Ma) avant de disparaître au sud (5,6 Ma) tout en demeurant un peu plus longtemps sur les rives de la mer Noire (4-3,5 Ma) ; les végétaux méga-mésothermes (subtropicaux) (Taxodiaceae, Sapotaceae, *Engelhardia*, etc.) ont suivi le même gradient nord-sud d'extinction avec toutefois une précocité en Afrique septentrionale (3,6 Ma), vraisemblablement à cause de la forte xéricité, et un maintien prolongé en Italie méridionale (relief proche du littoral) (<1,3 Ma) ; des végétaux mésothermes (tempérés-chauds) (*Parrotia*, *Carya*, *Pterocarya*, *Cedrus*, *Zelkova*, *Liquidambar*) ont disparu d'abord au nord de la région méditerranéenne mais certains d'entre eux subsistent encore en Sicile et en Crète (*Zelkova*), au Maroc, en Algérie et au Liban (*Cedrus*), enfin en Anatolie ou en Iran (*Liquidambar*, *Parrotia*).

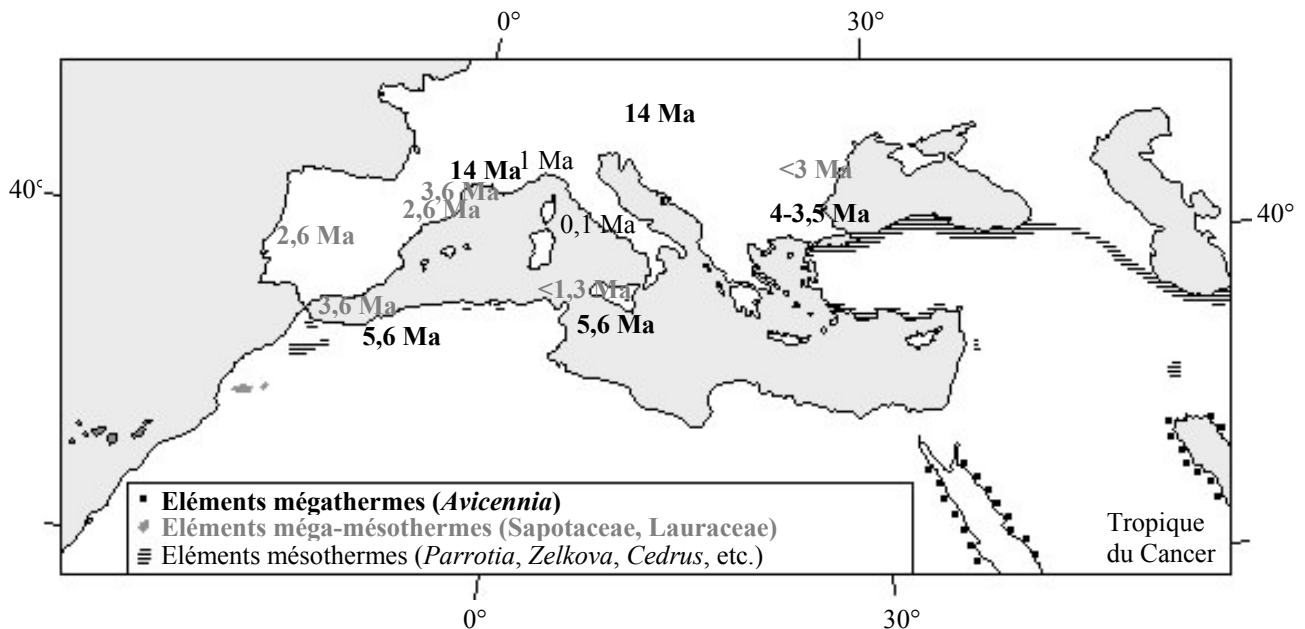


Fig. 6. Distribution actuelle des végétaux reliques mégathermes (tropicaux), méga-mésothermes (subtropicaux) et de quelques éléments mésothermes (tempérés-chauds) au voisinage du domaine méditerranéen. Les âges indiquent leur dernière présence respective.

Les grands domaines végétaux du Zancéen (5,33-3,6 Ma), période pour laquelle on dispose du plus grand nombre de données polliniques, ont été identifiés pour l'ensemble de l'Europe et le pourtour méditerranéen. On y distingue plusieurs provinces : atlantique (caractérisée par la prédominance des marécages à Taxodiaceae et les Ericaceae), nord-méditerranéenne (avec quelques marécages locaux à Taxodiaceae, des forêts à *Sequoia*, *Cathaya*, *Cedrus*, *Tsuga* sur les versants montagneux proches des littoraux), sud-méditerranéenne (dominée par les herbes incluant plusieurs éléments subdésertiques comme *Lygeum*, *Neurada*, *Nitraria*, *Calligonum*, etc.), est-européenne (avec des marécages à Taxodiaceae et à Cyperaceae comme de nos jours en Floride et dans le delta du Mississippi, et des forêts à *Abies* et *Picea* en altitude), anatolienne (végétation ouverte riche en *Artemisia*) (Suc *et al.*, 1995 ; Popescu, 2001a et sous presse). Les xérophytes méditerranéennes (*Olea*, *Phillyrea*, *Quercus sempervirens*, *Cistus*, *Ceratonia*, *Pistacia*, etc.) se trouvaient en abondance à la transition entre les régions nord- et sud-méditerranéenne. Les structures de végétation steppique existaient déjà sur les rives méridionales de la Méditerranée tandis que les formations à *Artemisia* d'Anatolie annonçaient déjà les steppes à Armoise qui envahiront le domaine méditerranéen dès l'apparition des cycles glaciaire-interglaciaire de

l'hémisphère Nord (2,6 Ma). Des cartes de paléovégétation sont en cours d'élaboration par interpolation des données polliniques ; un premier essai fructueux a porté sur le Zacléen de Méditerranée nord-occidentale (Charlet, 2002).

Les paramètres climatiques du Pliocène, du Messinien et du Tortonien, c'est-à-dire de 10 Ma environ à 1,77 Ma, d'Europe et du pourtour méditerranéen ont été quantifiés à partir d'une fonction de transfert construite sur les données polliniques (Fauquette *et al.*, 1998 et sous presse ; Fauquette et Bertini, 2003 ; Suc et Fauquette, 2003). Ils témoignent de conditions plus chaudes qu'actuellement sur l'ensemble du domaine mais plus humides au nord de la Méditerranée et plus sèches au sud qu'aujourd'hui (Fauquette *et al.*, 1999a et sous presse).

Ces quantifications ont aussi débouché sur l'estimation des paléoaltitudes des massifs montagneux. La méthode mise au point permet de restituer les paléoaltitudes minimales d'un massif proche d'un dépôt sédimentaire littoral riche en grains de pollen (Fauquette *et al.*, 1999). Elle se fonde sur l'identification de la structuration des paléoétages de la végétation néogène en fonction de l'altitude : l'étage à *Abies* et *Picea* est le plus élevé, il surmonte l'étage à *Cedrus* et *Tsuga* qui succède à son tour celui à *Cathaya*.

Si l'analyse pollinique d'un bassin sédimentaire situé au pied d'un massif révèle la présence voisine d'un ou plusieurs de ces groupements végétaux altitudinaux (c'est-à-dire avec des pourcentages polliniques significatifs), il est possible d'appliquer le gradient actuel d'élévation altitudinale des végétaux en fonction de la latitude dont les reconstitutions et les modèles paléoclimatiques ont montré qu'il était sensiblement équivalent au cours du Cénozoïque supérieur (M. Kageyama et A. Jost, communication personnelle). Ce gradient est, en moyenne, de 110 m en altitude par degré en latitude (Ozenda, 1989).

Ainsi, après avoir appliqué la fonction de transfert paléoclimatique qui permet la restitution des paléotempératures aux basses altitudes (les arbres d'altitude ne sont pas pris en compte pour cette estimation) (Fauquette *et al.*, 1998), on peut déterminer à quelle latitude on trouve aujourd'hui la paléotempérature moyenne annuelle restituée. Cette latitude "virtuelle" permet la transposition en termes de paléoaltitude de l'étage de végétation identifié dans le site pollinique (avec les fourchettes d'appréciation liées à la méthode "statistique" de la fonction de transfert paléoclimatique). S'il s'agit de l'étage (le plus élevé) à Sapin et Epicéa, cette appréciation de la paléoaltitude du massif voisin ne peut être que minimale dans la mesure où le palynologue ne peut pratiquement pas distinguer les herbes de l'étage alpin de celles de basse altitude ; il ne peut donc pas identifier clairement un étage alpin au-dessus de l'ultime étage arboré.

Cette méthode a été appliquée au site zancéen de Saint-Martin du Var se trouvant au pied du Massif du Mercantour (Alpes méridionales) (Fig. 7) où elle a reçu une solide validation de la part de la Géomorphologie quantitative sur la base des référentiels liés à l'épisode de la crise de salinité messinienne (Fauquette *et al.*, 1999b).

Un autre exemple de valorisation des herbiers par la Palynologie concerne le genre *Artemisia*. Son pollen, très reconnaissable, abonde dès le Zancéen en région anatolienne puis à partir de 2,6 Ma sur l'ensemble du pourtour méditerranéen et, dans une moindre mesure en Europe méridionale. *Artemisia* est caractéristique des formations végétales steppiques. Il existe toutefois deux types de steppes à Armoise, les steppes à déterminisme thermique (les steppes « froides ») et les steppes à déterminisme xérique (les steppes « chaudes ») (Quézel et Barbero, 1982).

Ces deux types de steppes à *Artemisia* ont été simultanément distingués au Pliocène final en région méditerranéenne, les premières se développant pendant les phases glaciaires (Calabre méridionale : Combourieu-Nebout et Vergnaud Grazzini, 1991), les secondes pendant les phases interglaciaires (île de Zakynthos : Subally *et al.*, 1999) grâce au guide climatique qu'est la courbe isotopique de l'oxygène (réalisée sur les mêmes échantillons que l'analyse pollinique).

Cette dualité dans la signification d'*Artemisia* interpelle les Palynologues (Subally et Quézel, 2002) et montre l'impérieuse nécessité de parvenir enfin à identifier les espèces d'*Artemisia* par leur pollen afin de pallier à l'absence ou à la défaillance éventuelles d'un enregistrement isotopique de l'oxygène comme guide climatique. C'est ainsi qu'un travail de longue haleine a été entrepris pour sélectionner les caractères morphologiques du pollen pouvant permettre de distinguer les espèces d'*Artemisia* ou, tout au moins, les grands groupes écologiques au sein de ce genre. L'inventaire pollinique complet du genre a exigé un grand nombre de prélèvements en herbiers et d'examens microscopiques.

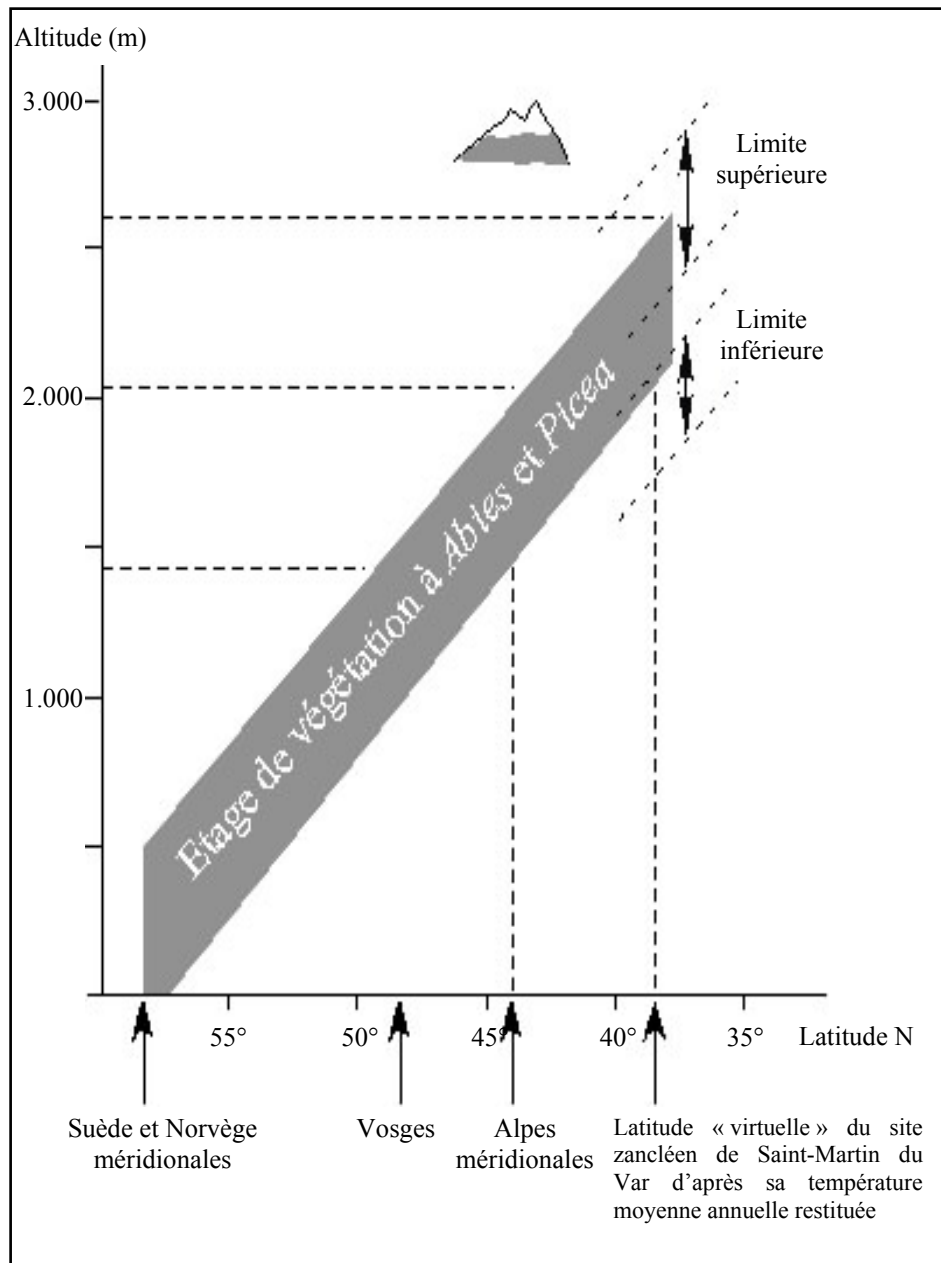


Fig.

7. Estimation de l'altitudes du Massif du Mercantour au Zancléen (comparée à sa latitude actuelle) d'après le déplacement altitudinal de l'étage à *Abies* et *Picea* en fonction de la latitude et de la température sur le littoral au Zancléen.

La Figure 8 montre le pollen au microscope électronique à balayage de 19 espèces d'*Artemisia* se distribuant selon l'indice de la température (espèces mégathermes à microthermes) avec également l'indication de conditions édaphiques (espèces halophiles ou psamophiles). On y voit que le pollen des espèces mégathermes possède des verrues modérément pointues mais assez larges donnant à l'ensemble une certaine ressemblance avec une ornementation verruqueuse. Le pollen des espèces méga-mésothermes, mésothermes et méso-microthermes (tempérées-froides) arborent plutôt des épines moins pointues entre lesquelles s'intercalent souvent des glomérules ou des micro-rugules. Le pollen des espèces microthermes (boréales) ont des épines émoussées reposant sur un mamelon. Les halophytes montrent un schéma où les épines sont plus espacées avec, semble-t-il, un gradient de décroissance de leur hauteur avec l'augmentation de la température (Fig. 8). On retrouve un peu la même tendance chez les espèces psamophiles mais beaucoup d'entre elles sont aussi des halophytes.

Le pollen d'*Artemisia* de sites polliniques s'étalant entre 6 Ma et le Dernier Glaciaire a ensuite été comparé (Fig. 9). L'*Artemisia* trouvé à Velona (Messinien) est probablement à relier à la xéricité engendrée lors de la crise de salinité; il s'agit vraisemblablement d'une espèce mégatherme. Les pollens d'*Artemisia* sont nombreux dans le site oriental de Lataquie daté du Pliocène basal. Ils représentent les steppes "chaudes" est-méditerranéennes qui ne se trouvent développées qu'au Moyen Orient avant les premiers cycles glaciaire-interglaciaire. Les pollens des premiers cycles glaciaire-interglaciaire évoquent des espèces mésothermes tandis que ceux des cycles les plus récents évoquent des espèces microthermes, tout au moins pour les sites de Vallo di Diano, Le Bouchet, Les Echets. Pour la dernière glaciation, les pollens du Portugal, du sud-est de l'Espagne et du sud de la France ressemblent au pollen d'espèces halophiles; cela n'est pas surprenant, s'agissant de pollens recueillis dans des sédiments marins.

La mise à l'écart délibérée de toute intention de dater les terrains cénozoïques à priori à partir de leur contenu pollinique (totalement irréaliste compte tenu des variations spatiales et temporelles dans la diversité floristique ; Suc et Bessedik, 1981) n'oblitére pas pour autant l'obtention de résultats très fins en matière de chronologie. En effet, dans notre approche, les couches sédimentaires sont datées par d'autres moyens très fiables : d'abord la biostratigraphie (foraminifères et nannoplancton pour les dépôts marins, mammifères pour les terrains continentaux) et(ou) les datations radiométriques ($^{39}\text{Ar}/^{40}\text{Ar}$ ou K/Ar s'il y a des intercalations volcaniques, ^{14}C pour la période la plus récente) fournissent un cadre chronologique général qui est ensuite affiné grâce aux mesures paléomagnétiques. Au sein de ce cadre déjà précis, les variations dans l'enregistrement pollinique permettent d'une part des corrélations climatostratigraphiques à grande distance (Suc et Zagwijn, 1983 ; Zagwijn, 1986 ; Popescu, 2001b et sous presse), d'autre part la mise en évidence des réponses de la végétation aux changements de climat (même

modestes) induits par les cyclicités orbitales. C'est ainsi qu'on a été montrées les réponses de la végétation (1) aux cycles glaciaire-interglaciaire de 100.000 ans (100 ka) de période depuis 1 Ma environ (Wijmstra et Groenhart, 1983 ; Hooghiemstra, 1989 ; Russo Ermolli, 1994 ; Kukla et Cilek, 1996) et à ceux de 41 ka de période entre 2,6 et 1 Ma environ (Hooghiemstra, 1989 ; Combourieu-Nebout et Vergnaud Grazzini, 1991 ; Subally *et al.*, 1999), (2) aux forçages antérieurs de l'excentricité (période de 100 ka) et de la précession (20 ka) dans certains sites privilégiés (Popescu, 2001 a et b).

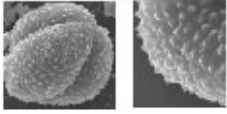
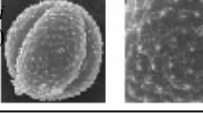
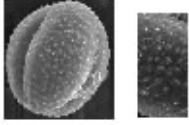
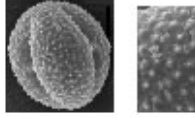
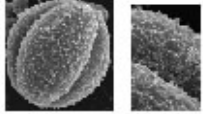

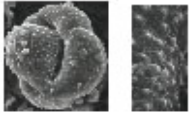
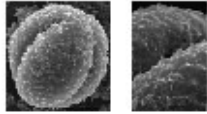
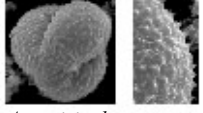
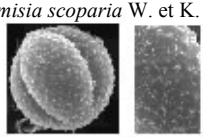
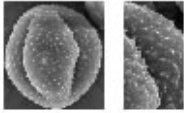
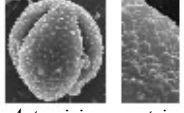
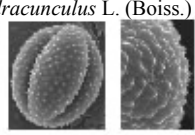
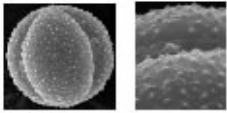
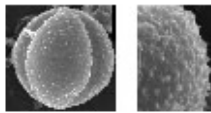
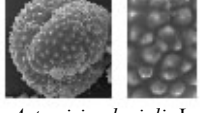
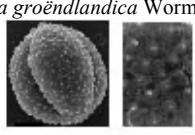
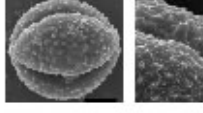
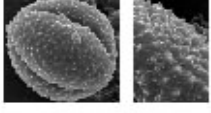
		HALOPHILES	PSAMOPHILES
MEGATHERME	 <i>Artemisia canariensis</i> Bess.  <i>Artemisia herba alba</i> Asso var. <i>Huguetii</i> (Caball.) Maire	 <i>Artemisia hispanica</i> Lam. et Roise	 <i>Artemisia judaica</i> L.
	 <i>Artemisia arborens</i> Bess.  <i>Artemisia barrelieri</i> Bess.	 <i>Artemisia crithmifolia</i> L.	 <i>Artemisia campestris</i> L. ssp. <i>glutinosa</i> Batt. et Trautv.
MESOTHERME	 <i>Artemisia desertorum</i>  <i>Artemisia scoparia</i> W. et K.	 <i>Artemisia caerulescens</i> ssp. <i>gallica</i> (Willd.) var. K. Persson	
	 <i>Artemisia rupestris</i> L.  <i>Artemisia dracunculoides</i> L. (Boiss.)	 <i>Artemisia lerchiana</i> Web. et Stechm.	 <i>Artemisia maritima</i> L.
MICROTHERME	 <i>Artemisia glacialis</i> L.  <i>Artemisia groenlandica</i> Wormlk. M.	 <i>Artemisia bottnica</i> Lundstr.	 <i>Artemisia stellerana</i> Bess.

Fig. 8. Gains de pollen au microscope électronique à balayage de quelques espèces d'*Artemisia* vivant dans des conditions thermiques et édaphiques différentes (les vues générales sont au grossissement 4.000, les vues de détail au gossissement 12.000).

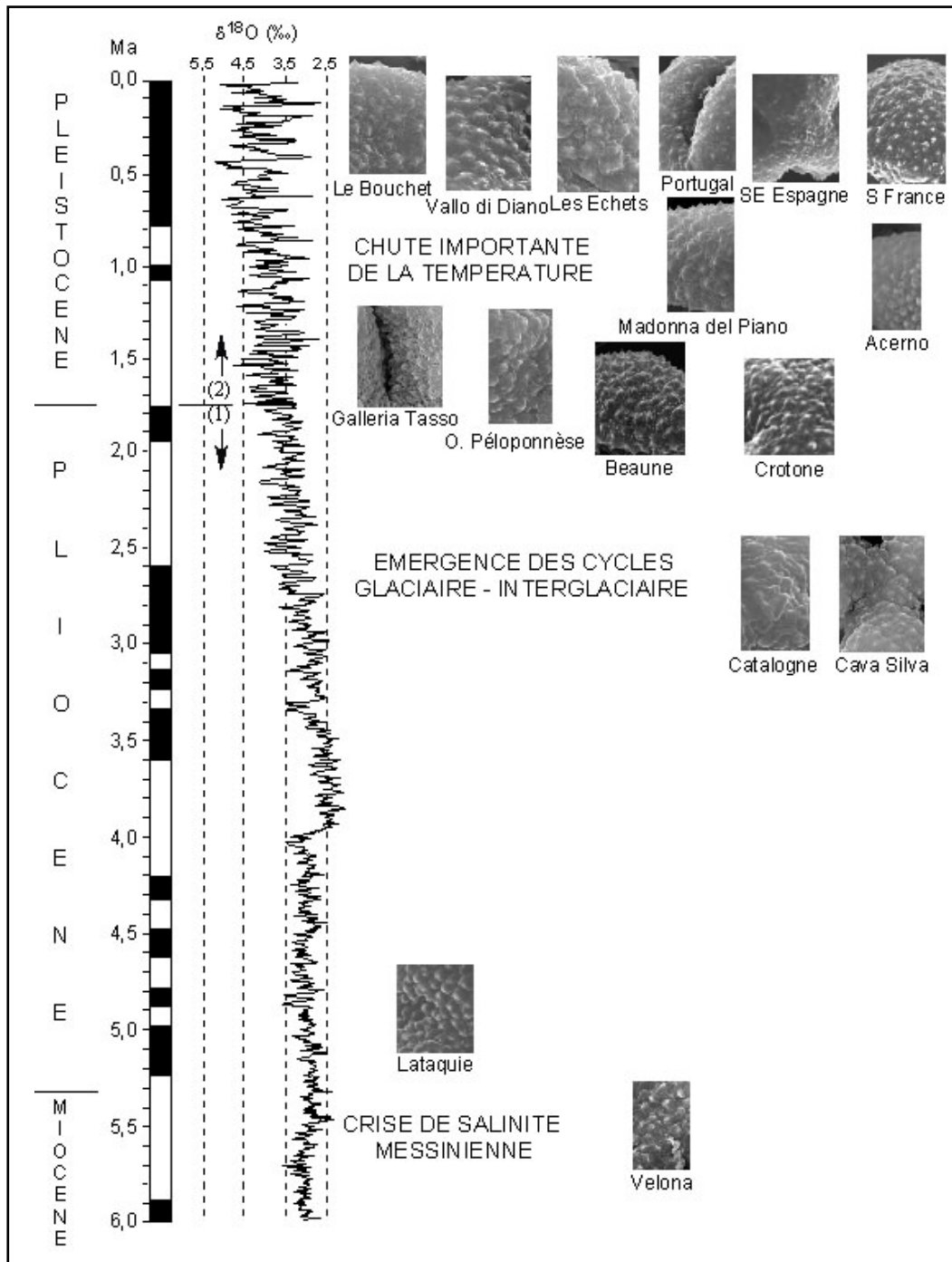


Fig. 9. Distribution chronologique du pollen d'*Artemisia* (ornementation de l'exine) provenant de quelques sites polliniques du pourtour de la Méditerranée allant du Messinien au Dernier Cycle Climatique (les vues en microscopie électronique à balayage sont au grossissement 12.000). La courbe isotopique de l'oxygène ici dessinée est une juxtaposition de deux courbes successives : (1) le Site ODP 846 (Shackleton *et al.*, 1995), (2) le Site ODP 659 (Tiedemann *et al.*, 1994).

CONCLUSION

Nous espérons que le lecteur aura mesuré toute l'importance des grains de pollen de référence provenant d'échantillons d'herbiers dans les travaux modernes en Palynologie. Même si certains travaux en analyse pollinique s'orientent hélas vers une voie plus technique et répétitive sans approfondissement des identifications, la référence aux grains de pollen des plantes actuelles ne cessera de se déployer au vu notamment des exigences au niveau de la connaissance de la diversité végétale et de son passé pour mieux prévoir son devenir. Il est sûr que les Palynologues qui se posent de véritables questions scientifiques ressentiront de plus en plus la nécessité de compléter leur listes floristiques. Les débouchés scientifiques s'intensifieront aussi par le biais de l'emploi des banques de données polliniques [par exemple l'*European Pollen Database* (<http://medias.obs-mip.fr/paleo/epd/>), l'*African Pollen Database* (<http://medias.obs-mip.fr/apd/>), la *Cenozoic Pollen database and Climatic values* (<http://medias.obs-mip.fr/cpc/>)] qui faciliteront les grandes synthèses.

Il faut enfin que les organismes abritant et gérant des herbiers cessent de les considérer comme des conservatoires représentatifs de notre patrimoine et prennent enfin conscience de leur très large utilité pour la recherche moderne en augmentant sensiblement les postes qui leur sont affectés. En effet, les Palynologues, entre autres, ont un besoin affirmé de la plus grande fiabilité dans l'identification des spécimens d'herbiers et cela passe par leur mise à jour taxinomique et leur révision constantes.

REMERCIEMENTS.

Il convient de souligner que certains des résultats évoqués ou présentés dans cet article proviennent de projets financés par des grands programmes (CRISEVOLE du CNRS, EEDEN de l'*European Science Foundation*) ou organismes (Institut Français de la Biodiversité). Nous remercions tout particulièrement P. Quézel et F. Médail pour leur aide dans les prélèvements en herbier ainsi que pour les informations transmises à propos de plusieurs espèces d'*Artemisia*, H. Méon qui a contribué aux photographies au microscope électronique à balayage. Cet article est pour nous l'occasion d'exprimer notre gratitude aux herbiers qui nous aident, certains depuis plus de trente ans comme l'Herbier de l'Université Montpellier 2, l'Herbier de l'Université Cl. Bernard - Lyon 1, l'Herbier de Genève, l'Herbier du Muséum national d'histoire naturelle de Paris, l'Herbier de la Faculté des Sciences de Saint-Jérôme de Marseille, et enfin l'Herbier de l'Université Sun Yat-sen de Canton en Chine.

Rappelons enfin que la banque PHOTOPAL a vu le jour grâce au soutien financier de plusieurs organismes publics (Département SDU du CNRS, D.I.S.T., Université Montpellier 2, Université Lyon 1) et privé (Elf).

BIBLIOGRAPHIE

- Bessedik M., 1981. Une mangrove à *Avicennia* L. en Méditerranée occidentale au Miocène inférieur et moyen. Implications paléogéographiques. *C. R. Acad. Sci. Paris*, sér. 2, 273 : 469-472.
- Bessedik M., 1985. *Reconstitution des environnements miocènes des régions nord-ouest méditerranéennes à partir de la palynologie*. Thèse, Univ. Montpellier 2, 162 p.
- Bonnefille R. et Riollet G., 1980. *Pollen des Savanes d'Afrique Orientale*.dit. CNRS, Paris, 140 p.
- Charlet V., 2002. Elaboration de paléocartes de végétation du Pliocène en région nord-ouest méditerranéenne. DEA Paléontologie et Environnements Sédimentaires, Univ. Lyon 1, 45 p.
- Combourieu-Nebout N. et Vergnaud Grazzini C. 1991. Late Pliocene Northern hemisphere glaciations: the continental and marine responses in the Central Mediterranean. *Quaternary Sci. Rev.*, 10 : 319-334.
- Erdtman G., 1966. *Pollen morphology and plant taxonomy. Angiosperms*. Hafner Publ. Comp., New York et Londres, 2^{ème} édit., 553 p.
- Fauquette S. et Bertini A., 2003. Quantification of the northern Italy Pliocene climate from pollen data – evidence for a very peculiar climate pattern. *Boreas*, 32, 2 : 361-369.
- Fauquette S., Guiot J. et Suc J.-P., 1998. A method for climatic reconstruction of the Mediterranean Pliocene using pollen data. *Palaeogeogr., Palaeoclimatol., Palaeoecol.*, 144 : 183-201.
- Fauquette S., Suc J.-P., Guiot J., Diniz F., Feddi N., Zheng Z., Bessais E. et Drivaliari A., 1999a. Climate and biomes in the West Mediterranean area during the Pliocene. *Palaeogeogr., Palaeoclimatol., Palaeoecol.*, 152 : 15-36.
- Fauquette S., Clauzon G., Suc J.-P. et Zheng Z., 1999b. A new approach for paleoaltitude estimates based on pollen records: example of the Mercantour Massif (southeastern France) at the earliest Pliocene. *Earth Planet. Sci. Lett.*, 170 : 35-47.
- Fauquette S., Suc J.-P., Bertini A., Popescu S.-M., Warny S., Bachiri Taouiq N., Perez Villa M., Chikhi H., Subally D., Feddi N., Clauzon G. et Ferrier J., sous presse. How much the climate forced the Messinian salinity crisis? Quantified climatic conditions from pollen records in the Mediterranean region. *Palaeogeogr., Palaeoclimatol., Palaeoecol.*
- Fuhsung W., Nanfen C., Yulong Z. et Huiqiu Y., 1997. *Pollen Flora of China*. Academia Sinica, 2^{ème} édit., 745 p.
- Gruas-Cavagnetto C., 1987. Nouveaux éléments mégathermes dans la palynoflore éocène du Bassin parisien. *Mém. Trav. E.P.H.E., Inst. Montpellier* : 207-233.
- Hooghiemstra H., 1989. Quaternary and Upper-Pliocene glaciations and forest development in the tropical Andes : evidence from a long high-resolution pollen

- record from the sedimentary basin of Bogota, Colombia. *Palaeogeogr., Palaeoclimatol., Palaeoecol.*, 72 : 11-26.
- Jones G.D., Bryant., Bryant V.M. Jr., Lieux M.H., Jones S.D. et Lingren P.D., 1995. Pollen of the Southeastern United States : with emphasis on Melissopalynology and Entomopalynology. *Amer. Ass. Stratigr. Palynologists Contr. Ser.*, 30 : 1-182.
- Krutzsch W., 1970. *Atlas der mittel- und jungtertiären dispersen Sporen- und Pollen- sowie der Mikroplanktonformen des nördlichen Mitteleuropas. 7, Monoporate, monocolpate, longicolpate, dicolpate und ephedroïde (polyplicate) Pollenformen.* VEB G. Fischer édit., 175 p.
- Krutzsch W., 1971. *Atlas der mittel- und jungtertiären dispersen Sporen- und Pollen- sowie der Mikroplanktonformen des nördlichen Mitteleuropas. 6, Coniferenpollen.* VEB G. Fischer édit., 234 p.
- Kukla G. et Cilek V., 1996. Plio-Pleistocene megacycles: record of climate and tectonics. *Palaeogeogr., Palaeoclimatol., Palaeoecol.*, 120 : 171-194.
- Kvacek Z., 2003. Do extant analogues of palaeotropical elements reliably reflect climatic signal? Workshop on "Tropical and Subtropical elements in the West Eurasian Neogene", Progr. "Environments and Ecosystem Dynamics of the Eurasian Neogene", Stuttgart, résumé, 1 p.
- Lobreau-Callen D. et Suc J.-P., 1972. Présence de pollens de *Microtropis fallax* (Celastraceae) dans le Pléistocène inférieur de Celleneuve (Hérault). *C. R. Acad. Sci. Paris*, sér. D, 275 : 1351-1354.
- Maley J., 1970. Contribution à l'étude du Bassin tchadien. Atlas de pollens du Tchad. *Bull. Jard. Bot. Nat. Belgique*, 40 : 29-48.
- Nilsson S., Praglowski J. et Nilsson L., 1977. *Airborne Pollen Grains and Spores in Northern Europe.* Natur och Kultur, Stockholm, 159 p.
- Ozenda P., 1989. Le déplacement vertical des étages de végétation en fonction de la latitude : un modèle simple et ses limites. *Bull. Soc. géol. France*, 8 : 535-540.
- Pons A., 1964. Contribution palynologique à l'étude de la flore et de la végétation pliocènes de la région rhodanienne. *Ann. Sci. nat., Bot.*, sér. 12, 5 : 499-722.
- Popescu S.-M., 2001a. *Végétation, climat et cyclostratigraphie en Paratéthys centrale au Miocène supérieur et au Pliocène inférieur d'après la palynologie.* Thèse, Univ. Lyon 1, 223 p.
- Popescu S.-M., 2001b. Repetitive changes in Early Pliocene vegetation revealed by high-resolution pollen analysis : revised cyclostratigraphy of southwestern Romania. *Rev. Palaeobot. Palynol.*, 120 : 181-202.
- Popescu S.-M., sous presse. Late Miocene and Early Pliocene environments in the southwestern Black Sea region from high-resolution palynology of DSDP Site 380A (Leg 42B). *Palaeogeogr., Palaeoclimatol., Palaeoecol.*
- Quézel P. et Barbero M. 1982. Definition and characterization of mediterranean-type ecosystems. *Ecol. Med.*, 8 : 15-29.
- Reille M., 1992. *Pollen et spores d'Europe et d'Afrique du Nord.* Lab. Botanique Historique et Palynologie, Marseille, 520 p.
- Reille M., 1995. *Pollen et spores d'Europe et d'Afrique du Nord.* Suppl. 1. Lab. Botanique Historique et Palynologie, Marseille, 327 p.
- Reille M., 1998. *Pollen et spores d'Europe et d'Afrique du Nord.* Suppl. 2. Lab. Botanique Historique et Palynologie, Marseille, 521 p.
- Richard P., 1970. Atlas pollinique des arbres et de quelques arbustes indigènes du Québec. *Naturaliste can.*, 97, 1 : -306.
- Russo Ermolli E., 1994. Analyse pollinique de la succession lacustre pléistocène du Vallo di Diano (Campanie, Italie). *Ann. Soc. géol. Belgique*, 117, 2 : 333-354.

- Schuler M., 1988. *Environnements et paléoclimats paléogènes. Palynologie et biostratigraphie de l'Eocène et de l'Oligocène inférieur dans les fossés rhénan, rhodanien et de Hesse*. Thèse, Univ. Strasbourg, 80 p.
- Shackleton N.J., Hall M.A. et Pate D., 1995 Pliocene stable isotope stratigraphy of ODP Site 846. *Proc. Ocean Drill. Progr., Sci. Res.*, 138 : 337-355.
- Subally D., Bilodeau G., Tamrat E., Ferry S., Debard E. et Hillaire-Marcel C., 1999. Cyclic climatic records during the Olduvai Subchron (Uppermost Pliocene) on Zakynthos Island (Ionian Sea). *Geobios*, 32, 6 : 793-803.
- Subally D. et Quézel P., 2002. Glacial or interglacial: *Artemisia* a plant indicator with dual responses. *Rev. Palaeobot. Palynol.*, 120 : 123-130.
- Suc J.-P., 1980. *Contribution à la connaissance du Pliocène et du Pléistocène inférieur des régions méditerranéennes d'Europe occidentale par l'analyse palynologique des dépôts du Languedoc-Roussillon (sud de la France) et de la Catalogne (nord-est de l'Espagne)*. Thèse, Univ. Montpellier 2, 2 vol., 198 p.
- Suc J.-P., 1996. Late Neogene vegetation changes in Europe and North Africa. *Europal Newslett.*, 10 : 27-28.
- Suc J.-P. et Bessais E., 1990. Pérennité d'un climat thermo-xérique en Sicile, avant, pendant, après la crise de salinité messinienne. *C.R. Acad. Sci. Paris*, sér. 2, 310 : 1701-1707.
- Suc J.-P. et Bessedik M., 1981. A methodology for Neogene palynostratigraphy. Intern. Symp. Concept. Meth. Paleo., Barcelone : 205-208.
- Suc J.-P., Bertini A., Combourieu-Nebout N., Diniz F., Leroy S., Russo-Ermolli E., Zheng Z., Bessais E. et Ferrier J., 1995. Structure of West Mediterranean vegetation and climate since 5.3 Ma. *Acta zool. cracov.*, 38, 1 : 3-16.
- Suc J.-P. et Fauquette S., 2003. An overview of Tortonian pollen records and the inferred climatic values around the Mediterranean. EEDEN Plenary Workshop « Birth of the New World », Stara Lesna (Slovaquie), résumés : 76-78.
- Suc J.-P. et Zagwijn W.H., 1983. Plio-Pleistocene correlations between the northwestern Mediterranean region and northwestern Europe according to recent biostratigraphic and paleoclimatic data. *Boreas*, 12 : 153-166.
- Thanikaimoni G., 1987. Mangrove Palynology. *Trav. Sect. Sci. Tech., Inst. Fr. Pondichéry*, 24 : 1-100.
- Thomson P.W. et Pflug H., 1953. Pollen und Sporen des mitteleuropäischen Tertiärs. *Paleontographica*, sér. B, 94, 1-4: 1-138.
- Tiedemann R., Sarthein M. et Shackleton N.J. 1994. Astronomic timescale for the Pliocene Atlantic $\delta^{18}\text{O}$ and dust flux records of Ocean Drilling Program Site 659. *Paleoceanography*, 9, 4 : 619-638.
- Tissot C., Chikhi H. et Nayar T.S., 1994. Pollen of evergreen forests of the Western Ghats, India. *Publ. Dép. Ecologie, Inst. Fr. Pondichéry*, 35 : 1-133.
- Wijmstra T.A. et Groenhart M.C., 1983. Record of 700,000 years vegetational history in Eastern Macedonia (Greece). *Rev. Acad. Colomb. Ciencias Ex., Fis. Natur.*, 15 : 87-98.
- Zagwijn W.H., 1960. Aspects of the Pliocene and early Pleistocene vegetation in The Netherlands. *Meded. Geol. Sticht*, sér. C, 3, 5 : 1-78.
- Zagwijn W.H., 1986. Plio-Pleistocene climatic change : evidence from pollen assemblages. *Mem. Soc. Geol. It.*, 31 : 145-152.

Stratigraphic architecture, sedimentology and structure of the Vouraikos Gilbert-type fan delta, Gulf of Corinth, Greece

MARY FORD*, EDWARD A. WILLIAMS†,
FABRICE MALARTRE‡ and SPERANTA-MARIA POPESCU§

*Ecole Nationale Supérieure de Géologie, CRPG, 15 Rue Notre-Dame des Pauvres, BP 20, 54501 Vandoeuvre-lès-Nancy, France
(Email : mford@crpg.cnrs-nancy.fr)

†'Geostandards and Geoanalytical Research', CRPG-CNRS, 15 rue Notre-Dame des Pauvres, BP 20, 54501 Vandoeuvre-lès-Nancy, France

‡Ecole Nationale Supérieure de Géologie, UMR 7566-G2R, Rue du Doyen Marcel Roubault, BP 40, 54501 Vandoeuvre-lès-Nancy, France

§Laboratoire Paléoenvironnements et Paléobiosphère, UMR 5125 CNRS, Université Claude Bernard – Lyon 1, 27–43 Boulevard du 11 novembre, 69622 Villeurbanne Cedex, France

ABSTRACT

In the Aegion to Kalavrita region of the Gulf of Corinth, Greece, Plio-Pleistocene syn-rift stratigraphy comprises a fluvial-dominated lower group and an upper group dominated by Gilbert-type deltas separated by an erosive unconformity. The lower group records substantial accumulation (1.3 km) of fluvial sediment across a broad area of fault-controlled grabens and half grabens, which was terminated by a marine transgression. The upper group records a great increase in accommodation space, the migration of the depocentre to the north and an increase in sediment supply. It is dominated by large gravel-rich systems that were sourced in the footwalls of active normal faults. The Vouraikos Delta is an exceptionally well-exposed Gilbert-type fan delta complex, which is > 800 m thick, with a surface area of 32 km². It lies in the hangingwall of the Pirgaki-Mamoussia Fault and has been exhumed in the footwall of the Eastern Helike Fault. Preliminary palynological results from topset and pro-delta fine-grained facies and from lower group strata indicate that the Vouraikos Delta began forming some time before 1.1 Ma and was terminated soon after 0.7 Ma. These preliminary Early to Middle Pleistocene age estimates are coherent with published models of the uplift history of the Eastern Helike Fault. Sedimentation rates are thus estimated between 1.3 and 2 mm yr⁻¹. While the earliest delta infilled an incised palaeovalley, accommodation space was primarily tectonically controlled, first by an extensional forced fold and later by a system of major normal faults (Pirgaki-Mamoussia Fault and its splays). Several families of syn-sedimentary and late normal faults cut the delta. A listric growth fault controlled a large rollover anticline in the lowest stratigraphic package. The delta prograded (to the north-northwest) into water that reached depths of 200–600 m. Topset limestones associated with coastal conglomerate facies indicate that the delta built into a water body that was wholly or periodically marine. Internally, the Vouraikos Delta comprises five stratigraphic packages each characterized by a distinctive organization of topsets, foresets, bottomsets and pro-delta facies and bounded by major stratigraphic surfaces. These packages are tentatively correlated with regressive glacio-eustatic interglacial periods. The trajectory of the offlap break in the centre of the Vouraikos reflects early progradation-dominated behaviour followed by increasingly aggradational behaviour.

Keywords Early to Middle Pleistocene, Vouraikos Gilbert-type delta, Corinth rift, Greece, normal faults.

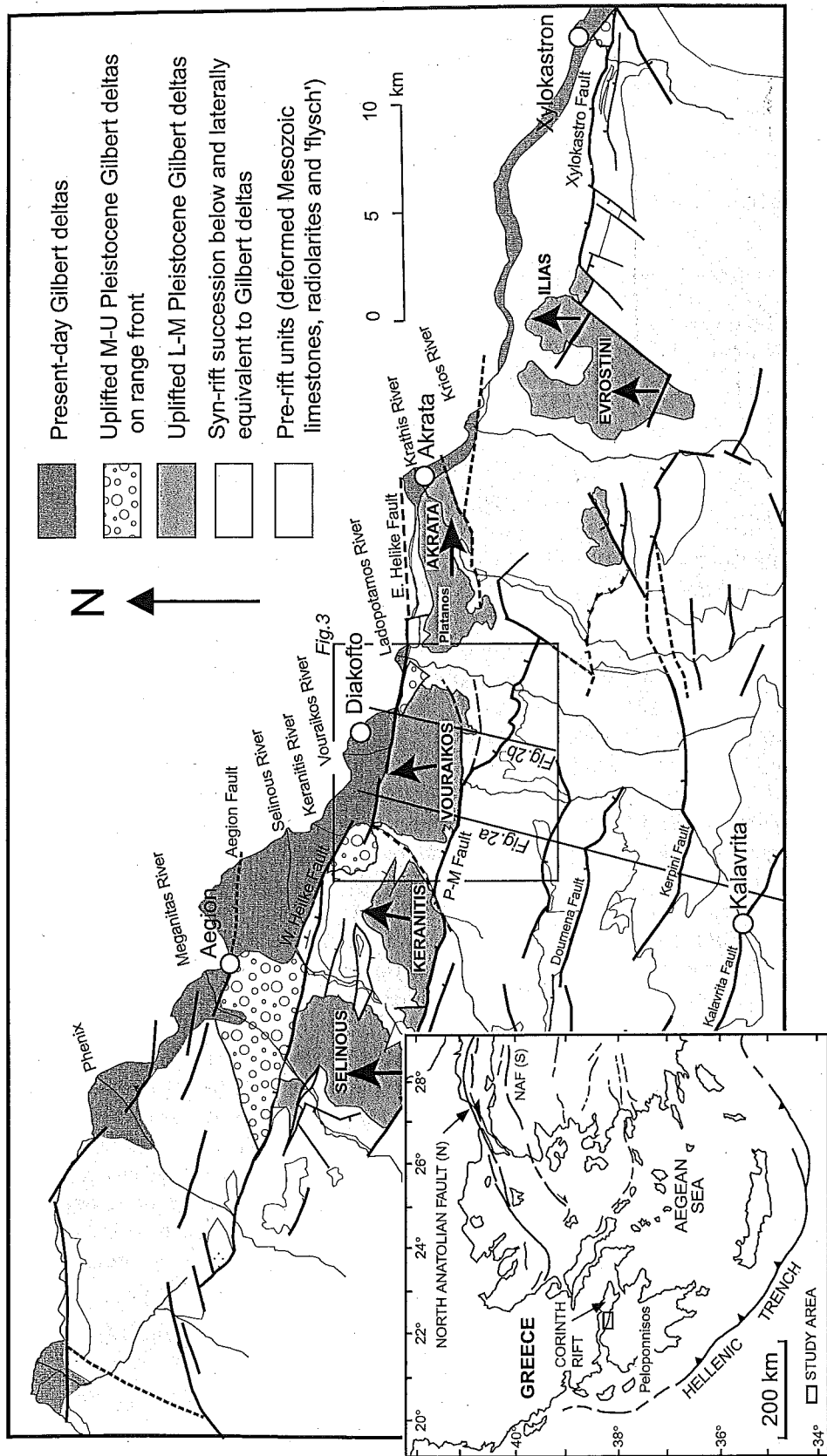


Fig. 1 Map of the southern coast of the Gulf of Corinth showing the distribution of pre-rift and syn-rift sequences. Three generations of syn-rift Gilbert-type deltas are distinguished. The principal normal faults are shown, with dip-direction and throw indicated by small ticks. The progradation directions of the principal Lower-Mid-Pleistocene Gilbert-type fan deltas are shown by large arrows. The location of the cross-sections of Fig. 2 are indicated. This map is based on Ghisetti & Vezzani (2004, 2005), Rohais *et al.* (in press) and authors' own work. Inset: Tectonic map of the Aegean region showing the Corinth rift and the location of the study area. NAF (S) is the southern branch of the North Anatolian Fault.

INTRODUCTION

Along the southern shore of the Gulf of Corinth (Fig. 1) high-relief outcrops expose some of the finest examples of ancient Gilbert-type deltas in an active extensional tectonic setting. Despite published research on several of this suite of deltas, there is little information on complete systems and some confusion about the relationships between several of the deltas. These conglomerate-rich Gilbert-type delta bodies are unusually large, varying in radius from 3 to 8 km (Fig. 1) and are up to 900 m thick. They have been uplifted to altitudes of over 800 m and are deeply incised by north-flowing rivers. While absolute and relative ages are as yet poorly constrained, various delta bodies have been attributed ages of between Pliocene and Holocene (Ori, 1989; Collier *et al.*, 1990; Ori *et al.*, 1991; Poulimenos *et al.*, 1993; Dart *et al.*, 1994). Recent provisional age estimates from palynofloras for the Vouraikos Delta give an Early Pleistocene age (Malartre *et al.*, 2004). Currently, major deltas of the same type are building out into the western Gulf, as modern rivers cannibalize their antecedent deltas (Fig. 1). The purpose of this paper is to present a detailed analysis of the Vouraikos Delta, one of the largest and best exposed of the giant Gilbert-type deltas of Corinth.

The Vouraikos Delta lies in the hangingwall of the Pargaki-Mamoussi (PM) Fault (Figs 1–3) and has been uplifted and incised in the footwall of the Eastern Helike (or East Eliki) Fault. Three river valleys, the Keranitis, Vouraikos and Ladopotamos, provide exceptional natural sections 3 to 4 km apart and with over 700 m of incision. These sections enable the detailed sedimentological and structural study of a substantially complete delta system. Additionally, the syn-rift stratigraphy and internal structure of the whole PM Fault block is described so that delta development can be placed in the context of rift evolution. The vertical and lateral stacking pattern of the delta (its internal architecture) is interpreted in terms of sequence stratigraphy and the creation of accommodation space in order to distinguish tectonic and eustatic controls.

Detailed analyses of major cliff sections using photographic panoramas form the backbone of this work. These sections were tied together by detailed

field mapping at various scales, integrating GPS technology, which forms the basis of ongoing three-dimensional database construction using GIS and gOcad. The stratigraphical architecture was established for each cliff, and key units and surfaces were correlated between cliffs. Facies associations for each stratigraphical unit were identified and detailed sedimentological analysis was carried out by logging at a scale of 1:25. Preliminary analysis of $\delta^{13}\text{C}$ and $\delta^{18}\text{O}$ isotopes was undertaken to characterize the chemical signature of critical stratigraphical horizons, and sampling for palynological analysis was carried out in order to biostratigraphically date the succession.

GROSS STRUCTURAL SETTING: THE GULF OF CORINTH

The Gulf of Corinth is an active rift that was initiated sometime in the past 5 Myr (Doutsos & Piper, 1990; Collier & Dart, 1991) in the upper plate of the Hellenic subduction zone (Fig. 1, inset). The rift is superimposed on the NNW–SSE trending Hellenide orogenic belt (Oligocene–Miocene) and is oriented 105°N . It is 120 km long, some 0.5 km wide in the west and is approximately 30 km at its widest point in the east. The basin has a maximum water depth of 900 m in the east and shallows westward to the Straits of Rion, where the water depth is only 62 m. WNW–ESE oriented north-dipping normal faults lie somewhat oblique and en échelon to the present southern coastline (Fig. 1). Active south-dipping faults, flanking the northern limit of the present graben, have recently been reported offshore (McNeill *et al.*, 2005). Seismic activity is concentrated at the western end of the basin, where geodetic measurements indicate a N–S extension rate of 1.2 cm yr^{-1} (Briole *et al.*, 2000). On the south shore, older syn-rift sediments have been uplifted and deeply incised over an area stretching south from the coast for 25–30 km (Fig. 1). Current uplift rates are estimated to be 1 to 1.5 mm yr^{-1} (De Martini *et al.*, 2004; McNeill & Collier, 2004). This unusual situation has generated superb vertical sections through the older syn-rift succession while active rifting takes place offshore.

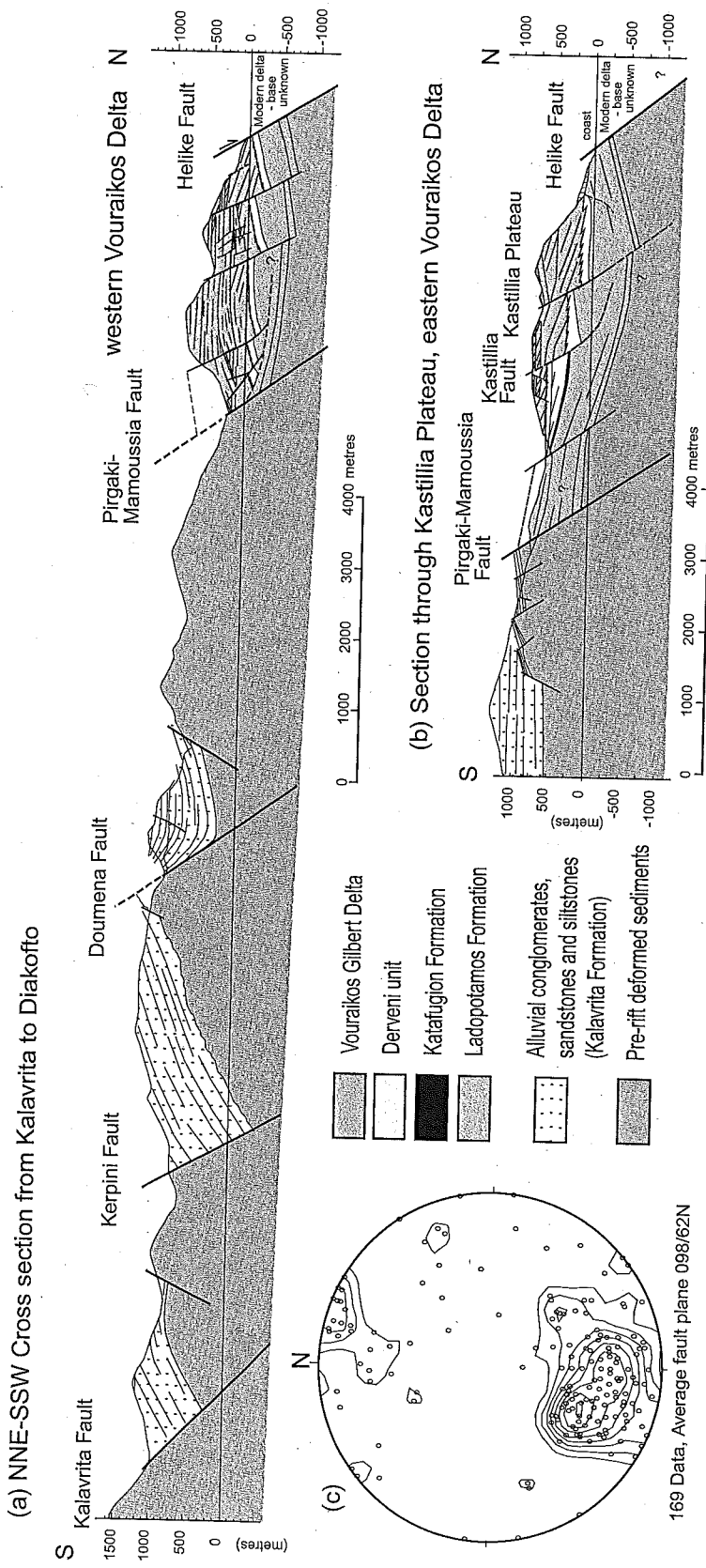


Fig. 2. Structural cross-sections through the central south coast of the Corinth Rift. (a) NNE-SSW cross-section from the Kalavrita Fault to the coast passing through the western Vouraikos Delta. (b) NNE-SSW cross-section from the Doumena Fault block to the coast passing through the eastern Vouraikos Delta. (c) Equal area stereonet of poles to fault planes cutting the eastern Vouraikos Delta. (c) Equal area stereonet of poles to fault planes cutting the eastern Vouraikos Delta, showing a dominance of north-dipping planes with an average plane of 098/62°N.

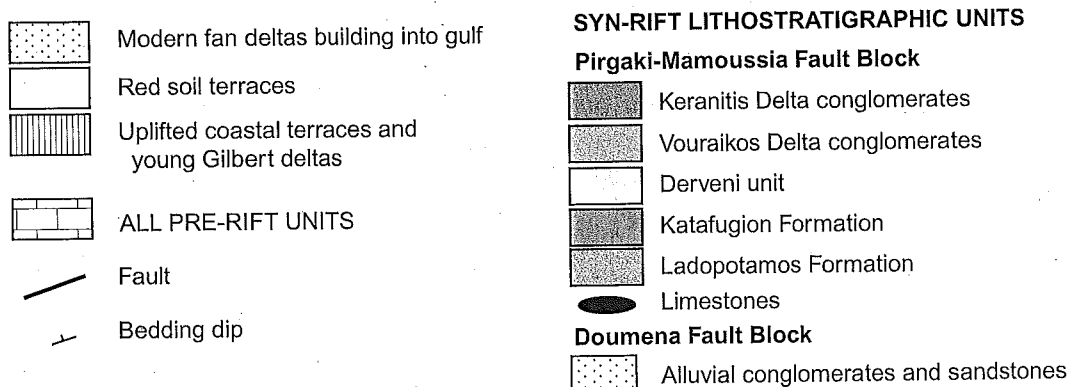
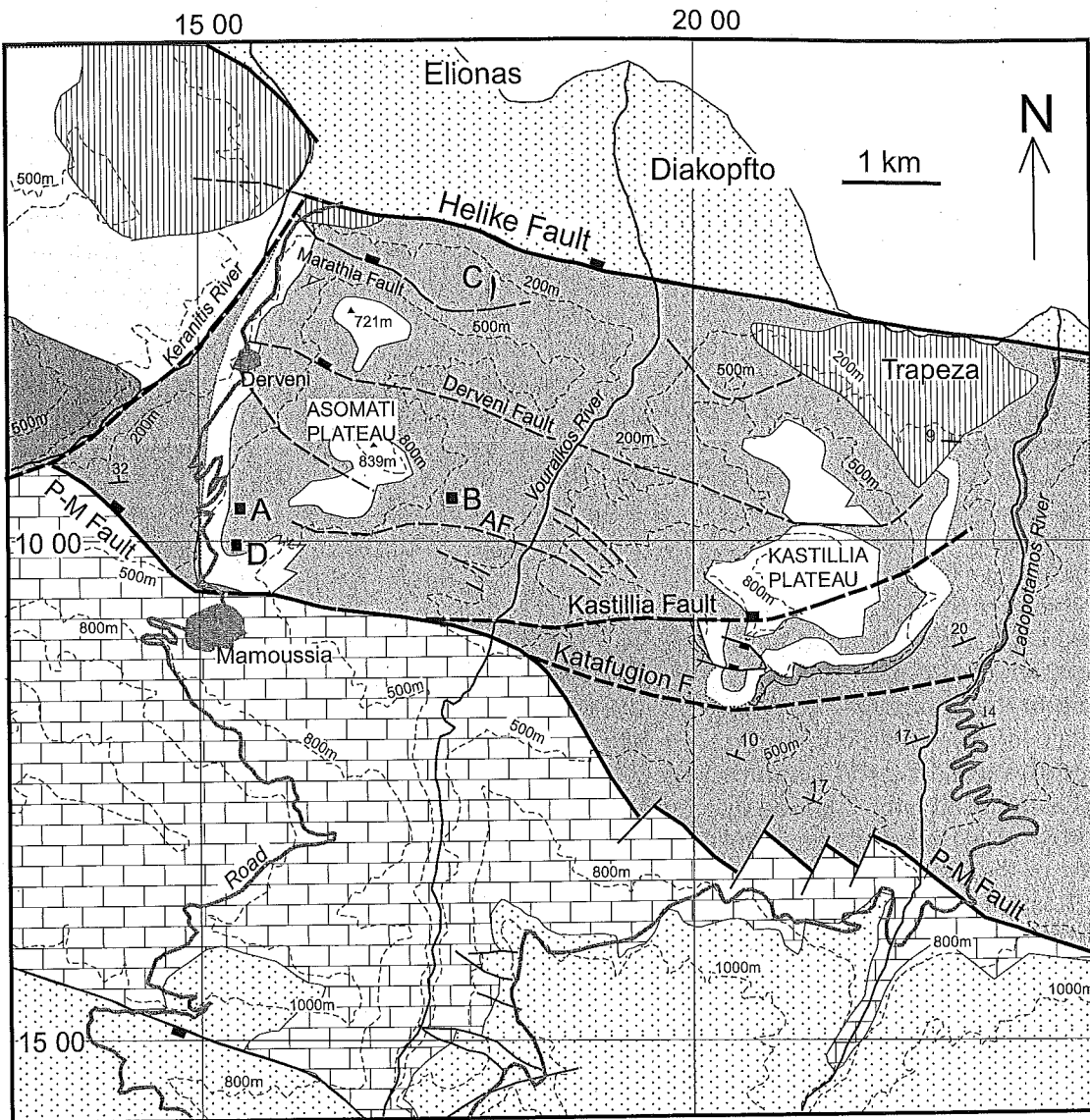


Fig. 3 Detailed geological map of the Vouraikos Delta in the Pargaki-Mamoussia Fault block based on new mapping by the authors, revised from fig. 1 of Malatre *et al.* (2004). A is the location of heterolithic fluvial topsets (Fig. 8), B is the location of outcrops of shoreline–shallow-marine topset association (Fig. 9), C is the location of the Marathia Limestone (Fig. 11a), and D is the location of the Mamoussia Limestone (Fig. 11b). AF is the Avriyiolaka Fault. Grid coordinates are from Greek topographic base map.

LOCAL STRUCTURAL SETTING

In the Aegion–Kalavrita region (Fig. 1) major, north-dipping normal faults with a mean trend of 110° and dipping 55°N define five principal fault blocks that are between 3 and 5 km wide (Goldsworthy & Jackson, 2001; Bourlange *et al.*, 2005). From south to north these blocks are delimited by the Kalavrita, Kerpini, Doumena, Pirgaki–Mamoussi (PM) and Helike faults (Fig. 2). Each block preserves a succession of coarse alluvial syn-rift sediments, generally tilted south, with thicknesses up to 1.3 km. The PM Fault block preserves a more complex syn-rift succession, comprising heterogeneous alluvial (and other) clastic rocks overlain by conglomeratic Gilbert-type fan delta sequences.

In the study area the PM Fault block is 5 km wide, and is bounded to the south by two fault segments: the Pirgaki Fault to the west and Mamoussia Fault to the east, which are hard-linked by a breached relay ramp in the Keranitis River Valley (trending 070°N , Figs 1 & 3). This oblique ramp probably extends northward along the Keranitis Valley. The PM Fault (specifically the Mamoussia Fault) accommodated at least 1.5 km of vertical displacement. East of the Vouraikos Gorge, the east–west trending Kastillia Fault and the Katafugion Fault branch from the ESE–WNW trending PM Fault (Fig. 3) and formed important bounding faults to the Vouraikos Delta for part of its history. Farther south, the PM Fault separates the older syn-rift succession from pre-rift carbonates in its footwall (Fig. 3).

Pre-rift strata comprise Mesozoic carbonates, radiolarites and clastic turbidites ('flysch') that record multiphase deformation at low metamorphic grades related to the westward emplacement of Hellenic nappes during the Oligo-Miocene (Doutsos *et al.*, 1993). These pre-rift strata are the source rocks for the Gilbert-type delta gravels. In the PM block, pre-rift carbonates are exposed in the Selinous River Valley and just to the east of the Ladopotamos River in the immediate footwall of the Eastern Helike Fault (Fig. 1). The lower syn-rift succession has a marked northward dip of up to 30° , while the top of the syn-rift succession (i.e. the uppermost conglomeratic units *above* the Gilbert delta succession) shows a shallow ($< 5^\circ$) tilt to the south.

REGIONAL SYN-RIFT STRATIGRAPHY

Published stratigraphical schemes

Two general schemes have been applied in this region (Ori, 1989; Doutsos & Piper, 1990); both differ significantly from that described here (Fig. 4). In the region around the Ilias and Evrostini deltas (Fig. 1), Ori (1989) reported a syn-rift stratigraphy that consists of a 1–3 km thick lower succession of alluvial plain–lacustrine–alluvial fan sediments (organized in a transgressive–regressive cycle), unconformably overlain by Gilbert-type fan deltas (but see Doutsos *et al.*, 1990). Doutsos & Piper (1990), working in an area to the southeast of that of Ori (1989, fig. 1), also described a two-unit stratigraphy comprising a lower unit of lacustrine and fluvial sands and silts of Middle to Late Pliocene age, and an upper unit of Quaternary conglomerates, the older part of which has been dated as 'Calabrian' (Lower Pleistocene; Doutsos & Piper, 1990, p. 815 and references therein). These conglomerates are of aerially contrasting facies, being: (i) terrestrial where they overlie basement rocks at the southern margin of the basin, and (ii) of Gilbert-type delta facies towards the north, where they are interbedded with marine, lacustrine and brackish 'marls' of locally Middle Pleistocene age.

More recently, Ghisetti & Vezzani (2005) presented a synthetic stratigraphic column for the study area, which they call the Aegion Basin, and another for the Derveni–Corinth Basin farther east. The Aegion Basin column corresponds very generally with our observations; however, we have not observed major clino-stratified conglomerates at the stratigraphic level they call 'Mid-Rift' (equivalent to our lower group). In the Evrostini–Akrata area (Fig. 1), Rohais *et al.* (in press) recognized three stratigraphic groups, which are a lower alluvial–lacustrine group, a middle group of Gilbert-type deltas and an upper group of recent small deltas and terrace deposits.

At present, there is a consensus that the onshore syn-rift stratigraphy comprises two main stratigraphical groups. The lower group of alluvial–lacustrine(?)–marine(?) clastics appears to vary rapidly in facies and thickness from west to east, so that attempts to generalize its component units across the south coast have led to some confusion. Detailed biostratigraphical dating is necessary to

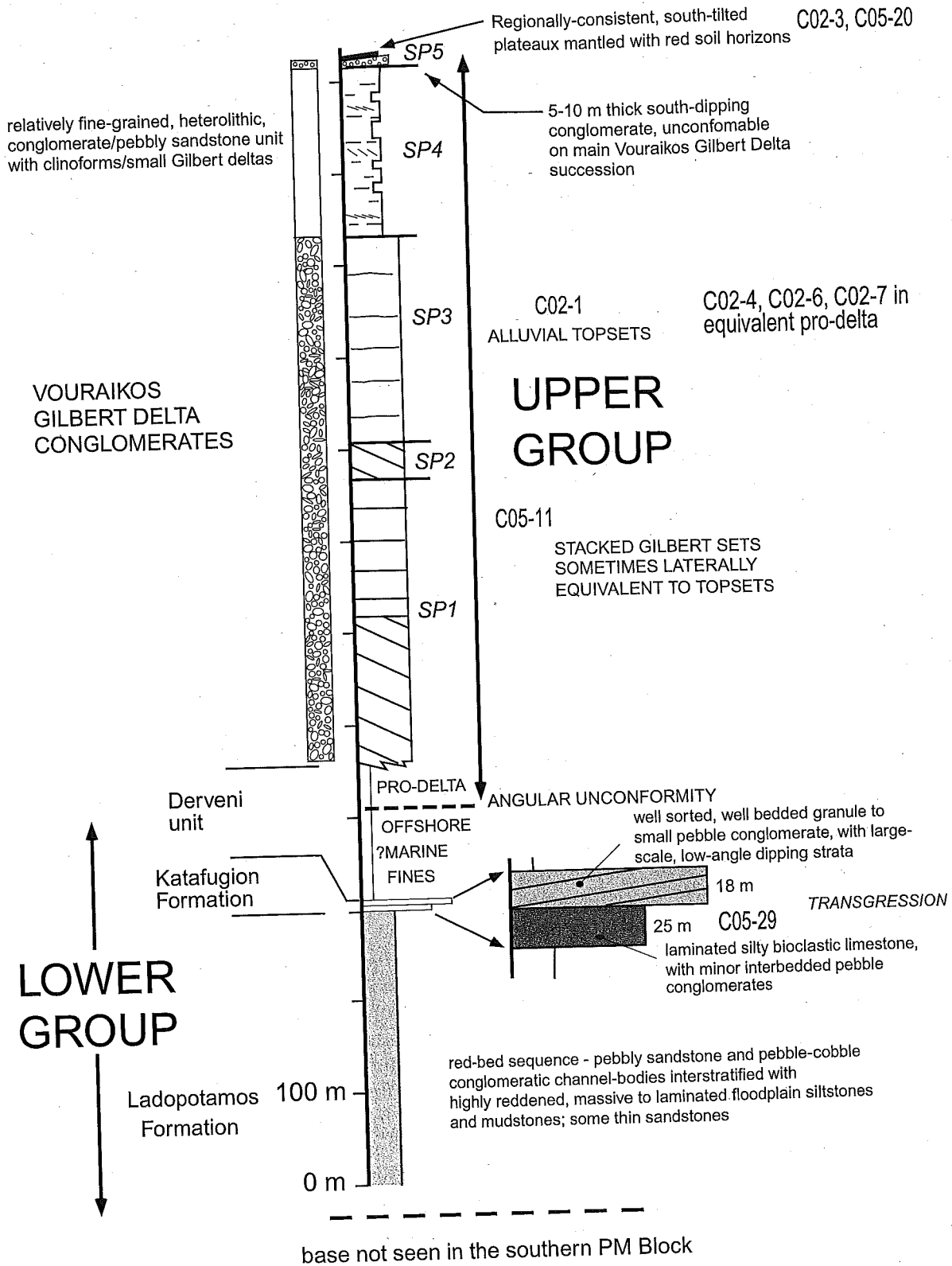


Fig. 4 Composite stratigraphical scheme for the syn-rift depositional sequence in the Pirgaki-Mamoussia Fault block between the Keranitis and Ladopotamos rivers. Note that due to poor exposure, the fine-grained offshore marine facies at the top of the lower group and the fine-grained pro-delta facies at the base of the upper group are here provisionally treated as a single mappable unit, the Derveni unit. The postulated erosive contact between the lower and upper groups lies within this unit. Pro-delta facies are equivalent to the SP1 to SP4 stratigraphic packages.

achieve good lateral correlation. A major unconformity probably separates the lower and upper groups, although some authors do not accept this. The upper group is dominated by the giant Gilbert-type fan deltas that are developed principally between Aegion and Xylokastron (Fig. 1). Equivalent stratigraphical levels to the east (and west?) appear to comprise thinner, smaller deltas and thick fine-grained marine clastics (e.g. Doutsos & Piper, 1990). A relatively small volume of young Gilbert-type fan deltas, fluvial deposits and terrace deposits locally unconformably overlie the main rift succession along the coastal strip, recording the late phase of surface uplift.

Stratigraphical age and dating

There is a lack of precise biostratigraphical dating of the various sedimentary successions in the Gulf of Corinth rift. This is mainly due to the dominance of conglomerates and sandstones in which biostratigraphical markers are poorly preserved. The oldest age published is Early Pliocene (Zanclean, 5.32–3.58 Ma, Papanicolaou *et al.*, 2000) from syn-rift coal-bearing rocks in the Kalavrita Basin (to the south of Vouraikos Delta), although details of the dating method are not specified. Andesites that represent the initiation of the Corinth Basin, in the east of the rift system, are dated as 4 Ma (Collier & Dart, 1991).

Along the south-eastern coast of the Gulf, brackish, lacustrine and fluvial siliciclastic sediment are dated as Middle to Late Pliocene to Quaternary (Kontopoulos & Doutsos, 1985; Frydas, 1987; Fernandez-Gonzalez *et al.*, 1994 and references therein). Thick Quaternary conglomerates (Gilbert-type deltas) overlie this lower series and in their lower levels contain mammalian fossils that have been dated as Calabrian (1.77–0.95 Ma) by Symeonidis *et al.* (1987). Intercalated marl levels within the conglomerates have yielded some calcareous nannofossils of Middle to Late Pleistocene age (Poulimenos *et al.*, 1993; Zelilidis & Kontopoulos, 1996). Gilbert-type deltas in the Xylokastron-Aegion area are capped by marine terraces that have been assigned ages from the top of Middle Pleistocene to Late Pleistocene (Keraudren & Sorel, 1987; Collier *et al.*, 1992; Dia *et al.*, 1997). Late Pleistocene to Holocene coral-algal reefal facies rocks are well developed within the eastern Gulf of Corinth (Kershaw *et al.*, 2005; Portman *et al.*, 2005).

SYN-RIFT STRATIGRAPHY IN THE PIRGAKI-MAMOSSI BLOCK

General

The syn-rift succession of the study area (Fig. 3) is here divided into two informal stratigraphical groups (Fig. 4). The *lower group* comprises two units: the Ladopotamos and Katafugion formations. The lowest syn-rift succession within the PM block is best exposed in the Ladopotamos Valley, represented by the dominantly coarse-grained clastic Ladopotamos Formation, which dips and youngs towards the northwest to north-northwest (Fig. 3). The Ladopotamos Formation comprises at least 300 m of reddish conglomerates, sandstones and siltstones (Fig. 4) unconformably overlying Mesozoic carbonate (basement) rocks (Fig. 1). An inlier of sandstones and conglomerates, previously regarded as part of the Keranitis Delta (Ori *et al.*, 1991, fig. 2 'topset beds'; Dart *et al.*, 1994, fig. 3a, b) that crops out in the Keranitis valley (Fig. 3), is considered to be part of the Ladopotamos Formation. The Katafugion Formation (40 m thick, Fig. 5) comprises a fine white calcareous unit (20–25 m thick) overlain by a package of fine-gravel clastics (18 m thick). This is followed by poorly exposed siltstones and mudstones (included in the Derveni unit). The Katafugion Formation is observed below the southeast part of the Vouraikos Delta to the south of the Kastillia Fault (Fig. 3). To the north of this fault the fine-grained pro-delta facies of the upper group directly overlie the Ladopotamos Formation. It is suggested that the unconformity at the base of the upper group has eroded down through the Katafugion Formation to the north of the Kastillia Fault. To the south of the fault the unconformity is located within the Derveni unit.

To the south of the PM Fault (Figs 1 & 2), markedly contrasting syn-rift successions can be traced for up to 15–20 km. Here, conglomerates (locally up to small boulder grade) with minor sandstones (and red siltstones) are organized in tilted fault blocks, locally reaching thicknesses of 1.3 km. Although precise dating is not yet available, this conglomerate succession is provisionally correlated with the lower group of the PM block.

The *upper group* comprises a relatively thin succession (< 50 m) of commonly beige-coloured

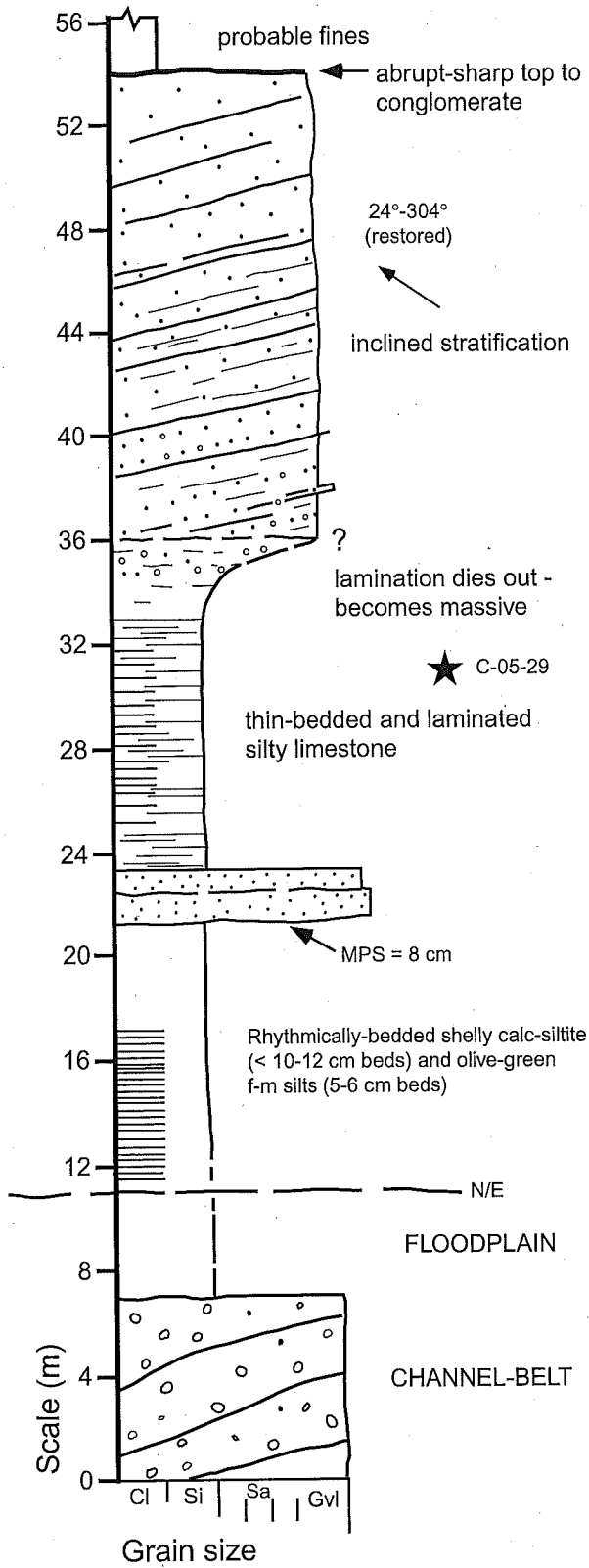


Fig. 5 Simplified graphic log of the limestone-clastic succession of the Katafugion Formation. MPS is maximum particle size.

siltstones and rarer mudstones (included in the Derveni unit; Fig. 4), overlain by a series of individual conglomeratic bodies (Gilbert-type fan deltas) that reach thicknesses of over 800 m. These are represented in the study area by the Vouraikos Delta, but also include the immediately flanking (western) Keranitis and (eastern) Plaka (or Platanos) deltas (Fig. 1). The top of the Vouraikos Delta succession is unconformably overlain by a thin (10–15 m) conglomerate unit, which is capped by recent red soils on the Asomati Plateau (Figs 3 & 4). Along the range front of the Eastern Helike Fault the upper group is incised and unconformably overlain by uplifted small Gilbert-type deltas (Fig. 3).

Lower group: Ladopotamos Formation

The Ladopotamos Formation consists of interbedded conglomerate/pebbly sandstone bodies and (minor) red siltstone/sandstone intervals. Typical conglomerate/pebbly sandstone bodies are about 2 m thick flat- and sharp-based, horizontally-bedded or more rarely cross-bedded sheets, or erosively based multi-storey bodies composed of similar sheets. Observed cross-stratification indicates north- and north-east-quadrant palaeoflows. Textures of the pebbly sandstone sheets are clast-supported, though rich in a matrix mixture of granules, sand and very small pebbles. Component clasts are extraformational, with rare instances of intraformational siltstone (pebbles and cobbles) lining basal erosive surfaces.

Coarse-grained conglomerate-sandstone bodies (5–7 m thick) observed near the top of the formation are markedly heterolithic, containing beds of medium-coarse-grained red sandstone, pebbly sandstone and small pebble to small cobble conglomerates. These show concordant channel-form structures, which incise into fine-grained red bed sequences, steep channel margins and meso- and macroscale inclined strata-sets (terminology of Bridge, 1993) with opposed dip-directions. Interbedded fine-grained sequences with the conglomerate-sandstone bodies are orange or red sandstones, small pebble conglomerates, small pebble-rich sandstones and blocky and faintly laminated red (dusky red) siltstones/mudstones. The latter contain occasional isolated small calcareous nodules and black charcolified wood fragments of 0.75 cm size.

Interpretation

The Ladopotamos Formation is considered to be fluvial in origin, with coarse-grained probably braided river conglomerate-sandstone bodies and relatively fine-grained overbank (floodplain) siltstones and interbedded sand and gravel sheets. No lacustrine facies have been observed, as are reported farther east in this fault block (see Ori, 1989; Dart *et al.*, 1994). Moreover, the basin-wide 'fan-glomerate' unit reported by Ori (1989) beneath the Gilbert-type delta sediment-bodies of the region does not occur in the study area.

Lower group: Katafugion Formation

The Katafugion Formation begins with a distinctive white-weathering flat- and parallel-laminated shelly siltstone/marly limestone (Fig. 5). Its basal contact, though not well exposed, is apparently conformable. Fresh exposures of the white-weathering facies reveal a rhythmical alternation of pale to white competent fossiliferous beds up to 10–12 cm in thickness, and olive green-coloured laminated silty to fine sandy beds that are 5–6 cm thick. The calcareous facies (typically a fine-grained, massive to faintly laminated bioclastic calcsiltite) contains distributed broken bivalve and gastropod shell material. Intact but disarticulated bivalves are concentrated on bedding planes. Much of the broken and intact bivalve material appears to be from a single genus, of small (< 1 cm) members of the suborder Pterioida. Intact small gastropods are as yet unidentified.

In thin-section, finer grained facies are finely laminated mudstones to wackestones with a high component of clay, seams of dark, fine-grained organic material and abundant calcitic microspar. Larger bioclasts include entire and broken ostracods, whereas smaller bioclasts include relatively abundant diatoms and possible coccoliths. A palynological study from the upper part of the carbonate member yielded dinoflagellate cysts. Apart from planar-horizontal lamination, these facies lack structures. Conformably interbedded in the fine-grained marly limestone facies at one interval is a bedset of 0.7–0.8 m thick small pebble conglomerate beds. Up-section within the fine calcareous unit, the horizontal lamination dies out, giving way to a massive texture that is

accompanied by the appearance of occasional small pebbles.

A preliminary stable isotope analysis of shell and rock matrix from the calcareous facies was undertaken (at the CRPG, Nancy, F. Palhol, personal communication). Results for $\delta^{13}\text{C}$ were 1.71 and 1.80‰ for shell and rock material respectively, and for $\delta^{18}\text{O}$ PDB, -3.69 and -3.64‰ respectively, the determinations being consistent for the differing materials. The values for $\delta^{13}\text{C}$ are typical for a large lake or the sea with open circulation. However, the extremely negative values for $\delta^{18}\text{O}$ suggest a water body of high salinity (typical values for the eastern Mediterranean are between -0.1 and +1.0‰).

Overlying the fine calcareous unit (although an exposure gap intervenes) is a distinctive moderately sorted, well-stratified 18 m thick unit of interbedded sandy-pebbly conglomerates, coarse to very-coarse (and granule-rich) sandstones and pebbly sandstones (Fig. 5) organized in beds of 30–50 cm thickness. The conglomerates are matrix-rich, and show matrix-support of the maximum clast size population. Gravel stringers that are one to three clasts thick are composed dominantly of pebbles with occasional small cobbles. The planar stratification has a (24°) depositional dip to the northwest with respect to the underlying calcareous unit (Fig. 5). Lineations defined by grain alignment (and possible obstacle shadows) on bedding planes show a near down-dip orientation. Although not well exposed, the top of the conglomerate unit is apparently extremely abrupt and sharp (?non-erosional) where very fine-grained lithologies replace the gravel. The poorly exposed overlying succession (?70–100 m) comprises laminated, poorly consolidated yellow to red-weathering siltstones, with possible very thin fine-very fine sandstones.

Interpretation

The transitional succession of the lower group, from fluvial channel and oxidized floodplain environments (Ladopotamos Formation) to a mixed fine-grained clastic-carbonate system capped by well-stratified fine gravel and finally much finer-grained sediments (Katafugion Formation), is thought to indicate a marine transgression. The Katafugion Formation is interpreted as representing a protected subtidal (dominantly carbonate)

lagoon in a microtidal regime (e.g. Anthony *et al.*, 1996), as no peritidal or obvious marsh facies were found. The restricted diversity of the mollusc-ostracod fauna plus the evidence of marine microfossils, allied to the preliminary geochemical data, suggests a saline coastal lagoon. The rare interbedded pebble gravel sheets within the lagoonal facies are likely to be storm-generated washovers or due to storm-generated flow through the barrier into the lagoon. The overlying conglomerates and sandstones suggest a high wave energy shoreface-barrier beach system (Nemec & Steel, 1984), probably at a ravinement surface. This is interpreted as part of a shoreface-shoreline retreat during transgression, leaving a seaward-dipping strata-set (Reinson, 1984). The termination of the coarse facies is thought to have occurred at a flooding surface, and the overlying fine-grained

possibly offshore marine clastics locally contain thin-bedded turbidites.

The upper group

The upper group (Fig. 4) is characterized by Gilbert-type fan delta conglomerates and their laterally equivalent facies. The Vouraikos Delta is one of the largest of these uplifted deltas, covering a (preserved) surface area of 32 km² (Fig. 3). It is at least 800 m thick in its central region but thins considerably to the east and west (Figs 4 & 6). The delta comprises conglomerate-dominated packages of topsets, foresets and bottomsets that are grouped together as a single mapping unit (Fig. 3; Vouraikos Delta conglomerates). These are underlain by a unit (< 50 m thick) of siltstones and fine sandstones with 'floating' gravel clasts) that are

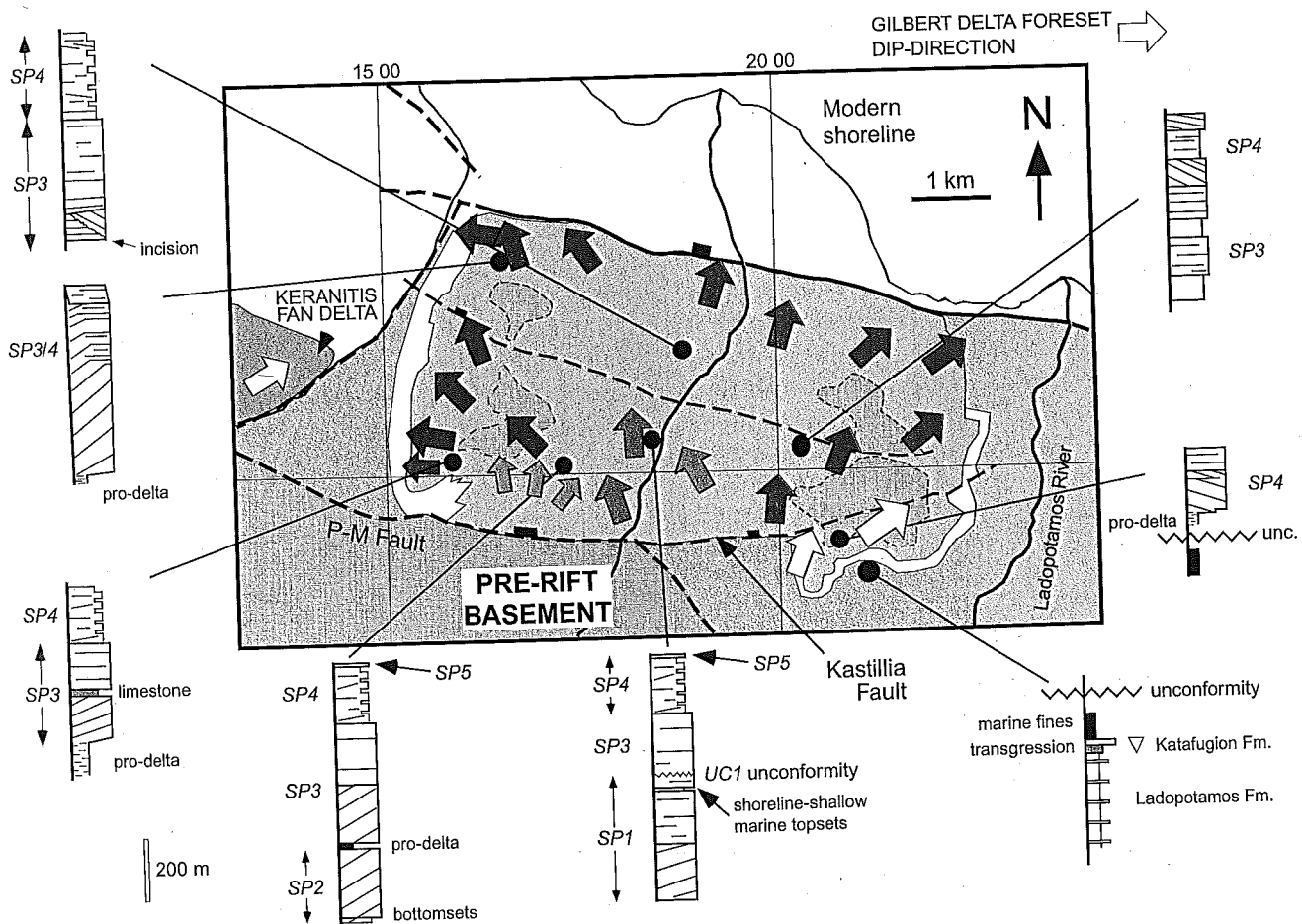


Fig. 6 Sketch map of the Vouraikos Delta showing simplified stratigraphies and foreset dip-directions. Key for Gilbert delta foreset dip-directions: green SP1, blue SP2, red SP3 and SP4, white SP4 (south of Kastilia Fault).

interpreted as proximal pro-delta facies. At several localities on the western and eastern borders of the delta, conglomeratic bottomsets are observed to pass laterally and asymptotically into these pro-delta facies. The pro-delta facies are distinguished as the Derveni unit (Fig. 3). The top of the Vouraikos Delta is characterized by two south-dipping plateaux (the Asomati to the west and the Kastillia to the east) at altitudes of between 750 and 820 m (Fig. 3). These plateaux are displaced by late secondary normal faults, and are capped by red soil deposits (Fig. 4). The detailed internal stratigraphy and sedimentology of the Vouraikos Delta are described below.

Basal contact of the upper group

The base of the Vouraikos Conglomerates can be traced on the eastern and western flanks of the delta. As the underlying pro-delta unit is consistently 20–50 m thick, it is assumed that the base of the upper group is subparallel to the base of the Vouraikos Conglomerates. In the Keranitis Valley the western base of the Vouraikos Conglomerates dips 8°N and rises southward to 600 m altitude. At the south-east edge of the delta in the Ladopotamos Valley this contact is also at 500 m altitude and locally dips 15°W (Fig. 7). However, the base of the delta is not exposed in the Vouraikos Gorge in the centre of the delta body, despite incision down to 120 m elevation.

The transverse change in elevation of the basal contact of the Vouraikos Conglomerates and, by implication, of the upper group (Fig. 7) is here interpreted as being due to incision and infill of a palaeovalley some 7–8 km wide by the Vouraikos Delta. No transverse faults that could explain the

lateral change in elevation of these contacts were detected. The general cusped base of the delta implies a relief of at least 300 m for this valley incised into the lower group. This cusped form, however, may have been enhanced by: (i) differential subsidence below the thicker central delta succession; and (ii) by progradation of foresets across older bottomsets, thus progressively raising the delta base basinward and laterally. The palaeovalley model implies that a major regression–transgression event occurred at the boundary between the lower and upper stratigraphic groups.

In the eastern delta block (Kastillia Plateau), in the footwall block of the Kastillia Fault (Fig. 5), the character of the basal contact is different. Approximately 100 m up-section from the Katafugion Formation are conglomerates and sandstones of foreset/bottomset facies associations of the Vouraikos Delta. The thickness of the upper group (Vouraikos Conglomerates) in the footwall block of the Kastillia Fault is only around 200 m, whereas in the hangingwall the Vouraikos Conglomerates are much thicker (> 800 m; Fig. 2b). This fault is therefore interpreted as a sealed growth fault, since there is no evidence for its surface trace. The implication of this relationship is that the Vouraikos Delta conglomerates in the footwall of the Kastillia Fault are some of the youngest sediments of the system, despite overlying the Katafugion Formation (Fig. 6). Furthermore, although a definite downlapping surface has not been identified, the structural observation that the approximately flat-lying Gilbert-type delta succession (from subhorizontal topsets) structurally overlies a panel of north-dipping lower group sediments strongly suggests an angular unconformity between these respective successions.

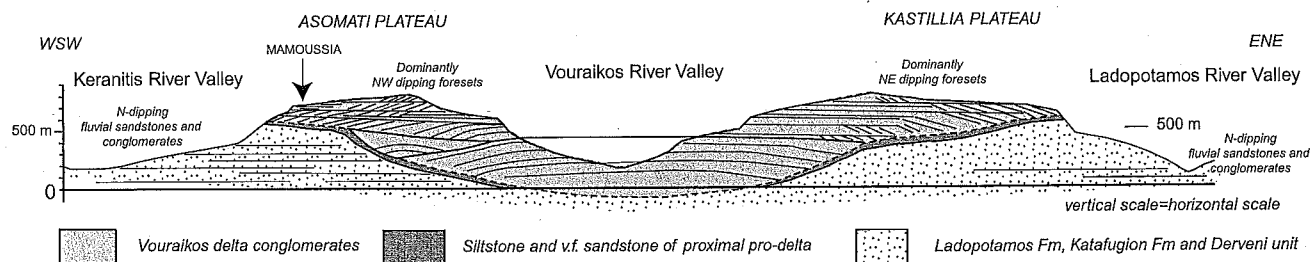


Fig. 7 Vertical ENE–WSW transverse section of the Vouraikos Delta orthogonal to its progradation direction (Fig. 6), located in the hangingwall of the Kastillia and Pirkaki-Mamoussia faults, showing incision of the delta into the lower group succession. No vertical exaggeration.

BIOSTRATIGRAPHY

Pollen content was used to date selected samples of fine-grained rocks from the lower and upper groups. The presence or absence of certain thermophilous plants that became successively extinct in this area during the past 2 Myr was used for this purpose. The chronological succession of their disappearance is relatively well known at latitude 36°–39°N in the eastern Mediterranean region based on several reference pollen successions covering the time-interval under consideration. These sections are at Croton [Vrica Santa (Combourieu-Nebout & Vergnaud Grazzini, 1991) and Santa Lucia], Citadel of Zakynthos (Subally *et al.*, 1999), Monte San Giorgio at Caltagirone (Dubois, 2001), Tsampika in the Rhodos Island (Joannin, 2003; Cornée *et al.*, 2006), Peloponnese localities [Megalopolis (Okuda *et al.*, 2002), Phlious (Urban & Fuchs, 2005) and the Argive Plain (Jahns, 1993)] and Oeniades (Gulf of Corinth; Fouache *et al.*, 2005).

A preliminary analysis has been performed on nine samples in which pollen grains are the most abundant. Their stratigraphical positions are indicated in Fig. 4. The pollen flora is represented by 58 taxa, which are generally at the genus level for the trees and the family level for the herbs. From an ecological point of view, these taxa belong to various groups:

- 1 subtropical trees (Taxodiaceae, *Cathaya*);
- 2 warm-temperate trees (deciduous *Quercus*, *Carpinus*, *Acer*, *Ulmus*, *Zelkova*, *Castanea*, *Taxus*, *Populus*, *Salix*, *Liquidambar*, *Fraxinus*, *Ligustrum*, *Betula*, *Alnus*, *Corylus*, *Tamarix*, Cupressaceae, *Carya*);
- 3 Mediterranean xerophytes (evergreen *Quercus*, *Pistacia*, *Olea*, *Phillyrea*, *Cistus*, *Vitis*);
- 4 cool-temperate (i.e. altitudinal) trees (*Cedrus*, *Tsuga*, *Abies*, *Picea*);
- 5 herbs and shrubs (Poaceae, Asteraceae Asteroideae, *Centaurea*, *Artemisia*, Asteraceae Cichorioideae, Brassicaceae, *Scabiosa*, *Knautia*, *Polygonum*, *Geranium*, *Mercurialis*, *Hippophae rhamnoides*, *Convolvulus*, *Catalpa*, *Jasminum*, *Ambrosia*, Fabaceae, Cyperaceae, Caryophyllaceae, *Plantago*, Ranunculaceae, Ericaceae, *Potamogeton*, *Ephedra*, Amaranthaceae-Chenopodiaceae);
- 6 *Pinus* and Rosaceae, which are non-significant elements because they can be related to many different biotopes;

7 *Tricolporopollenites sibiricum*, which has an artificial species name partly based on the pollen morphology because the corresponding plant is unknown.

The prevalence of tree pollen grains versus those of herbs indicates that all the samples represent interglacial phases. Some samples yielded very scarce dinoflagellate cysts (C05-11, C02-1, C05-29), indicative of a marine influence. The presence or absence of certain thermophilous plants allow the samples to be divided into two broad age groups.

1 Early Pleistocene. Five samples (C02-4, C02-7, C02-6, C05-29, C05-4) showed a significant percentage of thermophilous tree pollen, such as Taxodiaceae (in sample C02-4 only), *Cathaya* (in samples C02-4 and C02-7 only, which also include an unidentified pollen, the so-called *Tricolporopollenites sibiricum*), *Tsuga*, *Cedrus*, *Carya*, *Liquidambar*, and *Zelkova* (Table 1). Taxodiaceae and *Cathaya* simultaneously disappeared from the area at about 1.1 Ma, whereas *Carya* and *Tsuga* persisted up to about 0.9 Ma. The extinction of *Cedrus* occurred later (around 0.7 Ma), but is still present in South Turkey and Lebanon. *Liquidambar* and *Zelkova* became rare and disappeared very recently (during the Last Glacial); they are still present in some refuge territories in Turkey. Stratigraphically, two of these samples come from the lower group, C05-29 from the Katafugion Formation and C05-4 from the alluvial succession in the footwall of the PM Fault (Kalavrita conglomerates). The three other samples, two of which contain the oldest assemblages, are from the upper group, specifically in the fine-grained beds below the western edge of the Vouraikos Delta (pro-delta facies). These pro-delta beds are estimated to belong to the SP3 package in the Vouraikos Delta (see below). These five samples are grouped into an age bracket of Early Pleistocene (1.8–0.78 Ma; Gradstein *et al.*, 2004). No distinction can be made between the lower group samples and those from the lower parts of the upper group. Hence the basal unconformity of the upper group is not detectable.

2 Middle Pleistocene. Four samples (C02-3, C05-11, C02-1, C05-20) do not contain these thermophilous plants, except some rare pollen grains of *Cedrus* (samples C02-3 and C05-11) and *Carya* (C02-3) (Table 1). In addition, they show increased percentages of *Olea* and sometimes the presence of *Vitis* (Table 1), two Mediterranean elements that developed

Table 1 Nine samples (from the lower and upper groups) were analysed for pollen content. The presence/absence of the most significant thermophilous plants used for dating in the Pleistocene of the eastern Mediterranean are shown. Values are percentages based on the total number of pollen grains counted in each sample (between 150 and 300 grains per sample). See text for further details and interpretation. Most samples are located on Figs 4 and 14

Sample	Stratigraphic position	Coordinates	Taxa (%)										
			Taxodiaceae	Cathaya	Tsuga	Cedrus	Carya	Liquidambar	Zelkova	Tricolporo-pollenites sibiricum	Vitis	Olea	
C05-20	Vouraikos topsets (SP5)	N38 09.656' E22 12.412'	0	0	0	0	0	0	0	0	0	0.6	1.2
C02-3	Vouraikos topsets (SP5)	N38 09.88' E22 09.5'	0	0	0	1	1	0	0	0.5	0	0.5	0.5
C02-1	Vouraikos topsets (SP3)	N38 09.69' E22 08.56'	0	0	0	0	0	0	0	0	0	0	2.5
C05-11	Vouraikos topsets (SP1)	N38 09.58' E22 10.1'	0	0	0	0.8	0	0	0	0	0	0	9
C02-6	Vouraikos pro-delta (SP3)	N38 10.25' E22 08.63'	0	0	0.8	4	0	0	0	0.8	0	0	0.8
C02-7	Vouraikos pro-delta (SP3)	N38 10.25' E22 08.63'	0	0.8	0.4	21	0	0	0	2.1	0.4	0	0
C02-4	Vouraikos pro-delta siltstone/marine clastics	N38 10.83' E22 08.7'	1.6	0.8	0.8	5.3	1.2	0.8	0.8	0.8	0.8	0	0
C05-29	Katafugion Formation	N38 09' E22 12.8'	0	0	6.2	2.2	1.1	6.8	0.6	0	0	0	0
C05-4	Kalavrita Conglomerates	N38 08.12' E22 10.6'	0	0	1.5	0.7	0.7	2.3	0	0	0	0	0.7

during the Middle Pleistocene. Two samples come from within the delta itself: C05-11 comes from the upper topsets of SP1 in the centre of the delta and C02-1 comes from the western topsets of SP3. Two samples come from SP5 beds at the top of the delta (C02-3 and C05-20). These samples may be somewhat younger than those of the previous group and may belong to the Middle Pleistocene (i.e. after 0.78 Ma).

Although preliminary, these results indicate that the Vouraikos Delta was built mainly during the Early Pleistocene, beginning sometime before 1.1 Ma and probably during the beginning of the Middle Pleistocene (up to sometime after 0.6 Ma). These data indicate that the unconformity at the base of the upper group does not represent a major time gap.

VOURAIKOS DELTA SEDIMENTOLOGY

Previous work

Very little detailed stratigraphical or sedimentological research has been published on the Vouraikos Delta. Ori *et al.* (1991, fig. 2) regarded the Keranitis and Vouraikos deltas (Fig. 2) as a single system. They indicated that the sediments of the Vouraikos Delta (*sensu stricto* – as used in this paper) are composed of variously alternating sequences of topsets and foresets (their fig. 12), and the uppermost internal stratigraphical units to be 'foreset beds' (their fig. 2). Poulimenos *et al.* (1993) and Zelilidis & Kontopoulos (1996, fig. 1b and fig. 2a C–C') regarded the western part of the Vouraikos Delta (as defined herein) to be the eastern fan delta system in their 'Egio Subbasin'. They considered the delta to lack 'toesets' (bottomsets), describing it as a 'trapezoidal' delta on the basis of its longitudinal cross-section, and attributed this form to deposition in a 'protected' or narrow basin. Dart *et al.* (1994) did not report specifically on the sediments of the Vouraikos Delta system, but they showed the Vouraikos as being a separate system from the Keranitis, as did Malartre *et al.* (2004).

Facies and facies associations

Facies associations in Gilbert-type delta systems can be defined to a first-order by their position (and

attitude) in the tripartite structural division of these deltas: subhorizontal topsets, angle of repose foresets and low-angle ($< 10^\circ$) bottomsets. The range of facies associations defined (see also Malartre *et al.*, 2004) further includes the markedly finer grained (subhorizontal) pro-delta and the relatively thin shoreline/coastal heterolithic types. The distinction between bottomset and pro-delta environments differs from that of several other studies. Several of these gross divisions contain distinctive sub-associations, which are elaborated below.

Alluvial topset facies association

This consists of: (i) a heterolithic subassociation of sandstone, conglomerate and siltstone red-bed facies; and (ii) a volumetrically and areally dominant conglomerate-rich subassociation. Both have been observed to comprise only depositionally horizontal architectures (cf. Dart *et al.*, 1994, p. 549), and tend to occur in sequences of tens of metres thickness, although the conglomerate-rich association is consistently more thickly developed, and often reaches hundreds of metres of preserved thickness. Mean palaeoflow was towards the N–NNE.

Heterolithic subassociation. This consists of interbedded small-pebble to small-cobble conglomerates, pebbly sandstones, red or brown sandstones and reddened siltstones (Fig. 8). The small-pebble conglomerate facies are commonly horizontally stratified in sheet-like or lenticular beds, with erosive bases showing longitudinal scours. Coarser conglomerates (small cobble grade) tend to be massive, or locally cross-stratified. Normal grading has been observed in some 1 m thick beds. Subspherical carbonate nodules have been observed in red-brown siltstone facies, overlain by weakly undular-laminated carbonate (calcrete) in fine sandstone (forming a bedset > 0.7 m thick). The heterolithic subassociation is similar to 'topset facies association 2' of Dart *et al.* (1994), except that examples of their association 2 are traceable for distances up to 1 km across the fan delta top.

Conglomeratic subassociation. This is principally composed of matrix-rich (coarse sand to small pebbles) clast-supported conglomerates with modal grain sizes of medium pebble to small cobble grade. The modal grain populations are poorly sorted, and

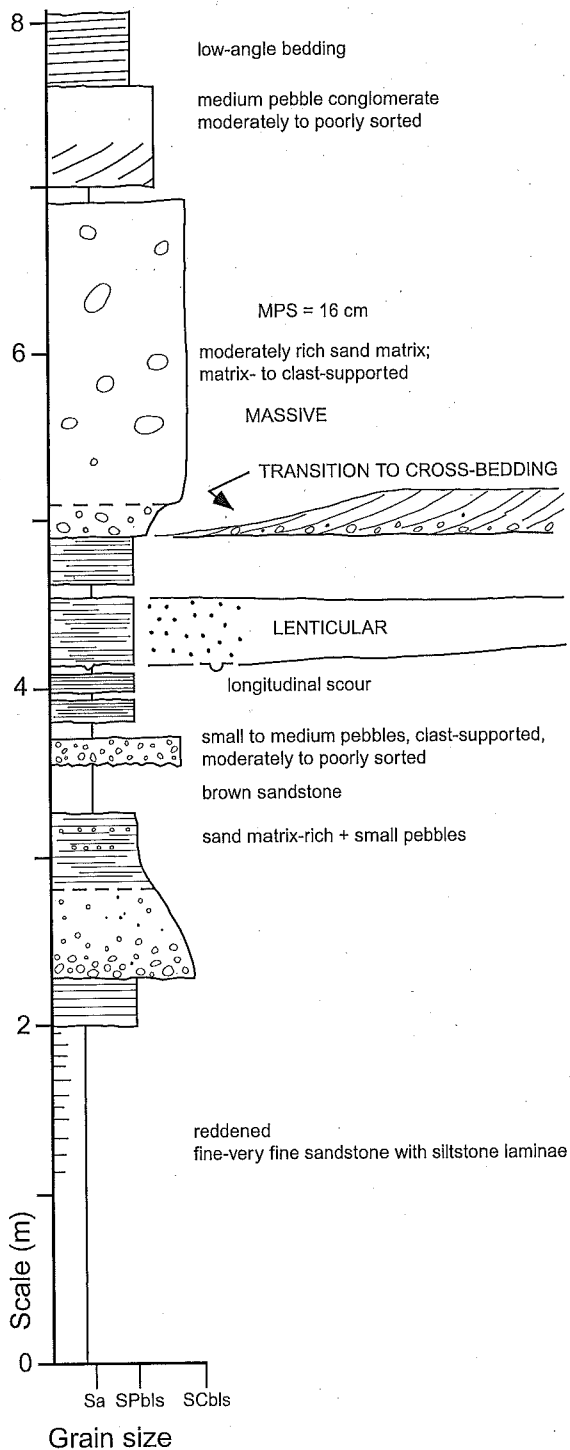


Fig. 8 Graphic log of a short section through the relatively fine-grained (heterolithic) alluvial topset facies association located on the southwest margin of the Vouraikos Delta at 675 m altitude (location A, Fig. 3), containing interbedded sandstone, conglomerate and siltstone red-bed facies. Road section to Asomati Plateau at co-ordinates 38°09'55.7"N/022°08'46.0"E.

maximum particle size is small boulder grade. Clasts are well rounded to rounded and shapes variable. Fabrics are dominantly unordered, with $a(t)b(i)$ imbrication being subordinate. Palaeoflow data from imbrication indicated north-quadrant vectors. Bed thicknesses of the typical conglomerates range from 1 to 5 m. Finer grained conglomerate facies (e.g. small-pebble conglomerates) can have bed thicknesses of < 0.5 m. Bases of coarse facies are generally prominent irregular-erosive surfaces lacking obvious large-scale relief, but with variably developed small-scale (0.1 m) longitudinal scours. Stratification within beds is very poorly developed, with a predominance of massive (structureless) to crudely horizontally stratified beds. Stratification is enhanced occasionally by very thin (often reddened) sandstones. Large-scale cross-stratified conglomerates occur rarely, and have been observed only as solitary sets, ranging from 1.5 to 4 m in thickness. Cryptic and very low-angle planar (cross) stratification has been occasionally observed, with surfaces having (north-quadrant) dip-directions similar to associated clast imbrication palaeocurrent indicators. Grading profiles in beds are not well developed and, although a detailed study has not been carried out, there is no obvious correlation between bed thickness and maximum particle size.

This subassociation is frequently organized in cyclical sequences, metres to tens of metres thick. Topset cycles are developed from prominent basal erosional surfaces, followed by massive, crudely bedded conglomerates and capped by thinner-bedded conglomerates with development of reddened sandstones (e.g. Fig. 9). Thus, there is a tendency towards fining- and thinning-upwards cycles. Other cycles between prominent basal surfaces are neutral in terms of grain size and bed thickness.

Interpretation. The texture (particularly $a(t)b(i)$ imbrication, clast-support and poor sorting) and bed geometry of the conglomerates (and subordinate sandstones) comprising the conglomeratic topset association are consistent with turbulent water (stream) flows (Nemec & Steel, 1984). Sheet-like geometries and the lack of channel forms suggest either deposition in wide, shallow low-sinuosity gravel rivers that occupied the subaerial fan delta top, or as unconfined high-magnitude sheet

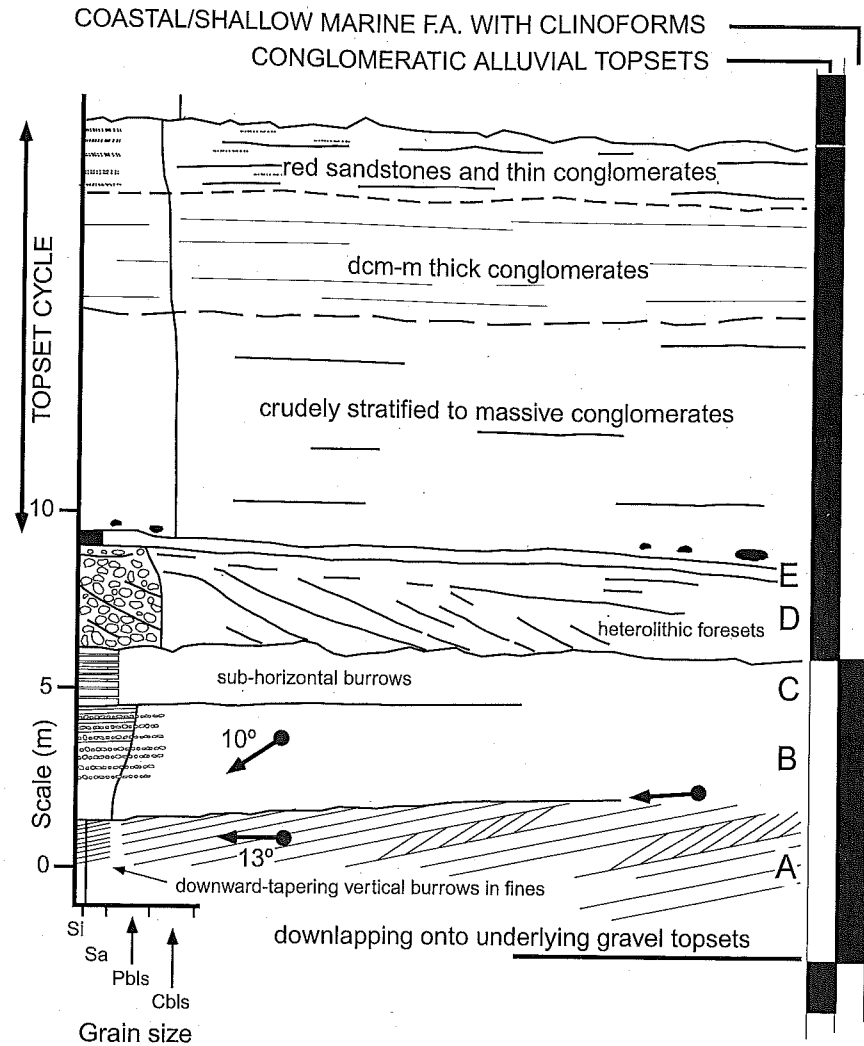


Fig. 9 Graphic log of well-stratified and sorted conglomerates and sandstones (SFA1) of the coastal-shallow-marine facies association organized in a west-dipping clinoform, and overlying flat-bedded and cross-stratified alluvial topset conglomerates (location B, Fig. 3).

floods (e.g. Young *et al.*, 2000). Occasionally preserved downstream-dipping low-angle inclined surfaces imply low-relief (?longitudinal) bars, on which gravel may have been accreted as diffuse gravel (bed load) sheets (Hein & Walker, 1977; Bridge, 2003); however, the preserved facies lack an openwork texture and well-developed grading profile typical of lower-stage plane beds (Bridge, 2003; see also Nemeč & Postma, 1993).

The stacked thinning- and fining-upwards topset cycles may be a reflection of declining accommodation modulated by high-frequency fluctuations in relative sea level, where thinner bedded units correspond to progradational episodes and basal thick-bedded topsets to aggradational episodes. The heterolithic subassociation is interstratified with the gravel-dominated topset sequences, and is thought

to represent subaerial, non-channelized (floodplain) environments on the delta top.

Shoreline-shallow-marine topset facies association

This lithologically and structurally diverse facies association occurs in grossly subhorizontal units and is therefore a 'topset' association. It is referred to as shoreline-shallow-marine based on evidence of distinctive textures, stratification and faunal/ichnofaunal content. It comprises four main subassociations, detailed below.

Very well sorted and stratified clinoform conglomerates (SFA1). Examples of this subassociation occur interstratified with texturally contrasting alluvial topsets (Fig. 9), in association with limestones (SFA3 below; Fig. 10c)

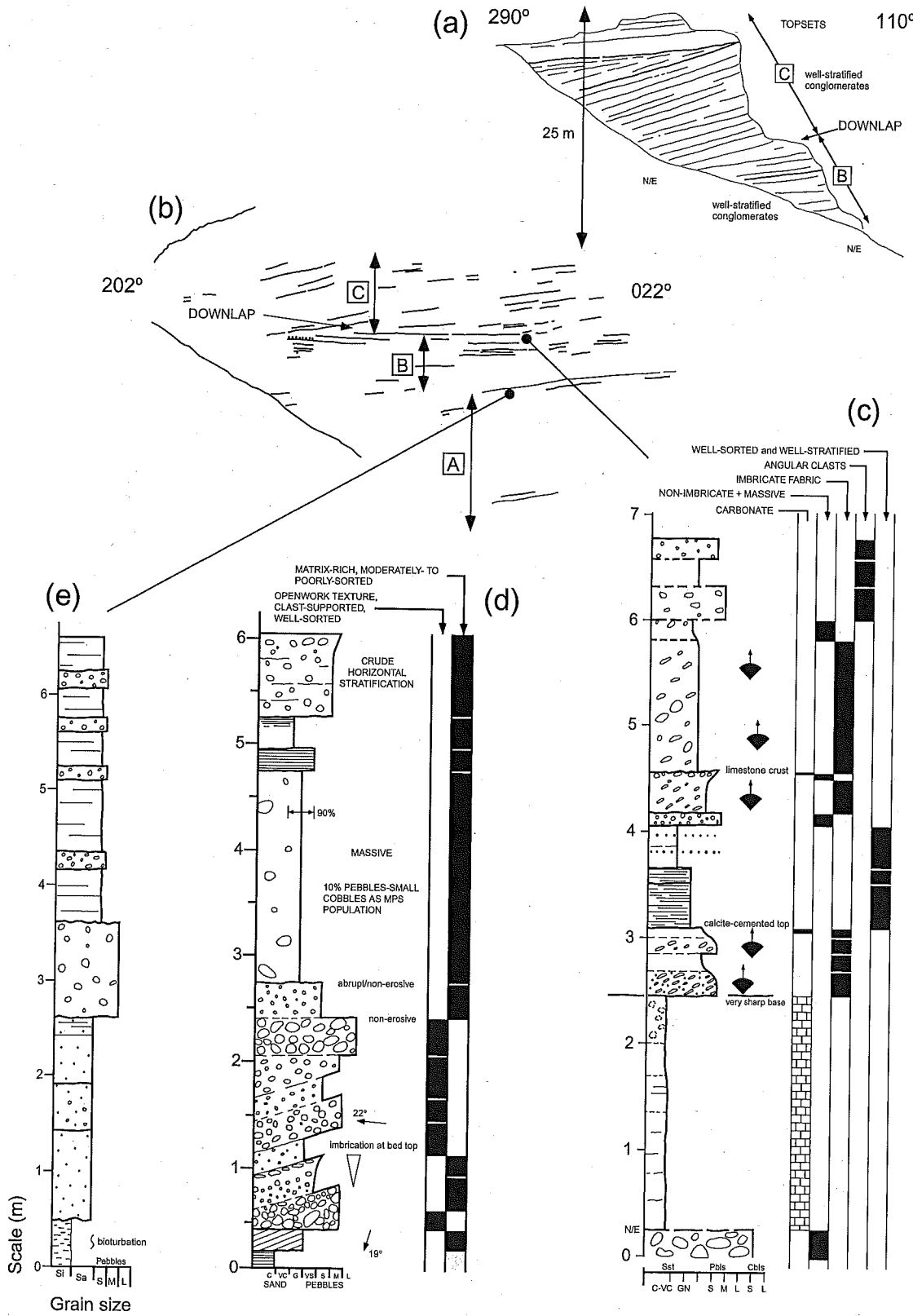


Fig. 10 (a,b) Line drawing of a valley side exposure (location C, Fig. 3) divisible into three macroscale units (A–C). Unit A contains variably sorted and structured examples of subdivision SFA1 of the shoreline–shallow-marine topset facies association (graphic logs d & e). Unit B shows an example of SFA3 (limestone) and SFA1 in erosive contact (graphic log c). Unit C comprises Gilbert delta foresets (overlain by topsets), which subtly downlap onto unit B.

and have also been observed to overlie the accretionary top lap association (SFA2, see below). This subassociation is exemplified by two detailed examples.

A well exposed 7–8 m thick sequence from the Vouraikos Gorge (Fig. 3, location B) consists of three inclined stratasesets (Fig. 9, A–C). The basal unit is heterolithic, with 5 cm thick, inclined, very well sorted small-pebble to granule conglomerates interbedded with laminated red, yellow and beige fine sandstones and siltstones. There are frequent downward-tapering burrows into the tops of the fine facies from the overlying fine gravels/sandstones. Unit B coarsens upwards, commencing with subhorizontally stratified, very well sorted granule to small-pebble conglomerates (bed thicknesses 4–6 cm), which are clast-supported and normally graded. The upper two-thirds of Unit B contains evenly spaced 'stringers' of large pebbles to small cobbles. Unit C is finer grained, composed of interbedded, very well stratified small-pebble conglomerates (9–38 cm in thickness) and red, medium to coarse sandstones (5–8 cm sheets) that contain granule to small-pebble laminae. The sandy facies contain a moderate frequency of subhorizontal, tube-like burrows.

The second example of SFA1 (Fig. 3, location C) shows several diverse metre-scale successions (Fig. 10a & b) comprising:

- 1 well imbricated, normally-graded small-pebble conglomerates, very well sorted parallel-laminated granule conglomerates, massive angular-shaped small-medium-pebble conglomerates (Fig. 10c);
- 2 steeply dipping (22°) openwork small- to large-pebble conglomerates, parallel-laminated coarse sandstone to granule conglomerates and massive bimodal conglomerates (Fig. 10d);
- 3 bioturbated siltstones, coarse sandstones and poorly sorted small-pebble conglomerates (Fig. 10e).

Additionally, the well-imbricated and stratified succession (1, described above) occurs in conjunction with a prominent limestone bed (SFA3, below), separated by an exceptionally sharp-planar surface (Fig. 10c), and comprises a package of sediment that has low-angle dips (5–10° restored), but was probably an overall subhorizontal unit. Two conglomerate beds within the section contain calcite-cemented and limestone-encrusted bed

tops (Fig. 10c). Observed clast imbrication indicated consistent north-quadrant palaeoflow.

Interpretation. SFA1 is considered to have been deposited subaqueously. The tightly packed conglomerate textures, stratified granule conglomerates and very coarse sandstones and seaward-dipping imbrication suggest moderate to high wave-energy conditions, and the lack of wave ripples in gravel sediments suggests that shallow depth conditions prevailed. The variable ichnofauna, thin carbonates, consistently directed clinofolds, and occasional cross-bedding with distinctive openwork textures again suggest wave-influenced and wave-reworked gravels in a shallow-marine shoreface to lower beachface setting (e.g. Nemec & Steel, 1984; Dabrio & Polo, 1988; Dabrio, 1990; Massari & Parea, 1990; Hart & Plint, 1995).

Accretionary top lap conglomerates/sandstones (SFA2). A suite of moderately distinctive facies is associated with accretionary top lap contacts where, rather than a single erosive contact between Gilbert foresets and flat-lying topsets, a series of areally restricted local contacts are arranged en-échelon, sometimes climbing upwards in the progradation direction (see Dart *et al.*, 1994, figs 7 & 8). Sequences arranged about accretionary top lap contacts (equivalent to the 'transition zone' of Colella, 1988; Gawthorpe & Colella, 1990) are around 5 m thick or less, and are characterized by showing moderately improved fabric development and stratification compared with alluvial topset conglomerates. The principal conglomerates' grain size varies typically from medium pebble to large cobble, and large cobble to small boulder sizes. Sorting is generally poor, with matrix-rich facies showing matrix- and local clast-support systems. Weak *a(t)b(i)* clast imbrication is recorded (with north-quadrant palaeoflows), but massive-unordered fabrics are the norm. Facies with matrices of coarse sand-granules to very small pebbles and outsize clasts are recorded, with variants being small- to medium-pebble conglomerates with small boulder outsize clasts. Stratification is characteristically enhanced in conglomerates of SFA2, being defined by either thin (5–10 cm thick) fine-grained conglomerates, equally thin medium-coarse (reddened) normally graded sandstones, or simply thin stratification in homogeneous gravelly sediments. Thicker interbedded sandstones within

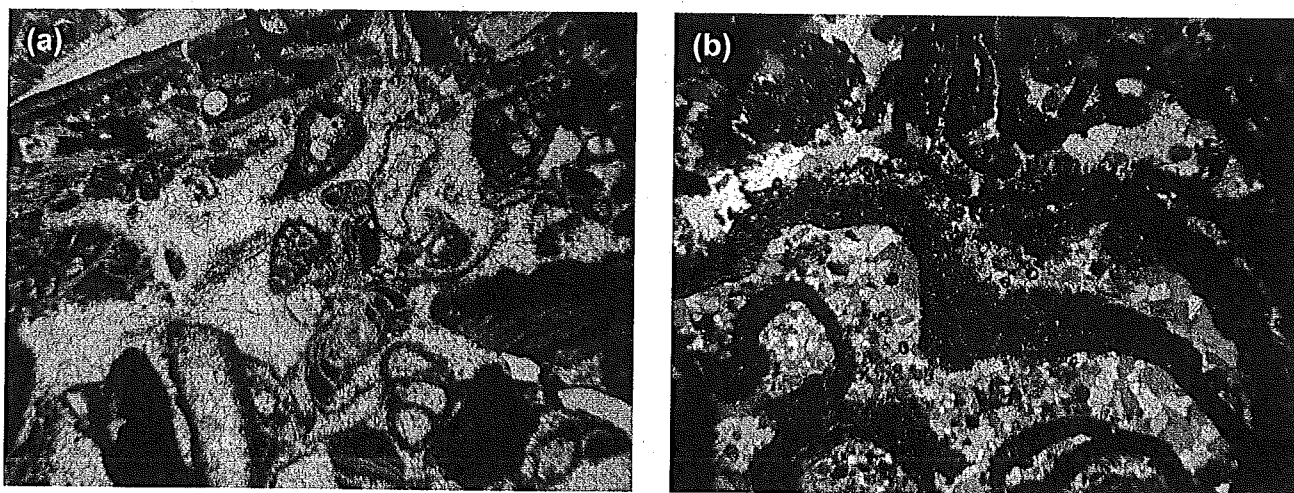


Fig. 11 (a) Photomicrograph of bioclastic grainstone carbonate facies at $38^{\circ}11'02.3''\text{N}/022^{\circ}10'28.1''\text{E}$ (Marathia Limestone). (b) Photomicrograph of algal packstone-grainstone facies from transitional section between foresets and topset facies association, at the SW extremity of the Mamoussia cliff section (location D, Fig. 3, Mamoussia Limestone). Plane-polarized light, with gypsum plate in (b). Each photomicrograph measures 5 mm across.

the accretionary toplap structure have been observed in inaccessible cliff sections, occupying the lower topset to upper foreset position. Apparently texturally distinct topset beds that overlie erosive toplap contacts have also been observed, but not directly examined. These are apparently massive and moderately to well sorted, tabular beds up to several metres thick.

Interpretation. The structural position of this subassociation alone suggests a contrasting emplacement process to alluvial topsets. The interpreted location is suggested to be a shallow subaqueous environment, which was affected by periodic flood-generated fluvial inputs of gravel (and sand) and reworking by moderate wave energy, equivalent to the 1 km wide shallow-marine topset of the modern Vouraikos Delta (Dart *et al.*, 1994, p. 549). The textural and stratification character of SFA2 contrasts with that of SFA1 where wave and current reworking of the sediment was considerably stronger. This may have been suppressed in SFA2 due to the dominance of fluvial supply during episodes of progradation and vertical accretion of the delta system. Occasionally observed distinct (single) beds erosionally overlying toplap contacts, which are apparently structureless and show closely packed textures, may represent wave-reworked gravels in a shoreline environment (see Colella, 1988).

Limestones (SFA3). Two limestone units were found in the Vouraikos Delta in this study, the Marathia and Mamoussia limestones (Figs 3, 6 & 10c). The Marathia Limestone is a bioclastic arenitic grainstone (Fig. 11a) to rudstone. It is massive to crudely horizontally stratified with a sandy texture in its lower part, and a 'rubby' 45 cm thick top (Fig. 10c). The limestone contains low-spire gastropods, fragmentary large, thick-shelled pecten bivalves, fragmentary small bivalves, ?tubiform bryozoa encrusting/cementing clasts, ostracods, foraminifera, echinoid spines, ?rhodophytic algae and other bryozoans (Fig. 11a).

The Marathia Limestone is associated with SFA1 sediments with low-angle ($7\text{--}10^{\circ}$) primary depositional dips (Fig. 10b & c). This limestone abruptly overlies a massive, pebble to cobble conglomerate, and is terminated by the exceptionally sharp, planar basal surface of a small-pebble conglomerate of SFA1 (Fig. 10c). The thickness of the limestone decreases southwards from 2.2 m to >1.4 m over a distance of 30 m, where the bed terminates in a low-relief (1.4 m) palaeocliff with a steep east-west striking orientation ($091/86^{\circ}$). Near the base of the palaeocliff there is a talus-like deposit with a northward-dipping inclined-curved fabric oriented $074/54^{\circ}$. However, the wall rocks of the palaeocliff have the same flat-lying bedding orientation of the main limestone, and are mixed

clastic-carbonate lithologies, in which sands and granule to pebbles are organized in typically 5–30 cm thick beds with white fine calcareous matrices.

The Mamoussia Limestone is located in the extreme south-west of the Vouraikos Delta in the western part of the Mamoussia cliff (Fig. 3, location D). This is a thin bed <2 m thick, stratigraphically located between the locally lowest Gilbert set and overlying topsets (Fig. 6). In thin section the limestone is seen to be very rich in fragmentary and complete algae (Fig. 11b). The lithology and texture is an arenitic bioclastic packstone to grainstone, containing probable peloids and extraformational clasts. Algal bioclasts have micritized envelopes. This facies, with its concentration of characteristic organisms, most closely resembles standard microfacies type 12 of Wilson (1975) and Flügel (1982).

Interpretation. The Marathia Limestone facies represents high-energy, shallow-water open-marine carbonate deposition on a flooded sector of the Vouraikos Delta top isolated from clastic input, following transgression. Similar facies from a Pliocene Gilbert-type delta setting have been described by Mortimer *et al.* (2005), where carbonate units represented marine transgression of the delta top. The Marathia palaeocliff and the contrasting mixed clastic and carbonate facies suggests an earlier phase of episodic carbonate-clastic deposition, followed by erosion and a later phase of sustained carbonate deposition lacking significant clastic input, which developed after minor fluctuations in relative sea level on the flooded delta top. The Mamoussia Limestone microfacies typifies wave-affected shelf edges (Tucker & Wright, 1990, table 1.1), which is analogous to the structural position of the unit at the seaward edge of the submerged delta topset. Carbonate sediments containing algal remains are reported in analogous shallow subaqueous (topset) settings, in (non-Gilbert) gravelly fan deltas (Ethridge & Wescott, 1984) and Gilbert-type deltas (Postma *et al.*, 1988; Young *et al.*, 2002, their facies 2b, c).

Laminated shelly siltstones and sandstones (SFA4). This rare subassociation consists of units up to 8 m thick of: (i) laminated fine-sandstone-siltstones with a uniform grain size profile; and (ii) laminated white-pale-grey siltstone (to mudstone), which

contains distributed fragmentary shelly fossils, as well as monospecific bivalve assemblages. Units may be sharp-based conformably overlying stratified pebble-cobble conglomerates. This fine facies is interbedded with rare <10–12 cm thick parallel-sided pebble conglomerates and pebbly sandstones, or interstratified with one-clast-thick layers of small pebbles.

Interpretation. This subassociation is considered to represent shallow-water back-barrier/lagoonal fines. The fine-grained laminated, weakly calcareous character plus the restricted diversity fauna point to a protected subaqueous environment at the margin of the flooded topset region of the delta. Small-pebble-clast layers and pebbly sands are interpreted to be storm washover sediments across coastal barriers or spits.

Gilbert-type delta foreset facies association

This facies association represents the largest volume of the Vouraikos fan delta. A compilation of large-scale (Gilbert) foreset orientations from the whole delta (Fig. 6) indicates a mean direction of progradation toward the north-northwest (345°, Fig. 12). The dispersion of the data suggests a convex (linguoid)-shaped sediment body. Dip values for foresets shown by the polar plot (Fig. 12; 10–35°) indicate a typical range for gravel-dominant Gilbert deltas (Nemec, 1990). It comprises well-bedded sequences of metre-scale pebble-cobble grade conglomerates, thinner bedded sand-matrix-rich very small- to small-pebble conglomerates, as well as coarse and pebbly sandstones. Notable are matrix-free openwork clast-supported pebble-cobble conglomerates (typically 10–20 cm in thickness), in units parallel to other facies.

Stratification includes types that are discordant, very low-angle planar strata and convex-up cross-stratification in single sets. Foreset stratification tends to be uniform and the texture homogeneous; subparallel, cross-cutting surfaces such as those described by Dart *et al.* (1994), or large-scale syn-sedimentary deformation features for the Keranitis Delta (described by Ori *et al.*, 1991), have not been observed. However, examples of interbedded fine-grained foreset intervals include mutually cross-cutting channel-form conglomerates <2 m thick with 10–15 m wide transverse sections, interbedded

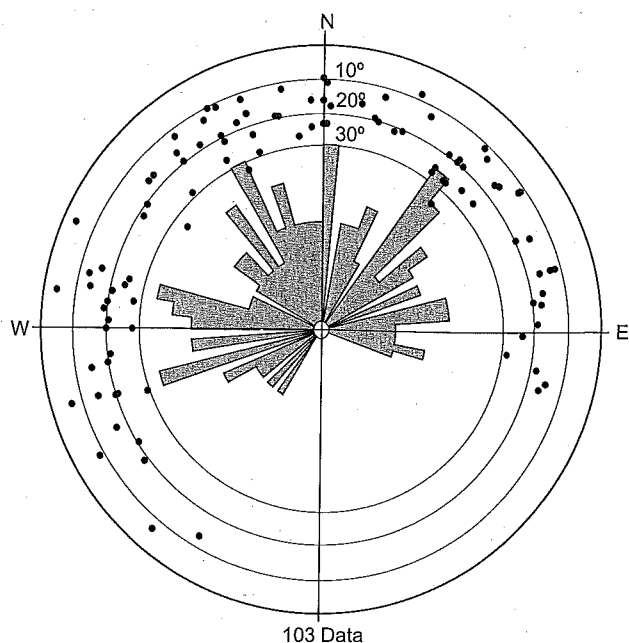


Fig. 12 Combined rose diagram and equal area polar dip-direction plot of the Vouraikos Delta foresets. Vector mean of foresets is 345° ($n = 103$). Rose diagram class interval is 3° .

with and eroding into red and brown laminated sandstones and red siltstones–mudstones. The shallow channel conglomerates are moderately to poorly sorted pebble to small cobble size with a sand matrix. Channel form bases are marked by scour structures in the form of occasional large-scale (10–15 cm thick), isolated flute marks. The channel form axes are oblique but dominantly down-dip of the foresets; interbedded associated fine-grained facies have been observed to contain small-scale down-dip verging soft sediment folds. Cliff-scale exposures of complete sets reveal very gently concave foresets, with clear reduction in dip as the bottomsets are approached.

Interpretation. Large-scale foresets represent bedload and mass-flow emplacement of gravel and sand into a standing water body (cf. Postma, 1990; Prior & Bornhold, 1990; Falk & Dorsey, 1998). The set thickness of the association indicates palaeowater depths in the range of 300–700 m. Clast-supported openwork foreset conglomerates were interpreted by Dart *et al.* (1994) as the tops of individual flow units, whereas the massive to crudely bedded, matrix-rich beds were considered as grain flows.

Bottomset facies association

This association is composed of thinly interbedded plane-laminated and rippled sandstones and conglomerates (Fig. 13a). Erosion surfaces and/or scours are common. In some places, soft-sediment deformation occurs with small-scale slump folds and/or dewatering structures (Fig. 13b). They represent the base of Gilbert foresets where low-angle slopes dip at values typically $5\text{--}10^\circ$.

Pro-delta facies association

This is an important facies association as it represents distal environments to the Gilbert-type delta, affected by basinal processes as well as sediment input from the delta. It is dominated by thinly bedded, beige and grey-green coloured, massive to finely parallel-laminated siltstones and silty sandstones with sharp bases (Fig. 13d), thin pebble conglomerates and laminated siltstones. Floating gravel clasts commonly occur in the fine (sand and silt) facies (Fig. 13c). This association is spatially related to the Gilbert-type delta bottomsets, and the two can be frequently mapped together in the field (Fig. 13e). Pro-delta and bottomsets share individual facies types (such as fine sandstones). Depositional dips are lower than those of bottomsets, and are generally undetectable.

Interpretation. These deposits can be interpreted as the products of processes ranging from suspension fallout deposits to turbidity current deposits that are *largely* beyond the influence of gravel input. They represent the deepest facies of all the associations observed in the Vouraikos fan delta system. This facies association is genetically related to the fan delta foreset–bottomset structure of the system, and results from emplacement of major increments of clastic sediment following periodic fluvial flood events. The pro-deltas of Type A feeder Gilbert-type fan deltas are affected by foreset-derived mass flows and density currents, as well as hemipelagic sedimentation (Postma, 1990; see also ‘basin plain’ deposits of Hwang & Chough, 2000).

VOURAIKOS DELTA ARCHITECTURE

Within the Vouraikos Delta, five internal stratigraphic packages have been defined, numbered *SP1*

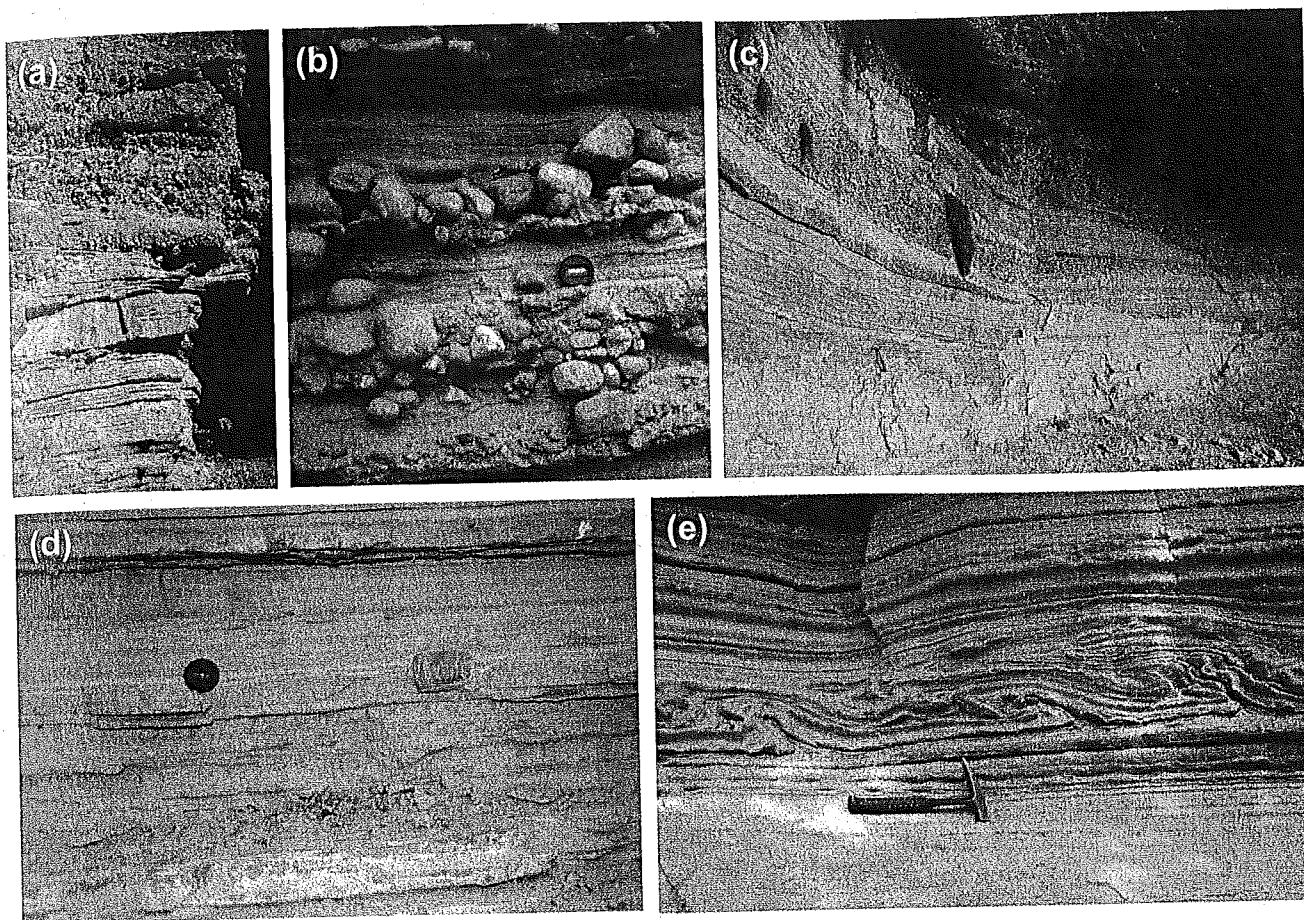


Fig. 13 Field photographs of bottomset and pro-delta facies associations of the Vouraikos Delta. (a) Bottomset conglomerates and sandstones from southwest base of delta (Keranitis Valley). (b) Coarse conglomerate levels within fine-grained pro-delta facies. (c) Conglomeratic bottomsets wedging downward into fine-grained pro-delta facies eastern base of delta (Ladopotamos Valley). (d) Floating pebble in pro-delta siltstones and fine sandstones (Ladopotamos Valley). (e) Slump folds showing basinward asymmetry from southwest base of delta (Keranitis Valley). Scales: hammer shaft = 28 cm; lens cap = 6 cm.

to SP5 (Fig. 4). A stratigraphic package is here defined as a distinct succession limited by prominent bounding surfaces. A stratigraphic package can comprise: (i) packages of topsets (representing palaeohorizontal); (ii) very large-scale foresets (at angles of repose of 20–35°); and/or (iii) multiple sets of topsets and foresets. Comparatively thin, but locally distinctive, bottomset, thin pro-delta and shallow-water coastal facies associations are occasionally found within the thicker stacked packages. There is considerable lateral variation in individual stratigraphic packages (see Fig. 6), related to: (i) thickness variations; (ii) transitions of topsets into foresets; and (iii) other variations due to intradeltaic growth faults. Detailed correlation is further complicated by changes in structural elevation

due to second-order extension faults, such as the Derveni Fault (Fig. 3). While bounding surfaces are clearly distinguishable in the proximal (topset) part of the delta, they can be lost distally, in particular within thick foreset sequences.

Despite this, good stratigraphic coherence is displayed, particularly in the southern and western parts of the delta. An analysis is presented principally of the western half of the delta (Asomati block) along two major NNE–SSW cross-sections (Fig. 14), and three east–west profiles in the Asomati block (south, centre and north). The eastern part of the delta (Kastillia block) is represented in less detail in the regional cross-section in Fig. 2b and in one natural east–west profile on the north-east side of the Kastillia block (Fig. 3).

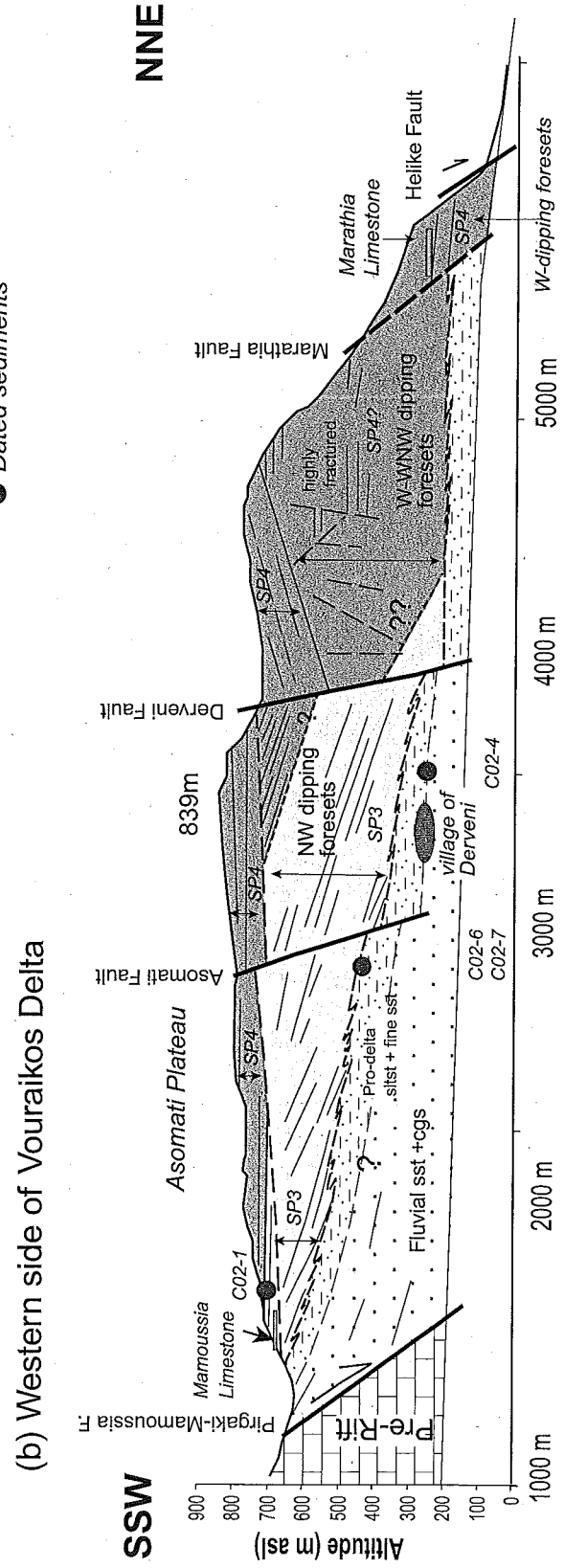
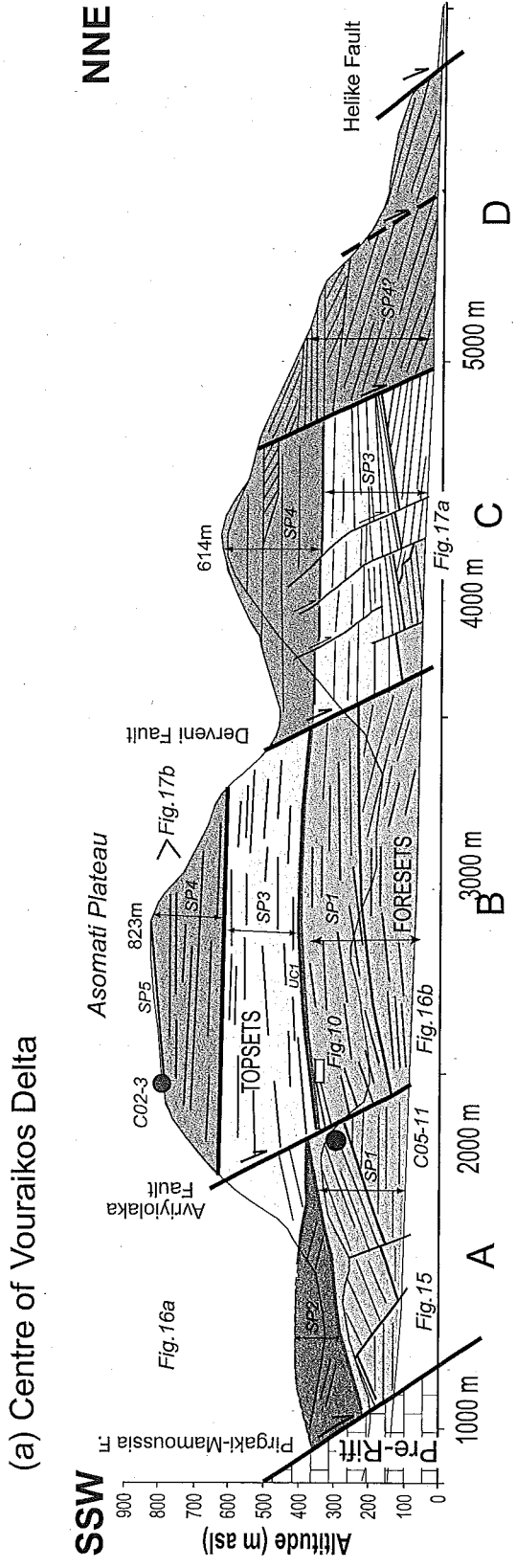


Fig. 14 Detailed SSW-NNE cross-section of (a) the western side of the Vouraikos Gorge, representing the centre of the delta and (b) east side of the Keranitis Valley, representing the western limit of the Vouraikos Delta. Circles indicate palynologically dated sample horizons (Table 1). AF is the Avryiolaka Fault.

Centre of delta – the Vouraikos Gorge

The Vouraikos Gorge, with a relief of > 700 m, provides the most complete section through the centre of the Vouraikos Delta. For convenience, the section along the western side of the gorge is divided into four sectors demarcated by major faults and labelled A to D (Fig. 14a). The base of the delta is not exposed anywhere along this section.

The lowest stratigraphic package *SP1* is found only in the centre of the delta (sectors A, B and C in Fig. 14a). It comprises a single set of major foresets at least 200 m thick (base not seen) overlain by 200–250 m of topsets that together describe a gentle rollover anticline dissected by secondary north-dipping normal faults. At the southern extremity of the fold, in the immediate hangingwall of the PM Fault, topsets have been rotated to dip

30°S and foresets have become horizontal (Figs 14a & 15). Fold amplitude decreases upward indicating that fold activity died out during deposition of *SP3*. A simple 'chevron' construction (Verrall, 1981) suggests that the controlling listric fault soled out about 100 m below the present erosion level (not shown on Fig. 14a). At the southern end of the section, tilted foresets lie within 20 m of the PM Fault and there is no evidence of extreme basin-margin proximal facies in the southernmost *SP1* packages. This implies that the topsets equivalent to these foresets must have lain farther south. The PM Fault, hitherto regarded as the basin-bounding fault for the whole Vouraikos Delta, is therefore here interpreted as a post-*SP1* fault. The southern topsets of *SP1* were thus uplifted and eroded in the footwall of the PM Fault. On this section line, the listric fault that generated the rollover anticline

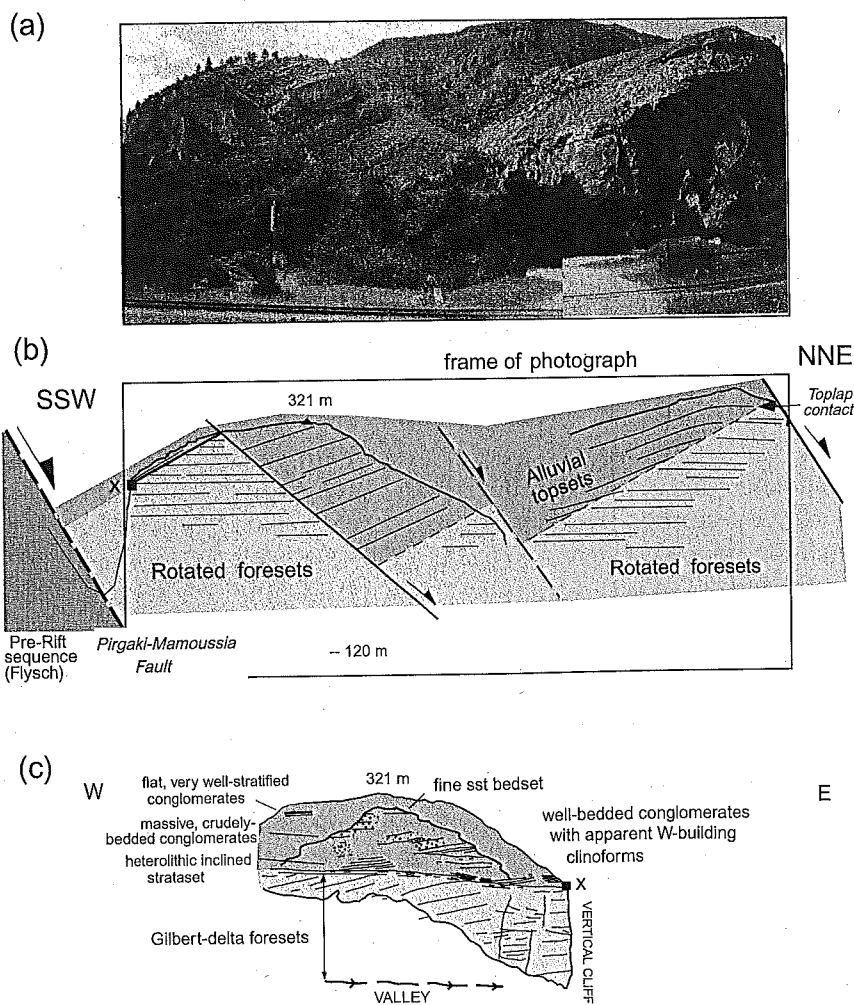


Fig. 15 Fault blocks in the Vouraikos Gorge. (a & b) View west of tilted fault blocks in *SP1* at the southern end of the gorge (located on Fig. 14a). (c) Line drawing of a cliff section at 90° to (a) viewed toward the north, showing foresets, toplap contact and overlying low-angle clinoforms. X is the common point to the two views.

was cut out by the later PM Fault, however, the Kastillia Fault identified in the eastern delta block is probably its lateral equivalent.

Across sector B, *SP1* foresets curve from horizontal to dip north, while *SP1* topsets become subhorizontal. These topsets are predominantly alluvial in character although a 12 m thick sequence of shallow-marine conglomeratic and sandy sediments occurs near the top (SFA1, Fig. 9). On the southern limb of the rollover anticline an angular unconformity of 12° marks the boundary between *SP1* and *SP3* (*UC1* on Figs 14a & 16). This unconformity disappears northward as the rollover anticline dies out. Toward the south *UC1* can be continued as the erosive boundary between *SP1* and *SP2*.

In the immediate hangingwall block of the Derveni Fault (Fig. 14a, panel C), the top of *SP1* is downthrown 300 m so that only the uppermost topsets are exposed. These south-tilted alluvial conglomerates are incised by an erosional scour with a (minimum) relief of 50 m (Fig. 17c, d) and oriented N–S. This surface is correlated with the *UC1* unconformity to the south and is overlain by a set of shallowly northwest dipping *SP3* foresets.

SP2 is an aerially restricted 200–220 m thick package of north-dipping foresets that lies between *SP1* and *SP3* in sector A (Figs 6, 7 & 14a, described below). It is found nowhere else in the delta. Northwest-dipping foresets of *SP3* abruptly overlie *SP2* foresets and locally preserve fine pro-delta facies at the *SP2*–*SP3* contact.

SP3 is a 200 m thick alluvial topset sequence showing a weakening rollover geometry up-section in sector B (Fig. 14a). These thickly-bedded conglomeratic topsets are laterally equivalent to major northwest-dipping foreset packages that are visible on the Mamoussia cliff and western profile (Fig. 14b).

Above *UC1* in sector C of the central profile, the *SP3* foresets (Fig. 14a) are cut by weakly curved faults, which have back-rotated the foresets to subhorizontal attitudes in places. The overlying *SP3* alluvial conglomerate topsets thicken southward toward the Derveni Fault indicating that it was active during their deposition.

In sectors B and C (Fig. 14a), *SP3* is abruptly terminated by a sharp, apparently horizontal bedding surface that forms the base to a finer-grained, and well-bedded, sequence of conglomerates and sandstones defined as *SP4* that includes alluvial topsets and small Gilbert-type delta packages of

10–20 m thickness all building out to the northwest (Fig. 17a, b). *SP4* thickens northward across panel B from 170 m to 200 m (top exposed). The unit also thickens abruptly across the Derveni Fault to form the upper 300 m of panel C (top eroded), implying syn-*SP4* activity on this fault.

Panel D (Fig. 14a) is demarcated to the south by a weakly listric, poorly exposed, growth fault of unknown displacement. The panel is dominated by a set of large foresets dipping shallowly toward the northwest and having a minimum thickness of 400 m. Above, at least two smaller sets occur as well as at one horizon of conglomeratic topsets of unverified environment. As correlation across the fault is unclear all these strata are assigned to *SP3/4*. The Eastern Helike Fault abruptly terminates the delta to the north. At the top of the cliff in sector B (Fig. 14a) a prominent, thin (5–10 m) south-dipping conglomerate unit (*SP5*) gives a wedge-shaped aspect to *SP4*.

Western limit of delta – Keranitis Valley

This N–S cliff section (Fig. 14b, shown as a mirror image for ease of comparison) forms the eastern side of the Keranitis River valley. The profile affords a near complete section of the western limit of the Vouraikos Delta, comprising a relatively simple architecture of upper topsets, a continuous foreset succession and thin (20–50 m) underlying pro-delta sediments (Malartre *et al.*, 2004, fig. 2). The architecture of this section is markedly different from the central Vouraikos Gorge section, which lies just 3 km to the east. The basal (diachronous) ‘enveloping surface’ of the delta conglomerates dips markedly (8°) to the north; this is a (largely) primary dip. As the topsets dip gently south, the delta body thickens northward. Bottomsets and foresets build toward the west and west-northwest (i.e. obliquely out of the plane of the section; Fig. 6).

North-dipping sediments of the Ladopotamos Formation are exposed below the delta in the southern Keranitis Valley. Correlation of stratigraphic packages from the Vouraikos Gorge identifies the lowest stratigraphical level of the delta at the southern end of this section as *SP3* foresets and topsets (compare with Fig. 16a & b). It is estimated that somewhere to the north of Derveni Village *SP3* foresets pass up into *SP4* foresets, however, it is not possible to pinpoint this transition.

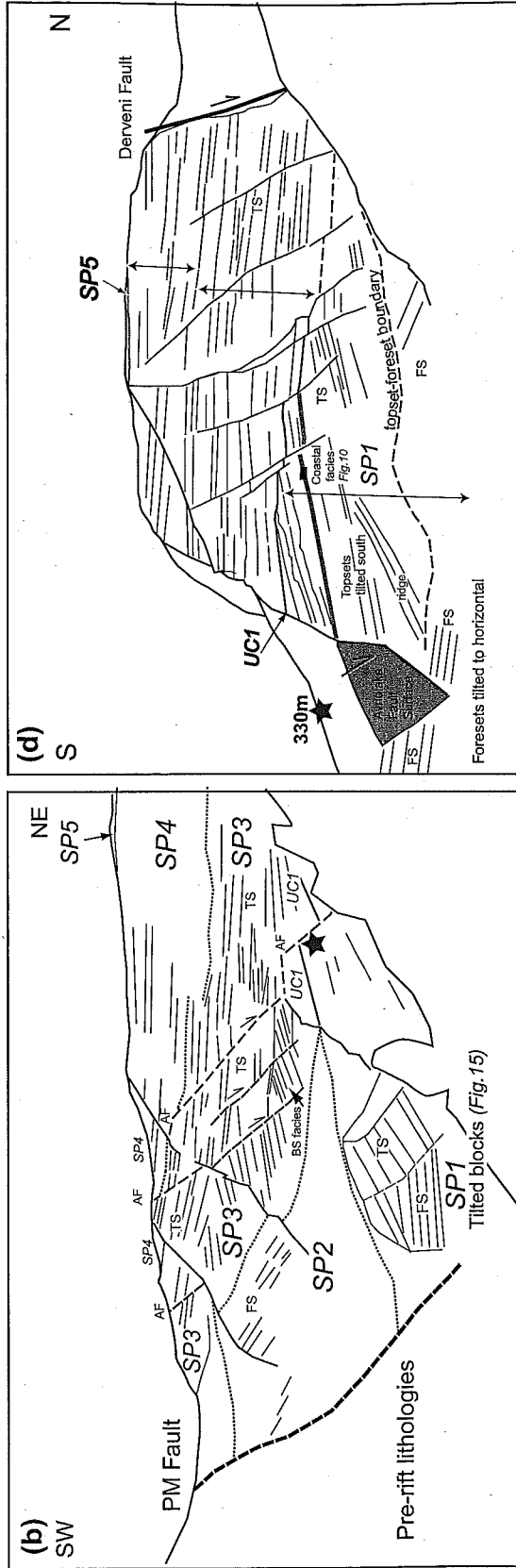
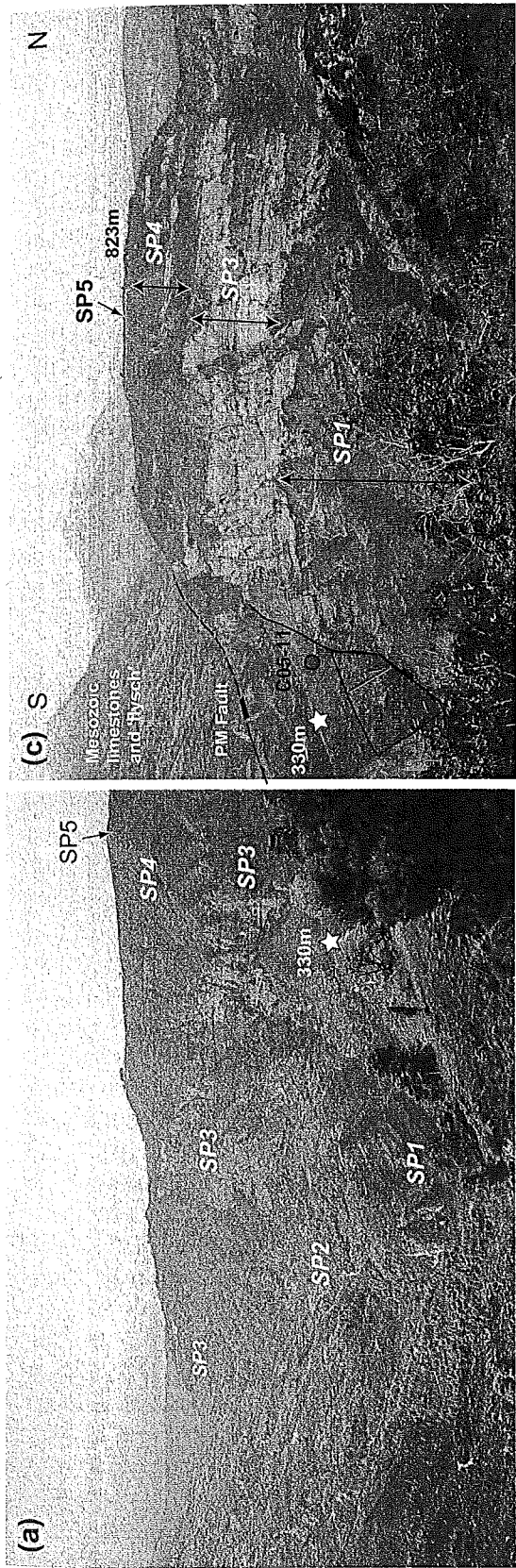


Fig. 16 Panoramas of the southern end of the Asomati Plateau and the Vouraikos Gorge. The star is a common point to the two views. (a) View westward of the southern margin of the Asomati Plateau. Relief on the section is 700 m. (b) Interpretation of (a) showing the organization of stratigraphic packages SP1 to SP4 in the immediate hangingwall of the Pirkaki-Mamoussia Fault. AF is the Avriyiolaka Fault. UCI is the unconformity between SP1 and SP3. TS, topsets; BS, bottomset to pro-delta facies; FS, foresets. SP3 foresets dip to the northwest. (c) Oblique view toward the west-southwest across the Vouraikos Gorge of the Asomati Plateau (sectors A and B of Fig. 14a). Relief in the gorge is over 700 m. (d) Interpretation of (c), showing stratigraphic packages, faults and the rollover anticline in SP1. The small secondary faults cutting SP3 are not represented in Fig. 14a. The heavy grey line in SP1 topsets is the coastal facies level (Fig. 10).

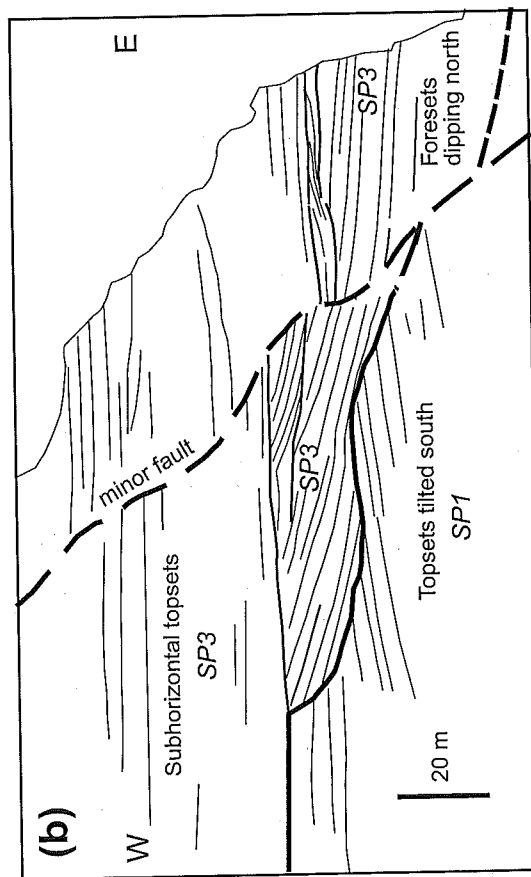
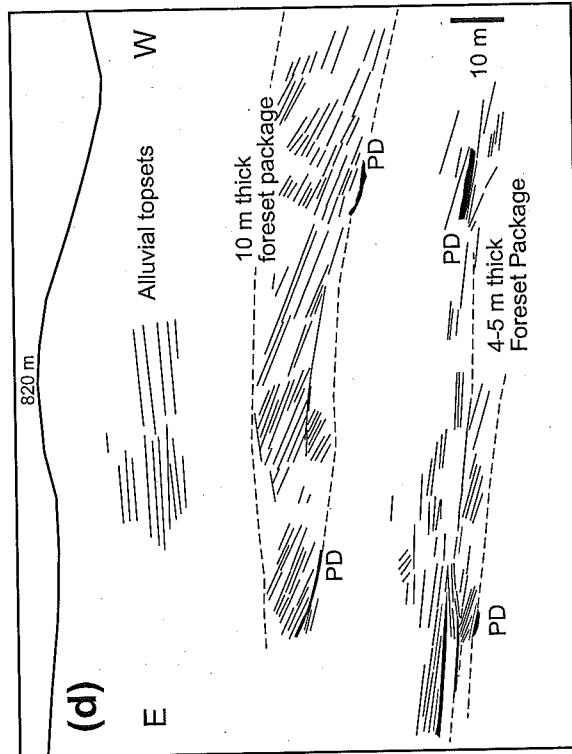
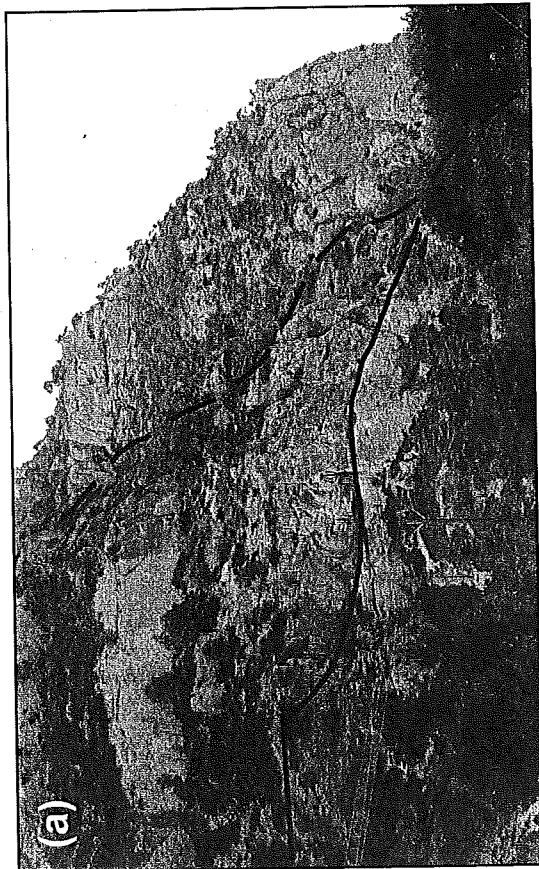
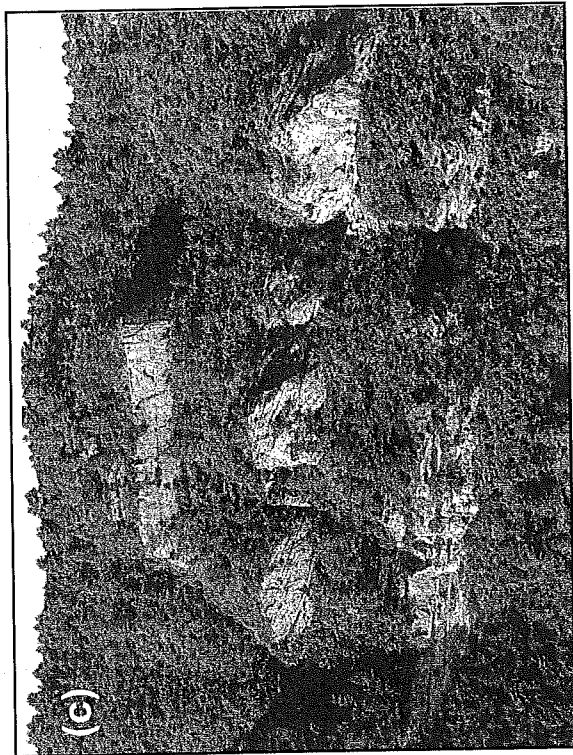


Fig. 17 (a) Photograph and (b) line drawing of major incision surface into SP1 topsets in the central Vouraikos Gorge (panel C, Fig. 14a). The incision is overlain by north-dipping foresets of SP3. (c) Photograph and (d) line drawing of a 110°-trending cliff in the immediate footwall of the Dervení Fault in the centre of the Asomati Plateau showing stacked Gilbert-type deltas of SP4 building out to the northwest. PD are bottomset to pro-delta facies at the base of individual Gilbert-type deltas.

Thus the *SP3* and *SP4* topsets observed in the Vouraikos Gorge (Fig. 14a) have passed distally (toward the NW–WNW) to foresets on this profile. Thin *SP3* topsets are only observed at the southern end of the western section where they include the Mamoussia algal limestone facies (SFA3, Figs 6 & 11b). Horizontal topsets above the main succession of foresets are assigned to *SP4* because they contain small Gilbert-type deltas of 5–10 m height interspersed with alluvial topset sequences. This package can also be traced around to the central profile along the cliffs in the immediate footwall of the Derveni Fault (see Fig. 17a & b). Therefore, the major toplap surface on this section is the *SP3–SP4* boundary. *SP5* is not visible on this section line. The marked contrast in geometry and stratigraphy between this section and that in Fig. 14a is because this section represents the younger western fringe of the delta, which has over-spilled the edge of the palaeovalley.

The minimum displacement on the PM Fault is considerably less on this profile than in the centre of the delta (Fig. 14a), implying that fault displacement decreases rapidly westward. The section is cut by three secondary extension faults, the Asomati, Derveni and Marathia faults. The Derveni Fault downthrows the toplap contact by 200 m to the north. Late displacement on the Derveni Fault has tilted topsets of the hangingwall block to 3°S. Between the Derveni Fault and the Helike Fault the delta conglomerates are highly fractured but comprise principally west-dipping *SP4* foresets of > 400 m height (see below).

The stratigraphic architecture of the western end of the Vouraikos Delta is quite distinct from that of the nearby eastern part of the Keranitis Delta (see Dart *et al.*, 1994, fig. 6). The bases of these deltas are separated by 400 m of altitude, while the tops are at the same level (detailed by Malartre *et al.*, 2004). This implies that they developed as independent delta systems separated by a transverse fault in the Keranitis Valley (Fig. 3).

Southwest proximal corner of delta – WSW–ENE Mamoussia section

This indented east–west cliff extends from the Vouraikos Gorge westward to just north of the village of Mamoussia (here referred to as the Mamoussia Pass, Figs 7 & 18b), a distance of

approximately 2 km, and links the proximal parts of the two sections described above. An oblique view of this cliff is shown in Fig. 18a. The cliff forms a gross depositional strike section in terms of the Vouraikos Delta as a whole, but for several of the constituent stratigraphical units it forms a dip and oblique section with respect to foreset building directions. The Avriyiolaka Fault, striking E–W, obliquely cuts the indented cliff and downthrows to the north by 30–40 m, with displacement dying out rapidly to the west (fault not seen on western section, Fig. 14b). Four stratigraphical packages, *SP2* to *SP5*, can be traced between the central and western cross-sections. No cross faults (i.e. striking around N–S) are detected in this cliff, however, the base of the delta clearly rises from below 120 m in the Vouraikos Gorge westward to an altitude of 600 m at Mamoussia Pass (Fig. 18b). At the same time, the delta edifice thins from over 800 m to less than 200 m westward. These observations are interpreted to mean that the delta gradually infilled a palaeovalley of around 500 m depth as represented in Fig. 18b. A similar configuration is observed on the eastern side of the delta between the Vouraikos Gorge and the Ladopotamos Valley.

SP2 is the smallest delta package, being 1.7 km wide and around 200–220 m thick (Fig. 18). It is limited to the southwest sector of the delta and comprises principally conglomeratic foresets, although its lowest, most easterly exposures include bottomset facies. The true base to the set is not exposed but it must erosionally overlie *SP1*. In the lowest part, foresets and bottomsets build towards 041°, however, the package is dominated by foresets with a mean building direction toward 357°. Foreset and bottomset inclinations suggest that little or no rotation has occurred. *SP2* can be followed westward to within 1 km of the Mamoussia pass. In its most westerly exposure it is overlain by bottomset and pro-delta facies of *SP3*. This delta package must terminate westward because, at the same elevation 2 km further west in the Keranitis Valley, north-dipping sandstones and conglomerates of the Ladopotamos Formation crop out.

The *SP3* package can be traced across the entire length of the cliff (Fig. 18a). It is dominated by a major set (180 m thick) of foresets with a true northwest-building direction. This set and its erosional toplap contact are downthrown to the north by the extensional Avriyiolaka Fault. *SP3* foresets

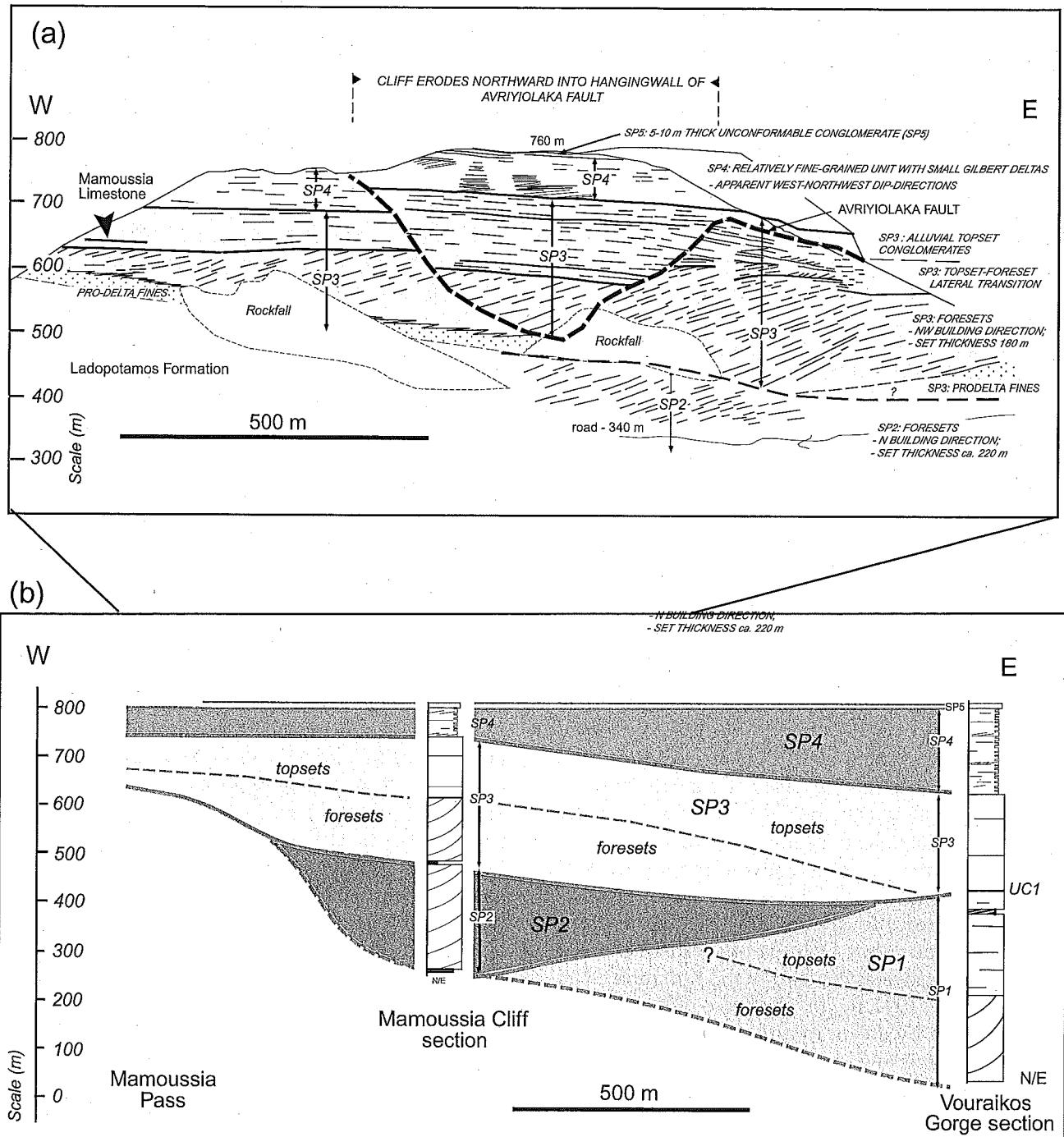


Fig. 18 (a) Field sketch of the east-west Mamoussia Cliff section representing the southwest side of the Vouraikos Delta viewed from Mamoussia village. (b) Correlation and geometry of stratigraphic packages within the proximal Vouraikos Delta from the Vouraikos Gorge (Fig. 14a) to the Keranitis Valley. The complex trace of the Avriyiolaka Fault in (a) is due to the indented cliff morphology.

pass eastward to flat-lying topset facies associations, which correlate with *SP3* alluvial topsets in the Vouraikos Gorge section (Figs 14b & 18b).

In the footwall of the Avriyiolaka Fault, fine-grained bottomset to pro-delta facies are exposed at around 500 m, marking the base of the *SP3* delta. This contact gradually rises westward in elevation to 600 m at Mamoussia Pass. *SP3* correspondingly thins rapidly to the west, where it comprises markedly curved-asymptotic foresets some 4–50 m high, passing into bottomsets and pro-delta beds (Fig. 18a).

The upper part of *SP3* (Fig. 18a) is a flat-lying sequence of horizontally stratified conglomerates of alluvial aspect. The facies are best seen in the mid-central part of the main cliff (hangingwall of the Avriyiolaka Fault), where they sharply truncate the underlying foresets. The package can be divided into three units by prominent sharp conformable bedding surfaces (Fig. 18a). The upper surface to the whole package is a very sharp, planar trace.

The uppermost major package in the profile, *SP4*, is finer grained than those units below, and contains facies showing well developed fine-scale stratification, heterolithic character, with (finer-grained) conglomerates, pebbly sandstone and sandstones. Overall it is horizontally stratified, but contains several levels comprising large-scale cross-stratification with consistent apparent inclinations to the west, which are interpreted as small-scale Gilbert-type deltas. The approximate thickness of these sets is 5–20 m. The gross horizontal stratification is conformable with the underlying *SP3* topsets. The unit is terminated by a notably continuous conglomerate bed at the top of the cliff (*SP5*), which dips to the south. *SP4* is 60–70 m thick in the Mamoussia cliff (Fig. 18a), indicating that it thins westward from 170 m at the southern end of the Vouraikos Gorge (Figs 14a & 18b).

SP5 is a 8–10 m thick grossly flat-bedded unit, comprising a variable sequence of facies that include matrix-rich, poorly sorted pebble- to cobble-grade massive conglomerates and matrix-poor, moderately sorted inclined- and flat-stratified conglomerates. Cross-bedded conglomerates occur, with sets up to 2 m thick and moderate to low-angle planar foresets. Finer-grained facies include interbedded reddish mudstones (8–10 cm bed

thickness) and 12–15 cm thick bioturbated fine sandstones (with bedding parallel burrows). Highly indurated very coarse sandstone–granule facies contain sparry calcite cements and ostracod and algal bioclasts.

Northern exposures of the delta: east and west frontal profiles

The Vouraikos Delta has been cut and exhumed in the footwall of the East Helike Fault to form a range front 7 km long and 700–800 m in height. At the northwest corner of the Asomati Plateau the youngest delta foresets belonging to *SP4* are well exposed in an east–west cliff in the footwall of the secondary Marathia Fault (Fig. 19a). These frontal foresets are at least 350 m high (being cut by the Marathia Fault) and dip predominantly 23–30° to the west-northwest and west. The overlying fluvial topsets at the northwest tip of the plateau dip 10–20°S–SW (Fig. 14b). The topset–foreset transition shows that the delta front prograded toward the west. Small Gilbert delta packages are seen to build out toward the west within the *SP4* topset complex.

Similarly, the youngest northeastern frontal part of the delta is visible on the E–W range front of the Kastillia Plateau (Fig. 19b). Here, two major packages of foresets are visible; a lower north-building package below Faghia, some 250 m high; and a larger upper package of consistently northeast-dipping foresets that are at least 600 m in height. This vast (unfaulted) foreset package forms the whole northeast and eastern side of the Vouraikos Delta. These foresets are probably the equivalent of *SP4*. Thin topsets of both packages dip shallowly south on the top of the Kastillia Plateau.

At the mouth of the Vouraikos Gorge on the western side of this section, a thick sequence of south-dipping fluvial sediments occurs in front of and below the delta foresets. It is not yet clear if these strata belong to the Ladopotamos Formation and thus truly underlie the delta, or if they are younger deposits deposited along the range front during late exhumation of the delta. These deposits are incised into and overlain by the youngest Gilbert-type deltas, the tops of which form depositional terraces dipping gently toward the northeast (Fig. 19b). These young deltas have themselves been uplifted

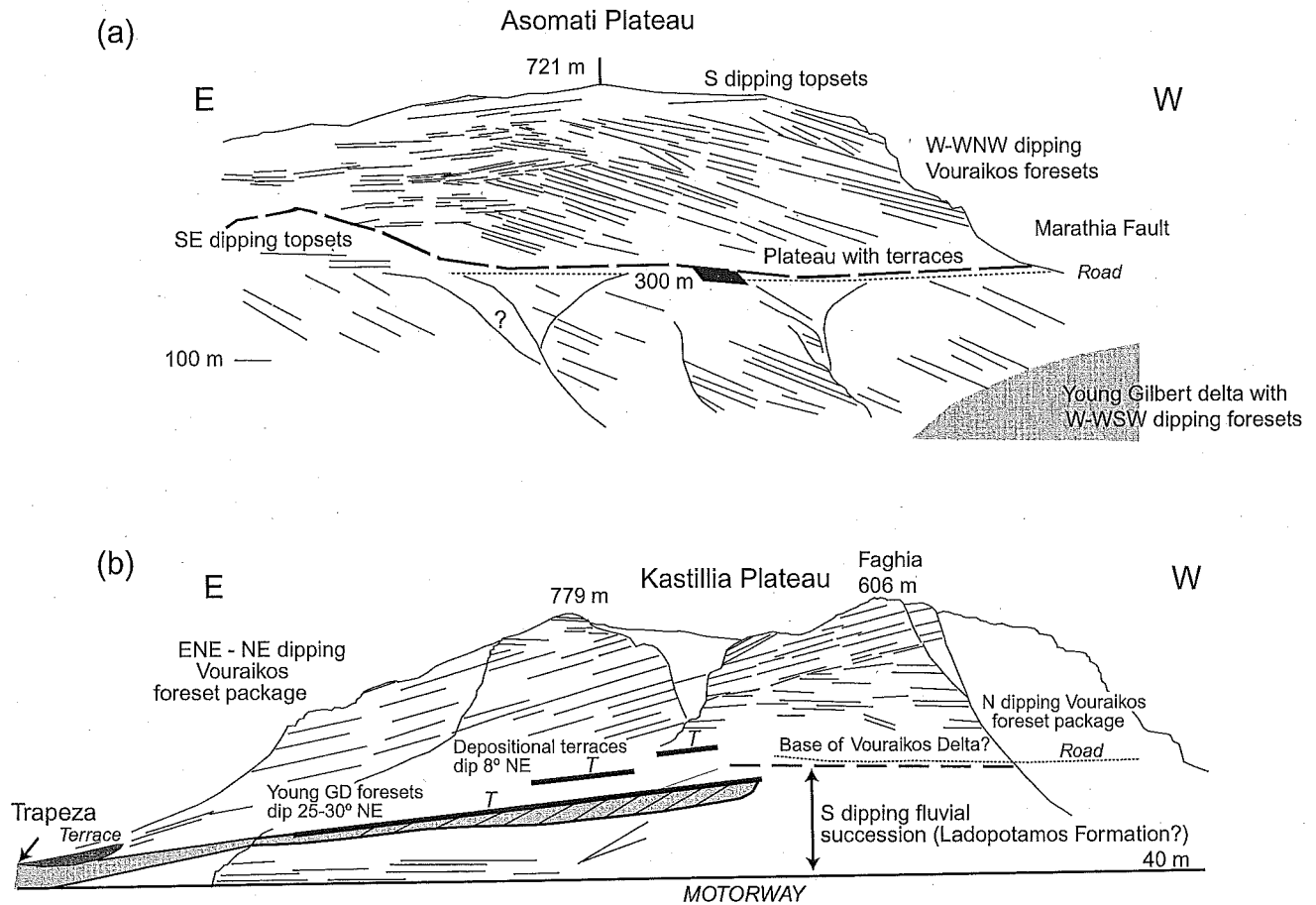


Fig. 19 Line drawing of the (a) northwest range front and (b) northeast range front of the Vouraikos Delta in the immediate footwall of the Eastern Helike Fault. Younger Gilbert deltas, deposited on the range front during its exhumation, are shown in light grey. The largest of these (100 m high) lies in the hangingwall of the Marathia Fault on the northwest range front and contains west-southwest-dipping foresets. Depositional terraces on the northeast range front dip 8° NE and are shown in heavy black lines with the letter *T* or in dark grey when dipping north.

in the footwall of the Eastern Helike Fault. Their foresets are up to 30 m high and dip predominantly to the northeast (Fig. 19b).

EVOLUTION OF THE VOURAIKOS DELTA

The data presented above are used to reconstruct the depositional history and character of the Vouraikos Delta and to identify the factors that controlled its evolution. Accommodation space was created principally by the PM normal fault system with displacement distributed on different branches at each stage of basin history (Fig. 20).

Delta deposition (800 m minimum) is estimated to have occurred during the early to mid-Pleistocene

from before 1.1 Ma to after 700 ka (600–400 kyr), implying a high sedimentation rate of between 1.3 and 2 mm yr^{-1} . The delta built northward in a radial fan fault-controlled basin. The carbonate facies (in *SP3* and *SP4*) and the isotope study (Katafugion Formation) described above indicate that this basin was wholly or periodically marine. High-resolution studies on Upper Pleistocene deposits in the Gulf of Corinth indicate that the salinity of the basin fluctuated between marine and fresh water, controlled by eustatic sea-level variations (Perissoratis *et al.*, 2000; Kershaw & Guo, 2003). In addition, biostratigraphic studies on Lower and Middle Pleistocene sediments record brackish, lacustrine and marine fauna (Frydas, 1989, 1991; Fernandez-Gonzalez *et al.*, 1994).

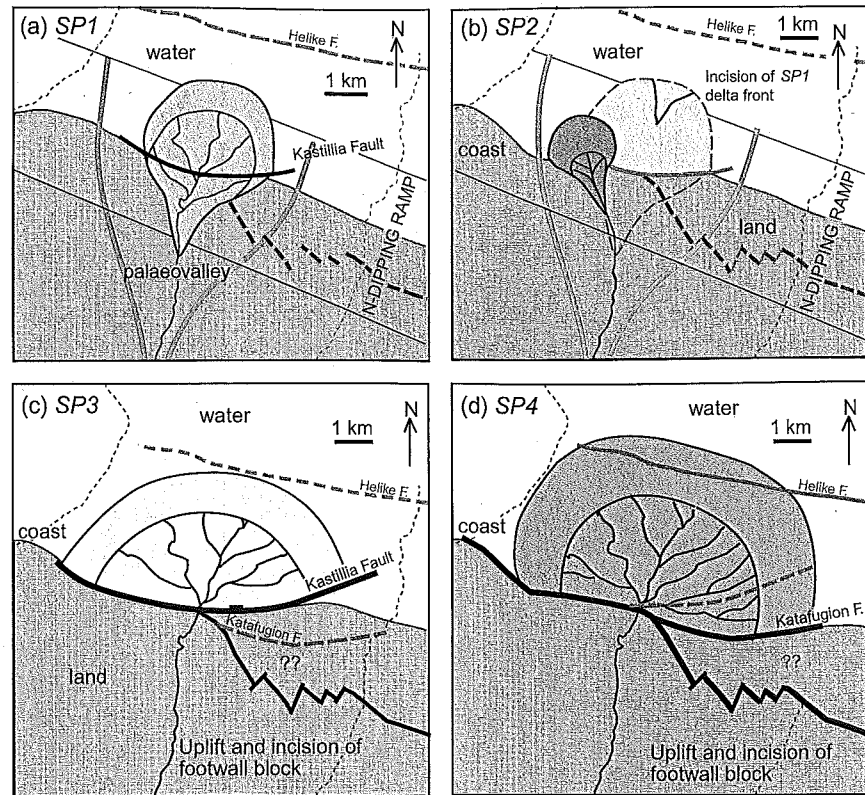


Fig. 20 Map view models for the four main stages in the evolution of the Vouraikos Delta corresponding to SP1 to SP4.

Reconstruction of the western half of the delta is divided into five stages, equivalent to the five stratigraphic packages SP1–SP5 described above. These are represented in scaled maps and in longitudinal and cross-sections (Figs 20 & 21). The cross-sections represent only the western half of the delta where the PM Fault consistently formed the basin bounding fault. It is not currently possible to define the duration of each of these stages due to lack of precise dating.

Early rifting (lower group and unconformity at base of upper group)

During the early phase of rifting (pre-1.1 Ma) the fluvial and alluvial successions of the lower group (Kalavrita conglomerates and the Ladopotamos Formation) were deposited in a series of half graben, controlled mainly by north-dipping faults spaced at between 4 and 5 km and with displacements of up to 1.5 km (Ghisetti & Vezzani, 2004, 2005; Bourlange *et al.*, 2005). The PM Fault was not active at this stage. Preliminary palaeocurrent data indicate that the main source areas lay to the

south and west. Towards the end of this period a base-level rise is recorded by deposition of the Katafugion Formation.

In the early Pleistocene, a major change occurred in the tectonic and depositional dynamics of the Corinth region. The main depocentre shifted northward and became narrower and the southern area (Kalavrita to Mamoussia) became uplifted. Sediment supply increased as major rivers began to transport large volumes of coarse sediment from the southern area to newly established Gilbert-type deltas. The establishment of new Gilbert-type delta systems requires high sediment supply and the creation of significant accommodation space below base level, requiring the activity on new normal faults. The northward dip of the Ladopotamos Formation indicates that a tectonic tilting took place before the major normal fault broke surface. This tilting is interpreted as being due to forced folding above the upward propagating PM Fault. The early delta (SP1) was therefore deposited above an active northward-tilting ramp, in a manner similar to that described by Young *et al.* (2000) in the Gulf of Suez and

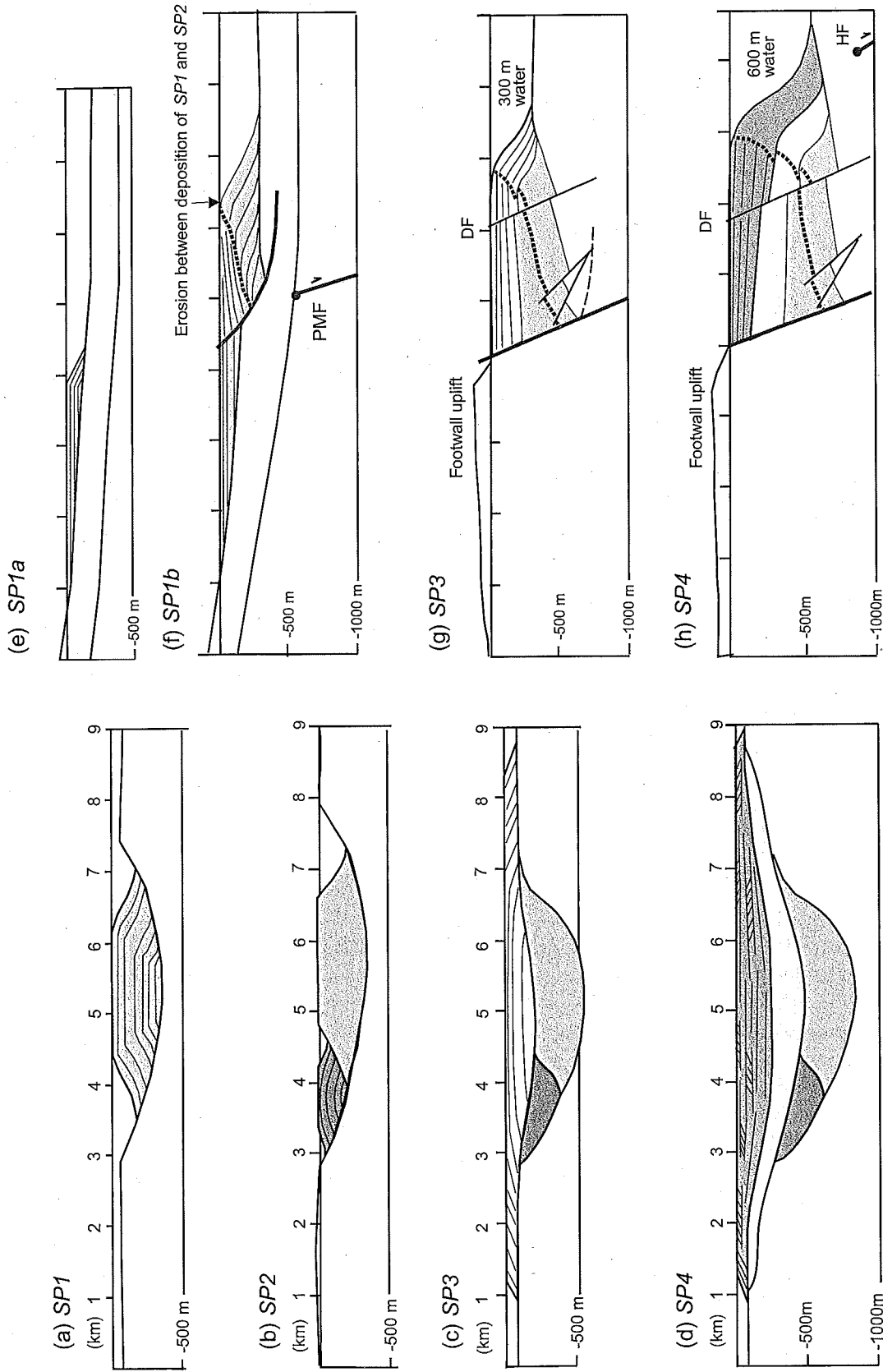


Fig. 21 Proximal longitudinal (a-d) and cross-sections through the centre of the Vouraikos Delta (e-h) representing the four stages in delta evolution corresponding to SP1 to SP4, using a vertical exaggeration of two. SP1 is represented in two cross-sections, while there is no cross-section for SP2 as this small delta is hardly seen on the central cross-section (Fig. 14a). The offlap break is shown as a blue dashed line. The upward propagating Pirgaki-Mamoussia Fault (PMF) is shown in (f), the upward propagating Helike Fault (HF) in (h) and the Dervenli Fault (DF) in (g) and (h).

as shown in the numerical models of Gawthorpe & Hardy (2002) and Ritchie *et al.* (2004a, b). Moreover, the concave erosive base of the Vouraikos Delta requires that the early delta (*SP1*) infilled a pre-existing palaeovalley of some 300 m relief. As this feature requires a major erosional (incision) event before initiation of delta deposition, a relative sea-level fall is inferred before the major relative sea-level rise.

The dramatic change in basin development between the lower and upper groups occurred sometime in the middle of the Early Pleistocene (before 1.1 Ma). The well-established change in Quaternary climate regime occurred between 0.9 and 0.6 Ma (Williams *et al.*, 1988), that is during deposition of the Vouraikos Delta. Therefore, tectonic forces must have been principally responsible for this change in basin regime.

Stage 1 of delta deposition (*SP1*)

The oldest delta package (*SP1*) was deposited in a palaeovalley incised into a gently north-dipping ramp (Figs 20a, 21a, e & f). The *SP1* delta had an estimated radius of less than 2 km. Foresets, up to 200 m high, prograded across the ramp. These foresets are overlain by alluvial topsets at an 'accretionary' toplap contact, suggesting regression and aggradation. Considerable aggradation then took place, until thin coastal facies (Fig. 9) record marine transgression across the top of the delta. Transgressive sediments over 12 m thick were deposited until terminated erosively by a return to alluvial facies *SP1* topsets. The topsets thicken southward to over 200 m across a syn-sedimentary rollover anticline generated above a listric fault that soled into a shallow décollement (Fig. 21f). This fault seems to have cut through an already well-established delta and was perhaps generated by gravitational instability on the basinward dipping ramp. Significant progradation and aggradation occurred implying rapid creation of accommodation space.

Stage 2 of delta deposition (*SP2*)

The top of *SP1* is marked by the erosional unconformity *UC1* implying a relative fall in sea level, which we correlate with the incision into the front of the *SP1* delta (Figs 14a & 17c, d). The following

SP2 package of foresets (no topsets preserved), over 200 m high, unconformably overlies the most southerly topsets of *SP1* in the southwest corner of the delta. In the map reconstruction these foresets represent the frontal part of a small northward-building delta of radius 1 km (Fig. 20c), most of which is now eroded. The delta front therefore stepped southward at the beginning of stage 2 requiring a significant relative rise in sea level. It is suggested that the *SP2* delta infilled the remaining bathymetry of the palaeovalley on the west side of the *SP2* delta (Fig. 20b). It is possible that the same phenomenon occurred in the east of the delta. While the *SP1* topsets are tilted, the *SP2* foresets do not appear to be significantly tilted, implying that the Kastillia Fault and its roll-over anticline were not active during deposition of *SP2*.

Stage 3 of delta deposition (*SP3*)

A significant unconformity separates *SP2* from *SP3*, and pro-delta and bottomset facies associations of *SP3* are seen directly above *SP2* foresets south of the Avriyiolaka Fault (Fig. 18). North of the Avriyiolaka Fault, *SP3* was deposited directly on *SP1* topsets. *SP3* topsets in the centre of the delta (Fig. 14a) pass westward into *SP3* foresets that record progradation (foresets reach heights of over 300 m) toward the NW and WNW during a relative sea-level (RSL) highstand (Figs 18 & 14b). The succeeding *SP3* topsets on the Mamoussia cliff (Fig. 18) indicate aggradation following erosional planation of the foresets probably accompanied by regression. The topsets are dominantly alluvial, although the Mamoussia Limestone may indicate a marine incursion across the (distal) delta top. The delta rapidly grew in E-W width to over 7 km and it significantly overspilled the palaeovalley (Fig. 21c). Its N-S extent, however, remained limited at just under 4 km. The significant increase in accommodation space at the *SP2* to *SP3* boundary may be explained by the emergence of the controlling normal fault. To the east of the Vouraikos Gorge displacement was distributed on two fault strands, principally on the Kastillia Fault to the north and probably on the PM Fault to the south (Fig. 20b). The Kastillia Fault formed the major bounding fault to the eastern half of the delta during Stage 3.

Stage 4 of delta deposition (SP4)

The SP4 sequence is conformable on SP3. It is however markedly different in character, with a finer average grain size, thinner bedding and small-scale Gilbert-type deltas interspersed with alluvial topsets (Fig. 17c & d). The change occurs across a key planar surface traceable over most of the western part of the delta (Figs 14, 16 & 18), which is interpreted as a major transgressive flooding surface across the previously subaerial delta. The small delta packages record regular high-frequency relative sea-level variations right across the delta top, implying that it was regularly flooded, in marked contrast to the earlier alluvial-dominated topsets. These small delta-top foresets built out until they spilled over the delta front into the large frontal foresets. These frontal foresets can be over 600 m high, indicating a very deep basin (Fig. 19). The N–S extent of the SP4 delta is estimated to have been at least 4.5 km (but cut by the Eastern Helike Fault), while its E–W width was over 8 km (Fig. 20d). The topsets are at least 300 m thick in the hangingwall of the Derveni Fault and are 200 m thick in its footwall, implying that this fault was active during deposition of SP4 (Fig. 14a). At the southeast side of the delta, the Kastillia Fault was sealed by 100 m high SP4 deltas that built north and northeast across its footwall from the Katafugion Fault (Figs 3 & 20d). It is possible that secondary point sources were active in the eastern part of the delta during this stage (Figs 20d & 21d, h),

Stage 5 of delta deposition (SP5)

Before the deposition of SP5, the Vouraikos Delta was effectively terminated during an episode when it was tilted north by 5–7° and eroded, due probably to a fault-related mechanism. This is exemplified by the SP4 sequence having a wedge-shape, thinning southward below SP5 (Figs 14a & 16). SP5 is itself tilted gently south, compatible with later extensional fault block uplift and rotation. SP5 comprises a distinctive marine-influenced (shallow-marine), dominantly conglomeratic sequence. This conglomerate is the last deposit of the Vouraikos Delta, and its planar sheet-like form represents the final approximate position of sea level prior to uplift. Following delta uplift (see below)

thick red soils developed above SP5, which now cover the Asomati and other plateaux.

Uplift of the Vouraikos Delta

Sometime in the Middle Pleistocene the Vouraikos Delta began to be exhumed in the footwall of the newly initiated Eastern Helike Fault (EHF). During exhumation the delta was cut and tilted by a number of secondary normal faults. The EHF is still active today and its displacement history continues to be intensively studied (Koukouvelas *et al.*, 2001, 2005; Leeder *et al.*, 2003; De Martini *et al.*, 2004; McNeill & Collier, 2004; Pavlides *et al.*, 2004; McNeill *et al.*, 2005). The range front preserves a series of erosional and depositional marine terraces (see Fig. 19), which have been used to model footwall uplift rates (assuming a constant uplift rate) giving estimates of between 1 and 1.5 mm yr⁻¹ (e.g. De Martini *et al.*, 2004 and references therein; McNeill & Collier, 2004). Assuming that the present-day plateau top (at around 800 m) is close to the original delta top, these rates would imply that uplift of the delta (and thus activity on the EHF) began some time between 530 and 800 ka. The biostratigraphic dates presented in this paper, bracketing the age of the Vouraikos Delta from before 1.1 Ma to sometime after 700 ka, are largely compatible with this exhumation history.

DISCUSSION

The symmetry of the gross building directions of its foresets suggests that the Vouraikos Delta had a fixed-point sediment supply from the footwall throughout its history (Type A feeder system of Postma, 1990, 1995). The approximate location of the input point, coincident with the present-day Vouraikos River, coincides with the intersection of the PM, the Katafugion and Kastillia faults, suggesting some structural control.

Although the Vouraikos was a footwall-derived delta, it has a preserved proximal profile more akin to a hangingwall delta (see e.g. Ritchie *et al.*, 2004a,b), probably due to a ramp-related steepening. This steepening during SP1, above the propagating footwall fault, may have achieved rapid deepening to give the high initial bathymetry modelled as being essential for the development

of deltas of this architectural style (Ulicny *et al.*, 2002).

The curved structure of the foresets, and the development of prominent bottomset and pro-delta facies associations, does not support the view of Zelilidis & Kontopoulos (1996) that the Vouraikos had a simple trapezoidal dip profile, nor that it built into a laterally restricted basin. The most distal facies of the delta do not suggest this, and it is more likely that downthrow on the Eastern Helike Fault disguises a considerable part of the distal delta. Early aggradational foresets are not notably preserved, except for one case. However, frequent transitions to interstratified thick sequences of topsets record significant regressive events and aggradational episodes. Transgressions of the sub-aerial delta also occurred, with limestones indicating that the delta built into a marine basin, and associated shoreline gravels indicating significant basinal wave energy. The marine carbonates indicate that the Corinth rift basin would have been affected by Pleistocene orbitally controlled glacio-eustatic sea-level cycles.

The overall form of the Vouraikos contrasts strongly with that of the flanking Keranitis Delta, in that the latter comprises a major proximal reach composed entirely of topset facies, with relatively limited foreset progradation (e.g. Ori *et al.*, 1991, fig. 9). The Vouraikos and Keranitis are regarded as separate delta systems (cf. Ori *et al.*, 1991) of similar age that are separated by a cross-fault in the Keranitis Valley. Correlation with events recorded in the foresets of the Keranitis Delta is not straightforward; the multiple depositional sequences defined by Dart *et al.* (1994) are not characteristic of the Vouraikos. However, the large relief incision surface above Sequence 2 of Dart *et al.* (1994, fig. 6) is of similar scale to the surface identified here at the base of *SP3* (*UC1*). Possible linkage of major surfaces would suggest basin-wide changes in RSL. Sedimentation rates derived for the Keranitis Delta (1.5 mm yr^{-1}) by Dart *et al.* (1994) are similar to our estimates based on consideration of the dating and sediment thickness. Finally, an interesting contrast between the deltas occurs in the degree to which syn- and post-depositional extensional faulting affected their development. The proximal rollover anticline affecting the Vouraikos, and the suite of planar and listric syn-sedimentary faults observed, have no apparent counterparts in

the Keranitis. The Keranitis also lacks the post-delta planar normal faults that disrupt the Vouraikos at a number of scales. This is probably because the Vouraikos Delta lies in the immediate footwall of the Eastern Helike Fault while the Keranitis lies farther south.

Based on the biostratigraphic dating, it is estimated that the delta was deposited within a period of ca. 0.4 to 0.6 Myr between $> 1.1 \text{ Ma}$ and $0.6\text{--}0.7 \text{ Ma}$. This age estimate implies that the whole Vouraikos Delta represents a third-order highstand systems tract (*sensu* Vail *et al.*, 1991). The five stratigraphic packages *SP1* to *SP5* therefore represent mainly fourth-order highstand system tracts. Each sedimentary cycle essentially comprises the regressive phase (progradation), with the vertical succession from pro-delta fines to bottomsets to foresets and finally to topsets (i.e. 'normal' regression *sensu* Posamentier *et al.*, 1992).

The development of each stratigraphic package is related to an interglacial period, which is consistent with the interglacial character of the palynological assemblages. If preserved, the lowstand deltas related to glacial periods may be situated to the north, below the present gulf. Each stratigraphic package comprises stacked fifth-order transgressive-regressive cycles, which are rarely detected in *SP1* to *SP3*. However, in *SP4* these fifth-order cycles are clearly recorded by the stacked small Gilbert deltas on the delta top.

Within the time period 1.1 to 0.6 Ma the oxygen isotope ^{18}O stages are MIS31 to MIS16. Potentially four or five major negative excursions may be recognized that could be correlated with the four stratigraphic packages *SP1* to *SP4*. This suggests that the stratigraphic packages were primarily controlled by eustasy superimposed on a high subsidence rate, in turn controlled by the PM Fault.

The bulk of this compact delta is made up of *SP1*, *SP3* and *SP4*. While *SP1* records significant progradation ($> 2 \text{ km}$) coupled with strong aggradation (200 m) across the early ramp (Fig. 21e & f), *SP3* and *SP4* each record limited frontal progradation ($< 1 \text{ km}$) of thick foresets coupled with strong aggradation (200–300 m) of topsets. This implies that rates of both sediment supply (*S*) and creation of accommodation space (*A*) were very high during deposition of *SP3* and *SP4* and that the ratio of *S/A* was about 1. The cyclic flooding of the delta top during *SP4* implies that *S/A* had

decreased either because sediment supply was waning or because creation of accommodation space was increasing.

CONCLUSIONS

1 The syn-rift stratigraphy in the Kalavrita to Aegion region of the southern Corinth rift shows a two-phase rifting history. The coarse alluvial succession of the lower group (up to 1.3 km thick) was deposited in a series of 4–5 km wide tilted blocks. This early rift phase ended with a marine transgression, preserved in the north. An erosional unconformity marks the base of the upper group, which records a great increase in accommodation space, the migration of the depocentre to the north and an increase in sediment supply. The upper group is characterized by Gilbert-type fan deltas.

2 The Vouraikos Delta is one of several giant fault-controlled Gilbert-type fan deltas that built into the Corinth rift during the Early to Middle Pleistocene, in response to a major change in basin dynamics. It is argued that this change in basin dynamics in the Early Pleistocene was not related to climate change but was probably due to a change in large-scale regional tectonics (Fig. 1, inset).

3 A limited number of palynological dates indicate that the Vouraikos Delta was initiated sometime in the middle of the Early Pleistocene and terminated in the Middle Pleistocene, sometime after 0.7 Ma. These preliminary age estimates are consistent with published models of the uplift history on the Eastern Helike Fault. Sedimentation rates are thus estimated to have been between 1.3 and 2 mm yr⁻¹.

4 The early Vouraikos Delta (SP1) was constructed on a basin-dipping ramp generated by an extensional forced-fold. Internally, it was affected by a listric normal fault and its rollover anticline. Later, the Vouraikos Delta was primarily controlled by displacement on the emergent Pargaki-Mamoussia Fault and its splays to the east (the Kastillia and Katafugion faults). Smaller planar and curved normal faults affected the delta throughout its history, and also during exhumation of the delta in the footwall of the Eastern Helike Fault.

5 The internal architecture of the conglomeratic delta records both tectonic and eustatic controls. Five stratigraphic packages (SP1–SP5) are separated by major surfaces. SP1, SP3 and SP4, which make up the bulk of the delta, are each characterized by thick topsets and thick foresets, and limited bottomset

and pro-delta facies. The stratigraphic packages are tentatively correlated with regressive glacio-eustatic interglacial periods. This model requires that the glacio-eustatic signal was superimposed on a relatively constant creation of accommodation space by normal faulting (by the Pargaki-Mamoussia Fault system). While this eustatic interpretation seems quite plausible, it is not possible to eliminate the possibility that the stratigraphic packages and their bounding surfaces may have been generated wholly or partly by pulses of high and low slip-rate on the Pargaki-Mamoussia Fault.

6 Topset limestones associated with coastal conglomerate facies indicate that the Vouraikos Gilbert-type Delta built mainly into a marine water body. Gravel-rich sediment prograded (to the north-northwest) into water that reached depths of 200–600 m.

7 The N–S radius of the 800 m thick fan delta increased only slowly (2–3.5 to 4.5 km) through time. The trajectory of the offlap break in a section through the centre of the Vouraikos Delta reflects early progradation-dominated behaviour (SP1), followed by increasingly aggradational behaviour during SP3 and SP4 deposition.

ACKNOWLEDGEMENTS

Thanks are due to F. Palhol (CRPG, Nancy) who kindly carried out stable isotope analyses. S.-M. Popescu carried out the palynological analyses. Thanks to D. Ulicny, J. ten Veen and G.J. Nichols for valuable comments on the first version of this paper. Fieldwork and dating for this project were funded by the 'Groupement de Recherche Corinthe' and by the project 'Dynamique de la Terre Interne' (DyTI) of the INSU (CNRS). MF and FM thank the following colleagues for fruitful and stimulating discussions: Nicolas Backert, Sylvain Bourlange, Rémi Eschard, Francois Guillocheau, David Jousselin, Christian Le Carlier de Veslud, Isabelle Moretti, Sébastien Rohais, and finally the students of the Nancy School of Geology (ENSG). CRPG Publication Number 1824.

REFERENCES

- Anthony, E.J., Lang, J. and Oyédé, L.M. (1996) Sedimentation in a tropical, microtidal, wave-dominated coastal-plain estuary. *Sedimentology*, **43**, 665–675.

- Bourlange, S., Joussetin, D., Ford, M. and Le Carlier, C. (2005) Evolution of a normal fault system on the southern flank of the Corinth Rift. *European Geophysical Union Congress, Vienna. Geophys. Res. Abstr.*, **7**, 07450, Sref-ID 107-7962/gra/EGU 05-A-07450.
- Bridge, J.S. (1993) Description and interpretation of fluvial deposits: a critical perspective. *Sedimentology*, **40**, 801–810.
- Bridge, J.S. (2003) *Rivers and Floodplains: Forms, Processes, and Sedimentary Record*. Blackwell Publishing, Oxford, 491 pp.
- Briole, P., Rigo, A., Lyon-Caen, H., et al. (2000) Active deformation of the Corinth rift, Greece: Results from repeated Global Positioning System surveys between 1990 and 1995. *J. Geophys. Res.*, **105**, 25,605–25,625.
- Colella, A. (1988) Pliocene–Holocene fan deltas and braid deltas in the Crati Basin, southern Italy: a consequence of varying tectonic conditions. In: *Fan Deltas: Sedimentology and Tectonic Settings* (Eds W. Nemeč and R.J. Steel), pp. 51–74. Blackie and Son, Glasgow.
- Collier, R.E.L.L. (1990) Eustatic and tectonic controls upon Quaternary coastal sedimentation in the Corinth Basin, Greece. *J. Geol. Soc. London*, **147**, 301–314.
- Collier, R.E.L.L. and Dart C.J. (1991) Neogene to Quaternary rifting, sedimentation and uplift in the Corinth Basin, Greece. *J. Geol. Soc. London*, **148**, 1049–1065.
- Collier, R.E.L.L., Leeder, M.R., Rowe, P.J. and Atkinson, T.C. (1992) Rates of tectonic uplift in the Corinth and Megara Basins, central Greece. *Tectonics*, **11**, 1159–1167.
- Combourieu-Nebout, N. and Vergnaud Grazzini, C. (1991) Late Pliocene northern hemisphere glaciations: the continental and marine responses in the central Mediterranean. *Quat. Sci. Rev.*, **10**, 319–334.
- Cornée, J.-J., Moissette, P., Joannin, S., et al. (2006) Tectonic and climatic controls on coastal sedimentation: the Late Pliocene–Middle Pleistocene of north-eastern Rhodes, Greece. *Sed. Geol.*, **187**, 159–181.
- Dabrio, C.J. (1990) Fan-delta facies associations in late Neogene and Quaternary basins of southeastern Spain. In: *Coarse-Grained Deltas* (Eds A. Colella and D.B. Prior), pp. 91–111. Special Publication 10, International Association of Sedimentologists. Blackwell Scientific Publications, Oxford.
- Dabrio, C.J. and Polo, M.D. (1988) Late Neogene fan deltas and associated coral reefs in the Almanzora Basin, Almería Province, southeastern Spain. In: *Fan Deltas: Sedimentology and Tectonic Settings* (Eds W. Nemeč and R.J. Steel), pp. 354–367. Blackie and Son, Glasgow.
- Dart, C.J., Collier, R.E.L.L., Gawthorpe, R.L., Keller, J.V.A. and Nichols, G. (1994) Sequence stratigraphy of (?)Pliocene–Quaternary synrift, Gilbert-type fan deltas, northern Peloponnesos, Greece. *Mar. Petrol. Geol.*, **11**, 545–560.
- De Martini, P.M., Pantosti, D., Palyvos, N., Lemeille, F., McNeill, L.C. and Collier, R. (2004) Slip rates of the Aigion and Eliki Faults from uplifted terraces, Corinth Gulf, Greece. *C. R. Acad. Sci. Paris*, **336**, 325–334.
- Dia, A.N., Cohen, A.S., O’Nions R.K. and Jackson J.A. (1997) Rates of uplift investigated through ^{230}Th dating in the Gulf of Corinth (Greece). *Chem. Geol.*, **138**, 171–184.
- Doutsos, T. and Piper, D.J.W. (1990) Listric faulting, sedimentation, and morphological evolution of the Quaternary eastern Corinth rift, Greece: First stages of continental rifting. *Geol. Soc. Am. Bull.*, **102**, 812–829.
- Doutsos, T., Kontopoulos, N., Poulimenos, G., Frydas, D. and Piper, D.J.W. (1990) Comment and Reply on ‘Geologic history of the extensional basin of the Gulf of Corinth (?Miocene–Pleistocene), Greece’. *Geology*, **18**, 1256–1257.
- Doutsos, T., Piper, G., Boronkay, K. and Koukouvelas, I.K. (1993) Kinematics of the central Hellenides. *Tectonics*, **12**, 936–953.
- Dubois, J.-M. (2001) *Cycles Climatiques et Paramètres Orbitaux vers 1 Ma. Etude de la Coupe de Monte San Giorgio (Caltagirone, Sicile): Palynologie, Isotopes Stables, Calcimétrie*. DEA Paléontologie et Environnements Sédimentaires, Univ. C. Bernard – Lyon 1, 54 pp.
- Ethridge, F.G. and Wescott, W.A. (1984) Tectonic setting, recognition and hydrocarbon reservoir potential of fan-delta deposits. In: *Sedimentology of Gravels and Conglomerates* (Eds E.H. Koster and R.J. Steel), pp. 217–235. Memoir 10, Canadian Society of Petroleum Geologists, Calgary.
- Falk, P.D. and Dorsey, R.J. (1998) Rapid development of gravely high-density turbidity currents in marine Gilbert-type fan deltas, Loreto Basin, Baja California Sur, Mexico. *Sedimentology*, **45**, 331–349.
- Fernandez-Gonzalez, M., Frydas, D., Guernet, C. and Mathieu, R. (1994) Foraminifères et ostracodes du Plio pléistocènes de la région de Patras (Grèce). Intérêt stratigraphique et paléogéographique. *Rev. Esp. Micropaleont.*, **26**, 89–108.
- Flügel, E. (1982) *Microfacies Analysis of Limestones*. Springer-Verlag, Berlin, 633 pp.
- Fouache, E., Dalongeville, R., Kunesch, S., et al. (2005) The environmental setting of the harbor of the classical site of Oeniades on the Acheloos Delta, Greece. *Geoarchaeol. Int. J.*, **20**, 285–302.
- Frydas, D. (1987) Kalkiges Nannoplankton aus dem Neogen von NW-Peloponnes. *Neues Jb. Geol. Paläont., Monat.*, **5**, 274–286.
- Frydas, D. (1989) Biostratigraphic investigations from the Neogene of the NW and W Peloponnes, Greece.

- (in German). *Neues Jb. Geol. Paläont. Monat.*, **6**, 321–344.
- Frydas, D. (1991) Paläoökologische und stratigraphische untersuchungen der diatomeen des Pleistozäns der N-Peloponnes, Griechenland. *Bull. Geol. Soc. Greece*, **25**, 499–513.
- Gawthorpe, R.L. and Colella, A. (1990) Tectonic controls on coarse-grained delta depositional systems in rift basins. In: *Coarse-Grained Deltas* (Eds A. Colella and D.B. Prior), pp. 113–127. Special Publication 10, International Association of Sedimentologists. Blackwell Scientific Publications, Oxford.
- Gawthorpe, R.L. and Hardy, S. (2002) Extensional fault-propagation folding and base-level change as controls on growth-strata geometries. *Sediment. Geol.*, **146**, 47–56.
- Ghisetti, F. and Vezzani, L. (2004) Plio-Pleistocene sedimentation and fault segmentation in the Gulf of Corinth (Greece) controlled by inherited structural fabric. *C. R. Acad. Sci. Paris*, **336**, 243–249.
- Ghisetti, F. and Vezzani, L. (2005) Inherited structural controls on normal fault architecture in the Gulf of Corinth (Greece). *Tectonics*, **24**, TC4016, doi:10.1029/2004TC001696, 2005.
- Goldsworthy, M. and Jackson, J. (2001) Migration of activity within normal fault systems: examples from the Quaternary of mainland Greece. *J. Struct. Geol.*, **23**, 489–506.
- Gradstein, F.M., Ogg, J.G. and Smith, A.G. (2004) *A Geological Time Scale 2004*. Cambridge University Press, 589 pp.
- Hart, B.S. and Plint, A.G. (1995) Gravelly shoreface and beachface deposits. In: *Clastic Facies Analysis – a Tribute to the Research and Teaching of Harold G. Reading* (Ed. A.G. Plint), pp. 75–99. Special Publication 22, International Association of Sedimentologists. Blackwell Scientific Publications, Oxford.
- Hein, F.J. and Walker, R.G. (1977) Bar evolution and development of stratification in the gravelly, braided, Kicking Horse River, British Columbia. *Can. J. Earth Sci.*, **14**, 562–570.
- Hwang, I.G. and Chough, S.K. (2000) The Maesan fan delta, Miocene Pohang Basin, SE Korea: architecture and depositional processes of a high-gradient fan-delta-fed slope system. *Sedimentology*, **47**, 995–1010.
- Jahns, S. (1993) On the Holocene history of the Argive Plain (Peloponnese, Southern Greece). *Veg. Hist. Archaeobot.*, **2**, 187–203.
- Joannin, S. (2003) *Forçage Climatique des Séquences Emboîtées du Pléistocène Inférieur et Moyen de Tsam-pika (Ile de Rhodes, Grèce)*. DEA Paléontologie et Environnements Sédimentaires, Univ. C. Bernard – Lyon 1, 52 pp.
- Keraudren, B. and Sorel, D. (1987) The terraces of Corinth (Greece). A detailed record of eustatic sea-level variations during the last 500 000 years. *Mar. Geol.*, **77**, 99–107.
- Kershaw, S. and Guo, L. (2003) Pleistocene cyanobacterial mounds in the Perachora Peninsula, Gulf of Corinth, Greece: structure and applications to interpreting sea-level history and terrace sequences in an unstable tectonic setting. *Palaeogeogr. Palaeoclimatol. Palaeoecol.*, **193**, 503–514.
- Kershaw, S., Guo, L. and Braga, J.C. (2005) A Holocene coral-algal reef at Mavra Litharia, Gulf of Corinth, Greece: structure, history, and applications in relative sea-level change. *Mar. Geol.*, **215**, 171–192.
- Kontopoulos, N. and Doutsos, T. (1985) Sedimentology and tectonics of the Antirion area (western Greece). *Bull. Geol. Soc. Ital.*, **104**, 479–489.
- Koukouvelas, I.K., Stamatopoulos, L., Katsonopoulou, D. and Pavlides, S.A. (2001) Palaeoseismological and geoarchaeological investigation of the Eliki Fault, Gulf of Corinth, Greece. *J. Struct. Geol.*, **23**, 531–543.
- Koukouvelas, I.K., Katsonopoulou, D., Soter, S. and Xypolias, P. (2005) Slip rates on the Helike Fault, Gulf of Corinth, Greece: new evidence from geoarchaeology. *Terra Nova*, **17**, 158–164.
- Leeder, M.R., McNeill, L.C., Collier, R.E.L., et al. (2003) Corinth rift margin uplift: New evidence from Late Quaternary marine shorelines. *Geophys. Res. Lett.*, **30**, 13-1–13-4.
- Malartre, F., Ford, M. and Williams, E.A. (2004) Preliminary biostratigraphy and 3D geometry of the Vouraikos Gilbert-type fan delta, Gulf of Corinth. *C. R. Acad. Sci. Paris*, **336**, 269–280.
- Massari, F. and Parea, G.C. (1990) Wave-dominated Gilbert-type gravel deltas in the hinterland of the Gulf of Taranto (Pleistocene, southern Italy). In: *Coarse-Grained Deltas* (Eds A. Colella and D.B. Prior), pp. 311–331. Special Publication 10, International Association of Sedimentologists. Blackwell Scientific Publications, Oxford.
- McNeill, L.C. and Collier, R.E.L. (2004) Uplift and slip rates of the eastern Eliki fault segment, Gulf of Corinth, Greece, inferred from Holocene and Pleistocene terraces. *J. Geol. Soc. London*, **161**, 81–92.
- McNeill, L.C., Cotterill, C.J., Henstock, T.J., et al. (2005) Active faulting within the offshore western gulf of Corinth, Greece: implications for models of continental rift deformation. *Geology*, **33**, 241–244.
- Mortimer, E., Gupta, S. and Cowie, P. (2005) Cliniform nucleation and growth in coarse-grained deltas, Loreto Basin, Baja California Sur, Mexico: a response to episodic accelerations in fault displacement. *Basin Res.*, **17**, 337–359.

- Nemec, W. (1990) Aspects of sediment movement on steep delta slopes. In: *Coarse-Grained Deltas* (Eds A. Colella and D.B. Prior), pp. 29–73. Special Publication 10, International Association of Sedimentologists. Blackwell Scientific Publications, Oxford.
- Nemec, W. and Postma, G. (1993) Quaternary alluvial fans in southwestern Crete: sedimentation processes and geomorphic evolution. In: *Alluvial Sedimentation* (Eds M. Marzo and C. Puigdefábregas), pp. 235–276. Special Publication 17, International Association of Sedimentologists. Blackwell Scientific Publications, Oxford.
- Nemec, W. and Steel, R.J. (1984) Alluvial and coastal conglomerates: their significant features and some comments on gravelly mass-flow deposits. In: *Sedimentology of Gravels and Conglomerates* (Eds E.H. Koster and R.J. Steel), pp. 1–31. Memoir 10, Canadian Society of Petroleum Geologists, Calgary.
- Okuda, M., van Vugt, N., Nakagawa, T., Ikeya, M., Hayashida, A. and Setoguchi, A. (2002) Palynological evidence for the astronomical origin of lignite-detritus sequence in the Middle Pleistocene Marathousa Member, Megalopolis, SW Greece. *Earth Planet. Sci. Lett.*, **201**, 143–157.
- Ori, G.G. (1989) Geologic history of the extensional basin of the Gulf of Corinth (?Miocene–Pleistocene), Greece. *Geology*, **17**, 918–921.
- Ori, G.G., Roveri, M. and Nichols, G. (1991) Architectural patterns in large-scale Gilbert-type delta complexes, Pleistocene, Gulf of Corinth, Greece. In: *The Three-dimensional Facies Architecture of Terrigenous Clastic Sediments and its Implications for Hydrocarbon Discovery and Recovery* (Eds A.D. Miall and N. Tyler), pp. 207–216. Concepts in Sedimentology and Paleontology, Vol. 3, Society of Economic Paleontologists and Mineralogists, Tulsa, OK.
- Papanicolaou, C., Dehmer, J. and Fowler, M. (2000) Petrological and organic geochemical characteristics of coal samples from Florina, Lava, Moscopotamos and Kalavryta coal fields. *Int. J. Coal Geol.*, **44**, 267–292.
- Pavlidis, S.B., Koukouvelas, I.K., Kokkalas, S., Stamatopoulos, L., Keramydas, D. and Tsodoulos, I. (2004) Late Holocene evolution of the East Eliki fault, Gulf of Corinth (Central Greece). *Quat. Int.*, **115–116**, 139–154.
- Perissoratis, C., Piper, D.J.W. and Lykousis, V. (2000) Alternating marine and lacustrine sedimentation during late Quaternary in the Gulf of Corinth Rift basin, central Greece. *Mar. Geol.*, **167**, 391–411.
- Portman C., Andrews J.E., Rowe P.J., Leeder M.R. and Hoogewerff J. (2005) Submarine-spring controlled calcification and growth of large *Rivularia* bioherms, Late Pleistocene (MIS 5e), Gulf of Corinth, Greece. *Sedimentology*, **52**, 441–465.
- Posamentier, H.W., Allen, G.P., James, D.P. and Tesson, M. (1992) Forced regressions in a sequence stratigraphic framework: concepts, examples and exploration significance. *Am. Assoc. Petrol. Geol. Bull.*, **76**, 1687–1709.
- Postma, G. (1990) Depositional architecture and facies of river and fan deltas: a synthesis. In: *Coarse-Grained Deltas* (Eds A. Colella and D.B. Prior), pp. 13–27. Special Publication 10, International Association of Sedimentologists. Blackwell Scientific Publications, Oxford.
- Postma, G. (1995) Sea-level-related architectural trends in coarse-grained delta complexes. *Sediment. Geol.*, **98**, 3–12.
- Postma, G., Babić, L., Zupanič, J. and Røe, S.-L. (1988) Delta-front failure and associated bottomset deformation in a marine, gravelly Gilbert-type fan delta. In: *Fan Deltas: Sedimentology and Tectonic Settings* (Eds W. Nemec and R.J. Steel), pp. 91–102. Blackie and Son, Glasgow.
- Poulimenos, G., Zeliidis, A., Kontopoulos, N. and Doutsos, T. (1993) Geometry of trapezoidal fan deltas and their relationship to the extensional faulting along the south-western active margins of the Corinth rift, Greece. *Basin Res.*, **5**, 179–192.
- Prior, D.B. and Bornhold, B.D. (1990) The underwater development of Holocene fan deltas. In: *Coarse-Grained Deltas* (Eds A. Colella and D.B. Prior), pp. 75–90. Special Publication 10, International Association of Sedimentologists. Blackwell Scientific Publications, Oxford.
- Reinson, G.E. (1984) Barrier island and associated strand-plain systems. In: *Facies Models* (Ed. R.G. Walker), pp. 119–140. Geological Association of Canada, St John's, Newfoundland.
- Ritchie, B.D., Gawthorpe, R.L. and Hardy, S. (2004a) Three dimensional modeling of deltaic depositional sequences 1: influence of the rate and magnitude of sea level change. *J. Sed. Res.*, **74**, 202–220.
- Ritchie, B.D., Gawthorpe, R.L. and Hardy, S. (2004b) Three dimensional modeling of deltaic depositional sequences 2: influence of local controls. *J. Sed. Res.*, **74**, 221–238.
- Rohais, S., Eschard, R., Ford, M., Guilloucheau, F. and Moretti, I. (In press) Stratigraphic architecture of the Plio-Pleistocene infill of the Corinth rift: implications for its structural evolution. *Tectonophysics*.
- Subally, D., Bilodeau, G., Tamrat, E., Ferry, S., Debard, E. and Hillaire-Marcel, C. (1999) Cyclic climatic records during the Olduvai Subchron (Uppermost Pliocene) on Zakynthos Island (Ionian Sea). *Geobios*, **32(6)**, 793–803.
- Symeonidis, N., Theodorou, G., Schutt, H. and Velitzelos, E. (1987) Paleontological and stratigraphic

- observations in the area of Achaia and Etoloakarnania (Western Greece). *Ann. Géol. Pays Hellén.*, **38**, 317–353.
- Tucker, M.E. and Wright, V.P. (1990) *Carbonate Sedimentology*. Blackwell Scientific Publications, Oxford, 482 pp.
- Ulicny, D., Nichols, G. and Waltham, D. (2002) Role of initial depth at basin margins in sequence architecture: field examples and computer models. *Basin Res.*, **14**, 347–360.
- Urban, B. and Fuchs, M. (2005) Late Pleistocene vegetation of the basin of Phlious, NE-Peloponnese, Greece. *Rev. Palaeobot. Palynol.*, **137**, 15–29.
- Vail, P.R., Audemard, F., Bowman, S.A., Eisner, P.N. and Perez-Cruz, C. (1991) The stratigraphic signatures of tectonics, eustasy and sedimentology – an overview. In: *Cycles and Events in Stratigraphy* (Eds G. Einsele, W. Ricken and A. Seilacher), pp. 617–659. Springer Verlag, Berlin.
- Verrall, P. (1981) *Structural Interpretation with Applications to North Sea Problems*. Course Notes No. 3, Joint Association for Petroleum Exploration Courses, London.
- Williams, D.F., Thunell, R.C., Tappa, E., Rio, D. and Raffi, I. (1988) Chronology of the Pleistocene oxygen isotope record: 0–1.88 m.y. B.P. *Palaeogeogr. Palaeoclimat. Palaeoecol.*, **64**, 221–240.
- Wilson, J.L. (1975) *Carbonate Facies in Geologic History*. Springer-Verlag, Berlin, 47 pp.
- Young, M.J., Gawthorpe, R.L. and Sharp, I.R. (2000) Sedimentology and sequence stratigraphy of a transfer zone coarse-grained delta, Miocene Suez Rift, Egypt. *Sedimentology*, **47**, 1081–1104.
- Young, M.J., Gawthorpe, R.L. and Sharp, I.R. (2002) Architecture and evolution of syn-rift clastic depositional systems towards the tip of a major fault segment, Suez Rift, Egypt. *Basin Res.*, **14**, 1–23.
- Zelilidis, A. and Kontopoulos, N. (1996) Significance of fan deltas without toe-sets within rift and piggy-back basins: examples from the Corinth graben and the Mesohellenic trough, Central Greece. *Sedimentology*, **43**, 253–262.

REFERENCES

- Agnihotri, R., K. Dutta, et al. (2002). "Evidence for solar forcing on the Indian monsoon during the last millennium." *Earth and Planetary Science Letters* 198(3-4): 521-527.
- Agusti, J., O. Oms, et al. (2006). "Introduction to the Late Miocene to Early Pliocene environment and climate change in the Mediterranean area." *Palaeogeography, Palaeoclimatology, Palaeoecology* 238(1): 1-4.
- Allen, M. B. and H. A. Armstrong (2008). "Arabia-Eurasia collision and the forcing of mid-Cenozoic global cooling." *Palaeogeography, Palaeoclimatology, Palaeoecology* 265(1): 52-58.
- Alley, R. B., J. Marotzke, et al. (2003). "Abrupt Climate Change." *Science* 299(5615): 2005-2010.
- Aksu, A. E., T. Abrajano, et al. (1999). "Organic geochemical and palynological evidence for terrigenous origin of the organic matter in Aegean Sea sapropel S1." *Marine Geology* 153: 303-318.
- Aksu, A. E., C. Yaltirak, et al. (2002). "Quaternary paleoclimatic-paleoceanographic and tectonic evolution of the Marmara Sea and environs." *Marine Geology* 190(1-2): 9-18.
- Andersen, M. B., C. H. Stirling, et al. (2008). "High-precision U-series measurements of more than 500,000 year old fossil corals." *Earth and Planetary Science Letters* 265(1-2): 229-245.
- An, Z., J.E. Kutzbach, et al. (2001) Evolution of Asian monsoons and phased uplift of the Himalaya-Tibet plateau since late Miocene times, *Nature* 411: 62-66.
- Anderson, R. Y. (1992). "Possible connection between surface winds, solar activity and the earth's magnetic field." *Nature* 358: 51-53.
- Asmerom, Y., V. Polyak, et al. (2007). "Solar forcing of Holocene climate: New insights from a speleothem record, southwestern United States." *Geology* 35(1): 1-4.
- Auclair, A. N. D. (1992). "Forest wildfire, atmospheric CO₂ and solar irradiance periodicity." *Eos Trans. Amer. Geophys. Union Suppl.*: 70.
- Bache, F., S-M. Popescu, et al. "Process of the reflooding of the Mediterranean Basin after the Messinian Salinity Crisis". *Basin Research* in progress.
- Bachiri Taoufiq, N. (2000). Les environnements marins et continentaux du corridor rifain au Miocène supérieur d'après la palynologie. Casablanca, Univ. Casablanca. PhD: 206.
- Ballantyne, A. P., N. Rybczynski, et al. (2006). "Pliocene Arctic temperature constraints from the growth rings and isotopic composition of fossil larch." *Palaeogeography, Palaeoclimatology, Palaeoecology* 242(3): 188-200.
- Bard, E., B. Hamelin, et al. (1990). "U-Th ages obtained by mass spectrometry in corals from Barbados: sea level during the past 130,000 years." *Nature* 346(6283): 456-458.
- Bard, E., G. M. Raisbeck, et al. (1997). "Solar modulation of cosmogenic nuclide production over the last millennium: comparison between ¹⁴C and ¹⁰Be records." *Earth and Planetary Science Letters* 150(3-4): 453-462.
- Barreiro, M., G. Philander, et al. (2006). "Simulations of warm tropical conditions with application to middle Pliocene atmospheres." *Climate Dynamics* 26(4): 349-365.
- Barrón, E. and C. Sansisteban (1999). "Estudio palinológico de la cuenca miocena de Rubielos de Mora (Teruel, España). Aspectos paleoecológicos y paleobiogeográficos." *Boletín Real Sociedad Española Historia Natural. (Sección Geología)* 95(67-82).
- Bartoli, G. (2005). "Final closure of Panama and the onset of northern hemisphere glaciation." *Earth Planet. Sci. Lett.* 237: 33-44.

- Baxter, M. S. and J. G. Farmer (1973). "Radiocarbon: Short-term variations." *Earth and Planetary Science Letters* 20(3): 295-299.
- Beer, J., A. Blinov, et al. (1990). "Use of ^{10}Be in polar ice to trace the 11-year cycle of solar activity." *Nature* 347(6289): 164-166.
- Beer, J., U. Siegenthaler, et al. (1988). "Information on past solar activity and geomagnetism from ^{10}Be in the Camp Century ice core." *Nature* 331(6158): 675-679
- Beer, J., M. Vonmoos, et al. (2006). "Solar Variability Over the Past Several Millennia." *Space Science Reviews* 125(1): 67-79.
- Berger, A. and M. F. Loutre (1991). "Insolation values for the climate of the last 10 million years." *Quat. Sci. Rev.* 10: 297-317.
- Berger, A. and M. F. Loutre (2004). "Théorie astronomique des paléoclimats." *Comptes Rendus Geosciences* 336(7-8): 701-709.
- Berger, A. L. (1978). "Long-term variations of daily insolation and Quaternary climatic change." *J. Atmos. Sci.* 35: 2362-2367.
- Berger, A. L., M. F. Loutre, et al. (2006b). "Equatorial insolation: from precession harmonics to excentricity frequencies." *Climate Past* 2: 131-136.
- Bertini, A., L. Londeix, et al. (1998). "Paleobiological evidence of depositional conditions in the Salt Member, Gessoso-Solfifera Formation (Messinian, Upper Miocene) of Sicily,." *Micropaleontology* 44(4): 413-433.
- Bertini A. (1992.). *Palinologia ed aspetti ambientali del versante adriatico dell'Appennino centro-settentrionale durante il Messiniano e lo Zancleano*. Firenze, Firenze University. PhD Thesis: 88
- Bessais E. and J. Cravatte, (1988). "Les écosystèmes végétaux pliocènes de Catalogne méridionale. Variations latitudinales dans le domaine nord-ouest méditerranéen ". *Geobios*, 21 : 49-63.
- Bessedik, M., 1985. Reconstitution des environnements miocènes des régions nord-ouest méditerranéennes à partir de la palynologie. Thesis, Univ. Montpellier 2, 162 pp.
- Bhattacharyya, S. and R. Narasimha (2007). "Regional differentiation in multidecadal connections between Indian monsoon rainfall and solar activity." *Journal of Geophysical Research* 112(D24).
- Billups, K. (2002a). "Late Miocene through early Pliocene deep water circulation and climate change viewed from the sub-Antarctic South Atlantic." *Palaeogeography, Palaeoclimatology, Palaeoecology* 185(3-4): 287-307.
- Billups, K., H. Pälike, et al. (2004). "Astronomic calibration of the late Oligocene through early Miocene geomagnetic polarity time scale." *Earth and Planetary Science Letters* 224(1-2): 33-44
- Billups, K., A. C. Ravelo, et al. (1998a). "Early Pliocene Climate: A Perspective from the Western Equatorial Atlantic Warm Pool." *Paleoceanography* 13(5): 459-470.
- Billups, K., A. C. Ravelo, et al. (1998b). "Early Pliocene Deep Water Circulation in the Western Equatorial Atlantic: Implications for High-Latitude Climate Change." *Paleoceanography* 13(1): 84-95.
- Billups, K. and D. P. Schrag (2002b). "Palaeotemperatures and ice volume of the past 27 Myr revisited with paired Mg/Ca and $^{18}\text{O}/^{16}\text{O}$ measurements on benthic foraminifera." *Paleoceanography* 17: 1-11.
- Blanc, P.-L. (2002). "The opening of the Plio-Quaternary Gibraltar Strait : assessing the size of a cataclysm." *Geodinamica Acta* 15: 303-317.
- Bond, G., B. Kromer, et al. (2001). "Persistent Solar Influence on North Atlantic Climate During the Holocene." *Science* 294(5549): 2130-2136.
- Bond GC, Lotti R (1997) "Iceberg discharges into the North Atlantic on millennial time scales during the last glaciation". *Science* 267:1005-1010

- Bonnefille, R., R. Potts, et al. (2004). "High-resolution vegetation and climate change associated with Pliocene *Australopithecus afarensis*." *Proceedings of the National Academy of Sciences of the United States of America* 101(33): 12125-12129.
- Bohn U., G. Gollub, et al. (2004) "Map of the Natural Vegetation of Europe at scale 1:2500000". Federal Agency for Nature Conservation, Bonn CD-ROM.
- Braun, H., M. Christl, et al. (2005). "Possible solar origin of the 1,470-year glacial climate cycle demonstrated in a coupled model." *Nature* 438(70695): 208-211.
- Brénac, P., 1984. Végétation et climat de la Campanie du Sud (Italie) au Pliocène final d'après l'analyse pollinique des dépôts de Camerota. *Ecologia Mediterranea*, 10, 3-4, 207-216.
- Brown, P., T. Sutikna, et al. (2004). "A new small-bodied hominin from the Late Pleistocene of Flores, Indonesia." *Nature* 431(7012): 1055-1061.
- Bruch, A. A., D. Uhl, et al. (2007). "Miocene climate in Europe -- Patterns and evolution: A first synthesis of NECLIME." *Palaeogeography, Palaeoclimatology, Palaeoecology* 253(1-2): 1-7.
- Burckle, L. H., R. Mortlock, et al. (1996). "No evidence for extreme, long term warming in early Pliocene sediments of the Southern Ocean." *Marine Micropaleontology* 27(1): 215-226.
- Caner, H. and O. Algan (2002). "Palynology of sapropelic layers from the Marmara Sea." *Marine Geology* 190: 35-46.
- Cagatay, M. N. and al (2000). "Late Glacial–Holocene palaeoceanography of the Sea of Marmara: timing of connections with the Mediterranean and the Black Seas." *Marine Geology* 167: 191–206.
- Cagatay, M. N., N. Gorur, et al. (2006). "Paratethyan-Mediterranean connectivity in the Sea of Marmara region (NW Turkey) during the Messinian." *Sedimentary Geology* 188: 171-187.
- Caldeira, K. and M. R. Rampino (1990). "Carbon dioxide emissions from Deccan volcanism and a K/T boundary greenhouse effect." *Geophys. Res. Lett* 17(9): 1é99-1302.
- Cane, M. A. (2005). "The evolution of El Niño, past and future." *Earth and Planetary Science Letters* 230(3-4): 227-240.
- Cane, M. A. and P. Molnar (2001). "Closing of the Indonesian seaway as a precursor to east African aridification around 3-4[thinsp]million years ago." *Nature* 411(6834): 157-162.
- Cazenave, A. (2005). "Global change: Sea level and volcanoes." *Nature* 438(7064): 35-36.
- Cerling, T. E., J. M. Harris, et al. (1997). "Global vegetation change through the Miocene/Pliocene boundary." *Nature* 389(6647): 153-158.
- Chambers, F. M. and J. J. Blackford (2001). "Mid- and late-Holocene climatic changes: a test of periodicity and solar forcing in proxy-climate data from blanket peat bogs." *Journal of Quaternary Science* 16(4): 329-338.
- Chandler, M., H. Dowsett, et al. (2008). "The PRISM Model/Data Cooperative: Mid-Pliocene data-model comparisons." *PAGES News* 16(2): 24-25.
- Chikhi, H. (1992). "Une palynoflore méditerranéenne à subtropicale au Messinien pré-évaporitique en Algérie." *Géol. Méditerr* 19(1): 19-30.
- Chow, J. M. and P. J. Bart (2003). "West Antarctic Ice Sheet grounding events on the Ross Sea outer continental shelf during the middle Miocene." *Palaeogeography, Palaeoclimatology, Palaeoecology* 198(1-2): 169-186.
- Chumakov, I., (1973). "Geological history of the Mediterranean at the end of the Miocene-the beginning of the Pliocene according to new data". In: *Leg 13* (Ed. by W.B.F. Ryan, K.J. Hsü *et al.*). *Initial Reports of the Deep Sea Drilling Project*, 13, 2, 1241-1242.
- Church, J. A., N. J. White, et al. (2005). "Significant decadal-scale impact of volcanic eruptions on sea level and ocean heat content." *Nature* 438(7064): 74-77.

- Clark, D. L. (1996). "The Pliocene record in the central Arctic Ocean." *Marine Micropaleontology* 27(1-4): 157-164.
- Claud, C., B. Duchiron, et al. (2008). "On associations between the 11-year solar cycle and the Indian Summer Monsoon system." *J. Geophys. Res* 113.
- Clauzon, G., (1973). "The eustatic hypothesis and the Pre-Pliocene cutting of the Rhône Valley". In: *Leg 13* (Ed. by W.B.F. Ryan & K.J. Hsü). *Initial Reports of the Deep Sea Drilling Project*, 13, 2, 1251-1256.
- Clauzon, G., J. P. Suc, et al. (1996). "Alternate interpretation of the Messinian salinity crisis: controversy resolved?" *Geology* 24: 363-366.
- Clauzon, G., J. P. Suc, et al. (2005). "Influence of Mediterranean sea level changes on the Dacic Basin (Eastern Paratethys) during the late Neogene: the Mediterranean Lago Mare facies deciphered." *Basin Research*(17): 437-462.
- Clauzon, G., Suc, J.-P., et al. (2007) "Chronology of the Messinian events and paleogeography of the Mediterranean region" *s.l. CIESM Workshop Monographs*, 33, 31-37.
- Clemens, S., W. Prell, et al. (1991). "Forcing mechanisms of the Indian Ocean monsoon." *Nature* 353(6346): 720-725.
- Clemens, S. C., D. W. Murray, et al. (1996). "Nonstationary Phase of the Plio-Pleistocene Asian Monsoon." *Science* 274(5289): 943-948
- Clet-Pellerin M., 1983. *Le Plio-Pléistocène en Normandie. Apports de la palynologie. Thèse, Univ. Caen : 135 p.*
- Combourieu-Nebout, N. (1993). "Vegetation Response to Upper Pliocene Glacial/Interglacial Cyclicity in the Central Mediterranean." *Quaternary Research* 40(2): 228-236.
- Combourieu-Nebout, N., Fauquette, S., Quézel, P., 2000. What was the late Pliocene Mediterranean climate like: a preliminary quantification from vegetation. *Bulletin de la Société géologique de France*, 171, 2, 271-277.
- Combourieu-Nebout, N. and C. Vergnaud Grazzini (1991). "Late Pliocene northern hemisphere glaciation: the continental and marine responses in the central Mediterranean." *Quat. Sci. Rev.* 10 319-334.
- Cour P (1974). "Nouvelles techniques de détection des flux et des retombées polliniques: études de la sédimentation des pollens et des spores à la surface du sol " *Pollen et Spores* 16 (1) :103–141.
- Cravatte J. and J.-P., Suc (1981). "Climatic evolution of North-Western Mediterranean area during Pliocene and Early Pleistocene by pollen-analysis and forams of drill Autan 1". *Chronostratigraphic correlations. Pollen et Spores*, 23(2): 247-258.
- Cronin, T. M., (1991). "Pliocene shallow water paleoceanography of the North Atlantic Ocean based on marine ostracodes." *Quaternary Science Reviews* 10: 175-188.
- Cronin, T. M., R. Whatley, et al. (1993). "Microfaunal evidence for elevated Pliocene temperature in the Arctic Ocean." *Paleoceanography* 8: 161-174.
- Crowley, T. J. (1996). "Pliocene climates: the nature of the problem." *Marine Micropaleontology* 27(1-4): 3-12.
- Crowley, T. J. and G. R. North (1988). "Abrupt Climate Change and Extinction Events in Earth History." *Science* 240(4855): 996-1002.
- Currie, R. G. and O'Brien (1988). "Periodic 18.6 year and cycle 10- to 11-year signals in northeast United States precipitation data." *Int. J. Climatol.* 8: 255-281.
- Dale, B. (1976). Cyst formation, sedimentation, and preservation: Factors affecting dinoflagellate assemblages in recent sediments from trondheimsfjord, Norway. *Review of Palaeobotany and Palynology* 22 (1) 39 -60.

- Dale B., (1986). Life cycle strategies of oceanic dinoflagellates, UNESCO Technical papers in Marine Science, 49: 29-34.
- Dale, B. "Dinoflagellate cyst ecology: modeling and geological applications". In: J. Jansonius and D.C. McGregor, Editors, *Palynology: Principles and Applications*, American Association of Stratigraphic Palynologists Foundation, Dallas (1996): 1249–1276.
- Dale, B. D. A. L. (2001). Environmental applications of dinoflagellate cysts and acritarchs. Quaternary Environmental Micropalaeontology. S. Haslett.
- Damon, P. E. and J. L. Jirikowic (1992). Solar forcing of global climate change? Berlin, Springer-Verlag.
- Damon, P. E. and J. L. Jirikowic (1994). Solar forcing of global climate change. . Cambridge, Cambridge University Press.
- Damon, P. E., A. Long, et al. (1973). "On the magnitude of the 11-year radiocarbon cycle." Earth and Planetary Science Letters 20(3): 300-306.
- Damon, P. E. and A. N. Peristykh (2005). "Solar forcing of global temperature change since AD 1400." Climatic Change 68: 101-111.
- Dansgaard, W. (1993). "Evidence for general instability of past climate from a 250-kyr ice-core record." Nature 364: 218-220.
- De Menocal, P. B. (1995). "Plio-Pleistocene African climate." Science 270(5233): 53-59.
- De Menocal, P. (2004). "African climate change and faunal evolution during the Pliocene-Pleistocene." Earth and Planetary Science Letters 220: 3-24.
- Dean, J. M. and A. E. S. Kemp (2004). "A 2100 year BP record of the Pacific Decadal Oscillation, El Niño Southern Oscillation and Quasi-Biennial Oscillation in marine production and fluvial input from Saanich Inlet, British Columbia." Palaeogeography, Palaeoclimatology, Palaeoecology 213(3-4): 207-229.
- DeConto, R. M. and D. Pollard (2003). "Rapid Cenozoic glaciation of Antarctica induced by declining atmospheric CO₂." Nature 421(6920): 245-249.
- DeLand, M. T., L. E. Floyd, et al. (2004). "Status of UARS solar UV irradiance data." Advances in Space Research 34(2): 243-250
- De Vernal A. and C. Hillaire-Marcel, (2000). "Sea-ice cover, sea-surface salinity and halo-/thermocline structure of the northwest North Atlantic: modern versus fullglacial conditions". Quaternary Science Reviews (19) : 65-85
- Demirbag, E., E. Gökasan, et al. (1999). "The last sea level changes in the Black Sea: evidence from the seismic data." Marine Geology 157: 249-265.
- Dettman, D. L., X. Fang, et al. (2003). "Uplift-driven climate change at 12 Ma: a long δO^{18} record from the NE margin of the Tibetan plateau." Earth and Planetary Science Letters 214(1): 267-277.
- Degens E.T. and D.A. Ross (1972) Chronology of the Black Sea over the last 25,000 years, Chem. Geol. 10: 1–16
- Dickens, G. R. and R. M. Owen (1996). "Sediment geochemical evidence for an early-middle Gilbert (early Pliocene) productivity peak in the North Pacific Red Clay Province." Marine Micropaleontology 27(1-4): 107-120.
- Diniz F. (1984). "Etude palynologique du bassin pliocène de Rio Maior". *Paléobiol. Cont.*, 14 (2) : 259-267.
- Dodson, R. E., M. D. Fuller, et al. (1977). "Paleomagnetic records of secular variation from Lake Michigan sediment cores." Earth and Planetary Science Letters 34(3): 387-395.
- Dowsett, H., J. Barron, et al. (1996). "Middle Pliocene sea surface temperatures: a global reconstruction." Marine Micropaleontology 27(1-4): 13-25.

- Dowsett, H., R. Thompson, et al. (1994). "Joint investigations of the Middle Pliocene climate I: PRISM paleoenvironmental reconstructions." *Global and Planetary Change* 9(3-4): 169-195.
- Dowsett, H. and D. Willard (1996). "Southeast Atlantic marine and terrestrial response to middle Pliocene climate change." *Marine Micropaleontology* 27(1-4): 181-193.
- Dowsett, H. J., M. A. Chandler, et al. (2005). "Middle Pliocene sea surface temperature variability." *Paleoceanography* 20(PA2014).
- Dowsett, H. J., T. M. Cronin, et al. (1992). "Micropaleontological evidence for increased meridional heat transport in the North Atlantic Ocean during the Pliocene." *Science* 258: 1133-1135.
- Dowsett, H. J. and R. Z. Poore (1991). "Pliocene sea surface temperatures of the North Atlantic Ocean at 3.0 Ma." *Quat. Sci. Rev.* 10: 189-204.
- Drivaliari A., Ticleanu N., et al., (1999.)
- Duplessy J.C., L. Labeyrie et al. (1992) "Changes in surface salinity of the North Atlantic Ocean, during the last deglaciation" *Nature* 358:485-488.
- Ellegaard, M. (2000). "Variations in dinoflagellate cysts morphology under conditions of changing salinity during the last 2000 years in the Limfjord, Denmark" *Review of Palaeobotany and Palynology* 109 (1):65-81.
- Elkibbi, M. and J. A. Rial (2001). "An outsider's review of the astronomical theory of the climate: is the eccentricity-driven insolation the main driver of the ice ages?" *Earth-Science Reviews* 56(1-4): 161-177.
- EPICACommunityMembers (2004). "Eight glacial cycles from an Antarctic ice core." *Nature* 429(6992): 623-628.
- Esu, D. (2007). "Latest Messinian "Lago-Mare" Lymnocyprinae from Italy: Close relations with the Pontian fauna from the Dacic Basin." *Geobios* 40(3): 291-302.
- Evitt, W.R. (1985). Sporopollenin dinoflagellate cyst. Their morphology and interpretation. American Association of Stratigraphic Palynologists Foundation, Dallas, 333p.
- Farrar, P. D. (2000). "Are Cosmic Rays Influencing Oceanic Cloud Coverage – Or Is It Only El Niño?" *Climatic Change* 47(1): 7-15.
- Fauquette, S., G. Clauzon, et al. (1999a). "A new approach for palaeoaltitude estimates based on pollen records: example of the Mercantour Massif (southeastern France) at the earliest Pliocene." *Earth and Planetary Science Letters* 170(1-2): 35-47.
- Fauquette, S., J. Guiot, et al. (1999b). "Vegetation and climate since the last interglacial in the Vienne area (France)." *Global and Planetary Change* 20(1): 1-17.
- Fauquette, S., J. Guiot, et al. (1998a). "A method for climatic reconstruction of the Mediterranean Pliocene using pollen data." *Palaeogeography, Palaeoclimatology, Palaeoecology* 144(1-2): 183-201.
- Fauquette, S., P. Quézel, et al. (1998b). "Signification bioclimatique de taxons-guides du Pliocène méditerranéen." *Geobios* 31(2): 151-169.
- Fauquette, S., J.-P. Suc, et al. (2006). "How much did climate force the Messinian salinity crisis? Quantified climatic conditions from pollen records in the Mediterranean region." *Palaeogeography, Palaeoclimatology, Palaeoecology* 238(1-4): 281-301.
- Fauquette, S., J.-P. Suc, et al. (1999b). "Climate and biomes in the West Mediterranean area during the Pliocene." *Palaeogeography, Palaeoclimatology, Palaeoecology* 152(1-2): 15-36.
- Favre, E., L. François, et al. (2007). "Messinian vegetation maps of the Mediterranean region using models and interpolated pollen data." *Geobios* 40(3): 433-443.

- Fedorov, A. V., P. S. Dekens, et al. (2006). "The Pliocene Paradox (Mechanisms for a Permanent El Niño)." *Science* 312(5779): 1485-1489.
- Fernández Marrón, T. and C. Alvarez Ramis (1988). Note préliminaire sur l'étude paléobotanique du gisement de Rubielos de Mora (Teruel, Espagne). Résumé Séminaire de Paléobotanique. Lille., OFP Informations 9: 14.
- Finkel, R. C. and K. Nishiizumi (1997). "Beryllium 10 concentrations in the Greenland Ice Sheet Project 2 ice core from 3-40 ka." *Journal of Geophysical Research* 102(C12): 26699-26706.
- Flecker, R. and R. M. Ellam (2006). "Identifying Late Miocene episodes of connection and isolation in the Mediterranean-Paratethyan realm using Sr isotopes." *Sedimentary Geology* 188: 189-203.
- Fleitmann, D., S. J. Burns, et al. (2003). "Holocene Forcing of the Indian Monsoon Recorded in a Stalagmite from Southern Oman." *Science* 300(5626): 1737-1739.
- Fleming, R. F. and J. A. Barron (1996). "Evidence of Pliocene *Nothofagus* in Antarctica from Pliocene marine sedimentary deposits (DSDP Site 274)." *Marine Micropaleontology* 27(1-4): 227-236.
- Flower, B. and J. Kennett (1995). "Middle Miocene deepwater paleoceanography in the southwest Pacific: Relations with East Antarctic Ice Sheet development." *Paleoceanography* 10(6).
- Flower, B. P. and J. P. Kennett (1993). "Middle Miocene Ocean-Climate Transition: High-Resolution Oxygen and Carbon Isotopic Records from Deep Sea Drilling Project Site 588A, Southwest Pacific." *Paleoceanography*, 8(6): 811-843.
- Flower, B. P. and J. P. Kennett (1994). "The middle Miocene climatic transition: East Antarctic ice sheet development, deep ocean circulation and global carbon cycling." *Palaeogeography, Palaeoclimatology, Palaeoecology* 108(3-4): 537-555.
- Fortelius, M., J. Eronen, et al. (2006). "Late Miocene and Pliocene large land mammals and climatic changes in Eurasia." *Palaeogeography, Palaeoclimatology, Palaeoecology* 238(1-4): 219-227.
- Foukal, P. (1994). "Stellar Luminosity Variations and Global Warming." *Science* 264(5156): 238-239.
- Foukal, P. (1998). "What Determines the Relative Areas of Spots and Faculae on Sun-like Stars?" *The Astrophysical Journal* 500(2): 958-965.
- Foukal, P., C. Frohlich, et al. (2006). "Variations in solar luminosity and their effect on the Earth's climate." *Nature* 443(7108): 161-166.
- François, L., M. Ghislain, et al. (2006). "Late Miocene vegetation reconstruction with the CARAIB model." *Palaeogeography, Palaeoclimatology, Palaeoecology* 238(1-4): 302-320.
- Fröhlich, C. (2006). "Solar irradiance variability since 1978. revision of the PMOD Composite during Solar Cycle 21." *Space Science Reviews*: 1-13.
- Garcin, Y., A. Vincens, et al. (2007). "Abrupt resumption of the African Monsoon at the Younger Dryas--Holocene climatic transition." *Quaternary Science Reviews* 26(5-6): 690-704.
- Georgieva, K., B. Kirov, et al. (2007). "Long-term variations in the correlation between NAO and solar activity: The importance of north-south solar activity asymmetry for atmospheric circulation." *Advances in Space Research* 40(7): 1152-1166.
- Ghebreab, W. (1998). "Tectonics of the Red Sea region reassessed." *Earth-Science Reviews* 45(1-2): 1-44.
- Gillet, H., G. Lericolais, et al. (2007). "Messinian event in the black sea: Evidence of a Messinian erosional surface." *Marine Geology* 244(1): 142-165.
- Gimeno, L., L. de la Torre, et al. (2003). "Changes in the relationship NAO-Northern hemisphere temperature due to solar activity." *Earth and Planetary Science Letters* 206(1-2): 15-20.
- Gleckler, P. J., T. M. L. Wigley, et al. (2006). "Volcanoes and climate: Krakatoa's signature persists in the ocean." *Nature* 439(7077): 675-675.

- Gliozzi, E., M. E. Ceci, et al. (2007). "Paratethyan Ostracod immigrants in Italy during the Late Miocene." *Geobios* 40(3): 325-337.
- Gordon, C. (2000). "The simulation of SST, sea ice extents and ocean heat transports in a version of the Hadley Centre coupled model without flux adjustments." *Clim. Dyn.* 16: 147-168.
- Gorini, C., Lofi, J., et al. (2005). "The Late Messinian salinity crisis and Late Miocene tectonism : Interaction and consequences on the physiography and post-rift evolution of the Gulf of Lions margin." *Marine and Petroleum Geology*, 22, 695-712.
- Görür, N., M. N. Cagatay, et al. (2001). "Is the abrupt drowning of the Black Sea shelf at 7150 yr BP at myth?" *Marine Geology* 176: 65-73.
- Goubert, E., Néraudeau, D., et al. (2001). "Foraminiferal record of environmental changes: Messinian of the Los Yesos area (Sorbas Basin, SE Spain)". *Palaeogeography, Palaeoclimatology, Palaeoecology*, 175: 61-78.
- Grainger, R. G. and E. J. Highwood (2003). "Changes in stratospheric composition, chemistry, radiation and climate caused by volcanic eruptions." Geological Society, London, Special Publications 213(1): 329-347.
- Greenwood, D. R. and S. L. Wing (1995). "Eocene continental climates and latitudinal temperature gradients." *Geology* 23: 1044-1048.
- Groeneveld (2005). Effect of the pliocene closure of the Panamanian Gateway on Caribbean and east Pacific sea surface temperatures and salinities by applying combined Mg/Ca and $\delta^{18}\text{O}$ measurements (5.6 - 2.2 Ma). PhD.
- Gökasan, E., E. Demirbag, et al. (1997). "On the origin of the Bosphorus." *Marine Geology* 140: 183-199.
- Grootes, P. M. and M. Stuiver (1997). "Oxygen 18/16 variability in Greenland snow and ice with 10^{-3} to 10^5 -year time resolution." *Journal of Geophysical Research*, 101(C12): 26455-26470.
- Gross, M. (2008). "A limnic ostracod fauna from the surroundings of the Central Paratethys (Late Middle Miocene/Early Late Miocene; Styrian." *Palaeogeography, Palaeoclimatology, Palaeoecology* 264(3): 263-276.
- Gussone, N., A. Eisenhauer, et al. (2004). "Reconstruction of Caribbean Sea surface temperature and salinity fluctuations in response to the Pliocene closure of the Central American Gateway and radiative forcing, using $\delta^{44}\text{Ca}$, $\delta^{18}\text{O}$ and Mg/Ca ratios." *Earth and Planetary Science Letters* 227(3-4): 201-214.
- Haggerty, S. E. (1994). "Superkimberlites: A geodynamic diamond window to the Earth's core." *Earth and Planetary Science Letters* 122(1-2): 57-69.
- Haig, J. D. (2003). "The effects of solar variability on the Earth's climate." *Philosophical Transactions of The Royal Society* 361(1802): 95-111.
- Halfman, J. D. and T. C. Johnson (1988). "High-resolution record of cyclic climatic change during the past 4 ka from Lake Turkana, Kenya." *Geology* 16: 496-500.
- Hall, R. (2002). "Cenozoic geological and plate tectonic evolution of SE Asia and the SW Pacific: computer-based reconstructions, model and animations." *Journal of Asian Earth Sciences* 20(4): 353-431.
- Hameed, S. (1984). "Fourier analysis of Nile flood levels." *Geophys. Res. Lett* 1: 843-845.
- Hameed, S., W. M. Yeh, et al. (1983). "An analysis of periodicities in the 1470 to 1974 Beijing precipitation record." *Geophys. Res. Lett* 10: 463-439.
- Hammen, T. van der, Wijnstra, T.A., Zagwijn, W.H., 1971. The floral record of the Late Cenozoic in Europe. In "The Late Cenozoic Glacial Ages", Turekian, K.K., ed., Yale Univ. Press, New Haven and London, 391-423.

- Hansen, J., M. Sato, et al. (2007). "Climate change and trace gases." *Philosophical Transactions of the Royal Society A: Mathematical, Physical and Engineering Sciences* 365(1856): 1925-1954.
- Hansen, J., M. Sato, et al. (1997). "The missing climate forcing." *Philosophical Transactions of the Royal Society B: Biological Sciences* 352(1350): 231-240.
- Hansen, J., A. Lacis et al. (1984). "Climate sensitivity : analysis of feedback mechanisms". *Geophys. Mono.* 29:130-163
- Haq, B. U., J. A. N. Hardenbol, et al. (1987). "Chronology of Fluctuating Sea Levels Since the Triassic." *Science* 235(4793): 1156-1167.
- Harris, N. (2006). "The elevation history of the Tibetan Plateau and its implications for the Asian monsoon." *Palaeogeography, Palaeoclimatology, Palaeoecology* 241(1): 4-15.
- Harrison S. P., I. Colin Prentice and Joël Guiot (1993) "Climatic controls on Holocene lake-level changes in Europe". *Climate Dynamics* 8(4): 189-200
- Harzhauser, M. and W. E. Piller (2007). "Benchmark data of a changing sea -- Palaeogeography, Palaeobiogeography and events in the Central Paratethys during the Miocene." *Palaeogeography, Palaeoclimatology, Palaeoecology* 253(1-2): 8-31.
- Harzhauser, M., W. E. Piller, et al. (2002). "Circum-Mediterranean Oligo-Miocene biogeographic evolution - the gastropods' point of view." *Palaeogeography, Palaeoclimatology, Palaeoecology* 183(1): 103-133.
- Haug, G. H., A. Ganopolski, et al. (2005). "North Pacific seasonality and the glaciation of North America 2.7million years ago." *Nature* 433(7028): 821-825.
- Haug, G. H. and R. Tiedemann (1998). "Effect of the formation of the Isthmus of Panama on Atlantic Ocean thermohaline circulation." *Nature* 393: 673-676.
- Haug, G. H., R. Tiedemann, et al. (2001). "Role of Panama uplift on oceanic freshwater balance." *Geology* 29(3): 207-210.
- Haug, G. H. and Tiedemann.R (1998). "Effect of the formation of the Isthmus of Panama on Atlantic Ocean thermohaline circulation." *Nature* 393(673-676).
- Hays, J. D., J. Imbrie, et al. (1976). "Variations in the Earth's Orbit: Pacemaker of the Ice Ages." *Science* 194(4270): 1121-1132.
- Haywood, A. M., P. Dekens, et al. (2005). "Warmer tropics during the mid-Pliocene? Evidence from alkenone paleothermometry and a fully coupled ocean-atmosphere GCM." *Geochem. Geophys. Geosyst.* 6.
- Haywood, A. M. and P. J. Valdes (2004). "Modelling Middle Pliocene warmth: contribution of atmosphere, oceans and cryosphere." *Earth Planet. Sci. Lett.* 218: 363-377.
- Haywood, A. M., P. J. Valdes, et al. (2007). "A permanent El Nino-like state during the Pliocene?" *Paleoceanography* 22.
- Haywood, A. M., P. J. Valdes, et al. (2002). "Antarctic climate during the middle Pliocene: model sensitivity to ice sheet variation." *Palaeogeography, Palaeoclimatology, Palaeoecology* 182(1): 93-115.
- Head, M.J. (1993). "Dinoflagellates, sporomorphs, and other palynomorphs from the Upper Pliocene St. Earth beds of Cornwall, South-western England". *Supplement to Journal of Paleontology*, 67 (3): 1-62.
- Head, M.J. (1994). "Morphology and paleoenvironmental significance of the Cenozoic dinoflagellate genera *Tectatodinium* and *Habibacysta*". *Micropaleontology*, 40(4):289-321.

- Head, M.J. (1996). "Late Cenozoic dinoflagellates from the Royal Society Borehole at Ludham, Norfolk, eastern England". *Journal of Paleontology*, 70(4): 543-570.
- Heusser, L. E. and J. J. Morley (1996). "Pliocene climate of Japan and environs between 4.8 and 2.8 Ma: A joint pollen and marine faunal study." *Marine Micropaleontology* 27(1-4): 85-106.
- Hilgen F.J. (1991). "Extension of the astronomically calibrated (polarity) time scale to the Miocene/Pliocene boundary". *Earth and Planetary Science Letters* 107: 349-368.
- Hiscott, R. N., A. E. Aksu, et al. (2002). "Deltas south of the Bosphorus Strait record persistent Black Sea outflow to the Marmara Sea since similar to 10 ka." *Marine Geology* 190(1-2): 95-118.
- Hiscott, R. N. and A. E. Aksu (2002). "Late Quaternary history of the Marmara Sea and Black Sea from high-resolution seismic and gravity-core studies." *Marine Geology* 190(1-2): 261-282.
- Holbourn, A., W. Kuhnt, et al. (2005). "Impacts of orbital forcing and atmospheric carbon dioxide on Miocene ice-sheet expansion." *Nature* 438(7067): 483-487.
- Holbourn, A., W. Kuhnt, et al. (2007). "Orbitally-paced climate evolution during the middle Miocene "Monterey" carbon-isotope excursion." *Earth and Planetary Science Letters* 261(3-4): 534-550.
- Hong, Y. T., H. B. Jiang, et al. (2000). "Response of climate to solar forcing recorded in a 6000-year - $\delta^{18}\text{O}$ time-series of Chinese peat cellulose." *The Holocene* 10(1): 1-7.
- Hong, Y. T., Z. G. Wang, et al. (2001). "A 6000-year record of changes in drought and precipitation in northeastern China based on a $\delta^{13}\text{C}$ time series from peat cellulose." *Earth and Planetary Science Letters* 185(1-2): 111-119.
- Hooghiemstra H., (1989). "Quaternary and Upper-Pliocene glaciations and forest development in the tropical Andes: evidence from a long high-resolution pollen record from the sedimentary basin of Bogota, Colombia". *Palaeogeography, Palaeoclimatology, Palaeoecology*, 72: 11-26.
- Hooghiemstra H. and E.T.H Ran. (1994). "Late Pliocene high resolution pollen sequence of Colombia: an overview of climate change". *Quaternary International*, 21: 63-80.
- Holmes P.L. (1994), in: A. Traverse (Eds.), "Sedimentation of Organic Particles", Cambridge University Press, Cambridge, UK, p9-32.
- Heusser L.E. and W.L. Balsam (1977) "Pollen distribution in the Northeast Pacific Ocean", *Quaternary Research* 7:45-62.
- Horiuchi, K., A. Ohta, et al. (2007). "Concentration of ^{10}Be in an ice core from the Dome Fuji station, Eastern Antarctica: Preliminary results from 1500 to 1810 yr AD." *Nuclear Instruments and Methods in Physics Research Section B: Beam Interactions with Materials and Atoms* 259(1): 584-587.
- Hsü K.J. (1978). "Correlation of Black Sea sequences". *In* Initial Report of the Deep Sea Drilling Project, Ross, D.A., Neprchnov, Y.P. *et al.* *édit.*, 42, 2, U.S. Gov. Print. Off: 489-497.
- Hsü K.J. and F.Giovanoli, 1979. "Messinian event in the Black Sea". *Palaeogeogr., Palaeoclimatol., Palaeoecol.*, 29, 1-2, 75-94.
- Hsü, K.J., and F Giovanoli (1979). "Messinian event in the Black Sea". *Palaeogeography, Palaeoclimatology, Palaeoecology*, 29, 75-93.
- Hsü, K. J., M. B. Cita, et al. (1973). The origine of the Mediterranean evaporites. Initial Reports of Deep Sea Drilling Project. W. B. F. Ryan, K. J. Hsü and al. Washington, (U.S. Government Printing Office). 13: 1203-1231.
- Hu, F. S., D. Kaufman, et al. (2003). "Cyclic Variation and Solar Forcing of Holocene Climate in the Alaskan Subarctic." *Science* 301(5641): 1890-1893.
- Imbrie, J. (1985). "A theoretical framework for the pleistocene ice ages." *Journal of the Geological Society London* 142: 417-432.

- Imbrie, J., E. A. Boyle, et al. (1993). "On the structure and origin of major glaciation cycles 2. The 100,000-year cycle." *Paleoceanography* 8(6): 669-735.
- Imbrie, J., E. A. Boyle, et al. (1992). "On the structure and origin of major glaciation cycles 1. Linear responses to Milankovich Forcing." *Paleoceanography* 7(6): 701-736.
- Imbrie, J. and J. Z. Imbrie (1980). "Modeling the climatic response to orbital variations." *Science* 207: 943-953.
- Ivanov, D., A. R. Ashraf, et al. (2002). "Palynological evidence for Miocene climate change in the Forecarpathian Basin (Central Paratethys, NW Bulgaria)." *Palaeogeography, Palaeoclimatology, Palaeoecology* 178(1): 19-37.
- Ivanov, D. A., A. R. Ashraf, et al. (2007). "Late Oligocene and Miocene climate and vegetation in the Eastern Paratethys area (northeast Bulgaria), based on pollen." *Palaeogeography, Palaeoclimatology, Palaeoecology* 255(3): 342-360.
- Jain, S. and L. S. Collins (2007). "Trends in Caribbean Paleoproductivity related to the Neogene closure of the Central American Seaway." *Marine Micropaleontology* 63(1-2): 57-74.
- Ji, J., J. Shen, et al. (2005). "Asian monsoon oscillations in the northeastern Qinghai-Tibet Plateau since the late glacial as interpreted from visible reflectance of Qinghai Lake sediments." *Earth and Planetary Science Letters* 233(1-2): 61-70.
- Jiang, H., J. Eiriksson, et al. (2005). "Evidence for solar forcing of sea-surface temperature on the North Icelandic Shelf during the late Holocene." *Geology* 33(1): 73-76.
- Jiang, X. and W. R. Peltier (1996). "Ten million year histories of obliquity and precession: The influence of the ice-age cycle." *Earth and Planetary Science Letters* 139(1-2): 17-32.
- Jimenez-Moreno, G. and J. P. Suc (2007d). "Middle Miocene latitudinal climatic gradient in Western Europe: Evidence from pollen records." *Palaeogeography, Palaeoclimatology, Palaeoecology* 253(1): 208-225.
- Jiménez- Moreno, G., S.-M. Popescu, et al. (2007c). Neogene flora, vegetation and climate dynamics in southeastern Europe and northeastern Mediterranean according to pollen records. *Deep-Time Perspectives on Climate Change: Marrying the Signal from Computer Models and Biological Proxies*. M. Williams and J. G. Haywood. London, The Micropalaeontological Society, Special Publications. The Geological Society, London: 503-516.
- Jimenez-Moreno, G. (2006). "Progressive substitution of a subtropical forest for a temperate one during the middle Miocene climate cooling in." *Review of Palaeobotany and Palynology* 142(1): 1-14.
- Jimenez-Moreno, G., H. A. Aziz, et al. (2007a). "Palynological evidence for astronomical forcing in Early Miocene lacustrine deposits from Rubielos de Mora Basin (NE)." *Palaeogeography, Palaeoclimatology, Palaeoecology* 252(3): 601-616.
- Jimenez-Moreno, G., S. Fauquette, et al. (2007b). "Early Miocene repetitive vegetation and climatic changes in the lacustrine deposits of the Rubielos de Mora Basin." *Palaeogeography, Palaeoclimatology, Palaeoecology* 250(1): 101-113.
- Jimenez-Moreno, G., F. J. Rodriguez-Tovar, et al. (2005). "High-resolution palynological analysis in late early-middle Miocene core from the Pannonian Basin, Hungary: climatic changes, astronomical forcing and eustatic fluctuations in the Central Paratethys." *Palaeogeography, Palaeoclimatology, Palaeoecology* 216(1-2): 73-97.
- Jiménez-Moreno, G., 2005. Utilización del análisis polínico para la reconstrucción de la vegetación, clima y estimación de paleoaltitudes a lo largo de arco alpino europeo durante el Miocene (21-8 Ma). Thesis, Univ. Granada, 310 pp.
- Joannin, S., Quillévéré, F., Suc, J.-P., Lécuyer, C., Martineau, F., 2007. Early Pleistocene climate changes in the central Mediterranean region as inferred from integrated pollen and planktonic foraminiferal stable isotope analyses. *Quaternary Research*, 67, 264-274.

- Johnsen, S. J., W. Dansgaard, et al. (1970). "Climatic Oscillations 1200-2000 AD." *Nature* 227(5257): 482-483.
- Jolivet, L., R. Augier, et al. (2006). "Lithospheric-scale geodynamic context of the Messinian salinity crisis." *Sedimentary Geology* 188-189: 9-33.
- Karl, T. R. and W. E. Riebsame (1984). "The identification of 10- to 20-year temperature and precipitation fluctuations in the contiguous United States. ." *J. Climate Appl. Meteor* 23: 950 - 966.
- Keigwin, L. (1982). "Isotopic paleoceanography of the Caribbean and east pacific: role of Panama uplift in late Neogene time." *Science* 217: 350-353.
- Kelly, P. M. and C. B. Sear (1984). "Climatic impact of explosive volcanic eruptions." *Nature* 311(5988): 740-743.
- Kennett, J. P. (1977). "Cenozoic Evolution of Antarctic Glaciation, the Circum-Antarctic Ocean, and Their Impact on Global Paleoceanograph." *Journal of Geophysical Research* 82(27): 3843-3860.
- Kennett, J. P., G. Keller, et al. (1985). Miocene planktonic foraminiferal biogeography and paleoceanographic development of the Indo-Pacific regio. *The Miocene Ocean*. K. J.P., GSA Mem. 163 197-236.
- Kirkby, J. (2007). "Cosmic Rays and Climate." *Surveys in Geophysics* 28(5): 333-375.
- Kofler, W., V. Krapf, et al. (2005). "Vegetation responses to the 8200 cal. BP cold event and to long-term climatic changes in the Eastern Alps: possible influence of solar activity and North Atlantic freshwater pulses." *The Holocene* 15(6): 779-788.
- Kokinos J. P. and D. M. Andersen (1995). "Morphological development of resting cysts in cultures of the marine dinoflagellate *Lingulodinium polyedrum* (=L. *machaerophorum*)". *Palynology* 19:143-166.
- Kovac, M., I. Barath, et al. (2006). "Late Miocene to Early Pliocene sedimentary environments and climatic changes in the Alpine-Carpathian-Pannonian junction." *Palaeogeography, Palaeoclimatology, Palaeoecology* 238(1): 32-52.
- Kovar-Eder, J., Z. Kvacek, et al. (2006). "Late Miocene to Early Pliocene vegetation of southern Europe (7-4 Ma) as reflected in the megafossil plant record." *Palaeogeography, Palaeoclimatology, Palaeoecology* 238(1-4): 321-339.
- Kowalke, T. and B. Reichenbacher (2005). "Early Miocene (Ottangian) Mollusca of the Western Paratethys-ontogenetic strategies and palaeo-environments." *Geobios* 38(5): 609-635.
- Krijgsman, W., F. J. Hilgen, et al. (1999). "Chronology, causes and progression of the Messinian salinity crisis." *Nature* 400(6745): 652-655.
- Kristjánsson, J. E., A. Staple, et al. (2002). "A new look at possible connections between solar activity, clouds and climate,." *Geophys. Res. Lett* 29(23): 2107.
- Kroh, A. (2007). "Climate changes in the Early to Middle Miocene of the Central Paratethys and the origin of its echinoderm fauna." *Palaeogeography, Palaeoclimatology, Palaeoecology* 253(1-2): 169-207.
- Kuhnt, W., A. Holbourn, et al. (2004). Neogene history of the Indonesian throughflow. *Continent-Ocean Interactions Within East Asian Marginal Seas*. P. Clift, P. Wang and W. Kuhnt, Geophysical Monograph Series. 149: 299-318.
- Kürschner, W. M., J. van der Burgh, et al. (1996). "Oak leaves as biosensors of late neogene and early pleistocene paleoatmospheric CO₂ concentrations." *Marine Micropaleontology* 27(1-4): 299-312.
- Latal, C., W. E. Piller, et al. (2004). "Palaeoenvironmental reconstructions by stable isotopes of Middle Miocene gastropods of the Central Paratethys." *Palaeogeography, Palaeoclimatology, Palaeoecology* 211(1): 157-169.
- LaViolette, P. A. (2005). "Solar cycle variations in ice acidity at the end of the last ice age: Possible marker of a climatically significant interstellar dust incursion." *Planetary and Space Science* 53(4): 385-393.

- Lawrence, K. T., Z. Liu, et al. (2006). "Evolution of the Eastern Tropical Pacific Through Plio-Pleistocene Glaciation." *Science* 312(5770): 79-83.
- Le Mouél, J.-L., V. Kossobokov, et al. (2005). "On long-term variations of simple geomagnetic indices and slow changes in magnetospheric currents: The emergence of anthropogenic global warming after 1990?" *Earth and Planetary Science Letters* 232(3-4): 273-286.
- Lean, J. and D. Rind (1998). "Climate Forcing by Changing Solar Radiation." *Journal of Climate* 11(12): 3069-3094.
- Lean, J. L., J. Cook, et al. (1998). "Magnetic Sources of the Solar Irradiance Cycle." *The Astrophysical Journal* 492(1): 390-401.
- Lean, J. L. and P. Foukal (1988). "A model of solar luminosity modulation by magnetic activity between 1954 and 1984." *Science* 240: 906.
- Lear, C. H., H. Elderfield, et al. (2000). "Cenozoic Deep-Sea Temperatures and Global Ice Volumes from Mg/Ca in Benthic Foraminiferal Calcite." *Science* 287(5451): 269-272.
- Lear, C. H., Y. Rosenthal, et al. (2003). "The closing of a seaway: ocean water masses and global climate change." *Earth and Planetary Science Letters* 210(3-4): 425-436.
- Ledbetter, M. T., D. F. Williams, et al. (1978). "Late Pliocene climate and south-west Atlantic abyssal circulation." *Nature* 272(5650): 237-239.
- Leever, K. A. (2007). Foreland of the Romanian Carpathians ; Controls on late orogenic sedimentary basin evolution and Paratethys paleogeography. Cloetingh, S.A.P.L. [Promotor]
- Leroy, S. and L. Dupont (1994). "Development of vegetation and continental aridity in northwestern Africa during the Late Pliocene: the pollen record of ODP site 658." *Palaeogeography, Palaeoclimatology, Palaeoecology* 109(2-4): 295-316.
- Lewis J. and R. Hallett (1997). "Lingulodinium polyedrum (Goniaulax polyedra) a blooming dinoflagellate". *Oceanogr. Mar. Biol. Ann. Rev.* 35: 97-161.
- Lewis J., Rochon A, et al. (1999) "Preliminary observations of cyst-theca relationships in *Spiniferites ramosus* and *Spiniferites membranaceus* (Dinophyceae)" *Grana* 38: 113-124.
- Lewis J., Ellegaard M., et al. (2003). "Environmental control of cyst morphology in *Gonyaulacoid* dinoflagellates". In: K. Matsuoka, M. Yoshida and M. Iwataki, Editors *Dino7, Seventh International Conference on Modern and fossil Dinoflagellates, Abstract Volume (2003) Additional Abstract*.
- Li, Q., B. Li, et al. (2006). "Late Miocene development of the western Pacific warm pool: Planktonic foraminifer and oxygen isotopic evidence." *Palaeogeography, Palaeoclimatology, Palaeoecology* 237(2-4): 465-482.
- Liew, P. M., C. Y. Lee, et al. (2006). "Holocene thermal optimal and climate variability of East Asian monsoon inferred from forest reconstruction of a subalpine pollen sequence, Taiwan." *Earth and Planetary Science Letters* 250(3-4): 596-605.
- Lifton, N. A., J. W. Bieber, et al. (2005). "Addressing solar modulation and long-term uncertainties in scaling secondary cosmic rays for in situ cosmogenic nuclide applications." *Earth and Planetary Science Letters* 239(1-2): 140-161.
- Lisiecki, L. E. and M. E. Raymo (2005). "A Pliocene-Pleistocene stack of 57 globally distributed benthic $\delta^{18}O$ records." *Paleoceanography* 20.
- Lisiecki, L. E. and M. E. Raymo (2007). "Plio-Pleistocene climate evolution: trends and transitions in glacial cycle dynamics." *Quaternary Science Reviews* 26(1-2): 56-69.
- Liu, X. and Z. Y. Yin (2002). "Sensitivity of East Asian monsoon climate to the uplift of the Tibetan Plateau." *Palaeogeography, Palaeoclimatology, Palaeoecology* 183(3): 223-245.
- Liu, Z. and T. D. Herbert (2004). "High-latitude influence on the eastern equatorial Pacific climate in the early Pleistocene epoch." *Nature* 427(6976): 720-723.

- Lockwood, M. and C. Fröhlich (2008). "Recent oppositely directed trends in solar climate forcings and the global mean surface air temperature. II. Different reconstructions of the total solar irradiance variation and dependence on response time scale." *Proceedings of the Royal Society A: Mathematical, Physical and Engineering Sciences* 464(2094): 1367-1385.
- Lofi, J., Gorini, C., et al. (2005). "Erosional processes and paleo-environmental changes in the western Gulf of Lions (SW France) during the Messinian Salinity Crisis". *Marine Geology*, 217, 1-30.
- Lunt, D. J., G. L. Foster, et al. (2008a). "Late Pliocene Greenland glaciation controlled by a decline in atmospheric CO₂ levels." *Nature* 454(7208): 1102-1105.
- Lunt, D. J., P. J. Valdes, et al. (2008b). "Closure of the Panama Seaway during the Pliocene: implications for climate and Northern Hemisphere glaciation." *Clim. Dyn.* 30: 1-18.
- Magyar, D.H. Geary and P. Müller, (1999). "Paleogeographic evolution of the Late Miocene Lake Pannon in Central Europe", *Paleogeography, Paleoclimatology, Paleocology*. 147:151–167.
- Magyar I., D.H. Geary, et al (1999). "Integrated bio-, magneto- and chronostratigraphic correlation of the Late Miocene Lake Pannon deposits" *Acta Geol. Hung.* 42:5–31
- Major, C., W. Ryan, et al. (2002). "Constraints on Black Sea outflow to the Sea of Marmara during the last glacial-interglacial transition." *Marine Geology* 190(1-2): 19-34.
- Major, C. O., S. L. Goldstein, et al. (2006). "The co-evolution of Black Sea level and composition through the last deglaciation and its paleoclimatic significance." *Quaternary Science Reviews* 25(17-18): 2031-2047.
- Mandic, O., M. Harzhauser, et al. (2002). "The paleoenvironment of an early Middle Miocene Paratethys sequence in NE Austria with special emphasis on paleoecology." *Geobios* 35: 193-206.
- Mann, M. E. (2007). "Climate Over the Past Two Millennia." *Annual Review of Earth and Planetary Sciences* 35(1): 111-136.
- Marret, F., and K.A.F. Zonneveld (2003) Atlas of modern organic-walled dinoflagellate cyst distribution, *Rev. Palaeobot. Palynol.* 125, 200 pp
- Marsh, N. D. and H. Svensmark (2000). "Low cloud properties influenced by cosmic rays." *Phys Rev Lett* 85(23): 5004-5007.
- Marsh, N. D. and H. Svensmark (2003). "Galactic cosmic ray and El Niño-Southern Oscillation trends in ISCCP-D2 low cloud properties." *Journal of Geophysical Research* 108(D6): 4195.
- Martinetto E. (1994). Paleocarpology and the *in situ* ancient plant communities of a few Italian Pliocene fossil forests. In "Studies on Ecology and Paleocology of Benthic Communities", *Boll. Soc. Paleontol. Ital.*, Special volume 2: 189-196.
- Marunteanu M. and I. Papaianopol, (1995). "L'association de nanoplancton dans les dépôts romaniens situés entre les vallées de Cosmina et de Cricovu Dulce (Munténie, bassin dacique, Roumanie)". *Romanian Journal of Paleontology*, 76.
- Marunteanu M. and I. Papaianopol, (1995). "The connection between the Dacic and Mediterranean Basins based on calcareous nanoplankton assemblages". *Romanian Journal of Stratigraphy*, 76 (7):169-170.
- Maslin, M. A., X. S. Li, et al. (1998). "The contribution of orbital forcing to the progressive intensification of Northern Hemisphere glaciation." *Quat. Sci. Rev.* 17: 411-426.
- McHargue, L. R. and P. E. Damon (1991). "The global Beryllium 10 cycle." *Reviews of Geophysics* 29: 141-158.
- Melinte-Dobrinescu, M.C., Suc, J.-P., et al. "The Messinian Salinity Crisis in the Dardanelles region: Chronostratigraphic constraints". *Palaeogeography, Palaeoclimatology, Palaeoecology*, submitted
- Menke B., 1975. Tertiäre Vegetationsgeschichte Europas. Methoden und Ergebnisse. Fischer G. édit., Jean-Stuttgart-New York : 691 p.

- Meulenkamp, J. E. and W. Sissingh (2003). "Tertiary palaeogeography and tectonostratigraphic evolution of the Northern and Southern Peri-Tethys platforms and the intermediate domains of the African-Eurasian convergent plate boundary zone." *Palaeogeography, Palaeoclimatology, Palaeoecology* 196(1-2): 209-228.
- Milankovitch, M. (1941). *Canon of insolation and ice-age problem* (English translation).
- Miller, K. G., R. G. Fairbanks, et al. (1987). "Tertiary oxygen isotope synthesis, sea level history, and continental margin erosion." *Paleoceanography* 2(1-19).
- Miller, K. G., M. D. Feigenson, et al. (1991a). "Miocene isotope reference section, DSDP Site 608: an evaluation of isotope and biostratigraphic resolution,." *Paleoceanography* 6(1): 33-52.
- Miller, K. G., J. D. Wright, et al. (1991b). "Unlocking the Ice House: Oligocene-Miocene Oxygen Isotopes, Eustasy, and Margin Erosion." *Journal of Geophysical Research* 96(B4): 6829-6848.
- Milovanovic, D. and D. Mihajlovic (1984). "A Miocene flora from Zagubica basin, eastern Serbia." *Annales Geologiques de la Peninsule Balkanique* 48 201-213.
- Minnis, P., E. F. Harrison, et al. (1993). "Radiative Climate Forcing by the Mount Pinatubo Eruption." *Science* 259(5100): 1411-1415.
- Miyahara, H., K. Masuda, et al. (2007). "Variation of solar activity from the Spörer to the Maunder minima indicated by radiocarbon content in tree-rings." *Advances in Space Research* 40(7): 1060-1063.
- Miyahara, H., Y. Yokoyama, et al. (2008). "Possible link between multi-decadal climate cycles and periodic reversals of solar magnetic field polarity." *Earth and Planetary Science Letters* 272(1-2): 290-295.
- Moissette, P., A. Dulai, et al. (2007). "Mosaic of environments recorded by bryozoan faunas from the Middle Miocene of Hungary." *Palaeogeography, Palaeoclimatology, Palaeoecology* 252(3): 530-556.
- Molnar, P. (2005). "Mio-Pliocene Growth of the Tibetan Plateau and Evolution of East Asian Climate." *Palaeontologia Electronica* 8(8.1.2.A): 1-23.
- Molnar, P., P. England, et al. (1993). "Mantle dynamics, the uplift of the Tibetan Plateau, and the Indian monsoon" *Reviews of Geophysics* 31: 357-396.
- Mosbrugger V., T. Utescher and D.L. Dilcher (2005) "Cenozoic continental climatic evolution of Central Europe". *Proceedings of the National Academy of Sciences* 102 (42):14964–14969.
- Montuire, S., O. Maridet, et al. (2006). "Late Miocene-Early Pliocene temperature estimates in Europe using rodents." *Palaeogeography, Palaeoclimatology, Palaeoecology* 238(1-4): 247-262.
- Mosbrugger V. and T. Utescher (1997) "The coexistence approach — a method for quantitative reconstructions of Tertiary terrestrial palaeoclimate data using plant fossils" *Palaeogeography, Palaeoclimatology, Palaeoecology*, 134 (1-4) :61-86
- Mudie, P. J., A. Rochon, et al. (2004). "Late glacial, Holocene and modern dinoflagellate cyst assemblages in the Aegean-Marmara-Black Sea corridor: statistical analysis and re-interpretation of the early Holocene Noah's Flood hypothesis." *Review of Palaeobotany and Palynology* 128(1-2): 143-167.
- Mudie, P. J., A. Rochon, et al. (2002a). "Pollen stratigraphy of Late Quaternary cores from Marmara Sea: land-sea correlation and paleoclimatic history." *Marine Geology* 190: 233-260.
- Mudie, P. J., A. Rochon, et al. (2002b). "Dinoflagellate cysts, freshwater algae and fungal spores as salinity indicators in Late Quaternary cores from Marmara and Black seas." *Marine Geology* 190(1-2): 203-231.
- Mudie, P. J., A. E. Aksu, et al. (2001). "Late Quaternary dinoflagellate cysts from the Black, Marmara and Aegean seas: variations in assemblages, morphology and paleosalinity." *Marine Micropaleontology* 43(1-2): 155-178.

- Muscheler, R., J. Beer, et al. (2004). "Changes in the carbon cycle during the last deglaciation as indicated by the comparison of ^{10}Be and ^{14}C records." *Earth and Planetary Science Letters* 219(3-4): 325-340.
- Naish, T. R., K. J. Woolfe, et al. (2001). "Orbitally induced oscillations in the East Antarctic ice sheet at the Oligocene/Miocene boundary." *Nature* 413(6857): 719-723.
- Neff, U., S. J. Burns, et al. (2001). "Strong coherence between solar variability and the monsoon in Oman between 9 and 6 kyr ago." *Nature* 411(6835): 290-293.
- Newell, N. E., R. E. Newell, et al. (1989). "Global marine temperature variation and the solar magnetic cycle." *Geophys. Res. Lett* 16: 311-314.
- Ninkovich, D., N. J. Shackleton, et al. (1978). "K-Ar age of the late Pleistocene eruption of Toba, north Sumatra." *Nature* 276(5688): 574-577.
- Oppenheimer, C. (2003). "Climatic, environmental and human consequences of the largest known historic eruption: Tambora volcano (Indonesia) 1815." *Progress in Physical Geography* 27(2): 230-259.
- Pagani, M., M. A. Arthur, et al. (1999). "Miocene Evolution of Atmospheric Carbon Dioxide." *Paleoceanography* 14(3): 273-292.
- Pagani, M., K. H. Freeman, et al. (1999). "Late Miocene atmospheric CO_2 concentrations and the expansion of C_4 grasses." *Science* 285: 876-879.
- Pantic, N. K. (1956). "Biostratigraphie des flores tertiaires de Serbie." *Annales Geologiques de la Peninsule Balkanique* 24: 199-317.
- Pearson, P. N. and M. R. Palmer (2000). "Atmospheric carbon dioxide concentrations over the past 60 million years." *Nature* 406(6797): 695-699.
- Pekar, S. F. and R. M. DeConto (2006). "High-resolution ice-volume estimates for the early Miocene: Evidence for a dynamic ice sheet in Antarctica." *Palaeogeography, Palaeoclimatology, Palaeoecology* 231(1-2): 101-109.
- Petit, J. R., J. Jouzel, et al. (1999). "Climate and atmospheric history of the past 420,000 years from the Vostok ice core, Antarctica." *Nature* 399(6735): 429-436.
- Philander, S. G. and A. V. Fedorov (2003). "Role of tropics in changing the response to Milankovich forcing some three million years ago." *Paleoceanography* 18.
- Pons, A., Suc, J.-P., Reille, M., Combourieu-Nebout, N., 1995. The history of dryness in regions with a mediterranean climate. In "Time-scales of water stress response of mediterranean biota", R.J. Aronson, D. di Castri édit., SPB Academic Publishing bv, Amsterdam, 169-188.
- Popescu, S.-M., Dalesme, F., et al., "*Galeacysta etrusca* complex, dinoflagellate cyst marker of Paratethyan influxes into the Mediterranean Sea before and after the peak of the Messinian Salinity Crisis". *Palynology* in press.
- Popescu, S.-M., Melinte, M.-C., et al. (2008). "Marine re-flooding of the Mediterranean after the Messinian Salinity Crisis predates the Zanclean GSSP". Reply to the "Comment o, 'Earliest Zanclean age for the Colombacci and uppermost Di Tetto formations of the "latest Messinian" northern Apennines: New palaeoenvironmental data from the Maccarone section (marche Province, Italy)' by Popescu et al. (2007) *Geobios* 40 (359-373)" authored by Roveri et al. *Geobios*, in press.
- Popescu, S.-M., Suc, J.-P., et al. (2007). "Earliest Zanclean age for the Colombacci and uppermost Di tetto formations of the "latest Messinian" northern Apennines: New palaeoenvironmental data from the Maccarone section (Marche Province, Italy)". *Geobios*, 40, 3, 359-373.
- Popescu, S.-M. (2006). "Late Miocene and early Pliocene environments in the southwestern Black Sea region from high-resolution palynology of DSDP Site 380A (Leg 42B)." *Palaeogeography, Palaeoclimatology, Palaeoecology* 238(1-4): 64-77.

- Popescu, S.-M., W. Krijgsman, et al. (2006a). "Pollen record and integrated high-resolution chronology of the early Pliocene Dacic Basin (southwestern Romania)." *Palaeogeography, Palaeoclimatology, Palaeoecology* 238(1-4): 78-90.
- Popescu, S.-M., J.-P. Suc, et al. (2006b). "Early Pliocene vegetation changes forced by eccentricity-precession. Example from Southwestern Romania." *Palaeogeography, Palaeoclimatology, Palaeoecology* 238(1-4): 340-348.
- Popescu, S. M. (2001). "Repetitive changes in Early Pliocene vegetation revealed by high-resolution pollen analysis: revised cyclostratigraphy." *Review of Palaeobotany and Palynology* 120(3): 181-202.
- S.-M. Popescu S.-M. (2001), Végétation, climat et cyclostratigraphie en Paratéthys centrale au Miocène supérieur et au Pliocène inférieur d'après la palynologie, Thesis Univ. C. Bernard–Lyon 1
- Popov, S.V., Rögl F., et al., (2003) "Lithological- paleogeographic maps of Paratethys" *Cour. Forsch.-Inst. Senckenberg* 250 : 1-46.
- Popov, S. V., I. G. Shcherba, et al. (2006). "Late Miocene to Pliocene palaeogeography of the Paratethys and its relation to the Mediterranean." *Palaeogeography, Palaeoclimatology, Palaeoecology* 238(1): 91-106.
- Quézel, P and F. Médail (2003). "Ecologie et biogéographie des forêts du bassin méditerranéen" Elsevier France 571 pp.
- Radan, S.C. and M. Radan (1998). "Study of the geomagnetic field structure in the Tertiary in the context of magnetostratigraphic scale elaboration. I – The Pliocene". *An. Inst. Geol. Rom.*, 70: 215-231
- Radulescu C., P.M. Samson and E., Stiuca (1989). Pliocene (Lower Romanian) micromammals in the Dacic Basin. *Misc. Speol. Rom.*, 1: 313-326
- Rampino, M. R. and S. Self (1984). "Sulphur-rich volcanic eruptions and stratospheric aerosols." *Nature* 310(5979): 677-679.
- Rampino, M. R. and S. Self (1992). "Volcanic winter and accelerated glaciation following the Toba super-eruption." *Nature* 359(6390): 50-52.
- Rampino, M. R. and S. Self,(1993). "Climate-volcanism feedback and the Toba eruption of ~74,000 years ago." *Quaternary Res* 40: 269-280.
- Raspopov, O. M., V. A. Dergachev, et al. (2004). "Periodicity of climate conditions and solar variability derived from dendrochronological and other palaeoclimatic data in high latitudes." *Palaeogeography, Palaeoclimatology, Palaeoecology* 209(1-4): 127-139.
- Ravelo, A. C., D. H. Andreasen, et al. (2004a). "Regional climate shifts caused by gradual global cooling in the Pliocene epoch." *Nature* 429(6989): 263-267.
- Ravelo, A. C., P. S. Dekens, et al. (2006). "Evidence for El Niño-like conditions during the Pliocene." *GSA Today* 16(3): 4-11.
- Rosignol-Strick M and M. Paterne (1999). "A synthetic pollen record of the eastern Mediterranean sapropels of the last 1 Ma: implications for the time-scale and formation of sapropels", *Marine Geology* 153: 221–237
- Ryan, W. B. F., W. C. P. III, et al. (1997). "An abrupt drowning of the Black Sea shelf." *Marine Geology* 138: 119-126.
- Ryan, W. B., C. O. Major, et al. (2003). Catastrophic flooding of the Black Sea. *Annual Review of Earth and Planetary Sciences* 31: 525-554.
- Raymo, M. E. (1994). "The Initiation of Northern Hemisphere Glaciation." *Annual Review of Earth and Planetary Sciences* 22(1): 353-383.
- Raymo, M. E., B. Grant, et al. (1996). "Mid-Pliocene warmth: stronger greenhouse and stronger conveyor." *Marine Micropaleontology* 27(1-4): 313-326.

- Raymo, M. E., W. F. Ruddiman, et al. (1989). "Late Pliocene Variation in Northern Hemisphere Ice Sheets and North Atlantic Deep Water Circulation." *Paleoceanography* 4(4): 413-446.
- Rea, D. K., H. Snoeckx, et al. (1998). "Late Cenozoic Eolian Deposition in the North Pacific: Asian Drying, Tibetan Uplift, and Cooling of the Northern Hemisphere." *Paleoceanography* 13(3): 215-224.
- Redfield, T. F., W. H. Wheeler, et al. (2003). "A kinematic model for the development of the Afar Depression and its paleogeographic implications." *Earth and Planetary Science Letters* 216(3): 383-398.
- Reid, G. C. (1987). "Influence of solar variability on global sea surface temperatures." *Nature* 329(6135): 142-143.
- Rigozo, N. R., H. E. da Silva, et al. (2008). "The Medieval and Modern Maximum solar activity imprints in tree ring data from Chile and stable isotope records from Antarctica and Peru." *Journal of Atmospheric and Solar-Terrestrial Physics* 70(7): 1012-1024.
- Rigozo, N. R., D. Jean Roger Nordemann, et al. (2007). "Solar and climate imprint differences in tree ring width from Brazil and Chile." *Journal of Atmospheric and Solar-Terrestrial Physics* 69(4-5): 449-458.
- Rhamstorf S. (1995) "Bifurcation of the Atlantic thermohaline circulation in response to changes in the hydrological cycle", *Nature* 378:145–149.
- Robock, A. (2000). "Volcanic eruptions and climate." *Reviews of Geophysics* 38(2): 191-219.
- Roiron P., 1992. Flores, végétations et climats du Néogène méditerranéen : apports des macroflores du sud de la France et du nord-est de l'Espagne. Thèse, Univ. Montpellier 2 : 296 p.
- Roiron, P., J. Ferrer, et al. (1999). "Les flores du bassin lacustre de Rubielos de Mora. Nouvelles données sur les conditions climatiques au Miocène inférieur dans la région de Teruel (Espagne)." *Comptes Rendus de l'Académie des Sciences - Series IIA - Earth and Planetary Science* 329(12): 897-904.
- Rögl F., (1998). "Palaeogeographic Considerations for mediterranean and Paratethys Seaways (Oligocene to Miocene)". *Ann. Naturhist. Mus. Wien*, 99, A : 279-310.
- Roth-Nebelsik et al., 2004
- Rouchy, J.M., and A. Caruso (2006). "The Messinian salinity crisis in the Mediterranean basin: A reassessment of the data and an integrated scenario". *Sedimentary Geology*, (188-189) 35-67.
- Roveri, M., Manzi, V., et al. (2008). "Recent advancements in the Messinian stratigraphy of Italy and their Mediterranean-scale implications". *Bollettino della Società Paleontologica Italiana*, 47, 2, 71-85.
- Ruddiman, W. F. (2003). "Orbital insolation, ice volume, and greenhouse gases." *Quaternary Science Reviews* 22(15-17): 1597-1629.
- Ruddiman, W. F. (2006a). "Orbital changes and climate." *Quaternary Science Reviews* 25(23-24): 3092-3112.
- Ruddiman, W. F. (2006b). "Ice – driven CO2 feedback on ice volume". *Climate of the Past* 2: 43-78.
- W.F. Ruddiman, M.E. Raymo and A. McIntyre (1986). "Matuyama 41,000-year cycles: North Atlantic Ocean and northern hemisphere ice sheets". *Earth and Planetary Science Letters* 80: 117–129
- Ruddiman, W. F. and J. E. Kutzbach (1989). "Forcing of Late Cenozoic northern hemisphere climate by plateau uplift in southern Asia and the American West." *Journal of Geophysical Research* 94(D15): 18409-18427.
- Ruddiman, W. F. and M. E. Raymo (2003). "A methane-based time scale for Vostok ice." *Quaternary Science Reviews* 22(2-4): 141-155.
- Sadler, J. P. and J. P. Grattan (1999). "Volcanoes as agents of past environmental change." *Global and Planetary Change* 21(1-3): 181-196.

- Sage, F., G. Von Gronefeld et al. (2005). "A record of the Messinian Salinity Crisis on the western Sardinia margin, Northwestern Mediterranean". *Marine and Petroleum Geology*, 22, 757-773.
- Sanz de Siria Catalán, A. (1993). "Datos sobre la paleoclimatología y paleoecología del Neógeno del Vallès-Penedès según las macrofloras halladas en la cuenca y zonas próximas." *Paleontologia i Evolució* 26-27: 281-289.
- Self, S. (2006). "The effects and consequences of very large explosive volcanic eruptions." *Philosophical Transactions of the Royal Society A: Mathematical, Physical and Engineering Sciences* 364(1845): 2073-2097.
- Self, S., M. R. Rampino, et al. (1981). "The possible effects of large 19th and 20th century volcanic eruptions on zonal and hemispheric surface temperatures." *Journal of Volcanology and Geothermal Research* 11(1): 41-60.
- Semenenko, V.N. and E.S. Olejnik (1995) "Stratigraphic correlation of the Eastern Paratethys Kimmerian and Dacian stages by molluscs, dinocyst and nannoplankton data". *Romanian Journal of Stratigraphy*, 76 (7):113-114.
- Shackleton, N. J. (1995). New data on the evolution of Pliocene climatic variability. *Paleoclimate and Evolution, with Emphasis on Human Origins*. G. H. D. a. T. C. P. E.S. Vrba. New Haven, Yale Univ. Press: 24-45.
- Shackleton, N. J. and J. P. Kennett (1975). Paleotemperature history of the Cainozoic and the initiation of Antarctic glaciation: oxygen and carbon analysis in DSDP sites 277, 279 and 281. *Initial Rep. Deep Sea Drill. Proj.* 29: 743-755.
- Shevenell, A. E., J. P. Kennett, et al. (2004). "Middle Miocene Southern Ocean Cooling and Antarctic Cryosphere Expansion." *Science* 305(5691): 1766-1770.
- Siddall M., E.J. Rohling, et al (2003) "Smeed, Sea-level fluctuations during the last glacial cycle" *Nature* 423: 853–858.
- Sigman, D. M., S. L. Jaccard, et al. (2004). "Polar ocean stratification in a cold climate." *Nature* 428(6978): 59-63.
- Sissingh, W. (1998). "Comparative Tertiary stratigraphy of the Rhine Graben, Bresse Graben and Molasse Basin: correlation of Alpine foreland events." *Tectonophysics* 300(1-4): 249-284.
- Sissingh, W. (2001). "Tectonostratigraphy of the West Alpine Foreland: correlation of Tertiary sedimentary sequences, changes in eustatic sea-level and stress regimes." *Tectonophysics* 333(3-4): 361-400.
- Sissingh, W. (2003). "Tertiary paleogeographic and tectonostratigraphic evolution of the Rhenish Triple Junction." *Palaeogeography, Palaeoclimatology, Palaeoecology* 196(1-2): 229-263.
- Sloan, T. and A. W. Wolfendale (2008). "Testing the proposed causal link between cosmic rays and cloud cover." *Environmental Research Letters* 3(2): 024001.
- Sluijs, A., Pross, J. et al., (2005). "From greenhouse to icehouse; organic-walled dinoflagellate cysts as paleoenvironmental indicators in the Paleogene". *Earth- Science Reviews* 68 (3-4):281-315.
- Snel, E., M. Marunteanu, et al. (2006b). "Late Miocene to Early Pliocene chronostratigraphic framework for the Dacic Basin, Romania." *Palaeogeography, Palaeoclimatology, Palaeoecology* 238(1): 107-124.
- Snel, E., M. Marunteanu, et al. (2006a). "Calcareous nannofossil biostratigraphy and magnetostratigraphy of the Upper Miocene and Lower Pliocene of the Northern." *Palaeogeography, Palaeoclimatology, Palaeoecology* 238(1): 125-150.
- Soden and Held, 2006
- Soden, B. J., R. T. Wetherald, et al. (2002). "Global Cooling After the Eruption of Mount Pinatubo: A Test of Climate Feedback by Water Vapor." *Science* 296(5568): 727-730.

- Solanki, S. K. and M. Fligge (2000). "Reconstruction of Past Solar Irradiance." *Space Science Reviews* 94(1): 127-138.
- Sorrel, P., S. M. Popescu, et al. (2006). "Corrigendum to "Hydrographic development of the Aral Sea during the last 2000 years based on a quantitative analysis of dinoflagellate cysts"." *Palaeogeography, Palaeoclimatology, Palaeoecology* 242(1-2): 137-137.
- Sorrel, P., S. M. Popescu, et al. (2006). "Hydrographic development of the Aral Sea during the last 2000 years based on a quantitative analysis of dinoflagellate cysts." *Palaeogeography, Palaeoclimatology, Palaeoecology* 234(2-4): 304-327.
- Sorrel, P., S.-M. Popescu, et al. (2007). "Climate variability in the Aral Sea basin (Central Asia) during the late Holocene based on vegetation changes." *Quaternary Research* 67(3): 357-370.
- Srinivasan, M. S. and D. K. Sinha (1998). "Early Pliocene closing of the Indonesian Seaway: evidence from north-east Indian Ocean and Tropical Pacific deep sea cores." *Journal of Asian Earth Sciences* 16(1): 29-44.
- Steig, E. J., P. J. Polissar, et al. (1996). "Large Amplitude Solar Modulation Cycles of ^{10}Be in Antarctica: Implications for Atmospheric Mixing Processes and Interpretation of the Ice Core Record." *Geophys. Res. Lett.* 23(5): 523-526.
- Steininger, F.F., Senes, J., et al. (1985). "Neogene of the Mediterranean Tethys and Paratethys". I.H. Peter Press. Inst. Paleont., Univ.Vienna. 1, 1-189 10 maps, 2. pp. 1-536.
- Stevanovic, M. P. and N. Pantic (1954). "O sarmatskoj flori i fauni iz zeleznickih useka kod Bozdarevca,." *Annals of the Geology Peninsula Balkan XXII*: 53-68.
- Stoica, M., I. Lazar, et al. (2007). "Mollusc assemblages of the Pontian and Dacian deposits from the Topolog-Arges area (southern Carpathian foredeep)." *Geobios* 40(3): 391-405.
- Stuiver, M. (1961). "Variations in radiocarbon concentrations and sunspot activity". *Journal of Geophysical Research*, 66 : 273-276.
- Stuiver M. and P.J. Reimer (1993). "Extended ^{14}C data base and revised CALIB 3.0 ^{14}C Age calibration program". *Radiocarbon* 35(1): 215-230.
- Studencka, B., I. A. Gontsharova, et al. (1998). "The bivalve faunas as a basis for reconstruction of the Middle Miocene history of the Paratethys." *Acta Geologica Polonica* 48(3): 285-342.
- Suc, J.-P. and J.Cravatte (1982). "Etude palynologique du Pliocène de Catalogne (nord-est de l'Espagne)". *Paléobiol. Cont.*, 13, 1: 1-31.
- Suc, J. P. (1984). "Origin and evolution of the Mediterranean vegetation and climate in Europe." *Nature* 307(5950): 429-432.
- Suc, J.-P., A. Bertini, et al. (1995a). "Structure of West Mediterranean and climate since 5,3 Ma." *Acta zool. Cracov* 38(1): 3-16.
- Suc, J.-P., F. Diniz, et al. (1995b). "Zanclean (~Brunsumian) to early Piacenzian (~early-middle Reuverian) climate from 4° to 54° north latitude (West Africa, West Europe and West Mediterranean areas)." *Meded. Rijks Geol. Dienst* 52: 43-56.
- Suc, J.-P. (1989). "Distribution latitudinale et étagement des associations végétales au Cénozoïque supérieur dans l'aire ouest-méditerranéenne." *Bull. Soc. Géol. Fr.Ser. 8 5 3*: 541-550.
- Suc, J.-P. and E. Bessais (1990). "Pérennité d'un climat thermoxérique en Sicile, avant, pendant et après la crise de salinité messinienne." *C. R. Acad. Sci.Paris* 310(II): 1701-1707.
- Suc, J.-P., Fauquette, S., Bessedik, M., Bertini, A., Zheng, Z., Clauzon, G., Suballyova, D., Diniz, F., Quézel, P., Feddi, N., Clet, M., Bessais, E., Bachiri Taoufiq, N., Méon, H., Combourieu-Nebout, N., 1999. Neogene vegetation changes in West European and West circum-Mediterranean areas. In "Hominid Evolution and Climate in Europe", 1 "Climatic and Environmental Change in the Neogene of Europe", Agusti J., Rook L., Andrews P. édit., Cambridge University Press: 370-385.

- Suc, J.-P., Popescu, S.-M., 2005. Pollen records and climatic cycles in the North Mediterranean region since 2.7 Ma. In "Early-Middle Pleistocene Transitions: The Land-Ocean Evidence", Head M.J., Gibbard P.L. eds., Geological Society of London, Spéc. Publ., 247, 147-158.
- Suc, J.-P., and W.H., Zagwijn, (1983). "Plio-Pleistocene correlations between the northwestern Mediterranean region and northwestern Europe according to recent biostratigraphic and palaeoclimatic data". *Boreas*, 12: 153-166.
- Sun, J., R. Zhu, et al. (2005). "Tectonic uplift in the northern Tibetan Plateau since 13.7 Ma ago inferred from molasse deposits along the Altyn Tagh." *Earth and Planetary Science Letters* 235(3): 641-653.
- Tapponnier, P., X. Zhiqin, et al. (2001). "Oblique Stepwise Rise and Growth of the Tibet Plateau." *Science* 294(5547): 1671-1677.
- Thiede, J. (1998). "Late Cenozoic history of the polar North Atlantic: Results from ocean drilling." *Quat. Sci. Rev.* 17: 185-208.
- Thompson, R. S. (1996). "Pliocene and early Pleistocene environments and climates of the western Snake River Plain, Idaho." *Marine Micropaleontology* 27(1-4): 141-156.
- Thompson, R. S. and R. F. Fleming (1996). "Middle Pliocene vegetation: reconstructions, paleoclimatic inferences, and boundary conditions for climate modeling." *Marine Micropaleontology* 27(1-4): 27-49.
- Thunell R.C. and D.F. Williams (1989) Glacial–Holocene salinity changes in the Mediterranean Sea: hydrographic and depositional effects, *Nature* 338 :493–496
- Tian, J., P. Wang, et al. (2004). "Development of the East Asian monsoon and Northern Hemisphere glaciation: oxygen isotope records from the South China Sea." *Quaternary Science Reviews* 23(18-19): 2007-2016.
- Tiedemann, R., M. Sarnthein, et al. (1994). "Astronomic Timescale for the Pliocene Atlantic $\delta^{18}O$ and Dust Flux Records of Ocean Drilling Program Site 659." *Paleoceanography* 9(4): 619-638.
- Traverse, A. (1978) "Palynological analysis of DSDP Leg 42B (1975) cores from the Black Sea". In Initial Report of the Deep Sea Drilling Project, Ross, D.A., Neprochnov, Y.P. *et al.* eds., 42, 2, U.S. Gov. Print. Off: 993-1015.
- Turco, E., A. M. Bambini, et al. (2002). "Middle Miocene high-resolution calcareous plankton biostratigraphy at Site 926 (Leg 154, equatorial Atlantic Ocean): palaeoecological and palaeobiogeographical implications." *Geobios* 35(Supplement 1): 257-276.
- Tzedakis, P.C., 2007. Seven ambiguities in the Mediterranean palaeoenvironmental narrative. *Quaternary Science Reviews*, 26, 2042-2066.
- Zohary, M. (1973) in: Fischer (Eds.), *Geobotanical foundations of the Middle East*, Stuttgart, 739 pp
- Zheng, Z., 1986. Contribution palynologique à la connaissance du Néogène du Sud-Est français et de Ligurie. Thesis, Univ. Montpellier 2, 142 pp.
- Uhl, D., S. Klotz, et al. (2007). "Cenozoic paleotemperatures and leaf physiognomy -- A European perspective." *Palaeogeography, Palaeoclimatology, Palaeoecology* 248(1-2): 24-31.
- Utescher, T., D. Djordjevic-Milutinovic, et al. (2007). "Palaeoclimate and vegetation change in Serbia during the last 30 Ma." *Palaeogeography, Palaeoclimatology, Palaeoecology* 253(1-2): 141-152.
- Utescher, T., V. Mosbrugger, et al. (2000). "Terrestrial Climate Evolution in Northwest Germany Over the Last 25 Million Years." *PALAIOS* 15(5): 430-449.
- Vai, G. B. and F. Ricci Lucchi (1977). "Algal crusts, autochthonous and clastic gypsum in a cannibalistic evaporite basin: a case history from the Messinian of Northern Apennines." *Sedimentology* 24(2): 211-244.
- van Geel, B., O. M. Raspopov, et al. (1999). "The role of solar forcing upon climate change." *Quaternary Science Reviews* 18(3): 331-338.

- Van Vugt, N., Steenbrink, J., et al. (1998). "Magnetostatigraphy-based astronomical tuning of the early Pliocene lacustrine sediments of Ptolemais (NW Greece) and bed-to-bed correlation with the marine record". *Earth Planetary Science Letters* (164): 535-551.
- van Vugt, N., C. G. Langereis et al. (2006) "Orbital forcing in Pliocene–Pleistocene Mediterranean lacustrine deposits: dominant expression of eccentricity versus precession". *Palaeogeography, Palaeoclimatology, Palaeoecology* 172(3-4):193-205.
- Vasiliev, I. (2006). A new chronology for the Dacian Basin (Romania) : Consequences for the kinematic and paleoenvironmental evolution of the.
- Vasiliev, I., W. Krijgsman, et al. (2004). "Towards an astrochronological framework for the eastern Paratethys Mio-Pliocene sedimentary sequences of the Focsani." *Earth and Planetary Science Letters* 227(3): 231-247.
- Vasiliev, S. S. and D. V.A. (2002). "The ~2400-year cycle in atmospheric radiocarbon concentration: bispectrum of 14C data over the last 8000 years." *Annales Geophysicae* 20: 115-120.
- Vidal, L., T. Bickert, et al. (2002). "Late Miocene stable isotope stratigraphy of SE Atlantic ODP Site 1085: Relation to Messinian events." *Marine Geology* 180(1-4): 71-85.
- Vincent, E. and W. H. Berger (1985). Carbon dioxide and polar cooling in the Miocene: The Monterey hypothesis. *The Carbon Cycle and Atmospheric CO₂: Natural Variations, Archean to Present*. E. T. Sundquist and W. S. Broecker, AGU Monogr. 32: 455-468.
- von der Heydt, A. and H. A. Dijkstra (2008). "The effect of gateways on ocean circulation patterns in the Cenozoic." *Global and Planetary Change* 62(1-2): 132-146.
- Vonmoos, M., J. Beer, et al. (2006). "Large variations in Holocene solar activity constraints from 10Be in the GRIP ice core." *J. Geophys. Res.*
- Wall, D., Dale, B. and Harada, K., 1973. "Descriptions of new fossil dinoflagellates from the Late Quaternary of the Black Sea". *Micropaleontology* (19):18-31.
- Wall D. and B. Dale (1974). "Dinoflagellates in late Quaternary deep-water sediments of Black Sea". In: E.T. Degens and D.A. Ross, Editors, *The Black Sea—Geology, Chemistry and Biology, Memoir - American Association of Petroleum Geologists* (1974), pp. 364–380.
- Wang, Y., H. Cheng, et al. (2005). "The Holocene Asian Monsoon: Links to Solar Changes and North Atlantic Climate." *Science* 308(5723): 854-857.
- Wara, M. W., A. C. Ravelo, et al. (2005). "Permanent El Nino-Like Conditions During the Pliocene Warm Period." *Science* 309(5735): 758-761.
- Warny, S. A., P. J. Bart, et al. (2003). "Timing and progression of climatic, tectonic and glacioeustatic influences on the Messinian Salinity Crisis." *Palaeogeography, Palaeoclimatology, Palaeoecology* 202(1-2): 59-66.
- Weaver, A. J., O. A. Saenko, et al. (2003). "Meltwater Pulse 1A from Antarctica as a Trigger of the Bolling-Allerod Warm Interval." *Science* 299(5613): 1709-1713.
- Wijmstra, T.A. and M.C. Groenhart (1983). "Record of 700,000 years vegetational history in Eastern Macedonia (Greece)". *Revista de la Academia Colombiana Ciencias Exactas, Fisicas y Naturales* 15: 87–98.
- Webb, P. N., D. M. Harwood, et al. (1996). "A marine and terrestrial Sirius Group succession, middle Beardmore Glacier-Queen Alexandra Range, Transantarctic Mountains, Antarctica." *Marine Micropaleontology* 27(1-4): 273-297.
- Westerhold, T., T. Bickert, et al. (2005). "Middle to late Miocene oxygen isotope stratigraphy of ODP site 1085 (SE Atlantic): new constrains on Miocene climate variability and sea-level fluctuations." *Palaeogeography, Palaeoclimatology, Palaeoecology* 217(3-4): 205-222.
- Willis, K. J., A. Kleczkowski, et al. (1999). "No Title." *Nature* 397(6721): 685-688.

- Winton, M. (2003). "On the Climatic Impact of Ocean Circulation." *Journal of Climate* 16(17): 2875-2889.
- Woodruff, F., Savin, S. (1989). "Miocene deepwater oceanography." *Paleoceanography* 4: 87-140.
- Woodruff, F. and S. Savin (1991). "Mid-Miocene Isotope Stratigraphy in the Deep Sea: High-Resolution Correlations, Paleoclimatic Cycles, and Sediment Preservation." *Paleoceanography* 6(6): 755-806.
- Wright, J. D. and K. G. Miller (1992). Miocene stable isotope stratigraphy, site 747, Kerguelen Plateau. *Proc. ODP, Sci. Results*. S. W. Wise Jr., R. Schlich and et al. College Station, TX. 120: 855– 866.
- Wright, J. D. and K. G. Miller (1993). Southern Ocean influence on late Eocene to Miocene deep-water circulation. *The Antarctic Paleoenvironment: A Perspective on Global Change, Part 2*. J. Kennett, Antarctic Research Series. 60: 1-25.
- Wright, J. D. and K. G. Miller (1996). "Control of North Atlantic Deep Water Circulation by the Greenland-Scotland Ridge." *Paleoceanography*, 11(2): 157-170.
- Wright, J. D., K. G. Miller, et al. (1992). "Early and Middle Miocene Stable Isotopes: Implications for Deepwater Circulation and Climate." *Paleoceanography* 7(3): 357-389.
- Yaltirak C., M. Sakinç, et al. (2002). "Late Pleistocene uplift history along the southwestern Marmara Sea determined from raised coastal deposits and global sea-level variations" *Marine Geology* 190: 283–305.
- Yang, F. and M. E. Schlesinger (2002). "On the surface and atmospheric temperature changes following the 1991 Pinatubo volcanic eruption: A GCM study" *J. Geophys. Res.* 107(D8).
- Yiou, F., G.M. Raisbeck, et al (1997). "Beryllium 10 in the Greenland Ice Core Project ice core at Summit, Greenland". *J. Geophysics. Res.* 102 : 26783–26794
- Yu, Z. and E. Ito (1999). "Possible solar forcing of century-scale drought frequency in the northern Great Plains." *Geology* 27(3): 263-266.
- Zachos, J., M. Pagani, et al. (2001a). "Trends, Rhythms, and Aberrations in Global Climate 65 Ma to Present." *Science* 292(5517): 686-693.
- Zagwijn W.H. (1960). "Aspects of the Pliocene and early Pleistocene vegetation in The Netherlands". *Meded. Geol. Sticht*, sér. C, 3, 5: 1-78.
- Zheng Z. and J. Cravatte (1986). "Etude palynologique du Pliocène de la Côte d'Azur (France) et du littoral ligure (Italie)". *Geobios*, 19(6) : 815-823.
- Zhisheng, A., J. E. Kutzbach, et al. (2001). "Evolution of Asian monsoons and phased uplift of the Himalaya-Tibetan plateau since Late Miocene times." *Nature* 411(6833): 62-66.